2

Stephen Wiggins

TEXTS IN APPLIED MATHEMATICS

Introduction to Applied Nonlinear Dynamical Systems and Chaos

Second Edition

Springer

Texts in Applied Mathematics 2

Springer
New York
Berlin
Heidelberg
Hong Kong
London
Milan
Paris
Tokyo

This page intentionally left blank

Stephen Wiggins

Introduction to Applied Nonlinear Dynamical Systems and Chaos

Second Edition

With 250 Figures

Springer

Stephen Wiggins
School of Mathematics
University of Bristol
Clifton, Bristol BS8 1TW
UK
S.Wiggins@bristol.ac.uk

Series Editors

J.E. Marsden
Control and Dynamical Systems, 107–81
California Institute of Technology
Pasadena, CA 91125
USA
marsden@cds.caltech.edu

L. Sirovich
Division of Applied Mathematics
Brown University
Providence, RI 02912
USA
chico@camelot.mssm.edu

S.S. Antman
Department of Mathematics
and
Institute for Physical Science
and Technology
University of Maryland
College Park, MD 20742-4015
USA
ssa@math.umd.edu

Mathematics Subject Classification (2000): 58Fxx, 34Cxx, 70Kxx

Library of Congress Cataloging-in-Publication Data
Wiggins, Stephen.
Introduction to applied nonlinear dynamical systems and chaos / Stephen Wiggins. – 2nd ed.
p. cm. – (Texts in applied mathematics ; 2)
Includes bibliographical references and index.
ISBN 0-387-00177-8 (alk. paper)
1. Differentiable dynamical systems. 2. Nonlinear theories. 3. Chaotic behavior in systems. I. Title. II. Texts in applied mathematics ; 2.
QA614.8.W544 2003
003′.85–dc21 2002042742

ISBN 0-387-00177-8 Printed on acid-free paper.

Printed in the United States of America.

9 8 7 6 5 4 3 2 1 SPIN 10901182

www.springer-ny.com

Springer-Verlag New York Berlin Heidelberg
A member of BertelsmannSpringer Science+Business Media GmbH

Series Preface

Mathematics is playing an ever more important role in the physical and biological sciences, provoking a blurring of boundaries between scientific disciplines and a resurgence of interest in the modern as well as the classical techniques of applied mathematics. This renewal of interest, both in research and teaching, has led to the establishment of the series Texts in Applied Mathematics (TAM).

The development of new courses is a natural consequence of a high level of excitement on the research frontier as newer techniques, such as numerical and symbolic computer systems, dynamical systems, and chaos, mix with and reinforce the traditional methods of applied mathematics. Thus, the purpose of this textbook series is to meet the current and future needs of these advances and to encourage the teaching of new courses.

TAM will publish textbooks suitable for use in advanced undergraduate and beginning graduate courses, and will complement the Applied Mathematical Sciences (AMS) series, which will focus on advanced textbooks and research-level monographs.

Pasadena, California — J.E. Marsden
Providence, Rhode Island — L. Sirovich
College Park, Maryland — S.S. Antman

This page intentionally left blank

Preface to the Second Edition

This edition contains a significant amount of new material. The main reason for this is that the subject of applied dynamical systems theory has seen explosive growth and expansion throughout the 1990s. Consequently, a student needs a much larger toolbox today in order to begin research on significant problems.

I also try to emphasize a broader and more unified point of view. My goal is to treat dissipative and conservative dynamics, discrete and continuous time systems, and local and global behavior, as much as possible, on the same footing. Many textbooks tend to treat most of these issues separately (e.g., dissipative, discrete time, local dynamics; global dynamics of continuous time conservative systems, etc.). However, in research one generally needs to have an understanding of each of these areas, and their inter-relations. For example, in studying a conservative continuous time system, one might study periodic orbits and their stability by passing to a Poincaré map (discrete time). The question of how stability may be affected by dissipative perturbations may naturally arise. Passage to the Poincaré map renders the study of periodic orbits a local problem (i.e., they are fixed points of the Poincaré map), but their manifestation in the continuous time problem may have global implications. An ability to put together a "big picture" from many (seemingly) disparate pieces of information is crucial for the successful analysis of nonlinear dynamical systems.

This edition has seen a major restructuring with respect to the first edition in terms of the organization of the chapters into smaller units with a single, common theme, and the exercises relevant to each chapter now being given at the end of the respective chapter.

The bulk of the material in this book can be covered in three ten week terms. This is an ambitious program, and requires relegating some of the material to background reading (described below). My goal was to have the necessary background material side-by-side with the material that I would lecture on. This tends to be more demanding on the student, but with the right guidance, it also tends to be more rewarding and lead to a deeper understanding and appreciation of the subject.

The mathematical prerequisites for the course are really not great; elementary analysis, multivariable calculus, and linear algebra are sufficient. In reality, this may not be enough on its own. A successful understanding of applied dynamical systems theory requires the students to have an inte-

grated knowledge of these prerequisites in the sense that they can fluidly manipulate and use the ideas between the subjects. This means they must possess the quality often referred to as "mathematical maturity." A study of dynamical systems theory can be a good way to obtain this. In addition, an ordinary differential equations course from the geometric point of view (e.g., the material in the books of Arnold [1973] or Hirsch and Smale [1974]) would be ideal.

Chapters 1-17 form the core of the first term material. It provides students with the basic concepts and tools for the study of dynamical systems theory. I tend to cover chapters 7, 11 and 12 at a brisk pace. The main point there is the ideas and main results. The details can be grasped over time, and in other settings. Chapters 13-17 could be viewed as belonging to the common theme of "dynamical systems with special structure." Chapter 14 is the most important of these chapters. The relation, and contrasts, between Hamiltonian and reversible systems is useful to understand, and is the reason for including chapter 16. I often just assign selected background reading from chapter 13, but knowledge of the relation between Lagrangian and Hamiltonian dynamical systems is of growing importance in applications. Gradient dynamical systems arise in numerous applications (e.g., in biologically related areas) and knowledge of the nature of their dynamics, and how it contrasts with, e.g., Hamiltonian dynamics, is important. Chapter 17 is short, but I have always felt that students should be aware of these results because there are numerous examples of systems arising in applications that experience a "transient temporal disturbance." Throughout the early chapters I discuss a number of results and theoretical frameworks for general nonautonomous vector fields (i.e., time-dependent vector fields whose time dependence is not periodic). This area traditionally has not been a part of dynamical systems from a geometric point of view, but this situation is changing rapidly, and I believe it will play an increasingly important role in applications in the near future.

Chapters 18-22 are covered in the second term. The subject is "local bifurcation theory." The two key tools for the local analysis of dynamical systems are center manifold theory and normal form theory, covered in chapters 18 and 19. The chapter on normal form theory is greatly expanded from the first edition. The main new material is the normal form work of Elphick, Tirapegui, Brachet, Coullet and Iooss, a discussion of Hamiltonian normal form theory (following Churchill, Kummer, and Rod), and some material on symmetries (whose possible existence, and implications, should be considered in the course of study of any dynamical system). Possibly sections 19.1-19.3 could have been omitted in this edition; however it has been my experience that students understand the later (and more difficult) material more easily once they have been exposed to this more pedestrian introduction. In chapters 20 and 21 I tend not to cover in much detail the material related to the codimension of a bifurcation and versal deformations. This is a standard language used in discussing the subject

and it is important that the students have all the details available to them for background reading and see it in the context of the material I lecture on. New material on Hamiltonian bifurcations and circle maps is included. The inclusion of introductory material on Hamiltonian bifurcations is an example of the effort to have a broader and more unified point of view as discussed earlier. For example, we first describe the "generic saddle-node bifurcation at a single zero eigenvalue." It is then natural to ask about the saddle-node bifurcation in a Hamiltonian system, which turns out to be rather different. Chapter 22 mainly serves as a warning that the way in which bifurcation phenomena are discussed in applications may not agree with the mathematical reality, and appropriate pointers to the literature are given.

Chapters 23-33 are covered in the third term. The subject is "global dynamics, bifurcations, and chaos." There is a sprinkling of new material throughout these chapters (e.g., a proof of a simple version of the lambda lemma and a proof of the shadowing lemma), but the structure is basically the same as the first edition.

There is not a great deal of overlap between the material in the individual terms, and with the appropriate prerequisites, each of these one term courses could be viewed as an independent course in itself. The textbook provides the necessary background for the students to make this a possibility.

Some material has been left out of this edition; in particular, material on averaging, the subharmonic Melnikov function, and lobe dynamics. The reason is that over time I have begun to cover averaging and the subharmonic Melnikov function as topics in a course solely devoted to perturbation methods. I cover lobe dynamics in a course devoted to transport phenomena in dynamical systems, which has developed in the last ten years to the point that it now justifies an independent course of its own, with applications taken from many diverse disciplines.

It has been my experience over time that a significant obstacle for students in their study of the subject is the sheer amount of (initially) unfamiliar jargon. In order to make this a bit easier to deal with I have now included a glossary of frequently used terms. The bibliography has also been updated and greatly expanded.

I would also like to take this opportunity to express my gratitude to the National Science Foundation and to Dr. Wen Masters and Dr. Reza Malek-Madani of the Office of Naval Research for their generous support of my research over the years. Research and teaching are two sides of the same coin, and it is only through an active and fruiful research program that the teaching becomes alive and relevant.

Bristol, England Stephen Wiggins
2003

This page intentionally left blank

Contents

Series Preface v

Preface to the Second Edition vii

Introduction 1

1 Equilibrium Solutions, Stability, and Linearized Stability 5
1.1 Equilibria of Vector Fields 5
1.2 Stability of Trajectories 7
1.2a Linearization 10
1.3 Maps 15
1.3a Definitions of Stability for Maps 15
1.3b Stability of Fixed Points of Linear Maps 15
1.3c Stability of Fixed Points of Maps via the Linear Approximation 15
1.4 Some Terminology Associated with Fixed Points 16
1.5 Application to the Unforced Duffing Oscillator 16
1.6 Exercises 16

2 Liapunov Functions 20
2.1 Exercises 25

3 Invariant Manifolds: Linear and Nonlinear Systems 28
3.1 Stable, Unstable, and Center Subspaces of Linear, Autonomous Vector Fields 29
3.1a Invariance of the Stable, Unstable, and Center Subspaces 32
3.1b Some Examples 33
3.2 Stable, Unstable, and Center Manifolds for Fixed Points of Nonlinear, Autonomous Vector Fields . . . 37
3.2a Invariance of the Graph of a Function: Tangency of the Vector Field to the Graph 39
3.3 Maps 40
3.4 Some Examples 41
3.5 Existence of Invariant Manifolds: The Main Methods of Proof, and How They Work 43

3.5a Application of These Two Methods to a Concrete Example: Existence of the Unstable Manifold 45
3.6 Time-Dependent Hyperbolic Trajectories and their Stable and Unstable Manifolds 52
3.6a Hyperbolic Trajectories 53
3.6b Stable and Unstable Manifolds of Hyperbolic Trajectories 56
3.7 Invariant Manifolds in a Broader Context 59
3.8 Exercises 62

4 Periodic Orbits **71**
4.1 Nonexistence of Periodic Orbits for Two-Dimensional, Autonomous Vector Fields 72
4.2 Further Remarks on Periodic Orbits 74
4.3 Exercises 76

5 Vector Fields Possessing an Integral **77**
5.1 Vector Fields on Two-Manifolds Having an Integral 77
5.2 Two Degree-of-Freedom Hamiltonian Systems and Geometry 82
5.2a Dynamics on the Energy Surface 83
5.2b Dynamics on an Individual Torus 85
5.3 Exercises 85

6 Index Theory **87**
6.1 Exercises 89

7 Some General Properties of Vector Fields: Existence, Uniqueness, Differentiability, and Flows **90**
7.1 Existence, Uniqueness, Differentiability with Respect to Initial Conditions 90
7.2 Continuation of Solutions 91
7.3 Differentiability with Respect to Parameters 91
7.4 Autonomous Vector Fields 92
7.5 Nonautonomous Vector Fields 94
7.5a The Skew-Product Flow Approach 95
7.5b The Cocycle Approach 97
7.5c Dynamics Generated by a Bi-Infinite Sequence of Maps 97
7.6 Liouville's Theorem 99
7.6a Volume Preserving Vector Fields and the Poincaré Recurrence Theorem 101
7.7 Exercises 101

8 Asymptotic Behavior **104**
8.1 The Asymptotic Behavior of Trajectories 104

8.2 Attracting Sets, Attractors, and Basins of Attraction . . . 107
8.3 The LaSalle Invariance Principle . . . 110
8.4 Attraction in Nonautonomous Systems . . . 111
8.5 Exercises . . . 114

9 The Poincaré-Bendixson Theorem 117
9.1 Exercises . . . 121

10 Poincaré Maps 122
10.1 Case 1: Poincaré Map Near a Periodic Orbit . . . 123
10.2 Case 2: The Poincaré Map of a Time-Periodic Ordinary Differential Equation . . . 127
10.2a Periodically Forced Linear Oscillators . . . 128
10.3 Case 3: The Poincaré Map Near a Homoclinic Orbit . . . 138
10.4 Case 4: Poincaré Map Associated with a Two Degree-of-Freedom Hamiltonian System . . . 144
10.4a The Study of Coupled Oscillators via Circle Maps . . . 146
10.5 Exercises . . . 149

11 Conjugacies of Maps, and Varying the Cross-Section 151
11.1 Case 1: Poincaré Map Near a Periodic Orbit: Variation of the Cross-Section . . . 154
11.2 Case 2: The Poincaré Map of a Time-Periodic Ordinary Differential Equation: Variation of the Cross-Section . . . 155

12 Structural Stability, Genericity, and Transversality 157
12.1 Definitions of Structural Stability and Genericity . . . 161
12.2 Transversality . . . 165
12.3 Exercises . . . 167

13 Lagrange's Equations 169
13.1 Generalized Coordinates . . . 170
13.2 Derivation of Lagrange's Equations . . . 172
13.2a The Kinetic Energy . . . 175
13.3 The Energy Integral . . . 176
13.4 Momentum Integrals . . . 177
13.5 Hamilton's Equations . . . 177
13.6 Cyclic Coordinates, Routh's Equations, and Reduction of the Number of Equations . . . 178
13.7 Variational Methods . . . 180
13.7a The Principle of Least Action . . . 180
13.7b The Action Principle in Phase Space . . . 182
13.7c Transformations that Preserve the Form of Hamilton's Equations . . . 184
13.7d Applications of Variational Methods . . . 186
13.8 The Hamilton-Jacobi Equation . . . 187

13.8a Applications of the Hamilton-Jacobi Equation . . . 192
13.9 Exercises . . . 192

14 Hamiltonian Vector Fields **197**
14.1 Symplectic Forms . . . 199
14.1a The Relationship Between Hamilton's Equations and the Symplectic Form . . . 199
14.2 Poisson Brackets . . . 200
14.2a Hamilton's Equations in Poisson Bracket Form . . . 201
14.3 Symplectic or Canonical Transformations . . . 202
14.3a Eigenvalues of Symplectic Matrices . . . 203
14.3b Infinitesimally Symplectic Transformations . . . 204
14.3c The Eigenvalues of Infinitesimally Symplectic Matrices . . . 206
14.3d The Flow Generated by Hamiltonian Vector Fields is a One-Parameter Family of Symplectic Transformations . . . 206
14.4 Transformation of Hamilton's Equations Under Symplectic Transformations . . . 208
14.4a Hamilton's Equations in Complex Coordinates . . . 209
14.5 Completely Integrable Hamiltonian Systems . . . 210
14.6 Dynamics of Completely Integrable Hamiltonian Systems in Action-Angle Coordinates . . . 211
14.6a Resonance and Nonresonance . . . 212
14.6b Diophantine Frequencies . . . 217
14.6c Geometry of the Resonances . . . 220
14.7 Perturbations of Completely Integrable Hamiltonian Systems in Action-Angle Coordinates . . . 221
14.8 Stability of Elliptic Equilibria . . . 222
14.9 Discrete-Time Hamiltonian Dynamical Systems: Iteration of Symplectic Maps . . . 223
14.9a The KAM Theorem and Nekhoroshev's Theorem for Symplectic Maps . . . 223
14.10 Generic Properties of Hamiltonian Dynamical Systems . . . 225
14.11 Exercises . . . 226

15 Gradient Vector Fields **231**
15.1 Exercises . . . 232

16 Reversible Dynamical Systems **234**
16.1 The Definition of Reversible Dynamical Systems . . . 234
16.2 Examples of Reversible Dynamical Systems . . . 235
16.3 Linearization of Reversible Dynamical Systems . . . 236
16.3a Continuous Time . . . 236
16.3b Discrete Time . . . 238

16.4 Additional Properties of Reversible Dynamical Systems . . . 239
16.5 Exercises . . . 240

17 Asymptotically Autonomous Vector Fields 242
17.1 Exercises . . . 244

18 Center Manifolds 245
18.1 Center Manifolds for Vector Fields . . . 246
18.2 Center Manifolds Depending on Parameters . . . 251
18.3 The Inclusion of Linearly Unstable Directions . . . 256
18.4 Center Manifolds for Maps . . . 257
18.5 Properties of Center Manifolds . . . 263
18.6 Final Remarks on Center Manifolds . . . 265
18.7 Exercises . . . 265

19 Normal Forms 270
19.1 Normal Forms for Vector Fields . . . 270
19.1a Preliminary Preparation of the Equations . . . 270
19.1b Simplification of the Second Order Terms . . . 272
19.1c Simplification of the Third Order Terms . . . 274
19.1d The Normal Form Theorem . . . 275
19.2 Normal Forms for Vector Fields with Parameters . . . 278
19.2a Normal Form for The Poincaré-Andronov-Hopf Bifurcation . . . 279
19.3 Normal Forms for Maps . . . 284
19.3a Normal Form for the Naimark-Sacker Torus Bifurcation . . . 285
19.4 Exercises . . . 288
19.5 The Elphick-Tirapegui-Brachet-Coullet-Iooss Normal Form . . . 290
19.5a An Inner Product on H_k . . . 291
19.5b The Main Theorems . . . 292
19.5c Symmetries of the Normal Form . . . 296
19.5d Examples . . . 298
19.5e The Normal Form of a Vector Field Depending on Parameters . . . 302
19.6 Exercises . . . 304
19.7 Lie Groups, Lie Group Actions, and Symmetries . . . 306
19.7a Examples of Lie Groups . . . 308
19.7b Examples of Lie Group Actions on Vector Spaces . . . 310
19.7c Symmetric Dynamical Systems . . . 312
19.8 Exercises . . . 312
19.9 Normal Form Coefficients . . . 314
19.10 Hamiltonian Normal Forms . . . 316

19.10a General Theory 316
19.10b Normal Forms Near Elliptic Fixed Points: The Semisimple Case 322
19.10c The Birkhoff and Gustavson Normal Forms 333
19.10d The Lyapunov Subcenter Theorem and Moser's Theorem 334
19.10e The KAM and Nekhoroshev Theorem's Near an Elliptic Equilibrium Point 336
19.10f Hamiltonian Normal Forms and Symmetries 338
19.10g Final Remarks 342
19.11 Exercises 342
19.12 Conjugacies and Equivalences of Vector Fields 345
19.12a An Application: The Hartman-Grobman Theorem 350
19.12b An Application: Dynamics Near a Fixed Point-Šošitaĭšvili's Theorem 353
19.13 Final Remarks on Normal Forms 353

20 Bifurcation of Fixed Points of Vector Fields 356
20.1 A Zero Eigenvalue 357
20.1a Examples 358
20.1b What Is A "Bifurcation of a Fixed Point"? 361
20.1c The Saddle-Node Bifurcation 363
20.1d The Transcritical Bifurcation 366
20.1e The Pitchfork Bifurcation 370
20.1f Exercises 373
20.2 A Pure Imaginary Pair of Eigenvalues: The Poincare-Andronov-Hopf Bifurcation 378
20.2a Exercises 386
20.3 Stability of Bifurcations Under Perturbations 387
20.4 The Idea of the Codimension of a Bifurcation 392
20.4a The "Big Picture" for Bifurcation Theory 393
20.4b The Approach to Local Bifurcation Theory: Ideas and Results from Singularity Theory 397
20.4c The Codimension of a Local Bifurcation 402
20.4d Construction of Versal Deformations 406
20.4e Exercises 415
20.5 Versal Deformations of Families of Matrices 417
20.5a Versal Deformations of Real Matrices 431
20.5b Exercises 435
20.6 The Double-Zero Eigenvalue: the Takens-Bogdanov Bifurcation 436
20.6a Additional References and Applications for the Takens-Bogdanov Bifurcation 446
20.6b Exercises 446

20.7 A Zero and a Pure Imaginary Pair of Eigenvalues: the Hopf-Steady State Bifurcation . . . 449
20.7a Additional References and Applications for the Hopf-Steady State Bifurcation . . . 477
20.7b Exercises . . . 477
20.8 Versal Deformations of Linear Hamiltonian Systems . . . 482
20.8a Williamson's Theorem . . . 482
20.8b Versal Deformations of Jordan Blocks Corresponding to Repeated Eigenvalues . . . 485
20.8c Versal Deformations of Quadratic Hamiltonians of Codimension ≤ 2 . . . 488
20.8d Versal Deformations of Linear, Reversible Dynamical Systems . . . 490
20.8e Exercises . . . 491
20.9 Elementary Hamiltonian Bifurcations . . . 491
20.9a One Degree-of-Freedom Systems . . . 491
20.9b Exercises . . . 494
20.9c Bifurcations Near Resonant Elliptic Equilibrium Points . . . 495
20.9d Exercises . . . 497

21 Bifurcations of Fixed Points of Maps 498
21.1 An Eigenvalue of 1 . . . 499
21.1a The Saddle-Node Bifurcation . . . 500
21.1b The Transcritical Bifurcation . . . 504
21.1c The Pitchfork Bifurcation . . . 508
21.2 An Eigenvalue of -1: Period Doubling . . . 512
21.2a Example . . . 513
21.2b The Period-Doubling Bifurcation . . . 515
21.3 A Pair of Eigenvalues of Modulus 1: The Naimark-Sacker Bifurcation . . . 517
21.4 The Codimension of Local Bifurcations of Maps . . . 523
21.4a One-Dimensional Maps . . . 524
21.4b Two-Dimensional Maps . . . 524
21.5 Exercises . . . 526
21.6 Maps of the Circle . . . 530
21.6a The Dynamics of a Special Class of Circle Maps-Arnold Tongues . . . 542
21.6b Exercises . . . 550

22 On the Interpretation and Application of Bifurcation Diagrams: A Word of Caution 552

23 The Smale Horseshoe **555**
23.1 Definition of the Smale Horseshoe Map 555
23.2 Construction of the Invariant Set 558
23.3 Symbolic Dynamics 566
23.4 The Dynamics on the Invariant Set 570
23.5 Chaos 573
23.6 Final Remarks and Observations 574

24 Symbolic Dynamics **576**
24.1 The Structure of the Space of Symbol Sequences 577
24.2 The Shift Map 581
24.3 Exercises 582

25 The Conley–Moser Conditions, or "How to Prove That a Dynamical System is Chaotic" **585**
25.1 The Main Theorem 585
25.2 Sector Bundles 602
25.3 Exercises 608

26 Dynamics Near Homoclinic Points of Two-Dimensional Maps **612**
26.1 Heteroclinic Cycles 631
26.2 Exercises 632

27 Orbits Homoclinic to Hyperbolic Fixed Points in Three-Dimensional Autonomous Vector Fields **636**
27.1 The Technique of Analysis 637
27.2 Orbits Homoclinic to a Saddle-Point with Purely Real Eigenvalues 640
27.2a Two Orbits Homoclinic to a Fixed Point Having Real Eigenvalues 651
27.2b Observations and Additional References 657
27.3 Orbits Homoclinic to a Saddle-Focus 659
27.3a The Bifurcation Analysis of Glendinning and Sparrow 666
27.3b Double-Pulse Homoclinic Orbits 676
27.3c Observations and General Remarks 676
27.4 Exercises 681

28 Melnikov's Method for Homoclinic Orbits in Two-Dimensional, Time-Periodic Vector Fields **687**
28.1 The General Theory 687
28.2 Poincaré Maps and the Geometry of the Melnikov Function 711
28.3 Some Properties of the Melnikov Function 713

28.4 Homoclinic Bifurcations 715
28.5 Application to the Damped, Forced Duffing Oscillator . . . 717
28.6 Exercises 720

29 Liapunov Exponents **726**
29.1 Liapunov Exponents of a Trajectory 726
29.2 Examples 730
29.3 Numerical Computation of Liapunov Exponents 734
29.4 Exercises 734

30 Chaos and Strange Attractors **736**
30.1 Exercises 745

31 Hyperbolic Invariant Sets: A Chaotic Saddle **747**
31.1 Hyperbolicity of the Invariant Cantor Set Λ Constructed in Chapter 25 747
31.1a Stable and Unstable Manifolds of the Hyperbolic Invariant Set 753
31.2 Hyperbolic Invariant Sets in $\mathbb{R}^n$ 754
31.2a Sector Bundles for Maps on $\mathbb{R}^n$ 757
31.3 A Consequence of Hyperbolicity: The Shadowing Lemma 758
31.3a Applications of the Shadowing Lemma 759
31.4 Exercises 760

32 Long Period Sinks in Dissipative Systems and Elliptic Islands in Conservative Systems **762**
32.1 Homoclinic Bifurcations 762
32.2 Newhouse Sinks in Dissipative Systems 774
32.3 Islands of Stability in Conservative Systems 776
32.4 Exercises 776

33 Global Bifurcations Arising from Local Codimension—Two Bifurcations **777**
33.1 The Double-Zero Eigenvalue 777
33.2 A Zero and a Pure Imaginary Pair of Eigenvalues 782
33.3 Exercises 790

34 Glossary of Frequently Used Terms **793**

Bibliography **809**

Index **836**

This page intentionally left blank

Introduction

In this book we will study equations of the following form

$$\dot{x} = f(x, t; \mu), \tag{0.0.1}$$

and

$$x \mapsto g(x; \mu), \tag{0.0.2}$$

with $x \in U \subset \mathbb{R}^n$, $t \in \mathbb{R}^1$, and $\mu \in V \subset \mathbb{R}^p$ where U and V are open sets in $\mathbb{R}^n$ and $\mathbb{R}^p$, respectively. The overdot in (0.0.1) means "$\frac{d}{dt}$," and we view the variables μ as parameters. In the study of dynamical systems the independent variable is often referred to as "time." We will use this terminology from time to time also. We refer to (0.0.1) as a *vector field* or *ordinary differential equation* and to (0.0.2) as a *map* or *difference equation*. Both will be termed *dynamical systems*. Before discussing what we might want to know about (0.0.1) and (0.0.2), we need to establish a bit of terminology.

By a solution of (0.0.1) we mean a map, x, from some interval $I \subset \mathbb{R}^1$ into $\mathbb{R}^n$, which we represent as follows

$$\begin{aligned} x &: I \to \mathbb{R}^n, \\ t &\mapsto x(t), \end{aligned}$$

such that $x(t)$ satisfies (0.1), i.e.,

$$\dot{x}(t) = f\big(x(t), t; \mu\big).$$

The map x has the geometrical interpretation of a curve in $\mathbb{R}^n$, and (0.0.1) gives the tangent vector at each point of the curve, hence the reason for referring to (0.0.1) as a vector field. We will refer to the space of dependent variables of (0.0.1) (i.e., $\mathbb{R}^n$) as the *phase space* of (0.0.1), and, abstractly, our goal will be to understand the geometry of solution curves in phase space. We remark that in many applications the structure of the phase space may be more general than $\mathbb{R}^n$; frequent examples are cylindrical, spherical, or toroidal phase spaces. We will discuss these situations as they are encountered; for now we incur no loss of generality if we take the phase space of our maps and vector fields to be open sets in $\mathbb{R}^n$.

We will see in Chapter 7 that solutions of differential equations have different properties depending on whether or not the ordinary differential equation depends explicity on time. Ordinary differential equations that depend explicity on time (i.e., $\dot{x} = f(x, t; \mu)$) are referred to as *nonautonomous* or *time dependent* ordinary differential equations, or vector fields, and ordinary differential equations that do not depend explicity on time (i.e., $\dot{x} = f(x; \mu)$) are referred to as *autonomous* or *time independent* ordinary differential equations, or vector fields.

It will often prove useful to build a little more information into our notation for solutions, which we describe below.

Dependence on Initial Conditions

It may be useful to distinguish a solution curve by a particular point in phase space that it passes through at a specific time, i.e., for a solution $x(t)$ we have $x(t_0) = x_0$. We refer to this as specifying an initial condition. This is often included in the expression for a solution by writing $x(t, t_0, x_0)$. In some situations explicitly displaying the initial condition may be unimportant, in which case we will denote the solution merely as $x(t)$. In still other situations the initial time may be always understood to be a specific value, say $t_0 = 0$; in this case we would denote the solution as $x(t, x_0)$.

Dependence on Parameters

Similarly, it may be useful to explicitly display the parametric dependence of solutions. In this case we would write $x(t, t_0, x_0; \mu)$, or, if we weren't interested in the initial condition, $x(t; \mu)$. If parameters play no role in our arguments we will often omit any specific parameter dependence from the notation.

Some Terminology

1. There are several different terms which are somewhat synonymous with the term *solution* of (0.0.1). $x(t, t_0, x_0)$ may also be referred to as the *trajectory* or *phase curve* through the point x_0 at $t = t_0$.

2. The graph of $x(t, t_0, x_0)$ over t is referred to as an *integral curve*. More precisely, graph $x(t, t_0, x_0) = \{ (x, t) \in \mathbb{R}^n \times \mathbb{R}^1 \mid x = x(t, t_0, x_0),\ t \in I \}$ where I is the time interval of existence.

3. Let x_0 be a point in the phase space of (0.1). By the *orbit through* x_0, denoted $O(x_0)$, we mean the set of points in phase space that lie on a trajectory passing through x_0. More precisely, for $x_0 \in U \subset \mathbb{R}^n$, the orbit through x_0 is given by $O(x_0) = \{ x \in \mathbb{R}^n \mid x = x(t, t_0, x_0),\ t \in I \}$. Note that for any $T \in I$, it follows that $O(x(T, t_0, x_0)) = O(x_0)$.

Let us now give an example that illustrates the difference between trajectories, integral curves, and orbits.

Example 0.0.1. Consider the equation

$$\begin{aligned} \dot{u} &= v, \\ \dot{v} &= -u, \qquad (u,v) \in \mathbb{R}^1 \times \mathbb{R}^1. \end{aligned} \tag{0.0.3}$$

The *solution* passing through the point $(u,v) = (1,0)$ at $t = 0$ is given by $\Big(u(t), v(t)\Big) = (\cos t, -\sin t)$. The *integral curve* passing through $(u,v) = (1,0)$ at $t = 0$ is given by $\{\, (u,v,t) \in \mathbb{R}^1 \times \mathbb{R}^1 \times \mathbb{R}^1 \mid \Big(u(t), v(t)\Big) = (\cos t, -\sin t)$, for all $t \in \mathbb{R}\,\}$. The *orbit* passing through $(u,v) = (1,0)$ is given by the circle $u^2 + v^2 = 1$. Figure 0.0.1 gives a geometrical interpretation of these different definitions for this example.

End of Example 0.0.1

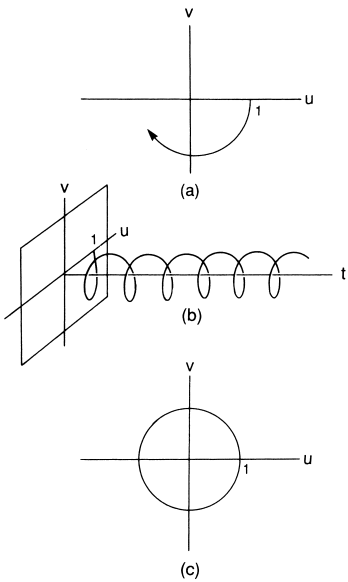

FIGURE 0.0.1. a) Solution through $(1,0)$ at $t = 0$. b) Integral curve through $(1,0)$ at $t = 0$. c) Orbit of $(1,0)$.

The astute reader will note that we have apparently gotten a bit ahead of ourselves in that we have tacitly assumed that (0.0.1) has solutions. Of course, this is by no means obvious, and apparently some conditions must be placed on $f(x,t;\mu)$ (as of yet, none have been stated) in order for solutions to exist. Moreover, additional properties of solutions, such as uniqueness and differentiability with respect to initial conditions and parameters, are necessary in applications. When we explicitly consider these

questions in Chapter 7, we will see that these properties also are inherited from conditions on $f(x,t;\mu)$. For now, we will merely state without proof that if $f(x,t;\mu)$ is $\mathbf{C}^r$ $(r \geq 1)$ in x, t, and μ then solutions through any $x_0 \in \mathbb{R}^n$ exist and are unique on some time interval. Moreover, the solutions themselves are $\mathbf{C}^r$ functions of t, t_0, x_0, and μ. (Note: recall that a function is said to be $\mathbf{C}^r$ if it is r times differentiable and each derivative is continuous; if $r = 0$ then the function is merely continuous.)

At this stage we have said nothing about maps, i.e., Equation (0.0.2). In a broad sense, we will study two types of maps depending on $g(x;\mu)$; *noninvertible* maps if $g(x;\mu)$ as a function of x for fixed μ has no inverse, and *invertible* maps if $g(x;\mu)$ has an inverse. The map will be referred to as a $\mathbf{C}^r$ *diffeomorphism* if $g(x;\mu)$ is invertible, with the inverse denoted $g^{-1}(x;\mu)$, and both $g(x;\mu)$ and $g^{-1}(x;\mu)$ are $\mathbf{C}^r$ maps (recall that a map is invertible if it is one-to-one and onto). Our goal will be to study the orbits of (0.0.2), i.e., the bi-infinite (if g is invertible) sequences of points

$$\{\cdots, g^{-n}(x_0;\mu), \cdots, g^{-1}(x_0;\mu), x_0, g(x_0;\mu), \cdots g^n(x_0;\mu), \cdots\}, \quad (0.0.4)$$

where $x_0 \in U$ and g^n is defined inductively by

$$g^n(x_0;\mu) \equiv g\big(g^{n-1}(x_0;\mu)\big), \qquad n \geq 2, \quad (0.0.5)$$

$$g^{-n}(x_0;\mu) \equiv g^{-1}\big(g^{-n+1}(x_0;\mu)\big), \qquad n \geq 2, \quad (0.0.6)$$

or the infinite (if g is noninvertible) sequences of points

$$\{x_0, g(x_0;\mu), \cdots, g^n(x_0;\mu), \cdots\}, \quad (0.0.7)$$

where $x_0 \in U$ and g^n is defined inductively by (0.0.5). (Note: it should be clear that we must assume $g^{n-1}(x_0;\mu)$, $g^{-n+1}(x_0;\mu) \in U$, $n \geq 2$, for (0.0.4) to make sense and $g^{n-1}(x_0;\mu) \in U$, $n \geq 2$, for (0.0.7) to make sense.) Notice that questions of existence and uniqueness of orbits for maps are obvious and that differentiability of orbits with respect to initial conditions and parameters is a consequence of the applicability of the chain rule of elementary calculus.

With these preliminaries out of the way, we can now turn to the main business of this book.

1

Equilibrium Solutions, Stability, and Linearized Stability

1.1 Equilibria of Vector Fields

Consider a general autonomous vector field

$$\dot{x} = f(x), \qquad x \in \mathbb{R}^n. \tag{1.1.1}$$

An *equilibrium solution* of (1.1.1) is a point $\bar{x} \in \mathbb{R}^n$ such that

$$f(\bar{x}) = 0,$$

i.e., a solution which does not change in time. Other terms often substituted for the term "equilibrium solution" are "fixed point," "stationary point," "rest point," "singularity," "critical point," or "steady state." In this book we will utilize the terms equilibrium point or fixed point exclusively.

Example 1.1.1 ("Equilibria" in Nonautonomous Vector Fields). What about the notion of equilibria for nonautonomous vector fields? This is a situation where doing what "seems right" (i.e.. using ideas that have only been developed for autonomous vector fields) can lead to incorrect results. Let is describe this in more detail
Consider a nonautonomous vector field

$$\dot{x} = f(x,t), \qquad x \in \mathbb{R}^n.$$

A common way of viewing this in applications is to view time as "frozen" and look at equilibria of the frozen time vector field (this is often done in fluid mechanics where the vector field has the interpretation as the velocity field). These "instantaneous" fixed points are given by

$$f(x,t) = 0.$$

If we can find a point $(\bar{x}, \bar{t})$ such that $f(\bar{x}, \bar{t}) = 0$ and $D_x f(\bar{x}, \bar{t}) \neq 0$, then by the implicit function theorem we can find a function $\bar{x}(t)$, with $\bar{x}(\bar{t}) = \bar{x}$ such that $f(\bar{x}(t), t) = 0$, for t in some interval about $\bar{t}$. However, these "frozen time equilibria" are not solutions of the nonautonomous vector field. In fact, it is easy

to see that if $\bar{x}(t)$ is a solution of the nonautonomous vector field, then it must be constant in time, i.e., $\dot{\bar{x}}(t) = 0$, see Exercise 11.
The following example from Szeri et al. [1991] is quite instructive. Consider the one dimensional nonautonomous vector field:

$$\dot{x} = -x + t, \tag{1.1.2}$$

The solution through the point x_0 at $t = 0$ is given by

$$x(t) = t - 1 + e^{-t}\,(x_0 + 1)\,, \tag{1.1.3}$$

from which it is clear that all solutions asymptotically approach the solution $t-1$ as $t \to \infty$.
The frozen time or "instantaneous" fixed points for (1.1.2) are given by

$$x = t. \tag{1.1.4}$$

At a fixed t, this is the unique point where the vector field is zero. However, $x = t$ is *not* a solution of (1.1.2). This is very different from the case of an autonomous vector field where a fixed point is a solution of the vector field.
In Fig. 1.1.1 we plot some of the trajectories of (1.1.2). In particular we plot the curve of instantaneous fixed points.

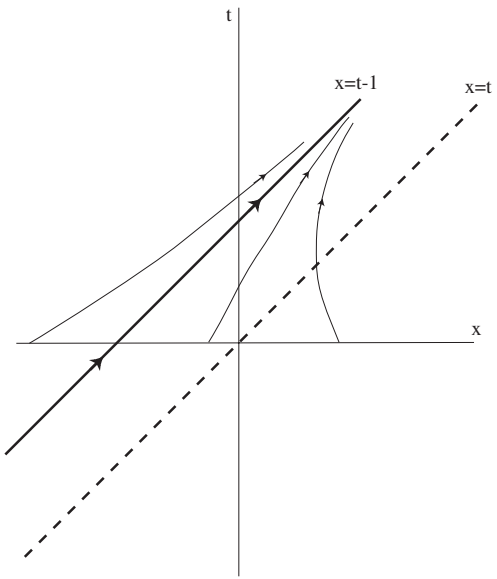

FIGURE 1.1.1. The trajectories of (1.1.2) plotted in $x - t$ space. The curve of instantaneous fixed points is plotted as a dashed line and given by $x = t$.

In Fig. 1.1.2 we plot the "frozen time" vector field at some time $t = \bar{t}$. In this figure we see something that seems somewhat counterintuitive. Trajectories to the right of the trajectory $x(t) = t - 1$ appear to be moving away from it according

to the direction of the instantaneous vector field, towards the instantaneous fixed point. However, we know from (1.1.3) that all trajectories decay to $x(t) = t - 1$ at an exponential rate. What we are "seeing" in Fig. 1.1.2 is an artifact of drawing incorrect conclusions from instantaneous vector fields. Trajectories to the immediate right of $x(t) = t - 1$ are indeed moving to the right (i.e., away from $x(t) = t - 1$). However, $x(t) = t - 1$ is moving to the right at a faster speed and it eventually overtakes these trajectories. Fig. 1.1.2 might also lead us to believe that trajectories converge to the instantaneous fixed point. But we know this is not true since we have the exact solutions.

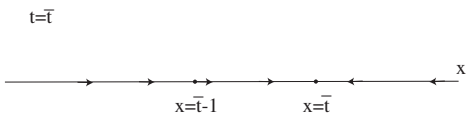

FIGURE 1.1.2. The "frozen time" vector field.

This example shows that it can be misleading and lead to incorrect conclusions if we try to think of nonautonomous vector fields as a "sequence" of frozen time autonomous vector fields.

End of Example 1.1.1

Once we find any solution of (1.1.1) it is natural to try to determine if the solution is stable.

1.2 Stability of Trajectories

Let $\bar{x}(t)$ be any solution of (1.1.1). Then, roughly speaking, $\bar{x}(t)$ is *stable* if solutions starting "close" to $\bar{x}(t)$ at a given time remain close to $\bar{x}(t)$ for all later times. It is *asymptotically stable* if nearby solutions not only stay close, but also converge to $\bar{x}(t)$ as $t \to \infty$. Let us formalize these ideas.

Definition 1.2.1 (Liapunov Stability.) *$\bar{x}(t)$ is said to be* stable *(or* Liapunov stable*) if, given $\varepsilon > 0$, there exists a $\delta = \delta(\varepsilon) > 0$ such that, for any other solution, $y(t)$, of (1.1.1) satisfying $|\bar{x}(t_0) - y(t_0)| < \delta$ (where $|\cdot|$ is a norm on $\mathbb{R}^n$), then $|\bar{x}(t) - y(t)| < \varepsilon$ for $t > t_0$, $t_0 \in \mathbb{R}$.*

We remark that a solution which is not stable is said to be *unstable*.

Definition 1.2.2 (Asymptotic Stability) *$\bar{x}(t)$ is said to be* asymptotically stable *if it is Liapunov stable and for any other solution, $y(t)$, of (1.1.1), there exists a constant $b > 0$ such that, if $|\bar{x}(t_0) - y(t_0)| < b$, then $\lim_{t\to\infty} |\bar{x}(t) - y(t)| = 0$.*

See Figure 1.2.1 for a geometrical interpretation of these two definitions. Notice that these two definitions imply that we have information on the

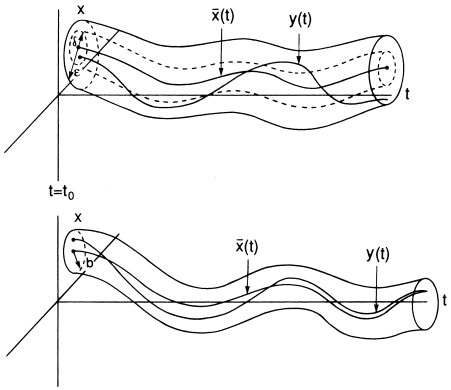

FIGURE 1.2.1. a) Liapunov stability. b) Asymptotic stability.

infinite time existence of solutions. This is obvious for equilibrium solutions but is not necessarily so for nearby solutions. Also, these definitions are for autonomous systems, since in the nonautonomous case it may be that δ and b depend explicitly on t_0 (more about this later).

Definition 1.2.2 may seem a bit strange in that we require stability in addition to the requirement that trajectories approach the solution as $t \to \infty$. One might think that the latter condition implies stability. However, this is not the case as is illustrated in the two phase portraits in Figure 1.2.2.

Both phase portraits show an equilibrium with the property that solutions in any arbitrarily small neighborhood leave the neighborhood. However, the *global* topology of the trajectories is such that all trajectories in a neighborhood asymptotically approach the equilibrium as $t \to \infty$. Thus, solutions can *attract* a neighborhood, but not be Liapunov stable.

Thus far we have discussed stability *of trajectories*. Now we define a slightly different, but important, notion of stability that will be generalized later on–*orbital stability* (recall the distinction between "trajectories" and "orbits" given in the introduction).

First, we define the *positive orbit through the point* x_0 *for* $t \geq t_0$ as:

$$O^+(x_0, t_0) = \{x \in \mathbb{R}^n \,|\, x = \bar{x}(t),\, t \geq t_0,\, \bar{x}(t_0) = x_0\}\,. \tag{1.2.1}$$

Next we need the notion of the distance between a point and a set. This is defined as follows. Let $S \in \mathbb{R}^n$ be an arbitrary set and $p \in \mathbb{R}^n$ be an arbitrary point. Then the distance between the point p and the set S is

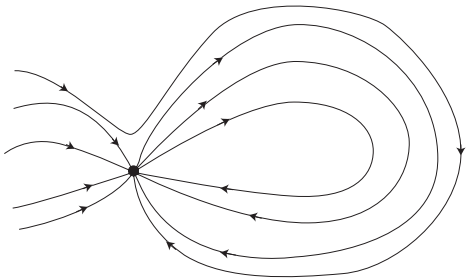

(a)

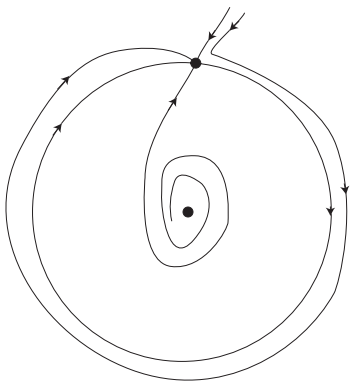

(b)

FIGURE 1.2.2. Phase portraits a) and b) illustrate the situation of an equilibrium point that is unstable, but all trajectories in a neighborhood of the equilibrium point approach it as $t \to \infty$.

denoted and defined as:

$$d(p, S) = \inf_{x \in S} |p - x|. \tag{1.2.2}$$

Now we can state the following definition.

Definition 1.2.3 (Orbital Stability) $\bar{x}(t)$ *is said to be* orbitally stable *if, given* $\varepsilon > 0$*, there exists a* $\delta = \delta(\varepsilon) > 0$ *such that, for any other solution,* $y(t)$*, of (1.1.1) satisfying* $|\bar{x}(t_0) - y(t_0)| < \delta$*, then* $d\,(y(t), O^+(x_0, t_0)) < \varepsilon$ *for* $t > t_0$*.*

We can also now define *asymptotic orbital stability.*

Definition 1.2.4 (Asymptotic Orbital Stability) $\bar{x}(t)$ *is said to be* asymptotically orbitally stable *if it is orbitally stable and for any other*

solution, $y(t)$, of (1.1.1), there exists a constant $b > 0$ such that, if $|\bar{x}(t_0) - y(t_0)| < b$, then $\lim_{t\to\infty} d\big(y(t), O^+(x_0, t_0)\big) = 0$.

Definitions 1.2.3 and 1.2.4 are stated in terms of orbital stability of a *trajectory*. In practice, variations in the terminology may arise. In particular, one could just as easily phrase these definitions in terms of the stability of the *orbit* (generated by the trajectory), rather than the trajectory. This is an example of where the distinction between "orbit" and "trajectory" is slightly blurred.

Definitions 1.2.1, 1.2.2, 1.2.3, 1.2.4 describe mathematically different types of stability; however, they do not provide us with a method for determining whether or not a given solution is stable. We now turn our attention to this question.

1.2A Linearization

In order to determine the stability of $\bar{x}(t)$ we must understand the nature of solutions near $\bar{x}(t)$. Let

$$x = \bar{x}(t) + y. \tag{1.2.3}$$

Substituting (1.2.3) into (1.1.1) and Taylor expanding about $\bar{x}(t)$ gives

$$\dot{x} = \dot{\bar{x}}(t) + \dot{y} = f\big(\bar{x}(t)\big) + Df\big(\bar{x}(t)\big)y + \mathcal{O}(|y|^2), \tag{1.2.4}$$

where Df is the derivative of f and $|\cdot|$ denotes a norm on $\mathbb{R}^n$ (note: in order to obtain (1.2.4) f must be at least twice differentiable). Using the fact that $\dot{\bar{x}}(t) = f\big(\bar{x}(t)\big)$, (1.2.4) becomes

$$\dot{y} = Df\big(\bar{x}(t)\big)y + \mathcal{O}(|y|^2). \tag{1.2.5}$$

Equation (1.2.5) describes the evolution of orbits near $\bar{x}(t)$. For stability questions we are concerned with the behavior of solutions arbitrarily close to $\bar{x}(t)$, so it seems reasonable that this question could be answered by studying the associated *linear system*

$$\dot{y} = Df\big(\bar{x}(t)\big)y. \tag{1.2.6}$$

Therefore, the question of stability of $\bar{x}(t)$ involves the following two steps:

1. Determine if the $y = 0$ solution of (1.2.6) is stable.
2. Show that stability (or instability) of the $y = 0$ solution of (1.2.6) implies stability (or instability) of $\bar{x}(t)$.

Step 1 may be equally as difficult as our original problem, since there are no general analytical methods for finding the solution of linear ordinary differential equations with time-dependent coefficients. However, if $\bar{x}(t)$ is

an equilibrium solution, i.e., $\bar{x}(t) = \bar{x}$, then $Df\big(\bar{x}(t)\big) = Df(\bar{x})$ is a matrix with constant entries, and the solution of (1.1.6) through the point $y_0 \in \mathbb{R}^n$ of $t = 0$ can immediately be written as

$$y(t) = e^{Df(\bar{x})t} y_0. \tag{1.2.7}$$

Thus, $y(t)$ is *asymptotically stable* if all eigenvalues of $Df(\bar{x})$ have negative real parts (cf. Exercise 7).

The answer to Step 2 can be obtained from the following theorem.

Theorem 1.2.5 *Suppose all of the eigenvalues of $Df(\bar{x})$ have negative real parts. Then the equilibrium solution $x = \bar{x}$ of the nonlinear vector field (1.1.1) is asymptotically stable.*

Proof: We will give the proof of this theorem in Chapter 2 when we discuss Liapunov functions. □

Example 1.2.1 (Stability and Eigenvalues of Time-Dependent Jacobians). For a general time dependent solution $\bar{x}(t)$ it might be tempting to infer stability properties of this solution from the eigenvalues of the Jacobian $Df(\bar{x}(t))$. The following example from Hale [1980] shows this can lead to wrong answers. Consider the following linear vector field with time-periodic coefficients

$$\begin{pmatrix} \dot{x}_1 \\ \dot{x}_2 \end{pmatrix} = A(t) \begin{pmatrix} x_1 \\ x_2 \end{pmatrix},$$

where

$$A(t) = \begin{pmatrix} -1 + \frac{3}{2}\cos^2 t & 1 - \frac{3}{2}\cos t \sin t \\ -1 - \frac{3}{2}\cos t \sin t & -1 + \frac{3}{2}\sin^2 t \end{pmatrix}. \tag{1.2.8}$$

The eigenvalues of $A(t)$ are found to be *independent of* t and are given by

$$\lambda_1(t) = \frac{-1 + i\sqrt{7}}{4}, \qquad \lambda_2(t) = \frac{-1 - i\sqrt{7}}{4}.$$

In particular, they have negative real parts *for all* t. However, one can verify that the following are two linearly independent solutions of this equation

$$v_1(t) = \begin{pmatrix} -\cos t \\ \sin t \end{pmatrix} e^{\frac{t}{2}}, \qquad v_2(t) = \begin{pmatrix} \sin t \\ \cos t \end{pmatrix} e^{-t}. \tag{1.2.9}$$

Hence, the solutions are unstable and of saddle type, a conclusion that does not follow from the eigenvalues of $A(t)$.

End of Example 1.2.1

Example 1.2.2. In this example we show that stability in the linear approximation does not necessarily imply stability. Consider the following vector field on $\mathbb{R}^2$

$$\begin{aligned} \dot{x} &= -y + x(x^2 + y^2), \\ \dot{y} &= x + y(x^2 + y^2). \end{aligned} \tag{1.2.10}$$

The origin is an equilibrium point for this equation, and the vector field linearized about this equilibrium is given by

$$\begin{aligned} \dot{x} &= -y, \\ \dot{y} &= x. \end{aligned} \tag{1.2.11}$$

The eigenvalues of the matrix associated with this linearization are $\pm i$, and the origin is stable in the linear approximation (but not asymptotically stable).

Next we examine nonlinear stability. We transform (1.2.10) to polar coordinates using

$$x = r\cos\theta, \qquad y = r\sin\theta,$$

to obtain

$$\begin{aligned} \dot{r} &= r^3, \\ \dot{\theta} &= 1. \end{aligned}$$

Since $r > 0$ we see that $\dot{r}$ is increasing, indicating that solutions spiral away from the origin.

End of Example 1.2.2

Sometimes the term "linearly stable" is used to describe a solution that is stable in the linear approximation. Thus, linearly stable solutions may be nonlinearly unstable.

In the following sections the reader will see many results that have a similar flavor to Theorem 1.2.5. Namely, if the eigenvalues of the associated linear vector field have nonzero real parts, then the orbit structure *near an equilibrium solution* of the nonlinear vector field is essentially the same as that of the linear vector field. Such equilibrium solutions are given a special name.

Definition 1.2.6 (Hyperbolic Fixed Point) *Let $x = \bar{x}$ be a fixed point of $\dot{x} = f(x)$, $x \in \mathbb{R}^n$. Then $\bar{x}$ is called a* hyperbolic *fixed point if none of the eigenvalues of $Df(\bar{x})$ have zero real part.*

It should be noted that the notion of "hyperbolicity of a fixed point" is defined in terms of the linearization about the fixed point. The notion of hyperbolicity extends to general trajectories, as well as to invariant sets and manifolds. In all of these cases hyperbolicity will also be defined in terms of the linearization about the trajectory, invariant set, or invariant manifold. Moreover, we will learn that hyperbolicity "persists under perturbations".

Historically, hyperbolicity has been a central concept in the development of dynamical systems theory.

It should be clear that in our studies of stability of equilibria in the linear approximation the nature of the linearized stability will boil down to a study of the nature of the roots of the characteristic polynomial of the matrix associated with the linearization about the equilibrium point of interest. Here we collect together a few very useful results about the roots of polynomials.
Consider a polynomial with real coefficients of the form:

$$p(\lambda) = a_0\lambda^n + a_1\lambda^{n-1} + \cdots + a_{n-1}\lambda + a_n, \qquad a_i \in \mathbb{R},\ a_0 \neq 0. \tag{1.2.12}$$

Theorem 1.2.7 (Fundamental Theorem of Algebra) *(1.2.12) has exactly n real or complex roots, $\lambda_1, \ldots, \lambda_n$, where repetition of roots is possible, i.e., $\lambda_i = \lambda_j$, for some i and j.*

Since we are considering the case of polynomials with *real coefficients*, it is easy to verify that if λ is a root of (1.2.12) then so is the complex conjugate of λ, $\bar{\lambda}$ (just substitute the root λ into (1.2.12) and take the complex conjugate of the result, using the fact that the coefficients are real). Hence, for polynomials with real coefficients the roots occur in complex conjugate pairs.
Next we describe a useful result that enables to get some information about the roots of polynomials just by "looking at" the coefficients.

Theorem 1.2.8 (Descartes' Rule of Signs) *Consider the sequence of coeficients of (1.2.12):*

$$a_n,\ a_{n-1},\ \cdots, a_1,\ a_0.$$

Let k be the total number of sign changes from one coefficient to the next in the sequence. Then the number of positive real roots of the polynomial is either equal to k, or k minus a positive even integer. (Note: if $k = 1$ then there is exactly one positive real root.)

Example 1.2.3. Consider the polynomial:

$$\lambda^2 - 2\lambda + 1 = 0.$$

There are two sign changes in the sequence of coefficients, and the roots are 1 and 1.

End of Example 1.2.3

Proofs of the fundamental theorem of algebra and Descartes' rule of signs can be found in many algebra textbooks.
We are interested in the location in the complex plane of the real parts of the roots of the polynomial (1.2.12). The famous *Routh-Hurwitz criterion* can be very useful for this purpose.

First we construct the *Routh table* associated with the polynomial (1.2.12). This is given by:

$$\begin{array}{ccccc} a_0 & a_2 & a_4 & a_6 & \cdots \\ a_1 & a_3 & a_5 & a_7 & \cdots \\ r_{3,1} & r_{3,2} & r_{3,3} & r_{3,4} & \cdots \\ r_{4,1} & r_{4,2} & r_{4,3} & r_{4,4} & \cdots \\ \vdots & \vdots & \vdots & \vdots & \cdots \\ r_{n+1,1} & r_{n+1,2} & r_{n+1,3} & r_{n+1,4} & \cdots \end{array} \tag{1.2.13}$$

where

$$(r_{i,1} \quad r_{i,2} \cdots) \equiv (r_{i-2,2} \quad r_{i-2,3} \cdots) - \frac{r_{i-2,1}}{r_{i-1,1}} (r_{i-1,2} \quad r_{i-1,3} \cdots), \qquad (i > 2). \tag{1.2.14}$$

(The notation $r_{i,j}$ stands for row i, column j.) Note that rows three and higher may not contain the same number of entries as rows one or two. This will be seen in an example below. Now we state the following test.

Theorem 1.2.9 (Routh-Hurwitz Test) *All of the roots of the polynomial (1.2.12) have real parts strictly less than zero if and only if all $n+1$ elements in the first column of the Routh table are nonzero and have the same sign.*

An elementary proof of the Routh-Hurwitz criterion can be found in Meinsma [1995]. A comprehensive reference is Gantmacher [1989], which also covers certain "singular" cases not covered by the result stated here (the so-called "regular case").

Example 1.2.4.
Consider the polynomial:

$$\lambda^3 + 6\lambda^2 + 11\lambda + 6 = 0. \tag{1.2.15}$$

The associated Routh table is given by:

$$\begin{array}{cc} 1 & 11 \\ 6 & 6 \\ 10 & \\ 6 & \end{array}$$

Hence, all of the roots of this polynomial lie in the left half plane (they are -1, -2, and -3).

End of Example 1.2.4

1.3 Maps

Everything discussed thus far applies also for maps; we mention some of the details explicitly.

Consider a $\mathbf{C}^r$ $(r \geq 1)$ map

$$x \mapsto g(x), \qquad x \in \mathbb{R}^n, \tag{1.3.1}$$

and suppose that it has a fixed point at $x = \bar{x}$, i.e., $\bar{x} = g(\bar{x})$. The associated linear map is given by

$$y \mapsto Ay, \qquad y \in \mathbb{R}^n, \tag{1.3.2}$$

where $A \equiv Dg(\bar{x})$.

1.3A Definitions of Stability for Maps

The definitions of stability and asymptotic stability for orbits of maps are very similar to the definitions for vector fields. We leave it as an exercise for the reader to formulate these definitions (cf. Exercise 4).

1.3B Stability of Fixed Points of Linear Maps

Choose a point $y_0 \in \mathbb{R}^n$. The orbit of y_0 under the linear map (1.3.2) is given by the bi-infinite sequence (if the map is a $\mathbf{C}^r$, $r \geq 1$, diffeomorphism)

$$\{\cdots, A^{-n}y_0, \cdots, A^{-1}y_0, y_0, Ay_0, \cdots, A^n y_0, \cdots\} \tag{1.3.3}$$

or the infinite sequence (if the map is $\mathbf{C}^r$, $r \geq 1$, but noninvertible)

$$\{y_0, Ay_0, \cdots, A^n y_0, \cdots\}. \tag{1.3.4}$$

From (1.3.3) and (1.3.4) it should be clear the fixed point $y = 0$ of the linear map (1.3.2) is asymptotically stable if all of the eigenvalues of A have moduli strictly less than one (cf. Exercise 9).

1.3C Stability of Fixed Points of Maps via the Linear Approximation

With the obvious modifications, Theorem 1.2.5 is valid for maps.

Before we apply these ideas to the unforced Duffing oscillator, let us first give some useful terminology.

1.4 Some Terminology Associated with Fixed Points

A hyperbolic fixed point of a vector field (resp., map) is called a *saddle* if some, but not all, of the eigenvalues of the associated linearization have real parts greater than zero (resp., moduli greater than one) and the rest of the eigenvalues have real parts less than zero (resp., moduli less than one). If all of the eigenvalues have negative real part (resp., moduli less than one), then the hyperbolic fixed point is called a *stable node* or *sink,* and if all of the eigenvalues have positive real parts (resp., moduli greater than one), then the hyperbolic fixed point is called an *unstable node* or *source.* If the eigenvalues are purely imaginary (resp., have modulus one) and nonzero (resp., are not real), the nonhyperbolic fixed point is said to be a *center* (resp., is said to be *elliptic*).

Let us now apply our results to the unforced Duffing oscillator.

1.5 Application to the Unforced Duffing Oscillator

The unforced Duffing oscillator is given by

$$\begin{aligned} \dot{x} &= y, \\ \dot{y} &= x - x^3 - \delta y, \qquad \delta \geq 0. \end{aligned}$$

It is easy to see that this equation has three fixed points given by

$$(x, y) = (0, 0), (\pm 1, 0). \tag{1.5.1}$$

The matrix associated with the linearized vector field is given by

$$\begin{pmatrix} 0 & 1 \\ 1 - 3x^2 & -\delta \end{pmatrix}. \tag{1.5.2}$$

Using (1.5.1) and (1.5.2) the eigenvalues λ_1 and λ_2 associated with the fixed point $(0, 0)$ are given by $\lambda_{1,2} = -\delta/2 \pm \frac{1}{2}\sqrt{\delta^2 + 4}$, and the eigenvalues associated with the fixed points $(\pm 1, 0)$ are the same for each point and are given by $\lambda_{1,2} = -\delta/2 \pm \frac{1}{2}\sqrt{\delta^2 - 8}$. Hence, for $\delta > 0$, $(0, 0)$ is unstable and $(\pm 1, 0)$ are asymptotically stable; for $\delta = 0$, $(\pm 1, 0)$ are stable in the linear approximation.

1.6 Exercises

1. Consider the following vector fields.

   a) $\begin{aligned} \dot{x} &= y, \\ \dot{y} &= -\delta y - \mu x, \end{aligned} \qquad (x, y) \in \mathbb{R}^2.$

b) $\begin{aligned}\dot{x} &= y,\\ \dot{y} &= -\delta y - \mu x - x^2,\end{aligned}$ $(x, y) \in \mathbb{R}^2$.

c) $\begin{aligned}\dot{x} &= y,\\ \dot{y} &= -\delta y - \mu x - x^3,\end{aligned}$ $(x, y) \in \mathbb{R}^2$.

d) $\begin{aligned}\dot{x} &= -\delta x - \mu y + xy,\\ \dot{y} &= \mu x - \delta y + \tfrac{1}{2}(x^2 - y^2),\end{aligned}$ $(x, y) \in \mathbb{R}^2$.

e) $\begin{aligned}\dot{x} &= -x + x^3,\\ \dot{y} &= x + y,\end{aligned}$ $(x, y) \in \mathbb{R}^2$.

f) $\begin{aligned}\dot{r} &= r(1 - r^2),\\ \dot{\theta} &= \cos 4\theta,\end{aligned}$ $(r, \theta) \in \mathbb{R}^+ \times S^1$.

g) $\begin{aligned}\dot{r} &= r(\delta + \mu r^2 - r^4),\\ \dot{\theta} &= 1 - r^2,\end{aligned}$ $(r, \theta) \in \mathbb{R}^+ \times S^1$.

h) $\begin{aligned}\dot{\theta} &= v,\\ \dot{v} &= -\sin\theta - \delta v + \mu,\end{aligned}$ $(\theta, v) \in S^1 \times \mathbb{R}$.

i) $\begin{aligned}\dot{\theta}_1 &= \omega_1,\\ \dot{\theta}_2 &= \omega_2 + \theta_1^n,\ n \geq 1,\end{aligned}$ $(\theta_1, \theta_2) \in S^1 \times S^1$.

j) $\begin{aligned}\dot{\theta}_1 &= \theta_2 - \sin\theta_1,\\ \dot{\theta}_2 &= -\theta_2,\end{aligned}$ $(\theta_1, \theta_2) \in S^1 \times S^1$.

k) $\begin{aligned}\dot{\theta}_1 &= \theta_1^2,\\ \dot{\theta}_2 &= \omega_2,\end{aligned}$ $(\theta_1, \theta_2) \in S^1 \times S^1$.

Find all fixed points and discuss their stability.

2. Consider the following maps.

a) $\begin{aligned}x &\mapsto x,\\ y &\mapsto x + y,\end{aligned}$ $(x, y) \in \mathbb{R}^2$.

b) $\begin{aligned}x &\mapsto x^2,\\ y &\mapsto x + y,\end{aligned}$ $(x, y) \in \mathbb{R}^2$.

c) $\begin{aligned}\theta_1 &\mapsto \theta_1,\\ \theta_2 &\mapsto \theta_1 + \theta_2,\end{aligned}$ $(\theta_1, \theta_2) \in S^1 \times S^1$.

d) $\begin{aligned}\theta_1 &\mapsto \sin\theta_1,\\ \theta_2 &\mapsto \theta_1,\end{aligned}$ $(\theta_1, \theta_2) \in S^1 \times S^1$.

e) $\begin{aligned}x &\mapsto \tfrac{2xy}{x+y},\\ y &\mapsto \left(\tfrac{2xy^2}{x+y}\right)^{1/2},\end{aligned}$ $(x, y) \in \mathbb{R}^2$.

f) $\begin{aligned}x &\mapsto \tfrac{x+y}{2},\\ y &\mapsto (xy)^{1/2},\end{aligned}$ $(x, y) \in \mathbb{R}^2$.

g) $\begin{aligned}x &\mapsto \mu - \delta y - x^2,\\ y &\mapsto x,\end{aligned}$ $(x, y) \in \mathbb{R}^2$.

h) $\begin{aligned}\theta &\mapsto \theta + v,\\ v &\mapsto \delta v - \mu\cos(\theta + v),\end{aligned}$ $(\theta, v) \in S^1 \times \mathbb{R}^1$.

Find all the fixed points and discuss their stability.

3. Consider a $\mathbf{C}^r$ $(r \geq 1)$ diffeomorphism

$$x \mapsto f(x), \qquad x \in \mathbb{R}^n.$$

Suppose f has a hyperbolic periodic orbit of period k. Denote the orbit by

$$O(p) = \Big\{p, f(p), f^2(p), \cdots, f^{k-1}(p), f^k(p) = p\Big\}.$$

Show that stability of $O(p)$ is determined by the linear map

$$y \mapsto Df^k(f^j(p))y$$

for any $j = 0, 1, \cdots, k-1$. Does the same result hold for periodic orbits of noninvertible maps?

4. Formulate the definitions of Liapunov stability and asymptotic stability for maps.

5. Show that hyperbolic fixed points of maps which are asymptotically stable in the linear approximation are nonlinearly asymptotically stable.

6. Give examples of fixed points of vector fields and maps that are stable in the linear approximation but are nonlinearly unstable.

7. Consider the linear vector field

$$\dot{x} = Ax, \qquad x \in \mathbb{R}^n,$$

where A is an $n \times n$ constant matrix. Suppose all the eigenvalues of A have negative real parts. Then prove that $x = 0$ is an asymptotically stable fixed point for this linear vector field. (*Hint:* utilize a linear transformation of the coordinates which transforms A into Jordan canonical form.)

8. Suppose that the matrix A in Exercise 7 has some eigenvalues with zero real parts (and the rest have negative real parts). Does it follow that $x = 0$ is stable? Answer this question by considering the following example.

$$\begin{pmatrix} \dot{x}_1 \\ \dot{x}_2 \end{pmatrix} = \begin{pmatrix} 0 & 1 \\ 0 & 0 \end{pmatrix} \begin{pmatrix} x_1 \\ x_2 \end{pmatrix}.$$

9. Consider the linear map

$$x \mapsto Ax, \qquad x \in \mathbb{R}^n,$$

where A is an $n \times n$ constant matrix. Suppose all of the eigenvalues of A have modulus less than one. Then prove that $x = 0$ is an asymptotically stable fixed point for this linear map (use the same hint given for Exercise 7).

10. Suppose that the matrix A in Exercise 9 has some eigenvalues having modulus one (with the rest having modulus less than one). Does it follow that $x = 0$ is stable? Answer this question by considering the following example.

$$\begin{pmatrix} x_1 \\ x_2 \end{pmatrix} \mapsto \begin{pmatrix} 1 & 1 \\ 0 & 1 \end{pmatrix} \begin{pmatrix} x_1 \\ x_2 \end{pmatrix}.$$

11. Consider a nonautonomous vector field

$$\dot{x} = f(x, t), \qquad x \in \mathbb{R}^n,$$

and suppose that $\bar{x}(t)$ is a function (defined for some interval of t) satisfying

$$f(\bar{x}(t), t) = 0.$$

Prove that if $\bar{x}(t)$ is a trajectory of the vector field then it must be constant in time.

12. Consider the following vector field (Yang [2001]):

$$\begin{aligned} \dot{x} &= -x, \\ \dot{\phi} &= 1, \\ \dot{\theta} &= \omega, \qquad\qquad (x, \phi, \theta) \in \mathbb{R} \times S^1 \times S^1, \end{aligned}$$

where ω is an irrational number. Show that every trajectory is asymptotically orbitally stable.

13. Consider the following vector field (Yang [2001]):

$$\begin{aligned} \dot{\theta} &= \sin^2 \theta + (1 - r)^2, \\ \dot{r} &= r(1 - r), \qquad\qquad (\theta, r) \in S^1 \times \mathbb{R}. \end{aligned}$$

Show that every trajectory, except $r = 0$, is asymptotically orbitally stable.

14. Does Descartes' rule of signs provide any information about the roots of the polynomial $p(-\lambda)$, where $p(\lambda)$ is given by (1.2.12)?

15. Use the Routh-Hurwitz test to determine the location of the roots of the following polynomials:

    (a) $\lambda^3 - 3\lambda^2 + 3\lambda - 1$,

    (b) $\lambda^3 + 3\lambda^2 - 4$,

    (c) $\lambda^3 + \lambda^2 + \lambda + 1$.

2

Liapunov Functions

The method of Liapunov can often be used to determine the stability of fixed points when the information obtained from linearization is inconclusive (i.e., when the fixed point is nonhyperbolic). Liapunov theory is a large area, and we will examine only an extremely small part of it; for more information, see Lasalle and Lefschetz [1961][1].

The basic idea of the method is as follows (the method works in n-dimensions and also infinite dimensions, but for the moment we will describe it pictorally in the plane). Suppose you have a vector field in the plane with a fixed point $\bar{x}$, and you want to determine whether or not it is stable. Roughly speaking, according to our previous definitions of stability it would be sufficient to find a neighborhood U of $\bar{x}$ for which orbits starting in U remain in U for all positive times (for the moment we don't distinguish between stability and asymptotic stability). This condition would be satisfied if we could show that the vector field is either tangent to the boundary of U or pointing inward toward $\bar{x}$ (see Figure 2.0.1). This situation should remain true even as we shrink U down onto $\bar{x}$. Now, Liapunov's method gives us a way of making this precise; we will show this for vector fields in the plane and then generalize our results to $\mathbb{R}^n$.

Suppose we have the vector field

$$\begin{aligned} \dot{x} &= f(x,y), \\ \dot{y} &= g(x,y), \qquad (x,y) \in \mathbb{R}^2, \end{aligned} \tag{2.0.1}$$

which has a fixed point at $(\bar{x},\bar{y})$ (assume it is stable). We want to show that in any neighborhood of $(\bar{x},\bar{y})$ the above situation holds. Let $V(x,y)$ be a scalar-valued function on $\mathbb{R}^2$, i.e., $V\colon \mathbb{R}^2 \to \mathbb{R}^1$ (and at least $\mathbf{C}^1$), with

[1]First, something should be said about the spelling of the name "Liapunov", also spelled as "Lyapunov", and , "Liapounoff". The book of Lasalle and Lefschetz [1961] uses "Liapunov". Hirsch and Smale [1974] use "Liapunov", while Arnold [1973] uses "Lyapunov". In the setting of "Lyapunov exponents" the "y" is more typically used (although the influential paper of Eckmann and Ruelle [1985] uses "i"). A random check of the journal *Systems & Control Letters* over the past few years found both "Liapunov" and "Lyapunov" both used about the same number of times. For this reason many references in the bibliography of this book will have different spellings of "L · apunov". From time to time we will also drift between different spellings when a particular spelling is more usually found in the area under discussion.

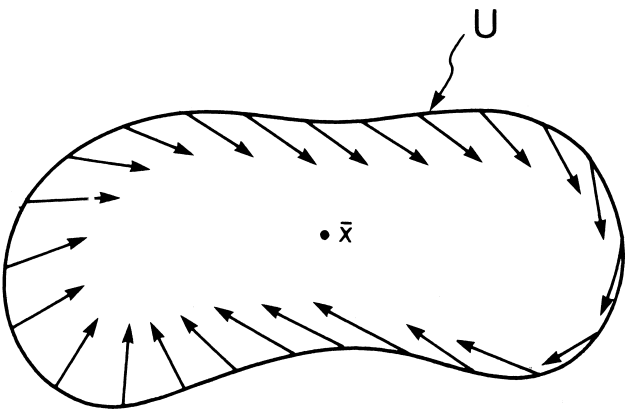

FIGURE 2.0.1. The vector field on the boundary of U.

$V(\bar{x}, \bar{y}) = 0$, and such that the locus of points satisfying $V(x, y) = C =$ constant form closed curves for different values of C encircling $(\bar{x}, \bar{y})$ with $V(x, y) > 0$ in a neighborhood of $(\bar{x}, \bar{y})$ (see Figure 2.0.2).

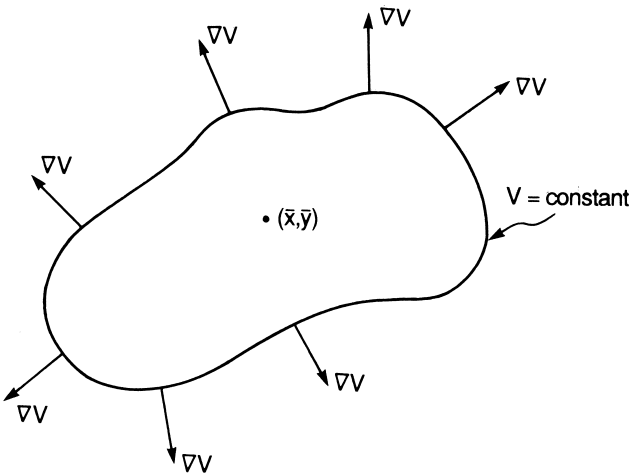

FIGURE 2.0.2. Level set of V and ∇V denoted at various points on the boundary.

Now recall that the gradient of V, ∇V, is a vector perpendicular to the tangent vector along each curve $V = C$ which points in the direction of increasing V (see Figure 2.0.3). So if the vector field were always to be either tangent or pointing inward for each of these curves surrounding $(\bar{x}, \bar{y})$, we would have

$$\nabla V(x, y) \cdot (\dot{x}, \dot{y}) \leq 0,$$

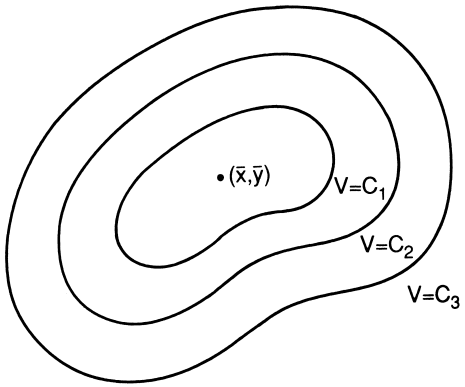

FIGURE 2.0.3. Level sets of V, $0 < C_1 < C_2 < C_3$.

where the "dot" represents the usual vector scalar product. (This is simply the derivative of V along orbits of (2.0.1), and is sometimes referred to as the *orbital derivative*.) We now state the general theorem which makes these ideas precise.

Theorem 2.0.1 *Consider the following vector field*

$$\dot{x} = f(x), \qquad x \in \mathbb{R}^n. \tag{2.0.2}$$

Let $\bar{x}$ be a fixed point of (2.0.2) and let $V : U \to \mathbb{R}$ be a $\mathbf{C}^1$ function defined on some neighborhood U of $\bar{x}$ such that

i) $V(\bar{x}) = 0$ *and* $V(x) > 0$ *if* $x \neq \bar{x}$.

ii) $\dot{V}(x) \leq 0$ *in* $U - \{\bar{x}\}$.

Then $\bar{x}$ is stable. *Moreover, if*

iii) $\dot{V}(x) < 0$ *in* $U - \{\bar{x}\}$

then $\bar{x}$ is asymptotically stable.

Proof: Consider a ball centered at $\bar{x}$ of radius δ, i.e.,

$$B_\delta(\bar{x}) \equiv \{x \in \mathbb{R}^n \,|\, |x - \bar{x}| \leq \delta\},$$

where δ is chosen so small that $B_\delta(\bar{x}) \subset U$. Let m be the minimum value of V on the boundary of $B_\delta(\bar{x})$. Then by i), $m > 0$. Then let

$$U_1 \equiv \{x \in B_\delta(\bar{x}) \,|\, V(x) < m\},$$

see Fig. 2.0.4. Now consider any trajectory starting in U_1. By ii), on such a trajectory V is non-increasing. Hence by our construction the trajectory cannot leave $B_\delta(\bar{x})$. This proves that $\bar{x}$ is stable since δ is arbitrary.

Now suppose that iii) holds, so that V is strictly decreasing on orbits in $U - \{\bar{x}\}$. Let $x(t)$ be a trajectory starting in $U_1 - \{\bar{x}\}$. Then since $B_\delta(\bar{x})$ is compact, and passing to a subsequence if necessary, we can find a sequence of times $\{t_n\}$, with $t_n \to \infty$ as $n \to \infty$ such that $x(t_n)$ converges to a point x_0 as $n \to \infty$. We now argue that $x_0 = \bar{x}$.

This can be seen as follows. We will give a proof by contradiction. Assume that $x_0 \neq \bar{x}$. Then there exists an ε sufficiently small such that $x_0 \notin B_\varepsilon(\bar{x})$. Repeating the same argument given above, one can then conclude that there exists a neighborhood of $\bar{x}$, $\tilde{U}_1 \subset B_\varepsilon(\bar{x})$, such that any trajectory starting in $\tilde{U}_1$ cannot leave $B_\varepsilon(\bar{x})$, see Fig. 2.0.4.

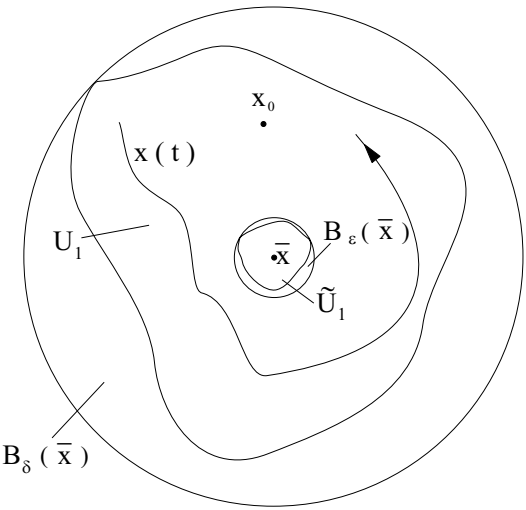

FIGURE 2.0.4. Geometry associated with the choice of neighborhoods in the proof of Theorem 2.0.1.

From this it follows that the trajectory $x(t)$ cannot enter $\tilde{U}_1$. Then, in $U_1 - \tilde{U}_1$, $\dot{V}$ is strictly bounded away from zero, i.e., we have the following estimate:

$$\dot{V} \leq -K < 0, \qquad \text{for some} \quad K > 0.$$

Since $x(t)$ cannot enter $\tilde{U}_1$ we can apply this estimate along the trajectory $x(t)$ to obtain the following inequality:

$$\begin{aligned} V(x(t_n)) - V(x(0)) &= \int_0^{t_n} \dot{V}(x(s))\, dt, \\ &\leq -Kt_n, \end{aligned}$$

or

$$V(x(t_n)) \leq V(x(0)) - Kt_n.$$

Now as $n \to \infty$ this inequality imples that $V\left(x(t_n)\right)$ must become negative. This is a contradiction, which came about by assuming $x_0 \neq \bar{x}$. Therefore $\bar{x} = x_0$. □

We remark that there is a slight gap in the proof of this theorem in that we have not proved that the trajectory $x(t)$ exists on the semi-infinite time interval $t \in [0, \infty)$. Indeed, we have not considered existence of solutions at all at this point in the book. Nevertheless, this fact is indeed true under our assumptions, see Theorem 7.2.1.

We refer to V as a *Liapunov function*. If $\dot{V} < 0$ on $U - \{\bar{x}\}$ the term *strict Liapunov function* is often used. We remark that if U can be chosen to be all of $\mathbb{R}^n$, then $\bar{x}$ is said to be *globally asymptotically stable,* if i) and iii) hold.

Example 2.0.1. Consider the following vector field

$$\dot{x} = y, \tag{2.0.3}$$

$$\dot{y} = -x + \varepsilon x^2 y. \tag{2.0.4}$$

It is easy to verify that (2.0.3) has a nonhyperbolic fixed point at $(x, y) = (0, 0)$. Our goal is to determine if this fixed point is stable.

Let $V(x, y) = (x^2 + y^2)/2$. Clearly $V(0, 0) = 0$ and $V(x, y) > 0$ in any neighborhood of $(0, 0)$. Then

$$\begin{aligned} \dot{V}(x, y) &= \nabla V(x, y) \cdot (\dot{x}, \dot{y}) \\ &= (x, y) \cdot (y, \varepsilon x^2 y - x) \\ &= xy + \varepsilon x^2 y^2 - xy \end{aligned}$$

and hence $\dot{V} = \varepsilon x^2 y^2$. Then, by Theorem 2.0.1, $(0, 0)$ is globally stable for $\varepsilon < 0$. Actually, with a little more work, one can show that $(0, 0)$ is globally asymptotically stable for $\varepsilon < 0$

End of Example 2.0.1

Let us now use Liapunov theory to give an outline of the proof of Theorem 1.2.5. We begin by recalling the set-up of the problem.

Consider the vector field

$$\dot{x} = f(x), \qquad x \in \mathbb{R}^n, \tag{2.0.5}$$

and suppose that (2.0.5) has a fixed point at $x = \bar{x}$, i.e., $f(\bar{x}) = 0$. We translate the fixed point to the origin via the coordinate shift $y = x - \bar{x}$ so that (1.1.17) becomes

$$\dot{y} = f(y + \bar{x}), \qquad y \in \mathbb{R}^n. \tag{2.0.6}$$

Taylor expanding (2.0.6) about $\bar{x}$ gives

$$\dot{y} = Df(\bar{x})y + R(y), \tag{2.0.7}$$

where $R(y) \equiv \mathcal{O}(|y|^2)$.

Now let us introduce the coordinate rescaling

$$y = \varepsilon u, \qquad 0 < \varepsilon < 1. \tag{2.0.8}$$

Thus, taking ε small implies making y small. Under (2.0.8) equation (2.0.7) becomes

$$\dot{u} = Df(\bar{x})u + \bar{R}(u, \varepsilon), \tag{2.0.9}$$

where $\bar{R}(u, \varepsilon) = R(\varepsilon u)/\varepsilon$. It should be clear that $\bar{R}(u, 0) = 0$ since $R(y) = \mathcal{O}(|y|^2)$. We choose as a Liapunov function

$$V(u) = \frac{1}{2}|u|^2.$$

Therefore,

$$\begin{aligned} \dot{V}(u) &= \nabla V(u) \cdot \dot{u} \\ &= \big(u \cdot Df(\bar{x})u\big) + \big(u \cdot \bar{R}(u, \varepsilon)\big). \end{aligned} \tag{2.0.10}$$

From linear algebra the reader should recall that if all eigenvalues of $Df(x_0)$ have negative real part, then there exists a basis such that

$$\big(u \cdot Df(\bar{x}_0)u\big) < k|u|^2 < 0 \tag{2.0.11}$$

for some real number k and for all u (see Arnold [1973] or Hirsch and Smale [1974] for a proof). Hence, by choosing ε sufficiently small, (2.0.10) is strictly negative, which implies that the fixed point $x = \bar{x}$ is asymptotically stable. We leave it to the reader to show that this result does not depend on the particular basis for which (2.0.11) holds. This latter point, while sounding simple in practice, is much more tricky than one might believe, see Arnold [1973] or Hirsch and Smale [1974] for details.

2.1 Exercises

1. Suppose $x = \bar{x}(t)$ is a solution of the nonautonomous equation

   $$\dot{x} = f(x, t), \qquad x \in \mathbb{R}^n.$$

   Show that this solution can be transformed to the "zero solution" by the shift

   $$x = y + \bar{x}(t).$$

   Hence, conclude that without loss of generality, the study of the stability of an arbitrary solution can be transformed to a study of the stability of the solution $x = 0$, even for time-dependent vector fields.

2. In this exercise we generalize Liapunov's theorem to nonautonomous systems. Consider a C^r, $r \geq 1$, vector field

   $$\dot{x} = f(x, t), \qquad x \in \mathbb{R}^n, \tag{2.1.1}$$

   satisfying

   $$f(0, t) = 0.$$

Definition 2.1.1 *A function $V(x,t)$ is called positive definite in a region $U \subset \mathbb{R}^n$ if there exists a function $W(x)$ with the following properties:*

1. *W is defined and continuous in U.*
2. *$0 < W(x) \leq V(x,t)$ for $x \neq 0$ and $t \geq t_0$.*

The derivative of V along trajectories of (2.1.1) is given by

$$\begin{aligned}\dot{V} &\equiv \frac{\partial V}{\partial t} + \nabla V \cdot \dot{x} \\ &= \frac{\partial V}{\partial t} + \nabla V \cdot f(x,t).\end{aligned}$$

This is the *orbital derivative* for nonautonomous systems. Prove the following theorem.

Theorem 2.1.2 *Suppose $V(x,t)$ is positive definite in a neighborhood U of $x = 0$ for $t \geq t_0$. Then*

i) *if $\dot{V}(x,t) \leq 0$ in U.*

$x = 0$ is stable. *Moreover, if*

ii) *$\dot{V}(x,t) < 0$ in U*

then $x = 0$ is asymptotically stable.

Hint: Since in the definition of positive definite $W(x)$ is independent of t, you should be able to mimic the proof of Theorem 2.0.1. For more information on Liapunov's method for nonautonomous systems see Aeyels [1995].

3. Prove Dirichlet's theorem (Siegel and Moser [1971]). Consider a $\mathbf{C}^r$ vector field ($r \geq 1$)

$$\dot{x} = f(x), \qquad x \in \mathbb{R}^n,$$

which has a fixed point at $x = \bar{x}$. Let $H(x)$ be a first integral of this vector field defined in a neighborhood of $x = \bar{x}$ such that $x = \bar{x}$ is a nondegenerate minimum of $H(x)$. Then $x = \bar{x}$ is stable.

4. Prove Liapunov's theorem for maps, i.e., consider a $\mathbf{C}^r$ diffeomorphism

$$x \mapsto f(x), \qquad x \in \mathbb{R}^n,$$

and suppose that we have a scalar-valued function

$$V : U \to \mathbb{R}^1$$

defined on some open set $U \in \mathbb{R}^n$ satisfying

i) $V(x_0) = 0$;

ii) $V(x) > 0$ for $x \neq x_0$;

iii) $V \circ f(x) \leq V(x)$ with equality if and only if $x = x_0$.

Then $x = x_0$ is a stable fixed point. Moreover, if strict inequality holds in iii), then $x = x_0$ is asymptotically stable. Does the same result hold for noninvertible maps?

5. Consider the vector field

$$\begin{aligned}\dot{x} &= -y - x(x^2 + y^2), \\ \dot{y} &= x - y(x^2 + y^2), \qquad (x,y) \in \mathbb{R}^2.\end{aligned}$$

Use Liapunov's method to show that the origin is globally asymptotically stable.

6. Consider the damped Duffing equation

$$\begin{aligned}\dot{x} &= y,\\ \dot{y} &= x - x^3 - \delta y, \qquad (x,y) \in \mathbb{R}^2, \quad \delta > 0.\end{aligned}$$

Use the function

$$V(x,y) = \frac{y^2}{2} - \frac{x^2}{2} + \frac{x^4}{4},$$

as a Liapunov function to show that the equilibrium points $(x,y) = (\pm 1, 0)$ are asymptotically stable.

7. Consider a particle of mass m moving in $\mathbb{R}^3$ under the influence of a potential field $\Phi(x,y,z)$. The equations of motion are given by

$$\begin{aligned}m\ddot{x} &= -\frac{\partial \Phi}{\partial x}(x,y,z),\\ m\ddot{y} &= -\frac{\partial \Phi}{\partial y}(x,y,z),\\ m\ddot{z} &= -\frac{\partial \Phi}{\partial z}(x,y,z),\end{aligned}$$

Prove that a minimum of the potential corresponds to a stable equilbrium point. Is it asymptotically stable? How differentiable must $\Phi(x,y,z)$ be?

8. Prove the following *instability theorem*. Let $x = \bar{x}$ be an equilibrium point of a C^r, $r \geq 1$, vector field $\dot{x} = f(x)$, $x \in \mathbb{R}^n$. Suppose $V(x)$ is a C^1 scalar valued function satisfying $V(\bar{x}) = 0$ and $\dot{V} > 0$ in $U - \{\bar{x}\}$, where U is a neighborhood of $\bar{x}$. If $V(x_n) > 0$ for some sequence $x_n \to \bar{x}$, then $\bar{x}$ is unstable.

3

Invariant Manifolds: Linear and Nonlinear Systems

We will see throughout this book that invariant manifolds, in particular stable, unstable, and center manifolds, play a central role in the analysis of dynamical systems. We will give a simultaneous discussion of these ideas for both vector fields

$$\dot{x} = f(x), \qquad x \in \mathbb{R}^n, \tag{3.0.1}$$

and maps

$$x \mapsto g(x), \qquad x \in \mathbb{R}^n. \tag{3.0.2}$$

Definition 3.0.3 (Invariant Set) *Let $S \subset \mathbb{R}^n$ be a set, then*

a) (Continuous time) S is said to be invariant *under the vector field $\dot{x} = f(x)$ if for any $x_0 \in S$ we have $x(t, 0, x_0) \in S$ for all $t \in \mathbb{R}$ (where $x(0, 0, x_0) = x_0$).*

b) (Discrete time) S is said to be invariant *under the map $x \mapsto g(x)$ if for any $x_0 \in S$ we have $g^n(x_0) \in S$ for all n.*

If we restrict ourselves to positive times (i.e., $t \geq 0$, $n \geq 0$) then we refer to S as a positively invariant set *and, for negative time, as a* negatively invariant set.

Stated succinctly, invariant sets have the property that trajectories starting in the invariant set, remain in the invariant set, for all of their future, and all of their past.

We remark that if g is noninvertible, then only $n \geq 0$ makes sense (although in some instances it may be useful to consider g^{-1} which does have a set theoretic meaning).

Definition 3.0.4 (Invariant Manifold) *An invariant set $S \subset \mathbb{R}^n$ is said to be a $\mathbf{C}^r$ ($r \geq 1$)* invariant manifold *if S has the structure of a $\mathbf{C}^r$ differentiable manifold. Similarly, a positively (resp., negatively) invariant set $S \subset \mathbb{R}^n$ is said to be a $\mathbf{C}^r$ ($r \geq 1$)* positively *(resp.,* negatively*)* invariant manifold *if S has the structure of a $\mathbf{C}^r$ differentiable manifold.*

Evidently, we need to say what we mean by the term "$\mathbf{C}^r$ differentiable manifold." However, this is the subject of a course in itself, so rather than

define the concept of a manifold in its full generality, we will describe only that portion of the vast theory that we will need.

Roughly speaking, a manifold is a set which *locally* has the structure of Euclidean space. In applications, manifolds are most often met as m-dimensional surfaces embedded in $\mathbb{R}^n$. If the surface has no singular points, i.e., the derivative of the function representing the surface has maximal rank, then by the implicit function theorem it can locally be represented as a graph. The surface is a $\mathbf{C}^r$ manifold if the (local) graphs representing it are $\mathbf{C}^r$ (note: for a thorough treatment of this particular representation of a manifold see Dubrovin, Fomenko, and Novikov [1985]).

Another example is even more basic. Let $\{s_1, \cdots, s_n\}$ denote the standard basis on $\mathbb{R}^n$. Let $\{s_{i_1}, \cdots, s_{i_j}\}$, $j < n$, denote any j basis vectors from this set; then the span of $\{s_{i_1}, \cdots, s_{i_j}\}$ forms a j-dimensional subspace of $\mathbb{R}^n$ which is trivially a $\mathbf{C}^\infty$ j-dimensional manifold. For a thorough introduction to the theory of manifolds with a view to applications see Abraham, Marsden, and Ratiu [1988].

The main reason for choosing these examples is that, in this book, when the term "manifold" is used, it will be sufficient to think of one of the following two situations:

1. *Linear Settings*: a linear vector subspace of $\mathbb{R}^n$;
2. *Nonlinear Settings*: a surface embedded in $\mathbb{R}^n$ which can be locally represented as a graph (which can be justified via the implicit function theorem).

3.1 Stable, Unstable, and Center Subspaces of Linear, Autonomous Vector Fields

Let us return to our study of the orbit structure near fixed points to see how some important invariant manifolds arise. We begin with vector fields. Let $\bar{x} \in \mathbb{R}^n$ be a fixed point of

$$\dot{x} = f(x), \qquad x \in \mathbb{R}^n. \tag{3.1.1}$$

Then, by the discussion in Chapter 1, it is natural to consider the associated linear system

$$\dot{y} = Ay, \qquad y \in \mathbb{R}^n, \tag{3.1.2}$$

where $A \equiv Df(\bar{x})$ is a constant $n \times n$ matrix. The solution of (3.1.2) through the point $y_0 \in \mathbb{R}^n$ at $t = 0$ is given by

$$y(t) = e^{At} y_0, \tag{3.1.3}$$

where

$$e^{At} = \mathrm{id} + At + \frac{1}{2!}A^2t^2 + \frac{1}{3!}A^3t^3 + \cdots \tag{3.1.4}$$

and "id" denotes the $n \times n$ identity matrix. We must assume sufficient background in the theory of linear constant coefficient ordinary differential equations so that (3.1.3) and (3.1.4) make sense to the reader. Excellent references for this theory are Arnold [1973] and Hirsch and Smale [1974]. Our goal here is to extract the necessary ingredients from this theory so as to give a geometrical interpretation to (3.1.3).

Now $\mathbb{R}^n$ can be represented as the direct sum of three subspaces denoted E^s, E^u, and E^c, which are defined as follows:

$$\begin{aligned} E^s &= \text{span}\{e_1, \cdots, e_s\}, \\ E^u &= \text{span}\{e_{s+1}, \cdots, e_{s+u}\}, \qquad s+u+c=n, \\ E^c &= \text{span}\{e_{s+u+1}, \cdots, e_{s+u+c}\}, \end{aligned} \tag{3.1.5}$$

where $\{e_1, \cdots, e_s\}$ are the (generalized) eigenvectors of A corresponding to the eigenvalues of A having *negative real part*, $\{e_{s+1}, \cdots, e_{s+u}\}$ are the (generalized) eigenvectors of A corresponding to eigenvalues of A having *positive real part*, and $\{e_{s+u+1}, \cdots, e_{s+u+c}\}$ are the (generalized) eigenvectors of A corresponding to the eigenvalues of A having *zero real part* (note: this is proved in great detail in Hirsch and Smale [1974]). E^s, E^u, and E^c are referred to as the stable, unstable, and center subspaces, respectively. They are also examples of invariant subspaces (or manifolds) since solutions of (3.1.2) with initial conditions entirely contained in either E^s, E^u, or E^c must forever remain in that particular subspace for all time (we will motivate this a bit more shortly). Moreover, solutions starting in E^s approach $y = 0$ asymptotically as $t \to +\infty$ and solutions starting in E^u approach $y = 0$ asymptotically as $t \to -\infty$.

We will now describe the linear algebra behind the definition of the stable, unstable, and center subspaces in more detail, largely following the discussion in Hirsch and Smale [1974], to which we refer the reader for proofs of some of the statements. We denote the eigenvalues of the (real) matrix A by

$$\{\lambda_{s,1}, \cdots, \lambda_{s,i}, \mu_{s,1}, \bar{\mu}_{s,1}, \cdots, \mu_{s,j}, \bar{\mu}_{s,j}\} \quad i + 2j = s,$$

$$\{\lambda_{u,1}, \cdots, \lambda_{u,k}, \mu_{u,1}, \bar{\mu}_{u,1}, \cdots, \mu_{u,l}, \bar{\mu}_{u,l}\} \quad k + 2l = u,$$

$$\{\lambda_{c,1}, \cdots, \lambda_{c,m}, \mu_{c,1}, \bar{\mu}_{c,1}, \cdots, \mu_{c,n}, \bar{\mu}_{c,n}\} \quad m + 2n = c,$$

where $\lambda_{\alpha,\gamma}$ denote the real eigenvalues and $\mu_{\alpha,\gamma}$ denotes complex eigenvalues. Since A is real, if $\mu_{\alpha,\gamma}$ is an eigenvalue of A so is $\bar{\mu}_{\alpha,\gamma}$.

The *generalized eigenspace corresponding to the (real) eigenvalue* $\lambda_{\alpha,\gamma}$ is defined as

$$V(A, \lambda_{\alpha,\gamma}) \equiv \text{Ker } (A - \lambda_{\alpha,\gamma}\,\text{id})^{n_{\alpha,\gamma}}, \qquad \alpha = s, u, c, \quad \gamma = i, k, m,$$

where $n_{\alpha,\gamma}$ is the (algebraic) multiplicity of the eigenvalue $\lambda_{\alpha,\gamma}$ (i.e., the number of times it appears as a root of the characteristic polynomial as-

sociated with A, $\det(A - \lambda\,\mathrm{id}) = 0$). The dimension of $V(A, \lambda_{\alpha,\gamma})$ is equal to $n_{\alpha,\gamma}$.

There is a bit of clumsiness with the notation here with respect to the eigenvalues with zero real part. The only way an eigenvalues can have zero real part, and be on the imaginary axis, is for it to be identically zero. Therefore $\lambda_{c,i} = 0$, $i = 1, \ldots, m$, and it follows that $n_{c,i} = m$, $i = 1, \ldots, m$.

Complex eigenvalues are a bit more difficult to treat (actually, the difficulty arises in the explanation; their treatment is fairly straightforward). Of course, the problem facing us is fairly evident. For a given complex eigenvalue $\mu_{\alpha,\gamma}$ we can define the corresponding generalized eigenspace in the usual way, i.e.,

$$V(A, \mu_{\alpha,\gamma}) \equiv \mathrm{Ker}\,(A - \mu_{\alpha,\gamma}\,\mathrm{id})^{n_{\alpha,\gamma}}, \qquad \alpha = s, u, c, \quad \gamma = j, l, n,$$

where $n_{\alpha,\gamma}$ is the (algebraic) multiplicity of the eigenvalue $\mu_{\alpha,\gamma}$. However, if one applies the same technique as one applies for real eigenvalues to compute the corresponding generalized eigenvectors one obtains *complex* generalized eigenvectors. Clearly, this is not a satisfactory situation since the phase space of our dynamical system is real. Nevertheless, one can derive a real basis for the generalized eigenspace corresponding to a complex eigenvalue from these "complex generalized eigenvectors" by adopting the complexification stratagem, which we now describe. First, we must give several definitions.

Let us think of $\mathbb{R}^n$ as a subset of $\mathbb{C}^n$ in the natural way, i.e., $\mathbb{R}^n$ is the set of complex n-tuples where each entry is a real number.

Definition 3.1.1 *Let F be a complex subspace of $\mathbb{C}^n$. Then $F_{\mathbb{R}} \equiv F \cap \mathbb{R}^n$ is the set of n-tuples in F that are real. $F_{\mathbb{R}}$ is referred to as* the set of real vectors in F.

It can easily be shown that $F_{\mathbb{R}}$ is closed under the operations of addition, as well as scalar multiplication by *real numbers*. Hence, $F_{\mathbb{R}}$ is a real vector space (a subspace of $\mathbb{R}^n$).

Definition 3.1.2 (Complexification of a Subspace) *Let E be a subspace of $\mathbb{R}^n$. Then*

$$E_{\mathbb{C}} \equiv \left\{ z \in \mathbb{C}^n \,|\, z = \sum \alpha_i x_i, \quad x_i \in E,\, \alpha_i \in \mathbb{C} \right\},$$

is called the complexification of E, *where the sum denotes arbitrary, but finite, linear combinations.*

It is not hard to show that $E_{\mathbb{C}}$ is a complex subspace of $\mathbb{C}^n$, and that $(E_{\mathbb{C}})_{\mathbb{R}} = E$.

Definition 3.1.3 (Complexification of a Real Linear Map) *Suppose $A : \mathbb{R}^n \to \mathbb{R}^n$ is a real linear map, and let E be a real subspace of $\mathbb{R}^n$ that*

is invariant under A. The complexification *of A, denoted $A_{\mathbb{C}}$, is a linear map of $E_{\mathbb{C}}$ into $E_{\mathbb{C}}$, and is defined as follows. By the definition of $E_{\mathbb{C}}$, any $z \in E_{\mathbb{C}}$ can be represented as*

$$z = \sum \alpha_i x_i, \qquad x_i \in E,\ \alpha_i \in \mathbb{C},$$

where the sum denotes arbitrary, but finite, linear combinations. Then we define

$$A_{\mathbb{C}} z \equiv \sum \alpha_i A x_i.$$

Finally, we are at the point where we can define the generalized eigenspace corresponding to a complex eigenvalue $\mu_{\alpha,\gamma}$. This is given by

$$V(A, \mu_{\alpha,\gamma}, \bar{\mu}_{\alpha,\gamma}) \equiv (V(A_{\mathbb{C}}, \mu_{\alpha,\gamma}) \oplus V(A_{\mathbb{C}}, \bar{\mu}_{\alpha,\gamma})) \cap \mathbb{R}^n,$$
$$\alpha = s, u, c, \quad \gamma = j, l, n,$$

where

$$V(A_{\mathbb{C}}, \mu_{\alpha,\gamma}) \equiv \mathrm{Ker}\ (A_{\mathbb{C}} - \mu_{\alpha,\gamma}\,\mathrm{id})^{n_{\alpha,\gamma}}.$$

We then define the stable, unstable, and center subspaces as follows

$$E^s \equiv \sum_{\gamma=1}^{i} V(A, \lambda_{s,\gamma}) + \sum_{\gamma=1}^{j} V(A, \mu_{s,\gamma}, \bar{\mu}_{s,\gamma}), \tag{3.1.6}$$

$$E^u \equiv \sum_{\gamma=1}^{k} V(A, \lambda_{u,\gamma}) + \sum_{\gamma=1}^{l} V(A, \mu_{u,\gamma}, \bar{\mu}_{u,\gamma}), \tag{3.1.7}$$

$$E^c \equiv V(A, 0) + \sum_{\gamma=1}^{n} V(A, \mu_{c,\gamma}, \bar{\mu}_{c,\gamma}), \tag{3.1.8}$$

where the sums are taken to be direct sums. By the primary decomposition theorem (Hirsch and Smale [1974]) we have

$$\mathbb{R}^n = E^s \oplus E^u \oplus E^c.$$

3.1A Invariance of the Stable, Unstable, and Center Subspaces

Let us outline how one ascertains the invariance of these subspaces under the linear flow given in (3.1.3) (this will provide some useful hints for the exercises). First, consider the matrix A associated with the linear vector field (3.1.2) as a linear map of $\mathbb{R}^n$ into $\mathbb{R}^n$. Clearly, E^s, E^u, and E^c are invariant subspaces for this linear map since each is the subspace spanned by a particular collection of generalized eigenvectors. We want to argue that they are invariant under the linear map e^{At}. This relies on the following three facts that are proven in a basic linear algebra course.

Suppose $V \subset \mathbb{R}^n$ is a subspace and invariant under the linear map A. Then

- For any $c \in \mathbb{R}$, V is invariant with respect to cA.
- For any integer $n > 1$, V is invariant with respect to A^n.
- Suppose A_1 and A_2 are linear maps on $\mathbb{R}^n$ and V is invariant with respect to both A_1 and A_2. Then V is invariant with respect to $A_1 + A_2$. From this result it also follows that for any finite number of linear maps A_i, $i = 1, \ldots, n$, with V invariant under each, V is also invariant under $\sum_{i=1}^{n} A_i$.

Using each of these facts one can easily conclude that V is invariant under the linear map

$$L_n(t) \equiv \mathrm{id} + At + \frac{1}{2}A^2t^2 + \cdots + \frac{1}{n!}A^nt^n = \sum_{i=0}^{n} \frac{1}{i!}A^it^i,$$

for any n, where id is the $n \times n$ identity matrix (and $0! \equiv 1$). Now using the fact that V is closed, and that $L_n(t)$ converges to e^{At} uniformly, we conclude that V is invariant with respect to e^{At}.

3.1B Some Examples

We now illustrate these ideas with three examples where for simplicity and easier visualization we will work in $\mathbb{R}^3$.

Example 3.1.1. Suppose the three eigenvalues of A are real and distinct and denoted by λ_1, $\lambda_2 < 0$, $\lambda_3 > 0$. Then A has three linearly independent eigenvectors e_1, e_2, and e_3 corresponding to λ_1, λ_2, and λ_3, respectively. If we form the 3×3 matrix T by taking as columns the eigenvectors e_1, e_2, and e_3, which we write as

$$T \equiv \begin{pmatrix} \vdots & \vdots & \vdots \\ e_1 & e_2 & e_3 \\ \vdots & \vdots & \vdots \end{pmatrix}, \tag{3.1.9}$$

then we have

$$\Lambda \equiv \begin{pmatrix} \lambda_1 & 0 & 0 \\ 0 & \lambda_2 & 0 \\ 0 & 0 & \lambda_3 \end{pmatrix} = T^{-1}AT. \tag{3.1.10}$$

Recall that the solution of (3.1.2) through $y_0 \in \mathbb{R}^3$ at $t = 0$ is given by

$$y(t) = e^{At}y_0 = e^{T\Lambda T^{-1}t}y_0. \tag{3.1.11}$$

Using (3.1.4), it is easy to see that (3.1.11) is the same as

$$\begin{aligned} y(t) &= Te^{\Lambda t}T^{-1}y_0 \\ &= T \begin{pmatrix} e^{\lambda_1 t} & 0 & 0 \\ 0 & e^{\lambda_2 t} & 0 \\ 0 & 0 & e^{\lambda_3 t} \end{pmatrix} T^{-1}y_0 \end{aligned}$$

$$= \begin{pmatrix} \vdots & \vdots & \vdots \\ e_1 e^{\lambda_1 t} & e_2 e^{\lambda_2 t} & e_3 e^{\lambda_3 t} \\ \vdots & \vdots & \vdots \end{pmatrix} T^{-1} y_0. \tag{3.1.12}$$

Now we want to give a geometric interpretation to (3.1.12). Recall from (3.1.5) that we have

$$E^s = \text{span}\{e_1, e_2\},$$
$$E^u = \text{span}\{e_3\}.$$

Invariance

Choose any point $y_0 \in \mathbb{R}^3$. Then T^{-1} is the transformation matrix which changes the coordinates of y_0 with respect to the standard basis on $\mathbb{R}^3$ (i.e., $(1,0,0)$, $(0,1,0)$, $(0,0,1)$) into coordinates with respect to the basis e_1, e_2, and e_3. Thus, for $y_0 \in E^s$, $T^{-1}y_0$ has the form

$$T^{-1}y_0 = \begin{pmatrix} \tilde{y}_{01} \\ \tilde{y}_{02} \\ 0 \end{pmatrix}, \tag{3.1.13}$$

and, for $y_0 \in E^u$, $T^{-1}y_0$ has the form

$$T^{-1}y_0 = \begin{pmatrix} 0 \\ 0 \\ \tilde{y}_{03} \end{pmatrix}. \tag{3.1.14}$$

Therefore, by substituting (3.1.13) (resp., (3.1.14)) into (3.1.12), it is easy to see that $y_0 \in E^s$ (resp., E^u) implies $e^{At}y_0 \in E^s$ (resp., E^u). Thus, E^s and E^u are *invariant* manifolds.

Asymptotic Behavior

Using (3.1.13) and (3.1.12), we can see that, for any $y_0 \in E^s$, we have $e^{At}y_0 \to 0$ as $t \to +\infty$ and, for any $y_0 \in E^u$, we have $e^{At}y_0 \to 0$ as $t \to -\infty$ (hence the reason behind the names stable and unstable manifolds).

See Figure 3.1.1 for an illustration of the geometry of E^s and E^u.

End of Example 3.1.1

Example 3.1.2. Suppose A has two complex conjugate eigenvalues $\rho \pm i\,\omega$, $\rho < 0$, $\omega \neq 0$ and one real eigenvalue $\lambda > 0$. Then A has three real generalized eigenvectors e_1, e_2, and e_3, which can be used as the columns of a matrix T in order to transform A as follows

$$\Lambda \equiv \begin{pmatrix} \rho & \omega & 0 \\ -\omega & \rho & 0 \\ 0 & 0 & \lambda \end{pmatrix} = T^{-1}AT. \tag{3.1.15}$$

From Example 3.1.1 it is easy to see that in this example we have

$$\begin{aligned} y(t) &= Te^{\Lambda t}T^{-1}y_0 \\ &= T \begin{pmatrix} e^{\rho t}\cos\omega t & e^{\rho t}\sin\omega t & 0 \\ -e^{\rho t}\sin\omega t & e^{\rho t}\cos\omega t & 0 \\ 0 & 0 & e^{\lambda t} \end{pmatrix} T^{-1}y_0. \end{aligned} \tag{3.1.16}$$

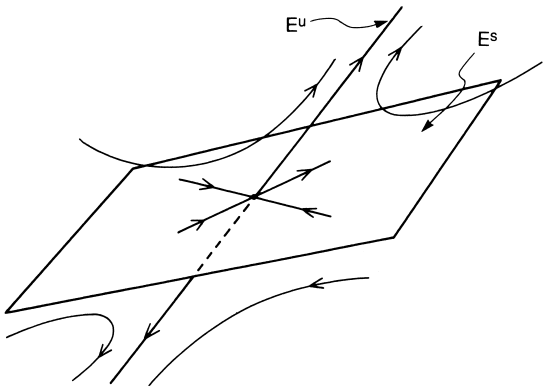

FIGURE 3.1.1. The geometry of E^s and E^u for Example 3.1.1.

Using the same arguments given in Example 3.1.1 it should be clear that $E^s = \text{span}\{e_1, e_2\}$ is an invariant manifold of solutions that decay exponentially to zero as $t \to +\infty$, and $E^u = \text{span}\{e_3\}$ is an invariant manifold of solutions that decay exponentially to zero as $t \to -\infty$ (see Figure 3.1.2).

End of Example 3.1.2

Example 3.1.3. Suppose A has two real repeated eigenvalues, $\lambda < 0$, and a third distinct eigenvalue $\gamma > 0$ such that there exist generalized eigenvectors e_1, e_2, and e_3 which can be used to form the columns of a matrix T so that A is transformed as follows

$$\Lambda = \begin{pmatrix} \lambda & 1 & 0 \\ 0 & \lambda & 0 \\ 0 & 0 & \gamma \end{pmatrix} = T^{-1}AT. \tag{3.1.17}$$

Following Examples 3.1.1 and 3.1.2, in this example the solution through the point $y_0 \in \mathbb{R}^3$ at $t = 0$ is given by

$$\begin{aligned} y(t) &= Te^{\Lambda t}T^{-1}y_0 \\ &= T \begin{pmatrix} e^{\lambda t} & te^{\lambda t} & 0 \\ 0 & e^{\lambda t} & 0 \\ 0 & 0 & e^{\gamma t} \end{pmatrix} T^{-1}y_0. \end{aligned} \tag{3.1.18}$$

Using the same arguments as in Example 3.1.1, it is easy to see that $E^s = \text{span}\{e_1, e_2\}$ is an invariant manifold of solutions that decay to $y = 0$ as $t \to +\infty$, and $E^u = \text{span}\{e_3\}$ is an invariant manifold of solutions that decay to $y = 0$ as $t \to -\infty$ (see Figure 3.1.3).

End of Example 3.1.3

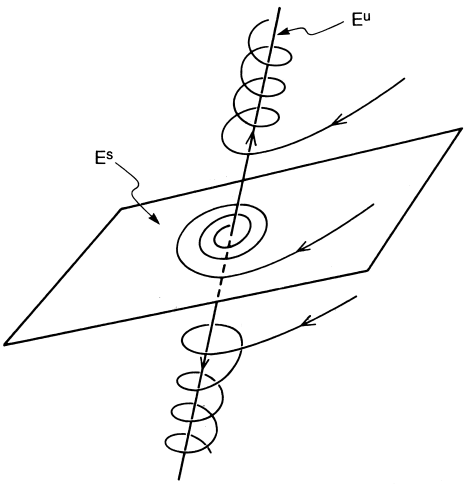

FIGURE 3.1.2. The geometry of E^s and E^u for Example 3.1.2(for $\omega < 0$).

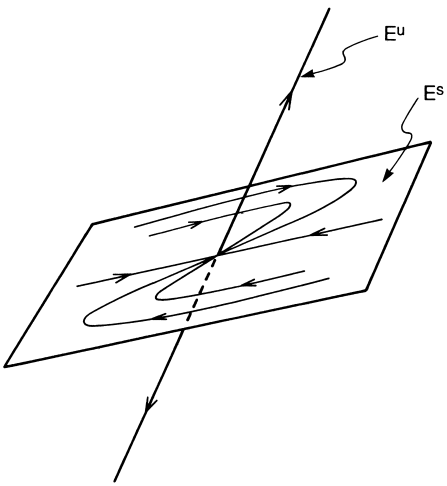

FIGURE 3.1.3. The geometry of E^s and E^u for Example 3.1.3

The reader should review enough linear algebra so that he or she can justify each step in the arguments given in these examples. We remark that we have not considered an example of a linear vector field having a center subspace. The reader can construct his or her own examples from Example 3.1.2 by setting $\rho = 0$ or from Example 3.1.3 by setting $\lambda = 0$; we leave these as exercises and now turn to the nonlinear system.

3.2 Stable, Unstable, and Center Manifolds for Fixed Points of Nonlinear, Autonomous Vector Fields

Recall that our original motivation for studying the linear system

$$\dot{y} = Ay, \qquad y \in \mathbb{R}^n, \tag{3.2.1}$$

where $A = Df(\bar{x})$, was to obtain information about the nature of solutions near the fixed point $x = \bar{x}$ of the nonlinear equation

$$\dot{x} = f(x), \qquad x \in \mathbb{R}^n. \tag{3.2.2}$$

The stable, unstable, and center manifold theorem provides an answer to this question; let us first transform (3.2.2) to a more convenient form.

We first transform the fixed point $x = \bar{x}$ of (3.2.2) to the origin via the translation $y = x - \bar{x}$. In this case (3.2.2) becomes

$$\dot{y} = f(\bar{x} + y), \qquad y \in \mathbb{R}^n. \tag{3.2.3}$$

Taylor expanding $f(\bar{x} + y)$ about $x = \bar{x}$ gives

$$\dot{y} = Df(\bar{x})y + R(y), \qquad y \in \mathbb{R}^n, \tag{3.2.4}$$

where $R(y) = \mathcal{O}(|y|^2)$ and we have used $f(\bar{x}) = 0$. From elementary linear algebra (see Hirsch and Smale [1974]) we can find a linear transformation T which transforms the linear equation (3.2.1) into block diagonal form

$$\begin{pmatrix} \dot{u} \\ \dot{v} \\ \dot{w} \end{pmatrix} = \begin{pmatrix} A_s & 0 & 0 \\ 0 & A_u & 0 \\ 0 & 0 & A_c \end{pmatrix} \begin{pmatrix} u \\ v \\ w \end{pmatrix}, \tag{3.2.5}$$

where $T^{-1}y \equiv (u, v, w) \in \mathbb{R}^s \times \mathbb{R}^u \times \mathbb{R}^c$, $s + u + c = n$, A_s is an $s \times s$ matrix having eigenvalues with negative real part, A_u is an $u \times u$ matrix having eigenvalues with positive real part, and A_c is an $c \times c$ matrix having eigenvalues with zero real part (note: we point out the (hopefully) obvious fact that the "0" in (3.2.5) are not scalar zero's but rather the appropriately sized block consisting of all zero's. This notation will be used throughout the book). Using this same linear transformation to transform the coordinates of the nonlinear vector field (3.2.4) gives the equation

$$\begin{aligned} \dot{u} &= A_s u + R_s(u, v, w), \\ \dot{v} &= A_u v + R_u(u, v, w), \\ \dot{w} &= A_c w + R_c(u, v, w), \end{aligned} \tag{3.2.6}$$

where $R_s(u, v, w)$, $R_u(u, v, w)$, and $R_c(u, v, w)$ are the first s, u, and c components, respectively, of the vector $T^{-1}R(T^y)$.

Now consider the linear vector field (3.2.5). From our previous discussion (3.2.5) has an s-dimensional invariant stable manifold, a u-dimensional invariant unstable manifold, and a c-dimensional invariant center manifold all intersecting in the origin. The following theorem shows how this structure changes when the nonlinear vector field (3.2.6) is considered.

Theorem 3.2.1 (Local Stable, Unstable, and Center Manifolds of Fixed Points) *Suppose (3.2.6) is $\mathbf{C}^r$, $r \geq 2$. Then the fixed point $(u, v, w) = 0$ of (3.2.6) possesses a $\mathbf{C}^r$ s-dimensional local, invariant stable manifold, $W^s_{loc}(0)$, a $\mathbf{C}^r$ u-dimensional local, invariant unstable manifold, $W^u_{loc}(0)$, and a $\mathbf{C}^r$ c-dimensional local, invariant center manifold, $W^c_{loc}(0)$, all intersecting at $(u, v, w) = 0$. These manifolds are all tangent to the respective invariant subspaces of the linear vector field (3.2.5) at the origin and, hence, are locally representable as graphs. In particular, we have*

$$W^s_{loc}(0) = \big\{(u,v,w) \in \mathbb{R}^s \times \mathbb{R}^u \times \mathbb{R}^c \,|\, v = h^s_v(u), w = h^s_w(u);$$
$$Dh^s_v(0) = 0, Dh^s_w(0) = 0; |u| \text{ sufficiently small}\big\}$$

$$W^u_{loc}(0) = \big\{(u,v,w) \in \mathbb{R}^s \times \mathbb{R}^u \times \mathbb{R}^c \,|\, u = h^u_u(v), w = h^u_w(v);$$
$$Dh^u_u(0) = 0, Dh^u_w(0) = 0; |v| \text{ sufficiently small}\big\}$$

$$W^c_{loc}(0) = \big\{(u,v,w) \in \mathbb{R}^s \times \mathbb{R}^u \times \mathbb{R}^c \,|\, u = h^c_u(w), v = h^c_v(w);$$
$$Dh^c_u(0) = 0, Dh^c_v(0) = 0; |w| \text{ sufficiently small}\big\}$$

where $h^s_v(u)$, $h^s_w(u)$, $h^u_u(v)$, $h^u_w(v)$, $h^c_u(w)$, and $h^c_v(w)$ are $\mathbf{C}^r$ functions. Moreover, trajectories in $W^s_{\rm loc}(0)$ and $W^u_{\rm loc}(0)$ have the same asymptotic properties as trajectories in E^s and E^u, respectively. Namely, trajectories of (3.2.6) with initial conditions in $W^s_{\rm loc}(0)$ (resp., $W^u_{\rm loc}(0)$) approach the origin at an exponential rate asymptotically as $t \to +\infty$ (resp., $t \to -\infty$).

Proof: See Fenichel [1971], Hirsch, Pugh, and Shub [1977], or Wiggins [1994] for details as well as for some history and further references on invariant manifolds. □

Some remarks on this important theorem are now in order.

Remark 1. First some terminology. Very often one hears the terms "stable manifold," "unstable manifold," or "center manifold" used alone; however, alone they are not sufficient to describe the dynamical situation. Notice that Theorem 3.2.1 is entitled stable, unstable, and center manifolds *of fixed points*. The phrase "of fixed points" is the key: one must say the stable, unstable, or center manifold *of something* in order to make sense. The "somethings" studied thus far have been fixed points; however, more

general invariant sets also have stable, unstable, and center manifolds. See Wiggins [1994] for a discussion.

Remark 2. The conditions $Dh_v^s(0) = 0$, $Dh_w^s(0) = 0$, etc., reflect that the nonlinear manifolds are tangent to the associated linear manifolds at the origin.

Remark 3. In the statement of the theorem the term *local*, invariant stable, unstable, or center manifold is used. This deserves further explanation. "Local" refers to the fact that the manifold is only defined in the neighborhood of the fixed point as a graph. Consequently, these manifolds have a boundary. They are therefore only *locally invariant* in the sense that trajectories that start on them may leave the local manifold, but *only* through crossing the boundary. Invariance is still manifested by the vector field being tangent to the manifolds, which we discuss further below.

Remark 4. Suppose the fixed point is hyperbolic, i.e., $E^c = \emptyset$. In this case an interpretation of the theorem is that trajectories of the nonlinear vector field in a sufficiently small neighborhood of the origin behave the same as trajectories of the associated linear vector field.

Remark 5. In general, the behavior of trajectories in in $W^c_{\text{loc}}(0)$ cannot be inferred from the behavior of trajectories in E^c.

Remark 6. Uniqueness of Stable, Unstable, and Center Manifolds. Typically the existence of these invariant manifolds are proved through a contraction mapping argument, where the invariant manifold turns out to be the unique fixed point of an appropriately constructed contraction map. From this construction the stable and unstable manifolds are unique. The center manifold is a bit more delicate. In that case, because of the nonhyperbolicity, a "cut-off" function is typically used in the construction of the appropriate contraction map. In this case the center manifold does depend upon the cut-off function. However, it can be shown that the center manifold is unique to all orders of its Taylor expansion. That is, center manifolds only differ by exponentially small functions of the distance from the fixed point. See Wan [1977], Sijbrand [1985] and Wiggins [1994].

3.2a Invariance of the Graph of a Function: Tangency of the Vector Field to the Graph

Suppose one has a general surface, or manifold and one wants to check if it is invariant with respect to the dynamics generated by a vector field. How can this be done?

Suppose the vector field is of the form

$$\begin{aligned} \dot{x} &= f(x, y), \\ \dot{y} &= g(x, y), \qquad (x, y) \in \mathbb{R}^n \times \mathbb{R}^m. \end{aligned}$$

Suppose that the surface in the phase space is represented by the graph of

a function

$$y = h(x),$$

This surface is invariant if the vector field is tangent to the surface. This tangency condition is expressed as follows

$$Dh(x)\dot{x} = \dot{y},$$

or,

$$Dh(x)f(x, h(x)) = g(x, h(x)). \tag{3.2.7}$$

Of course, one must take care that all the functions taking part in these expressions have common domains, and that the appropriate derivatives exist. It is also very important to appreciate the role that specific coordinate representations played in deriving this expression.

3.3 Maps

An identical theory can be developed for maps. We summarize the details below. Consider a $\mathbf{C}^r$ diffeomorphism

$$x \mapsto g(x), \qquad x \in \mathbb{R}^n. \tag{3.3.1}$$

Suppose (3.3.1) has a fixed point at $x = \bar{x}$ and we want to know the nature of orbits near this fixed point. Then it is natural to consider the associated linear map

$$y \mapsto Ay, \qquad y \in \mathbb{R}^n, \tag{3.3.2}$$

where $A = Dg(\bar{x})$. The linear map (3.3.2) has invariant manifolds given by

$$\begin{aligned} E^s &= \text{span}\{e_1, \cdots, e_s\}, \\ E^u &= \text{span}\{e_{s+1}, \cdots, e_{s+u}\}, \\ E^c &= \text{span}\{e_{s+u+1}, \cdots, e_{s+u+c}\}, \end{aligned}$$

where $s + u + c = n$ and $e_1, \cdots, e_s$ are the (generalized) eigenvectors of A corresponding to the eigenvalues of A having *modulus less than one*, $e_{s+1}, \cdots, e_{s+u}$ are the (generalized) eigenvectors of A corresponding to the eigenvalues of A having *modulus greater than one*, and $e_{s+u+1}, \cdots, e_{s+u+c}$ are the (generalized) eigenvectors of A corresponding to the eigenvalues of A having *modulus equal to one*. The reader should find it easy to prove this by putting A in Jordan canonical form and noting that the orbit of the linear map (3.3.2) through the point $y_0 \in \mathbb{R}^n$ is given by

$$\{\cdots, A^{-n}y_0, \cdots, A^{-1}y_0, y_0, Ay_0, \cdots, A^n y_0, \cdots\}. \tag{3.3.3}$$

Now we address the question of how this structure goes over to the nonlinear map (3.3.1). In the case of maps Theorem 3.2.1 holds identically.

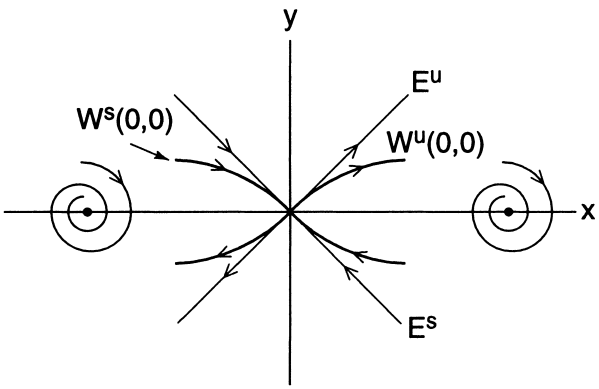

FIGURE 3.3.1. Local invariant manifold structure in the unforced Duffing oscillator, $0 < \delta < \sqrt{8}$.

Namely, the nonlinear map (3.3.1) has a $\mathbf{C}^r$ invariant s-dimensional stable manifold, a $\mathbf{C}^r$ invariant u-dimensional unstable manifold, and a $\mathbf{C}^r$ invariant c-dimensional center manifold all intersecting in the fixed point. Moreover, these manifolds are all tangent to the respective invariant manifolds of the linear map (3.3.2) at the fixed point.

Essentially, everything about stable, unstable, and center manifolds for fixed points of vector fields holds for fixed points of maps. We will give examples in the exercises. However, before completing our discussion of invariant manifolds let us apply our results to the unforced Duffing oscillator.

3.4 Some Examples

Example 3.4.1 (Application to the Unforced Duffing Oscillator). In Section 1 we have seen that the equation

$$\begin{aligned} \dot{x} &= y, \\ \dot{y} &= x - x^3 - \delta y, \qquad \delta > 0, \end{aligned}$$

has a saddle-type fixed point of $(x, y) = (0, 0)$, and sinks at $(\pm 1, 0)$ for $\delta > 0$. From Theorem 3.2.1 we now know that $(\pm 1, 0)$ have two-dimensional stable manifolds (this is obvious) and $(0, 0)$ has a one-dimensional stable manifold and a one-dimensional unstable manifold as shown in Figure 3.3.1 (note: we have drawn the figure for $0 < \delta < \sqrt{8}$. The reader should show how the solutions near the sinks are modified for $\delta > \sqrt{8}$). Note that Theorem 3.2.1 also tells us that a good local approximation to the stable and unstable manifolds of $(0, 0)$ is given by the corresponding invariant linear manifolds, which are relatively easy to calculate. The case $\delta = 0$ is treated in great detail in Chapter 5.

End of Example 3.4.1

Let us consider a final example from Guckenheimer and Holmes [1983].

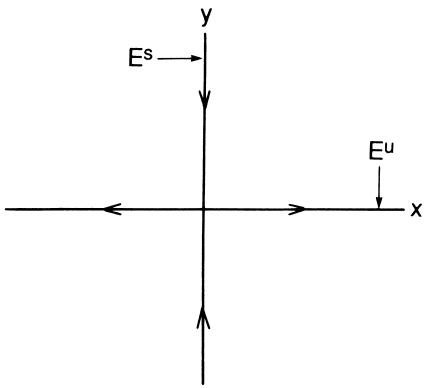

FIGURE 3.4.1. The stable and unstable subspaces in Example 3.4.2.

Example 3.4.2. Consider the planar vector field

$$\begin{aligned} \dot{x} &= x, \\ \dot{y} &= -y + x^2, \qquad (x, y) \in \mathbb{R}^1 \times \mathbb{R}^1, \end{aligned}$$

which has a hyperbolic fixed point at $(x, y) = (0, 0)$. The associated linearized system is given by

$$\begin{aligned} \dot{x} &= x, \\ \dot{y} &= -y, \end{aligned}$$

with stable and unstable subspaces given by

$$\begin{aligned} E^s &= \{\, (x, y) \in \mathbb{R}^2 \mid x = 0 \,\}, \\ E^u &= \{\, (x, y) \in \mathbb{R}^2 \mid y = 0 \,\} \end{aligned}$$

(see Figure 3.4.1).

Now we turn our attention to the nonlinear vector field for which, in this case, the solution can be obtained explicitly as follows. Eliminating time as the independent variable gives

$$\frac{\dot{y}}{\dot{x}} = \frac{dy}{dx} = \frac{-y}{x} + x,$$

which can be solved to obtain

$$y(x) = \frac{x^2}{3} + \frac{c}{x},$$

where c is some constant. Now $W^u_{\text{loc}}(0, 0)$ can be represented by a graph over the x variables, i.e., $y = h(x)$ with $h(0) = h'(0) = 0$. Varying c in the solution

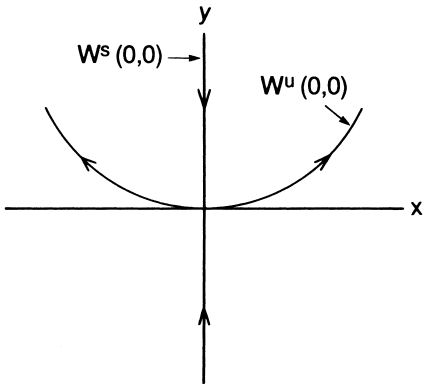

FIGURE 3.4.2. Stable and unstable manifolds of $(x, y) = (0, 0)$ in Example 3.4.2.

above takes us from orbit to orbit; we seek the value of c which corresponds to the unstable manifold—this is $c = 0$. Therefore, we have

$$W^u_{\text{loc}}(0,0) = \left\{ (x,y) \in \mathbb{R}^2 \;\middle|\; y = \frac{x^2}{3} \right\},$$

which is also the global unstable manifold of the origin. Finally, note that if we have initial conditions with the x component equal to zero, i.e., $(0, y)$ $\forall y$, then the solution stays on the y axis and approaches $(0, 0)$ as $t \uparrow \infty$; thus, $E^s = W^s(0,0) = \{ (x,y) \mid x = 0 \}$ (see Figure 3.4.2).

End of Example 3.4.2

3.5 Existence of Invariant Manifolds: The Main Methods of Proof, and How They Work

In this section we will describe the two main techniques for proving the existence of invariant manifolds. In particular, we will concentrate on how one proves the existence of stable, unstable, and center manifolds of fixed points, although the same approach works in more general settings. There are many excellent expositions of the proofs of these theorems. Our approach will be to show how they work in a concrete example where the answer is know explicitly. In this way we hope that the reader will be able to gain intuition concerning the key features of the problem that enables the procedure of the proof to work.

Of course, one might ask the question, "why do I need to know how to prove the stable and unstable manifold theorem?" There are two answers to this question. One is that the techniques of proof are often used as the basis for numerical approaches to computing stable and unstable manifolds. Even

if one has no interest in the details of the proof of the theorem, in using it in applications one often needs to numerically compute the manifolds. An overview of such numerical methods can be found in Moore and Hubert [1999] and Osinga [1996]. The other answer is that in a specific application the precise setting or hypotheses of the theorem may not be satisfied (e.g., the equilibrium point may be a saddle, but not hyperbolic, or the invariant set may be more complicated than an equilibrium point). In this situation it may be possible to prove a new theorem by following the same general approach, but with modifying certain details.

The main techniques for proving the existence of invariant manifolds are the following.

Hadamard's Method-The Graph Transform

Hadamard [1901] developed this method to prove the existence of stable and unstable manifolds of a fixed point of a C^r invertible map. The graph transform method is more geometrical in nature than the Liapunov-Perron method. In the context of a hyperbolic fixed point, the stable and unstable manifolds are constructed as graphs over the linearized stable and unstable subspaces, respectively–hence the name. Fenichel [1971], [1974], [1977] and Hirsch, Pugh, and Shub [1978] used this method in obtaining their general results on normally hyperbolic invariant manifolds. An elementary and detailed exposition of the graph transform method following Fenichel can be found in Wiggins [1994].

The Liapunov- Perron Method

Perron [1928], [1929], [1930] and Liapunov [1947] developed a method for proving the existence of stable and unstable manifolds of a hyperbolic equilbrium point. It deals with the integral equation formulation of the ordinary differential equations and constructs the invariant manifolds as a fixed point of an operator that is derived from this integral equation on a function space whose elements have the appropriate interpretation as stable and unstable manifolds. The Liapunov-Perron method has been used in many different situations. The book of Hale [1980] is a good reference point for surveying these applications. In this book Hale surveys the fundamental earlier work of Krylov and Bogoliubov, Bogoliubov and Mitropolski, Diliberto, Kyner, Kurzweil, and Pliss. In Chapter 7 of Hale [1980] several theorems related to various aspects of invariant manifolds are given which we refer to collectively as the "Hale invariant manifold theorem". These results can be viewed as a generalization and extension of much of the earlier work. Much of this work has recently been generalized in Yi [1993a,b]. Chicone [1999] has an excellent elementary and detailed exposition of the Liapunov-Perron method.

3.5A Application of These Two Methods to a Concrete Example: Existence of the Unstable Manifold

We recall Example 3.4.2:

$$\begin{aligned} \dot{x} &= x, \\ \dot{y} &= -y + x^2, \qquad (x, y) \in \mathbb{R}^2. \end{aligned} \tag{3.5.1}$$

This vector field has a hyperbolic fixed point at the origin with unstable manifold given by

$$y = \frac{x^2}{3}. \tag{3.5.2}$$

Now we will prove the existence of the unstable manifold by the graph transform method and the Liapunov-Perron method.

Application of the Graph Transform Method

The trajectory of (3.5.1) through the point (x_0, y_0) at $t = 0$ is easily calculated and found to be:

$$\begin{aligned} x(t; x_0, y_0) &= x_0 e^t, \\ y(t; x_0, y_0) &= y_0 e^{-t} + \frac{1}{3} x_0^2 e^{-t} \left(e^{3t} - 1\right). \end{aligned} \tag{3.5.3}$$

We view the trajectories as mapping initial conditions at $t = 0$ to points at the time t; often this is referred to as the *time-t map*.

Now consider a function $y = h(x)$, and we consider an initial condition (x_0, y_0) on the graph of this function, i.e., $y_0 = h(x_0)$. The image of this initial condition under the time-t map is given by

$$(x_0, h(x_0)) \to (x(t; x_0, h(x_0)), y(t; x_0, h(x_0))). \tag{3.5.4}$$

Now if the graph of $y = h(x)$ was an invariant manifold then, for any t, we would have:

$$y(t; x_0, h(x_0)) = h(x(t; x_0, h(x_0))). \tag{3.5.5}$$

This motivates us to define the following *graph transform*, $\mathcal{G}$:

$$\mathcal{G}h\left(x(t; x_0, h(x_0))\right) = y(t; x_0, h(x_0)), \tag{3.5.6}$$

where from (3.5.5) we see that the graph of a function $y = h(x)$ is invariant under the time-t map if it is a fixed point of the graph transform.

Now we are getting ahead of ourselves and we need to go back and develop the mathematical setting where the phrase "fixed point of the graph transform" makes sense.

We define the following space of functions:

$$S_\delta \equiv \{\text{the set of functions,} \quad h(x), \text{where} \quad |h(x) - h(x')| \leq \delta |x - x'|, \quad |x| \leq \epsilon,\ \delta > 0\}. \tag{3.5.7}$$

In other words, these are the set of Lipshitz functions with Lipschitz constant δ defined on the domain $|x| \leq \epsilon$. These two parameters, δ and ϵ are adjusted in order to make the proof work. We can put a norm on S_δ that is defined as follows:

$$\| h \| \equiv \sup_{|x| \leq \epsilon} |h(x)|.$$

With this norm S_δ becomes a Banach space, but more importantly, it becomes a complete metric space in the metric that is defined by this norm. This latter fact is important for using the contraction mapping principle.

The complete metric space S_δ will be the domain on which the graph transform is defined. Ultimately, we want to show that the graph transform has a fixed point in S_δ which, as we argued above, will be an invariant manifold. However first, several facts must be established.

The Graph Transform is Well-Defined:

We need to show that for any $h \in S_\delta$, $\mathcal{G}h$ is a function. Using (3.5.3) and (3.5.6), we have

$$\mathcal{G}h(x(t; x_0, h(x_0))) = h(x_0)e^{-t} + \frac{1}{3}x_0^2 e^{-t}\left(e^{3t} - 1\right).$$

Clearly, this is a well-defined function.

$\mathcal{G} : S_\delta \to S_\delta$:

This is the first step in showing that $\mathcal{G}$ is a contraction map on S_δ.

First, we need a preliminary result. Define

$$\xi = x(t; x_0, h(x_0)) = x_0 e^t, \qquad \xi' = x(t; x_0', h(x_0')) = x_0' e^t.$$

Then, for $t \geq 0$, we have

$$|\xi - \xi'| \geq |x_0 - x_0'|. \tag{3.5.8}$$

Next we calculate:

$$\begin{aligned}
|\mathcal{G}h(\xi) - \mathcal{G}h(\xi')| &\leq e^{-t}|h(x_0) - h(x_0')| + \frac{1}{3}e^{-t}\left(e^{3t} - 1\right)|x_0 + x_0'||x_0 - x_0'|, \\
&\leq \left(\delta e^{-t} + \frac{1}{3}e^{-t}\left(e^{3t} - 1\right)|x_0 + x_0'|\right)|x_0 - x_0'|, \\
&\leq \left(\delta e^{-t} + \frac{1}{3}e^{-t}\left(e^{3t} - 1\right)|x_0 + x_0'|\right)|\xi - \xi'|, \\
&\leq \left(\delta e^{-t} + \frac{2}{3}e^{-t}\left(e^{3t} - 1\right)\epsilon\right)|\xi - \xi'| \qquad (3.5.9)
\end{aligned}$$

Now for fixed $t > 0$, we can choose δ and ϵ small enough such that

$$\left(\delta e^{-t} + \frac{2}{3} e^{-t}\left(e^{3t} - 1\right)\epsilon\right) \leq \delta.$$

$\mathcal{G}$ is a Contraction Map on S_δ:

Choose x_0 and x_0' such that

$$\xi = x(t; x_0, h_1(x_0)) = x(t; x_0', h_2(x_0')). \tag{3.5.10}$$

Since $x(t; x_0, h_1(x_0)) = x_0 e^t$, $x(t; x_0', h_2(x_0')) = x_0' e^t$ this implies that

$$x_0 = x_0'. \tag{3.5.11}$$

Now for h_1, $h_2 \in S_\delta$ we have

$$\begin{aligned} |\mathcal{G}h_1(\xi) - \mathcal{G}h_2(\xi)| &\leq e^{-t}|h_1(x_0) - h_2(x_0)| \\ &\leq e^{-t} \parallel h_1 - h_2 \parallel, \end{aligned} \tag{3.5.12}$$

which is a contraction for $t > 0$. Therefore by the contraction mapping theorem, the graph transform has a unique fixed point, $\bar{h}(x)$, $|x| \leq \epsilon$. By construction, the graph of $\bar{h}(x)$ is invariant under the time-t map, for some *fixed* $t > 0$.

$y = \bar{h}(x)$ is Invariant:

There are two important points that need to be addressed related to the issue of *invariance*.

We have argued that $y = \bar{h}(x)$ is invariant under the discrete time-t map, for some fixed $t > 0$. [1] There is a technicality involved with this statement. One sees from the form of the trajectories of the vector field given in (3.5.3) that the x component of any trajectory grows exponentially in time. That means that any point starting on $y = \bar{h}(x)$ will eventually leave $y = \bar{h}(x)$ (for $t > 0$), but only by crossing the boundary, which is given by the two points $y_+ = \bar{h}(+\epsilon)$ and $y_- = \bar{h}(-\epsilon)$. The graph of $\bar{h}(x)$ is an example of a *locally invariant manifold*. That is, points starting on the graph of $\bar{h}(x)$ remain on the graph during time evolution, *except* they may leave

[1] Notice that the subscript "0" has disappeared from x_0 in our notation for the domain of the graph of the function which gives the local unstable manifold. This seemingly trivial point is one worth considering in a bit more detail. The subscript "0" makes explicit the fact that the invariant manifolds are manifolds of initial conditions for trajectories. This understanding is important and is similar to the understanding of how trajectories are different from orbits. Once this is made clear, the subscript "0" can be dropped since initial conditions are just points in the phase space. However, in setting up the problem, one needs to have the subscript so as not to confuse the notation for the initial condition with that for the trajectory itself.

the graph but only by crossing the boundary. This situation is typical for *local* stable, unstable, and center manifolds associated with fixed points since these manifolds are constructed in small neighborhoods of the fixed point as graphs over the respective linearized stable, unstable, and center subspaces. Therefore the domains of the graphs are finite, which generally gives rise to a boundary for these local invariant manifolds. Shortly we will show how one turns these local manifolds into global manifolds (and describe what that means).

The second important point concerning invariance is that we need to establish that points that start on $y = \bar{h}(x)$ stay on it for any time, unless they leave it by crossing the boundary. Our graph transform proof has only shown that the graph of $\bar{h}(x)$ is invariant with respect to the time-t map for some fixed $t > 0$. We leave the details of this as an exercise for the reader, but see Hartman [1964], Fenichel [1971], or Wiggins [1994] for details.

Continuation: The Global Unstable Manifold:

Once the existence of the local unstable manifold is established, we can then construct the global unstable manifold by letting the local unstable manifold evolve in time under the time-t map. More precisely, the global unstable manifold of the origin is given by:

$$W^u \equiv \bigcup_{\substack{t\geq 0 \\ |x|\leq \epsilon}} \left(x(t;x,\bar{h}(x)), y(t;x,\bar{h}(x))\right). \tag{3.5.13}$$

Clearly, this is object is invariant since it is a union of trajectories. It is also one dimensional, and trajectories with initial conditions in W^u approach the origin at an exponential rate as $t \to -\infty$.

Differentiability of the Unstable Manifold:

The local unstable manifold found by the graph transform is the graph of a Lipschitz function. However, the stable, unstable, and center manifold theorem for a fixed point states that if the vector field (or map) is C^r, then the unstable manifold should also be C^r (and our example is C^∞).

The procedure for showing that $y = \bar{h}(x)$ is C^1 is as follows. The fixed point of the graph transform satisfies (3.5.5). We formally differentiate (3.5.5) with respect to x_0 to obtain:

$$D\bar{h}\left(D_1 x + D_2 x\, D\bar{h}\right) = D_1 y + D_2 y\, D\bar{h},$$

or

$$D\bar{h} = \left(D_1 y + D_2 y\, D\bar{h}\right)\left(D_1 x + D_2 x\, D\bar{h}\right)^{-1}. \tag{3.5.14}$$

Here we are leaving out the arguments of all the functions in (3.5.5). The notation D denotes the derivative with respect to x_0, D_1 denotes the partial derivative with respect to x_0 and D_2 denotes the partial derivative with

respect to y_0. The phrase "formally differentiate' used above means to do exactly what we did to (3.5.5), which resulted in (3.5.14). We do not know that (3.5.14) has any meaning since it has not yet been shown that $\bar{h}(x)$ is differentiable.

Therefore we define the operator

$$\mathcal{H}v \equiv (D_1 y + D_2 y\, v)\,(D_1 x + D_2 x\, v)^{-1}, \tag{3.5.15}$$

where $v(\cdot)$ is the unknown function. Clearly, a fixed point of this operator is a solution of (3.5.14). We use contraction mapping techniques to show that $\mathcal{H}$ does have a fixed point. Then we show that this fixed point is actually the derivative of the fixed point of the graph transform. This will show that the fixed point of the graph transform is C^1. One then proceeds inductively to obtain higher order derivatives. The details can be found in Hartman [1964], Fenichel [1971], or Wiggins [1994].

This approach yields that the *local* unstable manifold is differentiable. What about the global unstable manifold defined in (3.5.13)? This will follow from Theorem 7.1.1 in Chapter 7 which says that the trajectories of a C^r vector field are C^r functions of the initial conditions. Since (3.5.13) is constructed by mapping the initial conditions of the local unstable manifold by the trajectories it will then follow that the global unstable manifold is C^r.

Application of the Liapunov-Perron Method

Now we develop the Liapunov-Perron method for proving the existence of the unstable manifold of the origin for the same example. The Liapunov-Perron method uses the integral equation form of the ordinary differential equation (3.5.1), since (3.5.1) can be equivalently written in the form:

$$\begin{aligned} x(t; x_0, y_0) &= x_0 e^t, \\ y(t; x_0, y_0) &= y_0 e^{-t} + e^{-t} \int_0^t e^{\tau} x^2(\tau; x_0, y_0) d\tau. \end{aligned} \tag{3.5.16}$$

Suppose the graph of a Lipschitz function $y = h(x)$, with $h(0) = 0$ and Lipschitz constant δ, is an invariant set for (3.5.1). Then $y(t; x_0, h(x_0)) = h(x(t; x_0, h(x_0)))$ is a solution of

$$\dot{y} = -y + x^2, \tag{3.5.17}$$

with $y(0; x_0, h(x_0)) = h(x_0)$. Using (3.5.16), (3.5.17) can be rewritten as

$$y(t; x_0, h(x_0)) = h(x_0)e^{-t} + e^{-t} \int_0^t e^{\tau} x^2(\tau; x_0, h(x_0)) d\tau, \tag{3.5.18}$$

or

$$h(x_0) = e^t y(t; x_0, h(x_0)) - \int_0^t e^{\tau} x^2(\tau; x_0, h(x_0)) d\tau. \tag{3.5.19}$$

Now

$$|y(t;x_0,h(x_0))| = |h(x(t;x_0,h(x_0)))| \leq \delta|x(t;x_0,h(x_0))| = \delta e^t|x_0|,$$

from which it follows that

$$\lim_{t\to-\infty} e^t y(t;x,h(x)) = 0.$$

Therefore, taking the limit as $t \to -\infty$ in (3.5.19) gives:

$$\begin{aligned} h(x_0) &= \int_{-\infty}^{0} e^{\tau}x^2(\tau;x_0,h(x_0))d\tau, \qquad (3.5.20)\\ &= \int_{-\infty}^{0} e^{\tau}x_0^2e^{2\tau}d\tau = \frac{x_0^2}{3}, \end{aligned}$$

which is exactly the unstable manifold of the origin. Conversely, one can show that if $h(x_0)$ satisfies (3.5.20), then the graph of $y = h(x)$ is invariant.

This motivates the following definition of the *Liapunov-Perron operator*:

$$\mathcal{P}h(x_0) = \int_{-\infty}^{0} e^{\tau}x^2(\tau;x_0,h(x_0))d\tau, \qquad (3.5.21)$$

which is defined on the complete metric space

$$S_\delta^0 \equiv \{\text{the set of functions,} \quad h(x), \text{where} \quad |h(x)-h(x')| \leq \delta|x-x'|, \; h(0)=0, \; |x| \leq \epsilon, \; \delta > 0\}, \qquad (3.5.22)$$

with metric derived from the following norm

$$\| \, h \, \| \equiv \sup_{|x|\leq\epsilon} |h(x)|.$$

By our construction, a fixed point of the Liapunov-Perron operator is the unstable manifold of the origin. We will show that the Liapunov- Perron operator is a contraction map on S_δ^0. As for the graph transform, several steps must be carried out in the course of establishing this fact. Of course, all of this is unneccessary for this example since we have already found the fixed point for the Liapunov- Perron operator, which is exactly the global unstable manifold of the origin. However, our goal here is to give a description of the method in general. With that in mind, we proceed accordingly.

$\mathcal{P}$ is Well-Defined:

This is obvious for this example from the form of (3.5.21).

$\mathcal{P} : S_\delta^0 \to S_\delta^0$:

Using (3.5.21) and the first equation of (3.5.16), we have

$$|\mathcal{P}h(x_0) - \mathcal{P}h(x_0')| \leq \frac{1}{3}|x_0 + x_0'|\,|x_0 - x_0'| \leq \frac{2\epsilon}{3}|x_0 - x_0'|, \tag{3.5.23}$$

so we need only choose ϵ small enough such that $\frac{2\epsilon}{3} \leq \delta$.

$\mathcal{P}$ is a Contraction Map on S_δ^0:

Using (3.5.21) and the first equation of (3.5.16), we have

$$|\mathcal{P}h_1(x_0) - \mathcal{P}h_2(x_0)| = 0, \tag{3.5.24}$$

So $\mathcal{P}$ is clearly a contraction map. By the contraction mapping theorem it therefore has a unique fixed point whose graph (by construction) is the invariant, local unstable manifold of the origin.

Once the existence of the local unstable manifold is established then it can be continued to a global unstable manifold in the same way as was done for the local unstable manifold obtained by the graph transform. It can also be shown that the unstable manifold is differentiable in a way that was similar to that described for the graph transform. That is, one formally differentiates the Lipaunov-Perron operator and derives equations that the derivatives must satisfy. Fixed point methods are then use to show that these equations have solutions, and that the solutions are indeed the derivatives. See Chicone [1999] for details.

Computing Invariant Manifolds using Taylor Expansions

Once we know the existence of a C^r invariant manifold we can use Taylor series methods to compute it. We will illustrate this in the context of example (3.5.1). Suppose the graph of $y = h(x)$ is an invariant manifold. Then

$$\dot{y} = Dh(x)\dot{x}, \tag{3.5.25}$$

or

$$Dh(x)\dot{x} - \dot{y} = 0. \tag{3.5.26}$$

Since $h(0) = 0$ (the invariant manifold passes through the fixed points at the origin) and $Dh(0) = 0$ (the invariant manifold is tangent to the unstable subspace of the origin, i.e., the x-axis), we can assume that $h(x)$ has the following form (provided the vector field is at least C^5, but our example is C^∞):

$$y = h(x) = ax^2 + bx^3 + cx^4 + \cdots. \tag{3.5.27}$$

Substituting the expression for $\dot{x}$ and $\dot{y}$ from (3.5.1) into (3.5.26) gives:

$$Dh(x)x - \left(-h(x) + x^2\right) = 0. \tag{3.5.28}$$

Substituting (3.5.27) into (3.5.28) gives

$$\left(2ax^2 + 3bx^3 + 4cx^4 + \mathcal{O}(5)\right) + ax^2 + bx^3 + cx^4 + \mathcal{O}(5) - x^2 = 0 \quad (3.5.29)$$

In order to solve this equation the coefficient multiplying each power of x must be zero. This implies:

$$\begin{array}{ll} x^2 \,:\, 2a + a - 1 = 0 & \Rightarrow a = \frac{1}{3} \\ x^3 \,:\, 3b + b = 0 & \Rightarrow b = 0 \\ x^4 \,:\, 4c + c = 0 & \Rightarrow c = 0 \end{array}$$

In fact, one easily sees that the coefficient on the nth order term, for any $n > 2$, must be zero. Hence we have

$$y = h(x) = \frac{x^2}{3}.$$

Simó [1990] and Beyn and Kless [1998] show how the Taylor method can be numerically implemented for computing invariant manifolds.

3.6 Time-Dependent Hyperbolic Trajectories and their Stable and Unstable Manifolds

In the previous sections we described the notion of hyperbolicity of a fixed point of an autonomous vector field, as well as the existence of stable, unstable, and center manifolds associated with a fixed point (a parallel theory for maps also exists, but at the moment we are considering the continuous time case of vector fields). All of these ideas and results were a result of the behavior of the vector field linearized about the fixed point. More precisely, they followed from the eigenvalue and generalized eigenspace structure of the *constant* matrix associated with the linearized vector field. Now we want to consider a general *time dependent* trajectory. What does it mean for such a trajectory to be hyperbolic? Does a hyperbolic trajectory have stable and unstable manifolds? These are questions that we now address.

We consider vector fields of the form

$$\dot{x} = f(x,t), \qquad x \in U \subset \mathbb{R}^n, \quad t \in \mathbb{R}, \tag{3.6.1}$$

where U is some open set in $\mathbb{R}^n$.

The basic existence and uniqueness results for particle trajectories to ordinary differential equations do not require very stringent requirements on the time dependence (these will be discussed in detail in Chapter 7) ; continuity in t is sufficient (see Hale [1980]). However, the dependence on x is more stringent. We describe this more precisely in the following assumption that will stand throughout this chapter, unless otherwise stated.

Regularity Assumptions

We assume that $f(x,t)$ is continuous in t, for all $t \in \mathbb{R}$, and C^r in x, $r \geq 1$. Moreover, all of the partial derivatives of $v(x,t)$, with respect to x, up to order r, are uniformly continuous and uniformly bounded in $K \times \mathbb{R}$, where K is an arbitrary, compact subset of U. These "regularity assumptions" on the velocity field will be sufficient for the invariant manifold theorems described below (Coddington and Levinson [1955], Hale [1980], or Yi [1993a,b]).

3.6A Hyperbolic Trajectories

We have seen that if the matrix associated with the linearization about a trajectory is time dependent, then the eigenvalues of this matrix need not give information about local stability of the trajectory. The appropriate notion for characterizing the local (linearized) behavior in this case is that of an *exponential dichotomy* (although Liapunov exponents are also relevant, which we will mention later), which we now define, and for which the standard reference is Coppel [1978].

Definition 3.6.1 (Exponential Dichotomy) *Consider the following linear ordinary differential equation with time dependent coefficients*

$$\dot{\xi} = A(t)\xi, \qquad \xi \in \mathbb{R}^n, \tag{3.6.2}$$

where $A(t)$ is a continuous function of $t \in \mathbb{R}$. Suppose $X(t)$ is the fundamental solution matrix *of (3.6.2), i.e., for any initial condition ξ_0, $\xi(t) = X(t)\xi_0$ is the solution of (3.6.2) passing through ξ_0 at $t = 0$, $X(0) = id$. Let $\| \cdot \|$ denote a norm on $\mathbb{R}^n$. Then (3.6.2) is said to possess an* exponential dichotomy *if there exists a projection operator P, $P^2 = P$, and constants K_1, K_2, λ_1, $\lambda_2 > 0$, such that*

$$\| X(t)PX^{-1}(\tau) \| \leq K_1 \exp\left(-\lambda_1(t-\tau)\right), \quad t \geq \tau, \tag{3.6.3}$$

$$\| X(t)\left(id - P\right)X^{-1}(\tau) \| \leq K_2 \exp\left(\lambda_2(t-\tau)\right), \quad t \leq \tau. \tag{3.6.4}$$

We now give a simple example of a linear autonomous vector field that illustrates this notion of exponential dichotomy. In this case we know that the eigenvalues of the matrix used to define the linear vector field give us information about the local stability. Therefore one can relate this notion with the new idea of an exponential dichotomy.

Example 3.6.1. Consider the following two dimensional, steady linear velocity field:

$$\begin{aligned} \dot{x} &= -\lambda x, \\ \dot{y} &= \lambda y, \qquad (x,y) \in \mathbb{R}^2, \qquad \lambda > 0. \end{aligned} \tag{3.6.5}$$

The fundamental solution matrix is given by

$$X(t) = \begin{pmatrix} e^{-\lambda t} & 0 \\ 0 & e^{\lambda t} \end{pmatrix} \tag{3.6.6}$$

and we take

$$P = \begin{pmatrix} 1\,0 \\ 0\,0 \end{pmatrix}.$$

(Clearly, $P^2 = P$.) Then we have

$$X(t)PX^{-1}(\tau) = \begin{pmatrix} e^{-\lambda(t-\tau)} & 0 \\ 0 & 0 \end{pmatrix},$$

and

$$X(t)\,(\mathrm{id} - P)\,X^{-1}(\tau) = \begin{pmatrix} 0 & 0 \\ 0 & e^{\lambda(t-\tau)} \end{pmatrix}.$$

We can take as a norm on the set of real 2×2 matrices the absolute value of the largest matrix element. In that case we see that the bounds given in (3.6.1) are obeyed for any $K_1 = K_2 > 1$.

End of Example 3.6.1

We now consider a less trivial time-dependent example.

Example 3.6.2.

Consider the following linear vector field with time-periodic coefficients that was earlier considered in Example 1.2.1:

$$\begin{pmatrix} \dot{x}_1 \\ \dot{x}_2 \end{pmatrix} = A(t) \begin{pmatrix} x_1 \\ x_2 \end{pmatrix},$$

where

$$A(t) = \begin{pmatrix} -1 + \frac{3}{2}\cos^2 t & 1 - \frac{3}{2}\cos t \sin t \\ -1 - \frac{3}{2}\cos t \sin t & -1 + \frac{3}{2}\sin^2 t \end{pmatrix}. \tag{3.6.7}$$

This is an example that we have seen earlier. The eigenvalues of $A(t)$ are found to be *independent of* t and are given by

$$\lambda_1(t) = \frac{-1 + i\sqrt{7}}{4}, \qquad \lambda_2(t) = \frac{-1 - i\sqrt{7}}{4}.$$

In particular, they have negative real parts *for all* t. However, one can verify that the following are two linearly independent solutions of this equation

$$v_1(t) = \begin{pmatrix} -\cos t \\ \sin t \end{pmatrix} e^{\frac{t}{2}}, \qquad v_2(t) = \begin{pmatrix} \sin t \\ \cos t \end{pmatrix} e^{-t}. \tag{3.6.8}$$

Therefore the fundamental solution matrix is given by:

$$X(t) = \begin{pmatrix} -e^{\frac{t}{2}}\cos t & e^{-t}\sin t \\ e^{\frac{t}{2}}\sin t & e^{-t}\cos t \end{pmatrix}, \tag{3.6.9}$$

with inverse

$$X^{-1}(\tau) = \begin{pmatrix} -e^{-\frac{\tau}{2}} \cos\tau & e^{-\frac{\tau}{2}} \sin\tau \\ e^{\tau} \sin\tau & e^{\tau} \cos\tau \end{pmatrix}. \tag{3.6.10}$$

We take as the projection operator:

$$P = \begin{pmatrix} 0 & 0 \\ 0 & 1 \end{pmatrix}. \tag{3.6.11}$$

Then we have

$$X(t)PX^{-1}(\tau) = \begin{pmatrix} e^{(\tau-t)} \sin\tau \sin t & e^{(\tau-t)} \cos\tau \sin t \\ e^{(\tau-t)} \sin\tau \cos t & e^{(\tau-t)} \cos\tau \cos t \end{pmatrix}, \tag{3.6.12}$$

from which it follows that

$$\| X(t)PX^{-1}(\tau) \| \leq e^{-(t-\tau)}, \qquad t \geq \tau, \tag{3.6.13}$$

where for a norm on the space of 2×2 matrices we have taken the maximum of the absolute value of the matrix elements.

Similarly, we have

$$X(t)\,(id - P)\,X^{-1}(\tau) = \begin{pmatrix} e^{\frac{1}{2}(-\tau+t)} \cos\tau \cos t & e^{\frac{1}{2}(-\tau+t)} \sin\tau \cos t \\ e^{\frac{1}{2}(-\tau+t)} \cos\tau \sin t & e^{\frac{1}{2}(-\tau+t)} \sin\tau \sin t \end{pmatrix}, \tag{3.6.14}$$

from which it follows that

$$\| X(t)\,(id - P)\,X^{-1}(\tau) \| \leq e^{\frac{1}{2}(t-\tau)}, \qquad t \leq \tau. \tag{3.6.15}$$

Taking $K_1 = K_2 = 1$ and $\lambda_1 = \lambda_2 = \frac{1}{2}$ we see from (3.6.1) that this equation has an exponential dichotomy.

We remark that this linear vector field is also interesting from the point of view that even though its coefficients are time periodic, it has no time dependent periodic solutions.

End of Example 3.6.2

With the notion of exponential dichotomy in hand we can now define the notion of a hyperbolic trajectory of a time dependent vector field.

Definition 3.6.2 (Hyperbolic Trajectory) *Let $\gamma(t)$ denote a trajectory of the vector field*

$$\dot{x} = f(x,t), \qquad x \in U \subset \mathbb{R}^n, \quad t \in \mathbb{R}, \tag{3.6.16}$$

where $U \subset \mathbb{R}^n$ is an open set, f is C^r, $r \geq 1$, in x, and continuous in t. Then $\gamma(t)$ is said to be a hyperbolic trajectory *if the associated linearized system*

$$\dot{\xi} = D_x f(\gamma(t), t)\xi, \tag{3.6.17}$$

has an exponential dichotomy.

We give a geometrical explanation of the notion of exponential dichotomy. For this, the picture is more easily understood in the *extended phase space*:

$$\mathcal{E} \equiv \{(x,t) \in \mathbb{R}^n \times \mathbb{R} \,|\, x \in U\}\,, \tag{3.6.18}$$

i.e., we append the dependent variable t to the phase space. We consider the velocity field defined on extended phase space by appending the (trivial) evolution of t to (3.6.16) as follows

$$\begin{aligned} \dot{x} &= f(x,t), \\ \dot{t} &= 1, \qquad\qquad x \in U \subset \mathbb{R}^n, \quad t \in \mathbb{R}, \end{aligned} \tag{3.6.19}$$

and the hyperbolic trajectory in the extended phase space $\mathcal{E}$ is denoted by

$$\Gamma(t) = (\gamma(t), t)\,. \tag{3.6.20}$$

We define a *time slice* of the extended phase space $\mathcal{E}$ as follows:

$$\Sigma_\tau \equiv \{(x,t) \in \mathcal{E} \,|\, t = \tau\}\,. \tag{3.6.21}$$

Then in the extended phase space the hyperbolic trajectory $\Gamma(t)$ intersects Σ_τ in the unique point $\gamma(\tau)$.

In Definition 3.6.1 suppose the projection operator P has rank k. Then (3.6.3) implies that on the phase slice Σ_τ, there is a k dimensional subspace of $\mathbb{R}^n$, $E^s(\tau)$, corresponding to trajectories of the linearized equations (3.6.17) that decay to zero at an exponential rate as $t \to \infty$. Similarly, (3.6.4) implies that on the phase slice Σ_τ, there is an $n-k$ dimensional subspace of $\mathbb{R}^n$, $E^u(\tau)$, corresponding to trajectories of the linearized equations (3.6.17) that decay to zero at an exponential rate as $t \to -\infty$. Moreover, the angle between $E^s(\tau)$ and $E^u(\tau)$ is bounded away from zero for all τ. We illustrate this geometrically in Fig. 3.6.1.

Next we examine how this situation carries over for the nonlinear equations.

3.6B Stable and Unstable Manifolds of Hyperbolic Trajectories

We can now state the result that says that tangent to these linearized eigenspaces we have invariant manifolds for the full nonlinear vector field.

Let $D_\rho(\tau) \in \Sigma_\tau$ denote the ball of radius ρ centered at $\gamma(\tau)$. Then

$$\mathcal{N}_\rho\left(\Gamma(t)\right) \equiv \cup_{\tau \in \mathbb{R}} \left(D_\rho(\tau), \tau\right),$$

is a *tubular neighborhood* of $\Gamma(t)$ in $\mathcal{E}$. We have the following theorem.

Theorem 3.6.3 (Local Stable and Unstable Manifolds) *For the set-up and hypotheses described above, there exists $k+1$ dimensional C^r manifold $W^s_{loc}(\Gamma(t)) \subset \mathcal{E}$, and an $n-k+1$ dimensional C^r manifold $W^u_{loc}(\Gamma(t)) \subset \mathcal{E}$ and ρ_0 sufficiently small such that for $\rho \in (0, \rho_0)$*

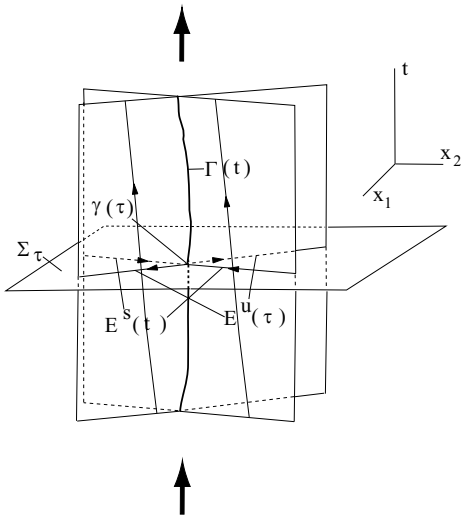

FIGURE 3.6.1. Geometry of the stable and unstable subspaces of the linearized system associated with the hyperbolic trajectory, both in the extended phase space and on a time slice, $n = 2$, $k = 1$. (The arrows are meant to indicate that the structure extends for all time.)

1. *$W^s_{loc}(\Gamma(t))$, the local stable manifold of $\Gamma(t)$, is invariant under the forward time evolution generated by (3.6.19), $W^u_{loc}(\Gamma(t))$, the local unstable manifold of $\Gamma(t)$, is invariant under the backward time evolution generated by (3.6.19).*

2. *$W^s_{loc}(\Gamma(t))$ and $W^u_{loc}(\Gamma(t))$ intersect along $\Gamma(t)$, and the angle between the manifolds is bounded away from zero uniformly for all $t \in \mathbb{R}$.*

3. *Every trajectory on $W^s_{loc}(\Gamma(t))$ can be continued to the boundary of $\mathcal{N}_\rho(\Gamma(t))$ in backward time, and every trajectory on $W^u_{loc}(\Gamma(t))$ can be continued to the boundary of $\mathcal{N}_\rho(\Gamma(t))$ in forward time.*

4. *Trajectories starting on $W^s_{loc}(\Gamma(t))$ at time $t = \tau$ approach $\Gamma(t)$ at an exponential rate $e^{-\lambda'(t-\tau)}$ as $t \to \infty$ and trajectories starting on $W^u_{loc}(\Gamma(t))$ at time $t = \tau$ approach $\Gamma(t)$ at an exponential rate $e^{-\lambda'|t-\tau|}$ as $t \to \infty$, for some constant $\lambda' > 0$.*

5. *Any trajectory in $\mathcal{N}_\rho(\Gamma(t))$* not *on either $W^s_{loc}(\Gamma(t))$ or $W^u_{loc}(\Gamma(t))$ will leave $\mathcal{N}_\rho(\Gamma(t))$ in both forward and backward time.*

Proof: In some sense this theorem has been known for some time, although the autonomous version is much more widely known. The theorem can be

obtained from simple modifications of results found in Coddington and Levinson [1955] and Hale [1980]. The theorem in this form can be found in the Ph. D. thesis of Kaper [1992], see also Yi [1993a,b]. A discrete time version can be found in Katok and Hasselblatt [1995]. For a different approach see Irwin [1973] and de Blasi and Schinas [1973]. □

The global stable and unstable manifolds, $W^s(\Gamma(t))$ and $W^u(\Gamma(t))$, are obtained in the usual way by evolving trajectories on $W^s_{loc}(\Gamma(t))$ and $W^u_{loc}(\Gamma(t))$ backward and forward in time, respectively. We illustrate this situation geometrically in Fig. 3.6.2.

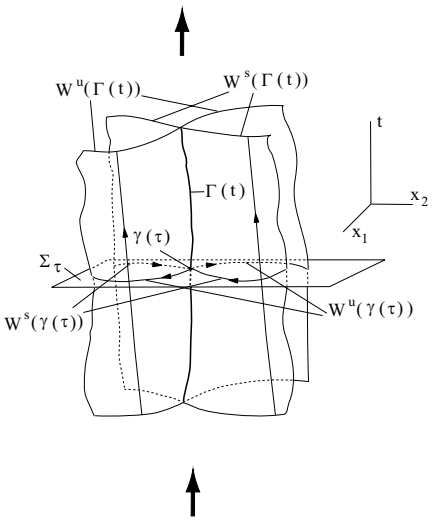

FIGURE 3.6.2. Geometry of the stable and unstable manifolds of the nonlinear system associated with the hyperbolic trajectory, both in the extended phase space and on a time slice. (The arrows are meant to indicate that the structure extends for all time.

Persistence of Hyperbolic Trajectories, and their Stable and Unstable Manifolds, Under Perturbation

We now want to consider what happens to this structure under perturbation. Consider the vector field

$$\begin{aligned} \dot{x} &= f(x,t;\epsilon), \\ \dot{t} &= 1, \qquad\qquad x \in U \subset \mathbb{R}^n, \quad t \in \mathbb{R}, \end{aligned} \tag{3.6.22}$$

where $\epsilon \in B_{\epsilon_0} \subset \mathbb{R}^p$ (with B_{ϵ_0} denoting the ball of radius ϵ_0 centered at 0), and

$$f(x,t;0) = f(x,t).$$

We assume that (3.6.22) depends upon the vector of parameters ϵ in a C^r manner, with all of the partial derivatives of $f(x,t,\epsilon)$, with respect to ϵ, up to order r, being uniformly continuous and uniformly bounded in $K \times \mathbb{R}$, where K is an arbitrary, compact subset of $\mathbb{R}^p$.

Theorem 3.6.4 (Persistence Under Perturbation) *Suppose that at $\epsilon = 0$ Theorem 3.6.3 holds for (3.6.22). Then there exists ϵ_0 sufficiently small such that for all $\epsilon \in B_{\epsilon_0}$ (3.6.22) possesses a hyperbolic trajectory $\Gamma_\epsilon(t)$, having a $k+1$ dimensional stable manifold, $W^s(\Gamma_\epsilon(t))$ and an $n-k+1$ dimensional unstable manifold, $W^u(\Gamma_\epsilon(t))$. These manifolds have the same properties as described in Theorem 3.6.3. Moreover, they depend on ϵ in a C^r manner.*

Proof: See Kaper [1992] or Yi [1993a,b]. □

An obvious question is how does one locate hyperbolic trajectories in vector fields having a general time dependence? Theorem 3.6.4 provides us with an easy way to do this if our problem is in the form of a time dependent perturbation of an autonomous vector field, i.e., consider a vector field of the form

$$\begin{aligned} \dot{x} &= f(x) + \epsilon g(x,t;\epsilon), \\ \dot{t} &= 1, \qquad\qquad x \in U \subset \mathbb{R}^n, \quad t \in \mathbb{R}. \end{aligned} \tag{3.6.23}$$

Suppose that for $\epsilon = 0$ the vector field $\dot{x} = v(x)$ has a hyperbolic fixed point. Then, by Theorem 3.6.4, for ϵ small this hyperbolic fixed point becomes a (generally) time varying hyperbolic trajectory with stable and unstable manifolds.

3.7 Invariant Manifolds in a Broader Context

In this chapter the invariant manifolds of interest have been the stable, unstable, and center manifolds of fixed points. Invariant manifold theory is a much broader and deeper subject and in this section we wish to describe some of the issues associated with invariant manifolds in a broader context.

Existence of Invariant Manifolds

Invariant manifold theory begins by *assuming* that some "basic" invariant manifold exists–the theory is then developed from this point onwards by building upon this basic invariant manifold. In particular, one is interested in the construction of stable, unstable, and center manifolds associated with these basic invariant manifolds. The types of basic invariant manifolds typically considered are:

1. Equilibrium points,

2. Periodic orbits,

3. Quasiperiodic or almost periodic orbits (invariant tori).

These manifolds all share an important property. Namely, they all admit a global coordinate description. In this case the dynamical system is typically subjected to a "preparatory" coordinate transformation that serves to localize the dynamical system about the invariant manifold. This amounts to deriving a normal form in the neighborhood of an invariant manifold and it greatly facilitates the various estimates that are required in the analysis. Sacker [1969], Fenichel [1971], and Hirsch, Pugh, and Shub [1977] were among the first to consider general invariant manifolds that are not described as graphs and required an atlas of local coordinate charts for their description. This is an important generalization since in recent years invariant manifolds that cannot be expressed globally as a graph have arisen in applications, see Wiggins [1990], Hoveijn [1992], and Haller and Wiggins [1996] for applications where invariant spheres arise.

The Persistence and Differentiability of Invariant Manifolds Under Perturbation

The question of whether or not an invariant manifold persists under perturbation and, if so, if it maintains, loses, or gains differentiabilty is also important. In considering these issues it is important to characterize the stability of the *unperturbed* invariant manifold. This is where the notion of *normal hyperbolicity* arises. Roughly speaking, a manifold is normally hyperbolic if, under the dynamics *linearized about the invariant manifold*, the growth rate of vectors transverse to the manifold dominates the growth rate of vectors tangent to the manifold. For equilibrium points, these growth rates can be characterized in terms of eigenvalues associated with the linearization at the equilibria that are not on the imaginary axis, for periodic orbits these growth rates can be characterized in terms of the Floquet multipliers associated with the linearization about the periodic orbit that are not on the unit circle, for invariant tori or more general invariant manifolds these growth rates can be characterized in terms of exponential dichotomies (see Coppel [1978] or Sacker and Sell [1974]) or by the notion of generalized Lyapunov type numbers (Fenichel [1971]), which is the approach that we will take in this book. A question of obvious importance for applications is how does one *compute* whether or not an invariant manifold is normally hyperbolic? The answer is not satisfactory. For equilibria, the problem involves finding the eigenvalues of a square matrix–an algebraic problem. For invariant manifolds on which the dynamics is nontrivial the issues are more complicated, and they are dealt with in this book. However, one important class of dynamical systems which may have nontrivial invariant manifolds on which the dynamics is also nontrivial are integrable Hamiltonian systems, see Wiggins [1988] for examples. Finally, we want to alert the reader

to an important characteristic of normal hyperbolicity that is of some importance for understanding the scope of possible applications. Namely, it is insensitive to the form of the dynamics on the invariant manifold, provided the dynamics transverse to the invariant manifold is dominant in the sense of normal hyperbolicity. Heuristically, one could think of the dynamics on the invariant manifold as being "slow" as compared to the "fast" dynamics off the invariant manifold. Hence, the dynamics on the invariant manifold could even be chaotic.

Characterizing growth rates in the fashion described above requires knowledge of the linearized dynamics near orbits on the invariant manifold as $t \to +\infty$ or $t \to -\infty$. Hence, if the invariant manifold has a boundary (which an equilibrium point, periodic orbit, or invariant torus *does not* have), then one must understand the nature of the dynamics at the boundary. Notions such as *overflowing invariance* or *inflowing invariance* are developed to handle this. Invariant manifolds with boundary arise very often in applications, see Wiggins [1988].

Behavior Near an Invariant Manifold–Stable, Unstable, and Center Manifolds

A "stable manifold theorem" asserts that the set of points that approach an invariant manifold at an exponential rate as $t \to +\infty$ is an invariant manifold in its own right. The exponential rate of approach is inherited from the linearized dynamics as the stable manifold is constructed as a graph over the linearized stable *subspace* or *subbundle*. An "unstable manifold theorem" asserts similar behavior in the limit as $t \to -\infty$. Obviously, one may have problems with both of these concepts if the invariant manifold has a boundary.

The notion of a center manifold is more subtle. For equilibrium points and periodic orbits a center manifold is an invariant manifold that is tangent to the linearized subspace corresponding to eigenvalues on the imaginary axis, and floquet multipliers on the unit circle, respectively. In contrast to the situation with stable and unstable manifolds, the asymptotic behavior of orbits in the nonlinear center manifold may be very different than the asymptotic behavior of orbits in the linearized center subspaces, under the linearized dynamics.

Questions related to persistence and differentiability of stable, unstable, and center manifolds also arise.

More Refined Behavior Near Invariant Manifolds–Foliations of Stable, Unstable, and Center Manifolds

One may be interested in which orbits in the stable manifold approach the invariant manifold at a specified *rate*. Under certain conditions these orbits may lie on submanifolds of the stable manifold which are not invariant, but make up an invariant family of submanifolds that *foliate* the

stable manifold. A similar situation may hold for the unstable manifold. Moreover, this foliation has the property that points in a *fiber* of the foliation asymptotically approach the trajectory in the invariant manifold that passes through the point of intersection of the fiber with the invariant manifold (the *basepoint* of the fiber). This is a generalization of the notion of *asymptotic phase*, that is familiar from studies of stability of periodic orbits, to arbitrary invariant manifolds. In recent years these foliations have seen many uses in applications. Fenichel [1979] has used them in his development of geometric singular perturbation theory. Kovačič and Wiggins [1992], Haller and Wiggins [1993], [1995], and McLaughlin *et al.* [1996] have used them in the development of new global perturbation methods. Finally, the recent monograph of Kirchgraber and Palmer [1990] proves a number of foliation results and shows how these can be used as coordinates in which the dynamical system becomes linear.

Invariant Manifolds for Stochastic Dynamical Systems

Invariant manifold theory for stochastic, or random dynamical systems is currently being developed. See Arnold [1998], Boxler [1989], [1991] and Schmalfuss [1998].

3.8 Exercises

1. Prove that the boundary, closure, interior, and complement of an invariant set are invariant.

2. Prove that the closure and interior of a positively invariant set are positively invariant.

3. Prove that the complement of a positively invariant set is negatively invariant.

4. Prove that the union and intersection of a family of invariant (resp. positively invariant) sets are invariant (resp. positively invariant).

5. Let $x \mapsto f(x), \quad x \in \mathbb{R}^n$, be a diffeomorphism and suppose $x = 0$ is a fixed point, i.e., $f(0) = 0$. We define the *stable set* of $x = 0$ as:

$$\mathcal{S} \equiv \left\{ y \in \mathbb{R}^n \mid f^n(y) \to 0, \text{ as } n \to \infty \right\}.$$

   Is $\mathcal{S}$ a manifold? (Be careful here, see McGehee [1973].)

6. Consider the linear vector field $\dot{x} = Ax$, A a constant matrix.

   (a) Verify that $x(t) = e^{At}x_0$ is a trajectory of this vector field passing through the point x_0 at $t = 0$.

   (b) Prove uniqueness of solutions, i.e., verify that this is the only solution passing through x_0 at $t = 0$.

   (c) Describe the dependence of trajectories on initial conditions and time (e.g., continuous, C^r, analytic, etc.).

   (d) Suppose A depends on parameters., i.e., $A = A(\mu)$. Describe the dependence of the solutions on parameters in terms of the parameter dependence of A (e.g., continuous, C^r, analytic, etc.).

   (e) Show that $x(t + \tau) = e^{A(t+\tau)}x_0$ is also a solution, for any $\tau \in \mathbb{R}$. Does this violate uniqueness of solutions?

(f) Prove that two different trajectories cannot intersect.

7. Prove that for any fixed t, the map

$$\begin{aligned}\phi_t \equiv e^{At} \,:\, \mathbb{R}^n &\to \mathbb{R}^n,\\ x &\mapsto \phi_t(x) \equiv e^{At}x,\end{aligned}$$

defines a diffeomorphism of $\mathbb{R}^n$ into $\mathbb{R}^n$.

8. Prove that $\phi_t(x) \equiv e^{At}x$ satisfies the following properties:

   (a) $\phi_0(x) = x$,
   (b) $\phi_{-t} \circ \phi_t(x) = x$,
   (c) $\phi_t \circ \phi_s(x) = \phi_{t+s}(x)$,

   for all $t \in \mathbb{R}$, $x \in \mathbb{R}^n$. A one-parameter family of diffeomorphisms satisfying these three properties is said to be a *flow*, and we say that the solutions of the vector field $\dot{x} = Ax$ define a flow on the phase space.

9. Prove that

$$V(A, \lambda_{\alpha,\gamma}) \equiv \text{Ker } (A - \lambda_{\alpha,\gamma}\,\text{id})^{n_{\alpha,\gamma}}, \qquad \alpha = s, u, c, \quad \gamma = i, k, m,$$

   is an invariant (under A) subspace of $\mathbb{R}^n$. Prove that it is also invariant under e^{At}.

10. Prove that $F_{\mathbb{R}}$ is a real vector space.

11. Prove that $E_{\mathbb{C}}$ is a complex subspace of $\mathbb{C}^n$.

12. Prove that $(E_{\mathbb{C}})_{\mathbb{R}} = E$.

13. Suppose $E \subset \mathbb{R}^n$ is a subspace with basis

$$\{e_1, \ldots, e_k\} \equiv e,$$

    and

$$A \,:\, E \to E,$$

    is a real linear map.

    (a) Prove that e is also a basis for $E_{\mathbb{C}}$.
    (b) Prove that the matrix representation of A with respect to e is the same as the matrix representation of $A_{\mathbb{C}}$ with respect to e.

14. Let E be a real vector space and A a linear map of E into E. Show that

    (a) $(\text{Ker})_{\mathbb{C}} = \text{Ker } (A_{\mathbb{C}})$,
    (b) $(\text{Im } A)_{\mathbb{C}} = \text{Im } (A_{\mathbb{C}})$,
    (c) $\left(A^{-1}\right)_{\mathbb{C}} = (A_{\mathbb{C}})^{-1}$, if A is invertible.

    In this exercise Ker denotes the kernel and Im denotes the image, or range.

15. Suppose $A \,:\, E \to E$ is a real linear map. Show that A and $A_{\mathbb{C}}$ have the same characteristic polynomial.

16. Prove that

$$V(A, \mu_{\alpha,\gamma}, \bar{\mu}_{\alpha,\gamma}),$$

    is an invariant (under A) subspace of $\mathbb{R}^n$. Prove that it is also invariant under e^{At}.

17. Prove that E^s, E^u, and E^c, defined in (3.1.6), (3.1.7), and (3.1.8), respectively, are each invariant under e^{At}.

    (a) Prove that trajectories with initial conditions in E^s approach zero at an exponential rate as $t \to \infty$.

    (b) Prove that trajectories with initial conditions in E^u approach zero at an exponential rate as $t \to -\infty$.

18. What can one say about trajectories with initial conditions in E^c under the following conditions on the eigenvalues:

    (a) there are no repeated eigenvalues,

    (b) there are no zero eigenvalues,

    (c) there are no zero eigenvalues, and no repeated eigenvalues.

19. Suppose that $E^c = \emptyset$. Prove that the only trajectories starting in a neighborhood of the origin that remain in that neighborhood for all time are those that start on E^s.

20. **The Variation of Constants Formula**. Consider the following *inhomogeneous* linear ordinary differential equation:

$$\dot{x} = Ax + g(t), \qquad x \in \mathbb{R}^n,$$

    where A is an $n \times n$-matrix of real numbers. Verify that the solution of this equation passing through x_0 at $t = 0$ is given by

$$x(t) = e^{At} \int_0^t e^{-As} g(s) ds + e^{At} x_0.$$

    Prove that this solution is unique. What conditions on $g(t)$ are required for this unique solution to exist?

21. Consider the block diagonal form of the linear vector field given in (3.2.5). Relate this block diagonal form of the vector field to the decomposition of the phase space as $\mathbb{R}^n = E^s \oplus E^u \oplus E^c$.

22. Consider the following linear vector fields on $\mathbb{R}^2$.

a) $\begin{pmatrix} \dot{x}_1 \\ \dot{x}_2 \end{pmatrix} = \begin{pmatrix} \lambda & 0 \\ 0 & \mu \end{pmatrix} \begin{pmatrix} x_1 \\ x_2 \end{pmatrix}, \qquad \begin{matrix} \lambda < 0 \\ \mu > 0 \end{matrix}.$

b) $\begin{pmatrix} \dot{x}_1 \\ \dot{x}_2 \end{pmatrix} = \begin{pmatrix} \lambda & 0 \\ 0 & \mu \end{pmatrix} \begin{pmatrix} x_1 \\ x_2 \end{pmatrix}, \qquad \begin{matrix} \lambda < 0 \\ \mu < 0 \end{matrix}.$

c) $\begin{pmatrix} \dot{x}_1 \\ \dot{x}_2 \end{pmatrix} = \begin{pmatrix} \lambda & -\omega \\ \omega & \lambda \end{pmatrix} \begin{pmatrix} x_1 \\ x_2 \end{pmatrix}, \qquad \begin{matrix} \lambda < 0 \\ \omega > 0 \end{matrix}.$

d) $\begin{pmatrix} \dot{x}_1 \\ \dot{x}_2 \end{pmatrix} = \begin{pmatrix} 0 & 0 \\ 0 & \lambda \end{pmatrix} \begin{pmatrix} x_1 \\ x_2 \end{pmatrix}, \qquad \lambda < 0.$

e) $\begin{pmatrix} \dot{x}_1 \\ \dot{x}_2 \end{pmatrix} = \begin{pmatrix} 0 & \lambda \\ 0 & 0 \end{pmatrix} \begin{pmatrix} x_1 \\ x_2 \end{pmatrix}, \qquad \lambda > 0.$

f) $\begin{pmatrix} \dot{x}_1 \\ \dot{x}_2 \end{pmatrix} = \begin{pmatrix} 0 & 0 \\ 0 & 0 \end{pmatrix} \begin{pmatrix} x_1 \\ x_2 \end{pmatrix}.$

    i. For each vector field compute all trajectories and illustrate them graphically on the phase plane. Describe the stable, unstable, and center manifolds of the origin.

    ii. For vector field a), discuss the cases $|\lambda| < \mu$, $|\lambda| = \mu$, and $|\lambda| > \mu$. What are the qualitative and quantitative differences in the dynamics for these three cases? Can the unstable manifold of the origin be considered an attracting set and/or an attractor and do the relative magnitudes of the eigenvalues affect these conclusions?

iii. For vector field b), discuss the cases $\lambda < \mu$, $\lambda = \mu$, $\lambda > \mu$. What are the qualitative and quantitative differences in the dynamics for these three cases? Describe all zero- and one-dimensional invariant manifolds for this vector field. Describe the nature of the trajectories at the origin. In particular, which trajectories are tangent to either the x_1 or x_2 axis?

iv. In vector field c), describe how the trajectories depend on the relative magnitudes of λ and ω. What happens when $\lambda = 0$? When $\omega = 0$?

v. Describe the effect of linear perturbations on each of the vector fields.

vi. Describe the effect *near the origin* of nonlinear perturbations on each of the vector fields. Can you say anything about the effects of nonlinear perturbations on the dynamics outside of a neighborhood of the origin?

We remark that vi) is a difficult problem for the nonhyperbolic fixed points. We will study this situation in great detail when we develop center manifold theory and bifurcation theory.

23. Give a characterization of the stable, unstable, and center subspaces for linear maps in terms of generalized eigenspaces along the same lines as we did for linear vector fields according to the formulae (3.1.6), (3.1.7), and (3.1.8).

24. For the following linear vector fields find the general solution, and compute the stable, unstable, and center subspaces and plot them in the phase space.

a) $\begin{pmatrix} \dot{x}_1 \\ \dot{x}_2 \end{pmatrix} = \begin{pmatrix} 1 & 2 \\ 3 & 2 \end{pmatrix} \begin{pmatrix} x_1 \\ x_2 \end{pmatrix}$

b) $\begin{pmatrix} \dot{x}_1 \\ \dot{x}_2 \\ \dot{x}_3 \end{pmatrix} = \begin{pmatrix} 3 & 0 & 0 \\ 0 & 2 & -5 \\ 0 & 1 & -2 \end{pmatrix} \begin{pmatrix} x_1 \\ x_2 \\ x_3 \end{pmatrix}$

c) $\begin{pmatrix} \dot{x}_1 \\ \dot{x}_2 \\ \dot{x}_3 \end{pmatrix} = \begin{pmatrix} 1 & -3 & 3 \\ 3 & -5 & 3 \\ 6 & -6 & 4 \end{pmatrix} \begin{pmatrix} x_1 \\ x_2 \\ x_3 \end{pmatrix}$

d) $\begin{pmatrix} \dot{x}_1 \\ \dot{x}_2 \\ \dot{x}_3 \end{pmatrix} = \begin{pmatrix} -3 & 1 & -1 \\ -7 & 5 & -1 \\ -6 & 6 & -2 \end{pmatrix} \begin{pmatrix} x_1 \\ x_2 \\ x_3 \end{pmatrix}$

e) $\begin{pmatrix} \dot{x}_1 \\ \dot{x}_2 \\ \dot{x}_3 \end{pmatrix} = \begin{pmatrix} 1 & 0 & 0 \\ 1 & 2 & 0 \\ 1 & 0 & -1 \end{pmatrix} \begin{pmatrix} x_1 \\ x_2 \\ x_3 \end{pmatrix}$

f) $\begin{pmatrix} \dot{x}_1 \\ \dot{x}_2 \\ \dot{x}_3 \end{pmatrix} = \begin{pmatrix} 1 & 0 & 1 \\ 0 & 0 & -2 \\ 0 & 1 & 0 \end{pmatrix} \begin{pmatrix} x_1 \\ x_2 \\ x_3 \end{pmatrix}$

g) $\begin{pmatrix} \dot{x}_1 \\ \dot{x}_2 \\ \dot{x}_3 \end{pmatrix} = \begin{pmatrix} 0 & 0 & 15 \\ 1 & 0 & -17 \\ 0 & 1 & 7 \end{pmatrix} \begin{pmatrix} x_1 \\ x_2 \\ x_3 \end{pmatrix}$

h) $\begin{pmatrix} \dot{x}_1 \\ \dot{x}_2 \\ \dot{x}_3 \end{pmatrix} = \begin{pmatrix} 0 & 0 & 1 \\ 0 & 1 & 2 \\ 0 & 3 & 2 \end{pmatrix} \begin{pmatrix} x_1 \\ x_2 \\ x_3 \end{pmatrix}$

25. Consider the following linear maps on $\mathbb{R}^2$.

a) $\begin{pmatrix} x_1 \\ x_2 \end{pmatrix} \mapsto \begin{pmatrix} \lambda & 0 \\ 0 & \mu \end{pmatrix} \begin{pmatrix} x_1 \\ x_2 \end{pmatrix}, \qquad \begin{matrix} |\lambda| < 1 \\ |\mu| > 1 \end{matrix}.$

b) $\begin{pmatrix} x_1 \\ x_2 \end{pmatrix} \mapsto \begin{pmatrix} \lambda & 0 \\ 0 & \mu \end{pmatrix} \begin{pmatrix} x_1 \\ x_2 \end{pmatrix}, \qquad \begin{matrix} |\lambda| < 1 \\ |\mu| < 1 \end{matrix}.$

c) $\begin{pmatrix} x_1 \\ x_2 \end{pmatrix} \mapsto \begin{pmatrix} \lambda & -\omega \\ \omega & \lambda \end{pmatrix} \begin{pmatrix} x_1 \\ x_2 \end{pmatrix}, \qquad \omega > 0.$

d) $\begin{pmatrix} x_1 \\ x_2 \end{pmatrix} \mapsto \begin{pmatrix} 1 & 0 \\ 0 & \lambda \end{pmatrix} \begin{pmatrix} x_1 \\ x_2 \end{pmatrix}, \qquad |\lambda| < 1.$

e) $\begin{pmatrix} x_1 \\ x_2 \end{pmatrix} \mapsto \begin{pmatrix} 1 & \lambda \\ 0 & 1 \end{pmatrix} \begin{pmatrix} x_1 \\ x_2 \end{pmatrix}, \qquad \lambda > 0.$

f) $\begin{pmatrix} x_1 \\ x_2 \end{pmatrix} \mapsto \begin{pmatrix} 1 & 0 \\ 0 & 1 \end{pmatrix} \begin{pmatrix} x_1 \\ x_2 \end{pmatrix}.$

i. For each map compute all the orbits and illustrate them graphically on the phase plane. Describe the stable, unstable, and center manifolds of the origin.

ii. For map a), discuss the cases $\lambda, \mu > 0$; $\lambda = 0$, $\mu > 0$; $\lambda, \mu < 0$; and $\lambda < 0$, $\mu > 0$. What are the qualitative differences in the dynamics for these four cases? Discuss how the orbits depend on the relative magnitudes of the eigenvalues. Discuss the attracting nature of the unstable manifold of the origin and its dependence on the relative magnitudes of the eigenvalues.

iii. For map b), discuss the cases $\lambda, \mu > 0$; $\lambda = 0$, $\mu > 0$; $\lambda, \mu < 0$; and $\lambda < 0$, $\mu > 0$. What are the qualitative differences in the dynamics for these four cases? Describe all zero- and one-dimensional invariant manifolds for this map. Do all orbits lie on invariant manifolds?

iv. For map c), consider the cases $\lambda^2 + \omega^2 < 1$, $\lambda^2 + \omega^2 > 1$, and $\lambda + i\omega = e^{i\alpha}$ for α rational and α irrational. Describe the qualitative differences in the dynamics for these four cases.

v. Describe the effect of linear perturbations on each of the maps.

vi. Describe the effect *near the origin* of nonlinear perturbations on each of the maps. Can you say anything about the effects of nonlinear perturbations on the dynamics outside of a neighborhood of the origin?

We remark that vi) is very difficult for nonhyperbolic fixed points (more so than the analogous case for vector fields in the previous exercise) and will be treated in great detail when we develop center manifold theory and bifurcation theory.

26. Consider the following vector fields.

a) $\begin{aligned} \dot{x} &= y, \\ \dot{y} &= -\delta y - \mu x, \end{aligned} \qquad (x, y) \in \mathbb{R}^2.$

b) $\begin{aligned} \dot{x} &= y, \\ \dot{y} &= -\delta y - \mu x - x^2, \end{aligned} \qquad (x, y) \in \mathbb{R}^2.$

c) $\begin{aligned} \dot{x} &= y, \\ \dot{y} &= -\delta y - \mu x - x^3, \end{aligned} \qquad (x, y) \in \mathbb{R}^2.$

d) $\begin{aligned} \dot{x} &= -\delta x - \mu y + xy, \\ \dot{y} &= \mu x - \delta y + \tfrac{1}{2}(x^2 - y^2), \end{aligned} \qquad (x, y) \in \mathbb{R}^2.$

e) $\begin{aligned} \dot{x} &= -x + x^3, \\ \dot{y} &= x + y, \end{aligned} \qquad (x, y) \in \mathbb{R}^2.$

f) $\begin{aligned} \dot{r} &= r(1 - r^2), \\ \dot{\theta} &= \cos 4\theta, \end{aligned} \qquad (r, \theta) \in \mathbb{R}^+ \times S^1.$

g) $\begin{aligned} \dot{r} &= r(\delta + \mu r^2 - r^4), \\ \dot{\theta} &= 1 - r^2, \end{aligned} \qquad (r, \theta) \in \mathbb{R}^+ \times S^1.$

h) $\begin{aligned} \dot{\theta} &= v, \\ \dot{v} &= -\sin\theta - \delta v + \mu, \end{aligned} \qquad (\theta, v) \in S^1 \times \mathbb{R}.$

i) $\begin{aligned} \dot{\theta}_1 &= \omega_1, \\ \dot{\theta}_2 &= \omega_2 + \theta_1^n, \ n \geq 1, \end{aligned} \qquad (\theta_1, \theta_2) \in S^1 \times S^1.$

j) $\begin{aligned} \dot{\theta}_1 &= \theta_2 - \sin\theta_1, \\ \dot{\theta}_2 &= -\theta_2, \end{aligned} \qquad (\theta_1, \theta_2) \in S^1 \times S^1.$

k) $\begin{aligned} \dot{\theta}_1 &= \theta_1^2, \\ \dot{\theta}_2 &= \omega_2, \end{aligned} \qquad (\theta_1, \theta_2) \in S^1 \times S^1.$

Describe the nature of the stable and unstable manifolds of the fixed points by drawing phase portraits. Can you determine anything about the global behavior of the manifolds?

In a), b), c), d), g), and h) consider the cases $\delta < 0$, $\delta = 0$, $\delta > 0$, $\mu < 0$, $\mu = 0$, and $\mu > 0$. In i) and k) consider $\omega_1 > 0$ and $\omega_2 > 0$.

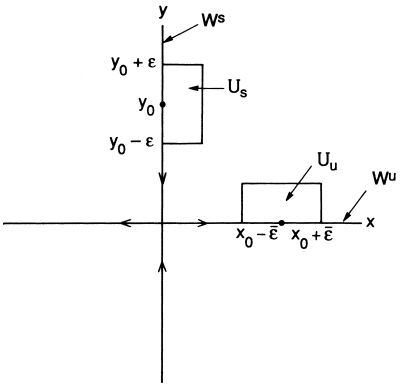

FIGURE 3.8.1.

27. Consider the following maps.

a) $\begin{aligned} x &\mapsto x, \\ y &\mapsto x + y, \end{aligned} \qquad (x, y) \in \mathbb{R}^2.$

b) $\begin{aligned} x &\mapsto x^2, \\ y &\mapsto x + y, \end{aligned} \qquad (x, y) \in \mathbb{R}^2.$

c) $\begin{aligned} \theta_1 &\mapsto \theta_1, \\ \theta_2 &\mapsto \theta_1 + \theta_2, \end{aligned} \qquad (\theta_1, \theta_2) \in S^1 \times S^1.$

d) $\begin{aligned} \theta_1 &\mapsto \sin\theta_1, \\ \theta_2 &\mapsto \theta_1, \end{aligned} \qquad (\theta_1, \theta_2) \in S^1 \times S^1.$

e) $\begin{aligned} x &\mapsto \tfrac{2xy}{x+y}, \\ y &\mapsto \left(\tfrac{2xy^2}{x+y}\right)^{1/2}, \end{aligned} \qquad (x, y) \in \mathbb{R}^2.$

f) $\begin{aligned} x &\mapsto \tfrac{x+y}{2}, \\ y &\mapsto (xy)^{1/2}, \end{aligned} \qquad (x, y) \in \mathbb{R}^2.$

g) $\begin{aligned} x &\mapsto \mu - \delta y - x^2, \\ y &\mapsto x, \end{aligned} \qquad (x, y) \in \mathbb{R}^2.$

h) $\begin{aligned} \theta &\mapsto \theta + v, \\ v &\mapsto \delta v - \mu\cos(\theta + v), \end{aligned} \qquad (\theta, v) \in S^1 \times \mathbb{R}^1.$

Describe the nature of the stable and unstable manifolds of the fixed points by drawing phase portraits. Can you determine any global behavior? Describe the nature of the In g) and h) consider the cases $\delta < 0$, $\delta = 0$, $\delta > 0$, $\mu < 0$, $\mu = 0$, and $\mu > 0$.

28. Consider the vector field

$$\begin{aligned} \dot{x} &= x, \\ \dot{y} &= -y, \qquad (x, y) \in \mathbb{R}^2. \end{aligned}$$

(see Fig. 3.8.1).

The origin is a hyperbolic fixed point with stable and unstable manifolds given by

$$W^s(0,0) = \Big\{(x, y) \,|\, x = 0\Big\}, \quad W^u(0,0) = \Big\{(x, y) \,|\, y = 0\Big\}.$$

Let

$$\begin{aligned} U_s &= \Big\{(x, y) \,|\, |y - y_0| \le \varepsilon, 0 \le x \le \varepsilon, \text{for some } \varepsilon > 0\Big\}, \\ U_u &= \Big\{(x, y) \,|\, |x - x_0| \le \bar{\varepsilon}, 0 \le y \le \bar{\varepsilon}, \text{for some } \bar{\varepsilon} > 0\Big\}; \end{aligned}$$

Show that you can find smaller closed sets $\tilde{U}_s \subset U_s$, $\tilde{U}_u \subset U_u$, such that $\tilde{U}_s$ maps onto $\tilde{U}_u$ under the time T flow map (T must be chosen carefully; it depends on the size of the $\tilde{U}_s$, $\tilde{U}_u$) *and* such that horizontal and vertical boundaries of $\tilde{U}_s$ correspond to horizontal and vertical boundaries of $\tilde{U}_u$. How would this problem be formulated and solved for maps?

(Note: This seemingly silly exercise is important for the understanding of chaotic invariant sets. We will use it later when we study the orbit structure near homoclinic orbits.)

29. Consider the vector field

$$\begin{aligned} \dot{x} &= -x + y^2, \\ \dot{y} &= -2x^2 + 2xy^2, \qquad (x, y) \in \mathbb{R}^2. \end{aligned}$$

(a) Show that $y = x^2$ is an invariant manifold.

(b) Show that there is a trajectory connecting the equilibrium points $(0, 0)$ and $(1, 1)$.

(c) Is $y = x^2$ the center manifold of the origin?

30. Consider the vector field

$$\begin{aligned} \dot{x} &= -x, \\ \dot{y} &= 2y - 5x^3, \qquad (x, y) \in \mathbb{R}^2. \end{aligned}$$

(a) Show that $y = x^3$ is an invariant manifold.

(b) Determine the global stable and unstable manifolds of the origin.

31. Consider a map

$$\begin{aligned} x &\mapsto f(x, y), \\ y &\mapsto g(x, y), \qquad (x, y) \in \mathbb{R}^n \times \mathbb{R}^m. \end{aligned}$$

Suppose the graph of $y = h(x)$ is an invariant manifold for this map. Derive the "tangency condition" for discrete time systems that is analogous to (3.2.7) for continuous time systems. How differentiable must the map be for the condition to hold?

32. Consider the map

$$\begin{aligned} x &\mapsto y^2, \\ y &\mapsto 2y - 2x^2 + x^4 y^2, \qquad (x, y) \in \mathbb{R}^2. \end{aligned}$$

(a) Is the map a diffeomorphism?

(b) Show that $y = x^2$ is an invariant manifold.

(c) Show that $(0, 0)$ and $(1, 1)$ are fixed points.

(d) Does there exist heteroclinic orbits between these fixed points?

33. Consider the graph transform proof of the existence of the local unstable manifold of the origin for (3.5.1).

(a) Show that S_δ is a complete metric space.

(b) The graph of $\bar{h}(x)$, $|x| \leq \epsilon$, was shown to be locally invariant for a fixed $t > 0$. Show that it is locally invariant for $t' \neq t$.

(c) Show that trajectories starting on the graph of $\bar{h}(x)$, $|x| \leq \epsilon$ decay to the origin at an exponential rate as $t \to -\infty$.

(d) Show that the global unstable manifold defined in (3.5.13) is invariant and one dimensional.

(e) Show that $\bar{h}(x)$, $|x| \leq \epsilon$ is C^1.

34. Consider the Liapunov-Perron proof of the existence of the local unstable manifold of the origin for (3.5.1).

    (a) Show that S^0_δ is a complete metric space.

    (b) Show that if $h(x_0)$ satisfies (3.5.20), then the graph of $h(x)$ is invariant.

    (c) Show that trajectories starting on the graph of $\bar{h}(x)$, $|x| \leq \epsilon$ decay to the origin at an exponential rate as $t \to -\infty$.

    (d) Show that unstable manifold found by this method is C^1.

35. Show that the conditions (3.6.3) and (3.6.4) in the definition of exponential dichotomy can be written in the equivalent form

$$\begin{aligned} \| X(t)Px \| &\leq K_1' \exp\left(-\lambda_1(t-\tau)\right) \| X(\tau)Px \|, \quad t \geq \tau, \\ \| X(t)\left(\mathrm{id} - P\right)x \| &\leq K_2' \exp\left(\lambda_2(t-\tau)\right) \| X(\tau)\left(\mathrm{id} - P\right)x \|, \quad t \leq \tau, \\ \| X(t)PX^{-1}(t) \| &\leq K_3', \quad \text{for all } t, \end{aligned}$$

    for constants K_1', K_2', $K_3' > 0$ and any x.

    Show that the stable subspace $E^s(\tau)$ is given by $X(\tau)Px$ for all x at time τ, and that the first of these conditions describes its evolution for $t > \tau$. Similarly, show that the second condition implies that there is a time-dependent, subspace $(E^u(\tau))$ of solutions that decay to zero at an exponential rate as $t \to -\infty$ and that it is given by $X(\tau)(\mathrm{id} - P)x$ for all x at time τ, and the second condition describes its evolution for $t < \tau$. Show that the third condition implies that the angle between these two subspaces stays bounded away from zero for all time.

36. In Example 3.6.2 compute and plot the time dependent stable and unstable subspaces in the extended phase space. Do they have any periodicity (in time) properties?

37. Consider the following linear, time dependent vector field:

$$\begin{aligned} \dot{x} &= -x + t, \\ \dot{y} &= y - x, \qquad (x, y) \in \mathbb{R}^2. \end{aligned} \tag{3.8.1}$$

    (a) Show that the general solution through an arbitrary point (x_0, y_0) at $t = 0$ is given by

$$\begin{aligned} x(t) &= t - 1 + e^{-t}\left(x_0 + 1\right), \\ y(t) &= t + e^{t}\left(y_0 + 2\right) + \frac{1}{2}\left(e^{-t} - e^{t}\right)\left(x_0 + 1\right). \end{aligned}$$

    (b) Show that the trajectory $(x(t), y(t)) = (t-1, t)$ has an exponential dichotomy.

    (c) Compute and plot the stable and unstable manifolds of the trajectory $(x(t), y(t)) = (t-1, t)$ in the extended phase space.

38. Consider the following vector field:

$$\begin{aligned} \dot{x} &= x, \\ \dot{y} &= -y + x^2\left(\frac{1}{3}\dot{a}(t) + a(t)\right), \end{aligned}$$

    where $a(t)$ is an arbitrary time dependent function.

    (a) Show that the origin is a hyperbolic trajectory.

    (b) Argue that the graph of $y = \frac{a(t)}{3}x^2$ is the global unstable manifold of the origin.

    What requirements must be made on the function $a(t)$ in order that these conclusions are true?

39. Consider the following modification of (3.5.1):

$$\begin{aligned} \dot{x} &= a(t)x, \\ \dot{y} &= -b(t)y + x^2, \end{aligned} \tag{3.8.2}$$

where

$$a(t),\ b(t) \geq \lambda > 0, \forall t,$$

where λ is a constant.

(a) Is the origin a trajectory of (3.8.2)?

(b) Consider (3.8.2) linearized about the origin. Discuss the stable and unstable subspaces associated with the origin and the nature of trajectories in these subspaces.

(c) Use the Liapunov-Perron method to show that the origin has a (time dependent) unstable manifold.

(d) Use the graph transform method to show that the origin has a time dependent unstable manifold.

4

Periodic Orbits

In this chapter we will describe a very important type of orbit for vector fields and maps: periodic orbits. In a certain sense, periodic orbits are the only types of orbits that we can ever hope to understand completely throughout their evolution from the distant past (i.e. as $t \to -\infty$) to the distant future (i.e., as $t \to \infty$) since the entire course of their evolution is determined by knowledge over a *finite* time interval, i.e., the period[1]. For this reason it is very tempting, and often quite advantageous, to try to understand the key features of a dynamical system in terms of the periodic orbits. We will discuss this a bit more at the end of this chapter. But now we begin with a definition.

We consider vector fields

$$\dot{x} = f(x,t), \qquad x \in \mathbb{R}^n, \tag{4.0.1}$$

and maps

$$x \mapsto g(x), \qquad x \in \mathbb{R}^n. \tag{4.0.2}$$

Definition 4.0.1 (Periodic Orbits) *(*Vector Fields*) A solution of (4.0.1) through the point x_0 is said to be* periodic of period T *if there exists $T > 0$ such that $x(t,t_0) = x(t+T,x_0)$ for all $t \in \mathbb{R}$. (*Maps*) The orbit of $x_0 \in \mathbb{R}^n$ is said to be* periodic of period $k > 0$ *if $g^k(x_0) = x_0$.*

We remark that if a solution of (4.0.1) is periodic of period T then evidently it is periodic of period nT for any integer $n > 1$. However, by the period of an orbit we mean the smallest possible $T > 0$ such that Definition 4.0.1 holds. A similar statement holds for periodic orbits of maps.

---

[1]This is not a completely accurate statement. One could make the same argument for fixed points, and orbits homoclinic or heteroclinic to fixed points and periodic orbits. However, one could argue that a fixed point is a particularly simple type of periodic orbit.

4.1 Nonexistence of Periodic Orbits for Two-Dimensional, Autonomous Vector Fields

Now we will learn a useful and easily applicable trick for establishing the nonexistence of periodic solutions of autonomous vector fields on the plane. We will denote these vector fields by

$$\begin{aligned} \dot{x} &= f(x,y), \\ \dot{y} &= g(x,y), \qquad (x,y) \in \mathbb{R}^2, \end{aligned} \tag{4.1.1}$$

where f and g are at least $\mathbf{C}^1$.

Theorem 4.1.1 (Bendixson's criterion) *If on a simply connected region $D \subset \mathbb{R}^2$ (i.e., D has no holes in it) the expression $\frac{\partial f}{\partial x} + \frac{\partial g}{\partial y}$ is not identically zero and does not change sign, then (4.1.1) has no closed orbits lying entirely in D.*

Proof: This is a simple result of Green's theorem on the plane; see Abraham, Marsden, and Ratiu [1988]. Using (4.1.1) and applying the chain rule we find that on any closed orbit Γ we have

$$\int_\Gamma f\,dy - g\,dx = 0. \tag{4.1.2}$$

By Green's theorem this implies

$$\int_S \left(\frac{\partial f}{\partial x} + \frac{\partial g}{\partial y} \right) dx\,dy = 0, \tag{4.1.3}$$

where S is the interior bounded by Γ. But if $\frac{\partial f}{\partial x} + \frac{\partial g}{\partial y} \neq 0$ and doesn't change sign, then this obviously can't be true. Therefore, there must be no closed orbits in D. □

A generalization of Bendixson's criterion due to Dulac is the following.

Theorem 4.1.2 *Let $B(x,y)$ be $\mathbf{C}^1$ on a simply connected region $D \subset \mathbb{R}^2$. If $\frac{\partial (Bf)}{\partial x} + \frac{\partial (Bg)}{\partial y}$ is not identically zero and does not change sign in D, then (4.1.1) has no closed orbits lying entirely in D.*

Proof: The proof is very similar to the previous theorem so we omit it and leave it as an exercise. □

Example 4.1.1 (Application to the Unforced Duffing Oscillator).
Consider the vector field

$$\begin{aligned} \dot{x} &= y \equiv f(x,y), \\ \dot{y} &= x - x^3 - \delta y \equiv g(x,y), \qquad \delta \geq 0. \end{aligned} \tag{4.1.4}$$

An easy calculation shows that

$$\frac{\partial f}{\partial x} + \frac{\partial g}{\partial y} = -\delta.$$

Thus, for $\delta > 0$, (4.1.4) has no closed orbits. We will answer the question of what happens when $\delta = 0$ in Chapter 5.

End of Example 4.1.1

The next example shows how Theorem 4.1.1 allows us to restrict regions in the plane where closed orbits might exist.

Example 4.1.2. Consider the following modification of the unforced Duffing oscillator

$$\begin{aligned} \dot{x} &= y \equiv f(x, y), \\ \dot{y} &= x - x^3 - \delta y + x^2 y \equiv g(x, y), \qquad \delta \geq 0. \end{aligned} \tag{4.1.5}$$

This equation has three fixed points at $(x, y) = (0, 0)$, $(\pm 1, 0)$ with the eigenvalues, $\lambda_{1,2}$, of the associated linearization about each fixed point given by

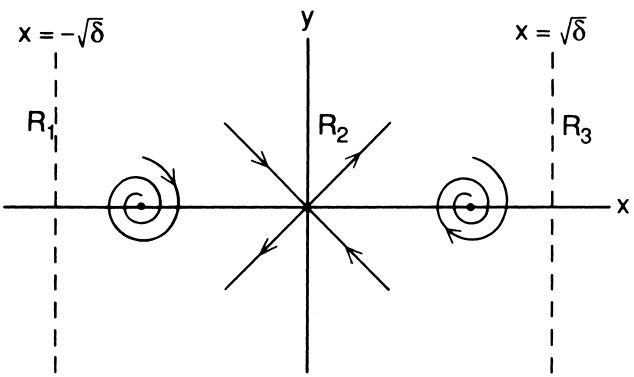

FIGURE 4.1.1. The regions defined by $x = \pm\sqrt{\delta}$ (the figure is drawn for $\delta > 1$).

$$(0, 0) \Rightarrow \lambda_{1,2} = \frac{-\delta}{2} \pm \frac{1}{2}\sqrt{\delta^2 + 4}, \tag{4.1.6}$$

$$(1, 0) \Rightarrow \lambda_{1,2} = \frac{-\delta + 1}{2} \pm \frac{1}{2}\sqrt{(-\delta + 1)^2 - 8}, \tag{4.1.7}$$

$$(-1, 0) \Rightarrow \lambda_{1,2} = \frac{-\delta + 1}{2} \pm \frac{1}{2}\sqrt{(-\delta + 1)^2 - 8}. \tag{4.1.8}$$

Thus, $(0, 0)$ is a saddle, and $(\pm 1, 0)$ are sinks for $\delta > 1$ and sources for $0 \leq \delta < 1$.

A simple calculation gives

$$\frac{\partial f}{\partial x} + \frac{\partial g}{\partial y} = -\delta + x^2. \tag{4.1.9}$$

Thus, (4.1.9) vanishes on the lines $x = \pm\sqrt{\delta}$. These two lines divide the plane into three disjoint regions which we label (from left to right) R_1, R_2, and R_3 as shown in Figure 4.1.1.

Now from Theorem 4.1.1, we can immediately conclude that (4.1.5) can have no closed orbits lying entirely in either region R_1, R_2, or R_3. However, we cannot rule out the existence of closed orbits which overlap these regions as shown in Figure 4.1.2. When we discuss index theory in Chapter 6 we will see how to reduce the number of possibilities even further. We finally remark that it is not a coincidence that the lines $x = \pm\sqrt{\delta}$ fall on the fixed points $(\pm 1, 0)$ when the real parts of the eigenvalues of these fixed points vanish. We will learn what is going on in this case when we study the Poincaré–Andronov–Hopf bifurcation.

End of Example 4.1.2

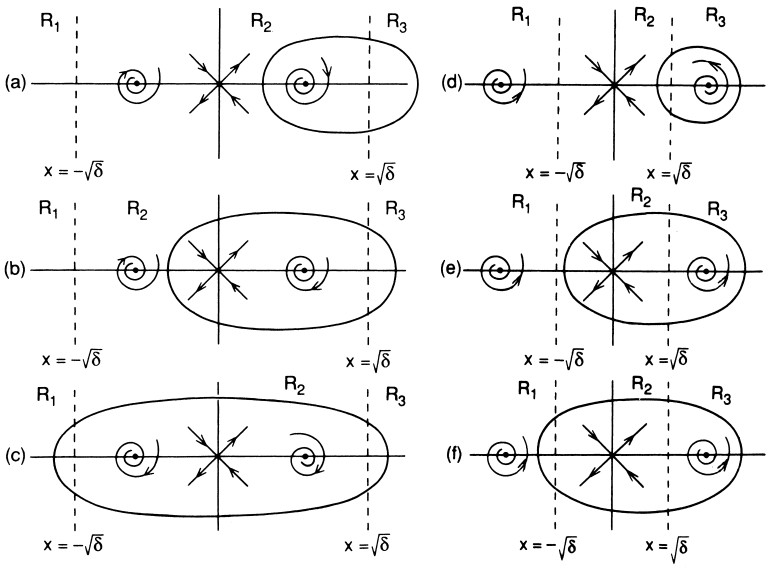

FIGURE 4.1.2. Some possibilities for the existence of close orbits in (4.1.4). a–c apply to the case for $\delta > 1$, d–f to $0 < \delta < 1$.

4.2 Further Remarks on Periodic Orbits

Below we describe a number of situations where periodic orbits are important.

Closing Lemmas: A "closing lemma" is a theorem that describes how "close" an orbit is to a periodic orbit. Hamiltonian systems and

chaotic systems tend to possess periodic orbits in abundance, and it is often possible to characterize "most" orbits in terms of periodic orbits. [2] One of the first closing lemmas is due to Pugh [1967]. Robinson [1978] provides an excellent introduction to the closing lemma. Recent references that describe the state of the art, as well as contain references to the previous work are Mañé [1982], Hayashi [1997], and Aranson et al. [1997]. However, a word of caution is in order, Herman [1991] has constructed examples of Hamiltonian systems that contain *no* periodic orbits. Moreover, this situation is structurally stable in the sense that small perturbations of Herman's examples also do not contain periodic orbits. This should be an indication of just how subtle these questions may be.

Dynamical Averaging: It is often more meaningful to characterize systems possessing complex dynamics through certain quantities involving asymptotic time averages of trajectories. Examples of such quantities are power spectra, generalized dimensions, Liapunov exponents, and Kolmogorov entropy. Cvitanović [1995] shows how under certain conditions such quantities can be calculated in terms of averages of periodic orbits.

Characterization of Chaos: Periodic orbits play a key role in understanding the structure of chaotic attractors. See Lai et al. [1997], Zoldi and Greenside [1998], and the references in these papers.

Semiclassical Mechanics: Periodic orbits play an important role as a bridge between classical and quantum mechanics. Unstable periodic orbits in classical systems may give rise to an extra, and unexpected, eigenstate density in their vicinity, which is referred to as a "scar" in the corresponding quantum mechanical system. See Kaplan and Heller [1999], and references therein.

Mathematical Biology: Periodic orbits are playing an increasingly important role in the understanding of certain biological phenomena. See, e.g., So. et al. [1998], Lesher, et al. [1999], and the references in these papers.

Time Series Analysis: Periodic orbits play a key role in distinguishing the difference between complicated time series generated by deterministic chaos, versus those generated by random noise. See Carroll [1999], and references therein.

---

[2] Proving closing lemmas for specific classes of dynamical systems requires precise hypotheses and rather technical arguments. The quotation marks around the words in this paragraph indicate that making these words mathematically precise is very important.

4.3 Exercises

1. Show that the following vector field on the cylinder

$$\begin{aligned} \dot{v} &= -v, \\ \dot{\theta} &= 1, \qquad (v, \theta) \in \mathbb{R}^1 \times S^1, \end{aligned}$$

has a periodic orbit. Explain why Bendixson's criterion does not hold.

2. Construct a vector field in $\mathbb{R}^3$ with negative divergence that possesses a periodic orbit. Construct a vector field in $\mathbb{R}^3$ with negative divergence that contains a continuous family of periodic orbits.

3. Prove Theorem 4.1.2.

4. The definition of periodic orbit for vector fields given in Definition 4.0.1 was given for the *nonautonomous* vector field (4.0.1). Suppose (4.0.1) is not periodic in time. That is, there is *no* constant $T > 0$ such that $f(x, t) = f(x, t + T)$ for all t, x in the domain of definition. We refer to such nonautonomous vector fields as *aperiodically time-dependent*. Can aperiodically time dependent vector fields have periodic orbits?

5

Vector Fields Possessing an Integral

For a general vector field

$$\dot{x} = f(x), \qquad x \in \mathbb{R}^n,$$

a scalar valued function $I(x)$ is said to be an *integral* (sometimes the term *first integral* is used) if it is constant on trajectories, i.e.,

$$\dot{I}(x) = \nabla I(x) \cdot \dot{x} = \nabla I(x) \cdot f(x) = 0,$$

where "$\cdot$" denotes the usual Euclidean inner product. From this relation we see that the level sets of $I(x)$ (which are generally $(n-1)$-dimensional) are invariant sets. For two-dimensional vector fields the level sets actually give the trajectories of the system. We examine this case in more detail.

5.1 Vector Fields on Two-Manifolds Having an Integral

In applications, three types of two-dimensional phase spaces occur frequently; they are (1) the plane, $\mathbb{R}^2 = \mathbb{R}^1 \times \mathbb{R}^1$, (2) the cylinder, $\mathbb{R}^1 \times S^1$, and (3) the two-torus, $T^2 = S^1 \times S^1$. The vector field can be written as

$$\begin{aligned} \dot{x} &= f(x, y), \\ \dot{y} &= g(x, y), \end{aligned} \tag{5.1.1}$$

where f and g are $\mathbf{C}^r$ $(r \geq 1)$, and as $(x, y) \in \mathbb{R}^1 \times \mathbb{R}^1$ for a vector field on the plane, as $(x, y) \in \mathbb{R}^1 \times S^1$ for a vector field on the cylinder, and as $(x, y) \in S^1 \times S^1$ for a vector field on the torus, where S^1 denotes the circle (which is sometimes referred to as a 1-torus, T^1). We now want to give some examples of how these different phase spaces arise and at the same time go into more detail concering the idea of an *integrable* vector field. We begin with the unforced Duffing oscillator.

Example 5.1.1 (The Unforced Duffing Oscillator). We have been slowly discovering the global structure of the phase space of the unforced Duffing oscillator given by

$$\ddot{x} - x + \delta\dot{x} + x^3 = 0, \tag{5.1.2}$$

or, written as a system,

$$\begin{aligned} \dot{x} &= y, \\ \dot{y} &= x - x^3 - \delta y, \end{aligned} \qquad (x, y) \in \mathbb{R}^1 \times \mathbb{R}^1, \quad \delta \geq 0. \tag{5.1.3}$$

Thus far we know the local structure near the three fixed points $(x, y) = (0, 0)$, $(\pm 1, 0)$ and that for $\delta > 0$ there are no closed orbits. The next step is to understand the geometry of the global orbit structure. In general, this is a formidable task. However, for the special parameter value $\delta = 0$, we can understand completely the global geometry, which, we will see, provides a framework for understanding the global geometry for $\delta \neq 0$.

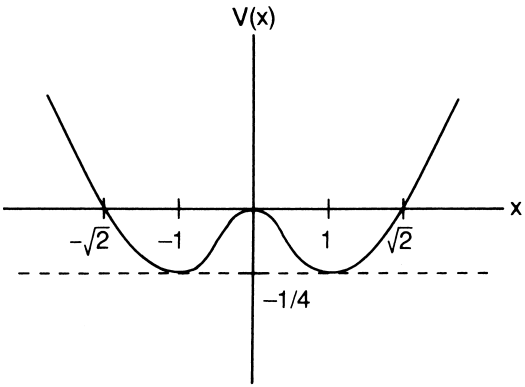

FIGURE 5.1.1. Graph of $V(x)$.

The reason we can do this is that, for $\delta = 0$, the unforced, undamped Duffing oscillator has a *first integral* or a function of the dependent variables whose level curves give the orbits. Alternately, in more physical terms, the unforced, undamped Duffing oscillator is a conservative system having an energy function which is constant on orbits. This can be seen as follows—take the unforced, undamped Duffing oscillator, multiply it by $\dot{x}$, and integrate as below.

$$\dot{x}\ddot{x} - \dot{x}x + \dot{x}x^3 = 0$$

or

$$\frac{d}{dt}\left(\frac{1}{2}\dot{x}^2 - \frac{x^2}{2} + \frac{x^4}{4}\right) = 0; \tag{5.1.4}$$

hence,

$$\frac{1}{2}\dot{x}^2 - \frac{x^2}{2} + \frac{x^4}{4} = h = \text{constant}$$

or

$$h = \frac{y^2}{2} - \frac{x^2}{2} + \frac{x^4}{4}. \tag{5.1.5}$$

This is a first integral for the unforced, undamped Duffing oscillator or, if you think of $y^2/2$ as the kinetic energy (mass has been scaled to be 1) and $-x^2/2 + x^4/4 \equiv V(x)$ as potential energy, h can be thought of as the total energy

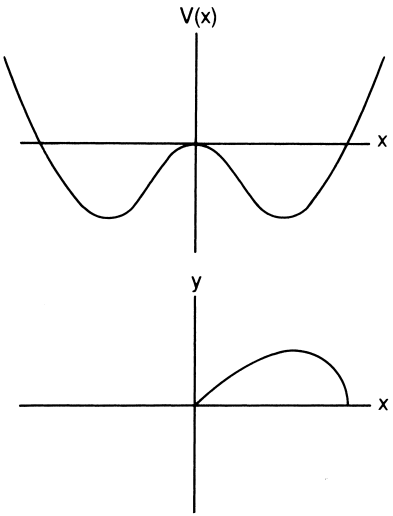

FIGURE 5.1.2.

of the system. Therefore, the level curves of this function give the global structure of the phase space.

End of Example 5.1.1

In general, for one-degree-of-freedom problems (i.e., vector fields on a two-dimensional phase space) that have a first integral that can be viewed as the sum of a kinetic and potential energy, there is an easy, graphical method for drawing the phase space.
We will illustrate the method for the unforced, undamped Duffing oscillator. As a preliminary step, we point out the shape of the graph of $V(x)$ in Figure 5.1.1.

Now suppose that the first integral is given by

$$h = \frac{y^2}{2} + V(x);$$

then

$$y = \pm\sqrt{2}\,\sqrt{h - V(x)}. \tag{5.1.6}$$

Our goal is to draw the level sets of h. Imagine sitting at the point $(0, 0)$, with h fixed. Now move toward the right (i.e., let x increase). A glance at the graph of $V(x)$ shows that V begins to decrease. Then, since $y = +\sqrt{2}\,\sqrt{h - V(x)}$ (we take the + sign for the moment) and h is fixed, y must increase until the minimum of the potential is reached, and then it decreases until the boundary of the potential is reached (why can't you

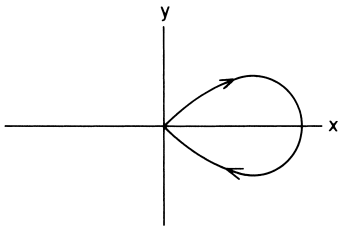

FIGURE 5.1.3.

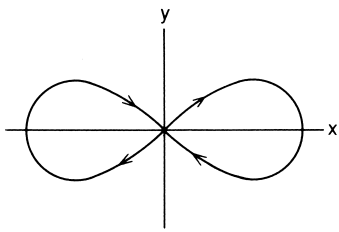

FIGURE 5.1.4.

go farther?) (see Figure 5.1.2). Now $y = +$ or $-\sqrt{2}\sqrt{h - V(x)}$; hence the entire orbit through $(0, 0)$ for fixed h is as in Figure 5.1.3.

(Note: why are the arrows drawn in their particular directions in Figure 5.1.3?) By symmetry, there is another *homoclinic orbit* to the left as in Figure 5.1.4, and if you repeat this procedure for different points you can draw the entire phase plane as shown in Figure 5.1.5.

The homoclinic orbit is sometimes called a *separatrix* because it is the boundary between two distinctly different types of motions. We will study homoclinic orbits in some detail later on.

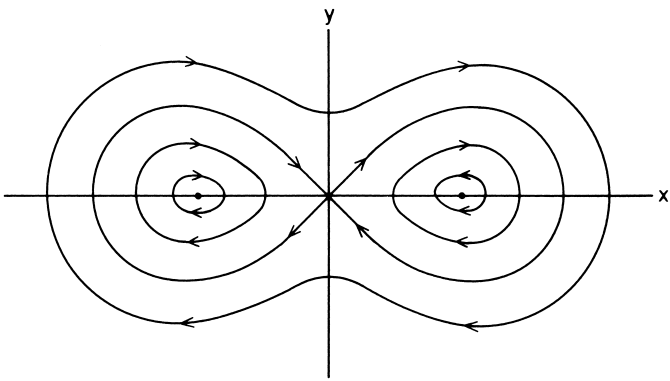

FIGURE 5.1.5. Orbits of the unforced, undamped Duffing oscillator.

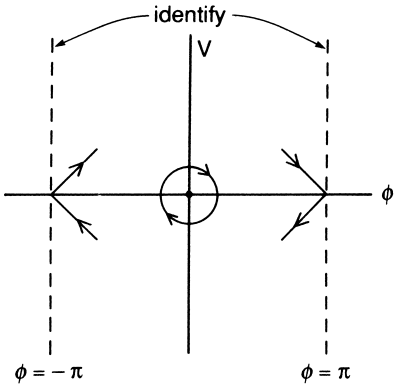

FIGURE 5.1.6. Fixed points of the pendulum.

Denoting the first integral of the unforced, undamped Duffing oscillator by h was meant to be suggestive. The unforced, undamped Duffing oscillator is actually a *Hamiltonian System*, i.e., there exists a function $h = h(x, y)$ such that the vector field is given by

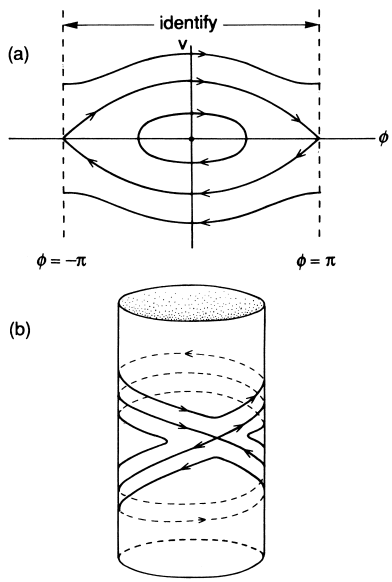

FIGURE 5.1.7. a) Orbits of the pendulum on $\mathbb{R}^2$ with $\phi = \pm\pi$ identified. b) Orbits of the pendulum on the cyliner.

$$\begin{aligned} \dot{x} &= \frac{\partial h}{\partial y}, \\ \dot{y} &= -\frac{\partial h}{\partial x} \end{aligned} \tag{5.1.7}$$

(we will study these in more detail later). Note that all the solutions lie on level curves of h which are topologically the same as S^1 (or T^1). This Hamiltonian system is an *integrable* Hamiltonian system and it has a characteristic of all n-degree-of-freedom integrable Hamiltonian systems in that its bounded motions lie on n-dimensional tori or homoclinic and heteroclinic orbits (see Arnold [1978] or Abraham and Marsden [1978]). (Note that all one-degree-of-freedom Hamiltonian systems are integrable.) More information on Hamiltonian vector fields can be found in Chapters 13 and 14.

Example 5.1.2 (The Pendulum). The equation of motion of a simple pendulum (again, all physical constants are scaled out) is given by

$$\ddot{\phi} + \sin\phi = 0 \tag{5.1.8}$$

or, written as a system,

$$\begin{aligned} \dot{\phi} &= v, \\ \dot{v} &= -\sin\phi, \end{aligned} \qquad (\phi, v) \in S^1 \times \mathbb{R}^1. \tag{5.1.9}$$

This equation has fixed points at $(0,0)$, $(\pm\pi, 0)$, and simple calculations show that $(0,0)$ is a *center* (i.e., the eigenvalues are purely imaginary) and $(\pm\pi, 0)$ are saddles, but since the phase space is the cylinder and not the plane, $(\pm\pi, 0)$ are really the same point (see Figure 5.1.6). (Think of the pendulum as a physical object and you will see that this is obvious.)

Now, just as in Example 5.1.1, the pendulum is a Hamiltonian system with a first integral given by

$$h = \frac{v^2}{2} - \cos\phi. \tag{5.1.10}$$

Again, as in Example 5.1.1, this fact allows the global phase portrait for the pendulum to be drawn, as shown in Figure 5.1.7a. Alternatively, by gluing the two lines $\phi = \pm\pi$ together, we obtain the orbits on the cylinder as shown in Figure 5.1.7b.

End of Example 5.1.2

5.2 Two Degree-of-Freedom Hamiltonian Systems and Geometry

We now give an example of a *two degree-of-freedom* Hamiltonian system that very concretely illustrates a number of more advanced concepts that we will discuss later on.

Consider two linearly coupled Harmonic oscillators that we write as a system as follows

$$\begin{aligned}
\dot{x}_1 &= y_1 = \frac{\partial H}{\partial y_1}, \\
\dot{y}_1 &= -\omega^2 x_1 - c(x_1 - x_2) = -\frac{\partial H}{\partial x_1}, \\
\dot{x}_2 &= y_2 = \frac{\partial H}{\partial y_2}, \\
\dot{y}_2 &= -\omega^2 x_2 - c(x_2 - x_1) = -\frac{\partial H}{\partial x_2},
\end{aligned}$$

where the Hamiltonian, H is given by,

$$H(x_1, y_1, x_2, y_2) = \frac{y_1^2}{2} + \frac{\omega^2 x_1^2}{2} + \frac{y_2^2}{2} + \frac{\omega^2 x_2^2}{2} + \frac{1}{2}c(x_1 - x_2)^2.$$

This is a linear system which can be transformed into real Jordan canonical form as follows

$$\begin{aligned}
\dot{u}_1 &= v_1 = \frac{\partial H}{\partial v_1}, \\
\dot{v}_1 &= -\Omega_1^2 u_1 = -\frac{\partial H}{\partial u_1}, \\
\dot{u}_2 &= v_2 = \frac{\partial H}{\partial v_2}, \\
\dot{v}_2 &= -\Omega_2^2 u_2 = -\frac{\partial H}{\partial u_2},
\end{aligned}$$

where

$$\Omega_1 = \omega, \qquad \Omega_2 = \sqrt{\omega^2 + 2c},$$

and

$$H(u_1, v_1, u_2, v_2) = \frac{v_1^2}{2} + \frac{\Omega_1^2 u_1^2}{2} + \frac{v_2^2}{2} + \frac{\Omega_2^2 u_2^2}{2}.$$

(Note that using the same symbol "H" for the Hamiltonian in two different sets of coordinates is not particularly good, and can lead to confusion.) Now one clearly sees that the level sets of the Hamiltonian are three-spheres, S^3. Thus the four dimensional phase space is foliated by a one-parameter family of invariant three-spheres. Next we will study the dynamics on these three-spheres.

5.2a Dynamics on the Energy Surface

First we transform to polar coordinates

$$u_i \;=\; \sqrt{\frac{2I_i}{\Omega_i}}\sin\theta_i,$$

$$\Longrightarrow \dot{u}_i = \sqrt{\frac{1}{2I_i\Omega_i}}\dot{I}_i \sin\theta_i + \sqrt{\frac{2I_i}{\Omega_i}}\dot{\theta}_i \cos\theta_i = \sqrt{2I_i\Omega_i}\cos\theta_i,$$

$$\begin{aligned} v_i &= \sqrt{2I_i\Omega_i}\cos\theta_i, \\ &\Longrightarrow \dot{v}_i = \sqrt{\frac{\Omega_i}{2I_i}}\dot{I}_i \cos\theta_i - \sqrt{2I_i\Omega_i}\dot{\theta}_i \sin\theta_i = \Omega_i^2\sqrt{\frac{2I_i}{\Omega_i}}\sin\theta_i, \\ i &= 1, 2. \end{aligned}$$

Combining these relations with the equations of motion in the $u_1 - v_1 - u_2 - v_2$ coordinates gives

$$\begin{aligned} \dot{I}_i &= 0 \\ \dot{\theta}_i &= \Omega_i, \quad i = 1, 2. \end{aligned}$$

Full Equations of Motion

The full equations of motion are given as

$$\dot{\theta}_1 = \Omega_1 = \tfrac{\partial H}{\partial I_1},$$

$$\dot{I}_1 = 0 = -\tfrac{\partial H}{\partial \theta_1},$$

$$\dot{\theta}_2 = \Omega_2 = \tfrac{\partial H}{\partial I_2},$$

$$\dot{I}_2 = 0 = -\tfrac{\partial H}{\partial \theta_2},$$

with Hamiltonian

$$H(I_1, I_2) = I_1\Omega_1 + I_2\Omega_2.$$

Equations of Motion Restricted to the Energy Surface

Since trajectories are restricted to lie in the three dimensional energy surface the dynamics is really three dimensional. Now we show how this can be realized in the equations of motion.

The equation for the energy surface is

$$H(I_1, I_2) = I_1\Omega_1 + I_2\Omega_2 = h = \text{constant},$$

which we can easily rearrange and explicitly exhibit I_2 as a function of I_1 and h

$$I_2 = \frac{h - I_1\Omega_1}{\Omega_2} = I_2(I_1, h).$$

Hence, if we know I_1 and h, we know I_2. Therefore, on the energy surface, the equations reduce to

$$\begin{aligned} \dot{\theta}_1 &= \Omega_1, \\ \dot{\theta}_2 &= \Omega_2, \\ \dot{I}_1 &= 0. \end{aligned} \tag{5.2.1}$$

From these equations we see that the energy surface is foliated by a one-parameter family of invariant two-tori.

5.2B Dynamics on an Individual Torus

Fixing h and I_1 chooses an individual two-torus. The trajectories on this torus are given by

$$\theta_1(t) = \Omega_1 t + \Omega_{10},$$
$$\theta_2(t) = \Omega_2 t + \Omega_{20}.$$

The nature of the trajectories depend on the number $\frac{\Omega_1}{\Omega_2}$. If this is a rational number then all trajectories are periodic. If it is irrational, then any trajectory densely covers the torus. These statements are proved in Section 10.4a.

For a more detailed study of the geometry of two coupled linear oscillators, which makes connections with many deeper topics such as the Hopf fibration of the three-sphere and knots, see the excellent paper of Meyer [1990].

5.3 Exercises

1. Consider the following vector fields.

   a) $\ddot{x} + \mu x = 0, \qquad x \in \mathbb{R}^1.$

   b) $\ddot{x} + \mu x + x^2 = 0, \qquad x \in \mathbb{R}^1.$

   c) $\ddot{x} + \mu x + x^3 = 0, \qquad x \in \mathbb{R}^1.$

   d) $\begin{aligned} \dot{x} &= -\mu y + xy, \\ \dot{y} &= \mu x + \tfrac{1}{2}(x^2 - y^2), \end{aligned} \qquad (x, y) \in \mathbb{R}^2.$

      i) Write a), b) and c) as systems.

      ii) Find and determine the nature of the stability of the fixed points.

      iii) Find the first integrals and draw all phase curves for $\mu < 0$, $\mu = 0$, and $\mu > 0$.

2. Euler's equations of motion for a free rigid body are

$$\begin{aligned} m_i &= I_i \omega_i, \qquad i = 1, 2, 3, \quad I_1 > I_2 > I_3 \\ \dot{m}_1 &= \frac{I_2 - I_3}{I_2 I_3} m_2 m_3, \\ \dot{m}_2 &= \frac{I_3 - I_1}{I_1 I_3} m_1 m_3, \qquad (m_1, m_2, m_3) \in \mathbb{R}^3, \\ \dot{m}_3 &= \frac{I_1 - I_2}{I_1 I_2} m_1 m_2, \end{aligned}$$

   a) Find and determine the nature of the stability of the fixed points.

   b) Show that the functions

$$H(m_1, m_2, m_3) = \frac{1}{2}\left[\frac{m_1^2}{I_1} + \frac{m_2^2}{I_2} + \frac{m_3^2}{I_3}\right],$$
$$L(m_1, m_2, m_3) = m_1^2 + m_2^2 + m_3^2$$

   are constants on orbits.

c) For fixed L, draw all phase curves.

3. At the beginning of this chapter we defined the notion of an integral for autonomous vector fields. An integral is a (scalar valued) function that is constant on trajectories, or more geometrically, it is a function having the property that the vector field is tangent to its level sets. Generalize these ideas for the case of nonautonomous vector fields.

4. Consider the a map:
$$x \mapsto g(x), \qquad x \in \mathbb{R}^n,$$
or
$$x_{n+1} = g(x_n).$$
Define the notion of an integral for maps.

6

Index Theory

Before we describe some of the uses of index theory, we will give a heuristic description of the idea.

Suppose we have a vector field defined in some simply connected region, $\mathcal{R}$,of the plane (this is a two-dimensional method only). Let Γ be any closed loop in $\mathcal{R}$ *which contains no fixed points* of the vector field. You can imagine at each point, p, on the loop Γ that there is an arrow representing the value of the vector field at p (see Figure 6.0.1).

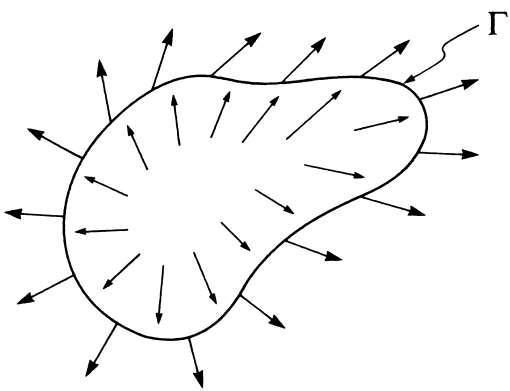

FIGURE 6.0.1. Vector field on the closed curve Γ.

Now as you move around Γ in the counter-clockwise sense (call this the positive direction), the vectors on Γ rotate, and when you get back to the point at which you started, they will have rotated through an angle $2\pi k$, where k is some integer. This integer, k, is called the *index of* Γ.

The index of a closed curve containing no fixed points can be calculated by integrating the change in the angle of the vectors at each point on Γ around Γ (this angle is measured with respect to some chosen coordinate system). For a vector field defined on some simply connected region, $\mathcal{R}$, of the plane given by

$$\begin{aligned} \dot{x} &= f(x,y), \\ \dot{y} &= g(x,y), \qquad (x,y) \in \mathcal{R} \subset \mathbb{R}^2, \end{aligned} \tag{6.0.1}$$

the index of Γ, k, is found by computing

$$k = \frac{1}{2\pi}\oint_\Gamma d\phi = \frac{1}{2\pi}\oint_\Gamma d\left(\tan^{-1}\frac{g(x,y)}{f(x,y)}\right)$$
$$= \frac{1}{2\pi}\oint_\Gamma \frac{f\,dg - g\,df}{f^2+g^2}. \tag{6.0.2}$$

This integral has several properties, one of the most important being that it retains the same value if Γ is smoothly deformed, as long as it is not deformed through some fixed point of the vector field. The index of a fixed point is defined to be the index of a closed curve which contains only this one fixed point, and where no fixed points are on the closed curve. From the definition of the index given above (if not by just drawing pictures), one can prove the following theorems.

Theorem 6.0.1 i) *The index of a sink, a source, or a center is* $+1$.

ii) *The index of a hyperbolic saddle point is* -1.

iii) *The index of a periodic orbit is* $+1$.

iv) *The index of a closed curve not containing any fixed points is 0.*

v) *The index of a closed curve is equal to the sum of the indices of the fixed points within it.*

An immediate corollary of this is the following.

Corollary 6.0.2 *Inside any periodic orbit* γ *there must be at least one fixed point. If there is only one, then it must be a sink, source, or center. If all the fixed points within* γ *are hyperbolic, then there must be an odd number,* $2n+1$, *of which* n *are saddles and* $n+1$ *either sinks or sources.*

For more information on index theory, see Andronov et al. [1971].

> A homoclinic orbit should *not* should not be treated as a periodic orbit for the purpose of the application of index theory. In fact, there are examples of vector fields on the two-sphere containing homoclinic orbits which in turn do not surround an equilibrium point. In particular, in Guillemin and Pollack [1974] there is a phase portrait of a vector field on the two sphere containing one saddle-type equlibrium point with *all* orbits homoclinic to this saddle point.

EXAMPLE 4.1.2 REVISITED Using the above results, the reader should be able to verify that the phase portraits shown in Figures 5.1.2b and 5.1.2e cannot occur. This example shows how Bendixson and Dulac's criteria used with index theory can go a long way toward describing the global structure of phase portraits on the plane. We remark that a higher dimensional generalization of index theory is *degree theory*. For an introduction to the use of degree theory in dynamical systems and bifurcation theory we refer the reader to Chow and Hale [1982] or Smoller [1983].

6.1 Exercises

1. There are six phase portraits of vector fields on the plane shown in Figure 6.1.1. Using various phase plane techniques, determine which phase portraits are correct and which are incorrect. Modify the incorrect phase portraits to make them correct, *not by deleting any orbits shown* but by changing the stability types of existing orbits or adding new orbits.

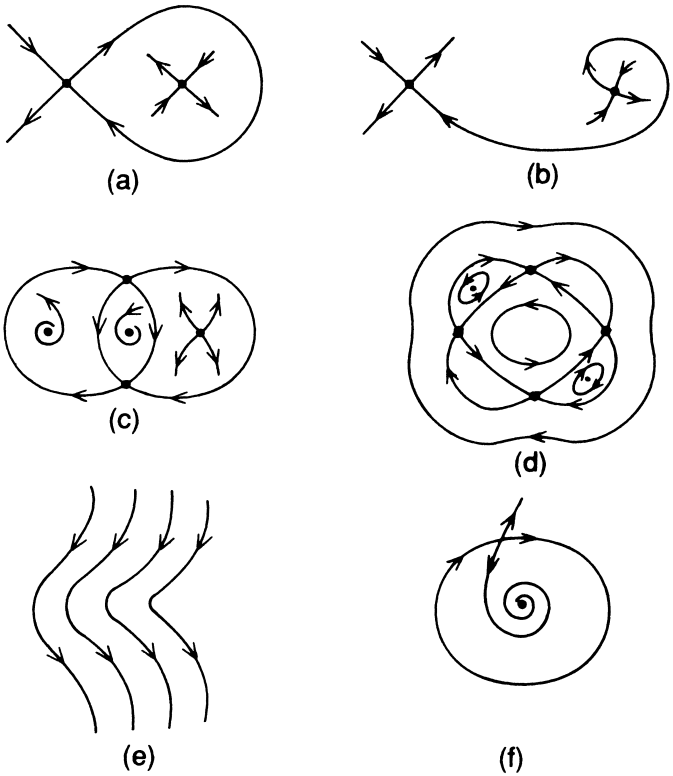

FIGURE 6.1.1.

7

Some General Properties of Vector Fields: Existence, Uniqueness, Differentiability, and Flows

In this section we want to give some of the basic theorems describing general properties of solutions of vector fields. Since it is just as easy to treat the nonautonomous case we will do so.

Consider the vector field

$$\dot{x} = f(x,t), \tag{7.0.1}$$

where $f(x,t)$ is $\mathbf{C}^r$, $r \geq 1$, on some open set $U \subset \mathbb{R}^n \times \mathbb{R}^1$.

7.1 Existence, Uniqueness, Differentiability with Respect to Initial Conditions

Theorem 7.1.1 *Let $(x_0, t_0) \in U$. Then there exists a solution of (7.0.1) through the point x_0 at $t = t_0$, denoted $x(t, t_0, x_0)$ with $x(t_0, t_0, x_0) = x_0$, for $|t - t_0|$ sufficiently small. This solution is unique in the sense that any other solution of (7.0.1) through x_0 at $t = t_0$ must be the same as $x(t, t_0, x_0)$ on their common interval of existence. Moreover, $x(t, t_0, x_0)$ is a $\mathbf{C}^r$ function of t, t_0, and x_0.*

Proof: See Arnold [1973], Hirsch and Smale [1974], or Hale [1980]. □

We remark that it is possible to weaken the assumptions on $f(x,t)$ and still obtain existence and uniqueness. We refer the reader to Hale [1980] for a discussion.

Theorem 7.1.1 only guarantees existence and uniqueness for sufficiently small time intervals. The following result allows us to uniquely extend the time interval of existence.

7.2 Continuation of Solutions

Let $C \subset U \subset \mathbb{R}^n \times \mathbb{R}^1$ be a compact set containing (x_0, t_0).

Theorem 7.2.1 *The solution $x(t, t_0, x_0)$ can be uniquely extended backward and forward in t up to the boundary of C.*

Proof: See Hale [1980]. □

Theorem 7.2.1 tells us how solutions fail to exist; namely, they "blow up." Consider the following example.

Example 7.2.1. Consider the equation

$$\dot{x} = x^2, \qquad x \in \mathbb{R}^1. \tag{7.2.1}$$

The solution of (7.2.1) through x_0 at $t = 0$ is given by

$$x(t, 0, x_0) = \frac{-x_0}{x_0 t - 1}. \tag{7.2.2}$$

It should be clear that (7.2.2) does not exist for all time, since it becomes infinite at $t = 1/x_0$. This example also shows that the time interval of existence may depend on x_0.

End of Example 7.2.1

In practice we often encounter vector fields depending on parameters, and it is often necessary to differentiate the solutions with respect to the parameters. The following result covers this situation.

7.3 Differentiability with Respect to Parameters

Consider the vector field

$$\dot{x} = f(x, t; \mu), \tag{7.3.1}$$

where $f(x, t; \mu)$ is $\mathbf{C}^r$ $(r \geq 1)$ on some open set $U \subset \mathbb{R}^n \times \mathbb{R}^1 \times \mathbb{R}^p$.

Theorem 7.3.1 *For $(t_0, x_0, \mu) \in U$ the solution $x(t, t_0, x_0, \mu)$ is a $\mathbf{C}^r$ function of t, t_0, x_0, and μ.*

Proof: See Arnold [1973] or Hale [1980]. □

At this stage we would like to point out some special properties of $\mathbf{C}^r$, $r \geq 1$, autonomous vector fields which will prove useful.

7.4 Autonomous Vector Fields

Consider the vector field

$$\dot{x} = f(x), \qquad x \in \mathbb{R}^n, \tag{7.4.1}$$

where $f(x)$ is $\mathbf{C}^r$, $r \geq 1$, on some open set $U \in \mathbb{R}^n$. For simplicity, let us suppose that the solutions exist for all time (we leave it as an exercise to make the necessary modifications when solutions exist only on finite time intervals). The following three results are very useful in applications.

Proposition 7.4.1 *If $x(t)$ is a solution of (7.4.1), then so is $x(t+\tau)$ for any $\tau \in \mathbb{R}$.*

Proof: By definition

$$\frac{dx(t)}{dt} = f\big(x(t)\big). \tag{7.4.2}$$

Hence, we have

$$\left.\frac{dx(t+\tau)}{dt}\right|_{t=t_0} = \left.\frac{dx(t)}{dt}\right|_{t=t_0+\tau} = f\big(x(t_0+\tau)\big) = \left. f\big(x(t+\tau)\big)\right|_{t=t_0}$$

or

$$\left.\frac{dx(t+\tau)}{dt}\right|_{t=t_0} = \left. f\big(x(t+\tau)\big)\right|_{t=t_0}. \tag{7.4.3}$$

Since (7.4.3) is true for any $t_0 \in \mathbb{R}$, the result follows. □

Note that Proposition 7.4.1 does not hold for nonautonomous vector fields. Consider the following example.

Example 7.4.1. Consider the nonautonomous vector field

$$\dot{x} = e^t, \qquad x \in \mathbb{R}^1. \tag{7.4.4}$$

The solution of (7.4.4) is given by

$$x(t) = e^t, \tag{7.4.5}$$

and it should be clear that

$$x(t+\tau) = e^{t+\tau} \tag{7.4.6}$$

is not a solution of (7.4.4) for $\tau \neq 0$.

End of Example 7.4.1

The following proposition lies at the heart of the Poincaré-Bendixson theorem.

Proposition 7.4.2 *For any $x_0 \in \mathbb{R}^n$ there exists only one solution of (7.4.1) passing through this point.*

Proof: We will show that if this proposition weren't true, then uniqueness of solutions would be violated.

Let $x_1(t)$, $x_2(t)$ be solutions of (7.4.1) satisfying

$$x_1(t_1) = x_0,$$
$$x_2(t_2) = x_0.$$

By Proposition 7.4.1

$$\tilde{x}_2(t) \equiv x_2\big(t - (t_1 - t_2)\big)$$

is also a solution of (7.4.1) satisfying

$$\tilde{x}_2(t_1) = x_0.$$

Hence, by Theorem 7.1.1, $x_1(t)$ and $x_2(t)$ must be identical. □

Since for autonomous vector fields time-translated solutions remain solutions (i.e., Proposition 7.4.1 holds), it suffices to choose a fixed initial time, say $t_0 = 0$, which is understood and therefore often omitted from the notation (as we do now).

Proposition 7.4.3 (Properties of a Flow)

i) $x(t, x_0)$ *is* $\mathbf{C}^r$.

ii) $x(0, x_0) = x_0$.

iii) $x(t + s, x_0) = x\big(t, x(s, x_0)\big)$.

Proof: i) follows from Theorem 7.1.1, ii) is by definition, and iii) follows from Proposition 7.4.2; namely, $\tilde{x}(t, x_0) \equiv x(t + s, x_0)$ and $x\big(t, x(s, x_0)\big)$ are both solutions of (7.4.1) satisfying the same initial conditions at $t = 0$. Hence, by uniqueness, they must coincide. □

Proposition 7.4.3 shows that the solutions of (7.4.1) form a one-parameter family of $\mathbf{C}^r$, $r \geq 1$, diffeomorphisms of the phase space (invertibility comes from iii)). This is referred to as a *phase flow* or just a *flow*. A common notation for flows is $\phi(t, x)$ or $\phi_t(x)$.

Let us comment a bit more on this notation $\phi_t(x)$. The part of Theorem 7.1.1 dealing with differentiability of solutions with respect to x_0 (regarding t and t_0 as fixed) allows us to think differently about the solutions of ordinary differential equations. More precisely, in the solution $x(t, t_0, x_0)$, we can think of t and t_0 as fixed and then study how the map $x(t, t_0, x_0)$ moves sets of points around in phase space. This is the global, geometrical

view of the study of dynamical systems. For a set $U \subset \mathbb{R}^n$, we would denote its image under this map by $x(t, t_0, U)$. Since points in phase space are also labeled by the letter x, it is often less confusing to change the notation for the solutions, which is why we use the symbol ϕ. This point of view will become more apparent when we study the construction of Poincaré maps.

Finally, let us note that in the study of ordinary differential equations one might believe the problem to be finished when the "solution" $x(t, t_0, x_0)$ is found. The rest of the book will show that this is not the case, but, on the contrary, that this is when the story begins to get really interesting.

7.5 Nonautonomous Vector Fields

It should be clear that Propositions 7.4.1, 7.4.2, and 7.4.3 do not hold for nonautonomous vector fields. However, we can always make a nonautonomous vector field autonomous by redefining time as a new dependent variable. This is done as follows.

By writing (7.0.1) as

$$\frac{dx}{dt} = \frac{f(x,t)}{1} \tag{7.5.1}$$

and using the chain rule, we can introduce a new independent variable s so that (7.5.1) becomes

$$\begin{aligned} \frac{dx}{ds} &\equiv x' = f(x,t), \\ \frac{dt}{ds} &\equiv t' = 1. \end{aligned} \tag{7.5.2}$$

If we define $y = (x,t)$ and $g(y) = (f(x,t), 1)$, we see that (7.5.2) becomes

$$y' = g(y), \qquad y \in \mathbb{R}^n \times \mathbb{R}^1. \tag{7.5.3}$$

Of course, knowledge of the solutions of (7.5.3) implies knowledge of the solutions of (7.0.1) and vice versa. For example, if $x(t)$ is a solution of (7.0.1) passing through x_0 at $t = t_0$, i.e., $x(t_0) = x_0$, then $y(s) = (x(s+t_0), t(s) = s + t_0)$ is a solution of (7.5.3) passing through $y_0 \equiv \big(x(t_0), t_0\big)$ at $s = 0$.

Every vector field can thus be viewed as an autonomous vector field. This apparently trivial trick is a great conceptual aid in the construction of Poincaré maps for time-periodic and quasiperiodic vector fields, as we shall see in Chapter 10. Notice, however, that in redefining time as a *dependent* variable, it may then be introduced in various situations requiring specification of initial positions (i.e., specifying x_0); in particular, the reader should reexamine the definition of stability given in Chapter 1. There are alternative, and more useful, views of nonautonomous vector fields that

we briefly describe since they are becoming more and more prominent in current developments in dynamical systems theory.

Let $x(t, t_0, x_0)$, denote a solution of (7.0.1) with $x(t_0, t_0, x_0) = x_0$. Then the analog of property *iii*) of Proposition 7.4.3 is the following:

$$x(t_2, t_0, x_0) = x(t_2, t_1, x(t_1, t_0, x_0)), \qquad \forall x_0 \in \mathbb{R}^n, \text{ and all } t_0 \leq t_1 \leq t_2, \tag{7.5.4}$$

which is called the *cocycle property*. The notion of a cocycle is central to current developments in ergodic theory (Katok and Hasselblatt [1995]), random dynamical systems (Arnold [1998]), and nonautonomous dynamical systems (Kloeden and Schmalfuss [1997]). We will describe the cocycle formalism in more generality, but we first describe the skew-product flow approach to nonautonomous vector fields.

7.5a The Skew-Product Flow Approach

The skew-product flow approach is a way of dealing with nonautonomous vector fields so as to retain the flow properties as described in Proposition 7.4.1. This approach has been pioneered by Sell [1967a, b], [1971].

The crucial observation leading to the development of the approach is the following. Suppose $x(t)$ is a solution of $\dot{x} = f(x, t)$. Then $x_\tau(t) \equiv x(t + \tau)$ is a solution of $\dot{x}_\tau(t) = f_\tau(x_\tau(t), t) \equiv f(x(t + \tau), t + \tau)$ (compare this with the proof of Proposition 7.4.1).

We first define the space of nonautonomous vector fields whose time translates remain within the space, i.e.,

$$\begin{aligned}\mathcal{F} \equiv \{&\text{Space of functions } f : \mathbb{R}^n \times \mathbb{R} \to \mathbb{R}^n \text{ such that} \\ &f_\tau(\cdot, \cdot) \equiv f(\cdot, \cdot + \tau) \in \mathcal{F} \text{ for all } \tau \in \mathbb{R}.\}\end{aligned}$$

We then define the group of shift operators on $\mathcal{F}$:

$$\begin{aligned}\theta_\tau &: \mathcal{F} \to \mathcal{F}, \\ &f \mapsto \theta_\tau f \equiv f_\tau, \quad \forall \tau \in \mathbb{R},\end{aligned} \tag{7.5.5}$$

and we define the product space:

$$\mathcal{X} \equiv \mathbb{R}^n \times \mathcal{F}.$$

A slight variation in notation is now useful. Let $x(t, x_0, f)$ denote a solution of $\dot{x} = f(x, t)$ with $x(0, x_0, f) = x_0$. Finally, we define the family of mappings:

$$\begin{aligned}&\Psi_t : \mathcal{X} \to \mathcal{X}, \\ &(x_0, f) \mapsto (x(t, x_0, f), \theta_t f).\end{aligned} \tag{7.5.6}$$

Ψ_t is a one-parameter family of mappings of $\mathcal{X}$ into $\mathcal{X}$, or flow [1]. This follows easily from the fact that the identity (i.e., the analog of (7.5.4)):

$$x(t+s, x_0, f) = x(t, x(s, x_0, f), \theta_s f), \tag{7.5.7}$$

is the same as

$$\Psi_{t+s}(x_0, f) = \Psi_t \circ \Psi_s(x_0, f). \tag{7.5.8}$$

It is easy to see that the role of the shift operators θ_τ is to advance the explicit time argument in the vector field. The reader should imagine this in the context of attempting to prove Proposition 7.4.1 for nonautonomous vector fields.

The notion of a skew-product flow derived from nonautonomous vector fields can be made general, and is referred to as a *skew-product dynamical system* (or just *skew dynamical system*). This is done as follows. Let M denote an n-dimensional manifold and S a metric space (or, possibly, something more general). Consider a map of the form:

$$\begin{aligned} f &: M \times S \to M \times S, \\ &(m, s) \mapsto (\phi(m, s), \sigma(s)) \,. \end{aligned} \tag{7.5.9}$$

Further, we will assume that for each fixed s, the map $\phi(\cdot, s) : M \to M$ is a C^r diffeomorphism. Then the system defined by (7.5.9) is referred to as a *skew dynamical system over the base* $\sigma : S \to S$.

Skew dynamical systems play a central role in dynamical systems in their own right. The following topics and references are representative of these areas and applications.

General Theory of Skew-Product Dynamical Systems: Sacker and Sell [1977], Sacker [1976], Shen and Yi [1998] develop many basic properties of skew-product dynamical systems.

Invariant Manifold Theorems: Chow and Yi [1994], Yi [1993a, b] prove invariant manifold theorems for nonautonomous vector fields by using the skew-product dynamical systems approach.

Global Stability: Meyer and Zhang [1996] develop many of the basic concepts of skew-product dynamical systems (e.g., stable and unstable manifolds of hyperbolic trajectories, hyperbolic sets, shadowing, basic sets, etc.) for studying global dynamics in much the same manner as described in, e.g. Shub [1987], for standard differential dynamical dynamical systems, i.e., dynamics defined by iterated diffeomorphisms or flows on manifolds. Johnson and Kloeden [2001] discuss attractors for skew-product dynamical systems.

---

[1] It is important (but not for our descriptive purposes here) to have a topology on $\mathcal{X}$ such that the map $(t, x_0, f) \mapsto x(t, x_0, f)$ is continuous, see Sell [1967a, b] for details.

7.5B The Cocycle Approach

The cocycle property can be expressed in a general formalism. Let P denote a *parameter space*. In different applications P could be a compact metric space, a function space, or a probability space. Let $\Theta = \{\theta_t \,|\, t \in \mathbb{R}\}$ denote a one-parameter family of mappings of P into itself, i.e.,

$$\begin{aligned} \theta_t \,:\, & P \to P, \\ & p \mapsto \theta_t p, \end{aligned}$$

with

$$\theta_t \circ \theta_s = \theta_{t+s}, \quad \forall t,\, s \in \mathbb{R},$$

and

$$\theta_0 = \mathrm{id}.$$

Then we have the following definition.

Definition 7.5.1 (Cocycle on $\mathbb{R}^n$) *A family of mappings*

$$\phi_{t,p} \,:\, \mathbb{R}^n \to \mathbb{R}^n, \quad t \in \mathbb{R},\, p \in P,$$

is called a cocycle on $\mathbb{R}^n$ with respect to a group Θ of mappings on P *if:*

1. $\phi_{0,p} = id$,
2. $\phi_{t+s,p} = \phi_{t,\theta_s p} \circ \phi_{s,p}$,

for all $t, s \in \mathbb{R}$, $p \in P$.

The reader should be able to verify that (7.5.7) is an example of a cocycle.

We show that the cocycle relation for nonautonomous vector fields given in (7.5.4) can be interpreted in terms of this general formalism. This can be seen as follows. Let $P = \mathbb{R}$, $\theta_t t_0 = t_0 + t$ and $t_0 \le t_0 + s \le t_0 + s + t$. Then we have:

$$\phi_{t+s,p} = x(t_0{+}s{+}t, t_0, x_0) = x(t_0{+}s{+}t, t_0{+}s, x(t_0{+}s, t_0, x_0)) = \phi_{t,\theta_s p} \circ \phi_{s,p}.$$

7.5C Dynamics Generated by a Bi-Infinite Sequence of Maps

There is yet another way to study the dynamics of nonautonomous vector fields. The dynamical systems point of view has taught us that it is often fruitful to study the trajectories of (7.0.1) by passing to an n-dimensional discrete time system, or *map*. We will explore this in some detail when we consider Poincaré maps in Chapter 10. In this setting the dynamical aspects of geometrical structures in phase space often appear more simple than in the continuous time setting. One reason for this is that the trajectories of time-dependent velocity fields may intersect themselves. The resulting

trajectory can appear very complicated, but when "sampled" at discrete time its discrete time analog may appear more simple, and any underlying geometrical structure may be more apparent.

There are a variety of ways of constructing a discrete time map from the trajectories of (7.0.1). However, the overriding issue is that the dynamics of the resulting discrete time system should somehow correlate with the dynamics of the continuous time system. The most straightforward way in which this connection can be made is if the trajectory of the velocity field interpolates the discrete set of points corresponding to the trajectory of the discrete time system.

With this in mind, we define the following n-dimensional map from trajectories of (7.0.1) as follows:

$$f_n(x_0) \equiv x\left(t_0 + nT,\, t_0 + (n-1)T,\, x_0\right), \tag{7.5.10}$$

where $T > 0$ is some fixed time increment and $n \in \mathbb{Z}$. We want to describe the evolution of x_0 in the vector field (7.0.1) in terms of the map (7.5.10). Unfortunately, this cannot be done in the case when the velocity field has an arbitrary time-dependence since generally

$$f_j(x_0) \neq f_k(x_0) \quad j \neq k.$$

Instead, we must use the bi-infinite sequence of maps

$$\{f_n(\cdot)\}, \quad n \in \mathbb{Z},$$

since the orbit of a point x_0 in the vector field (7.0.1), i.e.,

$$\{x \in \mathbb{R}^n \,|\, x = x(t, t_0, x_0),\, t \in \mathbb{R}\},$$

interpolates the following bi-infinite sequence of points.

$$\{\ldots, f_{-n} \circ f_{-n+1} \circ \cdots \circ f_{-1}(x_0), \ldots, f_{-1}(x_0),\, x_0,\, f_1(x_0), \\ \ldots, f_n \circ f_{n-1} \circ \cdots \circ f_1(x_0), \ldots\}.$$

We remark that in the usual situation studied in dynamical systems theory, if the velocity field is time periodic, with period T, then $f_j(\cdot) = f_k(\cdot), \quad \forall j,\, k \in \mathbb{Z}$. Some basic results for dynamics generated by sequences of maps (such as a stable and unstable manifold theorem) can be found in Katok and Hasselblatt [1995]; see also de Blasi and Schinas [1973] and Irwin [1973].

For the most part in this book we will be considering autonomous vector fields or maps constructed from nonautonomous vector fields (more specifically, maps constructed from time-periodic and quasiperiodic vector fields). Consequently, henceforth we will state definitions in the context of autonomous vector fields and maps.

7.6 Liouville's Theorem

Now we prove several results due to Liouville which describe the time evolution of volumes under a flow.

Consider a general autonomous vector field

$$\dot{x} = f(x), \qquad x \in \mathbb{R}^n,$$

and suppose that it generates a flow $\phi_t(\cdot)$. Let D_0 denote a domain in $\mathbb{R}^n$ and let $D_t \equiv \phi_t(D_0)$ denote the evolution of D_0 under the flow. Let $V(t)$ denote the volume of D_t. Then we have the following lemma.

Lemma 7.6.1

$$\left.\frac{dV}{dt}\right|_{t=0} = \int_{D_0} \nabla \cdot f dx,$$

where $\nabla \cdot f = \frac{\partial f_1}{\partial x_1} + \cdots + \frac{\partial f_n}{\partial x_n}$ *denotes the divergence of a vector field.*

Proof: From the definition of the Jacobian of a transformation we have

$$V(t) = \int_{D_0} \det \frac{\partial \phi_t(x)}{\partial x} dx. \tag{7.6.1}$$

By Taylor expanding the flow in t:

$$\phi_t(x) = x + f(x)t + \mathcal{O}(t^2),$$

it follows that

$$\frac{\partial \phi_t(x)}{\partial x} = \mathrm{id} + \frac{\partial f}{\partial x} t + \mathcal{O}(t^2),$$

where "id" denotes the $n \times n$ identity matrix. Using this relation, and a standard result from linear algebra on the expansion of the determinant (see, e.g., Arnold [1973], Sec. 16.3), we obtain

$$\begin{aligned} \det \frac{\partial \phi_t(x)}{\partial x} &= \det \left(id + \frac{\partial f}{\partial x} t \right) + \mathcal{O}(t^2), \\ &= 1 + \mathrm{tr} \left(\frac{\partial f}{\partial x} \right) t + \mathcal{O}(t^2). \end{aligned}$$

Substituting this expression into (7.6.1) gives

$$V(t) = V(0) + \int_{D_0} t \nabla \cdot f dx + \mathcal{O}(t^2),$$

from which the lemma follows immediately. □

Now there is nothing distinguished about the point $t = 0$. In particular, Lemma 7.6.1 can be written in the form

$$\left.\frac{dV}{dt}\right|_{t=t_0} = \int_{D_{t_0}} \nabla \cdot f dy, \tag{7.6.2}$$

for an arbitrary $t_0 \neq 0$. This can be seen as follows. Let

$$y = \phi_{t_0}(x),$$

for some arbirary $t_0 \neq 0$. Then

$$V(t) = \int_{D_{t_0}} \det \frac{\partial \phi_t(y)}{\partial y} dy.$$

Now

$$\phi_t(y) = y + f(y)t + \mathcal{O}(t^2),$$

and

$$\frac{\partial \phi_t(y)}{\partial y} = \mathrm{id} + \frac{\partial f}{\partial y} t + \mathcal{O}(t^2).$$

Using these three formulas we can repeat exactly the same steps as in the proof of Lemma 7.6.1 to conclude that (7.6.2) holds.

We can use these results to derive equations for the time evolution of volumes which can be explicitly solved in certain cases.

Suppose that the divergence is everywhere constant, i.e.,

$$\nabla \cdot f = c = \text{constant}.$$

Using (7.6.2), since t_0 is arbitrary the evolution equation for the volume is given by

$$\dot{V} = cV,$$

which has the obvious solution

$$V(t) = e^{ct} V(0). \tag{7.6.3}$$

In the case where the vector field is *divergence free* (i.e., $c = 0$), we have the following result that is typically referred to as *Liouville's Theorem*.

Theorem 7.6.2 (Liouville) *Suppose $\nabla \cdot f = 0$. Then for any region D_0,*

$$V(t) = V(0),$$

where $V(0)$ is the volume of D_0 and $V(t)$ is the volume of $\phi_t(D_0)$.

Proof: This follows immediately from (7.6.3) by setting $c = 0$. □

7.6A Volume Preserving Vector Fields and the Poincaré Recurrence Theorem

We refer to vector fields which have zero divergence as *divergence free* or *volume preserving* vector fields.

Volume preserving dynamical systems, which we think of as flows generated by divergence free vector fields or volume preserving maps, may have a certain recurrence property that is attributed to Poincaré. We now prove this Poincaré recurrence theorem.

Theorem 7.6.3 (Poincaré Recurrence Theorem) *Suppose $g : \mathbb{R}^n \to \mathbb{R}^n$ is a continuous, one-to-one mapping, and suppose that $D \subset \mathbb{R}^n$ is a compact invariant set, i.e., $g(D) = D$. Let $\bar{x}$ be any point in D and let U be any neighborhood of $\bar{x}$. Then there exists a point $x \in U$ such that $g^n(x) \in U$ for some $n > 0$.*

Proof: Consider the sets defined by the images of U under iteration by g:

$$U, g(U), g^2(U), \ldots, g^n(U), \ldots.$$

Since g is volume-preserving, each of these has the same volume. If they never intersected, then D would have infinite volume. But D is compact, therefore there must exist integers $k \geq 0$, $l \geq 0$, with $k > l$, such that

$$g^k(U) \cap g^l(U) \neq \emptyset.$$

Therefore

$$g^{k-l}(U) \cap U \neq \emptyset.$$

If we let $y = g^{k-l}(x)$, then $x \in U$ and $g^n(x) \in U$, where $n \equiv k - l$. □

7.7 Exercises

1. Consider the stable and unstable manifolds of a hyperbolic fixed point of saddle-type of a $\mathbf{C}^r$ $(r \geq 1)$ vector field.

   a) Can the stable (resp., unstable) manifold intersect itself?

   b) Can the stable (resp., unstable) manifold intersect the stable (resp., unstable) manifold of another fixed point?

   c) Can the stable manifold intersect the unstable manifold? If so, can the intersection consist of a discrete set of points?

   d) Can the stable (resp., unstable) manifold intersect a periodic orbit?

   These questions are independent of the dimension of the vector field (as long as it is finite); however, justify each of your answers with a geometrical argument for vector fields on $\mathbb{R}^2$. (*Hint:* the key to this problem is uniqueness of solutions.)

2. Consider the stable and unstable manifolds of a hyperbolic fixed point of saddle-type of a $\mathbf{C}^r$ $(r \geq 1)$ diffeomorphism.

   a) Can the stable (resp., unstable) manifold intersect itself?

b) Can the stable (resp., unstable) manifold intersect the stable (resp., unstable) manifold of another fixed point?

c) Can the stable manifold intersect the unstable manifold? If so, can the intersection consist of a discrete set of points?

These questions are independent of the dimension of the diffeomorphism (as long as it is finite); however, justify each of your answers with a geometrical argument for diffeomorphisms on $\mathbb{R}^2$. Are the arguments the same as for vector fields?

3. Consider the $\mathbf{C}^r$ $(r \geq 1)$ vector field

$$\dot{x} = f(x), \qquad x \in \mathbb{R}^n.$$

Let $\phi_t(x)$ denote the flow generated by this vector field, which we assume exists for all $t \in \mathbb{R}$, $x \in \mathbb{R}^n$. Suppose that the vector field has a hyperbolic fixed point at $x = \bar{x}$ having an s-dimensional stable manifold, $W^s(\bar{x})$, and a u-dimensional unstable manifold, $W^u(\bar{x})$ $(s+u=n)$. The typical way of proving their existence (see, e.g., Palis and deMelo [1982] or Fenichel [1971]) is to prove the existence of the local manifolds $W^s_{\rm loc}(\bar{x})$ and $W^u_{\rm loc}(\bar{x})$ via a contraction mapping type of argument. Then the global manifolds are defined by

$$W^s(\bar{x}) = \bigcup_{t \leq 0} \phi_t(W^s_{\rm loc}(\bar{x})),$$

$$W^u(\bar{x}) = \bigcup_{t \geq 0} \phi_t(W^u_{\rm loc}(\bar{x})).$$

a) Show that $W^s(\bar{x})$ and $W^u(\bar{x})$ defined in this way are invariant for *all* $t \in \mathbb{R}$.

b) If $W^s_{\rm loc}(\bar{x})$ and $W^u_{\rm loc}(\bar{x})$ are $\mathbf{C}^r$, does it follow by this definition that $W^s(\bar{x})$ and $W^u(\bar{x})$ are $\mathbf{C}^r$?

c) Discuss this definition of the stable and unstable manifolds in the context of how one might compute the manifolds numerically.

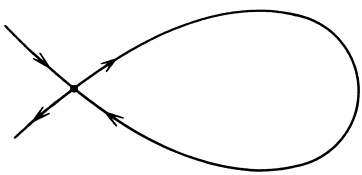

FIGURE 7.7.1.

4. Consider the situation described in the previous exercise in the context of $\mathbf{C}^r$ diffeomorphisms. Existence of stable and unstable manifolds of a hyperbolic fixed point is proved similarly (i.e., local manifolds are shown to exist via a contraction mapping argument), and the global manifolds are defined by

$$W^s(\bar{x}) = \bigcup_{n \leq 0} g^n(W^s_{\rm loc}(\bar{x})),$$

$$W^u(\bar{x}) = \bigcup_{n \geq 0} g^n(W^u_{\rm loc}(\bar{x})),$$

where g denotes the diffeomorphism and $\bar{x}$ the hyperbolic fixed point. Answer a), b), and c) from the previous exercise in the context of $\mathbf{C}^r$ diffeomorphisms.

5. Consider a hyperbolic fixed point of a $\mathbf{C}^r$ $(r \geq 1)$ vector field on $\mathbb{R}^2$ whose stable and unstable manifolds intersect along a homoclinic orbit, as shown in Figure 7.7.1. Show that any point on the homoclinic orbit cannot reach the fixed point in finite time.

6. Consider a periodic orbit (of either a $\mathbf{C}^r$ $(r \geq 1)$ vector field or map) that is contained in a compact region of phase space. Can the period of the orbit be infinite?

7. Consider the Lorenz equations:

$$\begin{aligned} \dot{x} &= \sigma(y - x), \\ \dot{y} &= \rho x - y - xz, \qquad \sigma, \beta, \rho \geq 0. \\ \dot{z} &= -\beta z + xy, \end{aligned}$$

   Describe the time evolution of volume elements under the flow generated by this vector field.

8. Does the divergence free property of a vector field imply that the vector field has a first integral?

9. Consider the vector field:

$$\dot{x} = -x + \sin t.$$

   The solution through the point x_0 at t_0 is given by:

$$x(t; t_0, x_0) = \frac{1}{2}(\sin t - \cos t) + \left(x_0 + \frac{1}{2}\cos t_0 - \frac{1}{2}\sin t_0\right) e^{-(t-t_0)}.$$

   Construct a skew-product flow.

10. Consider the vector field:

$$\dot{x} = -x + t.$$

   The solution through the point x_0 at t_0 is given by:

$$x(t; x_0, t_0) = t - 1 + (x_0 - t_0 + 1)e^{-(t-t_0)}.$$

   Construct a skew-product flow.

8

Asymptotic Behavior

We now develop a technical apparatus to deal with the notions of "long term" and "observable" behavior of orbits of dynamical systems. We will be concerned with $\mathbf{C}^r$ $(r \geq 1)$ maps and autonomous vector fields on $\mathbb{R}^n$ denoted as follows.

$$\textit{Vector Field:} \qquad \dot{x} = f(x), \qquad x \in \mathbb{R}^n, \tag{8.0.1}$$

$$\textit{Map:} \qquad x \mapsto g(x), \qquad x \in \mathbb{R}^n. \tag{8.0.2}$$

The *flow* generated by (8.0.1) (see Chapter 7) will be denoted as $\phi(t, x)$.

8.1 The Asymptotic Behavior of Trajectories

As we shall see in Chapter 9, the Poincaré-Bendixson theorem characterizes the nature of the ω and α limit sets of flows on certain two manifolds. We now define ω and α limit sets.

Definition 8.1.1 (ω and α Limit Points of Trajectories) *A point $x_0 \in \mathbb{R}^n$ is called an* ω limit point *of $x \in \mathbb{R}^n$, denoted $\omega(x)$, if there exists a sequence $\{t_i\}$, $t_i \longrightarrow \infty$, such that*

$$\phi(t_i, x) \longrightarrow x_0.$$

α limit points *are defined similarly by taking a sequence $\{t_i\}$, $t_i \longrightarrow -\infty$.*

Example 8.1.1. Consider a vector field on the plane with a hyperbolic saddle point, x, as shown in Figure 8.1.1. Then x is the ω limit point of any point on the stable manifold and the α limit point of any point on the unstable manifold.

End of Example 8.1.1

Example 8.1.2. This example shows why it is necessary to take a subsequence in time, $\{t_i\}$, and not to simply let $t \uparrow \infty$ in the definition of the α and ω limit point. Consider a vector field on the plane with a globally attracting closed orbit, γ, as shown in Figure 8.1.2. Then orbits not starting on γ "wrap onto" γ.

Now for each point on γ, we can find a subsequence $\{t_i\}$ such that $\phi(t_i, x)$, $x \in \mathbb{R}^2$, approaches that point as $i \uparrow \infty$. Therefore, γ is the ω limit set of x as you would expect. However, $\lim_{t \to \infty} \phi(t, x) \neq \gamma$.

End of Example 8.1.2

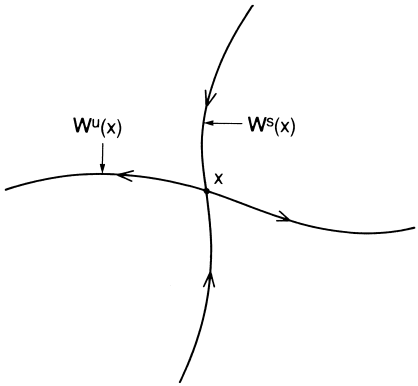

FIGURE 8.1.1. ω and α limit sets of the hyperbolic fixed point x.

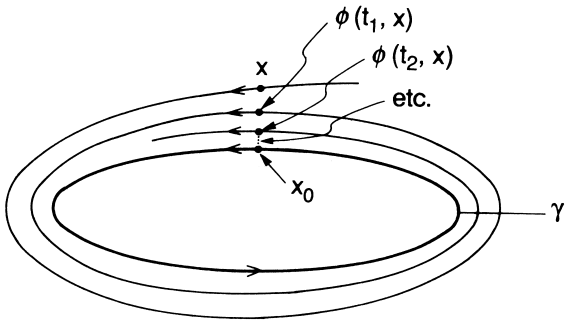

FIGURE 8.1.2. The point $x_0 \in \gamma$ is the ω limit point of x.

Definition 8.1.2 (ω and α Limit Sets of a Flow) *The set of all ω limit points of a flow or map is called the* ω limit set. *The α limit set is similarly defined.*

We will need the idea of α and ω limit sets in the context of flows only, so we leave it to the reader to modify Definition 8.1.2 for maps as an exercise. The following result describes some basic properties of α and ω limit sets of trajectories.

Proposition 8.1.3 (Properties of ω Limit Points) *Let $\phi_t(\cdot)$ be a flow generated by a vector field and let $\mathcal{M}$ be a positively invariant compact set for this flow. Then, for $p \in \mathcal{M}$, we have*

i) $\omega(p) \neq \emptyset$;

ii) $\omega(p)$ *is closed;*

iii) $\omega(p)$ *is invariant under the flow, i.e., $\omega(p)$ is a union of orbits;*

iv) $\omega(p)$ *is connected.*

Proof: i) Choose a sequence $\{t_i\}$, $\lim_{i\to\infty} t_i = \infty$, and let $\{p_i = \phi_{t_i}(p)\}$. Since $\mathcal{M}$ is compact, $\{p_i\}$ has a convergent subsequence whose limit belongs to $\omega(p)$. Thus, $\omega(p) \neq \emptyset$.

ii) It suffices to show that the complement of $\omega(p)$ is open. Choose $q \notin \omega(p)$. Then there must exist some neighborhood of q, $U(q)$, that is disjoint from the set of points $\{\, \phi_t(p) \mid t \geq T \,\}$ for some $T > 0$. Hence, q is contained in some open set that contains no points in $\omega(p)$. Since q is arbitrary, we are done.

iii) Let $q \in \omega(p)$ and $\tilde{q} = \phi_s(q)$. Choose a sequence $t_i \longrightarrow \infty$ as $i \uparrow \infty$ with $\phi_{t_i}(p) \to q$. Then $\phi_{t_i+s}(p) = \phi_s\big(\phi_{t_i}(p)\big)$ (cf. the notation for flows following Proposition 7.4.3) converges to $\tilde{q}$ as $i \to \infty$. Hence, $\tilde{q} \in \omega(p)$, and therefore $\omega(p)$ is invariant. However, there is a slight hole in this argument that needs to be filled; namely, it is not immediately obvious that $\phi_s(\cdot)$ exists for all s.

We begin by arguing that $\phi_s(q)$ exists for $s \in (-\infty, \infty)$ *when* $q \in \omega(p)$. It should be clear that this is true for $s \in (0, \infty)$ since $\mathcal{M}$ is a positively invariant compact set (cf. Theorem 1.1.9). Therefore, it suffices to show that this is true for $s \in (-\infty, 0]$.

Now $q \in \omega(p)$, so by definition we can find a sequence $\{t_i\}$, $t_i \longrightarrow \infty$ as $i \uparrow \infty$, such that $\phi_{t_i}(p) \to q$ as $i \to \infty$. Let us order the sequence so that $t_1 < t_2 < \cdots < t_n < \cdots$. Next consider $\phi_s\big(\phi_{t_i}(p)\big)$. By Proposition 7.4.3 this is valid for $s \in [-t_i, 0]$. Taking the limit as $i \to \infty$ and using continuity as well as the fact that $\phi_{t_i} \to q$ as $i \to \infty$, we see that $\phi_s(q)$ exists for $s \in (-\infty, 0]$.

iv) The proof is by contradiction. Suppose $\omega(p)$ is not connected. Then we can choose open sets V_1, V_2 such that $\omega(p) \subset V_1 \cup V_2$, $\omega(p) \cap V_1 \neq \emptyset$, $\omega(p) \cap V_2 \neq \emptyset$, and $\bar{V}_1 \cap \bar{V}_2 = \emptyset$. The orbit of p accumulates on points in both V_1 and V_2; hence, for any given $T > 0$, there exists $t > T$ such that $\phi_t(p) \in \mathcal{M} - (V_1 \cup V_2) = K$. Therefore we can find a sequence $\{t_n\}$, $t_n \longrightarrow \infty$ as $n \uparrow \infty$, with $\phi_{t_n}(p) \in K$. Passing to a subsequence, if necessary (K is compact), we have $\phi_{t_n}(p) \to q$, $q \in K$. But this implies that $q \in V_1 \cup V_2$. However, our construction indicates that q is also in $\omega(p)$. This is a contradiction. □

One can prove a similar result for α limit sets provided the hypotheses of the proposition are satisfied for the time reversed flow.

For maps, the notion of a nonwandering point has been more fashionable; however, we will explore the relationship between these two concepts in the exercises.

Definition 8.1.4 (Nonwandering Points) *A point x_0 is called* nonwandering *if the following holds.*

Flows: *For* any *neighborhood* U *of* x_0 *and* $T > 0$*, there exists some* $|t| > T$ *such that*

$$\phi(t, U) \cap U \neq \emptyset.$$

Maps: *For* any *neighborhood* U *of* x_0*, there exists some* $n \neq 0$ *such that*

$$g^n(U) \cap U \neq \emptyset.$$

Note that if the map is noninvertible, then we must take $n > 0$.

Fixed points and periodic orbits are nonwandering.

Definition 8.1.5 (Nonwandering Set) *The set of all nonwandering points of a map or flow is called the* nonwandering set *of that particular map or flow.*

8.2 Attracting Sets, Attractors, and Basins of Attraction

Definitions 8.1.2 and 8.1.4 do not address the question of stability of those asymptotic motions. For this we want to develop the idea of an attractor.

Definition 8.2.1 (Attracting Set) *A closed invariant set* $A \subset \mathbb{R}^n$ *is called an* attracting set *if there is some neighborhood* U *of* A *such that:*

flows: $\forall t \geq 0, \quad \phi(t, U) \subset U \quad$ *and* $\quad \bigcap_{t>0} \phi(t, U) = A.$

maps: $\forall n \geq 0, \quad g^n(U) \subset U \quad$ *and* $\quad \bigcap_{n>0} g^n(U) = A.$

Definition 8.2.2 (Trapping Region) *The open set* U *in Definition 8.2.1 is often referred to as a* trapping region.

A similar definition can be given for maps. By now the necessary modifications should be obvious, and we leave the details as an exercise for the reader.

It should be evident to the reader that finding a Liapunov function is equivalent to finding a trapping region (cf. Chapter 2). Also, let us mention a technical point; by Theorem 7.1.1 it follows that all solutions starting in a trapping region exist for all positive times. This is useful in noncompact phase spaces such as $\mathbb{R}^2$ for proving existence on semi-infinite time intervals.

In the continuous time case, one "tests" whether or not a region is a candidate to be a trapping region by evaluating the vector field on the boundary of the region in question. If, on the boundary of the region, the vector field is pointing toward the interior of the region, or is tangent to the boundary, then the region in question is a trapping region. However,

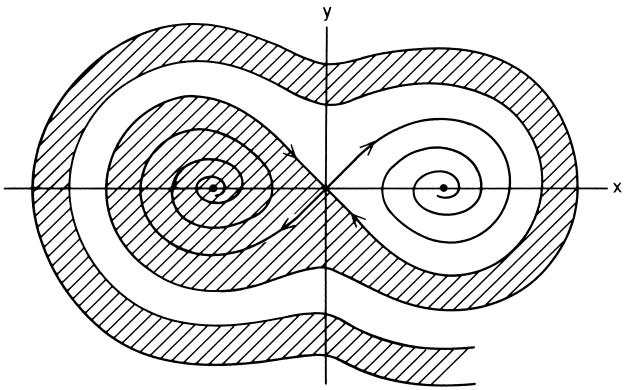

FIGURE 8.2.1. Basins of attractions of the sinks.

in order that this test can be carried out, one needs that the boundary of the region must be (at least) C^1.

There is another idea related to trapping regions that is becoming more commonly used in some areas. This is the notion of an *absorbing set*, which we now define.

Definition 8.2.3 (Absorbing set) *A positive invariant compact subset $B \subset \mathbb{R}^n$ is called an* absorbing set *if there exists a bounded subset of $\mathbb{R}^n$, U, with $U \supset B$, and:*

flows: *$t_U > 0$ such that $\phi(t, U) \subset B$, $\forall t \geq t_U$.*

maps: *$n_U > 0$ such that $g^n(U) \subset B$, $\forall n \geq n_U$.*

If we have an attracting set it is natural to ask which points in phase space approach the attracting set asymptotically.

Definition 8.2.4 (Basin of Attraction) *The* domain or basin of attraction *of an attracting set A is given by*

flows: $\displaystyle\bigcup_{t \leq 0} \phi(t, U),$

maps: $\displaystyle\bigcup_{n \leq 0} g^n(U),$

where U is any open set satisfying Definition 8.2.1.

We remark that the basin of attraction is independent of the choice of the open set U, provided that U satisfies Definition 8.2.1.

Note that even if g is noninvertible, g^{-1} still makes sense in a set theoretic sense. Namely, $g^{-1}(U)$ is the set of points in $\mathbb{R}^n$ that maps into U under g; g^{-n}, $n > 1$ is then defined inductively.

Example 8.2.1 (Application to the Unforced Duffing Oscillator).

As we've seen, the unforced Duffing oscillator has, for $\delta > 0$, two attractors which are fixed points. The boundaries of the domains of attraction for the two attractors are defined by the stable manifold of the saddle of the origin (see Figure 8.2.1).

End of Example 8.2.1

Now we want to motivate the idea of an *attractor* as opposed to attracting set. We do this with the following example taken from Guckenheimer and Holmes [1983].

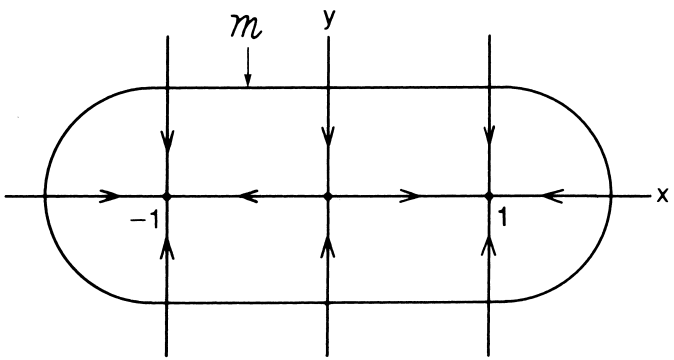

FIGURE 8.2.2. Attracting set of Example 1.8.3.

Example 8.2.2. Consider the planar autonomous vector field

$$\begin{aligned} \dot{x} &= x - x^3, \\ \dot{y} &= -y, \qquad (x, y) \in \mathbb{R}^1 \times \mathbb{R}^1. \end{aligned}$$

This vector field has a saddle at $(0, 0)$ and two sinks at $(\pm 1, 0)$. The y-axis is the stable manifold of $(0, 0)$. We choose an ellipse, $\mathcal{M}$, containing the three fixed points as shown in Figure 8.2.2.

It should be clear that $\mathcal{M}$ is a trapping region and that the closed interval $[-1, 1] = \bigcap_{t \geq 0} \phi(t, \mathcal{M})$ is an attracting set.

End of Example 8.2.2

Example 8.2.2 points out what some might regard as a possible deficiency in our Definition 8.2.1 of an attracting set. In this example, almost all points in the plane will *eventually* end up near one of the sinks. Hence, the attracting set, the interval $[-1, 1]$, contains two *attractors*, the sinks $(\pm 1, 0)$. Therefore, if we are interested in describing where most points in phase space ultimately go, the idea of an attracting set is not quite

precise enough. Somehow we want to incorporate into the definition of an attracting set the notion that it is not a collection of distinct *attractors*, but rather that all points in the attracting set eventually come arbitrarily close to every other point in the attracting set under the evolution of the flow or map. We now want to make this mathematically precise.

Definition 8.2.5 (Topological Transitivity) *A closed invariant set A is said to be* topologically transitive *if, for any two open sets U, $V \subset A$*

flows: $\exists\ t \in \mathbb{R} \ni \phi(t, U) \cap V \neq \emptyset$,

maps: $\exists\ n \in \mathbb{Z} \ni g^n(U) \cap V \neq \emptyset$.

Definition 8.2.6 (Attractor) *An* attractor *is a topologically transitive attracting set.*

We remark that the study of attractors and their basin boundaries in dynamical systems is rapidly evolving and, consequently, the theory is incomplete. For more information see Conley [1978], Guckenheimer and Holmes [1983], Milnor [1985], and Ruelle [1981].

8.3 The LaSalle Invariance Principle

Here we describe an application of the invariance of ω limit sets of a trajectory that is very useful for stability issues. It is referred to as the *LaSalle invariance principle* (LaSalle [1968]).

We first develop the set-up. Let

$$\dot{x} = f(x), \qquad x \in \mathbb{R}^n,$$

denote a C^r, $r \geq 1$ vector field. Let $\mathcal{M} \subset \mathbb{R}^n$ be a positively invariant compact set under the flow, $\phi_t(\cdot)$, generated by this vector field, which is the closure of some open set (so that it has nonempty interior) and whose boundary is (at least) C^1. Therefore $\mathcal{M}$ is a trapping region. Let $V(x)$ be a Liapunov function on $\mathcal{M}$. By this we mean that $\dot{V} \leq 0$ on $\mathcal{M}$. Note that we are using the term Liapunov function differently than was used in Chapter 2. There Liapunov function was a local notion defined in the neighborhood of an equilibrium point. Now we will consider a more global notion. Consider the following two sets.

$$E \equiv \left\{ x \in \mathcal{M} \,|\, \dot{V}(x) = 0 \right\},$$

$$M \equiv \left\{ \begin{array}{l} \text{The union of all trajectories that start in } E \\ \text{and remain in } E \text{ for all } t > 0. \end{array} \right\}$$

M is the "positively invariant part" of E. Now we can state the LaSalle invariance principle.

Theorem 8.3.1 (LaSalle, 1968) *For all $x \in \mathcal{M}$, $\phi_t(x) \to M$ as $t \to \infty$.*

Proof: First we argue that $V = \chi =$ constant on $\omega(x)$ (see also Theorem 15.0.3). This can be seen as follows. Suppose $\bar{x} \in \omega(x)$ and let $\chi = V(\bar{x})$, then χ is the greatest lower bound of the set $\{V(\phi_t(x)) \,|\, t \geq 0\}$. This follows from the fact that $V(x)$ decreases along trajectories (hence $V(\phi_{t_i}(x)) \geq V(\phi_t(x)) \geq V(\phi_{t_{i+1}}(x))$ for $t_i \leq t \leq t_{i+1}$) and by the continuity of $V(x)$. From Proposition 8.1.3 the omega limit set of a trajectory is invariant, hence $\phi_t(\bar{x})$ is also an omega limit point of $\phi_t(x)$. Then, since χ is the greatest lower bound of the set $\{V(\phi_t(x)) \,|\, t \geq 0\}$, $V(\phi_t(\bar{x})) = \chi$.

From this it follows that $\dot{V} = 0$ on $\omega(x)$. Then, by the definition of E, $\omega(x) \subset E$. Since $\omega(x)$ is invariant (Proposition 8.1.3), it follows by the definition of M that $\omega(x) \subset M$. Therefore, $\phi_t(x) \to M$ as $t \to \infty$. □

This result is particularly useful when one has information about M. For example, consider the Duffing equation

$$\begin{aligned} \dot{x} &= y, \\ \dot{y} &= x - x^3 - \delta y, \qquad (x, y) \in \mathbb{R}^2, \quad \delta > 0. \end{aligned}$$

Now consider the function

$$V(x, y) = \frac{y^2}{2} - \frac{x^2}{2} + \frac{x^4}{4}.$$

It is easy to verify that

$$\dot{V} = -\delta y^2.$$

Now consider the level set $V = c$ for c very large, but finite. This curve defines the boundary of a positively invariant compact set. E is given by the intersection of the x axis with this set and M is the three equilbrium points on the x axis. The LaSalle invariance principle states that all trajectories converge to one of the equilibrium points.

This example shows the relation between the Liapunov function V and the trapping region $\mathcal{M}$ that often arises in specific applications. One first constructs a candidate for a Liapunov function. Then certain level sets of this function may be used to define $\mathcal{M}$.

We remark that the LaSalle invariance principle can be generalized considerably. In particular, versions exist for situations where we have nonuniqueness of trajectories, finite time blow up of trajectories, and for discrete time dynamical systems, see LaSalle [1968] for details and references.

8.4 Attraction in Nonautonomous Systems

The notions of attracting set, basin of attraction, and attractor developed in this chapter may not be adequate to describe the same phenomena in

nonautonomous systems. [1] In the nonautonomous setting attracting sets and basins of attraction may vary in time and the attraction rates my be nonuniform. The paper of Kloeden and Schmalfuss [1997] is tutorial in nature and provides an excellent introduction to the main issues. See also Kloeden and Stonier [1998], Knyazhishche and Shavel [1995], Liu [1993], and Yoshizawa [1985].

We discuss some aspects of attraction in nonautonomous systems following Kloeden and Schmalfuss [1997] and Grüne and Kloeden [2001].

First, for nonautonomous systems a different notion of convergence of solutions to a specific solution arises. We begin with some motivation for this. Consider the following one-dimensional, linear nonautonomous vector field:

$$\dot{x} = -x + g(t), \quad x \in \mathbb{R}. \tag{8.4.1}$$

Using the variation of constants formula, it is easily computed that the trajectory through the point x_0 at $t = t_0$ is given by:

$$x(t, t_0, x_0) = x_0 e^{-(t-t_0)} + e^{-t} \int_{t_0}^{t} e^s g(s) ds, \tag{8.4.2}$$

where the function $g(s)$ needs to be defined in such a way that the integral makes sense, say continuous with no more than polynomial growth in s as $s \to \pm\infty$.

It is a simple matter to conclude by examining (8.4.2) that all trajectories of (8.4.1) converge to the trajectory

$$\phi(t) = e^{-t} \int_{-\infty}^{t} e^s g(s) ds, \tag{8.4.3}$$

as $t \to \infty$ (the reader should verify that (8.4.3) is indeed a trajectory of (8.4.1)). This is called *forward convergence* and is mathematically expressed as:

$$\lim_{t\to\infty} |x(t, t_0, x_0) - \phi(t)| = 0, \quad t_0,\, x_0 \quad \text{fixed.} \tag{8.4.4}$$

Hence, forward convergence is a property that is verified in the limit as $t \to \infty$. However, suppose we were interested in a different, but related question. Namely, for the trajectory $\phi(t)$, and a fixed, finite time t, characterize convergence of trajectories to $\phi(t)$ at the time t. This is a more practical question from the point of view of applications, as well as numerical analysis, and give rise to the notion of *pullback convergence*, which is mathematically expressed as follows:

$$\lim_{t_0\to-\infty} |x(t, t_0, x_0) - \phi(t)| = 0, \quad t,\, x_0 \quad \text{fixed.} \tag{8.4.5}$$

[1] Of course, if the vector field is time periodic then one can reduce the problem to the study of a Poincaré map (see Chapter 10) and then the results for maps apply immediately.

Notice that (8.4.3) is the only trajectory which all trajectories of (8.4.1) converge to as $t_0 \to \infty$ (with t fixed). However, there are many trajectories to which all trajectories of (8.4.1) converge to as $t \to \infty$ (with t_0 fixed). For example, all trajectories of (8.4.1) converge to

$$\bar{\phi}(t) = e^{-t} \int_{t_0}^{t} e^s g(s) ds,$$

for any fixed t_0.

For nonautonomous systems pullback convergence and forward convergence are independent notions (see Exercises 16 and 17). However, they are equivalent for autonomous systems. Essentially this follows from Proposition 7.4.1 which states that solutions of autonomous systems depend only on the "elapsed time", $t - t_0$. Hence, letting $t \to \infty$, with t_0 fixed, is equivalent to letting $t_0 \to -\infty$, with t fixed.

The history of pullback convergence is discussed briefly in Grüne and Kloeden [2001] who give much credit to the development of the idea to Krasnosel'skii [2001].

The notion of pullback convergence seems natural for defining attractors in nonautonomous systems, as we now describe. First, we establish some general notation. We begin by defining two notions of the distance between compact subsets of $\mathbb{R}^n$.

Definition 8.4.1 (Hausdorff Separation) *Let A and B be two nonempty, compact subsets of $\mathbb{R}^n$. The Hausdorff separation of A and B, denoted $H^*(A, B)$, is defined as:*

$$H^*(A, B) \equiv \max_{a \in A} \operatorname{dist}(\mathrm{a}, \mathrm{B}) = \max_{\mathrm{a} \in \mathrm{A}} \min_{\mathrm{b} \in \mathrm{B}} |\mathrm{a} - \mathrm{b}|. \tag{8.4.6}$$

Now we can define the Hausdorff metric.

Definition 8.4.2 (Hausdorff Metric)

$$H(A, B) \equiv \max \left(H^*(A, B), H^*(B, A) \right). \tag{8.4.7}$$

Now we can address the issue of attraction in the pullback sense using the language of cocycles developed in Chapter 7. Let $\phi_{t,p}$, $t \in \mathbb{R}$, $p \in P$ denote a cocycle on $\mathbb{R}^n$ with respect to the group Θ of mappings on P (see Definition 7.5.1).

Definition 8.4.3 (Pullback Attracting Set) *A family $\hat{A} = \{A_p, p \in P\}$ of compact subsets of $\mathbb{R}^n$ is called a* pullback attracting set of a cocycle $\{\phi_{t,p}, t \in \mathbb{R}, p \in P\}$ on $\mathbb{R}^n$ *if it is invariant in the sense that:*

$$\phi_{t,p}(A_p) = A_{\theta_t p}, \; t \in \mathbb{R}, \; p \in P,$$

and pullback attracting *in the sense that for every A_p there exists a bounded subset of $\mathbb{R}^n$, $D_p \supset A_p$, such that*

$$\lim_{t\to\infty} H^*\left(\phi_{t,\theta_{-t}p}(D_{\theta_{-t}p}), A_p\right) = 0.$$

The existence of a pullback attracting set is established through the notion of a *pullback absorbing family*, which we now define (compare with the definition of absorbing set given in Definition 8.2.3).

Definition 8.4.4 (Pullback Absorbing Family) *A family*

$$\hat{B} = \{B_p,\, p \in P\},$$

of compact subsets of $\mathbb{R}^n$ is called a pullback absorbing family for a cocycle $\{\phi_{t,p},\, t \in \mathbb{R}, p \in P\}$ on $\mathbb{R}^n$ if for each $p \in P$ there is a bounded subset of $\mathbb{R}^n$, U_p, satisfying $U_p \supset B_p$, and a time $t_{U_p} > 0$ such that:

$$\phi_{t,\theta_{-t}p}(U_{\theta_{-t}p}) \subset B_p, \quad \textit{for all} \quad t \geq t_{U_p}.$$

Now we can state the main theorem on the existence of pullback attracting sets.

Theorem 8.4.5 *Let $\{\phi_{t,p},\, t \in \mathbb{R}, p \in P\}$ be a cocycle of continuous mappings on $\mathbb{R}^n$ with a pullback absorbing family $\hat{B} = \{B_p,\, p \in P\}$. Then there exists a pullback attracting set $\hat{A} = \{A_p,\, p \in P\}$ with components uniquely determined by:*

$$A_p = \bigcap_{\tau\geq 0} \overline{\bigcup_{t\geq\tau} \phi_{t,\theta_{-t}p}\left(B_{\theta_{-t}p}\right)}.$$

Various versions of this theorem are discussed in Grüne and Kloeden [2001], where the notion of Lyapunov functions for pullback attracting sets is also discussed.

8.5 Exercises

1. Let $\phi_t(x)$ denote a flow generated by a $\mathbf{C}^r$ $(r \geq 1)$ vector field on $\mathbb{R}^n$ that exists for all $x \in \mathbb{R}^n$, $t \in \mathbb{R}$.

   1) Show that the α and ω limit sets of the flow are contained in the nonwandering set of the flow.

   2) Is the nonwandering set contained in the union of the α and ω limit set?

2. Prove that the basin of attraction is independent of the choice of the open set U, provided that U satisfies Definition 8.2.1.

3. Suppose A is an attracting set (of either a vector field or map), and suppose that $\bar{x} \in A$ is a hyperbolic fixed point of saddle-type. Must the following be true

1) $W^s(\bar{x}) \subset A$,
2) $W^u(\bar{x}) \subset A$?

4. Consider the union of the homoclinic orbit and the hyperbolic fixed point that it connects (shown in Figure 7.7.1). Can this set be an attracting set?

5. Consider the $\mathbf{C}^r$ $(r \geq 1)$ diffeomorphism

$$x \mapsto g(x), \qquad x \in \mathbb{R}^n.$$

Suppose that $\det Dg(x) = 1 \; \forall \, x \in \mathbb{R}^n$. Prove that the diffeomorphism preserves volume.

6. Consider the following vector field on $\mathbb{R}^2$.

$$\begin{pmatrix} \dot{x}_1 \\ \dot{x}_2 \end{pmatrix} = \begin{pmatrix} -\lambda & 0 \\ 0 & \lambda \end{pmatrix} \begin{pmatrix} x_1 \\ x_2 \end{pmatrix}, \qquad \lambda > 0.$$

The stable manifold of the origin is given by

$$W^s(0,0) = \Big\{ (x_1, x_2) \in \mathbb{R}^2 \,|\, x_2 = 0 \Big\}.$$

Consider a line segment contained in $W^s(0,0)$. Under the evolution of the flow generated by the vector field the length of the line segment shrinks to zero as $t \to \infty$. Does this violate the result of Exercise 5? Why or why not?

7. Consider the $\mathbf{C}^r$ $(r \geq 1)$ diffeomorphism

$$x \mapsto g(x), \qquad x \in \mathbb{R}^n.$$

Suppose $x = \bar{x}$ is a nonwandering point, i.e., for any neighborhood U of $\bar{x}$, there exists an $n \neq 0$ such that $g^n(U) \cap U \neq \emptyset$ (cf. Definition 8.1.4). Is it possible that there may exist only one such n, or, if there exists one n, must there be a countable (infinity?) of such n? Does the same result hold for flows?

8. Let B be an absorbing set. Show that:

$$\bigcap_{t \geq 0} \phi(t, B),$$

is an attracting set.

9. Describe the relation between trapping regions and absorbing sets.

10. Apply the LaSalle Invariance principle to the vector field

$$\begin{aligned} \dot{x} &= x - x^3, \\ \dot{y} &= -y, \qquad (x, y) \in \mathbb{R}^2, \end{aligned}$$

and conclude that all trajectories converge to one of the equilibrium points.

11. Consider the simple harmonic oscillator

$$\begin{aligned} \dot{x} &= y, \\ \dot{y} &= -x, \qquad (x, y) \in \mathbb{R}^2. \end{aligned}$$

Using

$$V(x, y) = \frac{1}{2} \left(x^2 + y^2 \right),$$

as a Liapunov function, what does the LaSalle invariance principle say about this system?

12. Suppose that $\mathcal{M}$ is a positively invariant compact set for a flow $\phi_t(\cdot)$, which is the closure of some open set and has a C^1 boundary, and that V is a strict Liapunov function on $\mathcal{M} - \{\text{equilibrium points}\}$. Then show that all trajectories converge to an equilibrium point.

13. With M and $\mathcal{M}$ defined as in the discussion of the LaSalle invariance principle, if V is a Liapunov function on $\mathcal{M}$ show that M is an attracting set and the interior of $\mathcal{M}$ is in the basin of attraction.

14. Suppose $x(t, t_0, x_0)$ is a trajectory of an autonomous vector field in $\mathbb{R}^n$ that exists for all time. Consider the set

$$\mathcal{T} = \left\{ x \in \mathbb{R}^n \mid x = x(t, t_0, x_0),\ t \in \mathbb{R} \right\}.$$

Prove that $\mathcal{T}$ is an invariant set.

15. Suppose $x(t, t_0, x_0)$ is a trajectory of an nonautonomous vector field in $\mathbb{R}^n$ that exists for all time. Consider the set

$$\mathcal{T} = \left\{ x \in \mathbb{R}^n \mid x = x(t, t_0, x_0),\ t \in \mathbb{R} \right\}.$$

Argue that $\mathcal{T}$ is not generally an invariant set.

16. Consider the vector field:

$$\dot{x} = -2tx, \quad x \in \mathbb{R}.$$

Show that all trajectories are forward, but not pullback, convergent to $x = 0$.

17. Consider the vector field:

$$\dot{x} = 2tx, \quad x \in \mathbb{R}.$$

Show that all trajectories are pullback, but not forward, convergent to $x = 0$.

18. Reformulate Definition 8.4.3 in terms of the trajectories of nonautonomous vector fields.

19. Reformulate Definition 8.4.4 in terms of the trajectories of nonautonomous vector fields.

20. Reformulate Theorem 8.4.5 in terms of the trajectories of nonautonomous vector fields.

21. Consider the vector field:

$$\dot{x} = -x + \sin t.$$

The solution through the point x_0 at t_0 is given by:

$$x(t; t_0, x_0) = \frac{1}{2}(\sin t - \cos t) + \left(x_0 + \frac{1}{2}\cos t_0 - \frac{1}{2}\sin t_0 \right) e^{-(t-t_0)}.$$

Construct the pullback attracting set.

22. Consider the vector field:

$$\dot{x} = -x + t.$$

The solution through the point x_0 at t_0 is given by:

$$x(t; x_0, t_0) = t - 1 + (x_0 - t_0 + 1)e^{-(t-t_0)}.$$

Construct the pullback attracting set.

23. Prove Theorem 8.4.5.

9

The Poincaré-Bendixson Theorem

The Poincaré-Bendixson theorem gives us a complete determination of the asymptotic behavior of a large class of flows on the plane, cylinder, and two-sphere. It is remarkable in that it assumes no detailed information about the vector field, only uniqueness of solutions, properties of ω limit sets, and some properties of the geometry of the underlying phase space. We begin by setting the framework and giving some preliminary definitions.

We will consider $\mathbf{C}^r$, $r \geq 1$, vector fields

$$\begin{aligned} \dot{x} &= f(x, y), \\ \dot{y} &= g(x, y), \qquad (x, y) \in \mathcal{P}, \end{aligned}$$

where $\mathcal{P}$ denotes the phase space, which may be the plane, cylinder, or two-sphere. We denote the flow generated by this vector field by

$$\phi_t(\cdot),$$

where the "$\cdot$" in this notation denotes a point $(x, y) \in \mathcal{P}$.

The following definition will be useful.

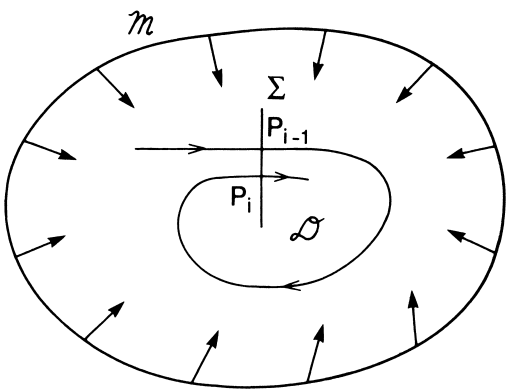

FIGURE 9.0.1.

Definition 9.0.1 *Let Σ be a continuous, connected arc in $\mathcal{P}$. Then Σ is said to be* transverse *to the vector field on $\mathcal{P}$ if the vector dot product of the unit normal at each point on Σ with the vector field at that point is not zero and does not change sign on Σ. Or equivalently, since the vector field is $\mathbf{C}^r$, $r \geq 1$, the vector field has no fixed points on Σ and is never tangent to Σ.*

Now we are in a position to actually prove the Poincaré-Bendixson theorem. We will first prove several lemmas from which the theorem will follow easily. Our presentation follows closely Palis and de Melo [1982]. In all that follows, $\mathcal{M}$ is understood to be a positively invariant compact set in $\mathcal{P}$. For any point $p \in \mathcal{P}$, we will denote the orbit of p under the flow $\phi_t(\cdot)$ *for positive times* $O_+(p)$ (also called the positive semiorbit of p).

Lemma 9.0.2 *Let $\Sigma \subset \mathcal{M}$ be an arc transverse to the vector field. The positive orbit through any point $p \in \mathcal{M}$, $O_+(p)$, intersects Σ in a monotone sequence; that is, if p_i is the i^{th} intersection of $O_+(p)$ with Σ, then $p_i \in [p_{i-1}, p_{i+1}]$.*

Proof: Consider the piece of the orbit $O_+(p)$ from p_{i-1} to p_i along with the segment $[p_{i-1}, p_i] \subset \Sigma$ (see Figure 9.0.1). (Note: of course, if $O_+(p)$ intersects Σ only once then we are done.)

This forms the boundary of a positively invariant region $\mathcal{D}$. Hence, $O_+(p_i) \subset \mathcal{D}$, and therefore we must have p_{i+1} (if it exists) contained in $\mathcal{D}$. Thus we have shown that $p_i \in [p_{i-1}, p_{i+1}]$. □

We remark that Lemma 9.0.2 does not apply immediately to toroidal phase spaces. This is because the piece of the orbit from p_{i-1} to p_i along with the segment $[p_{i-1}, p_i] \subset \Sigma$ needs to divide $\mathcal{M}$ into two "disjoint pieces." This would not be true for orbits completely encircling a torus. However, the lemma would apply to pieces of the torus that behave as $\mathcal{M}$ described above.

Corollary 9.0.3 *The ω-limit set of p ($\omega(p)$) intersects Σ in at most one point.*

Proof: The proof is by contradiction. Suppose $\omega(p)$ intersects Σ in two points, q_1 and q_2. Then by the definition of ω-limit sets, we can find sequences of points along $O_+(p)$, $\{p_n\}$ and $\{\bar{p}_n\}$, which intersect Σ such that $p_n \longrightarrow q_1$ as $n \uparrow \infty$ and $\bar{p}_n \longrightarrow q_2$ as $n \uparrow \infty$. However, if this were true, then it would contradict the previous lemma on monotonicity of the intersections of $O_+(p)$ with Σ. □

Lemma 9.0.4 *If $\omega(p)$ does not contain fixed points, then $\omega(p)$ is a closed orbit.*

Proof: The strategy is to choose a point $q \in \omega(p)$, show that the orbit of q is closed, and then show that $\omega(p)$ is the same as the orbit of q.

Choose $x \in \omega(q)$; then x is not a fixed point, since $\omega(p)$ closed and is a union of orbits containing no fixed points. Construct an arc transverse to the vector field at x (call it Σ). Now $O_+(q)$ intersects Σ in a monotone sequence, $\{q_n\}$, with $q_n \to x$ as $n \uparrow \infty$, but since $q_n \in \omega(p)$, by the previous corollary we must have $q_n = x$ for all n. Since $x \in \omega(q)$, the orbit of q must be a closed orbit.

It only remains to show that the orbit of q and $\omega(p)$ are the same thing. Taking a transverse arc, Σ, at q, we see by the previous corollary that $\omega(p)$ intersects Σ only at q. Since $\omega(p)$ is a union of orbits, contains no fixed points, and is connected, we know that $O(q) = \omega(p)$. □

Lemma 9.0.5 *Let p_1 and p_2 be distinct fixed points of the vector field contained in $\omega(p)$, $p \in \mathcal{M}$. Then there exists at most one orbit $\gamma \subset \omega(p)$ such that $\alpha(\gamma) = p_1$ and $\omega(\gamma) = p_2$. (Note: by $\alpha(\gamma)$ we mean the α limit set of every point on γ; similarly for $\omega(\gamma)$.)*

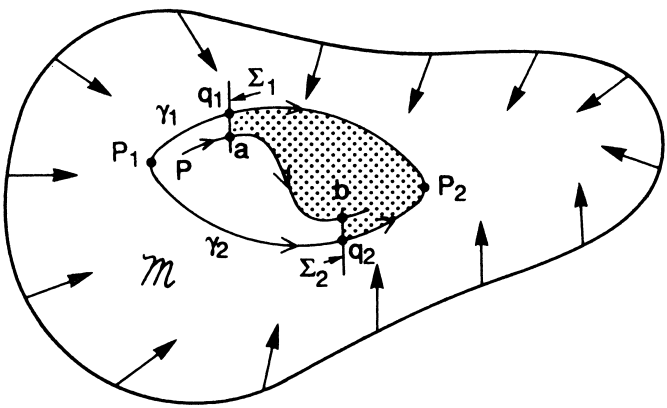

FIGURE 9.0.2.

Proof: The proof is by contradiction. Suppose there exist two orbits γ_1, $\gamma_2 \in \omega(p)$ such that $\alpha(\gamma_i) = p_1$, $\omega(\gamma_i) = p_2$, $i = 1, 2$. Choose points $q_1 \in \gamma_1$ and $q_2 \in \gamma_2$ and construct arcs Σ_1, Σ_2 transverse to the vector field at each of these points (see Figure 9.0.2).

Since γ_1, $\gamma_2 \subset \omega(p)$, $O_+(p)$ intersects Σ_1 in a point a and later intersects Σ_2 in a point b. Hence, the region bounded by the orbit segments and arcs connecting the points q_1, a, b, q_2, p_2 (shown in Figure 9.0.2) is a positively invariant region, but this leads to a contradiction, since γ_1, $\gamma_2 \subset \omega(p)$. □

Now we can finally prove the theorem.

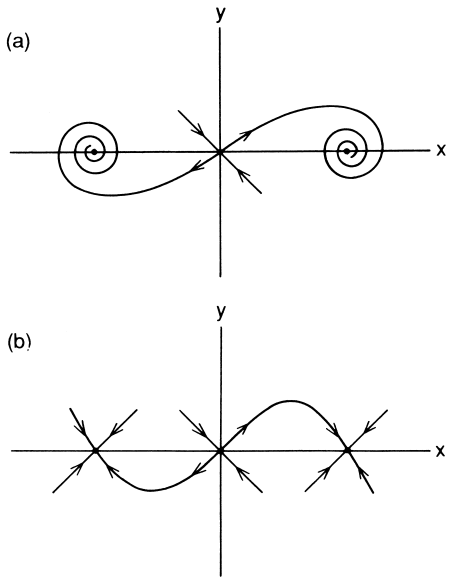

FIGURE 9.0.3. a) $0 < \delta < \sqrt{8}$; b) $\delta \geq \sqrt{8}$.

Theorem 9.0.6 (Poincaré-Bendixson) *Let $\mathcal{M}$ be a positively invariant region for the vector field containing a finite number of fixed points. Let $p \in \mathcal{M}$, and consider $\omega(p)$. Then one of the following possibilities holds.*

i) *$\omega(p)$ is a fixed point;*

ii) *$\omega(p)$ is a closed orbit;*

iii) *$\omega(p)$ consists of a finite number of fixed points $p_1, \cdots, p_n$ and orbits γ with $\alpha(\gamma) = p_i$ and $\omega(\gamma) = p_j$.*

Proof: If $\omega(p)$ contains only fixed points, then it must consist of a unique fixed point, since the number of fixed points in $\mathcal{M}$ is finite and $\omega(p)$ is a connected set.

If $\omega(p)$ contains no fixed points, then, by Lemma 9.0.4, it must be a closed orbit. Suppose that $\omega(p)$ contains fixed points and nonfixed points (sometimes called regular points). Let γ be a trajectory in $\omega(p)$ consisting of regular points. Then $\omega(\gamma)$ and $\alpha(\gamma)$ must be fixed points since, if they were not, then, by Lemma 9.0.4, $\omega(\gamma)$ and $\alpha(\gamma)$ would be closed orbits, which is absurd, since $\omega(p)$ is connected and contains fixed points.

We have thus shown that every regular point in $\omega(p)$ has a fixed point for an α and ω limit set. This proves iii) and completes the proof of the Poincaré-Bendixson theorem. □

For an example illustrating the necessity of a finite number of fixed

points in the hypotheses of Theorem 9.0.6 see Palis and de Melo [1982]. For generalizations of the Poincaré-Bendixson theorem to arbitrary closed two-manifolds see Schwartz [1963].

Example 9.0.1 (Application to the Unforced Duffing Oscillator).

We now want to apply the Poincaré-Bendixson theorem to the unforced Duffing oscillator which, we recall, is given by

$$\begin{aligned} \dot{x} &= y, \\ \dot{y} &= x - x^3 - \delta y, \qquad \delta > 0. \end{aligned}$$

Using the fact that the level sets of $V(x, y) = y^2/2 - x^2/2 + x^4/4$ bound positively invariant sets for $\delta > 0$, we see that the unstable manifold of the saddle must fall into the sinks as shown in Figure 9.0.3. The reader should convince him- or herself that Figure 9.0.3 is rigorously justified based on analytical techniques developed in this chapter. Note that we have not proved anything about the global behavior of the stable manifold of the saddle. Qualitatively, it behaves as in Figure 9.0.4, but, we stress, this has not been rigorously justified.

End of Example 9.0.1

9.1 Exercises

1. Use the Poincaré–Bendixson theorem to show that the vector field

$$\begin{aligned} \dot{x} &= \mu x - y - x(x^2 + y^2), \\ \dot{y} &= x + \mu y - y(x^2 + y^2), \qquad (x, y) \in \mathbb{R}^2, \end{aligned}$$

has a closed orbit for $\mu > 0$. (*Hint:* transform to polar coordinates.)

2. Prove that for $\delta > 0$ the unstable manifold of the saddle-type fixed point of the unforced Duffing oscillator falls into the sinks as shown in Figure 9.0.3.

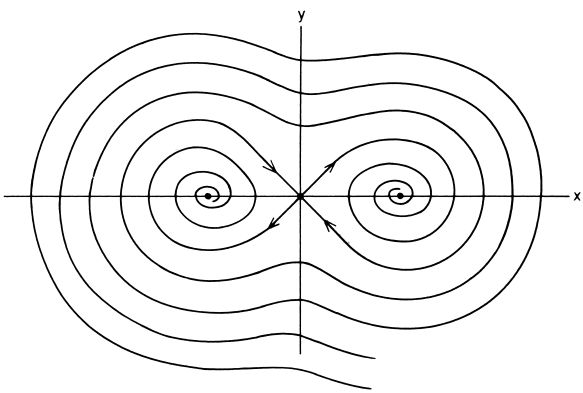

FIGURE 9.0.4.

10

Poincaré Maps

The idea of reducing the study of continuous time systems (flows) to the study of an associated discrete time system (map) is due to Poincaré [1899], who first utilized it in his studies of the three body problem in celestial mechanics. Nowadays virtually any discrete time system that is associated with an ordinary differential equation is referred to as a *Poincaré map*. This technique offers several advantages in the study of ordinary differential equations, including the following:

1. *Dimensional Reduction.* Construction of the Poincaré map involves the elimination of *at least* one of the variables of the problem resulting in the study of a lower dimensional problem.

2. *Global Dynamics*. In lower dimensional problems (say, dimension ≤ 4) numerically computed Poincaré maps provide an insightful and striking display of the global dynamics of a system; see Guckenheimer and Holmes [1983] and Lichtenberg and Lieberman [1982] for examples of numerically computed Poincaré maps.

3. *Conceptual Clarity*. Many concepts that are somewhat cumbersome to state for ordinary differential equations may often be succinctly stated for the associated Poincaré map. An example would be the notion of orbital stability of a periodic orbit of an ordinary differential equation (see Hale [1980]). In terms of the Poincaré map, this problem would reduce to the problem of the stability of a fixed point of the map, which is simply characterized in terms of the eigenvalues of the map linearized about the fixed point.

It would be useful to give methods for constructing the Poincaré map associated with an ordinary differential equation. Unfortunately, there exist no general methods applicable to arbitrary ordinary differential equations, since construction of the Poincaré map requires some knowledge of the geometrical structure of the phase space of the ordinary differential equation. Thus, construction of a Poincaré map requires ingenuity specific to the problem at hand; however, in four cases that come up frequently, the construction of a specific type of Poincaré map can in some sense be said to be canonical. The four cases are:

1. In the study of the orbit structure near a periodic orbit of an ordinary differential equation.

2. In the case where the phase space of an ordinary differential equation is periodic, such as in periodically forced oscillators.
3. In the study of the orbit structure near a homoclinic or heteroclinic orbit.
4. In the study of two degree-of-freedom Hamiltonian systems.

We begin by considering Case 1.

10.1 Case 1: Poincaré Map Near a Periodic Orbit

Consider the following ordinary differential equation

$$\dot{x} = f(x), \qquad x \in \mathbb{R}^n, \tag{10.1.1}$$

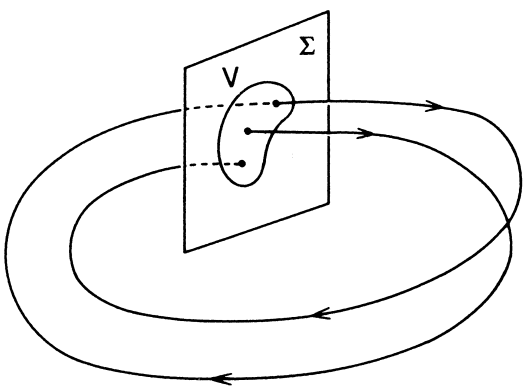

FIGURE 10.1.1. The geometry of the Poincaré map for a periodic orbit.

where $f: U \to \mathbb{R}^n$ is $\mathbf{C}^r$ on some open set $U \subset \mathbb{R}^n$. Let $\phi(t, \cdot)$ denote the flow generated by (10.1.1). Suppose that (10.1.1) has a periodic solution of period T which we denote by $\phi(t, x_0)$, where $x_0 \in \mathbb{R}^n$ is any point through which this periodic solution passes (i.e., $\phi(t + T, x_0) = \phi(t, x_0)$). Let Σ be an $n-1$ dimensional surface transverse to the vector field at x_0 (note: "transverse" means that $f(x) \cdot n(x) \neq 0$ where "$\cdot$" denotes the vector dot product and $n(x)$ is the normal to Σ at x); we refer to Σ as a cross-section to the vector field (10.1.1). Now in Theorem 7.1.1 we proved that $\phi(t, x)$ is $\mathbf{C}^r$ if $f(x)$ is $\mathbf{C}^r$; thus, we can find an open set $V \subset \Sigma$ such that the trajectories starting in V return to Σ in a time close to T. The map that associates points in V with their points of first return to Σ is called the *Poincaré map,* which we denote by P. To be more precise,

$$\begin{aligned} P&: V \to \Sigma, \\ &x \mapsto \phi\big(\tau(x), x\big), \end{aligned} \tag{10.1.2}$$

where $\tau(x)$ is the time of first return of the point x to Σ. Note that, by construction, we have $\tau(x_0) = T$ and $P(x_0) = x_0$.

Therefore, a fixed point of P corresponds to a periodic orbit of (10.1.1), and a period k point of P (i.e., a point $x \in V$ such that $P^k(x) = x$ provided $P^i(x) \in V$, $i = 1, \cdots, k$) corresponds to a periodic orbit of (10.1.1) that pierces Σ k times before closing; see Figure 10.1.1.

In applying this technique to specific examples, the following questions immediately arise.

1. How is Σ chosen?

2. How does P change as Σ is changed?

Question 1 cannot be answered in a general way, since in any given problem there will be many possible choices of Σ. This fact makes the answer to Question 2 even more important. However, for now we will postpone answering this question in order to consider a specific example.

Example 10.1.1. Consider the following vector field on $\mathbb{R}^2$

$$\begin{aligned} \dot{x} &= \mu x - y - x(x^2 + y^2), \\ \dot{y} &= x + \mu y - y(x^2 + y^2), \end{aligned} \qquad (x, y) \in \mathbb{R}^2, \tag{10.1.3}$$

where $\mu \in \mathbb{R}^1$ is a parameter. Our goal is to study (10.1.3) by constructing an associated one-dimensional Poincaré map and studying the dynamics of the map. According to our previous discussion, we need to find a periodic orbit of (10.1.3), construct a cross-section to the orbit, and then study how points on the cross-section return to the cross-section under the flow generated by (10.1.3). Considering (10.1.3) and thinking about how to carry out these steps should bring home the point stated at the beginning of this section — constructing a Poincaré map requires some knowledge of the geometry of the flow generated by (10.1.3). In this example the procedure is greatly facilitated by considering the vector field in a "more appropriate" coordinate system; in this case, polar coordinates.

Let

$$\begin{aligned} x &= r\cos\theta, \\ y &= r\sin\theta; \end{aligned} \tag{10.1.4}$$

then (10.1.3) becomes

$$\begin{aligned} \dot{r} &= \mu r - r^3, \\ \dot{\theta} &= 1. \end{aligned} \tag{10.1.5}$$

We will require $\mu > 0$, in which case the flow generated by (10.1.5) is given by

$$\phi_t(r_0, \theta_0) = \left(\left(\frac{1}{\mu} + \left(\frac{1}{r_0^2} - \frac{1}{\mu} \right) e^{-2\mu t} \right)^{-1/2}, t + \theta_0 \right). \tag{10.1.6}$$

It should be clear that (10.1.5) has a periodic orbit given by $\phi_t(\sqrt{\mu}, \theta_0)$. We now construct a Poincaré map near this periodic orbit.

We define a cross-section Σ to the vector field (10.1.5) by

$$\Sigma = \{ (r, \theta) \in \mathbb{R} \times S^1 \mid r > 0,\ \theta = \theta_0 \}. \tag{10.1.7}$$

The reader should verify that Σ is indeed a cross-section. From (10.1.5) we see that the "time of flight" for orbits starting on Σ to return to Σ is given by $t = 2\pi$. Using this information, the Poincaré map is given by

$$P\colon \Sigma \to \Sigma$$
$$(r_0, \theta_0) \mapsto \phi_{2\pi}(r_0, \theta_0) = \left(\left(\tfrac{1}{\mu} + \left(\tfrac{1}{r_0^2} - \tfrac{1}{\mu} \right) e^{-4\pi\mu} \right)^{-1/2}, \theta_0 + 2\pi \right), \tag{10.1.8}$$

or simply

$$r \mapsto \left(\frac{1}{\mu} + \left(\frac{1}{r^2} - \frac{1}{\mu} \right) e^{-4\pi\mu} \right)^{-1/2}, \tag{10.1.9}$$

where we have dropped the subscript '0' on r for notational convenience. The Poincaré map has a fixed point at $r = \sqrt{\mu}$. We can compute the stability of the fixed point by computing the eigenvalue (which is just the derivative for a one-dimensional map) of $DP(\sqrt{\mu})$. A simple calculation gives

$$DP(\sqrt{\mu}) = e^{-4\pi\mu}. \tag{10.1.10}$$

Therefore, the fixed point $r = \sqrt{\mu}$ is asymptotically stable.

Before leaving this example there are several points to make.

1. Viewing (10.1.3) in the correct coordinate system was the key to this problem. This made the choice of a cross-section virtually obvious and provided "nice" coordinates on the cross-section (i.e., r and θ "decoupled" as well). Later we will learn a general technique called *normal form theory* which can be used to transform vector fields into the "nicest possible" coordinate systems.
2. We know that the fixed point of P corresponds to a periodic orbit of (10.1.5) and that the fixed point of P is asymptotically stable. Does this imply that the corresponding periodic orbit of (10.1.5) is also asymptotically stable? It does, but we have not proved it yet (note: the reader should think about this in the context of this example until it feels "obvious"). We will consider this point when we consider how the Poincaré map changes when the cross-section is varied.

End of Example 10.1.1

Before leaving Case 1, let us illustrate how the study of Poincaré maps near periodic orbits may simplify the geometry.

Consider a vector field in $\mathbb{R}^3$ generating a flow given by $\phi_t(x)$, $x \in \mathbb{R}^3$. Suppose also that it has a periodic orbit, γ, of period $T > 0$ passing through the point $x_0 \in \mathbb{R}^3$, i.e.,

$$\phi_t(x_0) = \phi_{t+T}(x_0).$$

We construct in the usual way a Poincaré map, P, near this periodic orbit by constructing a cross-section, Σ, to the vector field through x_0 and considering the return of points to Σ under the flow generated by the vector field; see Figure 10.1.1.

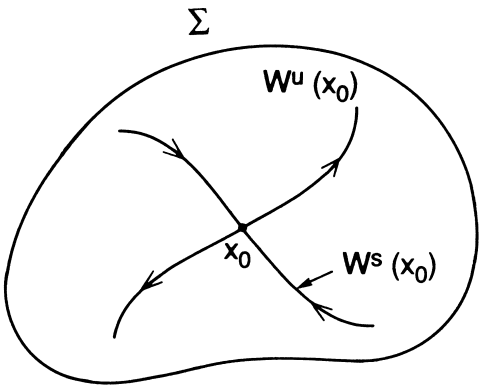

FIGURE 10.1.2. The geometry of the Poincaré map

Now consider the Poincaré map P. The map has a fixed point at x_0. Suppose that the fixed point is of saddle type having a one-dimensional stable manifold, $W^s(x_0)$, and a one-dimensional unstable manifold $W^u(x_0)$; see Figure 10.1.2. We now want to show how these manifolds are manifested in the flow and how they are related to γ. Very simply, using them as initial conditions, they generate the two-dimensional stable and unstable manifolds of γ. Mathematically, this is represented as follows

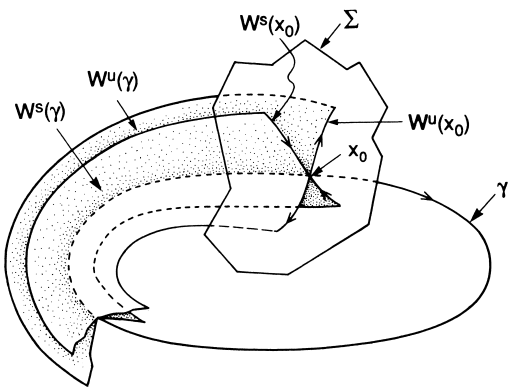

FIGURE 10.1.3.

$$W^s(\gamma) = \bigcup_{t \le 0} \phi_t(W^s_{\text{loc}}(x_0)),$$
$$W^u(\gamma) = \bigcup_{t \ge 0} \phi_t(W^u_{\text{loc}}(x_0)).$$

It should be clear that $W^s(\gamma)$ (resp. $W^u(\gamma)$) is just as differentiable as $W^s_{\text{loc}}(x_0)$ (resp. $W^u_{\text{loc}}(x_0)$), since $\phi_t(x)$ is differentiable with respect to x; see Figure 10.1.3 for an illustration of the geometry. Hence, in $\mathbb{R}^3$, $W^s(\gamma)$ and $W^u(\gamma)$ are two two-dimensional surfaces which intersect in the closed curve. This should serve to show that it is somewhat simpler geometrically to study periodic orbits and their associated stable and unstable manifolds by studying the associated Poincaré map.

We now turn to Case 2.

10.2 Case 2: The Poincaré Map of a Time-Periodic Ordinary Differential Equation

Consider the following ordinary differential equation

$$\dot{x} = f(x,t), \qquad x \in \mathbb{R}^n, \tag{10.2.1}$$

where $f: U \to \mathbb{R}^n$ is $\mathbf{C}^r$ on some open set $U \subset \mathbb{R}^n \times \mathbb{R}^1$. Suppose the time dependence of (10.2.1) is periodic with fixed period $T = 2\pi/\omega > 0$, i.e., $f(x,t) = f(x,t+T)$. We rewrite (10.2.1) in the form of an autonomous equation in $n+1$ dimensions (see Chapter 7) by defining the function

$$\begin{aligned} &\theta: \mathbb{R}^1 \to S^1, \\ &\quad t \mapsto \theta(t) = \omega t, \mod 2\pi. \end{aligned} \tag{10.2.2}$$

Using (10.2.2) equation (10.2.1) becomes

$$\begin{aligned} &\dot{x} = f(x,\theta), \\ &\dot{\theta} = \omega, \end{aligned} \qquad (x,\theta) \in \mathbb{R}^n \times S^1. \tag{10.2.3}$$

We denote the flow generated by (10.2.3) by $\phi(t) = \big(x(t), \theta(t) = \omega t + \theta_0 \pmod{2\pi}\big)$. We define a cross-section $\Sigma^{\bar{\theta}_0}$ to the vector field (10.2.3) by

$$\Sigma^{\bar{\theta}_0} = \{\, (x,\theta) \in \mathbb{R}^n \times S^1 \mid \theta = \bar{\theta}_0 \in (0, 2\pi] \,\}. \tag{10.2.4}$$

The unit normal to $\Sigma^{\bar{\theta}_0}$ in $\mathbb{R}^n \times S^1$ is given by the vector $(0,1)$, and it is clear that $\Sigma^{\bar{\theta}_0}$ is transverse to the vector field (10.2.3) for all $x \in \mathbb{R}^n$, since $\big(f(x,\theta),\omega\big) \cdot (0,1) = \omega \neq 0$. In this case $\Sigma^{\bar{\theta}_0}$ is called a *global cross-section*.

We define the Poincaré map of $\Sigma^{\bar{\theta}_0}$ as follows:

$$\begin{aligned} &P_{\bar{\theta}_0}: \Sigma^{\bar{\theta}_0} \to \Sigma^{\bar{\theta}_0}, \\ &\quad \left(x\left(\frac{\bar{\theta}_0 - \theta_0}{\omega} \right), \bar{\theta}_0 \right) \mapsto \left(x\left(\frac{\bar{\theta}_0 - \theta_0 + 2\pi}{\omega} \right), \bar{\theta}_0 + 2\pi \equiv \bar{\theta}_0 \right), \end{aligned}$$

or

$$x\left(\frac{\bar{\theta}_0 - \theta_0}{\omega} \right) \mapsto x\left(\frac{\bar{\theta}_0 - \theta_0 + 2\pi}{\omega} \right). \tag{10.2.5}$$

Thus, the Poincaré map merely tracks initial conditions in x at a fixed phase after successive periods of the vector field.

It should be clear that fixed points $P_{\bar{\theta}_0}$ correspond to $2\pi/\omega$-periodic orbits of (10.2.1) and k-periodic points of $P_{\bar{\theta}_0}$ correspond to periodic orbits of (10.2.1) that pierce $\Sigma^{\bar{\theta}_0}$ k times before closing. We will worry about the effect on the dynamics of the map caused by changing the cross-section later. Now we consider an example.

10.2A Periodically Forced Linear Oscillators

Consider the following ordinary differential equation

$$\ddot{x} + \delta\dot{x} + \omega_0^2 x = \gamma \cos \omega t. \tag{10.2.6}$$

This is an equation which most students learn to solve in elementary calculus courses. Our goal here is to study the nature of solutions of (1.2.17) from our more geometrical setting in the context of Poincaré maps. This will enable the reader to obtain a new point of view on something relatively familiar and, we hope, to see the value of this new point of view.

We begin by first obtaining the solution of (10.2.6). Recall (see, e.g., Arnold [1973] or Hirsch and Smale [1974]) that the general solution of (1.2.17) is the sum of the solution of the homogeneous equation (i.e., the solution for $\gamma = 0$), sometimes called the free oscillation, and a particular solution, sometimes called the forced oscillation. For $\delta > 0$ there are several possibilities for the homogeneous solution, which we state below.

$\delta > 0$: *The Homogeneous Solution, $x_h(t)$*

There are three cases depending on the sign of the quantity $\delta^2 - 4\omega_0^2$.

$$(a) \qquad \delta^2 - 4\omega_0^2 > 0 \Rightarrow x_h(t) = C_1 e^{r_1 t} + C_2 e^{r_2 t}, \tag{10.2.7}$$

where

$$r_{1,2} = -\delta/2 \pm (1/2)\sqrt{\delta^2 - 4\omega_0^2},$$

$$(b) \qquad \delta^2 - 4\omega_0^2 = 0 \Rightarrow x_h(t) = (C_1 + C_2 t)e^{-(\delta/2)t},$$

$$(c) \qquad \delta^2 - 4\omega_0^2 < 0 \Rightarrow x_h(t) = e^{-(\delta/2)t}(C_1 \cos \bar{\omega} t + C_2 \sin \bar{\omega} t),$$

and where $\bar{\omega} = (1/2)\sqrt{4\omega_0^2 - \delta^2}$. In all three cases C_1 and C_2 are unknown constants which are fixed when initial conditions are specified. Also, notice that in all three cases $\lim_{t\to\infty} x_h(t) = 0$. We now turn to the particular solution.

The Particular Solution, $x_p(t)$

The particular solution is given by

$$x_p(t) = A\cos\omega t + B\sin\omega t, \tag{10.2.8}$$

where

$$A \equiv \frac{(\omega_0^2 - \omega^2)\gamma}{(\omega_0^2 - \omega^2)^2 + (\delta\omega)^2}, \qquad B \equiv \frac{\delta\gamma\omega}{(\omega_0^2 - \omega^2)^2 + (\delta\omega)^2}.$$

Next we turn to the construction of the Poincaré map. For this we will consider only the case $\delta^2 - 4\omega_0^2 < 0$. The other two cases are similar, and we leave them as exercises for the reader.

The Poincaré Map: $\delta^2 - 4\omega_0^2 < 0$

Rewriting (10.2.6) as a system, we obtain

$$\begin{aligned} \dot{x} &= y, \\ \dot{y} &= -\omega_0^2 x - \delta y + \gamma\cos\omega t. \end{aligned} \tag{10.2.9}$$

By rewriting (10.2.9) as an autonomous system, as was described at the beginning of our discussion of Case 2, we obtain

$$\begin{aligned} \dot{x} &= y, \\ \dot{y} &= -\omega_0^2 x - \delta y + \gamma\cos\theta, \qquad (x, y, \theta) \in \mathbb{R}^1 \times \mathbb{R}^1 \times S^1. \\ \dot{\theta} &= \omega, \end{aligned} \tag{10.2.10}$$

The flow generated by (10.2.10) is given by

$$\phi_t(x_0, y_0, \theta_0) = \big(x(t), y(t), \omega t + \theta_0\big), \tag{10.2.11}$$

where, using (10.2.7c) and (10.2.8), $x(t)$ is given by

$$x(t) = e^{-(\delta/2)t}(C_1\cos\bar{\omega}t + C_2\sin\bar{\omega}t) + A\cos\omega t + B\sin\omega t$$

with

$$y(t) = \dot{x}(t). \tag{10.2.12}$$

The constants C_1 and C_2 are obtained by requiring

$$\begin{aligned} x(0) &= x_0, \\ y(0) &= y_0, \end{aligned}$$

which yield

$$\begin{aligned} C_1 &= x_0 - A, \\ C_2 &= \frac{1}{\bar{\omega}}\left(\frac{\delta}{2}x_0 + y_0 - \frac{\delta}{2}A - \omega B\right). \end{aligned} \tag{10.2.13}$$

Notice from (10.2.9) that we can set $\theta_0 = 0$ in (10.2.11) (cf. (10.2.5)).

We construct a cross-section at $\bar{\theta}_0 = 0$ (note: this is why we specified the initial conditions at $t = 0$) as follows

$$\Sigma^0 \equiv \Sigma = \{\, (x, y, \theta) \in \mathbb{R}^1 \times \mathbb{R}^1 \times S^1 \mid \theta = 0 \in [0, 2\pi) \,\}, \tag{10.2.14}$$

where we have dropped the subscript "0" on x, y, and θ for notational convenience. Using (10.2.12), the Poincaré map is given by

$$\begin{aligned} &P\colon \Sigma \to \Sigma, \\ &\quad \begin{pmatrix} x \\ y \end{pmatrix} \mapsto e^{-\delta\pi/\omega} \begin{pmatrix} \mathcal{C} + \frac{\delta}{2\bar{\omega}}\mathcal{S} & \frac{1}{\bar{\omega}}\mathcal{S} \\ -\frac{\omega_0^2}{\bar{\omega}}\mathcal{S} & \mathcal{C} - \frac{\delta}{2\bar{\omega}}\mathcal{S} \end{pmatrix} \begin{pmatrix} x \\ y \end{pmatrix} \\ &\quad + \begin{pmatrix} e^{-\delta\pi/\omega}\left[-A\mathcal{C} + \left(-\frac{\delta}{2\bar{\omega}}A - \frac{\omega}{\bar{\omega}}B\right)\mathcal{S}\right] + A \\ e^{-\delta\pi/\omega}\left[-\omega B\mathcal{C} + \left(\frac{\omega_0^2}{\bar{\omega}}A + \frac{\delta\omega}{2\bar{\omega}}B\right)\mathcal{S}\right] + \omega B \end{pmatrix}, \end{aligned} \tag{10.2.15}$$

where

$$\mathcal{C} \equiv \cos 2\pi\frac{\bar{\omega}}{\omega},$$

$$\mathcal{S} \equiv \sin 2\pi\frac{\bar{\omega}}{\omega}.$$

Equation (10.2.15) is an example of an *affine map*, i.e., it is linear map plus a translation.

The Poincaré map has a single fixed point given by

$$(x, y) = (A, \omega B) \tag{10.2.16}$$

(note: this should not be surprising). The next question is whether or not the fixed point is stable. A simple calculation shows that the eigenvalues of $DP(A, \omega B)$ are given by

$$\lambda_{1,2} = e^{-\delta\pi/\omega \pm i2\pi\bar{\omega}/\omega}. \tag{10.2.17}$$

Thus the fixed point is asymptotically stable with nearby orbits appearing as in Figure 10.2.1. (Note: the "spiraling" of orbits near the fixed point is due to the imaginary part of the eigenvalues.) Figure 10.2.1 is drawn for $A > 0$; see (10.2.8).

The Case of Resonance: $\bar{\omega} = \omega$

We now consider the situation where the driving frequency is equal to the frequency of the free oscillation. In this case the the Poincaré map becomes

$$\begin{aligned} &P\colon \Sigma \to \Sigma, \\ &\quad \begin{pmatrix} x \\ y \end{pmatrix} \mapsto e^{-\delta\pi/\omega} \begin{pmatrix} 1 & 0 \\ 0 & 1 \end{pmatrix} \begin{pmatrix} x \\ y \end{pmatrix} + \begin{pmatrix} A(1 - e^{-\delta\pi/\omega}) \\ \omega B(1 - e^{-\delta\pi/\omega}) \end{pmatrix}. \end{aligned} \tag{10.2.18}$$

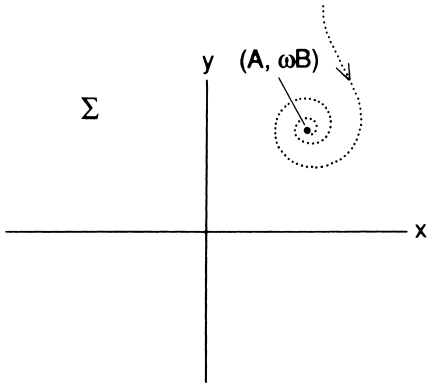

FIGURE 10.2.1.

This map has a unique fixed point at

$$(x, y) = (A, \omega B). \tag{10.2.19}$$

The eigenvalues of $DP(A, \omega B)$ are identical and are equal to

$$\lambda = e^{-\delta\pi/\omega}. \tag{10.2.20}$$

Thus, the fixed point is asymptotically stable with nearby orbits appearing as in Figure 10.2.2. (Note: in this case orbits do not spiral near the fixed point since the eigenvalues are purely real.)

For $\delta > 0$, in all cases the free oscillation dies out and we are left with the forced oscillation of frequency ω which is represented as an attracting fixed point of the Poincaré map. We will now examine what happens for $\delta = 0$.

$\delta = 0$: Subharmonics, Ultraharmonics, and Ultrasubharmonics

In this case the equation becomes

$$\begin{aligned} \dot{x} &= y, \\ \dot{y} &= -\omega_0^2 x + \gamma \cos\theta, \\ \dot{\theta} &= \omega. \end{aligned} \tag{10.2.21}$$

Using (10.2.7c) and (10.2.8), we see that the general solution of (10.2.21) is given by

$$\begin{aligned} x(t) &= C_1 \cos\omega_0 t + C_2 \sin\omega_0 t + \bar{A}\cos\omega t, \\ y(t) &= \dot{x}(t), \end{aligned} \tag{10.2.22}$$

where

$$\bar{A} \equiv \frac{\gamma}{\omega_0^2 - \omega^2}, \tag{10.2.23}$$

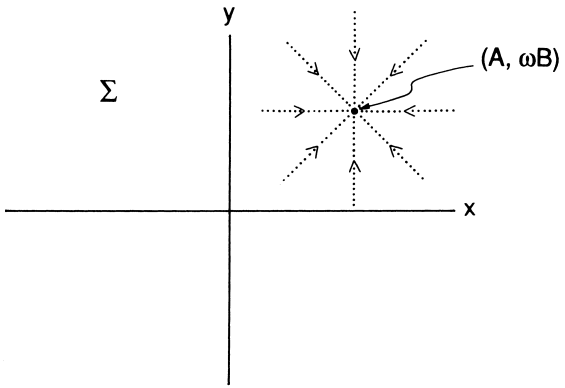

FIGURE 10.2.2.

and C_1 and C_2 are found by solving

$$\begin{aligned} x(0) &\equiv x_0 = C_1 + \bar{A}, \\ y(0) &\equiv y_0 = C_2\omega_0. \end{aligned} \tag{10.2.24}$$

It should be evident that, for now, we must require $\omega \neq \omega_0$ in order for (10.2.22) to be valid.

Before writing down the Poincaré map, there is an important distinction to draw between the cases $\delta > 0$ and $\delta = 0$. As mentioned above, for $\delta > 0$, the free oscillation eventually dies out leaving only the forced oscillation of frequency ω. This corresponds to the associated Poincaré map having a single asymptotically stable fixed point. In the case $\delta = 0$, by examining (10.2.22), we see that this does not happen. In general, for $\delta = 0$, it should be clear that the solution is a superposition of solutions of frequencies ω and ω_0. The situation breaks down into several cases depending on the relationship of ω to ω_0. We will first write down the Poincaré map and then consider each case individually.

The Poincaré map is given by

$$\begin{aligned} &P\colon \Sigma \to \Sigma, \\ &\begin{pmatrix} x \\ y \end{pmatrix} \mapsto \begin{pmatrix} \cos 2\pi\frac{\omega_0}{\omega} & \frac{1}{\omega_0}\sin 2\pi\frac{\omega_0}{\omega} \\ -\omega_0 \sin 2\pi\frac{\omega_0}{\omega} & \cos 2\pi\frac{\omega_0}{\omega} \end{pmatrix} \begin{pmatrix} x \\ y \end{pmatrix} \\ &\qquad + \begin{pmatrix} \bar{A}\left(1 - \cos 2\pi\frac{\omega_0}{\omega}\right) \\ \omega_0 \bar{A} \sin 2\pi\frac{\omega_0}{\omega} \end{pmatrix}. \end{aligned} \tag{10.2.25}$$

Our goal is to study the orbits of P. As mentioned above, this will depend on the relationship of ω and ω_0. We begin with the simplest case.

Harmonic Response

Consider the point

$$(x, y) = (\bar{A}, 0). \tag{10.2.26}$$

It is easy to verify that this is a fixed point of P corresponding to a solution of (10.2.21) having frequency ω.

We now want to describe a somewhat more geometrical way of viewing this solution which will be useful later on. Using (10.2.26), (10.2.24) and (10.2.22), the fixed point (10.2.26) corresponds to the solution

$$\begin{aligned} x(t) &= \bar{A}\cos\omega t, \\ y(t) &= -\bar{A}\omega\sin\omega t. \end{aligned} \tag{10.2.27}$$

If we view this solution in the x–y plane, it traces out a circle which closes after time $2\pi/\omega$.
If we view this solution in the x-y-θ phase space, it traces out a spiral which can be viewed as lying on the surface of a cylinder.

The cylinder can be thought of as an extension of the circle traced out by (10.2.27) in the x-y plane into the θ-direction. Since θ is periodic, the ends of the cylinder are joined to become a torus, and the trajectory traces out a curve on the surface of the torus which makes *one* complete revolution on the torus before closing. The torus can be parameterized by two angles; the angle θ is the longitudinal angle. We will call the latitudinal angle θ_0, which is the angle through which the circular trajectory turns in the x-y plane. This situation is depicted geometrically in Figure 10.2.3.

Trajectories which wind many times around the torus may be somewhat difficult to draw, as in Figure 10.2.3; we now want to show an easier way to represent the same information. First, we cut open the torus and identify the two ends as shown in Figure 10.2.4. Then we cut along the longitudinal angle θ and flatten it out into a square as shown in Figure 10.2.5. This square is really a torus if we identify the two vertical sides and the two horizontal sides.

This means that a trajectory that runs off the top of the square reappears at the bottom of the square at the same θ value where it intersected the top edge. For a more detailed description of trajectories on a torus, see Abraham and Shaw [1984]. We stress that this construction works because *all* trajectories of (10.2.21) lie on circles in the x-y plane. Motion on tori is a characteristic of multifrequency systems.

Subharmonic Response of Order m

Suppose we have

$$\omega = m\omega_0, \qquad m > 1, \tag{10.2.28}$$

where m is an integer. Consider all points on Σ *except* $(x, y) = (\bar{A}, 0)$ (we already know about this point). Using (10.2.22) and the expression for the Poincaré map given in (10.2.25), it is easy to see that all points *except* $(x, y) = (\bar{A}, 0)$ are *period m points*, i.e., they are fixed points of the m^{th} iterate of the Poincaré map (note: this statement assumes that by the phrase "period of a point" we mean the smallest possible period). Let us now see what they correspond to in terms of motion on the torus.

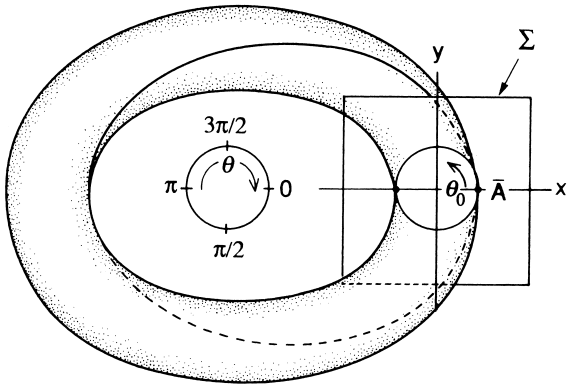

FIGURE 10.2.3.

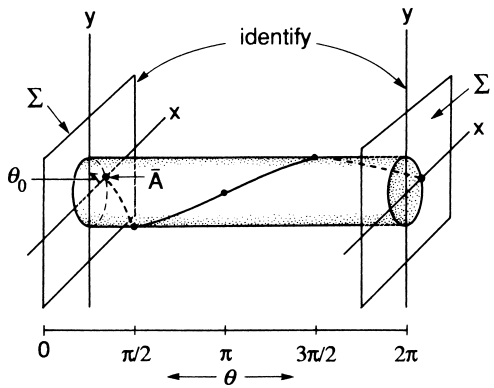

FIGURE 10.2.4.

Using (10.2.28) and (10.2.22) it should be clear that $x(t)$ and $y(t)$ have frequency ω/m. Thus, after a time $t = 2\pi/\omega$, the solution has turned through an angle $2\pi/m$ in the x-y plane, i.e., θ_0 has changed by $2\pi/m$. Therefore, the solution makes m longitudinal circuits and one latitudinal circuit around the torus before closing up. The m distinct points of intersection that the trajectory makes with $\theta = 0$ are all period m points of P, or equivalently, fixed points of the m^{th} iterate of P. Such solutions are called *subharmonics of order m*. In Figure 10.2.6 we show examples for $m = 2$ and $m = 3$.

Ultraharmonic Response of Order n

Suppose we have

$$n\omega = \omega_0, \qquad n > 1, \tag{10.2.29}$$

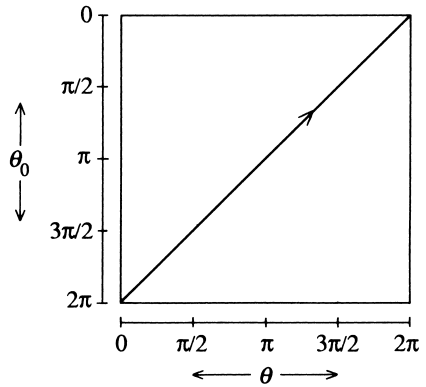

FIGURE 10.2.5.

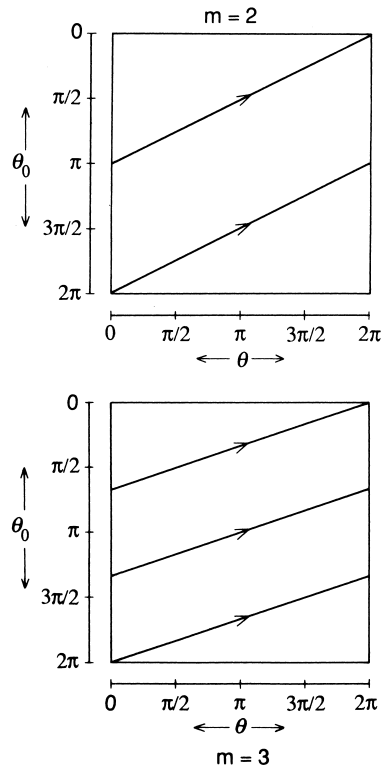

FIGURE 10.2.6.

where n is an integer. Consider all points on Σ *except* $(x, y) = (\bar{A}, 0)$. Using (10.2.29) and (10.2.22) it is easy to see that every point is a fixed point of

the Poincaré map. Let us see what this corresponds to in terms of motion on the torus.

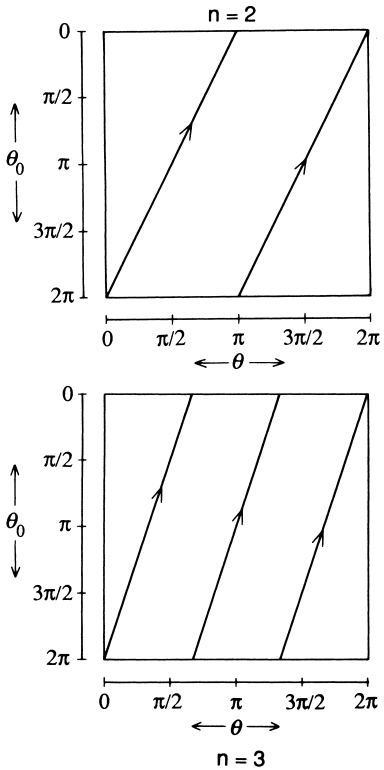

FIGURE 10.2.7.

Using (10.2.22) and (10.2.29), we see that $x(t)$ and $y(t)$ have frequency $n\omega$. This means that after a time $t = 2\pi/\omega$, the solution has turned through an angle $2\pi n$ in the x-y plane before closing up. Since $2\pi n = 2\pi \pmod{2\pi}$, this explains the nature of these fixed points of P: they correspond to solutions which make n latitudinal and one longitudinal circuits around the torus before closing up. We illustrate the situation geometrically for $n = 2$ and $n = 3$ in Figure 10.2.7. Such solutions are referred to as *ultraharmonics of order n*.

Ultrasubharmonic Response of Order m, n

Suppose we have

$$n\omega = m\omega_0, \qquad m,\ n > 1, \tag{10.2.30}$$

where m and n are *relatively prime integers*, which means that all common factors of n/m have been divided out. Using exactly the same argu-

ments as those given above, it is easy to show that all points in Σ *except* $(x, y) = (\bar{A}, 0)$ are period m points which correspond to trajectories making m longitudinal and n latitudinal circuits around the torus before closing up. These solutions are referred to as *ultrasubharmonics of order m, n*. We illustrate the situation for $(n, m) = (2, 3)$ and $(n, m) = (3, 2)$ in Figure 10.2.8.

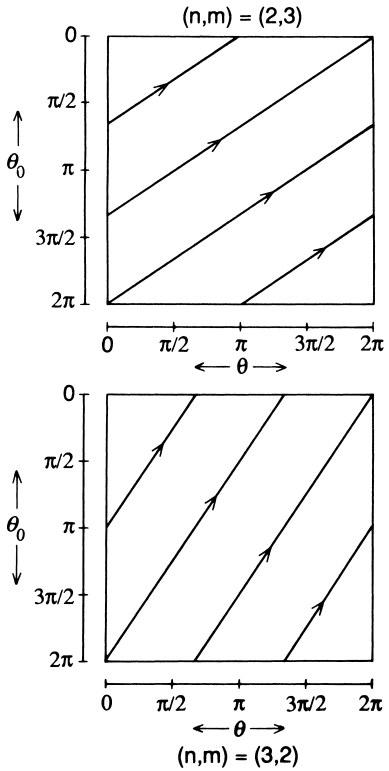

FIGURE 10.2.8.

Quasiperiodic Response

For the final case, suppose we have

$$\frac{\omega}{\omega_0} = \text{irrational number.} \tag{10.2.31}$$

Then for all points in Σ *except* $(x, y) = (\bar{A}, 0)$, the orbit of the point densely fills out a circle on Σ which corresponds to an invariant two-torus in x-y-θ space. We will prove this rigorously in Section 10.4a.

10.3 Case 3: The Poincaré Map Near a Homoclinic Orbit

We now want to give an example of the construction of a Poincaré map in the neighborhood of a homoclinic orbit. Rather than getting entangled in technical details, we will concentrate on a specific example in two dimensions which illustrates the main ideas.

Consider the ordinary differential equation

$$\begin{aligned} \dot{x} &= \alpha x + f_1(x, y; \mu), \\ \dot{y} &= \beta y + f_2(x, y; \mu), \end{aligned} \qquad (x, y, \mu) \in \mathbb{R}^1 \times \mathbb{R}^1 \times \mathbb{R}^1, \tag{10.3.1}$$

with $f_1,\ f_2 = \mathcal{O}(|x|^2 + |y|^2)$ and $\mathbf{C}^r$, $r \geq 2$ and where μ is regarded as a parameter. We make the following hypotheses on (10.3.1).

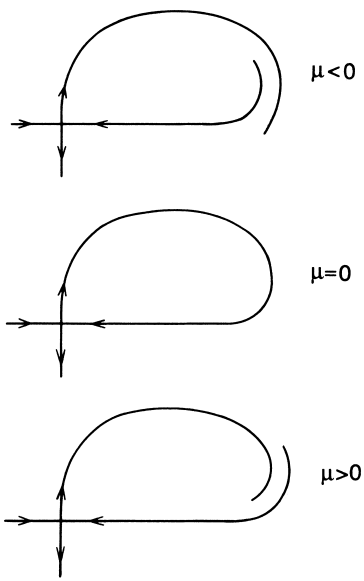

FIGURE 10.3.1. Behavior of the homoclinic orbit as μ is varied.

Hypothesis 1. $\alpha < 0$, $\beta > 0$, and $\alpha + \beta \neq 0$.

Hypothesis 2. At $\mu = 0$ (10.3.1) possesses a homoclinic orbit connecting the hyperbolic fixed point $(x, y) = (0, 0)$ to itself, and on both sides of $\mu = 0$ the homoclinic orbit is broken. Furthermore, the homoclinic orbit breaks in a transverse manner in the sense that the stable and unstable manifolds have different orientations on different sides of $\mu = 0$. For definiteness, we will assume that, for $\mu < 0$, the stable manifold lies inside the unstable

manifold, for $\mu > 0$, the stable manifold lies outside the stable manifold and, for $\mu = 0$, they coincide; see Figure 10.3.1.

Hypothesis 1 is of a local nature, since it concerns the nature of the eigenvalues of the vector field linearized about the fixed point. Hypothesis 2 is global in nature, since it supposes the existence of a homoclinic orbit and describes the nature of the parameter dependence of the homoclinic orbit.

Now an obvious question is why this scenario? Why not stable inside for $\mu > 0$ and unstable inside for $\mu < 0$? Certainly this could happen; however, this is not important for us to consider at the moment. We need to know only that, on one side of $\mu = 0$, the stable manifold lies inside the unstable manifold, and on the other side of $\mu = 0$, the unstable manifold lies inside the stable manifold. Of course, in applications, we would want to determine which case actually occurs, and later on we will learn a method for doing this (Melnikov's method); however, now we will simply study the consequences of a homoclinic orbit to a hyperbolic fixed point of a planar vector field breaking in the manner described above.

Let us remark that it is certainly possible for the eigenvalues α and β to depend on the parameter μ. However, this will be of no consequence provided that Hypothesis 1 is satisfied for each parameter value and that this is true for μ sufficiently close to zero.

The question we ask is the following: *What is the nature of the orbit structure near the homoclinic orbit for μ near $\mu = 0$?* We will answer this question by computing a Poincaré map near the homoclinic orbit and studying the orbit structure of the Poincaré map. The Poincaré map that we construct will be very different from those we constructed in Cases 1 and 2 in that it will be the composition of two maps. One of the maps, P_0, will be constructed from the flow near the origin (which we will take to be the flow generated by the linearization of (10.3.1) about the origin). The other map, P_1, will be constructed from the flow outside of a neighborhood of the fixed point, which, if we remain close enough to the homoclinic orbit, can be made to be as close to a rigid motion as we like. The resulting Poincaré map, P, will then be given by $P \equiv P_1 \circ P_0$. Evidently, with these approximations, our Poincaré map will be valid (meaning that its dynamics reflect the dynamics of (10.3.1)) only when it is defined sufficiently close to the (broken) homoclinic orbit. We will discuss the validity of our approximations later on, but for now we begin our analysis.

The analysis will proceed in several steps.

Step 1. Set up the domain for the Poincaré map.

Step 2. Compute P_0.

Step 3. Compute P_1.

Step 4. Examine the dynamics of $P = P_1 \circ P_0$.

Step 1: *Set Up the Domain for the Poincaré Map.* For the domain of P_0 we choose

$$\Sigma_0 = \{\, (x, y) \in \mathbb{R}^2 \mid x = \varepsilon > 0,\ y > 0 \,\}, \tag{10.3.2}$$

and for the domain P_1 we choose

$$\Sigma_1 = \{\, (x, y) \in \mathbb{R}^2 \mid x > 0,\ y = \varepsilon > 0 \,\}. \tag{10.3.3}$$

We will take ε small; the need for this will become apparent later on. See Figure 10.3.2 for an illustration of the geometry of Σ_0 and Σ_1.

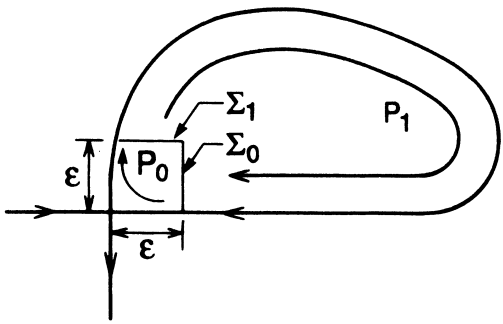

FIGURE 10.3.2.

Step 2: *Compute* P_0. We will use the flow generated by the linear vector field

$$\begin{aligned} \dot{x} &= \alpha x, \\ \dot{y} &= \beta y, \end{aligned} \tag{10.3.4}$$

in order to compute the map, P_0, of points on Σ_0 to Σ_1. For this to be a good approximation, it should be clear that we must take ε and y small. We will discuss the validity of this approximation later.

The flow generated by (10.3.4) is given by

$$\begin{aligned} x(t) &= x_0 e^{\alpha t}, \\ y(t) &= y_0 e^{\beta t}. \end{aligned} \tag{10.3.5}$$

The time of flight, T, needed for a point $(\varepsilon, y_0) \in \Sigma_0$ to reach Σ_1 under the action of (10.3.5) is given by solving

$$\varepsilon = y_0 e^{\beta T} \tag{10.3.6}$$

to obtain

$$T = \frac{1}{\beta} \log \frac{\varepsilon}{y_0}. \tag{10.3.7}$$

From (10.3.7) it is clear that we must require $y_0 \leq \varepsilon$.

$$\begin{aligned} P_0 &: \Sigma_0 \to \Sigma_1, \\ &(\varepsilon, y_0) \mapsto \left(\varepsilon \left(\frac{\varepsilon}{y_0} \right)^{\alpha/\beta}, \varepsilon \right). \end{aligned} \tag{10.3.8}$$

Step 3: *Compute* P_1. Using Theorem 7.1.1, by smoothness of the flow with respect to initial conditions and the fact that it only takes a finite time to flow from Σ_1 to Σ_0 along the homoclinic orbit, we can find a neighborhood $U \subset \Sigma_1$ which is mapped onto Σ_0 under the flow generated by (10.3.4). We denote this map by

$$P_1(x, \varepsilon; \mu) = \big(P_{11}(x, \varepsilon; \mu), P_{12}(x, \varepsilon; \mu)\big) : U \subset \Sigma_1 \to \Sigma_0, \tag{10.3.9}$$

where $P_1(0, \varepsilon; 0) = (\varepsilon, 0)$. Taylor expanding (10.3.9) about $(x, \varepsilon; \mu) = (0, \varepsilon; 0)$ gives

$$P_1(x, \varepsilon; \mu) = (\varepsilon, ax + b\mu) + \mathcal{O}(2). \tag{10.3.10}$$

The expression "$\mathcal{O}(2)$" in (10.3.10) represents higher order nonlinear terms which can be made small by taking ε, x, and μ small. For now, we will neglect these terms and take as our map

$$\begin{aligned} P_1 &: U \subset \Sigma_1 \to \Sigma_0, \\ &(x, \varepsilon) \mapsto (\varepsilon, ax + b\mu), \end{aligned} \tag{10.3.11}$$

where $a > 0$ and $b > 0$. The reader should study Figure 10.3.1 to determine why we must have a, $b > 0$.

Step 4: *Examine the Dynamics of* $P = P_1 \circ P_0$. We have

$$\begin{aligned} P = P_1 \circ P_0 &: V \subset \Sigma_0 \to \Sigma_0, \\ &(\varepsilon, y_0) \mapsto \left(\varepsilon, a\varepsilon \left(\frac{\varepsilon}{y_0} \right)^{\alpha/\beta} + b\mu \right), \end{aligned} \tag{10.3.12}$$

where $V = (P_0)^{-1}(U)$, or

$$P(y; \mu) : y \to Ay^{|\alpha/\beta|} + b\mu, \tag{10.3.13}$$

where $A \equiv a\varepsilon^{1+(\alpha/\beta)} > 0$ (we have left the subscript "0" off the y_0 for the sake of a less cumbersome notation). (Note: of course, we are assuming also that U is sufficiently small so that $(P_0)^{-1}(U) \subset \Sigma_0$.)

Let $\delta = |\alpha/\beta|$; then $\alpha + \beta \neq 0$ implies $\delta \neq 1$. We will seek fixed points of the Poincaré map, i.e., $y \in V$ such that

$$P(y; \mu) = Ay^{\delta} + b\mu = y. \tag{10.3.14}$$

The fixed points can be displayed graphically as the intersection of the graph of $P(y; \mu)$ with the line $y = P(y; \mu)$ for fixed μ.

There are two distinct cases.

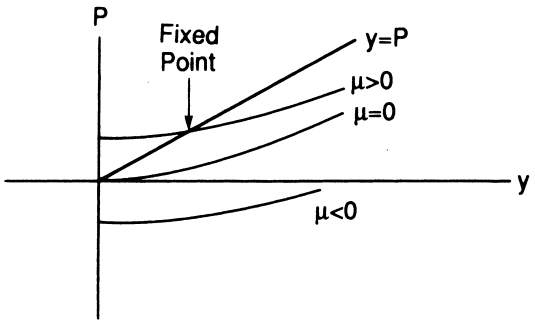

FIGURE 10.3.3. Graph of P for $\mu > 0$, $\mu = 0$, and $\mu < 0$ with $\delta > 1$.

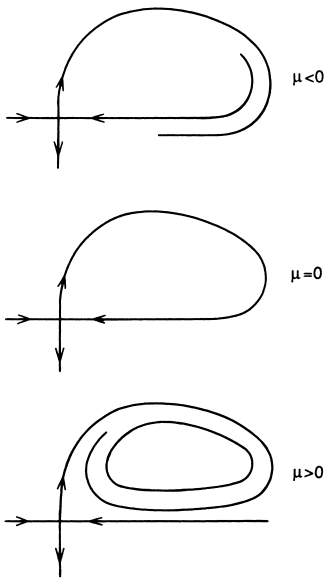

FIGURE 10.3.4. Phase plane of (10.3.1) for $\delta > 1$.

Case 1: $|\alpha| > |\beta|$ *or* $\delta > 1$

For this case $D_y P(0;0) = 0$, and the graph of P appears as in Figure 10.3.3 for $\mu > 0$, $\mu = 0$, and $\mu < 0$. Thus, for $\mu > 0$ and small μ, (10.3.13) has a fixed point.

The fixed point is stable and hyperbolic, since $0 < D_y P < 1$ for μ sufficiently small. By construction we therefore see that this fixed point corresponds to an attracting periodic orbit of (10.3.1) (provided that we can justify our approximations); see Figure 10.3.4. We remark that if the homoclinic orbit were to break in the manner opposite to that shown in Figure

10.3.1, then the fixed point of (10.3.13) would occur for $\mu < 0$.

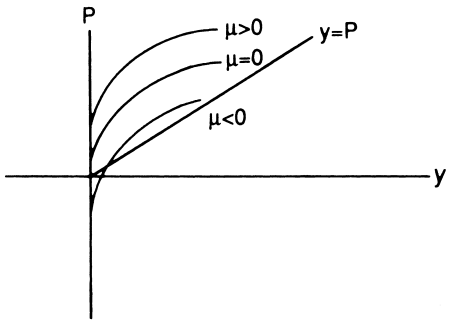

FIGURE 10.3.5. Graph of P for $\mu > 0$, $\mu = 0$, and $\mu < 0$ with $\delta < 1$.

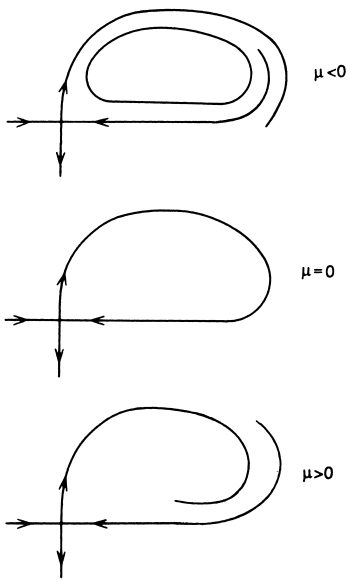

FIGURE 10.3.6. Phase plane of (1.2.50) for $\delta < 1$.

Case 2: $|\alpha| < |\beta|$ *or* $\delta < 1$

For this case, $D_y P(0;0) = \infty$, and the graph of P appears as in Figure 10.3.5. Thus, for $\mu < 0$, (10.3.13) has a repelling fixed point. By construction we can therefore conclude that this corresponds to a repelling periodic orbit for (10.3.1); see Figure 10.3.6. We remark that if the homoclinic orbit

were to break in the manner opposite to that shown in Figure 10.3.1, then the fixed point of (10.3.13) would occur for $\mu > 0$.

We summarize our results in the following theorem.

Theorem 10.3.1 *Consider a system where Hypothesis 1 and Hypothesis 2 hold. Then we have, for μ sufficiently small:* i) *If $\alpha + \beta < 0$, there exists a unique stable periodic orbit on one side of $\mu = 0$; on the opposite side of μ there are no periodic orbits.* ii) *If $\alpha + \beta > 0$, the same conclusion holds as in* i), *except that the periodic orbit is unstable.*

We remark that if the homoclinic orbit breaks in the manner opposite that shown in Figure 10.3.1, then Theorem 10.3.1 still holds except that the periodic orbits occur for μ values having the opposite sign as those given in Theorem 10.3.1. Theorem 10.3.1 is a classical result which can be found in Andronov et al. [1971]. Additional proofs can be found in Guckenheimer and Holmes [1983] and Chow and Hale [1982].

Before leaving this example we must address an important point, which is that we have not rigorously proven Theorem 10.3.1, since the Poincaré map we computed was only an approximation. We must therefore show that the dynamics of the exact Poincaré map are contained in the dynamics of the approximate Poincaré map. Because our main goal is to demonstrate how to construct a Poincaré map near a homoclinic orbit, we refer the reader to Wiggins [1988] and Bakaleinikov and Silbergleit [1995a, b] for the proof of this fact under the condition that we remain sufficiently close to the (broken) homoclinic orbit, i.e., for ϵ and μ sufficiently small.

10.4 Case 4: Poincaré Map Associated with a Two Degree-of-Freedom Hamiltonian System

The study of two degree-of-freedom Hamiltonian systems can often be reduced to the study of two-dimensional maps, although this reduction is typically local in the phase space. Here we describe how this can be done.

Consider a two degree-of-freedom Hamiltonian system with Hamiltonian given by

$$H(x_1, x_2, y_1, y_2), \qquad (x_1, x_2, y_1, y_2) \in \mathbb{R}^4,$$

where $x_i - y_i$, $i = 1, 2$, are the canonically conjugate pairs of variables. The level set of the Hamiltonian, or *energy surface*, i.e.,

$$H(x_1, x_2, y_1, y_2) = h, \tag{10.4.1}$$

is *typically* three-dimensional. In particular, if

$$\frac{\partial H}{\partial y_2} \neq 0, \tag{10.4.2}$$

then it is three-dimensional and, by the implicit function theorem, on a fixed energy surface we can solve for y_2 as a function of x_1, x_2, y_1, and h, i.e.,

$$y_2 = y_2(x_1, x_2, y_1, h). \tag{10.4.3}$$

Hence, locally the level set of the Hamiltonian is represented by the graph of this function.

Now consider the three-dimensional hyperplane given by $x_2 =$ constant. Then a vector normal to this hyperplane is given by

$$N = (0, 1, 0, 0),$$

and a vector normal to the energy surface is given by

$$\nabla H = \left(\frac{\partial H}{\partial x_1}, \frac{\partial H}{\partial x_2}, \frac{\partial H}{\partial y_1}, \frac{\partial H}{\partial y_2} \right).$$

Hence, we see that (10.4.2) implies that ∇H and N cannot be parallel, and therefore the three-dimensional hyperplane $x_2 =$ constant intersects the three-dimensional energy surface transversely in a two-dimensional surface, which we denote by Σ. Σ, or some subset of it, is our candidate for the Poincaré section. Since the energy surface is locally represented by the graph of (10.4.3), we can take x_1 and y_1 as coordinates on Σ. Let $\tilde{\Sigma} \subset \Sigma$ denote the subset of Σ for which $N \cdot \nabla H$ is nonzero and of one sign, and trajectories with initial conditions on $\tilde{\Sigma}$ return to Σ. This latter condition is the most problematic. It is certainly true if x_2 is an angular variable, and it is reasonable to expect it to be true if the energy surface is bounded, but insuring that this condition holds is part of the art of constructing Poincaré sections. Once all these conditions are satisfied the Poincaré map is given by

$$\begin{aligned} P &: \tilde{\Sigma} \to \tilde{\Sigma}, \\ (x_1(0), y_1(0)) &\mapsto (x_1(\tau), y_1(\tau)), \end{aligned} \tag{10.4.4}$$

where $\tau = \tau\,(x_1(0), y_1(0); h)$ is the time for a trajectory with initial condition $(x_1(0), y_1(0))$ on $\tilde{\Sigma}$ to return to $\tilde{\Sigma}$.

Let us carry out this procedure for the two-degree-of-freedom Hamiltonian system given in Example 5.2b, where all the calculations can be done explicitly. From (5.2.1), the equations restricted to the energy surface are given by

$$\begin{aligned} \dot{I}_1 &= 0, \\ \dot{\theta}_1 &= \Omega_1, \\ \dot{\theta}_2 &= \Omega_2, \end{aligned}$$

with the energy surface given by the graph of the function

$$I_2 = \frac{h - I_1 \Omega_1}{\Omega_2} = I_2(I_1; h).$$

The Poincaré section is parametrized by the coordinates $I_1 - \theta_1$ and, since θ_2 is an angular coordinate, all points on Σ return to Σ after time $\frac{2\pi}{\Omega_2}$. Hence the Poincaré map is given by

$$P : \Sigma \to \Sigma,$$
$$(I_1, \theta_1) \mapsto (I_1, \theta_1 + 2\pi\frac{\Omega_1}{\Omega_2}).$$

Therefore Σ is foliated by invariant circles given by $I_1 = \text{constant}$ and the dynamics on each invariant circle is given by $\theta_1 \mapsto \theta_1 + 2\pi\frac{\Omega_1}{\Omega_2}$.

10.4a The Study of Coupled Oscillators via Circle Maps

In both Section 10.4 and Section 5.2b we saw that (for I_1, $I_2 \neq 0$) the study of two linearly coupled, linear undamped oscillators in a four-dimensional phase space could be reduced to the study of the following two-dimensional vector field

$$\begin{aligned} \dot{\theta}_1 &= \omega_1, \\ \dot{\theta}_2 &= \omega_2, \end{aligned} \qquad (\theta_1, \theta_2) \in S^1 \times S^1. \tag{10.4.5}$$

The flow generated by (10.4.5) is defined on the two-torus, $S^1 \times S^1 \equiv T^2$, and θ_1 and θ_2 are called the longitude and latitude; see Figure 10.4.1. As in Example 10.2a, it is often easier to visualize flows on tori by cutting open the torus, flattening it out, and identifying horizontal and vertical sides of the resulting square as shown in Figure 10.4.2. The flow generated by (10.4.5) is simple to compute and is given by

$$\begin{aligned} \theta_1(t) &= \omega_1 t + \theta_{10}, \\ \theta_2(t) &= \omega_2 t + \theta_{20}, \end{aligned} \qquad (\text{mod}\, 2\pi). \tag{10.4.6}$$

However, orbits under this flow will depend on how ω_1 and ω_2 are related.

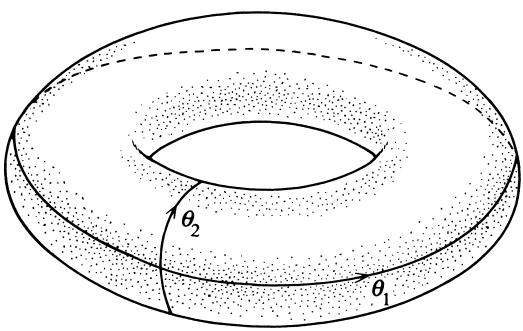

FIGURE 10.4.1.

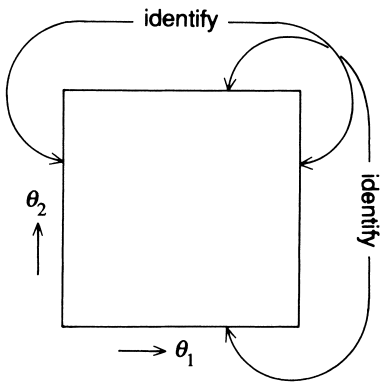

FIGURE 10.4.2.

Definition 10.4.1 *ω_1 and ω_2 are said to be* incommensurate *if the equation*

$$m\omega_1 + n\omega_2 = 0$$

has no solutions consisting of n, $m \in \mathbb{Z}$ (integers). Otherwise, ω_1 and ω_2 are commensurate.

Theorem 10.4.2 *If ω_1 and ω_2 are commensurate, then every phase curve of (10.4.5) is closed. However, if ω_1 and ω_2 are incommensurate, then every phase curve of (10.4.5) is everywhere dense on the torus.*

To prove this theorem, we need the following lemma.

Lemma 10.4.3 *Suppose the circle S^1 is rotated through an angle α, and α is incommensurate with 2π. Then the sequence*

$$S = \{\theta, \theta + \alpha, \theta + 2\alpha, \cdots, \theta + n\alpha, \cdots, (\mathrm{mod}\, 2\pi)\}$$

is everywhere dense on the circle (note: n is an integer).

Proof:

$$\theta + m\alpha(\mathrm{mod}\, 2\pi) = \begin{cases} \theta + m\alpha & \text{if} \quad m\alpha - 2\pi < 0, \\ \theta + (m\alpha - 2\pi k) & \text{if} \quad m\alpha - 2\pi k > 0, k > 1 \\ & \quad \text{and } m\alpha - 2\pi(k+1) < 0, \end{cases}$$

so, in particular, since α and 2π are incommensurate, the sequence S is infinite and never repeats.

We will use the "pigeonhole principle," i.e., if you have n holes and $n+1$ pigeons, then one hole must contain at least two pigeons.

Divide the circle into k half-open intervals of equal length $2\pi/k$. Then, among the first $k+1$ elements of the sequence S, at least two must be in the same half-open interval; call these points $\theta + p\alpha$, $\theta + q\alpha(\mathrm{mod}\, 2\pi)$ with

$p > q$. Thus, $(p-q)\alpha \equiv s\alpha < 2\pi/k (\mathrm{mod}\, 2\pi)$. Any two consecutive points of the sequence $\bar{S}$ given by

$$\bar{S} = \{\theta, \theta + s\alpha, \theta + 2s\alpha, \cdots, \theta + ns\alpha, \cdots, (\mathrm{mod}\, 2\pi)\}$$

are therefore the same distance d apart, where $d < 2\pi/k$ (note that $\bar{S} \subset S$).

Now choose any point on S^1 and construct an ε-neighborhood around it. If k is chosen such that $2\pi/k < \varepsilon$, then at least one of the elements of $\bar{S}$ will lie in the ε-neighborhood. This proves the lemma. □

Now we prove Theorem 10.4.2.

Proof: First, suppose ω_1 and ω_2 are commensurate, i.e., $\exists\ n,\ m \in \mathbb{Z}$ such that $\omega_1 = (n/m)\omega_2$. We construct a Poincaré map as follows. Let the cross-section Σ be defined as

$$\Sigma^{\theta_{10}} = \{\, (\theta_1, \theta_2) \mid \theta_1 = \theta_{10} \,\}. \tag{10.4.7}$$

Then, using (10.4.7), we have

$$\begin{aligned} P_{\theta_{10}} &: \Sigma^{\theta_{10}} \to \Sigma^{\theta_{10}}, \\ &\theta_2 \mapsto \theta_2 + \omega_2 \frac{2\pi}{\omega_1}. \end{aligned} \tag{10.4.8}$$

However, $\omega_2/\omega_1 = m/n$; hence, we have

$$\theta_2 \mapsto \theta_2 + 2\pi \frac{m}{n} (\mathrm{mod}\, 2\pi). \tag{10.4.9}$$

This is a map of the circle onto itself (called a *circle map*); the number ω_2/ω_1 is called the *rotation number*. (Rotation numbers are also defined for nonlinear circle maps, as we shall see later.)

It is clear that the n^{th} iterate of this map is given by

$$\theta_2 \mapsto \theta_2 + 2\pi m (\mathrm{mod}\, 2\pi) = \theta_2. \tag{10.4.10}$$

Thus, every θ_2 is a periodic point; hence the flow consists entirely of closed orbits. This proves the first part of the theorem.

Now suppose ω_1 and ω_2 are incommensurate; then $\omega_2/\omega_1 = \alpha$, where α is irrational. The Poincaré map is then given by

$$\theta_2 \mapsto \theta_2 + 2\pi\alpha (\mathrm{mod}\, 2\pi); \tag{10.4.11}$$

thus, by Lemma 10.4.3, the orbit of any point θ_2 is dense in the circle.

Next choose any point p on T^2 and construct an ε-neighborhood of p. To finish the proof of Theorem 10.4.2 we need to show that, given any orbit on T^2, it eventually passes through this ε-neighborhood of p. This is done as follows.

First, we are able to construct a new cross-section $\Sigma^{\bar{\theta}_{10}}$ which passes through the ε-neighborhood of p; see Figure 10.4.3. We have seen that the orbits of $P_{\theta_{10}}: \Sigma^{\theta_{10}} \to \Sigma^{\theta_{10}}$ are all dense on $\Sigma^{\theta_{10}}$ *for any* θ_{10}. Therefore, we can take any point on $\Sigma^{\theta_{10}}$ and look at its first intersection point with $\Sigma^{\bar{\theta}_{10}}$ under the flow (10.4.6). From this it follows that the iterates of this point under $P_{\bar{\theta}_{10}}$ are dense in $\Sigma^{\bar{\theta}_{10}}$. This completes the proof. □

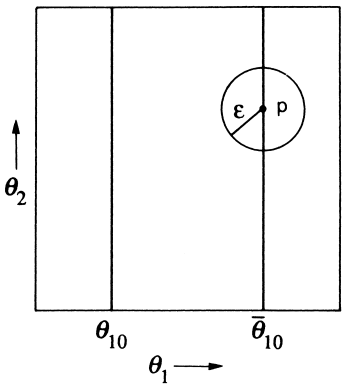

FIGURE 10.4.3.

Let us make a final remark before leaving this example. In our introductory motivational remarks we stated that Poincaré maps allow a dimensional reduction of the problem by *at least one*. In this example, we have seen how the study of a four-dimensional system can be reduced to the study of a one-dimensional system. This was possible because of our understanding of the geometry of the phase space; i.e., the phase space was made up of families of two-tori. It will be a common theme throughout this book that a good qualitative feel for the geometry of the phase space will put us in the best position for quantitative analysis.

Finally, we note that these results for linear vector fields on T^2 actually remain true for nonlinear differentiable vector fields on T^2, namely, that the ω limit sets for vector fields with no singular points are either closed orbits or the entire torus; see Hale [1980].

10.5 Exercises

Exercises $1-3$ *are concerned with the properties of the following Poincaré map.*
Consider the Poincaré map given in (10.2.15)

$$\begin{pmatrix} x \\ y \end{pmatrix} \mapsto e^{-\delta\pi/\omega} \begin{pmatrix} \mathcal{C} + \frac{\delta}{2\omega}\mathcal{S} & \frac{1}{\omega}\mathcal{S} \\ -\frac{\omega_0^2}{\omega}\mathcal{S} & \mathcal{C} - \frac{\delta}{2\omega}\mathcal{S} \end{pmatrix} \begin{pmatrix} x \\ y \end{pmatrix}$$

$$+\begin{pmatrix} e^{-\delta\pi/\omega}[-A\mathcal{C}+(\frac{-\delta}{2\bar\omega}A-\frac{\omega}{\bar\omega}B)\mathcal{S}]+A \\ e^{-\delta\pi/\omega}[-\omega B\mathcal{C}+(\frac{\omega_0^2}{\bar\omega}A+\frac{\delta\omega}{2\bar\omega}B)\mathcal{S}]+\omega B \end{pmatrix},$$

where

$$\mathcal{C}=\cos 2\pi\frac{\bar\omega}{\omega},\qquad \mathcal{S}=\sin 2\pi\frac{\bar\omega}{\omega},$$

and

$$\bar\omega=\frac{1}{2}\sqrt{4\omega_0^2-\delta^2},\quad A=\frac{(\omega_0^2-\omega^2)\gamma}{(\omega_0^2-\omega^2)^2+(\delta\omega)^2},\quad B=\frac{\delta\gamma\omega}{(\omega_0^2-\omega^2)^2+(\delta\omega)^2}.$$

1. Show that $(x,y)=(A,\omega B)$ is the only fixed point for this map and, hence, argue that it is a global attractor.

2. Discuss the nature of the orbit structure near $(x,y)=(A,\omega B)$ for different values of $\bar\omega/\omega$.

3. Show how the fixed point of the Poincaré map changes as the cross-section (i.e., phase angle) is varied.

4. Construct and study the Poincaré map for

$$\begin{aligned}\dot x &= y,\\ \dot y &= -\omega_0^2 x+\gamma\cos\theta,\\ \dot\theta &= \omega_0.\end{aligned}$$

Exercises $5-9$ *are concerned with the properties of the following Poincaré map.* Consider the Poincaré map ($\omega\neq\omega_0$) given in (10.2.25)

$$\begin{pmatrix}x\\y\end{pmatrix}\mapsto\begin{pmatrix}\cos 2\pi\frac{\omega_0}{\omega} & \frac{1}{\omega_0}\sin 2\pi\frac{\omega_0}{\omega}\\ -\omega_0\sin 2\pi\frac{\omega_0}{\omega} & \cos 2\pi\frac{\omega_0}{\omega}\end{pmatrix}\begin{pmatrix}x\\y\end{pmatrix}+\begin{pmatrix}\bar A(1-\cos 2\pi\frac{\omega_0}{\omega})\\ \omega_0\bar A\sin 2\pi\frac{\omega_0}{\omega}\end{pmatrix}.$$

5. For $\omega=m\omega_0$, $m>1$, show that all points except $(x,y)=(\bar A,0)$ are period m points.

6. For $n\omega=\omega_0$, $n>1$, show that all points are fixed points.

7. Discuss the orbit structure of the Poincaré map when ω/ω_0 is an irrational number.

8. Discuss stability of the harmonics, subharmonics, ultraharmonics, and ultrasubharmonics.

9. Recall that a $\mathbf{C}^1$ map, f, preserves orientation when $\det Df>0$. Show that the four types of Poincaré maps discussed in this section preserve orientation. What would be the consequences if they did not?

10. Consider an n degree-of-freedom Hamiltonian system. Following the discussion in Section 10.4, discuss how it can be studied via a $2n-2$ dimensional Poincaré map.

11. Show that the Poincaré maps for Hamiltonian systems described in Section 10.4 and Exercise 10 preserve volume.

11

Conjugacies of Maps, and Varying the Cross-Section

We now turn to answering the question of how the choice of cross-section affects the Poincaré map. The point of view that we develop will be that Poincaré maps defined on different cross-sections are related by a (in general, nonlinear) coordinate transformation. The importance of coordinate transformations in the study of dynamical systems cannot be overestimated. For example, in the study of systems of linear constant coefficient ordinary differential equations, coordinate transformations allow one to decouple the system and hence reduce the system to a set of decoupled linear first-order equations which are easily solved. In the study of completely integrable Hamiltonian systems, the transformations to action-angle coordinates results in a trivially solvable system (see Arnold [1978]), and these coordinates are also useful in the study of near integrable systems. If we consider general properties of dynamical systems, coordinate transformations provide us with a way of classifying dynamical systems according to properties which remain unchanged after a coordinate transformation. In Chapter 12 we will see that the notion of structural stability is based on such a classification scheme.

Before considering Poincaré maps, we want to discuss coordinate transformations, or, to use the more general mathematical term, *conjugacies,* giving some results that describe properties which must be retained by a map or vector field after a coordinate transformation of a specific differentiability class. Let us begin with an example which should be familiar to the reader.

Example 11.0.1. We want to motivate how coordinate transformations affect the orbits of maps.

Consider two linear, invertible maps

$$x \mapsto Ax, \qquad x \in \mathbb{R}^n \tag{11.0.1}$$

$$y \mapsto By, \qquad y \in \mathbb{R}^n. \tag{11.0.2}$$

For $x_0 \in \mathbb{R}^n$, we denote the orbit of x_0 under A by

$$O_A(x_0) = \{\cdots, A^{-n}x_0, \cdots, A^{-1}x_0, x_0, Ax_0, \cdots, A^n x_0, \cdots\}, \tag{11.0.3}$$

and, for $y_0 \in \mathbb{R}^n$, we denote the orbit of y_0 under B by

$$O_B(y_0) = \{\cdots, B^{-n}y_0, \cdots, B^{-1}y_0, y_0, By_0, \cdots, B^n y_0, \cdots\}. \tag{11.0.4}$$

Now suppose A and B are related by a similarity transformation, i.e., there is an invertible matrix T such that

$$B = TAT^{-1}. \tag{11.0.5}$$

We could think of T as transforming A into B, and, hence, since it does no harm in the linear setting to confuse the map with the matrix that generates it, T transforms (11.0.1) into (11.0.2). We represent this in the following diagram

$$\begin{array}{ccc} \mathbb{R}^n & \xrightarrow{A} & \mathbb{R}^n \\ \Big\downarrow{\scriptstyle T} & & \Big\downarrow{\scriptstyle T}. \\ \mathbb{R}^n & \xrightarrow{B} & \mathbb{R}^n \end{array} \tag{11.0.6}$$

The question we want to answer is this: when (11.0.1) is transformed into (11.0.2) via (11.0.5), how are orbits of A related to orbits of B? To answer this question, note that from (11.0.5) we have

$$B^n = TA^nT^{-1} \qquad \text{for all } n. \tag{11.0.7}$$

Hence, using (11.0.7) and comparing (11.0.1) and (11.0.5), we see that orbits of A are mapped to orbits of B under the transformation $y = Tx$. Moreover, we know that since similar matrices have the same eigenvalues, the stability types of these orbits coincide under the transformation T.

End of Example 11.0.1

Now we want to consider coordinate transformation in a more general, nonlinear setting. However, the reader will see that the essence of the ideas is contained in this example.

Let us consider two $\mathbf{C}^r$ diffeomorphisms $f\colon \mathbb{R}^n \to \mathbb{R}^n$ and $g\colon \mathbb{R}^n \to \mathbb{R}^n$, and a $\mathbf{C}^k$ diffeomorphism $h\colon \mathbb{R}^n \to \mathbb{R}^n$.

Definition 11.0.1 (Conjugacy) *f and g are said to be* $\mathbf{C}^k$ conjugate *($k \le r$) if there exists a $\mathbf{C}^k$ diffeomorphism $h\colon \mathbb{R}^n \to \mathbb{R}^n$ such that $g \circ h = h \circ f$. If $k = 0$, f and g are said to be* topologically conjugate.

The conjugacy of two diffeomorphisms is often represented by the following diagram.

$$\begin{array}{ccc} \mathbb{R}^n & \xrightarrow{f} & \mathbb{R}^n \\ \Big\downarrow{\scriptstyle h} & & \Big\downarrow{\scriptstyle h}. \\ \mathbb{R}^n & \xrightarrow{g} & \mathbb{R}^n \end{array} \tag{11.0.8}$$

The diagram is said to *commute* if the relation $g \circ h = h \circ f$ holds, meaning that you can start at a point in the upper left-hand corner of the diagram and reach the same point in the lower right-hand corner of the diagram by either of the two possible routes. We note that h need not be defined on all of $\mathbb{R}^n$ but possibly only locally about a given point. In such cases, f and g are said to be *locally* $\mathbf{C}^k$ *conjugate*.

If f and g are $\mathbf{C}^k$ conjugate, then we have the following results.

Proposition 11.0.2 *If f and g are $\mathbf{C}^k$ conjugate, then orbits of f map to orbits of g under h.*

Proof: Let $x_0 \in \mathbb{R}^n$; then the orbit of x_0 under f is given by

$$O(x_0) = \{\cdots, f^{-n}(x_0), \cdots, f^{-1}(x_0), x_0, f(x_0), \cdots, f^n(x_0), \cdots\}. \quad (11.0.9)$$

From Definition 11.0.1, we have that $f = h^{-1} \circ g \circ h$, so for a given $n > 0$ we have

$$\begin{aligned} f^n(x_0) &= \underbrace{(h^{-1} \circ g \circ h) \circ (h^{-1} \circ g \circ h) \circ \cdots \circ (h^{-1} \circ g \circ h)}_{n \text{ factors}}(x_0) \\ &= h^{-1} \circ g^n \circ h(x_0) \end{aligned} \quad (11.0.10)$$

or

$$h \circ f^n(x_0) = g^n \circ h(x_0). \quad (11.0.11)$$

Also from Definition 1.2.2, we have that $f^{-1} = h^{-1} \circ g^{-1} \circ h$, so by the same argument, for $n > 0$ we obtain

$$h \circ f^{-n}(x_0) = g^{-n} \circ h(x_0). \quad (11.0.12)$$

Therefore, from (11.0.10) and (11.0.12) we see that the orbit of x_0 under f is mapped by h to the orbit of $h(x_0)$ under g. □

Proposition 11.0.3 *If f and g are $\mathbf{C}^k$ conjugate, $k \geq 1$, and x_0 is a fixed point of f, then the eigenvalues of $Df(x_0)$ are equal to the eigenvalues of $Dg\big(h(x_0)\big)$.*

Proof: From Definition 11.0.1, $f(x) = h^{-1} \circ g \circ h(x)$. Note that since x_0 is a fixed point then $h^{-1} \circ g \circ h(x_0) = x_0$. Also, by the inverse function theorem, we have $Dh^{-1} = (Dh)^{-1}$. Using this and the fact that h is differentiable, we have

$$Df\big|_{x_0} = Dh^{-1}\big|_{x_0} Dg\big|_{h(x_0)} Dh\big|_{x_0}. \quad (11.0.13)$$

Therefore, recalling that similar matrices have equal eigenvalues gives the result. □

Now we will return to the specific question of what happens to the Poincaré map when the cross-section is changed. We begin with Case 1, a Poincaré map defined near a periodic orbit.

11.1 Case 1: Poincaré Map Near a Periodic Orbit: Variation of the Cross-Section

Let x_0 and x_1 be two points on the periodic solution of (10.1.1), and let Σ_0 and Σ_1 be two $(n-1)$-dimensional surfaces at x_0 and x_1, respectively, which are transverse to the vector field, and suppose that Σ_1 is chosen such that it is the image of Σ_0 under flow generated by (10.1.1); see Figure 11.1.1. By Theorem 7.1.1, this defines a $\mathbf{C}^r$ diffeomorphism

$$h\colon \Sigma_0 \to \Sigma_1. \tag{11.1.1}$$

We define Poincaré maps P_0 and P_1 as in the previous construction.

$$\begin{aligned} &P_0\colon V_0 \to \Sigma_0, \\ &\quad x_0 \mapsto \phi\big(\tau(\bar{x}_0), \bar{x}_0\big), \qquad \bar{x}_0 \in V_0 \subset \Sigma_0, \end{aligned} \tag{11.1.2}$$

$$\begin{aligned} &P_1\colon V_1 \to \Sigma_1, \\ &\quad x_1 \mapsto \phi\big(\tau(\bar{x}_1), \bar{x}_1\big), \qquad \bar{x}_1 \in V_1 \subset \Sigma_1. \end{aligned} \tag{11.1.3}$$

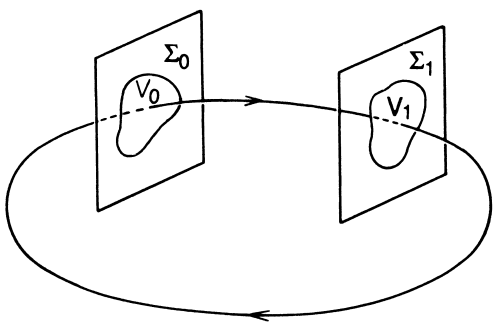

FIGURE 11.1.1. The cross-sections Σ_0 and Σ_1.

Then we have the following result.

Proposition 11.1.1 *P_0 and P_1 are locally $\mathbf{C}^r$ conjugate.*

Proof: We need to show that

$$P_1 \circ h = h \circ P_0,$$

from which the result follows immediately since h is a $\mathbf{C}^r$ diffeomorphism. However, we need to worry a bit about the domains of the maps. We have

$$\begin{aligned} &h(\Sigma_0) = \Sigma_1, \\ &P_0(V_0) \subset \Sigma_0, \\ &P_1(V_1) \subset \Sigma_1. \end{aligned} \tag{11.1.4}$$

Thus, $h \circ P_0 \colon V_0 \to \Sigma_1$ is well defined but $P_1 \circ h$ need not be defined, since P_1 is not defined on all of Σ_1; however, this problem is solved if we choose Σ_1 such that $V_1 = h(V_0)$ and take V_0 sufficiently small. □

11.2 Case 2: The Poincaré Map of a Time-Periodic Ordinary Differential Equation: Variation of the Cross-Section

Consider the Poincaré map $P_{\bar{\theta}_0}$ defined on the cross-section $\Sigma^{\bar{\theta}_0}$ as defined in (10.2.5). Suppose we construct a different Poincaré map, $P_{\bar{\theta}_1}$, in the same manner but on the cross-section

$$\Sigma^{\bar{\theta}_1} = \left\{ (x, \theta) \in \mathbb{R}^n \times S^1 \mid \theta = \bar{\theta}_1 \in (0, 2\pi] \right\}. \tag{11.2.1}$$

Then we have the following result.

Proposition 11.2.1 *$P_{\bar{\theta}_0}$ and $P_{\bar{\theta}_1}$ are $\mathbf{C}^r$ conjugate.*

Proof: The proof follows a construction similar to that given in Proposition 11.1.1. We construct a $\mathbf{C}^r$ diffeomorphism, h, of $\Sigma^{\bar{\theta}_0}$ into $\Sigma^{\bar{\theta}_1}$ by mapping points on $\Sigma^{\bar{\theta}_0}$ into $\Sigma^{\bar{\theta}_1}$ under the action of the flow generated by (10.2.3). Points starting on $\Sigma^{\bar{\theta}_0}$ have initial time $t_0 = (\bar{\theta}_0 - \theta_0)/\omega$, and they reach $\Sigma^{\bar{\theta}_1}$ after time

$$t = \frac{\bar{\theta}_1 - \bar{\theta}_0}{\omega};$$

thus we have

$$\begin{aligned} &h \colon \Sigma^{\bar{\theta}_0} \to \Sigma^{\bar{\theta}_1}, \\ &\left(x \left(\frac{\bar{\theta}_0 - \theta_0}{\omega} \right), \bar{\theta}_0 \right) \mapsto \left(x \left(\frac{\bar{\theta}_1 - \theta_0}{\omega} \right), \bar{\theta}_1 \right). \end{aligned} \tag{11.2.2}$$

Using (11.2.2) and the expression for the Poincaré maps defined on the different cross-sections, we obtain

$$\begin{aligned} &h \circ P_{\bar{\theta}_0} \colon \Sigma^{\bar{\theta}_0} \to \Sigma^{\bar{\theta}_1}, \\ &\left(x \left(\frac{\bar{\theta}_0 - \theta_0}{\omega} \right), \bar{\theta}_0 \right) \mapsto \left(x \left(\frac{\bar{\theta}_1 - \theta_0 + 2\pi}{\omega} \right), \bar{\theta}_1 + 2\pi \equiv \bar{\theta}_1 \right), \end{aligned} \tag{11.2.3}$$

and

$$\begin{aligned} &P_{\bar{\theta}_1} \circ h \colon \Sigma^{\bar{\theta}_0} \to \Sigma^{\bar{\theta}_1}, \\ &\left(x \left(\frac{\bar{\theta}_0 - \theta_0}{\omega} \right), \bar{\theta}_0 \right) \mapsto \left(x \left(\frac{\bar{\theta}_1 - \theta_0 + 2\pi}{\omega} \right), \bar{\theta}_1 + 2\pi \equiv \bar{\theta}_1 \right). \end{aligned} \tag{11.2.4}$$

Thus, from (11.2.3) and (11.2.4), we have that

$$h \circ P_{\bar{\theta}_0} = P_{\bar{\theta}_1} \circ h. \quad \square \tag{11.2.5}$$

Therefore, Propositions 11.0.2 and 11.0.3 imply that, as long as we remain sufficiently close to the periodic orbit, changing the cross-section does not have any dynamical effect in the sense that we will still have the same orbits with the same stability type. However, geometrically there may be an apparent difference in the sense that the locations of the orbits as well as their stable and unstable manifolds may "move around" under a change in cross-section. It may also be possible that an intelligent choice of the cross-section could result in a "more symmetric" Poincaré map which could facilitate the analysis. We will see an example of this later.

We note that the case of a Poincaré map near a homoclinic orbit can be treated in the same way with the same results. We leave this as an exercise for the reader.

We remark that it should be clear from these results that a Poincaré map constructed according to Case 2 (i.e., the global cross-section) has information concerning all possible dynamics of the vector field. When only a local cross-section can be constructed, then the Poincaré map will not, in general, contain information on all possible dynamics of the vector field. Different Poincaré maps defined on different cross-sections may not have the same dynamics.

12

Structural Stability, Genericity, and Transversality

The mathematical models we devise to make sense of the world around and within us can only be approximations. Therefore, it seems reasonable that if they are to accurately reflect reality, the models themselves must be somewhat insensitive to perturbations and have properties that are "not atypical", in a sense that is not easy to characterize in a way that is useful in applications. The attempts to give mathematical substance to these rather vague ideas have led to the concept of *structural stability* and *genericity*, which have played an important role historically in the development of dynamical systems theory as a *mathematical* subject. Another concept that we define in this chapter is *transversality*. This is an example of a "typical property" arising in a number of settings that is amenable to concrete calculations. We will see that it will play an important role in local and global bifurcation theory, as well as in characterizing chaotic dynamics.

Before defining structural stability and genericity, let us consider a specific example which illustrates many of the issues that need to be addressed.

Example 12.0.1. Consider the simple harmonic oscillator

$$\begin{aligned} \dot{x} &= y, \\ \dot{y} &= -\omega_0^2 x, \end{aligned} \qquad (x, y) \in \mathbb{R}^2. \tag{12.0.1}$$

We know everything about this system. It has a nonhyperbolic fixed point of $(x, y) = (0, 0)$ surrounded by a one-parameter family of periodic orbits, each having frequency ω_0. The phase portrait of (12.0.1) is shown in Figure 12.0.1 (note: strictly speaking, the phase curves are circles for $\omega_0 = 1$ and ellipses otherwise). Is (12.0.1) stable with respect to perturbations (note: this is a new concept of stability, as opposed to the idea of stability of specific solutions discussed in Chapter 1)? Let us try a few perturbations and see what happens.

Linear, Dissipative Perturbation

Consider the perturbed system

$$\begin{aligned} \dot{x} &= y, \\ \dot{y} &= -\omega_0^2 x - \varepsilon y. \end{aligned} \tag{12.0.2}$$

It is easy to see that the origin is a hyperbolic fixed point, a sink for $\varepsilon > 0$ and a source for $\varepsilon < 0$. However, all the periodic orbits are destroyed (use Bendixson's criteria). Thus, this perturbation radically alters the structure of the phase space of (12.0.1); see Figure 12.0.2.

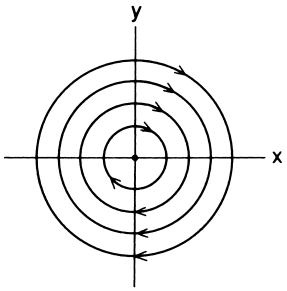

FIGURE 12.0.1.

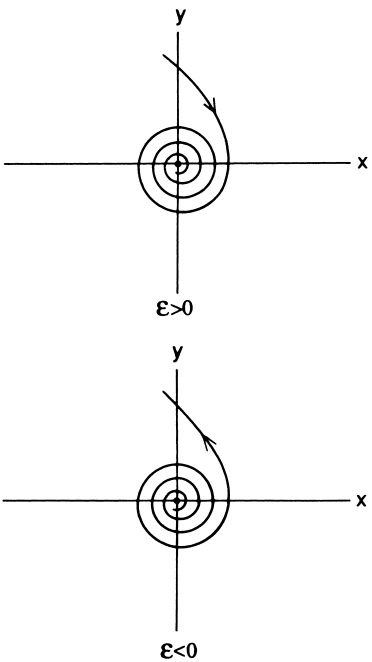

FIGURE 12.0.2.

Nonlinear Perturbation

Consider the perturbed system

$$\begin{aligned} \dot{x} &= y, \\ \dot{y} &= -\omega_0^2 x + \varepsilon x^2. \end{aligned} \tag{12.0.3}$$

The perturbed system now has two fixed points given by

$$\begin{aligned} (x, y) &= (0, 0), \\ (x, y) &= (\omega_0^2/\varepsilon, 0). \end{aligned} \tag{12.0.4}$$

The origin is still a center (i.e., unchanged by the perturbation), and the new fixed point is a saddle and far away for ε small.

This particular perturbation has the property of preserving a first integral. In particular, (12.0.3) has a first integral given by

$$h(x,y) = \frac{y^2}{2} + \frac{\omega_0^2 x^2}{2} - \varepsilon \frac{x^3}{3}. \tag{12.0.5}$$

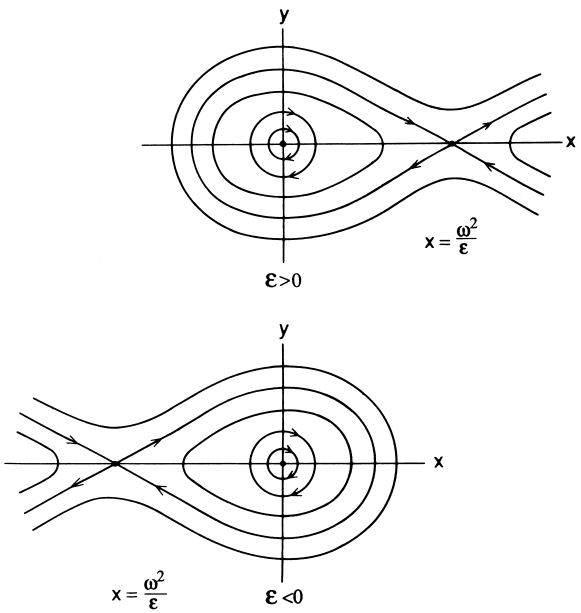

FIGURE 12.0.3.

This enables us to draw all phase curves for (12.0.3), which are shown in Figure 12.0.2. From Figure 12.0.3, we make the following observations.

1. This particular perturbation preserves the symmetry of (12.0.3) implied by the existence of a first integral. Therefore, sufficiently close to $(x, y) = (0, 0)$ the phase portraits of (12.0.1) and (12.0.3) look the same. However, for (12.0.3), it is important to note that the frequency of the periodic orbits changes with distance from the origin, as opposed to (12.0.1).
2. The phase space of (12.0.1) is unbounded. Therefore, no matter how small we take ε, far enough away from the origin the perturbation is no longer a small perturbation. This is evidenced in Figure 12.0.3 by the saddle point and the homoclinic orbit connecting it to itself. Thus, there is a problem in discusing perturbations of vector fields on unbounded phase spaces.

Time-Dependent Perturbation

Consider the system

$$\begin{aligned} \dot{x} &= y, \\ \dot{y} &= -\omega_0^2 x + \varepsilon x \cos t. \end{aligned} \tag{12.0.6}$$

This perturbation is of a very different character than the previous two. Writing (12.0.6) as an autonomous system (see Chapter 7)

$$\begin{aligned} \dot{x} &= y, \\ \dot{y} &= -\omega_0^2 x + \varepsilon x \cos\theta, \\ \dot{\theta} &= 1, \end{aligned} \tag{12.0.7}$$

we see that the time-dependent perturbation has the effect of enlarging the dimension of the system. However, in any case, $(x, y) = (0, 0)$ is still a fixed point of (12.0.6), although it is interpreted as a periodic orbit of (12.0.7). We now ask what the nature of the flow is near $(x, y) = (0, 0)$, which is a difficult question to answer due to the time dependence. Equation (12.0.6) is known as the Mathieu equation, and for $\omega_0 = n/2$, n an integer, it is possible for the system to exhibit parametric resonance resulting in a solution starting near the origin that grows without bound. Thus, the flow of (12.0.7) near the origin differs very much from the flow of (12.0.1) near the origin. For more information on the Mathieu equation see Nayfeh and Mook [1979].

End of Example 12.0.1

This simple example illustrates several points that need to be considered when discussing whether or not a system is stable under perturbations.

Specification of the Space of Dynamical Systems: It is important to specify the type of perturbations that are allowed. For example, if the system has a symmetry, then one might want to consider only perturbations which preserve the symmetry. The idea of structural stability thus depends on the type of dynamical system under consideration.

Quantifying "Closeness" of Dynamical Systems: In discussing the idea of a perturbation of a dynamical system, it is necessary to specify what it means for two vector fields or maps to be "close." In our example we used an ε and required ε to be small. However, we saw that this did not work well when the phase space was unbounded.

Quantifying Qualitatively Similar Dynamics: It is necessary to quantify the statement "two dynamical systems have qualitatively the same dynamics." This must be specified if one is to decide when a system is structurally stable.

Up to this point our discussion has been very heuristic. Indeed, our main purpose has been to get the reader to worry about whether the systems they are studying are stable under perturbations. We will see throughout this

book, especially when we study bifurcation theory, that a consideration of this question often reveals much about the underlying dynamics of dynamical systems. However, now we want to say a little about the mathematical formulation of the notion of structural stability.

12.1 Definitions of Structural Stability and Genericity

The concept of structural stability was introduced by Andronov and Pontryagin [1937] and has played a central role in the development of dynamical systems theory. Roughly speaking, a dynamical system (vector field or map) is said to be structurally stable if nearby systems have qualitatively the same dynamics. Therefore, in defining structural stability one must provide a recipe for determining when two systems are "close," and then one must specify what is meant by saying that, qualitatively, two systems have the same dynamics. We will discuss each question separately.

Let $\mathbf{C}^r(\mathbb{R}^n, \mathbb{R}^n)$ denote the space of $\mathbf{C}^r$ maps of $\mathbb{R}^n$ into $\mathbb{R}^n$. In terms of dynamical systems, we can think of the elements of $\mathbf{C}^r(\mathbb{R}^n, \mathbb{R}^n)$ as being vector fields. We denote the subset of $\mathbf{C}^r(\mathbb{R}^n, \mathbb{R}^n)$ consisting of the $\mathbf{C}^r$ diffeomorphisms by $\mathrm{Diff}^r(\mathbb{R}^n, \mathbb{R}^n)$. We remark that if one is studying dynamical systems that have certain symmetries, then additional constraints must be put on these spaces.

Two elements of $\mathbf{C}^r(\mathbb{R}^n, \mathbb{R}^n)$ are said to be $\mathbf{C}^r$ ε-close ($k \leq r$), or just $\mathbf{C}^k$ close, if they, along with their first k derivatives, are within ε as measured in some norm. There is a problem with this definition; namely, $\mathbb{R}^n$ is unbounded, and the behavior at infinity needs to be brought under control. The reader should consider this in the context of the example described at the beginning of this chapter. This explains why most of the mathematical theory of dynamical systems has been developed using compact phase spaces; however, in applications this is not sufficient and appropriate modifications must be made.

There are several ways of handling this difficulty. For the purpose of our discussion we will choose the usual way and assume that our maps act on compact, boundaryless n-dimensional differentiable manifolds, M, rather than all of $\mathbb{R}^n$. The topology induced on $\mathbf{C}^r(M, M)$ by this measure of distance between two elements of $\mathbf{C}^r(M, M)$ is called the $\mathbf{C}^k$ *topology*, and we refer the reader to Palis and de Melo [1982] or Hirsch [1976] for a more thorough discussion.

The question of what is meant by saying that two dynamical systems are close is usually answered in terms of conjugacies. Specifically, $\mathbf{C}^0$ conjugate maps have qualitatively the same orbit structure in the sense of the propositions given in Chapter 11. For vector fields there is a similar notion to $\mathbf{C}^k$ conjugacies for maps called a $\mathbf{C}^k$ equivalence. We will discuss this in more

detail in Chapter 20 when we study bifurcation theory (note: in some sense the study of bifurcation theory will be the study of structural instability). In this section we will state the definitions for maps along with vector fields; the reader should refer back to these definitions when we study the related ideas for vector fields.

We are now at the point where we can formally define structural stability.

Definition 12.1.1 (Structural Stability) *Consider a map $f \in \mathrm{Diff}^r(M, M)$ (resp. a $\mathbf{C}^r$ vector field in $\mathbf{C}^r(M, M)$); then f is said to be* structurally stable *if there exists a neighborhood $\mathcal{N}$ of f in the $\mathbf{C}^k$ topology such that f is $\mathbf{C}^0$ conjugate (resp. $\mathbf{C}^0$ equivalent) to every map (resp. vector field) in $\mathcal{N}$.*

Now that we have defined structural stability, it would be nice if we could determine the characteristics of a specific system which result in that system being structurally stable. From the point of view of the applied scientist, this would be useful, since one might presume that a dynamical system used to model phenomena occurring in nature should possess the property of structural stability. Unfortunately, such a characterization does not exist, although some partial results are known, which we will describe shortly. One approach to the characterization of structural stability has been through the identification of typical or generic properties of dynamical systems, and we now discuss this idea.

Naively, one might expect a typical or generic property of a dynamical system to be one that is common to a dense set of dynamical systems in $\mathbf{C}^r(M, M)$. This is not quite adequate, since it is possible for a set and its complement to both be dense. For example, the set of rational numbers is dense in the real line, and so is its complement, the set of irrational numbers. However, there are many more irrational numbers than rational numbers, and one might expect the irrationals to be more typical than the rationals in some sense. The proper *topological* sense in which this is true is captured by the idea of a *residual set*.

Definition 12.1.2 (Residual Set) *Let X be a topological space, and let U be a subset of X. U is called a* residual set *if it contains the intersection of a countable number of sets, each of which are open and dense in X. If every residual set in X is itself dense in X, then X is called a* Baire space.

We remark that $\mathbf{C}^r(M, M)$ equipped with the $\mathbf{C}^r$ topology ($k \leq r$) is a Baire space (see Palis and deMelo [1982]). We now give the definition of a generic property.

Definition 12.1.3 (Generic Property) *A property of a map (resp. vector field) is said to be $\mathbf{C}^k$* generic *if the set of maps (resp. vector fields) possessing that property contains a residual subset in the $\mathbf{C}^k$ topology.*

Residual sets have played the central role in characterizing genericity in the development of dynamical systems theory as a mathematical subject. Upon an initial consideration of the definition, one would expect that residual sets capture "most" of the points in a space. However, the manner in which one mathematically captures the concept of "most", is rather subtle. Residual sets are a topological notion. One might also consider a probabilistic or measure theoretic notion of "typical". For example, on the unit interval the rational numbers have Lebesgue meaure zero and the irrational numbers have Lebesgue measure one (full measure). Such a characterization is not equivalent to the topological characterization since a residual set can have Lebesgue measure zero and an open and dense subset of $\mathbb{R}^n$ can have arbitrarily small Lebesgue measure. Hence, certain generic properties could occur with zero probability. An excellent discussion of these ideas, as well as a development of these ideas in a measure-theoretic framework, can be found in Hunt *et al.* [1992].

Below we list some generic properties of dynamical systems (in the sense of the property holding for a residual subset of the appropriately defined space).

Example 12.1.1 (Examples of Structurally Stable and Generic Properties).

- Hyperbolic fixed points and periodic orbits are structurally stable and generic.
- The transversal intersection (see Section 12.2) of the stable and unstable manifolds of hyperbolic fixed points and periodic orbits is structurally stable and generic.

End of Example 12.1.1

The proof of these statements in a carefully defined class of dynamical systems comprises the Kupka-Smale Theorem. Details of the proof of this theorem can be found in Palis and de Melo [1992].

In utilizing the idea of a generic property to characterize the structurally stable systems, one first identifies some generic property. Then, since a structurally stable system is $\mathbf{C}^0$ conjugate (resp. equivalent for vector fields) to all nearby systems, structurally stable systems must have this property if the property is one that is preserved under $\mathbf{C}^0$ conjugacy (resp. equivalence for vector fields). One would like to go the other way with this argument; namely, it would be nice to show that structurally stable systems are generic. For two-dimensional vector fields on compact manifolds, we have the following result due to Peixoto [1962].

Theorem 12.1.4 (Peixoto's Theorem) *A $\mathbf{C}^r$ vector field on a compact boundaryless two-dimensional manifold M is structurally stable if and only if*

i) *the number of fixed points and periodic orbits is finite and each is hyperbolic;*

ii) *there are no orbits connecting saddle points;*

iii) *the nonwandering set consists of fixed points and periodic orbits.*

Moreover, if M is orientable, then the set of such vector fields is open and dense in $\mathbf{C}^r(M, M)$ (note: this is stronger than generic).

This theorem is useful because it spells out precise conditions under which the dynamics of a vector field on a compact boundaryless two manifold are structurally stable. Unfortunately, we do not have a similar theorem in higher dimensions. This is in part due to the presence of complicated recurrent motions (e.g., the Smale horseshoe; see Chapter 23) which are not possible for two-dimensional vector fields. Even more disappointing is the fact that structural stability is not a generic property for n-dimensional diffeomorphisms ($n \geq 2$) or n-dimensional vector fields ($n \geq 3$). This fact was first demonstrated by Smale [1966].

At this point we will conclude our brief discussion of the ideas of structural stability and genericity. For more information, we refer the reader to Chillingworth [1976], Hirsch [1976], Arnold [1983], Nitecki [1971], Smale [1967], and Shub [1987]. However, before ending this section, we want to comment on the relevance of these ideas to the applied scientist, i.e., someone who must discover what types of dynamics are present in a specific dynamical system.

Genericity and structural stability as defined above have been guiding forces behind much of the development of dynamical systems theory. The approach often taken has been to postulate some "reasonable" form of dynamics for a certain class of dynamical systems and then to prove that this form of dynamics is structurally stable and/or generic within this class. If one is persistent with this approach one is occasionally successful and eventually a significant catalogue of generic and structurally stable dynamical properties is obtained. This catalogue is useful to the applied scientist in that it gives some idea of what dynamics to expect in a specific dynamical system. However, this is hardly adequate. Given a specific dynamical system, is it structurally stable and/or generic?

We would like to give computable conditions under which a specific dynamical system is structurally stable and/or generic. For certain special types of motions such as periodic orbits and fixed points, this can be done in terms of the eigenvalues of the linearized system. However, for more general, global motions such as homoclinic orbits and quasiperiodic orbits, this cannot be done so easily, since the nearby orbit structure may be exceedingly complicated and defy any local description. What this boils down to is that to determine whether or not a specific dynamical system is structurally stable, one needs a fairly complete understanding of its orbit structure, or

to put it more cynically, one needs to know the answer before asking the question. It might therefore seem that these ideas are of little use to the applied scientist; however, this is not exactly true, since the theorems describing structural stability and generic properties do give one a good idea of what to *expect*, although they cannot tell what is precisely happening in a specific system. Also, the reader should always ask him or herself whether or not the dynamics are stable and/or typical in some sense. Probably the best way of mathematically quantifying these two notions for the applied scientist has yet to be determined.

12.2 Transversality

Before leaving this section let us introduce the idea of *transversality*, which will play a central role in many of our geometrical arguments.

Transversality is a geometric notion which deals with the intersection of surfaces or manifolds. Let M and N be differentiable (at least $\mathbf{C}^1$) manifolds in $\mathbb{R}^n$.

Definition 12.2.1 (Transversality) *Let p be a point in $\mathbb{R}^n$; then M and N are said to be* transversal at p *if $p \notin M \cap N$; or, if $p \in M \cap N$, then $T_pM + T_pN = \mathbb{R}^n$, where T_pM and T_pN denote the tangent spaces of M and N, respectively, at the point p. M and N are said to be* transversal *if they are transversal at every point $p \in \mathbb{R}^n$; see Figure 12.2.1.*

Whether or not the intersection is transversal can be determined by knowing the dimension of the intersection of M and N. This can be seen as follows. Using the formula for the dimension of the intersection of two

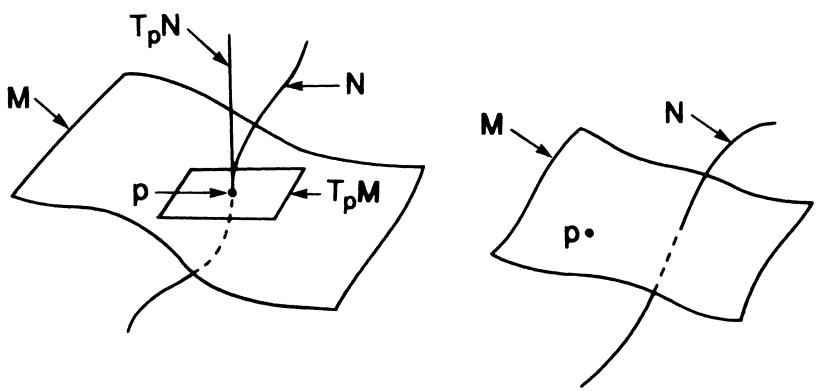

FIGURE 12.2.1. M and N transversal at p.

vector subspaces we have

$$\dim(T_pM + T_pN) = \dim T_pM + \dim T_pN - \dim(T_pM \cap T_pN). \quad (12.2.1)$$

From Definition 12.2.1, if M and N intersect transversely at p, then we have

$$n = \dim T_pM + \dim T_pN - \dim(T_pM \cap T_pN). \quad (12.2.2)$$

Since the dimensions of M and N are known, then knowing the dimension of their intersection allows us to determine whether or not the intersection is transversal.

Note that transversality of two manifolds at a point requires more than just the two manifolds geometrically piercing each other at the point. Consider the following example.

Example 12.2.1. Let M be the x axis in $\mathbb{R}^2$, and let N be the graph of the function $f(x) = x^3$; see Figure 12.2.2. Then M and N intersect at the origin in $\mathbb{R}^2$, but they are not transversal at the origin, since the tangent space of M is just the x axis and the tangent space of N is the span of the vector $(1, 0)$; thus, $T_{(0,0)}N = T_{(0,0)}M$ and, therefore, $T_{(0,0)}N + T_{(0,0)}M \neq \mathbb{R}^2$.

End of Example 12.2.1

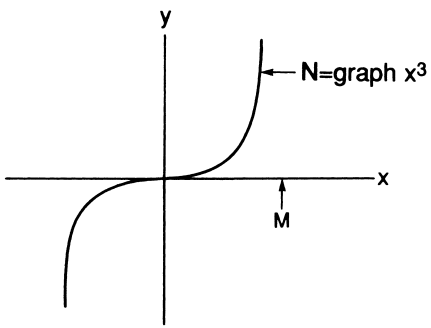

FIGURE 12.2.2. Nontransversal manifolds.

The most important characteristic of transversality is that it persists under sufficiently small perturbations. This fact will play a useful role in many of our geometric arguments; we remark that a term often used synonymously for transversal is *general position*, i.e., two or more manifolds which are transversal are said to be in general position.

Let us end this section by giving a few "dynamical" examples of transversality.

Example 12.2.2. Consider a hyperbolic fixed point of a $\mathbf{C}^r$, $r \geq 1$, vector field on $\mathbb{R}^n$. Suppose the matrix associated with the linearization of the vector

field about the fixed point has $n-k$ eigenvalues with positive real part and k eigenvalues with negative real part. Thus this fixed point has an $(n-k)$-dimensional unstable manifold and a k-dimensional stable manifold. If these two manifolds intersect in a point, other than the fixed point, then by uniqueness of solutions and invariance of the manifolds, they must intersect along a (at least) one-dimensional orbit. Hence, by (12.2.2), the intersection *cannot* be transverse.

End of Example 12.2.2

Example 12.2.3. Suppose the vector field of Example 12.2.2 is Hamiltonian so that all orbits are restricted to lie in $(n-1)$-dimensional "energy" surfaces given by the level sets of the Hamiltonian. Then it is possible for the stable and unstable manifolds of the hyperbolic fixed point to intersect transversely *in the* $(n-1)$*-dimensional energy surface.*

End of Example 12.2.3

Example 12.2.4. Consider a hyperbolic periodic orbit of a $\mathbf{C}^r$, $r \geq 1$, vector field on $\mathbb{R}^n$. Suppose that the Poincaré map associated with the periodic orbit linearized about the fixed point has $n-k-1$ eigenvalues with modulus greater than one and k eigenvalues with modulus less than one. Then the periodic orbit has an $(n-k)$-dimensional unstable manifold and a $(k+1)$-dimensional stable manifold. Therefore, by (12.2.2), if these manifolds intersect transversely, the dimension of the intersection must be one. This is possible without violating uniqueness of solutions and invariance of the manifolds.

End of Example 12.2.4

12.3 Exercises

1. Consider the space of linear, autonomous vector fields on $\mathbb{R}^2$.
   (a) Give a rigorous definition of this space. Define a norm on this space.
   (b) Describe the set of structurally stable vector fields on this space. Is this set a residual set?
2. Consider the unit interval in $\mathbb{R}$. Show that the irrational numbers are a residual subset. Show that the rational numbers are not a residual subset.
3. Consider the unit interval in $\mathbb{R}$. Construct an open and dense subset having Lebesgue measure smaller than any specified number. Construct a residual subset with Lebesgue measure zero. (Hint: for help, see Hunt *et al.* [1992].)
4. Discuss the idea of structural stability of the following vector fields and maps.

   a) $\begin{aligned} \dot{\theta}_1 &= \omega_1, \\ \dot{\theta}_2 &= \omega_2, \end{aligned} \qquad (\theta_1, \theta_2) \in S^1 \times S^1.$

   b) $\begin{aligned} \dot{x} &= 1, \\ \dot{y} &= 2, \end{aligned} \qquad (x, y) \in \mathbb{R}^2.$

   c) $\begin{aligned} \dot{x} &= y, \\ \dot{y} &= x - x^3, \end{aligned} \qquad (x, y) \in \mathbb{R}^2.$

d) $\begin{aligned} \dot{x} &= y, \\ \dot{y} &= x - x^3 - y, \end{aligned} \qquad (x, y) \in \mathbb{R}^2.$

e) $\theta \mapsto \theta + \omega, \qquad \theta \in S^1.$

f) $\theta \mapsto \theta + \omega + \varepsilon \sin\theta, \qquad \varepsilon \text{ small}, \quad \theta \in S^1.$

5. Consider an autonomous vector field on $\mathbb{R}^2$ having a hyperbolic sink equilibrium point and a hyperbolic saddle equilibrium point.

   (a) Can the unstable manifold of the saddle intersect the stable manifold of the sink transversely?

   (b) Can the stable manifold of the saddle intersect the stable manifold of the sink transversely?

6. Consider an autonomous vector field on $\mathbb{R}^3$ having a hyperbolic periodic orbit and a hyperbolic saddle equilibrium point having a one dimensional stable manifold and a two dimensional unstable manifold.

   (a) Can the unstable manifold of the saddle intersect the stable manifold of the periodic orbit transversely?

   (b) Can the stable manifold of the saddle intersect the unstable manifold of the periodic orbit transversely?

13

Lagrange's Equations

Up to this point in the book we have been studying general dynamical systems, e.g., , $\dot{x} = f(x)$, where $f(x)$ is just C^r. In this, and the following four chapters, we will study dynamical systems with *special structure*; Lagrangian systems, Hamiltonian systems, gradient vector fields, reversible systems, and asymptotically autonomous vector fields. We will see that the particular special structure greatly constrains the types of dynamics that are allowed, and it also provides techniques of analysis that are particular to the special structure. These particular types of structure are important because they do arise in a variety of applications.

In this chapter we will derive and discuss the properties of Lagrange's euations of motion or *Lagrangian dynamical systems* for a system of P particles each having constant mass m_p and located at position $\mathbf{r}_p = (x_p, y_p, z_p)$, $p = 1, \ldots, P$, where (x_p, y_p, z_p) denote the standard cartesian coordinates.

The issue of the correct choice of coordinates is central to the understanding of many problems in dynamical systems theory. Indeed, many techniques, such as normal form theory and invariant manifold theory, are primarily concerned with finding a coordinate system in which the dynamical system assumes the "simplest" form, or the dimensionality (i.e., in this context, we mean the number of equations) of the system is reduced.

For a system of P point masses moving under the influence of external and internal forces it may be that there are certain functional relations among some of the coordinate components. In this case we say that the motion of the point masses is subject to certain *constraints*. For example, a particle could be constrained to move on the surface of a sphere, on an inclined plane, etc.

Suppose the system of P particles is such that C functional relations must be satisfied by the coordinates of the particles. We represent these *constraints* as follows:

$$\phi_i \left(x_1, y_1, z_1, \ldots, x_P, y_P, z_P, t\right), \qquad i = 1, \ldots, C. \tag{13.0.1}$$

Constraints that are represented as functions of the coordinates and time in this manner are referred to as *holonomic constraints*. In this case we say that the system has $N = 3P - C$ *degrees of freedom*. That is, the position of all the particles in the system can be specified by choosing N *independent* coordinates. In other words, the number of degrees of freedom of a system is the number of independent coordinates needed to specify the positions

of all the components (in our case, particles) of the system. Choosing such a system of independent coordinates brings up the notion of *generalized coordinates*, which we now discuss.

13.1 Generalized Coordinates

We introduce the notion of generalized coordinates by first considering an example.

Example 13.1.1 (The Double Pendulum).

The double pendulum consists of two mass points moving in the $x - y$ plane. The mass point m_1 is located at a fixed distance, l_1, from a fixed point O, and m_2 is located a fixed distance l_2 from m_1, see Fig. 13.1.1.

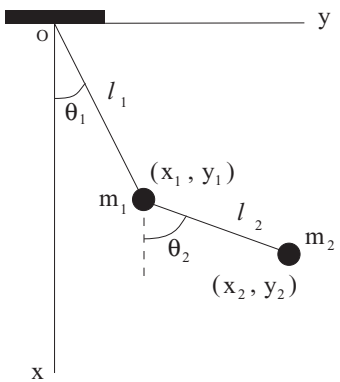

FIGURE 13.1.1. Geometry of the double pendulum.

The location of m_1 is given by the cartesian coordinates (x_1, y_1) and the location of m_2 is given by (x_2, y_2). However, one sees that four coordinates are not necessary for describing the location of all the particles in this system. In fact, the location of each point can be described by a single angle, as shown in Fig. 13.1.1. This is because each mass point must remain a fixed distance from a given point. This results in us being able to describe the location of the mass point by the angle around the point from which it remains a fixed distance. Moreover, we can write down the relation between the coordinates (x_1, y_1, x_2, y_2) and (θ_1, θ_2) as follows:

$$\begin{aligned} x_1 &= l_1 \cos\theta_1, & y_1 &= l_1 \sin\theta_1, \\ x_2 &= l_1 \cos\theta_1 + l_2 \cos\theta_2, & y_2 &= l_1 \sin\theta_1 + l_2 \sin\theta_2. \end{aligned} \tag{13.1.1}$$

In this example (θ_1, θ_2) are generalized coordinates for the double pendulum.

End of Example 13.1.1

A set of coordinates that contain the minimum number of independent coordinates needed to specify all the positions of a set of particles is referred to as *generalized coordinates*, and denoted by $(q_1, \ldots, q_N)$. Generalized coordinates may be distances, angles, or quantities relating them. The integer N is referred to as the number of *degrees-of-freedom* of a system. So a system is said to have N degrees-of-freedom if the positions of all its components can be described by N independent (generalized) coordinates. The space of generalized coordinates of a system is often referred to as the *configuration space* of the system (the reader should contrast this with the notion of "phase space"). Furthermore, we refer to $(\dot{q}_1, \ldots, \dot{q}_N)$ as *generalized velocities*.

Getting back to the notion of constraints, one could also say that the constraints imposed on a system are holonomic if it is possible to choose a set of *independent* generalized coordinates to describe the position of the set of particles. The issue of constraints is very important in dynamics, and is beyond the scope of this book. Excellent discussions of constraints, both holonomic and non-holonomic, can be found in Sommerfeld [1952], Whittaker [1904], and Arnold [1978]. One of the strengths of the Lagrangian form of dynamics is that it deals with constraints in a very simple manner, especially holonomic constraints. In this chapter we will deal exclusively with holonomic constraints.

The relationship between the original cartesian position coordinates of each particle and the generalized coordinates (see, as an example, eq. (13.1.1)) is expressed in the following form:

$$\begin{aligned} x_p &= x_p(q_1, \ldots, q_N, t), \\ y_p &= y_p(q_1, \ldots, q_N, t), \\ z_p &= z_p(q_1, \ldots, q_N, t), \qquad p = 1, \ldots, P, \end{aligned} \tag{13.1.2}$$

or, in vector notation

$$\mathbf{r}_p = \mathbf{r}_p(q_1, \ldots, q_N, t), \qquad p = 1, \ldots, P. \tag{13.1.3}$$

In the derivation of Lagrange's equations of motion two relationships between the derivatives of the coordinates and velocities and the corresponding generalized coordinates and velocities will be particularly useful, so we want to derive them now.

Differentiating (13.1.3) with respect to time gives:

$$\dot{\mathbf{r}}_p = \frac{\partial \mathbf{r}_p}{\partial q_1}\dot{q}_1 + \cdots + \frac{\partial \mathbf{r}_p}{\partial q_N}\dot{q}_N + \frac{\partial \mathbf{r}_p}{\partial t} = \sum_{i=1}^{N}\left(\frac{\partial \mathbf{r}_p}{\partial q_i}\dot{q}_i + \frac{\partial \mathbf{r}_p}{\partial t}\right), \tag{13.1.4}$$

from which it follows that

$$\frac{\partial \dot{\mathbf{r}}_p}{\partial \dot{q}_i} = \frac{\partial \mathbf{r}_p}{\partial q_i}. \tag{13.1.5}$$

If we assume that the second order partial derivative of (13.1.3) exist and are continuous then the order of differentiation with respect to any two variables can be interchanged. In this case we have

$$\frac{d}{dt}\left(\frac{\partial \mathbf{r}_p}{\partial q_i}\right) = \frac{\partial \dot{\mathbf{r}}_p}{\partial q_i}, \tag{13.1.6}$$

which can be derived directly from (13.1.4) with a bit of work, which we leave for the reader.

13.2 Derivation of Lagrange's Equations

Now we are ready to derive Lagrange's equations of motion. Newton's second law of motion for the point mass m_p acted on by the force $\mathbf{F}_p$ is given by

$$m_p \ddot{\mathbf{r}}_p = \mathbf{F}_p. \tag{13.2.1}$$

Here the force $\mathbf{F}_p$ acting on the particle p could be due to internal forces of interaction amongst the particles (such as electrical or gravitational interactions) or external forces. This distinction is not important in the derivation of Lagrange's equations.

Imagine each point p is subject to a displacement $d\mathbf{r}_p$. Then the work done on the *system of particles* is given by

$$\sum_{p=1}^{P} m_p \ddot{\mathbf{r}}_p \cdot d\mathbf{r}_p = \sum_{p=1}^{P} \mathbf{F}_p \cdot d\mathbf{r}_p. \tag{13.2.2}$$

This is the key expression in our derivation of Lagrange's equations (although there are other ways in which Lagrange's equations may be derived, see Sommerfeld [1952]). Computing the differential of (13.1.3) gives:

$$d\mathbf{r}_p = \sum_{i=1}^{N} \left(\frac{\partial \mathbf{r}_p}{\partial q_i} dq_i + \frac{\partial \mathbf{r}_p}{\partial t} dt\right). \tag{13.2.3}$$

Substituting (13.2.3) into the left hand side of (13.2.2) gives:

$$\begin{aligned}
\sum_{p=1}^{P} m_p \ddot{\mathbf{r}}_p \cdot d\mathbf{r}_p &= \sum_{p=1}^{P}\sum_{i=1}^{N} m_p \ddot{\mathbf{r}}_p \cdot \left(\frac{\partial \mathbf{r}_p}{\partial q_i} dq_i + \frac{\partial \mathbf{r}_p}{\partial t} dt\right) \\
&= \sum_{p=1}^{P}\sum_{i=1}^{N} m_p \left(\frac{d}{dt}\left(\dot{\mathbf{r}}_p \cdot \frac{\partial \dot{\mathbf{r}}_p}{\partial \dot{q}_i}\right) - \dot{\mathbf{r}}_p \cdot \frac{d}{dt}\frac{\partial \mathbf{r}_p}{\partial q_i}\right) dq_i \\
&\qquad + m_p \ddot{\mathbf{r}}_p \cdot \frac{\partial \mathbf{r}_p}{\partial t} dt \qquad \text{using (13.1.5) and (13.1.6)}
\end{aligned}$$

$$= \sum_{p=1}^{P} \sum_{i=1}^{N} \left(\frac{d}{dt} \frac{\partial}{\partial \dot{q}_i} \left(\frac{1}{2} m_p \dot{\mathbf{r}}_p \cdot \dot{\mathbf{r}}_p \right) - \frac{\partial}{\partial q_i} \left(\frac{1}{2} m_p \dot{\mathbf{r}}_p \cdot \dot{\mathbf{r}}_p \right) \right) dq_i$$

$$+ m_p \ddot{\mathbf{r}}_p \cdot \frac{\partial \mathbf{r}_p}{\partial t} dt,$$

$$= \sum_{i=1}^{N} \left(\frac{d}{dt} \left(\frac{\partial T}{\partial \dot{q}_i} \right) - \frac{\partial T}{\partial q_i} \right) dq_i + \sum_{p=1}^{P} m_p \ddot{\mathbf{r}}_p \cdot \frac{\partial \mathbf{r}_p}{\partial t} dt, \quad (13.2.4)$$

where

$$T = \frac{1}{2} \sum_{p=1}^{P} m_p \dot{\mathbf{r}}_p \cdot \dot{\mathbf{r}}_p, \quad (13.2.5)$$

is the *kinetic energy* of the system of P particles.

Substituting (13.2.3) into the right hand side of (13.2.2) gives:

$$\sum_{p=1}^{P} \mathbf{F}_p \cdot d\mathbf{r}_p = \sum_{i=1}^{N} \sum_{p=1}^{P} \mathbf{F}_p \cdot \frac{\partial \mathbf{r}_p}{\partial q_i} dq_i + \sum_{p=1}^{P} \mathbf{F}_p \cdot \frac{\partial \mathbf{r}_p}{\partial t} dt,$$

$$= \sum_{i=1}^{N} \Phi_i dq_i + \sum_{p=1}^{P} \mathbf{F}_p \cdot \frac{\partial \mathbf{r}_p}{\partial t} dt, \quad (13.2.6)$$

where

$$\Phi_i \equiv \sum_{p=1}^{P} \mathbf{F}_p \cdot \frac{\partial \mathbf{r}_p}{\partial q_i}, \quad (13.2.7)$$

is referred to as the *generalized force* associated with the generalized coordinate q_i.

Since (13.2.6) and (13.2.4) are equal (from (13.2.2)), subtracting these two equations gives:

$$\sum_{i=1}^{N} \left(\left(\frac{d}{dt} \left(\frac{\partial T}{\partial \dot{q}_i} \right) - \frac{\partial T}{\partial q_i} \right) - \Phi_i \right) dq_i = 0. \quad (13.2.8)$$

Since we are considering only holonomic constraints the dq_i are all independent displacements. Then we must have:

$$\frac{d}{dt} \left(\frac{\partial T}{\partial \dot{q}_i} \right) - \frac{\partial T}{\partial q_i} = \Phi_i, \qquad i = 1, \ldots, N. \quad (13.2.9)$$

These are Lagrange's equations of motion.

If the forces are derivable from a potential function, i.e.,

$$\Phi_i = -\frac{\partial V}{\partial q_i}, \quad (13.2.10)$$

then we can write Lagrange's equations in a more compact form. We define the *Lagrangian function* (or, just the "Lagrangian") as

$$L = T - V. \tag{13.2.11}$$

Then, since V is only a function of the q_i, we have

$$\frac{\partial L}{\partial \dot{q}_i} = \frac{\partial T}{\partial \dot{q}_i},$$

and Lagrange's equations become:

$$\frac{d}{dt}\left(\frac{\partial L}{\partial \dot{q}_i}\right) - \frac{\partial L}{\partial q_i} = 0, \qquad i = 1, \ldots, N. \tag{13.2.12}$$

From (13.1.3), (13.1.4), (13.2.5), and (13.2.7) we see that the Lagrangian has the following functional dependencies with respect to the generalized coordinates:

$$L = L(q_1, \ldots, q_N, \dot{q}_1, \ldots, \dot{q}_N, t). \tag{13.2.13}$$

In some cases it may be convenient to adopt a shorthand notation for (13.2.12). Let

$$q \equiv (q_1, \ldots, q_N), \qquad \dot{q} \equiv (\dot{q}_1, \ldots, \dot{q}_N).$$

Then we write (13.2.12) as

$$\frac{d}{dt}\left(\frac{\partial L}{\partial \dot{q}}\right) - \frac{\partial L}{\partial q} = 0, \tag{13.2.14}$$

where (13.2.12) is the definition of (13.2.14).

We now give an example where we derive the equations of motion of a system using Lagrange's equations.

Example 13.2.1 (The Pendulum).

As an example, we compute the Lagrangian, and Lagrange's equations of motion, for the pendulum, as illustrated in Fig. 13.2.1. We assume that all forces acting on the pendulum are conservative (e.g., there is no drag force as the pendulum moves through air).

We choose as the generalized coordinate (the reader should convince him or herself that this is a one degree-of-freedom system) the angle θ between the vertical line OA and the string, OB, of the pendulum. If l denotes the length of OB then the kinetic energy is given by

$$T = \frac{1}{2}mv^2 = \frac{1}{2}m(l\dot{\theta})^2 = \frac{1}{2}ml^2\dot{\theta}^2.$$

Next we compute the potential energy, V, We take as a reference line the horizontal line through the lowest point of the pendulum, denoted A. Then the potential energy due to gravity is given by

$$V = mg\,(OA - OC) = mg\,(l - l\cos\theta) = mgl(1 - \cos\theta).$$

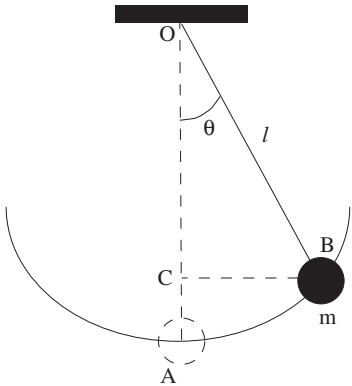

FIGURE 13.2.1. Geometry of the pendulum.

Hence, the Lagrangian is given by

$$L = T - V = \frac{1}{2}ml^2\dot{\theta}^2 - mgl(1 - \cos\theta).$$

Recall that Lagrange's equations of motion are given by:

$$\frac{d}{dt}\left(\frac{\partial L}{\partial \dot{\theta}}\right) - \frac{\partial L}{\partial \theta} = 0.$$

Therefore

$$\frac{\partial L}{\partial \theta} = -mgl\sin\theta,$$

and

$$\frac{\partial L}{\partial \dot{\theta}} = ml^2\dot{\theta}.$$

Hence, Lagrange's equations for the pendulum are given by:

$$ml^2\ddot{\theta} + mgl\sin\theta = 0,$$

or

$$\ddot{\theta} + \frac{g}{l}\sin\theta = 0.$$

End of Example 13.2.1

13.2A The Kinetic Energy

We now want to make a few remarks about the kinetic energy function in generalized coordinates. From (13.2.5), we see that the kinetic energy is a quadratic function when expressed in the original cartesian coordinates. We now want to express the kinetic energy in the $(q, \dot{q})$ coordinates. This

is done by substituting (13.1.4) into (13.2.5), and then after some routine algebra we obtain:

$$T = \sum_{i=1}^{N}\sum_{j=1}^{N} m_{i,j}(q,t)\dot{q}_i\dot{q}_j + \sum_{i=1}^{N} n_i(q,t)\dot{q}_i + f(q,t), \tag{13.2.15}$$

where

$$m_{i,j}(q,t) = \sum_{p=1}^{P} \frac{\partial \mathbf{r}_p}{\partial q_i} \cdot \frac{\partial \mathbf{r}_p}{\partial q_j},$$

$$n_i(q,t) = 2\sum_{p=1}^{P} \frac{\partial \mathbf{r}_p}{\partial q_i} \cdot \frac{\partial \mathbf{r}_p}{\partial t},$$

$$f(q,t) = \sum_{p=1}^{P} \frac{\partial \mathbf{r}_p}{\partial t} \cdot \frac{\partial \mathbf{r}_p}{\partial t}.$$

Note that if the transformation between the original coordinates and the generalized coordinates (i.e., (13.1.3)) is independent of time, then the last two sums in (13.2.15) do not occur.

13.3 The Energy Integral

In the case where the generalized forces are derivable from a potential function (so that Lagrange's equations are given by (13.2.12)), and the Lagrangian is independent of time, Lagrange's equations possess and integral of the motion, called the *energy integral*, which is given by:

$$E = \sum_{i=1}^{N} \frac{\partial L}{\partial \dot{q}_i}\dot{q}_i - L. \tag{13.3.1}$$

We prove this quantity is an integral for Lagrange's equations through the following calculation:

$$\begin{aligned}
\frac{dE}{dt} &= \sum_{i=1}^{N}\left(\left(\frac{d}{dt}\left(\frac{\partial L}{\partial \dot{q}_i}\right)\right)\dot{q}_i + \frac{\partial L}{\partial \dot{q}_i}\frac{d}{dt}\dot{q}_i\right) - \frac{dL}{dt}, \\
&= \sum_{i=1}^{N}\left(\left(\frac{d}{dt}\left(\frac{\partial L}{\partial \dot{q}_i}\right)\right)\dot{q}_i + \frac{\partial L}{\partial \dot{q}_i}\ddot{q}_i - \frac{\partial L}{\partial \dot{q}_i}\ddot{q}_i - \frac{\partial L}{\partial q_i}\dot{q}_i\right) - \frac{\partial L}{\partial t}, \\
&= \sum_{i=1}^{N}\left(\left(\frac{d}{dt}\frac{\partial L}{\partial \dot{q}_i}\right) - \frac{\partial L}{\partial q_i}\right)\dot{q}_i - \frac{\partial L}{\partial t}, \\
&= -\frac{\partial L}{\partial t}, \qquad \text{using (13.2.12)},
\end{aligned} \tag{13.3.2}$$

So if L does not depend on time then we have

$$\frac{dE}{dt} = 0.$$

13.4 Momentum Integrals

In the previous section we saw that when the Lagrangian is time independent there is an integral for the system, the energy integral. Similarly, we will now see that when the Lagrangian does not depend upon a certain coordinate, say q_k (although it may depend on $\dot{q}_k$), then there is also an integral for the system, called a *momentum integral*. The coordinate q_k is referred to as a *cyclic* or *ignorable* coordinate.

In particular, suppose

$$L = L(q_1, \ldots, q_{k-1}, q_{k+1}, \ldots, q_N, \dot{q}_1, \ldots, \dot{q}_N, t).$$

Then clearly

$$\frac{\partial L}{\partial q_k} = 0,$$

and therefore it follows from Lagrange's equations that

$$\frac{d}{dt}\left(\frac{\partial L}{\partial \dot{q}_k}\right) = 0.$$

Hence

$$\frac{\partial L}{\partial \dot{q}_k} = \beta_k = \text{constant}.$$

In general the quantity $\frac{\partial L}{\partial \dot{q}_k}$ is referred to as the kth *component of momentum* (or *generalized momentum*), and is denoted by p_k. It plays an important role in Hamilton's equations, which we now discuss.

13.5 Hamilton's Equations

Now we will show how Hamilton's equations can be derived using the Lagrangian.

The function

$$H(q, p, t) = \sum_{i=1}^{N} p_i \dot{q}_i - L(q, \dot{q}, t), \tag{13.5.1}$$

is defined to be the Hamiltonian function (or just "Hamiltonian") of the system. Note that it is just the energy integral given in (13.3.1) where

$$p_i \equiv \frac{\partial L}{\partial \dot{q}_i}, \qquad \text{and} \quad p = (p_1, \ldots, p_N). \tag{13.5.2}$$

This is an important point because the left hand side of (13.5.1) is denoted as a function of q, p, and t, rather than q, $\dot{q}$, and t. This is accomplished by using (13.5.2) to solve for $\dot{q}$ as a function of p, and then substituting the result for $\dot{q}$ into (13.5.1), resulting in a function depending on q, p, and t. Note that differentiating (13.5.2) with respect to time and using (13.1.5) gives

$$\dot{p}_i = \frac{\partial L}{\partial q_i}. \tag{13.5.3}$$

Computing the differential of (13.5.1) gives:

$$\begin{aligned} dH(q,p,t) &= \sum_{i=1}^{N} d\left(p_i \dot{q}_i\right) - dL, \\ &= \sum_{i=1}^{N} \dot{q}_i dp_i + p_i d\dot{q}_i - \frac{\partial L}{\partial q_i} dq_i - \frac{\partial L}{\partial \dot{q}_i} d\dot{q}_i - \frac{\partial L}{\partial t} dt, \\ &= \sum_{i=1}^{N} \dot{q}_i dp_i - \dot{p}_i dq_i - \frac{\partial L}{\partial t} dt, \quad \text{using (13.5.2) and (13.5.3).} \end{aligned} \tag{13.5.4}$$

Since, as described above, the Hamiltonian is a function of q, p, and t, we have, in general:

$$dH(q,p,t) = \sum_{i=1}^{N} \frac{\partial H}{\partial q_i} dq_i + \frac{\partial H}{\partial p_i} dp_i + \frac{\partial H}{\partial t} dt. \tag{13.5.5}$$

The expressions given in (13.5.4) and (13.5.5) must be equal. Since the q_i and p_i are independent (holonomic constraints), equating the coefficients of dq_i and dp_i immediately leads to Hamilton's equations

$$\begin{aligned} \dot{q}_i &= \frac{\partial H}{\partial p_i}, \\ \dot{p}_i &= -\frac{\partial H}{\partial q_i}, \qquad i = 1, \ldots, N, \end{aligned} \tag{13.5.6}$$

with the relation

$$\frac{\partial H}{\partial t} = -\frac{\partial L}{\partial t}. \tag{13.5.7}$$

13.6 Cyclic Coordinates, Routh's Equations, and Reduction of the Number of Equations

Now we will describe an elegant procedure due to Routh for reducing the number of equations that need to be integrated in the case where we have cyclic coordinates in the Lagrangian.

Suppose we have r cyclic coordinates. Without loss of generality (through relabeling the coordinates, if necessary) we can suppose these are the first r coordinates:

$$\left(\underbrace{q_1, \ldots, q_r}_{\text{cyclic}}, q_{r+1}, \ldots, q_N \right). \tag{13.6.1}$$

Then the Lagrangian has the form

$$L = L(q_{r+1}, \ldots, q_N, \dot{q}_1, \ldots, \dot{q}_N), \tag{13.6.2}$$

and, as we described earlier,

$$\frac{\partial L}{\partial \dot{q}_i} = \beta_i = \text{constant}, \qquad i = 1, \ldots, r. \tag{13.6.3}$$

Using (13.6.3) we can solve for $\dot{q}_i$, $i = 1, \ldots, r$, as a function of $q_{r+1}, \ldots, q_N, \dot{q}_{r+1}, \ldots, \dot{q}_N, \beta_1, \ldots, \beta_r, t$, i.e., we have

$$\dot{q}_i = \dot{q}_i(q_{r+1}, \ldots, q_N, \dot{q}_{r+1}, \ldots, \dot{q}_N, \beta_1, \ldots, \beta_r, t) \qquad i = 1, \ldots, r. \tag{13.6.4}$$

We then form Routh's function, or the *Routhian*, defined as follows:

$$R = L - \sum_{i=1}^{r} p_i \dot{q}_i, \tag{13.6.5}$$

Computing the differential of (13.6.5) gives:

$$\begin{aligned} dR &= \sum_{i=r+1}^{N} \frac{\partial L}{\partial q_i} dq_i + \sum_{i=1}^{N} \frac{\partial L}{\partial \dot{q}_i} d\dot{q}_i + \frac{\partial L}{\partial t} dt - \sum_{i=1}^{r} \left(p_i d\dot{q}_i + \dot{q}_i dp_i \right), \\ &= \sum_{i=r+1}^{N} \frac{\partial L}{\partial q_i} dq_i + \sum_{i=r+1}^{N} \frac{\partial L}{\partial \dot{q}_i} d\dot{q}_i + \frac{\partial L}{\partial t} dt - \sum_{i=1}^{r} \dot{q}_i dp_i. \end{aligned} \tag{13.6.6}$$

However, as we described above, in general the Routhian is a function of $q_{r+1}, \ldots, q_N, \dot{q}_{r+1}, \ldots, \dot{q}_N, \beta_1, \ldots, \beta_r, t$, where $\beta_i = p_i$, $i = 1, \ldots, r$. Computing the differential of the Routhian with these functional dependencies gives:

$$dR = \sum_{i=r+1}^{N} \left(\frac{\partial R}{\partial q_i} dq_i + \frac{\partial R}{\partial \dot{q}_i} d\dot{q}_i \right) + \sum_{i=1}^{r} \frac{\partial R}{\partial p_i} dp_i + \frac{\partial R}{\partial t} dt, \tag{13.6.7}$$

Now (13.6.6) and (13.6.7) must be equal. Since the coordinates q_i, $\dot{q}_i$ and p_i are independent we can then equate the coefficients on dq_i, $d\dot{q}_i$ and dp_i to obtain Routh's equations:

$$\begin{aligned} \frac{\partial L}{\partial q_i} &= \frac{\partial R}{\partial q_i}, \\ \frac{\partial L}{\partial \dot{q}_i} &= \frac{\partial R}{\partial \dot{q}_i}, \qquad i = r+1, \ldots, N, \end{aligned} \tag{13.6.8}$$

with the relation

$$\dot{q}_i = -\frac{\partial R}{\partial p_i}, \qquad i = 1, \ldots, r. \tag{13.6.9}$$

Substituting (13.6.8) into Lagrange's equations (13.2.14) gives:

$$\frac{d}{dt}\left(\frac{\partial R}{\partial \dot{q}_i}\right) - \frac{\partial R}{\partial q_i} = 0, \qquad i = r+1, \ldots, N. \tag{13.6.10}$$

Hence we solve the $N-r$ equations for $q_{r+1}, \ldots, q_N, \dot{q}_{r+1}, \ldots, \dot{q}_N$. We then substitute the result into (13.6.9) to obtain $\dot{q}_i$, $i = 1, \ldots, r$. In turn, these can then be integrated (since, now in principle they are known functions of time once (13.6.10) are solved) to give q_i, $i = 1, \ldots, r$. So we see that in the case where there are r cyclic coordinates the solution of Lagrange's equations can be "reduced" to the solution of $N-r$ (second order) differential equations.

13.7 Variational Methods

Trajectories of Lagrange's and Hamilton's equations can also be characterized as extrema of a certain functional defined on paths in configuration and phase space, respectively. This leads to the variational principles of mechanics, which we now describe. Excellent references with historical surveys can be found in Sommerfeld [1952] and Arnold [1978][1].

13.7A The Principle of Least Action

Let $\mathcal{C}$ denote the set of curves in the configuration space with fixed end points, i.e., a "point" in $\mathcal{C}$ is a map

$$t \mapsto (q_1(t), \ldots, q_N(t)) \equiv q(t), \qquad t_0 \le t \le t_1,$$

and the fixed endpoint condition means that every $q(t) \in \mathcal{C}$ satisfies $q(t_0) = q_0$ and $q(t_1) = q_1$. We equip $\mathcal{C}$ with the following norm. For $q \in \mathcal{C}$, the norm of q is defined as

$$\| q \| \equiv \sup_{t \in [t_0, t_1],\, 1 \le i \le N} \left(|q_i(t)| + |\dot{q}_i(t)| \right). \tag{13.7.1}$$

We will need the curves in $\mathcal{C}$ to have at least one continuous derivative.

---

[1] In most dynamics textbooks the action functional is stated and then it is shown that the extrema correspond to solutions of Lagrange's equations. Sommerfeld [1952] provides an insightful derivation of the action functional by beginning from the principle of virtual work (a differential variational principle, as opposed to the integral variational principles discussed here). See also Arnold [1978] for a similar argument in more modern mathematical language.

If $L(q, \dot{q}, t)$ denotes the Lagrangian of a system then the expression defined by

$$\Phi(q) = \int_{t_0}^{t_1} L(q, \dot{q}, t)dt = \int_{t_0}^{t_1} L(q_1, \ldots, q_N, \dot{q}_1, \ldots, \dot{q}_N, t)dt, \qquad (13.7.2)$$

is called the *action*. The action is an example of a functional, i.e., a map from $\mathcal{C}$ to $\mathbb{R}$. Now we want to define the notion of differentiability of this functional.

Definition 13.7.1 *The functional $\Phi(q)$ is said to be differentiable at q if $\Phi(q+h) - \Phi(q) = F + R$, where $F = F(q, h)$ is a linear function of h (with $h(t_0) = h(t_1) = 0$ in order to satisfy the fixed end point constraint, and regarding q as fixed), and $R = \mathcal{O}(\| h \|^2)$. The term linear in h, $F(q, h)$, is called the differential of Φ.*

We now define the notion of an *extremal* for the action.

Definition 13.7.2 *An extremal of the action Φ is a curve q such that $F(q, h) = 0$ for all h.*

Now we compute the differential of the action functional:

$$\begin{aligned}
&= \int_{t_0}^{t_1} \Big(L(q + h, \dot{q} + \dot{h}, t)dt - L(q, \dot{q}, t) \Big)\, dt, \\
&= \int_{t_0}^{t_1} \sum_{i=1}^{N} \left(\frac{\partial L}{\partial q_i} h_i + \frac{\partial L}{\partial \dot{q}_i} \dot{h}_i \right) dt + \mathcal{O}(\| h \|^2), \\
&= \int_{t_0}^{t_1} \sum_{i=1}^{N} \left(\frac{\partial L}{\partial q_i} - \frac{d}{dt}\frac{\partial L}{\partial \dot{q}} \right) h_i dt + \sum_{i=1}^{N} \frac{\partial L}{\partial \dot{q}_i} h_i \Big|_{t_0}^{t_1} + \mathcal{O}(\| h \|^2), \\
&\qquad\qquad \text{after integration by parts.} \qquad (13.7.3)
\end{aligned}$$

Now since $h(t_0) = h(t_1) = 0$ we see that the differential of the action is given by

$$\int_{t_0}^{t_1} \sum_{i=1}^{N} \left(\frac{\partial L}{\partial q_i} - \frac{d}{dt}\frac{\partial L}{\partial \dot{q}} \right) h_i dt. \qquad (13.7.4)$$

Now we set the differential of the action to zero and we can then appeal to a classical result from the calculus of variations (see, e.g., Arnold [1978]) that says that (13.7.4) is zero for all h_i if and only if

$$\frac{\partial L}{\partial q_i} - \frac{d}{dt}\frac{\partial L}{\partial \dot{q}} = 0, \qquad i = 1, \ldots N.$$

Now these are just Lagrange's equations of motion, and we arrive at the following result, which is referred to as *Hamilton's principle of least action*[2].

Theorem 13.7.3 (Hamilton's Principle of Least Action) *The curve $q(t)$, $t_0 \le t \le t_1$ is a solution of Lagrange's equations:*

$$\frac{d}{dt}\left(\frac{\partial L}{\partial \dot{q}_i}\right) - \frac{\partial L}{\partial q_i} = 0, \qquad i = 1, \ldots, N,$$

if and only if it is an extremal of the action:

$$\Phi(q) = \int_{t_0}^{t_1} L(q, \dot{q}, t)dt.$$

Despite the name "principle of *least* action" we remark that an extremal of the action need not be a minimum. The only requirement is that the differential of the action must vanish on a trajectory.

In the classical mechanics literature there is another common notation for the differential of the action. Namely,

$$\delta \int_{t_0}^{t_1} L(q, \dot{q}, t)dt, \tag{13.7.5}$$

and the phrase "first variation' or just "variation" of the action is used.

13.7B The Action Principle in Phase Space

The action principle can also be formulated in phase space.

Let $\mathcal{P}$ denote the set of curves in the phase space where the q coordinates have fixed end points, i.e., a "point" in $\mathcal{P}$ is a map

$$t \mapsto (q_1(t), \ldots, q_N(t), p_1(t), \ldots, p_N(t)) \equiv (q(t), p(t)), \qquad t_0 \le t \le t_1,$$

and the fixed endpoint condition means that for every curve $(q(t), p(t))$, the $q(t)$ component satisfies $q(t_0) = q_0$ and $q(t_1) = q_1$. We equip $\mathcal{P}$ with the following norm. For $(q(t), p(t)) \in \mathcal{P}$, the norm of $(q(t), p(t))$ is defined as

$$\| (q(t), p(t)) \| \equiv \sup_{t \in [t_0, t_1],\, 1 \le i \le N} \left(|q_i(t)| + |\dot{q}_i(t)|,\, |p_i(t)| + |\dot{p}_i(t)| \right). \tag{13.7.6}$$

We will need the curves in $\mathcal{P}$ to have at least one continuous derivative.

---

[2]While the name of Hamilton is associated with this integral variational principle in configuration space, Leibniz, Maupertuis, Euler, and Lagrange also made significant contributions. See Sommerfeld [1952].

Since $L = \sum_{i=1}^{N} p_i \dot{q}_i - H$ we can rewrite (13.7.2) and define the following functional on $\mathcal{P}$:

$$\int_{t_0}^{t_1} \left(\sum_{i=1}^{N} p_i \dot{q}_i - H(q,p,t) \right) dt = \int_{t_0}^{t_1} \left(\sum_{i=1}^{N} p_i dq_i - H(q,p,t)dt \right). \quad (13.7.7)$$

Next we compute the differential of this functional:

$$\begin{aligned} &\int_{t_0}^{t_1} \left(\sum_{i=1}^{N} (p_i + k_i)(\dot{q}_i + \dot{h}_i) - p_i \dot{q}_i - H(q+h, p+k, t) + H(q,p,t) \right) dt, \\ &= \int_{t_0}^{t_1} \sum_{i=1}^{N} \left(\dot{q}_i k_i + p_i \dot{h}_i - \frac{\partial H}{\partial q_i} h_i - \frac{\partial H}{\partial p_i} k_i \right) dt + \mathcal{O}(\| \ (h,k) \ \|^2), \\ &= \int_{t_0}^{t_1} \left(\sum_{i=1}^{N} \left(\dot{q}_i - \frac{\partial H}{\partial p_i} \right) k_i - \left(\dot{p}_i + \frac{\partial H}{\partial q_i} \right) h_i \right) dt + \sum_{i=1}^{N} p_i h_i \Big|_{t_0}^{t_1} \\ &\qquad + \mathcal{O}(\| \ (h,k) \ \|^2), \end{aligned} \quad (13.7.8)$$

where the passage from the second to the third line in (13.7.8) is effected by integration by parts. Since $h(t_0) = h(t_1) = 0$ we see that the differential of this functional is given by

$$\int_{t_0}^{t_1} \left(\sum_{i=1}^{N} \left(\dot{q}_i - \frac{\partial H}{\partial p_i} \right) k_i - \left(\dot{p}_i + \frac{\partial H}{\partial q_i} \right) h_i \right) dt. \quad (13.7.9)$$

Clearly, trajectories of Hamilton's equations are extrema of (13.7.7). However, the argument that extrema of (13.7.7) are trajectories of Hamilton's equations requires a bit more care since p_i and q_i are related in time through the equation $p_i = \frac{\partial L}{\partial \dot{q}_i}$. Sommerfeld [1952] and Arnold [1978] both address this issue. Sommerfeld resolves the issue by noting that upon differentiating (13.5.1) with respect to p_i one obtains $\frac{\partial H}{\partial p_i} = \dot{q}_i$. Hence the first term in braces in (13.7.9) vanishes. Since the h_i are independent for each i, the second term in braces in (13.7.9) must also vanish (applying the same argument as was used to deduce Hamilton's principle of least action in configuration space). Hence, we have the following result. [3]

Theorem 13.7.4 (Hamilton's Principle of Least Action in Phase Space) *The curve $(q(t), p(t))$, $t_0 \le t \le t_1$ is a solution of Hamilton's equations:*

$$\dot{q}_i = \frac{\partial H}{\partial p_i}(q,p,t), \quad \dot{p}_i = -\frac{\partial H}{\partial q_i}(q,p,t), \qquad i = 1, \ldots, N,$$

[3] Poincaré and Hilbert also studied this functional.

if and only if it is an extremal of the functional:

$$\int_{t_0}^{t_1} \left(\sum_{i=1}^{N} p_i \dot{q}_i - H(q,p,t) \right) dt.$$

Rather than the phrase "Hamilton's principle of least action", often the shorter phrase "Hamilton's principle" is used instead. This applies in both the configuration space and phase space formulations.

13.7c Transformations that Preserve the Form of Hamilton's Equations

We now consider an application of the action principle in phase space. Consider the Hamiltonian

$$H(q,p,t), \tag{13.7.10}$$

and the associated Hamilton's equations:

$$\begin{aligned} \dot{q} &= \frac{\partial H}{\partial p}(q,p,t), \\ \dot{p} &= -\frac{\partial H}{\partial q}(q,p,t). \end{aligned} \tag{13.7.11}$$

Suppose we have a transformation of coordinates of the form

$$\begin{aligned} Q &= Q(q,p,t), \\ P &= P(q,p,t), \end{aligned} \tag{13.7.12}$$

which we assume can be inverted (viewing t as fixed) to yield

$$\begin{aligned} q &= q(Q,P,t), \\ p &= p(Q,P,t). \end{aligned} \tag{13.7.13}$$

Clearly, (13.7.13) can be substituted into (13.7.10) so that the Hamiltonian in the original (q,p) coordinates can be written as a function of the (Q,P) coordinates:

$$H(q,p,t) = \bar{H}(Q,P,t). \tag{13.7.14}$$

However, it is not at all clear that this transformation preserves the form of Hamilton's equations in the sense that

$$\begin{aligned} \dot{Q} &= \frac{\partial \bar{H}}{\partial P}(Q,P,t), \\ \dot{P} &= -\frac{\partial \bar{H}}{\partial Q}(Q,P,t). \end{aligned} \tag{13.7.15}$$

Now we want to derive conditions on the transformation (13.7.12) so that (13.7.15) holds, and we will do this using Hamilton's principle of least action in phase space.

If (13.7.15) holds in the (Q, P) coordinates then we must have

$$\delta \int_{t_0}^{t_1} \sum_{i=1}^{N} P_i dQ_i - \bar{H} dt = 0,$$

and therefore

$$\delta \int_{t_0}^{t_1} \sum_{i=1}^{N} p_i dq_i - H dt = \delta \int_{t_0}^{t_1} \sum_{i=1}^{N} P_i dQ_i - \bar{H} dt = 0, \tag{13.7.16}$$

or

$$\delta \int_{t_0}^{t_1} \sum_{i=1}^{N} p_i dq_i - P_i dQ_i - (H - \bar{H}) dt = 0,$$

from which it follows that

$$dF(q, Q, t) = \sum_{i=1}^{N} p_i dq_i - \sum_{i=1}^{N} P_i dQ_i + (H - \bar{H}) dt, \tag{13.7.17}$$

for some function $F(q, Q, t)$. This function is referred to as the *generating function* of the transformation (13.7.12). Writing out the terms of the differential of the left hand side of (13.7.17) gives

$$\sum_{i=1}^{N} \frac{\partial F}{\partial q_i} dq_i + \sum_{i=1}^{N} \frac{\partial F}{\partial Q_i} dQ_i + \frac{\partial F}{\partial t} dt = \sum_{i=1}^{N} p_i dq_i - \sum_{i=1}^{N} P_i dQ_i + (H - \bar{H}) dt,$$

from which it follows that

$$\begin{aligned} p_i &= \frac{\partial F}{\partial q_i}, \\ P_i &= -\frac{\partial F}{\partial Q_i}, \\ \bar{H} &= H + \frac{\partial F}{\partial t}, \end{aligned} \tag{13.7.18}$$

So when F is known (13.7.18) gives the relation between the "old" coordinates (q, p), the "new" coordinates (P, Q), and the Hamiltonian. Note that if the system does not depend explicitly on time then the "new" Hamiltonian function is the same as the "old" Hamiltonian function. Transformations of coordinates given by (13.7.18) which preserve the form of Hamilton's equations as described above are referred to as *canonical transformations* or *symplectic transformations* (cf. Section 14.4). [4]

[4]The reader should be aware of how the terms and phrases "function", "map", "coordinate transformation", and "operator" are often used interchangeably.

In some situations it may be more convenient to express the generating function not in terms of the old and new coordinates (i.e., in terms of q and Q), but rather in terms of the old coordinates q and the new momenta P. This can be accomplished by rewriting (13.7.17) as

$$d\left(F + \sum_{i=1}^{N} P_i Q_i\right) = \sum_{i=1}^{N} p_i dq_i + \sum_{i=1}^{N} Q_i dP_i + (H - \bar{H})dt, \qquad (13.7.19)$$

We express the argument of the differential on the left hand side of (13.7.19) as a function of q, P, t, which can be viewed as a new generating function $G(q, P, t)$. Applying the same argument as above gives the relations

$$\begin{aligned} p_i &= \frac{\partial G}{\partial q_i}, \\ Q_i &= \frac{\partial G}{\partial P_i}, \\ \bar{H} &= H + \frac{\partial G}{\partial t}. \end{aligned} \qquad (13.7.20)$$

The reader should compare the discussion in this section with that in Section 14.4.

13.7D Applications of Variational Methods

In recent years variational methods have been developed into a powerful and rigorous mathematical tool. Examples of some applications are given below. Kozlov [1985] provides an excellent survey of the application of variational methods in mechanics.

Existence of Periodic Orbits. There is a vast literature on the use of variational methods for proving the existence of periodic orbits. See Rabinowitz [1978] and Struwe [1990] and the references therein.

Existence of Homoclinic Orbits. In recent years variational methods have been developed for proving the existence of homoclinic orbits. See, e.g., Zelati et al. [1990]

Existence of Invariant Tori. A proof of the KAM theorem (which is concerned with the existence of invariant tori in perturbations of integrable Hamiltonian systems) by variational methods is given by Salamon and Zehnder [1989].

Existence of Heteroclinic Orbits. The existence of heteroclinic orbits are believed by many to be a key mechanism for global instabilities in Hamiltonian systems (such as "Arnold diffusion"). See, e.g., Mather [1993] and Bessi [1997].

Existence of Chaos. Séré [1993] has used variational methods to construct a chaotic invariant set modeled on the Bernoulli shift.

Numerical Integration of Lagrange's Equations. Hamilton's principle can be used to derive a class of numerical methods for solving Lagrange's equations. An excellent background for this subject, as well as a literature review, can be found in Lewis and Kostelic [1996]

13.8 The Hamilton-Jacobi Equation

We now consider the action integral (or functional) defined in (13.7.2) from a different point of view. The action as defined in (13.7.2) is a functional defined on the set of curves in configuration space having the same endpoints. We now want to view this integral as defined on extremals (i.e., on trajectories of Lagrange's equations) and as a function of the endpoint of the extremal. In order to make this precise we will need to adopt a slightly different notation.

Let $\tilde{q}(t)$ denote an extremal of (13.7.2) with $\tilde{q}(t_0) = q_0$ and $\tilde{q}(t) = q$. Then we define

$$S(q,t) = \int_{t_0}^{t} L(\tilde{q}(\tau), \dot{\tilde{q}}(\tau), \tau) d\tau. \tag{13.8.1}$$

In this way we view the action as a function of the endpoint of an extremal of (13.7.2) (and we view q_0 and t_0 as fixed). Arnold [1978] discusses a number of technical difficulties that can arise in this definition.

Recalling (13.7.3), the differential of (13.8.1) (where variations in q, but not t are considered) is given by

$$dS(q,t)h = \int_{t_0}^{t} \sum_{i=1}^{N} \left(\frac{\partial L}{\partial q_i} - \frac{d}{dt}\frac{\partial L}{\partial \dot{q}_i} \right) h_i dt + \sum_{i=1}^{N} \frac{\partial L}{\partial \dot{q}_i} h_i \Big|_{t_0}^{t}. \tag{13.8.2}$$

Now since $\tilde{q}(t)$ is an extremal the first term vanishes, and since $\tilde{q}(t_0) = q_0$ is fixed for each extremal under consideration, (13.8.2) reduces to

$$dS(q,t)h = \sum_{i=1}^{N} \frac{\partial L}{\partial \dot{q}_i} h_i = \sum_{i=1}^{N} p_i h_i. \tag{13.8.3}$$

Since only q (and not t) was varied in computing the differential of $S(q,t)$ we immediately obtain the relation

$$p_i = \frac{\partial S}{\partial q_i}, \qquad i = 1, \ldots, N. \tag{13.8.4}$$

From (13.8.1) we have

$$\frac{dS}{dt} = L, \tag{13.8.5}$$

and therefore

$$\frac{dS}{dt} = L = \sum_{i=1}^{N} \frac{\partial S}{\partial q_i}\dot{q}_i + \frac{\partial S}{\partial t},$$
$$= \sum_{i=1}^{N} p_i \dot{q}_i + \frac{\partial S}{\partial t}, \tag{13.8.6}$$

Equation (13.8.6) can be rewritten as

$$\frac{\partial S}{\partial t} + H(q, p, t) = 0, \tag{13.8.7}$$

or

$$\frac{\partial S}{\partial t} + H\left(q, \frac{\partial S}{\partial q}, t\right) = 0, \tag{13.8.8}$$

Equation (13.8.8) is a partial differential equation for the function $S(q, t)$ which is known as the *Hamilton-Jacobi equation*. From a solution of the Hamilton-Jacobi equation one can obtain the trajectories of the corresponding Hamilton's canonical equations. We now describe this procedure, but first we need a definition.

Definition 13.8.1 (Complete Integral of the Hamilton-Jacobi Equation) *If*

$$\phi(q_1, \ldots, q_N, t; a_1, \ldots, a_N) \equiv \phi(q, t; a),$$

is a solution of (13.8.8), depending on the N constants $a = (a_1, \ldots, a_N)$ such that

$$\det\left(\frac{\partial^2 \phi}{\partial q \partial a}\right) \neq 0,$$

in the domain of interest, then

$$S \equiv \phi + \alpha,$$

where α is a constant, is said to be a complete integral *of (13.8.8).*

Now we prove the theorem that also provides a procedure for constructing the trajectories of Hamilton's canonical equations from a complete integral of the Hamilton-Jacobi equation.

Theorem 13.8.2 *If a complete integral:*

$$S \equiv \phi(q_1, \ldots, q_N, t; a_1, \ldots, a_N) + \alpha,$$

is known for the Hamilton-Jacobi equation (13.8.8):

$$\frac{\partial S}{\partial t} + H\left(q, \frac{\partial S}{\partial q}, t\right) = 0,$$

then from the equations

$$\frac{\partial \phi}{\partial a_i} = b_i, \qquad \frac{\partial \phi}{\partial q_i} = p_i, \quad i = 1, \ldots, N, \tag{13.8.9}$$

with the $2N$ arbitrary constants a_i, b_i, one obtains (implicitly) the $2N$-parameter family of solutions of Hamilton's equations:

$$\dot{q}_i = \frac{\partial H}{\partial p_i}, \qquad \dot{p}_i = -\frac{\partial H}{\partial q_i}, \qquad i = 1, \ldots, N. \tag{13.8.10}$$

Proof: The proof is taken from Courant and Hilbert [1962]. Since we are assuming that

$$\det\left(\frac{\partial^2 \phi}{\partial q \partial a}\right) \neq 0,$$

then we can solve the N equations

$$\frac{\partial \phi}{\partial a_i} = b_i,$$

for q_i as a function of t and the $2N$ constants a_i, b_i. If we substitute these functions into

$$\frac{\partial \phi}{\partial q_i} = p_i,$$

then we obtain p_i as functions of t and the $2N$ constants a_i, b_i.

Now we need to show that the solutions obtained in this way are solutions of Hamilton's equations.

We begin by differentiating the equation $\frac{\partial \phi}{\partial a_i} = b_i$ with respect to t to obtain:

$$\frac{\partial^2 \phi}{\partial t \partial a_i} + \sum_{j=1}^{N} \frac{\partial^2 \phi}{\partial q_j \partial a_i} \frac{dq_j}{dt} = 0. \tag{13.8.11}$$

We next differentiate $\frac{\partial \phi}{\partial t} + H(q, \frac{\partial \phi}{\partial q}, t) = 0$ with respect to a_i to obtain:

$$\frac{\partial^2 \phi}{\partial t \partial a_i} + \sum_{j=1}^{N} \frac{\partial H}{\partial p_j} \frac{\partial^2 \phi}{\partial q_j \partial a_i} = 0. \tag{13.8.12}$$

Now we subtract (13.8.11) from (13.8.12), and use the fact that $\det\left(\frac{\partial^2 \phi}{\partial q \partial a}\right) \neq 0$ to obtain

$$\dot{q}_j = \frac{\partial H}{\partial p_j}, \; j = 1, \ldots, N.$$

Next we need to show that the functions we obtained satisfy $\dot{p}_i = -\frac{\partial H}{\partial q_i}$. The argument is similar to the one just given. We first differentiate the equation $\frac{\partial \phi}{\partial q_i} = p_i$ with respect to t to obtain:

$$\frac{dp_i}{dt} = \frac{\partial^2 \phi}{\partial t \partial q_i} + \sum_{j=1}^{N} \frac{\partial^2 \phi}{\partial q_i \partial q_j} \frac{dq_j}{dt}. \tag{13.8.13}$$

We next differentiate $\frac{\partial \phi}{\partial t} + H(q, \frac{\partial \phi}{\partial q}, t) = 0$ with respect to q_i to obtain:

$$0 = \frac{\partial^2 \phi}{\partial t \partial q_i} + \sum_{j=1}^{N} \frac{\partial H}{\partial p_j} \frac{\partial^2 \phi}{\partial q_j \partial q_i} + \frac{\partial H}{\partial q_i}, \tag{13.8.14}$$

We have already shown that our functions satisfy $\dot{q}_j = \frac{\partial H}{\partial p_j}$, which we substitute into (13.8.14). Then we subtract (13.8.14) from (13.8.13) to immediately obtain:

$$\dot{p}_i = -\frac{\partial H}{\partial q_i},\ i = 1, \ldots, N.$$

This completes the proof of the theorem. □

Example 13.8.1. Now we will give an application of the Hamilton-Jacobi method by solving for the trajectories of the simple harmonic oscillator.

The Hamiltonian for the simple harmonic oscillator is given by:

$$H = \frac{p^2}{2} + \frac{\omega^2}{2} q^2. \tag{13.8.15}$$

Substituting $p = \frac{\partial S}{\partial q}$ into (13.8.15), the Hamilton-Jacobi equation is found to be:

$$\frac{\partial S}{\partial t} + \frac{1}{2} \left(\frac{\partial S}{\partial q} \right)^2 + \frac{1}{2} \omega^2 q^2 = 0. \tag{13.8.16}$$

Now we need to find a complete integral of the Hamilton-Jacobi equation. We assume a solution of the form:

$$S(q, t) = S_1(q) + S_2(t). \tag{13.8.17}$$

Substituting (13.8.17) into (13.8.16) gives:

$$-\frac{dS_2}{dt} = \frac{1}{2} \left(\frac{dS_1}{dq} \right)^2 + \frac{1}{2} \omega^2 q^2.$$

Now the left hand side of this equation is a function of t and the right hand side is a function of q. For equality to hold, each side must be equal to a constant, a:

$$-\frac{dS_2}{dt} = \frac{1}{2} \left(\frac{dS_1}{dq} \right)^2 + \frac{1}{2} \omega^2 q^2 = a.$$

Then

$$\frac{1}{2}\left(\frac{dS_1}{dq}\right)^2 + \frac{1}{2}\omega^2 q^2 = a,$$

yields

$$S_1 = \int \sqrt{2\left(a - \frac{1}{2}\omega^2 q^2\right)}\, dq,$$

and

$$-\frac{dS_2}{dt} = a,$$

yields

$$S_2 = -at.$$

Therefore

$$S(q,t;a) = \int \sqrt{2\left(a - \frac{1}{2}\omega^2 q^2\right)}\, dq - at. \tag{13.8.18}$$

With a solution of the Hamilton-Jacobi equation in hand, we can now follow the procedure described in Theorem 13.8.2 and obtain the solutions of Hamilton's equations.

We set

$$\frac{\partial S}{\partial a} = b = \frac{1}{\sqrt{2}} \int \frac{dq}{\sqrt{a - \frac{1}{2}\omega^2 q^2}} - t. \tag{13.8.19}$$

Computing the integral gives:

$$\frac{1}{\omega} \sin^{-1}\left(q\frac{\omega}{\sqrt{2a}}\right) = t + b,$$

or,

$$q(t) = \frac{\sqrt{2a}}{\omega} \sin \omega(t+b).$$

The expression for $p(t)$ is obtained through the relation

$$p = \frac{\partial S}{\partial q}.$$

The constants a and b are determined when the initial conditions for the trajectory are chosen[5].

End of Example 13.8.1

[5]In deriving the equation for S_1 we took a square root, for which there is a choice of sign. The reader should check that we have not missed something here and, if not, why not?

13.8A Applications of the Hamilton-Jacobi Equation

The main reason for developing the Hamilton-Jacobi equation is that it has plays a role in a large variety of applications nowadays. Accordingly, it is impossible to make more than a feeble attempt at a survey of the applications[6]. Nevertheless, we will provide a few pointers to the literature that are relevant to dynamical systems theory.

Courant and Hilbert [1962] provides a mathematically gentle, and straightforward, introduction to the Hamilton-Jacobi partial differential equation. The books of Benton [1977] and Rund [1966] provide further references and the monographs of Lions [1982] and Barles [1994] provide a deeper look at the mathematics. Recent papers describing the asymptotic behavior of solution of the Hamilton-Jacobi equation are Barles and Souganidis [2000a,b], and Roquejoffre [2001]. Recently there has been very interesting work involving generalizing the work of Aubry [1983a,b] and Mather [1982], [1984], [1986] on twist maps to other settings. See Fathi [1997], Evans and Gomes [2001], and Gomes [2001 a,b,c]. The Hamilton-Jacobi equation has been used to study the existence of homoclinic and heteroclinic orbits in near integrable systems. See Fathi [1998], Gallavotti et al. [2000], Rudnev and Wiggins [1999], [2000], and Sauzin [2001].

13.9 Exercises

1. Give a set of generalized coordinates needed to completely specify the motion of each of the following systems:

   (a) a particle constrained to move on an ellipse,

   (b) a particle constrained to move on the surface of a sphere,

   (c) a pendulum that is not confined to a plane, i.e., it can move in three dimensional space.

2. Derive (13.1.6) directly from (13.1.4).

3. For the double pendulum described in Example 13.1.1:

   (a) compute the Lagrangian,

   (b) compute Lagrange's equations of motion.

4. Suppose that the transformation between the original coordinates and the generalized coordinates (i.e., (13.1.3)) is independent of time and let T denote the kinetic energy. Show that
$$2T = \sum_{i=1}^{N} \dot{q}_i \frac{\partial T}{\partial \dot{q}_i}.$$

5. Compute the energy integral (13.3.1) for the simple pendulum described in Example 13.2.1. Show that it is constant on trajectories.

---

[6]Indeed, typing "Hamilton Jacobi" into the MathSciNet search engine yielded 842 references, Web of Science gave 1229, and Google gave 19,400.

6. Compute the energy integral (13.3.1) for the double pendulum described in Example 13.1.1. Show that it is constant on trajectories.

7. Consider the simple harmonic oscillator with Hamiltonian given by

$$H = \frac{p^2}{2} + \frac{\omega^2}{2} q^2.$$

   (a) Compute the Lagrangian and Lagrange's equations.

   (b) Show that the transformation

$$q = \sqrt{\frac{2P}{\omega}} \sin Q, \qquad p = \sqrt{2P\omega} \cos Q,$$

   is canonical.

   (c) Show that in the $Q - P$ coordinates Q is a cyclic coordinate.

   (d) Compute the Routhian and Routh's equations.

8. Consider a simple harmonic oscillator of mass m and spring constant k free to move in a plane. In plane polar coordinates the kinetic and potential energies are given by

$$T = \frac{1}{2} m \left(\dot{r}^2 + r^2 \dot{\theta}^2 \right),$$
$$V = \frac{1}{2} k r^2.$$

   Compute the Lagrangian and Lagrange's equations of motion. Show that this system has two independent integrals.

9. Compute the Hamiltonian and Hamilton's equations of motion for the simple pendulum described in Example 13.2.1.

10. Compute the Hamiltonian and Hamilton's equations of motion for the double pendulum described in Example 13.1.1.

11. Consider a simple harmonic oscillator of mass m and spring constant k free to move in a plane. In plane polar coordinates the kinetic and potential energies are given by

$$T = \frac{1}{2} m \left(\dot{r}^2 + r^2 \dot{\theta}^2 \right),$$
$$V = \frac{1}{2} k r^2.$$

   Compute the Routhian and Routh's equations for this system.

12. The Hénon-Heiles Hamiltonian for a three dimensional potential is given by (Ferrer et al. [1998]):

$$H = \frac{1}{2} \left(p_x^2 + p_y^2 + p_z^2 \right) + \frac{1}{2} \omega^2 \left(x^2 + y^2 + z^2 \right) + \epsilon \omega^2 \left((x^2 + y^2) z - \frac{1}{3} z^3 \right),$$

   where ϵ, $\omega > 0$ are constants.

   (a) Compute the Lagrangian and Lagrange's equations for this system.

   (b) The potential for this problem is said to be an *axisymmetric potential*. Construct a canonical transformation for which $x - y$ are transformed to cylindrical coordinates, and the z coordinate is left alone. Verify that the coordinate transformation is canonical and write the Hamiltonian in these new coordinates. Show that one obtains a cyclic coordinate in these new coordinates.

(c) Using the cyclic coordinate obtained in the previous exercise, compute the Routhian and Routh's equations.

13. This exercise comes from Sommerfeld [1952]. Calculate the value of the action between the limits $t = 0$ and $t = t_1$:

(a) for the real motion of a falling partcle, $z = \frac{1}{2}gt^2$,

(b) for two fictitious motions $z = ct$ and $z = at^3$, where the constants c and a must be so determined that the initial and end conditions coincide with those of the real path, in agreement with the rules for variations of paths in the action principle. Show that the integral has a smaller value for the real motion than for the fictitious motions.

14. Show that the following transformations are canonical:

(a) $Q = p, \qquad P = -q,$

(b) $Q = q \tan p, \qquad P = \log(\sin p).$

15. Show that the transformation

$$q_1 = r\cos\chi, \;\; p_1 = P\cos\chi - I\sin\left(\frac{\chi}{r}\right),$$
$$q_2 = r\sin\chi, \;\; p_2 = P\sin\chi + I\cos\left(\frac{\chi}{r}\right),$$

is canonical.

16. This exercise requires some knowledge of the method of characteristics from the theory of partial differential equations (see, e.g., Courant and Hilbert [1962]). Consider the Hamilton-Jacobi equation:

$$\frac{\partial S}{\partial t} + H\left(q, \frac{\partial S}{\partial q}, t\right) = 0.$$

Show that the characteristics for this partial differential equation are given by the trajectories of Hamilton's canonical equations:

$$\dot{q} = \frac{\partial H}{\partial p},$$
$$\dot{p} = -\frac{\partial H}{\partial q}.$$

17. Consider a particle of mass m moving in the $x - y$ plane under the influence of a central force that depends only on the distance from the origin. Use polar coordinates to describe the configuration space and let $V(r)$ denote the potential due to the central force.

(a) Compute the Lagrangian and Lagrange's equations.

(b) Compute the Hamiltonian and Hamilton's equations.

(c) Suppose that the central force has the form of an inverse square force, i.e.,

$$V(r) = \frac{K}{r},$$

for some constant K. Use the Hamilton-Jacobi method to solve for the trajectories of Hamilton's equations.

18. Show that if the function H in the Hamilton-Jacobi equation is independent of time then the solution S has the form

$$S(q) = S_0(q) - Et.$$

Furthermore, show that the corresponding Hamilton-Jacobi equation has the form

$$H\left(q, \frac{\partial S_0}{\partial q}\right) = E,$$

where E is a constant representing the total energy of the system.

19. This exercise requires some preliminary motivation. Consider a Hamiltonian system with Hamiltonian $H = H(q,p)$, $(q,p) \in \mathbb{R}^{2N}$. Suppose we make a *canonical* coordinate transformation:

$$Q = Q(q,p), \qquad P = P(q,p),$$

with inverse

$$q = q(Q,P), \qquad p = p(Q,P),$$

such that in the (Q,P) coordinates the new Hamiltonian depends only on the Q variables, i.e.,

$$H(q,p) = \bar{H}(Q).$$

Since the transformation is canonical Hamilton's equations become:

$$\dot{Q} = \frac{\partial \bar{H}}{\partial P}(Q) = 0,$$
$$\dot{P} = -\frac{\partial \bar{H}}{\partial Q}(Q).$$

These equations can be easily integrated, and the expression for the trajectories is:

$$Q(t) = Q(0) = Q_0,$$
$$P(t) = P(0) - t\,\frac{\partial \bar{H}}{\partial Q}(Q_0).$$

Now all we need is the appropriate canonical transformation that "simplifies" the Hamiltonian in the manner described above. Accordingly, we seek a generating function, $S(q,Q)$, satisfying:

$$H\left(q, \frac{\partial S}{\partial q}\right) = \bar{H}(Q). \tag{13.9.1}$$

Now viewing Q as constants, this is exactly the form of the Hamilton- Jacobi equation (for a time-independent Hamiltonian). Hence, finding a solution of the Hamilton-Jacobi equation of the form of (13.9.1) leads to the integration of Hamilton's equations.

This result is due to Jacobi, and is summarized in the following theorem.

Theorem 13.9.1 (Jacobi's Theorem) *If a solution $S(q,Q)$ is found to the Hamilton-Jacobi equation (13.9.1) depending on the N parameters Q such that*

$$\det\left(\frac{\partial^2 S}{\partial q \partial Q}\right) \neq 0,$$

then Hamilton's equations

$$\dot{q} = \frac{\partial H}{\partial p}(q,p),$$
$$\dot{p} = -\frac{\partial H}{\partial q}(q,p), \tag{13.9.2}$$

can be be solved explicitly. The functions $Q(q,p)$ *determined by the equations*

$$p = \frac{\partial S}{\partial q}(q,Q),$$

are first integrals of (13.9.2).

Provide all the details to the proof of Jacobi's theorem.

20. Consider the Hamilton-Jacobi equation for a time independent function H:

$$H\left(q, \frac{\partial S}{\partial q}\right) = E, \qquad q \in \mathbb{R}^n, \tag{13.9.3}$$

Suppose that it has a solution of the form

$$S = S_1(q_1, a_1, \ldots, a_N) + \cdots + S_N(q_N, a_1, \ldots, a_N) - Et, \tag{13.9.4}$$

where $(a_1, \ldots, a_N)$ are constants. A Hamilton-Jacobi equation possessing a solution of this form is said to be *separable*. Let C_i denote a simple closed curve in the $q_i - p_i$ plane. Then the integral

$$J_i \equiv \oint_{C_i} p_i dq_i, \tag{13.9.5}$$

is referred to as the *phase integral* or *action variable*.

(a) Show that the J_i are functions of $a_1, \ldots, a_N$ only and, hence, we can write $S = S_1(q_1, J_1, \ldots, J_N) + \cdots + S_N(q_N, J_1, \ldots, J_N) - Et$.

(b) Define

$$w_i = \frac{\partial S}{\partial J_i}, \tag{13.9.6}$$

and consider the canonical transformation from the $q-p$ coordinates to the $w-J$ coordinates defined by this generating function. Let $\bar{H}$ denote the Hamiltonian in these coordinates. Show that Hamilton's equations can be integrated in these coordinates and that the trajectories are given by

$$J_i(t) = J_i(0) = \text{constant}, \qquad w_i(t) = w_i(0) + \frac{\partial \bar{H}}{\partial J_i}(J(0))t, \tag{13.9.7}$$

where $J(0) \equiv (J_1(0), \ldots, J_N(0))$.

14

Hamiltonian Vector Fields

In this section we will develop some of the basic properties of canonical Hamiltonian vector fields. Background on Hamilton's equations can be found in any book on classical mechanics (see, e.g., Whittaker [1904] or Goldstein [1980]). Over the past 15 years there has been a great deal of research on Hamilton's equations. Most of the research has occurred along two directions. One direction is concerned with the *geometrical* structure of Hamilton's equations. The other direction is concerned with the dynamical properties of the flow generated by Hamiltonian vector fields. Excellent references for both viewpoints are Abraham and Marsden [1978], Arnold [1978], Guillemin and Sternberg [1984], and Meyer and Hall [1992].

For a C^r, $r \geq 2$, real valued function on some open set $U \subset \mathbb{R}^{2n}$ Hamilton's canonical equations are given by

$$\begin{aligned} \dot{q} &= \frac{\partial H}{\partial p}(q,p), \\ \dot{p} &= -\frac{\partial H}{\partial q}(q,p), \qquad (q,p) \in U \subset \mathbb{R}^{2n}. \end{aligned} \tag{14.0.1}$$

It will often be convenient to write these in a more compact notation. Defining $x \equiv (q,p)$, then (14.0.1) can be written as

$$\dot{x} = JDH(x), \tag{14.0.2}$$

where

$$J = \begin{pmatrix} 0 & \text{id} \\ -\text{id} & 0 \end{pmatrix},$$

"id" denotes the $n \times n$ identity matrix, and $DH(x) \equiv (\frac{\partial H}{\partial q}, \frac{\partial H}{\partial p})$.

> *In this section we will develop a number of ideas related to the trajectories generated by Hamiltonian vector fields. In this context, we will assume that the trajectories exist for the length of time required in order for the ideas under discussion to "make sense". Of course, in specific applications this should be verified.*

Before proceeding further it will be useful to first establish notation that we will frequently use throughout our discussion.

Notation

Coordinates. Points in the phase space $\mathbb{R}^{2n}$ will be denoted by $x \equiv (q,p) \equiv (q_1,\dots,q_n,p_1,\dots,p_n)$.

Derivatives of Real Valued Functions. For a real valued function H on $\mathbb{R}^{2n}$ we will use the following notation for the derivative with respect to the q coordinate:

$$\frac{\partial H}{\partial q} \equiv \left(\frac{\partial H}{\partial q_1},\dots,\frac{\partial H}{\partial q_n}\right).$$

Moreover, we will also use the following shorthand notation:

$$\frac{\partial H}{\partial q}\frac{\partial G}{\partial q} \equiv \sum_{i=1}^{n} \frac{\partial H}{\partial q_i}\frac{\partial G}{\partial q_i},$$

with a similar notation for $\frac{\partial H}{\partial q}\frac{\partial G}{\partial p}$, etc.

Maps of the Phase Space into Itself. We will denote C^r, $r \geq 1$ maps of $\mathbb{R}^{2n}$ into $\mathbb{R}^{2n}$ by

$$f \equiv (Q,P) : \mathbb{R}^{2n} \to \mathbb{R}^{2n},$$
$$x \equiv (q,p) \mapsto y = f(x) \equiv (Q(q,p),P(q,p)),$$

where

$$(Q(q,p),P(q,p)) = (Q_1(q,p),\dots,Q_n(q,p),P_1(q,p),\dots,P_n(q,p)).$$

By the symbol $\frac{\partial Q}{\partial q}$ we mean the following $n \times n$ matrix:

$$\frac{\partial Q}{\partial q} \equiv \begin{pmatrix} \frac{\partial Q_1}{\partial q_1} & \cdots & \frac{\partial Q_1}{\partial q_n} \\ \vdots & & \vdots \\ \frac{\partial Q_n}{\partial q_1} & \cdots & \frac{\partial Q_n}{\partial q_n} \end{pmatrix}.$$

$\frac{\partial Q}{\partial q}\frac{\partial Q}{\partial p}$ will denote the $n \times n$ matrix whose $i-j$ entry is given by

$$\left(\frac{\partial Q}{\partial q}\frac{\partial Q}{\partial p}\right)_{i,j} \equiv \sum_{k=1}^{n} \frac{\partial Q_i}{\partial q_k}\frac{\partial Q_k}{\partial p_j}.$$

General Notation for Hamiltonian Vector Fields. For the sake of a more compact notation we will occasionally denote the Hamiltonian vector field derived from a function H by

$$X_H(x) \equiv \left(\frac{\partial H}{\partial p},-\frac{\partial H}{\partial q}\right).$$

14.1 Symplectic Forms

By a *symplectic form* on $\mathbb{R}^{2n}$ we mean a skew-symmetric, nondegenerate bilinear form. By nondegenerate we mean that the matrix representation of the bilinear form is nonsingular. A vector space equipped with a symplectic form is called a *symplectic vector space*. For our phase space $\mathbb{R}^{2n}$ a symplectic form is given by

$$\Omega(u, v) \equiv \langle u, Jv \rangle, \qquad u, v \in \mathbb{R}^{2n}, \tag{14.1.1}$$

where $\langle \cdot, \cdot \rangle$ denotes the standard Euclidean inner product on $\mathbb{R}^{2n}$. This particular symplectic form is referred to as the *canonical symplectic form* for reasons that we will now explain.

> *Throughout this section our symplectic vector space will be $\mathbb{R}^{2n}$ equipped with the canonical symplectic form. However, virtually every result that we derive is valid for Hamilton's equations arising from general symplectic forms on finite dimensional vector spaces. The reader should consult Abraham and Marsden [1978] for the details of this more general theory.*

Note that nondegeneracy of the canonical symplectic form follows from the nondegeneracy of the Euclidean inner product and the invertibility of J.

14.1A The Relationship Between Hamilton's Equations and the Symplectic Form

We next look at Hamilton's equations from a different point of view, and one that is more in line with much current mathematical research in Hamiltonian mechanics.

We say that the symplectic form $\Omega(\cdot, \cdot)$ defines a *symplectic structure* on the phase space $\mathbb{R}^{2n}$. For a given Hamiltonian function H, the corresponding Hamilton's equations are then derived from the symplectic structure through the following formula

$$\Omega\left(X_H(x), v\right) = \langle DH(x), v \rangle, \qquad x \in U \subset \mathbb{R}^{2n},\ v \in \mathbb{R}^{2n}. \tag{14.1.2}$$

One can think of (14.1.2) as an equation for $X_H(x)$, for a given $H(x)$. Often, (14.1.2) is written in the following shorthand notation

$$i_{X_H}\Omega = DH, \tag{14.1.3}$$

where $i_{X_H}\Omega \equiv \Omega\left(X_H, \cdot\right)$ and the pointwise nature of the formula is not explicitly denoted. The symbol $i_{X_H}\Omega$ is referred to as the *interior product* of the vector field X_H with the bilinear form Ω. This operation creates a *linear form* which makes the left-hand-side of (14.1.2) compatible with the linear form $\langle DH, \cdot \rangle$ on the right-hand-side of the formula.

Now we return to the question of deriving Hamilton's equations from this formula. Let $X = (\dot{q}, \dot{p})$ denote an arbitrary vector field on $U \subset \mathbb{R}^{2n}$ with $DH = \left(\frac{\partial H}{\partial q}, \frac{\partial H}{\partial p}\right)$. Then (14.1.2) becomes

$$\Omega\left((\dot{q}, \dot{p}), v\right) = \langle (\dot{q}, \dot{p}), Jv \rangle = \left\langle \left(\frac{\partial H}{\partial q}, \frac{\partial H}{\partial p}\right), v \right\rangle. \tag{14.1.4}$$

It is a simple calculation to verify that $J^T = -J$ and, thus, that

$$\langle (\dot{q}, \dot{p}), Jv \rangle = \langle -J(\dot{q}, \dot{p}), v \rangle = \langle (-\dot{p}, \dot{q}), v \rangle. \tag{14.1.5}$$

Substituting (14.1.5) into (14.1.4) gives

$$\langle (-\dot{p}, \dot{q}), v \rangle = \left\langle \left(\frac{\partial H}{\partial q}, \frac{\partial H}{\partial p}\right), v \right\rangle. \tag{14.1.6}$$

Now we are practically done, we need only appeal to nondegeneracy of the symplectic form. For fixed v, using linearity, we can rewrite (14.1.6) as

$$\left\langle (-\dot{p}, \dot{q}) - \left(\frac{\partial H}{\partial q}, \frac{\partial H}{\partial p}\right), v \right\rangle = 0, \tag{14.1.7}$$

which holds for all $v \in \mathbb{R}^{2n}$. Hence by nondegeneracy of the symplectic form we must have

$$(-\dot{p}, \dot{q}) - \left(\frac{\partial H}{\partial q}, \frac{\partial H}{\partial p}\right) = 0,$$

or,

$$\begin{aligned} \dot{q} &= \frac{\partial H}{\partial p}, \\ \dot{p} &= -\frac{\partial H}{\partial q}, \end{aligned}$$

which are Hamilton's canonical equations.

14.2 Poisson Brackets

Let $H, G : U \to \mathbb{R}$ denote two C^r, $r \geq 2$, functions. Then the *Poisson bracket* of these two functions is another function, and it is defined through the symplectic form as follows:

$$\{H, G\} \equiv \Omega(X_H, X_G) \equiv \langle X_H, JX_G \rangle. \tag{14.2.1}$$

It follows immediately that the Poisson bracket is antisymmetric. Using the definitions of X_H, X_G, as well as the canonical symplectic form, we easily see that (14.2.1) assumes the following "coordinate" form:

$$\{H, G\} \equiv \sum_{i=1}^{n} \frac{\partial H}{\partial q_i} \frac{\partial G}{\partial p_i} - \frac{\partial H}{\partial p_i} \frac{\partial G}{\partial q_i}. \tag{14.2.2}$$

14.2A Hamilton's Equations in Poisson Bracket Form

For a scalar valued C^r, $r \geq 2$, function $F : U \to \mathbb{R}$, $U \subset \mathbb{R}^{2n}$, the rate of change of this function along the trajectories generated by the Hamiltonian vector field $X_H = (\frac{\partial H}{\partial p}, -\frac{\partial H}{\partial q})$ is given by

$$\begin{aligned}\dot{F} &= \sum_{i=1}^{n} \frac{\partial F}{\partial q_i}\dot{q}_i + \frac{\partial F}{\partial p_i}\dot{p}_i, \\ &= \sum_{i=1}^{n} \frac{\partial F}{\partial q_i}\frac{\partial H}{\partial p_i} - \frac{\partial F}{\partial p_i}\frac{\partial H}{\partial q_i}, \\ &= \{F, H\}.\end{aligned}$$

Hamilton's equations are alternately written as follows:

$$\dot{F} = \{F, H\}, \qquad \forall F : U \to \mathbb{R}. \tag{14.2.3}$$

To see that (14.2.3) implies (14.0.1) we can substitute the "coordinate functions" $(q, p) \mapsto q_i$ and $(q, p) \mapsto p_i$ into (14.2.3), which will yield (14.0.1).

It follows easily from (14.2.2) that for any scalar valued C^r, $r \geq 1$, function $F : U \to \mathbb{R}$, $U \subset \mathbb{R}^{2n}$ we have

$$\{F, F\} = 0.$$

Using this fact, as well (14.2.3), we obtain the following result.

Proposition 14.2.1 *The Hamiltonian $H(q, p)$ is constant along trajectories of the Hamiltonian vector field X_H.*

More generally, we refer to any function F satisfying

$$\{F, H\} = 0,$$

as an *integral* or *constant of the motion* with respect to the dynamics generated by the vector field X_H. Integrals have a nice geometric interpretation which can be deduced from the following simple calculation:

$$\begin{aligned}\{F, H\} &= \langle X_F, JX_H \rangle, \\ &= -\langle JX_F, X_H \rangle = 0.\end{aligned}$$

Now

$$JX_F = J \begin{pmatrix} \frac{\partial F}{\partial p} \\ \\ -\frac{\partial F}{\partial q} \end{pmatrix} = - \begin{pmatrix} \frac{\partial F}{\partial q} \\ \\ \frac{\partial F}{\partial p} \end{pmatrix},$$

and the vector $-\left(\frac{\partial F}{\partial q}, \frac{\partial F}{\partial p}\right)$ is just a vector perpendicular to the level set of F, at each point at which it is evaluated. Hence, an integral has the property that the vector field is tangent to the surface given by the level set of the integral.

14.3 Symplectic or Canonical Transformations

Symplectic, or canonical, transformations and their properties play a very important role in Hamiltonian mechanics. We begin with a definition.

Definition 14.3.1 (Symplectic or Canonical Transformations) *Consider a C^r, $r \geq 1$, diffeomorphism $f : \mathbb{R}^{2n} \to \mathbb{R}^{2n}$. Then f is said to be a* canonical *or* symplectic *transformation if*

$$\Omega(u, v) = \Omega(Df(x)u, Df(x)v), \qquad \forall x, u, v \in \mathbb{R}^{2n}. \tag{14.3.1}$$

We remark that Definition 14.3.1 could have been much more general. In particular, the transformation could be between spaces of different dimensions (and therefore also not invertible). However, for our purposes this definition will be sufficient.

For the canonical symplectic form (14.3.1) takes the form

$$\begin{aligned} \langle u, Jv\rangle &= \langle Df(x)u, JDf(x)v\rangle \\ &= \langle u, (Df(x))^T JDf(x)v\rangle, \end{aligned} \tag{14.3.2}$$

where $(Df(x))^T$ denotes the transpose of the matrix $Df(x)$. Since (14.3.2) must hold for all $u, v\, \mathbb{R}^{2n}$ we have

$$(Df(x))^T JDf(x) = J, \tag{14.3.3}$$

which provides a computable means for determining whether or not a transformation is symplectic *with respect to the canonical symplectic form*. If we take the determinant of (14.3.3), and use the easily verifiable facts that $\det J = 1$ and $\det (Df(x))^T = \det Df(x)$, we obtain

$$(\det Df(x))^2 = 1.$$

Hence,

$$\det Df(x) = \pm 1,$$

and we see that symplectic transformations are volume preserving. Actually, it can be shown that $\det Df(x) = 1$, so that symplectic transformations are also orientation preserving (see the exercises).

For later purposes it will be useful to write out (14.3.3) using the $q - p$ local coordinates that we defined earlier. Writing the symplectic transformation f as

$$f : (q, p) \mapsto (Q(q, p), P(q, p)),$$

the Jacobian of f is given by

$$A = \begin{pmatrix} \frac{\partial Q}{\partial q} & \frac{\partial Q}{\partial p} \\ \\ \frac{\partial P}{\partial q} & \frac{\partial P}{\partial p} \end{pmatrix},$$

and (14.3.3) takes the form

$$A^T J A = J. \tag{14.3.4}$$

We refer to a matrix satisfying (14.3.4) as a *symplectic matrix.*

14.3A Eigenvalues of Symplectic Matrices

Proposition 14.3.2 *Suppose that A is a symplectic matrix and that $\lambda \in \mathbb{C}$ is an eigenvalue of A. Then $\frac{1}{\lambda}$, $\bar{\lambda}$, and $\frac{1}{\bar{\lambda}}$ are also eigenvalues of A. If λ is an eigenvalue of multiplicity k, then $\frac{1}{\lambda}$ is also an eigenvalue of multiplicity k. Moreover, the multiplicities of the eigenvalues $+1$ and -1, if they occur, are even.*

Proof: We begin with the following algebraic manipulations of the characteristic polynomial of A using simple properties of determinants (where $\mathbb{1}$ denotes the $2n \times 2n$ identity matrix):

$$\begin{aligned}
p(\lambda) &= det\,(A - \lambda\mathbb{1}) \\
&= det\,\left(J(A - \lambda\mathbb{1})J^{-1}\right), \\
&= det\,\left(\left(A^{-1^T}\right) - \lambda\mathbb{1}\right), \qquad \text{using (14.3.4)}, \\
&= det\,\left(A^{-1} - \lambda\mathbb{1}\right), \qquad \text{since } det\,A^{-1} = det\,A^{-1^T}, \\
&= det\,\left(A^{-1}\left(\mathbb{1} - \lambda A\right)\right), \\
&= det\,A^{-1}\,det\,\left(\mathbb{1} - \lambda A\right), \\
&= det\,\left(-\lambda\left(A - \frac{1}{\lambda}\mathbb{1}\right)\right), \qquad \text{since } det\,A^{-1} = \frac{1}{det\,A} = 1, \\
&= \lambda^{2n}\,det\,\left(A - \frac{1}{\lambda}\mathbb{1}\right), \\
&= \lambda^{2n} p\left(\frac{1}{\lambda}\right).
\end{aligned} \tag{14.3.5}$$

Since $det\,A = 1$ it follows that 0 is not an eigenvalue of A. Therefore from (14.3.5) it follows that if λ is an eigenvalue so is $\frac{1}{\lambda}$. Moreover, since the coefficients of the characteristic polynomial are real (A is real), then if λ is an eigenvalue so is its complex conjugate, $\bar{\lambda}$.

Next we consider the issue of the multiplicity of the eigenvalues. Suppose λ_0 is an eigenvalue of multiplicity k. Then the characteristic polynomial can be factored as follows

$$p(\lambda) = (\lambda - \lambda_0)^k\, Q(\lambda), \tag{14.3.6}$$

where $Q(\lambda)$ is a polynomial in λ of degree $2n - k$. Using (14.3.5) and some trivial algebra, (14.3.6) can be written as

$$p\left(\frac{1}{\lambda}\right)\lambda^{2n} = (\lambda - \lambda_0)^k\, Q(\lambda) = (\lambda\lambda_0)^k \left(\frac{1}{\lambda_0} - \frac{1}{\lambda}\right)^k Q(\lambda), \tag{14.3.7}$$

or

$$p\left(\frac{1}{\lambda}\right) = \lambda_0^k \left(\frac{1}{\lambda_0} - \frac{1}{\lambda}\right)^k \frac{Q(\lambda)}{\lambda^{2n-k}}. \tag{14.3.8}$$

Now $\frac{Q(\lambda)}{\lambda^{2n-k}}$ is a polynomial in $\frac{1}{\lambda}$ of degree $2n-k$. So it follows from (14.3.8) that $\frac{1}{\lambda_0}$ is an eigenvalue of multiplicity $\ell \geq k$.

Next, we reverse the roles of λ_0 and $\frac{1}{\lambda_0}$, use the fact that $\frac{1}{\lambda_0}$ is an eigenvalue of multiplicity ℓ, and go through the same argument. After some trivial algebra we obtain

$$p\left(\frac{1}{\lambda}\right) = \left(1 - \frac{1}{\lambda\lambda_0}\right)^\ell \frac{\bar{Q}(\lambda)}{\lambda^{2n-\ell}}. \tag{14.3.9}$$

Now $\frac{\bar{Q}(\lambda)}{\lambda^{2n-\ell}}$ is a polynomial in $\frac{1}{\lambda}$ of degree $2n-\ell$. Substituting $\frac{1}{\lambda_0}$ for λ in (14.3.9), and using the fact that λ_0 is a zero of the right hand side of (14.3.9) of multiplicity k, we see that $\frac{1}{\lambda_0}$ has multiplicity $\ell \leq k$. Therefore $\ell = k$ and we are done.

Now 1 or -1 is an eigenvalue if and only if $\lambda_0 = \frac{1}{\lambda_0}$. It follows from the above result that the multiplicity of the eigenvalues 1 and -1 is even. However, $\det A = 1$, therefore the multiplicity of each must be even. □

14.3B Infinitesimally Symplectic Transformations

Definition 14.3.3 (Infinitesimally Symplectic Transformations) *Consider a C^r, $r \geq 1$, map $f : \mathbb{R}^{2n} \to \mathbb{R}^{2n}$. Then f is said to be an* infinitesimally symplectic *or* Ω skew *transformation if*

$$\Omega(Df(x)u, v) = -\Omega(u, Df(x)v), \qquad \forall x, u, v \in \mathbb{R}^{2n}. \tag{14.3.10}$$

In terms of the canonical symplectic form, (14.3.10) becomes

$$\langle Df(x)u, Jv\rangle = -\langle u, JDf(x)v\rangle. \tag{14.3.11}$$

Using the same manipulations as above, (14.3.11) can be transformed into the following form

$$\langle J^T Df(x)u, v\rangle = -\langle (JDf(x))^T u, v\rangle,$$

which holds for all u, $v \in \mathbb{R}^{2n}$. Hence, using $J^T = -J$, we have

$$JDf(x) + Df(x)^T J = 0. \tag{14.3.12}$$

We refer to a matrix satisfying (14.3.12) as an *infinitesimally symplectic matrix*. It can be shown that the exponential of an infinitesimally symplectic matrix is a symplectic matrix, see Guillemin and Sternberg [1984]. There is a connection here with Lie algebras and groups which the reader can

find fully developed in Abraham and Marsden [1978] or Guillemin and Sternberg [1984].

The importance of the notion of "infinitesimally symplectic" follows from the following proposition.

Proposition 14.3.4 *Let $X : U \to \mathbb{R}^{2n}$ denote a C^r, $r \geq 1$ vector field on some open, convex set $U \subset \mathbb{R}^{2n}$. Then $X = X_H$, for some Hamiltonian $H : U \to \mathbb{R}$ if and only if $DX(x)$ is an infinitesimally symplectic matrix for all $x \in U$.*

Proof: Differentiating (14.1.2) with respect to x in the direction u, and using bilinearity of Ω gives

$$\Omega\left(DX_H(x)u, v\right) = D^2H(x)(v, u). \tag{14.3.13}$$

From this, and the symmetry of the second partial derivative matrix, we obtain

$$\begin{aligned}\Omega\left(DX_H(x)u, v\right) &= D^2H(x)(v, u),\\ &= \Omega\left(DX_H(x)v, u\right),\\ &= -\Omega\left(u, DX_H(x)v\right) \quad \text{(using skew symmetry).}\end{aligned} \tag{14.3.14}$$

From this calculation it follows that if $X_H(x)$ is Hamiltonian, then $DX_H(x)$ is an infinitesimally symplectic matrix.

Now suppose that $DX(x)$ is an infinitesimally symplectic matrix. Using convexity of U, we define

$$H(x) = \int_0^1 \Omega(X(tx), x)dt + \text{constant}, \tag{14.3.15}$$

and claim that $X = X_H$. This is deduced from the following calculation

$$\begin{aligned}\langle DH(x), v\rangle &= \int_0^1 \left(\Omega(DX(tx)tv, x) + \Omega(X(tx), v)\right) dt\\ &= \int_0^1 \left(-\Omega(v, tDX(tx)x) + \Omega(X(tx), v)\right) dt,\\ &= \int_0^1 \left(\Omega(tDX(tx)x, v) + \Omega(X(tx), v)\right) dt,\\ &= \Omega\left(\int_0^1 \frac{d}{dt}\left(tX(tx)\right) dt, v\right)\\ &= \Omega\left(X(x), v\right).\end{aligned} \tag{14.3.16}$$

Hence, by the definition in (14.1.2), X is Hamiltonian with respect to the Hamiltonian (14.3.15). □

14.3c The Eigenvalues of Infinitesimally Symplectic Matrices

It follows from the previous proposition that the matrices associated with the linearization about equilibria of Hamiltonian vector fields are infinitesimally symplectic. The following result is therefore useful for the study of stability of equilibria of Hamiltonian vector fields.

Proposition 14.3.5 *Suppose A is an infinitesimally symplectic matrix. Then if $\lambda \in \mathbb{C}$ is an eigenvalue of A so are $-\lambda$, $\bar{\lambda}$, and $-\bar{\lambda}$. If λ is an eigenvalue of multiplicity k, then $-\lambda$ is also an eigenvalue of multiplicity k. Moreover, if 0 is an eigenvalue then it has even multiplicity.*

Proof: As in the proof of proposition 14.3.2, we begin with the following algebraic manipulations of the characteristic polynomial of A using simple properties of determinants (where $\mathbb{1}$ denotes the $2n \times 2n$ identity matrix):

$$\begin{aligned} p(\lambda) &= det\ (A - \lambda \mathbb{1}), \\ &= det\ \left(J\,(A - \lambda \mathbb{1})\,J^{-1}\right), \\ &= det\ \left(-A^T - \lambda \mathbb{1}\right), \qquad \text{using} \quad (14.3.12), \\ &= det\ \left(-A - \lambda \mathbb{1}\right)^T, \\ &= det\ \left(-\left(A + \lambda \mathbb{1}\right)\right) = (-1)^{2n}\, p(-\lambda) = p(-\lambda). \end{aligned}$$

From this equality, and the fact that A is real, the first part of the proposition follows. The rest of the proposition follows from arguments identical to those of proposition 14.3.2. □

14.3d The Flow Generated by Hamiltonian Vector Fields is a One-Parameter Family of Symplectic Transformations

Theorem 14.3.6 *Let $\phi_t(\cdot)$ denote the flow generated by the Hamiltonian vector field X_H defined on some open, convex set $U \in \mathbb{R}^{2n}$. Then for each t ϕ_t is a symplectic transformation. Conversely, if the flow generated by a vector field consists of symplectic transformations for each t, then the vector field is a Hamiltonian vector field.*

Proof: We begin with two preliminary calculations. First we derive the following *first variational equation* that the linearized flow of an arbitrary vector field $X(x)$ must satisfy

$$\begin{aligned} \frac{d}{dt}\left(D\phi_t(x)v\right) &= D\left(\frac{d}{dt}\phi_t(x)v\right), \\ &= D\left(X(\phi_t(x))v\right), \\ &= DX(\phi_t(x))\left(D\phi_t(x)v\right), \end{aligned} \tag{14.3.17}$$

which holds for any $v \in \mathbb{R}^{2n}$.
Secondly, we use (14.3.17) to derive the following identity

$$\begin{aligned}
&\tfrac{d}{dt}\langle D\phi_t(x)u, JD\phi_t(x)v\rangle \\
&\quad = \langle DX\left(\phi_t(x)\right)\left(D\phi_t(x)u\right), JD\phi_t(x)v\rangle \\
&\qquad\qquad + \langle D\phi_t(x)u, JDX\left(\phi_t(x)\right)\left(D\phi_t(x)v\right)\rangle, \\
&\quad = -\langle JDX\left(\phi_t(x)\right)\left(D\phi_t(x)u\right), D\phi_t(x)v\rangle \\
&\qquad\qquad - \langle DX\left(\phi_t(x)\right)^T JD\phi_t(x)u, D\phi_t(x)v\rangle, \\
&\quad = -\langle \Big(JDX\left(\phi_t(x)\right) + DX\left(\phi_t(x)\right)^T J \Big)\left(D\phi_t(x)u\right), D\phi_t(x)v\rangle.
\end{aligned} \tag{14.3.18}$$

Now, let's assume that the flow is generated by a Hamiltonian vector field, X_H. Then, from Proposition 14.3.4, DX_H is infinitesimally symplectic, therefore

$$JDX_H + DX_H^T J = 0,$$

Hence, (14.3.18) reduces to

$$\frac{d}{dt}\langle D\phi_t(x)u, JD\phi_t(x)v\rangle = 0. \tag{14.3.19}$$

Integrating (14.3.19) with respect to t, between 0 and t, and using $D\phi_t(x)|_{t=0} = \mathrm{id}$, we obtain

$$\langle D\phi_t(x)u, JD\phi_t(x)v\rangle = \langle u, Jv\rangle. \tag{14.3.20}$$

Therefore ϕ_t is a symplectic transformation for each t (recall (14.3.2)).

Conversely, suppose ϕ_t is a symplectic transformation for each t. Then, tracing our steps backwards, (14.3.20) holds, and hence (14.3.18) is zero, i.e.,

$$-\langle \Big(JDX_H\left(\phi_t(x)\right) + DX_H\left(\phi_t(x)\right)^T J \Big)\left(D\phi_t(x)u\right), D\phi_t(x)v\rangle = 0. \tag{14.3.21}$$

Using nondegeneracy of the Euclidean inner product and the invertibility of $D\phi_t$, the fact that (14.3.21) folds for all u, $v \in \mathbb{R}^{2n}$ implies that

$$JDX_H + DX_H^T J = 0.$$

Hence, DX_H is infinitesimally symplectic, and it therefore follows from Proposition 14.3.4 that X_H is Hamiltonian. □

14.4 Transformation of Hamilton's Equations Under Symplectic Transformations

We now discuss the transformation of Hamilton's equations under symplectic coordinate changes. However, first we discuss coordinate transformations for nonlinear ordinary differential equations in general. Consider the following vector field

$$\dot{x} = G(x), \qquad x \in \mathbb{R}^n. \tag{14.4.1}$$

Suppose we want to transform from the "x" coordinates to the "y" coordinates, where the x and y coordinates are related through the following diffeomorphism (which in general we would like to be as differentiable as possible)

$$y = f(x). \tag{14.4.2}$$

Differentiating (14.4.2) with respect to t gives

$$\dot{y} = Df(f^{-1}(y))\dot{x}. \tag{14.4.3}$$

Substituting (14.4.1) into (14.4.3) gives

$$\dot{y} = Df(f^{-1}(y))G(f^{-1}(y)), \tag{14.4.4}$$

which is the vector field in the y coordinates. The right-hand-side of (14.4.4) gives the rule for how vector fields transform under a coordinate change given by (14.4.2). We will use this general result on the way to determining how Hamilton's equations transform under symplectic coordinate changes. However, initially we will determine how the Poisson bracket transforms under symplectic coordinate changes. This will bring us close to our goal since Hamiltonian dynamics can be defined through the Poisson bracket.

We use the general notation introduced earlier in this section. Suppose

$$\begin{aligned} f \equiv (Q, P) &: \mathbb{R}^{2n} \to \mathbb{R}^{2n} \\ x \equiv (q, p) &\mapsto y = f(x) \equiv (Q(q,p), P(q,p)) \end{aligned}$$

is a symplectic transformation. The Poisson bracket with respect to the $x \equiv (q, p)$ coordinates is given by

$$\{H, G\}_{q,p} = \langle X_H(x), JX_G(x) \rangle. \tag{14.4.5}$$

Next we want to determine the Poisson bracket with respect to the $y \equiv (Q, P)$ coordinates. This can be obtained from (14.4.5) and the rule for the general transformation of vector fields given in (14.4.4). Using (14.4.4) to describe the transformation of X_H and X_G, we have

$$\{H, G\}_{Q,P} = \langle Df(f^{-1}(y))X_H(f^{-1}(y)), JDf(f^{-1}(y))X_G(f^{-1}(y)) \rangle. \tag{14.4.6}$$

Since the transformation is symplectic, the right-hand-sides of (14.4.5) and (14.4.6) are equal and we have

$$\{H, G\}_{q,p} = \{H, G\}_{Q,P}\,. \tag{14.4.7}$$

Referring back to the Poisson bracket formulation of Hamilton's equations, (14.4.7) shows that the form of Hamilton's equations is unchanged under symplectic transformations. More practically speaking, suppose we have a Hamiltonian $H = H(Q, P)$ and a symplectic change of coordinates $(Q(q, p), P(q, p))$. Then the Hamiltonian vector field in the (Q, P) coordinates is also a Hamiltonian vector field in the (q, p) coordinates with the Hamiltonian given by $H = H(Q(q, p), P(q, p))$. Or, saying this still another way, under symplectic coordinate transformations Hamiltonian vector fields transform to Hamiltonian vector fields, and the transformed Hamiltonian vector field can be computed by taking the appropriate derivatives with respect to the "new" coordinates of the "old" Hamiltonian , which is expressed as a function of the "new" coordinates by expressing the "old" coordinates as functions of the "new" coordinates.

The reader should compare the discussion in this section with that in Section 13.7c.

14.4a Hamilton's Equations in Complex Coordinates

For certain calculations we will see that it is easier to use Hamilton's equations defined on $\mathbb{C}^n$ rather than $\mathbb{R}^{2n}$. We will consider the Hamiltonian as a real valued function of the complex variables z a nd $\bar{z}$ where

$$z_j = q_j + ip_j, \qquad \bar{z}_j = q_j - ip_j, \quad j = 1, \ldots, n, \tag{14.4.8}$$

where partial derivatives are related through the following expressions

$$\frac{\partial}{\partial z_j} = \frac{1}{2}\left(\frac{\partial}{\partial q_j} - i\frac{\partial}{\partial p_j}\right), \quad \frac{\partial}{\partial \bar{z}_j} = \frac{1}{2}\left(\frac{\partial}{\partial q_j} + i\frac{\partial}{\partial p_j}\right). \tag{14.4.9}$$

The Poisson Bracket of two real valued C^1 functions of z and $\bar{z}$ takes the following form in complex coordinates

$$\{G, H\} = 2i\sum_{j=1}^{n}\left(\frac{\partial G}{\partial \bar{z}_j}\frac{\partial H}{\partial z_j} - \frac{\partial G}{\partial z_j}\frac{\partial H}{\partial \bar{z}_j}\right).$$

This can be verified from (14.2.2) by using (14.4.8) and (14.4.9). Hamilton's equations in complex coordinates then take the form

$$\dot{z}_j = \{z_j, H\} = -2i\frac{\partial H}{\partial \bar{z}_j}, \quad j = 1, \ldots, n. \tag{14.4.10}$$

14.5 Completely Integrable Hamiltonian Systems

An n degree of freedom Hamiltonian system

$$\begin{aligned} \dot{q} &= \frac{\partial H}{\partial p}(q,p), \\ \dot{p} &= -\frac{\partial H}{\partial q}(q,p), \qquad (q,p) \in U \subset \mathbb{R}^{2n}, \end{aligned} \tag{14.5.1}$$

is said to be *completely integrable* if there exists n functions (called *integrals*)

$$F_1 \equiv H, F_2, \cdots, F_n,$$

which satisfy the following conditions.

1. The F_i, $i = 1, \cdots, n$, are functionally independent on U, with the possible exception of sets of measure zero.
2. $\{F_i, F_j\} = 0$, for all i and j.

Completely integrable Hamiltonian systems can be "solved" in some sense. In particular, they can be reduced to quadratures (this is a result due to Liouville and Jacobi, see Arnold [1978]). If the sets defined by

$$\begin{aligned} F_1 &= f_1, \\ F_2 &= f_2, \\ &\vdots \quad \vdots \\ F_n &= f_n, \end{aligned}$$

where f_i, $i = 1, \cdots, n$ are constants, are compact and connected manifolds, then it can be proved that they are actually n-tori on which action-angle variables can be introduced. This was proved by Arnold (see Arnold [1978]), and we state his theorem below. First, we define the notation

$$M_f \equiv \left\{(q,p) \in \mathbb{R}^{2n} \,|\, F_i(q,p) = f_i,\, i = 1, \ldots n\right\}. \tag{14.5.2}$$

Theorem 14.5.1 (Liouville-Arnold)

1. *M_f is a manifold, as differentiable as the least differentiable integral, and is invariant under the dynamics generated by (14.5.1).*
2. *If M_f is compact and connected then it is diffeomorphic to the n-dimensional torus*

$$T^n = \{(\phi_1, \ldots, \phi_n)\, mod 2\pi\}.$$

3. *The flow generated by (14.5.1) gives rise to quasiperiodic motion on T^n , i.e. in angular coordinates on M_f we have*

$$\frac{d\phi}{dt} = \omega, \qquad \omega(f) = (\omega_1(f), \ldots, \omega_n(f)).$$

4. *Hamilton's equations can be integrated by quadratures. More precisely, in a neighborhood of M_f we can construct a symplectic coordinate transformation*

$$(I, \theta) \mapsto (q(I, \theta), p(I, \theta)),$$

where $I \in B \subset \mathbb{R}^n$, B is an open set, and $\theta \in T^n$. In these coordinates the Hamiltonian takes the form

$$H(q(I, \theta), p(I, \theta)) \equiv K(I),$$

with Hamilton's equations given by

$$\begin{aligned} \dot{I} &= -\frac{\partial K}{\partial \theta}(I) = 0, \\ \dot{\theta} &= \frac{\partial K}{\partial I}(I) \equiv \omega(I). \end{aligned} \tag{14.5.3}$$

These equations can be trivially integrated

$$\begin{aligned} I &= \textit{constant}, \\ \theta(t) &= \omega(I)t + \theta_0. \end{aligned} \tag{14.5.4}$$

14.6 Dynamics of Completely Integrable Hamiltonian Systems in Action-Angle Coordinates

In this section we want to consider a number of geometrical and analytical issues associated with completely integrable Hamiltonian systems expressed in action-angle variables, i.e., Hamiltonians of the form

$$H = H^0(I),$$

which give rise to the Hamiltonian vector field

$$\dot{I} = -\frac{\partial H^0}{\partial \theta}(I) = 0, \tag{14.6.1}$$

$$\dot{\theta} = \frac{\partial H^0}{\partial I}(I) \equiv \omega(I), \qquad (I, \theta) \in B \times T^n, \tag{14.6.2}$$

where B is the ball of radius R in $\mathbb{R}^n$ and T^n is the n-torus.

It follows immediately from the form of these equations that

$$\{I = I_0 = \text{constant}\} \times T^n,$$

is an invariant manifold for this system. In particular, as a result of the nature of the coordinates, it is an invariant n-torus. Thus the phase space is foliated by an n-parameter family of n-tori. Moreover, the trajectories on these tori are given by

$$I(t) = I_0 = \text{constant}, \tag{14.6.3}$$
$$\theta(t) = \omega(I_0)t + \theta_0. \tag{14.6.4}$$

In the remainder of this section we want to examine in more detail the nature of this foliation of phase space by n-tori.

Before proceeding we need to take care of a technical detail. Many of the results will require that the Hamiltonian be *non-degenerate* in a way that we now describe.

Definition 14.6.1 (Nondegenerate) *The Hamiltonian is said to be* nondegenerate *if the* frequency map

$$I \mapsto \omega(I)$$

is a diffeomorphism. A sufficient condition for this is

$$det\left(\frac{\partial^2 H^0}{\partial I^2}(I)\right) \neq 0.$$

14.6A Resonance and Nonresonance

The n-parameter family of tori in the foliation of the phase space are either *resonant* or *nonresonant*, and we now define these notions.

Definition 14.6.2 (Resonance) *The frequency vector ω is said to be* resonant *if there exists $k \in \mathbb{Z}^n - \{0\}$ such that $k \cdot \omega = 0$. If no such $k \in \mathbb{Z}^n - \{0\}$ exists, ω is said to be* nonresonant.

The n-dimensional *nonresonant* tori have the property that trajectories on the tori densely fill out the torus. More precisely, this means that given *any* point on a nonresonant torus, and *any* neighborhood of that point, the trajectory through that point will re-intersect that neighborhood after leaving it. Moreover, given any other point and any other neighborhood of that point, the same trajectory will also intersect that neighborhood. This is a classical result that goes back to Kronecker (the flow on a nonresonant torus is often referred to as *Kronecker flow*). Chapter 23 of Hardy and Wright [1938] gives an excellent and detailed exposition of the proof from

the number theory viewpoint. A proof of this fact can also be found in Arnold [1978].

There are different types of resonant tori. One way of describing this is through the notion of the *multiplicity* of a resonance.

Definition 14.6.3 (Multiplicity of a Resonance) *A resonant frequency vector is said to be of multiplicity $m < n$ if there exist independent $k^i \in \mathbb{Z}^n - \{0\}, i = 1, \ldots, m$, such that $k^i \cdot \omega = 0$.*

We will discuss the some of the geometrical meanings of the multiplicity of resonant tori shortly. However, in a rough sense, resonances of high multiplicity are more difficult to analyze and lead to more complicated dynamics when perturbed from the integrable setting. The notion of the *order of a resonance* will also play an important role in our studies.

Definition 14.6.4 (Order of a Resonance) *Suppose $k \cdot \omega = 0$ for some $k \in \mathbb{Z}^n - \{0\}$. Then the order of this resonance is defined to be $|k| = \sum_i |k_i|$.*

Roughly speaking, resonances of high order are less complicated than those of low order. This will be quantified later on.

The following proposition describes some aspects of the dynamics on resonant tori of multiplicity m.

Proposition 14.6.5 (Foliation of Resonant Tori) *Suppose the n- torus $I = I^*$ is resonant of multiplicity $m < n$, i.e., $\omega(I^*)$ is a multiplicity m frequency vector. Then the dynamics on the n-torus $I = I^*$ is such that it is foliated by invariant tori of dimension $n - m$ with trajectories densely filling out these lower dimensional tori.*

Proof: On a resonant invariant n-torus $I = I^*$ of multiplicity m the dynamics is given by

$$\dot{\theta} = \frac{\partial H^0}{\partial I}(I^*) \equiv \omega(I^*), \quad \theta \in T^n.$$

and the resonance relations are

$$k_i \cdot \omega(I^*) \equiv k_{i1}\omega_1(I^*) + \cdots + k_{in}\omega_n(I^*) = 0, \quad k_i \in \mathbb{Z}^n - \{0\}, i = 1, \ldots, m,$$

with the k_i's being linearly independent over the integers. Therefore, the $m \times n$ matrix

$$K = \begin{pmatrix} k_{11} & \ldots & k_{1n} \\ \vdots & \ddots & \vdots \\ k_{m1} & \ldots & k_{mn} \end{pmatrix}$$

has maximal rank m. Without loss of generality we may assume that the first m columns of the matrix K are linearly independent, and write

$$K_1 = \begin{pmatrix} k_{11} & \ldots & k_{1m} \\ \vdots & \ddots & \vdots \\ k_{m1} & \ldots & k_{mm} \end{pmatrix},$$

and

$$K_2 = \begin{pmatrix} k_{1,m+1} & \dots & k_{1n} \\ \vdots & \ddots & \vdots \\ k_{m,m+1} & \dots & k_{mn} \end{pmatrix}.$$

Then K_1 is non-singular. Introduce the linear transformation of coordinates $\theta \mapsto \phi$ on T^n by

$$\begin{aligned} \phi_i &= k_{i1}\theta_1 + \ldots + k_{in}\theta_n, \qquad i = 1, \ldots, m, \\ \phi_i &= \theta_i, \qquad i = m+1, \ldots, n. \end{aligned}$$

This transformation is a diffeomorphism because it is linear and nonsingular, as the following calculation demonstrates:

$$\det \begin{pmatrix} K_1 & K_2 \\ 0 & \mathrm{id}_{(n-m)\times(n-m)} \end{pmatrix} = \det(K_1) \neq 0.$$

where $\mathrm{id}_{(n-m)\times(n-m)}$ denotes the $(n-m)\times(n-m)$ identity matrix. In these new coordinates, the dynamics on the resonant n-torus of multiplicity m are given

$$\begin{aligned} \dot{\phi}_i &= (K\,\omega(I^*))_i = 0, \qquad i = 1, \ldots, m, \\ \dot{\phi}_i &= \omega_i(I^*), \qquad i = m+1, \ldots, n. \end{aligned}$$

These equations are easily solved to yield the trajectories

$$\begin{aligned} \phi_i &= \phi_i^* = \text{constant}, \qquad i = 1, \ldots, m, \\ \phi_i &= = \omega_i(I^*)t + \phi_{i0}, \qquad i = m+1, \ldots, n. \end{aligned}$$

Hence, for a fixed $\psi^* \equiv (\phi_1^*, \ldots, \phi_m^*)$, $(\phi_{m+1}^*, \ldots, \phi_n^*) \in \mathrm{T}^{n-m}$ parametrize a torus of dimension $n-m$. Thus, the n-torus T^n specified by $I = I^*$ is foliated into an m-parameter family of $(n-m)$ tori.

To show that the trajectories are dense in the $(n-m)$-tori, we only need to verify that the frequencies $\omega_{m+1}(I^*), \ldots, \omega_n(I^*)$ are not in resonance. Suppose it is not so, then there exist $k'_{m+1}, \ldots, k'_n$ not all being zero such that

$$k'_{m+1}\omega_{m+1}(I^*) + \ldots + k'_n\omega_n(I^*) = 0.$$

Without loss of generality we may assume that $k'_{m+1} \neq 0$. Let k' be the n vector $(0, \ldots, 0, k'_{m+1}, \ldots, k'_n)$. Then k' and $k_i, i = 1, \ldots, m$ are linearly independent because the matrix

$$\begin{pmatrix} K \\ k' \end{pmatrix}$$

has a nonsingular $(m+1)\times(m+1)$ submatrix

$$\begin{pmatrix} k_{11} & \dots & k_{1m} & k_{1,m+1} \\ \vdots & \ddots & \vdots & \vdots \\ k_{m1} & \dots & k_{mm} & k_{m,m+1} \\ 0 & \dots & 0 & k'_{m+1} \end{pmatrix}$$

This contradicts the assumption that $\omega(I^*)$ is resonant of multiplicity m.

Since $\omega_{m+1}(I^*)\ldots,\omega_n(I^*)$ are nonresonant and constants, the corresponding trajectories of $(\phi^*_{m+1},\ldots,\phi^*_n)$ on T^{n-m} are quasiperiodic windings which fill the torus densely. The proof can be found in many references, see the comment following Definition 14.6.2. □

Tori of multiplicity $n-1$ are often referred to as *periodic tori* since they are foliated by 1-tori, i.e., periodic orbits.

> **The Notion of Measure.** The term *measure* of a set will be used in various places throughout this book. By this we will mean nothing more than ordinary Lebesgue measure on $\mathbb{R}^n$. Most of the sets of interest will be quite well-behaved so that "measure" and "area" or "volume" will be synonomous. For any set $U \in \mathbb{R}^n$, we will denote the measure of U by mes(U).

Proposition 14.6.6 *Suppose that*

$$det\left\{\frac{\partial^2 H^0}{\partial I_i \partial I_j}\right\} \neq 0$$

in B. Then the nonresonant *values of I are dense in B and occupy a set of full measure. Moreover, the I values corresponding to* nonresonant *tori of dimension $n-k$ are also dense in B, but occupy a set of zero measure, for $k = 1,\cdots,n-1$.*

Proof: We introduce the following notation:

$$\begin{aligned}
&\Omega_B = \{\omega \in \mathbb{R}^n \,|\, \omega = \omega(I), \text{ for some } I \in B\},\\
&\Omega_r = \{\omega \in \mathbb{R}^n - \{0\} \,|\, k\cdot\omega = 0 \text{ for some } k \in \mathbb{Z}^n - \{0\}\},\\
&\Omega_q = \{\omega \in Q^n - \{0\}\}.
\end{aligned}$$

Namely, Ω_B is the set of all frequencies under consideration, Ω_r is the set of all resonant frequencies and Ω_q is the set of all frequencies with rational components.

First we argue that Ω_r is dense in $\mathbb{R}^n$. This follows immediately from the following facts.

1. $\Omega_q \subset \Omega_r$.
2. Ω_q is dense in $\mathbb{R}^n - \{0\}$.

To show that the set $P_r = \{I \in B \,|\, \omega(I) \in \Omega_r\}$ is dense in B, we only need to note that

$$\det\left(\frac{\partial \omega_i}{\partial I_j}\right) = \det\left(\frac{\partial^2 H^0}{\partial I_i \partial I_j}\right) \neq 0.$$

Hence the map

$$g : I \in B \mapsto \omega(I) \in \Omega_B$$

is a diffeomorphism on B so that $\mathrm{P}_r = g^{-1}(\Omega_r) \cap B$ is dense in $B \cap \mathbb{R}^n$ follows.

To show that

$$\mathrm{mes}(\mathrm{P}_r) = 0$$

we define the map

$$f_k : I \in B \mapsto k_1\omega_1(I) + \ldots + k_n\omega_n(I) \in \mathbb{R}$$

for each fixed $k \in \mathbb{Z}^n - \{0\}$, and denote the set of I corresponding to this particular resonance relation as

$$\mathrm{P}_r^k = \{I \in \mathrm{P}_r \,|\, f_k(I) = 0, \quad \text{for the given}\, k \in \mathbb{Z}^n - \{0\}\}.$$

Then P_r^k is the zero set of f_k

$$f_k(I^*) = k_1\omega_1(I^*) + \ldots + k_n\omega_n(I^*) = 0, \quad I^* \in \mathrm{P}_r^k,$$

and $\mathrm{P}_r^k \subset \mathrm{P}_r$. We have

$$\frac{\partial f_k}{\partial I}(I^*) = k\frac{\partial \omega}{\partial I}(I^*) = k\frac{\partial^2 H^0}{\partial I^2}(I^*) \neq 0$$

since

$$\det\left(\frac{\partial^2 H^0}{\partial I^2}(I^*)\right) \neq 0,\ k \neq 0, \text{ and } \left(\frac{\partial^2 H^0}{\partial I^2}(I^*)\right) = \left(\frac{\partial^2 H^0}{\partial I^2}(I^*)\right)^T.$$

Hence, 0 is a regular value of f_k so that the zero set of f, P_r^k is a manifold of dimension $n-1$. Then

$$\mathrm{mes}(\mathrm{P}_r^k) = 0.$$

Notice that

$$\mathrm{P}_r = \bigcup_{\substack{k \in \mathbb{Z}^n - \{0\} \\ k\cdot\omega(I) = 0}} \mathrm{P}_r^k,$$

and the set $\mathbb{Z}^n - \{0\}$ is countable. Then

$$\mathrm{mes}(\mathrm{P}_r) = 0$$

follows.

The rest of the proposition is straightforward. Note that the nonresonant set

$$\mathrm{P} = \{I \in B \,|\, k \cdot \omega(I) = 0 \Longleftrightarrow k = 0 \in \mathbb{Z}^n\}$$

is complementary to the resonant set P_r in B, hence

$$\mathrm{mes}(\mathrm{P}) = \mathrm{mes}(B).$$

so that P has the full measure so it is dense in B. □

14.6B Diophantine Frequencies

Certain nonresonant frequencies play an important role in the proof of the KAM theorem. These are the *diophantine* frequencies, which we now define. For $\tau, \gamma > 0$

$$\Omega(\tau,\gamma) \equiv \left\{\omega \in \mathbb{R}^n \mid |\omega \cdot k| \geq \gamma |k|^{-\tau} \, \forall k \in \mathbb{Z}^n - \{0\}\right\} \tag{14.6.5}$$

where

$$|k| \equiv \sup_i |k_i|,$$

and we set

$$\Omega(\tau) \equiv \bigcup_{\gamma>0} \Omega(\tau,\gamma).$$

It is important to note that the frequencies satisfying (14.6.5) satisfy a countable infinity of inequalities. These inequalities quantify the characteristic of these frequencies not being close to resonance.

The following proposition is classical. All pieces of the proof can be found in Cassels [1957], Schmidt [1980], Arnold [1963], Russmann [1975], and Lochak and Meunier [1988]. For completeness, we provide a few additional details.

Proposition 14.6.7

1. *For* $0 < \tau < n-1$, $\Omega(\tau) = \emptyset$.
2. *For* $\tau = n-1$, $\Omega(\tau)$ *has Lebesgue measure zero.*
3. *For* $\tau > n-1$, $\mathbb{R}^n - \Omega(\tau)$ *has Lebesgue measure zero, and more precisely*
$$mes\{(\mathbb{R}^n - \Omega(\tau,\gamma)) \cap B_R\} \leq C(\tau)\gamma R^{n-1},$$
where B_R *denotes the ball of radius* R *in* $\mathbb{R}^n$.

Proof:

Proof of 1. The proof of 1 relies on the following result that we state without proof.

Theorem 14.6.8 (Dirichlet's Theorem, Cassels) [1957], *pg. 14*
For any $\theta \equiv (\theta_1, \cdots, \theta_m) \in \mathbb{R}^m$ *the inequality*

$$\| \, p \cdot \theta \, \| \equiv \| \, p_1\theta_1 + \cdots + p_m\theta_m \, \| < |p|^{-m}$$

is satisfied by infinitely many $p \in \mathbb{Z}^m$, *where the notation* $\| \cdot \|$ *is defined by*

$$\forall \theta \in \mathbb{R}, \qquad \| \, \theta \, \| \equiv \inf_{q \in \mathbb{Z}} |\theta - q|. \tag{14.6.6}$$

Without loss of generality we can assume $\omega_n \neq 0$. We set $\theta_i \equiv \frac{\omega_i}{\omega_n}$, $i = 1, \cdots, n-1$. Then, applying Dirichlet's theorem, for any $\left(\frac{\omega_1}{\omega_n}, \cdots, \frac{\omega_{n-1}}{\omega_n}\right) \in \mathbb{R}^{n-1}$ the inequality

$$\| k_1 \frac{\omega_1}{\omega_n} + \cdots + k_{n-1} \frac{\omega_{n-1}}{\omega_n} \| < |k|^{-(n-1)}, \tag{14.6.7}$$

is satisfied by infinitely many $k \equiv (k_1, \cdots, k_{n-1}) \in \mathbb{Z}^{n-1}$. This implies that (14.6.7) has solutions for arbitrarily large $|k|$.

Now we are interested in solutions of the following inequality (viewing $(\omega_1, \cdots, \omega_n)$ as given)

$$\| k_1 \frac{\omega_1}{\omega_n} + \cdots + k_{n-1} \frac{\omega_{n-1}}{\omega_n} \| > \gamma |k|^{-\tau}, \qquad 0 < \tau < n-1. \tag{14.6.8}$$

Then, for a given $(\omega_1, \cdots, \omega_n)$, simultaneous solution of (14.6.7) and (14.6.8) implies

$$0 < \gamma |k|^{-\tau} < \| k_1 \frac{\omega_1}{\omega_n} + \cdots + k_{n-1} \frac{\omega_{n-1}}{\omega_n} \| < |k|^{(n-1)},$$

or

$$\gamma < \frac{\| k_1 \frac{\omega_1}{\omega_n} + \cdots + k_{n-1} \frac{\omega_{n-1}}{\omega_n} \|}{|k|^{-\tau}} < |k|^{-n+1+\tau}. \tag{14.6.9}$$

Now for fixed $\gamma > 0$ the right-hand-side of this bound can be made smaller than the left-hand-side for sufficiently large $|k|$, provided $0 < \tau < n-1$. Hence, we conclude that for any $0 < \tau < n-1$, and for any $\left(\frac{\omega_1}{\omega_n}, \cdots, \frac{\omega_{n-1}}{\omega_n}\right)$ the inequality

$$\| k_1 \frac{\omega_1}{\omega_n} + \cdots + k_{n-1} \frac{\omega_{n-1}}{\omega_n} \| > \gamma |k|^{-\tau}, \tag{14.6.10}$$

does not hold for *all* $k \in \mathbb{Z}^{n-1}$.

From (14.6.6) we have

$$\begin{aligned} |k_1 \frac{\omega_1}{\omega_n} + \cdots + k_{n-1} \frac{\omega_{n-1}}{\omega_n} + k_n| &> \min_{k_n \in \mathbb{Z}} |k_1 \frac{\omega_1}{\omega_n} + \cdots + k_{n-1} \frac{\omega_{n-1}}{\omega_n} + k_n| \\ &\equiv \| k_1 \frac{\omega_1}{\omega_n} + \cdots + k_{n-1} \frac{\omega_{n-1}}{\omega_n} \| > \gamma |k|^{-\tau}, \\ &\quad k \in \mathbb{Z}^{n-1}. \end{aligned} \tag{14.6.11}$$

Now recall $|k| \equiv \max |k_i|$, and for $k \neq 0$ $|k| \geq 1$. Then if we define

$$k^{n-1} \equiv (k_1, \cdots, k_{n-1}),$$

and

$$k^n \equiv (k_1, \cdots, k_n),$$

where the first $n-1$ elements of k^n are the same as k^{n-1}, we have

$$|k^n| \geq |k^{n-1}|,$$

and, thus,

$$|k^{n-1}|^{-\tau} \geq |k^n|^{-\tau}.$$

Using this fact, along with (14.6.11), we conclude that the inequality

$$|k_1\omega_1 + \cdots + k_{n-1}\omega_{n-1} + k_n\omega_n| > \omega_n\gamma|k|^{-\tau}, \quad k \in \mathbb{Z}^n,\ 0 < \tau < n-1, \tag{14.6.12}$$

is not solved for all $k \in \mathbb{Z}^n$. We have shown that $\Omega(\tau, \omega_n\gamma) = \emptyset$ for any γ, $\omega_n \neq 0$.

Proof of 2. This is the difficult case, and the reader is referred to Schmidt [1980].

Proof of 3. Here we follow Arnold [1963] and Lochak and Meunier [1988].

$\omega \cdot k = 0$ is a resonant plane passing through the origin in $\mathbb{R}^n$ (and the integer vector k is perpendicular to the plane). A neighborhood of this plane is given by

$$\left\{\omega \in \mathbb{R}^n \,|\, |\omega \cdot k| \leq \gamma|k|^{-\tau}\right\}, \tag{14.6.13}$$

and the width of this neighborhood is given by

$$2\gamma|k|^{-\tau-1}.$$

It is only in these neighborhoods of the resonant planes that the inequality

$$|\omega \cdot k| > \gamma|k|^{-\tau},$$

does *not* hold. The volume of one of these neighborhoods is given by

$$\operatorname{mes}\left\{\left\{\omega \in \mathbb{R}^n \,|\, |\omega \cdot k| \leq \gamma|k|^{-\tau}\right\} \cap B_R\right\} = 2C\gamma R^{n-1}|k|^{\tau-1}, \tag{14.6.14}$$

where C is a constant depending on B_R. Hence we have

$$\begin{aligned}\operatorname{mes}\left\{(\mathbb{R}^n - \Omega(\tau,\gamma)) \cap B_R\right\} &= 2C\gamma R^{n-1} \sum_{k \in \mathbb{Z}^n - \{0\}} |k|^{-\tau-1} \\ &\equiv C(\tau)\gamma R^{n-1}\end{aligned} \tag{14.6.15}$$

which goes to zero as $\gamma \to 0$ and where

$$C(\tau) \equiv 2C \sum_{k \in \mathbb{Z}^n - \{0\}} |k|^{-\tau-1}.$$

This sum converges only if $\tau > n-1$, we leave the details of this last fact to the reader. □

14.6c Geometry of the Resonances

Here we describe a few features associated with the *geometry of resonances*. Essentially, these amount to properties of the equation(s)

$$k \cdot \omega(I) = 0, \quad k \in \mathbb{Z}^n - \{0\}.$$

We can view these properties as manifested either in *action space* or *frequency space* by use of the frequency map

$$I \mapsto \omega(I), \qquad I \in B. \tag{14.6.16}$$

Action Space

In action space we make the following observations.

- The solutions of the equation $k \cdot \omega(I) = 0,\ k$ fixed, generically form a hypersurface in B.
- The solutions of the $r < n$ equations $k^i \cdot \omega(I) = 0, i = 1, \ldots, r$, generically form a surface of codimension r in B.

We also easily conclude that *resonances are nested* – a resonance of multiplicity r is contained in a resonance of multiplicity $r-1$.

Frequency Space

In frequency space the equation(s) $k \cdot \omega = 0$ represent a system of linear equations. It is natural to leave out the explicit dependence of ω on I in this representation.

Energy Conservation

In frequency space the resonance relation restricted to $H^0(I) = h = \text{constant}$ can be written as

$$k_1 \frac{\omega_1}{\omega_n} + \ldots + k_{n-1} \frac{\omega_{n-1}}{\omega_n} + k_n = 0$$

where we suppose (without loss of generality) $\omega_n(I)$ does not vanish in the region of interest.

Resonance Structure Versus the Number of Angles

n=1 In this case resonance implies $\omega = 0$.

n=2 In this case the resonance relation restricted to the energy surface is given by

$$k_1 \frac{\omega_1}{\omega_2} + k_2 = 0.$$

Thus the resonances occur at *isolated* points in $\frac{\omega_1}{\omega_2}$ space. Moreover, for nondegenerate systems they have different energies (i.e., different values for the Hamiltonian). We say that for two degree-of-freedom systems the resonances are *energetically isolated*.

n=3 In this case the resonance relation restricted to the energy surface is given by

$$k_1\frac{\omega_1}{\omega_3} + k_2\frac{\omega_2}{\omega_3} + k_3 = 0.$$

The resonance relation defines lines in $\frac{\omega_1}{\omega_3} - \frac{\omega_2}{\omega_3}$ space. For a fixed (k_1, k_2, k_3) the line corresponds to a multiplicity one resonance. Generically, if two lines intersect they do so in an isolated point. Such a point corresponds to a multiplicity two resonance. As (k_1, k_2, k_3) runs through $\mathbb{Z}^3$ the resulting lines are dense in $\frac{\omega_1}{\omega_3} - \frac{\omega_2}{\omega_3}$ space. This is a significant difference between two degree-of-freedom systems and systems with three or more degrees-of-freedom. In the former case the resonances are (generically) energetically isolated. In the latter case they are not.

14.7 Perturbations of Completely Integrable Hamiltonian Systems in Action-Angle Coordinates

This is a huge area, a good up-to-date and general reference is Arnold et al. [1988]. However, the two most important theorems are those due to Kolmogorov [1954]-Arnold [1963] -Moser [1962] (KAM) and Nekhoroshev. Here we state them. The Hamiltonian we consider is of the form

$$H(I,\theta) = H^0(I) + \varepsilon H^1(I,\theta), \qquad (I,\theta) \in B \times T^n. \tag{14.7.1}$$

Below is the statement of the KAM theorem due to Pöschel [1982].

Theorem 14.7.1 (KAM) *Let the integrable Hamiltonian H^0 be real analytic and nondegenerate, and let the perturbed Hamiltonian $H = H^0 + \varepsilon H^1$ be of class C^r with $r > 2n$. Then, for sufficiently small ε proportional to γ^2, the perturbed system possesses smooth invariant n-tori with linear flow for all $\omega \in \Omega(n,\gamma)$, i.e., restricted to the invariant n-tori, the vector field is analytically conjugate to $\dot{\phi} = \omega$.*

What about the lower dimensional tori described in Proposition 14.6.5? Recent results of Eliasson [1988], and Pöschel [1989] prove the persistence of lower-dimensional "elliptic" tori, and results of de la Llave and Wayne [1990], and Treschev [1991] prove the persistence of lower-dimensional "hyperbolic" (or "whiskered") tori.

The following theorem is originally due to Nekhoroshev [1977], but it has recently been sharpened considerably in the work of Lochak [1992],

Lochak and Neishtadt [1992], and Pöschel [1993]. It is a result that requires analyticity of the Hamiltonian, as well as either convexity or quasiconvexity of the unperturbed Hamiltonian.

The function $H^0(I)$ is said to be *convex* if

$$\| \nabla^2 H^0(I)v \| \leq M \| v \|, \quad \nabla^2 H^0(I)v \cdot v \geq m \| v \|^2, \qquad \forall I \in B,\, v \in \mathbb{R}^n,$$

and where $0 < m \leq M$. *Quasiconvexity* is convexity restricted to the level set of the Hamiltonian.

Theorem 14.7.2 (Nekhoroshev) *For any initial condition $(I(0), \theta(0))$ one has*

$$|I(t) - I(0)| \leq C_1 \epsilon^b \qquad \text{for} \qquad |t| \leq C_2 \exp(C_3 \epsilon^{-a}) \ ,$$

where $a = b = 1/2n$, C_1, C_2, and C_3 are constants, and provided ϵ is small enough.

14.8 Stability of Elliptic Equilibria

Suppose (14.0.1) has an equilibrium point, which without loss of generality, we can assume to be at $(q, p) = (0, 0)$. We are interested in the stability of the equilibrium. Therefore, as a first step, we linearize (14.0.1) about the equilibrium and examine the eigenvalues of the matrix associated with the equilibrium. This matrix is an infinitesimally symplectic matrix and so Proposition 14.3.5 describes the nature of the eigenvalues. If all eigenvalues lie on the imaginary axis, *but none are zero*, then the equilibrium is said to be an *elliptic equilibrium*. Morse theory can be used to prove Liapunov stability of a large class of elliptic equilibria. We begin by developing the necessary background to prove this result.

Definition 14.8.1 (Nondegenerate Critical Point) *Suppose $F : \mathbb{R}^n \to \mathbb{R}$ is a C^r, $r \geq 3$, or analytic function. Suppose $x = x_0$ is a point such that $\frac{\partial F}{\partial x}(x_0) = 0$. Then x_0 is said to be a* critical point. *If x_0 is such that $\det \frac{\partial^2 F}{\partial x^2}(x_0) \neq 0$ then it is said to be a* nondegenerate critical point.

Definition 14.8.2 (Morse Function) *If $x = x_0$ is a nondegenerate critical point of $F(x)$ then $F(x)$ is said to be a* Morse function *in a neighborhood of x_0.*

Suppose we Taylor expand $F(x)$ about $x = 0$. The $n \times n$ matrix associated with the second derivatives is symmetric. Therefore it can always be diagonalized by a linear transformation. We assume that this has been done, after which the Taylor expansion assumes the form

$$F(x) = F(0) - c_1 x_1^2 - \cdots - c_k x_k^2 + c_{k+1} x_{k+1}^2 + \cdots + c_n x_n^2 + \mathcal{O}(3),$$

where $c_i \geq 0$, $i = 1, \ldots, n$. The integer k is called the *index of the critical point*. Then we have the following *Morse lemma*.

Lemma 14.8.3 (Morse) *If F is a C^r, $r \geq 3$, or analytic Morse function near $x = 0$, then in a neighborhood of $x = 0$ there exists a C^{r-2}, or analytic diffeomorphism, which transforms F to the form*

$$G(x) = G(0) - y_1^2 - \cdots - y_k^2 + y_{k+1}^2 + \cdots + y_n^2.$$

Proof: See Golubitsky and Marsden [1983]. □

One now should be able to guess how these results are used to study stability of elliptic equilibria in Hamiltonian systems. At an elliptic equilibrium the Hamiltonian is a Morse function. Now suppose the matrix associated with the second derivative of the Hamiltonian, evaluated at the equilibrium point, is positive definite. Then the equilibrium point has index zero and the Hamiltonian is locally conjugate to a Hamiltonian of the form

$$H(q, p) - H(0, 0) = q_1^2 + \cdots + q_n^2 + p_1^2 + \cdots + p_n^2.$$

Hence the energy surfaces are locally diffeomorphic to a family of spheres that shrink down to the point $(0, 0)$ as $H \to H(0, 0)$. Since the trajectories are tangent to the energy surfaces Liapunov stability follows. In the case that the matrix associated with the second derivative of the Hamiltonian, evaluated at the equilibrium point, is negative definite we apply the same reasoning to the time reversed vector field (i.e., let $H \to -H$) and obtain the same result.

14.9 Discrete-Time Hamiltonian Dynamical Systems: Iteration of Symplectic Maps

The dynamics of symplectic maps can be viewed as a discrete time analog of the dynamics generated by Hamiltonian vector fields. Proposition 14.3.2 gives us information about linearized stability of periodic orbits of symplectic maps and, hence, the local invariant manifold structure (i.e. existence and dimensions of stable, unstable, and center manifolds of periodic orbits). There are also discrete analogs of the KAM theorem and Nekoroshev's theorem, which we now describe.

14.9A The KAM Theorem and Nekhoroshev's Theorem for Symplectic Maps

As in the continuous time case, the setting for these theorems is that of perturbations of integrable symplectic maps. Before stating the results we must develop the appropriate setting.

Let B_δ denote the open ball in $\mathbb{R}^n$ of radius δ. Then the $2n$-dimensional annulus is denoted by $A_\delta = B_\delta \times T^n$. We define the following map on A_δ:

$$f_0 : A_\delta \to A_\delta$$

$$(I, \theta) \mapsto (I, \theta + \omega(I)) = f_0(I, \theta). \tag{14.9.1}$$

(14.9.2)

It should be clear that A_δ is foliated by an n-parameter family of invariant n-tori. We assume that ω is given by the gradient of a function, i.e.,

$$\omega = \nabla h.$$

In this case f_0 is a globally symplectic map with generating function h.

Now we want to consider perturbations of f_0, but not just any perturbations. Rather, we only wish to consider perturbations where the resulting perturbed map is also symplectic. This can be achieved through the use of *generating functions*, for which we refer the reader to Whittaker [1904], Goldstein [1980], Abraham and Marsden [1978], Arnold [1978], or Section 13.7c for more background. For our limited purposes one could just take the following as the definition of the maps under consideration.

We consider the map generated by a perturbation of h:

$$\Sigma(I', \theta) = h(I') + \sigma(I', \theta),$$

where σ is small, with $\| \sigma \| \equiv \epsilon$. Then the perturbed map $f : A_\delta \to A_\delta$ is implicitly defined by

$$f : A_\delta \to A_\delta,$$

$$(I', \theta') = \left(I - \frac{\partial \sigma}{\partial \theta}, \theta + \omega(I') + \frac{\partial \sigma}{\partial I'} \right), \tag{14.9.3}$$

where primes denote the image of the respective coordinate under the map.

Nekhoroshev Theorem for Symplectic Maps

The discrete version of Nekhoroshev's theorem was first announced in Nekhoroshev [1977]. Details first appeared in Kuksin and Pöschel [1994], but see also Bazzani et al. [1990] and Lochak [1992]. We first establish some notation. Let $f^s(I, \theta) \equiv (I_s, \theta_s)$, with $(I_0, \theta_0) \equiv (I, \theta)$. We assume that (I_s, θ_s) remains in A_δ for all times under consideration.

Theorem 14.9.1 *Suppose h and σ are analytic and h is a convex function. If $\epsilon \equiv \| \sigma \| \leq \epsilon_0$, then $\| I_s - I \| \leq c\epsilon^b$ when $|s| \leq c \exp(\epsilon^{-a})$, $s \in \mathbb{Z}$, and where $a = b = \frac{1}{2n+2}$.*

Proof: See Kuksin and Pöschel [1994]. □

KAM Theorem for Symplectic Maps

The discrete version of the KAM theorem was first worked out in the analytic setting by Douady [1982] (although the two dimensional Moser twist theorem in the finitely differentiable case was obtained much earlier). Kuksin and Pöschel [1994] provide a new proof. First we establish some notation.

We assume that the unperturbed map is nondegenerate in the following sense:

$$\det \nabla^2 h(I) = \det \frac{\partial \omega}{\partial I} \neq 0.$$

This condition is often referred to as the *twist condition*. We are concerned with the preservation tori whose unperturbed frequency vectors satisfy the following diophantine condition:

$$|2\pi p + q_1\omega_1 + \cdots + q_n\omega_n| > c\left(|q_1| + \cdots + |q_n|\right)^{-\gamma}, \tag{14.9.4}$$

for all $q \in \mathbb{Z}^n - \{0\}$ and $p \in \mathbb{Z}$, and where $c > 0$ and $\gamma > n$ are constants.

Theorem 14.9.2 *For analytic f, and for ϵ sufficiently small, the perturbed map f possesses analytic invariant n-tori for all ω satisfying (14.9.4). Moreover, the dynamics restricted to the invariant n-tori is analytically conjugate to the rigid rotation $\phi \mapsto \phi + \omega$.*

Proof: See Kuksin and Pöschel [1994]. □

14.10 Generic Properties of Hamiltonian Dynamical Systems

The special structure of Hamiltonian dynamical systems (both continuous and discrete time) give rise to additional generic properties than those described in the usual Kupka-Smale theorems discussed in Chapter 12. The classic papers on this subject are Robinson [1970a, b], Takens [1970], [1972], Newhouse [1977], and Pugh and Robinson [1983]. Here we content ourselves with just stating a few of these properties, which we will expand upon when we learn more about global dynamics later in the book.

For C^1 Hamiltonian systems the following properties are generic (in the sense of holding for a residual subset in the appropriate "space of dynamical systems").

Hyperbolic periodic orbits are dense in the phase space (Pugh and Robinson [1983]).

Every hyperbolic periodic orbit has a transverse homoclinic point in any neighborhood of any point in the phase space (Taken [1970], [1972], Newhouse [1977]).

The reader should take great care in applying these generic results to specific dynamical systems following the caveats described in Chapter 12. In a measure theoretic sense, residual sets can be "small". Herman [1991] has constructed an explicit example of a Hamiltonian system with *no* periodic orbits. Another important point for applications is that "generic type theorems" are typically proved in a C^r setting. In many applications the dynamical systems are analytic. The C^r techniques generally make the results inapplicable in an analytic setting.

14.11 Exercises

1. Prove that $\langle \cdot, J\cdot \rangle$ is a symplectic form on $\mathbb{R}^{2n}$.

2. Suppose a $2n \times 2n$ matrix of real numbers A satisfies

$$A^T J A = J,$$

where A has the form

$$\begin{pmatrix} a & b \\ c & d \end{pmatrix},$$

and a, b, c, d are $n \times n$ matrices. Show that

   (a) The $n \times n$ matrices $a^T c$ and $b^T d$ are symmetric,
   (b) $a^T d - c^T b = \mathrm{id}$,
   (c) $\det A = 1$.

3. Prove that the composition of two symplectic transformations is a symplectic transformation.

4. Consider a (real), canonical autonomous Hamiltonian vector field having an equilibrium point.

   (a) Can the equilibrium point be asymptotically stable?
   (b) Can the equilibrium point have an odd dimensional center manifold?

5. Consider a (real), symplectic map having a periodic orbit.

   (a) Can the periodic orbit be asymptotically stable?
   (b) Can the periodic orbit have an odd dimensional center manifold?

6. Prove that the flow generated by a Hamiltonian vector field is volume preserving.

7. Prove that symplectic maps preserve volume.

8. Prove that two dimensional volume preserving vector fields are Hamiltonian.

9. Construct an example of a vector field in dimension $2n$, $n \geq 2$, that is volume preserving but not Hamiltonian.

10. Consider a Hamiltonian vector field in the plane having a hyperbolic equlibrium point connected to itself by a homoclinic orbit. Is the homoclinic orbit structurally stable? Consider a heteroclinic connection between two hyperbolic equlibrium points. Is this situation structurally stable? Do the results change if the equilibria are not hyperbolic? Do the results hold in higher dimensions?

11. Consider the following vector field in complex coordinates $z_z = x_1 + iy_1$, $z_2 = x_2 + iy_2$:

$$\begin{aligned}\dot{z}_1 &= i[-(\sigma-\beta)z_1 + \Delta\bar{z}_1 + \pi_1 z_1^2\bar{z}_1 + \pi_2 z_1 z_2\bar{z}_2 + \pi_3\bar{z}_1 z_2^2],\\ \dot{z}_2 &= i[-(\sigma+\beta)z_2 + \Delta\bar{z}_2 + \pi_1 z_2^2\bar{z}_2 + \pi_2 z_1 z_2\bar{z}_1 + \pi_3\bar{z}_2 z_1^2].\end{aligned}$$

This equation is a normal form that arises in the study of a variety of two degree-of-freedom parametrically forced mechanical systems (see Feng and Wiggins [1993]). The parameters represent

- σ – difference between the forcing frequency and the sum of the two natural frequencies.
- β – difference between the two natural frequencies.
- Δ – amplitude of the sinusoidal excitation.
- $\pi_1,\ \pi_2,\ \pi_3$–coefficients of the nonlinear terms depending on the mode numbers and geometrical properties.

(a) Show that this vector field is Hamiltonian.

(b) Show that through rescaling we can set

$$\Delta = 1, \quad \pi_1 = -1,$$

and that it the rescaled *cartesian* coordinates the vector field is given by

$$\begin{aligned}\dot{x_1} &= (\sigma - \pi_1 E + 1)y_1 - 2\pi_3 L x_2 - \beta y_1 + C y_1(x_2^2 + y_2^2)\\ \dot{y_1} &= (-\sigma + \pi_1 E + 1)x_1 - 2\pi_3 L y_2 + \beta x_1 - C x_1(x_2^2 + y_2^2)\\ \dot{x_2} &= (\sigma - \pi_1 E + 1)y_2 + 2\pi_3 L x_1 + \beta y_2 + C y_2(x_1^2 + y_1^2)\\ \dot{y_2} &= (-\sigma + \pi_1 E + 1)x_2 + 2\pi_3 L y_1 - \beta x_2 - C x_2(x_1^2 + y_1^2)\end{aligned} \tag{14.11.1}$$

where

$$\begin{aligned}E &= x_1^2 + y_1^2 + x_2^2 + y_2^2,\\ L &= x_1 y_2 - x_2 y_1,\\ C &= \pi_1 - \pi_2 - \pi_3.\end{aligned}$$

The parameters are now reduced to

$$d,\ \sigma,\ \beta,\ C,\ \pi_3.$$

(c) Show that (14.11.1) is Hamiltonian with Hamiltonian given by

$$\begin{aligned}H = &\frac{\sigma}{2}E + \frac{1}{4}E^2 + \pi_3 L^2 + \frac{1}{2}(y_1^2 + y_2^2 - x_1^2 - x_2^2)\\ &+ \frac{\beta}{2}(x_2^2 + y_2^2 - x_1^2 - y_1^2) + \frac{C}{2}(x_1^2 + y_1^2)(x_2^2 + y_2^2).\end{aligned}$$

(d) Consider the transformation

$$\begin{aligned}x_1 &= q_1\cos q_2,\\ x_2 &= q_1\sin q_2,\\ y_1 &= p_1\cos q_2 - p_2 q_1^{-1}\sin q_2,\\ y_2 &= p_1\sin q_2 + p_2 q_1^{-1}\cos q_2,\end{aligned} \tag{14.11.2}$$

with inverse

$$\begin{aligned} q_1 &= \sqrt{x_1^2 + x_2^2}, \\ p_1 &= \frac{x_1 y_1 + x_2 y_2}{\sqrt{x_1^2 + x_2^2}}, \\ q_2 &= \tan^{-1} \frac{x_2}{x_1}, \\ p_2 &= x_1 y_2 - x_2 y_1. \end{aligned} \tag{14.11.3}$$

Show that this transformation is canonical.

(e) Show that in this new coordinate system the vector field is Hamiltonian with Hamiltonian given by

$$\begin{aligned} \tilde{H} \equiv H_0 + \epsilon H_1 = \frac{\sigma}{2}\tilde{E} + \frac{1}{4}\tilde{E}^2 + \pi_3 p_2^2 + \frac{1}{2}(p_1^2 + p_2^2 q_1^{-2} - q_1^2) \\ + \left(\frac{\beta}{2} D + \frac{C}{8}(\tilde{E}^2 - D^2)\right) \end{aligned} \tag{14.11.4}$$

where

$$\tilde{E} = q_1^2 + p_1^2 + p_2^2 q_1^{-2},$$

$$D = 2p_1 p_2 q_1^{-1} \sin 2q_2 + (p_2^2 q_1^{-2} - q_1^2 - p_1^2)\cos 2q_2.$$

(f) Show that for $\beta = C = 0$ this system is completely integrable.

12. Consider the following two degree-of-freedom system in complex coordinates

$$\begin{aligned} -i\dot{c} + (\frac{1}{2}|c|^2 + \frac{1}{2}|b|^2 - 1)c + \frac{1}{2}(c\bar{b} + b\bar{c})b = 0, \\ -i\dot{b} + (\frac{1}{2}|c|^2 + \frac{3}{4}|b|^2 - (1 + k^2))b + \frac{1}{2}(c\bar{b} + b\bar{c})c = 0, \end{aligned}$$

where k is a real parameter. This equation arises in the study of a two-mode truncation of the nonlinear Schrödinger equation, see Bishop et al. [1990] and Kovačič and Wiggins [1992].

(a) Show that this system is Hamiltonian.

(b) Show that the coordinate transformation

$$c = |c|e^{i\theta}, \qquad b = (x + iy)e^{i\theta},$$

is canonical, and be careful to describe where it is defined.

(c) Show that in these new coordinates the vector field takes the form

$$\begin{aligned} \dot{x} &= -k^2 y - \frac{3}{4}x^2 y + \frac{1}{4}y^3, \\ \dot{y} &= (k^2 - 2I)x + \frac{7}{4}x^3 + \frac{3}{4}xy^2, \\ \dot{I} &= 0, \\ \dot{\theta} &= 1 - I - x^2, \end{aligned} \tag{14.11.5}$$

and it is Hamiltonian with Hamiltonian given by

$$H = \frac{1}{2}I^2 - I - \frac{7}{16}x^4 - \frac{3}{8}x^2 y^2 + \frac{1}{16}y^4 + (I - \frac{1}{2}k^2)x^2 - \frac{1}{2}k^2 y^2. \tag{14.11.6}$$

(d) Show that the system is completely integrable.

(e) Sketch the phase portrait of the $x-y$ component of (14.11.5) as a function of I and k.

13. Consider the following three degree-of-freedom Hamiltonian given in complex coordinates

$$H_c = \frac{1}{2}\left(1+\varepsilon d\right)|z_1|^2 + |z_2|^2 + \frac{1}{2}\omega_3|z_3|^2 + \epsilon\frac{a}{2}\mathrm{Re}\left(z_1^2\bar{z}_2\right). \tag{14.11.7}$$

where d, ϵ, ω_3, and a are real parameters. This Hamiltonian arises in the study of dynamics near an elliptic equilibrium point in $1:2:2$ resonance, see Haller and Wiggins [1996].

(a) Show that it is completely integrable with integrals given by

$$H_c, \quad J_1 = \frac{1}{2}|z_1|^2 + |z_2|^2, \quad J_2 = \frac{1}{2}|z_3|^2. \tag{14.11.8}$$

(b) We define the following coordinate transformations:

$$z_k = \sqrt{2I_k}e^{i\phi_k}, \quad \bar{z}_k = \sqrt{2I_k}e^{-i\phi_k}, \qquad k=1,2,3, \tag{14.11.9}$$

$$\begin{array}{ll} \psi_1 = \phi_1, & K_1 = I_1 + 2I_2 + \omega_3 I_3, \\ \psi_2 = \phi_3 - \omega_3\phi_1, & K_2 = I_3, \\ x_1 = \sqrt{2I_2}\sin\left(\phi_2 - 2\phi_1\right), & x_2 = \sqrt{2I_2}\cos\left(\phi_2 - 2\phi_1\right), \end{array} \tag{14.11.10}$$

Composing these two transformations gives us a map

$$(z,\bar{z}) \to (x,K,\psi).$$

Show that the resulting transformation is canonical.

(c) Show that in the (x,K,ψ) coordinates the Hamiltonian takes the form

$$H_c(x,K,\psi) = K_1 + \epsilon\left(d + ax_2\right)\left(K_1 - \omega_3 K_2 - |x|^2\right). \tag{14.11.11}$$

(d) Show that the vector field corresponding to H_c takes the form

$$\begin{aligned} \dot{x}_1 &= \epsilon[a(K_1 - \omega_3 K_2 - x_1^2 - x_2^2) - 2\left(d + ax_2\right)x_2], \\ \dot{x}_2 &= \epsilon 2x_1\left(d + ax_2\right), \\ \dot{K}_2 &= 0, \\ \dot{\psi}_2 &= -\epsilon\omega_3\left(d + ax_2\right), \\ \dot{K}_1 &= 0, \\ \dot{\psi}_1 &= 1 + \epsilon\left(d + ax_2\right). \end{aligned} \tag{14.11.12}$$

(e) Sketch the phase portrait of the $x_1 - x_2$ component of (14.11.12) as a function of $K_1 - \omega_3 K_2$ and d.

14. The following two degree-of-freedom Hamiltonian is the normal form (through third order) describing the behavior near an elliptic equilibrium point in $1:2$ resonance:

$$H(z_1,\bar{z}_1,z_2,\bar{z}_2) = \frac{1}{2}|z_1|^2 + |z_2|^2 + 2a\,\mathrm{Re}\,z_1^2\bar{z}_2 - 2b\,\mathrm{Im}\,z_1^2\bar{z}_2, \tag{14.11.13}$$

where a and b are real. Let

$$c \equiv a + ib, \qquad c = |c|e^{i\,arg\,c},$$

and consider the coordinate transformation

$$(z_1,\bar{z},z_2,\bar{z}_2) \mapsto \left(e^{\frac{-i\,arg\,c}{2}}z_1, e^{\frac{i\,arg\,c}{2}}\bar{z}_1, z_2, \bar{z}_2\right).$$

Show that this transformation is canonical, and that the Hamiltonian becomes

$$H(z_1,\bar{z}_1,z_2,\bar{z}_2) = \frac{1}{2}|z_1|^2 + |z_2|^2 + 2|c|\,\mathrm{Re}\,z_1^2\bar{z}_2. \tag{14.11.14}$$

15. Show that the Poincaré map constructed in section 10.4 is symplectic.

16. Consider the following frequency vectors

    (a) $\omega = 0$.
    (b) $\omega = 1$.
    (c) $\omega = (1, 0)$.
    (d) $\omega = (\sqrt{2}, 0)$.
    (e) $\omega = (\sqrt{2}, 1)$.
    (f) $\omega = (\sqrt{2}, 0, 0)$.
    (g) $\omega = (\sqrt{2}, 0, 1)$.
    (h) $\omega = (\sqrt{2}, 1, 1)$.
    (i) $\omega = (\sqrt{2}, \sqrt{2}, 1)$.
    (j) $\omega = (\sqrt{2}, \sqrt{2}, \sqrt{2})$.
    (k) $\omega = (\sqrt{2}, 2, 1)$.
    (l) $\omega = (1, 1, 1)$.
    (m) $\omega = (1, 2, 1)$.
    (n) $\omega = (1, 2, 3)$.
    (o) $\omega = (1, 2, 8)$.

    Which of these is resonant? For the the resonant frequency vectors, compute the multiplicity of the resonance.

17. Compare the Liouville-Arnold Theorem (Theorem 14.5.1)with the results obtained in Exercise 20 of Chapter 13.

15

Gradient Vector Fields

In this chapter we consider vector fields that are given by the gradient of a scalar valued function, which are referred to as *gradient vector fields*. Gradient vector fields arise in a variety of applications. For example, they arise in the study of neural networks (Haykin [1994]) and in the study of electrical circuits and networks (see Hirsch and Smale [1974]).

Consider a vector field of the form

$$\dot{x} = -\nabla V(x), \qquad x \in \mathbb{R}^n, \tag{15.0.1}$$

where $V(x)$ is a scalar valued function on $\mathbb{R}^n$ that is C^r, $r \geq 2$. The minus sign in front of the gradient is traditional and imposes no restriction as we can always redefine $V(x)$ as $-V(x)$. The special structure of this vector field, i.e., the fact that it is a gradient of a scalar valued function, imposes strict constraints on the nature of the dynamics, as we shall see.

First, it should be clear that equilibrium points of (15.0.1) are relative extrema of $V(x)$. Moreover, at any point *except* for an equilibrium point, the vector field (15.0.1) is perpendicular to the level sets of $V(x)$. We can get more information by differentiating $V(x)$ along trajectories of (15.0.1), i.e.,

$$\begin{aligned} \dot{V}(x) &= \nabla V(x) \cdot \dot{x}, \\ &= \nabla V(x) \cdot (-\nabla V(x)), \\ &= -|\nabla V(x)|^2, \end{aligned} \tag{15.0.2}$$

where "$\cdot$" is the Euclidean inner product and $|\cdot|$ is the induced Euclidean norm. The next result follows immediately from this calculation.

Proposition 15.0.1 *$\dot{V}(x) \leq 0$ and $\dot{V}(x) = 0$ if and only if x is an equilibrium point of (15.0.1).*

Using $V(x)$ to construct an appropriate Liapunov function, we can obtain stability information about certain equilibrium points.

Proposition 15.0.2 *Suppose $\bar{x}$ is an isolated minimum of $V(x)$, i.e., there is a neighborhood of $\bar{x}$ that contains no other minima of $V(x)$. Then $\bar{x}$ is an asymptotically stable equilibrium point of (15.0.1).*

Proof: A simple calculation shows that $V(x) - V(\bar{x})$ is an appropriate Liapunov function from which the result follows by applying Theorem 2.0.1. □

It is also easy to see that the matrix associated with the linearization about an equilibrium point of a gradient vector field can have only real eigenvalues. This follows from the fact that $-\nabla^2 V(x)$ is a symmetric matrix, and symmetric matrices have only real eigenvalues.

Trajectories of gradient dynamical systems have very simple asymptotic behavior, as the following theorem shows.

Theorem 15.0.3 *Suppose $\bar{x}$ is an ω limit point of a trajectory of (15.0.1). Then $\bar{x}$ is an equilibrium point of (15.0.1).*

Proof: If $\bar{x}$ is an omega limit point of a trajectory, say $\phi_t(x)$, then we can show that $V(x)$ is constant along the trajectory through $\bar{x}$. Hence, $\dot{V}(\bar{x}) = 0$. It then follows from (15.0.2) that $\bar{x}$ is an equilibrium point.

So we show that $V(x)$ is constant along the trajectory through $\bar{x}$. By the definition of omega limit point, there exists a sequence $\{t_i\}$, $t_i \to \infty$ as $i \to \infty$ such that

$$\lim_{i \to \infty} \phi_{t_i}(x) = \bar{x}.$$

Let $\chi = V(\bar{x})$, then χ is the greatest lower bound of the set $\{V(\phi_t(x)) \,|\, t \geq 0\}$. This follows from the fact that $V(x)$ decreases along trajectories (hence $V(\phi_{t_i}(x)) \geq V(\phi_t(x)) \geq V(\phi_{t_{i+1}}(x))$ for $t_i \leq t \leq t_{i+1}$) and by the continuity of $V(x)$. From Proposition 8.1.3 the omega limit set of a trajectory is invariant, hence $\phi_t(\bar{x})$ is also an omega limit point of $\phi_t(x)$. Then, since χ is the greatest lower bound of the set $\{V(\phi_t(x)) \,|\, t \geq 0\}$, $V(\phi_t(\bar{x})) = \chi$. □

15.1 Exercises

1. Show that gradient vector fields cannot have:
   (a) periodic orbits,
   (b) homoclinic orbits, or
   (c) heteroclinic cycles.
2. Can gradient vector fields have heteroclinic orbits?
3. Give sufficient conditions on $V(x)$ so that the trajectories of (15.0.1) exist for all time.
4. Describe the time evolution of the volume of a region of the phase space under the flow generated by a gradient vector field.
5. Consider the vector field

$$\begin{aligned} \dot{\theta}_1 &= \omega_1 + w \sin(\theta_2 - \theta_1), \\ \dot{\theta}_2 &= \omega_2 + w \sin(\theta_1 - \theta_2), \qquad (\theta_1, \theta_2) \in S^1 \times S^1, \end{aligned}$$

   where ω_1, ω_2, and w are parameters.

(a) Show that this is a gradient vector field.

(b) Determine the phase portrait for this vector field.

(c) Can this vector field have periodic orbits? Would the existence of periodic orbits contradict Theorem 15.0.3?

16

Reversible Dynamical Systems

In this section we introduce the notion of *reversible dynamical systems*. Another example of a class of dynamical systems with "special structure" that constrains the dynamics. Such systems often arise in applications (see Roberts and Quispel [1992] for many examples, as well as the exercises at the end of this chapter) and may have the seemingly peculiar property of simultaneously possessing Hamiltonian-like dynamics (e.g. KAM tori) and dissipative dynamics (e.g. attractors). We begin by defining reversibility in both the continuous and discrete time settings. Comprehensive references are Sevryuk [1986], [1992], and Roberts and Quispel [1992].

16.1 The Definition of Reversible Dynamical Systems

Consider the following continuous and discrete time dynamical systems:

$$\dot{x} = f(x), \qquad x_{n+1} = g(x_n), \qquad x \in \mathbb{R}^n,$$

which we assume to be C^r, $r \geq 1$. Next consider a C^r map

$$G : \mathbb{R}^n \mapsto \mathbb{R}^n,$$

satisfying

$$G \circ G = id,$$

where id stands for the identity map. G is called an *involution*. Then a vector field is said to be *reversible* if

$$\frac{d}{dt}(G(x)) = -f(G(x)). \tag{16.1.1}$$

From this definition we can see the motivation for the term *reversible*. A vector field, $\dot{x} = f(x)$, is reversible if the dynamics on the phase space $G \cdot \mathbb{R}^n$ is given by the time reversed vector field. Using the chain rule on the left hand side of (16.1.1), as well as the identity $\dot{x} = f(x)$, we see that the definition of reversibility for a vector field reduces to the following relationship between G and f:

$$DG \cdot f = -f \circ G, \tag{16.1.2}$$

where in this section the "$\cdot$" notation means ordinary matrix multiplication, with a matrix to the left of $\cdot$ and a vector to the right of $\cdot$.

Next we consider maps. A map is said to be reversible if

$$g(G(x_{i+1})) = G(x_i). \tag{16.1.3}$$

The motivation for the term reversible should be apparent. In the transformed phase space, $G\cdot\mathbb{R}^n$, g reverses the temporal direction of trajectories. Substituting $x_{i+1} = g(x_i)$ into the left hand side of (16.1.3), we obtain the following relationship between G and g that is required for g to be reversible:

$$g \circ G \circ g = G. \tag{16.1.4}$$

16.2 Examples of Reversible Dynamical Systems

We now consider some explicit examples of reversible dynamical systems.

Example 16.2.1. Consider a canonical Hamiltonian vector field where the Hamiltonian is even in the momenta, i.e.,

$$H(q,p) = H(q,-p), \qquad (q,p) \in \mathbb{R}^n \times \mathbb{R}^n.$$

Hamilton's equations are given by

$$\begin{aligned} \dot{q} &= \frac{\partial H}{\partial p}, \\ \dot{p} &= -\frac{\partial H}{\partial q}. \end{aligned} \tag{16.2.1}$$

It is easy to verify that the map

$$G : (q,p) \mapsto (q,-p),$$

is an involution of $\mathbb{R}^{2n}$ and that (16.2.1) satisfies (16.1.1).

End of Example 16.2.1

Example 16.2.2. The following example is from Roberts and Quispel [1992]. Consider the vector field

$$\dot{x} = x(1-x), \qquad x \in \mathbb{R}.$$

This vector field is reversible with respect to the involution

$$G : x \mapsto 1 - x.$$

Also, this vector field is *not* Hamiltonian, and it is *not* volume preserving. It has a repelling fixed point at $x = 0$ and an attracting fixed point at $x = 1$.

End of Example 16.2.2

16.3 Linearization of Reversible Dynamical Systems

Suppose $x = x_0$ is a fixed point. We now consider the structure of reversible dynamical systems linearized about fixed points.

16.3A Continuous Time

Letting $x = x_0 + \xi$, (16.1.1) becomes

$$\frac{d}{dt}\left(G(x_0+\xi)\right) = -f\left(G(x_0+\xi)\right).$$

Taylor expanding each side in ξ gives

$$\begin{aligned} DG(x_0+\xi)\left(\dot{x}_0+\dot{\xi}\right) &= -f\left(G(x_0)+DG(x_0)\xi+\mathcal{O}(|\xi|^2)\right) \\ &= -f\left(G(x_0)\right) - Df\left(G(x_0)\right)DG(x_0)\xi + \mathcal{O}\left(|\xi|^2\right). \end{aligned}$$

It follows from (1.15.2) that if x_0 is a fixed point, then $G(x_0)$ is a fixed point, and therefore $f\left(G(x_0)\right) = 0$. Then this relation becomes

$$\begin{aligned} DG(x_0)\dot{\xi} = &-Df\left(G(x_0)\right)DG(x_0)\xi \\ &+ \mathcal{O}(|\xi|^2) + \mathcal{O}(|\xi||\dot{\xi}|). \end{aligned}$$

Note that $\dot{\xi} = Df(x_0)\xi + \mathcal{O}(|\xi|^2)$. Substituting this expression into the left-hand-side of the equation, and dropping the $\mathcal{O}(|\xi|^2)$ terms, we obtain

$$DG(x_0)Df(x_0) = -Df\left(G(x_0)\right)DG(x_0). \tag{16.3.1}$$

Suppose $G(x_0) = x_0$. Then x_0 is said to be a *symmetric fixed point*. For symmetric fixed points (16.3.1) has the form

$$DG(x_0)Df(x_0) = -Df(x_0)DG(x_0), \tag{16.3.2}$$

and the matrix $Df(x_0)$ is said to be *infinitesimally reversible*. In general, we have the following definition.

Definition 16.3.1 (Infinitesimally Reversible) *Suppose $G : \mathbb{R}^n \to \mathbb{R}^n$ is a linear involution and $A : \mathbb{R}^n \to \mathbb{R}^n$ is a linear map. Then A is said to be* infinitesimally reversible *if*

$$AG + GA = 0.$$

Note that this linearization condition is defined at a symmetric *fixed point.*

Note that we have not proven that if G is an involution, so is DG. This is true for DG evaluated at a symmetric fixed point, as can be easily verified with a simple calculation using the definition of involution and the chain rule that we leave to the reader.

Sevryuk [1986], [1992] has studied the spectra of infinitesimally reversible linear maps. It can be shown that if $\lambda \in \mathbb{C}$ is an eigenvalue of an infinitesimally reversible linear map then so is $-\lambda$. Moreover, all nonzero eigenvalues occur in real pairs $(x, -x)$, $x \in \mathbb{R}$, purely imaginary pairs, $(iy, -iy)$, $y \in \mathbb{R}$, and quadruplets, $\pm x \pm iy$. This is made precise in the following proposition (courtesy of Jerry Marsden).

Proposition 16.3.2 *Suppose A is an $n \times n$ infinitesimally reversible linear matrix. Then the characteristic polynomial $p(\lambda)$ of A satisfies*

$$p(-\lambda) = (-1)^n p(\lambda), \qquad \lambda \in \mathbb{C}.$$

In particular, if λ is an eigenvalue of A so is $-\lambda$. If A is nonsingular, then n is even. In any case, the spectrum of A is symmetric with respect to the real and imaginary axes.

Proof: By definition 16.3.1 we have $AG + GA = 0$, which implies

$$GAG^{-1} = -A,$$

and $p(\lambda) = \det(A - \lambda \mathbb{1})$, where $\mathbb{1}$ denotes the $n \times n$ identity matrix (note that $G^{-1} = G$ since G is an involution). Using these two equations, we obtain

$$\begin{aligned} p(\lambda) &= \det\,(A - \lambda \mathbb{1}) \\ &= \det\,\left(G\,(A - \lambda \mathbb{1})\,G^{-1}\right) \\ &= \det\,\left(GAG^{-1} - \lambda \mathbb{1}\right) \\ &= \det\,(-A - \lambda \mathbb{1}) \\ &= (-1)^n \det\,(A + \lambda \mathbb{1}) \\ &= (-1)^n\, p(-\lambda). \end{aligned}$$

It follows immediately that the spectrum of A is symmetric with respect to the real and imaginary axes. Moreover, if n is odd, then p is an odd function of λ, and so 0 is an eigenvalue. Then if n is odd, A cannot be invertible. □

Note that the proof of this proposition is identical to the proof of Proposition 14.3.5 which described the eigenvalues of infinitesimally symplectic matrices.

16.3B Discrete Time

We carry out the same procedure for maps as we carried out for vector fields above. Substituting $x = x_0 + \xi$ into (16.1.3)

$$g \circ G(x_0 + \xi_{i+1}) = G(x_0 + \xi_i),$$

and Taylor expanding in ξ gives

$$g \circ G(x_0) + Dg(G(x_0)) \cdot DG(x_0)\xi_{i+1} + \mathcal{O}(|\xi_{i+1}|^2)$$

$$= G(x_0) + DG(x_0)\xi_i + \mathcal{O}(|\xi_i|^2).$$

If we substitute the following expression for ξ_{i+1} into this expression

$$\xi_{i+1} = Dg(x_0)\xi_i,$$

then the terms of order ξ_i give us the following relation:

$$Dg\left(G(x_0)\right) DG(x_0) Dg(x_0) = DG(x_0). \tag{16.3.3}$$

If x_0 is a symmetric fixed point (16.3.3) becomes

$$Dg(x_0) DG(x_0) Dg(x_0) = DG(x_0), \tag{16.3.4}$$

and the matrix $Dg(x_0)$ is said to be *reversible*. In general, we have the following definition.

Definition 16.3.3 (Reversible) *Suppose $G : \mathbb{R}^n \to \mathbb{R}^n$ is a linear involution and $A : \mathbb{R}^n \to \mathbb{R}^n$ is a linear map. Then A is said to be* reversible *if*

$$AGA = G.$$

Note that this linearization condition is defined at a symmetric *fixed point.*

Sevryuk [1986], [1992] has also studied the spectra of reversible linear maps. It can be shown that if $\lambda \in \mathbb{C}$ is an eigenvalue of a reversible linear map then so is $\frac{1}{\lambda}$. Moreover, all eigenvalues different from 1 and -1 occur in real pairs $(x, \frac{1}{x})$, $x \in \mathbb{R}$, unitary pairs, (e^{iy}, e^{-iy}), $y \in \mathbb{R}$, and quadruplets, $x^{\pm 1} e^{\pm iy}$. We prove this in the following proposition.

Proposition 16.3.4 *Suppose $A : \mathbb{R}^n \to \mathbb{R}^n$ is a linear operator that is reversible with respect to the linear involution $G : \mathbb{R}^n \to \mathbb{R}^n$. Then if λ is an eigenvalue of A so is $\frac{1}{\lambda}$, $\bar{\lambda}$, and $\frac{1}{\bar{\lambda}}$. If A does not have 1 and -1 as eigenvalues, then n is even.*

Proof: First, note that it follows from the relation $AGA = G$ that $\det A = \pm 1$. Hence, 0 is not an eigenvalue of A. Moreover, $AGA = G$ is equivalent to $A = GA^{-1}G$, where we have used the fact that G is an involution, i.e., $G = G^{-1}$. Using these results, we have

$$\begin{aligned} p(\lambda) &= \det\left(A - \lambda \mathbb{1}\right), \\ &= \det\left(GA^{-1}G - \lambda \mathbb{1}\right), \\ &= \det\left(G\left(A^{-1} - \lambda \mathbb{1}\right)G\right), \\ &= \det\left(A^{-1} - \lambda \mathbb{1}\right), \\ &= \det\left(A^{-1}\left(\mathbb{1} - \lambda A\right)\right), \\ &= \det A^{-1} \det\left(\mathbb{1} - \lambda A\right), \\ &= \pm 1 \det\left(-\lambda\left(-\frac{1}{\lambda}\mathbb{1} + A\right)\right), \\ &= \pm 1 \left(\lambda\right)^n p\left(\frac{1}{\lambda}\right). \end{aligned}$$

Hence, it immediately follows that if λ is an eigenvalue of A so is $\frac{1}{\lambda}$. Since A is real, it also follows that $\bar{\lambda}$ and $\frac{1}{\bar{\lambda}}$ are also eigenvalues. From this is follows that if 1 and -1 are not eigenvalues, the eigenvalues occur in pairs or quartets. Hence n must be even. □

16.4 Additional Properties of Reversible Dynamical Systems

We end this section with a few general remarks about reversible dynamical systems. Additional properties are developed in the exercises.

1. We saw that near symmetric fixed points the spectra of the associcated linearized dynamical systems is very similar to that of Hamiltonian dynamical systems. There are many more similarities between reversible dynamical systems and Hamiltonian systems. An extensive outline, with references, can be found in Sevryuk [1991]. Most notably, there is a KAM theory for reversible dynamical systems (but, interestingly enough, there is no analog of Nekhoroshev's theorem).

2. Despite the similarities between reversible and Hamiltonian dynamical systems, reversible dynamical systems can simultaneously display non-Hamiltonian behavior (odd-dimensionality notwithstanding). For example, numerical simulations of dynamical systems that display KAM-type behavior, as well as possess attractors and repellers, can be found in Roberts and Quispel [1992] and Politi et al. [1986].

16.5 Exercises

Exercises 1-4 are examples given in the review paper of Roberts and Quispel [1992].

1. The following vector field arises in laser physics (Arecchi [1987]):

$$\begin{aligned}\dot{x} &= zx + y + C_1,\\ \dot{y} &= zy - x,\\ \dot{z} &= C_2 - x^2 - y^2, \qquad (x, y, z) \in \mathbb{R}^3,\end{aligned}$$

   where C_1 and C_2 are parameters. Prove that this is a reversible vector field. Is the vector field volume-preserving?

2. The following vector field arises in the study of non-equilibrium thermodynamics (Hoover et al. [1987]):

$$\begin{aligned}\dot{x} &= y,\\ \dot{y} &= F - \epsilon \sin x - zy,\\ \dot{z} &= \alpha(y^2 - 1), \qquad (x, y, z) \in \mathbb{R}^3,\end{aligned}$$

   where F, α, and ϵ are parameters. Prove that this is a reversible vector field.

3. The following vector field is an idealized model describing the sedimentation of small particles in a fluid (see Golubitsky et al. [1991]):

$$\dot{r}_i = \sum_{k=1}^{n-2} \left[U(r_{i+1} + \cdots + r_{i+k}) - U(r_{i-1} + \cdots + r_{i-k})\right], \ i = 1, \ldots, n,$$

   where

$$U(r) = \frac{e_z}{|r|} + \frac{(e_z \cdot r)r}{|r|^3},$$

   the indices are taken mod n, $r_1, \ldots, r_n \in \mathbb{R}^3$ denote the consecutive edges of an n-sided polygon in $\mathbb{R}^3$, and e_z is a unit vector in the z direction (in which gravity is acting). Prove that this is a volume-preserving, reversible vector field.

4. The following vector field models a series array of Josephson junctions in parallel with a single resistor (Tsang et al. [1991]):

$$\dot{\theta}_k = \Omega + a \cos \theta_k + \frac{1}{N} \sum_{i=1}^{N} \cos \theta_i, \qquad k = 1, \ldots, N,$$

   where θ_k are the phase angles (defined mod 2π), and Ω and a are parameters. Prove that this is a reversible vector field.

5. Suppose $G : \mathbb{R}^n \to \mathbb{R}^n$ is a C^r, $r \geq 1$, involution. Prove that at a symmetric fixed point DG is also an involution.

6. Suppose a map $g : \mathbb{R}^n \to \mathbb{R}^n$ is reversible with respect to the involution $G : \mathbb{R}^n \to \mathbb{R}^n$. Then show that g can be written as the product of two involutions, i.e.,

$$g = H \circ G, \qquad H \circ H = \mathrm{id}.$$

7. Suppose a map $g : \mathbb{R}^n \to \mathbb{R}^n$ is reversible with respect to the involution $G : \mathbb{R}^n \to \mathbb{R}^n$. Then show that g is invertible.

8. Consider the so-called Chirikov-Taylor or Standard map:

$$\begin{aligned} x' &= x + y, \\ y' &= y + \frac{K}{2\pi} \sin 2\pi x', \qquad (x, y) \in \mathbb{R}^2, \end{aligned}$$

where K is a parameter. Show that it can be written as the product of two involutions $H \circ G$.

9. Consider the following area-preserving Hénon map:

$$\begin{aligned} x' &= y, \\ y' &= -x + 2Cy + 2y^2, \qquad (x, y) \in \mathbb{R}^2, \end{aligned}$$

where C is a parameter. Show that it can be written as the product of two involutions $H \circ G$.

10. Suppose a map $g : \mathbb{R}^n \to \mathbb{R}^n$ is reversible with respect to the involution $G : \mathbb{R}^n \to \mathbb{R}^n$. Suppose $\Gamma \subset \mathbb{R}^n$ is an invariant set for g, i.e., $g(\Gamma) = \Gamma$. Then show that $G(\Gamma)$ is also an invariant set for g.

11. Suppose a map $g : \mathbb{R}^n \to \mathbb{R}^n$ is reversible with respect to the involution $G : \mathbb{R}^n \to \mathbb{R}^n$. Let x_0 be a hyperbolic saddle point for g with stable and unstable manifolds denoted $W^s(x_0)$ and $W^u(x_0)$, respectively. Show that $G\left(W^s(x_0)\right) = W^u\left(G(x_0)\right)$ and $G\left(W^u(x_0)\right) = W^s\left(G(x_0)\right)$

12. Suppose a map $g : \mathbb{R}^n \to \mathbb{R}^n$ is reversible with respect to the involution $G : \mathbb{R}^n \to \mathbb{R}^n$. Let x_0 be a hyperbolic saddle point for g with stable and unstable manifolds denoted $W^s(x_0)$ and $W^u(x_0)$, respectively. Let $\mathrm{Fix}(G)$ denote the fixed point set of G and suppose $W^s(x_0)$ intersects $\mathrm{Fix}(G)$. If $G(x_0) = x_0$ show that the intersection point is a homoclinic point and if $G(x_0) \neq x_0$ show that the intersection point is a heteroclinic point.

13. Suppose a map $g : \mathbb{R}^n \to \mathbb{R}^n$ is reversible with respect to the involution $G : \mathbb{R}^n \to \mathbb{R}^n$. Show that reversibility is preserved under conjugacy.

14. Suppose the C^r, $r \geq 1$ vector field $\dot{x} = f(x)$, $x \in \mathbb{R}^n$, is reversible with respect to the involution $G : \mathbb{R}^n \to \mathbb{R}^n$. Let $\phi_t(\cdot)$ denote the flow generated by this vector field. Show that $\phi_t(\cdot)$ is a one-parameter family of reversible diffeomorphisms.

15. Show that a linear map represented by a symplectic matrix is reversible.

16. Show that a linear map represented by an infinitesimally symplectic matrix is infinitesimally reversible.

17

Asymptotically Autonomous Vector Fields

Imagine a system that is subjected to some type of time-dependent disturbance that "dies away" in time. Mathematically, this might be represented by a nonautonomous vector field that becomes autonomous as time increases. Now many dynamical properties are only defined in the limit as $t \to \infty$. Therefore, in order to study the long time behavior of such a system would it be sufficient to study the long time behavior of the autonomous vector field obtained in the limit as $t \to \infty$? This is one of the questions we will address in our discussion in this chapter of *asymptotically autonomous vector fields*, which we now define more precisely.

Consider the following nonautonomous vector field

$$\dot{x} = f(x,t), \qquad x \in \mathbb{R}^n, \tag{17.0.1}$$

which we assume to be C^r, $r \geq 1$ (this can be weakened to continuity in t, and locally Lipschitz in x). Suppose that (17.0.1) is *asymptotically autonomous* in the sense that

$$f(x,t) \to g(x), \qquad t \to \infty,$$

where the convergence is locally uniform in $x \in \mathbb{R}^n$, i.e., convergence occurs for any x in any compact subset of $\mathbb{R}^n$. We denote the *autonomous limit equation* by

$$\dot{x} = g(x), \qquad x \in \mathbb{R}^n. \tag{17.0.2}$$

For both (17.0.1) and (17.0.2) we assume that the trajectory through any point $x \in \mathbb{R}^n$ exists for all positive time.

It is natural to conjecture that the asymptotic behavior of trajectories of (17.0.1) can be inferred from the asymptotic behavior of trajectories of (17.0.2). The first results along these lines were obtained by Markus [1956]. We summarize his results, but first we begin with a definition.

Definition 17.0.1 (ω Limit Set of A Nonautonomous System) *Suppose $x(t,t_0,x_0)$ is the solution of (17.0.1) satisfying $x(t_0,t_0,x_0) = x_0$. A point y is said to be an* ω limit point *of $x(t,t_0,x_0)$, denoted $\omega(x_0,t_0)$, if there exists a sequence of times $\{t_j\}$, $t_j \to \infty$ as $j \to \infty$, such that*

$$\lim_{j\to\infty} x(t_j,t_0,x_0) = y.$$

The set of all ω limit points of a given trajectory is called the omega limit set *of the trajectory. The set of all ω limit sets for all trajectories is called the omega* limit set *of the system.*

We now state Markus's main results on this problem.

Theorem 17.0.2 (Markus) *The ω limit set ω of a trajectory $x(t, t_0, x_0)$ of (17.0.1) is non-empty, compact, and connected. ω attracts $x(t, t_0, x_0)$ in the sense that*

$$dist\,(x(t, t_0, x_0), \omega) \to 0, \qquad t \to \infty,$$

where dist$(\cdot, \cdot)$ is a metric on $\mathbb{R}^n$. Moreover, ω is invariant under (17.0.2).

Proof: See Markus [1956]. □

Note that this result does *not* imply that ω limit sets of (17.0.1) are unions of ω limit sets of (17.0.2). Thieme [1994] gives several examples showing that this is not the case.

Theorem 17.0.3 (Markus) *Suppose $\bar{x}$ is an asymptotically stable equilibrium of (17.0.2) and let ω denote the ω limit set of a trajectory $x(t, t_0, x_0)$ of (17.0.1). If ω contains a point $\tilde{x}$ such that a trajectory of (17.0.2) starting at $\tilde{x}$ converges to $\bar{x}$ as $t \to \infty$ then $\omega = \bar{x}$, i.e., $x(t, t_0, x_0) \to \bar{x}$ as $t \to \infty$.*

Proof: See Markus [1956]. □

If one restricts attention to two-dimensional systems, then an analog of the *Poincaré-Bendixson theorem* is available.

Theorem 17.0.4 (Markus) *Suppose $n = 2$, and let ω denote the ω limit set of a trajectory $x(t, t_0, x_0)$ of (17.0.1). Then ω contains at least one equilibrium of (17.0.2), or ω is the union of periodic orbits of (17.0.2).*

Proof: See Markus [1956]. □

Thieme [1992], [1994] has strengthened this result. Moreover, his paper describes a variety of applications where asymptotically autonomous equations arise.

Theorem 17.0.5 (Thieme) *Let $n = 2$, and let ω denote the ω limit set of a trajectory $x(t, t_0, x_0)$ of (17.0.1). Assume that there exists a neighborhood of ω which contains at most finitely many equilibria of (17.0.2). Then* one *of the following holds.*

1. *ω consists of an equilibrium point of (17.0.2).*
2. *ω is the union of periodic orbits of (17.0.2), and possibly of center type equilibria of (17.0.2) that are surrounded by periodic orbits of (17.0.2) lying in ω.*

3. *ω consists of equilibria of (17.0.2) that are cyclically connected to each other in a* heteroclinic cycle. *In the case of only one equilibrium it would be connected by a homoclinic orbit.*

Proof: See Thieme [1992]. □

Further information on asymptotically autonomous systems can be found in Thieme [1994], as well as the original work of Markus [1956]. Thieme [1994] contains a number of examples that appear to be somewhat counter-intuitive. Holmes and Stuart [1992] study the existence of homoclinic orbits in asymptotically autonomous vector fields. Asymptotically autonomous equations also naturally arise in the study of the approach of trajectories to a low dimensional invariant manifold in autonomous systems, see Robinson [1996].

17.1 Exercises

1. Consider the following asymptotically autonomous vector field in the plane:

$$\begin{aligned} \dot{x} &= y, \\ \dot{y} &= x - x^3 - \delta y + \gamma e^{-t}, \qquad (x, y) \in \mathbb{R}^2, \quad \delta, \gamma > 0. \end{aligned}$$

   Describe the ω limit sets for trajectories.

2. This example is from Thieme [1994]. Consider the following planar vector field

$$\begin{aligned} \dot{x} &= (-x(1-x) + y)(2+x), \\ \dot{y} &= -y. \end{aligned} \tag{17.1.1}$$

   The y component of the vector field is independent of the x component and the solution of this can be solved and substituted into the x component to yield the following asymptotically autonomous system

$$\dot{x} = \left(-x(1-x) + y_0 e^{-t}\right)(2+x), \tag{17.1.2}$$

   and the asymptotically autonomous limit of this equation is

$$\dot{x} = -x(1-x)(2+x). \tag{17.1.3}$$

   (a) Show that $x = 0$ is an attracting equilibrium of (17.1.3), and that the basin of attraction is the open interval between $x = 1$ and $x = -2$.

   (b) For (17.1.2), show that the basin of attraction of $x = 0$ becomes arbitrarily small as y_0 is chosen arbitrarily large.

18

Center Manifolds

When one thinks of simplifying dynamical systems, two approaches come to mind: one, reduce the dimensionality of the system and two, eliminate the nonlinearity. Two rigorous mathematical techniques that allow substantial progress along both lines of approach are center manifold theory and the method of normal forms. These techniques are the most important, generally applicable methods available in the local theory of dynamical systems, and they will form the foundation of our development of bifurcation theory in Chapters 20 and 21.

The center manifold theorem in finite dimensions can be traced to the work of Pliss [1964], Šošitaĭšvili [1975], and Kelley [1967]. Additional valuable references are Guckenheimer and Holmes [1983], Hassard, Kazarinoff, and Wan [1980], Marsden and McCracken [1976], Carr [1981], Henry [1981], and Sijbrand [1985].

The method of normal forms can be traced to the Ph.D thesis of Poincaré [1929]. The books by van der Meer [1985] and Bryuno [1989] give valuable historical background.

Let us begin our discussion of center manifold theory with some motivation. Consider the linear systems

$$\dot{x} = Ax, \tag{18.0.1}$$

$$x \longmapsto Ax, \qquad x \in \mathbb{R}^n, \tag{18.0.2}$$

where A is an $n \times n$ matrix. Recall from Chapter 3 that each system has invariant subspaces E^s, E^u, E^c, corresponding to the span of the generalized eigenvectors, which in turn correspond to eigenvalues having

***Flows*:** negative real part, positive real part, and zero real part, respectively.

***Maps*:** modulus < 1, modulus > 1, and modulus $= 1$, respectively.

The subspaces were so named because orbits starting in E^s decayed to zero as t (resp. n for maps) $\uparrow \infty$, orbits starting in E^u became unbounded as t (resp. n for maps) $\uparrow \infty$, and orbits starting in E^c neither grew nor decayed *exponentially* as t (resp. n for maps) $\uparrow \infty$.

If we suppose that $E^u = \emptyset$, then we find that any orbit will rapidly decay to E^c. Thus, if we are interested in long-time behavior (i.e., stability) we need only to investigate the system restricted to E^c.

It would be nice if a similar type of "reduction principle" applied to the study of the stability of nonhyperbolic fixed points of nonlinear vector fields and maps, namely, that there were an invariant *center manifold* passing through the fixed point to which the system could be restricted in order to study its asymptotic behavior in the neighborhood of the fixed point. That this is the case is the content of the center manifold theory.

18.1 Center Manifolds for Vector Fields

We will begin by considering center manifolds for vector fields. The set-up is as follows. We consider vector fields of the following form

$$\begin{aligned} \dot{x} &= Ax + f(x,y), \\ \dot{y} &= By + g(x,y), \qquad (x,y) \in \mathbb{R}^c \times \mathbb{R}^s, \end{aligned} \tag{18.1.1}$$

where

$$\begin{aligned} f(0,0) &= 0, \quad Df(0,0) = 0, \\ g(0,0) &= 0, \quad Dg(0,0) = 0. \end{aligned} \tag{18.1.2}$$

(See Chapter 3 for a discussion of how a general vector field is transformed to the form of (18.1.1) in the neighborhood of a fixed point.)

In the above, A is a $c \times c$ matrix having eigenvalues with zero real parts, B is an $s \times s$ matrix having eigenvalues with negative real parts, and f and g are $\mathbf{C}^r$ functions ($r \geq 2$).

Definition 18.1.1 (Center Manifold) *An invariant manifold will be called a center manifold for (18.1.1) if it can locally be represented as follows*

$$W^c(0) = \{\, (x,y) \in \mathbb{R}^c \times \mathbb{R}^s \mid y = h(x), |x| < \delta, h(0) = 0, Dh(0) = 0 \,\}$$

for δ sufficiently small.

We remark that the conditions $h(0) = 0$ and $Dh(0) = 0$ imply that $W^c(0)$ is tangent to E^c at $(x,y) = (0,0)$. The following three theorems are taken from the excellent book by Carr [1981].

The first result on center manifolds is an existence theorem.

Theorem 18.1.2 (Existence) *There exists a $\mathbf{C}^r$ center manifold for (18.1.1). The dynamics of (18.1.1) restricted to the center manifold is, for u sufficiently small, given by the following c-dimensional vector field*

$$\dot{u} = Au + f(u, h(u)), \qquad u \in \mathbb{R}^c. \tag{18.1.3}$$

Proof: See Carr [1981]. □

The "u" Notation. Since the center manifold of an equilibrium point is locally represented as a graph, i.e., $y = h(x)$, the reader may be wondering why we substituted u for x in the restriction of the vector field to the center manifold given in (18.1.3). This is to emphasize that the restriction of the vector field to the center manifold is, generally, a vector field on a *nonlinear surface*. If we had used x, since $(x, y) \in \mathbb{R}^c \times \mathbb{R}^s$ are the original coordinates for the vector field, this point might have been be obscured. Once this point of interpretation is understood, there is no harm in using x (or, for that matter, any other symbol), and this is typically done in the literature.

The next result implies that the dynamics of (18.1.3) near $u = 0$ determine the dynamics of (18.1.1) near $(x, y) = (0, 0)$.

Theorem 18.1.3 (Stability) i) *Suppose the zero solution of (18.1.3) is stable (asymptotically stable) (unstable); then the zero solution of (18.1.1) is also stable (asymptotically stable) (unstable).* ii) *Suppose the zero solution of (18.1.3) is stable. Then if* $\big(x(t), y(t)\big)$ *is a solution of (18.1.1) with* $\big(x(0), y(0)\big)$ *sufficiently small, there is a solution* $u(t)$ *of (18.1.3) such that as* $t \to \infty$

$$\begin{aligned} x(t) &= u(t) + \mathcal{O}\big(e^{-\gamma t}\big), \\ y(t) &= h(u(t)) + \mathcal{O}\big(e^{-\gamma t}\big), \end{aligned}$$

where $\gamma > 0$ *is a constant.*

Proof: See Carr [1981]. □

Dynamics Captured by the Center Manifold

Stated in words, this theorem says that for initial conditions of the *full system* sufficiently close to the origin, trajectories through them asymptotically approach a trajectory on the center manifold. In particular, equilibrium points sufficiently close to the origin, sufficiently small amplitude periodic orbits, as well as "small" homoclinic and heteroclinic orbits *are contained in the center manifold.*

The obvious question now is how do we compute the center manifold so that we can reap the benefits of Theorem 18.1.3? To answer this question we will derive an equation that $h(x)$ must satisfy in order for its graph to be a center manifold for (18.1.1).

Suppose we have a center manifold

$$W^c(0) = \{(x, y) \in \mathbb{R}^c \times \mathbb{R}^s \mid y = h(x), |x| < \delta, h(0) = 0,\ Dh(0) = 0\}, \tag{18.1.4}$$

with δ sufficiently small. Using invariance of $W^c(0)$ under the dynamics of (18.1.1), we derive a quasilinear partial differential equation that $h(x)$ must satisfy. This is done as follows:

1. The (x, y) coordinates of any point on $W^c(0)$ must satisfy
$$y = h(x). \tag{18.1.5}$$

2. Differentiating (18.1.5) with respect to time implies that the $(\dot{x}, \dot{y})$ coordinates of any point on $W^c(0)$ must satisfy
$$\dot{y} = Dh(x)\dot{x}. \tag{18.1.6}$$

3. Any point on $W^c(0)$ obeys the dynamics generated by (18.1.1). Therefore, substituting
$$\dot{x} = Ax + f\big(x, h(x)\big), \tag{18.1.7}$$
$$\dot{y} = Bh(x) + g\big(x, h(x)\big) \tag{18.1.8}$$
into (18.1.6) gives
$$Dh(x)\big[Ax + f\big(x, h(x)\big)\big] = Bh(x) + g\big(x, h(x)\big) \tag{18.1.9}$$
or
$$\mathcal{N}\big(h(x)\big) \equiv Dh(x)\big[Ax + f\big(x, h(x)\big)\big] - Bh(x) - g\big(x, h(x)\big) = 0. \tag{18.1.10}$$

Equation (18.1.10) is a quasilinear partial differential equation that $h(x)$ must satisfy in order for its graph to be an invariant center manifold. To find a center manifold, all we need do is solve (18.1.10).

Unfortunately, it is probably more difficult to solve (18.1.10) than our original problem; however, the following theorem gives us a method for computing an approximate solution of (18.1.10) to any desired degree of accuracy.

Theorem 18.1.4 (Approximation) *Let $\phi : \mathbb{R}^c \to \mathbb{R}^s$ be a $\mathbf{C}^1$ mapping with $\phi(0) = D\phi(0) = 0$ such that $\mathcal{N}\big(\phi(x)\big) = \mathcal{O}(|x|^q)$ as $x \to 0$ for some $q > 1$. Then*
$$|h(x) - \phi(x)| = \mathcal{O}(|x|^q) \qquad \text{as } x \to 0.$$

Proof: See Carr [1981]. □

This theorem allows us to compute the center manifold to any desired degree of accuracy by solving (18.1.10) to the same degree of accuracy. For this task, power series expansions will work nicely. Let us consider a concrete example.

Example 18.1.1. Consider the vector field

$$\begin{aligned} \dot{x} &= x^2 y - x^5, \\ \dot{y} &= -y + x^2, \qquad (x, y) \in \mathbb{R}^2. \end{aligned} \tag{18.1.11}$$

The origin is obviously a fixed point for (18.1.11), and the question we ask is whether or not it is stable. The eigenvalues of (18.1.11) linearized about $(x, y) = (0, 0)$ are 0 and -1. Thus, since the fixed point is not hyperbolic, we cannot make any conclusions concerning the stability or instability of $(x, y) = (0, 0)$ based on linearization (note: in the linear approximation the origin is stable but not asymptotically stable). We will answer the question of stability using center manifold theory.

From Theorem 18.1.2, there exists a center manifold for (18.1.11) which can locally be represented as follows

$$W^c(0) = \left\{ (x, y) \in \mathbb{R}^2 \mid y = h(x), |x| < \delta,\ h(0) = Dh(0) = 0 \right\} \tag{18.1.12}$$

for δ sufficiently small. We now want to compute $W^c(0)$. We assume that $h(x)$ has the form

$$h(x) = ax^2 + bx^3 + \mathcal{O}(x^4), \tag{18.1.13}$$

and we substitute (18.1.13) into equation (18.1.10), which $h(x)$ must satisfy to be a center manifold. We then equate equal powers of x, and in that way we can compute $h(x)$ to any desired order of accuracy. In practice, computing only a few terms is usually sufficient to answer questions of stability.

We recall from (18.1.10) that the equation for the center manifold is given by

$$\mathcal{N}(h(x)) = Dh(x)\left[Ax + f(x, h(x))\right] - Bh(x) - g(x, h(x)) = 0, \tag{18.1.14}$$

where, in this example, we have $(x, y) \in \mathbb{R}^2$,

$$\begin{aligned} A &= 0, \\ B &= -1, \\ f(x, y) &= x^2 y - x^5, \\ g(x, y) &= x^2. \end{aligned} \tag{18.1.15}$$

Substituting (18.1.13) into (18.1.14) and using (18.1.15) gives

$$\begin{aligned} \mathcal{N}(h(x)) = (2ax + 3bx^2 + \cdots)(ax^4 + bx^5 - x^5 + \cdots) \\ + ax^2 + bx^3 - x^2 + \cdots = 0. \end{aligned} \tag{18.1.16}$$

In order for (18.1.16) to hold, the coefficients of each power of x must be zero; see Exercise 2. Thus, equating coefficients on each power of x to zero gives

$$\begin{aligned} &x^2 : a - 1 = 0 \Rightarrow a = 1, \\ &x^3 : b = 0, \\ &\ \vdots \quad\ \vdots \end{aligned} \tag{18.1.17}$$

and we therefore have

$$h(x) = x^2 + \mathcal{O}(x^4). \tag{18.1.18}$$

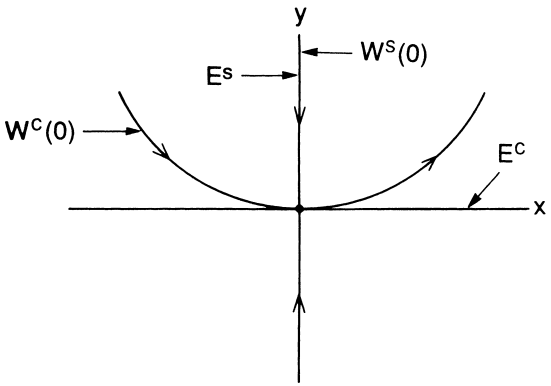

FIGURE 18.1.1.

Using (18.1.18) along with Theorem 18.1.2, the vector field restricted to the center manifold is given by

$$\dot{x} = x^4 + \mathcal{O}(x^5). \tag{18.1.19}$$

For x sufficiently small, $x = 0$ is thus unstable in (2.1.19). Hence, by Theorem 18.1.2, $(x, y) = (0, 0)$ is unstable in (18.1.11); see Figure 18.1.1 for an illustration of the geometry of the flow near $(x, y) = (0, 0)$.

This example illustrates an important phenomenon, which we now describe.

The Failure of the Tangent Space Approximation

The idea is as follows. Consider (18.1.11). One might expect that the y components of orbits starting near $(x, y) = (0, 0)$ should decay to zero exponentially fast. Therefore, the question of stability of the origin should reduce to a study of the x component of orbits starting near the origin. One might thus be very tempted to set $y = 0$ in (18.1.11) and study the reduced equation

$$\dot{x} = -x^5. \tag{18.1.20}$$

This corresponds to approximating $W^c(0)$ by E^c. However, $x = 0$ is stable for (18.1.20) and, therefore, we would arrive at the *wrong* conclusion that $(x, y) = (0, 0)$ is stable for (18.1.20). The tangent space approximation might sometimes work, but, as this example shows, it does not always do so.

End of Example 18.1.1

Example 18.1.2. The previous example showed a situation where an equilibrium point was unstable, but the tangent space approximation to its center manifold indicated that it was stable. One could ask the following question. "Suppose the equilibrium point is stable, will the tangent space approximation to the center manifold also show stability"? Here we give an example showing that the answer is "no".

Consider the vector field

$$\begin{aligned}\dot{x} &= -xy - x^6,\\ \dot{y} &= -y + x^2, \qquad (x,y) \in \mathbb{R}^2.\end{aligned}$$

The origin is an equilibrium point, and the eigenvalues of the matrix associated with the linearization are 0 and -1. The tangent space to the center manifold is the x axis. Hence, the restriction of the vector field to the center manifold *in the tangent space approximation* is given by

$$\dot{x} = -x^6,$$

for which the origin is unstable.

The center manifold can be calculated, and it is given by the graph of the following function

$$h(x) = x^2 + \mathcal{O}(4).$$

The vector field restricted to the center manifold is given by

$$\dot{x} = -x^3 + \mathcal{O}(5),$$

which indicates that the origin is stable.

End of Example 18.1.2

18.2 Center Manifolds Depending on Parameters

Suppose (18.1.1) depends on a vector of parameters, say $\varepsilon \in \mathbb{R}^p$. In this case we write (2.1.2) in the form

$$\begin{aligned}\dot{x} &= Ax + f(x,y,\varepsilon),\\ \dot{y} &= By + g(x,y,\varepsilon), \qquad (x,y,\varepsilon) \in \mathbb{R}^c \times \mathbb{R}^s \times \mathbb{R}^p, \quad (18.2.1)\end{aligned}$$

where

$$\begin{aligned} f(0,0,0) &= 0, \qquad Df(0,0,0) = 0,\\ g(0,0,0) &= 0, \qquad Dg(0,0,0) = 0,\end{aligned}$$

and we have the same assumptions on A and B as in (18.1.1), with f and g also being $\mathbf{C}^r$ $(r \geq 2)$ functions in some neighborhood of $(x,y,\varepsilon) = (0,0,0)$. An obvious question is why do we not allow the matrices A and B to depend on ε? This will be answered shortly.

The way in which we will handle parametrized systems is to include the parameter ε as a new *dependent variable* as follows

$$\begin{aligned}\dot{x} &= Ax + f(x,y,\varepsilon),\\ \dot{\varepsilon} &= 0,\\ \dot{y} &= By + g(x,y,\varepsilon), \qquad (x,\varepsilon,y) \in \mathbb{R}^c \times \mathbb{R}^p \times \mathbb{R}^s. \quad (18.2.2)\end{aligned}$$

At first glance it might appear that nothing is really gained from this action, but we will argue otherwise.

Let us suppose we are considering (18.2.2) afresh. It obviously has a fixed point at $(x, \varepsilon, y) = (0, 0, 0)$. The matrix associated with the linearization of (18.2.2) about this fixed point has $c + p$ eigenvalues with zero real part and s eigenvalues with negative real part. Now let us apply center manifold theory. Modifying Definition 18.1.1, a center manifold will be represented as a graph over the *x and ε variables*, i.e., the graph of $h(x, \varepsilon)$ for x and ε sufficiently small. Theorem 18.1.2 still applies, with the vector field reduced to the center manifold given by

$$\begin{aligned} \dot{u} &= Au + f(u, h(u, \varepsilon), \varepsilon), \\ \dot{\varepsilon} &= 0, \qquad\qquad (u, \varepsilon) \in \mathbb{R}^c \times \mathbb{R}^p. \end{aligned} \tag{18.2.3}$$

Theorems 18.1.3 and 18.1.4 also follow (we will worry about any modifications to computing the center manifold shortly). Thus, adding the parameter as a new dependent variable merely acts to augment the matrix A in (18.1.1) by adding p new center directions that have no dynamics, and the theory goes through just the same. However, there is a new concept which will be important when we study *bifurcation theory*; namely, the center manifold exists for all ε in a sufficiently small neighborhood of $\varepsilon = 0$. We will learn in Chapters 20 and 21 that it is possible for solutions to be created or destroyed by perturbing nonhyperbolic fixed points. Thus, since the invariant center manifold exists in a sufficiently small neighborhood in both x and ε of $(x, \varepsilon) = (0, 0)$, all bifurcating solutions will be contained in the lower dimensional center manifold.

Let us now worry about computing the center manifold. From the existence theorem for center manifolds, locally we have

$$\begin{aligned} W^c_{\text{loc}}(0) = \big\{ (x, \varepsilon, y) \in \mathbb{R}^c \times \mathbb{R}^p \times \mathbb{R}^s \mid y = h(x, \varepsilon), |x| < \delta, \\ |\varepsilon| < \bar{\delta},\ h(0, 0) = 0,\ Dh(0, 0) = 0 \big\} \end{aligned} \tag{18.2.4}$$

for δ and $\bar{\delta}$ sufficiently small. Using invariance of the graph of $h(x, \varepsilon)$ under the dynamics generated by (18.2.2) we have

$$\dot{y} = D_x h(x, \varepsilon)\dot{x} + D_\varepsilon h(x, \varepsilon)\dot{\varepsilon} = Bh(x, \varepsilon) + g\left(x, h(x, \varepsilon), \varepsilon\right). \tag{18.2.5}$$

However,

$$\begin{aligned} \dot{x} &= Ax + f\left(x, h(x, \varepsilon), \varepsilon\right), \\ \dot{\varepsilon} &= 0; \end{aligned} \tag{18.2.6}$$

hence substituting (18.2.6) into (18.2.5) results in the following quasilinear partial differential equation that $h(x, \varepsilon)$ must satisfy in order for its graph to be a center manifold.

$$\begin{aligned} \mathcal{N}\left(h(x, \varepsilon)\right) = D_x h(x, \varepsilon)\left[Ax + f\left(x, h(x, \varepsilon), \varepsilon\right)\right] \\ - Bh(x, \varepsilon) - g\left(x, h(x, \varepsilon), \varepsilon\right) = 0. \end{aligned} \tag{18.2.7}$$

Thus, we see that (18.2.7) is very similar to (18.1.10).

Before considering a specific example we want to point out an important fact. By considering ε as a new dependent variable, terms such as

$$x_i\varepsilon_j, \qquad 1 \le i \le c, \quad 1 \le j \le p,$$

or

$$y_i\varepsilon_j, \qquad 1 \le i \le s, \quad 1 \le j \le p,$$

become *nonlinear terms*. In this case, returning to a question asked at the beginning of this section, the parts of the matrices A and B depending on ε are now viewed as nonlinear terms and are included in the f and g terms of (18.2.2), respectively. We remark that in applying center manifold theory to a given system, it must first be transformed into the standard form (either (18.1.1) or (18.2.2)).

Example 18.2.1 (The Lorenz Equations). Consider the Lorenz equations

$$\begin{aligned} \dot{x} &= \sigma(y - x), \\ \dot{y} &= \bar{\rho}x + x - y - xz, \qquad (x, y, z) \in \mathbb{R}^3, \\ \dot{z} &= -\beta z + xy, \end{aligned} \tag{18.2.8}$$

where σ and β are viewed as fixed positive constants and $\bar{\rho}$ is a parameter (note: in the standard version of the Lorenz equations it is traditional to put $\bar{\rho} = \rho - 1$). It should be clear that $(x, y, z) = (0, 0, 0)$ is a fixed point of (18.2.9). Linearizing (18.2.9) about this fixed point, we obtain the associated matrix

$$\begin{pmatrix} -\sigma & \sigma & 0 \\ 1 & -1 & 0 \\ 0 & 0 & -\beta \end{pmatrix}. \tag{18.2.9}$$

(Note: recall, $\bar{\rho}x$ is a nonlinear term.)

Since (18.2.9) is in block form, the eigenvalues are particularly easy to compute and are given by

$$0, -\sigma - 1, -\beta, \tag{18.2.10}$$

with eigenvectors

$$\begin{pmatrix} 1 \\ 1 \\ 0 \end{pmatrix}, \begin{pmatrix} \sigma \\ -1 \\ 0 \end{pmatrix}, \begin{pmatrix} 0 \\ 0 \\ 1 \end{pmatrix}. \tag{18.2.11}$$

Our goal is to determine the nature of the stability of $(x, y, z) = (0, 0, 0)$ for $\bar{\rho}$ near zero. First, we must put (18.2.9) into the standard form (18.2.2). Using the eigenbasis (18.2.11), we obtain the transformation

$$\begin{pmatrix} x \\ y \\ z \end{pmatrix} = \begin{pmatrix} 1 & \sigma & 0 \\ 1 & -1 & 0 \\ 0 & 0 & 1 \end{pmatrix} \begin{pmatrix} u \\ v \\ w \end{pmatrix} \tag{18.2.12}$$

with inverse

$$\begin{pmatrix} u \\ v \\ w \end{pmatrix} = \frac{1}{1+\sigma} \begin{pmatrix} 1 & \sigma & 0 \\ 1 & -1 & 0 \\ 0 & 0 & 1+\sigma \end{pmatrix} \begin{pmatrix} x \\ y \\ z \end{pmatrix}, \tag{18.2.13}$$

which transforms (18.2.9) into

$$\begin{pmatrix} \dot{u} \\ \dot{v} \\ \dot{w} \end{pmatrix} = \begin{pmatrix} 0 & 0 & 0 \\ 0 & -(1+\sigma) & 0 \\ 0 & 0 & -\beta \end{pmatrix} \begin{pmatrix} u \\ v \\ w \end{pmatrix} + \frac{1}{1+\sigma} \begin{pmatrix} \sigma\bar{\rho}(u+\sigma v) - \sigma w(u+\sigma v) \\ -\bar{\rho}(u+\sigma v) + w(u+\sigma v) \\ (1+\sigma)(u+\sigma v)(u-v) \end{pmatrix},$$
$$\dot{\bar{\rho}} = 0. \tag{18.2.14}$$

Thus, from center manifold theory, the stability of $(x, y, z) = (0, 0, 0)$ near $\bar{\rho} = 0$ can be determined by studying a one-parameter family of first-order ordinary differential equations on a center manifold, which can be represented as a graph over the u and $\bar{\rho}$ variables, i.e.,

$$W^c(0) = \Big\{ (u, v, w, \bar{\rho}) \in \mathbb{R}^4 \mid v = h_1(u, \bar{\rho}), w = h_2(u, \bar{\rho}), \\ h_i(0, 0) = 0, Dh_i(0, 0) = 0, i = 1, 2 \Big\} \tag{18.2.15}$$

for u and $\bar{\rho}$ sufficiently small.

We now want to compute the center manifold and derive the vector field on the center manifold. Using Theorem 18.1.4, we assume

$$\begin{aligned} h_1(u, \bar{\rho}) &= a_1 u^2 + a_2 u\bar{\rho} + a_3\bar{\rho}^2 + \cdots, \\ h_2(u, \bar{\rho}) &= b_1 u^2 + b_2 u\bar{\rho} + b_3\bar{\rho}^2 + \cdots. \end{aligned} \tag{18.2.16}$$

Recall from (2.1.27) that the center manifold must satisfy

$$\mathcal{N}\Big(h(x,\varepsilon)\Big) = D_x h(x,\varepsilon)\,[Ax + f(x, h(x,\varepsilon), \varepsilon)] \\ - Bh(x,\varepsilon) - g(x, h(x,\varepsilon), \varepsilon) = 0, \tag{18.2.17}$$

where, in this example,

$$\begin{aligned} &x \equiv u, \qquad y \equiv (v, w), \qquad \varepsilon \equiv \bar{\rho}, \qquad h = (h_1, h_2), \\ &A = 0, \\ &B = \begin{pmatrix} -(1+\sigma) & 0 \\ 0 & -\beta \end{pmatrix}, \\ &f(x, y, \varepsilon) = \frac{1}{1+\sigma}[\sigma\bar{\rho}(u+\sigma v) - \sigma w(u+\sigma v)], \\ &g(x, y, \varepsilon) = \frac{1}{1+\sigma} \begin{pmatrix} -\bar{\rho}(u+\sigma v) + w(u+\sigma v) \\ (1+\sigma)(u+\sigma v)(u-v) \end{pmatrix}. \end{aligned} \tag{18.2.18}$$

Substituting (18.2.16) into (18.2.17) and using (18.2.19) gives the two components of the equation for the center manifold.

$$(2a_1 u + a_2\bar{\rho} + \cdots) \left[\frac{\sigma}{1+\sigma} \Big(\bar{\rho}(u + \sigma h_1) - h_2(u + \sigma h_1) \Big) \right] \\ + (1+\sigma)h_1 + \frac{\bar{\rho}}{1+\sigma}(u + \sigma h_1) - \frac{h_2}{1+\sigma}(u + \sigma h_1) = 0,$$

$$(2b_1u + b_2\bar{\rho} + \cdots)\left[\frac{\sigma}{1+\sigma}\Big(\bar{\rho}(u+\sigma h_1) - h_2(u+\sigma h_1)\Big)\right]$$
$$+ \beta h_2 - (u+\sigma h_1)(u-h_1) = 0. \tag{18.2.19}$$

Equating terms of like powers to zero gives

$$\begin{aligned} u^2 &: a_1(1+\sigma) = 0 \Rightarrow a_1 = 0, \\ &\beta b_1 - 1 = 0 \Rightarrow b_1 = \frac{1}{\beta}, \\ u\bar{\rho} &: (1+\sigma)a_2 + \frac{1}{1+\sigma} = 0 \Rightarrow a_2 = \frac{-1}{(1+\sigma)^2}, \\ &\beta b_2 = 0 \Rightarrow b_2 = 0. \end{aligned} \tag{18.2.20}$$

Then, using (18.2.21) and (18.2.16), we obtain

$$\begin{aligned} h_1(u,\bar{\rho}) &= -\frac{1}{(1+\sigma)^2}u\bar{\rho} + \cdots, \\ h_2(u,\bar{\rho}) &= \frac{1}{\beta}u^2 + \cdots. \end{aligned} \tag{18.2.21}$$

Finally, substituting (18.2.21) into (18.2.14) we obtain the vector field reduced to the center manifold

$$\begin{aligned} \dot{u} &= \frac{\sigma}{1+\sigma}u\left(\bar{\rho} - \frac{1}{\beta}u^2 + \cdots\right), \\ \dot{\bar{\rho}} &= 0. \end{aligned} \tag{18.2.22}$$

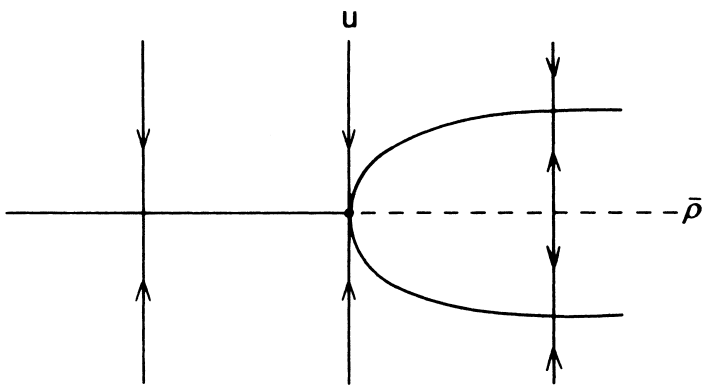

FIGURE 18.2.1.

In Figure 18.2.1 we plot the fixed points of (18.2.22) *neglecting* higher order terms such as $\mathcal{O}(\bar{\rho}^2)$, $\mathcal{O}(u\bar{\rho}^2)$, $\mathcal{O}(u^3)$, etc. It should be clear that $u = 0$ is always a fixed point and is stable for $\bar{\rho} < 0$ and unstable for $\bar{\rho} > 0$. At the point of exchange of stability (i.e., $\bar{\rho} = 0$) two new stable fixed points are created and are given by

$$\bar{\rho} = \frac{1}{\beta}u^2. \tag{18.2.23}$$

A simple calculation shows that these fixed points are stable. In Chapter 20 we will see that this is an example of a *pitchfork bifurcation*.

Before leaving this example two comments are in order.

1. Figure 18.2.1 shows the advantage of introducing the parameter as a new dependent variable. In a full neighborhood in parameter space new solutions are "captured" on the center manifold. In Figure 18.2.1, for each fixed $\bar{\rho}$ we have a flow in the u direction; this is represented by the vertical lines with arrows.
2. We have not considered the effects of the higher order terms in (18.2.22) on Figure 18.2.1. In Chapter 20 we will show that they do not qualitatively change the figure (i.e., they do not create, destroy, or change the stability of any of the fixed points) near the origin.

End of Example 18.2.1

18.3 The Inclusion of Linearly Unstable Directions

Suppose we consider the system

$$\begin{aligned} \dot{x} &= Ax + f(x,y,z), \\ \dot{y} &= By + g(x,y,z), \\ \dot{z} &= Cz + h(x,y,z), \qquad (x,y,z) \in \mathbb{R}^c \times \mathbb{R}^s \times \mathbb{R}^u, \end{aligned} \tag{18.3.1}$$

where

$$\begin{aligned} f(0,0,0) &= 0, \qquad Df(0,0,0) = 0, \\ g(0,0,0) &= 0, \qquad Dg(0,0,0) = 0, \\ h(0,0,0) &= 0, \qquad Dh(0,0,0) = 0, \end{aligned}$$

and f, g, and h are $\mathbf{C}^r (r \geq 2)$ in some neighborhood of the origin, A is a $c \times c$ matrix having eigenvalues with zero real parts, B is an $s \times s$ matrix having eigenvalues with negative real parts, and C is a $u \times u$ matrix having eigenvalues with positive real parts.

In this case $(x,y,z) = (0,0,0)$ is unstable due to the existence of a u-dimensional unstable manifold. However, much of the center manifold theory still applies, in particular Theorem 18.1.2 concerning existence, with the center manifold being locally represented by

$$\begin{aligned} W^c(0) = \big\{ (x,y,z) \in \mathbb{R}^c \times \mathbb{R}^s \times \mathbb{R}^u \mid y = h_1(x), z = h_2(x), \\ h_i(0) = 0, Dh_i(0) = 0, i = 1,2 \big\} \end{aligned} \tag{18.3.2}$$

for x sufficiently small. The vector field restricted to the center manifold is given by

$$\dot{u} = Au + f\big(u, h_1(u), h_2(u)\big), \qquad u \in \mathbb{R}^c. \tag{18.3.3}$$

Using the fact that the center manifold is invariant under the dynamics generated by (18.3.1), we obtain

$$\begin{aligned}
\dot{x} &= Ax + f\big(x, h_1(x), h_2(x)\big),\\
\dot{y} &= Dh_1(x)\dot{x} = Bh_1(x) + g\big(x, h_1(x), h_2(x)\big),\\
\dot{z} &= Dh_2(x)\dot{x} = Ch_2(x) + h\big(x, h_1(x), h_2(x)\big),
\end{aligned} \tag{18.3.4}$$

which yields the following quasilinear partial differential equation for $h_1(x)$ and $h_2(x)$

$$\begin{aligned}
&Dh_1(x)\big[Ax + f\big(x, h_1(x), h_2(x)\big)\big]\\
&\qquad - Bh_1(x) - g\big(x, h_1(x), h_2(x)\big) = 0,\\
&Dh_2(x)\big[Ax + f\big(x, h_1(x), h_2(x)\big)\big]\\
&\qquad - Ch_2(x) - h\big(x, h_1(x), h_2(x)\big) = 0.
\end{aligned} \tag{18.3.5}$$

Theorem 18.1.4 also holds in order that we may justify solving (18.3.5) approximately via power series expansions. We can also include parameters in exactly the same way as in Section 18.2.

Of course, Theorem 18.1.3 does not hold as a result of the presence of the exponentially linearly unstable directions. Nevertheless, the formulation of the theory with the inclusion of the linearly unstable directions is still useful. It is often important to know the nature of solutions having saddle-type stability since their stable manifolds may play a role in forming the boundaries of the basins of attraction of attracting sets. In the context of bifurcation theory, the creation of unstable solutions may be important since it may be possible for them to undergo secondary bifurcations and, consequently, become stable.

18.4 Center Manifolds for Maps

The center manifold theory can be modified so that it applies to maps with only a slight difference in the method by which the center manifold is calculated. We outline the theory below.

Suppose we have the map

$$\begin{aligned}
&x \longmapsto Ax + f(x, y),\\
&y \longmapsto By + g(x, y), \qquad (x, y) \in \mathbb{R}^c \times \mathbb{R}^s,
\end{aligned} \tag{18.4.1}$$

or

$$\begin{aligned}
x_{n+1} &= Ax_n + f(x_n, y_n),\\
y_{n+1} &= By_n + g(x_n, y_n),
\end{aligned}$$

where

$$f(0,0) = 0, \qquad Df(0,0) = 0,$$
$$g(0,0) = 0, \qquad Dg(0,0) = 0,$$

and f and g are $\mathbf{C}^r (r \geq 2)$ in some neighborhood of the orgin, A is a $c \times c$ matrix with eigenvalues of modulus one, and B is an $s \times s$ matrix with eigenvalues of modulus less than one.

Evidently $(x, y) = (0, 0)$ is a fixed point of (18.4.1), and the linear approximation is not sufficient for determining its stability. We have the following theorems, which are completely analogous to Theorems 18.1.2, 18.1.3, and 18.1.4.

Theorem 18.4.1 (Existence) *There exists a* $\mathbf{C}^r$ *center manifold for (18.4.1) which can be locally represented as a graph as follows*

$$W^c(0) = \{(x, y) \in \mathbb{R}^c \times \mathbb{R}^s \mid y = h(x), |x| < \delta, h(0) = 0, Dh(0) = 0\} \tag{18.4.2}$$

for δ *sufficiently small. Moreover, the dynamics of (18.4.1) restricted to the center manifold is, for* u *sufficiently small, given by the c-dimensional map*

$$u \longmapsto Au + f\big(u, h(u)\big), \qquad u \in \mathbb{R}^c. \tag{18.4.3}$$

Proof: See Carr [1981]. □

The next theorem allows us to conclude that $(x, y) = (0, 0)$ is stable or unstable based on whether or not $u = 0$ is stable or unstable in (18.4.3).

Theorem 18.4.2 (Stability) i) *Suppose the zero solution of (18.4.3) is stable (asymptotically stable) (unstable). Then the zero solution of (18.4.1) is stable (asymptotically stable) (unstable).* ii) *Suppose that the zero solution of (18.4.3) is stable. Let* (x_n, y_n) *be a solution of (18.4.1) with* (x_0, y_0) *sufficiently small. Then there is a solution* u_n *of (18.4.3) such that* $|x_n - u_n| \leq k\beta^n$ *and* $|y_n - h(u_n)| \leq k\beta^n$ *for all* n *where* k *and* β *are positive constants with* $\beta < 1$.

Proof: See Carr [1981]. □

Next we want to compute the center manifold so that we can derive (18.4.3). This is done in exactly the same way as for vector fields, i.e., by deriving a nonlinear functional equation that the graph of $h(x)$ must satisfy in order for it to be invariant under the dynamics generated by (18.4.1). In this case we have

$$\begin{aligned} x_{n+1} &= Ax_n + f\big(x_n, h(x_n)\big), \\ y_{n+1} &= h(x_{n+1}) = Bh(x_n) + g\big(x_n, h(x_n)\big), \end{aligned} \tag{18.4.4}$$

or

$$\mathcal{N}\big(h(x)\big) = h\big(Ax + f\big(x, h(x)\big)\big) - Bh(x) - g\big(x, h(x)\big) = 0. \qquad (18.4.5)$$

(Note: the reader should compare (18.4.5) with (18.1.10).) The next theorem justifies the approximate solution of (18.4.5) via power series expansions.

Theorem 18.4.3 (Approximation) *Let $\phi : \mathbb{R}^c \to \mathbb{R}^s$ be a $\mathbf{C}^1$ map with $\phi(0) = 0, \phi'(0) = 0$, and $\mathcal{N}\big(\phi(x)\big) = \mathcal{O}(|x|^q)$ as $x \to 0$ for some $q > 1$. Then*

$$h(x) = \phi(x) + \mathcal{O}(|x|^q) \qquad \text{as } x \to 0.$$

Proof: See Carr [1981]. □

We now give an example.

Example 18.4.1. Consider the map

$$\begin{pmatrix} u \\ v \\ w \end{pmatrix} \mapsto \begin{pmatrix} -1 & 0 & 0 \\ 0 & -\frac{1}{2} & 0 \\ 0 & 0 & \frac{1}{2} \end{pmatrix} \begin{pmatrix} u \\ v \\ w \end{pmatrix} + \begin{pmatrix} vw \\ u^2 \\ -uv \end{pmatrix}, \quad (u, v, w) \in \mathbb{R}^3. \qquad (18.4.6)$$

It should be clear that $(u, v, w) = (0, 0, 0)$ is a fixed point of (18.4.6), and the eigenvalues associated with the map linearized about this fixed point are $-1, -\frac{1}{2}, \frac{1}{2}$. Thus, the linear approximation does not suffice to determine the stability or instability. We will apply center manifold theory to this problem.

The center manifold can locally be represented as follows

$$W^c(0) = \Big\{(u, v, w) \in \mathbb{R}^3 \mid v = h_1(u), w = h_2(u), h_i(0) = 0, \\ Dh_i(0) = 0, i = 1, 2\Big\} \qquad (18.4.7)$$

for u sufficiently small. Recall that the center manifold must satisfy the following equation

$$\mathcal{N}\Big(h(x)\Big) = h\Big(Ax + f\Big(x, h(x)\Big)\Big) - Bh(x) - g\Big(x, h(x)\Big) = 0, \qquad (18.4.8)$$

where, in this example,

$$\begin{aligned} x &= u, \quad y \equiv (v, w), \quad h = (h_1, h_2), \\ A &= -1, \\ B &= \begin{pmatrix} -\frac{1}{2} & 0 \\ 0 & \frac{1}{2} \end{pmatrix}, \\ f(u, v, w) &= vw, \\ g(u, v, w) &= \begin{pmatrix} u^2 \\ -uv \end{pmatrix}. \end{aligned} \qquad (18.4.9)$$

We assume a center manifold of the form

$$h(u) = \begin{pmatrix} h_1(u) \\ h_2(u) \end{pmatrix} = \begin{pmatrix} a_1u^2 + b_1u^3 + \mathcal{O}(u^4) \\ a_2u^2 + b_2u^3 + \mathcal{O}(u^4) \end{pmatrix}. \qquad (18.4.10)$$

Substituting (18.4.10) into (18.4.8) and using (18.4.9) yields

$$\begin{aligned}\mathcal{N}\Big(h(u)\Big) &= \begin{pmatrix} a_1u^2 - b_1u^3 + \mathcal{O}(u^5) \\ a_2u^2 - b_2u^3 + \mathcal{O}(u^5) \end{pmatrix} \\ &\quad - \begin{pmatrix} -1/2 & 0 \\ 0 & 1/2 \end{pmatrix} \begin{pmatrix} a_1u^2 + b_1u^3 + \cdots \\ a_2u^2 + b_2u^3 + \cdots \end{pmatrix} - \begin{pmatrix} u^2 \\ -uh_1(u) \end{pmatrix} \\ &= \begin{pmatrix} 0 \\ 0 \end{pmatrix}. \end{aligned} \tag{18.4.11}$$

Balancing powers of coefficients for each component gives

$$\begin{aligned} u^2 : \begin{pmatrix} a_1 + \frac{1}{2}a_1 - 1 \\ a_2 - \frac{1}{2}a_2 \end{pmatrix} = \begin{pmatrix} 0 \\ 0 \end{pmatrix} &\Rightarrow \begin{array}{rcl} a_1 &=& \frac{2}{3} \\ a_2 &=& 0 \end{array}, \\ u^3 : \begin{pmatrix} -b_1 + \frac{1}{2}b_1 \\ -b_2 - \frac{1}{2}b_2 + a_1 \end{pmatrix} = \begin{pmatrix} 0 \\ 0 \end{pmatrix} &\Rightarrow \begin{array}{rcccl} b_1 &=& 0 & & \\ b_2 &=& a_1\frac{2}{3} &=& \frac{4}{9} \end{array}; \end{aligned} \tag{18.4.12}$$

hence, the center manifold is given by the graph of $\Big(h_1(u), h_2(u)\Big)$, where

$$\begin{aligned} h_1(u) &= \frac{2}{3}u^2 + \mathcal{O}(u^4), \\ h_2(u) &= \frac{4}{9}u^3 + \mathcal{O}(u^4). \end{aligned} \tag{18.4.13}$$

The map on the center manifold is given by

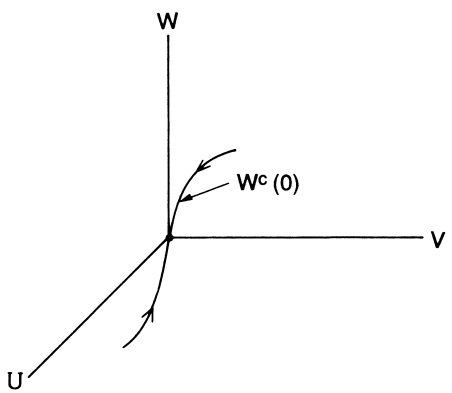

FIGURE 18.4.1.

$$u \longmapsto -u + \frac{8}{27}u^5 + \mathcal{O}(u^6); \tag{18.4.14}$$

thus, the origin is attracting; see Figure 18.4.1.

End of Example 18.4.1

Example 18.4.2. Consider the map

$$\begin{pmatrix} x \\ y \end{pmatrix} \mapsto \begin{pmatrix} 0 & 1 \\ -\frac{1}{2} & \frac{3}{2} \end{pmatrix} \begin{pmatrix} x \\ y \end{pmatrix} + \begin{pmatrix} 0 \\ -y^3 \end{pmatrix}, \qquad (x, y) \in \mathbb{R}^2. \tag{18.4.15}$$

The origin is a fixed point of the map. Computing the eigenvalues of the map linearized about the origin gives

$$\lambda_{1,2} = 1, \frac{1}{2}.$$

Therefore, there is a one-dimensional center manifold and a one-dimensional stable manifold with the orbit structure in a neighborhood of $(0, 0)$ determined by the orbit structure on the center manifold.

We wish to compute the center manifold, but first we must put the linear part in block diagonal form as given in (18.4.1). The matrix associated with the linear transformation has columns consisting of the eigenvectors of the linearized map and is easily calculated. It is given by

$$T = \begin{pmatrix} 1 & 2 \\ 1 & 1 \end{pmatrix} \quad \text{with } T^{-1} = \begin{pmatrix} -1 & 2 \\ 1 & -1 \end{pmatrix}. \tag{18.4.16}$$

Thus, letting

$$\begin{pmatrix} x \\ y \end{pmatrix} = T \begin{pmatrix} u \\ v \end{pmatrix},$$

our map becomes

$$\begin{pmatrix} u \\ v \end{pmatrix} \mapsto \begin{pmatrix} 1 & 0 \\ 0 & \frac{1}{2} \end{pmatrix} \begin{pmatrix} u \\ v \end{pmatrix} + \begin{pmatrix} -2(u+v)^3 \\ (u+v)^3 \end{pmatrix}. \tag{18.4.17}$$

We seek a center manifold

$$W^c(0) = \{\, (u, v) \mid v = h(u); h(0) = Dh(0) = 0 \,\} \tag{18.4.18}$$

for u sufficiently small. The next step is to assume $h(u)$ of the form

$$h(u) = au^2 + bu^3 + \mathcal{O}(u^4) \tag{18.4.19}$$

and substitute (18.4.19) into the center manifold equation

$$\mathcal{N}\Big(h(u)\Big) = h\Big(Au + f\Big(u, h(u)\Big)\Big) - Bh(u) - g\Big(u, h(u)\Big) = 0, \tag{18.4.20}$$

where, in this example, we have

$$\begin{aligned} A &= 1, \\ B &= \frac{1}{2}, \\ f(u, v) &= -2(u+v)^3, \\ g(u, v) &= (u+v)^3, \end{aligned} \tag{18.4.21}$$

and (18.4.20) becomes

$$\begin{aligned} & a\Big(u-2\Big(u+au^2+bu^3+\mathcal{O}(u^4)\Big)^3\Big)^2 \\ & + \ b\Big(u-2\Big(u+au^2+bu^3+\mathcal{O}(u^4)\Big)^3\Big)^3 \\ & + \ \cdots-\frac{1}{2}\Big(au^2+bu^3+\mathcal{O}(u^4)\Big)-\Big(u+au^2+bu^3+\mathcal{O}(u^4)\Big)^3=0. \end{aligned} \tag{18.4.22}$$

or

$$au^2+bu^3-\frac{1}{2}au^2-\frac{1}{2}bu^3-u^3+\mathcal{O}(u^4)=0. \tag{18.4.23}$$

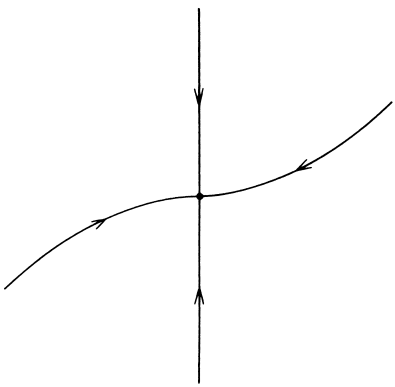

FIGURE 18.4.2.

Equating coefficients of like powers to zero gives

$$\begin{aligned} u^2 &: a-\frac{1}{2}a=0 \Rightarrow a=0, \\ u^3 &: b-\frac{1}{2}b-1=0 \Rightarrow b=2. \end{aligned} \tag{18.4.24}$$

Thus, the center manifold is given by the graph of

$$h(u)=2u^3+\mathcal{O}(u^4), \tag{18.4.25}$$

and the map restricted to the center manifold is given by

$$u \mapsto u-2\Big(u+2u^3+\mathcal{O}(u^4)\Big)^3 \tag{18.4.26}$$

or

$$u \mapsto u-2u^3+\mathcal{O}(u^4). \tag{18.4.27}$$

Therefore, the orbit structure in the neighborhood of $(0,0)$ appears as in Figure 18.4.2 and $(0,0)$ is stable.

End of Example 18.4.2

Some remarks are now in order.

Remark 1. Parametrized Families of Maps. Parameters can be included as new dependent variables for maps in exactly the same way as for vector fields in Section 18.2.

Remark 2. Inclusion of Linearly Unstable Directions. The case where the origin has an unstable manifold can be treated in exactly the same way as for vector fields in Section 18.3.

18.5 Properties of Center Manifolds

In this brief section we would like to discuss a few properties of center manifolds. More information can be obtained from Carr [1981] or Sijbrand [1985].

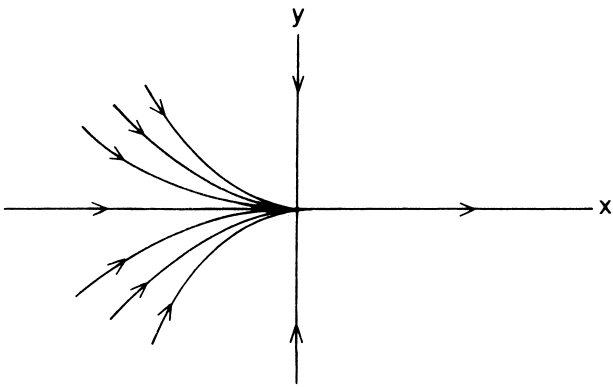

FIGURE 18.5.1.

Uniqueness

Although center manifolds exist, they need not be unique. This can be seen from the following example due to Anosov (see Sijbrand [1985]). Consider the vector field

$$\begin{aligned} \dot{x} &= x^2, \\ \dot{y} &= -y, \qquad (x, y) \in \mathbb{R}^2. \end{aligned} \tag{18.5.1}$$

Clearly, $(x, y) = (0, 0)$ is a fixed point with stable manifold given by $x = 0$. It should also be clear that $y = 0$ is an invariant center manifold, but there are other center manifolds.

Eliminating t as the independent variable in (18.5.1), we obtain

$$\frac{dy}{dx} = \frac{-y}{x^2}. \tag{18.5.2}$$

The solution of (18.5.2) (for $x \neq 0$) is given by

$$y(x) = \alpha e^{1/x} \tag{18.5.3}$$

for any real constant α. Thus, the curves given by

$$W^c_\alpha(0) = \left\{(x, y) \in \mathbb{R}^2 \mid y = \alpha e^{1/x} \text{ for } x < 0, y = 0 \text{ for } x \geq 0\right\} \tag{18.5.4}$$

are a one-parameter (parametrized by α) family of center manifolds of $(x, y) = (0, 0)$; see Figure 18.5.1.

This example immediately brings up two questions.

1. In approximating the center manifold via power series expansions according to Theorem 18.1.4, which center manifold is actually being approximated?

2. Is the dynamical behavior the "same" on all of the center manifolds of a given fixed point?

Regarding Question 1, it can be proven (see Wan [1977], Carr [1981] or Sijbrand [1985]) that any two center manifolds of a given fixed point differ by (at most) transcendentally small terms (cf. (18.5.4)). Thus, the Taylor series expansions of any two center manifolds agree to all orders.

This fact emphasizes the importance of Question 2 from a practical point of view. However, it can be shown that due to the attractive nature of the center manifold, certain orbits that remain close to the origin for all time must be on *every* center manifold of a given fixed point, for example, fixed points, periodic orbits, homoclinic orbits, and heteroclinic orbits.

Differentiability

From Theorem 18.1.2 we have that if the vector field is $\mathbf{C}^r$, then the center manifold is also $\mathbf{C}^r$. However, if the vector field is analytic, then the center manifold need not be analytic; see Sijbrand [1985].

Preservation of Symmetry

Suppose that the vector field (18.1.1) possesses certain symmetries (e.g., it is Hamiltonian). Does the vector field restricted to the center manifold possess the same symmetries? See Ruelle [1973] for a discussion of these issues.

Preservation of Hamiltonian Structure

For a Hamiltonian vector field, the restriction of the vector field to the center manifold gives rise to a Hamiltonian vector field. A proof of this can be found in Mielke [1991].

18.6 Final Remarks on Center Manifolds

A Coordinate Independent Center Manifold Reduction. We developed center manifold theory by assuming that the linear part of the vector field was in block diagonal form, see, e.g., (18.1.1). However, Leen [1993] has developed a coordinate independent approach to the center manifold reduction.

Center Manifolds for Stochastic Dynamical Systems. A center manifold theory for stochastic dynamical systems has been developed by Boxler [1989], [1991].

18.7 Exercises

1. Consider the $\mathbf{C}^r$ $(r \geq 1)$ map

$$x \mapsto f(x), \qquad x \in \mathbb{R}^n. \tag{18.7.1}$$

Suppose that the map has a fixed point at $x = x_0$, i.e.,

$$x_0 = f(x_0).$$

Next consider the vector field

$$\dot{x} = f(x) - x. \tag{18.7.2}$$

Clearly (18.7.2) has a fixed point, and $x = x_0$. What can you determine about the orbit structure near the fixed point of the map (18.7.1) based on knowledge of the orbit structure near the fixed point $x = x_0$ of the vector field (18.7.2)?

2. Consider the $\mathbf{C}^r$ map

$$f\colon \mathbb{R}^1 \to \mathbb{R}^1$$

and denote the Taylor expansion of f by

$$f(x) = a_0 + a_1 x + \cdots + a_{r-1} x^{r-1} + \mathcal{O}(|x|^r).$$

Suppose f is identically zero. Then show that $a_i = 0$, $i = 0, \ldots, r-1$. Does the same result hold for the $\mathbf{C}^r$ map

$$f\colon \mathbb{R}^n \to \mathbb{R}^n, \qquad n > 1?$$

3. Study the dynamics near the origin for each of the following vector fields. Draw phase portraits. Compute the center manifolds and describe the dynamics on the center manifold. Discuss the stability or instability of the origin.

a) $\begin{aligned} \dot{\theta} &= -\theta + v^2, \\ \dot{v} &= -\sin\theta, \end{aligned} \qquad (\theta, v) \in S^1 \times \mathbb{R}^1.$

b) $\begin{aligned} \dot{x} &= \frac{1}{2}x + y + x^2 y, \\ \dot{y} &= x + 2y + y^2, \end{aligned} \qquad (x, y) \in \mathbb{R}^2.$

c) $\begin{aligned} \dot{x} &= x - 2y, \\ \dot{y} &= 3x - y - x^2, \end{aligned} \qquad (x, y) \in \mathbb{R}^2.$

d) $\begin{aligned} \dot{x} &= 2x + 2y, \\ \dot{y} &= x + y + x^4, \end{aligned} \qquad (x, y) \in \mathbb{R}^2.$

e) $\begin{aligned}\dot{x} &= -y - y^3,\\ \dot{y} &= 2x,\end{aligned}$ $(x, y) \in \mathbb{R}^2$.

f) $\begin{aligned}\dot{x} &= -2x + 3y + y^3,\\ \dot{y} &= 2x - 3y + x^3,\end{aligned}$ $(x, y) \in \mathbb{R}^2$.

g) $\begin{aligned}\dot{x} &= -x - y - xy,\\ \dot{y} &= 2x + y + 2xy,\end{aligned}$ $(x, y) \in \mathbb{R}^2$.

h) $\begin{aligned}\dot{x} &= -x + y,\\ \dot{y} &= -e^x + e^{-x} + 2x,\end{aligned}$ $(x, y) \in \mathbb{R}^2$.

i) $\begin{aligned}\dot{x} &= -2x + y + z + y^2 z,\\ \dot{y} &= x - 2y + z + xz^2,\\ \dot{z} &= x + y - 2z + x^2 y,\end{aligned}$ $(x, y, z) \in \mathbb{R}^3$.

j) $\begin{aligned}\dot{x} &= -x - y + z^2,\\ \dot{y} &= 2x + y - z^2,\\ \dot{z} &= x + 2y - z,\end{aligned}$ $(x, y, z) \in \mathbb{R}^3$.

k) $\begin{aligned}\dot{x} &= -x - y - z - yz,\\ \dot{y} &= -x - y - z - xz,\\ \dot{z} &= -x - y - z - xy,\end{aligned}$ $(x, y, z) \in \mathbb{R}^3$.

l) $\begin{aligned}\dot{x} &= y + x^2,\\ \dot{y} &= -y - x^2,\end{aligned}$ $(x, y) \in \mathbb{R}^3$.

m) $\begin{aligned}\dot{x} &= x^2,\\ \dot{y} &= -y - x^2,\end{aligned}$ $(x, y) \in \mathbb{R}^2$.

n) $\begin{aligned}\dot{x} &= -x + 2y + x^2 y + x^4 y^5,\\ \dot{y} &= y - x^4 y^6 + x^8 y^9,\end{aligned}$ $(x, y) \in \mathbb{R}^2$.

4. Consider the following parametrized families of vector fields with parameter $\varepsilon \in \mathbb{R}^1$. For $\varepsilon = 0$, the origin is a fixed point of each vector field. Study the dynamics near the origin for ε small. Draw phase portraits. Compute the one-parameter family of center manifolds and describe the dynamics on the center manifolds. How do the dynamics depend on ε? Note that, for $\varepsilon = 0$, e.g., a) and a′) reduce to a) in the previous exercise. Discuss the role played by a parameter by comparing these cases. In, for example, a) and a′), the parameter ε multiplies a linear and nonlinear term, respectively. Discuss the differences in these two cases in the most general setting possible.

a) $\begin{aligned}\dot{\theta} &= -\theta + \varepsilon v + v^2,\\ \dot{v} &= -\sin\theta,\end{aligned}$ $(\theta, v) \in S^1 \times \mathbb{R}^1$.

a′) $\begin{aligned}\dot{\theta} &= -\theta + v^2 + \varepsilon v^2,\\ \dot{v} &= -\sin\theta\end{aligned}$

b) $\begin{aligned}\dot{x} &= \frac{1}{2}x + y + x^2 y,\\ \dot{y} &= x + 2y + \varepsilon y + y^2,\end{aligned}$ $(x, y) \in \mathbb{R}^2$.

b′) $\begin{aligned}\dot{x} &= \frac{1}{2}x + y + x^2 y,\\ \dot{y} &= x + 2y + y^2 + \varepsilon y^2,\end{aligned}$

c) $\begin{aligned}\dot{x} &= x - 2y + \varepsilon x,\\ \dot{y} &= 3x - y - x^2,\end{aligned}$ $(x, y) \in \mathbb{R}^2$.

c′) $\begin{aligned}\dot{x} &= x - 2y + \varepsilon x^2,\\ \dot{y} &= 3x - y - x^2,\end{aligned}$

d) $\begin{aligned}\dot{x} &= 2x + 2y + \varepsilon y,\\ \dot{y} &= x + y + x^4,\end{aligned}$ $(x, y) \in \mathbb{R}^2$.

d′) $\begin{aligned}\dot{x} &= 2x + 2y,\\ \dot{y} &= x + y + x^4 + \varepsilon y^2,\end{aligned}$

e) $\begin{aligned}\dot{x} &= -y - \varepsilon x - y^3,\\ \dot{y} &= 2x,\end{aligned}$ $(x,y) \in \mathbb{R}^2$.

e′) $\begin{aligned}\dot{x} &= -y - y^3,\\ \dot{y} &= 2x + \varepsilon x^2,\end{aligned}$

f) $\begin{aligned}\dot{x} &= -2x + 3y + \varepsilon x + y^3,\\ \dot{y} &= 2x - 3y + x^3,\end{aligned}$ $(x,y) \in \mathbb{R}^2$.

f′) $\begin{aligned}\dot{x} &= -2x + 3y + y^3 + \varepsilon x^2,\\ \dot{y} &= 2x - 3y + x^3,\end{aligned}$

g) $\begin{aligned}\dot{x} &= -x - y + \varepsilon x - xy,\\ \dot{y} &= 2x + y + 2xy,\end{aligned}$ $(x,y) \in \mathbb{R}^2$.

g′) $\begin{aligned}\dot{x} &= -x - y - xy + \varepsilon x^2,\\ \dot{y} &= 2x + y + 2xy,\end{aligned}$

h) $\begin{aligned}\dot{x} &= -x + y,\\ \dot{y} &= -e^x + e^{-x} + 2x + \varepsilon y,\end{aligned}$ $(x,y) \in \mathbb{R}^2$.

h′) $\begin{aligned}\dot{x} &= -x + y + \varepsilon x^2,\\ \dot{y} &= -e^x + e^{-x} + 2x,\end{aligned}$

i) $\begin{aligned}\dot{x} &= -2x + y + z + \varepsilon x - y^2 z,\\ \dot{y} &= x - 2y + z + \varepsilon x + x z^2,\\ \dot{z} &= x + y - 2z + \varepsilon x + x^2 y,\end{aligned}$ $(x,y,z) \in \mathbb{R}^3$.

i′) $\begin{aligned}\dot{x} &= -2x + y + z + \varepsilon x^2 + y^2 z,\\ \dot{y} &= x - 2y + z + \varepsilon xy + x z^2,\\ \dot{z} &= x + y - 2z + x^2 y.\end{aligned}$

j) $\begin{aligned}\dot{x} &= -x - y + z^2,\\ \dot{y} &= 2x + y + \varepsilon y - z^2,\\ \dot{z} &= x + 2y - z,\end{aligned}$ $(x,y,z) \in \mathbb{R}^3$.

j′) $\begin{aligned}\dot{x} &= -x - y + \varepsilon x^2 + z^2,\\ \dot{y} &= 2x + y - z^2 + \varepsilon y^2,\\ \dot{z} &= x + 2y - z.\end{aligned}$

k) $\begin{aligned}\dot{x} &= -x - y - z + \varepsilon x - yz,\\ \dot{y} &= -x - y - z - xz,\\ \dot{z} &= -x - y - z - yz,\end{aligned}$ $(x,y,z) \in \mathbb{R}^3$.

k′) $\begin{aligned}\dot{x} &= -x - y - z - yz + \varepsilon x^2,\\ \dot{y} &= -x - y - z - xz,\\ \dot{z} &= -x - y - z - xy.\end{aligned}$

l) $\begin{aligned}\dot{x} &= y + x^2 + \varepsilon y,\\ \dot{y} &= -y - x^2,\end{aligned}$ $(x,y) \in \mathbb{R}^2$.

l′) $\begin{aligned}\dot{x} &= y + x^2 + \varepsilon y^2,\\ \dot{y} &= -y - x^2,\end{aligned}$

m) $\begin{aligned}\dot{x} &= x^2 + \varepsilon y,\\ \dot{y} &= -y - x^2,\end{aligned}$ $(x,y) \in \mathbb{R}^2$.

m′) $\begin{aligned}\dot{x} &= x^2 + \varepsilon y^2,\\ \dot{y} &= -y - x^2.\end{aligned}$

5. Study the dynamics near the origin for each of the following maps. Draw phase portraits. Compute the center manifold and describe the dynamics on the center manifold. Discuss the stability or instability of the origin.

a) $\begin{aligned}x &\mapsto -\frac{1}{2}x - y - xy^2,\\ y &\mapsto -\frac{1}{2}x + x^2,\end{aligned}$ $(x,y) \in \mathbb{R}^2$.

b) $\begin{aligned} x &\mapsto x + 2y + x^3, \\ y &\mapsto 2x + y, \end{aligned} \qquad (x, y) \in \mathbb{R}^2.$

c) $\begin{aligned} x &\mapsto -x + y - xy^2, \\ y &\mapsto y + x^2 y, \end{aligned} \qquad (x, y) \in \mathbb{R}^2.$

d) $\begin{aligned} x &\mapsto 2x + y, \\ y &\mapsto 2x + 3y + x^4, \end{aligned} \qquad (x, y) \in \mathbb{R}^2.$

e) $\begin{aligned} x &\mapsto x, \\ y &\mapsto x + 2y + y^2, \end{aligned} \qquad (x, y) \in \mathbb{R}^2.$

f) $\begin{aligned} x &\mapsto 2x + 3y, \\ y &\mapsto x + x^2 + xy^2, \end{aligned} \qquad (x, y) \in \mathbb{R}^2.$

g) $\begin{aligned} x &\mapsto x - z^3, \\ y &\mapsto 2x - y, \\ z &\mapsto x + \frac{1}{2}z + x^3, \end{aligned} \qquad (x, y, z) \in \mathbb{R}^3.$

h) $\begin{aligned} x &\mapsto x + z^4, \\ y &\mapsto -x - 2y - x^3, \\ z &\mapsto y - \frac{1}{2}z + y^2, \end{aligned} \qquad (x, y, z) \in \mathbb{R}^3.$

i) $\begin{aligned} x &\mapsto y + x^2, \\ y &\mapsto y + xy, \end{aligned} \qquad (x, y) \in \mathbb{R}^2.$

j) $\begin{aligned} x &\mapsto x^2, \\ y &\mapsto y + xy, \end{aligned} \qquad (x, y) \in \mathbb{R}^2.$

6. Consider the following parametrized families of maps with parameter $\varepsilon \in \mathbb{R}^1$. For $\varepsilon = 0$, the origin is a fixed point of each vector field. Study the dynamics near the origin for ε small. Draw phase portraits. Compute the one-parameter family of center manifolds and describe the dynamics on the center manifolds. How do the dynamics depend on ε? Note that, for $\varepsilon = 0$, e.g., a) and a′) reduce to a) in the previous exercise. Discuss the role played by a parameter by comparing these cases. In, e.g., a) and a′), the parameter ε multiplies a linear and nonlinear term, respectively. Discuss the differences in these two cases in the most general possible setting.

a) $\begin{aligned} x &\mapsto -\frac{1}{2}x - y - xy^2, \\ y &\mapsto -\frac{1}{2}x + \varepsilon y + x^2, \end{aligned} \qquad (x, y) \in \mathbb{R}^2.$

a′) $\begin{aligned} x &\mapsto -\frac{1}{2}x - y - xy^2, \\ y &\mapsto -\frac{1}{2}y + \varepsilon y^2 + x^2. \end{aligned}$

b) $\begin{aligned} x &\mapsto x + 2y + x^3, \\ y &\mapsto 2x + y + \varepsilon y, \end{aligned} \qquad (x, y) \in \mathbb{R}^2.$

b′) $\begin{aligned} x &\mapsto x + 2y + x^3, \\ y &\mapsto 2x + y + \varepsilon y^2. \end{aligned}$

c) $\begin{aligned} x &\mapsto -x + y - xy^2, \\ y &\mapsto y + \varepsilon y + x^2 y, \end{aligned} \qquad (x, y) \in \mathbb{R}^2.$

c′) $\begin{aligned} x &\mapsto -x + y - xy^2, \\ y &\mapsto y + \varepsilon y^2 + x^2 y. \end{aligned}$

d) $\begin{aligned} x &\mapsto 2x + y, \\ y &\mapsto 2x + 3y + \varepsilon x + x^4, \end{aligned} \qquad (x, y) \in \mathbb{R}^2.$

d′) $\begin{aligned} x &\mapsto 2x + y + \varepsilon x^2, \\ y &\mapsto 2x + 3y + x^4. \end{aligned}$

e) $\begin{aligned} x &\mapsto x + \varepsilon y, \\ y &\mapsto x + 2y + y^2, \end{aligned} \qquad (x, y) \in \mathbb{R}^2.$

e′) $\begin{aligned} x &\mapsto x + \varepsilon y^2, \\ y &\mapsto x + 2y + y^2. \end{aligned}$

f) $\begin{aligned} x &\mapsto 2x + 3y, \\ y &\mapsto x + \varepsilon y + x^2 + xy^2, \end{aligned} \qquad (x, y) \in \mathbb{R}^2.$

f′) $\begin{aligned} x &\mapsto 2x + 3y, \\ y &\mapsto x + x^2 + \varepsilon y^2 + xy^2. \end{aligned}$

g) $\begin{aligned} x &\mapsto x - z^3, \\ y &\mapsto 2x - y + \varepsilon y, \\ z &\mapsto x + \frac{1}{2}z + x^3, \end{aligned} \qquad (x, y, z) \in \mathbb{R}^3.$

g′) $\begin{aligned} x &\mapsto x - z^3, \\ y &\mapsto 2x - y + \varepsilon y^2, \\ z &\mapsto x + \frac{1}{2}z + x^3. \end{aligned}$

h) $\begin{aligned} x &\mapsto x + \varepsilon z^4, \\ y &\mapsto -x - 2y - x^3, \\ z &\mapsto y - \frac{1}{2}z + y^2, \end{aligned} \qquad (x, y, z) \in \mathbb{R}^3.$

h′) $\begin{aligned} x &\mapsto x + \varepsilon x + z^4, \\ y &\mapsto -x - 2y - x^3, \\ z &\mapsto y - \frac{1}{2}z + y^2. \end{aligned}$

i) $\begin{aligned} x &\mapsto y + \varepsilon x + x^2, \\ y &\mapsto y + xy, \end{aligned} \qquad (x, y) \in \mathbb{R}^2.$

i′) $\begin{aligned} x &\mapsto y + x^2, \\ y &\mapsto y + xy + \varepsilon x^2. \end{aligned}$

j) $\begin{aligned} x &\mapsto \varepsilon x + x^2, \\ y &\mapsto y + xy, \end{aligned} \qquad (x, y) \in \mathbb{R}^2.$

j′) $\begin{aligned} x &\mapsto x^2 + \varepsilon y, \\ y &\mapsto y + xy. \end{aligned}$

7. In Chapter 3 we illustrated the graph transform method and the Liapunov-Perron method for proving the existence of stable and unstable manifolds associated with a hyperbolic fixed point by applying the techniques to the specific vector field:

$$\begin{aligned} \dot{x} &= x, \\ \dot{y} &= -y + x^2, \end{aligned} \qquad (x, y) \in \mathbb{R}^2.$$

Now let's consider a slight modification of this example:

$$\begin{aligned} \dot{x} &= x^2, \\ \dot{y} &= -y + x^2, \end{aligned} \qquad (x, y) \in \mathbb{R}^2.$$

For this example the origin is a nonhyperbolic fixed point with a one dimensional center manifold and a one dimensional stable manifold. Use the graph transform, Liapunov-Perron, and Taylor series methods to prove the existence of a center manifold of the origin.

Recall from Example 7.2.1 of Chapter 7 that the equation $\dot{x} = x^2$ is an example of a vector field whose solutions "blow up in finite time". Does this fact have any bearing on the existence of a center manifold? (Note: this provides another setting where the reader should think of the difference between "trajectories" and "manifolds made up of trajectories". One is a dynamical object, the other is a geometrical object.)

19

Normal Forms

The method of normal forms provides a way of finding a coordinate system in which the dynamical system takes the "simplest" form, where the term "simplest" will be defined as we go along. As we develop the method, three important characteristics should become apparent.

1. The method is local in the sense that the coordinate transformations are generated in a neighborhood of a known solution. For our purposes, the known solution will be a fixed point. However, when we develop the theory for maps, the results will have immediate applications to periodic orbits of vector fields by considering the associated Poincaré map (cf. Chapter 10).

2. In general, the coordinate transformations will be nonlinear functions of the dependent variables. However, the important point is that these coordinate transformations are found by solving a sequence of *linear* problems.

3. The structure of the normal form is determined entirely by the nature of the linear part of the vector field.

We now begin the development of the method.

19.1 Normal Forms for Vector Fields

Consider the vector field

$$\dot{w} = G(w), \qquad w \in \mathbb{R}^n, \tag{19.1.1}$$

where G is $\mathbf{C}^r$, with r to be specified as we go along (note: in practice we will need $r \geq 4$). Suppose (19.1.1) has a fixed point at $w = w_0$.

19.1A Preliminary Preparation of the Equations

We first want to perform a few simple (linear) coordinate transformations that will put (19.1.1) into a form which is easier to work with.

1. First we transform the fixed point to the origin by the translation

$$v = w - w_0, \qquad v \in \mathbb{R}^n,$$

under which (19.1.1) becomes

$$\dot{v} = G(v + w_0) \equiv H(v). \tag{19.1.2}$$

2. We next "split off" the linear part of the vector field and write (19.1.2) as follows

$$\dot{v} = DH(0)v + \bar{H}(v), \tag{19.1.3}$$

where $\bar{H}(v) \equiv H(v) - DH(0)v$. It should be clear that $\bar{H}(v) = \mathcal{O}(|v|^2)$.

3. Finally, let T be the matrix that transforms the matrix $DH(0)$ into (real) Jordan canonical form. Then, under the transformation

$$v = Tx, \tag{19.1.4}$$

(19.1.3) becomes

$$\dot{x} = T^{-1}DH(0)Tx + T^{-1}\bar{H}(Tx). \tag{19.1.5}$$

Denoting the (real) Jordan canonical form of $DH(0)$ by J, we have

$$J \equiv T^{-1}DH(0)T, \tag{19.1.6}$$

and we define

$$F(x) \equiv T^{-1}\bar{H}(Tx)$$

so that (19.1.4) is alternately written as

$$\dot{x} = Jx + F(x), \qquad x \in \mathbb{R}^n. \tag{19.1.7}$$

We remark that the transformation (19.1.4) has simplified the linear part of (19.1.3) as much as possible. We now begin the task of simplifying the nonlinear part, $F(x)$.

First, we Taylor expand $F(x)$ so that (19.1.7) becomes

$$\dot{x} = Jx + F_2(x) + F_3(x) + \cdots + F_{r-1}(x) + \mathcal{O}(|x|^r), \tag{19.1.8}$$

where $F_i(x)$ represent the order i terms in the Taylor expansion of $F(x)$.

19.1B Simplification of the Second Order Terms

We next introduce the coordinate transformation

$$x = y + h_2(y), \tag{19.1.9}$$

where $h_2(y)$ is second order in y. Substituting (19.1.9) into (19.1.8) gives

$$\begin{aligned}\dot{x} = \big(\mathrm{id} + Dh_2(y)\big)\dot{y} = Jy + Jh_2(y) + F_2\big(y + h_2(y)\big) \\ + F_3\big(y + h_2(y)\big) + \cdots + F_{r-1}\big(y + h_2(y)\big) + \mathcal{O}(|y|^r),\end{aligned} \tag{19.1.10}$$

where "id" denotes the $n \times n$ identity matrix. Note that each term

$$F_k\big(y + h_2(y)\big), \qquad 2 \le k \le r-1, \tag{19.1.11}$$

can be written as

$$F_k(y) + \mathcal{O}(|y|^{k+1}) + \cdots + \mathcal{O}(|y|^{2k}), \tag{19.1.12}$$

so that (19.1.10) becomes

$$\begin{aligned}\big(\mathrm{id} + Dh_2(y)\big)\dot{y} = Jy + Jh_2(y) + F_2(y) + \tilde{F}_3(y) \\ + \cdots + \tilde{F}_{r-1}(y) + \mathcal{O}(|y|^r),\end{aligned} \tag{19.1.13}$$

where the change of notation for the $\mathcal{O}(|y|^k)$ terms, to $\tilde{F}_k(y)$, serves to denote that they have been modified as a result of the coordinate transformation.

Now, for y sufficiently small,

$$\big(\mathrm{id} + Dh_2(y)\big)^{-1} \tag{19.1.14}$$

exists and can be represented in a series expansion as follows (see Exercise 3)

$$\big(\mathrm{id} + Dh_2(y)\big)^{-1} = \mathrm{id} - Dh_2(y) + \mathcal{O}(|y|^2). \tag{19.1.15}$$

Substituting (19.1.15) into (19.1.13) gives

$$\begin{aligned}\dot{y} = Jy + Jh_2(y) - Dh_2(y)Jy + F_2(y) + \tilde{F}_3(y) \\ + \cdots + \tilde{F}_{r-1}(y) + \mathcal{O}(|y|^r).\end{aligned} \tag{19.1.16}$$

Up to this point $h_2(y)$ has been completely arbitrary. However, now we will choose a specific form for $h_2(y)$ so as to simplify the $\mathcal{O}(|y|^2)$ terms as much as possible. Ideally, this would mean choosing $h_2(y)$ such that

$$Dh_2(y)Jy - Jh_2(y) = F_2(y), \tag{19.1.17}$$

which would eliminate $F_2(y)$ from (19.1.16). Equation (19.1.17) can be viewed as an equation for the unknown $h_2(y)$. We want to motivate the fact that, when viewed in the correct way, it is in fact a linear equation acting on a linear vector space. This will be accomplished by 1) defining the appropriate linear vector space; 2) defining the linear operator on the vector space; and 3) describing the equation to be solved in this linear vector space (which will turn out to be (19.1.17)). We begin with Step 1.

Step 1. The Space of Vector-Valued Homogeneous Polynomials of Degree k, H_k

Let $\{s_1, \cdots, s_n\}$ denote a basis of $\mathbb{R}^n$, and let $y = (y_1, \cdots, y_n)$ be coordinates with respect to this basis. Now consider those basis elements with coefficients consisting of homogeneous polynomials of degree k, i.e.,

$$(y_1^{m_1} y_2^{m_2} \cdots y_n^{m_n}) s_i, \quad \sum_{j=1}^{n} m_j = k, \tag{19.1.18}$$

where $m_j \geq 0$ are integers. We refer to these objects as *vector-valued homogeneous polynomials of degree k*. The set of all vector-valued homogeneous polynomials of degree k forms a linear vector space, which we denote by H_k. An obvious basis for H_k consists of elements formed by considering all possible homogeneous polynomials of degree k that multiply each s_i. The reader should verify these statements. Let us consider a specific example.

Example 19.1.1. We consider the standard basis

$$\begin{pmatrix} 1 \\ 0 \end{pmatrix}, \begin{pmatrix} 0 \\ 1 \end{pmatrix} \tag{19.1.19}$$

on $\mathbb{R}^2$ and denote the coordinates with respect to this basis by x and y, respectively. Then we have

$$H_2 = \text{Span} \left\{ \begin{pmatrix} x^2 \\ 0 \end{pmatrix}, \begin{pmatrix} xy \\ 0 \end{pmatrix}, \begin{pmatrix} y^2 \\ 0 \end{pmatrix}, \begin{pmatrix} 0 \\ x^2 \end{pmatrix}, \begin{pmatrix} 0 \\ xy \end{pmatrix}, \begin{pmatrix} 0 \\ y^2 \end{pmatrix} \right\}. \tag{19.1.20}$$

End of Example 19.1.1

Step 2. The Linear Map on H_k

Now let us reconsider equation (19.1.17). It should be clear that $h_2(y)$ can be viewed as an element of H_2. The reader should easily be able to verify that the map

$$h_2(y) \longmapsto Dh_2(y)Jy - Jh_2(y) \tag{19.1.21}$$

is a linear map of H_2 into H_2. Indeed, for any element $h_k(y) \in H_k$, it similarly follows that

$$h_k(y) \longmapsto Dh_k(y)Jy - Jh_k(y) \tag{19.1.22}$$

is a linear map of H_k into H_k.

Let us mention some terminology associated with Eq. (19.1.17) that has become traditional. Due to its presence in Lie algebra theory (see, e.g., Olver [1986]) this map is often denoted as

$$L_J^{(k)}\big(h_k(y)\big) \equiv -\big(Dh_k(y)Jy - Jh_k(y)\big) \tag{19.1.23}$$

or

$$-\big(Dh_k(y)Jy - Jh_k(y)\big) \equiv [h_k(y), Jy], \tag{19.1.24}$$

where $[\cdot,\cdot]$ denotes the Lie bracket operation on the vector fields $h_k(y)$ and Jy.

Step 3. The Solution of (19.1.17)

We now return to the problem of solving (19.1.17). It should be clear that $F_2(y)$ can be viewed as an element of H_2. From elementary linear algebra, we know that H_2 can be (nonuniquely) represented as follows

$$H_2 = L_J^{(2)}(H_2) \oplus G_2, \tag{19.1.25}$$

where G_2 represents a space complementary to $L_J^{(2)}(H_2)$. Solving (19.1.17) is like solving the equation $Ax = b$ from linear algebra. If $F_2(y)$ is in the range of $L_J^{(2)}(\cdot)$, then all $\mathcal{O}(|y|^2)$ terms can be eliminated from (19.1.17). In any case, we can choose $h_2(y)$ so that only $\mathcal{O}(|y|^2)$ terms that are in G_2 remain. We denote these terms by

$$F_2^r(y) \in G_2 \tag{19.1.26}$$

(note: the superscript r in (19.1.26) denotes the term "resonance," which will be explained shortly).

Thus, (19.1.16) can be simplified to

$$\dot{y} = Jy + F_2^r(y) + \tilde{F}_3(y) + \cdots + \tilde{F}_{r-1}(y) + \mathcal{O}(|y|^r). \tag{19.1.27}$$

At this point the meaning of the phrase "simplify the second-order terms" should be clear. It means the introduction of a coordinate change such that, in the new coordinate system, the only second-order terms are in a space complementary to $L_J^{(2)}(H_2)$. If $L_J^{(2)}(H_2) = H_2$, then all second-order terms can be eliminated.

19.1c Simplification of the Third Order Terms

Next let us simplify the $\mathcal{O}(|y|^3)$ terms. Introducing the coordinate change

$$y \longmapsto y + h_3(y), \tag{19.1.28}$$

where $h_3(y) = \mathcal{O}(|y|^3)$ (note: we will retain the same variables y in our equation), and performing the same algebraic manipulations as in dealing with the second-order terms, (19.1.27) becomes

$$\begin{aligned}\dot{y} = Jy + F_2^r(y) + Jh_3(y) - Dh_3(y)Jy + \tilde{F}_3(y) + \tilde{\tilde{F}}_4(y)\\ + \cdots + \tilde{\tilde{F}}_{r-1}(y) + \mathcal{O}(|y|^r),\end{aligned} \tag{19.1.29}$$

where the terms $\tilde{\tilde{F}}_k(y)$, $4 \leq k \leq r-1$, indicate, as before, that the coordinate transformation has modified the terms of order higher than three. Now, simplifying the third-order terms involves solving

$$Dh_3(y)Jy - Jh_3(y) = \tilde{F}_3(y). \tag{19.1.30}$$

The same comments as for second-order terms apply here. The map

$$h_3(y) \longmapsto Dh_3(y)Jy - Jh_3(y) \equiv -L_J^{(3)}(h_3(y)) \tag{19.1.31}$$

is a linear map of H_3 into H_3. Thus, we can write

$$H_3 = L_J^{(3)}(H_3) \oplus G_3, \tag{19.1.32}$$

where G_3 is some space complementary to $L_J^{(3)}(H_3)$. Thus, the third-order terms can be simplified to

$$F_3^r(y) \in G_3. \tag{19.1.33}$$

If $L_J^{(3)}(H_3) = H_3$, then the third-order terms can be eliminated.

19.1D The Normal Form Theorem

Clearly, this procedure can be iterated so that we obtain the following *normal form theorem.*

Theorem 19.1.1 (Normal Form Theorem) *By a sequence of analytic coordinate changes (19.1.8) can be transformed into*

$$\dot{y} = Jy + F_2^r(y) + \cdots + F_{r-1}^r(y) + \mathcal{O}(|y|^r), \tag{19.1.34}$$

where $F_k^r(y) \in G_k$, $2 \leq k \leq r-1$, *and* G_k *is a space complementary to* $L_J^{(k)}(H_k)$. *Equation (19.1.34) is said to be in* normal form through order $r-1$.

Several comments are now in order.

1. The terms $F_k^r(y)$, $2 \leq k \leq r-1$, are referred to as *resonance terms* (hence the superscript r). We will explain what this means in Section 19.12.

2. The structure of the nonlinear terms in (19.1.34) is determined entirely by the linear part of the vector field (i.e., J).

3. It should be clear that simplifying the terms at order k does not modify any lower order terms. However, terms of order higher than k are modified. This happens at each step of the application of the method. If one wanted to actually calculate the coefficients on each term of the normal form in terms of the original vector field, it would be necessary to keep track of how the higher order terms are modified by the successive coordinate transformations.

Example 19.1.2 (The Takens-Bogdanov Normal Form). We want to compute the normal form for a vector field on $\mathbb{R}^2$ in the neighborhood of a fixed point where the linear part is given by

$$J = \begin{pmatrix} 0 & 1 \\ 0 & 0 \end{pmatrix}. \tag{19.1.35}$$

Second-Order Terms

We have

$$H_2 = \text{span}\left\{ \begin{pmatrix} x^2 \\ 0 \end{pmatrix}, \begin{pmatrix} xy \\ 0 \end{pmatrix}, \begin{pmatrix} y^2 \\ 0 \end{pmatrix}, \begin{pmatrix} 0 \\ x^2 \end{pmatrix}, \begin{pmatrix} 0 \\ xy \end{pmatrix}, \begin{pmatrix} 0 \\ y^2 \end{pmatrix} \right\}. \tag{19.1.36}$$

We want to compute $L_J^{(2)}(H_2)$. We do this by computing the action of $L_J^{(2)}(\cdot)$ on each basis element on H_2

$$\begin{aligned}
L_J^{(2)} \begin{pmatrix} x^2 \\ 0 \end{pmatrix} &= \begin{pmatrix} 0 & 1 \\ 0 & 0 \end{pmatrix} \begin{pmatrix} x^2 \\ 0 \end{pmatrix} - \begin{pmatrix} 2x & 0 \\ 0 & 0 \end{pmatrix} \begin{pmatrix} y \\ 0 \end{pmatrix} = \begin{pmatrix} -2xy \\ 0 \end{pmatrix} \\
&= -2 \begin{pmatrix} xy \\ 0 \end{pmatrix}, \\
L_J^{(2)} \begin{pmatrix} xy \\ 0 \end{pmatrix} &= \begin{pmatrix} 0 & 1 \\ 0 & 0 \end{pmatrix} \begin{pmatrix} xy \\ 0 \end{pmatrix} - \begin{pmatrix} y & x \\ 0 & 0 \end{pmatrix} \begin{pmatrix} y \\ 0 \end{pmatrix} = \begin{pmatrix} -y^2 \\ 0 \end{pmatrix} \\
&= -1 \begin{pmatrix} y^2 \\ 0 \end{pmatrix}, \\
L_J^{(2)} \begin{pmatrix} y^2 \\ 0 \end{pmatrix} &= \begin{pmatrix} 0 & 1 \\ 0 & 0 \end{pmatrix} \begin{pmatrix} y^2 \\ 0 \end{pmatrix} - \begin{pmatrix} 0 & 2y \\ 0 & 0 \end{pmatrix} \begin{pmatrix} y \\ 0 \end{pmatrix} = \begin{pmatrix} 0 \\ 0 \end{pmatrix}, \\
L_J^{(2)} \begin{pmatrix} 0 \\ x^2 \end{pmatrix} &= \begin{pmatrix} 0 & 1 \\ 0 & 0 \end{pmatrix} \begin{pmatrix} 0 \\ x^2 \end{pmatrix} - \begin{pmatrix} 0 & 0 \\ 2x & 0 \end{pmatrix} \begin{pmatrix} y \\ 0 \end{pmatrix} = \begin{pmatrix} x^2 \\ -2xy \end{pmatrix} \\
&= \begin{pmatrix} x^2 \\ 0 \end{pmatrix} - 2 \begin{pmatrix} 0 \\ xy \end{pmatrix}, \\
L_J^{(2)} \begin{pmatrix} 0 \\ xy \end{pmatrix} &= \begin{pmatrix} 0 & 1 \\ 0 & 0 \end{pmatrix} \begin{pmatrix} 0 \\ xy \end{pmatrix} - \begin{pmatrix} 0 & 0 \\ y & x \end{pmatrix} \begin{pmatrix} y \\ 0 \end{pmatrix} = \begin{pmatrix} xy \\ -y^2 \end{pmatrix} \\
&= \begin{pmatrix} xy \\ 0 \end{pmatrix} - \begin{pmatrix} 0 \\ y^2 \end{pmatrix}, \\
L_J^{(2)} \begin{pmatrix} 0 \\ y^2 \end{pmatrix} &= \begin{pmatrix} 0 & 1 \\ 0 & 0 \end{pmatrix} \begin{pmatrix} 0 \\ y^2 \end{pmatrix} - \begin{pmatrix} 0 & 0 \\ 0 & 2y \end{pmatrix} \begin{pmatrix} y \\ 0 \end{pmatrix} = \begin{pmatrix} y^2 \\ 0 \end{pmatrix}.
\end{aligned} \tag{19.1.37}$$

From (19.1.37) we have

$$\begin{aligned}
L_J^{(2)}(H_2) = \text{span}\Bigg\{ &\begin{pmatrix} -2xy \\ 0 \end{pmatrix}, \begin{pmatrix} -y^2 \\ 0 \end{pmatrix}, \begin{pmatrix} 0 \\ 0 \end{pmatrix}, \begin{pmatrix} x^2 \\ -2xy \end{pmatrix}, \\
&\begin{pmatrix} xy \\ -y^2 \end{pmatrix}, \begin{pmatrix} y^2 \\ 0 \end{pmatrix} \Bigg\}.
\end{aligned} \tag{19.1.38}$$

Clearly, from this set, the vectors

$$\begin{pmatrix} -2xy \\ 0 \end{pmatrix}, \begin{pmatrix} y^2 \\ 0 \end{pmatrix}, \begin{pmatrix} x^2 \\ -2xy \end{pmatrix}, \begin{pmatrix} xy \\ -y^2 \end{pmatrix} \tag{19.1.39}$$

are linearly independent and, hence, second-order terms that are linear combinations of these four vectors can be eliminated. To determine the nature of the second-order terms that cannot be eliminated (i.e., $F_2^r(y)$), we must compute a space complementary to $L_J^{(2)}(H_2)$. This space, denoted G_2, will be two dimensional.

In computing G_2 it will be useful to first obtain a matrix representation for the linear operator $L_J^{(2)}(\cdot)$. This is done with respect to the basis given in (19.1.36) by constructing the columns of the matrix from the coefficients multiplying each basis element that are obtained when $L_J^{(2)}(\cdot)$ acts individually on each basis element of H_2 given in (19.1.36). Using (19.1.37), the matrix representation of $L_J^{(2)}(\cdot)$ is given by

$$\begin{pmatrix} 0 & 0 & 0 & 1 & 0 & 0 \\ -2 & 0 & 0 & 0 & 1 & 0 \\ 0 & -1 & 0 & 0 & 0 & 1 \\ 0 & 0 & 0 & 0 & 0 & 0 \\ 0 & 0 & 0 & -2 & 0 & 0 \\ 0 & 0 & 0 & 0 & -1 & 0 \end{pmatrix}. \tag{19.1.40}$$

One way of finding a complementary space G_2 would be to find two "6-vectors" that are linearly independent and orthogonal (using the standard inner product in $\mathbb{R}^6$) to each column of the matrix (19.1.40), or, in other words, two linearly independent left eigenvectors of zero for (19.1.40). Due to the fact that most entries of (19.1.40) are zero, this is an easy calculation, and two such vectors are found to be

$$\begin{pmatrix} 1 \\ 0 \\ 0 \\ 0 \\ \frac{1}{2} \\ 0 \end{pmatrix}, \begin{pmatrix} 0 \\ 0 \\ 0 \\ 1 \\ 0 \\ 0 \end{pmatrix}. \tag{19.1.41}$$

Hence, the vectors

$$\begin{pmatrix} x^2 \\ \frac{1}{2}xy \end{pmatrix}, \begin{pmatrix} 0 \\ x^2 \end{pmatrix} \tag{19.1.42}$$

span a two-dimensional subspace of H_2 that is complementary to $L_J^{(2)}(H_2)$. This implies that the normal form through second-order is given by

$$\begin{aligned} \dot{x} &= y + a_1 x^2 + \mathcal{O}(3), \\ \dot{y} &= a_2 xy + a_3 x^2 + \mathcal{O}(3), \end{aligned} \tag{19.1.43}$$

where a_1, a_2, and a_3 represent constants.

Now our choice of G_2 is certainly not unique. Another choice might be

$$G_2 = \text{span}\left\{ \begin{pmatrix} x^2 \\ 0 \end{pmatrix}, \begin{pmatrix} 0 \\ x^2 \end{pmatrix} \right\}. \tag{19.1.44}$$

This complementary space can be obtained by taking the vector

$$\begin{pmatrix} x^2 \\ \frac{1}{2}xy \end{pmatrix} \tag{19.1.45}$$

given in (19.1.42) and adding to it the vector

$$\begin{pmatrix} \frac{1}{4}x^2 \\ -\frac{1}{2}xy \end{pmatrix} \tag{19.1.46}$$

contained in $L_J^{(2)}(H_2)$. This gives the vector

$$\begin{pmatrix} \frac{5}{4}x^2 \\ 0 \end{pmatrix}, \tag{19.1.47}$$

(and the multiplicative constant $\frac{5}{4}$ is irrelevant). For the other basis element of the complementary space, we simply retain the vector

$$\begin{pmatrix} 0 \\ x^2 \end{pmatrix} \tag{19.1.48}$$

given in (19.1.42). With this choice of G_2 the normal form becomes

$$\begin{aligned} \dot{x} &= y + a_1 x^2 + \mathcal{O}(3), \\ \dot{y} &= a_2 x^2 + \mathcal{O}(3). \end{aligned} \tag{19.1.49}$$

This normal form near a fixed point of a planar vector field with linear part given by (19.1.35) was first studied by Takens [1974].

Another possibility for G_2 is given by

$$G_2 = \text{span}\left\{ \begin{pmatrix} 0 \\ x^2 \end{pmatrix}, \begin{pmatrix} 0 \\ xy \end{pmatrix} \right\}, \tag{19.1.50}$$

where the second vector is obtained obtained by subtracting the third vector in (19.1.39) from the first vector in (19.1.42). With this choice of G_2 the normal form becomes

$$\begin{aligned} \dot{x} &= y + \mathcal{O}(3), \\ \dot{y} &= a_1 x^2 + b_2 xy + \mathcal{O}(3); \end{aligned} \tag{19.1.51}$$

this is the normal form for a vector field on $\mathbb{R}^2$ near a fixed point with linear part given by (19.1.35) that was first studied by Bogdanov [1975].

End of Example 19.1.2

19.2 Normal Forms for Vector Fields with Parameters

Now we want to extend the normal form techniques to systems with parameters. Consider the vector field

$$\dot{x} = f(x, \mu), \qquad x \in \mathbb{R}^n, \quad \mu \in I \subset \mathbb{R}^p, \tag{19.2.1}$$

where I is some open set in $\mathbb{R}^p$ and f is $\mathbf{C}^r$ in each variable. Suppose that

$$f(0,0) = 0 \tag{19.2.2}$$

(note: the reader should recall from the beginning of Section 19.1 that there is no loss of generality in assuming that the fixed point is located at $(x,\mu) = (0,0)$). The goal is to transform (19.2.1) into normal form near the fixed point in both phase space and parameter space. The most straightforward way to put (19.2.1) into normal form would be to follow the same procedure as for systems with no parameters except to allow the coefficients of the transformation to depend on the parameters. Rather than develop the general theory along these lines, we illustrate the idea with a specific example which will be of much use later on.

19.2A Normal Form for The Poincaré-Andronov-Hopf Bifurcation

Suppose $x \in \mathbb{R}^2$ and $Df(0,0)$ has two pure imaginary eigenvalues $\lambda(0) = \pm i\omega(0)$. Then we can find a linear transformation which puts $D_x f(0,\mu)$ in the following form

$$D_x f(0,\mu) = \begin{pmatrix} \text{Re } \lambda(\mu) & -\text{Im } \lambda(\mu) \\ \text{Im } \lambda(\mu) & \text{Re } \lambda(\mu) \end{pmatrix} \tag{19.2.3}$$

for μ sufficiently small. Also, by the implicit function theorem, the fixed point varies in a $\mathbf{C}^r$ manner with μ (for μ sufficiently small) such that, if necessary, we can introduce a parameter-dependent coordinate transformation so that $x = 0$ is a fixed point for all μ sufficiently small. We will assume that this has been done.

Letting

$$\begin{aligned} \text{Re } \lambda(\mu) &= |\lambda(\mu)| \cos(2\pi\theta(\mu)), \\ \text{Im } \lambda(\mu) &= |\lambda(\mu)| \sin(2\pi\theta(\mu)), \end{aligned} \tag{19.2.4}$$

it is easy to see that (19.2.3) can be put in the form

$$D_x f(0,\mu) = |\lambda(\mu)| \begin{pmatrix} \cos 2\pi\theta(\mu) & -\sin 2\pi\theta(\mu) \\ \sin 2\pi\theta(\mu) & \cos 2\pi\theta(\mu) \end{pmatrix}. \tag{19.2.5}$$

Now we want to put the following equation into normal form

$$\begin{aligned} \begin{pmatrix} \dot{x} \\ \dot{y} \end{pmatrix} = |\lambda(\mu)| &\begin{pmatrix} \cos 2\pi\theta(\mu) & -\sin 2\pi\theta(\mu) \\ \sin 2\pi\theta(\mu) & \cos 2\pi\theta(\mu) \end{pmatrix} \begin{pmatrix} x \\ y \end{pmatrix} \\ &+ \begin{pmatrix} f^1(x,y;\mu) \\ f^2(x,y;\mu) \end{pmatrix}, \qquad (x,y) \in \mathbb{R}^2, \end{aligned} \tag{19.2.6}$$

where the f^i are nonlinear in x and y.

We remark that we will frequently omit the explicit parameter dependence of λ, θ, and possibly other quantities from time to time for the sake of a less cumbersome notation.

In dealing with linear parts of vector fields having complex eigenvalues, it is often easier to calculate the normal form using complex coordinates. We will illustrate this procedure for this example.

We make the following linear transformation

$$\begin{pmatrix} x \\ y \end{pmatrix} = \frac{1}{2}\begin{pmatrix} 1 & 1 \\ -i & i \end{pmatrix}\begin{pmatrix} z \\ \bar{z} \end{pmatrix}; \qquad \begin{pmatrix} z \\ \bar{z} \end{pmatrix} = \begin{pmatrix} 1 & i \\ 1 & -i \end{pmatrix}\begin{pmatrix} x \\ y \end{pmatrix} \tag{19.2.7}$$

to obtain

$$\begin{pmatrix} \dot{z} \\ \dot{\bar{z}} \end{pmatrix} = |\lambda| \begin{pmatrix} e^{2\pi i\theta} & 0 \\ 0 & e^{-2\pi i\theta} \end{pmatrix}\begin{pmatrix} z \\ \bar{z} \end{pmatrix} + \begin{pmatrix} F^1(z,\bar{z};\mu) \\ F^2(z,\bar{z};\mu) \end{pmatrix}, \tag{19.2.8}$$

where

$$F^1(z,\bar{z};\mu) = f^1(x(z,\bar{z}),y(z,\bar{z});\mu) + if^2(x(z,\bar{z}),y(z,\bar{z});\mu),$$

$$F^2(z,\bar{z};\mu) = f^1(x(z,\bar{z}),y(z,\bar{z});\mu) - if^2(x(z,\bar{z}),y(z,\bar{z});\mu).$$

Therefore, all we really need to study is

$$\dot{z} = |\lambda|\, e^{2\pi i\theta} z + F^1(z,\bar{z};\mu), \tag{19.2.9}$$

since the second component of (19.2.8) is simply the complex conjugate of the first component. We will therefore put (19.2.9) in normal form and then transform back to the x, y variables.

Expanding (19.2.9) in a Taylor series gives

$$\dot{z} = |\lambda|\, e^{2\pi i\theta} z + F_2 + F_3 + \cdots + F_{r-1} + \mathcal{O}(|z|^r, |\bar{z}|^r), \tag{19.2.10}$$

where the F_j are homogeneous polynomials in $z, \bar{z}$ of order j *whose coefficients depend on* μ.

Simplify Second-Order Terms

We make the transformation

$$z \longmapsto z + h_2(z,\bar{z}), \tag{19.2.11}$$

where $h_2(z,\bar{z})$ is second-order in z and $\bar{z}$ *with coefficients depending on* μ. We neglect displaying the explicit μ dependence.

Under (19.2.11), (19.2.10) becomes

$$\dot{z}\left(1 + \frac{\partial h_2}{\partial z}\right) + \frac{\partial h_2}{\partial \bar{z}}\dot{\bar{z}} = \lambda z + \lambda h_2 + F_2(z,\bar{z}) + \mathcal{O}(3) \tag{19.2.12}$$

or

$$\dot{z} = \left(1 + \frac{\partial h_2}{\partial z}\right)^{-1} \left[\lambda z + \lambda h_2 - \frac{\partial h_2}{\partial \bar{z}} \dot{\bar{z}} + F_2 + \mathcal{O}(3)\right].$$

Note that we have

$$\dot{\bar{z}} = \bar{\lambda}\bar{z} + \bar{F}_2 + \mathcal{O}(3) \tag{19.2.13}$$

and, for $z, \bar{z}$ sufficiently small

$$\left(1 + \frac{\partial h_2}{\partial z}\right)^{-1} = 1 - \frac{\partial h_2}{\partial z} + \mathcal{O}(2). \tag{19.2.14}$$

Thus, using (19.2.13) and (19.2.14), (19.2.12) becomes

$$\dot{z} = \lambda z - \lambda \frac{\partial h_2}{\partial z} z - \bar{\lambda} \frac{\partial h_2}{\partial \bar{z}} \bar{z} + \lambda h_2 + F_2 + \mathcal{O}(3), \tag{19.2.15}$$

so that we can eliminate all second-order terms if

$$\lambda h_2 - \left(\lambda \frac{\partial h_2}{\partial z} z + \bar{\lambda} \frac{\partial h_2}{\partial \bar{z}} \bar{z}\right) + F_2 = 0. \tag{19.2.16}$$

Equation (19.2.16) is very similar to Eq. (19.1.17) derived earlier. The map

$$h_2 \longmapsto \lambda h_2 - \left(\lambda \frac{\partial h_2}{\partial z} \bar{z} + \bar{\lambda} \frac{\partial h_2}{\partial \bar{z}} \bar{z}\right) \tag{19.2.17}$$

is a linear map of the space of homogeneous polynomials in z and $\bar{z}$ of degree 2 into itself. We denote this space by H_2. F_2 can also be viewed as an element in this space. Thus, solving (19.2.16) is a problem from linear algebra.

Now we have

$$H_2 = \text{span}\left\{z^2, z\bar{z}, \bar{z}^2\right\}. \tag{19.2.18}$$

Computing the action of the linear map (19.2.17) on each of these basis elements gives

$$\begin{aligned}
\lambda z^2 - \left[\lambda \left(\frac{\partial}{\partial z} z^2\right) z + \bar{\lambda} \left(\frac{\partial}{\partial \bar{z}} z^2\right) \bar{z}\right] &= -\lambda z^2, \\
\lambda z\bar{z} - \left[\lambda \left(\frac{\partial}{\partial z} z\bar{z}\right) z + \bar{\lambda} \left(\frac{\partial}{\partial \bar{z}} z\bar{z}\right) \bar{z}\right] &= -\bar{\lambda} z\bar{z}, \\
\lambda \bar{z}^2 - \left[\lambda \left(\frac{\partial}{\partial z} \bar{z}^2\right) z + \bar{\lambda} \left(\frac{\partial}{\partial \bar{z}} \bar{z}^2\right) \bar{z}\right] &= (\lambda - 2\bar{\lambda})\bar{z}^2.
\end{aligned}$$

Thus, (19.2.17) is diagonal in this basis with a matrix representation given by

$$\begin{pmatrix} -\lambda(\mu) & 0 & 0 \\ 0 & -\bar{\lambda}(\mu) & 0 \\ 0 & 0 & \lambda(\mu) - 2\bar{\lambda}(\mu) \end{pmatrix}. \tag{19.2.19}$$

For $\mu = 0$, it should be clear that $\lambda(0) \neq 0$ and $\lambda(0) = -\bar{\lambda}(0)$; hence, for μ sufficiently small, $\lambda(\mu) \neq 0$ and $\lambda(\mu) - 2\bar{\lambda}(\mu) \neq 0$. Therefore, for μ sufficiently small, all second-order terms can be eliminated from (19.2.10).

Simplify Third-Order Terms

We have

$$\dot{z} = \lambda z + F_3 + \mathcal{O}(4). \tag{19.2.20}$$

Let $z \longmapsto z + h_3(z, \bar{z})$; then we obtain

$$\begin{aligned}\dot{z} &= \left(1 + \frac{\partial h_3}{\partial z}\right)^{-1} \left[\lambda z - \frac{\partial h_3}{\partial \bar{z}}\dot{\bar{z}} + \lambda h_3 + F_3(z, \bar{z}) + \mathcal{O}(4)\right] \\ &= \lambda z - \lambda \frac{\partial h_3}{\partial z} z - \bar{\lambda}\frac{\partial h_3}{\partial \bar{z}}\bar{z} + \lambda h_3 + F_3 + \mathcal{O}(4).\end{aligned}$$

We want to solve

$$\lambda h_3 - \lambda \frac{\partial h_3}{\partial z} z - \bar{\lambda}\frac{\partial h_3}{\partial \bar{z}}\bar{z} + F_3 = 0. \tag{19.2.21}$$

Note that we have

$$H_3 = \text{span}\left\{z^3, z^2\bar{z}, z\bar{z}^2, \bar{z}^3\right\}. \tag{19.2.22}$$

We compute the action of the linear map

$$h_3 \longmapsto \lambda h_3 - \left[\lambda \frac{\partial h_3}{\partial z} z + \bar{\lambda}\frac{\partial h_3}{\partial \bar{z}}\bar{z}\right] \tag{19.2.23}$$

on each basis element of H_3 and obtain

$$\begin{aligned}\lambda z^3 - \left[\lambda\left(\frac{\partial}{\partial z} z^3\right) z + \bar{\lambda}\left(\frac{\partial}{\partial \bar{z}} z^3\right)\bar{z}\right] &= -2\lambda z^3, \\ \lambda z^2\bar{z} - \left[\lambda\left(\frac{\partial}{\partial z} z^2\bar{z}\right) z + \bar{\lambda}\left(\frac{\partial}{\partial \bar{z}} z^2\bar{z}\right)\bar{z}\right] &= -\left(\lambda + \bar{\lambda}\right) z^2\bar{z}, \\ \lambda z\bar{z}^2 - \left[\lambda\left(\frac{\partial}{\partial z} z\bar{z}^2\right) z + \bar{\lambda}\left(\frac{\partial}{\partial \bar{z}} z\bar{z}^2\right)\bar{z}\right] &= -2\bar{\lambda} z\bar{z}^2, \\ \lambda \bar{z}^3 - \left[\lambda\left(\frac{\partial}{\partial z} \bar{z}^3\right) z + \bar{\lambda}\left(\frac{\partial}{\partial \bar{z}} \bar{z}^3\right)\bar{z}\right] &= \left(\lambda - 3\bar{\lambda}\right)\bar{z}^3.\end{aligned} \tag{19.2.24}$$

Therefore, a matrix representation for (19.2.23) is given by

$$\begin{pmatrix} -2\lambda(\mu) & 0 & 0 & 0 \\ 0 & -(\lambda(\mu) + \bar{\lambda}(\mu)) & 0 & 0 \\ 0 & 0 & -2\bar{\lambda}(\mu) & 0 \\ 0 & 0 & 0 & \lambda(\mu) - 3\bar{\lambda}(\mu) \end{pmatrix}. \tag{19.2.25}$$

Now, at $\mu = 0$,

$$\lambda(0) + \bar{\lambda}(0) = 0; \tag{19.2.26}$$

however, none of the remaining columns in (19.2.25) are identically zero at $\mu = 0$. Therefore, for μ sufficiently small, third-order terms that are not of the form

$$z^2\bar{z} \tag{19.2.27}$$

can be eliminated.

Thus, the normal form through third-order is given by

$$\dot{z} = \lambda z + c(\mu) z^2 \bar{z} + \mathcal{O}(4), \tag{19.2.28}$$

where $c(\mu)$ is a constant depending on μ.

Next we simplify the fourth-order terms. However, notice that, at each order, simplification depends on whether

$$\lambda h - \left(\lambda z \frac{\partial h}{\partial z} + \bar{\lambda} \bar{z} \frac{\partial h}{\partial \bar{z}} \right) = 0 \tag{19.2.29}$$

for some $h = z^n \bar{z}^m$, where $m + n$ is the order of the term that we want to simplify. Substituting this into (19.2.29) gives

$$\begin{aligned} \lambda z^n \bar{z}^m - \left(n\lambda z^n \bar{z}^m + m\bar{\lambda} z^n \bar{z}^m \right) = 0, \\ \left(\lambda - n\lambda - m\bar{\lambda} \right) z^n \bar{z}^m = 0. \end{aligned} \tag{19.2.30}$$

At $\mu = 0$, $\lambda = -\bar{\lambda}$; hence we must not have

$$1 + m - n = 0. \tag{19.2.31}$$

It is easily seen that this can never happen if m and n are even numbers. Therefore, all even-order terms can be removed, and the normal form is given by

$$\dot{z} = \lambda z + c(\mu) z^2 \bar{z} + \mathcal{O}(5) \tag{19.2.32}$$

for μ in some neighborhood of $\mu = 0$.

We can write this in cartesian coordinates as follows. Let $\lambda(\mu) = \alpha(\mu) + i\omega(\mu)$, and $c(\mu) = a(\mu) + ib(\mu)$. Then

$$\begin{aligned} \dot{x} &= \alpha x - \omega y + (ax - by)(x^2 + y^2) + \mathcal{O}(5), \\ \dot{y} &= \omega x + \alpha y + (bx + ay)(x^2 + y^2) + \mathcal{O}(5). \end{aligned} \tag{19.2.33}$$

In polar coordinates, it can be expressed as

$$\begin{aligned} \dot{r} &= \alpha r + a r^3 + \cdots, \\ \dot{\theta} &= \omega + b r^2 + \cdots. \end{aligned} \tag{19.2.34}$$

We will study the dynamics associated with this normal form in great detail in Chapter 20 when we study the Poincaré–Andronov–Hopf bifurcation.

Differentiability

We make the important remark that in order to obtain the normal form (19.2.32) the vector field must be at least $\mathbf{C}^5$.

19.3 Normal Forms for Maps

We now want to develop the method of normal forms for maps. We will see that it is very much the same as for vector fields with only a slight modification.

Suppose we have a $\mathbf{C}^r$ map which has a fixed point at the origin and is written as follows

$$x \longmapsto Jx + F_2(x) + \cdots + F_{r-1}(x) + \mathcal{O}(|x|^r)$$

or

$$x_{n+1} = Jx_n + F_2(x_n) + \cdots + F_{r-1}(x_n) + \mathcal{O}(|x_n|^r), \tag{19.3.1}$$

where $x \in \mathbb{R}^n$, and the F_j are vector-valued homogeneous polynomials of degree j. We introduce the change of coordinates

$$x = y + h_2(y), \tag{19.3.2}$$

where $h_2(y)$ is a vector valued homogeneous polynomial of degree 2. After this transformation (19.3.1) becomes

$$x_{n+1} = y_{n+1} + h_2(y_{n+1}) = Jy_n + Jh_2(y_n) + F_2(y_n) + \mathcal{O}(3)$$

or

$$(\mathrm{id} + h_2)(y_{n+1}) = Jy_n + Jh_2(y_n) + F_2(y_n) + \mathcal{O}(3). \tag{19.3.3}$$

Now, for y sufficiently small, the function $(\mathrm{id} + h_2)(\cdot)$ is invertible so that (19.3.3) can be written as

$$y_{n+1} = (\mathrm{id} + h_2)^{-1}\big(Jy_n + Jh_2(y_n) + F_2(y_n) + \mathcal{O}(3)\big). \tag{19.3.4}$$

For y sufficiently small, $(\mathrm{id} + h_2)^{-1}(\cdot)$ can be expressed as follows (see Exercise 3)

$$(\mathrm{id} + h_2)^{-1}(\cdot) = (\mathrm{id} - h_2 + \mathcal{O}(4))(\cdot), \tag{19.3.5}$$

so that (19.3.4) becomes

$$y_{n+1} = Jy_n + Jh_2(y_n) - h_2(Jy_n) + F_2(y_n) + \mathcal{O}(3). \tag{19.3.6}$$

Thus, we can eliminate the second-order terms if

$$Jh_2(y) - h_2(Jy) + F_2(y) = 0. \tag{19.3.7}$$

(Compare this with the situation for vector fields.)

This process can be repeated, but it should be clear that the ability to eliminate terms of order j depends upon the operator

$$h_j(y) \longmapsto Jh_j(y) - h_j(Jy) \equiv M_J^{(j)}(h_j(y)), \tag{19.3.8}$$

which (the reader should verify) is a linear map of H_j into H_j, where H_j is the linear vector space of vector-valued homogeneous polynomials of degree j. The analysis proceeds as in the case for vector fields except the equation to solve is slightly different (it has a term involving a composition rather than a matrix multiplication). Let us consider an example which can be viewed as the discrete time analog of this example.

19.3a Normal Form for the Naimark-Sacker Torus Bifurcation

Suppose we have a $\mathbf{C}^r$ map of the plane

$$x \longmapsto f(x,\mu), \qquad x \in \mathbb{R}^2, \quad \mu \in I \in \mathbb{R}^p, \tag{19.3.9}$$

where I is some open set in $\mathbb{R}^p$. Suppose also that (19.3.9) has a fixed point at $x = 0$ for μ sufficiently small (cf. Example 19.2a) and that the eigenvalues of $Df(0,\mu)$, μ small, are given by

$$\lambda_1 = |\lambda(\mu)|\, e^{2\pi i\theta(\mu)}, \qquad \lambda_2 = |\lambda(\mu)|\, e^{-2\pi i\theta(\mu)}, \tag{19.3.10}$$

i.e., $\bar{\lambda}_1 = \lambda_2$. Furthermore, we assume that at $\mu = 0$ the two eigenvalues lie on the unit circle, i.e., $|\lambda(0)| = 1$. As in Example 19.2a, with a linear change of coordinates we can put the map in the form

$$\begin{pmatrix} x \\ y \end{pmatrix} \longmapsto |\lambda| \begin{pmatrix} \cos 2\pi\theta & -\sin 2\pi\theta \\ \sin 2\pi\theta & \cos 2\pi\theta \end{pmatrix} \begin{pmatrix} x \\ y \end{pmatrix} + \begin{pmatrix} f^1(x,y;\mu) \\ f^2(x,y;\mu) \end{pmatrix}, \tag{19.3.11}$$

where $f^i(x,y;\mu)$ are nonlinear in x and y.

Utilizing the same complex linear transformation as in Example 19.2a, we reduce the study of the two-dimensional map to the study of the one-dimensional complex map

$$z \longmapsto \lambda(\mu)z + F^1(z,\bar{z};\mu), \tag{19.3.12}$$

where $F^1 = f^1 + if^2$ and $\lambda(\mu) = |\lambda(\mu)|\, e^{2\pi i\theta(\mu)}$.

We want to put this complex map into normal form. As a preliminary transformation, we expand $F^1(z,\bar{z};\mu)$ in a Taylor expansion in z and $\bar{z}$ with *coefficients depending on* μ so that (19.3.12) becomes

$$z_{n+1} = \lambda(\mu)z_n + F_2 + \cdots + F_{r-1} + \mathcal{O}(r), \tag{19.3.13}$$

where F_j is a homogeneous polynomial of order j in z and $\bar{z}$.

Simplify Second-Order Terms

Introducing the transformation

$$z \longmapsto z + h_2(z,\bar{z}), \tag{19.3.14}$$

where $h_2(z,\bar{z})$ is a second-order polynomial in z and $\bar{z}$ with *coefficients depending on* μ, (19.3.13) becomes

$$z_{n+1} + h_2(z_{n+1},\bar{z}_{n+1}) = \lambda z_n + \lambda h_2(z_n,\bar{z}_n) + F_2(z_n,\bar{z}_n) + \mathcal{O}(3)$$

or

$$z_{n+1} = \lambda z_n + \lambda h_2(z_n,\bar{z}_n) - h_2(z_{n+1},\bar{z}_{n+1}) + F_2(z_n,\bar{z}_n) + \mathcal{O}(3). \tag{19.3.15}$$

Let us simplify further the term

$$h_2(z_{n+1}, \bar{z}_{n+1}) \tag{19.3.16}$$

in the right-hand side of (19.3.15). Clearly we have

$$\begin{aligned} z_{n+1} &= \lambda z_n + \mathcal{O}(2), \\ \bar{z}_{n+1} &= \bar{\lambda}\bar{z}_n + \mathcal{O}(2), \end{aligned} \tag{19.3.17}$$

so that

$$h_2(z_{n+1}, \bar{z}_{n+1}) = h_2(\lambda z_n, \bar{\lambda}\bar{z}_n) + \mathcal{O}(3). \tag{19.3.18}$$

Substituting (19.3.18) into (19.3.15) gives

$$z_{n+1} = \lambda z_n + \lambda h_2(z_n, \bar{z}_n) - h_2(\lambda z_n, \bar{\lambda}\bar{z}_n) + F_2 + \mathcal{O}(3). \tag{19.3.19}$$

Therefore, we can eliminate all second-order terms provided we can find $h_2(z, \bar{z})$ so that

$$\lambda h_2(z, \bar{z}) - h_2(\lambda z, \bar{\lambda}\bar{z}) + F_2 = 0. \tag{19.3.20}$$

As in all other situations involving normal forms that we have encountered thus far, this involves a problem from elementary linear algebra. This is because the map

$$h_2(z, \bar{z}) \longmapsto \lambda h_2(z, \bar{z}) - h_2(\lambda z, \bar{\lambda}\bar{z}) \tag{19.3.21}$$

is a linear map of H_2 into H_2 where

$$H_2 = \text{span}\left\{z^2, z\bar{z}, \bar{z}^2\right\}. \tag{19.3.22}$$

In order to compute a matrix representation for (19.3.21) we need to compute the action of (19.3.21) on each basis element in (19.3.22). This is given as follows

$$\begin{aligned} \lambda z^2 - \lambda^2 z^2 &= \lambda(1-\lambda)z^2, \\ \lambda z\bar{z} - \lambda\bar{\lambda} z\bar{z} &= \lambda(1-\bar{\lambda})z\bar{z}, \\ \lambda\bar{z}^2 - \bar{\lambda}^2\bar{z}^2 &= (\lambda - \bar{\lambda}^2)\bar{z}^2. \end{aligned} \tag{19.3.23}$$

Using (19.3.23), the matrix representation for (19.3.21) with respect to the basis (19.3.22) is

$$\begin{pmatrix} \lambda(\mu)\big(1-\lambda(\mu)\big) & 0 & 0 \\ 0 & \lambda(\mu)\big(1-\bar{\lambda}(\mu)\big) & 0 \\ 0 & 0 & \lambda(\mu) - \bar{\lambda}(\mu)^2 \end{pmatrix}. \tag{19.3.24}$$

Now, by assumption, we have

$$|\lambda(0)| = 1 \qquad \text{and} \qquad \bar{\lambda}(0) = \frac{1}{\lambda(0)}. \tag{19.3.25}$$

Therefore, (19.3.24) is invertible at $\mu = 0$ provided

$$\begin{aligned} &\lambda(0) \neq 1, \\ &\lambda(0) \neq \frac{1}{\lambda(0)^2} \Rightarrow \lambda(0)^3 \neq 1. \end{aligned} \tag{19.3.26}$$

If (19.3.26) are satisfied at $\mu = 0$, then they are also satisfied in a sufficiently small neighborhood of $\mu = 0$. Therefore, if (19.3.26) are satisfied, then all second-order terms can be eliminated from the normal form for μ sufficiently small.

Simplify Third-Order Terms

Using an argument exactly like that given above, third-order terms can be eliminated provided

$$\lambda h_3(z, \bar{z}) - h_3(\lambda z, \bar{\lambda}\bar{z}) + F_3 = 0. \tag{19.3.27}$$

The map

$$h_3(z, \bar{z}) \longmapsto \lambda h_3(z, \bar{z}) - h_3(\lambda z, \bar{\lambda}\bar{z}) \tag{19.3.28}$$

is a linear map of H_3 into H_3 where

$$H_3 = \text{span}\left\{z^3, z^2\bar{z}, z\bar{z}^2, \bar{z}^3\right\}. \tag{19.3.29}$$

The action of (19.3.28) on each element of (19.3.29) is given by

$$\begin{aligned} \lambda z^3 - \lambda^3 z^3 &= \lambda(1 - \lambda^2)z^3, \\ \lambda z^2\bar{z} - \lambda^2\bar{\lambda}z^2\bar{z} &= \lambda(1 - \lambda\bar{\lambda})z^2\bar{z}, \\ \lambda z\bar{z}^2 - \bar{\lambda}^2\lambda z\bar{z}^2 &= \lambda(1 - \bar{\lambda}^2)z\bar{z}^2, \\ \lambda\bar{z}^3 - \bar{\lambda}^3\bar{z}^3 &= (\lambda - \bar{\lambda}^3)\bar{z}^3. \end{aligned} \tag{19.3.30}$$

Thus, a matrix representation of (19.3.28) with respect to the basis (19.3.29) is given by

$$\begin{pmatrix} \lambda(\mu)\big(1 - \lambda(\mu)^2\big) & 0 & 0 & 0 \\ 0 & \lambda(\mu)\big(1 - \lambda(\mu)\bar{\lambda}(\mu)\big) & 0 & 0 \\ 0 & 0 & \lambda(\mu)\big(1 - \bar{\lambda}(\mu)^2\big) & 0 \\ 0 & 0 & 0 & \lambda(\mu) - \bar{\lambda}(\mu)^3 \end{pmatrix} \tag{19.3.31}$$

Recall that at $\mu = 0$ we have

$$|\lambda(0)| = 1, \qquad \bar{\lambda}(0) = \frac{1}{\lambda(0)}, \tag{19.3.32}$$

so that at $\mu = 0$ the second column of (19.3.31) is all zero's. The reader can easily check that the remaining columns are all linearly independent at $\mu = 0$ provided

$$\lambda^2(0) \neq 1, \qquad \lambda^4(0) \neq 1. \tag{19.3.33}$$

This situation will also hold for μ sufficiently small. Therefore, the normal form is as follows

$$z \longmapsto \lambda(\mu)z + c(\mu)z^2\bar{z} + \mathcal{O}(4), \tag{19.3.34}$$

where $c(\mu)$ is a constant, provided

$$\lambda^n(0) \neq 1, \qquad n = 1, 2, 3, 4$$

for μ sufficiently small.

More generally, simplification at order k depends on how the linear operator

$$h_k(z, \bar{z}) \longmapsto \lambda h_k(z, \bar{z}) - h_k(\lambda z, \bar{\lambda}\bar{z}) \tag{19.3.35}$$

acts on elements like $h = z^n\bar{z}^m$ where $m + n$ is the order of the term one wishes to simplify. Substituting this into the above equation gives

$$\lambda z^n\bar{z}^m - \lambda^n\bar{\lambda}^m z^n\bar{z}^m = \lambda(1 - \lambda^{n-1}\bar{\lambda}^m)z^n z^m. \tag{19.3.36}$$

At $\mu = 0$, $\bar{\lambda} = 1/\lambda$; hence, we cannot have

$$\lambda^{n-m-1}(0) = 1. \tag{19.3.37}$$

We leave it to the reader to work out general conditions for the elimination of higher order terms based on (19.3.37).

Differentiability

We make the important remark that in order to obtain the normal form (19.3.34) the map must be at least $\mathbf{C}^4$.

19.4 Exercises

1. Prove that H_k is a linear vector space.
2. Suppose $h_k(x) \in H_k$ ($x \in \mathbb{R}^n$), and J is an $n \times n$ matrix of real numbers. Then prove that the maps

   a) $h_k(x) \mapsto Jh_k(x) - Dh_k(x)Jx \equiv L_J^{(k)}(h_k(x))$,

   b) $h_k(x) \mapsto Jh_k(x) - h_k(Jx) \equiv M_J^{(k)}(h_k(x))$,

   are linear maps of H_k into H_k.
3. Argue that, for $y \in \mathbb{R}^n$ sufficiently small,

   a) $(\mathrm{id} + Dh_k(y))^{-1}$ exists

   and

   b) $(\mathrm{id} + Dh_k(y))^{-1} = \mathrm{id} - Dh_k(y) + \cdots$

   for $h_k(y) \in H_k$. Similarly, show that for $y \in \mathbb{R}^n$ sufficiently small

   c) $(\mathrm{id} + h_k)^{-1}(y)$ exists

and

d) $(\mathrm{id}+h_k)^{-1}(y) = (\mathrm{id}-h_k+\cdots)(y)$.

4. Compute a normal form for a map in the neighborhood of a fixed point having the linear part

$$\begin{pmatrix} 1 & 1 \\ 0 & 1 \end{pmatrix}$$

through second-order terms.

Compare the resulting normal form with the normal form of a vector field near a fixed point having linear part

$$\begin{pmatrix} 0 & 1 \\ 0 & 0 \end{pmatrix}$$

(see Example 19.1.2). Explain the results.

5. Consider a third-order autonomous vector field near a fixed point having linear part

$$\begin{pmatrix} 0 & -\omega & 0 \\ \omega & 0 & 0 \\ 0 & 0 & 0 \end{pmatrix}$$

with respect to the standard basis in $\mathbb{R}^3$. Show that in cylindrical coordinates a normal form is given by

$$\begin{aligned} \dot{r} &= a_1 rz + a_2 r^3 + a_3 rz^2 + \mathcal{O}(4), \\ \dot{z} &= b_1 r^2 + b_2 z^2 + b_3 r^2 z + b_4 z^3 + \mathcal{O}(4), \\ \dot{\theta} &= \omega + c_1 z + \mathcal{O}(2), \end{aligned}$$

where a_1, a_2, a_3, b_1, b_2, b_3, b_4, and c_1 are constants. (*Hint:* lump the two coordinates associated with the block

$$\begin{pmatrix} 0 & -\omega \\ \omega & 0 \end{pmatrix}$$

into a single complex coordinate.)

6. Consider a four-dimensional $\mathbf{C}^r$ (r as large as necessary) vector field having a fixed point where the matrix associated with the linearization is given by

$$\begin{pmatrix} 0 & -\omega_1 & 0 & 0 \\ \omega_1 & 0 & 0 & 0 \\ 0 & 0 & 0 & -\omega_2 \\ 0 & 0 & \omega_2 & 0 \end{pmatrix}.$$

Compute the normal form through third order. (*Hint:* use two complex variables.) You should find that certain "resonance" problems arise; namely, the normal form will depend on $m\omega_1 + n\omega_2 \neq 0$, $|m| + |n| \leq 4$. Give the normal form for the cases

a) $m\omega_1 + n\omega_2 = 0, \qquad |m| + |n| = 1.$

b) $m\omega_1 + n\omega_2 = 0, \qquad |m| + |n| = 2.$

c) $m\omega_1 + n\omega_2 = 0, \qquad |m| + |n| = 3.$

d) $m\omega_1 + n\omega_2 = 0, \qquad |m| + |n| = 4.$

e) $m\omega_1 + n\omega_2 \neq 0, \qquad |m| + |n| \leq 4.$

7. Consider the normal form for a map of $\mathbb{R}^2$ in the neighborhood of a fixed point where the eigenvalues of the matrix associated with the linearization, denoted λ_1 and λ_2, are complex conjugates, i.e., $\lambda_1 = \overline{\lambda}_2$, and have modulus one, i.e., $|\lambda_1| = |\lambda_2| \equiv |\lambda| = 1$ (cf. Example 19.3a). Compute the normal form for the cases.

a) $\lambda = 1$.

b) $\lambda^2 = 1$.

c) $\lambda^3 = 1$.

d) $\lambda^4 = 1$.

8. Compute the normal form of a map of $\mathbb{R}^2$ in the neighborhood of a fixed point where the matrix associated with the linearization has the following form

a) $\begin{pmatrix} 1 & 1 \\ 0 & 1 \end{pmatrix}$.

b) $\begin{pmatrix} 1 & 0 \\ 0 & 1 \end{pmatrix}$.

c) $\begin{pmatrix} -1 & 1 \\ 0 & -1 \end{pmatrix}$.

d) $\begin{pmatrix} -1 & 0 \\ 0 & -1 \end{pmatrix}$.

Compare your normal forms with those obtained in parts a) and b) of Exercise 7.

9. Consider a $\mathbf{C}^r$ $(r \geq 2)$ vector field

$$\dot{x} = f(x, \mu), \qquad x \in \mathbb{R}^2, \quad \mu \in \mathbb{R}^1,$$

defined on a sufficiently large open set in $\mathbb{R}^2 \times \mathbb{R}^1$. Suppose that $(x, \mu) = (0, 0)$ is a fixed point of this vector field and that $D_x f(0, 0)$ has a pair of purely imaginary eigenvalues.

a) Show that there exists a curve of fixed points of the vector field, denoted $x(\mu)$, $x(0) = 0$, for μ sufficiently small.

b) By using this curve of fixed points as a parameter-dependent coordinate transformation, show that one can choose coordinates so that the origin in phase space remains a fixed point for μ sufficiently small.

19.5 The Elphick-Tirapegui-Brachet-Coullet-Iooss Normal Form

In this section we will describe the work of Elphick et al. [1987]. A key feature of their work is that they introduce an inner product on H_k. This inner product can be used to construct the *orthogonal* complement to $L_J^{(k)}$. The resulting normal form has a number of nice properties. Moreover, their method seems to be computationally very efficient. Similar work by Cushman and Sanders [1986] appeared simultaneously, however all of the results described in this section are taken from Elphick et al. [1987].

For easier reference we recall (19.1.8), which we wish to transform into *normal form*:

$$\begin{aligned} \dot{x} &= Jx + F_2(x) + F_3(x) + \cdots + F_{r-1}(x) + \mathcal{O}(|x|^r), \\ &\equiv Jx + \mathcal{F}(x) + \mathcal{O}(|x|^r), \end{aligned} \tag{19.5.1}$$

where $F_i(x)$ represent the order i terms in the Taylor expansion of $F(x)$ and $\mathcal{F}(x)$ represents the nonlinear terms in this expansion through order $r - 1$.

19.5A An Inner Product on H_k

First we define an inner product on the scalar valued homogeneous polynomials of degree k, and then use this to construct an inner product on H_k. Let $x = (x_1, \ldots, x_n)$ and let $p(x)$, $q(x)$ denote scalar valued homogeneous polynomials in x of degree k. For example,

$$p(x) = \sum_{\substack{m_1+\cdots+m_n=k \\ m_i \in \mathbb{Z}^+ \cup \{0\}}} a_{m_1 \cdots m_n} x_1^{m_1} \cdots x_n^{m_n}, \tag{19.5.2}$$

where $\mathbb{Z}^+$ denotes the positive integers, and $a_{m_1 \cdots m_n}$ denotes a scalar. Following Bargmann [1961], Elphick et al. [1987] define the following inner product on the space of scalar valued homogeneous polynomials in x of degree k

$$\langle p, q \rangle \equiv p(\partial) q(x)|_{x=0}, \tag{19.5.3}$$

where $p(\partial)$ is the symbol for a homogeneous polynomial of degree k in $(\partial_1, \cdots, \partial_n)$ with $\partial_i \equiv \frac{\partial}{\partial x_i}$. For example, for $p(x)$ as defined in (19.5.2), we have

$$p(\partial) = \sum_{\substack{m_1+\cdots+m_n=k \\ m_i \in \mathbb{Z}^+ \cup \{0\}}} a_{m_1 \cdots m_n} \frac{\partial^{m_1}}{\partial x_1^{m_1}} \cdots \frac{\partial^{m_n}}{\partial x_n^{m_n}}. \tag{19.5.4}$$

The following example computation is instructive. Let

$$p(x) = x_1^{m_1} \cdots x_n^{m_n}, \quad q(x) = x_1^{\bar{m}_1} \cdots x_n^{\bar{m}_n}, \qquad \sum_{i=1}^n m_i = \sum_{i=1}^n \bar{m}_i.$$

Then

$$\langle p, q \rangle = \left(\frac{\partial^{m_1}}{\partial x_1^{m_1}} \cdots \frac{\partial^{m_n}}{\partial x_n^{m_n}} \right) \left(x_1^{\bar{m}_1} \cdots x_n^{\bar{m}_n} \right) = \prod_{i=1}^n \frac{\partial^{m_i}}{\partial x_i^{m_i}} x_i^{\bar{m}_i} = \prod_{i=1}^n \delta_{m_i, \bar{m}_i} m_i!.$$

There are two basic properties of this inner product that we now derive.

Property One

Let $p(x)$, $q(x)$, $r(x)$ denote scalar valued homogeneous polynomials in x of degree k. Then it follows from (19.5.3) that

$$\begin{aligned} \langle qr, p \rangle &= q(\partial) r(\partial) p(x)|_{x=0}, \\ &= r(\partial) q(\partial) p(x)|_{x=0}, \\ &= \langle r, q(\partial) p \rangle. \end{aligned} \tag{19.5.5}$$

This equation states that multiplication by the polynomial $q(x)$ is the adjoint of differentiation by $q(\partial)$.

Property Two

Another key property is the following.

Suppose $A : \mathbb{R}^n \to \mathbb{R}^n$ is a linear, invertible operator. Then the second basic property is the following

$$\langle p(Ax), q(x)\rangle = \langle p(x), q(A^*x)\rangle, \tag{19.5.6}$$

where A^* denotes the adjoint of A. We will leave the proof of this property to the exercises.

Now we construct an inner product on H_k. With respect to the chosen basis on $\mathbb{R}^n$, the corresponding coordinates of a point $x \in \mathbb{R}^n$ are denoted $x = (x_1, \ldots, x_n)$. Then, with respect to this same basis, a vector valued homogeneous polynomial of degree k (i.e., an element of H_k) is denoted $h_k(x) = \left(h_k^1(x), \ldots, h_k^n(x)\right)$, where $h_k^i(x)$ is a scalar valued homogeneous polynomial of degree k for each i. Then an inner product on H_k is defined as follows. For h_k, $g_k \in H_k$, the inner product of these two vectors is defined by

$$\langle h_k, g_k\rangle_{H_k} = \sum_{i=1}^{n} \langle h_k^i, g_k^i\rangle. \tag{19.5.7}$$

Since we are dealing with real vector fields note that A^* is the adjoint with respect to the standard Euclidean inner product on $\mathbb{R}^n$, i.e., it is the transpose of A, denoted A^T. We could have just as easily developed the theory for vector fields on $\mathbb{C}^n$. In that case A^* would be the adjoint with respect to the usual inner product on $\mathbb{C}^n$. Then the inner product (19.5.3) would be modified as follows:

$$\langle p, q\rangle \equiv p(\partial)\bar{q}(x)|_{x=0}.$$

The complex case will be useful when we have imaginary eigenvalues and perform calculations using the complexification of the real case.

19.5B The Main Theorems

With this inner product in hand, we can now prove the main results that describe the structure of the normal form.

Suppose h_k, $g_k \in H_k$ and $A : \mathbb{R}^n \to \mathbb{R}^n$ is a linear invertible operator. Then

$$\begin{aligned}\left\langle A^{-1} g_k\left(Ax\right), h_k\left(x\right)\right\rangle_{H_k} &= \left\langle g_k\left(Ax\right), A^{*-1} h_k\left(x\right)\right\rangle_{H_k}, \\ &= \left\langle g_k\left(x\right), A^{*-1}\left(h_k\left(A^*x\right)\right)\right\rangle_{H_k}, \text{ using (19.5.6).}\end{aligned} \tag{19.5.8}$$

In (19.5.8) substitute $A = e^{Jt}$. Then (19.5.8) becomes

$$\left\langle e^{-Jt} g_k\left(e^{Jt}x\right), h_k\left(x\right)\right\rangle_{H_k} = \left\langle g_k\left(x\right), e^{-J^*t} h_k\left(e^{J^*t}x\right)\right\rangle_{H_k}, \tag{19.5.9}$$

where we have used $\left(e^{Jt}\right)^* = e^{J^*t}$. Next we differentiate (19.5.9) with respect to t and evaluate the result at $t = 0$ to obtain

$$\langle -Jg_k(x) + Dg_k(x)Jx, h_k(x)\rangle_{H_k} = \langle g_k(x), -J^*h_k(x) + Dh_k(x)J^*x\rangle_{H_k}, \tag{19.5.10}$$

or, using the notation developed in (19.1.23) and (19.1.24),

$$\langle [g_k, Jx], h_k\rangle_{H_k} = \langle g_k, [h_k, J^*x]\rangle_{H_k}, \tag{19.5.11}$$

or

$$\langle L_J^{(k)}(g_k), h_k\rangle_{H_k} = \langle g_k, L_{J^*}^{(k)}(h_k)\rangle_{H_k}, \tag{19.5.12}$$

from which it follows that

$$\left(L_J^{(k)}\right)^* = L_{J^*}^{(k)}.$$

But most importantly, this expression implies that if $h_k \in \operatorname{Ker} L_{J^*}^{(k)}$ then h_k is in the orthogonal complement of the image of $L_J^{(k)}$, denoted $\operatorname{Im} L_J^{(k)}$. This is a key feature of the normal form, but before summarizing this in a theorem we want to develop a useful characterization of $\operatorname{Ker} L_{J^*}^{(k)}$.

First, we argue that

$$e^{L_{J^*}^{(k)}t}h_k(x) = e^{-J^*t}h_k\left(e^{J^*t}x\right). \tag{19.5.13}$$

This can be seen as follows. Consider the following linear ordinary differential equation on H_k:

$$\dot{h_k} = L_{J^*}^{(k)}h_k, \qquad h_k \in H_k.$$

It is a straightforward calculation to verify that

$$m_k(t) = e^{-J^*t}h_k\left(e^{J^*t}x\right),$$
$$n_k(t) = e^{L_{J^*}^{(k)}t}h_k(x),$$

are both solutions of this equation satisfying

$$m_k(0) = h_k(x),$$
$$n_k(0) = h_k(x).$$

Hence, by existence and uniqueness of solutions of linear ordinary differential equations with constant coefficients, it follows that $m_k(t) = n_k(t)$ for all t. Therefore (19.5.13) holds.

Now $e^{L_{J^*}^{(k)}t}$ acts as the identity map on $\operatorname{Ker} L_{J^*}^{(k)}$. Hence it follows that

$$\operatorname{Ker} L_{J^*}^{(k)} = \left\{h_k \in H_k \,|\, e^{-J^*t}h_k\left(e^{J^*t}x\right) = h_k(x), \quad \forall t \in \mathbb{R}\right\}. \tag{19.5.14}$$

We can summarize these results in the following theorem.

Theorem 19.5.1 (Elphick-Tirapegui-Brachet-Coullet-Iooss) *H_k can be decomposed as follows:*

$$H_k = Im\, L_J^{(k)} \oplus Ker\, L_{J^*}^{(k)},$$

where

$$Ker\, L_{J^*}^{(k)} = \left\{ h_k \in H_k \,|\, e^{-J^*t} h_k \left(e^{J^*t} x \right) = h_k(x), \quad \forall t \in \mathbb{R} \right\}.$$

Applying this result to successive orders of the Taylor expansion of (19.5.1), we can immediately state a theorem characterizing what we mean by the normal form of (19.5.1)

Theorem 19.5.2 (Elphick-Tirapegui-Brachet-Coullet-Iooss) *The vector field (19.5.1) is said to be in* normal form through order $r-1$ *if the nonlinear terms $\mathcal{F}(x)$ commutes with e^{J^*t} is the sense that*

$$e^{-J^*t} \mathcal{F} \left(e^{J^*t} x \right) = \mathcal{F}(x). \tag{19.5.15}$$

Or, equivalently, if $\mathcal{F}(x)$ satisfies the following partial differential equation

$$D\mathcal{F}(x) J^* x - J^* \mathcal{F}(x) = 0. \tag{19.5.16}$$

Note that the partial differential equation (19.5.16) can be solved by the method of characteristics. Writing (19.5.16) out in components gives

$$\sum_{j,l=1}^{n} \frac{\partial \mathcal{F}_i}{\partial x_j} \bar{J}_{lj} x_l - \sum_{j=1}^{n} \bar{J}_{ji} \mathcal{F}_j = 0, \quad i = 1, \ldots, n. \tag{19.5.17}$$

The characteristic system associated with (19.5.17) is given by

$$\frac{dx_j}{\sum_l \bar{J}_{lj} x_l} = \frac{d\mathcal{F}_i}{\sum_l \bar{J}_{li} \mathcal{F}_l}, \quad i,\, j = 1, \ldots, n. \tag{19.5.18}$$

It follows immediately that the characteristic curves in $\mathbb{R}^n$ are given by

$$x(t) = e^{J^*t} x_0. \tag{19.5.19}$$

This result is useful for giving another characterization of the nonlinear terms of the normal form.

Theorem 19.5.3 (Elphick-Tirapegui-Brachet-Coullet-Iooss) *The nonlinear terms of the normal form can be written in the following form:*

$$\mathcal{F}(x) = \sum_{i=1}^{n} \alpha_j(x) \mathcal{L}_i x, \tag{19.5.20}$$

where $\mathcal{L}_i$, $i = 1, \ldots, n$ are linear operators commuting with J^* in $\mathbb{R}^n$ (to be explicitly constructed in the proof), and the scalar functions $\alpha_i(x)$, $i = 1, \ldots, n$, are rational functions that are first integrals of the characteristic system $\dot{x} = J^* x$.

Proof: First we construct the linear operators $\mathcal{L}_1, \ldots, \mathcal{L}_n$. To do this, we will assume that J^* is in Jordan canonical form. Then it has r Jordan blocks, with each block J_j^* corresponding to an invariant subspace of $\mathbb{R}^n$, denoted E_j, and to an eigenvalue λ_j, $j = 1, \ldots, r$. Let ν_j denote the dimension of E_j and P_j denote the projection onto E_j. Then

$$\sum_{i=1}^{r} P_j = \mathrm{id}.$$

To each Jordan block we associate ν_j linear operators

$$P_j, \left(J_j^* - \lambda_j \,\mathrm{id}\right) P_j, \ldots, \left(J_j^* - \lambda_j \,\mathrm{id}\right)^{\nu_j - 1} P_j, \quad j = 1, \ldots, r.$$

This is a set of n linearly independent operators, with each commuting with J^*, which we denote by $\mathcal{L}_j$. Now we choose any $x \in \mathbb{R}^n$ having the property that it has a nonzero component in each of the E_j. Then $\mathcal{L}_j x$, $j = 1, \ldots, n$ forms a basis for $\mathbb{R}^n$. We express $\mathcal{F}(x)$ in this basis to obtain (19.5.20). Next we examine the properties of the coefficients in this expansion, $\alpha_j(x)$.

Since

$$J^* \mathcal{L}_j = \mathcal{L}_j J^*, \quad j = 1, \ldots, n,$$

it follows that

$$e^{J^* t} \mathcal{L}_j = \mathcal{L}_j e^{J^* t}, \quad j = 1, \ldots, n. \tag{19.5.21}$$

Now using (19.5.15), we obtain

$$\begin{aligned} e^{-J^* t} \mathcal{F}\left(e^{J^* t} x\right) &= \sum_{j=1}^{n} e^{-J^* t} \alpha_j \left(e^{J^* t} x\right) \mathcal{L}_j e^{J^* t} x, \\ &= \sum_{j=1}^{n} e^{-J^* t} \alpha_j \left(e^{J^* t} x\right) e^{J^* t} \mathcal{L}_j x, \\ &= \sum_{j=1}^{n} \alpha_j \left(e^{J^* t} x\right) \mathcal{L}_j x, \\ &= \mathcal{F}(x) = \sum_{j=1}^{n} \alpha_j(x) \mathcal{L}_j x. \end{aligned}$$

Hence

$$\alpha_j \left(e^{J^* t} x\right) = \alpha_j(x). \tag{19.5.22}$$

Therefore the functions $\alpha_j(x)$ are first integrals of the characteristic system. □

19.5c Symmetries of the Normal Form

Suppose $T : \mathbb{R}^n \to \mathbb{R}^n$ is a linear invertible operator. Consider an arbitrary vector field

$$\dot{x} = f(x), \qquad x \in \mathbb{R}^n. \tag{19.5.23}$$

We say that T is a *symmetry* of (19.5.23) if

$$f(Tx) = Tf(x). \tag{19.5.24}$$

If (19.5.23) has an equilibrium point at $x = 0$, and J is the matrix associated with the linearization about this equilibrium, then by differentiating (19.5.24) we obtain

$$JT = TJ. \tag{19.5.25}$$

The terminology "T commutes with the vector field" is also used.

From our construction of the normal form we see immediately that the one-parameter group of transformations $\left\{e^{J^*t}, \quad t \in \mathbb{R}\right\}$ is a symmetry for the normal form. In this section we will prove that if the vector field has an additional symmetry, denoted by the linear invertible operator $T : \mathbb{R}^n \to \mathbb{R}^n$, then the normal form as constructed above, also has the symmetry T.

To begin with, we define the following linear operator on H_k:

$$T_* h_k(x) = T^{-1} h_k(Tx), \tag{19.5.26}$$

which will be useful for proving the following lemma.

Lemma 19.5.4 *The image of $L_J^{(k)}$, $Im L_J^{(k)}$, and the kernel of $L_J^{(k)}$, $Ker L_J^{(k)}$, are invariant under T_*.*

Proof: First we show that T_* commutes with $L_J^{(k)}$ in the following sense:

$$\begin{aligned} L_J^{(k)}\left(T_* h_k(x)\right) = L_J^{(k)}\left(T^{-1} h_k(Tx)\right) &= JT^{-1} h_k(Tx) - D\left(T^{-1} h_k(Tx)\right) Jx \\ &= JT^{-1} h_k(Tx) - T^{-1} Dh_k(Tx) TJx \\ &= T^{-1} Jh_k(Tx) - T^{-1} Dh_k(Tx) JTx \\ &= T^{-1}\left(Jh_k(Tx) - Dh_k(Tx) JTx\right) \\ &= T^{-1} L_J^{(k)}\left(h_k(Tx)\right) = T_* L_J^{(k)}\left(h_k(x)\right), \end{aligned} \tag{19.5.27}$$

where in this calculation we have used

$$JT = TJ \Rightarrow T^{-1}J = JT^{-1}.$$

The lemma follows directly from this calculation. □

Now assume that T is unitary, i.e., $T^* = T^{-1}$. Then we have the following lemma.

Lemma 19.5.5 *The image of* $L^{(k)}_{J^*}$, $Im L^{(k)}_{J^*}$, *and the kernel of* $L^{(k)}_{J^*}$, $Ker L^{(k)}_{J^*}$, *are invariant under* T_*.

Proof: First we show that T_* commutes with $L^{(k)}_{J^*}$ in the following sense:

$$\begin{aligned} L^{(k)}_{J^*}\left(T_* h_k(x)\right) &= L^{(k)}_{J^*}\left(T^{-1}h_k(Tx)\right) \\ &= J^*T^{-1}h_k(Tx) - D\left(T^{-1}h_k(Tx)\right)J^*x \\ &= J^*T^{-1}h_k(Tx) - T^{-1}Dh_k(Tx)TJ^*x \\ &= T^{-1}J^*h_k(Tx) - T^{-1}Dh_k(Tx)J^*Tx \\ &= T^{-1}\left(J^*h_k(Tx) - Dh_k(Tx)J^*Tx\right) \\ &= T^{-1}L^{(k)}_{J^*}\left(h_k(Tx)\right) = T_*L^{(k)}_{J^*}\left(h_k(x)\right), \end{aligned} \tag{19.5.28}$$

where in this calculation we have used

$$J^*T = TJ^* \Rightarrow T^{-1}J^* = J^*T^{-1}.$$

The lemma follows directly from this calculation. □

The two lemmas show that both $\mathrm{Im}\, L^{(k)}_J$ and $\mathrm{Ker}\, L^{(k)}_{J^*}$ are invariant under T_*. We will use these two facts to show that the normal form, as constructed above, commutes with T.

First, suppose the vector field (19.5.1) has the symmetry T. Then we must have

$$\begin{aligned} \dot{x} &= T^{-1}JTx + T^{-1}F_2(Tx) + T^{-1}F_3(Tx) + \cdots, \\ &= Jx + F_2(x) + F_3(x) + \cdots. \end{aligned}$$

Now we consider simplifying the second order terms. Making the change of coordinates

$$x \mapsto x + h_2(x),$$

gives

$$\dot{x} = Jx + L^{(2)}_J\left(h_2(x)\right) + F_2(x) + \mathcal{O}(3),$$

or

$$\dot{x} = Jx + L^{(2)}_J\left(h_2(x)\right) + \Pi^{\mathrm{Im}\, L^{(2)}_J}F_2(x) + \Pi^{\mathrm{Ker}\, L^{(2)}_{J^*}}F_2(x) + \mathcal{O}(3),$$

where $\Pi^{\mathrm{Im}\, L^{(2)}_{J^*}}$ denotes the projection onto $\mathrm{Im}\, L^{(2)}_J$ and $\Pi^{\mathrm{Ker}\, L^{(2)}_{J^*}}$ denotes the projection onto $\mathrm{Ker}\, L^{(2)}_{J^*}$.

We next apply the symmetry transformation to this equation, i.e., we let $x \mapsto Tx$, and act on the equation from the left with T^{-1} to obtain

$$\begin{aligned} \dot{x} = {} & T^{-1}JTx + T^{-1}L^{(2)}_J\left(h_2(Tx)\right) + T^{-1}\Pi^{\mathrm{Im}\, L^{(2)}_J}F_2(Tx) \\ & + T^{-1}\Pi^{\mathrm{Ker}\, L^{(2)}_{J^*}}F_2(Tx) + \mathcal{O}(3). \end{aligned}$$

Now $\operatorname{Ker} L_{J^*}^{(2)}$ and $\operatorname{Im} L_{J^*}^{(2)}$ are invariant under T_*. Hence T_* commutes with the projection operators, which allows us to rewrite this equation as

$$\dot{x} = Jx + T_* \left(L_J^{(2)} \left(h_2(x) \right) + \Pi^{\operatorname{Im} L_J^{(2)}} F_2(x) \right) + \Pi^{\operatorname{Ker} L_{J^*}^{(2)}} T^{-1} F_2(Tx) + \mathcal{O}(3).$$

Since $h_2(x)$ can be chosen such that

$$L_J^{(2)} \left(h_2(x) \right) + \Pi^{\operatorname{Im} L_J^{(2)}} F_2(x) = 0,$$

it follows that

$$\dot{x} = Jx + \Pi^{\operatorname{Ker} L_{J^*}^{(2)}} T^{-1} F_2(Tx) + \mathcal{O}(3),$$

or

$$\dot{x} = Jx + \Pi^{\operatorname{Ker} L_{J^*}^{(2)}} F_2(x) + \mathcal{O}(3),$$

Hence, through $\mathcal{O}(2)$ terms, the normal form has the symmetry T. Clearly, this same argument can be continued at subsequent higher orders. In this way, we arrive at the following theorem.

Theorem 19.5.6 (Elphick-Tirapegui-Brachet-Coullet-Iooss) *Suppose $T : \mathbb{R}^n \to \mathbb{R}^n$ is unitary, and the vector field (19.5.1) has the symmetry T. Then the normal form also has the symmetry T.*

19.5D Examples

Now we will give some examples of normal forms computed with this method.

Example 19.5.1 (The "Double-Hopf" Bifurcation).

We will compute the normal form for the so-called "double Hopf bifurcation". By this we mean that the matrix associated with the linearization about an equilibrium has a pair of pure imaginary eigenvalues, $\pm i\omega_0$, $\pm i\omega_1$, and we will assume that the matrix associated with the linearization is diagonalizable in a complex basis (semisimple). In this case the Jordan canonical form for the matrix is

$$J = \begin{pmatrix} i\omega_0 & 0 & 0 & 0 \\ 0 & -i\omega_0 & 0 & 0 \\ 0 & 0 & i\omega_1 & 0 \\ 0 & 0 & 0 & -i\omega_1 \end{pmatrix}, \tag{19.5.29}$$

with

$$e^{J^* t} = \begin{pmatrix} e^{-i\omega_0 t} & 0 & 0 & 0 \\ 0 & e^{i\omega_0 t} & 0 & 0 \\ 0 & 0 & e^{-i\omega_1 t} & 0 \\ 0 & 0 & 0 & e^{i\omega_1 t} \end{pmatrix}. \tag{19.5.30}$$

Since the first and second components are complex conjugates, as well as the third and fourth, we only need to be concerned with the first and third components of the normal form.

The i^{th} component ($i = 1, \ldots, 4$) of a typical element of $H_{p+q+r+s}$ is of the form

$$g_i(z_0, \bar{z}_0, z_1, \bar{z}_1) = z_0^p \bar{z}_0^q z_1^r \bar{z}_1^s.$$

We want to determine the conditions on the nonnegative integers p, q, r, s such that the commutation relation holds, i.e., we must compute

$$\left(e^{-J^* t}\right)_{j,i} g_i(e^{J^* t} z) = g_j(z), \quad j = 1, \ldots, 4,$$

where $z \equiv (z_0, \bar{z}_0, z_1, \bar{z}_1)$. Since $e^{-J^* t}$ is diagonal, and the first and second components of the normal form are complex conjugates, as well as the third and fourth, the computation reduces to

$$\left(e^{-J^* t}\right)_{i,i} g_i(e^{J^* t} z) = g_i(z), \quad i = 1, 3.$$

The first and third components of this commutation relation are easily found to be:

First Component:

$$e^{-i((p-q-1)\omega_0 + (r-s)\omega_1)t} z_0^p \bar{z}_0^q z_1^r \bar{z}_1^s = z_0^p \bar{z}_0^q z_1^r \bar{z}_1^s, \tag{19.5.31}$$

Third Component:

$$e^{-i((p-q)\omega_0 + (r-s-1)\omega_1)t} z_0^p \bar{z}_0^q z_1^r \bar{z}_1^s = z_0^p \bar{z}_0^q z_1^r \bar{z}_1^s. \tag{19.5.32}$$

These conditions give rise to the following relations between p, q, r, s:

First Component:

$$(p - q - 1)\omega_0 + (r - s)\omega_1 = 0, \tag{19.5.33}$$

Third Component:

$$(p - q)\omega_0 + (r - s - 1)\omega_1 = 0. \tag{19.5.34}$$

There are two general situations to consider; the nonresonant and the resonant cases.

Nonresonance: $\frac{\omega_0}{\omega_1}$ Irrational

In this case, since ω_0 and ω_1 are independent over the rational numbers, (19.5.33) has the unique solution $p = q + 1$ and $r = s$. From this it follows that the terms in the first component of the normal form have the form

$$z_0 |z_0|^{2q} |z_1|^{2r}.$$

Similarly, (19.5.34) has the unique solution $p = q$ and $r = s + 1$, and from this it follows that the terms in the third component of the normal form have the form

$$z_1 |z_0|^{2q} |z_1|^{2r}.$$

Thus the normal form for the nonresonant double Hopf bifurcation is of the form

$$\begin{aligned} \dot{z}_0 &= i\omega_0 z_0 + z_0 P_0(|z_0|^2, |z_1|^2), \\ \dot{z}_1 &= i\omega_1 z_1 + z_1 P_1(|z_0|^2, |z_1|^2), \end{aligned} \tag{19.5.35}$$

where P_0 and P_1 are polynomials in $|z_0|^2$ and $|z_1|^2$.

Resonance: $\frac{\omega_0}{\omega_1}$ Rational

Suppose $\frac{\omega_0}{\omega_1} = \frac{m}{n}$, where m and n are integers with all common factors cancelled from the ratio (in this case we say that m and n are *relatively prime* or *coprime*, and write $(m, n) = 1$). In this case the solution to (19.5.33) is

$$p = q + 1 + kn, \quad r = s - km, \qquad k \in \mathbb{Z},$$

which leads to terms of the form

$$z_0 |z_0|^{2q} |z_1|^{2s} z_0^{kn} z_1^{-km}. \tag{19.5.36}$$

For this expression we must consider the cases $k > 0$ and $k < 0$.

$\boxed{k > 0:}$ Using

$$z_1^{-1} = \frac{\bar{z}_1}{|z_1|^2},$$

(19.5.36) can be rewritten as

$$z_0 |z_0|^{2q} |z_1|^{2r} z_0^{kn} \bar{z}_1^{km}.$$

$\boxed{k < 0:}$ Using

$$z_0 = \bar{z}_0^{-1} |z_0|^2,$$

(19.5.36) can be rewritten as

$$z_0 |z_0|^{2(p-1)} |z_1|^{2s} \bar{z}_0^{-kn} z_1^{-km},$$

or

$$\bar{z}_0^{n-1} z_1^m |z_0|^{2p} |z_1|^{2s} \bar{z}_0^{-(k+1)n} z_1^{-(k+1)m}.$$

The solution to (19.5.34) is

$$r = s + 1 + km, \quad p = q - kn, \qquad k \in \mathbb{Z},$$

which leads to terms of the form

$$z_1 |z_0|^{2q} |z_1|^{2s} z_0^{-kn} z_1^{km}. \tag{19.5.37}$$

For this expression we must consider the cases $k > 0$ and $k < 0$.

$\boxed{k > 0:}$ Using

$$z_0^{-1} = \frac{\bar{z}_0}{|z_0|^2},$$

(19.5.37) can be rewritten as

$$z_1 |z_1|^{2s} |z_0|^{2p} \bar{z}_0^{kn} \bar{z}_1^{km}.$$

$\boxed{k < 0:}$ Using

$$z_1 = \bar{z}_1^{-1} |z_1|^2,$$

(19.5.36) can be rewritten as

$$z_1 |z_1|^{2(r-1)} |z_0|^{2q} z_0^{-kn} \bar{z}_1^{-km},$$

or

$$z_0^n \bar{z}_1^{m-1} |z_0|^{2q} |z_1|^{2r} z_0^{-(k+1)n} \bar{z}_1^{-(k+1)m}.$$

Hence, the normal form takes the following form

$$\begin{aligned} \dot{z}_0 &= i\omega_0 z_0 + z_0 P_0(|z_0|^2, |z_1|^2, z_0^n \bar{z}_1^m) + \bar{z}_0^{n-1} z_1^m P_1(|z_0|^2, |z_1|^2, \bar{z}_0^n z_1^m), \\ \dot{z}_1 &= i\omega_1 z_1 + z_1 Q_0(|z_0|^2, |z_1|^2, \bar{z}_0^n z_1^m) + z_0^n \bar{z}_1^{m-1} Q_1(|z_0|^2, |z_1|^2, z_0^n \bar{z}_1^m), \end{aligned} \tag{19.5.38}$$

where P_0, P_1, Q_0 and Q_1 are polynomials in their arguments.

End of Example 19.5.1

Example 19.5.2. We compute the normal form for a two-dimensional vector field with linear part given by

$$J = \begin{pmatrix} 0 & 1 \\ 0 & 0 \end{pmatrix}.$$

We will compute the normal form by solving the characteristic system (19.5.18), which for this example is given by

$$x \frac{\partial F_1}{\partial y} = 0, \quad x \frac{\partial F_2}{\partial y} = F_1.$$

The solution is given by

$$\begin{aligned} F_1(x, y) &= x\phi_1(x), \\ F_2(x, y) &= y\phi_1(x) + \phi_2(x), \end{aligned} \tag{19.5.39}$$

where ϕ_1 and ϕ_2 are polynomials in x (this is proved in Elphick et al. [1987], but it can easily be verified by substitution). Hence, $\operatorname{Ker} L_{J^*}^{(k)}$ is two dimensional, and a general vector in this space is given by

$$\left(ax^k, ayx^{k-1} + bx^k\right).$$

Hence, the normal form is given by

$$\begin{aligned} \dot{x} &= y + \tilde{P}_0(x), \\ \dot{y} &= xy\tilde{P}_1(x) + x^2 \tilde{P}_2(x), \end{aligned} \tag{19.5.40}$$

where $\tilde{P}_i(x)$, $i = 0, 1, 2$, are polynomials in x.

The normal form can be simplified if we add to $\operatorname{Ker} L_{J^*}^{(k)}$ the vector

$$\left(-ax^k, kax^{k-1}y\right),$$

which is orthogonal to $\operatorname{Ker} L_{J^*}^{(k)}$. This amounts to choosing a different space complementary to $\operatorname{Im} L_{J^*}^{(k)}$. The resulting complementary space has the form

$$\left(0, a'yx^{k-1} + bx^k\right),$$

and the normal form is given by

$$\begin{aligned} \dot{x} &= y, \\ \dot{y} &= xyP_1(x) + x^2P_2(x), \end{aligned} \tag{19.5.41}$$

where $P_1(x)$ and $P_2(x)$ are polynomials in x.

End of Example 19.5.2

19.5E The Normal Form of a Vector Field Depending on Parameters

Essentially the same theory goes through for vector fields depending on parameters, but with a few interesting twists.

We rewrite the vector field (19.5.1), where $\mathcal{F}$ is $\mathcal{O}(r-1)$ in x:

$$\dot{x} = Jx + \mathcal{F}(x,\mu), \qquad x \in \mathbb{R}^n,\ \mu \in \mathbb{R}^p, \tag{19.5.42}$$

with J in Jordan canonical form, and *not* depending on μ, and

$$\mathcal{F}(0,\mu) = \mathcal{O}(|\mu|), \quad D_x\mathcal{F}(0,0) = 0.$$

Theorem 19.5.7 *The vector field (19.5.42) can be transformed to a normal form in which $\mathcal{F}(x,\mu)$ satisfies*

$$e^{-J^*t}\mathcal{F}\left(e^{J^*t}x,\mu\right) = \mathcal{F}(x,\mu), \tag{19.5.43}$$

and

$$\mathcal{F}(0,\mu) \in Ker\, J^*, \tag{19.5.44}$$

$$J^*D_x\mathcal{F}(0,\mu) - D_x\mathcal{F}(0,\mu)J^* = 0. \tag{19.5.45}$$

Proof: The basic idea here, as we mentioned earlier, is that we Taylor expand in x and view the coefficients as functions of the parameters μ. In this way, the previous theory goes through in exactly the same way and the parameters "just go along for the ride". However, two new terms do arise in this way, but they cause little difficulty as we will now see.

Taylor expanding (19.5.42) in x gives

$$\dot{x} = Jx + \mathcal{F}(0,\mu) + D_x\mathcal{F}(0,\mu)x + \mathcal{O}(|x|^2). \tag{19.5.46}$$

As in the situation with no parameters, we choose the $(|x|^p)$ terms to be in Ker $L_{J^*}^{(p)}$. In the case with parameters there are two new terms; $\mathcal{F}(0,\mu) \in H_0$ (constant terms) and $D_x\mathcal{F}(0,\mu) \in H_1$ (linear terms). Now

$$L_{J^*}^{(0)}\left(\mathcal{F}(0,\mu)\right) = J^*\mathcal{F}(0,\mu) = 0 \Rightarrow \mathcal{F}(0,\mu) \in \text{Ker}\, J^*,$$

and

$$L_{J^*}^{(1)}\left(D_x\mathcal{F}(0,\mu)\right) \Rightarrow J^* D_x\mathcal{F}(0,\mu) - D_x\mathcal{F}(0,\mu)J^* = 0.$$

Requiring the $\mathcal{O}(|x|^p)$ terms to be in $\operatorname{Ker} L_{J^*}^{(p)}$, $p \geq 2$ immediately leads to

$$e^{-J^*t}\mathcal{F}\left(e^{J^*t}x,\mu\right) = \mathcal{F}(x,\mu).$$

This completes the proof of the theorem. □

Example 19.5.3.

We consider the example of the double-zero eigenvalue with non-semisimple linear part

$$J = \begin{pmatrix} 0 & 1 \\ 0 & 0 \end{pmatrix},$$

with the vector field in the form

$$\begin{pmatrix} \dot{x} \\ \dot{y} \end{pmatrix} = J\begin{pmatrix} x \\ y \end{pmatrix} + \begin{pmatrix} \mathcal{F}_1(0,\mu) \\ \mathcal{F}_2(0,\mu) \end{pmatrix} + \begin{pmatrix} \mathcal{F}_{1x}(0,\mu) & \mathcal{F}_{1y}(0,\mu) \\ \mathcal{F}_{2x}(0,\mu) & \mathcal{F}_{2y}(0,\mu) \end{pmatrix}\begin{pmatrix} x \\ y \end{pmatrix} + \mathcal{O}(|x|^2, |y|^2).$$

Then we have

$$\begin{pmatrix} 0 & 0 \\ 1 & 0 \end{pmatrix}\begin{pmatrix} \mathcal{F}_1(0,\mu) \\ \mathcal{F}_2(0,\mu) \end{pmatrix} = \begin{pmatrix} 0 \\ \mathcal{F}_1(0,\mu) \end{pmatrix} \Rightarrow \mathcal{F}_1(0,\mu) = 0,$$

and

$$\begin{pmatrix} 0 & 0 \\ 1 & 0 \end{pmatrix}\begin{pmatrix} \mathcal{F}_{1x}(0,\mu) & \mathcal{F}_{1y}(0,\mu) \\ \mathcal{F}_{2x}(0,\mu) & \mathcal{F}_{2y}(0,\mu) \end{pmatrix} - \begin{pmatrix} \mathcal{F}_{1x}(0,\mu) & \mathcal{F}_{1y}(0,\mu) \\ \mathcal{F}_{2x}(0,\mu) & \mathcal{F}_{2y}(0,\mu) \end{pmatrix}\begin{pmatrix} 0 & 0 \\ 1 & 0 \end{pmatrix} = \begin{pmatrix} 0 & 0 \\ 0 & 0 \end{pmatrix}$$

$$\Rightarrow \mathcal{F}_{1y}(0,\mu) = 0, \quad \mathcal{F}_{1x}(0,\mu) = \mathcal{F}_{2y}(0,\mu).$$

Then the vector field takes the form

$$\begin{aligned} \dot{x} &= y + \mathcal{F}_{1x}(0,\mu)x, \\ \dot{y} &= \mathcal{F}_2(0,\mu) + \mathcal{F}_{2x}(0,\mu)x + \mathcal{F}_{1x}(0,\mu)y + \mathcal{O}(|x|^2, |y|^2). \end{aligned}$$

End of Example 19.5.3

We make some final remarks concerning extensions of the Elphick-Tirapegui-Brachet-Coullet-Iooss approach to normal forsm.

Normal Form for a Vector Field Near a Periodic Orbit

Iooss [1988] has extended the work of Elphick et al. [1987] to the situation of computing the normal form of a vector field in the neighborhood of a periodic orbit.

Normal Form for a Map Near a Fixed Point

Chen and Della Dora [1999] have extended the work of Elphick et al. [1987] to the situation of computing the normal form of a map near a fixed point.

19.6 Exercises

1. Prove that
$$\langle p(Ax), q(x)\rangle = \langle p(x), q(A^*x)\rangle.$$
(Hint: Apply the chain rule and show that $\partial_x = A\partial_y$ where $y = A^*x$.)

2. Prove that
$$\langle A^{-1}g_k\left(Ax\right), h_k\left(x\right)\rangle_{H_k} = \langle g_k\left(x\right), A^{*-1}\left(h_k\left(A^*x\right)\right)\rangle_{H_k}.$$

3. Prove that $\langle\cdot,\cdot\rangle_{H_k}$ is an inner product on H_k.

4. Let $\{e_i\}_{i=1}^n$ denote the standard basis on $\mathbb{R}^n$ and let $(x_1,\ldots,x_n)$ denote coordinates with respect to this basis. We denote two arbitrary elements of H_k by
$$h_k = \sum_{i=1}^n \sum_{m_1+\cdots+m_n=k} h^i_{k:m_1,\ldots,m_n} x_1^{m_1}x_2^{m_2}\cdots x_n^{m_n} e_i,$$
$$g_k = \sum_{i=1}^n \sum_{m_1+\cdots+m_n=k} g^i_{k:m_1,\ldots,m_n} x_1^{m_1}x_2^{m_2}\cdots x_n^{m_n} e_i.$$
Compute the inner product of h_k and g_k.

5. Prove the following result from Elphick et al. [1987]. If J is diagonalizable, then
$$\operatorname{Ker} L^{(k)}_{J^*} = \operatorname{Ker} L^{(k)}_J,$$
and the normal form can be constructed so that it commutes with e^{Jt}, $t\in\mathbb{R}$.

6. Consider a two-dimensional vector field having an equilibrium point at the origin with the linear part of the vector field given by
$$J = \begin{pmatrix} 0 & 1\\ 0 & 0\end{pmatrix}.$$
Suppose also that the vector field commutes with the linear map defined by the following matrix
$$T = \begin{pmatrix} -1 & 0\\ 0 & -1\end{pmatrix}.$$
Compute the normal form.

7. Consider a three-dimensional vector field having an equilibrium point at the origin with the linear part of the vector field given by
$$J = \begin{pmatrix} 0 & \omega & 0\\ -\omega & 0 & 0\\ 0 & 0 & 0\end{pmatrix},$$
where $\omega > 0$ is a real number. Suppose also that the vector field commutes with the linear map defined by the following matrix
$$T = \begin{pmatrix} 1 & 0 & 0\\ 0 & 1 & 0\\ 0 & 0 & -1\end{pmatrix}.$$
Compute the normal form.

8. Consider the non-semisimple double-Hopf bifurcation at $1:1$ resonance, i.e., a four-dimensional vector field having an equilibrium point at the origin with the linear part of the vector field, with respect to a complex basis, is given by

$$J = \begin{pmatrix} i\omega & 1 & 0 & 0 \\ 0 & i\omega & 0 & 0 \\ 0 & 0 & -i\omega & 1 \\ 0 & 0 & 0 & -i\omega \end{pmatrix},$$

where $\omega > 0$ is a real number. Show that in complex coordinates the normal form can be written as follows

$$\begin{aligned} \dot{z}_1 &= i\omega z_1 + z_2, \\ \dot{z}_2 &= i\omega z_2 + z_1\phi_1\left(|z_1|, z_1\bar{z}_2 - \bar{z}_1 z_2\right) + z_2\phi_2\left(|z_1|, z_1\bar{z}_2 - \bar{z}_1 z_2\right), \end{aligned}$$

where ϕ_1 and ϕ_2 are polynomials in their two arguments.

9. Recall the example of the non-semisimple double-zero eigenvalue depending on parameters. We showed that the normal form could be transformed into the following form

$$\begin{aligned} \dot{x} &= y + \mathcal{F}_{1x}(0,\mu)x, \\ \dot{y} &= \mathcal{F}_2(0,\mu) + \mathcal{F}_{2x}(0,\mu)x + \mathcal{F}_{1x}(0,\mu)y + +\mathcal{O}(|x|^2, |y|^2). \end{aligned}$$

"Re-parametrize" by letting

$$\begin{aligned} \mathcal{F}_2(0,\mu) &\to \mu_1, \\ \mathcal{F}_{1x}(0,\mu) &\to \mu_2, \\ \mathcal{F}_{2x}(0,\mu) &\to \mu_3. \end{aligned}$$

Show that the $\mu_2 x$ and $\mu_3 x$ term cans be eliminated by appropriate linear transformations.

10. Consider the "double-Hopf bifurcation" as described above, both the resonant and non-resonant cases. Suppose the associated vector field depends on parameters. Compute the terms (19.5.44) and (19.5.45).

11. Consider a two-dimensional vector field having an equilibrium point at the origin with the linear part of the vector field given by

$$J = \begin{pmatrix} 0 & 1 \\ 0 & 0 \end{pmatrix}.$$

Suppose also that the vector field commutes with the linear map defined by the following matrix

$$T = \begin{pmatrix} -1 & 0 \\ 0 & -1 \end{pmatrix}.$$

Now consider the situation where the vector field depends on parameters. Compute the terms (19.5.44) and (19.5.45).

12. Consider a three-dimensional vector field having an equilibrium point at the origin with the linear part of the vector field given by

$$J = \begin{pmatrix} 0 & \omega & 0 \\ -\omega & 0 & 0 \\ 0 & 0 & 0 \end{pmatrix},$$

where $\omega > 0$ is a real number. Suppose that the vector field depends on parameters. Compute the terms (19.5.44) and (19.5.45).

Suppose also that the vector field commutes with the linear map defined by the following matrix

$$T = \begin{pmatrix} 1 & 0 & 0 \\ 0 & 1 & 0 \\ 0 & 0 & -1 \end{pmatrix}.$$

Compute the terms (19.5.44) and (19.5.45).

13. Consider the non-semisimple double-Hopf bifurcation at 1 : 1 resonance, i.e., a four-dimensional vector field having an equilibrium point at the origin with the linear part of the vector field, with respect to a complex basis, is given by

$$J = \begin{pmatrix} i\omega & 1 & 0 & 0 \\ 0 & i\omega & 0 & 0 \\ 0 & 0 & -i\omega & 1 \\ 0 & 0 & 0 & -i\omega \end{pmatrix},$$

where $\omega > 0$ is a real number. Suppose that the vector field depends on parameters and compute the terms (19.5.44) and (19.5.45).

14. Develop the Elphick-Tirapegui-Brachet-Coullet-Iooss normal form for maps.

19.7 Lie Groups, Lie Group Actions, and Symmetries

In this section we develop some of the terminology and tools to discuss issues related to symmetries in dynamical systems, which we will visit from time-to-time throughout the rest of this book. We begin by recalling the definition of a group.

Definition 19.7.1 (Group) *A group is a set, G, equipped with a binary operation on the group elements, denoted "$*$" and referred to as* group multiplication*, which satisfies the following three properties.*

1. *G is closed under group multiplication, i.e., $g_1, g_2 \in G \Rightarrow g_1 * g_2 \in G$.*
2. *There exists a multiplicative identity element in G, i.e., there exists an element $e \in G$ such that $e * g = g * g = g$, for any $g \in G$.*
3. *For every element of G there exists a multiplicative inverse, i.e., for every $g \in G$, there exists an element, denoted g^{-1}, such that $g * g^{-1} = g^{-1} * g = e$.*
4. *Multiplication is associative, i.e., $(g_1 * g_2) * g_3 = g_1 * (g_2 * g_3)$, for any $g_1, g_2, g_3 \in G$.*

Most of the groups which we encounter will be *Lie groups*. Roughly speaking, a Lie group is a group that also has the structure of a differentiable manifold. However, rather than developing the necessary machinery for the theory of differentiable manifolds, we will introduce the notion of

Lie groups from a more elementary point of view (following Golubitsky et al. [1988]) that will be more than adequate for our purposes.

Let $GL(\mathbb{R}^n)$ denote the group of linear, invertible transformations of $\mathbb{R}^n$ into $\mathbb{R}^n$, which we can view as the group of nonsingular $n \times n$ matrices over $\mathbb{R}$. Then we have the following definition.

Definition 19.7.2 (Lie Group) *A Lie group is a closed subgroup of $GL(\mathbb{R}^n)$, which we will denote by Γ.*

Recall that a subgroup is a subset of a group, which obeys the same axioms as a group (but with the important point that it is the subset that is closed with respect to group multiplication). The term "closed" in the definition of a Lie group needs clarification. We can identify the space of all $n \times n$ matrices with R^{n^2}. Then $GL(\mathbb{R}^n)$ is an open subset of R^{n^2}. Γ is said to be a *closed subgroup* if it is a closed subset of $GL(\mathbb{R}^n)$, as well as a subgroup of $GL(\mathbb{R}^n)$. If this closed subset is *compact* or *connected* then the associated Lie group is also said to be compact or connected.

In the context of symmetry properties of dynamical systems, we will be concerned with transformations of the phase space (and, in some situations, parameter space) under a Lie group. This brings us to the idea of a *group action*.

Definition 19.7.3 (Lie Group Action on a Vector Space) *Let Γ denote a Lie group and V a vector space. We say that Γ acts linearly on V if there is a continuous mapping, referred to as the* action*:*

$$\begin{aligned} &\Gamma \times V \to V, \\ &(\gamma, v) \mapsto \gamma \cdot v, \end{aligned}$$

such that

1. *For each $\gamma \in \Gamma$ the mapping*

$$\begin{aligned} \rho_\gamma \; : \; & V \to V, \\ & v \mapsto \gamma \cdot v \equiv \rho_\gamma(v). \end{aligned}$$

   is linear.

2. *(a) For any $\gamma_1, \gamma_2 \in \Gamma$,*

$$\gamma_1 \cdot (\gamma_2 \cdot v) = (\gamma_1 * \gamma_2) \cdot v.$$

   (b) $e \cdot v = v$.

Closely related to the notion of a Lie group action on a vector space is the notion of a representation of Γ with respect to a vector space V. Let $GL(V)$ denote the group of invertible linear transformations of V into V. Then we have the following definition.

Definition 19.7.4 (Representation of Γ on V) *The map*

$$\rho : \Gamma \to GL(V),$$
$$\gamma \mapsto \rho_\gamma,$$

is called a representation of Γ *on* V*.*

A group is an abstract object. A representation of a group gives rise to a more concrete manifestation of the group in terms of specific types of transformations on a vector space. This enables us to be able to perform calculations for a specific representation. This is (loosely) analogous to the situation with a linear map on a vector space. The map itself is an abstract object. However, in order to perform certain calculations we often have to choose a basis in order to obtain a representation for the map. The map has an abstract existence that is independent of any choice of basis for the vector space on which it acts. Similarly, a given group can have different representations.

19.7A Examples of Lie Groups

We now give some examples of concrete Lie groups. Following our discussion above, note that in some of the examples we can define the Lie group in a rather abstract way. Yet when we mathematically describe a Lie group in terms of the way in which it transforms a vector space (e.g., such as rotations, reflections, etc.) we typically resort to writing down formulae, which is equivalent to choosing a specific representation. Often this (seemingly) subtle point is of little consequence in elementary applications of these ideas. However, the appropriate representation for a group of symmetries can greatly simplify computations in specific problems.

$O(n)$**: The n-dimensional Orthogonal Group.** This is the set of $n \times n$ matrices, A, satisfying

$$AA^T = id.$$

$SO(n)$**: The Special Orthogonal Group.** This is the set of matrices $A \in O(n)$ such that $\det A = 1$.

Z_n**: The Cyclic Group of Order** n**.** [1] This is the set of rotational symmetries of a regular n-sided polygon. It consists of rotations of the plane through the angles

$$0,\ \theta,\ 2\theta,\ \ldots,\ (n-1)\theta, \qquad \theta = \frac{2\pi}{n}.$$

[1] Recall that the *order* of a finite group is the number of elements in the group.

Hence, it can be identified with the set of 2×2 matrices generated [2] by

$$R_{\frac{2\pi}{n}} = \begin{pmatrix} \cos\frac{2\pi}{n} & -\sin\frac{2\pi}{n} \\ \sin\frac{2\pi}{n} & \cos\frac{2\pi}{n} \end{pmatrix}.$$

D_n**: The Dihedral Group of Order** $2n$**.** This is the set of all symmetries of a regular n-sided polygon. It consists of rotations of the plane through the angles

$$0,\, \theta,\, 2\theta,\, \ldots,\, (n-1)\theta, \qquad \theta = \frac{2\pi}{n},$$

as well reflection in the x-axis (which is referred to as a "flip").

It can be identified with the set of 2×2 matrices generated by $R_{\frac{2\pi}{n}}$, along with the flip

$$\kappa = \begin{pmatrix} 1 & 0 \\ 0 & -1 \end{pmatrix}.$$

Z_n is a subgroup of D_n.

$U(n)$**: The n-dimensional Unitary Group.** This is the set of $n \times n$ matrices, A, satisfying

$$AA^* = id.$$

$SU(n)$**: The Special Unitary Group.** This is the set of matrices $A \in U(n)$ such that $\det A = 1$.

$Sp(2n)$**: The symplectic Group.** Let Ω denote a nondegenerate, skew-symmetric, bilinear form on $\mathbb{R}^{2n}$. The set of linear transformations $A : \mathbb{R}^{2n} \to \mathbb{R}^{2n}$ which preserve Ω, i.e.,

$$\Omega(Au, Av) = \Omega(u, v), \quad \forall u, v \in \mathbb{R}^{2n},$$

forms a group, which is called the *Symplectic group.*

T^n**: The n-dimensional torus.** The n dimensional torus

$$T^n = \underbrace{S^1 \times \cdots \times S^1}_{n\,times},$$

[2] Recall that a collection of elements is said to *generate* a group if all elements of the group can be expressed in terms of those elements.

can be viewed as a Lie group by identifying $\theta \in T^n$ with the matrix

$$\begin{pmatrix} R_{\theta_1} & 0 & 0 & \cdots & 0 \\ 0 & R_{\theta_2} & 0 & \cdots & 0 \\ 0 & 0 & R_{\theta_3} & \cdots & 0 \\ \vdots & \vdots & \vdots & \ddots & \vdots \\ 0 & 0 & 0 & \cdots & R_{\theta_n} \end{pmatrix},$$

which is an element of $GL(\mathbb{R}^{2n})$.

19.7B Examples of Lie Group Actions on Vector Spaces

Now we consider some examples of group actions.

$SO(2)$ **acting on** $\mathbb{R}^2$**.** We identify $SO(2)$ with the one- parameter family of matrices

$$R_\theta = \begin{pmatrix} \cos\theta & -\sin\theta \\ \sin\theta & \cos\theta \end{pmatrix}, \qquad 0 \le \theta < 2\pi,$$

and let it act on points in $\mathbb{R}^2$ via standard matrix multiplication.

Equivalently, we identify points $(x, y) \in \mathbb{R}^2$ with complex numbers $z = x + iy \in \mathbb{C}$. We can also identify a point $R_\theta \in SO(2)$ with a point θ in the circle group, S^1. Then we can view S^1 acting on $\mathbb{C}$ as follows:

$$\theta \cdot z = e^{i\theta} z.$$

$O(2)$ **acting on** $\mathbb{R}^2$**.** The same as above, however we append to the matrices R_θ the flip

$$\kappa = \begin{pmatrix} 1 & 0 \\ 0 & -1 \end{pmatrix}.$$

In the complex setting, we append to $e^{i\theta}$ the flip, which is defined by the complex conjugation operation

$$\kappa \cdot z = \bar{z}.$$

$SO(2)$ **acting on** $\mathbb{R}^3$**.** We define an $SO(2)$ action on $\mathbb{R}^3$ by allowing matrices of the form

$$R_\theta = \begin{pmatrix} \cos\theta & -\sin\theta & 0 \\ \sin\theta & \cos\theta & 0 \\ 0 & 0 & 1 \end{pmatrix}, \qquad 0 \le \theta < 2\pi,$$

to act on elements of $\mathbb{R}^3$ via the usual matrix multiplication.

Equivalently, we can identify $\mathbb{R}^3$ with $\mathbb{C} \times \mathbb{R}$ and define a S^1 action on $\mathbb{C} \times \mathbb{R}$ by

$$\theta \cdot (z, x) = (e^{i\theta} z, x).$$

$SO(2)$ **acting on** $\mathbb{R}^4$**.** We express this group action in complex coordinates by identifying $\mathbb{R}^4$ with $\mathbb{C}^2$. For a group element $\phi \in SO(2)$, we define an action on $\mathbb{C}^2$:

$$\phi \cdot (z_1, z_2) = \left(e^{i\phi} z_1, e^{i\phi} z_2)\right).$$

$O(2)$ **acting on** $\mathbb{R}^4$**.** We express this group action in complex coordinates by identifying $\mathbb{R}^4$ with $\mathbb{C}^2$. Recall that $O(2)$ is the same as $SO(2)$, together with a flip. We define the following action of $O(2)$ on $\mathbb{C}^2$:

$$\begin{aligned} \phi \cdot (z_1, z_2) &= \left(e^{i\phi} z_1, e^{i\phi} z_2)\right), \quad (\phi \in SO(2)), \\ \kappa \cdot (z_1, z_2) &= (\bar{z}_1, \bar{z}_2), \quad (\kappa = \text{flip in } O(2)). \end{aligned}$$

D_n **acting on** $\mathbb{R}^2$**.** We identify $\mathbb{R}^2$ with $\mathbb{C}$ in the usual way. Then an action of D_n on $\mathbb{C}$ is given by

$$\theta \cdot z = e^{i\theta} z, \quad (\theta = \frac{2\pi}{n}), \quad \text{and} \quad \kappa \cdot z = \bar{z}.$$

Z_n **acting on** $\mathbb{R}^2$**.** We identify $\mathbb{R}^2$ with $\mathbb{C}$ in the usual way. Then an action of D_n on $\mathbb{C}$ is given by

$$\theta \cdot z = e^{i\theta} z, \quad \left(\theta = \frac{2\pi}{n}\right).$$

T^2 **action on** $\mathbb{C}^2$**.** We define a two-torus action on $\mathbb{C}^2$ as follows:

$$(\theta, \phi) \cdot (z_1, z_2) = (e^{i\theta} z_1, e^{i\phi} z_2), \quad (\theta, \phi) \in T^2.$$

$D_n \times S^1$ **acting on** $\mathbb{R}^4$**.** We express this group action in complex coordinates by identifying $\mathbb{R}^4$ with $\mathbb{C}^2$.

$$\begin{aligned} \gamma \cdot (z_1, z_2) &= \left(e^{i\gamma} z_1, e^{i\gamma} z_2\right), \quad (\gamma \in Z_n) \\ \kappa \cdot (z_1, z_2) &= (\bar{z}_1, \bar{z}_2), \\ \theta \cdot (z_1, z_2) &= \left(e^{i\theta} z_1, e^{i\theta} z_2\right), \quad (\theta \in S^1), \end{aligned}$$

where

$$\gamma = 0,\ \phi,\ 2\phi,\ \ldots,\ (n-1)\phi, \qquad \phi = \frac{2\pi}{n},$$

$O(2) \times S^1$ acting on $\mathbb{R}^4$. We express this group action in complex coordinates by identifying $\mathbb{R}^4$ with $\mathbb{C}^2$. Using the action of $O(2)$ on $\mathbb{C}^2$ as defined above, we define the following action of $O(2) \times S^1$ on $\mathbb{C}^2$:

$$\begin{aligned}
\theta \cdot (z_1, z_2) &= \left(e^{i\theta} z_1, e^{i\theta} z_2)\right), \quad (\theta \in S^1), \\
\phi \cdot (z_1, z_2) &= \left(e^{i\phi} z_1, e^{i\phi} z_2)\right), \quad (\phi \in SO(2)), \\
\kappa \cdot (z_1, z_2) &= (\bar{z}_1, \bar{z}_2), \quad (\kappa = \text{flip in } O(2)).
\end{aligned}$$

$Z_2 \oplus Z_2$ acting on $\mathbb{R}^2$. The group $Z_2 \oplus Z_2$ has four elements (ε, δ), where $\varepsilon = \pm 1$, $\delta = \pm 1$. We define a group action on $\mathbb{R}^2$. For any $(x, y) \in \mathbb{R}^2$ the group element (ε, δ) acts on it as follows:

$$(\varepsilon, \delta) \cdot (x, y) = (\varepsilon x, \delta y).$$

19.7c Symmetric Dynamical Systems

Now we can give the definitions that specify precisely what we mean by a symmetric dynamical system.

Definition 19.7.5 (Γ-Equivariant Map) *Now let $f : V \to V$ denote a mapping of a vector space V into V. Let Γ denote a compact Lie group with a specified action on V. We say that f is* Γ-equivariant with respect to this action *if*

$$f(\gamma x) = \gamma f(x), \quad \forall \gamma \in \Gamma,\, x \in V.$$

If f is a vector field then we will refer to it as a Γ- equivariant vector field. It follows that if $x(t)$ is a solution of a Γ-equivariant vector field $\dot{x} = f(x)$, then $\gamma x(t)$ is also a solution, for each $\gamma \in \Gamma$.

Definition 19.7.6 (Γ-Invariant Function) *Now let $f : V \to \mathbb{R}$ denote a mapping of a vector space V into $\mathbb{R}$. Let Γ denote a compact Lie group with a specified action on V. We say that f is* Γ-invariant with respect to this action *if*

$$f(\gamma x) = f(x), \quad \forall \gamma \in \Gamma,\, x \in V.$$

19.8 Exercises

1. Prove that the transformations

$$\begin{aligned}
(x_1, y_1, x_2, y_2) &\to (-x_1, -y_1, x_2, y_2) \to (x_1, y_1, -x_2, -y_2) \\
&\to (x_1, y_1, x_2, y_2) \to (x_2, y_2, x_1, y_1),
\end{aligned}$$

   define a D_4 action on $\mathbb{R}^4$.

2. Prove that the transformations

$$(x_1, y_1, x_2, y_2) \to (-x_1, -y_1, x_2, y_2) \to (x_1, y_1, -x_2, -y_2),$$

   define a $Z_2 \oplus Z_2$ action on $\mathbb{R}^4$.

3. Prove that the transformations

$$(z_1, z_2) \to (\cos\theta z_1 + \sin\theta z_2, -\sin\theta z_1 + \cos\theta z_2), \qquad \theta \in [0, 2\pi).$$

define an $SO(2)$ action on $\mathbb{C}^2$.

4. Prove that the following transformations

$$z \mapsto \bar{z},$$
$$z \mapsto iz,$$

define a D_4 action on $\mathbb{C}$.

5. The following exercise comes from Sethna and Feng [1991]. Consider the following vector field on $\mathbb{C} \times \mathbb{C}$:

$$\begin{aligned}\dot{z_j} = {} & i\omega z_j + a_j|z_1|^2 z_1 + b_j z_1^2 \bar{z}_2 \\ & + c_j|z_1|^2 z_2 + d_j z_1|z_2|^2 + e_j \bar{z}_1 z_2^2 + f_j|z_2|^2 z_2, j = 1, 2,\end{aligned}$$

where a_j, b_j, c_j, d_j, e_j, f_j are complex coefficients, where $z_j = x_j + iy_j$. Derive conditions on the coefficients under which the vector field is equivariant with respect to the following group actions.

(a) D_4:

$$\begin{aligned}(x_1, y_1, x_2, y_2) &\to (-x_1, -y_1, x_2, y_2) \to (x_1, y_1, -x_2, -y_2) \\ &\to (x_1, y_1, x_2, y_2) \to (x_2, y_2, x_1, y_1).\end{aligned}$$

(b) $Z_2 \oplus Z_2$:

$$(x_1, y_1, x_2, y_2) \to (-x_1, -y_1, x_2, y_2) \to (x_1, y_1, -x_2, -y_2).$$

(c) $O(2)$:

$$\begin{aligned}&(z_1, z_2) \mapsto (\cos\theta z_1 + \sin\theta z_2, -\sin\theta z_1 + \cos\theta z_2), \theta \in [0, 2\pi), \\ &(z_1, z_2) \mapsto (\bar{z}_1, \bar{z}_2)\end{aligned}$$

6. Consider a vector field having an equilibrium point at the origin with the (real) Jordan canonical form of the matrix associated with the linear part given by

$$\begin{pmatrix} 0 & -\omega_1 & 0 & 0 \\ \omega_1 & 0 & 0 & 0 \\ 0 & 0 & 0 & -\omega_2 \\ 0 & 0 & \omega_2 & 0 \end{pmatrix},$$

where ω_1, $\omega_2 > 0$.

(a) Suppose $m\omega_1 + n\omega_2 \neq 0$ for any nonzero integers n and m. Prove that the normal form, computed up to any finite order, is equivariant with respect to T^2.

(b) Suppose $m\omega_1 + n\omega_2 = 0$ for some nonzero integers n and m, with n and m relatively prime. Prove that the normal form, computed up to any finite order, is equivariant with respect to S^1.

7. Consider a vector field having an equilibrium point at the origin where the matrix associated with the linear part is given by

$$\begin{pmatrix} 0 & 1 \\ 0 & 0 \end{pmatrix}.$$

Suppose the vector field is equivariant with respect to a D_2 action. Compute the normal form through third order terms.

8. Consider a vector field having an equilibrium point at the origin where the matrix associated with the linear part is given by

$$\begin{pmatrix} 0 & -\omega \\ \omega & 0 \end{pmatrix}, \qquad \omega > 0.$$

Transforming to complex coordinates, consider the following D_4 action on $\mathbb{C}$:

$$\begin{aligned} z &\mapsto \bar{z}, \\ z &\mapsto iz. \end{aligned}$$

Compute a normal form for the vector field that is equivariant with respect to this group action.

9. Prove that:

$$\begin{aligned} \theta \cdot (z_1, z_2) &= \left(e^{i\theta} z_1, e^{i\theta} z_2)\right), \quad (\theta \in S^1), \\ \phi \cdot (z_1, z_2) &= \left(e^{-i\phi} z_1, e^{i\phi} z_2)\right), \quad (\phi \in SO(2)), \\ \kappa \cdot (z_1, z_2) &= (z_2, z_1), \quad (\kappa = \text{flip in } O(2)), \end{aligned}$$

defines an $O(2) \times S^1$ action on $\mathbb{C}^2$. (This result is due to van Gils [1984], see also Golubitsky et al. [1988]. *Hint: Use the coordinates* $z_2(1, i) + \bar{z}_1(1, -i)$.)

10. Consider an autonomous vector field on $\mathbb{R}^4$ having an equilibrium point at the origin where the matrix associated with the linearization is given by

$$\begin{pmatrix} 0 & -\omega_1 & 0 & 0 \\ \omega_1 & 0 & 0 & 0 \\ 0 & 0 & 0 & -\omega_2 \\ 0 & 0 & \omega_2 & 0 \end{pmatrix}, \qquad \omega > 0.$$

Compute a normal form, up to some finite order, that is equivariant with respect to $O(2) \times S^1$. (Note: two $O(2) \times S^1$ actions were described above. Consider each.)

19.9 Normal Form Coefficients

Up to now we have only been concerned with calculating the form of the nonlinear terms in the normal form. However, in applications once will need to know the coefficents on each nonlinear term in the normal form as a function of the Taylor coefficients of the original vector field. Fortunately, this is the type of problem that only needs to be once. Below we summarize some of the known results for the normal forms of autonomous vector fields near non-hyperbolic equilibria.

The Non-Semisimple Double Zero Eigenvalue:

The following results are due to Knobloch [1986a]. Consider a two- dimensional autonomous vector field having an equilibrium point at the origin where the Jordan canonical form of the matrix associated with the linearization is given by

$$J = \begin{pmatrix} 0 & 1 \\ 0 & 0 \end{pmatrix}.$$

Taylor expanding about the origin, the vector field has the following general form

$$\begin{pmatrix} \dot{x} \\ \dot{y} \end{pmatrix} = \begin{pmatrix} y \\ 0 \end{pmatrix} + \begin{pmatrix} a_1\ x^2 + b_1\ x\ y + c_1\ y^2 \\ a_2\ x^2 + b_2\ x\ y + c_2\ y^2 \end{pmatrix} + \begin{pmatrix} d_1\ x^3 + e_1\ x^2\ y + f_1\ x\ y^2 + g_1\ y^3 \\ d_2\ x^3 + e_2\ x^2\ y + f_2\ x\ y^2 + g_2\ y^3 \end{pmatrix} + \mathcal{O}(4)$$

We know that through a sequence of nonlinear coordinate transformations the vector field can be transformed into the following form

$$\begin{pmatrix} \dot{u} \\ \dot{v} \end{pmatrix} = \begin{pmatrix} v \\ 0 \end{pmatrix} + \begin{pmatrix} 0 \\ A\ u^2 + B\ u\ v \end{pmatrix} + \begin{pmatrix} 0 \\ C\ u^3 + D\ u^2\ v \end{pmatrix} + \mathcal{O}(4).$$

Knobloch [1986a] has computed the coefficients of the normal form in terms of the original Taylor coefficients of the vector field. These are summarized in the following table where it is assumed that the coefficients C and D are nonzero, unless otherwise indicated.

Case	Conditions	A	B	C	D
1A	$A \neq 0, B \neq 0$	a_2	$2a_1 + b_2$	$d_2 + b_1 a_2 - a_1 b_2$	0
2A	$A \neq 0, B = 0$	a_2	0	$d_2 + b_1 a_2 + 2a_1^2$	0
3A	$A = 0, B \neq 0$	0	$2a_1 + b_2$	$d_2 - a_1 b_2$	$e_2 + 3d_1 - a_1 c_2 + b_2(b_1 + c_2)/2$
4A	$A = 0, B = 0$	0	0	$d_2 + 2a_1^2$	$e_2 + 3d_1 - 2a_1 c_2 - a_1 b_1$

For the next case the expressions for the normal form coefficients are so long that we do not reproduce them here. Rather, we refer the reader to the appropriate papers in the published literature.

A Zero and a Pair of Pure Imaginary Eigenvalues:

Consider a three- dimensional autonomous vector field having an equilibrium point at the origin where the real Jordan canonical form of the matrix associated with the linearization is given by

$$J = \begin{pmatrix} 0 & -\omega & 0 \\ \omega & 0 & 0 \\ 0 & 0 & 0 \end{pmatrix}, \qquad \omega > 0.$$

Coefficients for the normal form can be found in Wittenberg and Holmes [1997].

A Pair of Pure Imaginary Pairs of Eigenvalues:

Consider a four- dimensional autonomous vector field having an equilibrium point at the origin where the real Jordan canonical form of the matrix associated with the linearization is given by

$$J = \begin{pmatrix} 0 & -\omega_1 & 0 & 0 \\ \omega_1 & 0 & 0 & 0 \\ 0 & 0 & 0 & -\omega_2 \\ 0 & 0 & \omega_2 & 0 \end{pmatrix}, \qquad \omega_1 > 0,\, \omega_2 > 0.$$

For the nonresonant case defined by $m\omega_1 + n\omega_2 \neq 0$, $0 < |m| + |n| \leq 4$ normal form coefficients have been calculated by Knobloch [1986b]. For the case of $1:1$ resonance in the non-semisimple case normal form coefficients have been calculated by Namachchivaya et al. [1994].

19.10 Hamiltonian Normal Forms

In this section we want to describe the procedure for transforming a Hamiltonian vector field into normal form in the neighborhood of a fixed point. In particular, most of our attention will be focussed on *elliptic fixed points*, i.e., fixed points having the property that the eigenvalues of the matrix associated with the linearization are purely imaginary, with nonzero imaginary parts. This is a very old subject where the original results are often attributed to Birkhoff [1966] (for the nonresonant situation) and Gustavson [1966] (for the resonant situation). Many books and papers contain expositions of the theory of Hamiltonian normal forms in one form or another, and with varying degrees of completeness. See, e.g., Abraham and Marsden [1978], Guillemin and Sternberg [1984], Meyer and Hall [1992], Arnold *et al.* [1988], Sanders and Verhulst [1985], and Sáenz *et al.* [1986]. Our exposition follows that given in Churchill *et al.* [1983].

19.10a General Theory

Our calculations will be greatly simplified if we use the form of Hamilton's equations in complex variables given in Chapter 14. We begin by developing some notation. Let $\mathcal{P}_r$ denote the set of *real valued* homogeneous polynomials of degree $r \geq 2$ in the complex variables $z_j = x_j + iy_j$, $\bar{z}_j = x_j - iy_j$, $j = 1, \cdots, n$. We want to consider a formal power series of the following form

$$H = H_2 + H_3 + \cdots + H_m + \cdots, \qquad H_r \in \mathcal{P}_r. \tag{19.10.1}$$

We denote the space of formal power series by $\mathcal{P}$ and, as a result of the form of (19.10.1), we use the notation

$$\mathcal{P} = \oplus_{r=2}^{\infty} \mathcal{P}_r,$$

to denote the space of formal power series under consideration. This rather abstract notation will allow us to very succinctly discuss certain algebraic structures that would be very cumbersome to express in coordinates.

However, keeping with the subject matter of this section, you can think of H as a real Hamiltonian expressed in complex variables and having the value zero at the origin, with the corresponding Hamiltonian vector field having a fixed point at the origin. Issues such as convergence and differentiability will not play a role in the formal algebraic manipulations, so we will address these later on.

For a fixed $F \in \mathcal{P}$ we define the linear map

$$\begin{aligned} \mathrm{ad}_F &: \mathcal{P} \to \mathcal{P}, \\ &H \mapsto \mathrm{ad}_F(H) \equiv [F, H], \end{aligned} \tag{19.10.2}$$

for any $H \in \mathcal{P}$, where

$$[H, G] = -2i \sum_{j=1}^{n} \left(\frac{\partial H}{\partial \bar{z}_j} \frac{\partial G}{\partial z_j} - \frac{\partial H}{\partial z_j} \frac{\partial G}{\partial \bar{z}_j} \right), \tag{19.10.3}$$

and

$$\frac{\partial}{\partial z_j} = \frac{1}{2} \left(\frac{\partial}{\partial x_j} - i \frac{\partial}{\partial y_j} \right), \quad \frac{\partial}{\partial \bar{z}_j} = \frac{1}{2} \left(\frac{\partial}{\partial x_j} + i \frac{\partial}{\partial y_j} \right).$$

Note that

$$\mathrm{ad}_F(H) = -\mathrm{ad}_H(F). \tag{19.10.4}$$

$[\cdot, \cdot]$ is an example of a *Lie bracket*; note that it is the negative of the usual Poisson bracket of two functions, i.e., $[\cdot, \cdot] = -\{\cdot, \cdot\}$. It is easy to verify that for $F \in \mathcal{P}_2$ we have

$$\mathrm{ad}_F|_{\mathcal{P}_r} : \mathcal{P}_r \to \mathcal{P}_r.$$

We also define

$$\begin{aligned} \mathrm{ad}_F^0 &\equiv \text{identity mapping on } \mathcal{P}, \\ \mathrm{ad}_F^1 &\equiv \mathrm{ad}_F \end{aligned} \tag{19.10.5}$$

and, inductively,

$$\mathrm{ad}_F^j \equiv \mathrm{ad}_F \circ \mathrm{ad}_F^{j-1},\ j > 1.$$

For $F \in \mathcal{P}_s$, $H_r \in \mathcal{P}_r$, using (19.10.2) and (19.10.3) we can show

$$\mathrm{ad}_F(H_r) \in \mathcal{P}_{r+s-2}. \tag{19.10.6}$$

Using this relation, we can inductively verify that

$$\mathrm{ad}_F^j(H_r) \in \mathcal{P}_{r+j(s-2)}. \tag{19.10.7}$$

The *exponential map* will also play an important role for Hamiltonian normal forms. For $K \in \mathcal{P}_s$ we define

$$\begin{aligned} \exp(\mathrm{ad}_K) \,:\, \mathcal{P} &\to \mathcal{P} \\ H &\mapsto \sum_{j=0}^{\infty} \frac{1}{j!} \mathrm{ad}_K^j(H) \equiv \exp\left(\mathrm{ad}_K\right)(H)) \,. \end{aligned} \tag{19.10.8}$$

We now define what we mean by the term *normal form* of a Hamiltonian.

Definition 19.10.1 (Normal Form) *An element $H = \oplus_{r=2}^{\infty} H_r \in \mathcal{P}$ is said to be* in normal form through terms of order $m \geq 2$ with respect to $F \in \mathcal{P}$ *if $ad_F(H_r) = 0$ for $2 \leq r \leq m$.*

The following definition is important for the procedure of computing the normal form.

Definition 19.10.2 (Splitting) *$F \in \mathcal{P}_r$ is said to* split *$\mathcal{P}$ if for $r \geq 2$ we have*

$$\mathcal{P}_r = N_r \oplus R_r$$

where $N_r = Ker(ad_F|_{\mathcal{P}_r})$ and $R_r = Im(ad_F|_{\mathcal{P}_r})$. When F splits $\mathcal{P}$ then $ad_F|_{R_r}$ is an isomorphism and we let $\Gamma_r : R_r \to R_r$ denote the inverse.

The following is the main *normal form theorem* and provides an algorithm for transforming a Hamiltonian into normal form order-by-order.

Theorem 19.10.3 *Let $H = \oplus_{r=2}^{\infty} H_r \in \mathcal{P}$ be in normal form through terms of order $(m-1) \geq 2$ with respect to H_2, and assume that H_2 splits $\mathcal{P}$. Let $H_m = \hat{H}_m + \tilde{H}_m$, where $\hat{H}_m \in N_m$ and $\tilde{H}_m \in R_m$, and set $K_m = \Gamma_m\left(\tilde{H}_m\right)$. Then $\exp\left(ad_{K_m}\right)(H)$ is in normal form through terms of order m with respect to H_2, it agrees with H through terms of order $m-1$, and it has $\hat{H}_m$ as the m^{th} term.*

Proof: From (19.10.8) we have

$$\begin{aligned} \exp\left(\mathrm{ad}_{K_m}\right)(H) &= \sum_{j=0}^{\infty} \frac{1}{j!} \mathrm{ad}_{K_m}^j(H) \\ &= H + \mathrm{ad}_{K_m}(H) + \{\text{terms in } \mathcal{P}_j,\, j \geq 2m-2\} \\ &= H_2 + H_3 + \cdots + H_{m-1} + H_m + \mathrm{ad}_{K_m}(H_2) \\ &\quad + \{\text{terms in } \mathcal{P}_j,\, j \geq m+1\} \,, \end{aligned} \tag{19.10.9}$$

which one easily sees agrees with H through terms of order $m-1$.

Next we want to show that (19.10.9) is in normal form through order m with respect to H_2. For this to be true, by definition 19.10.1 we must have

$$\mathrm{ad}_{H_2}\left(H_m + \mathrm{ad}_{K_m}(H_2)\right) = 0.$$

This can be verified through the following simple calculations:

$$\begin{aligned}
\mathrm{ad}_{H_2}\left(H_m + \mathrm{ad}_{K_m}(H_2)\right) &= \mathrm{ad}_{H_2}(H_m) + \mathrm{ad}_{H_2}\left(\mathrm{ad}_{K_m}(H_2)\right) \\
&= \mathrm{ad}_{H_2}(H_m) - \mathrm{ad}_{H_2}\left(\mathrm{ad}_{H_2}(K_m)\right) \\
&= \mathrm{ad}_{H_2}\left(H_m - \mathrm{ad}_{H_2}(K_m)\right) \\
&= \mathrm{ad}_{H_2}\left(H_m - \mathrm{ad}_{H_2}(\mathrm{ad}_{H_2}^{-1}(\tilde{H_m})\right) \\
&= \mathrm{ad}_{H_2}(H_m - \tilde{H}_m) \\
&= \mathrm{ad}_{H_2}(\hat{H}_m) = 0, \qquad (19.10.10)
\end{aligned}$$

since $\hat{H}_m \in N_m$. This calculation also reveals that the order m term in the normal form is $\hat{H}_m$. More precisely, the order m term of (19.10.9) is given by

$$\begin{aligned}
H_m + \mathrm{ad}_{K_m}(H_2) &= H_m - \mathrm{ad}_{H_2}(K_m) \\
&= H_m - \tilde{H}_m = \hat{H}_m. \qquad (19.10.11)
\end{aligned}$$

The theorem is now proved. □

The following results show how the normalization transformations are related to symplectic or canonical transformations.

Proposition 19.10.4 *Let $H(z,\bar{z}) = \sum_{j=2}^{\infty} H_j(z,\bar{z})$ converge in some neighborhood U of the origin in $\mathbb{R}^{2n}$. Assume that H, considered as an element of $\mathcal{P}$, is in normal form with respect to H_2 through terms of order $(m-1) \geq 2$. Denote $H_m = \hat{H}_m + \tilde{H}_m$, where $\hat{H}_m \in N_m$ and $\tilde{H}_m \in R_m$, set $K_m = \Gamma_m(\tilde{H}_m)$, and let ϕ_t denote the flow generated by the Hamiltonian vector field $\dot{z} = -2i\frac{\partial K_m}{\partial \bar{z}}$. Then*

1. *There is a neighborhood $V \subset U$ of the origin such that ϕ_t is defined in V for all $|t| \leq 2$; and*
2. *$exp(ad_{K_m})(H) = H \circ \phi_1$.*

We remark that coordinate transformations generated by the time-one flow map of the solutions of Hamilton's equations are often referred to as *Lie transforms*.

Proof:

1. The origin is an equilibrium point, hence the flow exists at this point for all t. Since flows have open domains, there is an open set containing the origin such that the flow is defined for $|t| \leq 2$.

2. Let $F(t) = H \circ \phi_t$. Taylor expanding $F(t)$ about $t = 0$ gives

$$F(t) = F(0) + F'(0)t + \frac{1}{2!}F''(0)t^2 + \cdots + \frac{1}{n!}F^{(n)}t^n + \cdots. \quad (19.10.12)$$

Now we want to evaluate the Taylor coefficients. Recall that

$$\mathrm{ad}_{K_m}(H) = [K_m, H] = -\{K_m, H\} = \{H, K_m\},$$

hence, from the formula for the time evolution of a function under the flow generated by a Hamiltonian vector field (see Chapter 14), we have

$$F'(t) = \frac{d}{dt}(H \circ \phi_t) = \mathrm{ad}_{K_m}(H) \circ \phi_t.$$

Repeatedly differentiating this expression, we find

$$\begin{aligned} F''(t) &= \mathrm{ad}^2_{K_m}(H) \circ \phi_t \\ F'''(t) &= \mathrm{ad}^3_{K_m}(H) \circ \phi_t \\ &\vdots \\ F^{(n)}(t) &= \mathrm{ad}^n_{K_m}(H) \circ \phi_t \\ &\vdots \end{aligned}$$

and substituting these expressions into (19.10.12) gives

$$\begin{aligned} F(1) = H \circ \phi_1 &= \mathbb{1} + \mathrm{ad}_{K_m}(H) \\ &\quad + \frac{1}{2!}\mathrm{ad}^2_{K_m}(H) + \cdots + \frac{1}{n!}\mathrm{ad}^n_{K_m}(H) + \cdots \\ &= \sum_{j=0}^{\infty} \frac{1}{j!}\mathrm{ad}^j_{K_m}(H) \equiv \exp\left(\mathrm{ad}_{K_m}\right)(H), \quad (19.10.13) \end{aligned}$$

which proves the result. □

Corollary 19.10.5 *$exp(ad_{K_m})$ is a symplectic transformation.*

Proof: This follows immediately from Theorem 14.3.6 in Chapter 14 since $\exp(\mathrm{ad}_{K_m})(H) = H \circ \phi_1$, and ϕ_1 is the time-one map obtained from a Hamiltonian flow. □

An Example Calculation: Normalization Through Terms of $\mathcal{O}(3)$

We will now illustrate the use of Theorem 19.10.3 by beginning with a Hamiltonian of the form

$$H = H_2 + H_3 + H_4 + \cdots + H_m + \cdots,$$

and *normalizing* it through terms of $\mathcal{O}(3)$. From Theorem 19.10.3 we have

$$\begin{aligned}\exp\left(\mathrm{ad}_{K_3}\right)(H) &= H + \mathrm{ad}_{K_3}(H) + \frac{1}{2}\mathrm{ad}^2_{K_3}(H) \\ &\quad + \{\text{terms in}\, \mathcal{P}_j, j \geq 5\} \\ \\ &= H_2 + \hat{H}_3 + \tilde{H}_3 + \mathrm{ad}_{K_3}(H_2) \\ &\quad + \underbrace{H_4 + \mathrm{ad}_{K_3}(H_3) + \frac{1}{2}\mathrm{ad}^2_{K_3}(H_2)}_{\mathcal{O}(4)\,\text{terms}} + \mathcal{O}(5)\end{aligned} \tag{19.10.14}$$

Now

$$\mathrm{ad}_{H_2}(K_3) = \mathrm{ad}_{H_2}\left(\mathrm{ad}^{-1}_{H_2}(\tilde{H}_3)\right) = \tilde{H}_3 = -\mathrm{ad}_{K_3}(H_2),$$

from which it also follows that

$$\mathrm{ad}^2_{K_3}(H_2) = -\mathrm{ad}_{K_3}\left(\tilde{H}_3\right),$$

Using these to relations, (19.10.14) can be written as

$$\exp\left(\mathrm{ad}_{K_3}(H)\right) = H_2 + \hat{H}_3 + \underbrace{H_4 + \mathrm{ad}_{K_3}(H_3) - \frac{1}{2}\mathrm{ad}_{K_3}(\tilde{H}_3)}_{\mathcal{O}(4)\,\text{terms}} + \mathcal{O}(5). \tag{19.10.15}$$

This equation can be further simplified. Note that

$$\begin{aligned}\mathrm{ad}_{K_3}(H_3) - \frac{1}{2}\mathrm{ad}_{K_3}(\tilde{H}_3) &= \mathrm{ad}_{K_3}(H_3) - \mathrm{ad}_{K_3}(\tilde{H}_3) \\ &\quad + \frac{1}{2}\mathrm{ad}_{K_3}(\tilde{H}_3) \\ &= \mathrm{ad}_{K_3}(H_3 - \tilde{H}_3) + \frac{1}{2}\mathrm{ad}_{K_3}(\tilde{H}_3) \\ &= \mathrm{ad}_{K_3}(\hat{H}_3) + \frac{1}{2}\mathrm{ad}_{K_3}(\tilde{H}_3)\end{aligned} \tag{19.10.16}$$

Substituting this expression into (19.10.15) gives

$$\exp\left(\mathrm{ad}_{K_3}(H)\right) = H_2 + \hat{H}_3 + \underbrace{H_4 + \mathrm{ad}_{K_3}(\hat{H}_3) + \frac{1}{2}\mathrm{ad}_{K_3}(\tilde{H}_3)}_{\mathcal{O}(4)\,\text{terms}} + \mathcal{O}(5). \tag{19.10.17}$$

By Theorem 19.10.3, (19.10.17) is in normal form with respect to H_2 through terms of order 3.

We make several remarks concerning this computation.

1. Normalizing the $\mathcal{O}(3)$ terms modified the $\mathcal{O}(4)$ terms, but did *not* modify the $\mathcal{O}(2)$ terms.

2. Note that in deriving explicit expressions for the normal form we will need to compute K_m. We will address this issue in a more explicit context in the next subsection.

3. How might one use a partially normalized Hamiltonian such as (19.10.17)? One situation is if the normalized part possesses some special solutions or structure, e.g. it possesses periodic orbits it is integrable. In that case, by appropriate scaling, one may be able to consider the unnormalized part of the Hamiltonian, or "tail" as a perturbation to the normalized part. The advantage of this lies in the fact that there are a great deal of techniques for studying perturbations of periodic orbits and completely integrable Hamiltonian systems.

19.10B Normal Forms Near Elliptic Fixed Points: The Semisimple Case

Now we specialize to the case that will be our primary interest. Henceforth we will assume that

$$H_2(z, \bar{z}) = \sum_{j=1}^{n} \frac{\omega_j}{2} |z_j|^2 \in \mathcal{P}_2. \tag{19.10.18}$$

This is the Hamiltonian corresponding to a linear Hamiltonian vector field having an *elliptic fixed point* at the origin, i.e., the eigenvalues of the matrix associated with the linear vector field are $\pm i\omega_1, \cdots, \pm i\omega_n$, $\omega_i \neq 0$. This form assumes that the linearization is semisimple, i.e, it's complexification is diagonalizable, which is true if the ω_i, $i = 1, \cdots, n$, are distinct.

Definition 19.10.6 *An elliptic fixed point is said to be* resonant *if there exists a nonzero integer n-vector, i.e., $k \in \mathbb{Z}^n - \{0\}$, such that*

$$\langle k, \omega \rangle \equiv \sum_{i=1}^{n} k_i \omega_i = 0. \tag{19.10.19}$$

The order of the resonance *is defined to be*

$$|k| \equiv \sum_{i=1}^{n} |k_i|.$$

For fixed ω, the number of independent integer vectors that solve (19.10.19) is referred to as the multiplicity *of the resonance. If (19.10.19) has no integer solutions, then the elliptic fixed point is said to be* nonresonant.

The following abbreviated notation will be used throughout the remainder of this section

$$z^k \bar{z}^l \equiv z_1^{k_1} \cdots z_n^{k_n} \bar{z}_1^{l_1} \cdots \bar{z}_n^{l_n}, \quad k_i,\, l_i \geq 0,\, i = 1, \cdots, n, \tag{19.10.20}$$

and

$$\langle k - l, \omega \rangle \equiv \sum_{j=1}^{n} (k_j - l_j)\, \omega_j. \tag{19.10.21}$$

Next we give a proposition that shows why the method of normalization is often referred to as *averaging*, since we will show that the terms that cannot be removed by the normal form transformation are averages over trajectories of the Hamiltonian vector field corresponding to $H_2(z, \bar{z}) = \sum_{j=1}^{n} \frac{\omega_j}{2} |z_j|^2$.

Proposition 19.10.7 *Let ρ_t denote the flow generated by the Hamiltonian vector field $\dot{z} = -2i \frac{\partial H_2}{\partial \bar{z}}$. Then*

$$\hat{H}_m(z, \bar{z}) = \lim_{T \to \infty} \frac{1}{T} \int_0^T (H_m \circ \rho_t)(z, \bar{z}) dt.$$

Proof: By definition 19.10.1 we have $\mathrm{ad}_{H_2}(\hat{H}_m) = 0$, hence

$$\frac{d}{dt} \left(\hat{H}_m \circ \rho_t \right) = \mathrm{ad}_{H_2}(\hat{H}_m) \circ \rho_t = 0, \tag{19.10.22}$$

which implies that $\hat{H}_m$ is constant on trajectories generated by the Hamiltonian vector field corresponding to H_2. Recall also that

$$\frac{d}{dt} (K_m \circ \rho_t) = \mathrm{ad}_{H_2} \left(\Gamma_m(\tilde{H}_m) \right) \circ \rho_t = \tilde{H}_m \circ \rho_t. \tag{19.10.23}$$

Now we consider the following calculation

$$\begin{aligned} &\lim_{T \to \infty} \frac{1}{T} \int_0^T (H_m \circ \rho_t)(z, \bar{z}) dt \\ &= \lim_{T \to \infty} \frac{1}{T} \int_0^T \left(\hat{H}_m \circ \rho_t \right)(z, \bar{z}) dt + \lim_{T \to \infty} \frac{1}{T} \int_0^T \left(\tilde{H}_m \circ \rho_t \right)(z, \bar{z}) dt \end{aligned} \tag{19.10.24}$$

From (19.10.22), the first term in (19.10.24) is given by

$$\lim_{T \to \infty} \frac{1}{T} \int_0^T \left(\hat{H}_m \circ \rho_t \right)(z, \bar{z}) dt = \hat{H}_m(z, \bar{z}). \tag{19.10.25}$$

It remains to show that the second expression in (19.10.24) is zero, i.e.,

$$\lim_{T\to\infty}\frac{1}{T}\int_0^T\left(\tilde{H}_m\circ\rho_t\right)(z,\bar{z})dt=0. \tag{19.10.26}$$

From (19.10.23), we have (using $\phi_0=\mathbb{1}$)

$$\frac{1}{T}\int_0^T\left(\tilde{H}_m\circ\rho_t\right)(z,\bar{z})dt=\frac{1}{T}\left(K_m\circ\rho_T-K_m\right). \tag{19.10.27}$$

Equation (19.10.26) will follow if we show that show that $K_m\circ\rho_T$ is bounded for all T. But this is true since the components of $\rho_t(z,\bar{z})$ are given by $z_j(t)=z_je^{i\omega_jt}$, $j=1,\ldots,n$. □

Real Hamiltonians as Functions of Complex Variables: Some Properties

For explicit calculations we will need more concrete notation. We will express our Hamiltonians in the form of a power series

$$H(z,\bar{z})=\sum_{|k|+|l|=2}^{\infty}c_{kl}z^k\bar{z}^l,$$

with

$$|k|+|l|\equiv k_1+\cdots+k_n+l_1+\cdots+l_n,\qquad k_i,\,l_i\geq 0.$$

For real Hamiltonians several relations between the coefficients of the power series hold. Moreover, certain algebraic simplifications of terms are possible. We now want to catalog these for future reference.

$\boxed{\bar{c}_{kl}=c_{lk}}$ This can be seen as follows. For real Hamiltonians we have

$$H(z,\bar{z})=\overline{H(z,\bar{z})}.$$

The Hamiltonians that we are now considering have the following representation

$$H(z,\bar{z})=\sum_{|k|+|l|=2}^{\infty}c_{kl}z^k\bar{z}^l, \tag{19.10.28}$$

and, hence, their complex conjugates are given by

$$\overline{H(z,\bar{z})}=\sum_{|k|+|l|=2}^{\infty}\bar{c}_{kl}\overline{z^k\bar{z}^l}=\sum_{|k|+|l|=2}^{\infty}\bar{c}_{kl}\bar{z}^kz^l. \tag{19.10.29}$$

Reality implies that (19.10.28) and (19.10.29) are equal. Equating the coefficients of each term in (19.10.28) and (19.10.29) gives

$$\bar{c}_{kl}=c_{lk}. \tag{19.10.30}$$

If $k = l$ then c_{lk} is real This is an immediate consequence of (19.10.30).

Algebraic Simplification, I The following relation will be useful later on in simplifying normal forms that we compute. Suppose that the Hamiltonian has two terms of the same order having the following form

$$c_{kl} z^k \bar{z}^l + c_{lk} z^l \bar{z}^k,$$

where

$$c_{kl} \equiv a + ib.$$

Then this term can be simplified as follows

$$\begin{aligned}
& c_{kl} z^k \bar{z}^l + c_{lk} z^l \bar{z}^k, \\
& = c_{kl} z^k \bar{z}^l + \bar{c}_{kl} z^l \bar{z}^k, \qquad \text{using (19.10.30)}, \\
& = c_{kl} z^k \bar{z}^l + \bar{c}_{kl} \overline{z^k \bar{z}^l}, \\
& = (a + ib)(\mathrm{Re}\, z^k \bar{z}^l + i \mathrm{Im}\, z^k \bar{z}^l) \\
& \quad + (a - ib)(\mathrm{Re}\, z^k \bar{z}^l - i \mathrm{Im}\, z^k \bar{z}^l), \\
& = 2a \mathrm{Re}\, z^k \bar{z}^l - 2b \mathrm{Im} z^k \bar{z}^l.
\end{aligned} \tag{19.10.31}$$

Algebraic Simplification, II In the case where $k_j \neq l_j$, for some $1 \leq j \leq n$ with at least one of these two exponents nonzero, this last term can be simplified even further:

$$\begin{aligned}
& 2a \mathrm{Re}\, z^k \bar{z}^l - 2b \mathrm{Im} z^k \bar{z}^l \\
& = \mathrm{Re}\, \left[2a \mathrm{Re}\, z^k \bar{z}^l + i 2a \mathrm{Im}\, z^k \bar{z}^l + i 2b \mathrm{Re}\, z^k \bar{z}^l - 2b \mathrm{Im}\, z^k \bar{z}^l \right] \\
& = \mathrm{Re}\, \left[2(a + ib)(\mathrm{Re} z^k \bar{z}^l + i \mathrm{Im}\, z^k \bar{z}^l) \right] \\
& = 2 \mathrm{Re} \left[(a + ib) z^k \bar{z}^l \right].
\end{aligned} \tag{19.10.32}$$

Now denote

$$a + ib = c, \qquad c = |c| e^{i \arg c}.$$

Suppose that in the term

$$z_1^{k_1} \cdots z_n^{k_n} \bar{z}_1^{l_1} \cdots \bar{z}_n^{l_n}$$

there exists exponents such that $k_j \neq l_j$, for some $1 \leq j \leq n$, with at least one of the two nonzero.

Then we transform the z_j and $\bar{z}_j$ terms as follows (and leave the remaining $2n-2$ terms unchanged)

$$z_j \mapsto e^{-\frac{i\,arg\,c}{k_j - l_j}} z_j,$$
$$\bar{z}_j \mapsto e^{\frac{i\,arg\,c}{k_j - l_j}} z_j.$$

Under this transformation we obtain

$$\begin{aligned} &2\mathrm{Re}\left[(a+ib)z^k\bar{z}^l\right], \\ &= 2\mathrm{Re}\left[|c|e^{i\,arg\,c}e^{-i\,arg\,c}z^k\bar{z}^l\right], \\ &= 2|c|\mathrm{Re}\, z^k\bar{z}^l. \end{aligned} \tag{19.10.33}$$

THE DECOMPOSITION OF H_m

In relation to our more general notation, it should be clear that

$$\sum_{|k|+|l|=m} c_{kl} z^k \bar{z}^l = H_m \in \mathcal{P}_m.$$

Moreover, $\mathcal{P}_m$ is spanned by the homogeneous polynomials $z^k\bar{z}^l$, $|k|+|l| = m$. Given H_m, we will want to determine the decomposition $H_m = \hat{H}_m + \tilde{H}_m$. The following calculation will be be crucial for this.

$$\begin{aligned} \mathrm{ad}_{H_2}\left(z^k\bar{z}^l\right) &= \left[H_2, z^k\bar{z}^l\right] \\ &= \left[\sum_{k=1}^n \frac{\omega_k}{2} z_k\bar{z}_k,\, z_1^{k_1}\cdots z_n^{k_n}\bar{z}_1^{l_1}\cdots\bar{z}_n^{l_n}\right] \\ &= -2i\sum_{j=1}^n \left(\frac{\partial}{\partial\bar{z}_j}\left(\sum_{k=1}^n \frac{\omega_k}{2} z_k\bar{z}_k\right)\frac{\partial}{\partial z_j}\left(z_1^{k_1}\cdots z_n^{k_n}\bar{z}_1^{l_1}\cdots\bar{z}_n^{l_n}\right)\right. \\ &\qquad \left. - \frac{\partial}{\partial z_j}\left(\sum_{k=1}^n \frac{\omega_k}{2} z_k\bar{z}_k,\right)\frac{\partial}{\partial\bar{z}_j}\left(z_1^{k_1}\cdots z_n^{k_n}\bar{z}_1^{l_1}\cdots\bar{z}_n^{l_n}\right)\right) \\ &= -2i\sum_{j=1}^n \left(\left(\frac{\omega_j}{2} z_j\right)\left(k_j z_1^{k_1}\cdots z_j^{k_j-1}\cdots z_n^{k_n}\bar{z}_1^{l_1}\cdots\bar{z}_n^{l_n}\right)\right. \\ &\qquad \left. - \left(\frac{\omega_j}{2}\bar{z}_j\right)\left(l_j z_1^{k_1}\cdots z_n^{k_n}\bar{z}_1^{l_1}\cdots\bar{z}_j^{l_j-1}\cdots\bar{z}_n^{l_n}\right)\right) \\ &= -i\sum_{j=1}^n \left(\omega_j k_j - \omega_j l_j\right) z_1^{k_1}\cdots z_n^{k_n}\bar{z}_1^{l_1}\cdots\bar{z}_n^{l_n} \\ &= -i\langle k-l,\omega\rangle z^k\bar{z}^l. \end{aligned} \tag{19.10.34}$$

Thus, from (19.10.34) we see that $z^k\bar{z}^l$, $|k|+|l|=m$, are eigenvectors of $\mathrm{ad}_{H_2}|_{\mathcal{P}_m}$, corresponding to the eigenvalues $-i\langle k-l,\omega\rangle$.

So, for

$$H_m(z,\bar{z}) = \sum_{|k|+|l|=m} c_{kl} z^k \bar{z}^l, \tag{19.10.35}$$

we have $H_m = \hat{H}_m + \tilde{H}_m$, where

$$\hat{H}_m(z,\bar{z}) = \sum_{\substack{|k|+|l|=m \\ \langle k-l,\omega\rangle=0}} c_{kl} z^k \bar{z}^l, \tag{19.10.36}$$

and

$$\tilde{H}_m(z,\bar{z}) = \sum_{\substack{|k|+|l|=m \\ \langle k-l,\omega\rangle\neq 0}} c_{kl} z^k \bar{z}^l. \tag{19.10.37}$$

From (19.10.34) we also can conclude the following

$$\Gamma_m\left(\tilde{H}_m(z,\bar{z})\right) = i \sum_{\substack{|k|+|l|=m \\ \langle k-l,\omega\rangle\neq 0}} \langle k-l,\omega\rangle^{-1} c_{kl} z^k \bar{z}^l. \tag{19.10.38}$$

Examples: Normal Forms for Resonant Elliptic Fixed Points of Two Degree-of-Freedom Systems

We will now compute the leading order terms for several normal forms associated with resonant elliptic fixed points of two degree-of-freedom Hamiltonian systems. We will assume that the quadratic part of the Hamiltonian has the following form

$$H(z_1,\bar{z}_1,z_2,\bar{z}_2) = \frac{\omega_1}{2}|z_1|^2 + \frac{\omega_2}{2}|z_2|^2.$$

For two degree-of-freedom systems the resonance condition (19.10.19) can be stated much more simply: the elliptic fixed point is resonant if $\frac{\omega_1}{\omega_2}$ is a rational number and nonresonant if $\frac{\omega_1}{\omega_2}$ is an irrational number. For the former case we use the phrase "$\omega_1 : \omega_2$ resonance".

In the following examples we will compute the terms that cannot be removed by the normal form transformation, i.e., the terms in $N_m = \ker\left(\mathrm{ad}_{H_2}|_{\mathcal{P}_m}\right)$. These terms have the form of (19.10.36), which can be deduced from (19.10.34) (cf. (19.10.20) and (19.10.21)). Hence, to find the terms at order m in N_m, we proceed as follows. Find a solution to

$$(k_1-l_1)\omega_1 + (k_2-l_2)\omega_2 = 0, \quad k_i,\, l_i \geq 0, \tag{19.10.39}$$

which satisfies

$$k_1+k_2+l_1+l_2 = m, \tag{19.10.40}$$

and is subject to the constraint

$$0 \leq |k_1 - l_1|,\, |k_2 - l_2| \leq m. \tag{19.10.41}$$

The existence of such a solution implies that there is an order m term of the form

$$z_1^{k_1} z_2^{k_2} \bar{z}_1^{l_1} \bar{z}_2^{l_2}.$$

All such solutions will give all order m terms. These are the terms that *cannot* be removed by the normalization procedure.

1:1 Resonance

To normalize the Hamiltonian at order m, the solutions of the following equations play the key role

$$k_1 - l_1 + k_2 - l_2 = 0, \tag{19.10.42}$$

$$k_1 + k_2 + l_1 + l_2 = m, \tag{19.10.43}$$

$$0 \leq |k_1 - l_1|,\, |k_2 - l_2| \leq m, \tag{19.10.44}$$

Equation (19.10.42) is the $1:1$ resonance condition and (19.10.43) and (19.10.44) are constraints placed on the exponents by the particular order of the terms being normalized. There is one immediate conclusion that we can make. Combining (19.10.42) and (19.10.43) gives

$$k_1 + k_2 = \frac{m}{2}.$$

Hence, the normal form contains no odd order terms.

We then turn to determining the order 4 terms. In this case (19.10.39), (19.10.40), and (19.10.41) become

$$k_1 - l_1 + k_2 - l_2 = 0, \tag{19.10.45}$$

$$k_1 + k_2 + l_1 + l_2 = 4, \tag{19.10.46}$$

$$0 \leq |k_1 - l_1|,\, |k_2 - l_2| \leq 4. \tag{19.10.47}$$

The solutions of (19.10.45) compatible with (19.10.47) are given by

$$\begin{aligned}
&a)\ \ k_1 - l_1 = 0, \quad k_2 - l_2 = 0,\\
&b)\ \ k_1 - l_1 = 1, \quad k_2 - l_2 = -1,\\
&b')\ \ k_1 - l_1 = -1, \quad k_2 - l_2 = 1,\\
&c)\ \ k_1 - l_1 = 2, \quad k_2 - l_2 = -2,\\
&c')\ \ k_1 - l_1 = -2, \quad k_2 - l_2 = 2,\\
&d)\ \ k_1 - l_1 = 3, \quad k_2 - l_2 = -3,\\
&d')\ \ k_1 - l_1 = -3, \quad k_2 - l_2 = 3,\\
&e)\ \ k_1 - l_1 = 4, \quad k_2 - l_2 = -4,\\
&e')\ \ k_1 - l_1 = -4, \quad k_2 - l_2 = 4.
\end{aligned}$$

Next we take each of these pairs of solutions and combine them with (19.10.46).

a) and (19.10.46) : This yields the solutions

$$(k_1, k_2, l_1, l_2) = (1, 1, 1, 1),\ (0, 2, 0, 2),\ (2, 0, 2, 0),$$

which correspond to the terms

$$|z_1|^2|z_2|^2, \quad |z_2|^4, \quad |z_1|^4,$$

respectively.

b) and (19.10.46) : This yields the solutions

$$(k_1, k_2, l_1, l_2) = (2, 0, 1, 1),\ (1, 1, 0, 2),$$

which correspond to the terms

$$z_1^2 \bar{z}_1 \bar{z}_2, \quad z_1 z_2 \bar{z}_2^2,$$

respectively.

b') and (19.10.46) : This yields the solutions

$$(k_1, k_2, l_1, l_2) = (1, 1, 2, 0),\ (0, 2, 1, 1),$$

which correspond to the terms

$$z_1 z_2 \bar{z}_1^2, \quad z_2^2 \bar{z}_1 \bar{z}_2,$$

respectively.

Notice that the terms corresponding to the solutions of b) and (19.10.46) are the complex conjugates of the terms corresponding to the solutions of b') and (19.10.46). This is generally true of the primed and unprimed equations corresponding to the same letters; henceforth we will only simultaneously solve the equation corresponding to the unprimed letter and (19.10.46).

c) and (19.10.46) : This yields the solution

$$(k_1, k_2, l_1, l_2) = (2, 0, 0, 2),$$

which corresponds to the term

$$z_1^2 \bar{z}_2^2.$$

d) and (19.10.46) : This yields no solutions since we must have $l_i,\ k_i \geq 0$.

e) and (19.10.46) : This yields no solutions since we must have $l_i,\ k_i \geq 0$.

Hence, the normal form through order 4 terms has the form (where we have remembered to put in the complex conjugate terms)

$$\begin{aligned} H(z_1,\bar{z}_1,z_2,\bar{z}_2) = &\frac{1}{2}|z_1|^2+\frac{1}{2}|z_2|^2 \\ &+c_{1111}|z_1|^2|z_2|^2+c_{0202}|z_2|^4+c_{2020}|z_1|^4 \\ &+2ac_{2011}z_1^2\bar{z}_1\bar{z}_2+c_{1120}\bar{z}_1^2z_1z_2 \\ &+c_{1102}z_1z_2\bar{z}_2^2+c_{0211}\bar{z}_1\bar{z}_2z_2^2 \\ &+c_{2002}z_1^2\bar{z}_2^2+c_{0220}\bar{z}_1^2z_2^2+\mathcal{O}(6), \end{aligned} \tag{19.10.48}$$

Using "algebraic simplification, II" given in Section 19.10b, the normal form can be written as

$$\begin{aligned} H(z_1,\bar{z}_1,z_2,\bar{z}_2) = &\frac{1}{2}|z_1|^2+\frac{1}{2}|z_2|^2 \\ &+c_{1111}|z_1|^2|z_2|^2+c_{0202}|z_2|^4+c_{2020}|z_1|^4 \\ &+2a\mathrm{Re}z_1^2\bar{z}_1\bar{z}_2-2b\mathrm{Im}z_1^2\bar{z}_1\bar{z}_2 \\ &+2c\mathrm{Re}z_1z_2\bar{z}_2^2-2d\mathrm{Im}z_1z_2\bar{z}_2^2 \\ &+2e\mathrm{Re}z_1^2\bar{z}_2^2-2f\mathrm{Im}\bar{z}_1^2z_2^2+\mathcal{O}(6), \end{aligned} \tag{19.10.49}$$

where

$$\begin{aligned} c_{2011} &= a+ib, \\ c_{1102} &= c+id, \\ c_{2002} &= e+if. \end{aligned} \tag{19.10.50}$$

Using "algebraic simplication, II" given in 19.10b, the normal form can be written as

$$\begin{aligned} &H(z_1,\bar{z}_1,z_2,\bar{z}_2) = \tfrac{1}{2}|z_1|^2+\tfrac{1}{2}|z_2|^2 \\ &+c_{1111}|z_1|^2|z_2|^2+c_{0022}|z_2|^4+c_{2200}|z_1|^4 \\ &+2|c_{2011}|\mathrm{Re}z_1^2\bar{z}_1\bar{z}_2+2|c_{1102}|\mathrm{Re}z_1z_2\bar{z}_2^2+2|c_{2002}|\mathrm{Re}z_1^2\bar{z}_2^2 \\ &+\mathcal{O}(6). \end{aligned}$$

1:2 Resonance

Following the same procedure as in the $1:1$ resonance case, we seek nonnegative integer solutions of the following equations

$$k_1-l_1+2(k_2-l_2)=0, \tag{19.10.51}$$

$$k_1+k_2+l_1+l_2=3, \tag{19.10.52}$$

$$0\leq|k_1-l_1|,\ |k_2-l_2|\leq 3. \tag{19.10.53}$$

Solutions of (19.10.51) compatible with (19.10.53) are given by

$$\begin{aligned} a)\quad & k_1 - l_1 = 0, \quad k_2 - l_2 = 0, \\ b)\quad & k_1 - l_1 = 2, \quad k_2 - l_2 = -1, \\ b')\quad & k_1 - l_1 = -2, \quad k_2 - l_2 = 1, \end{aligned}$$

We next seek simultaneous solutions of each of these pairs equations with (19.10.52).

a) and (19.10.52) : This yields no solutions since we must have $l_i,\ k_i \geq 0$.

b) and (19.10.52) : This yields the solution

$$(k_1, k_2, l_1, l_2) = (2, 0, 0, 1),$$

which corresponds to the term

$$z_1^2 \bar{z}_2.$$

Solving b') and (19.10.52) simultaneously gives rise to the complex conjugate of the term arising from the simultaneous solution of b) and (19.10.52).

Hence, the normal form through order 3 terms is given by (where we have remembered to put in the complex conjugate terms)

$$H(z_1, \bar{z}_1, z_2, \bar{z}_2) = \frac{1}{2}|z_1|^2 + |z_2|^2 + c_{2001} z_1^2 \bar{z}_2 + c_{0120} \bar{z}_1^2 z_2 + \mathcal{O}(4), \quad (19.10.54)$$

Using "algebraic simplification, I" given in section 19.10b, the normal form can be written as

$$H(z_1, \bar{z}_1, z_2, \bar{z}_2) = \frac{1}{2}|z_1|^2 + |z_2|^2 + 2a\mathrm{Re} z_1^2 \bar{z}_2 - 2b\mathrm{Im} z_1^2 \bar{z}_2 + \mathcal{O}(4), \quad (19.10.55)$$

where

$$c_{2001} = a + ib.$$

Using "algebraic simplification, II" given in section 19.10b, the normal form can be written as

$$H(z_1, \bar{z}_1, z_2, \bar{z}_2) = \frac{1}{2}|z_1|^2 + |z_2|^2 + 2|c_{2001}|\mathrm{Re} z_1^2 \bar{z}_2 + \mathcal{O}(4), \quad (19.10.56)$$

1:3 Resonance

Following the same procedure as in the previous two cases, we find that there are no third order terms. The fourth order terms can be obtained through solution of the following equations

$$k_1 - l_1 + 3(k_2 - l_2) = 0, \quad (19.10.57)$$

$$k_1 + k_2 + l_1 + l_2 = 4, \quad (19.10.58)$$

$$0 \leq |k_1 - l_1|,\ |k_2 - l_2| \leq 4. \quad (19.10.59)$$

Solutions of (19.10.57) compatible with (19.10.59) are given by

$$\begin{aligned} &a)\ \ k_1 - l_1 = 0, \quad k_2 - l_2 = 0, \\ &b)\ \ k_1 - l_1 = 3, \quad k_2 - l_2 = -1, \\ &b')\ \ k_1 - l_1 = -3, \quad k_2 - l_2 = 1. \end{aligned}$$

We next solve each of these pairs of equations simultaneously with (19.10.58).

a) and (19.10.52) : This yields the solutions

$$(k_1, k_2, l_1, l_2) = (0, 2, 0, 2),\ (2, 0, 2, 0),\ (1, 1, 1, 1),$$

which correspond to the terms

$$|z_2|^4,\ |z_1|^4,\ |z_1|^2|z_2|^2,$$

respectively.

b) and (19.10.52) : This yields the solutions

$$(k_1, k_2, l_1, l_2) = (3, 0, 0, 1),$$

which correspond to the terms

$$z_1^3 \bar{z}_2.$$

Solution of b') and (19.10.58) yields the complex conjugate of this term.

Hence, the normal form through order 4 terms is given by (where we have remembered to put in the complex conjugate terms)

$$\begin{aligned} H(z_1, \bar{z}_1, z_2, \bar{z}_2) = &\frac{1}{2}|z_1|^2 + \frac{3}{2}|z_2|^2 \\ &+ c_{0202}|z_2|^4 + c_{2020}|z_1|^4 + c_{1111}|z_1|^2|z_2|^2 \\ &+ c_{3001} z_1^3 \bar{z}_2 + c_{0130} \bar{z}_1^3 z_2 + \mathcal{O}(5), \end{aligned} \tag{19.10.60}$$

Using "algebraic simplification, I" given in section 19.10b, the normal form can be written as

$$\begin{aligned} H(z_1, \bar{z}_1, z_2, \bar{z}_2) = &\frac{1}{2}|z_1|^2 + \frac{3}{2}|z_2|^2 \\ &+ c_{0202}|z_2|^4 + c_{2020}|z_1|^4 + c_{1111}|z_1|^2|z_2|^2 \\ &+ 2a\mathrm{Re} z_1^3 \bar{z}_2 - 2b\mathrm{Im} z_1^3 \bar{z}_2 + \mathcal{O}(5), \end{aligned} \tag{19.10.61}$$

where

$$c_{3001} = a + ib.$$

Using "algebraic simplification, II" given in section 19.10b, the normal form can be written as

$$\begin{aligned} H(z_1, \bar{z}_1, z_2, \bar{z}_2) = \frac{1}{2}|z_1|^2 + \frac{3}{2}|z_2|^2 \\ + c_{0202}|z_2|^4 + c_{2020}|z_1|^4 + c_{1111}|z_1|^2|z_2|^2 \\ + 2|c_{3001}|\mathrm{Re} z_1^3 \bar{z}_2 + \mathcal{O}(5). \end{aligned} \tag{19.10.62}$$

There is a large literature on the analysis of the dynamics near resonant elliptic fixed points in two degree-of-freedom Hamiltonian systems; see, e.g., Arnold *et al.* [1988], Sanders and Verhulst [1985], Henrard [1970], Meyer and Hall [1992], and Golubitsky *et al.* [1995].

19.10c The Birkhoff and Gustavson Normal Forms

We now describe the *Birkhoff normal form* and the *Gustavson normal form.* These are normal forms in the neighborhood of an elliptic fixed point in the nonresonant and resonant cases, respectively. We begin with some definitions.

First we recall the form of the Hamiltonian in the neighborhood of an elliptic fixed point that we described earlier:

$$H(z, \bar{z}) = \frac{1}{2}\sum_{i=1}^{n} \omega_i |z_1|^2 + H_3(z, \bar{z}) + H_4(z, \bar{z}) + \cdots. \tag{19.10.63}$$

Near an elliptic equilibrium point symplectic polar coordinates provide a useful coordinate system. These are related to the complex coordinates by

$$z_k \equiv \sqrt{2\rho_k} e^{i\varphi_k}, \qquad \bar{z}_k \equiv \sqrt{2\rho_k} e^{-i\varphi_k}, \qquad k = 1, \ldots, n.$$

However, one must be aware that singularities may arise as $\rho_k \to 0$. Next we define the notion of *Birkhoff normal form* near an elliptic equilibrium point.

Definition 19.10.8 (Birkhoff Normal Form) *The Hamiltonian (19.10.63) is said to be in* Birkhoff normal form of degree r *if it is a polynomial of degree r in z_i, $\bar{z}_i$, which is actually a polynomial of degree $\left[\frac{r}{2}\right]$ in the variables $\rho_i = \frac{1}{2}|z_i|^2$, where $\left[\frac{r}{2}\right]$ denotes the integer part of the number $\frac{r}{2}$.*

Example 19.10.1. Consider the two degree-of-freedom version of (19.10.63) with terms through order 4. Then the Birkhoff normal form of degree 4 has the form

$$H = \omega_1\rho_1 + \omega_2\rho_2 + a\rho_1^2 + b\rho_1\rho_2 + c\rho_2^2.$$

End of Example 19.10.1

Now we can state Birkhoff's theorem (Birkhoff [1966]).

Theorem 19.10.9 (Birkhoff) *Suppose the ω_i in (19.10.63) satisfy no resonance relations of order less than or equal to r. Then there exists a symplectic change of coordinates defined in a neighborhood of the origin such that in the new coordinates the Hamiltonian is reduced to Birkhoff normal form of degree r up to terms of order $r+1$, i.e.,*

$$H = \mathcal{H}_r(\rho) + \mathcal{O}(|z|, |\bar{z}|)^{r+1}.$$

Proof: See Exercise 3. □

Next we consider the case where there are some resonances of order less than or equal to r. In this case we first define what we mean by a *resonant normal form* near an elliptic equilibrium point.

Definition 19.10.10 (Resonant Normal Form) *Let K be a subgroup of the lattice of integers $\mathbb{Z}^n$. A* resonant normal form of degree r under resonances from K *(or, a K resonant normal form of degree r) is a polynomial of degree r in z_i, $\bar{z}_i$ which, when expressed in terms of polar coordinates, depends only on the phases through the combinations $k \cdot \varphi$, with $k \in K$.*

Now we can state Gustavson's theorem on resonant normal forms (Gustavson [1966]).

Theorem 19.10.11 (Gustavson) *Suppose the ω_i in (19.10.63) satisfy no resonance relations of order less than or equal to r, except, possibly, for relations $k \cdot \omega = 0$, $k \in K$. Then there exists a symplectic change of coordinates defined in a neighborhood of the origin such that in the new coordinates the Hamiltonian is reduced to a K resonant normal form of degree r up to terms of order $r+1$.*

Proof: See Exercise 4. □

19.10D The Lyapunov Subcenter Theorem and Moser's Theorem

We now describe two classical results that describe the behavior near equilibrium points of Hamiltonian systems.

Consider an n degree-of-freedom Hamiltonian having the following form

$$H(x,y) = H_2(x,y) + H_3(x,y) + H_4(x,y) + \cdots, \tag{19.10.64}$$

where

$$x \equiv (x_1, \ldots, x_n) \in \mathbb{R}^n, \qquad y \equiv (y_1, \ldots, y_n) \in \mathbb{R}^n,$$

and

$$H_2(x,y) = \frac{\omega_1}{2}(x_1^2 + y_1^2) + \cdots + \frac{\omega_n}{2}(x_n^2 + y_n^2), \tag{19.10.65}$$

and H_r denotes a homogeneous polynomial of degree r in x and y. We must further assume that H is analytic in a neighborhood of the origin, which is an elliptic equilibrium point for the corresponding Hamiltonian vector field.

Theorem 19.10.12 (Lyapunov Subcenter Theorem) *If for all $s > 1$ the ratio $\frac{\omega_s}{\omega_1}$ is not an integer, then there exists an invertible, analytic, canonical transformation $(x, y) \mapsto (\xi, \eta)$ which transforms the Hamiltonian $H(x, y)$ to the form*

$$H(\xi, \eta) = \Phi(\rho) + \mathcal{O}(|\zeta|^2), \tag{19.10.66}$$

where Φ is a function of the single variable $\rho = \xi_1^2 + \eta_1^2$, and $\zeta = (\xi_2, \ldots, \xi_n, \eta_2, \ldots, \eta_n)$.

Proof: See Siegel and Moser [1971] and Moser [1958]. □

From the form of the transformed Hamiltonian one sees immediately that $\zeta = 0$ is a two dimensional invariant manifold, with the dynamics on this manifold given by

$$\dot{\xi}_1 = 2\frac{d\Phi}{d\rho}(\rho)\eta_1,$$
$$\dot{\eta}_1 = -2\frac{d\Phi}{d\rho}(\rho)\xi_1.$$

If one multiplies the first equation by ξ_1, the second by η_1, adds them together and uses the definition of ρ one sees immediately that ρ is a constant of the motion on this two dimensional invariant manifold. Since $\rho = \xi_1^2 + \eta_1^2$, we see that this two dimensional invariant manifold is filled with periodic orbits. Moreover, the form of the equations, *restricted to the periodic orbit ρ=constant*, is that of a linear harmonic oscillator with frequency $\frac{d\Phi}{d\rho}(\rho)$.

The Lyapunov subcenter theorem states that under the nonresonance assumptions given by the theorem, the corresponding two dimensional invariant subspace of the linearized Hamiltonian vector field filled with periodic orbits, all having frequency ω_1, persists for the full nonlinear problem, however the frequencies may change slightly. (Keep in mind that this is a local result valid in a neighborhood of the equilibrium point.) If the nonresonance condition is violated then the result does not hold in the sense that a manifold of periodic solutions does not exist for the nonlinear Hamiltonian vector field (Roels [1971a], [1971b]). Periodic orbits may persist from the linearized problem. However, analytic manifolds of such solutions do not exist. See Weinstein [1973], Moser [1976], [1978], and Ito [1989].

There is one other point to be made. As mentioned in the remarks at the end of our discussion of normal forms, generically normal form transformations are divergent when taken to all orders. However, it may be that

the transformation is convergent on a lower dimensional submanifold, as it is in the situation described by the Lyapunov subcenter theorem.

Moser [1958] has generalized the Lyapunov subcenter theorem to the case where there is exactly one pair of real eigenvalues, λ and $-\lambda$. We state his theorem.

Theorem 19.10.13 (Moser's Theorem) *Suppose H_2 in the Hamiltonian (19.10.64) has the form*

$$H_2(x,y) = \lambda x_1 y_1 + \frac{\omega_2}{2}(x_2^2 + y_2^2) + \cdots + \frac{\omega_n}{2}(x_n^2 + y_n^2). \tag{19.10.67}$$

Then there exists an invertible, analytic, canonical transformation $(x,y) \mapsto (\xi,\eta)$ which transforms the Hamiltonian $H(x,y)$ to the form

$$H(\xi,\eta) = \Phi(\rho) + \mathcal{O}(|\zeta|^2), \tag{19.10.68}$$

where Φ is a function of the single variable $\rho = \xi_1\eta_1$, and $\zeta = (\xi_2,\ldots,\xi_n,\eta_2,\ldots,\eta_n)$.

Proof: See Moser [1958]. □

From the form of the transformed Hamiltonian one sees immediately that $\zeta = 0$ is a two dimensional invariant manifold, with the dynamics on this manifold given by

$$\dot{\xi}_1 = \frac{d\Phi}{d\rho}(\rho)\xi_1,$$
$$\dot{\eta}_1 = -\frac{d\Phi}{d\rho}(\rho)\eta_1.$$

If one multiplies the first equation by η_1, the second by ξ_1, adds them together and uses the definition of ρ one sees immediately that ρ is a constant of the motion on this two dimensional invariant manifold, and the trajectories are given by the hyperbolae defined by ρ=constant.

19.10E The KAM and Nekhoroshev Theorem's Near an Elliptic Equilibrium Point

Suppose the ω_i in (19.10.63) satisfy no resonance relations of order less than or equal to 4. Then, in a neighborhood of the origin, the Hamiltonian can be transformed to Birkhoff normal form through degree 4:

$$H = H_0(\rho) + \mathcal{O}(5), \tag{19.10.69}$$

where

$$H_0(\rho) = \sum_{i=1}^{n} \omega_i \rho_i + \frac{1}{2}\sum_{i,j=1}^{n} a_{i,j}\rho_i\rho_j.$$

The Hamiltonian $H_0(\rho)$ defines a completely integrable Hamiltonian system where the trajectories lie on the invariant tori ρ = constant. Now for ρ sufficently small one could view the $\mathcal{O}(5)$ terms as a perturbation of $H_0(\rho)$. In this case it is natural to think of trying to apply the KAM theorem to see if any of the invariant tori of $H_0(\rho)$ are preserved when the effect of the $\mathcal{O}(5)$ terms is considered. This can be done if $H_0(\rho)$ is appropriately nondegenerate, which we describe in more detail.

As is typical in KAM type arguments, we need a nondegeneracy assumption on the unperturbed Hamiltonian. The Hamiltonian $H_0(\rho)$ is said to be *nondegenerate* if

$$\det\left(\frac{\partial^2 H_0}{\partial \rho^2}\right) \neq 0,$$

and *isoenergetically nondegenerate* if

$$\det\begin{pmatrix} \frac{\partial^2 H_0}{\partial \rho^2} & \frac{\partial H_0}{\partial \rho} \\ \frac{\partial H_0}{\partial \rho} & 0 \end{pmatrix} \neq 0.$$

We now have the following theorem due to Arnold [1963].

Theorem 19.10.14 (Arnold) *For $H_0(\rho)$ either nondegenerate or isoenergetically nondegnerate, in a sufficently small neighborhood of the origin there exists invariant tori for $H_0(\rho) + \mathcal{O}(5)$ having freqencies close to the linearized frequencies ω_i.*

Proof: See Arnold [1963]. □

As one might suspect, there is also a version of Nekhoroshev's theorem that is valid in the neighborhood of an elliptic equilbrium point, the ω_i in (19.10.63) satisfy no resonance relations of order less than or equal to 4. In addition, we assume that the matrix $A \equiv (a_{ij})$ is sign definite, say positive (if not, then multiply the Hamiltonian by -1), with spectrum bounded from below by $m > 0$ and bounded from above by $M > 0$.

Theorem 19.10.15 (Lochak) *Consider a trajectory $(z(t), \bar{z}(t))$ of the Hamiltonian vector field generated by the Hamiltonian (19.10.69), written in complex coordinates $(z, \bar{z})$. There is a constant $\nu > 0$ such that if $(z(0), \bar{z}(0))$ is small enough and satisfies*

$$|z_j(0)| \geq \nu \parallel z(0) \parallel^{2+\frac{1}{n+2}}, \qquad j = 1, \ldots, n,$$

where $\| \cdot \|$ is the Euclidean norm, then one has

$$\parallel z_j(t) - z(0) \parallel \leq \frac{\nu}{2} \parallel z(0) \parallel^{2+\frac{1}{n+2}}, \qquad j = 1, \ldots, n,$$

provided that t satisfies

$$|t| \leq \mathcal{T} \exp\left(\parallel z(0) \parallel^{-\frac{1}{n+2}}\right),$$

where $\mathcal{T}$ is some strictly positive constant.

Proof: See Lochak [1992]. □

Polar coordinates are the natural "action-angle" coordinates in the neighborhood of an elliptic equilibrium point. However, using polar coordinates can present difficulties when studying trajectories in a neighborhood of an equilibrium point. The reason for this is that a singularity develops when a component of the radius vector goes to zero. This problem has been overcome in the recent work of Niederman [1998] and Fasso et al. [1998].

19.10f Hamiltonian Normal Forms and Symmetries

In this subsection we will deal with the situation where the Hamiltonian which we are transforming to normal form has a symmetry. The main result is that the normal form, through any finite order which we wish to calculate, will have the same symmetry. All the results in this subsection are from Churchill et al. [1983].

We recall our earlier notation. Let

$$\mathcal{P} = \oplus_{r=2}^{\infty} \mathcal{P}_r,$$

denote the space of (scalar valued) form power series, and $\mathcal{P}_r$ will denote the real valued homogeneous polynomials of order r. We assume that $H_2 \in \mathcal{P}_2$ splits $\mathcal{P}$ (recall definition 19.10.2).

The following is our assumption on the nature of the group action.

Assumption 19.10.1 (The Group Action) *Let $\mathcal{G}$ denote a group. We assume that it acts linearly (on the right) on $\mathcal{P}$ as follows. For any $g \in \mathcal{G}$, H, $F \in \mathcal{P}$:*

1. $\mathcal{P}_r \cdot g \subset \mathcal{P}_r$,
2. $H_2 \cdot g = H_2$,
3. $\{H \cdot g, F \cdot g\} = \pm\{H, F\} \cdot g$.

Remarks on the Group Action Assumption:

Let us now make several remarks intended to related to the group action assumption.

1. Our viewpoint here is that the group elements act on the functions $F \in \mathcal{P}$, and they do so by ordinary composition of functions, which is what "$\cdot$" stands for. This is consistent with our view of the normal form procedure, where we are successively modifying the original Hamiltonian.

2. Regarding condition 2 above, if $F \cdot g = F$ for some $g \in \mathcal{G}$ we say that g *fixes* F, or that it is *invariant with respect to* g. The group element is said to be a *symmetry of* F. If $F \cdot g = F$ for all $g \in \mathcal{G}$ we say that $\mathcal{G}$ *fixes* F, or that it is *invariant with respect to the group* $\mathcal{G}$, or that it is $\mathcal{G}$ *invariant*.

3. Regarding condition 3 above, the choice of sign requires some explanation. The plus sign indicates that we are considering a *symplectic group action*, and the minus sign indicates that we are considering a *reversing group action*. In a specific application the appropriate sign is chosen and then fixed thereafter. The theory is developed in exactly the same way for each case.

Since we have assumed that H_2 splits $\mathcal{P}$ we have

$$\mathcal{P}_r = R_r \oplus N_r,$$

where

$$R_r = \operatorname{Im} \operatorname{ad}_{H_2}|_{\mathcal{P}_r}, \qquad N_r = \operatorname{Ker} \operatorname{ad}_{H_2}|_{\mathcal{P}_r},$$

(and, recall, $\operatorname{ad}_{H_2}(\cdot) \equiv -\{H_2, \cdot\}$, where $\{H_2, \cdot\}$ denotes the Poisson bracket). Then we have the following lemma.

Lemma 19.10.16

1. *N_r and R_r are both $\mathcal{G}$ invariant.*

2. *$E \in N_r$ and $F \in R_r$ are both fixed by an element $g \in \mathcal{G}$ if and only if $E + F$ is fixed by g.*

3. *Let $H = ad_{H_2}(F)$ for $F \in R_r$. Then $H \in R_r$, and H is fixed by $g \in \mathcal{G}$ if and only if $F \cdot g = \pm F$.*

4. *Let $H \cdot g = H$ and $F \cdot g = \pm F$ for some $g \in \mathcal{G}$. Then $ad_F^j(H)$ is fixed by g for all $j \geq 0$.*

5. *Let $F \cdot g = F$ for some $g \in \mathcal{G}$. Then $H = \oplus_{r=2}^{\infty} H_r$ is in normal form through terms of order m with respect to F if and only if $H \cdot g$ has this property.*

Proof:

1. Suppose $E \in N_r$, then we have

$$\{H_2, E \cdot g\} = \{H_2 \cdot g, E \cdot g\} = \pm\{H_2, E\} \cdot g = 0,$$

since $E \in N_r$. Hence we have shown that $E \cdot g \in N_r$. This establishes that N_r is $\mathcal{G}$ invariant.

Now suppose that $F \in R_r$. Then there exists some $K \in R_r$ such that $\mathrm{ad}_{H_2}(K) = F = -\{H_2, K\}$. We use this fact in the following calculation

$$\begin{aligned} F \cdot g = -\{H_2, K\} \cdot g &= \mp\{H_2 \cdot g, K \cdot g\}, \\ &= \{H_2, (\mp K) \cdot g\}, \\ &= \mathrm{ad}_{H_2}((\mp K) \cdot g) \in R_r. \end{aligned}$$

This establishes that R_r is $\mathcal{G}$ invariant.

2. This follows from 1 and the uniqueness of the direct sum decomposition.

3. First, suppose $H \in R_r$ and H is fixed by g, i.e., $H \cdot g = H$. Then

$$\begin{aligned} H \cdot g = -\{H_2, F\} \cdot g &= \mp\{H_2 \cdot g, F \cdot g\}, \\ &= -\{H_2, (\pm F) \cdot g\}. \end{aligned}$$

Since $H = H \cdot g$ we have

$$-\{H_2, F\} = -\{H_2, (\pm F) \cdot g\},$$

and since $\mathrm{ad}_{H_2}|_{R_r}$ is an isomorphism it follows that

$$F = \pm F \cdot g.$$

Now suppose $F = \pm F \cdot g$. Using our assumption on the group action we have

$$\begin{aligned} H \cdot g &= -\{H_2, F\} \cdot g, \\ &= \mp\{H_2 \cdot g, F \cdot g\}, \\ &= -\{H_2 \cdot g, \pm F \cdot g\}, \\ &= -\{H_2, F\} = H. \end{aligned}$$

4. The proof is by induction.

j=0: By definition, $\mathrm{ad}_F^0 = \text{identity}$. Hence $\mathrm{ad}_F^0(H) \cdot g = \mathrm{ad}_F^0(H)$ since $H \cdot g = H$.

j=1: For this case we have:

$$\begin{aligned} \mathrm{ad}_F^1(H) \cdot g = -\{F, H\} \cdot g &= \{H, F\} \cdot g, \\ &= \pm\{H \cdot g, F \cdot g\}, \\ &= \{H \cdot g, \pm F \cdot g\}, \\ &= -\{\pm F \cdot g, H \cdot g\}, \\ &= -\{F, H\} = \mathrm{ad}_F^1(H). \end{aligned}$$

Induction Assumption: We assume that the result holds for $j = n-1$, i.e., $\mathrm{ad}_F^{n-1}(H) \cdot g = \mathrm{ad}_F^{n-1}(H)$.

$j = n$**:** We now show that the result holds for $j = n$:

$$\begin{aligned}
\mathrm{ad}_F^n(H) \cdot g &= \left(\mathrm{ad}_F\left(\mathrm{ad}_F^{n-1}(H)\right)\right) \cdot g, \\
&= -\{F, \mathrm{ad}_F^{n-1}(H)\} \cdot g, \\
&= \mp\{F \cdot g, \mathrm{ad}_F^{n-1}(H) \cdot g\}, \\
&= -\{\pm F \cdot g, \mathrm{ad}_F^{n-1}(H) \cdot g\}, \\
&= -\{F, \mathrm{ad}_F^{n-1}(H)\}, \\
&= \mathrm{ad}_F^n(H).
\end{aligned}$$

5. It follows that if $F \cdot g = F$ for some $g \in \mathcal{G}$ then

$$-\{F, H_j\} \cdot g = \mp\{F, H_j \cdot g\}, \quad j = 1, \cdots.$$

Now suppose that $H = \oplus_{r=2}^{\infty} H_r$ is in normal form with respect to F through terms of order m, i.e., $\mathrm{ad}_F(H_r) = 0$, $r = 2, \cdots, m$. Then we have

$$-\{F, H_r\} \cdot g = \mp\{F, H_r \cdot g\} = \pm \mathrm{ad}_F(H_r \cdot g) = 0, \quad r = 2, \cdots, m.$$

Hence, $H \cdot g$ is in normal form with respect to F through terms of order m.

□

Theorem 19.10.17 *Let $H = \oplus_{r=2}^{\infty} H_r \in \mathcal{P}_r$ be in normal form with respect to H_2 through terms of order $(m-1) \geq 2$, and assume H_2 splits $\mathcal{P}$. Let $H_m = \tilde{H}_m + \hat{H}_m$, where $\tilde{H}_m \in R_m$, $\hat{H}_m \in N_m$, and set $K_m = \Gamma_m(\tilde{H}_m)$. We assume that Assumption 19.10.1 holds and that $g \in \mathcal{G}$ fixes H. Then g also fixes* $\exp(ad_{K_m})(H)$.

Proof: Since $H \cdot g = H$, it follows from part 1 of Lemma 19.10.16 $H_m = \tilde{H}_m + \hat{H}_m$ is fixed by g. Part 2 of the lemma then implies that $\hat{H}_m$ is fixed by g and $\tilde{H}_m$ is fixed by g. It follows from part 3 of the lemma that if $\tilde{H}_m = -\{H_2, K_m\}$, where $K_m = \Gamma_m(\tilde{H}_m)$, then $K_m \cdot g = \pm K_m$. The theorem then follows from part 4 of Lemma 19.10.16. □

Summary:

We summarize the main ideas in this section. Recall that we say that $H = \oplus_{r=2}^{\infty} H_r$ admits a symmetry corresponding to $g \in \mathcal{G}$ if $H \cdot g = H$.

- We have shown that each H_r admits the same symmetry.
- When H_2 splits $\mathcal{P}$, we have shown that $\tilde{H}_r$ and $\hat{H}_r$ each admit the same symmetry.

- When H is converted into normal form with respect to H_2 through terms of order $(m-1) \geq 2$, we have shown that the normal form through terms of order $(m-1) \geq 2$ will have the same symmetry.

19.10G Final Remarks

We want to end this section with some final remarks.

Convergence. Convergence of the normalizing transformation is discussed in Ito [1989], see also the classic work of Siegel [1941]. A good review of these issues can be found in Arnold et al. [1988]. The following results are known.

1. If (19.10.63) is completely integrable, then the transformation to Birkhoff normal form is a convergent transformation ((Rüssmann [1964]).
2. For "most" Hamiltonians of the form (19.10.63), the transformation to Birkhoff normal form is a divergent transformation (Siegel [1954]).

See also Bryuno [1988], [1989a], [1989b].

Stability of Elliptic Equilbria. In Chapter 14 we saw that if the second derivative of the Hamiltonian at the elliptic equilbrium point was sign definite, then the equlibrium point is Liapunov stable. In the case that it is not sign definite (e.g., some frequencies have opposite signs), then *for the two-degree-of-freedom case*, the KAM theorem can be applied to study stability, since, in that case, KAM tori are codimension one in the energy surface and therefore bound trajectories, see Arnold [1961] and Meyer and Schmidt [1986]. A good general reference for results on this subject is Bryuno [1989c].

Invariants. As we saw in our development of the approach of Elphick et al. [1987] to general normal forms, the normal form can be expressed as polynomials that are invariant under some group action. Similar results hold for the Hamiltonian case. For general background see Golubitsky et al. [1988]. For examples specific to the Hamiltonian case see Kirk et al. [1996], Hoveijn [1992].

19.11 Exercises

1. Show that for $F \in \mathcal{P}_s$, $H_r \in \mathcal{P}_r$,

$$\mathrm{ad}_F(H_r) \in \mathcal{P}_{r+s-2}.$$

Using this relation, inductively verify that

$$\mathrm{ad}_F^j(H_r) \in \mathcal{P}_{r+j(s-2)}.$$

2. Consider a two degree-of-freedom Hamiltonian in the neighborhood of an elliptic equilibrium. Prove that the normal form, through terms of order r, is completely integrable. Does the same argument apply to Hamiltonian systems with three or more degrees-of-freedom?

3. Consider the Hamiltonian

$$H = H_2 + H_3 + \cdots + H_m + \cdots, \qquad H_r \in \mathcal{P}_r,$$

where

$$H_2 = \sum_{i=1}^{n} \frac{\omega_i}{2} |z_i|^2.$$

Suppose that the Hamiltonian is transformed to normal form through order m terms. Prove that the normal form through order m terms is invariant with respect to the flow generated by linear Hamiltonian vector field with Hamiltonian given by H_2. Describe the group action defined by this flow? Can you relate this to the averaging result described in Proposition 19.10.7?

4. Recall the definition of a Lie group action on a vector space V given in Definition 19.7.3. Let $V = \mathbb{R}^{2n}$ be a symplectic vector space with respect to the canonical symplectic form (or, in some instances we will consider $\mathbb{C}^n$ as a symplectic vector space with respect to the complex version of the canonical symplectic form). The Lie group action is said to be symplectic if the map

$$\begin{aligned} \rho_\gamma \,:\, \mathbb{R}^{2n} &\to \mathbb{R}^{2n}, \\ v &\mapsto \gamma \cdot v \equiv \rho_\gamma(v), \end{aligned}$$

is symplectic for each $\gamma \in \Gamma$. Consider the following group actions.

Z_2 acting on $\mathbb{R}^2$:

$$(x, y) \mapsto (-x, -y).$$

$SO(2)$ acting on $\mathbb{C}$:

$$\theta \cdot z = e^{\pm\theta} z.$$

Z_m acting on $\mathbb{C}$:

$$\phi \cdot z = e^{i\phi} z, \quad z = \frac{2\pi}{m}.$$

S^1 acting on $\mathbb{C}^2$:

$$\theta \cdot (z_1, z_2) = (e^{im\theta} z_1, e^{in\theta} z_2), \quad m,\, n \in \mathbb{Z}^+.$$

Are these group actions symplectic?

5. Consider the symplectic group action described in Assumption 19.10.1. Relate this to the notion of a symplectic group action described in the previous exercise.

6. Consider one degree-of-freedom Hamiltonians near an equilibrium point where the leading order terms in the Hamiltonian are quadratic and given by

$$\begin{aligned} H_2 &= \frac{\omega}{2}(p^2 + q^2), \quad \omega > 0, \\ H_2 &= \lambda pq, \quad \lambda > 0. \end{aligned}$$

Compute the normal forms in each case. Can you say anything about convergence of the normal form?

7. Consider two degree-of-freedom Hamiltonians near an equilibrium point where the leading order terms in the Hamiltonian are quadratic and given by

$$H_2 = \lambda p_1 q_1 + \frac{\omega}{2}(p_2^2 + q_2^2), \quad \lambda, \omega > 0,$$
$$H_2 = \lambda_1 p_1 q_1 + \lambda_2 p_2 q_2, \quad \lambda_1, \lambda_2 > 0.$$

Compute the normal forms in each case. For the second Hamiltonian consider both the cases $\frac{\lambda_1}{\lambda_2}$ rational and $\frac{\lambda_1}{\lambda_2}$ irrational.

8. Consider three degree-of-freedom Hamiltonians near an equilibrium point where the leading order terms in the Hamiltonian are quadratic and given by

$$H_2 = \lambda p_1 q_1 + \frac{\omega_2}{2}(p_2^2 + q_2^2) + \frac{\omega_3}{2}(p_3^2 + q_3^2) \quad \omega_2, \omega_3 > 0,$$
$$H_2 = \lambda_1 p_1 q_1 + \lambda_2 p_2 q_2 + \frac{\omega}{2}(p_3^2 + q_3^2), \quad \lambda_1, \lambda_2 > 0.$$

Compute the normal forms in each case. For the first Hamiltonian consider both the cases $\frac{\omega_1}{\omega_2}$ rational and $\frac{\omega_1}{\omega_2}$ irrational. For the second Hamiltonian consider both the cases $\frac{\lambda_1}{\lambda_2}$ rational and $\frac{\lambda_1}{\lambda_2}$ irrational.

9. Consider one degree-of-freedom Hamiltonians defined on $\mathbb{R}^2$ (or $\mathbb{C}$. Compute the normal forms (through order 4) for Hamiltonians that are invariant with respect to the Z_m ($m = 2, 3, 4$) and $SO(2)$ actions described above.

10. Prove Theorem 19.10.9.

11. Prove Theorem 19.10.11.

12. Consider a two-degree-of-freedom Hamiltonian system near an elliptic equilibrium point where the lowest order (quadratic) part of the Hamiltonian is given by

$$H_2(z_1, \bar{z}_1, z_2, \bar{z}_2) = \frac{\omega_1}{2}|z_1|^2 + \frac{\omega_2}{2}|z_2|^2, \qquad \omega_1, \omega_2 > 0.$$

The "Hopf variables", are defined as;

$$W_1 = 2\,\mathrm{Re}\,\left(z_1^{\omega_2}\bar{z}_2^{\omega_1}\right),$$
$$W_2 = 2\,\mathrm{Im}\,\left(z_1^{\omega_2}\bar{z}_2^{\omega_1}\right),$$
$$W_3 = \omega_1|z_1|^2 - \omega_2|z_2|^2,$$
$$W_4 = \omega_1|z_1|^2 + \omega_2|z_2|^2.$$

$$\frac{1}{4}\left(W_1^2 + W_2^2\right) = \left(\frac{W_4 + W_3}{2\omega_1}\right)^{\omega_2}\left(\frac{W_4 - W_3}{2\omega_2}\right)^{\omega_1}.$$

   (a) Show that if ω_1 and ω_2 are resonant, $\mathrm{ad}_{H_2}(H) = 0$ if and only if H can be written as a polynomial in the Hopf variables.

   (b) Show that if ω_1 and ω_2 are not resonant, $\mathrm{ad}_{H_2}(H) = 0$ if and only if H can be written as a polynomial in the Hopf variables W_3 and W_4, i.e., as a polynomial in $|z_1|^2$ and $|z_2|^2$.

   (c) Show that in the resonant case the normal form is invariant with respect to S^1, and in the nonresonant case it is invariant with respect to T^2.

13. Show that the truncated normal form associated with the Hamiltonian near an elliptic equilibrium point is completely integrable if the elliptic equilibrium point is resonant of multiplicity one.

14. Consider the $1:2:2$ resonant elliptic equilibrium point of a three degre-of-freedom Hamiltonian system.

    (a) Show that this is a multiplicity two resonance.

    (b) Show that the normal form, through terms of order three, has the following form

$$H = \frac{1}{2}|z_1|^2 + |z_2|^2 + |z_3|^2 + \frac{a}{2}\,\mathrm{Re}\, z_1^2 \bar{z}_2, \quad a \in \mathbb{R}.$$

    (c) Show that this normal form defines a completely integrable Hamiltonian system. This result is due to R. Cushman. For more information on this problem see Haller and Wiggins [1996].

15. Develop the Elphick-Tirapegui-Brachet-Coullet-Iooss normal form approach for Hamiltonian normal forms.

16. For both the Lyapunov subcenter theorem and Moser's theorem derive conditions under which the orbits on the invariant two-dimensional manifold have different energies. In this case we say that they are "energetically isolated".

17. Using Hamiltonian normal form theory, for H_2 given by (19.10.65), show that the Hamiltonian (19.10.64) can be formally transformed to the form (19.10.66).

18. Using Hamiltonian normal form theory, for H_2 given by (19.10.67), show that the Hamiltonian (19.10.64) can be formally transformed to the form (19.10.68).

19. Can Moser's theorem be generalized to the case of more than one pair of real eigenvalues?

19.12 Conjugacies and Equivalences of Vector Fields

In Chapter 11 we discussed the idea of a $\mathbf{C}^r$ conjugacy or coordinate transformation for maps. This was motivated by the question of how the dynamics of a Poincaré map were affected as the cross-section on which the map was defined was changed. The change in cross-section could be viewed as a change of coordinates for the map. A similar question arises here in the context of the method of normal forms; namely, the normal form of a vector field or map is obtained through a coordinate transformation. How does this coordinate transformation modify the dynamics? For maps, the discussion in Chapter 11 applies; however, we did not discuss the notion of conjugacies of vector fields. To address that topic, we begin with a definition.

Let

$$\dot{x} = f(x), \qquad x \in \mathbb{R}^n, \tag{19.12.1}$$

$$\dot{y} = g(y), \qquad y \in \mathbb{R}^n, \tag{19.12.2}$$

be two $\mathbf{C}^r$ $(r \geq 1)$ vector fields defined on $\mathbb{R}^n$ (or sufficiently large open sets of $\mathbb{R}^n$).

Definition 19.12.1 *The dynamics generated by the vector fields f and g are said to be* $\mathbf{C}^k$ equivalent $(k \leq r)$ *if there exists a* $\mathbf{C}^k$ *diffeomorphism h which takes orbits of the flow generated by f, $\phi(t,x)$, to orbits of the flow generated by g, $\psi(t,y)$, preserving orientation but not necessarily parameterization by time. If h does preserve parameterization by time, then the dynamics generated by f and g are said to be* $\mathbf{C}^k$ conjugate.

We remark that, as for maps, the conjugacies do not need to be defined on all of $\mathbb{R}^n$ but, rather, on appropriately chosen open sets in $\mathbb{R}^n$. In this case f and g are said to be *locally* $\mathbf{C}^k$ equivalent or *locally* $\mathbf{C}^k$ conjugate.

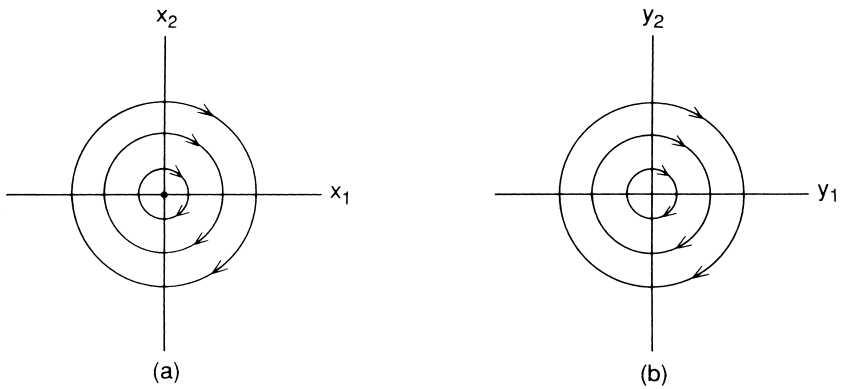

FIGURE 19.12.1. (a) Phase portrait of (2.2.124). (b) Phase portrait of (2.2.125).

Definition 19.12.1 is slightly different than the analogous definition for maps (see Chapter 11). Indeed, in Definition 19.12.1 we have introduced an additional concept: the idea of $\mathbf{C}^k$ *equivalence*. These differences all stem from the fact that in vector fields the independent variable (time) is continuous and in maps time is discrete. Let us illustrate these differences with an example. However, we exhort the reader to keep the following in mind.

The purpose of Definition 19.12.1 *is to provide us with a way of characterizing when two vector fields have qualitatively the same dynamics.*

Example 19.12.1. Consider the two vector fields

$$\begin{aligned} \dot{x}_1 &= x_2, \\ \dot{x}_2 &= -x_1, \end{aligned} \qquad (x_1, x_2) \in \mathbb{R}^2, \tag{19.12.3}$$

and

$$\begin{aligned} \dot{y}_1 &= y_2, \\ \dot{y}_2 &= -y_1 - y_1^3, \end{aligned} \qquad (y_1, y_2) \in \mathbb{R}^2. \tag{19.12.4}$$

The phase portraits of each vector field are shown in Figure 21.1.1. Each vector field possesses only a single fixed point, a center at the origin. In each case the fixed point is surrounded by a one-parameter family of periodic orbits. Note also from Figure 21.1.1 that in each case the direction of motion along the periodic orbits is in the same sense; therefore, qualitatively these two vector fields have the same dynamics—the phase portraits appear identical. However, let us see if this is reflected by the idea of $\mathbf{C}^k$ *conjugacy*.

Let us denote the flow generated by (19.12.3) as

$$\phi(t, x), \qquad x \equiv (x_1, x_2),$$

and the flow generated by (19.12.4) as

$$\psi(t, y), \qquad y \equiv (y_1, y_2).$$

Suppose we have found a $\mathbf{C}^k$ *diffeomorphism*, h, taking orbits of the flow generated by (19.12.3) into orbits of the flow generated by (19.12.4). Then we have

$$h \circ \phi(t, x) = \psi\Big(t, h(x)\Big). \tag{19.12.5}$$

Equation (19.12.5) reveals an immediate problem; namely, if $\phi(t, x)$ and $\psi(t, y)$ are periodic in t, then $h \circ \phi(t, x)$ and $\psi\Big(t, h(x)\Big)$ must have the same period in order for (19.12.5) to hold. However, in general, (19.12.5) cannot be satisfied. Consider (19.12.3) and (19.12.4). The vector field (19.12.3) is linear; therefore, all the periodic orbits have the same period. The vector field (19.12.4) is nonlinear; therefore, the period of the periodic orbits varies with the distance from the fixed point. Thus, (19.12.3) and (19.12.4) are not $\mathbf{C}^k$ *conjugate* (note: one can actually compute the period of the orbits of (19.12.4) since it is a Hamiltonian vector field. It is a tedious exercise involving elliptic integrals).

End of Example 19.12.1

It is precisely this situation from which the idea of $\mathbf{C}^k$ *equivalence* can rescue us, for rather than only having a $\mathbf{C}^k$ *diffeomorphism* that maps orbits to orbits, we at the same time allow a reparametrization of time along the orbit. We make this idea more quantitative as follows. Let $\alpha(x, t)$ be an increasing function of t along orbits (note: it must be increasing in order to preserve orientations of orbits). Then (19.12.3) and (19.12.4) are $\mathbf{C}^k$ *equivalent* if the following holds

$$h \circ \phi(t, x) = \psi\big(\alpha(x, t), h(x)\big). \tag{19.12.6}$$

Equation (19.12.6) shows that orbits of the flow generated by (19.12.3) are mapped to orbits of the flow generated by (19.12.4); however, the time dependence of the image of an orbit under h may be reparametrized in an orbitally dependent manner. Finally, we remark that the term "preserving orientation" in Definition 19.12.1 refers to the fact that the direction of motion along an orbit is unchanged under $\mathbf{C}^k$ equivalence.

Let us now consider some of the dynamical consequences of Definition 19.12.1.

Proposition 19.12.2 *Suppose f and g are $\mathbf{C}^k$* conjugate. *Then*

i) *fixed points of f are mapped to fixed points of g;*

ii) *T-periodic orbits of f map to T-periodic orbits of g.*

Proof: That f and g are $\mathbf{C}^k$ conjugate under h implies the following

$$h \circ \phi(t,x) = \psi\big(t, h(x)\big), \tag{19.12.7}$$

$$Dh\dot{\phi} = \dot{\psi}. \tag{19.12.8}$$

The proof of i) follows from (19.12.8) and the proof of ii) follows from (19.12.7). □

Proposition 19.12.3 *Suppose f and g are $\mathbf{C}^k$* conjugate *($k \geq 1$) and $f(x_0) = 0$; then $Df(x_0)$ has the same eigenvalues as $Dg\big(h(x_0)\big)$.*

Proof: We have the two vector fields $\dot{x} = f(x)$, $\dot{y} = g(y)$. By differentiating (19.12.7) with respect to t we have

$$Dh|_x\, f(x) = g\big(h(x)\big). \tag{19.12.9}$$

Differentiating (19.12.9) gives

$$D^2h\big|_x\, f(x) + Dh|_x\, Df|_x = Dg|_{h(x)}\, Dh|_x\,. \tag{19.12.10}$$

Evaluating (19.12.10) at x_0 gives

$$Dh|_{x_0}\, Df|_{x_0} = Dg|_{h(x_0)}\, Dh|_{x_0} \tag{19.12.11}$$

or

$$Df|_{x_0} = (Dh)^{-1}\big|_{x_0}\, Dg|_{h(x_0)}\, Dh|_{x_0}\,, \tag{19.12.12}$$

and, since similar matrices have equal eigenvalues, the proof is complete. □

The previous two propositions dealt with $\mathbf{C}^k$ *conjugacies*. We next examine the consequences of $\mathbf{C}^k$ *equivalence* under the assumption that the change in parameterization by time along orbits is $\mathbf{C}^1$. The validity of this assumption must be verified in any specific application.

Proposition 19.12.4 *Suppose f and g are $\mathbf{C}^k$* equivalent*; then*

i) *fixed points of f are mapped to fixed points of g;*

ii) *periodic orbits of f are mapped to periodic orbits of g, but the periods need not be equal.*

Proof: If f and g are $\mathbf{C}^k$ *equivalent*, then

$$h \circ \phi(t,x) = \psi\big(\alpha(x,t), h(x)\big), \tag{19.12.13}$$

where α is an increasing function of time along orbits (note: α must be increasing in order to preserve orientations of orbits).

Differentiating (19.12.13) gives

$$Dh\dot{\phi} = \frac{\partial \alpha}{\partial t}\frac{\partial \psi}{\partial \alpha}. \tag{19.12.14}$$

Therefore, (19.12.14) implies i), and ii) follows automatically since $\mathbf{C}^k$ *diffeomorphisms* map closed curves to closed curves. (If this were not true, then the inverse would not be continuous.) □

Proposition 19.12.5 *Suppose f and g are $\mathbf{C}^k$* equivalent *($k \geq 1$) and $f(x_0) = 0$; then the eigenvalues of $Df(x_0)$ and the eigenvalues of $Dg\big(h(x_0)\big)$ differ by a positive multiplicative constant.*

Proof: Proceeding as in the proof of Proposition 19.12.3, we have

$$Dh|_x\, f(x) = \frac{\partial \alpha}{\partial t} g\big(h(x)\big). \tag{19.12.15}$$

Differentiating (19.12.15) gives

$$D^2h\big|_x\, f(x) + Dh|_x\, Df|\, x = \frac{\partial \alpha}{\partial t}\, Dg|_{h(x)}\, Dh|_x + \left.\frac{\partial^2 \alpha}{\partial x \partial t}\right|_x g\big(h(x)\big). \tag{19.12.16}$$

Evaluating at x_0 gives

$$Dh|_{x_0}\, Df|_{x_0} = \frac{\partial \alpha}{\partial t}\, Dg|_{h(x_0)}\, Dh|_{x_0}\,; \tag{19.12.17}$$

thus, $Df|_{x_0}$ and $Dg|_{h(x_0)}$ are similar up to the multiplicative constant $\partial\alpha/\partial t$, which is positive, since α is increasing on orbits. □

Example 19.12.2. Consider the vector fields

$$\begin{aligned} \dot{x}_1 &= x_1, \\ \dot{x}_2 &= x_2, \end{aligned} \qquad (x_1, x_2) \in \mathbb{R}^2,$$

and

$$\begin{aligned} \dot{y}_1 &= y_1, \\ \dot{y}_2 &= 2y_2, \end{aligned} \qquad (y_1, y_2) \in \mathbb{R}^2.$$

Qualitatively these two vector fields have the same dynamics. However, by Proposition 19.12.3 they are not $\mathbf{C}^k$ *equivalent*, $k \geq 1$.

End of Example 19.12.2

19.12A An Application: The Hartman-Grobman Theorem

An underlying theme throughout the first chapter of this book was that the orbit structure near a hyperbolic fixed point was qualitatively the same as the orbit structure given by the associated linearized dynamical system. A theorem proved independently by Hartman [1960] and Grobman [1959] makes this precise. We will describe the situation for vector fields.

Consider a $\mathbf{C}^r$ $(r \geq 1)$ vector field

$$\dot{x} = f(x), \qquad x \in \mathbb{R}^n, \tag{19.12.18}$$

where f is defined on a sufficiently large open set of $\mathbb{R}^n$. Suppose that (19.12.18) has a *hyperbolic* fixed point at $x = x_0$, i.e.,

$$f(x_0) = 0,$$

and $Df(x_0)$ has no eigenvalues on the imaginary axis. Consider the associated linear vector field

$$\dot{\xi} = Df(x_0)\xi, \qquad \xi \in \mathbb{R}^n. \tag{19.12.19}$$

Then we have the following theorem.

Theorem 19.12.6 (Hartman and Grobman) *The flow generated by (19.12.18) is* $\mathbf{C}^0$ conjugate *to the flow generated by (19.12.19) in a neighborhood of the fixed point* $x = x_0$.

Proof: See Arnold [1973] or Palis and deMelo [1982]. □

We remark that the theorem can be modified so that it applies to hyperbolic fixed points of maps, and we leave it to the reader to reformulate the theorem along these lines.

A point to note concerning Theorem 19.12.6 is that the conjugacy transforming the nonlinear flow into the linear flow near the hyperbolic fixed point is not differentiable; rather, it is a homeomorphism. This makes the generation of the transformation via, for example, normal form theory, not possible since the coordinate transformations constructed via that theory were power series expansions and, hence, differentiable. However, a closer look at normal form theory will reveal the heart of the problem with "differentiable linearization." Let us expand on this with a brief discussion.

Recall equation (19.1.8)

$$\dot{x} = Jx + F_2(x) + \cdots + F_{r-1}(x) + \mathcal{O}(|x|^r), \qquad x \in \mathbb{R}^n. \tag{19.12.20}$$

A sufficient condition for eliminating the $\mathcal{O}(|x|^k)$ terms $(2 \leq k \leq r-1)$ from (19.12.20) is that the linear operator $L_J^{(k)}(\cdot)$ is invertible on H_k. We want to explore why $L_J^{(k)}(\cdot)$ is noninvertible.

Recall

$$L_J^{(k)}\big(h_k(x)\big) \equiv Jh_k(x) - Dh_k(x)Jx, \tag{19.12.21}$$

with $h_k(x) \in H_k$, where H_k is the linear vector space of vector-valued homogeneous polynomials of degree k. Let us choose a basis for H_k. Suppose J is diagonal with eigenvalues $\lambda_1, \cdots, \lambda_n$ (note: if J is not diagonalizable, then the following argument is still valid, but with slight modifications; see Arnold [1983] or Bryuno [1989a]). Let e_i, $1 \le i \le n$, be the standard basis of $\mathbb{R}^n$, i.e., e_i is an n vector with a 1 in the i^{th} component and zeros in the remaining components. Then we have

$$Je_i = \lambda_i e_i. \tag{19.12.22}$$

As a basis for H_k we take the set of elements

$$x_1^{m_1} \cdots x_n^{m_n} e_i, \qquad \sum_{j=1}^{n} m_j = k, \quad m_j \ge 0, \tag{19.12.23}$$

where we consider all possible terms $x_1^{m_1} \cdots x_n^{m_n}$ of degree k multiplying each e_i, $1 \le i \le n$.

Next we consider the action of $L_J^{(k)}(\cdot)$ on each of these basis elements of H_k. Let

$$h_k(x) = x_1^{m_1} \cdots x_n^{m_n} e_i, \qquad \sum_{j=1}^{n} m_j = k, \qquad m_j \ge 0; \tag{19.12.24}$$

then a simple calculation shows that

$$L_J^{(k)}\big(h_k(x)\big) = Jh_k(x) - Dh_k(x)Jx = \left[\lambda_i - \sum_{j=1}^{n} m_j \lambda_j\right] h_k(x). \tag{19.12.25}$$

Thus, the linear operator $L_J^{(k)}(\cdot)$ is diagonal in this basis, with eigenvalues given by

$$\lambda_i - \sum_{j=1}^{n} m_j \lambda_j. \tag{19.12.26}$$

Now we can see the problem. The linear operator $L_J^{(k)}(\cdot)$ will fail to be invertible if it has a zero eigenvalue, which in this case means

$$\lambda_i = \sum_{j=1}^{n} m_j \lambda_j. \tag{19.12.27}$$

Equation (19.12.27) is called a *resonance* and is the origin of the name "resonance terms" for the unremovable nonlinear terms in the normal form described in Theorem 19.1.1. The integer

$$\sum_{j=1}^{n} m_j$$

is called the *order of the resonance*. Thus, the difficulty in finding a differentiable coordinate change that will linearize a vector field in the neighborhood of a hyperbolic fixed point lies in the fact that an eigenvalue of the linearized part may be equal to a linear combination over the nonnegative integers of elements from the set of eigenvalues of the linearized part. Much work has been done on the geometry of the resonances in the complex plane and on differentiable linearizations in the situations where the resonances are avoided. For more information we refer the reader to the fundamental papers by Sternberg [1957], [1958] and also Arnold [1983] and Bryuno [1989a].

Let us consider the following example due to Sternberg (see also Meyer [1986]). Consider the vector field

$$\begin{aligned} \dot{x} &= 2x + y^2, \\ \dot{y} &= y, \qquad (x, y) \in \mathbb{R}^2. \end{aligned} \tag{19.12.28}$$

This vector field clearly has a hyperbolic fixed point at the origin. The vector field linearized about the origin is given by

$$\begin{aligned} \dot{x} &= 2x, \\ \dot{y} &= y. \end{aligned} \tag{19.12.29}$$

Eliminating t as the independent variable, (19.12.29) can be written as

$$\frac{dx}{dy} = \frac{2x}{y}, \qquad y \neq 0. \tag{19.12.30}$$

Solving (19.12.30), the orbits of (19.12.29) are given by

$$x = cy^2, \tag{19.12.31}$$

where c is a constant. Clearly (19.12.31) are analytic curves at the origin.

Now consider the nonlinear vector field (19.12.28). Eliminating t as the independent variable, (19.12.28) can be written as

$$\frac{dx}{dy} = \frac{2x}{y} + y, \qquad y \neq 0. \tag{19.12.32}$$

Equation (19.12.32) is a standard first-order linear equation which can be solved via elementary methods (see, e.g., Boyce and DiPrima [1977]). The solution of (19.12.32) is given by

$$x = y^2 \left[k + \log |y|\right], \tag{19.12.33}$$

where k is a constant. Clearly (19.12.33) are $\mathbf{C}^1$ but not $\mathbf{C}^2$ at the origin. Since the property of lying on $\mathbf{C}^2$ curves must be preserved under a $\mathbf{C}^2$ change of coordinates (the chain rule), we conclude that (19.12.28) and (19.12.29) are $\mathbf{C}^1$ but not $\mathbf{C}^2$ conjugate.

In terms of resonances, the problem involves a second-order resonance (hence the problem with $\mathbf{C}^2$ linearization). This can be seen as follows. Let

$$\lambda_1 = 1,$$
$$\lambda_2 = 2,$$

be the eigenvalues of the linearization. Then we have

$$\lambda_2 = m_1\lambda_1 + m_2\lambda_2,$$

with $m_1 = 2$, $m_2 = 0$, and $\sum_{j=1}^{2} m_j = 2$.

19.12B An Application: Dynamics Near a Fixed Point-Šošitaĭšvili's Theorem

Consider the parameter-dependent vector field

$$\begin{aligned} \dot{x} &= Ax + f(x, y, z, \varepsilon), \\ \dot{y} &= By + g(x, y, z, \varepsilon), \qquad (x, y, z, \varepsilon) \in \mathbb{R}^c \times \mathbb{R}^s \times \mathbb{R}^u \times \mathbb{R}^p, \\ \dot{z} &= Cz + h(x, y, z, \varepsilon), \end{aligned} \tag{19.12.34}$$

where

$$\begin{aligned} f(0,0,0,0) &= 0, \qquad Df(0,0,0,0) = 0, \\ g(0,0,0,0) &= 0, \qquad Dg(0,0,0,0) = 0, \\ h(0,0,0,0) &= 0, \qquad Dh(0,0,0,0) = 0, \end{aligned}$$

and f, g, and h are $\mathbf{C}^r$ $(r \geq 2)$ in some neighborhood of the orgin, A is a $c \times c$ matrix having eigenvalues with zero real parts, B is a $s \times s$ matrix having eigenvalues with negative real parts, and C is a $u \times u$ matrix having eigenvalues with positive real parts.

The center manifold theorem tells us that near the orgin in $\mathbb{R}^c \times \mathbb{R}^s \times \mathbb{R}^u \times \mathbb{R}^p$, the flow generated by (19.12.34) is $\mathbf{C}^0$ *conjugate* to the flow generated by the following vector field

$$\begin{aligned} \dot{x} &= w(x, \varepsilon), \\ \dot{y} &= -y, \qquad (x, y, z, \varepsilon) \in \mathbb{R}^c \times \mathbb{R}^s \times \mathbb{R}^u \times \mathbb{R}^p, \\ \dot{z} &= z, \end{aligned} \tag{19.12.35}$$

where $w(x, \varepsilon)$ represents the $\mathbf{C}^r$ vector field on the center manifold. The result in this form is due to Šošitaĭšvili [1975].

19.13 Final Remarks on Normal Forms

Nonuniqueness of Normal Forms. It should be clear from our discussion that normal forms need not be unique. However, it may happen

that certain properties of a vector field (e.g., symmetries) must be possessed by any normal form. Such questions are explored in Kummer [1971], Bryuno [1989a], van der Meer [1985], Baider and Churchill [1988], and Baider [1989].

Divergence of the Normalizing Transformations. In general, normal forms are divergent. This is discussed in detail in Siegel [1941] and Bryuno [1989a]. However, this does not affect considerations of local stability.

Computation of Normal Forms. The book of Rand and Armbruster [1987] describes how one may implement the computation of normal forms using computer algebra. Chow et al. [1990] provide an algorithm for computing normal forms, as well as a MACSYMA code. Ashkenazi et al. [1992] provide the same for Hamiltonian normal forms.

The Method of Amplitude Expansions. This method has been used for many years in studies of hydrodynamic stability and has much in common with the center manifold reduction. This situation has been clarified by Coullet and Spiegel [1983].

The Homological Equation. We want to remark on some terminology. In computing the normal form of vector fields near a fixed point, the equation

$$Dh_k(y)Jy - Jh_k(y) = F_k(y)$$

must be solved in order to simplify the order k terms in the Taylor expansion of the vector field. This equation is called the *homological equation* (see Arnold [1983]). The analogous equation for maps is also called the homological equation.

Nonautonomous Systems. Consider the situation of $\mathbf{C}^r$ (with r as large as necessary) vector fields

$$\dot{x} = f(x), \qquad x \in \mathbb{R}^n. \tag{19.13.1}$$

The method of normal forms as developed in this chapter can be viewed as a method for simplifying the vector field in the neighborhood of a *fixed point.* However, suppose $x(t) = \bar{x}(t)$ is a trajectory of this vector field. Can the method of normal forms then be used to simplify the vector field in the neighborhood of a general (time-dependent) solution? The answer is "sometimes," but there are associated difficulties. Let

$$x = \bar{x}(t) + y;$$

then (19.13.1) becomes

$$\dot{y} = A(t)y + \mathcal{O}(|y|^2), \tag{19.13.2}$$

where

$$A(t) \equiv Df(\bar{x}(t)).$$

In applying the method of normal forms to (19.13.2), the fact that $A(t)$ is time dependent causes problems. If $\bar{x}(t)$ is periodic in t, then $A(t)$ is periodic. Hence, Floquet theory can be used to transform (19.13.2) to a vector field where the linear part is constant (this is described in Arnold [1983]). In this case the method of normal forms as developed in this chapter can then be applied. Recently, Floquet theory has been generalized to the quasiperiodic case by Johnson [1986, 1987]; using these ideas, the normal form theory can be applied in this case also. Recent results along these lines have also been obtained by Jorba and Simo [1992], Treshchev [1995], and Jorba et al [1997]. Their results also apply to linear systems with quasiperiodically varying coefficients, and are computationally very efficient.

Concerning center manifold theory, Sell [1978] has proved existence theorems for stable, unstable, and center manifolds in nonautonomous systems.

Some very interesting work of Siegmund [2002] has recently appeared that develops the method of normal forms for very general nonautonomous vector fields.

Smooth Linearization. There exists a number of results concerning differentiable coordinate changes that linearize a dynamical system (vector field or diffeomorphism) in the neighborhood of an invariant manifold. A recent review of these results can be found in Bronstein and Kopanskii [1994].

Real Normal Forms and Complex Coordinates. We have seen numerous examples in this chapter where the use of complex coordinates simplifies normal form calculations. A systematic development of this approach can be found in Menck [1993].

Normal Forms for Stochastic Systems. Normal form theory for stochastic dynamical systems has been worked out in Namachchivaya and Leng [1990] and Namachchivaya and Lin [1991].

20

Bifurcation of Fixed Points of Vector Fields

Consider the parameterized vector field

$$\dot{y} = g(y, \lambda), \qquad y \in \mathbb{R}^n, \quad \lambda \in \mathbb{R}^p, \tag{20.0.1}$$

where g is a $\mathbf{C}^r$ function on some open set in $\mathbb{R}^n \times \mathbb{R}^p$. The degree of differentiability will be determined by our need to Taylor expand (20.0.1). Usually $\mathbf{C}^5$ will be sufficient.

Suppose (20.0.1) has a fixed point at $(y, \lambda) = (y_0, \lambda_0)$, i.e.,

$$g(y_0, \lambda_0) = 0. \tag{20.0.2}$$

Two questions immediately arise.

1. Is the fixed point stable or unstable?
2. How is the stability or instability affected as λ is varied?

To answer Question 1, the first step to take is to examine the linear vector field obtained by linearizing (20.0.1) about the fixed point $(y, \lambda) = (y_0, \lambda_0)$. This linear vector field is given by

$$\dot{\xi} = D_y g(y_0, \lambda_0)\xi, \qquad \xi \in \mathbb{R}^n. \tag{20.0.3}$$

If the fixed point is hyperbolic (i.e., none of the eigenvalues of $D_y g(y_0, \lambda_0)$ lie on the imaginary axis), we know that the stability of (y_0, λ_0) in (20.0.1) is determined by the linear equation (20.0.3) (cf. Chapter 1). This also enables us to answer Question 2, because since hyperbolic fixed points are structurally stable (cf. Chapter 12), varying λ slightly does not change the nature of the stability of the fixed point. This should be clear intuitively, but let us belabor the point slightly.

We know that

$$g(y_0, \lambda_0) = 0, \tag{20.0.4}$$

and that

$$D_y g(y_0, \lambda_0) \tag{20.0.5}$$

has no eigenvalues on the imaginary axis. Therefore, $D_y g(y_0, \lambda_0)$ is invertible. By the implicit function theorem, there thus exists a *unique* $\mathbf{C}^r$ function, $y(\lambda)$, such that

$$g(y(\lambda), \lambda) = 0 \tag{20.0.6}$$

for λ sufficiently close to λ_0 with

$$y(\lambda_0) = y_0. \tag{20.0.7}$$

Now, by continuity of the eigenvalues with respect to parameters, for λ sufficiently close to λ_0,

$$D_y g(y(\lambda), \lambda) \tag{20.0.8}$$

has no eigenvalues on the imaginary axis. Therefore, for λ sufficiently close to λ_0, the hyperbolic fixed point (y_0, λ_0) of (20.0.1) persists and its stability type remains unchanged. To summarize, in a neighborhood of λ_0 an isolated fixed point of (20.0.1) persists and always has the same stability type.

The real fun starts when the fixed point (y_0, λ_0) of (20.0.1) is not hyperbolic, i.e., when $D_y g(y_0, \lambda_0)$ has some eigenvalues on the imaginary axis. In this case, for λ very close to λ_0 (and for y close to y_0), radically new dynamical behavior can occur. For example, fixed points can be created or destroyed and time-dependent behavior such as periodic, quasiperiodic, or even chaotic dynamics can be created. In a certain sense (to be clarified later), the more eigenvalues on the imaginary axis, the more exotic the dynamics will be.

We will begin our study by considering the simplest way in which $D_y g(y_0, \lambda_0)$ can be nonhyperbolic. This is the case where $D_y g(y_0, \lambda_0)$ has a single zero eigenvalue with the remaining eigenvalues having nonzero real parts. The question we ask in this situation is what is the nature of this nonhyperbolic fixed point for λ close to λ_0? It is under these circumstances where the real power of the center manifold theory becomes apparent, since we know that this question can be answered by studying the vector field (20.0.1) restricted to the associated center manifold (cf. Section 18.2). In this case the vector field on the center manifold will be a p-parameter family of one-dimensional vector fields. This represents a vast simplification of (20.0.1).

20.1 A Zero Eigenvalue

Suppose that $D_y g(y_0, \lambda_0)$ has a single zero eigenvalue with the remaining eigenvalues having nonzero real parts; then the orbit structure near (y_0, λ_0) is determined by the associated center manifold equation, which we write as

$$\dot{x} = f(x, \mu), \qquad x \in \mathbb{R}^1, \quad \mu \in \mathbb{R}^p, \tag{20.1.1}$$

where $\mu = \lambda - \lambda_0$. Furthermore, we know that (20.1.1) must satisfy

$$f(0, 0) = 0, \tag{20.1.2}$$

$$\frac{\partial f}{\partial x}(0, 0) = 0. \tag{20.1.3}$$

Equation (20.1.2) is simply the fixed point condition and (20.1.3) is the zero eigenvalue condition. We remark that (20.1.1) is $\mathbf{C}^r$ if (20.0.1) is $\mathbf{C}^r$. Let us begin by studying a few specific examples. In these examples we will assume

$$\mu \in \mathbb{R}^1.$$

If there are more parameters in the problem (i.e., $\mu \in \mathbb{R}^p$, $p > 1$), we will consider all, except one, as fixed. Later we will consider more carefully the role played by the number of parameters in the problem. We remark also that we have not yet precisely defined what we mean by the term "bifurcation." We will consider this after the following series of examples.

20.1A Examples

Example 20.1.1. Consider the vector field

$$\dot{x} = f(x, \mu) = \mu - x^2, \qquad x \in \mathbb{R}^1, \quad \mu \in \mathbb{R}^1. \tag{20.1.4}$$

It is easy to verify that

$$f(0, 0) = 0 \tag{20.1.5}$$

and

$$\frac{\partial f}{\partial x}(0, 0) = 0, \tag{20.1.6}$$

but in this example we can determine much more. The set of all fixed points of (20.1.4) is given by

$$\mu - x^2 = 0$$

or

$$\mu = x^2. \tag{20.1.7}$$

This represents a parabola in the $\mu - x$ plane as shown in Figure 20.1.1.

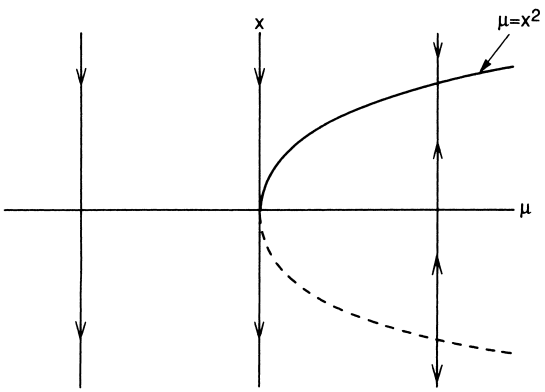

FIGURE 20.1.1.

In the figure the arrows along the vertical lines represent the flow generated by (20.1.4) along the x-direction. Thus, for $\mu < 0$, (20.1.4) has no fixed points,

and the vector field is decreasing in x. For $\mu > 0$, (20.1.4) has two fixed points. A simple linear stability analysis shows that one of the fixed points is stable (represented by the solid branch of the parabola), and the other fixed point is unstable (represented by the broken branch of the parabola). However, we hope that it is obvious to the reader that, given a $\mathbf{C}^r$ $(r \geq 1)$ vector field on $\mathbb{R}^1$ having only two *hyperbolic* fixed points, one must be stable and the other unstable.

This is an example of *bifurcation*. We refer to $(x, \mu) = (0, 0)$ as a *bifurcation point* and the parameter value $\mu = 0$ as a *bifurcation value*.

Figure 20.1.1 is referred to as a *bifurcation diagram*. This particular type of bifurcation (i.e., where on one side of a parameter value there are no fixed points and on the other side there are two fixed points) is referred to as a *saddle-node bifurcation*. Later on we will worry about seeking precise conditions on the vector field on the center manifold that define the saddle-node bifurcation unambiguously.

End of Example 20.1.1

Example 20.1.2. Consider the vector field

$$\dot{x} = f(x, \mu) = \mu x - x^2, \qquad x \in \mathbb{R}^1, \quad \mu \in \mathbb{R}^1. \tag{20.1.8}$$

It is easy to verify that

$$f(0, 0) = 0 \tag{20.1.9}$$

and

$$\frac{\partial f(0, 0)}{\partial x} = 0. \tag{20.1.10}$$

Moreover, the fixed points of (20.1.8) are given by

$$x = 0 \tag{20.1.11}$$

and

$$x = \mu \tag{20.1.12}$$

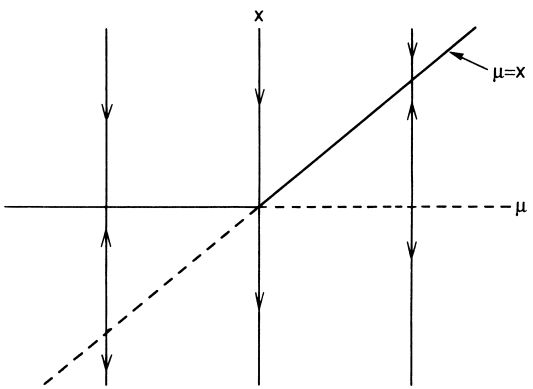

FIGURE 20.1.2.

and are plotted in Figure 20.1.2. Hence, for $\mu < 0$, there are two fixed points; $x = 0$ is stable and $x = \mu$ is unstable. These two fixed points coalesce at $\mu = 0$ and, for $\mu > 0$, $x = 0$ is unstable and $x = \mu$ is stable. Thus, an exchange of stability has occurred at $\mu = 0$. This type of bifurcation is called a *transcritical bifurcation.*

End of Example 20.1.2

Example 20.1.3. Consider the vector field

$$\dot{x} = f(x, \mu) = \mu x - x^3, \qquad x \in \mathbb{R}^1, \quad \mu \in \mathbb{R}^1. \tag{20.1.13}$$

It is clear that we have

$$f(0, 0) = 0, \tag{20.1.14}$$

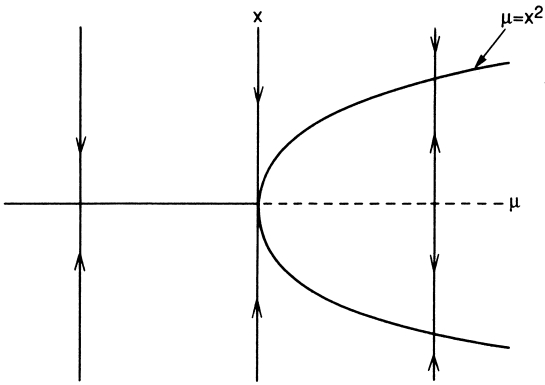

FIGURE 20.1.3.

$$\frac{\partial f}{\partial x}(0, 0) = 0. \tag{20.1.15}$$

Moreover, the fixed points of (20.1.13) are given by

$$x = 0 \tag{20.1.16}$$

and

$$x^2 = \mu \tag{20.1.17}$$

and are plotted in Figure 20.1.3.

Hence, for $\mu < 0$, there is one fixed point, $x = 0$, which is stable. For $\mu > 0$, $x = 0$ is still a fixed point, but two new fixed points have been created at $\mu = 0$ and are given by $x^2 = \mu$. In the process, $x = 0$ has become unstable for $\mu > 0$, with the other two fixed points stable. This type of bifurcation is called a *pitchfork bifurcation.*

End of Example 20.1.3

Example 20.1.4. Consider the vector field

$$\dot{x} = f(x, \mu) = \mu - x^3, \qquad x \in \mathbb{R}^1, \quad \mu \in \mathbb{R}^1. \tag{20.1.18}$$

It is trivial to verify that

$$f(0, 0) = 0 \tag{20.1.19}$$

and

$$\frac{\partial f}{\partial x}(0, 0) = 0. \tag{20.1.20}$$

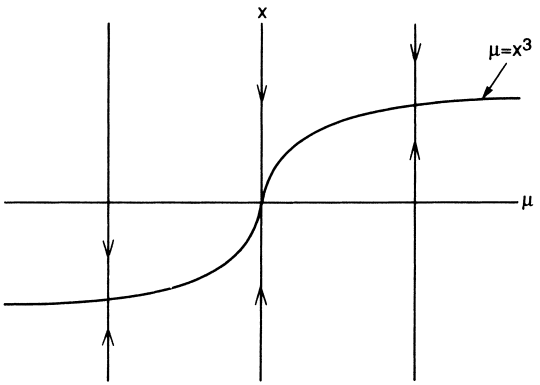

FIGURE 20.1.4.

Moreover, all fixed points of (20.1.18) are given by

$$\mu = x^3 \tag{20.1.21}$$

and are shown in Figure 20.1.4.

However in this example, despite (20.1.19) and (20.1.20), the dynamics of (20.1.18) are qualitatively the same for $\mu > 0$ and $\mu < 0$. Namely, (20.1.18) possesses a unique, stable fixed point.

End of Example 20.1.4

20.1B What Is A "Bifurcation of a Fixed Point"?

The term "bifurcation" is extremely general. We will begin to learn its uses in dynamical systems by understanding its use in describing the orbit structure near nonhyperbolic fixed points. Let us consider what we learned from the previous examples.

In all four examples we had

$$f(0, 0) = 0$$

and

$$\frac{\partial f}{\partial x}(0,0) = 0,$$

and yet the orbit structure near $\mu = 0$ was different in all four cases. Hence, knowing that a fixed point has a zero eigenvalue for $\mu = 0$ is not sufficient to determine the orbit structure for λ near zero. Let us consider each example individually.

1. (*Example 20.1.1*). In this example a *unique* curve (or branch) of fixed points passed through the origin. Moreover, the curve lay entirely on one side of $\mu = 0$ in the $\mu - x$ plane.

2. (*Example 20.1.2*). In this example two curves of fixed points intersected at the origin in the $\mu - x$ plane. Both curves existed on either side of $\mu = 0$. However, the stability of the fixed point along a given curve changed on passing through $\mu = 0$.

3. (*Example 20.1.3*). In this example two curves of fixed points intersected at the origin in the $\mu - x$ plane. Only one curve ($x = 0$) existed on both sides of $\mu = 0$; however, its stability changed on passing through $\mu = 0$. The other curve of fixed points lay entirely to one side of $\mu = 0$ and had a stability type that was the opposite of $x = 0$ for $\mu > 0$.

4. (*Example 20.1.4*). This example had a unique curve of fixed points passing through the origin in the $\mu - x$ plane and existing on both sides of $\mu = 0$. Moreover, all fixed points along the curve had the same stability type. Hence, despite the fact that the fixed point $(x, \mu) = (0, 0)$ was nonhyperbolic, the orbit structure was qualitatively the same for all μ.

We want to apply the term "bifurcation" to Examples 20.1.1, 20.1.2, and 20.1.3 but not to Example 20.1.4 to describe the change in orbit structure as μ passes through zero. We are therefore led to the following definition.

Definition 20.1.1 (Bifurcation of a Fixed Point) *A fixed point* $(x, \mu) = (0, 0)$ *of a one-parameter family of one-dimensional vector fields is said to undergo a* bifurcation *at* $\mu = 0$ *if the flow for* μ *near zero and* x *near zero is* not *qualitatively the same as the flow near* $x = 0$ *at* $\mu = 0$.

Several remarks are now in order concerning this definition.

Remark 1. The phrase "qualitatively the same" is a bit vague. It can be made precise by substituting the term "$\mathbf{C}^0$-equivalent" (cf. Section 19.12), and this is perfectly adequate for the study of the bifurcation of fixed points of *one-dimensional* vector fields. However, we will see that as we explore higher dimensional phase spaces and global bifurcations, how to

make mathematically precise the statement "two dynamical systems have qualitatively the same dynamics" becomes more and more ambiguous.

Remark 2. Practically speaking, a fixed point (x_0, μ_0) of a one-dimensional vector field is a bifurcation point if either more than one curve of fixed points passes through (x_0, μ_0) in the $\mu - x$ plane or if only one curve of fixed points passes (x_0, μ_0) in the $\mu - x$ plane; then it (locally) lies entirely on one side of the line $\mu = \mu_0$ in the $\mu - x$ plane.

Remark 3. It should be clear from Example 20.1.4 that the condition that a fixed point is nonhyperbolic is a necessary but not sufficient condition for bifurcation to occur in one-parameter families of vector fields.

We next turn to deriving general conditions on one-parameter families of one-dimensional vector fields which exhibit bifurcations exactly as in Examples 20.1.1, 20.1.2, and 20.1.3.

20.1c The Saddle-Node Bifurcation

We now want to derive conditions under which a general one-parameter family of one-dimensional vector fields will undergo a saddle-node bifurcation exactly as in Example 20.1.1. These conditions will involve derivatives of the vector field evaluated at the bifurcation point and are obtained by a consideration of the geometry of the curve of fixed points in the $\mu - x$ plane in a neighborhood of the bifurcation point.

Let us recall Example 20.1.1. In this example a *unique* curve of fixed points, parameterized by x, passed through $(\mu, x) = (0, 0)$. We denote the curve of fixed points by $\mu(x)$. The curve of fixed points satisfied two properties.

1. It was tangent to the line $\mu = 0$ at $x = 0$, i.e.,

$$\frac{d\mu}{dx}(0) = 0. \tag{20.1.22}$$

2. It lay entirely to one side of $\mu = 0$. Locally, this will be satisfied if we have

$$\frac{d^2\mu}{dx^2}(0) \neq 0. \tag{20.1.23}$$

Now let us consider a general, one-parameter family of one-dimensional vector fields.

$$\dot{x} = f(x, \mu), \qquad x \in \mathbb{R}^1, \quad \mu \in \mathbb{R}^1. \tag{20.1.24}$$

Suppose (20.1.24) has a fixed point at $(x, \mu) = (0, 0)$, i.e.,

$$f(0, 0) = 0. \tag{20.1.25}$$

Furthermore, suppose that the fixed point is not hyperbolic, i.e.,

$$\frac{\partial f}{\partial x}(0,0) = 0. \tag{20.1.26}$$

Now, if we have

$$\frac{\partial f}{\partial \mu}(0,0) \neq 0, \tag{20.1.27}$$

then, by the implicit function theorem, there exists a unique function

$$\mu = \mu(x), \qquad \mu(0) = 0 \tag{20.1.28}$$

defined for x sufficiently small such that $f(x, \mu(x)) = 0$. (Note: the reader should check that (20.1.27) holds in Example 20.1.1.) Now we want to derive conditions in terms of derivatives of f evaluated at $(\mu, x) = (0,0)$ so that we have

$$\frac{d\mu}{dx}(0) = 0, \tag{20.1.29}$$

$$\frac{d^2\mu}{dx^2}(0) \neq 0. \tag{20.1.30}$$

Equations (20.1.29) and (20.1.30), along with (20.1.25), (20.1.26), and (20.1.27), imply that $(\mu, x) = (0,0)$ is a bifurcation point at which a saddle-node bifurcation occurs.

We can derive expressions for (20.1.29) and (20.1.30) in terms of derivatives of f at the bifurcation point by implicitly differentiating f along the curve of fixed points.

Using (20.1.27), we have

$$f(x, \mu(x)) = 0. \tag{20.1.31}$$

Differentiating (20.1.31) with respect to x gives

$$\frac{df}{dx}(x, \mu(x)) = 0 = \frac{\partial f}{\partial x}(x, \mu(x)) + \frac{\partial f}{\partial \mu}(x, \mu(x))\frac{d\mu}{dx}(x). \tag{20.1.32}$$

Evaluating (20.1.32) at $(\mu, x) = (0,0)$, we obtain

$$\frac{d\mu}{dx}(0) = \frac{-\dfrac{\partial f}{\partial x}(0,0)}{\dfrac{\partial f}{\partial \mu}(0,0)}; \tag{20.1.33}$$

thus we see that (20.1.26) and (20.1.27) imply that

$$\frac{d\mu}{dx}(0) = 0, \tag{20.1.34}$$

i.e., the curve of fixed points is tangent to the line $\mu = 0$ at $x = 0$.

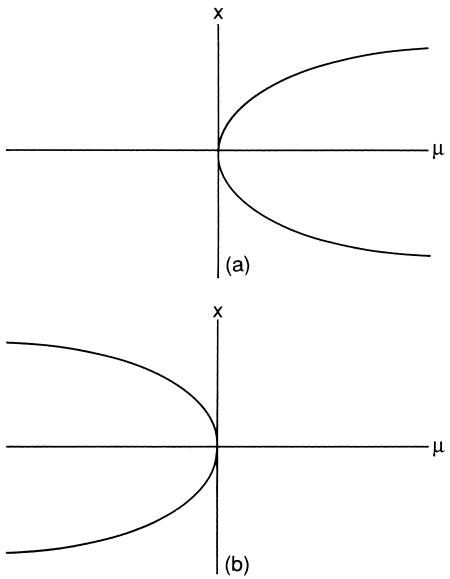

FIGURE 20.1.5.
a) $\left(-\frac{\partial^2 f}{\partial x^2}(0,0)/\frac{\partial f}{\partial \mu}(0,0)\right) > 0$; b) $\left(-\frac{\partial^2 f}{\partial x^2}(0,0)/\frac{\partial f}{\partial \mu}(0,0)\right) < 0$.

Next, let us differentiate (20.1.32) once more with respect to x to obtain

$$\begin{aligned}\frac{d^2 f}{dx^2}(x,\mu(x)) = 0 = &\frac{\partial^2 f}{\partial x^2}(x,\mu(x)) + 2\frac{\partial^2 f}{\partial x \partial \mu}(x,\mu(x))\frac{d\mu}{dx}(x) \\ &+ \frac{\partial^2 f}{\partial \mu^2}(x,\mu(x))\left(\frac{d\mu}{dx}(x)\right)^2 \\ &+ \frac{\partial f}{\partial \mu}(\mu,\mu(x))\frac{d^2\mu}{dx^2}(x). \end{aligned} \tag{20.1.35}$$

Evaluating (20.1.35) at $(\mu, x) = (0,0)$ and using (20.1.33) gives

$$\frac{\partial^2 f}{\partial x^2}(0,0) + \frac{\partial f}{\partial \mu}(0,0)\frac{d^2\mu}{dx^2}(0) = 0$$

or

$$\frac{d^2\mu}{dx^2}(0) = \frac{-\dfrac{\partial^2 f}{\partial x^2}(0,0)}{\dfrac{\partial f}{\partial \mu}(0,0)}. \tag{20.1.36}$$

Hence, (20.1.36) is nonzero provided we have

$$\frac{\partial^2 f}{\partial x^2}(0,0) \neq 0. \tag{20.1.37}$$

Let us summarize. In order for (20.1.24) to undergo a saddle-node bifurcation we must have

$$\left.\begin{aligned} &f(0,0)=0\\ &\frac{\partial f}{\partial x}(0,0)=0 \end{aligned}\right\} \quad \text{nonhyperbolic fixed point} \tag{20.1.38}$$

and

$$\frac{\partial f}{\partial \mu}(0,0)\neq 0, \tag{20.1.39}$$

$$\frac{\partial^2 f}{\partial x^2}(0,0)\neq 0. \tag{20.1.40}$$

Equation (20.1.39) implies that a unique curve of fixed points passes through $(\mu, x) = (0, 0)$, and (20.1.40) implies that the curve lies locally on one side of $\mu = 0$. It should be clear that the sign of (20.1.36) determines on which side of $\mu = 0$ the curve lies. In Figure 20.1.5 we show both cases without indicating stability and leave it as an exercise for the reader to verify the stability types of the different branches of fixed points emanating from the bifurcation point.

Let us end our discussion of the saddle-node bifurcation with the following remark. Consider a general one-parameter family of one-dimensional vector fields having a nonhyperbolic fixed point at $(x, \mu) = (0, 0)$. The Taylor expansion of this vector field is given as follows

$$f(x,\mu)=a_0\mu+a_1x^2+a_2\mu x+a_3\mu^2+\mathcal{O}(3). \tag{20.1.41}$$

Our computations show that the dynamics of (20.1.41) near $(\mu, x) = (0, 0)$ are qualitatively the same as one of the following vector fields

$$\dot{x}=\mu\pm x^2. \tag{20.1.42}$$

Hence, (20.1.42) can be viewed as the *normal form* for saddle-node bifurcations.

This brings up another important point. In applying the method of normal forms there is always the question of truncation of the normal form; namely, how are the dynamics of the normal form including only the $\mathcal{O}(k)$ terms modified when the higher order terms are included? We see that, in the study of the saddle-node bifurcation, all terms of $\mathcal{O}(3)$ and higher could be neglected and the dynamics would not be qualitatively changed. The implicit function theorem was the tool that enabled us to verify this fact.

20.1D The Transcritical Bifurcation

We want to follow the same strategy as in our discussion and derivation of general conditions for the saddle-node bifurcation given in the previous

section, namely, to use the implicit function theorem to characterize the geometry of the curves of fixed points passing through the bifurcation point in terms of derivatives of the vector field evaluated at the bifurcation point.

For the example of transcritical bifurcation discussed in Example 20.1.2, the orbit structure near the bifurcation point was characterized as follows.

1. Two curves of fixed points passed through $(x, \mu) = (0, 0)$, one given by $x = \mu$, the other by $x = 0$.
2. Both curves of fixed points existed on both sides of $\mu = 0$.
3. The stability along each curve of fixed points changed on passing through $\mu = 0$.

Using these three points as a guide, let us consider a general one-parameter family of one-dimensional vector fields

$$\dot{x} = f(x, \mu), \qquad x \in \mathbb{R}^1, \quad \mu \in \mathbb{R}^1. \tag{20.1.43}$$

We assume that at $(x, \mu) = (0, 0)$, (20.1.43) has a nonhyperbolic fixed point, i.e.,

$$f(0, 0) = 0 \tag{20.1.44}$$

and

$$\frac{\partial f}{\partial x}(0, 0) = 0. \tag{20.1.45}$$

Now, in Example 20.1.2 we had two curves of fixed points passing through $(\mu, x) = (0, 0)$. In order for this to occur it is necessary to have

$$\frac{\partial f}{\partial \mu}(0, 0) = 0, \tag{20.1.46}$$

or else, by the implicit function theorem, only one curve of fixed points could pass through the origin.

Equation (20.1.46) presents a problem if we wish to proceed as in the case of the saddle-node bifurcation; in that situation we used the condition $\frac{\partial f}{\partial \mu}(0, 0) \neq 0$ in order to conclude that a unique curve of fixed points, $\mu(x)$, passed through the bifurcation point. We then evaluated the vector field on the curve of fixed points and used implicit differentiation to derive local characteristics of the geometry of the curve of fixed points based on properties of the derivatives of the vector field evaluated at the bifurcation point. However, if we use Example 20.1.2 as a guide, we can extricate ourselves from this difficulty.

In Example 20.1.2, $x = 0$ was a curve of fixed points passing through the bifurcation point. We will *require* that to be the case for (20.1.43), so that (20.1.43) has the form

$$\dot{x} = f(x, \mu) = xF(x, \mu), \qquad x \in \mathbb{R}^1, \quad \mu \in \mathbb{R}^1, \tag{20.1.47}$$

where, by definition, we have

$$F(x,\mu) \equiv \left\{ \begin{array}{ll} \frac{f(x,\mu)}{x}, & x \neq 0 \\ \\ \frac{\partial f}{\partial x}(0,\mu), & x = 0 \end{array} \right\}. \tag{20.1.48}$$

Since $x = 0$ is a curve of fixed points for (20.1.47), in order to obtain an additional curve of fixed points passing through $(\mu, x) = (0, 0)$ we need to seek conditions on F whereby F has a curve of zeros passing through $(\mu, x) = (0, 0)$ (that is not given by $x = 0$). These conditions will be in terms of derivatives of F which, using (20.1.48), can be expressed as derivatives of f.

Using (20.1.48), it is easy to verify the following

$$F(0,0) = 0, \tag{20.1.49}$$

$$\frac{\partial F}{\partial x}(0,0) = \frac{\partial^2 f}{\partial x^2}(0,0), \tag{20.1.50}$$

$$\frac{\partial^2 F}{\partial x^2}(0,0) = \frac{\partial^3 f}{\partial x^3}(0,0), \tag{20.1.51}$$

and (most importantly)

$$\frac{\partial F}{\partial \mu}(0,0) = \frac{\partial^2 f}{\partial x \partial \mu}(0,0). \tag{20.1.52}$$

Now let us assume that (20.1.52) is *not* zero; then by the implicit function theorem there exists a function, $\mu(x)$, defined for x sufficiently small, such that

$$F(x, \mu(x)) = 0. \tag{20.1.53}$$

Clearly, $\mu(x)$ is a curve of fixed points of (20.1.47). In order for $\mu(x)$ to not coincide with $x = 0$ and to exist on both sides of $\mu = 0$, we must require that

$$0 < \left| \frac{d\mu}{dx}(0) \right| < \infty.$$

Implicitly differentiating (20.1.53) exactly as in the case of the saddle-node bifurcation we obtain

$$\frac{d\mu}{dx}(0) = \frac{-\frac{\partial F}{\partial x}(0,0)}{\frac{\partial F}{\partial \mu}(0,0)}. \tag{20.1.54}$$

Using (20.1.49), (20.1.50), (20.1.51), and (20.1.52), (20.1.54) becomes

$$\frac{d\mu}{dx}(0) = \frac{-\frac{\partial^2 f}{\partial x^2}(0,0)}{\frac{\partial^2 f}{\partial x \partial \mu}(0,0)}. \tag{20.1.55}$$

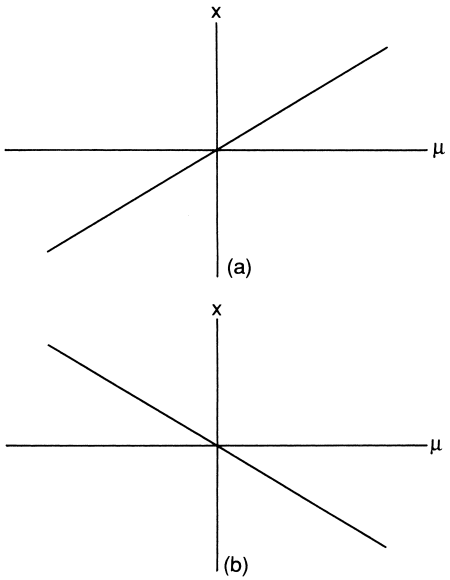

FIGURE 20.1.6.
a) $\left(-\frac{\partial^2 f}{\partial x^2}(0,0)/\frac{\partial^2 f}{\partial x \partial \mu}(0,0)\right) > 0$; b) $\left(-\frac{\partial^2 f}{\partial x^2}(0,0)/\frac{\partial^2 f}{\partial x \partial \mu}(0,0)\right) < 0$.

We now summarize our results. In order for a vector field

$$\dot{x} = f(x,\mu), \qquad x \in \mathbb{R}^1, \quad \mu \in \mathbb{R}^1, \tag{20.1.56}$$

to undergo a transcritical bifurcation, we must have

$$\left.\begin{aligned} &f(0,0) = 0 \\ &\frac{\partial f}{\partial x}(0,0) = 0 \end{aligned}\right\} \quad \text{nonhyperbolic fixed point} \tag{20.1.57}$$

and

$$\frac{\partial f}{\partial \mu}(0,0) = 0, \tag{20.1.58}$$

$$\frac{\partial^2 f}{\partial x \partial \mu}(0,0) \neq 0, \tag{20.1.59}$$

$$\frac{\partial^2 f}{\partial x^2}(0,0) \neq 0. \tag{20.1.60}$$

We note that the slope of the curve of fixed points not equal to $x = 0$ is given by (20.1.55). These two cases are shown in Figure 20.1.6; however, we do not indicate stabilities of the different branches of fixed points. We leave it as an exercise to the reader to verify the stability types of the different curves of fixed points emanating from the bifurcation point.

Thus, (20.1.57), (20.1.58), (20.1.59), and (20.1.60) show that the orbit structure near $(x, \mu) = (0, 0)$ is qualitatively the same as the orbit structure near $(x, \mu) = (0, 0)$ of

$$\dot{x} = \mu x \mp x^2. \tag{20.1.61}$$

Equation (20.1.61) can be viewed as a normal form for the transcritical bifurcation.

20.1E The Pitchfork Bifurcation

The discussion and derivation of conditions under which a general one-parameter family of one-dimensional vector fields will undergo a bifurcation of the type shown in Example 20.1.3 follows very closely our discussion of the transcritical bifurcation.

The geometry of the curves of fixed points associated with the bifurcation in Example 20.1.3 had the following characteristics.

1. Two curves of fixed points passed through $(\mu, x) = (0, 0)$, one given by $x = 0$, the other by $\mu = x^2$.
2. The curve $x = 0$ existed on both sides of $\mu = 0$; the curve $\mu = x^2$ existed on one side of $\mu = 0$.
3. The fixed points on the curve $x = 0$ had different stability types on opposite sides of $\mu = 0$. The fixed points on $\mu = x^2$ all had the same stability type.

Now we want to consider conditions on a general one-parameter family of one-dimensional vector fields having two curves of fixed points passing through the bifurcation point in the $\mu - x$ plane that have the properties given above.

We denote the vector field by

$$\dot{x} = f(x, \mu), \qquad x \in \mathbb{R}^1, \quad \mu \in \mathbb{R}^1, \tag{20.1.62}$$

and we suppose

$$f(0, 0) = 0, \tag{20.1.63}$$

$$\frac{\partial f}{\partial x}(0, 0) = 0. \tag{20.1.64}$$

As in the case of the transcritical bifurcation, in order to have more than one curve of fixed points passing through $(\mu, x) = (0, 0)$ we must have

$$\frac{\partial f}{\partial \mu}(0, 0) = 0. \tag{20.1.65}$$

Proceeding further along these lines, we *require* $x = 0$ to be a curve of fixed points for (20.1.62) by assuming the vector field (20.1.62) has the form

$$\dot{x} = xF(x, \mu), \qquad x \in \mathbb{R}^1, \quad \mu \in \mathbb{R}^1, \tag{20.1.66}$$

where

$$F(x,\mu) \equiv \left\{ \begin{array}{ll} \frac{f(x,\mu)}{x}, & x \neq 0 \\ \\ \frac{\partial f}{\partial x}(0,\mu), & x = 0 \end{array} \right\}. \tag{20.1.67}$$

In order to have a second curve of fixed points passing through $(\mu, x) = (0,0)$ we must have

$$F(0,0) = 0 \tag{20.1.68}$$

with

$$\frac{\partial F}{\partial \mu}(0,0) \neq 0. \tag{20.1.69}$$

Equation (20.1.69) insures that only *one* additional curve of fixed points passes through $(\mu, x) = (0,0)$. Also, using (20.1.69), the implicit function theorem implies that for x sufficiently small there exists a unique function $\mu(x)$ such that

$$F(x, \mu(x)) = 0. \tag{20.1.70}$$

In order for the curve of fixed points, $\mu(x)$, to satisfy the above-mentioned characteristics, it is sufficient to have

$$\frac{d\mu}{dx}(0) = 0 \tag{20.1.71}$$

and

$$\frac{d^2\mu}{dx^2}(0) \neq 0. \tag{20.1.72}$$

The conditions for (20.1.71) and (20.1.72) to hold in terms of the derivatives of F evaluated at the bifurcation point can be obtained via implicit differentiation of (20.1.70) along the curve of fixed points exactly as in the case of the saddle-node bifurcation. They are given by

$$\frac{d\mu}{dx}(0) = \frac{-\frac{\partial F}{\partial x}(0,0)}{\frac{\partial F}{\partial \mu}(0,0)} = 0 \tag{20.1.73}$$

and

$$\frac{d^2\mu}{dx^2}(0) = \frac{-\frac{\partial^2 F}{\partial x^2}(0,0)}{\frac{\partial F}{\partial \mu}(0,0)} \neq 0. \tag{20.1.74}$$

Using (20.1.67), (20.1.73) and (20.1.74) can be expressed in terms of derivatives of f as follows

$$\frac{d\mu}{dx}(0) = \frac{-\frac{\partial^2 f}{\partial x^2}(0,0)}{\frac{\partial^2 f}{\partial x \partial \mu}(0,0)} = 0 \tag{20.1.75}$$

and

$$\frac{d^2\mu}{dx^2}(0) = \frac{-\frac{\partial^3 f}{\partial x^3}(0,0)}{\frac{\partial^2 f}{\partial x \partial \mu}(0,0)} \neq 0. \tag{20.1.76}$$

We summarize as follows. In order for the vector field

$$\dot{x} = f(x, \mu), \qquad x \in \mathbb{R}^1, \quad \mu \in \mathbb{R}^1, \tag{20.1.77}$$

to undergo a pitchfork bifurcation at $(x, \mu) = (0, 0)$, it is sufficient to have

$$\left.\begin{aligned} &f(0,0) = 0 \\ &\frac{\partial f}{\partial x}(0,0) = 0 \end{aligned}\right\} \quad \text{nonhyperbolic fixed point} \tag{20.1.78}$$

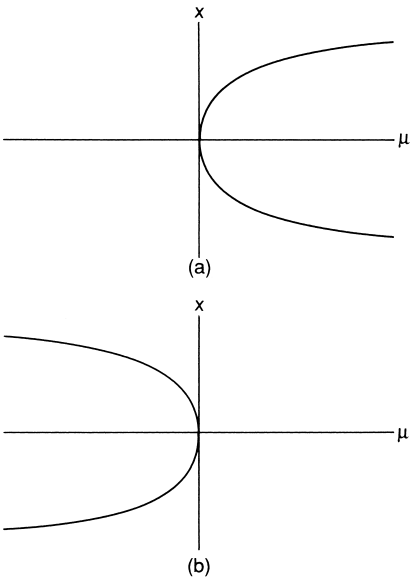

FIGURE 20.1.7.
a) $\left(-\frac{\partial^3 f}{\partial x^3}(0,0)/\frac{\partial^2 f}{\partial x \partial \mu}(0,0)\right) > 0$; b) $\left(-\frac{\partial^3 f}{\partial x^3}(0,0)/\frac{\partial^2 f}{\partial x \partial \mu}(0,0)\right) < 0$.

with

$$\frac{\partial f}{\partial \mu}(0,0) = 0, \tag{20.1.79}$$

$$\frac{\partial^2 f}{\partial x^2}(0,0) = 0, \tag{20.1.80}$$

$$\frac{\partial^2 f}{\partial x \partial \mu}(0,0) \neq 0, \tag{20.1.81}$$

$$\frac{\partial^3 f}{\partial x^3}(0,0) \neq 0. \tag{20.1.82}$$

There are two possibilities for the disposition of the two branches of fixed points depending on the sign of (20.1.76). These two possibilities are shown

in Figure 20.1.7 without indicating stabilities. We leave it as an exercise for the reader to verify the stability types for the different branches of fixed points emanating from the bifurcation point.

We conclude by noting that (20.1.78), (20.1.79), (20.1.80), (20.1.81), and (20.1.82) imply that the orbit structure near $(x, \mu) = (0, 0)$ is qualitatively the same as the orbit structure near $(x, \mu) = (0, 0)$ in the vector field

$$\dot{x} = \mu x \mp x^3. \tag{20.1.83}$$

Thus, (20.1.83) can be viewed as a normal form for the pitchfork bifurcation.

20.1F Exercises

1. In our development of the transcritical and pitchfork bifurcations we assumed that $x = 0$ was a trivial solution. Was this necessary? In particular, would the conditions for transcritical and pitchfork bifurcations change if this were not the case?

2. Consider a $\mathbf{C}^r$ $(r \geq 1)$ autonomous vector field on $\mathbb{R}^1$ having precisely two *hyperbolic* fixed points. Can you infer the nature of the stability of the two fixed points? How does the situation change if one of the fixed points is not hyperbolic? Can both fixed points be nonhyperbolic? Construct explicit examples illustrating each situation.

3. Consider the saddle-node bifurcation for vector fields and Figure 20.1.5. For the case $\left(-\frac{\partial^2 f}{\partial x^2}(0,0)/\frac{\partial f}{\partial \mu}(0,0)\right) > 0$, give conditions under which the upper part of the curve of fixed points is stable and the lower part is unstable. Alternatively, give conditions under which the upper part of the curve of fixed points is unstable and the lower part is stable.

   Repeat the exercise for the case $\left(-\frac{\partial^2 f}{\partial x^2}(0,0)/\frac{\partial f}{\partial \mu}(0,0)\right) < 0$.

4. Consider the transcritical bifurcation for vector fields and Figure 20.1.6. For the case $\left(-\frac{\partial^2 f}{\partial x^2}(0,0)/\frac{\partial^2 f}{\partial x \partial \mu}(0,0)\right) > 0$, give conditions for $x = 0$ to be stable for $\mu > 0$ and unstable for $\mu < 0$. Alternatively, give conditions for $x = 0$ to be unstable for $\mu > 0$ and stable for $\mu < 0$.

   Repeat the exercise for the case $\left(-\frac{\partial^2 f}{\partial x^2}(0,0)/\frac{\partial^2 f}{\partial x \partial \mu}(0,0)\right) < 0$.

5. Consider the pitchfork bifurcation for vector fields and Figure 20.1.7. For the case $\left(-\frac{\partial^3 f}{\partial x^3}(0,0)/\frac{\partial^2 f}{\partial x \partial \mu}(0,0)\right) > 0$, give conditions for $x = 0$ to be stable for $\mu > 0$ and unstable for $\mu < 0$. Alternatively, give conditions for $x = 0$ to be unstable for $\mu > 0$ and stable for $\mu < 0$.

   Repeat the exercise for the case $\left(-\frac{\partial^3 f}{\partial x^3}(0,0)/\frac{\partial^2 f}{\partial x \partial \mu}(0,0)\right) < 0$.

6. In Exercise 4 following Chapter 18 we computed center manifolds near the origin for the following one-parameter families of vector fields. Describe the bifurcations of the origin. In, for example, a) and a′) the parameter ε multiplies a linear and nonlinear term, respectively. In terms of bifurcations, is there a qualitative difference in the two cases? What kinds of general statements can you make?

   a) $\dot{\theta} = -\theta + \varepsilon v + v^2$, $\quad (\theta, v) \in S^1 \times \mathbb{R}^1$.
   $\dot{v} = -\sin\theta$,

   a′) $\dot{\theta} = -\theta + v^2 + \varepsilon v^2$,
   $\dot{v} = -\sin\theta$.

b) $\begin{aligned}\dot{x} &= \frac{1}{2}x + y + x^2 y,\\ \dot{y} &= x + 2y + \varepsilon y + y^2,\end{aligned}$ $(x, y) \in \mathbb{R}^2$.

b′) $\begin{aligned}\dot{x} &= \frac{1}{2}x + y + x^2 y,\\ \dot{y} &= x + 2y + y^2 + \varepsilon y^2.\end{aligned}$

d) $\begin{aligned}\dot{x} &= 2x + 2y + \varepsilon y,\\ \dot{y} &= x + y + x^4,\end{aligned}$ $(x, y) \in \mathbb{R}^2$.

d′) $\begin{aligned}\dot{x} &= 2x + 2y,\\ \dot{y} &= x + y + x^4 + \varepsilon y^2.\end{aligned}$

f) $\begin{aligned}\dot{x} &= -2x + 3y + \varepsilon x + y^3,\\ \dot{y} &= 2x - 3y + x^3,\end{aligned}$ $(x, y) \in \mathbb{R}^2$.

f′) $\begin{aligned}\dot{x} &= -2x + 3y + y^3 + \varepsilon x^2,\\ \dot{y} &= 2x - 3y + x^3.\end{aligned}$

h) $\begin{aligned}\dot{x} &= -x + y,\\ \dot{y} &= -e^x + e^{-x} + 2x + \varepsilon y,\end{aligned}$ $(x, y) \in \mathbb{R}^2$.

h′) $\begin{aligned}\dot{x} &= -x + y + \varepsilon x^2,\\ \dot{y} &= -e^x + e^{-x} + 2x.\end{aligned}$

i) $\begin{aligned}\dot{x} &= -2x + y + z + \varepsilon x + y^2 z,\\ \dot{y} &= x - 2y + z + \varepsilon x + x z^2,\\ \dot{z} &= x + y - 2z + \varepsilon x + x^2 y,\end{aligned}$ $(x, y, z) \in \mathbb{R}^3$.

i′) $\begin{aligned}\dot{x} &= -2x + y + z + \varepsilon x^2 + y^2 z,\\ \dot{y} &= x - 2y + z + \varepsilon x y + x z^2,\\ \dot{z} &= x + y - 2z + x^2 y.\end{aligned}$

j) $\begin{aligned}\dot{x} &= -x - y + z^2,\\ \dot{y} &= 2x + y + \varepsilon y - z^2,\\ \dot{z} &= x + 2y - z,\end{aligned}$ $(x, y, z) \in \mathbb{R}^3$.

j′) $\begin{aligned}\dot{x} &= -x - y + \varepsilon x^2 + z^2,\\ \dot{y} &= 2x + y - z^2 + \varepsilon y^2,\\ \dot{z} &= x + 2y - z.\end{aligned}$

k) $\begin{aligned}\dot{x} &= -x - y - z + \varepsilon x - yz,\\ \dot{y} &= -x - y - z - xz,\\ \dot{z} &= -x - y - z - yz,\end{aligned}$ $(x, y, z) \in \mathbb{R}^3$.

k′) $\begin{aligned}\dot{x} &= -x - y - z - yz + \varepsilon x^2,\\ \dot{y} &= -x - y - z - xz,\\ \dot{z} &= -x - y - z - xy.\end{aligned}$

l) $\begin{aligned}\dot{x} &= y + x^2 + \varepsilon y,\\ \dot{y} &= -y - x^2,\end{aligned}$ $(x, y) \in \mathbb{R}^2$.

l′) $\begin{aligned}\dot{x} &= y + x^2 + \varepsilon y^2,\\ \dot{y} &= -y - x^2.\end{aligned}$

m) $\begin{aligned}\dot{x} &= x^2 + \varepsilon y,\\ \dot{y} &= -y - x^2,\end{aligned}$ $(x, y) \in \mathbb{R}^2$.

m′) $\begin{aligned}\dot{x} &= x^2 + \varepsilon y^2,\\ \dot{y} &- -y - x^2.\end{aligned}$

7. *Center Manifolds at a Saddle-node Bifurcation Point for Vector Fields*

In developing the center manifold theory for parametrized families of vector fields, we dealt with equations of the following form

$$\begin{aligned} \dot{x} &= Ax + f(x, y, \varepsilon), \\ \dot{y} &= By + g(x, y, \varepsilon), \end{aligned} \qquad (x, y, \varepsilon) \in \mathbb{R}^c \times \mathbb{R}^s \times \mathbb{R}^p, \tag{20.1.84}$$

where A is a $c \times c$ matrix whose eigenvalues all have zero real parts, B is an $s \times s$ matrix whose eigenvalues all have negative real parts, and

$$\begin{aligned} f(0,0,0) &= 0, \qquad Df(0,0,0) = 0, \\ g(0,0,0) &= 0, \qquad Dg(0,0,0) = 0. \end{aligned} \tag{20.1.85}$$

The conditions $Df(0,0,0) = 0$, $Dg(0,0,0) = 0$ do not allow for terms that are linear in the parameter ε. Clearly, this *may not* be the case at a saddle-node bifurcation point, and we want to consider this issue in this exercise. Although this could have been done in Chapter 18, in that chapter we were introducing only center manifold theory and were not really concerned with bifurcations. In this case the form of the equations given by (20.1.84) and (20.1.85) was the "cleanest and quickest" way to introduce the notion of parametrized families of center manifolds.

We will start at a very basic level. Consider the $\mathbf{C}^r$ (r as large as necessary) vector field

$$\dot{z} = F(z, \varepsilon), \qquad (z, \varepsilon) \in \mathbb{R}^{c+s} \times \mathbb{R}^p. \tag{20.1.86}$$

Suppose that $(z, \varepsilon) = (0, 0)$ is a fixed point of (20.1.86) at which the matrix

$$D_z F(0, 0) \tag{20.1.87}$$

has c eigenvalues with zero real parts and s eigenvalues with negative real parts. Our goal is to apply the center manifold theory in order to examine the dynamics of (20.1.86) near $(z, \varepsilon) = (0, 0)$.

We rewrite Equation (20.1.86) as follows

$$\dot{z} = D_z F(0, 0)z + D_\varepsilon F(0, 0)\varepsilon + G(z, \varepsilon), \tag{20.1.88}$$

where

$$G(z, \varepsilon) = \Big[F(z, \varepsilon) - D_z F(0, 0)z - D_\varepsilon F(0, 0)\varepsilon\Big] = \mathcal{O}(2) \tag{20.1.89}$$

in z and ε. Note that the term "$D_\varepsilon F(0, 0)\varepsilon$" in (20.1.88) is the new wrinkle—it was zero under our previous assumptions. For notational purposes we let

$$\begin{aligned} D_z F(0, 0) &\equiv M \qquad -(c + s) \times (c + s) \text{ matrix}, \\ D_\varepsilon F(0, 0) &\equiv \Lambda \qquad -(c + s) \times p \text{ matrix}, \end{aligned}$$

so that (20.1.88) becomes

$$\dot{z} = Mz + \Lambda\varepsilon + G(z, \varepsilon). \tag{20.1.90}$$

Now let T be the $(s+c) \times (s+c)$ matrix that puts M into the following block diagonal form

$$T^{-1}MT = \begin{pmatrix} A & 0 \\ 0 & B \end{pmatrix}, \tag{20.1.91}$$

where A is a $(c \times c)$ matrix with all eigenvalues having zero real parts and B is an $(s \times s)$ matrix with all eigenvalues having negative real parts. If we let

$$z = Tw, \qquad (x, y) \in \mathbb{R}^c \times \mathbb{R}^s, \tag{20.1.92}$$

where $w = (x, y)$, and apply this linear transformation to (20.1.90), we obtain

$$\begin{pmatrix} \dot{x} \\ \dot{y} \end{pmatrix} = \begin{pmatrix} A & 0 \\ 0 & B \end{pmatrix} \begin{pmatrix} x \\ y \end{pmatrix} + \overline{\Lambda}\varepsilon + \begin{pmatrix} f(x, y, \varepsilon) \\ g(x, y, \varepsilon) \end{pmatrix}, \tag{20.1.93}$$

where

$$\overline{\Lambda} \equiv T^{-1}\Lambda,$$

$$\begin{pmatrix} f(x,y,\varepsilon) \\ g(x,y,\varepsilon) \end{pmatrix} \equiv T^{-1}G(T(x,y),\varepsilon).$$

Note that $f(0,0,0)=0$, $g(0,0,0)=0$, $Df(0,0,0)=0$, and $Dg(0,0,0)=0$. Next, let

$$\overline{\Lambda} = \begin{pmatrix} \overline{\Lambda}_c \\ \overline{\Lambda}_s \end{pmatrix},$$

where Λ_c corresponds to the first c rows of Λ, and Λ_s corresponds to the last s rows of Λ. Then (20.1.93) can be rewritten as

$$\begin{pmatrix} \dot{x} \\ \dot{\varepsilon} \\ \dot{y} \end{pmatrix} = \begin{pmatrix} A & \overline{\Lambda}_c & 0 \\ 0 & 0 & 0 \\ 0 & \overline{\Lambda}_s & B \end{pmatrix} \begin{pmatrix} x \\ \varepsilon \\ y \end{pmatrix} + \begin{pmatrix} f(x,y,\varepsilon) \\ 0 \\ g(x,y,\varepsilon) \end{pmatrix}. \tag{20.1.94}$$

The reader should recognize that (20.1.94) is "almost" in the standard normal form for application of the center manifold theory. The final step would be to introduce a linear transformation that block diagonalizes the linear part of (20.1.94) into a $(c+p)\times(c+p)$ matrix with eigenvalues all having zero real parts (and p identically zero) and an $(s\times s)$ matrix with all eigenvalues having negative real parts.

a) Carry out this final step and discuss applying the center manifold theorem to the resulting system. In particular, do the relevant theorems from Chapter 18 go through?

Before we work out some specific problems, let us first answer an example.

Consider the vector field

$$\begin{aligned} \dot{x} &= \varepsilon + x^2 + y^2, \\ \dot{y} &= -y + x^2, \end{aligned} \qquad (x,y,\varepsilon) \in \mathbb{R}^3. \tag{20.1.95}$$

It should be clear that $(x,y,\varepsilon)=(0,0,0)$ is a fixed point of (20.1.95). We want to study the orbit structure near this fixed point for ε small. Rewriting (20.1.95) in the form of (20.1.94) gives

$$\begin{pmatrix} \dot{x} \\ \dot{\varepsilon} \\ \dot{y} \end{pmatrix} = \begin{pmatrix} 0 & 1 & 0 \\ 0 & 0 & 0 \\ 0 & 0 & -1 \end{pmatrix} \begin{pmatrix} x \\ \varepsilon \\ y \end{pmatrix} + \begin{pmatrix} x^2+y^2 \\ 0 \\ x^2 \end{pmatrix}. \tag{20.1.96}$$

We seek a center manifold of the form

$$h(x,\varepsilon) = ax^2 + bx\varepsilon + c\varepsilon^2 + \mathcal{O}(3).$$

Utilizing the usual procedure for calculating the center manifold, we obtain

$$h(x,\varepsilon) = x^2 - 2x\varepsilon + 2\varepsilon^2 + \mathcal{O}(3).$$

The vector field restricted to the center manifold is then given by

$$\begin{aligned} \dot{x} &= \varepsilon + x^2 + \mathcal{O}(4), \\ \dot{\varepsilon} &= 0. \end{aligned}$$

Hence, a saddle-node bifurcation occurs at $\varepsilon = 0$.

Now consider the following vector fields

b) $\begin{aligned} \dot{x} &= \varepsilon + x^4 + y^2, \\ \dot{y} &= -y + x^3, \end{aligned} \qquad (x,y,\varepsilon) \in \mathbb{R}^3.$

c) $\begin{aligned} \dot{x} &= \varepsilon + x^2 - y^3, \\ \dot{y} &= \varepsilon - y + x^2. \end{aligned}$

d) $\begin{aligned} \dot{x} &= \varepsilon + \varepsilon x + x^2, \\ \dot{y} &= -y + x^2. \end{aligned}$

e) $\dot{x} = \varepsilon + \varepsilon x + x^2,$
$\dot{y} = \varepsilon - y + x^2.$

f) $\dot{x} = \varepsilon + \frac{1}{2}x + y + x^3,$
$\dot{y} = x + 2y - xy.$

g) $\dot{x} = 2\varepsilon + 2x + 2y,$
$\dot{y} = \varepsilon + x + y + y^2.$

h) $\dot{x} = \varepsilon - 2x + 2y - x^4,$
$\dot{y} = 2x - 2y.$

i) $\dot{x} = \varepsilon - 2x + y + z + yz,$
$\dot{y} = x - 2y + z + zx,$ $(x, y, z, \varepsilon) \in \mathbb{R}^4.$
$\dot{z} = x + y - 2z + xy,$

For each vector field, construct the center manifold and discuss the dynamics near the origin for ε small. What types of bifurcations occur?

8. Consider the vector field

$$\begin{aligned} \dot{x} &= \varepsilon + x^2 + y^2, \\ \dot{y} &= -y + x^2, \end{aligned} \qquad (x, y, \varepsilon) \in \mathbb{R}^3.$$

For this vector field the tangent space approximation is sufficient for approximating the center manifold of the origin. Verify this statement and discuss conditions under which the tangent space approximation might work in general. Consider your ideas in the context of the following examples.

a) $\dot{x} = \varepsilon x + x^2 + y^2,$
$\dot{y} = -y + x^2.$

b) $\dot{x} = \varepsilon + x^2 + xy,$
$\dot{y} = -y + x^2.$

c) $\dot{x} = \varepsilon + y^2,$
$\dot{y} = -y + x^2.$

d) $\dot{x} = \varepsilon + xy + y^2,$
$\dot{y} = -y + x^2.$

9. Consider the block diagonal "normal form" of (20.1.84) to which we first transformed the vector field in order to apply the center manifold theory. Discuss why (or why not) this preliminary transformation was necessary. Is this preliminary transformation necessary for equations of the form of (20.1.94) in order to apply the center manifold theory? Work out several examples to support your views and illustrate the relevant points. (*Hint:* consider the coordinatization of the center manifold and how the invariance condition is manifested in those coordinates.)

10. Consider the following one-parameter family of two-dimensional $\mathbf{C}^r$ (r as large as necessary) vector fields

$$\dot{x} = f(x; \mu), \qquad (x, \mu) \in \mathbb{R}^2 \times \mathbb{R}^1,$$

where $f(0; 0) = 0$ and $D_x f(0, 0)$ has a zero eigenvalue and a negative eigenvalue. Suppose the vector field has the following symmetry

$$f(x, \mu) = -f(-x, \mu).$$

What can you then conclude concerning the symmetry of the vector field restricted to the center manifold for x and μ small? Can the vector field undergo a saddle-node bifurcation at $(x, \mu) = (0, 0)$? Can the vector field undergo a saddle-node bifurcation at other points $(x, \mu) \in \mathbb{R}^2 \times \mathbb{R}^1$?

20.2 A Pure Imaginary Pair of Eigenvalues: The Poincare-Andronov-Hopf Bifurcation

We now turn to the next most simple way that a fixed point can be nonhyperbolic; namely, that the matrix associated with the vector field linearized about the fixed point has a pair of purely imaginary eigenvalues, with the remaining eigenvalues having nonzero real parts. Let us be more precise.

Recall (20.0.1), which we restate here;

$$\dot{y} = g(y, \lambda), \qquad y \in \mathbb{R}^n, \quad \lambda \in \mathbb{R}^p, \tag{20.2.1}$$

where g is $\mathbf{C}^r$ $(r \geq 5)$ on some sufficiently large open set containing the fixed point of interest. The fixed point is denoted by $(y, \lambda) = (y_0, \lambda_0)$, i.e.,

$$0 = g(y_0, \lambda_0). \tag{20.2.2}$$

We are interested in how the orbit structure near y_0 changes as λ is varied. In this situation the first thing to examine is the linearization of the vector field about the fixed point, which is given by

$$\dot{\xi} = D_y g(y_0, \lambda_0)\xi, \qquad \xi \in \mathbb{R}^n. \tag{20.2.3}$$

Suppose that $D_y g(y_0, \lambda_0)$ has two purely imaginary eigenvalues with the remaining $n - 2$ eigenvalues having nonzero real parts. We know (cf. the remarks at the beginning of this chapter) that since the fixed point is not hyperbolic, the orbit structure of the linearized vector field near $(y, \lambda) = (y_0, \lambda_0)$ may reveal little (and, possibly, even incorrect) information concerning the nature of the orbit structure of the nonlinear vector field (20.2.1) near $(y, \lambda) = (y_0, \lambda_0)$.

Fortunately, we have a systematic procedure for analyzing this problem. By the center manifold theorem, we know that the orbit structure near $(y, \lambda) = (y_0, \lambda_0)$ is determined by the vector field (20.2.1) restricted to the center manifold. This restriction gives us a p-parameter family of vector fields on a two-dimensional center manifold. For now we will assume that we are dealing with a single, scalar parameter, i.e., $p = 1$. If there is more than one parameter in the problem, we will consider all but one of them as fixed.

On the center manifold the vector field (20.2.1) has the following form

$$\begin{pmatrix} \dot{x} \\ \dot{y} \end{pmatrix} = \begin{pmatrix} \text{Re } \lambda(\mu) & -\text{Im } \lambda(\mu) \\ \text{Im } \lambda(\mu) & \text{Re } \lambda(\mu) \end{pmatrix} \begin{pmatrix} x \\ y \end{pmatrix} + \begin{pmatrix} f^1(x, y, \mu) \\ f^2(x, y, \mu) \end{pmatrix},$$
$$(x, y, \mu) \in \mathbb{R}^1 \times \mathbb{R}^1 \times \mathbb{R}^1, \tag{20.2.4}$$

where f^1 and f^2 are nonlinear in x and y and $\lambda(\mu)$, $\overline{\lambda(\mu)}$ are the eigenvalues of the vector field linearized about the fixed point at the origin.

Equation (20.2.4) was first discussed in Section 19.2. The reader should recall that in performing the center manifold reduction to obtain (20.2.4),

several preliminary steps were first implemented. Namely, first we transformed the fixed point to the origin and, then, if necessary, performed a linear transformation of the coordinates so that the vector field (20.2.1) was in the form of (20.2.4). We further remark that the eigenvalue, denoted $\lambda(\mu)$, should not be confused with the general vector of parameters in (20.2.1), denoted $\lambda \in \mathbb{R}^p$, which we subsequently restricted to a scalar and labeled μ. We will henceforth denote

$$\lambda(\mu) = \alpha(\mu) + i\omega(\mu), \tag{20.2.5}$$

and note that by our assumptions we have

$$\begin{aligned} \alpha(0) &= 0, \\ \omega(0) &\neq 0. \end{aligned} \tag{20.2.6}$$

The next step is to transform (20.2.4) into normal form. This was done in Section 19.2. The normal form was found to be

$$\begin{aligned} \dot{x} &= \alpha(\mu)x - \omega(\mu)y + (a(\mu)x - b(\mu)y)(x^2 + y^2) + \mathcal{O}(|x|^5, |y|^5), \\ \dot{y} &= \omega(\mu)x + \alpha(\mu)y + (b(\mu)x + a(\mu)y)(x^2 + y^2) + \mathcal{O}(|x|^5, |y|^5). \end{aligned} \tag{20.2.7}$$

We will find it more convenient to work with (20.2.7) in polar coordinates. In polar coordinates (20.2.7) is given by

$$\begin{aligned} \dot{r} &= \alpha(\mu)r + a(\mu)r^3 + \mathcal{O}(r^5), \\ \dot{\theta} &= \omega(\mu) + b(\mu)r^2 + \mathcal{O}(r^4). \end{aligned} \tag{20.2.8}$$

Because we are interested in the dynamics near $\mu = 0$, it is natural to Taylor expand the coefficients in (20.2.8) about $\mu = 0$. Equation (20.2.8) thus becomes

$$\begin{aligned} \dot{r} &= \alpha'(0)\mu r + a(0)r^3 + \mathcal{O}(\mu^2 r, \mu r^3, r^5), \\ \dot{\theta} &= \omega(0) + \omega'(0)\mu + b(0)r^2 + \mathcal{O}(\mu^2, \mu r^2, r^4), \end{aligned} \tag{20.2.9}$$

where " $'$ " denotes differentiation with respect to μ and we have used the fact that $\alpha(0) = 0$.

Our goal is to understand the dynamics of (20.2.9) for r small and μ small. This will be accomplished in two steps.

Step 1. Neglect the higher order terms of (20.2.9) and study the resulting "truncated" normal form.

Step 2. Show that the dynamics exhibited by the truncated normal form are qualitatively unchanged when one considers the influence of the previously neglected higher order terms.

Step 1. Neglecting the higher order terms in (20.2.9) gives

$$\begin{aligned} \dot{r} &= d\mu r + ar^3, \\ \dot{\theta} &= \omega + c\mu + br^2, \end{aligned} \tag{20.2.10}$$

where, for ease of notation, we define

$$\begin{aligned} \alpha'(0) &\equiv d, \\ a(0) &\equiv a, \\ \omega(0) &\equiv \omega, \\ \omega'(0) &\equiv c, \\ b(0) &\equiv b. \end{aligned} \tag{20.2.11}$$

In analyzing the dynamics of vector fields we have always started with the simplest situation; namely, we have found the fixed points and studied the nature of their stability. In regard to (20.2.10), however, we proceed slightly differently because of the nature of the coordinate system. To be precise, values of $r > 0$ and μ for which $\dot{r} = 0$, but $\dot{\theta} \neq 0$, correspond to periodic orbits of (20.2.10). We highlight this in the following lemma.

Lemma 20.2.1 *For $-\infty < \frac{\mu d}{a} < 0$ and μ sufficiently small*

$$(r(t), \theta(t)) = \left(\sqrt{\frac{-\mu d}{a}}, \left[\omega + \left(c - \frac{bd}{a} \right) \mu \right] t + \theta_0 \right) \tag{20.2.12}$$

is a periodic orbit for (20.2.10).

Proof: In order to interpret (20.2.12) as a periodic orbit, we need only to insure that $\dot{\theta}$ is not zero. Since ω is a constant independent of μ, this immediately follows by taking μ sufficiently small. □

We address the question of stability in the following lemma.

Lemma 20.2.2 *The periodic orbit is*

i) *asymptotically stable for $a < 0$;*

ii) *unstable for $a > 0$.*

Proof: The way to prove this lemma is to construct a one-dimensional Poincaré map along the lines of Chapter 10 (and in particular, Example 10.1.1), from which the results of this lemma follow. □

We note that since we must have $r > 0$, (20.2.12) is the only periodic orbit possible for (20.2.10). Hence, for $\mu \neq 0$, (20.2.10) possesses a unique periodic orbit having amplitude $\mathcal{O}(\sqrt{\mu})$. Concerning the details of stability of the periodic orbit and whether it exists for $\mu > 0$ or $\mu < 0$, from (20.2.12) it is easy to see that there are four possibilities:

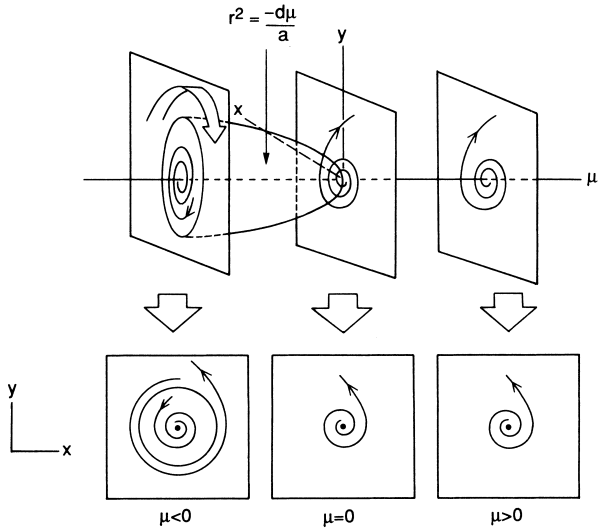

FIGURE 20.2.1. $d > 0$, $a > 0$.

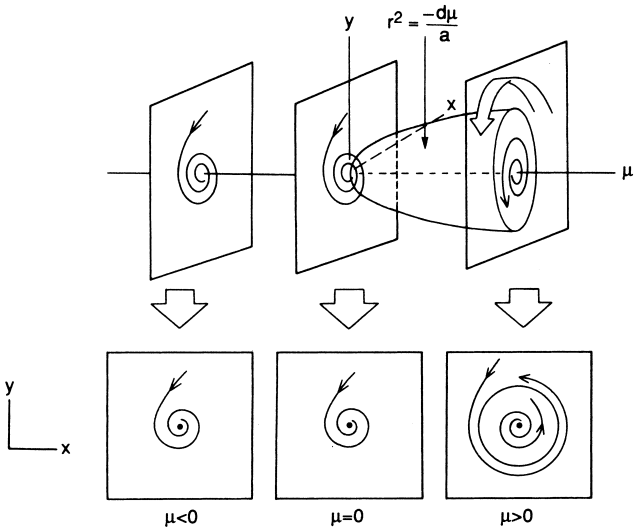

FIGURE 20.2.2. $d > 0$, $a < 0$.

1. $d > 0$, $a > 0$;
2. $d > 0$, $a < 0$;
3. $d < 0$, $a > 0$;

4. $d < 0$, $a < 0$.

We will examine each case individually; however, we note that in all cases the origin is a fixed point which is

$$\text{stable at } \mu = 0 \quad \text{for } a < 0,$$

$$\text{unstable at } \mu = 0 \quad \text{for } a > 0.$$

Case 1: $d > 0$, $a > 0$. In this case the origin is an unstable fixed point for $\mu > 0$ and an asymptotically stable fixed point for $\mu < 0$, with an unstable periodic orbit for $\mu < 0$ (note: the reader should realize that if the origin is stable for $\mu < 0$, then the periodic orbit should be unstable); see Figure 20.2.1.

Case 2: $d > 0$, $a < 0$. In this case the origin is an asymptotically stable fixed point for $\mu < 0$ and an unstable fixed point for $\mu > 0$, with an asymptotically stable periodic orbit for $\mu > 0$; see Figure 20.2.2.

Case 3: $d < 0$, $a > 0$. In this case the origin is an unstable fixed point for $\mu < 0$ and an asymptotically stable fixed point for $\mu > 0$, with an unstable

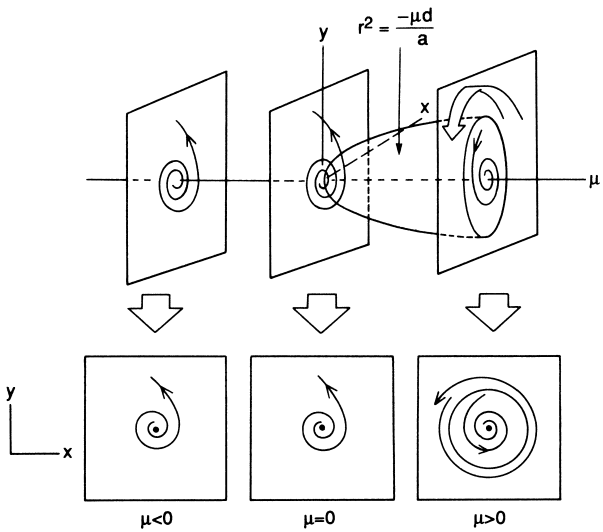

FIGURE 20.2.3. $d < 0$, $a > 0$.

periodic orbit for $\mu > 0$; see Figure 20.2.3.

Case 4: $d < 0$, $a < 0$. In this case the origin is an asymptotically stable fixed point for $\mu < 0$ and an unstable fixed point for $\mu > 0$, with an asymptotically stable periodic orbit for $\mu < 0$; see Figure 20.2.4.

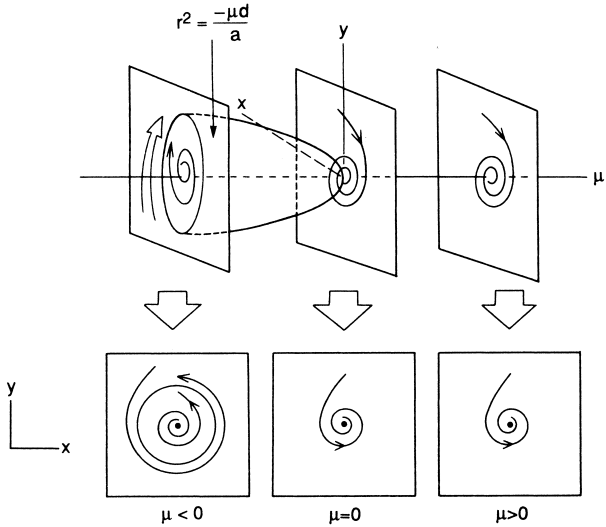

FIGURE 20.2.4. $d < 0$, $a < 0$.

From these four cases we can make the following general remarks.

Remark 1. For $a < 0$ it is possible for the periodic orbit to exist for either $\mu > 0$ (Case 2) or $\mu < 0$ (Case 4); however, in each case the periodic orbit is asymptotically stable. Similarly, for $a > 0$ it is possible for the periodic orbit to exist for either $\mu > 0$ (Case 3) or $\mu < 0$ (Case 1); however, in each case the periodic orbit is unstable. Thus, the number a tells us whether the bifurcating periodic orbit is stable ($a < 0$) or unstable ($a > 0$). The case $a < 0$ is referred to as a *supercritical* bifurcation, and the case $a > 0$ is referred to as a *subcritical* bifurcation.

Remark 2. Recall that

$$d = \frac{d}{d\mu}(\mathrm{Re}\lambda(\mu))\bigg|_{\mu=0}.$$

Hence, for $d > 0$, the eigenvalues cross from the left half-plane to the right half-plane as μ increases and, for $d < 0$, the eigenvalues cross from the right half-plane to the left half-plane as μ increases. For $d > 0$, it follows that the origin is asymptotically stable for $\mu < 0$ and unstable for $\mu > 0$. Similarly, for $d < 0$, the origin is unstable for $\mu < 0$ and asymptotically stable for $\mu > 0$.

Step 2. At this point we have a fairly complete analysis of the orbit structure of the truncated normal form near $(r, \mu) = (0, 0)$. We now must consider Step 2 in our analysis of the normal form (20.2.9); namely, are the dynamics that we have found in the truncated normal form changed when the effects

of the neglected higher order term are considered? Fortunately, the answer to this question is no and is the content of the following theorem.

Theorem 20.2.3 (Poincaré-Andronov-Hopf Bifurcation) *Consider the full normal form (20.2.9). Then, for μ sufficiently small, Case 1, Case 2, Case 3, and Case 4 described above hold.*

Proof: We will outline a proof that uses the Poincaré-Bendixson Theorem. We begin by considering the truncated normal form (20.2.10) and the case $a < 0$, $d > 0$. In this case the periodic orbit is stable and exists for $\mu > 0$, and the r coordinate is given by

$$r = \sqrt{\frac{-d\mu}{a}}.$$

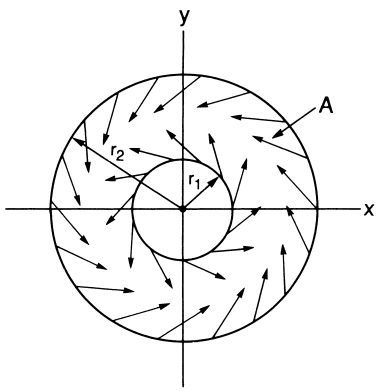

FIGURE 20.2.5.

We next choose $\mu > 0$ sufficiently small and consider the annulus in the plane, A, given by

$$A = \{(r, \theta) |\ r_1 \leq r \leq r_2\},$$

where r_1 and r_2 are chosen such that

$$0 < r_1 < \sqrt{\frac{-d\mu}{a}} < r_2.$$

By (20.2.10), it is easy to verify that on the boundary of A, the vector field given by the truncated normal form (20.2.10) is pointing *strictly* into the interior of A. Hence, A is a positive invariant region (cf. Definition 3.0.3, Chapter 3); see Figure 20.2.5.

It is also easy to verify that A contains no fixed points so, by the Poincaré-Bendixson theorem, A contains a stable periodic orbit. Of course we already

knew this; our goal is to show that this situation still holds when the full normal form (20.2.9) is considered.

Now consider the full normal form (20.2.9). By taking μ and r sufficiently small, the $\mathcal{O}(\mu^2 r, \mu r^3, r^5)$ terms can be made much smaller than the rest of the normal form (i.e., the truncated normal form (20.2.10). Therefore, by taking r_1 and r_2 sufficiently small, A is still a positive invariant region containing no fixed points. Hence, by the Poincaré-Bendixson theorem, A contains a stable periodic orbit. The remaining three cases can be treated similarly; however, in the cases where $a > 0$, the time-reversed flow (i.e., letting $t \to -t$) must be considered. □

To apply this theorem to specific systems, we need to know d (which is easy) and a. In principle, a is relatively straightforward to calculate. We simply carefully keep track of the coefficients in the normal form transformation in terms of our original vector field. However, in practice, the algebraic manipulations are horrendous. The explicit calculation can be found in Hassard, Kazarinoff, and Wan [1980], Marsden and McCracken[1976], and Guckenheimer and Holmes [1983]; here we will just state the result.

At bifurcation (i.e., $\mu = 0$), (20.2.4) becomes

$$\begin{pmatrix} \dot{x} \\ \dot{y} \end{pmatrix} = \begin{pmatrix} 0 & -\omega \\ \omega & 0 \end{pmatrix} \begin{pmatrix} x \\ y \end{pmatrix} + \begin{pmatrix} f^1(x, y, 0) \\ f^2(x, y, 0) \end{pmatrix}, \tag{20.2.13}$$

and the coefficient $a(0) \equiv a$ is given by

$$\begin{aligned} a = & \frac{1}{16}\left[f^1_{xxx} + f^1_{xyy} + f^2_{xxy} + f^2_{yyy}\right] \\ & + \frac{1}{16\omega}\left[f^1_{xy}\left(f^1_{xx} + f^1_{yy}\right) - f^2_{xy}\left(f^2_{xx} + f^2_{yy}\right)\right. \\ & \left. - f^1_{xx} f^2_{xx} + f^1_{yy} f^2_{yy}\right], \end{aligned} \tag{20.2.14}$$

where all partial derivatives are evaluated at the bifurcation point, i.e., $(x, y, \mu) = (0, 0, 0)$.

We end this section with some historical remarks. Usually Theorem 20.2.3 goes by the name of the "Hopf bifurcation theorem." However, as has been pointed out repeatedly by V. Arnold [1983], this is inaccurate, since examples of this type of bifurcation can be found in the work of Poincaré [1892]. The first specific study and formulation of a theorem was due to Andronov [1929]. However, this is not to say that E. Hopf did not make an important contribution; while the work of Poincaré and Andronov was concerned with two-dimensional vector fields, the theorem due to E. Hopf [1942] is valid in n dimensions (note: this was before the discovery of the center manifold theorem). For these reasons we refer to Theorem 20.2.3 as the Poincaré-Andronov-Hopf bifurcation theorem.

20.2A Exercises

1. This exercise comes from Marsden and McCracken [1976]. Consider the following vector fields

   a) $\dot{r} = -r(r-\mu)^2, \quad (r,\theta) \in \mathbb{R}^+ \times S^1.$
   $\dot{\theta} = 1,$

   b) $\dot{r} = r(\mu - r^2)(2\mu - r^2)^2,$
   $\dot{\theta} = 1.$

   c) $\dot{r} = r(r+\mu)(r-\mu),$
   $\dot{\theta} = 1.$

   d) $\dot{r} = \mu r(r^2 - \mu),$
   $\dot{\theta} = 1.$

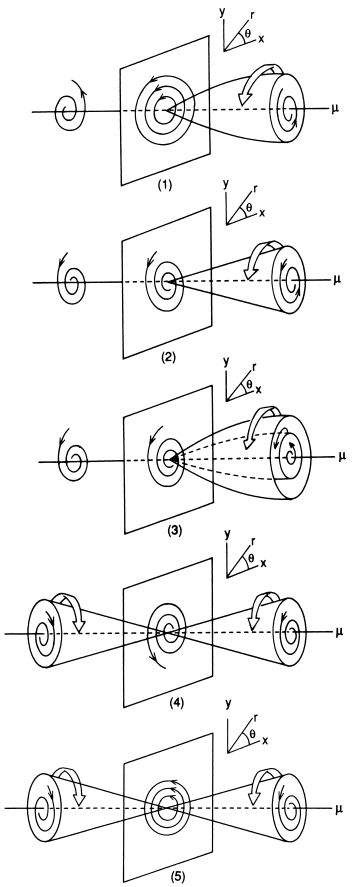

FIGURE 20.2.6.

   e) $\dot{r} = -\mu^2 r(r+\mu)^2(r-\mu)^2,$
   $\dot{\theta} = 1.$

Match each of these vector fields to the appropriate phase portrait in Figure 20.2.6 and explain which hypotheses (if any) of the Poincaré–Andronov–Hopf bifurcation theorem are violated.

2. Consider the Poincaré–Andronov–Hopf bifurcation theorem (Theorem 20.2.3). Work out all of the details of the proof outlined that uses the Poincaré–Bendixson theorem.

3. For the Poincaré–Andronov–Hopf bifurcation, compute the expression for the coefficient a given in (20.2.14).

20.3 Stability of Bifurcations Under Perturbations

Let us recall the central motivational question raised at the beginning of this chapter; namely, what is the nature of the orbit structure *near* a nonhyperbolic fixed point of a vector field? The key word to focus on in this question is "near." We have seen that a nonhyperbolic fixed point can be either asymptotically stable or unstable. However, most importantly, we have seen that "nearby vector fields" can have very different orbit structures. The phrase "nearby vector fields" was made concrete by considering parameterized families of vector fields; at a certain parameter value the fixed point was not hyperbolic, and a qualitatively different orbit structure existed for nearby parameter values (i.e., new solutions were created as the parameter was varied). There is an important, general lesson to be learned from this, which we state as follows.

Pure Mathematical Lesson

From the point of view of stability of nonhyperbolic fixed points of vector fields, one should not only study the orbit structure near the fixed point but also the local orbit structure of nearby vector fields.

Applied Mathematical Lesson

From the point of view of "robustness" of mathematical models, suppose one has a vector field possessing a nonhyperbolic fixed point. The vector field should then possess enough (independent) parameters so that, as the parameters are varied, all possible *local* dynamical behavior is realized in this particular parameterized family of vector fields.

Before making these somewhat vague ideas more precise, let us consider how they are manifested in the saddle-node, transcritical, pitchfork, and Poincaré-Andronov-Hopf bifurcations of vector fields that we have already studied.

Example 20.3.1 (The Saddle-Node Bifurcation). Consider the one-parameter family of one-dimensional vector fields

$$\dot{x} = f(x, \mu), \qquad y \in \mathbb{R}^1, \quad \mu \in \mathbb{R}^1, \tag{20.3.1}$$

with

$$f(0, 0) = 0, \tag{20.3.2}$$

$$\frac{\partial f}{\partial x}(0,0) = 0. \tag{20.3.3}$$

We saw in Section 20.1c that the conditions

$$\frac{\partial f}{\partial \mu}(0,0) \neq 0, \tag{20.3.4}$$

$$\frac{\partial^2 f}{\partial x^2}(0,0) \neq 0, \tag{20.3.5}$$

were sufficient conditions in order for the vector field (20.3.1) to undergo a saddle-node bifurcation at $\mu = 0$. The question we ask is the following.

> If a one-parameter family of one-dimensional vector fields satisfying (20.3.2), (20.3.3), (20.3.4), and (20.3.5) is "perturbed," will the resulting family of one-dimensional vector fields have qualitatively the same dynamics?

We will have essentially answered this question once we have explained what we mean by the term "perturbed."

We do this by first eliminating the parameters entirely. Consider a one-dimensional vector field

$$\dot{x} = f(x) = a_0 x^2 + \mathcal{O}(x^3), \qquad x \in \mathbb{R}^1, \tag{20.3.6}$$

where, in the Taylor expansion of $f(x)$, we have omitted the constant and $\mathcal{O}(x)$ terms, since we want (20.3.6) to have a nonhyperbolic fixed point at $x = 0$. Because $x = 0$ is a nonhyperbolic fixed point, the orbit structure near $x = 0$ of vector fields near (20.3.6) may be very different. We consider vector fields close to (20.3.6) by embedding (20.3.6) in a one-parameter family of vector fields as follows

$$\dot{x} = f(x,\mu) = \mu + a_0 x^2 + \mathcal{O}(x^3). \tag{20.3.7}$$

The addition of the term "μ" in (20.3.7) can be viewed as a perturbation of (20.3.6) via adding lower-order terms in the Taylor expansion of the vector field about the nonhyperbolic fixed point (note: "lower-order terms" means terms of order lower than the first nonvanishing term in the Taylor expansion). Clearly, (20.3.7) satisfies (20.3.2), (20.3.3), (20.3.4), and (20.3.5); hence, $(x,\mu) = (0,0)$ is a saddle-node bifurcation point. What about further perturbations of (20.3.7)? If we add terms of $\mathcal{O}(x^3)$ and larger, we see that this has no effect on the nature of the bifurcation, since the saddle-node bifurcation is completely determined by (20.3.2), (20.3.3), (20.3.4), and (20.3.5), i.e., by terms of $\mathcal{O}(x^2)$ and lower. We could perturb (20.3.7) further by adding lower-order terms. For example,

$$\dot{x} = f(x,\mu,\varepsilon) = \mu + \varepsilon x + a_0 x^2 + \mathcal{O}(x^3). \tag{20.3.8}$$

In this case we have a two-parameter family of one-dimensional vector fields having a nonhyperbolic fixed point at $(x,\mu,\varepsilon) = (0,0,0)$. However, the nature of the saddle-node bifurcation (i.e., the geometry of the curve(s) of fixed points passing through the bifurcation point) is completely determined by (20.3.2), (20.3.3), (20.3.4), and (20.3.5). Hence, the addition of the term "εx" in (20.3.8) does not introduce any new dynamical phenomena into (20.3.7) (provided $\mu \neq 0$).

End of Example 20.3.1

Example 20.3.2 (The Transcritical Bifurcation). Consider the one-parameter family of one-dimensional vector fields

$$\dot{x} = f(x, \mu), \qquad x \in \mathbb{R}^1, \quad \mu \in \mathbb{R}^1, \tag{20.3.9}$$

with

$$f(0, 0) = 0, \tag{20.3.10}$$

$$\frac{\partial f}{\partial x}(0, 0) = 0. \tag{20.3.11}$$

We saw in Section 20.1d that if (20.3.9) also satisfies

$$\frac{\partial f}{\partial \mu}(0, 0) = 0, \tag{20.3.12}$$

$$\frac{\partial^2 f}{\partial \mu \partial x}(0, 0) \neq 0, \tag{20.3.13}$$

$$\frac{\partial^2 f}{\partial x^2}(0, 0) \neq 0, \tag{20.3.14}$$

then a transcritical bifurcation occurs at $(x, \mu) = (0, 0)$. The conditions (20.3.12), (20.3.13), and (20.3.14) imply that, in the study of the orbit structure near the bifurcation point, terms of $\mathcal{O}(x^3)$ and larger in the Taylor expansion of the vector field about the bifurcation point do not qualitatively affect the nature of the bifurcation (i.e., they do not affect the geometry of the curves of fixed points passing through the bifurcation point). From this we concluded that a normal form for the transcritical bifurcation was given by

$$\dot{x} = \mu x \mp x^2. \tag{20.3.15}$$

Now let us consider a perturbation of the transcritical bifurcation by perturbing this normal form. Following our discussion of the perturbation of the saddle-node bifurcation and upon examining the defining conditions for the transcritical bifurcation given in (20.3.12), (20.3.13), and (20.3.14), we see that the only way to perturb (20.1.31) that may lead to qualitatively new dynamics is as follows

$$\dot{x} = \varepsilon + \mu x \mp x^2. \tag{20.3.16}$$

In Figure 20.3.1 we show what becomes of the transcritical bifurcation for $\varepsilon < 0$, $\varepsilon = 0$, and $\varepsilon > 0$.

From this we see that the two curves of fixed points which pass through the origin for $\varepsilon = 0$ break apart into either a pair of curves of fixed points on which no bifurcation happens on passing through $\mu = 0$ or a pair of saddle-node bifurcations.

End of Example 20.3.2

Example 20.3.3 (The Pitchfork Bifurcation). From (20.1.83), the normal form for the pitchfork bifurcation was found to be

$$\dot{x} = \mu x \mp x^3, \qquad x \in \mathbb{R}^1, \quad \mu \in \mathbb{R}^1. \tag{20.3.17}$$

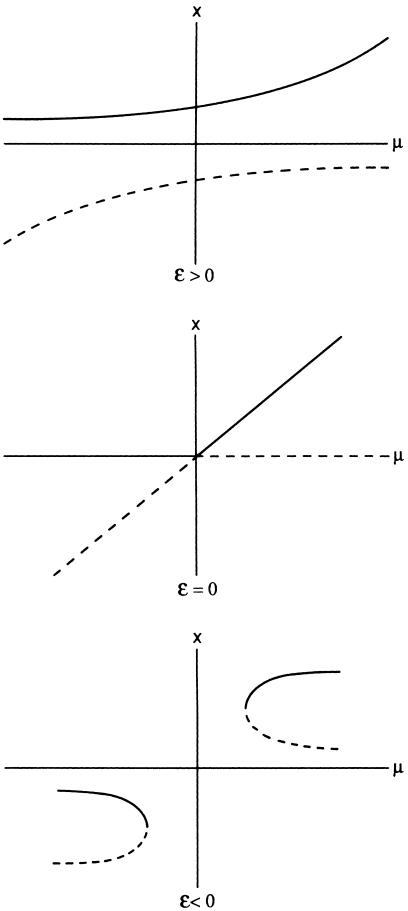

FIGURE 20.3.1.

Using arguments exactly like those used in Examples 20.3.1 and 20.3.2, we can see that the only perturbations able to affect the orbit structure near $\mu = 0$ of (20.3.17) are

$$\dot{x} = \varepsilon + \mu x \mp x^3, \qquad \varepsilon \in \mathbb{R}^1. \tag{20.3.18}$$

In Figure 20.3.2 we show bifurcation diagrams for $\varepsilon < 0$, $\varepsilon = 0$, and $\varepsilon > 0$.

As in the case of transcritical bifurcation, we see that, upon perturbation, the two curves of fixed points which pass through $(x, \mu) = (0, 0)$ for $\varepsilon = 0$ break up into either curves of fixed points exhibiting no bifurcation as μ varies through 0 or saddle-node bifurcations for $\varepsilon \neq 0$.

End of Example 20.3.3

Example 20.3.4. Recall the one-parameter family of one-dimensional vector

fields discussed in Example 20.1.4

$$\dot{x} = \mu - x^3, \qquad x \in \mathbb{R}^1, \quad \mu \in \mathbb{R}^1. \tag{20.3.19}$$

The vector fields in this example have a nonhyperbolic fixed point at $(x, \mu) = (0, 0)$, but the orbit structure is qualitatively the same for all μ, i.e., no bifurcation occurs at $(x, \mu) = (0, 0)$.

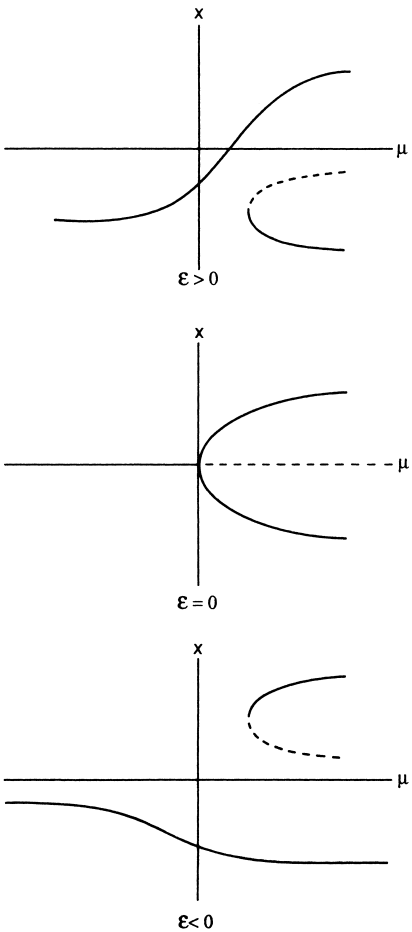

FIGURE 20.3.2.

Now consider the following perturbation of (20.3.19)

$$\dot{x} = \mu + \varepsilon x - x^3, \qquad \varepsilon \in \mathbb{R}^1. \tag{20.3.20}$$

From Figure 20.3.2 (with the roles of ε and μ reversed), it should be evident that

(20.3.20) does exhibit saddle-node bifurcations for $\varepsilon \neq 0$.

End of Example 20.3.4

Example 20.3.5 (The Poincaré-Andronov-Hopf Bifurcation). From Theorem 20.2.3, the normal form for the Poincaré-Andronov-Hopf bifurcation was given by

$$\dot{r} = \mu d r + a r^3, \qquad (r, \theta) \in \mathbb{R}^+ \times S^1, \quad \mu \in \mathbb{R}^1, \tag{20.3.21}$$

$$\dot{\theta} = \omega + c\mu + b r^2. \tag{20.3.22}$$

We want to consider how the bifurcation near $(r, \mu) = (0, 0)$ studied in Section 20.2 changes as (20.3.21) is perturbed. Three points should be considered.

1. Theorem 20.2.3 tells us that, for $a \neq 0$, $d \neq 0$, higher order terms (i.e., $\mathcal{O}(r^4)$) will not affect the dynamics of (20.3.21) near $(r, \mu) = (0, 0)$.
2. Since ω is a constant, for (r, μ) small, in order to determine the nature of solutions bifurcating from the origin we need only worry about the $\dot{r}$ component of the vector field (20.3.21).
3. Due to the structure of the linear part of the vector field, $r = 0$ is a fixed point for μ sufficiently small and *no terms of even order in* r are present in the $\dot{r}$ component of the normal form.

Using these three points, we see that, for $a \neq 0$, $d \neq 0$, no perturbations allowed by the structure of the vector field (cf. the third point above) will qualitatively alter the nature of the bifurcation near $(r, \mu) = (0, 0)$.

End of Example 20.3.5

From Examples 20.3.1–20.3.5 we might conclude that, in one-parameter families of vector fields, the most "typical" bifurcations are saddle-node and Poincaré-Andronov-Hopf. This is indeed the case, as we will show in Section 20.4. Moreover, these examples show that some nonhyperbolic fixed points are more degenerate than others in the sense that more parameters are needed in order to capture all possible nearby behavior. In Section 20.4 we explore the idea of the codimension of a bifurcation, which will enable us to quantify these ideas. A complete theory is given by Golubitsky and Schaeffer [1985] and Golubitsky, Stewart, and Schaeffer [1988].

20.4 The Idea of the Codimension of a Bifurcation

We have seen that some types of bifurcations (e.g., transcritical, pitchfork) are more degenerate than others (e.g., saddle-node). In this section we will attempt to make this more precise by introducing the idea of the codimension of a bifurcation. We will do this by starting with a heuristic discussion

of the "big picture" of bifurcation theory. This will serve to show just how little is actually understood about bifurcation theory at this stage of the mathematical development of nonlinear dynamical systems theory.

20.4a The "Big Picture" for Bifurcation Theory

The first step is to eliminate the consideration of all parameters from the problem; instead, we consider the infinite-dimensional space of all dynamical systems, either vector fields or maps. Within this space we consider the subset of all *structurally stable* dynamical systems, which we denote as S. By the definition of structural stability (cf. Chapter 12), perturbations of structurally stable dynamical systems do not yield qualitatively new dynamical phenomena. Thus, from the point of view of bifurcation theory, it is not dynamical systems in S that are of interest but rather dynamical systems in the complement of S, denoted S^c, since perturbations of dynamical systems in S^c can result in systems exhibiting radically different dynamical behavior. Thus, in order to understand the types of bifurcations that may occur in a class of dynamical systems, it is necessary to understand the structure of S^c.

Presumably, in order for a dynamical system to be in S^c, the system must satisfy a certain number of extra conditions or constraints. When viewed geometrically in the infinite-dimensional function space setting, this can be interpreted as implying that S^c is a lower-dimensional "surface" contained in the space of dynamical systems. Here we use the word "surface" in a heuristic sense. More specifically, it would be nice if we could show that S^c is a codimension one submanifold. In practice, however, S^c may have singular regions and therefore be more appropriately described as an *algebraic variety* (see Arnold [1983]). In any case, for our heuristic discussion, it does no harm for the reader to visualize S^c as a surface. Before proceeding with this picture, let us first make a slight digression and define the notion of the "codimension of a submanifold."

The Codimension of a Submanifold

Let M be an m-dimensional manifold and let N be an n-dimensional submanifold contained in M; then the codimension of N is defined to be $m-n$. Equivalently, in a coordinate setting, the codimension of N is the number of independent equations needed to define N. Thus, the codimension of a submanifold is a measure of the avoidability of the submanifold as one moves about the ambient space; in particular, the codimension of a submanifold N is equal to the minimum dimension of a submanifold $P \subset M$ that intersects N such that the intersection is transversal. We have defined codimension in a finite-dimensional setting, which permits some intuition to be gained; now we move to the infinite-dimensional setting. Let M be an infinite-dimensional manifold and let N be a submanifold contained in

M. (Note: for the definition of an infinite-dimensional manifold see Hirsch [1976]. Roughly speaking, an infinite-dimensional manifold is a set which is locally diffeomorphic to an infinite-dimensional Banach space. Because infinite-dimensional manifolds are discussed in this section only, and then mainly in a heuristic fashion, we refer the reader to the literature for the proper definitions.) We say that N is of codimension k if every point of N is contained in some open set in M which is diffeomorphic to $U \times \mathbb{R}^k$, where U is an open set in N. This implies that k is the smallest dimension of a submanifold $P \subset M$ that intersects N such that the intersection is transversal. Thus, the definition of codimension in the infinite-dimensional case has the same geometrical connotations as in the finite-dimensional case. Now we return to our main discussion. (For the case of "codimension ∞", $\mathbb{R}^k$ in this definition is replaced with an infinite dimensional Banach space.)

Suppose S^c is a codimension one submanifold or, more generally, an algebraic variety. We might think of S^c as a surface dividing the infinite-dimensional space of dynamical systems as depicted in Figure 20.4.1. Bifurcations (i.e., topologically distinct orbit structures) occur as one passes through S^c. Thus, in the infinite-dimensional space of dynamical systems, one might define a *bifurcation point* as being any dynamical system which is structurally unstable.

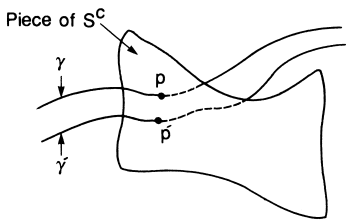

FIGURE 20.4.1.

In this setting one might initially conclude that bifurcations seldom occur and are unimportant, since any point p on S^c may be perturbed to S by (most) arbitrarily small perturbations. One might also conclude from a practical point of view that dynamical systems contained in S^c might not be very good models for physical systems, since any model is only an approximation to reality and therefore should be structurally stable. However, suppose we have a curve γ of dynamical systems transverse to S^c, i.e., a one-parameter family of dynamical systems. Then any sufficiently small perturbation of this curve γ still results in a curve γ' transverse to S^c. Thus, although any particular point on S^c may be removed from S^c by (most) arbitrarily small perturbations, a curve transverse to S^c remains transverse to S^c under perturbation. Bifurcation may therefore be unavoidable in a parameterized family of dynamical systems. This is an important point.

Now, even if we are able to show that S^c is a codimension one submanifold or algebraic variety, S^c itself may be divided up into objects of higher codimension corresponding to more degenerate types of bifurcations. A particular type of codimension k bifurcation in S^c would then be persistent in a k-parameter family of dynamical systems transverse to the codimension k submanifold.

This is essentially the program for bifurcation theory originally outlined by Poincaré. In order to utilize it in practice one would proceed as follows.

1. Given a specific dynamical system, determine whether or not it is structurally stable.

2. If it is not structurally stable, compute the codimension of the bifurcation.

3. Embed the system in a parameterized family of systems transverse to the bifurcation surface with the number of parameters equal to the codimension of the bifurcation. These parameterized systems are called *unfoldings* or *deformations* and, if they contain all possible qualitative dynamics that can occur near the bifurcation, they are called *universal unfoldings* or *versal deformations*; see Arnold [1983] and our discussion to follow.

4. Study the dynamics of the parametrized systems.

In this way one obtains structurally stable *families* of systems. Moreover, this provides a method for gaining a complete understanding of the qualitative dynamics of the space of dynamical systems with as little work as possible; namely, one uses the degenerate bifurcation points as "organizing centers" around which one studies the dynamics. Because elsewhere the dynamical systems are structurally stable, there is no need to worry about the details of their dynamics; qualitatively, they will be topologically conjugate to the structurally stable dynamical systems in a neighborhood of the bifurcation point.

This program is far from complete, and many of the problems associated with its completion are exactly those encountered in our discussion of structural stability in Chapter 12. First, we must specify what we mean by the "infinite-dimensional space of dynamical systems." (Usually this does not present any major difficulties.) Next, we must equip the space with a topology in order to define what we mean by a perturbation of a dynamical system. We have already seen (cf. Example 12.0.1 of Chapter 12) that there can be problems with this if the phase space is unbounded; nevertheless, these difficulties can usually be brought under control. The real difficulty is the following. Given a dynamical system, what does one need to know about it in order to determine whether it is in S or S^c? For vector fields on compact, boundaryless two-dimensional manifolds Peixoto's theorem gives

us an answer to this question (see Theorem 12.1.4 , Chapter 12), but, in higher dimensions, we do not have nice analogs of this theorem. Moreover, the detailed structure of S^c is certainly beyond our reach at this time. Although the situation appears hopeless, some progress has been made along two fronts:

1. Local bifurcations;

2. Global bifurcations of specific orbits.

Since the subject of this chapter is local bifurcations we will discuss only this aspect. In Chapter 33 we will see examples of global bifurcations; for more information see Wiggins [1988].

Local bifurcation theory is concerned with the bifurcation of fixed points of vector fields and maps or with situations in which the problem can be cast into this form, such as in the study of bifurcations of periodic motions. For vector fields one can construct a local Poincaré map (see Chapter 10) near the periodic orbit, thus reducing the problem to one of studying the bifurcation of a fixed point of a map, and for maps with a k periodic orbit one can consider the k^{th} iterate of the map, thus reducing the problem to one of studying the bifurcation of a fixed point of the k^{th} iterate of the map. Utilizing a procedure such as the center manifold theorem or the Lyapunov-Schmidt reduction (see Chow and Hale [1982]), one can usually reduce the problem to that of studying an equation of the form

$$f(x, \lambda) = 0, \tag{20.4.1}$$

where $x \in \mathbb{R}^n$, $\lambda \in \mathbb{R}^p$ are the system parameters and $f : \mathbb{R}^n \times \mathbb{R}^p \to \mathbb{R}^n$ is assumed to be sufficiently smooth. The goal is to study the nature of the solutions of (20.4.1) as λ varies. In particular, it would be interesting to know for what parameter values solutions disappear or are created. These particular parameters are called *bifurcation values*, and there exists an extensive mathematical machinery called *singularity theory* (see Golubitsky and Guillemin [1973]) that deals with such questions. Singularity theory is concerned with the local properties of smooth functions near a zero of the function. It provides a classification of the various cases based on codimension in a spirit similar to that described in the beginning of the section. The reason this is possible is that the codimension k submanifolds in the space of all smooth functions having zeroes can be described algebraically by imposing conditions on derivatives of the functions. This gives us a way of classifying the various possible bifurcations and of computing the proper unfoldings or deformations. From this one might be led to believe that local bifurcation theory is a well-understood subject; however, this is not the case. The problem arises in the study of degenerate local bifurcations, specifically, in codimension k ($k \geq 2$) bifurcations of vector fields. Fundamental work of Takens [1974], Langford [1979], and Guckenheimer

[1981] has shown that, arbitrarily near these degenerate bifurcation points, complicated global dynamical phenomena such as invariant tori and Smale horseshoes may arise. These phenomena cannot be described or detected via singularity theory techniques. Nevertheless, when one reads or hears the phrase "codimension k bifurcation" in the context of bifurcations of fixed points of dynamical systems, it is the singularity theory recipe that is used to compute the codimension. For this reason we want to describe the singularity theory approach.

20.4B The Approach to Local Bifurcation Theory: Ideas and Results from Singularity Theory

We now want to give a brief account of the techniques from singularity theory that are used to determine the codimension of a *local* bifurcation and the correspondingly appropriate unfolding or versal deformation. Our discussion follows closely Arnold [1983].

We begin by specifying the infinite-dimensional space of dynamical systems of interest. This will be the set of $\mathbf{C}^r$ maps of $\mathbb{R}^n$ into $\mathbb{R}^m$, denoted $\mathbf{C}^r(\mathbb{R}^n, \mathbb{R}^m)$. At this stage we can think of the elements of $\mathbf{C}^r(\mathbb{R}^n, \mathbb{R}^m)$ as either vector fields or maps; we will draw a distinction only when required by context. Several technical issues involving $\mathbf{C}^r(\mathbb{R}^n, \mathbb{R}^m)$ must now be addressed.

1. Since we are interested only in local behavior, our maps need not be defined on all of $\mathbb{R}^n$, but rather they need only be defined on open sets containing the region of interest (i.e., the fixed point). Along these same lines, we can be more general and consider maps of $\mathbf{C}^\infty$ manifolds. However, since we are concerned with local questions this will not be an issue; the reader should consult Arnold [1983].

2. As mentioned in our discussion of structural stability in Chapter 12, there can be technical difficulties in deciding when two dynamical systems are "close" when the phase space is unbounded (as is $\mathbb{R}^n$). Since we are interested only in the behavior near fixed points, we will be able to avoid this unpleasant issue.

3. As we have mentioned several times, we will be interested in the orbit structure of dynamical systems in a *sufficiently small neighborhood of a fixed point*. This phrase is a bit ambiguous, so at this point, we want to spend a little effort to try to make it clearer.

We begin by studying an example which will illustrate some of the salient points. Consider the vector field

$$\dot{x} = \mu - x^2 + \varepsilon x^3, \qquad x \in \mathbb{R}^1, \quad \mu \in \mathbb{R}^1, \tag{20.4.2}$$

where we view the term "εx^3" in (20.4.2) as a perturbation term. It should be evident (see Section 20.1c) that (20.4.2) undergoes a saddle-node bifurcation at $(x, \mu) = (0, 0)$ so that, in the $x - \mu$ plane, *in a sufficiently small neighborhood of the origin*, the curve of fixed points of (20.4.2) appear as in Figure 20.4.2.

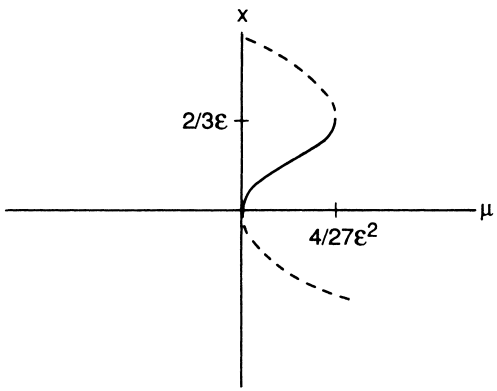

FIGURE 20.4.2.

However, (20.4.2) is so simple that we can actually compute the global curve of fixed points, which is given by

$$\mu = x^2 - \varepsilon x^3 \tag{20.4.3}$$

and is shown in Figure 20.4.2. Thus, we see that, besides the saddle-node bifurcation point at $(x, \mu) = (0, 0)$, (20.4.2) has an additional saddle-node bifurcation point at $(x, \mu) = (2/3\varepsilon, 4/27\varepsilon^2)$. Clearly these two saddle-node bifurcation points are far apart for ε small; however, this example shows that the size of a "sufficiently small neighborhood of a point" can vary from situation to situation. In this example, the "sufficiently small neighborhood" of $(x, \mu) = (0, 0)$ shrinks to a point as $\varepsilon \to \infty$. The idea of a "germ" of a differentiable function has been invented in order to handle this ambiguity, and we refer the interested reader to Arnold [1983] for an introduction to this formalism. However, in this book we will not utilize the idea of germs but rather the less mathematically precise and more verbose approach of reminding the reader that we are always working in a *sufficiently small neighborhood of a fixed point.*

Now that we have specified the infinite-dimensional space of dynamical systems, next we need some way of understanding the geometry of the "degenerate" dynamical systems. This is afforded by the notions of *jets and jet spaces.* We will first give some definitions and then explanations.

Definition 20.4.1 (k-jet of a Map) *Consider $f \in \mathbf{C}^r(\mathbb{R}^n, \mathbb{R}^m)$. The k-*

jet of f at x *($k \leq r$) is given by the following* $(k+2)$*-tuple*

$$(x, f(x), Df(x), \cdots, D^k f(x)).$$

Thus we see that the k-jet of a map at a point is simply the Taylor coefficients through order k plus the point at which they are evaluated. We denote the k-jet of f at x by

$$J^k_x(f).$$

Although it may seem a bit silly to dress up something as commonplace as a Taylor expansion in a new formalism, the reader will see that there is a definite payoff. We next consider the set of all k-jets of $\mathbf{C}^r$ $(k \leq r)$ maps of $\mathbb{R}^n$ into $\mathbb{R}^m$ at all points of $\mathbb{R}^n$.

Definition 20.4.2 (The Space of k-jets) *The set of all k-jets of $\mathbf{C}^r$ ($k \leq r$) maps of $\mathbb{R}^n$ into $\mathbb{R}^m$ at all points of $\mathbb{R}^n$ is called the* space of k-jets *and is denoted by*

$$J^k(\mathbb{R}^n, \mathbb{R}^m) = \{\textit{The space of } k\textit{-jets of } \mathbf{C}^\infty \textit{ maps of } \mathbb{R}^n \textit{ into } \mathbb{R}^m\}.$$

The spaces $J^k(\mathbb{R}^n, \mathbb{R}^m)$ have a nice linear vector space structure. In fact, we can identify $J^k(\mathbb{R}^n, \mathbb{R}^m)$ with $\mathbb{R}^p$ for an appropriate choice of p. We illustrate this in the following examples.

Example 20.4.1. $J^0(\mathbb{R}^n, \mathbb{R}^m) = \mathbb{R}^n \times \mathbb{R}^m$.

End of Example 20.4.1

Example 20.4.2. $J^1(\mathbb{R}^1, \mathbb{R}^1)$ is three dimensional, because points in $J^1(\mathbb{R}^1, \mathbb{R}^1)$ can be assigned the coordinates

$$\left(x, f(x), \frac{\partial f}{\partial x}(x)\right).$$

End of Example 20.4.2

Example 20.4.3. $J^1(\mathbb{R}^2, \mathbb{R}^2)$ is eight dimensional, because points in $J^1(\mathbb{R}^2, \mathbb{R}^2)$ can be assigned the coordinates

$$(x, f(x), Df(x)),$$

where $Df(x)$ is a 2×2 matrix.

End of Example 20.4.3

In a certain sense, the spaces $J^k(\mathbb{R}^n, \mathbb{R}^m)$ can be thought of as finite-dimensional approximations of $\mathbf{C}^r(\mathbb{R}^n, \mathbb{R}^m)$.

We now introduce a map that will play an important role when we discuss the notion of versal deformations.

Definition 20.4.3 (The k-jet Extension of a Map) *For any map $f \in \mathbf{C}^r(\mathbb{R}^n, \mathbb{R}^m)$ we define a map*

$$\hat{f} : \mathbb{R}^n \to J^k(\mathbb{R}^n, \mathbb{R}^m),$$

$$x \mapsto J^k_x(f) \equiv \hat{f}(x),$$

which we call the k-jet extension of f *$(k \leq r)$.*

Thus, the k-jet extension of f merely associates to each point in the phase space of the dynamical system (f) the k-jet of f at the point. We also remark that the k-jet extension of f can be viewed as a map of the phase space of the dynamical system (f) into $J^k(\mathbb{R}^n, \mathbb{R}^m)$. This remark will be important later on. We next introduce a new notion of transversality.

Recall from Chapter 12 the notion of two manifolds being transversal. We now introduce a similar idea: the notion of a map being transverse to a manifold.

Definition 20.4.4 (Transversality of a Map to a Submanifold) *Consider a map $f \in \mathbf{C}^r(\mathbb{R}^n, \mathbb{R}^m)$ and a submanifold $M \subset \mathbb{R}^m$. The map is said to be* transversal to M at a point $x \in \mathbb{R}^n$ *if either $f(x) \notin M$ or the tangent space to M at $f(x)$ and the image of the tangent space to $\mathbb{R}^n$ at x under $Df(x)$ are transversal, i.e.,*

$$Df(x) \cdot T_x\mathbb{R}^n + T_{f(x)}M = T_{f(x)}\mathbb{R}^m.$$

The map is said to be transversal to M *if it is transversal to M at any point $x \in \mathbb{R}^n$.*

Let us consider an example.

Example 20.4.4. Consider the map

$$\begin{aligned} f : \mathbb{R}^1 &\to \mathbb{R}^2, \\ x &\mapsto (x, x^2). \end{aligned}$$

When viewed geometrically, the image of $\mathbb{R}^1$ under f is only the parabola $y = x^2$; see Figure 20.4.3. We ask the following questions.

1. Thinking of the x-axis as a one-dimensional submanifold of $\mathbb{R}^2$, is f transverse to the x-axis?
2. Similarly for the y-axis, is f transverse to the y-axis?

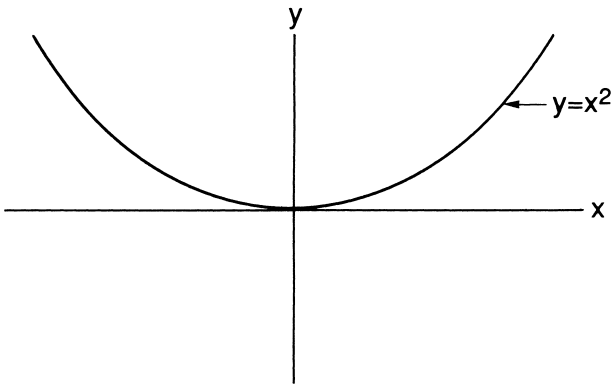

FIGURE 20.4.3.

The only point at which the image of $\mathbb{R}^1$ under f intersects either the x-axis or y-axis is at the origin; therefore, this is the only point at which we need to check transversality. Let us denote the x-axis by X and the y-axis by Y. Then, using the standard coordinates on $\mathbb{R}^2$, we can take

$$T_{(0,0)}X = (\mathbb{R}^1, 0), \tag{20.4.4}$$

$$T_{(0,0)}Y = (0, \mathbb{R}^1). \tag{20.4.5}$$

We have that $Df(0) = (1, 0)$; thus, on recalling Definition 20.4.4 and examining (20.4.4) and (20.4.5), it follows that f is transverse to Y but not transverse to X.

End of Example 20.4.4

We now state the Thom transversality theorem, which will guide the construction of candidates for versal deformations of degenerate dynamical systems.

Theorem 20.4.5 (Thom) *Let $U \subset \mathbb{R}^n$, $V \subset \mathbb{R}^m$ be open sets and $\mathbf{C}$ be a submanifold of $J^k(U, V)$. The set of maps $f : U \to V$ whose k-jet extensions are transversal to $\mathbf{C}$ is an everywhere dense countable intersection of open sets in $\mathbf{C}^r(U, V)$, where $r \geq r_0(k, n, m)$ (where r_0 is some function of the indicated variables).*

Proof: See Arnold [1983]. □

This theorem allows us to work in finite dimensions, where geometrical intuition is more apparent, and to draw conclusions concerning the geometry in the infinite-dimensional space of dynamical systems, $\mathbf{C}^r(U, V)$, where $U \subset \mathbb{R}^n$, $V \subset \mathbb{R}^m$ are open sets . At this point we have developed enough machinery from singularity theory to discuss the idea of the codimension of a local bifurcation. We now turn to this question.

20.4c The Codimension of a Local Bifurcation

As mentioned in our discussion of the "big picture" of bifurcation theory, the problem we are immediately faced with is determining whether a dynamical system is structurally stable. If we limit ourselves to the study of the behavior of fixed points, then the problem is much easier, because we know how to characterize structurally unstable fixed points—they are simply the nonhyperbolic fixed points. The techniques from singularity theory we developed in 20.4 will enable us to characterize the degree of "structural instability" of a fixed point in a way that is similar in spirit to our discussion of the "big picture" of bifurcation theory given in that section. However, the reader should realize that these ideas are concerned with fixed point behavior only and as such we must often do additional work to determine whether nearby *dynamical* phenomena are properly taken into account. We will see several examples of this as we go along.

Thus far we have been using the term "dynamical system" to refer to vector fields and maps interchangeably. At this stage we need to draw a slight distinction. We will be studying the fixed points of dynamical systems. For vector fields

$$\dot{x} = f(x), \qquad x \in \mathbb{R}^n, \tag{20.4.6}$$

this means studying the equation

$$f(x) = 0, \tag{20.4.7}$$

and for maps

$$x \mapsto g(x), \qquad x \in \mathbb{R}^n, \tag{20.4.8}$$

this means studying the equation

$$g(x) - x = 0. \tag{20.4.9}$$

It should be clear that from an analytic point of view, (20.4.7) and (20.4.9) are essentially the same. However, for the remainder of this section we will deal solely with vector fields and leave the trivial modifications for maps as exercises.

For vector fields the space of dynamical systems will be $\mathbf{C}^r(U, V)$ and the associated jet spaces $J^k(U, V)$, where $U \subset \mathbb{R}^n$, $V \subset \mathbb{R}^m$ are open sets. In particular, we will work solely in the finite-dimensional space $J^k(U, V)$. Within $J^k(U, V)$ we will be interested in the subset consisting of k-jets of vector fields having fixed points. We denote this subset by F (for fixed points) and note that F has codimension n. Within F we will be interested in the k-jets of vector fields having nonhyperbolic fixed points. We denote this subset by B (for bifurcation) and note the B has codimension $n + 1$. We remark that the codimension of F and B is independent of k; however, the dimension of F and B is *not* independent of k. Let us now consider some specific examples.

Example 20.4.5 (One-Dimensional Vector Fields). As our space of vector fields we take $\mathbf{C}^r(\mathbb{R}^1, \mathbb{R}^1)$. In this case $J^k(\mathbb{R}^1, \mathbb{R}^1)$ is $(k+2)$-dimensional with coordinates of points in $J^k(\mathbb{R}^n, \mathbb{R}^n)$ given by the $(k+2)$-tuples

$$\left(x, f(x), \frac{\partial f}{\partial x}(x), \frac{\partial^2 f}{\partial x^2}(x), \cdots, \frac{\partial^k f}{\partial x^k}(x)\right), \quad x \in \mathbb{R}^1,\ f \in \mathbf{C}^r(\mathbb{R}^1, \mathbb{R}^1),$$

F is $(k+1)$-dimensional (codimension 1) with coordinates of points in F given by

$$\left(x, 0, \frac{\partial f}{\partial x}(x), \frac{\partial^2 f}{\partial x^2}(x), \cdots, \frac{\partial^k f}{\partial x^k}(x)\right), \qquad x \in \mathbb{R}^1,\ f \in \mathbf{C}^r(\mathbb{R}^1, \mathbb{R}^1),$$

and B is k-dimensional (codimension 2) with coordinates of points in B given by

$$\left(x, 0, 0, \frac{\partial^2 f}{\partial x^2}(x), \cdots, \frac{\partial^k f}{\partial x^k}(x)\right), \qquad x \in \mathbb{R}^1,\ f \in \mathbf{C}^r(\mathbb{R}^1, \mathbb{R}^1).$$

End of Example 20.4.5

Example 20.4.6 (n-Dimensional Vector Fields). As our space of vector fields we take $\mathbf{C}^r(\mathbb{R}^n, \mathbb{R}^n)$. In this case coordinates of $J^k(\mathbb{R}^n, \mathbb{R}^n)$ are given by

$$\left(x, f(x), Df(x), \cdots, D^k f(x)\right), \qquad x \in \mathbb{R}^n, \quad f \in \mathbf{C}^r(\mathbb{R}^n, \mathbb{R}^n).$$

F is codimension n, with points in F having coordinates

$$\left(x, 0, Df(x), \cdots, D^k f(x)\right), \qquad x \in \mathbb{R}^n, \quad f \in \mathbf{C}^r(\mathbb{R}^n, \mathbb{R}^n),$$

and B is codimension $n+1$, with points in B having coordinates

$$\left(x, 0, \widetilde{Df(x)}, \cdots, D^k f(x)\right), \qquad x \in \mathbb{R}^n, \quad f \in \mathbf{C}^r(\mathbb{R}^n, \mathbb{R}^n),$$

where $\widetilde{Df(x)}$ represents a nonhyperbolic matrix which lies on a surface of codimension 1 in the n^2-dimensional space of $n \times n$ matrices. This is explained in great detail in Section 20.5.

End of Example 20.4.6

We are now at the point where we can define the *codimension of a fixed point*. There are two possibilities for the choice of this number, and we closely follow the discussion of Arnold [1972].

Definition 20.4.6 (The Codimension of a Fixed Point) *Consider $J^k(\mathbb{R}^n, \mathbb{R}^n)$ and the subset of $J^k(\mathbb{R}^n, \mathbb{R}^n)$ consisting of k-jets of elements of $\mathbf{C}^r(\mathbb{R}^n, \mathbb{R}^n)$ that have fixed points. We denote this subset by F and note that F has codimension n in $J^k(\mathbb{R}^n, \mathbb{R}^n)$. Consider the k-jet of an element of $\mathbf{C}^r(\mathbb{R}^n, \mathbb{R}^n)$ that has a nonhyperbolic fixed point. Then this k-jet lies in a subset of F defined by conditions on the derivatives. Suppose this subset of F has codimension b in $J^k(\mathbb{R}^n, \mathbb{R}^n)$. Then we define the codimension of the fixed point to be $b - n$.*

Before giving examples we want to make a few general remarks concerning this definition.

Remark 1. Evidently k must be taken sufficiently large so that the degree of degeneracy of the nonhyperbolic fixed point can be specified.

Remark 2. This definition says that the codimension of a fixed point is equal to the codimension of the subset of F specified by the degeneracy of the fixed point minus n. Thus, hyperbolic fixed points have codimension zero by this definition. This seems reasonable, since the notion of the codimension of a fixed point should somehow specify the degree of "nongenericity" of the fixed point.

Remark 3. There is another way of describing the reasons why we chose this way of defining the codimension of a fixed point. The dynamical system induces a map of the phase space, $\mathbb{R}^n$, into $J^k(\mathbb{R}^n, \mathbb{R}^n)$. This map is only the k-jet extension map (cf. Definition 20.4.3). At hyperbolic fixed points this map is transverse to the subset F of $J^k(\mathbb{R}^n, \mathbb{R}^n)$. Thus, hyperbolic fixed points cannot be destroyed by small perturbations. Hence, if the notion of codimension is to quantify the amount of "degeneracy" of nonhyperbolic fixed points, then the generic elements of F should be regarded as codimension zero. Practically speaking, this also implies that *generically* the fixed points move if they are perturbed.

Now we consider several examples where we will compute the codimension.

Example 20.4.7. Consider the vector field

$$\dot{x} = f(x) = ax^2 + \mathcal{O}(x^3), \qquad x \in \mathbb{R}^1. \tag{20.4.10}$$

We are interested in studying (20.4.10) near the nonhyperbolic fixed point $x = 0$. At this point we see that the k-jet of (20.4.10) is a typical element of the set B described in Example 20.4.5. Hence, using Definition 20.4.6, we conclude that $x = 0$ is codimension 1.

End of Example 20.4.7

Example 20.4.8. Consider the vector field

$$\dot{x} = f(x) = ax^3 + \mathcal{O}(x^4), \qquad x \in \mathbb{R}^1. \tag{20.4.11}$$

We are interested in (20.4.11) near the nonhyperbolic fixed point $x = 0$. As in Example 20.4.7, the k-jet of (20.4.11) is contained in the set B described in Example 20.4.5. However, (20.4.11) is more degenerate than the typical element of B in that (20.4.11) also has

$$\frac{\partial^2 f}{\partial x^2}(0) = 0.$$

Hence, the k-jet of (20.4.11) lies in a lower dimensional subset of B, denoted B', which has codimension 3 in $J^k(\mathbb{R}^1, \mathbb{R}^1)$, with points in B' having coordinates

$$\left(x, 0, 0, 0, \frac{\partial^3 f}{\partial x^2}(x), \cdots, \frac{\partial^k f}{\partial x^k}(x)\right), \qquad x \in \mathbb{R}^n, \quad f \in \mathbf{C}^r(\mathbb{R}^n, \mathbb{R}^n).$$

Using Definition 20.4.6 we can thus conclude that $x = 0$ is codimension 2.

End of Example 20.4.8

Example 20.4.9. In Section 20.5 we show the following.

1. In the four-dimensional space of 2×2 real matrices the matrices

$$\begin{pmatrix} 0 & -\omega \\ \omega & 0 \end{pmatrix} \tag{20.4.12}$$

and

$$\begin{pmatrix} 0 & 1 \\ 0 & 0 \end{pmatrix} \tag{20.4.13}$$

lie on surfaces of codimension 2.

2. In the nine-dimensional space of 3×3 real matrices the matrix

$$\begin{pmatrix} 0 & -\omega & 0 \\ \omega & 0 & 0 \\ 0 & 0 & 0 \end{pmatrix} \tag{20.4.14}$$

lies on a surface of codimension 3.

Hence, using Example 20.4.6 and Definition 20.4.6, we might conclude that the codimension of a fixed point of a vector field whose 1-jet in (real) Jordan canonical form is given by (20.4.12), (20.4.13), or (20.4.14) is 2, 2, and 3, respectively. However, this is not quite true. By a re-parametrization of time, we can show that cases (20.4.12), and (20.4.14) are codimension 1 and 2, respectively. This is another way in which *dynamics* enters to slightly cloud the singularity theory approach to classifying the degeneracy of an equilibrium point of a *vector field*.

End of Example 20.4.9

We end this section with two remarks.

Remark 1. The codimensions computed in these examples are for generic vector fields. In particular, we have not considered the possibility of symmetries which would put extra constraints on eigenvalues and of derivatives which would result in a modification of the codimension; see Golubitsky and Schaeffer [1985] and Golubitsky, Stewart, and Schaeffer [1988].

Remark 2. We have referred to the sets F and B as "subsets" of $J^k(\mathbb{R}^n, \mathbb{R}^n)$. In applying the Thom transversality theorem the question of whether or not they are actually submanifolds arises. The same question is also of interest for the higher codimension subsets of B corresponding to more

degenerate fixed points. In general, these subsets may have singular points and, thus, they will not have the structure of a submanifold. However, these singularities can be removed by slight perturbations and, hence, for our purposes, they can be treated as submanifolds. This technical point is treated in great detail in Gibson [1979].

20.4D Construction of Versal Deformations

We now want to develop the necessary definitions in order to discuss *versal deformations* of vector fields. We follow Arnold [1972], [1983] very closely. We remark the the phrase "unfolding" is often used to refer to a similar procedure; see, e.g., Guckenheimer and Holmes [1983] (where the term "universal unfolding" is taken to be virtually synonymous with the phrase "versal deformation") or Golubitsky and Schaeffer [1985] (where various subtleties in the definitions are thoroughly explored).

Consider the following $\mathbf{C}^r$, parameter-dependent vector fields

$$\dot{x} = f(x, \lambda), \qquad x \in \mathbb{R}^n, \quad \lambda \in \mathbb{R}^\ell, \tag{20.4.15}$$

$$\dot{y} = g(y, \lambda), \qquad y \in \mathbb{R}^n, \quad \lambda \in \mathbb{R}^\ell. \tag{20.4.16}$$

We will be concerned with local behavior of these vector fields near fixed points. Therefore, we assume that (20.4.15) and (20.4.16) have fixed points at (x_0, λ_0) and (y_0, λ_0), respectively, and we will be concerned with the dynamics in a *sufficiently small neighborhood* of these points. We now give a parametric version of the notion of $\mathbf{C}^0$-equivalence given in Definition 19.12.1.

Definition 20.4.7 (Parametric Version of $\mathbf{C}^0$-Equivalence) *Equations (20.4.15) and (20.4.16) are said to be $\mathbf{C}^0$-equivalent (or topologically equivalent) if there exists a continuous map*

$$h : U \to V,$$

with U a neighborhood of (x_0, λ_0) and V a neighborhood of y_0 such that, for λ sufficiently close to λ_0,

$$h(\cdot, \lambda),$$

with $h(x_0, \lambda_0) = y_0$, is a homeomorphism that takes orbits of the flow generated by (20.4.15) onto orbits of the flow generated by (20.4.16), preserving orientation but not necessarily parameterization by time. If h does preserve parameterization by time, then (20.4.15) and (20.4.16) are said to be $\mathbf{C}^0$ conjugate (or topologically conjugate).

In the construction of versal deformations we will be concerned with having the minimum number of parameters (for reasons to be discussed later), not too many or too few. The following definition is the first step toward formalizing this notion.

Consider the following $\mathbf{C}^r$ vector field

$$\dot{x} = u(x, \mu), \qquad x \in \mathbb{R}^n, \quad \mu \in \mathbb{R}^m, \tag{20.4.17}$$

with

$$u(x_0, \mu_0) = 0.$$

Then we have the following definition.

Definition 20.4.8 (Family Induced from a Deformation) *Let $\lambda = \phi(\mu)$ be a continuous map defined for μ sufficiently close to μ_0 with $\lambda_0 = \phi(\mu_0)$. We say that (20.4.17) is induced from (20.4.15) if*

$$u(x, \mu) = f(x, \phi(\mu)).$$

We now can give our main definition.

Definition 20.4.9 (Versal Deformation) *Equation (20.4.15) is called a* $\mathbf{C}^0$-equivalent versal deformation *(or just versal deformation) of*

$$\dot{x} = f(x, \lambda_0) \tag{20.4.18}$$

at the point x_0 if every other parameterized family of $\mathbf{C}^r$ vector fields that reduces to (20.4.18) for a particular choice of parameters is equivalent to a family of vector fields induced from (20.4.15).

At this point we again remind the reader that we are working in a *sufficiently small neighborhood* of (x_0, λ_0). We are now at the stage where we can construct versal deformations of dynamical systems. We will deal with vector fields and merely state the simple modifications needed for dealing with maps.

Once we have a vector field having a nonhyperbolic fixed point there are four steps necessary in order to construct a versal deformation.

Steps in the Construction of a Versal Deformation

Step 1. Put the vector field in normal form to reduce the number of cases that need to be considered.

Step 2. Truncate the normal form and embed the resulting k-jet of the normal form in a parameterized family having the number of parameters equal to the codimension of the bifurcation such that the parameterized family of k-jets is transverse to the appropriate subset of degenerate k-jets.

Step 3. Appeal to the Thom transversality theorem (Theorem 20.4.5) to argue that in this way one has constructed a generic family. By the term *generic family* we mean a family from an everywhere dense set in the space of all families.

Step 4. Prove that the parametrized family constructed in this manner is actually a versal deformation.

It should be apparent that Step 4 is by far the most difficult. Steps 1 through 3 merely give us a procedure for constructing a parameterized family that we hope will be a versal deformation. The reason why it may not be is related to *dynamics*. The whole procedure is static only in nature; it takes into account only the nature of the fixed point. For one-dimensional vector fields we will see that the method will yield versal deformations, since the only possible orbits distinguished by $\mathbf{C}^0$ equivalence are fixed points. However, for higher dimensional vector fields we will see that the method may not yield versal deformations and, indeed, no such versal deformation may exist.

Elimination of a Parameter in One-Dimensional Vector Fields. Before constructing candidates for versal deformations of vector fields we mention a technical point relevant to one dimensional vector fields that enables us to eliminate a parameter in some circumstances. Consider an n-parameter family of one-dimensional vector fields of the form

$$f(x,\mu) = \mu_1 + \mu_2 x + \mu_3 x^2 + \cdots + \mu_n x^{n-1} \pm a x^n, \tag{20.4.19}$$

where

$$x \in \mathbb{R}^1, \quad a \neq 0, \quad \mu \equiv (\mu_1, \ldots, \mu_n) \in \mathbb{R}^n.$$

Let us suppose that we make the following coordinate shift:

$$x \mapsto x + c,$$

with c to be chosen shortly. Then (20.4.19) can be rewritten as

$$\begin{aligned} f(x,\mu) = {} & \mu_1 + \mu_2(x+c) + \mu_3(x^2 + 2cx + c^2) \\ & + \cdots + \mu_n(c^{n-1} + (n-1)c^{n-2}x + \cdots + x^{n-1}) \\ & \pm a(c^n + nc^{n-1}x + \cdots + ncx^{n-1} + x^n), \end{aligned} \tag{20.4.20}$$

where the coefficients multiplying each μ_i can be computed using the binomial formula. The terms can then be rearranged, yielding a polynomial in x of degree n. It is easy to see that after this is done the coefficient multiplying x^{n-1} is given by

$$\mu_n \pm anc.$$

Then if we choose

$$c = \mp \frac{\mu_n}{an},$$

the x^{n-1} term does not appear.
Hence, we have shown that given an n-parameter family of one-dimensional vector fields of the form

$$f(x,\mu) = \mu_1 + \mu_2 x + \mu_3 x^2 + \cdots + \mu_n x^{n-1} \pm a x^n, \tag{20.4.21}$$

with a translation of x given by

$$x \mapsto x \mp \frac{\mu_n}{an},$$

it can be rewritten in the form

$$f(x, \tilde{\mu}) = \tilde{\mu}_1 + \tilde{\mu}_2 x + \tilde{\mu}_3 x^2 + \cdots + \tilde{\mu}_{n-1} x^{n-2} \pm a x^n, \tag{20.4.22}$$

where the $\tilde{\mu}_i$, $i = 1, \ldots, n-1$, can be computed in terms of the μ_i, $i = 1, \ldots, n$, if desired.

Let us now consider some examples. In all of the following examples the origin will be the degenerate fixed point.

Example 20.4.10 (One-Dimensional Vector Fields).
a) Consider the vector field

$$\dot{x} = a x^2 + \mathcal{O}(x^3). \tag{20.4.23}$$

We follow the steps described above for constructing a versal deformation of (20.4.23).

Step 1. Equation (20.4.23) is already in a sufficient normal form.

Step 2. We truncate (20.4.23) to obtain

$$\dot{x} = a x^2, \quad a \neq 0. \tag{20.4.24}$$

From Example 20.4.7, we know that $x = 0$ is a degenerate fixed point of (20.4.24) having *codimension* 1. Now recall the definitions of the subsets F and B of $J^2(\mathbb{R}^1, \mathbb{R}^1)$ described in Section 20.4. For reference, we denote below these submanifolds of $J^2(\mathbb{R}^1, \mathbb{R}^1)$ and to their right a typical coordinate in the submanifold

$$J^2(\mathbb{R}^1, \mathbb{R}^1) - \left(x, f(x), \frac{\partial f}{\partial x}(x), \frac{\partial^2 f}{\partial x^2}(x) \right), \tag{20.4.25}$$

$$F - \left(x, 0, \frac{\partial f}{\partial x}(x), \frac{\partial^2 f}{\partial x^2}(x) \right), \tag{20.4.26}$$

$$B - \left(x, 0, 0, \frac{\partial^2 f}{\partial x^2}(x) \right). \tag{20.4.27}$$

Now the 2-jet of (20.4.23) at $x = 0$ is a typical point in B. A two-parameter family of vector fields transverse to B and F is given by

$$\dot{x} = \mu_1 + \mu_2 x + a x^2. \tag{20.4.28}$$

However, this is a codimension one singularity. From the technical remark above, we know that through a shift of coordinates (20.4.28) can be written as

$$\dot{x} = \mu + a x^2, \tag{20.4.29}$$

and we take this as our candidate for a versal deformation.

Step 3. It follows from the Thom transversality theorem (Theorem 20.4.5) that (20.4.29) is a generic family. The reader should perform the simple calculation necessary to verify this fact.

Step 4. In Section 20.1c we showed that higher order terms do not affect the dynamics of (20.4.29) near $(x, \mu) = (0, 0)$. Hence, the deformation is versal.

We can conclude from this that the saddle-node bifurcation is generic in one-parameter families of vector fields.

b) Consider the vector field

$$\dot{x} = ax^3 + \mathcal{O}(x^4). \tag{20.4.30}$$

Step 1. Equation (20.4.30) is already in a sufficient normal form.

Step 2. We truncate (20.4.30) to obtain

$$\dot{x} = ax^3. \tag{20.4.31}$$

From Example 20.4.8, $x = 0$ is a codimension 2 fixed point. For reference, we denote below the subsets B', B, and F of $J^3(\mathbb{R}^1, \mathbb{R}^1)$ discussed in Example 20.4.8 with typical coordinates immediately to the right.

$$J^3(\mathbb{R}^1, \mathbb{R}^1) - \left(x, f(x), \frac{\partial f}{\partial x}(x), \frac{\partial^2 f}{\partial x^2}(x), \frac{\partial^3 f}{\partial x^3}(x)\right), \tag{20.4.32}$$

$$F - \left(x, 0, \frac{\partial f}{\partial x}(x), \frac{\partial^2 f}{\partial x^2}(x), \frac{\partial^3 f}{\partial x^3}(x)\right), \tag{20.4.33}$$

$$B - \left(x, 0, 0, \frac{\partial^2 f}{\partial x^2}(x), \frac{\partial^3 f}{\partial x^3}(x)\right), \tag{20.4.34}$$

$$B' - \left(x, 0, 0, 0, \frac{\partial^3 f}{\partial x^3}(x)\right). \tag{20.4.35}$$

Since this is a codimension two singularity we want to embed (20.4.31) in a two-parameter generic family transverse. Following the same reasoning given in the previous example, we obtain

$$\dot{x} = \mu_1 + \mu_2 x + ax^3, \tag{20.4.36}$$

as a candidate for a versal deformation.

Step 3. It is an immediate consequence of the Thom transversality theorem (Theorem 20.4.5) that (20.4.36) is a generic family. The reader should perform the calculations necessary to verify this statement.

Step 4. In Section 20.1e, we proved that higher order terms do not qualitatively effect the local dynamics of (20.4.36). Hence, we have found a versal deformation of (20.4.30).

End of Example 20.4.10

Example 20.4.11 (Two-Dimensional Vector Fields).

a) *The Poincaré-Andronov-Hopf Bifurcation*

Consider the vector field

$$\begin{aligned} \dot{x} &= -\omega y + \mathcal{O}(2), \\ \dot{y} &= \omega x + \mathcal{O}(2). \end{aligned} \tag{20.4.37}$$

Step 1. From Example 19.2a, the normal form for this vector field in cartesian coordinates is

$$\begin{aligned} \dot{x} &= -\omega y + (ax - by)(x^2 + y^2) + \mathcal{O}(5), \\ \dot{y} &= \omega x + (bx + ay)(x^2 + y^2) + \mathcal{O}(5). \end{aligned} \tag{20.4.38}$$

We note the important fact that due to the structure of the linear part of the vector field the normal form (20.4.38) contains no even-order terms.

Step 2. We take as the truncated normal form

$$\begin{aligned} \dot{x} &= -\omega y + (ax - by)(x^2 + y^2), \\ \dot{y} &= \omega x + (bx + ay)(x^2 + y^2). \end{aligned} \tag{20.4.39}$$

From Example 20.5.5 in Section 20.5 we note that $(x, y) = (0, 0)$ is a codimension 2 fixed point. From Example 20.4.6 we recall the subsets B and F of $J^2(\mathbb{R}^2, \mathbb{R}^2)$ and denote typical coordinates on these subsets to the right.

$$J^2(\mathbb{R}^2, \mathbb{R}^2) - \left(x, f(x), Df(x), D^2 f(x)\right), \tag{20.4.40}$$

$$F - \left(x, 0, Df(x), D^2 f(x)\right), \tag{20.4.41}$$

$$B - \left(x, 0, \widetilde{Df}(x), D^2 f(x)\right), \tag{20.4.42}$$

where $\widetilde{Df}(x)$ represents nonhyperbolic matrices. Now we want to embed (20.4.39) in a one-parameter family transverse to B, but due to the structure of the linear part of the vector field, we want the origin to remain a fixed point. From Section 20.5, Example 20.5.5, the matrix

$$\begin{pmatrix} 0 & -\omega \\ \omega & 0 \end{pmatrix} \tag{20.4.43}$$

lies on a surface of codimension 2 in the four-dimensional space of 2×2 real matrices. Moreover, a versal deformation for (20.4.43) is given by

$$\begin{pmatrix} \mu & -\omega - \gamma \\ \omega + \gamma & \mu \end{pmatrix}. \tag{20.4.44}$$

Using (20.4.44), we take as our transverse family

$$\begin{aligned} \dot{x} &= \mu x - (\omega + \gamma) y + (ax - by)(x^2 + y^2), \\ \dot{y} &= (\omega + \gamma) x + \mu y + (bx + ay)(x^2 + y^2). \end{aligned} \tag{20.4.45}$$

This is a two-parameter family. But it is "well known" that the Poincaré-Andronov-Hopf bifurcation is a codimension one bifurcation. However, as we mentioned earlier, one parameter can be removed by a re-parametrization of time and the coefficients on the nonlinear terms. This is done as follows.

Let

$$t \to \frac{\omega}{\omega + \gamma} t, \qquad \lambda = \frac{\mu\omega}{\omega + \gamma}.$$

where we view ω as $\mathcal{O}(1)$ and fixed, and the deformation parameter γ as small. In this way $\omega + \gamma$ is bounded away from zero. Under this rescaling of time and re-parametrization (20.4.45) becomes

$$\dot{x} = \lambda x - \omega y + \frac{\omega}{\omega + \gamma}(ax - by)(x^2 + y^2),$$
$$\dot{y} = \omega x + \lambda y + \frac{\omega}{\omega + \gamma}(bx + ay)(x^2 + y^2).$$

and the factor $\frac{\omega}{\omega+\gamma}$ can be absorbed into the constants a and b by a re-definition of the constants multiplying the nonlinear terms.

This "elimination of a parameter by re-parametrization of time" can be viewed in another way. Let us work first in the complex setting. The normal form in complex coordinates is given by

$$\dot{z} = i\omega z + cz^2\bar{z} + \mathcal{O}(5),$$

where ω is real, $c = a + ib$. From Example 20.5.5 of Section 20.5, this is a *complex* codimension one fixed point, and we can take as a versal deformation

$$\dot{z} = (i\omega + \mu + i\gamma)z + cz^2\bar{z} + \mathcal{O}(5),$$

where μ and γ are real. Re-writing this equation in real polar coordinates gives

$$\dot{r} = \mu r + ar^3 + \mathcal{O}(5),$$
$$\dot{\theta} = \omega + \gamma + br^2 + \mathcal{O}(4).$$

Hence, we see that for $\omega + \gamma$ bounded away from zero (which we are assuming to be true with ω $\mathcal{O}(1)$ and fixed, with γ the small deformation parameter), the small parameter γ has no qualitative effect on the dynamics.

Step 3. It follows from the Thom transversality theorem (Theorem 20.4.5) that (20.4.45) is a generic family (when we take into account that the origin must remain a fixed point in the one-parameter family). The reader should perform the necessary calculations to verify this statement.

Step 4. Theorem 20.2.3 implies that the higher order terms in the normal form do not qualitatively change the dynamics of (20.4.45). Hence, we have constructed a versal deformation of (20.4.37).

Thus, we can conclude that, like saddle-node bifurcations, Poincaré-Andronov-Hopf bifurcations are also generic in one-parameter families of vector fields.

Due to the importance of the Poincaré-Andronov-Hopf bifurcation, before ending our discussion let us re-examine it from a slightly different point of view.

In polar coordinates, the normal form is given by (cf. (20.2.9))

$$\dot{r} = ar^3 + \mathcal{O}(r^5),$$
$$\dot{\theta} = \omega + \mathcal{O}(r^2). \tag{20.4.46}$$

Our goal is to construct a versal deformation of (20.4.46). It is in this context that we see yet another example of the power and conceptual clarity that results upon transforming the system to normal form.

In our study of the dynamics of (20.4.46) we have seen (see Section 20.2, Lemma 20.2.1) that, for r sufficiently small, we need only to study

$$\dot{r} = ar^3 + \mathcal{O}(r^5) = 0, \tag{20.4.47}$$

since $\theta(t)$ merely increases monotonically in t.

Equation (20.4.47) looks very much like the degenerate one-dimensional vector field studied in Example 20.4.10 whose versal deformation yielded the pitchfork bifurcation. However, there is an important difference; namely, due to the structure of the linear part of the vector field in (20.4.37), the $\dot{r}$ component of the vector field must have no even-order terms in r and must be zero at $r = 0$. Hence, this degenerate fixed point is codimension 1 rather than codimension 2 as in the pitchfork bifurcation, and a natural candidate for a versal deformation is

$$\begin{aligned} \dot{r} &= \mu r + ar^3, \\ \dot{\theta} &= \omega. \end{aligned} \tag{20.4.48}$$

It is the content of Theorem 20.2.3 that (20.4.48) is indeed a versal deformation.

b) *A Double-Zero Eigenvalue*

Consider the vector field

$$\begin{aligned} \dot{x} &= y + \mathcal{O}(2), \\ \dot{y} &= \mathcal{O}(2). \end{aligned} \tag{20.4.49}$$

Step 1. From Example 19.1.2, the normal form for (20.4.49) is given by

$$\begin{aligned} \dot{x} &= y + \mathcal{O}(3), \\ \dot{y} &= axy + by^2 + \mathcal{O}(3). \end{aligned} \tag{20.4.50}$$

Step 2. We take as the truncated normal form

$$\begin{aligned} \dot{x} &= y, \\ \dot{y} &= axy + by^2. \end{aligned} \tag{20.4.51}$$

From Example 20.4.9, recall that $(x, y) = (0, 0)$ is a codimension 2 fixed point. From Example 20.4.6 we denote the subsets B and F of $J^2(\mathbb{R}^2, \mathbb{R}^2)$ with typical coordinates of points in these sets to the right.

$$J^1(\mathbb{R}^2, \mathbb{R}^2) - (x, f(x), Df(x)), \tag{20.4.52}$$

$$F - (x, 0, Df(x)), \tag{20.4.53}$$

$$B - \left(x, 0, \widetilde{Df}(x)\right), \tag{20.4.54}$$

where $\widetilde{Df}(x)$ represent nonhyperbolic matrices. In Appendix 1 we show that these matrices form a three-dimensional surface in the four-dimensional space of 2×2 matrices. We also show in this appendix that matrices with Jordan canonical form given by

$$\begin{pmatrix} 0 & 1 \\ 0 & 0 \end{pmatrix} \tag{20.4.55}$$

form a two-dimensional surface, B', with $B' \subset B \subset F \subset J^1(\mathbb{R}^1, \mathbb{R}^1)$. We now seek to embed (20.4.51) in a two-parameter family transverse to B'. In Appendix 1 we show that a versal deformation of (20.4.55) is given by

$$\begin{pmatrix} 0 & 1 \\ \mu_1 & \mu_2 \end{pmatrix}. \tag{20.4.56}$$

Thus, one might take as a transverse family

$$\begin{aligned} \dot{x} &= y, \\ \dot{y} &= \mu_1 x + \mu_2 y + ax^2 + bxy. \end{aligned} \tag{20.4.57}$$

However, recall the remarks following the definition of codimension (Definition 20.4.6). Generically, we expect the fixed points to move as the parameters are varied. This does not happen in (20.4.57); the origin always remains a fixed point. This situation is easy to remedy.

Notice from the form of (20.4.57) that any fixed point must have $y = 0$. If we make the coordinate transformation

$$\begin{aligned} x &\to x - x_0, \\ y &\to y, \end{aligned} \tag{20.4.58}$$

and take as a versal deformation of the linear part

$$\begin{pmatrix} 0 & 1 \\ \mu_1 & \mu_2 \end{pmatrix} \begin{pmatrix} x - x_0 \\ y \end{pmatrix}, \tag{20.4.59}$$

then a simple reparameterization allows us to transform (20.4.57) into

$$\begin{aligned} \dot{x} &= y, \\ \dot{y} &= \mu_1 + \mu_2 y + axy + by^2, \end{aligned} \tag{20.4.60}$$

see exercise 5 at the end of this section. We remark that in some cases it may be necessary for the origin to remain a fixed point as the parameters are varied; for example, in the case where the normal form is invariant under the transformation $(x, y) \to (-x, -y)$.

Step 3. It follows from the Thom transversality theorem that (20.4.60) is a generic family. The reader should perform the necessary calculation to verify this statement.

Step 4. Bogdanov [1975] proved that (20.4.60) is a versal deformation. We will consider this question in great detail in Section 20.6.

End of Example 20.4.11

Practical Remarks on the Location of Parameters

For a specific dynamical system arising in applications the number of parameters and their locations in the equation are usually fixed. The theory developed in this section tells us that too many parameters (i.e., more than the codimension of the fixed point) are permissible provided they result in

a transverse family. Having more parameters than the codimension of the fixed point will simply require more work in enumerating all the cases. However, one must verify that the parameters are in the correct location so as to form a transverse family. We have seen that there is some freedom in where the parameters may be; in one dimension it is fairly obvious, in higher dimensions it is not as obvious, but the reader should keep in mind that transversality is the typical situation.

20.4E Exercises

1. Let $L^j_{sym}(\mathbb{R}^n, \mathbb{R}^m)$ denote the set of symmetric j-linear maps of $\mathbb{R}^n$ into $\mathbb{R}^n$. Prove that it is a linear vector space.

2. Let
$$P(\mathbb{R}^n, \mathbb{R}^m) \equiv \mathbb{R}^m \times \prod_{j=1}^{k} L^j_{sym}(\mathbb{R}^n, \mathbb{R}^m).$$
Prove that
$$J^k(\mathbb{R}^n, \mathbb{R}^m) = \mathbb{R}^n \times P(\mathbb{R}^n, \mathbb{R}^m).$$
Show that $J^k(\mathbb{R}^n, \mathbb{R}^m)$ is a linear vector space.

3. Let $U \subset \mathbb{R}^n$ and $V \subset \mathbb{R}^m$ be open sets. Show that $J^k(U, V)$ is an open subset of $J^k(\mathbb{R}^n, \mathbb{R}^m)$.

4. **a)** Consider the following three-parameter family of one-dimensional vector fields
$$\dot{x} = x^3 + \mu_3 x^2 + \mu_2 x + \mu_1, \qquad x \in \mathbb{R}^1. \tag{20.4.61}$$
Show that by a parameter-dependent shift of x, (20.4.61) can be written as a two-parameter family
$$\dot{\overline{x}} = \overline{x}^3 + \overline{\mu}_2 \overline{x} + \overline{\mu}_1.$$
What are $\overline{x}$, $\overline{\mu}_2$, and $\overline{\mu}_1$ in terms of x, μ_1, μ_2, and μ_3?

b) Consider the following two-parameter family of one-dimensional vector fields
$$\dot{x} = x^2 + \mu_2 x + \mu_1, \qquad x \in \mathbb{R}^1. \tag{20.4.62}$$
Show that by a parameter-dependent shift of x, (20.4.62) can be written as a one-parameter family
$$\dot{\overline{x}} = \overline{x}^2 + \overline{\mu}_1.$$
What are $\overline{x}$ and $\overline{\mu}_1$ in terms of x, μ_1, and μ_2?

Discuss the results of a) and b) in terms of the codimension of a bifurcation and the number of parameters.

In particular, consider part b) and address these issues in relation to a comparison of the saddle-node bifurcation
$$\dot{x} = x^2 + \mu$$
and the transcritical bifurcation
$$\dot{x} = x^2 + \mu x.$$

5. Consider the following two-parameter family of planar vector fields

$$\begin{aligned} \dot{x} &= y, \\ \dot{y} &= \mu_1 x + \mu_2 y + a x^2 + bxy. \end{aligned} \tag{20.4.63}$$

Under the shift of coordinates

$$\begin{aligned} x &\to x + x_0, \\ y &\to y, \end{aligned}$$

(20.4.63) becomes

$$\begin{aligned} \dot{x} &= y, \\ \dot{y} &= \mu_1 x_0 + \mu_1 x + \mu_2 y + a(x^2 + 2xx_0 + x_0^2) + b(x_0 + x)y. \end{aligned} \tag{20.4.64}$$

Show that by a parameter-dependent shift of y (but not x), (20.4.63) can be transformed to the form

$$\begin{aligned} \dot{x} &= y, \\ \dot{y} &= \overline{\mu}_1 + \overline{\mu}_2 y + a x^2 + bxy. \end{aligned} \tag{20.4.65}$$

What are $\overline{\mu}_1$ and $\overline{\mu}_2$ in terms of x_0, μ_1, μ_2, a, and b?

6. Consider the "Hopf-steady state interaction", i.e., a three dimensional vector field having a fixed point where the (real) Jordan canonical form of the matrix is given by

$$\begin{pmatrix} 0 & -\omega & 0 \\ \omega & 0 & 0 \\ 0 & 0 & 0 \end{pmatrix}, \quad \omega > 0.$$

Show that this is a codimension two bifurcation and compute a candidate for a versal deformation. (*Hint: Use Example 20.5.6 from Section 20.5.*)

7. Consider the "double-Hopf bifurcation" or the "mode interaction", i.e., a four dimensional vector field having a fixed point where the (real) Jordan canonical form of the matrix is given by

$$\begin{pmatrix} 0 & -\omega_1 & 0 & 0 \\ \omega_1 & 0 & 0 & 0 \\ 0 & 0 & 0 & -\omega_2 \\ 0 & 0 & \omega_2 & 0 \end{pmatrix}, \quad \omega_1, \omega_2 > 0.$$

   (a) For the nonresonant case, compute the codimension and a candidate for a versal deformation.

   (b) For the resonant case (except for $1:1$ resonance), compute the codimension and a candidate for a versal deformation.

   (c) For the $1:1$ resonant case (both semisimple and non-semisimple), compute the codimension and a candidate for a versal deformation.

   (*Hint: Use Examples 20.5.7 and 20.5.8 from Section 20.5.*)

8. Survey the literature and find five applications where the "Hopf- steady state" bifurcation arises.

9. Survey the literature and find five applications where the a) non- resonant double-Hopf bifurcation arises, b) where the resonant double- Hopf bifurcation arises. In particular, find an example of a $1:1$ resonant double-Hopf bifurcation in both the semsimple and non- semisimple case.

20.5 Versal Deformations of Families of Matrices

In this section we develop the theory of versal deformations of matrices which we use in computing versal deformations of fixed points of dynamical systems. Our discussion follows Arnold [1983]. Let M be the space of $n \times n$ matrices with complex entries. The relation of similarity of matrices partitions the entire space into manifolds consisting of matrices having the same eigenvalues and dimensions of Jordan blocks; this partitioning is continuous, since the eigenvalues vary continuously.

Suppose we have a matrix having some identical eigenvalues, and we want to reduce it to Jordan canonical form. This process is not stable, because the slightest perturbation might destroy the Jordan canonical form completely. Thus, if the matrix is only approximately known (or the reduction is attempted by computer), then the procedure may yield nonsense.

We give an example. Consider the matrix

$$A(\lambda) = \begin{pmatrix} 0 & \lambda \\ 0 & 0 \end{pmatrix}.$$

The Jordan canonical form is given by

$$\begin{pmatrix} 0 & 1 \\ 0 & 0 \end{pmatrix}, \qquad \lambda \neq 0,$$

with conjugating matrix

$$C(\lambda) = \begin{pmatrix} 1 & 0 \\ 0 & 1/\lambda \end{pmatrix}, \qquad \lambda \neq 0.$$

Now, at $\lambda = 0$, the Jordan canonical form of $A(\lambda)$ is given by

$$\begin{pmatrix} 0 & 0 \\ 0 & 0 \end{pmatrix},$$

with conjugating matrix

$$C(0) = \begin{pmatrix} 1 & 0 \\ 0 & 1 \end{pmatrix}.$$

Therefore, $C(\lambda)$ is discontinuous at $\lambda = 0$.

However, even though multiple eigenvalues is an unstable situation for individual matrices, it is stable for parametrized families of matrices, i.e., perturbing the family does not remove the multiple eigenvalue matrix from the family. Thus, while we can reduce every member of the family to Jordan canonical form (as in the example above), in general, the transformation will depend discontinuously on the parameter. The problem we address is the following:

What is the simplest form to which a family of matrices can be reduced depending differentiably on the parameters by a change of parameters depending differentiably on the parameters?

In the following we will construct such families and determine the minimum number of parameters, but first we must begin with some definitions and develop some necessary machinery.

We will consider $n \times n$ matrices whose entries are complex numbers. Let A_0 be such a matrix. The reason that we will be dealing (initially) with complex matrices is that the Jordan canonical form is more simple in this setting. Afterwards, we will show how the results obtained in the complex setting can be used for matrices with real entries.

We first need to introduce several definitions.

Definition 20.5.1 (Deformation of a Matrix) *A* deformation *of A_0 is a $\mathbf{C}^r$ $(r \geq 1)$ mapping*

$$\begin{aligned} A : \Lambda &\to \mathbb{C}^{n^2}, \\ \lambda &\to A(\lambda), \end{aligned}$$

where $\Lambda \in \mathbb{C}^\ell$ is some parameter space and

$$A(\lambda_0) = A_0.$$

A deformation is also called a family*, the variables λ_i, $i = 1, \cdots, \ell$, are called the parameters, and Λ is called the* base *of the family.*

Definition 20.5.2 (Equivalence of Deformations) *Two deformations $A(\lambda)$, $B(\lambda)$ of A_0 are called* equivalent *if there exists a deformation of the identity matrix $C(\lambda)$ $(C(\lambda_0) = id)$ with the same base such that*

$$B(\lambda) = C(\lambda)A(\lambda)C^{-1}(\lambda).$$

The following idea will be useful for reparametrizing families of matrices in order to reduce the number of parameters.

Definition 20.5.3 (Family Induced from a Deformation) *Let $\Sigma \subset \mathbb{C}^m$, $\Lambda \subset \mathbb{C}^\ell$ be open sets. Consider the $\mathbf{C}^r$ $(r \geq 1)$ mapping*

$$\begin{aligned} \phi : \Sigma &\to \Lambda, \\ \mu &\to \phi(\mu), \end{aligned}$$

with $\phi(\mu_0) = \lambda_0$.

The family induced from A by the mapping ϕ *is called $(\phi^* A)(\mu)$ and is defined by*

$$(\phi^* A)(\mu) \equiv A(\phi(\mu)), \qquad \mu \in \mathbb{C}^m.$$

Definition 20.5.4 (Versal, Miniversal, and Universal Deformations) *A deformation $A(\lambda)$ of a matrix A_0 is said to be* versal *if any deformation $B(\mu)$ of A_0 is equivalent to a deformation induced from A, i.e.,*

$$B(\mu) = C(\mu)A(\phi(\mu))C^{-1}(\mu)$$

for some change of parameters

$$\phi : \Sigma \to \Lambda,$$

with $C(\mu_0) = id$ and $\phi(\mu_0) = \lambda_0$.

A versal deformation is said to be universal *if the inducing mapping (i.e., change of parameters map) is determined uniquely by the deformation B.*

A versal deformation is said to be miniversal *if the dimension of the parameter space is the smallest possible for a versal deformation.*

At this stage it is useful to consider an example.

Example 20.5.1. Consider the matrix

$$A_0 = \begin{pmatrix} 0 & 1 \\ 0 & 0 \end{pmatrix}.$$

It should be clear that a versal deformation of A_0 is given by

$$B(\mu) \equiv \begin{pmatrix} 0 & 1 \\ 0 & 0 \end{pmatrix} + \begin{pmatrix} \mu_1 & \mu_2 \\ \mu_3 & \mu_4 \end{pmatrix},$$

where $\mu \equiv (\mu_1, \mu_2, \mu_3, \mu_4) \in \mathbb{C}^4$. However, $B(\mu)$ is not miniversal; a miniversal deformation is given by

$$A(\lambda) = \begin{pmatrix} 0 & 1 \\ 0 & 0 \end{pmatrix} + \begin{pmatrix} 0 & 0 \\ \lambda_1 & \lambda_2 \end{pmatrix},$$

where $\lambda = (\lambda_1, \lambda_2) \in \mathbb{C}^2$. This can be seen by showing that $B(\mu)$ is equivalent to a deformation induced from $A(\lambda)$. If we let

$$C(\mu) = \begin{pmatrix} 1+\mu_2 & 0 \\ -\mu_1 & 1 \end{pmatrix}, \qquad C^{-1}(\mu) = \frac{1}{1+\mu_2}\begin{pmatrix} 1 & 0 \\ \mu_1 & 1+\mu_2 \end{pmatrix},$$

then it follows that

$$\begin{aligned} A(\lambda) = A(\phi(\mu)) &= C^{-1}(\mu)B(\mu)C(\mu) \\ &= \begin{pmatrix} 0 & 1 \\ 0 & 0 \end{pmatrix} + \begin{pmatrix} 0 & 0 \\ \mu_3(1+\mu_2) - \mu_1\mu_4 & \mu_1 + \mu_4 \end{pmatrix}, \end{aligned}$$

where we take

$$\phi(\mu) = (\phi_1(\mu), \phi_2(\mu)) = (\mu_3(1+\mu_2) - \mu_1\mu_4, \mu_1 + \mu_4) \equiv (\lambda_1, \lambda_2) \equiv \lambda$$

as the inducing mapping.

End of Example 20.5.1

Now that we have the necessary definitions out of the way we can proceed toward our goal, which is to construct normal forms (miniversal deformations) of matrices having multiple eigenvalues. It is important to know the number of parameters necessary and to know the conditions that the normal form must satisfy for versality. To reach that point we must develop some machinery in order that the result does not appear to be "pulled out of the air."

We denote the set of all $n \times n$ matrices with complex entries by M. M is isomorphic to $\mathbb{C}^{n^2}$; however, we will simply write $M = \mathbb{C}^{n^2}$.

Now let us consider the Lie group $G = GL(n, \mathbb{C})$ of all nonsingular $n \times n$ matrices with complex entries. $GL(n, \mathbb{C})$ is a submanifold of $\mathbb{C}^{n^2}$.

Definition 20.5.5 (The Adjoint Action) *The group G acts on M according to the formula*

$$Ad_g m = gmg^{-1}, \qquad (m \in M, \quad g \in G) \tag{20.5.1}$$

(Ad stands for adjoint).

Definition 20.5.6 (Orbit Under the Adjoint Action) *Consider the orbit of an arbitrary fixed matrix $A_0 \in M$ under the action of G; this is the set of points $m \in M$ such that $m = gA_0g^{-1}$ for all $g \in G$. The orbit of A_0 under G forms a smooth submanifold of M, which we denote by N. Thus, from (20.5.1), the orbit, N, of A_0 consists of all matrices similar to A_0.*

We next restate the notion of *transversality of a map.* (cf. Definition 20.4.4).

Definition 20.5.7 (Transversality of a Map) *Let $N \subset M$ be a smooth submanifold of a manifold M. Consider a $\mathbf{C}^r$ $(r \geq 1)$ mapping of another manifold Λ into M and let λ be a point in Λ such that $A(\lambda) \in N$. Then the mapping A is called* transversal to N at λ *if the tangent space to M at $A(\lambda)$ is the sum*

$$TM_{A(\lambda)} = TN_{A(\lambda)} + DA(\lambda) \cdot T\Lambda_\lambda, \tag{20.5.2}$$

where $DA(\lambda)$ denotes the derivative of A at λ; see Figure 20.5.1.

With these two notions we can state and prove the proposition that provides the key for constructing miniversal deformations of Jordan matrices.

Proposition 20.5.8 *If the mapping A is transversal to the orbit of A_0 at $\lambda = \lambda_0$, then $A(\lambda)$ is a versal deformation. If the dimension of the parameter space is equal to the codimension of the orbit of A_0, then the deformation is miniversal.*

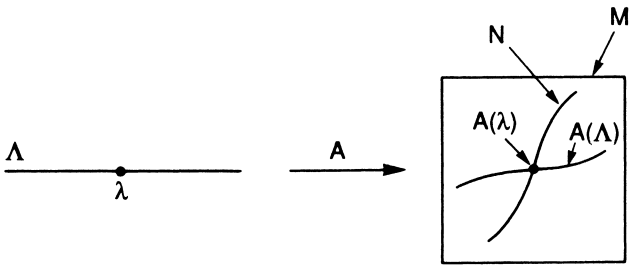

FIGURE 20.5.1.

Proof: Unfortunately we cannot proceed to the proof directly but must go in a rather roundabout way through several steps and definition. First note, however, that a geometrical picture of Proposition 20.5.8 is given in Figure 20.5.2.

In Figure 20.5.2 N is codimension 2; hence, we choose the dimension of λ to be 2. Since $A(\lambda)$ is transverse to N at $\lambda = \lambda_0$, we thus represent it as a two-dimensional surface passing through A_0. We want to show that $A(\lambda)$ satisfying this geometrical picture is actually a miniversal deformation of A_0. To do this we will need to develop a local coordinate structure near A_0 which describes points along the orbit of A_0 and points off of the orbit of A_0. We begin with a definition.

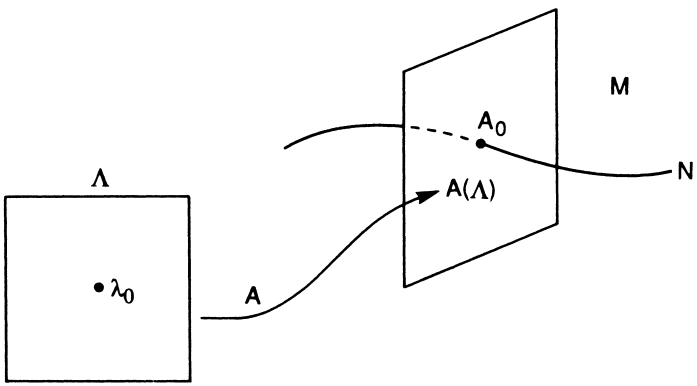

FIGURE 20.5.2.

Definition 20.5.9 (Centralizer of a Matrix) *The* centralizer of a matrix u *is the set of all matrices commuting with* u *denoted*

$$Z_u = \{v : [u, v] = 0\}, \qquad [u, v] \equiv uv - vu. \tag{20.5.3}$$

It is easy to show that the centralizer of any matrix of order n is a linear subspace of $M = \mathbb{C}^{n^2}$. We leave this as an exercise for the reader.

Now we want to develop the geometrical structure of M near $A(\lambda_0) \equiv A_0$. Let $\mathcal{Z}$ be the centralizer of the matrix A_0. Consider the set of nonsingular matrices that contain the identity matrix (which we denote by "id"). Clearly this set has dimension n^2. Within this set consider a smooth submanifold, P, intersecting the subspace $\mathrm{id} + \mathcal{Z}$ transversely at id and having dimension equal to the codimension of the centralizer; see Figure 20.5.3.

With Figure 20.5.3 in mind, consider the mapping

$$\Phi : P \times \Lambda \to \mathbb{C}^{n^2},$$

$$\Phi : (p, \lambda) \to pA(\lambda)p^{-1} \equiv \Phi(p, \lambda) \tag{20.5.4}$$

(we will worry about dimensions shortly).

The following lemma will provide us with local coordinates near A_0.

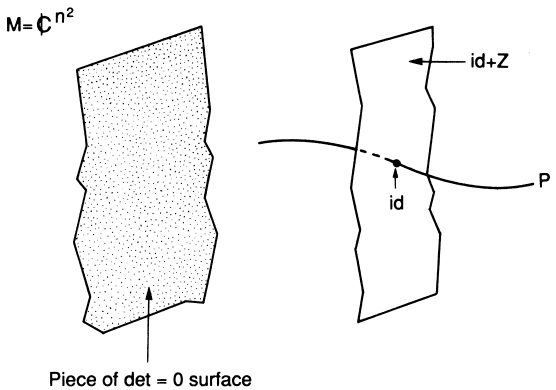

FIGURE 20.5.3.

Lemma 20.5.10 *In a neighborhood of* (id, λ_0) Φ *is a local diffeomorphism.*

Proof: Before proving lemma this we need to state several facts.

1) Consider the mapping

$$\psi : G \to \mathbb{C}^{n^2},$$
$$b \to bA_0b^{-1} \equiv \psi(b).$$

The derivative of ψ at the identity is a linear mapping of $T_{\mathrm{id}}G$ onto $T_{A_0}\mathbb{C}^{n^2}$. Without loss of generality, we can take $T_{\mathrm{id}}G = \mathbb{C}^{n^2}$ and $T_{A_0}\mathbb{C}^{n^2} = \mathbb{C}^{n^2}$. Denoting the derivative of ψ at id by $D\psi(\mathrm{id})$, we want to show that, for

$u \in \mathbb{C}^{n^2}$, $D\psi(\mathrm{id})u$ is given by the operation of commutation of u with A_0, i.e., $D\psi(\mathrm{id})u = [u, A_0]$.

This is easily calculated as follows

$$\begin{aligned} D\psi(\mathrm{id})u &= \lim_{\varepsilon \to 0} \frac{(\mathrm{id} + \varepsilon u)A_0(\mathrm{id} + \varepsilon u)^{-1} - A_0}{\varepsilon} \\ &= \lim_{\varepsilon \to 0} \frac{(A_0 + \varepsilon u A_0)(\mathrm{id} - \varepsilon u) + \mathcal{O}(\varepsilon^2) - A_0}{\varepsilon} \\ &= \lim_{\varepsilon \to 0} \frac{A_0 - \varepsilon A_0 u + \varepsilon u A_0 + \mathcal{O}(\varepsilon^2) - A_0}{\varepsilon} \\ &= uA_0 - A_0 u \equiv [u, A_0]; \end{aligned}$$

therefore,

$$\begin{aligned} D\psi(\mathrm{id}) : \mathbb{C}^{n^2} &\to \mathbb{C}^{n^2}, \\ u &\to [u, A_0]. \end{aligned} \tag{20.5.5}$$

We make the following observation. Since $\dim G = \dim M = n^2$, the dimension of the centralizer is equal to the codimension of the orbit of A_0. This is because, roughly speaking, from (20.5.1) and (20.5.4) we can think of the centralizer of A_0 to be the matrices that do not change A_0. Thus, we have

$$\dim \mathcal{Z} = \dim \Lambda, \tag{20.5.6}$$

$$\dim P = \dim N, \tag{20.5.7}$$

and

$$\dim \Lambda + \dim N = n^2.$$

Now, returning to Φ,

$$\Phi : P \times \Lambda \to \mathbb{C}^{n^2}.$$

From (20.5.6) and (20.5.7) we see that the dimensions are consistent (i.e., $\dim(P \times \Lambda) = \dim \mathbb{C}^{n^2}$) for Φ to be a diffeomorphism.

We can now finally prove Lemma 20.5.10. We compute the derivative of Φ at (id, λ_0), denoted $D\Phi(\mathrm{id}, \lambda_0)$, and examine how it acts on a typical element of $T_{(\mathrm{id},\lambda_0)}(P \times \Lambda)$. Let $(u, \lambda) \in T_{(\mathrm{id},\lambda_0)}(P \times \Lambda)$; then we have

$$D\Phi(\mathrm{id}, \lambda_0)(u, \lambda) = (D_p\Phi(\mathrm{id}, \lambda_0), D_\lambda\Phi(\mathrm{id}, \lambda_0))(u, \lambda). \tag{20.5.8}$$

Using (20.5.4) and (20.5.5) it is easy to see that (20.5.8) is given by

$$D\Phi(\mathrm{id}, \lambda_0)(u, \lambda) = ([u, A_0], DA(\lambda_0)\lambda). \tag{20.5.9}$$

By construction of the submanifold P, $D_p\Phi(\mathrm{id}, \lambda_0)$ maps $T_{\mathrm{id}}P$ isomorphically to a space tangent to the orbit N at A_0 (check dimensions and the fact that $[u, A_0] \neq 0$). Also by the hypothesis of Proposition 20.5.8, $DA(\lambda_0)$ maps $T_{\lambda_0}\Lambda$ isomorphically to a space transverse to N at $A(\lambda_0) = A_0$. Consequently, $D\Phi(\mathrm{id}, \lambda_0)$ is an isomorphism between linear spaces of dimension

n^2; thus, by the inverse function theorem, Φ is a local diffeomorphism. This completes our proof of Lemma 20.5.10. □

This lemma tells us that we have a local product structure (in terms of coordinates) near A_0 in M (note: this is for a sufficiently small neighborhood of (id, λ_0), since the inverse function theorem is only a local result); see Figure 20.5.4.

Now we can finish the proof of Proposition 20.5.8.

Let $B(\mu)$ for some fixed $\mu \in \Sigma \subset \mathbb{C}^m$ be an arbitrary deformation of A_0 (i.e., for some $\mu_0 \in \Sigma \subset \mathbb{C}^m$, $B(\mu_0) = A_0$). In the local coordinates near A_0, we know that any matrix sufficiently close to A_0 can be represented as

$$\Phi(p, \lambda) = pA(\lambda)p^{-1}, \qquad p \in P, \quad \lambda \in \Lambda \subset \mathbb{C}^\ell.$$

Hence, for $\mu - \mu_0$ sufficiently small, $B(\mu)$ has the representation

$$B(\mu) = \Phi(p, \lambda) = pA(\lambda)p^{-1}$$

for some $p \in P$, $\lambda \in \Lambda \subset \mathbb{C}^\ell$.

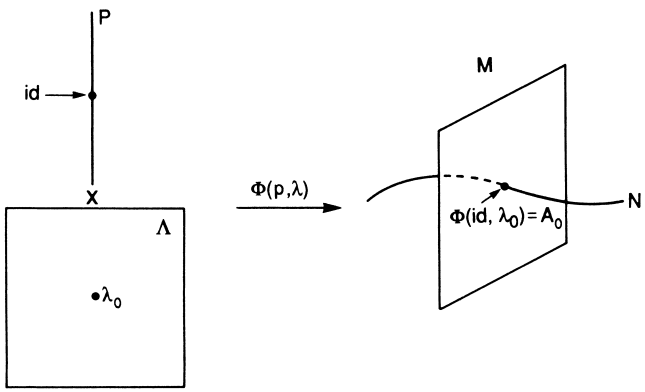

FIGURE 20.5.4.

Now let π_1 and π_2 be the projections onto P and Λ of $P \times \Lambda$, respectively. Then it follows by definition of Φ that

$$\lambda = \pi_2 \Phi^{-1}(B(\mu)),$$
$$p = \pi_1 \Phi^{-1}(B(\mu)).$$

Thus, letting

$$\phi(\mu) = \pi_2 \Phi^{-1}(B(\mu)),$$
$$C(\mu) = \pi_1 \Phi^{-1}(B(\mu)),$$

it follows that

$$B(\mu) = C(\mu)A(\phi(\mu))C^{-1}(\mu).$$

This proves Proposition 20.5.8. □

We remark that it should be clear from the argument that the deformation is miniversal, i.e., we have used the smallest number of parameters.

Thus, the proposition tells us that, in order to construct a miniversal deformation of A_0, we may take the family of matrices

$$A_0 + B,$$

where B is in the orthogonal complement of the orbit of A_0, and the entries of B are the deformation parameters. An obvious question therefore is how do you compute B?

Lemma 20.5.11 *A vector B in the tangent space of $\mathbb{C}^{n^2}$ at the point A_0 is perpendicular to the orbit of A_0 if and only if*

$$[B^*, A_0] = 0$$

where B^* denotes the adjoint of B.

Proof: Vectors tangent to the orbit are matrices representable in the form

$$[x, A_0], \qquad x \in M.$$

Orthogonality of B to the orbit of A_0 means that, for any $x \in M$,

$$\langle [x, A_0], B \rangle = 0, \tag{20.5.10}$$

where $\langle\ ,\ \rangle$ is the inner product on the space of matrices, which we take as

$$\langle A, B \rangle = \mathrm{tr}(AB^*). \tag{20.5.11}$$

Using (20.5.10), (20.5.11) becomes

$$\begin{aligned} 0 &= \mathrm{tr}\left([x, A_0]B^*\right) \\ &= \mathrm{tr}\left(xA_0B^* - A_0xB^*\right). \end{aligned}$$

Using the fact that

$$\begin{aligned} \mathrm{tr}(AB) &= \mathrm{tr}(BA), \\ \mathrm{tr}(A+B) &= \mathrm{tr}A + \mathrm{tr}B, \end{aligned}$$

we obtain

$$\begin{aligned} \mathrm{tr}(xA_0B^* - A_0xB^*) &= \mathrm{tr}(xA_0B^*) - \mathrm{tr}(A_0xB^*) \\ &= \mathrm{tr}(A_0B^*x) - \mathrm{tr}(xB^*A_0) \\ &= \mathrm{tr}(A_0B^*x) - \mathrm{tr}(B^*A_0x) \\ &= \mathrm{tr}((A_0B^* - B^*A_0)x) \\ &= \mathrm{tr}([A_0, B^*]x) \\ &= \langle [A_0, B^*], x^* \rangle = 0. \end{aligned}$$

Since x was arbitrary, this implies

$$[A_0, B^*] = 0. \qquad \square$$

This lemma actually allows us to "read off" the form of B if A_0 is in Jordan canonical form.

Suppose A_0 has been transformed to Jordan canonical form and has distinct eigenvalues

$$\alpha_i, \qquad i = 1, \cdots, s,$$

and to each eigenvalue there corresponds a finite number of Jordan blocks of order n_i

$$n_1(\alpha_i) \geq n_2(\alpha_i) \geq \cdots .$$

For the moment, to simplify our arguments, we will assume that our matrix has only one distinct eigenvalue, α, and let us say three Jordan blocks $n_1(\alpha) \geq n_2(\alpha) \geq n_3(\alpha)$. The matrices which commute with A_0 then have the structure shown in Figure 20.5.5, where *each oblique segment in each separate Jordan block* denotes a sequence of equal entries.

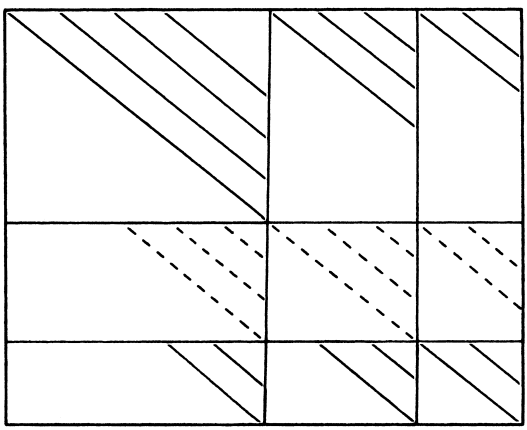

FIGURE 20.5.5.

Thus, a matrix B^* in the orthogonal complement of A_0 has the structure shown in Figure 20.5.6. The general proofs of these statements can be found in Gantmacher [1977], [1989] for the case of an arbitrary number of eigenvalues and Jordan blocks; however, we will not need such generality, since we will be concerned with 2×2, 3×3, and 4×4 matrices only and, in these cases, it is relatively easy to verify the structures shown in Figures 20.5.5 and 20.5.6 by direct calculation. We will do this shortly.

Therefore, a matrix of the structure shown in Figure 20.5.6 is orthogonal to A_0. Now in general we only desire transversality, not orthogonality, and

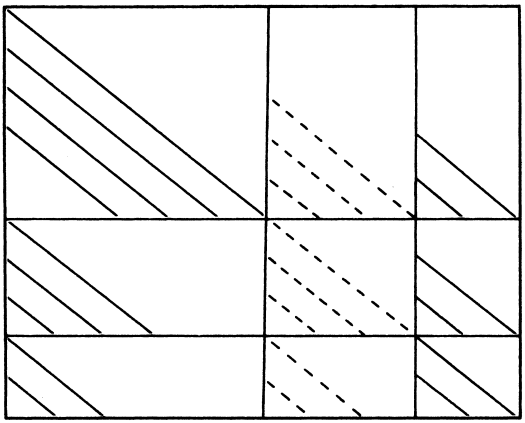

FIGURE 20.5.6.

it may simplify matters (i.e., reduce the number of matrix elements) to choose a basis not orthogonal but transverse to A_0 so that B^* appears as simply as possible. This can be accomplished by taking a matrix of the form shown in Figure 20.5.6 as B^* and replacing every slanted line by one independent parameter and the rest of the entries on the slanted line by zeros.

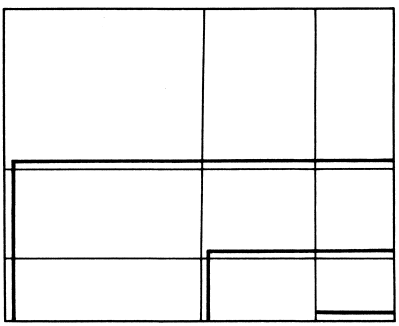

FIGURE 20.5.7.

The nonzero entry (independent parameter) can be placed at any position along the slanted line. Thus, matrices transverse to A_0 would have the structure shown in Figure 20.5.7, where the horizontal and vertical lines in the figure represent the positions where the required number of independent parameters are placed. From the above form of the matrices commuting with A_0, and only *one distinct eigenvalue*, the number of

parameters needed for a miniversal deformation is given by the formula

$$n_1(\alpha) + 3n_2(\alpha) + 5n_3(\alpha) + \cdots . \tag{20.5.12}$$

We now will state the general case for an arbitrary number of eigenvalues α_i, $i = 1, \cdots, s$, and then work out some explicit examples.

Theorem 20.5.12 *The smallest number of parameters of a versal deformation of the matrix A_0 is equal to*

$$d = \sum_{i=1}^{s} [n_1(\alpha_i) + 3n_2(\alpha_i) + 5n_3(\alpha_i) + \cdots] . \tag{20.5.13}$$

Proof: See Arnold [1983] and Gantmacher [1977], [1989]. □

We now sum up everything in our main theorem.

Theorem 20.5.13 *Every matrix A_0 has a miniversal deformation; the number of its parameters is equal to the codimension of the orbit of A_0 or, equivalently, to the dimension of the centralizer of A_0.*

If A_0 is in Jordan normal form, then for a miniversal deformation we may take a d-parameter normal form (with d given in Theorem A.1.4) $A_0 + B$, where the blocks of B have the previously described form.

In other words, any complex matrix close to a given matrix can be reduced to the above d-parameter normal form $A_0 + B$ (where A_0 is the Jordan canonical form of the given matrix), so that the reducing mapping and the parameters of the normal form depend in a $\mathbf{C}^r$ manner on the elements of the original matrix.

Now we will compute some examples.

Example 20.5.2. Consider the matrix

$$A_0 = \begin{pmatrix} \alpha & 1 \\ 0 & \alpha \end{pmatrix}, \qquad \alpha^2. \tag{20.5.14}$$

This matrix is denoted α^2, where α refers to the eigenvalue and two refers to the size of the Jordan block. In the context of bifurcations of fixed points of vector fields, we take $\alpha = 0$ and, for fixed points of maps, we take $\alpha = 1$. From (20.5.12) it follows that a versal deformation of (20.5.14) has at least two parameters; hence, matrices having Jordan canonical form A_0 (i.e., from (20.5.1), the orbit of A_0) form a codimension 2 submanifold of $\mathbb{C}^4$.

We now want to compute a versal deformation for A_0. First we compute a matrix which commutes with A_0.

$$\begin{aligned} &\begin{pmatrix} a & b \\ c & d \end{pmatrix} \begin{pmatrix} \alpha & 1 \\ 0 & \alpha \end{pmatrix} - \begin{pmatrix} \alpha & 1 \\ 0 & \alpha \end{pmatrix} \begin{pmatrix} a & b \\ c & d \end{pmatrix} \\ &= \begin{pmatrix} a\alpha & a + b\alpha \\ c\alpha & c + d\alpha \end{pmatrix} - \begin{pmatrix} a\alpha + c & b\alpha + d \\ \alpha c & \alpha d \end{pmatrix} \\ &= \begin{pmatrix} -c & a - d \\ 0 & c \end{pmatrix} = \begin{pmatrix} 0 & 0 \\ 0 & 0 \end{pmatrix}; \end{aligned}$$

thus,

$$c = 0, \qquad a = d, \qquad \text{and} \quad b = \text{arbitrary}.$$

Therefore, we obtain

$$B^* = \begin{pmatrix} a & b \\ 0 & a \end{pmatrix}.$$

From Lemma 20.5.11, we have that a matrix *orthogonal* to A_0 is given by

$$B = \begin{pmatrix} \bar{a} & 0 \\ \bar{b} & \bar{a} \end{pmatrix},$$

where $\bar{a}, \bar{b}$ are arbitrary complex numbers.

A family of matrices that is transverse to A_0 and that simplifies our expression for a versal deformation would be

$$\tilde{B} = \begin{pmatrix} 0 & 0 \\ \bar{b} & \bar{a} \end{pmatrix}.$$

We can check whether or not $\tilde{B}$ is transverse to A_0 by showing that

$$\langle \tilde{B}, B \rangle \equiv \operatorname{tr}(\tilde{B}B^*) \neq 0.$$

In our case we have

$$\tilde{B}B^* = \begin{pmatrix} 0 & 0 \\ \bar{b} & \bar{a} \end{pmatrix} \begin{pmatrix} a & 0 \\ b & a \end{pmatrix} = \begin{pmatrix} 0 & 0 \\ \bar{b}a + \bar{a}b & |a|^2 \end{pmatrix}$$

so that

$$\langle \tilde{B}, B \rangle \equiv \operatorname{tr}(\tilde{B}B^*) = |a|^2 \neq 0.$$

Relabeling by letting $\bar{b} = \lambda_1$ and $\bar{a} = \lambda_2$, we obtain the following versal deformation

$$\begin{pmatrix} \alpha & 1 \\ 0 & \alpha \end{pmatrix} + \begin{pmatrix} 0 & 0 \\ \lambda_1 & \lambda_2 \end{pmatrix}.$$

End of Example 20.5.2

Example 20.5.3. Consider the matrix

$$A_0 = \begin{pmatrix} \alpha & 0 \\ 0 & \alpha \end{pmatrix}, \qquad \alpha\alpha. \tag{20.5.15}$$

From (20.5.12), it follows that a versal deformation of (20.5.15) has four parameters; hence, matrices having Jordan normal form A_0 form a codimension 4 submanifold of $\mathbb{C}^4$.

We next compute a family orthogonal to the orbit of A_0 as follows

$$\begin{pmatrix} a & b \\ c & d \end{pmatrix} \begin{pmatrix} \alpha & 0 \\ 0 & \alpha \end{pmatrix} - \begin{pmatrix} \alpha & 0 \\ 0 & \alpha \end{pmatrix} \begin{pmatrix} a & b \\ c & d \end{pmatrix} = \begin{pmatrix} 0 & 0 \\ 0 & 0 \end{pmatrix}.$$

or

$$\begin{pmatrix} a\alpha & b\alpha \\ c\alpha & d\alpha \end{pmatrix} - \begin{pmatrix} \alpha a & \alpha b \\ \alpha c & \alpha d \end{pmatrix} = \begin{pmatrix} 0 & 0 \\ 0 & 0 \end{pmatrix}.$$

Thus, a, b, c, d can be anything; this situation is therefore codimension 4 with a versal deformation given by

$$\begin{pmatrix} \alpha & 0 \\ 0 & \alpha \end{pmatrix} + \begin{pmatrix} \lambda_1 & \lambda_2 \\ \lambda_3 & \lambda_4 \end{pmatrix},$$

where we have relabeled the parameters as in Example 20.5.2.

End of Example 20.5.3

Example 20.5.4. Consider the matrix

$$A_0 = \begin{pmatrix} \alpha & 1 & 0 \\ 0 & \alpha & 0 \\ 0 & 0 & \alpha \end{pmatrix}, \qquad \alpha^2\alpha. \tag{20.5.16}$$

From (20.5.12), it follows that a versal deformation of (20.5.16) has at least five parameters; hence, matrices having Jordan canonical form A_0 form a codimension 5 submanifold of $\mathbb{C}^9$.

We compute a family of matrices orthogonal to the orbit of A_0 as follows

$$\begin{pmatrix} a & b & c \\ d & e & f \\ g & h & i \end{pmatrix} \begin{pmatrix} \alpha & 1 & 0 \\ 0 & \alpha & 0 \\ 0 & 0 & \alpha \end{pmatrix} - \begin{pmatrix} \alpha & 1 & 0 \\ 0 & \alpha & 0 \\ 0 & 0 & \alpha \end{pmatrix} \begin{pmatrix} a & b & c \\ d & e & f \\ g & h & i \end{pmatrix}$$
$$= \begin{pmatrix} 0 & 0 & 0 \\ 0 & 0 & 0 \\ 0 & 0 & 0 \end{pmatrix}$$

$$\begin{pmatrix} a\alpha & a+b\alpha & c\alpha \\ d\alpha & d+e\alpha & f\alpha \\ g\alpha & g+h\alpha & i\alpha \end{pmatrix} - \begin{pmatrix} a\alpha+d & \alpha b+e & \alpha c+f \\ \alpha d & \alpha e & \alpha f \\ \alpha g & \alpha h & \alpha i \end{pmatrix}$$
$$= \begin{pmatrix} -d & a-e & -f \\ 0 & d & 0 \\ 0 & g & 0 \end{pmatrix} = \begin{pmatrix} 0 & 0 & 0 \\ 0 & 0 & 0 \\ 0 & 0 & 0 \end{pmatrix};$$

we thus obtain $d = 0$, $g = 0$, $f = 0$, $a = e$, and $b, c, h, i =$ arbitrary.

Therefore, we obtain

$$B = \begin{pmatrix} \overline{a} & 0 & \overline{0} \\ \overline{b} & \overline{a} & \overline{h} \\ \overline{c} & 0 & \overline{i} \end{pmatrix}$$

or a simpler form, transverse to the orbit of A_0, given by

$$\tilde{B} = \begin{pmatrix} 0 & 0 & 0 \\ \lambda_1 & \lambda_2 & \lambda_3 \\ \lambda_4 & 0 & \lambda_5 \end{pmatrix},$$

where we have relabeled the parameters as in Example 20.5.2. Hence, a versal deformation of A_0 is given by

$$\begin{pmatrix} \alpha & 1 & 0 \\ 0 & \alpha & 0 \\ 0 & 0 & \alpha \end{pmatrix} + \begin{pmatrix} 0 & 0 & 0 \\ \lambda_1 & \lambda_2 & \lambda_3 \\ \lambda_4 & 0 & \lambda_5 \end{pmatrix}.$$

We leave it to the reader to verify the transversality of $\tilde{B}$ to the orbit of A_0.

End of Example 20.5.4

To summarize, the first few low codimension matrices have versal deformations given by

$$\boxed{\alpha^2} \qquad \begin{pmatrix} \alpha & 1 \\ 0 & \alpha \end{pmatrix} + \begin{pmatrix} 0 & 0 \\ \lambda_1 & \lambda_2 \end{pmatrix},$$

$$\boxed{\alpha\alpha} \qquad \begin{pmatrix} \alpha & 0 \\ 0 & \alpha \end{pmatrix} + \begin{pmatrix} \lambda_1 & \lambda_2 \\ \lambda_3 & \lambda_4 \end{pmatrix},$$

$$\boxed{\alpha^2\alpha} \qquad \begin{pmatrix} \alpha & 1 & 0 \\ 0 & \alpha & 0 \\ 0 & 0 & \alpha \end{pmatrix} + \begin{pmatrix} 0 & 0 & 0 \\ \lambda_1 & \lambda_2 & \lambda_3 \\ \lambda_4 & 0 & \lambda_5 \end{pmatrix}.$$

These are the simplest forms to which these parametrized families of matrices containing multiple eigenvalues can be reduced by a *transformation depending differentiably on the parameters.*

20.5A Versal Deformations of Real Matrices

Before leaving this section there is a very important point we should address, namely, that all of our work in this section has dealt with complex numbers. The reason for this is simple; it is much easier to deal with the Jordan canonical form when dealing with matrices of complex numbers. However, throughout this book we are mainly interested in real-valued vector fields. Thus it is fortunate that the results for versal deformations of matrices of complex numbers go over immediately to the situation of versal deformations of matrices of real numbers. The main idea is the following (Galin [1972], Arnold [1983]).

> The decomplexification of a versal deformation with the minimum number of parameters of a complex matrix, $\tilde{A}_0$, can be chosen to be a versal deformation with the minimum number of parameters of the real matrix A_0, where A_0 is the decomplexification of $\tilde{A}_0$.

This statement should be almost obvious after reviewing some definitions and terminology. We will discuss only what is necessary for our purposes and refer the reader to Arnold [1973], Hirsch and Smale [1974], or Chapter 3 for more information.

It should be clear that the decomplexification of $\mathbb{C}^n$; is $\mathbb{R}^{2n}$. Moreover, if $e_1, \cdots, e_n$ is a basis of $\mathbb{C}^n$, then $e_1, \cdots, e_n$, $ie_1, \ldots, ie_n$ is a basis for the decomplexification of $\mathbb{C}^n$, $\mathbb{R}^{2n}$. Now, let $A = A_r + iA_i$ be a matrix

representation of some complex linear operator mapping $\mathbb{C}^n$ into itself. Then the decomplexification of this matrix is given by the $2n \times 2n$ matrix

$$\begin{pmatrix} A_r & -A_i \\ A_i & A_r \end{pmatrix}. \tag{20.5.17}$$

Now we show how we can use these ideas to construct a versal deformation of a real matrix. As in the complex case, the construction of a versal deformation of a matrix in Jordan canonical form is carried out "Jordan block by Jordan block". Therfore we really only need to understand the case of a real matrix having exactly two complex eigenvalues (complex conjugate pairs).

Consider a real matrix

$$A_0 : \mathbb{R}^{2n} \to \mathbb{R}^{2n},$$

and suppose that it has exactly two eigenvalues

$$\alpha \pm i\beta, \quad \beta \neq 0,$$

and each eigenvalue has corresponding Jordan blocks of dimension

$$n_1 \geq n_2 \geq n_3 \geq \cdots, \qquad \text{with} \quad n_1 + n_2 + n_3 + \cdots = n.$$

Using the theory of the real Jordan canonical form, we can construct a real basis in $\mathbb{R}^{2n}$ with respect to which A_0 has the form of the matrix of the decomplexification of the Jordan canonical form of the complex matrix

$$\tilde{A}_0 : \mathbb{C}^n \to \mathbb{C}^n,$$

where $\tilde{A}_0$ has only one eigenvalue, $\alpha + i\beta$, with Jordan blocks of dimensions $n_1 \geq n_2 \geq n_3 \geq \cdots$, with $n_1 + n_2 + n_3 + \cdots = n$, i.e.,

$$A_0 = \begin{pmatrix} J & -\beta\mathrm{id} \\ \beta\mathrm{id} & J \end{pmatrix},$$

where id denotes the $n \times n$ identity matrix and J is the upper triangular real Jordan matrix with eigenvalue α and blocks of dimension $n_1 \geq n_2 \geq n_3 \geq \cdots$, with $n_1 + n_2 + n_3 + \cdots = n$. Then a versal deformation for A_0 is constructed from a versal deformation of $\tilde{A}_0$ as follows.

> With $\tilde{A}_0$ in Jordan canonical form, construct the versal deformation according the the methods for complex matrices developed above. Then decomplexify the result according to (20.5.17).

As we have noted, the construction of a versal deformation of a matrix in Jordan canonical form is carried out "Jordan block by Jordan block". Therefore if the eigenvalues of a matrix are all real, we see that there is

no difference with the theory developed for the case of complex matrices. If there are complex eigenvalues, versal deformations for the corresponding Jordan blocks are constructed as described above.

Moreover, we also see immediately that the minimum number of parameters of a real versal deformation are also given by the formula:

$$d = \sum_{\lambda} \left(n_1(\lambda) + 3n_2(\lambda) + 5n_3(\lambda) \cdots \right),$$

where the summation is over all s eigenvalues, both real and complex.

We next consider some examples.

Example 20.5.5 (An Imaginary Pair of Eigenvalues).

Consider a 2×2 real matrix having eigenvalues $\rho + i\tau$. Then with respect to an appropriate basis it has the form

$$A_0 = \begin{pmatrix} \rho & -\tau \\ \tau & \rho \end{pmatrix}.$$

We want to construct a versal deformation of this matrix.

The complexification of A_0 is given by

$$\tilde{A}_0 = (\alpha), \quad \alpha \equiv \rho + i\tau.$$

According to Theorem 20.5.12, a versal deformation for $\tilde{A}_0$ can be constructed with one (complex) parameter, $\lambda = \mu + i\gamma$, i.e, the versal deformation of $\tilde{A}_0$ is given by

$$(\alpha) + (\lambda).$$

With this result, and (20.5.17), a versal deformation of A_0 is given by

$$\begin{pmatrix} \rho & -\tau \\ \tau & \rho \end{pmatrix} + \begin{pmatrix} \mu & -\gamma \\ \gamma & \mu \end{pmatrix}.$$

End of Example 20.5.5

Examples 20.5.6, and 20.5.7 use the fact that versal deformations are constructed Jordan block-by-block, versal deformations of Jordan blocks corresponding to real eigenvalues are exactly the same as in the complex case (with real parameters), and example 20.5.5.

Example 20.5.6 (One Real, and A Pure Imaginary Pair of Eigenvalues).

Consider a 3×3 real matrix having eigenvalues $\rho \pm i\tau$, β, $\tau \neq 0$. Then with respect to an appropriate basis it has the form

$$A_0 = \begin{pmatrix} \rho & -\tau & 0 \\ \tau & \rho & 0 \\ 0 & 0 & \beta \end{pmatrix}.$$

A versal deformation requires three real parameters and is given by

$$\begin{pmatrix} \rho & -\tau & 0 \\ \tau & \rho & 0 \\ 0 & 0 & \beta \end{pmatrix} + \begin{pmatrix} \mu & -\gamma & 0 \\ \gamma & \mu & 0 \\ 0 & 0 & \delta \end{pmatrix}.$$

End of Example 20.5.6

Example 20.5.7 (A Pair of Distinct, Imaginary Pairs of Eigenvalues).

Consider a 4×4 real matrix having eigenvalues $\alpha_i = \rho_i + i\tau_i$, $i = 1, 2$, with $\alpha_1 \neq \alpha_2$. Then with respect to an appropriate basis it has the form

$$A_0 = \begin{pmatrix} \rho_1 & -\tau_1 & 0 & 0 \\ \tau_1 & \rho_1 & 0 & 0 \\ 0 & 0 & \rho_2 & -\tau_2 \\ 0 & 0 & \tau_2 & \rho_2 \end{pmatrix}.$$

This matrix is simple two Jordan blocks of example 20.5.5. Hence, using the result from example 20.5.5, a versal deformation of A_0 requires four real parameters and is given by

$$\begin{pmatrix} \rho_1 & -\tau_1 & 0 & 0 \\ \tau_1 & \rho_1 & 0 & 0 \\ 0 & 0 & \rho_2 & -\tau_2 \\ 0 & 0 & \tau_2 & \rho_2 \end{pmatrix} + \begin{pmatrix} \mu_1 & -\gamma_1 & 0 & 0 \\ \gamma_1 & \mu_1 & 0 & 0 \\ 0 & 0 & \mu_2 & -\gamma_2 \\ 0 & 0 & \gamma_2 & \mu_2. \end{pmatrix}$$

End of Example 20.5.7

Example 20.5.8 (A Repeated Complex Pair of Eigenvalues: The Semisimple and Non-Semisimple Cases).

$$\begin{pmatrix} \alpha & 1 \\ 0 & \alpha \end{pmatrix} + \begin{pmatrix} 0 & 0 \\ \lambda_1 & \lambda_2 \end{pmatrix}, \tag{20.5.18}$$

$$\begin{pmatrix} \alpha & 0 \\ 0 & \alpha \end{pmatrix} + \begin{pmatrix} \lambda_1 & \lambda_2 \\ \lambda_3 & \lambda_4 \end{pmatrix}. \tag{20.5.19}$$

Letting

$$\begin{aligned} \alpha &= \rho + i\tau, \\ \lambda_i &= \mu_i + i\gamma_i, \end{aligned}$$

where ρ, τ, μ_i, and γ_i are real, (20.5.17) implies that the decomplexification of these matrices is given by

$$\begin{pmatrix} \rho & 1 & -\tau & 0 \\ 0 & \rho & 0 & -\tau \\ \tau & 0 & \rho & 1 \\ 0 & \tau & 0 & \rho \end{pmatrix} + \begin{pmatrix} 0 & 0 & 0 & 0 \\ \mu_1 & \mu_2 & -\gamma_1 & -\gamma_2 \\ 0 & 0 & 0 & 0 \\ \gamma_1 & \gamma_2 & \mu_1 & \mu_2 \end{pmatrix}, \tag{20.5.20}$$

$$\begin{pmatrix} \rho & 0 & -\tau & 0 \\ 0 & \rho & 0 & -\tau \\ \tau & 0 & \rho & 0 \\ 0 & \tau & 0 & \rho \end{pmatrix} + \begin{pmatrix} \mu_1 & \mu_2 & -\gamma_1 & -\gamma_2 \\ \mu_3 & \mu_4 & -\gamma_3 & -\gamma_4 \\ \gamma_1 & \gamma_2 & \mu_1 & \mu_2 \\ \gamma_3 & \gamma_4 & \mu_3 & \mu_4 \end{pmatrix}. \tag{20.5.21}$$

End of Example 20.5.8

20.5B Exercises

1. Let M denote the set of all $n \times n$ matrices with complex entries. Show that M can be identified as $\mathbb{C}^{n^2}$ (note: see Dubrovin, Fomenko, and Novikov [1984] for an excellent discussion of matrix groups as surfaces).

2. Show that $GL(n, \mathbb{C})$ is a submanifold of $\mathbb{C}^{n^2}$.

3. Show that the orbit of a matrix $A_0 \in M$ under the action of $GL(n, \mathbb{C})$ defined by

$$gA_0g^{-1}, \qquad g \in GL(n, \mathbb{C}),$$

is a submanifold of M.

4. Show that the centralizer of any matrix of order n (with complex entries) is a linear subspace of $\mathbb{C}^{n^2}$.

5. Prove that the dimension of the centralizer is equal to the codimension of the orbit of A_0.

6. Explain why that, in the local coordinates near A_0 constructed in Lemma 20.5.10, any matrix sufficiently close to A_0 can be represented in the form

$$pA(\lambda)p^{-1}, \qquad p \in P, \quad \lambda \in \Lambda \subset \mathbb{C}^{\ell}.$$

Can you give a more intuitive explanation of this based on elementary notions from linear algebra?

7. Explain why the deformation constructed in Proposition 20.5.8 is miniversal.

8. Prove the following statement:

> The decomplexification of a versal deformation with the minimum number of parameters of a complex matrix, $\tilde{A}_0$, can be chosen to be a versal deformation with the minimum number of parameters of the real matrix A_0, where A_0 is the decomplexification of $\tilde{A}_0$.

9. Prove that the decomplexification of $\mathbb{C}^n$ is $\mathbb{R}^{2n}$ and that if $e_1, \cdots, e_n$ is a basis of $\mathbb{C}^n$, then $e_1, \cdots e_n$, $ie_1, \cdots, ie_n$ is a basis for the decomplexification of $\mathbb{C}^n$, $\mathbb{R}^{2n}$.

10. Suppose $A = A_r + iA_i$ is the matrix representation of some linear mapping of $\mathbb{C}^n$ into $\mathbb{C}^n$. Then show that

$$\begin{pmatrix} A_r & -A_i \\ A_i & A_r \end{pmatrix}$$

is the decomplexification of this matrix.

11. Compute miniversal deformations of the following *real* matrices.

a) $\begin{pmatrix} 0 & -\omega & 0 \\ \omega & 0 & 0 \\ 0 & 0 & 0 \end{pmatrix}$

b) $\begin{pmatrix} 0 & -\omega_1 & 0 & 0 \\ \omega_1 & 0 & 0 & 0 \\ 0 & 0 & 0 & -\omega_2 \\ 0 & 0 & \omega_2 & 0 \end{pmatrix}$

c) $\begin{pmatrix} 1 & 0 \\ 0 & 1 \end{pmatrix}$

d) $\begin{pmatrix} 1 & 0 \\ 0 & -1 \end{pmatrix}$

e) $\begin{pmatrix} 0 & 1 & 0 \\ 0 & 0 & 0 \\ 0 & 0 & 0 \end{pmatrix}$

f) $\begin{pmatrix} 0 & 1 & 0 \\ 0 & 0 & 1 \\ 0 & 0 & 0 \end{pmatrix}$

g) $\begin{pmatrix} 0 & 0 & 0 \\ 0 & 0 & 1 \\ 0 & 0 & 0 \end{pmatrix}$

h) $\begin{pmatrix} 0 & -\omega & 0 \\ \omega & 0 & 0 \\ 0 & 0 & 1 \end{pmatrix}$

i) $\begin{pmatrix} 0 & 0 \\ 1 & 0 \end{pmatrix}$

j) $\begin{pmatrix} 0 & -\omega \\ \omega & 1 \end{pmatrix}$.

12. Relate Theorem 19.5.7 from Chapter 19 (especially equations (19.5.44) and (19.5.45)) to the miniversal deformation of a matrix and, more generally, the construction of versal deformations developed in this chapter.

20.6 The Double-Zero Eigenvalue: the Takens-Bogdanov Bifurcation

Suppose we have a vector field on $\mathbb{R}^n$ having a fixed point at which the matrix associated with the linearization of the vector field about the fixed point has two zero eigenvalues bounded away from the imaginary axis. In this case we know that the study of the dynamics near this nonhyperbolic fixed point can be reduced to the study of the dynamics of the vector field restricted to the associated two-dimensional center manifold (cf. Chapter 18).

We assume that the reduction to the two-dimensional center manifold has been made, and the Jordan canonical form of the linear part of the vector field is given by

$$\begin{pmatrix} 0 & 1 \\ 0 & 0 \end{pmatrix}. \tag{20.6.1}$$

Our goal is to study the dynamics near a nonhyperbolic fixed point having linear part given by (20.6.1). The procedure is fairly systematic and will be accomplished in the following steps.

1. Compute a normal form and truncate.

2. Rescale the normal form so as to reduce the number of cases to be studied.
3. Embed the truncated normal form in an appropriate two-parameter family (see Example 20.4.11b)
4. Study the local dynamics of the two-parameter family of vector fields.
   - 4a. Find the fixed points and study the nature of their stability.
   - 4b. Study the bifurcations associated with the fixed points.
   - 4c. Based on a consideration of the local dynamics, infer if global bifurcations must be present.
5. Analyze the global bifurcations.
6. Study the effect of the neglected higher order terms in the normal form on the dynamics of the truncated normal form.

We remark that Step 4c is a new phenomenon. However, we will see that it is not uncommon for global effects to be associated with *local* codimension k ($k \geq 2$) bifurcations. Moreover, we will see that it is often possible to "guess" their existence from a thorough local analysis. We will discuss this in more detail later on. Now we begin our analysis with Step 1.

Step 1: The Normal Form. In Example 19.1.2 we saw that a normal form associated with a fixed point of a vector field having linear part (20.6.1) is given by

$$\begin{aligned} \dot{x} &= y + \mathcal{O}(|x|^3, |y|^3), \\ \dot{y} &= ax^2 + bxy + \mathcal{O}(|x|^3, |y|^3), \qquad (x, y) \in \mathbb{R}^2. \end{aligned} \tag{20.6.2}$$

At this stage we will neglect the $\mathcal{O}(3)$ terms in (20.6.2) and study the resulting truncated normal form

$$\begin{aligned} \dot{x} &= y, \\ \dot{y} &= ax^2 + bxy. \end{aligned} \tag{20.6.3}$$

Step 2: Rescaling. Letting

$$\begin{aligned} x &\to \alpha x, \\ y &\to \beta y, \\ t &\to \gamma t, \qquad \gamma > 0, \end{aligned}$$

(20.6.3) becomes

$$\begin{aligned} \dot{x} &= \left(\frac{\gamma\beta}{\alpha}\right) y, \\ \dot{y} &= \left(\frac{\gamma a \alpha^2}{\beta}\right) x^2 + (\gamma b \alpha) xy. \end{aligned} \tag{20.6.4}$$

Now we want to choose γ, β, and α so that the coefficients of (20.6.4) are as simple as possible. Ideally, they would all be unity; we will see that this is not possible but that we can come close.

We will require

$$\frac{\gamma\beta}{\alpha} = 1 \tag{20.6.5}$$

or

$$\gamma = \frac{\alpha}{\beta}.$$

Equation (20.6.5) fixes γ. We require α and β to have the same signs so that stability will not be affected under the rescaling (since γ scales time).

Next, we require that

$$\frac{\gamma a \alpha^2}{\beta} = 1. \tag{20.6.6}$$

Using (20.6.5), (20.6.6) becomes

$$\frac{a\alpha^3}{\beta^2} = a\alpha\left(\frac{\alpha^2}{\beta^2}\right) = 1. \tag{20.6.7}$$

Equation (20.6.7) fixes α/β.

We finally require

$$\gamma b \alpha = 1 \tag{20.6.8}$$

but, using (20.6.5), (20.6.8) becomes

$$\frac{b\alpha^2}{\beta} = b\beta\left(\frac{\alpha^2}{\beta^2}\right) = 1. \tag{20.6.9}$$

We can see that a and b can have either sign and that α and β must have the same sign. From (20.6.7) we can further see that a and α must have the same sign. Therefore, if (20.6.9) is to hold, we conclude that b and a have the same sign. This is too restrictive—the best we can do and still retain full generality is to require

$$b\beta\left(\frac{\alpha^2}{\beta^2}\right) = \pm 1, \tag{20.6.10}$$

so that, in the rescaled variables, the normal form is

$$\begin{aligned} \dot{x} &= y, \\ \dot{y} &= x^2 \pm xy. \end{aligned} \tag{20.6.11}$$

Step 3: Construct a Candidate for a Versal Deformation. From Example 20.4.11b, a likely candidate for a versal deformation is

$$\begin{aligned} \dot{x} &= y, \\ \dot{y} &= \mu_1 + \mu_2 y + x^2 + bxy, \qquad b = \pm 1. \end{aligned} \tag{20.6.12}$$

Step 4: Study the Local Dynamics of (20.6.12). We take the case $b = +1$.

Step 4a: Fixed Points and Their Stability. It is easy to see that the fixed points of (20.6.12) are given by

$$(x, y) = (\pm\sqrt{-\mu_1}, 0). \tag{20.6.13}$$

In particular, there are no fixed points for $\mu_1 > 0$.

Next we check the stability of these fixed points.

The Jacobian of the vector field evaluated at the fixed point is given by

$$\left.\begin{pmatrix} 0 & 1 \\ 2x & \mu_2 + x \end{pmatrix}\right|_{(\pm\sqrt{-\mu_1},0)} = \begin{pmatrix} 0 & 1 \\ \pm 2\sqrt{-\mu_1} & \mu_2 \pm \sqrt{-\mu_1} \end{pmatrix}. \tag{20.6.14}$$

The eigenvalues are given by

$$\lambda_{1,2} = \frac{\mu_2 \pm \sqrt{-\mu_1}}{2} \pm \frac{1}{2}\sqrt{(\mu_2 \pm \sqrt{-\mu_1})^2 \pm 8\sqrt{-\mu_1}}. \tag{20.6.15}$$

If we denote the two branches of fixed points by $(x^+, 0) \equiv (+\sqrt{-\mu_1}, 0)$ and $(x^-, 0) = (-\sqrt{-\mu_1}, 0)$, we see from (20.6.15) that $(x^+, 0)$ is a *saddle* for $\mu_1 < 0$ and all μ_2, while for $\mu_1 = 0$ the eigenvalues of $(x^+, 0)$ are given by

$$\lambda_{1,2} = \mu_2, 0.$$

The fixed point $(x^-, 0)$ is a *source* for $\{\mu_2 > \sqrt{-\mu_1}, \mu_1 < 0\}$ and a sink for $\{\mu_2 < \sqrt{-\mu_1}, \mu_1 < 0\}$; for $\mu_1 = 0$, the eigenvalues of $(x^-, 0)$ are given by

$$\lambda_{1,2} = \mu_2, 0$$

and, for $\mu_2 = \sqrt{-\mu_1}$, $\mu_1 < 0$, the eigenvalues on $(x^-, 0)$ are given by

$$\lambda_{1,2} = \pm i\sqrt{2\sqrt{-\mu_1}}.$$

Thus, we might expect that $\mu_1 = 0$ is a bifurcation curve on which $(x^\pm, 0)$ are born in a saddle-node bifurcation and $\mu_2 = \sqrt{-\mu_1}$, $\mu_1 < 0$, is a bifurcation curve on which $(x^-, 0)$ undergoes a Poincaré–Andronov–Hopf bifurcation. We now turn to verifying this and studying the orbit structure associated with these bifurcations.

Step 4b: The Bifurcations of the Fixed Points. We begin by examining the orbit structure near $\mu_1 = 0$, μ_2 arbitrary. We will use the center manifold theorem (Theorem 18.1.2).

First we put the system into the "normal form" for the center manifold theorem. We treat μ_2 as a fixed constant in the problem and think of μ_1 as a parameter, and we examine bifurcations from $\mu_1 = 0$.

To transform (20.6.12) into the form in which the center manifold can be applied, we use the following linear transformation

$$\begin{pmatrix} x \\ y \end{pmatrix} = \begin{pmatrix} 1 & 1 \\ 0 & \mu_2 \end{pmatrix} \begin{pmatrix} u \\ v \end{pmatrix}, \qquad \begin{pmatrix} u \\ v \end{pmatrix} = \frac{1}{\mu_2} \begin{pmatrix} \mu_2 & -1 \\ 0 & 1 \end{pmatrix} \begin{pmatrix} x \\ y \end{pmatrix}, \tag{20.6.16}$$

which transforms (20.6.12) into

$$\begin{pmatrix} \dot{u} \\ \dot{v} \end{pmatrix} = \begin{pmatrix} 0 & 0 \\ 0 & \mu_2 \end{pmatrix} \begin{pmatrix} u \\ v \end{pmatrix} + \frac{1}{\mu_2} \begin{pmatrix} -\mu_1 \\ \mu_1 \end{pmatrix} + \frac{1}{\mu_2} \begin{pmatrix} -(u^2 + (2+\mu_2)uv + (1+\mu_2)v^2) \\ u^2 + (2+\mu_2)uv + (1+\mu_2)v^2 \end{pmatrix}$$

or

$$\begin{aligned} \dot{u} &= -\frac{\mu_1}{\mu_2} - \frac{1}{\mu_2}\left[u^2 + (2+\mu_2)uv + (1+\mu_2)v^2\right], \\ \dot{v} &= \mu_2 v + \frac{\mu_1}{\mu_2} + \frac{1}{\mu_2}\left[u^2 + (2+\mu_2)uv + (1+\mu_2)v^2\right]. \end{aligned} \tag{20.6.17}$$

Without actually computing the center manifold, we can argue as follows.

The center manifold will be given as a graph over u and μ_1, $v(u, \mu_1)$, and be at least $\mathcal{O}(2)$. Thus, from this we can immediately see that the reduced system is given by

$$\dot{u} = -\frac{1}{\mu_2}(\mu_1 + u^2) + \mathcal{O}(3), \tag{20.6.18}$$

and thus it undergoes a saddle-node bifurcation at $\mu_1 = 0$.

We can immediately conclude that the stable (unstable) manifold of the node connects to the unstable (stable) manifold of the saddle, since this always occurs for one-dimensional flows. This points out another advantage of the center manifold analysis, since such results are nontrival in dimensions ≥ 2.

We next want to examine in more detail the nature of the flow on the center manifold and what it implies for the full two-dimensional flow. Recall that the eigenvalues of the linearized two-dimensional vector field on the bifurcation curve are given by

$$\lambda_{1,2} = \mu_2, 0.$$

In transforming (20.6.12) to (20.6.17), we see from (20.6.16) that the coordinate axes have be transformed as in Figure 20.6.1.

Now the flow on the center manifold is given by

$$\dot{u} = -\frac{1}{\mu_2}(\mu_1 + u^2) + \mathcal{O}(3), \tag{20.6.19}$$

and in the (u, μ_1) coordinates appear as in Figure 20.6.2.

Using the information in Figures 20.6.1 and 20.6.2 and recalling that the eigenvalues of the vector field linearized about the fixed point at $\mu_1 = 0$ are $\lambda_{1,2} = \mu_2, 0$, we can easily obtain phase portraits near the origin that show the bifurcation in the two-dimensional phase space on crossing the μ_2-axis; see Figure 20.6.3.

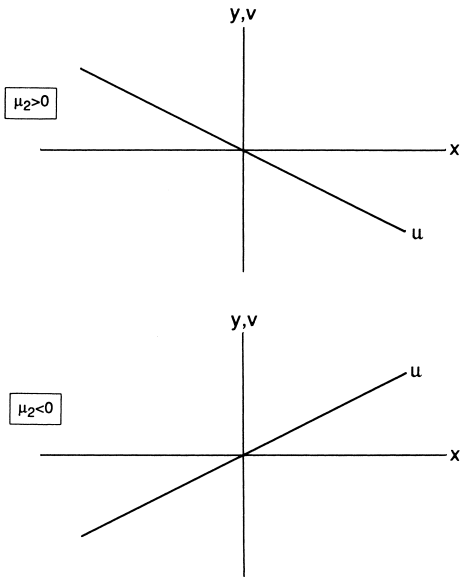

FIGURE 20.6.1.

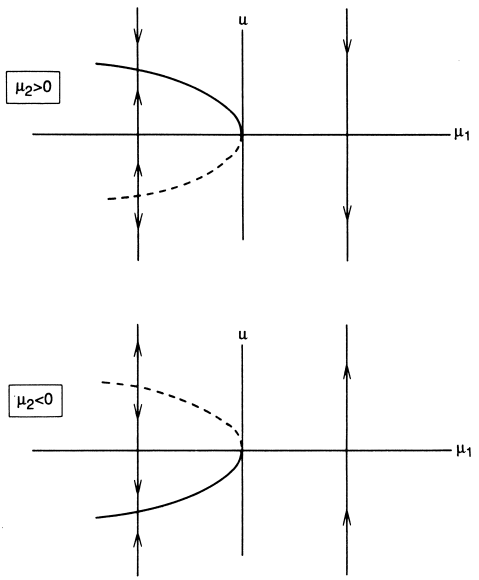

FIGURE 20.6.2.

In the cases μ_1 slightly negative, notice the reversals of position for the stable and unstable manifolds of the saddle for $\mu_2 > 0$ and $\mu_2 < 0$.

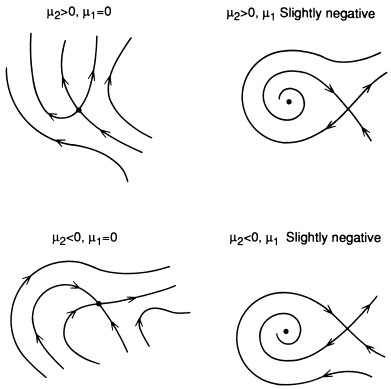

FIGURE 20.6.3.

We next examine the change of stability of the fixed points $(x^-, 0)$ on $\mu_2 = \sqrt{-\mu_1}$, $\mu_1 < 0$. From (20.6.15), the eigenvalues associated with the linearization about this curve of fixed points are

$$\lambda_{1,2} = \pm i\sqrt{2\sqrt{-\mu_1}}.$$

If we view μ_2 as a parameter, then using (20.6.15) we obtain

$$\frac{d}{d\mu_2}\mathrm{Re}\,\lambda_{1,2}\bigg|_{\mu_2=\sqrt{-\mu_1}} = \frac{1}{2} \neq 0.$$

Thus, it appears that a Poincaré-Andronov-Hopf bifurcation occurs on $\mu_2 = \sqrt{-\mu_1}$.

Next we check the stability of the bifurcating periodic orbits. Recall from Theorem 20.2.3 that this involves putting the equation in a certain "normal form" and then computing a coefficient, a, which is given by derivatives of functions occuring in this normal form.

First we transform the fixed point to the origin via

$$\begin{aligned}\bar{x} &= x - x^-,\\ \bar{y} &= y,\end{aligned}$$

so that (3.1.198) becomes

$$\begin{pmatrix}\dot{\bar{x}}\\ \dot{\bar{y}}\end{pmatrix} = \begin{pmatrix}0 & 1\\ -2\sqrt{-\mu_1} & 0\end{pmatrix}\begin{pmatrix}\bar{x}\\ \bar{y}\end{pmatrix} + \begin{pmatrix}0\\ \bar{x}\bar{y} + \bar{x}^2\end{pmatrix}. \tag{20.6.20}$$

Then we put the linear part of (20.6.20) in normal form via the linear transformation

$$\begin{pmatrix}\bar{x}\\ \bar{y}\end{pmatrix} = \begin{pmatrix}0 & 1\\ \sqrt{-2\sqrt{-\mu_1}} & 0\end{pmatrix}\begin{pmatrix}u\\ v\end{pmatrix}, \tag{20.6.21}$$

under which (20.6.20) becomes

$$\begin{pmatrix} \dot{u} \\ \dot{v} \end{pmatrix} = \begin{pmatrix} 0 & -\sqrt{-2\sqrt{-\mu_1}} \\ \sqrt{-2\sqrt{-\mu_1}} & 0 \end{pmatrix} \begin{pmatrix} u \\ v \end{pmatrix} + \begin{pmatrix} uv + \frac{1}{\sqrt{-2\sqrt{-\mu_1}}} v^2 \\ 0 \end{pmatrix}. \tag{20.6.22}$$

Notice that (20.6.23) is exactly in the form of (20.2.13), in which the coefficient a was given as follows

$$a = \frac{1}{16}\left[f_{uuu} + f_{uvv} + g_{uuv} + g_{vvv}\right] + \frac{1}{16\sqrt{-2\sqrt{-\mu_1}}}\left[f_{uv}(f_{uu} + f_{vv}) - g_{uv}(g_{uu} + g_{vv}) - f_{uu}g_{uu} + f_{vv}g_{vv}\right],$$

where all partial derivatives are evaluated at the origin. In our case,

$$f = uv + \frac{1}{\sqrt{-2\sqrt{-\mu_1}}} v^2,$$
$$g = 0;$$

thus, an easy calculation gives

$$a = \frac{1}{16\sqrt{-\mu_1}} > 0,$$

indicating a *subcritical* Poincaré-Andronov-Hopf bifurcation to an unstable periodic orbit below $\mu_2^2 = -\mu_1$.

This completes the local analysis, and we summarize the results in the bifurcation diagram in Figure 20.6.4.

Step 4c: Global Dynamics. At this stage we have analyzed all possible local bifurcations; however, a careful study of Figure 20.6.4 reveals that there must be additional bifurcations. This conclusion is based on the following facts.

1. Note the stable and unstable manifolds of the saddle point. For the case $\mu_2 > \sqrt{-\mu_1}$, $\mu_1 < 0$, the stable and unstable manifolds have the opposite "orientation" compared with the case $\mu_2 < 0$, $\mu_1 < 0$. It appears as if the manifolds have "passed through each other" as μ_2 decreases.

2. Using index theory, it is easy to verify that (20.6.12) ($b = +1$) has no periodic orbits for $\mu_1 > 0$ (since there are no fixed points in this region). Hence, in traversing the $\mu_1 - \mu_2$ plane in an arc around the origin starting on the curve $\mu_2 = -\mu_1^2$ and ending in $\mu_1 > 0$ (see Figure 20.6.5), we must somehow cross a bifurcation curve(s) which results in the annihilation of all periodic orbits. This cannot be a local bifurcation, because these have all been taken into account.

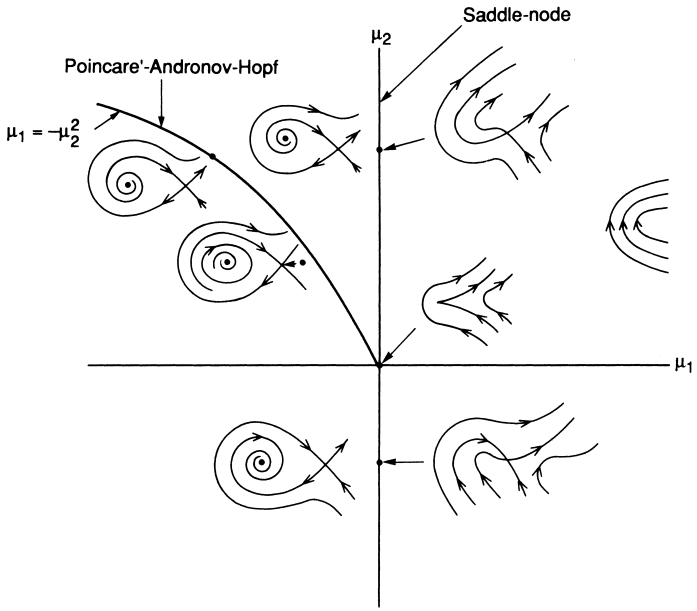

FIGURE 20.6.4.

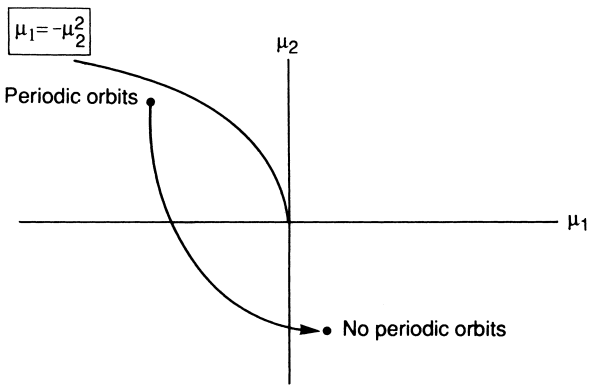

FIGURE 20.6.5.

Step 5: Analysis of Global Bifurcations. We postpone an analysis of the global bifurcation in this case until Volume 4 and merely state the result for now.

In this case a likely candidate for the global bifurcation which will complete the bifurcation diagram is a *saddle-connection* or *homoclinic bifurca-*

tion. In Chapter 33 we show that this occurs on the curve

$$\mu_1 = -\frac{49}{25}\mu_2^2 + \mathcal{O}(\mu_2^{5/2}),$$

which we shown in Figure 20.6.6. From this figure one can see that the saddle-connection or homoclinic bifurcation is described by the periodic orbit created in the subcritical Poincaré-Andronov-Hopf bifurcation growing in amplitude as μ_2 is decreased until it collides with the saddle point, creating a homoclinic orbit. As μ_2 is further decreased, the homoclinic orbit breaks. This explains the reversal in orientation of the stable and unstable manifolds of the saddle point described above, and it also explains how the periodic orbits created in the subcritical Poincaré-Andronov-Hopf bifurcation are destroyed.

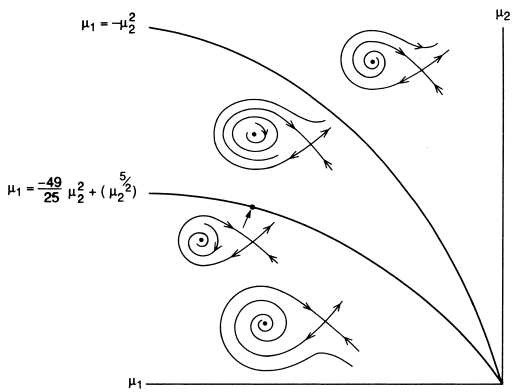

FIGURE 20.6.6.

Step 6: Effects of Higher Order Terms in the Normal Form. Takens [1974] and Bogdanov [1975] proved that the dynamics of (20.6.12) are not qualitatively changed by the higher order terms in the normal form. Hence, (20.6.12) is a versal deformation. We will discuss the issues involved with proving this more thoroughly in Chapter 33. For this reason, the bifurcation associated with the non-semisimple souble zero eigenvalue is often referred to as the *Takens-Bogdanov bifurcation.*

This completes our analysis of the case $b = +1$; the case $b = -1$ is very similar, so we leave it as an exercise. Before leaving the double-zero eigenvalue, we want to make some final remarks.

Remark 1. The reader should note the generality of this analysis. The normal form is completely determined by the structure of the linear part of the vector field.

Remark 2. Global dynamics arose from a local bifurcation analysis. For two-dimensional vector fields these dynamics cannot be very complicated, but for three-dimensional vector fields chaotic dynamics may occur.

Remark 3. When one speaks of the "double-zero eigenvalue" for vector fields, one usually means a vector field whose linear part (in Jordan canonical form) is given by

$$\begin{pmatrix} 0 & 1 \\ 0 & 0 \end{pmatrix}.$$

However, the linear part

$$\begin{pmatrix} 0 & 0 \\ 0 & 0 \end{pmatrix}$$

is also a double-zero eigenvalue. This case is *codimension 4* and is consequently more difficult to analyze.

20.6A Additional References and Applications for the Takens-Bogdanov Bifurcation

The Takens-Bogdanov bifurcation arises in a variety of applications and is still a current topic of research. Recent references are Kertesz [2000], Belhaq et al. [2000], Algaba et al. [1998], [1999a,b,c,d], Batiste et al. [1999], Renardy et al. [1999], Champneys et al. [1999], Ramanan et al. [1999], Nikolaev et al. [1999], Degtiarev et al. [1998], Needham and McAllister [1998], Skeldon and Moroz [1998], Tracy and Tang [1998], Tracy et al. [1998], Kertesz [1997], Golubitsky et al. [1997], and Labate et al. [1997].

20.6B Exercises

1. *The Double-Zero Eigenvalue with Symmetry.* Consider a $\mathbf{C}^r$ (r as large as necessary) vector field on $\mathbb{R}^2$ having a fixed point at which the matrix associated with the linearization has the following Jordan canonical form

$$\begin{pmatrix} 0 & 1 \\ 0 & 0 \end{pmatrix}.$$

Let (x, y) denote coordinates on $\mathbb{R}^2$, and suppose further that the vector field is equivariant under the coordinate transformation

$$(x, y) \mapsto (-x, -y).$$

This exercise is concerned with the bifurcations near such a degenerate fixed point.

a) Show that a normal form for this vector field near this nonhyperbolic fixed point is given by

$$\begin{aligned} \dot{x} &= y + \mathcal{O}(5), \\ \dot{y} &= ax^3 + bx^2y + \mathcal{O}(5). \end{aligned}$$

b) Following the procedure described earlier, show that a candidate for a versal deformation is given by

$$\begin{aligned} \dot{x} &= y + \mathcal{O}(5), \\ \dot{y} &= \mu_1 x + \mu_2 y + ax^3 + bx^2y + \mathcal{O}(5). \end{aligned}$$

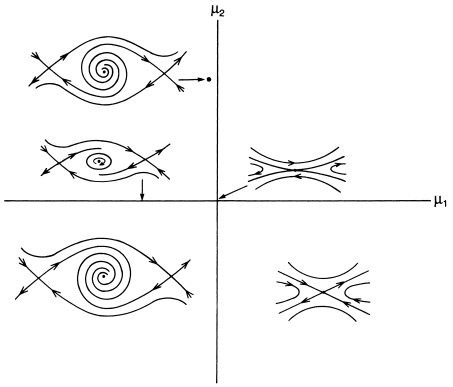

FIGURE 20.6.7.

In the following we will be concerned with the dynamics of the truncated normal form

$$\begin{aligned} \dot{x} &= y, \\ \dot{y} &= \mu_1 x + \mu_2 y + a x^3 + b x^2 y. \end{aligned}$$

c) Show that by rescaling, the number of cases to be considered can be reduced to the following

$$\begin{aligned} \dot{x} &= y, \\ \dot{y} &= \mu_1 x + \mu_2 y + c x^3 - x^2 y, \end{aligned} \tag{20.6.23}$$

where $c = \pm 1$.

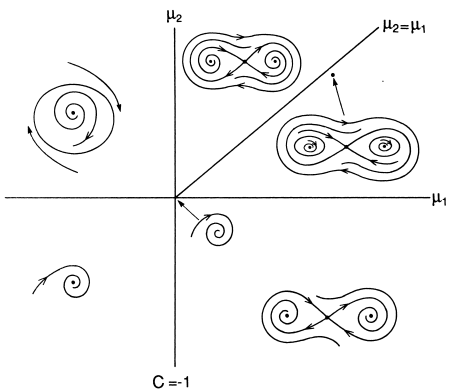

FIGURE 20.6.8.

d) For $\mu_1 = \mu_2 = 0$, show that the flow near the origin appears as in Figure 20.6.7 for $c = +1$ and as in Figure 20.6.8 for $c = -1$.

e) Show that (20.6.23) has the following fixed points

$$\begin{array}{ll} \underline{c = +1}: & (0,0), \quad (\pm\sqrt{-\mu_1}, 0), \\ \underline{c = -1}: & (0,0), \quad (\pm\sqrt{\mu_1}, 0). \end{array}$$

f) Compute the linearized stability for the fixed points for both $c = +1$ and $c = -1$ and show that the following bifurcations occur.

$$\underline{c = +1}: \quad \begin{array}{l} \text{pitchfork} \quad \text{on } \mu_1 = 0, \\ \text{supercritical Poincaré–Andronov–Hopf} \\ \quad \text{on } \mu_1 < 0,\ \mu_2 = 0. \end{array}$$

$$\underline{c = -1}: \quad \begin{array}{l} \text{pitchfork} \quad \text{on } \mu_1 = 0, \\ \text{subcritical Poincaré–Andronov–Hopf} \\ \quad \text{on } \mu_1 = \mu_2,\ \mu_1 > 0. \end{array}$$

g) Show that (20.6.23) has no periodic orbits for

$$\underline{c = +1}: \quad \begin{array}{l} \mu_1 > 0; \\ \mu_1 < 0,\ \mu_2 < 0; \\ \mu_2 > -\mu_1/5,\ \mu_1 < 0. \end{array}$$

$$\underline{c = -1}: \quad \mu_2 < 0.$$

(*Hint:* use Bendixson's criterion and index theory.)

h) Use the results obtained in d) $\rightarrow$ e) and *completely justify* the local bifurcation diagrams shown in Figure 20.6.7 for $c = +1$ and in Figure 20.6.8 for $c = -1$.

i) Based on an examination of Figures 20.6.7 and 20.6.8, can you infer the necessity of the existence of global bifurcations? What scenarios are most likely?

We will return to this exercise in Chapter 33 to study possible global bifurcations in more detail.

2. The averaged equations for the forced van der Pol oscillator (See Holmes and Rand [1978]) are given by:

$$\begin{aligned} \dot{u} &= u - \sigma v - u(u^2 + v^2), \\ \dot{v} &= \sigma u + v - v(u^2 + v^2) - \gamma. \end{aligned} \tag{20.6.24}$$

Consider the bifurcation diagram in Figure 20.6.9.

The object of this exercise is to derive the bifurcation diagram.

a) Show that (20.6.24) has a single fixed point in regions I and III (a sink in I, a source in III). Show that in region II there are two sinks and a saddle, and in region IVa $\cup$ IVb there is a sink, a saddle, and a source.

b) Show that (20.6.24) undergoes a saddle-node bifurcation on

$$\frac{\gamma^4}{4} - \frac{\gamma^2}{27}(1 + 9\sigma^2) + \frac{\sigma^2}{27}(1 + \sigma^2)^2 = 0.$$

This is the curve DAC marked B_S in Figure 20.6.9.

c) Show that (20.6.24) undergoes a Poincaré–Andronov–Hopf bifurcation on

$$8\gamma^2 = 4\sigma^2 + 1, \qquad |\sigma| > \frac{1}{2}.$$

This is the curve OE marked B_H in Figure 20.6.9.

d) In Figure 20.6.9, consider the broken lines $- - -$ crossing the curves OA, OD, AB, BE, and OB. Draw phase portraits representing the flow on and to each side of the indicated curve; see the example in Figure 20.6.9.

e) OS is a curve on which homoclinic orbits occur (sometimes called saddle connections). Give an intuitive argument as to why such a curve should exist. (Is it obvious that it should be a smooth curve?)

f) Discuss the nature of (20.6.24) near the points A, O, and C.

g) (20.6.24) is an autonomous equation whose flow gives an approximation to the Poincaré map of the original forced van der Pol equation in a sense made precise by the averaging theorem. Using the previously obtained results, interpret Parts i) $\rightarrow$ vi) in terms of the dynamics of the original forced van der Pol equation. In particular, list the structurally stable motions and bifurcations along with the structurally unstable bifurcations.

If you need help you may consult Holmes and Rand [1978], where these results were first worked out.

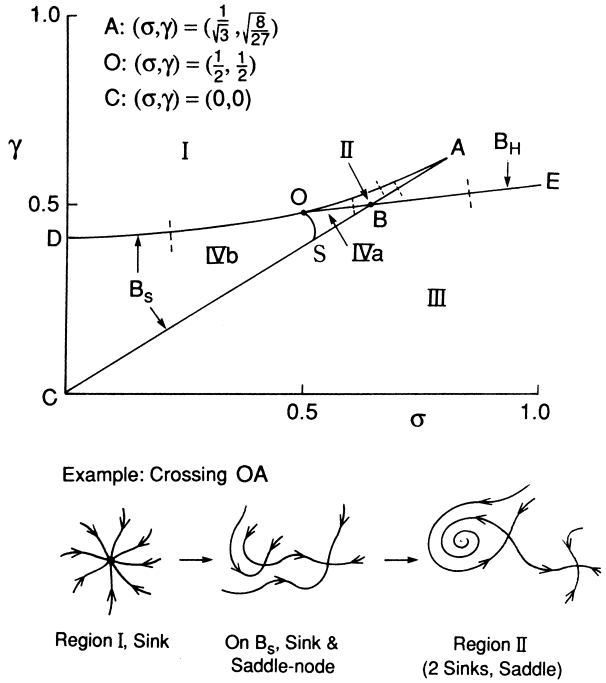

FIGURE 20.6.9.

20.7 A Zero and a Pure Imaginary Pair of Eigenvalues: the Hopf-Steady State Bifurcation

Suppose that the linear part of the vector field (after a possible center manifold reduction) has the following form

$$\begin{pmatrix} 0 & -\omega & 0 \\ \omega & 0 & 0 \\ 0 & 0 & 0 \end{pmatrix} \begin{pmatrix} x \\ y \\ z \end{pmatrix}. \tag{20.7.1}$$

The bifurcation associated with this nonhyperbolic equilibrium point is sometimes referred to as the *Hopf-steady state bifurcation*, since it is a combination of a Hopf bifurcation (i.e, there is a pure imaginary pair of eigenvalues) and a steady state bifurcation (i.e., a zero eigenvalue associated with a bifurcation of an equilibrium point, or "steady state").

The normal form for this case is given by:

$$\begin{aligned} \dot{r} &= a_1 rz + a_2 r^3 + a_3 rz^2 + \mathcal{O}(|r|^4, |z|^4), \\ \dot{z} &= b_1 r^2 + b_2 z^2 + b_3 r^2 z + \mathcal{O}(|r|^4, |z|^4), \\ \dot{\theta} &= \omega + c_1 z + \mathcal{O}(|r|^2, |z|^2), \end{aligned} \tag{20.7.2}$$

(see Exercise 5 in Section 19.4 in Chapter 19). This is the vector field we will study. Notice that the θ-dependence in the r and z components of the vector field can be removed to order k for k arbitrarily large (note: exactly the same thing occurred when analyzing the normal form for the Poincaré-Andronov-Hopf bifurcation). This is important. because it is a major tool in facilitating the analysis of this system. Specifically, recall that our analysis is only local (i.e., r, z sufficiently small), so that we have, for r, z sufficiently small, $\dot{\theta} \neq 0$. Thus, we will truncate our equation at some order and, ignoring the $\dot{\theta}$ part of our vector field, perform a phase plane analysis on the r, z part of the vector field. For r, z sufficiently small, in some sense (to be made precise later) the $r - z$ phase plane can be thought of as a Poincaré map for the full three-dimensional system. Also, we must consider the effects of higher order terms on our analysis, since it is not necessarily true that in the actual vector field the (r, z) components are independent of θ; we only push the θ-dependence up to higher order with the method of normal forms.

Our analysis will follow the same steps as our analysis of the double-zero eigenvalue in Section 20.6.

Step 1: Compute and Truncate the Normal Form. The normal form is given by (20.7.2). For now we will neglect terms of $\mathcal{O}(3)$ and higher and, as described above, the $\dot{\theta}$ component of (20.7.2). Thus, the vector field we will study is

$$\begin{aligned} \dot{r} &= a_1 r z, \\ \dot{z} &= b_1 r^2 + b_2 z^2. \end{aligned} \tag{20.7.3}$$

Step 2: Rescaling to Reduce the Number of Cases. Rescaling by letting $\bar{r} = \alpha r$ and $\bar{z} = \beta z$, we obtain

$$\dot{\bar{r}} = \alpha \left[a_1 \frac{\bar{r}\bar{z}}{\alpha\beta} \right],$$

$$\dot{\bar{z}} = \beta \left[\frac{b_1}{\alpha^2} \bar{r}^2 + \frac{b_2}{\beta^2} \bar{z}^2 \right].$$

Now, letting $\beta = -b_2$, $\alpha = -\sqrt{|b_1 b_2|}$, and dropping the bars on $\bar{r}, \bar{z}$, we obtain

$$\begin{aligned} \dot{r} &= -\frac{a_1}{b_2} r z, \\ \dot{z} &= \frac{-b_1 b_2}{|b_1 b_2|} r^2 - z^2, \end{aligned}$$

or

$$\begin{aligned} \dot{r} &= a r z, \\ \dot{z} &= b r^2 - z^2, \end{aligned} \tag{20.7.4}$$

where $a = \frac{-a_1}{b_2}$ is arbitrary (except that it is nonzero and bounded) and $b = \pm 1$.

Next we want to determine the topologically distinct phase portraits of (20.7.4) which occur for the various choices of a and b. We will find that there are six different types, which (following Guckenheimer and Holmes [1983]) we label I, IIa, IIb, III, IVa, IVb, because the versal deformation of IIa and IIb as well as the versal deformation of IVa and IVb are essentially the same.

The key idea in determining these classifications involves finding certain invariant lines (separatrices) for the flow given by $z = kr$ (note that $r \geq 0$). Substituting this into our equation gives

$$\frac{dz}{dr} = k = \frac{br^2 - k^2 r^2}{akr^2} = \frac{b - k^2}{ak}$$

or

$$k = \pm\sqrt{\frac{b}{a+1}}; \tag{20.7.5}$$

hence, the condition for such invariant lines to exist is $\frac{b}{a+1} > 0$.

Note that $r = 0$ is always invariant, and the equation is invariant under the transformation $z \to -z$, $t \to -t$.

Therefore, for $b = 1$ there are two distinct cases

$$a \leq -1, \qquad a > -1,$$

and, for $b = -1$, there are two distinct cases

$$a < -1, \qquad a \geq -1.$$

The direction of the flow on these invariant lines can be calculated by taking the dot product of the vector field with a radial vector field evaluated on the invariant line.

$$\begin{aligned} s &\equiv (arz, br^2 - z^2) \cdot (r, z)\big|_{z=kr} \\ &= r^3 k(a + b - k^2). \end{aligned} \tag{20.7.6}$$

Substituting (20.7.5) into (20.7.6) (and taking the '+' sign in (20.7.5), which will give the direction of flow along $z = kr$ in the first quadrant) gives

$$s = \frac{ar^2 z}{1+a}(a + b + 1). \tag{20.7.7}$$

If this quantity s is > 0 (take $z, k > 0$), then the flow is directed radially outward for $z > 0$. If $s < 0$, then the flow is directed inward for $z > 0$. The opposite case occurs for $z, k < 0$. We summarize this information below.

$\underline{b = +1,\ a \leq -1}$. There are no invariant lines except $r = 0$.

$b = +1,\ a > -1$. From (20.7.5) we see that, in this case, we do have an invariant line and, from (20.7.7), that the direction of flow along this line is governed by the sign of

$$\frac{a}{1+a}.$$

Hence, we have two cases

$$\frac{a}{1+a} > 0 \qquad \text{for} \quad a > 0,$$

$$\frac{a}{1+a} < 0 \qquad \text{for} \quad -1 < a < 0.$$

We will not consider the degenerate $a = 0$ case, since this will necessitate the consideration of higher order terms in the normal form.

$b = -1,\ a \geq -1$. There are no invariant lines except $r = 0$.

$b = -1,\ a < -1$. From (20.7.5) and (20.7.7) we see that, in this case, we do have an invariant line with $s < 0$.

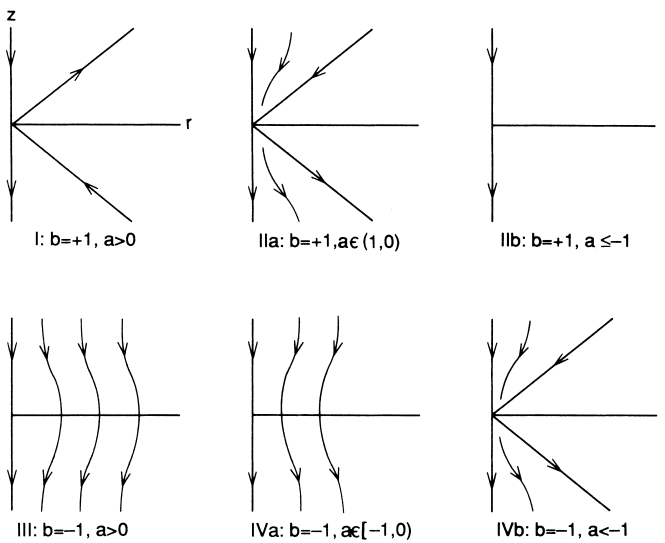

FIGURE 20.7.1.

We summarize the information obtained concerning the orbit structure of (20.7.4) in Figure 20.7.1. There are thus six topologically distinct cases. However, we are still not quite finished with their phase portraits. Notice that (20.7.4) has the first integral

$$I(r,z) = \frac{a}{2} r^{2/a} \left[\frac{br^2}{1+a} - z^2 \right]. \tag{20.7.8}$$

The reader can check this by showing

$$\frac{\partial I}{\partial r}\dot{r} + \frac{\partial I}{\partial z}\dot{z} = 0,$$

where $\dot{r}$ and $\dot{z}$ are obtained from (20.7.4).

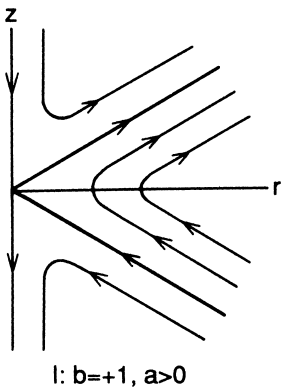

FIGURE 20.7.2.

Now this first integral can give us information concerning whether or not there are closed orbits in our phase portraits and, of course, the level curves give us all the trajectories. We will thus examine the level curves of $I(r, z)$ for each of our six cases. Also, we will only analyze the $r \geq 0$, $z \geq 0$ quadrant of the (r, z) plane, since knowledge of the flow in this quadrant is sufficient due to the symmetry $z \to -z$, $t \to -t$.

Case I. We begin with Case I for which we have $b = +1$ and $a > 0$, which implies that $k = \sqrt{\frac{1}{1+a}} < 1$.

Recall that, in this case, the vector field is given by

$$\dot{r} = arz,$$
$$\dot{z} = r^2 - z^2,$$

from which we see that, in $r \geq 0$, $z \geq 0$, we have

$$\dot{r} > 0 \Rightarrow r \qquad \text{is increasing on orbits,}$$

$$\dot{z} = 0 \qquad \text{on the line} \quad r = z.$$

For $z > 0, z$ below the line $r = z$, we have $\dot{z} > 0$, which implies that z is increasing on orbits with initial z values below the line $r = z$. The opposite conclusion holds for orbits starting above $r = z$. Also, since the line $z = kr$ is invariant and thus cannot be crossed by trajectories, and since $z = kr$

lies below $z = r$, we conclude that trajectories below the line $z = kr$ must have z and r components increasing montonically. These observations allow us to sketch the phase portrait shown in Figure 20.7.2.

Case IIa. We have $b = +1$, $a \in (-1, 0)$, which implies $k = \sqrt{\frac{1}{1+a}} > 1$.

1. In this case the line $z = r$ lies below the invariant line $z = kr$; therefore, the only place where $\dot{z}$ can vanish (besides the origin) is below $z = kr$.

2. Also, due to the fact that $a \in (-1, 0)$, in the quadrant $r > 0$, $z > 0$, we always have $\dot{r} < 0$; hence, r is always decreasing on orbits.

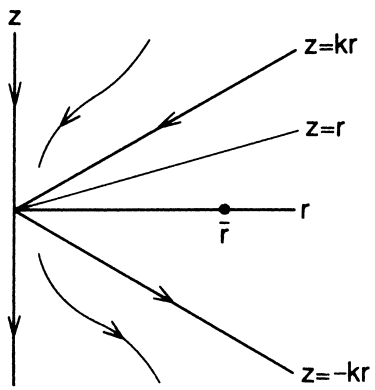

FIGURE 20.7.3.

Now we will consider our first integral

$$I(r, z) = \frac{a}{2} r^{2/a} \left[\frac{r^2}{1+a} - z^2 \right].$$

The level curves of this function are trajectories of (20.7.4). The following lemma will prove useful.

Lemma 20.7.1 *A level curve of $I(r, z)$ may intersect the line $z = r$ only once in $r > 0$, $z > 0$.*

Proof: At this stage of our analysis of Case IIa the orbit structure shown in Figure 20.7.3 has been verified. Note that at the point $(\bar{r}, 0)$ shown in Figure 20.7.3 we have

$$\dot{r} = 0, \qquad \dot{z} = \bar{r}^2 \qquad \text{at} \quad (\bar{r}, 0).$$

By the comments 1 and 2 above, since $\dot{r} < 0$ everywhere in $z > 0$, $r > 0$, and $\dot{z} > 0$ at $(\bar{r}, 0)$, the trajectory starting at $(\bar{r}, 0)$ must eventually cross the line $z = r$.

Now the trajectory starting at $(\bar{r}, 0)$ lies on the level curve given by

$$I(\bar{r}, 0) = \frac{a\bar{r}^{2+\frac{2}{a}}}{2(1+a)} \equiv \bar{c}. \tag{20.7.9}$$

It intersects the line $z = r$, and we can compute the r coordinate of the intersection as follows on $z = r$

$$\begin{aligned} I(r, r) = \bar{c} &= \frac{a}{2} r^{2/a} \left[\frac{r^2}{1+a} - \frac{r^2(1+a)}{1+a} \right] \\ &= \frac{a}{2} r^{2/a} \left[-\frac{ar^2}{1+a} \right] = -\frac{a^2}{2(1+a)} r^{2+(2/a)}. \end{aligned} \tag{20.7.10}$$

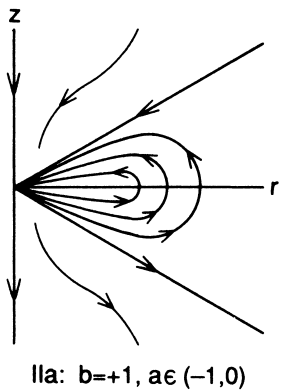

FIGURE 20.7.4.

We can compute the r coordinate of the intersection point in terms of the starting point $\bar{r}$ by equating (20.7.9) and (20.7.10)

$$-\frac{a^2}{2(1+a)} r^{2+(2/a)} = \frac{a\bar{r}^{2+(2/a)}}{2(1+a)},$$

and solving for

$$r = \left(-\frac{1}{a} \right)^{a/(2a+2)} \bar{r}.$$

Thus, given $(\bar{r}, 0)$ as an initial condition for a trajectory, we conclude that this trajectory can intersect the line $z = r$ only at the unique value of r given above (and hence also at a unique value of z). This proves the lemma. □

This lemma therefore tells us that once a trajectory crosses the $z = r$ line it is forever trapped between the lines $z = r$, $z = kr$ and, since $\dot{r} < 0$, it must approach $(0, 0)$ asymptotically. Putting together these results and using the symmetry $z \to -z$, $t \to -t$, we obtain the phase portrait for Case IIa shown in Figure 20.7.4.

Case IIb. There are no invariant lines in this case; however, the arguments given in Case IIa can be slightly modified to yield the phase portrait shown in Figure 20.7.5.

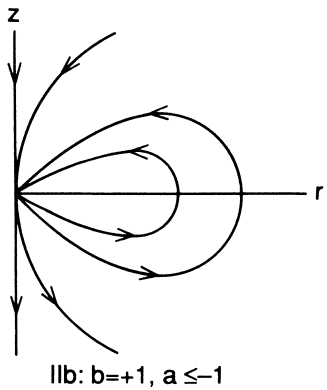

FIGURE 20.7.5.

We now proceed to the $b = -1$ cases. In these cases z is always decreasing.

Cases III and IVa. These cases are easy since there are no invariant lines; hence, there is no additional orbit structure beyond that shown in Figure 20.7.1 (note: the reader should verify the different "dimples" exhibited by phase curves in these figures upon crossing the r-axis).

Case IVb. We have $b = -1$ and $a < -1$ with $k = \sqrt{\frac{-1}{1+a}}$. Since $\dot{z}$ is decreasing and $\dot{r}$ is decreasing we have the phase portrait shown in Figure 20.7.6. This completes the classification of the possible local phase portraits. We now show them together in Figure 20.7.7 for comparative purposes.

Step 3: Construct a Candidate for a Versal Deformation. From Section 20.4 and, in particular, Example 20.5.6 from Section 20.5, a candidate for a versal deformation is given by

$$\begin{aligned} \dot{r} &= \mu_1 r + arz, \\ \dot{z} &= \mu_2 + br^2 - z^2, \qquad b = \pm 1. \end{aligned} \tag{20.7.11}$$

Step 4: Study the Local Dynamics of (20.7.11).

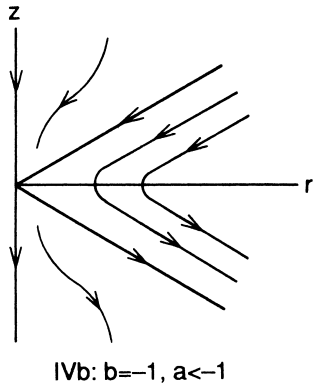

FIGURE 20.7.6.

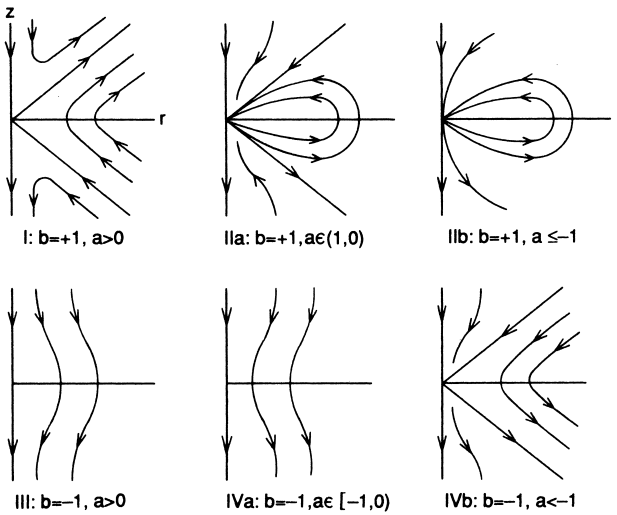

FIGURE 20.7.7.

Step 4a. Fixed Points and Their Stability. It is easy to see that there are three branches of fixed points of (20.7.11) given by

$$(r, z) = (0, \pm\sqrt{\mu_2}),$$
$$(r, z) = \left(\sqrt{\frac{1}{b}(\frac{\mu_1^2}{a^2} - \mu_2)}, \frac{-\mu_1}{a}\right) \tag{20.7.12}$$

(note: $r \geq 0$).

We next examine the stability of these fixed points. The matrix associ-

ated with the linearized vector field is given by

$$J = \begin{pmatrix} \mu_1 + az & ar \\ 2br & -2z \end{pmatrix}. \tag{20.7.13}$$

Before analyzing the stability of each branch of fixed points, we want to work out a general result that will save much time.

The eigenvalues of (20.7.13) are given by

$$\lambda_{1,2} = \frac{\operatorname{tr} J}{2} \pm \frac{1}{2}\sqrt{(\operatorname{tr} J)^2 - 4 \det J}. \tag{20.7.14}$$

Using (20.7.14), we notice the following facts

$$\begin{aligned}
&\text{if } \operatorname{tr} J > 0,\ \det J > 0, && \text{then } \lambda_1 > 0, \lambda_2 > 0 \Rightarrow \text{ source},\\
&\text{if } \operatorname{tr} J > 0,\ \det J < 0, && \text{then } \lambda_1 > 0, \lambda_2 < 0 \Rightarrow \text{ saddle},\\
&\text{if } \operatorname{tr} J < 0,\ \det J > 0, && \text{then } \lambda_1 < 0, \lambda_2 < 0 \Rightarrow \text{ sink},\\
&\text{if } \operatorname{tr} J < 0,\ \det J < 0, && \text{then } \lambda_1 > 0, \lambda_2 < 0 \Rightarrow \text{ saddle},\\
&\text{if } \operatorname{tr} J = 0,\ \det J < 0, && \text{then } \lambda_{1,2} = \pm\sqrt{|\det J|} \Rightarrow \text{ saddle},\\
&\text{if } \operatorname{tr} J = 0,\ \det J > 0, && \text{then } \lambda_{1,2} = \pm i\sqrt{|\det J|}, \Rightarrow \text{ center},\\
&\text{if } \operatorname{tr} J > 0,\ \det J = 0, && \text{then } \lambda_1 = \operatorname{tr} J, \lambda_2 = 0,\\
&\text{if } \operatorname{tr} J < 0,\ \det J = 0, && \text{then } \lambda_1 = \operatorname{tr} J, \lambda_2 = 0.
\end{aligned} \tag{20.7.15}$$

We now analyze each branch of fixed points individually.

$\underline{(0, \sqrt{\mu_2})}$. On this branch of fixed points we have

$$\begin{aligned}
\operatorname{tr} J &= (\mu_1 + a\sqrt{\mu_2}) - 2\sqrt{\mu_2},\\
\det J &= -2\sqrt{\mu_2}(\mu_1 + a\sqrt{\mu_2}),
\end{aligned}$$

from which we conclude

$$\begin{aligned}
\operatorname{tr} J > 0 \Rightarrow &\quad \mu_1 + a\sqrt{\mu_2} > 2\sqrt{\mu_2},\\
\operatorname{tr} J < 0 \Rightarrow &\quad \mu_1 + a\sqrt{\mu_2} < 2\sqrt{\mu_2},\\
\det J > 0 \Rightarrow &\quad \mu_1 + a\sqrt{\mu_2} < 0,\\
\det J < 0 \Rightarrow &\quad \mu_1 + a\sqrt{\mu_2} > 0.
\end{aligned}$$

Appealing to (20.7.14) and using (20.7.15), we make the following con-

clusions concerning stability of the branch of fixed points $(0, \sqrt{\mu_2})$

$$\begin{aligned}
&\operatorname{tr} J > 0,\ \det J > 0, && \text{cannot occur,}\\
&\text{if } \operatorname{tr} J > 0,\ \det J < 0, && \text{then } \mu_1 + a\sqrt{\mu_2} > 2\sqrt{\mu_2} \Rightarrow \text{ saddle,}\\
&\text{if } \operatorname{tr} J < 0,\ \det J > 0, && \text{then } \mu_1 + a\sqrt{\mu_2} < 0 \Rightarrow \text{ sink,}\\
&\text{if } \operatorname{tr} J < 0,\ \det J < 0, && \text{then } 0 < \mu_1 + a\sqrt{\mu_2} < 2\sqrt{\mu_2},\\
&\text{if } \operatorname{tr} J = 0,\ \det J < 0, && \text{then } \begin{matrix}\mu_1 + a\sqrt{\mu_2} = 2\sqrt{\mu_2}\\ \mu_1 + a\sqrt{\mu_2} > 0\end{matrix} \Rightarrow \text{ saddle,}\\
&\operatorname{tr} J = 0,\ \det J > 0, && \text{cannot occur,}\\
&\text{if } \operatorname{tr} J > 0,\ \det J = 0, && \mu_2 = 0, \mu_1 > 0 \Rightarrow \text{ bifurcation,}\\
&\text{if } \operatorname{tr} J < 0,\ \det J = 0, && \text{then } \mu_1 + a\sqrt{\mu_2} = 0 \text{ or } \mu_2 = 0,\\
& && \mu_1 < 0 \Rightarrow \text{ bifurcation.}
\end{aligned}$$

Thus, $(0, \sqrt{\mu_2})$ is a

$$\begin{aligned}
&\text{sink} && \text{for } \mu_1 + a\sqrt{\mu_2} < 0,\\
&\text{saddle} && \text{for } \mu_1 + a\sqrt{\mu_2} > 0.
\end{aligned}$$

Later we will examine the nature of the bifurcation occurring on $\mu_1 + a\sqrt{\mu_2} = 0$ and $\mu_2 = 0$.

Next we examine the branch $(0, -\sqrt{\mu_2})$.

$\underline{(0, -\sqrt{\mu_2})}$. On this branch we have

$$\begin{aligned}
\operatorname{tr} J &= \mu_1 - a\sqrt{\mu_2} + 2\sqrt{\mu_2},\\
\det J &= 2\sqrt{\mu_2}(\mu_1 - a\sqrt{\mu_2}),
\end{aligned}$$

from which we conclude

$$\begin{aligned}
\operatorname{tr} J > 0 &\Rightarrow\ \mu_1 - a\sqrt{\mu_2} > -2\sqrt{\mu_2},\\
\operatorname{tr} J < 0 &\Rightarrow\ \mu_1 - a\sqrt{\mu_2} < -2\sqrt{\mu_2},\\
\det J > 0 &\Rightarrow\ \mu_1 - a\sqrt{\mu_2} > 0,\\
\det J < 0 &\Rightarrow\ \mu_1 - a\sqrt{\mu_2} < 0.
\end{aligned}$$

Appealing to (20.7.14) and using (20.7.15), we make the following con-

clusions concerning the stability of the branch of fixed points $(0, -\sqrt{\mu_2})$:

if $\operatorname{tr} J > 0,\ \det J > 0,$ then $\mu_1 - a\sqrt{\mu_2} > 0 \Rightarrow$ source,

if $\operatorname{tr} J > 0,\ \det J < 0,$ then $0 > \mu_1 - a\sqrt{\mu_2} > -2\sqrt{\mu_2} \Rightarrow$ saddle,

$\operatorname{tr} J < 0,\ \det J > 0,$ cannot occur,

if $\operatorname{tr} J < 0,\ \det J < 0,$ then $\mu_1 - a\sqrt{\mu_2} < -2\sqrt{\mu_2} \Rightarrow$ saddle,

$\operatorname{tr} J = 0,\ \det J > 0$ cannot occur,

if $\operatorname{tr} J = 0,\ \det J < 0,$ then $\mu_1 - a\sqrt{\mu_2} = -2\sqrt{\mu_2} \Rightarrow$ saddle,

if $\operatorname{tr} J > 0,\ \det J = 0,$ then $\mu_1 = a\sqrt{\mu_2} \Rightarrow$ bifurcation,

$\operatorname{tr} J < 0,\ \det J = 0$ cannot occur.

We thus conclude that $(0, -\sqrt{\mu_2} > 0)$ has the following stability characteristics.

source for $\mu_1 - a\sqrt{\mu_2} > 0$,
saddle for $\mu_1 - a\sqrt{\mu_2} < 0$.

Later we will examine the bifurcation occuring on $\mu_1 - a\sqrt{\mu_2} = 0$.

Now we turn to an examination of the remaining branch of fixed points (note that our previous analysis did not depend on b)

$$(r, z) = \left(\sqrt{\frac{1}{b}\left(\frac{\mu_1^2}{a^2} - \mu_2\right)}, \frac{-\mu_1}{a} \right).$$

We examine the cases $b = +1$ and $b = -1$ separately.

$b = +1$, $\left(\sqrt{\dfrac{\mu_1^2}{a^2} - \mu_2}, \dfrac{-\mu_1}{a} \right)$. This branch exists only for $\dfrac{\mu_1^2}{a^2} > \mu_2$, and on this branch we have

$$\operatorname{tr} J = \frac{2\mu_1}{a}, \tag{20.7.16}$$

$$\det J = -2a\left(\frac{\mu_1^2}{a^2} - \mu_2\right). \tag{20.7.17}$$

We now must consider Cases I and IIa and b individually.

Case I: $a > 0$. From (20.7.17), for $a > 0$ we have $\det J \leq 0$. Using (20.7.15), for $\det J \leq 0$, the fixed point is always a saddle.

Cases IIa,b: $a < 0$. From (20.7.17), for $a < 0$ we have $\det J \geq 0$. Hence, using (20.7.15), we conclude the following

$$\mu_1 > 0, \qquad \frac{\mu_1^2}{a^2} - \mu_2 > 0 \Rightarrow \text{ source},$$
$$\mu_1 < 0, \qquad \frac{\mu_1^2}{a^2} - \mu_2 > 0 \Rightarrow \text{ sink}.$$

We might guess that on $\mu_1 = 0$, $\mu_2 < 0$, a Poincaré-Andronov-Hopf bifurcation occurs.

Next we examine the case $b = -1$.

$b = -1$, $\left(\sqrt{\mu_2 - \dfrac{\mu_1^2}{a^2}}, \dfrac{-\mu_1}{a}\right)$. For this case we have

$$\operatorname{tr} J = \frac{2\mu_1}{a}, \tag{20.7.18}$$
$$\det J = 2a\left(\mu_2 - \frac{\mu_1^2}{a^2}\right). \tag{20.7.19}$$

(Note that $\mu_2 - \dfrac{\mu_1^2}{a^2} \geq 0$.)

We will examine Cases III and IVa and b individually.

Case III: $a > 0$. Using (20.7.19), it follows that $\det J \geq 0$ which, when used with (20.7.18) and (20.7.15), allows us to conclude that

$$\mu_1 > 0 \Rightarrow \text{ source},$$
$$\mu_1 < 0 \Rightarrow \text{ sink}.$$

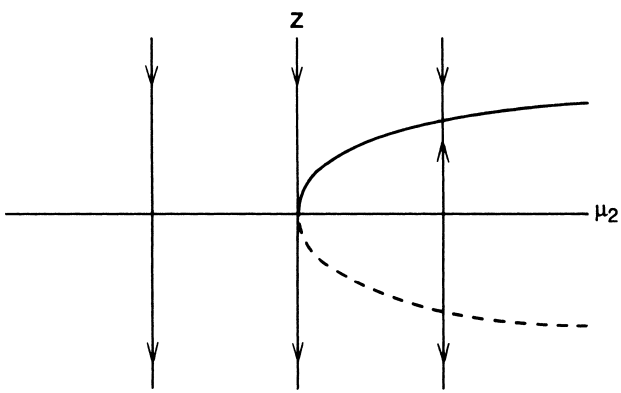

FIGURE 20.7.8.

Hence, we might guess that a Poincaré-Andronov-Hopf bifurcation is possible on $\mu_1 = 0$, $\mu_2 > 0$.

Cases IVa,b: $a < 0$. Using (20.7.19), we see that $\det J \leq 0$, which, when used with (20.7.18) and (20.7.15), allows us to conclude that

$$\begin{aligned} \mu_1 < 0 &\Rightarrow \text{ saddle,} \\ \mu_1 > 0 &\Rightarrow \text{ saddle.} \end{aligned}$$

Hence, no Poincaré-Andronov-Hopf bifurcations occur.

This completes the stability analysis of the fixed points. We next examine the nature of the various possible bifurcations.

Step 4b: The Bifurcations of the Fixed Points. First we examine the two branches

$$(0, \pm\sqrt{\mu_2}) .$$

These branches exist only for $\mu_2 \geq 0$, coalescing at $\mu_2 = 0$. We thus expect them to bifurcate from $(0, 0)$ in a *saddle-node* bifurcation. Since these branches start on $r = 0$ and remain on $r = 0$, the center manifold analysis is particulary simple—we simply set $r = 0$ in our original equations and obtain

$$\dot{z} = \mu_2 - z^2.$$

(Note that the equation is independent of b with bifurcation diagram shown in Figure 20.7.8.)

Next we examine the bifurcation of the branches $(0, \pm\sqrt{\mu_2})$, $\mu_2 > 0$, which occurs on $\mu_1 \pm a\sqrt{\mu_2} = 0$.

We will do a center manifold analysis. First we transform the fixed point to the origin.

Letting $\xi = z \mp \sqrt{\mu_2}$, (20.7.11) becomes

$$\begin{aligned} \dot{r} &= \mu_1 r + ar(\xi \pm \sqrt{\mu_2}), \\ \dot{\xi} &= \mu_2 + br^2 - (\xi \pm \sqrt{\mu_2})^2, \qquad \mu_2 > 0. \end{aligned} \tag{20.7.20}$$

We are interested in the flow in a neighborhood of the curve $\mu_1 \pm a\sqrt{\mu_2} = 0$; we illustrate this curve in the $(\mu_1 - \mu_2)$-parameter plane in Figure 20.7.9.

Therefore, we will set $\mu_1 =$ constant and $\sqrt{\mu_2} = \mp\frac{\mu_1}{a} - \varepsilon$. This corresponds to crossing the parabola vertically for fixed μ_1. We will have to pay close attention to the direction in which we cross the curve by varying ε; we will come back to this later. Substituting $\sqrt{\mu_2} = \mp\frac{\mu_1}{a} - \varepsilon$ into (20.7.20) gives

$$\begin{aligned} \dot{r} &= \mu_1 r + ar\left(\xi \pm \left(\mp\frac{\mu_1}{a} - \varepsilon\right)\right), \\ \dot{\xi} &= \left(\mp\frac{\mu_1}{a} - \varepsilon\right)^2 + br^2 - \left(\xi \pm \left(\mp\frac{\mu_1}{a} - \varepsilon\right)\right)^2, \end{aligned}$$

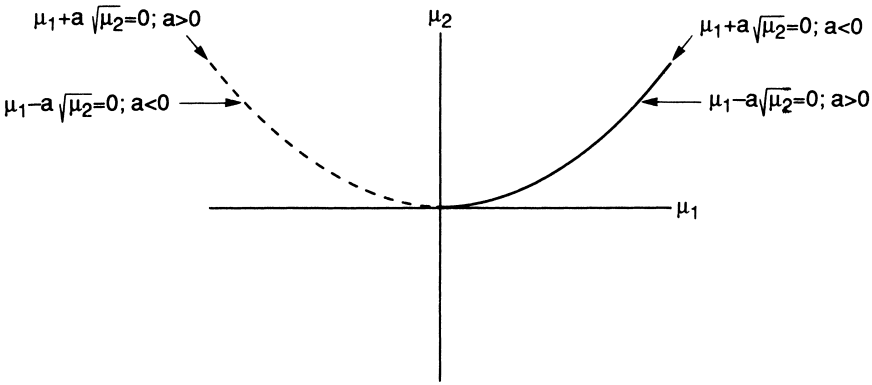

FIGURE 20.7.9.

or

$$\dot{r} = ar\xi \mp ar\varepsilon,$$
$$\dot{\xi} = 2\left(\frac{\mu_1}{a} \pm \varepsilon\right)\xi + br^2 - \xi^2;$$

in matrix form (including the parameters as a dependent variable in anticipation of applying center manifold theory), it gives

$$\begin{pmatrix} \dot{r} \\ \dot{\xi} \end{pmatrix} = \begin{pmatrix} 0 & 0 \\ 0 & \frac{2\mu_1}{a} \end{pmatrix} + \begin{pmatrix} ar\xi \mp ar\varepsilon \\ \pm 2\varepsilon\xi + br^2 - \xi^2 \end{pmatrix},$$
$$\dot{\varepsilon} = 0. \tag{20.7.21}$$

Fortunately, (20.7.21) is already in the standard form for application of the center manifold theorem. From Theorem 18.1.2, the center manifold can be represented as follows

$$W^c = \{\,(r,\varepsilon,\xi)|\,\xi = h(r,\varepsilon), h(0,0) = 0; Dh(0,0) = 0\}$$

for r and ε sufficiently small where h satisfies

$$Dh(x)[Bx + f(x,h(x))] - Ch(x) - g(x,h(x)) = 0, \tag{20.7.22}$$

with

$$x \equiv (r,\varepsilon), \qquad B = \begin{pmatrix} 0 & 0 \\ 0 & 0 \end{pmatrix}, \qquad C = \frac{2\mu_1}{a},$$
$$f = \begin{pmatrix} ar\xi \mp ar\varepsilon \\ 0 \end{pmatrix}, \qquad g = \pm 2\varepsilon\xi + br^2 - \xi^2.$$

Substituting $h(r,\varepsilon) = \alpha r^2 + \beta r\varepsilon + \gamma\varepsilon^2 + \mathcal{O}(3)$ into (20.7.22) gives

$$(2\alpha r + \beta\varepsilon + \mathcal{O}(3), \beta r + 2\gamma\varepsilon + \mathcal{O}(3)) \begin{pmatrix} arh \mp ar\varepsilon \\ 0 \end{pmatrix}$$

$$-\frac{2\mu_1}{a}(\alpha r^2 + \beta r\varepsilon + \gamma\varepsilon^2 + \mathcal{O}(3)) - (\pm 2\varepsilon h + br^2 - h^2) = 0. \tag{20.7.23}$$

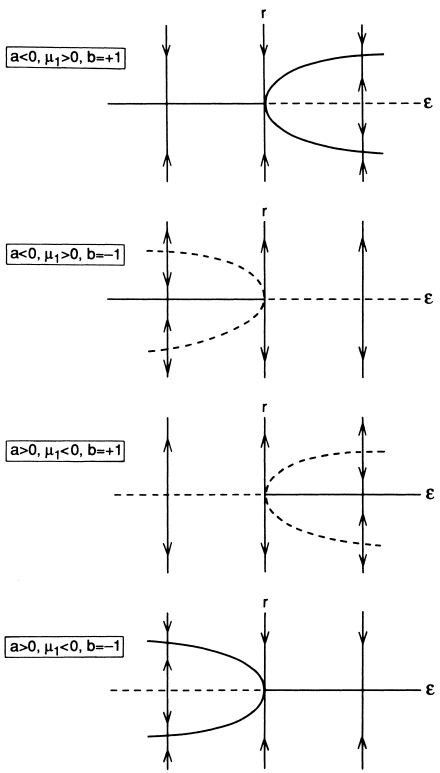

FIGURE 20.7.10. Bifurcations on the center manifold for $(0, +\sqrt{\mu_2})$.

Balancing coefficients on powers of r and ε in (20.7.23) gives

$$\begin{aligned} r^2 &: -\frac{2\mu_1}{a}\alpha - b = 0 \Rightarrow \alpha = -\frac{ab}{2\mu_1}, \\ \varepsilon r &: \frac{2\mu_1}{a}\beta = 0 \Rightarrow \beta = 0, \\ \varepsilon^2 &: \frac{2\mu_1}{a}\gamma = 0 \Rightarrow \gamma = 0; \end{aligned}$$

hence, the center manifold is the graph of

$$h(r, \varepsilon) = -\frac{ab}{2\mu_1}r^2 + \mathcal{O}(3)$$

and, therefore, the vector field (3.1.227) restricted to the center manifold is given by

$$\dot{r} = ar\left(-\frac{ab}{2\mu_1}r^2 + \mathcal{O}(3)\right) \mp ar\varepsilon$$

or

$$\dot{r} = r\left(-\frac{a^2b}{2\mu_1}r^2 \mp a\varepsilon\right) + \cdots . \tag{20.7.24}$$

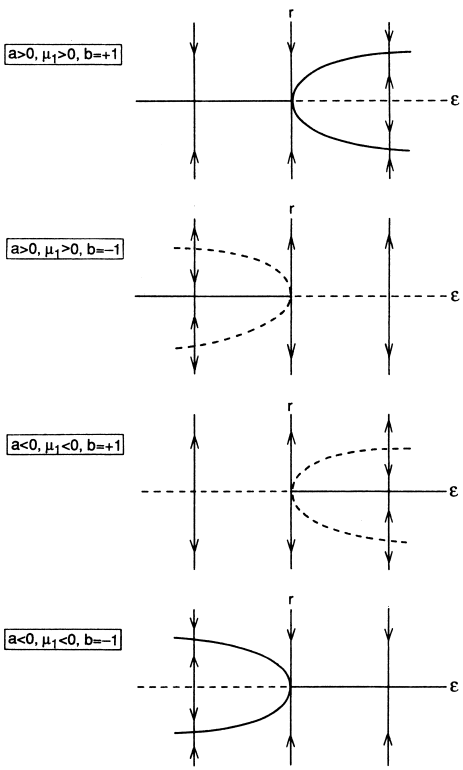

FIGURE 20.7.11. Bifurcations on the center manifold for $(0, -\sqrt{\mu_2})$.

This equation indicates that pitchfork bifurcations occur at $\varepsilon = 0$, but note that, for us, the only bifurcating solution that has meaning is the $r > 0$ solution.

We now use (20.7.24) to derive bifurcation diagrams for each branch of fixed points.

$(0, +\sqrt{\mu_2})$. The bifurcation curve is given by

$$\sqrt{\mu_2} = -\frac{\mu_1}{a},$$

and ε increasing from negative to positive corresponds to decreasing μ_2 across the bifurcation curve.

The vector field restricted to the center manifold is

$$\dot{r} = r\left(-\frac{a^2 b}{2\mu_1} r^2 - a\varepsilon\right) + \cdots,$$

from which we easily obtain the bifurcation diagrams shown in Figure 20.7.10.

$(0, -\sqrt{\mu_2})$. The bifurcation curve is given by

$$\sqrt{\mu_2} = -\frac{\mu_1}{a}.$$

The vector field restricted to the center manifold is

$$\dot{r} = r\left(-\frac{a^2 b}{2\mu_1} r^2 + a\varepsilon\right) + \cdots,$$

from which we easily obtain the bifurcation diagrams shown in Figure 20.7.11.

Now we want to translate these center manifold pictures into phase portraits for the two-dimensional flows. Recall that the eigenvalues for the direction normal to the center manifold is given by $\frac{\pm 2\mu_1}{a}$. We draw separate diagrams for each branch in Figures 20.7.12 and 20.7.13.

At this point we will summarize our results thus far.

A *saddle-node* bifurcation occurs at $\mu_2 = 0$, giving us two branches of fixed points $(0, \pm\sqrt{\mu_2})$.

1. $(0, +\sqrt{\mu_2})$ undergoes a pitchfork bifurcation on $\sqrt{\mu_2} + \frac{\mu_1}{a} = 0$ with a new fixed point being born above the curve for $b = -1$ and below the curve for $b = +1$.

2. $(0, -\sqrt{\mu_2})$ undergoes a pitchfork bifurcation on $\sqrt{\mu_2} - \frac{\mu_1}{a} = 0$ with a new fixed point being born above the curve for $b = -1$ and below the curve for $b = +1$.

Detailed stability diagrams can be obtained from the previously given diagrams.

To complete the local analysis we must examine the nature of the possible Poincaré-Andronov-Hopf bifurcations in Cases IIa,b and III.

We examine each case individually.

Cases IIa,b. The branch of fixed points is given by

$$(r, z) = \left(+\sqrt{\frac{\mu_1^2}{a^2} - \mu_2}, \frac{-\mu_1}{a}\right), \tag{20.7.25}$$

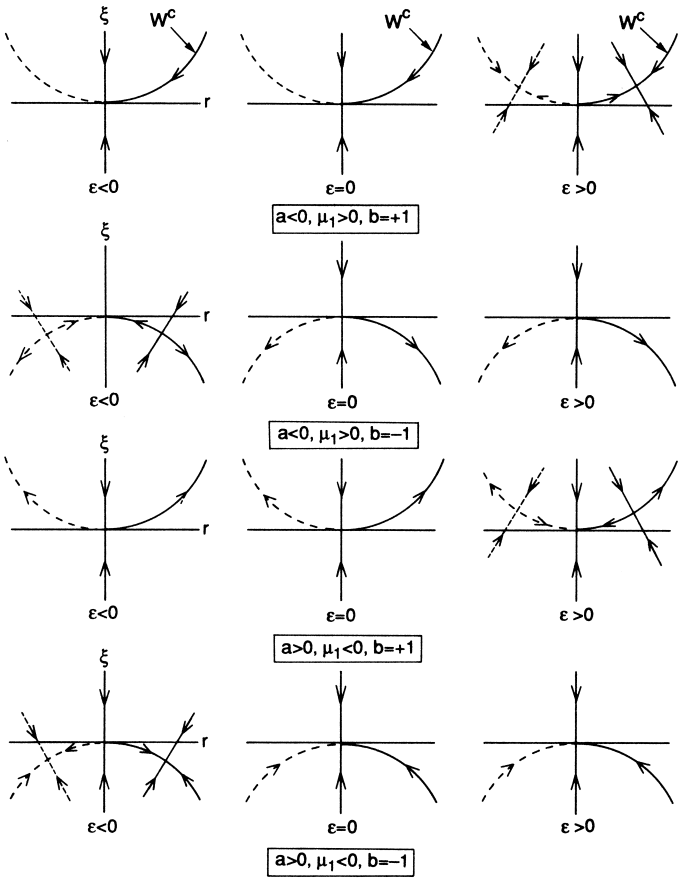

FIGURE 20.7.12. Bifurcations in the $r - \xi$ plane for $(0, +\sqrt{\mu_2})$.

where $a < 0$ and $\dfrac{\mu_1^2}{a^2} \geq \mu_2$.

Our candidate for the Poincaré-Andronov-Hopf bifurcation curve is given by

$$\mu_1 = 0, \qquad \mu_2 < 0.$$

On this curve the eigenvalues of the vector field linearized about a fixed point on the branch (20.7.25) are

$$\lambda_{1,2} = \pm i\sqrt{|2a\mu_2|}.$$

The reader should recall from Theorem 20.2.3 that there are two quantities which need to be determined.

1. The eigenvalues cross the imaginary axis transversely.

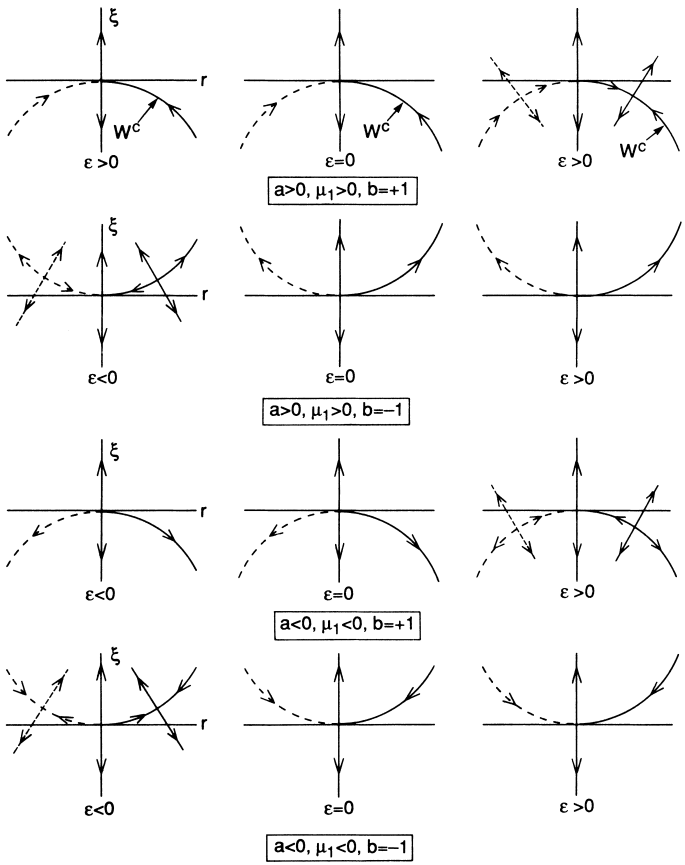

FIGURE 20.7.13. Bifurcations in the $r - \xi$ plane for $(0, -\sqrt{\mu_2})$.

2. The coefficient a in the Poincaré-Andronov-Hopf normal form is nonzero. (Note: this should not be confused with the coefficient a in the normal form that we are presently studying, which we have assumed to be nonzero.)

We begin by verifying statement 1.

The general expression for the eigenvalues is

$$\lambda_{1,2} = \frac{\operatorname{tr} J}{2} \pm \frac{1}{2}\sqrt{(\operatorname{tr} J)^2 - 4 \det J},$$

where in our case

$$\operatorname{tr} J = \frac{2\mu_1}{a},$$

$$\det J = -2a\left(\frac{\mu_1^2}{a^2} - \mu_2\right).$$

We will view μ_2 as fixed and μ_1 as a parameter; since we are interested only in the behavior of the eigenvalues near $\mu_1 = 0$, $\mu_2 < 0$, we can take the real part of $\lambda_{1,2}$ to be $\frac{\operatorname{tr} J}{2}$ and thus obtain

$$\frac{d}{d\mu_1}\operatorname{Re}\lambda = \frac{2}{a} \neq 0.$$

Next we check statement 2.

We set $b = +1$ in (20.7.11) and obtain

$$\begin{aligned}\dot{r} &= \mu_1 r + arz,\\ \dot{z} &= \mu_2 + r^2 - z^2.\end{aligned}$$

We next put this system into the normal form so that the coefficient a in the Poincaré-Andronov-Hopf normal form can be computed. First we translate the fixed point to the origin by letting

$$\rho = r - \sqrt{\frac{\mu_1^2}{a} - \mu_2}, \qquad \xi = z + \frac{\mu_1}{a},$$

and hence obtain

$$\begin{aligned}\dot{\rho} &= \mu_1\left(\rho + \sqrt{\frac{\mu_1^2}{a^2} - \mu_2}\right) + a\left(\rho + \sqrt{\frac{\mu_1^2}{a^2} - \mu_2}\right)\left(\xi - \frac{\mu_1}{a}\right),\\ \dot{\xi} &= \mu_2 + \left(\rho + \sqrt{\frac{\mu_1^2}{a^2} - \mu_2}\right)^2 - \left(\xi - \frac{\mu_1}{a}\right)^2,\end{aligned}$$

or

$$\begin{aligned}\dot{\rho} &= a\xi\sqrt{\frac{\mu_1^2}{a^2} - \mu_2} + a\rho\xi,\\ \dot{\xi} &= 2\rho\sqrt{\frac{\mu_1^2}{a^2} - \mu_2} + \frac{2\mu_1}{a}\xi + \rho^2 - \xi^2.\end{aligned}$$

We next evaluate this equation on the bifurcation curve $\mu_1 = 0$, $\mu_2 < 0$ and get

$$\begin{aligned}\dot{\rho} &= a\sqrt{|\mu_2|}\xi + a\rho\xi,\\ \dot{\xi} &= 2\sqrt{|\mu_2|}\rho + \rho^2 - \xi^2.\end{aligned}$$

The matrix associated with the linear part of this equation is given by

$$\begin{pmatrix} 0 & a\sqrt{|\mu_2|} \\ 2\sqrt{|\mu_2|} & 0 \end{pmatrix}.$$

Introducing the linear tranformation

$$\begin{pmatrix}\rho\\ \xi\end{pmatrix} = \begin{pmatrix} 0 & -\sqrt{\frac{|a|}{2}} \\ 1 & 0 \end{pmatrix}\begin{pmatrix}u\\ v\end{pmatrix};$$

$$\begin{pmatrix} u \\ v \end{pmatrix} = \frac{1}{\sqrt{\frac{|a|}{2}}} \begin{pmatrix} 0 & \sqrt{\frac{|a|}{2}} \\ -1 & 0 \end{pmatrix} \begin{pmatrix} \rho \\ \xi \end{pmatrix},$$

the equation becomes

$$\begin{pmatrix} \dot{u} \\ \dot{v} \end{pmatrix} = \begin{pmatrix} 0 & -\sqrt{|2a\mu_2|} \\ \sqrt{|2a\mu_2|} & 0 \end{pmatrix} \begin{pmatrix} u \\ v \end{pmatrix} + \begin{pmatrix} \frac{|a|}{2}v^2 - u^2 \\ -|a|uv \end{pmatrix}.$$

This is the standard form given in (20.2.13) from which the coefficient a in the Poincaré-Andronov-Hopf normal form can be computed.

From (20.2.14), this coefficient is given by

$$\frac{1}{16}\left[f_{uuu} + f_{uvv} + g_{uuv} + g_{vvv}\right] + \frac{1}{16\sqrt{|2a\mu_2|}}[f_{uv}(f_{uu} + f_{vv})$$

$$- g_{uv}(g_{uu} + g_{vv}) - f_{uu}g_{uu} + f_{vv}g_{vv}],$$

and all partial derivatives are evaluated at $(0, 0)$.

In our case

$$f \equiv \frac{|a|}{2}v^2 - u^2,$$
$$g \equiv -|a|uv.$$

Now we work out the partial derivatives (note all third derivatives vanish)

$$\begin{aligned} f_{uu} &= -2, & g_{uu} &= 0, \\ f_{uv} &= 0, & g_{uv} &= -|a|, \\ f_{vv} &= |a|, & g_{vv} &= 0. \end{aligned}$$

Thus, the coefficient a is identically zero. This tells us that we must retain (at least) cubic terms in our normal form in order to get any stability information concerning the Poincaré-Andronov-Hopf bifurcation. (Note: we might have guessed that this would be the case. Why?) We will complete this analysis in Chapter 33.

Now we must examine Poincaré-Andronov-Hopf bifurcations in the remaining case.

Case III, $a > 0$. It is straightforward to verify that Poincaré-Andronov-Hopf bifurcations occur on $\mu_1 = 0$, $\mu_2 > 0$ for the branch of fixed points given by

$$\left(\sqrt{\mu_2 - \frac{\mu_1^2}{a^2}}, \frac{-\mu_1}{a}\right)$$

and that, unfortunately, in this case also, the coefficient in the Poincaré-Andronov-Hopf normal form is identically zero.

We now want to summarize these results in the following bifurcation diagrams.

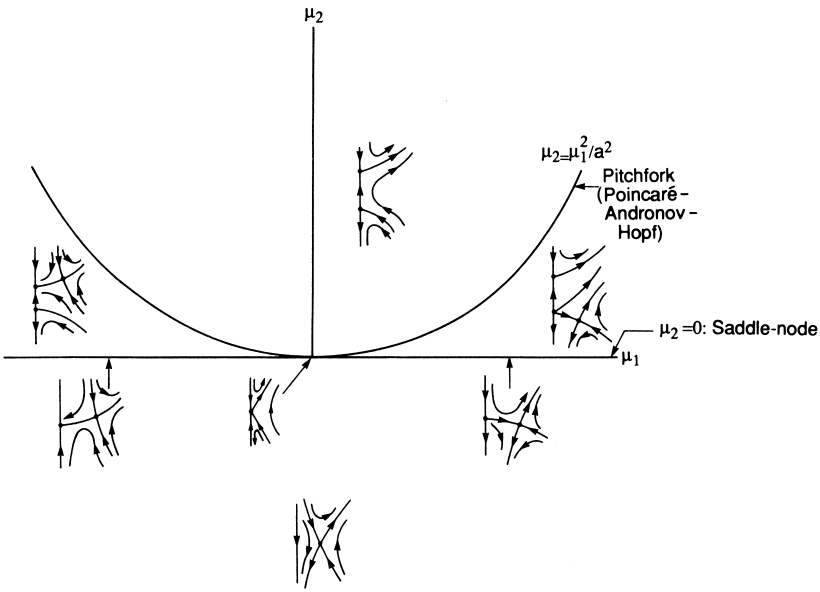

FIGURE 20.7.14. Case I: $b = +1$, $a > 0$.

Case I: $b = +1$, $a > 0$. In Figure 20.7.14 we show phase portraits for different regions in the $\mu_1 - \mu_2$ plane. Note that by index theory there can be no periodic orbits in Case I (which might arise via some global bifurcation). This is because we must have $r > 0$, and the only fixed point in $r > 0$ is a saddle point. Thus, Figure 20.7.14 represents the complete story for Case I. It remains only to interpret the $r - z$ phase plane results in terms of the full three-dimensional vector field and consider the effects of the higher order terms of the normal form. We will do this later in this section.

Case IIa,b: $b = +1$, $a > 0$. We show phase portraits for this case in different regions of the $\mu_1 - \mu_2$ plane in Figure 20.7.15. Note that the eigenvalues of the matrix associated with the vector field linearized about $\left(\sqrt{\frac{\mu_1^2}{a^2} - \mu_2}, \frac{-\mu_1}{a}\right)$ are given by

$$\lambda_{1,2} = \frac{\mu_1}{a} \pm \sqrt{\frac{\mu_1^2}{a^2} + \frac{2}{a}(\mu_1^2 - a^2\mu_2)},$$

and that these eigenvalues have nonzero imaginary part for

$$\mu_2 < \mu_1^2 \left(2 + \frac{1}{a}\right)/2a^2, \qquad \mu_2 < 0.$$

This gives us a better idea of the local orbit structure near these fixed points, and we illustrate this curve with a dotted line in Figure 20.7.15. We caution, however, that it is *not* a bifurcation curve.

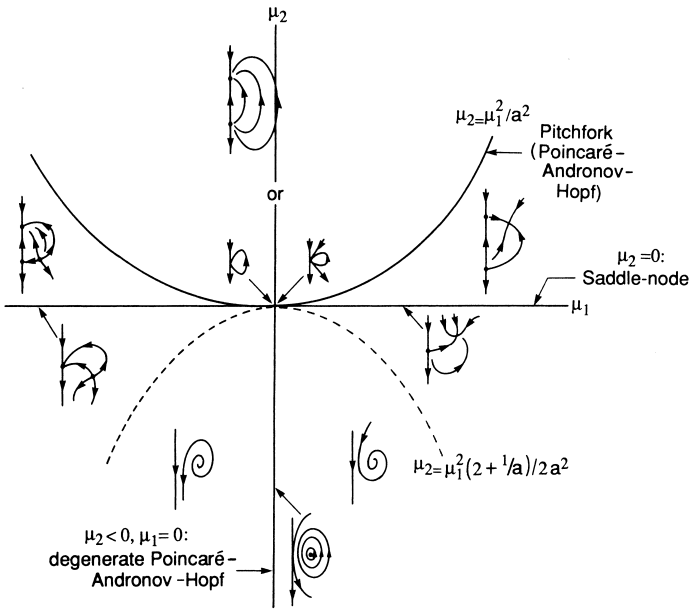

FIGURE 20.7.15. Case IIa,b: $b = +1$, $a > 0$.

Note that on $\mu_1 = 0$ the truncated normal form has the first integral

$$F(r,z) = \frac{a}{2} r^{2/a} \left[\mu_2 + \frac{r^2}{1+a} - z^2 \right]. \tag{20.7.26}$$

This should give some insight into the "degenerate" Poincaré-Andronov-Hopf bifurcation, since (20.7.26) implies that on $\mu_1 = 0$ the truncated normal form has a one-parameter family of periodic orbits. We expect that this degenerate situation will dramatically change when the effects of the higher order terms in the normal form are taken into account. In particular, we would expect that a finite number of these periodic orbits survive. Exactly how many is a delicate issue that we will examine in Chapter 33.

Case III: $b = -1$, $a > 0$. We show phase portraits in different regions of the $\mu_1 - \mu_2$ plane in Figure 20.7.16. This case suffers from many of the same difficulties of Cases IIa,b. In particular, the truncated normal form has the first integral

$$G(r,z) = \frac{a}{2} r^{2/a} \left(\mu_2 - \frac{1}{1+a} r^2 - z^2 \right) \tag{20.7.27}$$

on $\mu_1 = 0$. An examination of the first integral shows that, for $\mu_2 > 0$, the truncated normal form has a one-parameter family of periodic orbits which limit on a heteroclinic cycle as shown in Figure 20.7.16. In Chapter 33 we will consider the effects of the higher order terms in the normal form on this degenerate phase portrait.

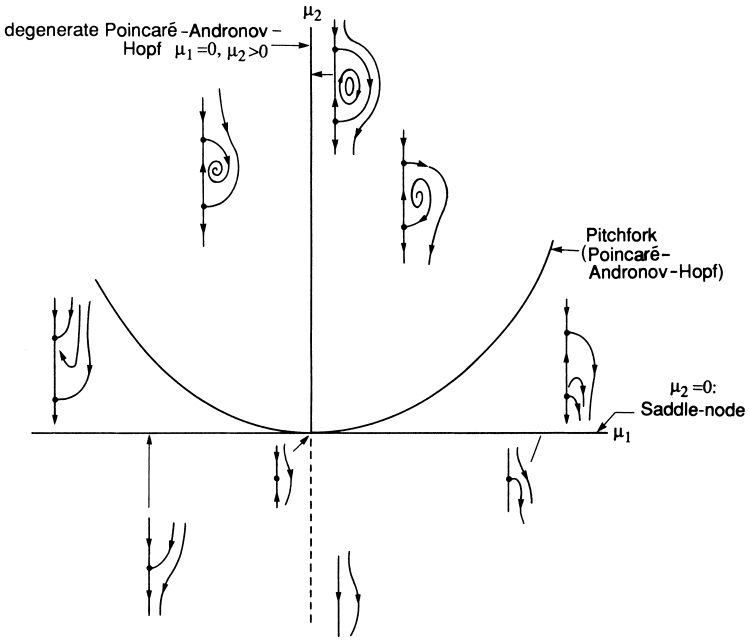

FIGURE 20.7.16. Case III: $b = +1$, $a > 0$.

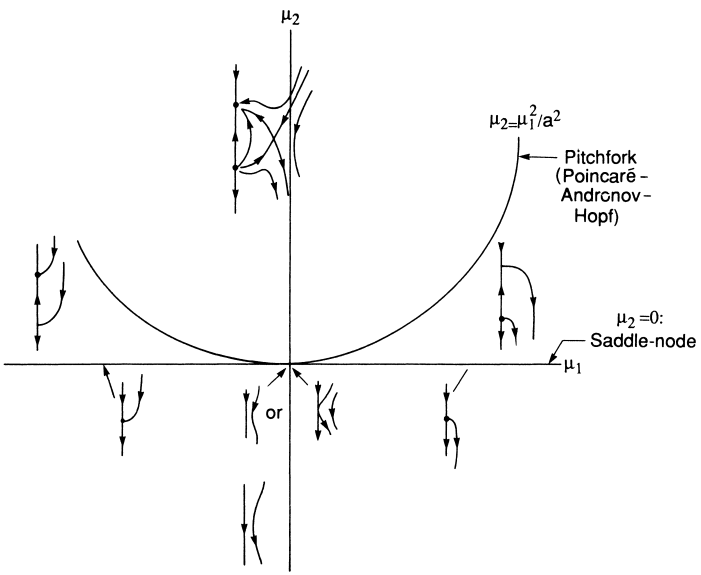

FIGURE 20.7.17. Case IVa,b: $b = -1$, $a < 0$.

Case IVa,b: $b = -1$, $a < 0$. We show phase portraits in the different regions in the $\mu_1 - \mu_2$ plane in Figure 20.7.17. Using index theory, it is easy to argue that these cases have no periodic orbits. Hence, Figure 20.7.17 represents the complete story for the $r-z$ phase plane analysis of the truncated normal form.

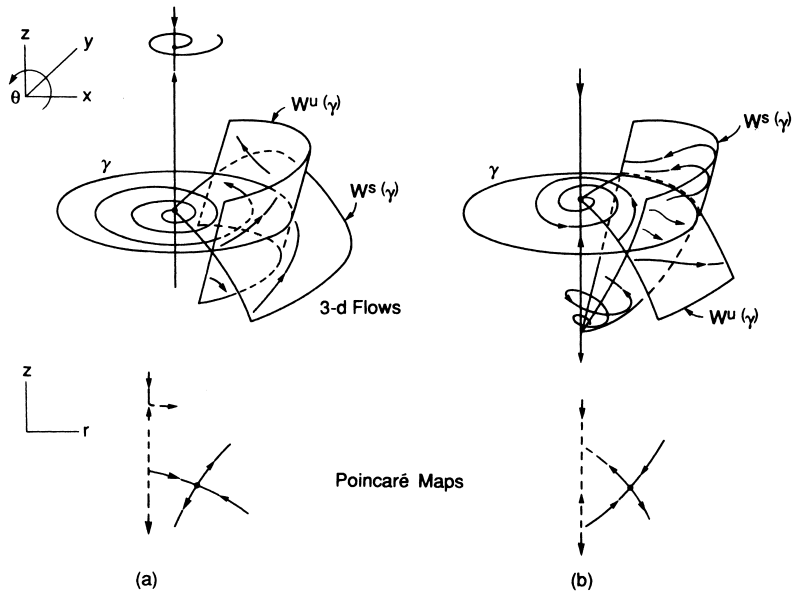

FIGURE 20.7.18. a) From Case I, b) From Case IVa,b.

Relation of the Dynamics in the $r - z$ Phase Plane to the Full Three-Dimensional Vector Field

We now want to discuss how the dynamics of

$$\begin{aligned} \dot{r} &= \mu_1 r + arz, \\ \dot{z} &= \mu_2 + br^2 - z^2, \end{aligned} \tag{20.7.28}$$

relate to

$$\begin{aligned} \dot{r} &= \mu_1 r + arz, \\ \dot{z} &= \mu_2 + br^2 - z^2, \\ \dot{\theta} &= \omega + \cdots . \end{aligned} \tag{20.7.29}$$

We are interested in three types of invariant sets studied in (3.1.233). They are fixed points, periodic orbits, and heteroclinic cycles. We consider each case separately.

Fixed Points

There are two cases, fixed points with $r = 0$ and fixed points with $r > 0$. It is easy to see (returning to the definition of r and θ in terms of the original Cartesian coordinates) that fixed points of (20.7.28) with $r = 0$ correspond to fixed points of (20.7.29). *Hyperbolic* fixed points of (20.7.28) with $r > 0$ correspond to periodic orbits of (20.7.29). This follows immediately by applying the method of averaging. See Figure 20.7.18 for a geometrical description.

Periodic Orbits

We have not developed the theoretical tools to treat this situation rigorously; this will be done in Volume 3. However, for now we will give a heuristic description of what is happening. Notice that the r and z components of (20.7.29) are independent of θ. This implies that the periodic orbit in the $r - z$ plane is manifested as an invariant two-torus in the $r - z - \theta$ phase space; see Figure 20.7.19. This is a very delicate situation regarding the higher order terms in the normal form, since they could dramatically affect the flow on the torus, in particular, whether or not we get quasiperiodic motion or phase locking (periodic motion).

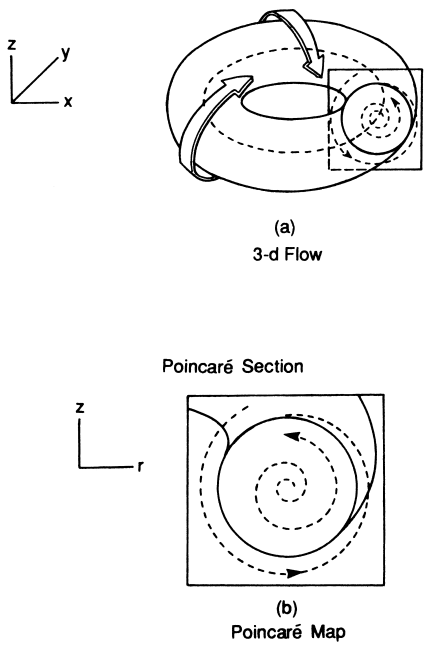

FIGURE 20.7.19. a) Three-dimensional flow, b) Poincaré section.

Heteroclinic Cycles

Following the discussion for periodic orbits given above, the part of the heteroclinic cycle in Case III ($\mu_2 > 0$) on the z axis is manifested as an invariant line in $r - z - \theta$ space, and the part of the heteroclinic cycle having $r > 0$ is manifested as an invariant sphere in $r - z - \theta$ space; see Figure 20.7.20. This is a very degenerate situation and could be dramatically affected by the higher order terms of the normal form.

Step 5: Analysis of Global Bifurcations. As we have mentioned, this will be completed in Chapter 33 after we have developed the necessary theoretical tools.

Step 6: Effects of the Higher Order Terms in the Normal Form. In Cases I and IVa,b the method of averaging essentially enables us to conclude that the higher order terms do not qualitatively change the dynamics. Thus we have found a versal deformation. The details of proving this, however, are left to the exercises.

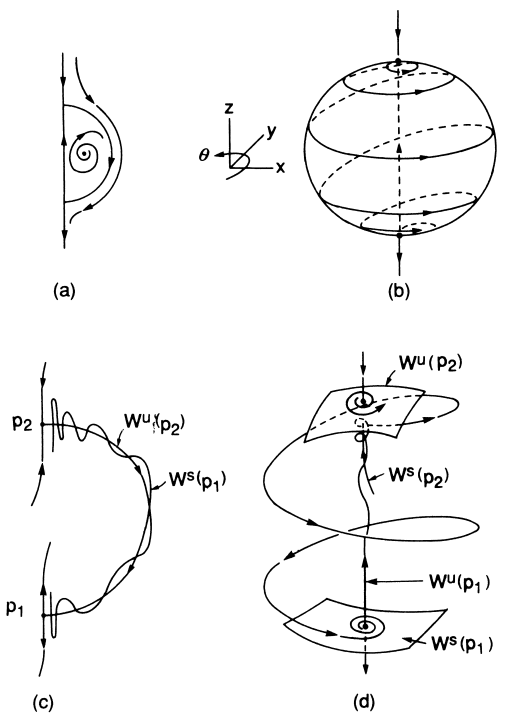

FIGURE 20.7.20.

The remaining cases are more difficult and, ultimately, we will argue that versal deformations may not exist in some circumstances.

Before leaving this section we want to make some final remarks.

Remark 1. This analysis reemphasizes the power of the method of normal forms. As we will see throughout the remainder of this book, vector fields having phase spaces of dimension three or more can exhibit very complicated dynamics. In our case the method of normal forms utilized the structure of the vector field to naturally "separate" the variables. This enabled us to "get our foot in the door" by using powerful phase plane techniques.

Remark 2. From the double-zero eigenvalue and now this case, a lesson to be learned is that Poincaré-Andronov-Hopf bifurcations always cause us trouble in the sense of how they relate to global bifurcations and/or how they are affected by the consideration of the higher order terms of the normal form.

20.7A Additional References and Applications for the Hopf-Steady State Bifurcation

The Hopf-steady state bifurcation arises in a variety of applications and is still a current topic of research. Recent references are Arnold et al. [1988], Dawes [2000], Moore and Weiss [2000], Algaba et al. [1999a,b,d], Campbell [1999], Wu and Kupper [1998], Murphy and Lee [1998], Zimmermann et al. [1997], Allen and Moroz [1997], Wu and Kupper [1996], Solari and Oppo [1994], and Summers and Savage [1992].

20.7B Exercises

1. Consider a three-dimensional autonomous $\mathbf{C}^r$ (r as large as necessary) vector field having a fixed point where the linear part, in Cartesian coordinates, takes the form

$$\begin{pmatrix} 0 & -\omega & 0 \\ \omega & 0 & 0 \\ 0 & 0 & 0 \end{pmatrix} \begin{pmatrix} x \\ y \\ z \end{pmatrix}.$$

The versal deformation of this nonhyperbolic fixed point was studied in some detail earlier. Suppose now we assume that the vector field is equivariant under the coordinate transformation

$$(x, y, z) \mapsto (x, y, -z).$$

a) Show that the normal form in cylindrical coordinates is given by

$$\begin{aligned} \dot{r} &= r(a_1 r^2 + a_2 z^2) + \cdots, \\ \dot{z} &= z(b_1 r^2 + b_2 z^2) + \cdots, \\ \dot{\theta} &= \omega + \cdots. \end{aligned}$$

b) Show that a candidate for a versal deformation is given by

$$\begin{aligned} \dot{r} &= r(\mu_1 + a_1 r^2 + a_2 z^2), \\ \dot{z} &= z(\mu_2 + b_1 r^2 + b_2 z^2), \\ \dot{\theta} &= \omega + \cdots. \end{aligned}$$

c) Following the steps in the analysis of the nonsymmetric case, analyze this versal deformation completely, addressing all issues discussed for the nonsymmetric case.

For an excellent review and bibliography of this nonhyperbolic fixed point with various symmetries see Langford [1985].

2. Consider a four-dimensional autonomous $\mathbf{C}^r$ (r as large as necessary) vector field having a nonhyperbolic fixed point at which the linear part has the form

$$\begin{pmatrix} 0 & -\omega_1 & 0 & 0 \\ \omega_1 & 0 & 0 & 0 \\ 0 & 0 & 0 & -\omega_2 \\ 0 & 0 & \omega_2 & 0 \end{pmatrix} \begin{pmatrix} w \\ x \\ y \\ z \end{pmatrix}.$$

a) Suppose $m\omega_1 + n\omega_2 \neq 0$, $|m| + |n| \leq 4$. Then show that in polar coordinates a normal form is given by

$$\begin{aligned} \dot{r}_1 &= a_1 r_1^3 + a_2 r_1 r_2^2 + \cdots, \\ \dot{r}_2 &= b_1 r_1^2 r_2 + b_2 r_1^3 + \cdots, \\ \dot{\theta}_1 &= \omega_1 + \cdots, \\ \dot{\theta}_2 &= \omega_2 + \cdots. \end{aligned}$$

b) Show that a candidate for a versal deformation is given by

$$\begin{aligned} \dot{r}_1 &= \mu_1 r_1 + a_1 r_1^3 + a_2 r_1 r_2^2, \\ \dot{r}_2 &= \mu_2 r_2 + b_1 r_1^2 r_2 + b_2 r_1^3, \\ \dot{\theta}_1 &= \omega_1 + \cdots, \\ \dot{\theta}_2 &= \omega_2 + \cdots. \end{aligned}$$

c) Analyze this versal deformation completely and address all issues raised in this section. In particular, under what conditions may "three-tori" arise?

d) For each of the resonant cases

$$m\omega_1 + n\omega_2 = 0, \qquad |m| + |n| \leq 4,$$

discuss the codimension of the bifurcation and candidates for versal deformations.

3. Consider the following ordinary differential equation

$$\begin{aligned} \dot{x} &= \frac{\omega}{\sqrt{3}}(y - z) + [\varepsilon - \mu(x^2 - yz)]x, \\ \dot{y} &= \frac{\omega}{\sqrt{3}}(z - x) + [\varepsilon - \mu(y^2 - xz)]y, \qquad (x, y, z) \in \mathbb{R}^3 \\ \dot{z} &= \frac{\omega}{\sqrt{3}}(x - y) + [\varepsilon - \mu(z^2 - xy)]z, \end{aligned} \tag{20.7.30}$$

where $\varepsilon > 0$, $\mu > 0$, and ω are parameters. This system is useful for modeling and simulating synchronous machine systems in the study of power system dynamics; see Kaplan and Yardeni [1989] and Kaplan and Kottick [1983], [1985], [1987].

It should be obvious that

$$(x, y, z) = (0, 0, 0)$$

is a fixed point of (20.7.30) for all parameter values. We are interested in studying the bifurcations associated with this fixed point.

a) Show that for $\varepsilon = 0$ the eigenvalues of the matrix associated with the linearized vector field are given by

$$0, \pm i\omega.$$

b) Study the bifurcations associated with this fixed point for $\varepsilon = 0$, $\omega \neq 0$, and $\varepsilon = 0$, $\omega = 0$.

4. Consider the following class of feedback control systems studied by Holmes [1985].

$$\begin{aligned} &\ddot{x} + \delta\dot{x} + g(x) = -z, \\ &\dot{z} + \alpha z = \alpha\gamma(x - r), \end{aligned} \tag{20.7.31}$$

where x and $\dot{x}$ represent the displacement and velocity, respectively, of an oscillatory system with nonlinear stiffness $g(x)$ and linear damping $\delta\dot{x}$ subject to negative feedback control z. The controller has first-order dynamics with time constant $\frac{1}{\alpha}$ and gain γ. A constant or time-varying bias r can be applied. This system provides the simplest possible model for a nonlinear elastic system whose position is controlled by a servomechanism with negligible inertia; see Holmes and Moon [1983] for details.

For this exercise we will assume

$$g(x) = x(x^2 - 1)$$

and

$$r = 0.$$

Rewriting (20.7.31) as a system gives

$$\begin{aligned} &\dot{x} = y, \\ &\dot{y} = x - x^3 - \delta y - z, \qquad (x, y, z) \in \mathbb{R}^3 \\ &\dot{z} = \alpha\gamma x - \alpha z, \end{aligned} \tag{20.7.32}$$

with scalar parameters δ, α, $\gamma > 0$. This exercise is concerned with studying local bifurcations of (20.7.32).

a) Show that (20.7.32) has fixed points at

$$(x, y, z) = (0, 0, 0) \equiv \underline{0}$$

and

$$(x, y, z) = \left(\pm\sqrt{1 - \gamma}, 0, \pm\gamma\sqrt{1 - \gamma}\right) \equiv \underline{p}_{\pm}, \qquad (\gamma < 1).$$

b) Linearize about these three fixed points and show that (20.7.32) has the following *bifurcation surfaces* in (α, δ, γ) space.

$\gamma = 1$	one eigenvalue is zero for $\underline{0}$
$\gamma = \frac{\delta}{\alpha}(\alpha^2 + \alpha\delta - 1)$, $\gamma > 1$	a pair of eigenvalues is pure imaginary for $\underline{0}$
$\gamma = \frac{\delta}{\alpha+3\delta}(\alpha^2 + \alpha\delta + 2)$, $0 < \gamma < 1$	a pair of eigenvalues is pure imaginary for $\underline{p}_{\pm}$.

c) Show that these three surfaces meet on the curve

$$\gamma = 1, \quad \delta = \frac{1}{\alpha},$$

where there is a double-zero eigenvalue with the third eigenvalue being $-(1 + \alpha^2)/\alpha$.

d) Fix $\alpha > 0$ and study the bifurcations from the double-zero eigenvalue in the (δ, γ) plane.

e) Describe all attractors as a function of δ and γ. Discuss the implications for the control problem.

We remark that, although this exercise is concerned with local nonlinear analysis, global techniques for studying problems of the form (20.7.31) have been developed in Wiggins and Holmes [1987a], [1987b] and Wiggins [1988].

5. Consider the following partial differential equation known as the *complex Ginzburg–Landau* (CGL) *equation*

$$iA_t + \hat{\alpha}A_{xx} = \hat{\beta}A - \hat{\gamma}|A|^2 A, \tag{20.7.33}$$

where $(x,t) \in \mathbb{R}^1 \times \mathbb{R}^1$, $A(x,t)$ is complex and $\hat{\alpha} = \alpha_R + i\alpha_I$, $\hat{\beta} = \beta_R + i\beta_I$, and $\gamma = \gamma_R + i\gamma_I$ are complex numbers.

If we set $\alpha_I = 0$, $\gamma_I = 0$, and $\hat{\beta} = 0$, (20.7.33) reduces to

$$iA_t + \alpha_R A_{xx} = -\gamma_R |A|^2 A, \tag{20.7.34}$$

which is a famous *completely integrable* partial differential equation known as the *nonlinear Schrödinger* (NLS) *equation.* We refer the reader to Newell [1985] for background material and a discussion of the physical circumstances in which (20.7.33) and (20.7.34) arise. We will comment on this in more detail at the end of this exercise.

a) Show that (20.7.33) is invariant under translations in space and time, i.e., under the transformation
$$(x,t) \mapsto (x + x_0, t + t_0).$$
Show also that (20.7.33) is invariant under multiplication by a complex number of unit modulus, i.e., under the transformation
$$A \mapsto Ae^{i\psi_0}.$$

Our goal in this exercise will be to study solutions of (20.7.33) that have the form

$$A(x,t) = a(x)e^{i\omega t}. \tag{20.7.35}$$

b) Substitute (20.7.35) into (20.7.33) and show that $a(x)$ satisfies the following *complex Duffing equation*

$$a'' - (\alpha + i\beta)a + (\gamma + i\delta)|a|^2 a = 0, \tag{20.7.36}$$

where

$$\begin{aligned}
\alpha &= [\alpha_R(\omega + \beta_R + \alpha_I\beta_I]/\Delta,\\
\beta &= [\alpha_R\beta_I - \alpha_I(\omega + \beta_R)]/\Delta,\\
\gamma &= [\alpha_R\gamma_R + \alpha_I\gamma_I]/\Delta,\\
\delta &= [\alpha_R\gamma_I - \alpha_I\gamma_R]/\Delta,
\end{aligned}$$

and
$$\Delta = \alpha_R^2 + \alpha_I^2.$$

c) Letting $a = b + ic$, show that (20.7.36) can be written as

$$\begin{aligned}
b' &= d,\\
d' &= \alpha b - \beta c - (\gamma b - \delta c)(b^2 + c^2),\\
c' &= e,\\
e' &= \beta b + \alpha c - (\delta b + \gamma c)(b^2 + c^2).
\end{aligned} \tag{20.7.37}$$

d) Show that, for $\beta = \delta = 0$, (20.7.37) is a completely integrable Hamiltonian system with integrals

$$\begin{aligned}
H &= \frac{d^2 + e^2}{2} - \frac{\alpha}{2}(c^2 + b^2) + \frac{\gamma}{4}(c^2 + b^2)^2,\\
m &= be - cd.
\end{aligned}$$

e) Using the transformation

$$a = \rho e^{i\varphi},$$

show that (20.7.36) can be written in the form

$$\begin{aligned} &\rho'' - \rho(\varphi')^2 = \alpha\rho - \gamma\rho^3, \\ &(\rho^2\varphi')' = (\beta - \delta\rho^2)\rho^2. \end{aligned} \tag{20.7.38}$$

f) Let

$$\begin{aligned} r &= \rho^2, \\ v &= \rho'/\rho, \end{aligned}$$

and

$$m = \rho^2\varphi',$$

and show that (20.7.38) can be written in the form

$$\begin{aligned} r' &= 2rv, \\ v' &= \frac{m^2}{r^2} - v^2 + \alpha - \gamma r, \\ m' &= (\beta - \delta r)r. \end{aligned} \tag{20.7.39}$$

g) For $\beta = \delta = 0$, show that (20.7.39) has the form of a one-parameter family (with m playing the role of the parameter) of two-dimensional Hamiltonian systems with Hamiltonian function

$$H(r, v; m) = rv^2 + \frac{m^2}{r} - \alpha r + \frac{\gamma}{2}r^2. \tag{20.7.40}$$

h) Using (20.7.40), give a complete description of the orbit structure of (20.7.39) for $\beta = \delta = 0$.

i) Consider the symmetries of the CGL equation described in a). Discuss how these symmetries are manifested in (20.7.36), (20.7.37), (20.7.38), and (20.7.39).

j) For $\beta\gamma = \alpha\delta$, the point

$$(r, v, m) = \left(\frac{\alpha}{\gamma} = \frac{\beta}{\delta}, 0, 0\right)$$

is a fixed point of (20.7.39) where the eigenvalues of the matrix associated with the linearization are given by

$$0, \pm i\sqrt{2\alpha}.$$

Study the bifurcations associated with this fixed point (take $\alpha > 0$).

k) Discuss the implications of the results obtained concerning the dynamics of the ordinary differential equations for the spatial and temporal structure of solutions to the CGL equation.

l) In our original discussion of the CGL and NLS equations, we did not mention initial or boundary conditions. Discuss this issue in the context of the solutions we found.

The CGL equation is a fundamental equation that arises in a variety of physical situations. See Newell [1985], where it is derived in the context of nonlinear waves, and Landman [1987], where it is used to understand the transition to turbulence in Poiseuille flow. Most of this exercise is based on results in Holmes [1986]; see also Holmes and Wood [1985] and Newton and Sirovich [1986a,b].

20.8 Versal Deformations of Linear Hamiltonian Systems

In this section we describe versal deformation theory for linear Hamiltonian systems that is very similar to the theory developed for matrices in Section 20.5.

The versal deformation theory for matrices used the Jordan canonical form in a variety of ways. Similarly, we need something like a Jordan canonical form theory for the matrices associated with linear Hamiltonian systems, or *infinitesimally symplectic matrices*. First, we establish some notation. We will be concerned with linear Hamiltonian vector fields. Hence, the Hamiltonians are quadratic forms of the following form:

$$H_0(x) = \frac{1}{2}\langle A_0 x, x\rangle, \tag{20.8.1}$$

where

$$x \equiv (q_1, \ldots, q_n, p_1, \ldots, p_n),$$

and A_0 is a $2n \times 2n$ real symmetric matrix. The associated Hamiltonian vector field is then given by

$$\dot{x} = JA_0 x,$$

where

$$J = \begin{pmatrix} 0 & \mathrm{id} \\ -\mathrm{id} & 0 \end{pmatrix},$$

and "id" denotes the $n \times n$ identity matrix. By the term *eigenvalues of the Hamiltonian* we will mean the eigenvalues of the infinitesimally symplectic matrix JA_0, and by the term *Jordan block of the Hamiltonian* we will mean Jordan block of the infinitesimally symplectic matrix JA_0.

20.8A Williamson's Theorem

According to Proposition 14.3.5 from Chapter 14, the eigenvalues of the infinitesimally symplectic matrix JA_0 occur in four possible ways:

1. real pairs: $(a, -a)$,
2. purely imaginary pairs: $(ia, -ia)$,

3. complex quartets: $(\pm a \pm ib)$,

4. zero eigenvalues, with even multiplicity.

This eigenvalue structure is reflected in the Jordan block structure. For example, if there is a Jordan block of dimension k corresponding to the real eigenvalue a, then there is a Jordan block of dimension k corresponding to the real eigenvalue $-a$. Similarly, if there is a Jordan block of dimension k corresponding to the complex eigenvalue $a + ib$, then there are three other Jordan blocks of dimension k corresponding to the remaining three eigenvalues in the quartet. In the case of purely imaginary eigenvalues we have to distinguish between Jordan blocks of even and odd dimension. For zero eigenvalues there can also be Jordan blocks of even and odd dimension, but if they are odd they occur in pairs.

Williamson [1936] showed that the following is a complete list of normal forms corresponding to the different possible Jordan blocks.

Pair of Jordan Blocks of Dimension k Corresponding to Real Eigenvalues $\pm a$

$$H_0 = -a \sum_{i=1}^{k} p_i q_i + \sum_{i=1}^{k-1} p_i q_{i+1}. \tag{20.8.2}$$

Quartet of Jordan Blocks of Dimension k with Eigenvalues $\pm a \pm ib$

$$H_0 = -a \sum_{i=1}^{2k} p_i q_i + b \sum_{i=1}^{k} (p_{2i-1} q_{2i} - p_{2i} q_{2i-1}) + \sum_{i=1}^{2k-2} p_i q_{i+2}. \tag{20.8.3}$$

Pair of Jordan Blocks with Odd Dimension k Corresponding to Eigenvalue 0

$$H = \sum_{i=1}^{k-1} p_i q_{i+1}. \tag{20.8.4}$$

For $k = 1$, $H_0 = 0$.

Pair of Jordan Blocks with Even Dimension k Corresponding to Eigenvalue 0

$$H_0 = \pm\frac{1}{2}\left(\sum_{i=1}^{l-1} p_i p_{l-i} - \sum_{i=1}^{l} q_i q_{l+1-i}\right) - \sum_{i=1}^{l-1} p_i q_{i+1}, \tag{20.8.5}$$

where $l = \frac{k}{2}$. For $k = 2$, $H_0 = \pm\frac{1}{2}q_1^2$.

Pair of Jordan Blocks with Odd Dimension k Corresponding to Eigenvalues $\pm ia$

$$\begin{aligned} H_0 = \mp\frac{1}{2}\Bigg(&\sum_{i=1}^{l}\left(a^2 p_{2i-1}p_{2l+1-2i} + q_{2i-1}q_{2l+1-2i}\right) \\ &- \sum_{i=1}^{l-1}\left(a^2 p_{2i}p_{2l-2i} + q_{2i}q_{2l-2i}\right)\Bigg) - \sum_{i=1}^{2l-2} p_i q_{i+1}, \end{aligned} \tag{20.8.6}$$

where $l = \frac{k+1}{2}$. For $k = 1$, $H_0 = \pm\frac{1}{2}\left(a^2p_1^2 + q_1^2\right)$.

Pair of Jordan Blocks with Even Dimension k Corresponding to Eigenvalues $\pm ia$

$$\begin{aligned} H_0 = \mp\frac{1}{2}\Bigg(&\sum_{i=1}^{l-1}\left(a^2 p_{2i+1}p_{2l+1-2i} + p_{2i+2}p_{2l+2-2i}\right) \\ &- \sum_{i=1}^{l}\left(\frac{1}{a^2}q_{2i-1}q_{2l+1-2i} + q_{2i}q_{2l+2-2i}\right)\Bigg) \\ &- a^2\sum_{i=1}^{l} p_{2i-1}q_{2i} + \sum_{i=1}^{l} p_{2i}q_{2i-1}, \end{aligned} \tag{20.8.7}$$

where $l = \frac{k}{2}$. For $k = 2$, $H_0 = \pm\frac{1}{2}\left(\frac{1}{a^2}q_1^2 + q_2^2\right) - a^2 p_1 q_2 + p_2 q_1$.

We can now state Williamson's theorem.

Theorem 20.8.1 (Williamson) *A real symplectic vector space with a given quadratic form H_0 can be decomposed into a direct sum of skew orthogonal real symplectic subspaces in such a way that the quadratic form*

H_0 is represented as a sum of quadratic forms of the types listed above on these subspaces.

Williamson's list of normal forms is not unique. Slightly different lists are given by Bryuno [1988], and Laub and Meyer [1974]. Bryuno [1988] gives an excellent history of the subject. Other relevant work is Burgoyne and Cushman [1977a], [1977b]. A version of Williamson's theorem that applies to Hamiltonians invariant with respect to a compact Lie group can be found in Melbourne and Dellnitz [1993]. Churchill and Kummer [1999] give an algorithm for computing Williamson's normal forms. Their paper also surveys and discusses a variety of issues associated with the computation of normal forms for Hamiltonian systems.

20.8B Versal Deformations of Jordan Blocks Corresponding to Repeated Eigenvalues

We next describe versal deformations of the Jordan blocks corresponding to repeated eigenvalues described above classified according to codimension. These results are due to Galin [1982] (see also Kocak [1984] and Hoveijn [1996]). The theory is very similar to the theory developed in our discussion of versal deformations of matrices in Section 20.5. We begin by describing the modifications required for the definitions from that section.

We denote the set of all $2n \times 2n$ infinitesimally symplectic matrices (with real entries) by $M = sp(2n, \mathbb{R})$. M is a $n(2n+1)$ dimensional manifold. Matrices in M can be represented by

$$JA,$$

where

$$J = \begin{pmatrix} 0 & \mathrm{id} \\ -\mathrm{id} & 0 \end{pmatrix},$$

and A is a $2n \times 2n$ symmetric matrix. We also consider the Lie group $G = Sp(2n, \mathbb{R})$ of $2n \times 2n$ symplectic matrices with real entries.

Definition 20.8.2 (Adjoint Action) *The group G acts on M according to the formula*

$$Ad_S JA = S\,JA\,S^{-1}, \qquad (JA \in M, \quad S \in G).$$

(Ad stands for adjoint.)

Definition 20.8.3 (Orbit Under the Adjoint Action) *Consider the orbit of an arbitrary fixed matrix $JA_0 \in M$ under the adjoint action of G on M; this is the set of points $JA \in M$ such that $JA = S\,JA_0\,S^{-1}$ for all $S \in G$.*

The orbit of JA_0 under G forms a smooth submanifold of M, which we denote by N. Hence, the orbit, N, of JA_0 consists of all matrices similar to JA_0.

Definition 20.8.4 (Deformation of an Infinitesimally Symplectic Matric) *A* deformation *of JA_0 is a C^r ($r \geq 1$) mapping*

$$\begin{aligned} JA : \Lambda &\to M, \\ \lambda &\to JA(\lambda), \end{aligned}$$

where $\Lambda \in \mathbb{R}^\ell$ is some parameter space and

$$JA(\lambda_0) = JA_0.$$

A deformation is also called a family, *the variables λ_i, $i = 1, \cdots, \ell$, are called the parameters, and Λ is called the* base *of the family.*

Definition 20.8.5 (Equivalence of Deformations) *Two deformations $JA(\lambda)$, $JB(\lambda)$ of JA_0 are called* equivalent *if there exists a deformation of the identity matrix $C(\lambda)$ ($C(\lambda_0) = id$), where $C(\lambda)$ is symplectic for each value of λ, with the same base, such that*

$$JB(\lambda) = C(\lambda)JA(\lambda)C^{-1}(\lambda).$$

Definition 20.8.6 (Induced Family) *Let $\Sigma \subset \mathbb{R}^m$, $\Lambda \subset \mathbb{R}^\ell$ be open sets. Consider the C^r ($r \geq 1$) mapping*

$$\begin{aligned} \phi : \Sigma &\to \Lambda, \\ \mu &\to \phi(\mu), \end{aligned}$$

with $\phi(\mu_0) = \lambda_0$.

The family induced from JA by the mapping ϕ *is called $(\phi^* JA)(\mu)$ and is defined by*

$$(\phi^* JA)(\mu) \equiv JA(\phi(\mu)), \qquad \mu \in \mathbb{R}^m.$$

Definition 20.8.7 (Versal, Universal, and Miniversal Deformation) *A deformation $JA(\lambda)$ of an infinitesimally symplectic matrix JA_0 is said to be* versal *if any deformation $JB(\mu)$ of JA_0 is equivalent to a deformation induced from JA, i.e.,*

$$JB(\mu) = C(\mu)JA(\phi(\mu))C^{-1}(\mu)$$

for some change of parameters

$$\phi : \Sigma \to \Lambda,$$

with $C(\mu_0) = id$ and $\phi(\mu_0) = \lambda_0$.

A versal deformation is said to be universal *if the inducing mapping (i.e., change of parameters map) is determined uniquely by the deformation JB.*

A versal deformation is said to be miniversal *if the dimension of the parameter space is the smallest possible for a versal deformation.*

Versal deformations for infinitesimally symplectic matrices are constructed in essentially the same way as for arbitrary matrices in Section 20.5. The centralizer of a matrix played a key role.

Definition 20.8.8 (Centralizer) *The centralizer of an infinitesimally symplectic matrix JA is the set Z of all infinitesimally symplectic matrices JC such that*

$$JCJA = JAJC.$$

The dimension of the centralizer can be computed by the formula given in the following lemma.

Lemma 20.8.9 *The dimension of the centralizer of an infinitesimally symplectic matrix JA_0 depends on the Jordan form of the matrix, and is given by the formula*

$$\begin{aligned} dim\, Z = &\frac{1}{2}\sum_{z\neq 0}\left[\sum_{j=1}^{s(z)}(2j-1)n_j(z)-1\right] + \frac{1}{2}\sum_{j=1}^{u}(2j-1)m_j \\ &+ \sum_{j=1}^{v}[2(2j-1)\tilde{m}_j+1] + 2\sum_{j=1}^{u}\sum_{k=1}^{v} min\{m_j, \tilde{m}_k\}, \end{aligned}$$

where $n_1(z) \geq n_2(z) \geq \cdots \geq n_s(z)$ are the dimensions of the Jordan blocks with eigenvalue $z \neq 0$, $m_1 \geq m_2 \geq \cdots \geq m_u$, $\tilde{m}_1 \geq \tilde{m}_2 \geq \cdots \geq \tilde{m}_v$ are

the dimensions of the Jordan blocks with eigenvalue $z = 0$, the numbers m_j being even, while $\tilde{m}_j$ are odd (only one block out of each pair of Jordan blocks of odd dimension is taken into account).

The relationship between the dimension of the centralizer and the orbit of an infinitesimally symplectic matrix under the adjoint action of G is given in the following proposition.

Proposition 20.8.10 *The dimension of the centralizer of an arbitrary infinitesimally symplectic matrix JA_0 is equal to the codimension of its orbit in the space M of infinitesimally symplectic matrices.*

The following proposition is analogous to Proposition 20.5.8, and proven in the same way.

Proposition 20.8.11 *A deformation $JA(\lambda)$ of an arbitrary infinitesimally symplectic matrix JA_0 is versal if and only if the mapping $JA(\lambda)$ is transversal to N at the point $\lambda = \lambda_0$.*

Versal deformations for infinitesimally symplectic matrices are computed in exactly the same way as for arbitrary matrices as described in Section 20.5. For a Jordan block JA_0, a versal deformation is of the form

$$JA_0 + JB,$$

where B is symmetric, and has entries consisting of the appropriate number of parameters (as given by Lemma 20.8.9), with the parameters occurring in such a way that JB is *not* in the tangent space of N. Lemma 20.5.11 and the inner product on the space of matrices (equation (20.5.11)) can be used to verify that JB has this property. Once this has been done, we can also recover $A_0 + B$ (by multiplying by J^{-1}, and write a corresponding versal deformation of the Hamiltonian, or quadratic form (20.8.1). Galin [1982] has made a list of these quadratic forms for codimension ≤ 2, which we now reproduce.

20.8c Versal Deformations of Quadratic Hamiltonians of Codimension ≤ 2

First, we introduce some notation. For a given eigenvalue λ, we will denote the corresponding Jordan block of dimension (or order) k by $(\lambda)^k$.

The following will be our shorthand notation denoting the Jordan block structure associated with the pairs or quartets of eigenvalues that occur for infinitesimally symplectic matrices (a and b stand for real numbers):

$$(+a)^k(-a)^k \equiv (\pm a)^k,$$
$$(+ia)^k(-ia)^k \equiv (\pm ia)^k,$$
$$(+a+ib)^k(+a-ib)^k(-a+ib)^k(-a-ib)^k \equiv (\pm a \pm ib)^k.$$

Codimension Zero

This is the situation when there are no multiple eigenvalues.

Codimension One

There are three cases of codimension one Jordan blocks.

$\boxed{(\pm a)^2}$

$$H(\lambda) = -a\,(p_1q_1 + p_2q_2) + p_1q_2 + \lambda_1 p_2q_1. \tag{20.8.8}$$

$\boxed{(\pm ia)^2}$

$$H(\lambda) = p_2q_1 - a^2p_1q_2 \pm \frac{1}{2}\left(\frac{1}{a^2}q_1^2 + q_2^2\right) + \frac{\lambda_1}{2}p_1^2. \tag{20.8.9}$$

$\boxed{0^2}$

$$H(\lambda) = \mp\frac{1}{2}q_1^2 + \frac{\lambda_1}{2}p_1^2 \tag{20.8.10}$$

Codimension Two

There are nine cases of codimension two Jordan blocks.

$\boxed{(\pm a)^3}$

$$\begin{aligned} H(\lambda) = &-a\,(p_1q_1 + p_2q_2 + p_3q_3) + (p_1q_2 + p_2q_3) \\ &+ \lambda_1 p_2q_1 + \lambda_2 p_3q_1 \end{aligned} \tag{20.8.11}$$

$\boxed{(\pm ia)^3}$

$$\begin{aligned} H(\lambda) = &-(p_1q_2 + p_2q_3) \mp \frac{1}{2}\left(2a^2p_1p_3 - a^2p_2^2 + 2q_1q_3 - q_2^2\right) \\ &+ \lambda_1 p_2q_1 + \frac{\lambda_2}{2}q_1^2 \end{aligned} \tag{20.8.12}$$

$\boxed{(\pm a \pm ib)^2}$

$$\begin{aligned} H(\lambda) = &-a\,(p_1q_1 + p_2q_2 + p_3q_3 + p_4q_4) \\ &+ b\,(p_1q_2 - p_2q_1 + p_3q_4 - p_4q_3) \\ &+ (p_1q_3 + p_2q_4) + \lambda_1 p_3 q_1 + \lambda_2 p_4 q_1 \end{aligned} \tag{20.8.13}$$

$\boxed{0^4}$

$$H(\lambda) = -p_1q_2 \pm \frac{1}{2}\left(p_1^2 - 2q_1q_2\right) + \lambda_1 p_1 p_2 + \frac{\lambda_2}{2}p_2^2 \tag{20.8.14}$$

$\boxed{(\pm a)^2\,(\pm b)^2}$

$$\begin{aligned} H(\lambda) = &-a\,(p_1q_1 + p_2q_2) + p_1q_2 - b\,(p_3q_3 + p_4q_4) \\ &+ p_3q_4 + \lambda_1 p_2 q_1 + \lambda_2 p_4 q_3 \end{aligned} \tag{20.8.15}$$

$\boxed{(\pm ia)^2\,(\pm ib)^2}$

$$\begin{aligned} H(\lambda) = &\, p_2q_1 - a^2 p_1 q_2 \pm \frac{1}{2}\left(\frac{1}{a^2}q_1^2 + q_2^2\right) + p_4q_3 \\ &- b^2 p_3 q_4 \pm \frac{1}{2}\left(\frac{1}{b^2}q_3^2 + q_4^2\right) + \frac{\lambda_1}{2}p_1^2 + \frac{\lambda_2}{2}p_3^2 \end{aligned} \tag{20.8.16}$$

$\boxed{(\pm a)^2\,(\pm ib)^2}$

$$\begin{aligned} H(\lambda) = &-a\,(p_1q_1 + p_2q_2) + p_1q_2 + p_4q_3 \\ &- b^2 p_3 q_4 \pm \frac{1}{2}\left(\frac{1}{b^2}q_3^2 + q_4^2\right) + \lambda_1 p_2 q_1 + \frac{\lambda_2}{2}p_3^2 \end{aligned} \tag{20.8.17}$$

$\boxed{(\pm a)^2\,0^2}$

$$H(\lambda) = -a\,(p_1q_1 + p_2q_2) + p_1q_2 \mp \frac{1}{2}q_3^2 + \lambda_1 p_2 q_1 + \frac{\lambda_2}{2}p_3^2 \tag{20.8.18}$$

$\boxed{(\pm ia)^2\,0^2}$

$$H(\lambda) = p_2q_1 - a^2 p_1 q_2 \pm \frac{1}{2}\left(\frac{1}{a^2}q_1^2 + q_2^2\right) \mp \frac{1}{2}q_3^2 + \frac{\lambda_1}{2}p_1^2 + \frac{\lambda_2}{2}p_3^2 \tag{20.8.19}$$

20.8D Versal Deformations of Linear, Reversible Dynamical Systems

Versal deformations for linear, reversible systems have been worked out by Sevryuk [1986], [1992], and Hoveijn [1996].

20.8e Exercises

1. Compute the form of the quadratic Hamiltonians in the codimension zero cases. Also compute the associated infinitesimally symplectic matrices.

2. For the codimension one versal deformations, compute the associated infinitesimally symplectic matrices.

3. Prove that the three codimension one cases in Galin's list are indeed versal deformations.

4. **Eigenvalue Movement.** For the codimension one versal deformations, sketch the positions of the eigenvalues in the complex plane for $\lambda_1 < 0$, $\lambda_1 = 0$, and $\lambda_1 > 0$. Indicate how the eigenvalues move as λ_1 is varied from positive to negative. The case $(\pm ia)^2$ is known as the *Hamiltonian Hopf bifurcation*. However, as pointed out in Meyer and Hall [1992], Hopf had nothing to do with the study of the bifurcations associated with this case. van der Meer [1985] and Meyer and Hall [1992] give discussions that put this in the correct historical context. An elementary exposition of the Hamiltonian Hopf bifurcation is given by Lahiri and Roy [2001].

5. Compute the normal form (the leading order terms beyond quadratic) for the Hamiltonian Hopf bifurcation.

6. Compute the normal form (the leading order terms beyond quadratic) for the the case $(\pm a)^2$.

20.9 Elementary Hamiltonian Bifurcations

In this section we describe some of the basic elementary Hamiltonian bifurcations. Hamiltonian bifurcation theory is a rapidly developing area. The articles of Meyer [1975], [1986], and Golubitsky *et al.* [1995] and the books of Arnold *et al.* [1988] and Meyer and Hall [1992] provide a good overview of the subject of Hamiltonian bifurcations of equilibrium points and periodic orbits, with and without symmetry.

20.9a One Degree-of-Freedom Systems

We now describe three elementary bifurcations of equilibrium points in one-degree-of-freedom Hamiltonian systems in the spirit of the saddle-node, pitchfork, and Hopf bifurcations for general vector fields that we described earlier. The following discussion is taken from Golubitsky and Stewart [1987].

Hamiltonian Saddle Node

The analog of the saddle-node bifurcation for Hamiltonian systems is a situation where as a parameter is varied two equilibria, a saddle and a center,

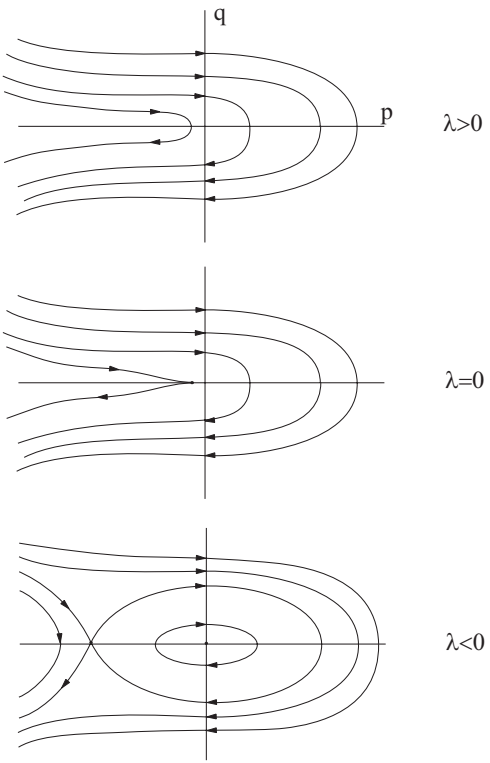

FIGURE 20.9.1. Phase portraits corresponding to the Hamiltonian saddle-node bifurcation.

collide and disappear, leaving no fixed points. Since the system is Hamiltonian it is (at least) two dimensional, and one would expect the center to be surrounded by periodic orbits and the saddle to have a separatrix (or homoclinic orbit). The normal form for this bifurcation is given by

$$H(p, q, \lambda) = \lambda p + q^2 + p^3, \quad (p, q, \lambda) \in \mathbb{R}^1 \times \mathbb{R}^1 \times \mathbb{R}^1. \tag{20.9.1}$$

The phase portraits are shown in Figure 20.9.1.

Hamiltonian Pitchfork: Z_2 Symmetry

The standard pitchfork bifurcation of equilibria is generic in one parameter families of vector fields equivariant with respect to a Z_2 action. Similarly, the Hamiltonian analog of the pitchfork occurs generically in one parameter families of Hamiltonians that are invariant with respect to a Z_2 action. The normal form is given by

$$H(p,q,\lambda) = \lambda p^2 + q^2 + p^4, \quad (p,q,\lambda) \in \mathbb{R}^1 \times \mathbb{R}^1 \times \mathbb{R}^1. \tag{20.9.2}$$

The phase portraits are shown in Figure 20.9.2.

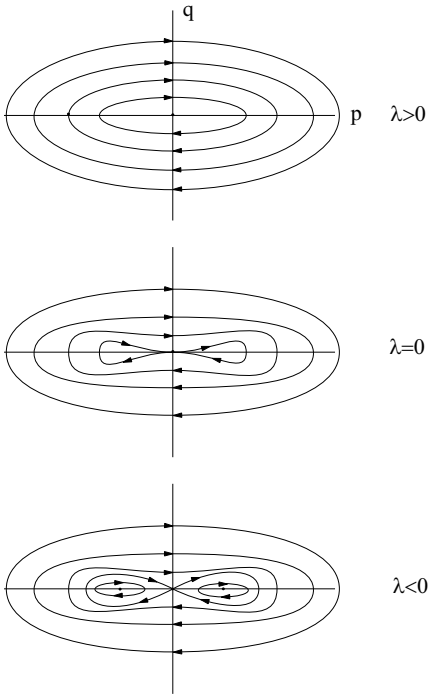

FIGURE 20.9.2. Phase portraits corresponding to the Hamiltonian pitchfork bifurcation.

S^1 Symmetry

The Poincaré-Andronov-Hopf bifurcation is a generic bifurcation of equilibria for one parameters families of two-dimensional vector fields having an S^1 symmetry. The normal form for a one-degree-of-freedom Hamiltonian in the neighborhood of an equilibrium point, and invariant with respect to an S^1 symmetry is given by

$$H(p,q,\lambda) = \lambda(p^2 + q^2) + (p^2 + q^2)^2, \quad (p,q,\lambda) \in \mathbb{R}^1 \times \mathbb{R}^1 \times \mathbb{R}^1. \tag{20.9.3}$$

However, the term Hamiltonian Hopf bifurcation is *not* applied to this situation. The phase portraits are shown in Figure 20.9.3.

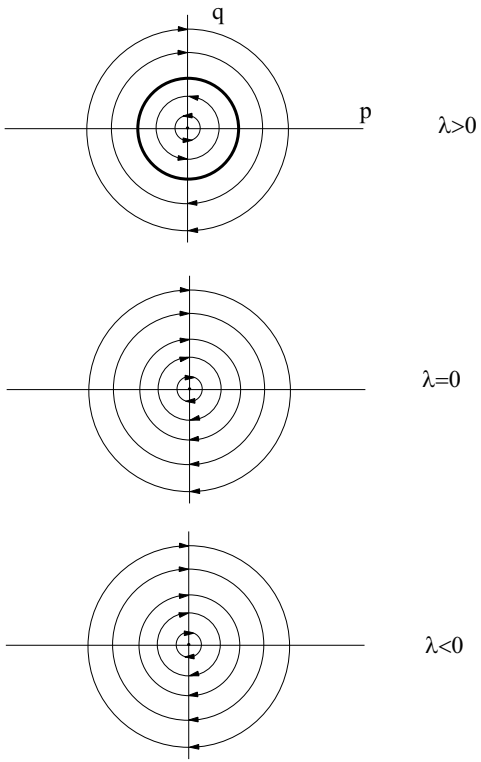

FIGURE 20.9.3. Phase portraits corresponding to the Hamiltonian invariant with respect to an S^1 symmetry. The heavy circle represents a circle of equilibrium points.

20.9B Exercises

1. Verify that the phase portraits shown in the Figures 20.9.1, 20.9.2, and 20.9.3 are correct.

2. For the Hamiltonian pitchfork bifurcation, an elliptic equilibrium point became a saddle (as the parameter passed through zero) with a symmetric pair of elliptic equilibria branching from it. Can you write down a normal form where a saddle type equilibrium point becomes an elliptic equilibrium point with two saddle type equilibria branching from it?

3. Prove that these three normal forms (20.9.1), (20.9.2), and (20.9.3) are indeed versal deformations for the situations described.

20.9c Bifurcations Near Resonant Elliptic Equilibrium Points

Bifurcations near resonant elliptic equilibrium points have been studied in detail by a number of authors. Arnold *et al.* [1988] and Meyer and Hall [1992] give excellent surveys. A great deal is known about bifurcations near resonant elliptic equilibria in the two degree-of-freedom case. There are two natural bifurcation parameters. One is the energy and the other is the "detuning", which allows one to study the passage through the resonance. The main reason so much is known in the two degree-of-freedom case is that the truncated normal form is integrable. Very little is known about bifurcations in resonant elliptic equilibria in n degree- of-freedom systems, $n \geq 3$, when the multiplicity of the resonance is larger than two (the truncated normal forms associated with multiplicity one resonances are still integrable, regardless of the number of degrees of freedom, provided it is finite). Hoveijn [1992] and Haller and Wiggins [1996] give recent surveys of the literature related to resonant elliptic equilibria with three or more degrees-of-freedom.

We now describe how one analyzes bifurcations near resonant equilibria in two degree-of-freedom Hamiltonian systems.

First we recall some basic results from Section 19.10b. The quadratic part of the Hamiltonian is given by

$$H(z_1, \bar{z}_1, z_2, \bar{z}_2) = \frac{\omega_1}{2}|z_1|^2 + \frac{\omega_2}{2}|z_2|^2,$$

and is said to be in resonance provided $\frac{\omega_1}{\omega_2}$ is a rational number. The truncated normal forms for the $1:1$ (semisimple), $1:2$, and $1:3$ resonances were computed and found to be:

1:1 Resonance

$$\begin{aligned} H(z_1, \bar{z}_1, z_2, \bar{z}_2) = &\frac{1}{2}(1+\delta_1)|z_1|^2 + \frac{1}{2}(1+\delta_2)|z_2|^2 \\ &+ c_{1111}|z_1|^2|z_2|^2 + c_{0022}|z_2|^4 + c_{2200}|z_1|^4 \\ &+ 2|c_{2011}|\mathrm{Re}z_1^2\bar{z}_1\bar{z}_2 + 2|c_{1102}|\mathrm{Re}z_1z_2\bar{z}_2^2 + 2|c_{2002}|\mathrm{Re}z_1^2\bar{z}_2^2, \end{aligned}$$

1:2 Resonance

$$H(z_1, \bar{z}_1, z_2, \bar{z}_2) = \frac{1}{2}(1+\delta_1)|z_1|^2 + (1+\delta_2)|z_2|^2 + 2|c_{2001}|\mathrm{Re}z_1^2\bar{z}_2,$$

1:3 Resonance

$$H(z_1, \bar{z}_1, z_2, \bar{z}_2) = \frac{1}{2}(1+\delta_1)|z_1|^2 + \frac{3}{2}(1+\delta_2)|z_2|^2 + c_{0202}|z_2|^4 + c_{2020}|z_1|^4 + c_{1111}|z_1|^2|z_2|^2 + 2|c_{3001}|\mathrm{Re}z_1^3\bar{z}_2.$$

These expressions differ slightly from the expressions computed in Section 19.10b in that we have included the (small) detuning parameters δ_1 and δ_2 which allow for the variation of the resonant frequencies.

Following Arnold et al. [1988], each of these normal forms can be transformed into a parametrized family of one degree-of-freedom Hamiltonian systems plus an "action-angle pair". The interesting dynamical information is contained in the family of one degree-of-freedom systems. In this way the entire phase space stucture can be uncovered. Moreover, the one degree-of-freedom bifurcations described in the previous section are particularly relevant for the analysis of the family of one degree-of-freedom systems.

The transformation is carried out as follows. First one transforms the normal form to symplectic polar coordinates via the transformation

$$z_k = \sqrt{\rho_k}e^{i\varphi_k}, \qquad \bar{z}_k = \sqrt{\rho_k}e^{-i\varphi_k}, \quad k = 1, 2.$$

If the resonance relation between ω_1 and ω_2 is expressed in the form

$$k_1\omega_1 + k_2\omega_2 = 0,$$

where k_1 and k_2 are relatively prime (and not *both* zero), then we choose relatively prime integers l_1 and l_2 satisfying

$$k_1 l_2 - k_2 l_1 = 1.$$

Then the following symplectic transformation casts the truncated normal form into the desired form

$$\begin{aligned} \varphi_1 &= l_2\psi - k_2\chi, \\ \varphi_2 &= -l_1\psi + k_1\chi, \\ \rho_1 &= k_1 G + l_1 I, \\ \rho_2 &= k_2 G + l_2 I. \end{aligned} \tag{20.9.4}$$

20.9D Exercises

1. Prove that (20.9.4) is a symplectic transformation.

2. Recast the truncated normal forms for the $1:1$ (semisimple), $1:2$, and $1:3$ resonances into the $I - G - \psi - \chi$ coordinates defined in (20.9.4). In these coordinates show that δ_1 and δ_2 can be effectively combined as one parameter, and give an interpretation of this parameter in terms of the resonance frequencies. Analyze the bifurcations (as a function of "energy" and "detuning"), and describe the phase space structure for the $1:1$ (semisimple), $1:2$, and $1:3$ resonances.

3. Show that for a general resonance, i.e.,

$$k_1\omega_1 + k_2\omega_2 = 0,$$

where k_1 and k_2 are relatively prime (and not *both* zero), the truncated normal form has the general form

$$H_{k_1,k_2} = \omega_1\rho_1 + \omega_2\rho_2 + F(\rho_1,\rho_2) + B\rho_1^{\frac{|k_1|}{2}}\rho_2^{\frac{|k_2|}{2}}\cos\left(k_1\varphi_1 + k_2\varphi_2 + \psi_0\right).$$

See Arnold *et al.* [1988] for an analysis of this normal form.

4. Using the coordinate transformations given above, analyze the truncated normal form associated with the Hamiltonian Hopf bifurcation (i.e., the case $(\pm ia)^2$) derived in the previous section.

5. Using the coordinate transformations given above, analyze the truncated normal form associated with the case $(\pm a)^2$ derived in the previous section.

6. Survey the literature and find five applications where bifurcations associated with the case $(\pm ia)^2$ arise.

7. Survey the literature and find five applications where bifurcations associated with the case $(\pm a)^2$ arise.

21

Bifurcations of Fixed Points of Maps

The theory for bifurcations of fixed points of maps is very similar to the theory for vector fields. Therefore, we will not include as much detail but merely highlight the differences when they occur.

Consider a p-parameter family of maps of $\mathbb{R}^n$ into $\mathbb{R}^n$

$$y \mapsto g(y, \lambda), \qquad y \in \mathbb{R}^n, \quad \lambda \in \mathbb{R}^p \tag{21.0.1}$$

where g is $\mathbf{C}^r$ (with r to be specified later, usually $r \geq 5$ is sufficient) on some sufficiently large open set in $\mathbb{R}^n \times \mathbb{R}^p$. Suppose (21.0.1) has a fixed point at $(y, \lambda) = (y_0, \lambda_0)$, i.e.,

$$g(y_0, \lambda_0) = y_0. \tag{21.0.2}$$

Then, just as in the case for vector fields, two questions naturally arise.

1. Is the fixed point stable or unstable?
2. How is the stability or instability affected as λ is varied?

As in the case for vector fields, an examination of the associated linearized map is the first place to start in order to answer these questions. The associated linearized map is given by

$$\xi \mapsto D_y g(y_0, \lambda_0)\xi, \qquad \xi \in \mathbb{R}^n, \tag{21.0.3}$$

and, from Chapter 1, we know that if the fixed point is hyperbolic (i.e., none of the eigenvalues of $D_y g(y_0, \lambda_0)$ have unit modulus), then stability (resp. instability) in the linear approximation implies stability (resp. instability) of the fixed point of the nonlinear map. Moreover, using an implicit function theorem argument exactly like that given at the beginning of Section 20, it can be shown that, in a sufficiently small neighborhood of (y_0, λ_0), for each λ there is a unique fixed point having the same stability type as (y_0, λ_0). Thus, hyperbolic fixed points are locally dynamically dull!

The fun begins when we consider Questions 1 and 2 above in the situation when the fixed point is *not hyperbolic*. Just as in the case for vector fields, the linear approximation cannot be used to determine stability, and varying λ can result in the creation of new orbits (i.e., bifurcation). The simplest ways in which a fixed point of a map can be nonhyperbolic are the following.

1. $D_y g(y_0, \lambda_0)$ has a single eigenvalue equal to 1 with the remaining $n-1$ eigenvalues having moduli not equal to 1.
2. $D_y g(y_0, \lambda_0)$ has a single eigenvalue equal to -1 with the remaining $n-1$ eigenvalues having moduli not equal to 1.
3. $D_y g(y_0, \lambda_0)$ has two complex conjugate eigenvalues having modulus 1 (which are *not* one of the first four roots of unity) with the remaining $n-2$ eigenvalues having moduli not equal to 1.

Using the center manifold theory, the analysis of the above situations can be reduced to the analysis of a p-parameter family of one-, one-, and two-dimensional maps, respectively.

Moreover, all of our results also apply immediately to periodic points of maps. Suppose the map $y \mapsto g(y, \lambda)$, $y \in \mathbb{R}^n$, $\lambda \in \mathbb{R}^p$ has a period k orbit for $\lambda = \lambda_0$, i.e., there is a sequence of length k, denoted $\{y_0, y_1, \ldots, y_{k-1}, y_k\}$, with $y_k = y_0$, such that $g(y_i, \lambda_0) = g(y_{i+1}, \lambda_0)$, $i = 0, \ldots, k-1$. Then y_i is a fixed point for the kth iterate of g, i.e., $g^k(y_i, \lambda_0) = y_i$, $i = 0, \ldots, k-1$. In other words, a periodic k orbit for a map gives rise to k fixed points for the kth iterate of the map and our results can be applied to each point individually for the kth iterate.

We begin with the case of an eigenvalue equal to one.

21.1 An Eigenvalue of 1

In this case, the study of the orbit structure near the fixed point can be reduced to the study of a parametrized family of maps on the one-dimensional center manifold. We suppose that the map on the center manifold is given by

$$x \mapsto f(x, \mu), \qquad x \in \mathbb{R}^1, \quad \mu \in \mathbb{R}^1, \tag{21.1.1}$$

where, for now, we will consider only one parameter (if there is more than one parameter in the problem, we will consider all but one as fixed constants). In making the reduction to the center manifold, the fixed point

$(y_0, \lambda_0) \in \mathbb{R}^n \times \mathbb{R}^p$ has been transformed to the origin in $\mathbb{R}^1 \times \mathbb{R}^1$ (cf. Section 18.1) so that we have

$$f(0,0) = 0, \tag{21.1.2}$$

$$\frac{\partial f}{\partial x}(0,0) = 1. \tag{21.1.3}$$

21.1a The Saddle-Node Bifurcation

Consider the map

$$x \mapsto f(x,\mu) = x + \mu \mp x^2, \qquad x \in \mathbb{R}^1, \quad \mu \in \mathbb{R}^1. \tag{21.1.4}$$

It is easy to verify that $(x,\mu) = (0,0)$ is a nonhyperbolic fixed point of (21.1.4) with eigenvalue 1, i.e.,

$$f(0,0) = 0, \tag{21.1.5}$$

$$\frac{\partial f}{\partial x}(0,0) = 1. \tag{21.1.6}$$

We are interested in the nature of the fixed points for (21.1.4) near $(x,\mu) = (0,0)$. Since (21.1.4) is so simple, we can solve for the fixed points directly as follows

$$f(x,\mu) - x = \mu \mp x^2 = 0. \tag{21.1.7}$$

We show the two curves of fixed points in Figure 21.1.1 and leave it as an exercise for the reader to verify the stability types of the different branches of fixed points shown in this figure. We refer to the bifurcation occuring at $(x,\mu) = (0,0)$ as a *saddle-node* bifurcation.

In analogy with the situation for vector fields (see Section 20.1c) we want to find general conditions (in terms of derivatives evaluated at the bifurcation point) under which a map will undergo a saddle-node bifurcation, i.e.,

> the map possesses a unique curve of fixed points in the $x - \mu$ plane passing through the bifurcation point which locally lies on one side of $\mu = 0$.

We proceed using the implicit function theorem exactly as in the case for vector fields.

Consider a general one-parameter family of one-dimensional maps

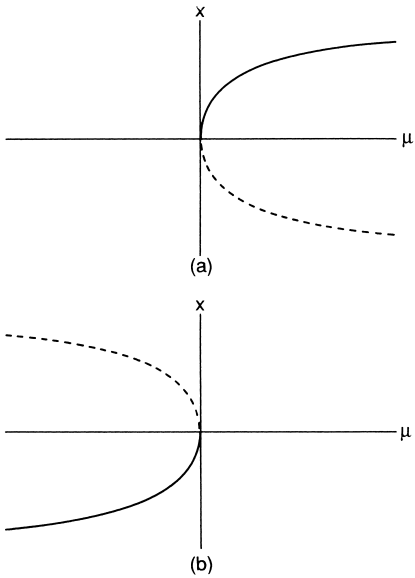

FIGURE 21.1.1. a) $f(x,\mu) = x + \mu - x^2$; b) $f(x,\mu) = x + \mu + x^2$.

$$x \mapsto f(x,\mu), \qquad x \in \mathbb{R}^1, \quad \mu \in \mathbb{R}^1, \tag{21.1.8}$$

with

$$f(0,0) = 0, \tag{21.1.9}$$

$$\frac{\partial f}{\partial x}(0,0) = 1. \tag{21.1.10}$$

The fixed points of (3.2.11) are given by

$$f(x,\mu) - x \equiv h(x,\mu) = 0. \tag{21.1.11}$$

We seek conditions under which (21.1.11) defines a curve in the $x - \mu$ plane with the properties described above. By the implicit function theorem,

$$\frac{\partial h}{\partial \mu}(0,0) = \frac{\partial f}{\partial \mu}(0,0) \neq 0 \tag{21.1.12}$$

implies that a single curve of fixed points passes through $(x,\mu) = (0,0)$; moreover, for x sufficiently small, this curve of fixed points can be represented as a graph over the x variables, i.e., there exists a unique $\mathbf{C}^r$ function, $\mu(x)$, x sufficiently small, such that

$$h(x,\mu(x)) \equiv f(x,\mu(x)) - x = 0. \tag{21.1.13}$$

Now we simply require that

$$\frac{d\mu}{dx}(0) = 0, \tag{21.1.14}$$

$$\frac{d^2\mu}{dx^2}(0) \neq 0. \tag{21.1.15}$$

As was the case for vector fields (Section 20.1c), we obtain (21.1.14) and (21.1.15) in terms of derivatives of the map at the bifurcation point by implicitly differentiating (3.2.16). Following (20.1.32) and (20.1.35), we obtain

$$\frac{d\mu}{dx}(0) = \frac{-\frac{\partial h}{\partial x}(0,0)}{\frac{\partial h}{\partial \mu}(0,0)} = -\frac{\left(\frac{\partial f}{\partial x}(0,0) - 1\right)}{\frac{\partial f}{\partial \mu}(0,0)} = 0, \tag{21.1.16}$$

$$\frac{d^2\mu}{dx^2}(0) = \frac{-\frac{\partial^2 h}{\partial x^2}(0,0)}{\frac{\partial h}{\partial \mu}(0,0)} = \frac{-\frac{\partial^2 f}{\partial x^2}(0,0)}{\frac{\partial f}{\partial \mu}(0,0)}. \tag{21.1.17}$$

To summarize, a general one-parameter family of $\mathbf{C}^r$ $(r \geq 2)$ one-dimensional maps

$$x \mapsto f(x, \mu), \qquad x \in \mathbb{R}^1, \quad \mu \in \mathbb{R}^1$$

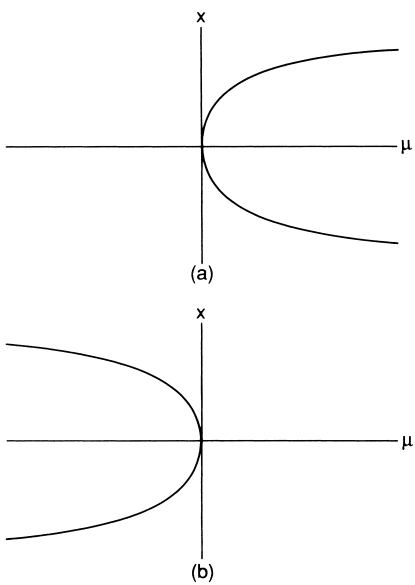

FIGURE 21.1.2.

undergoes a *saddle-node* bifurcation at $(x, \mu) = (0, 0)$ if

$$\left.\begin{array}{l} f(0,0) \quad = 0 \\ \frac{\partial f}{\partial \mu}(0,0) = 1 \end{array}\right\} \qquad \text{nonhyperbolic fixed point} \tag{21.1.18}$$

with

$$\frac{\partial f}{\partial \mu}(0,0) \neq 0, \tag{21.1.19}$$

$$\frac{\partial^2 f}{\partial x^2}(0,0) \neq 0. \tag{21.1.20}$$

Moreover, the sign of (21.1.17) tells us on which side of $\mu = 0$ the curve of fixed points is located; we show the two cases in Figure 21.1.2 and leave it as an exercise for the reader to compute the possible stability types of the branches of fixed points shown in the figure. Thus, (21.1.4) can be viewed as a normal form for the saddle-node bifurcation of maps. Notice that, with the exception of the condition $\frac{\partial f}{\partial x}(0,0) = 1$, the conditions for a one-parameter family of one-dimensional maps to undergo a saddle-node bifurcation in terms of derivatives of the map at the bifurcation point are exactly the same as those for vector fields (cf. (20.1.38), (20.1.39) and (20.1.40)). The reader should consider the implications of this.

Before finishing our discussion of the saddle-node bifurcation we want to describe a way of geometrically visualizing the bifurcation which will be useful later on. In the $x - y$ plane, the graph of $f(x, \mu)$ (thinking of μ as fixed) is given by

$$\text{graph } f(x,\mu) = \{\, (x,y) \in \mathbb{R}^2 \big|\, y = f(x,\mu)\}.$$

The graph of the function $g(x) = x$ is given by

$$\text{graph } g(x) = \{\, (x,y) \in \mathbb{R}^2 \big|\, y = x\}.$$

The intersection of these two graphs is given by

$$\{(x,y) \in \mathbb{R}^2 \big|\, y = x = f(x,\mu)\},$$

i.e., this is simply the set of fixed points for the map $x \mapsto f(x, \mu)$. The latter is simply a more mathematically complete way of saying that we draw the curve $y = f(x, \mu)$ (μ fixed) and the line $y = x$ in the $x - y$ plane and look for their intersections. We illustrate this for the map

$$x \mapsto x + \mu - x^2$$

in Figure 21.1.3 for different values of μ that graphically demonstrate the saddle-node bifurcation.

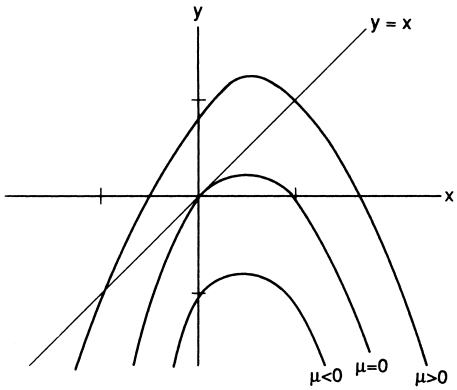

FIGURE 21.1.3.

21.1B The Transcritical Bifurcation

Consider the maps

$$x \mapsto f(x,\mu) = x + \mu x \mp x^2, \qquad x \in \mathbb{R}^1, \quad \mu \in \mathbb{R}^1. \tag{21.1.21}$$

It is easy to verify that $(x,\mu) = (0,0)$ is a nonhyperbolic fixed point of (21.1.21) with eigenvalue 1, i.e.,

$$f(0,0) = 0, \tag{21.1.22}$$

$$\frac{\partial f}{\partial x}(0,0) = 1. \tag{21.1.23}$$

The simplicity of (21.1.21) allows us to calculate all the fixed points relatively easily. They are given by

$$f(x,\mu) - x = \mu x \mp x^2 = 0. \tag{21.1.24}$$

Hence, there are two curves of fixed points passing through the bifurcation point,

$$x = 0 \tag{21.1.25}$$

and

$$\mu = \pm x. \tag{21.1.26}$$

We illustrate the two cases in Figure 21.1.4 and leave it as an exercise for the reader to compute the stability types of the different curves of fixed points shown in this figure. We refer to this type of bifurcation as a *transcritical* bifurcation.

We now want to find conditions for a general one-parameter family of $\mathbf{C}^r$ $(r \geq 2)$ one-dimensional maps to undergo a transcritical bifurcation, i.e.,

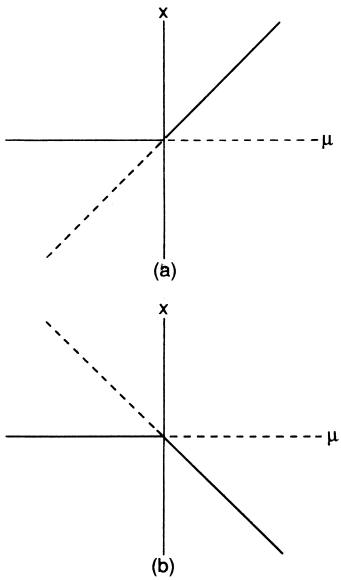

FIGURE 21.1.4. a) $f(x,\mu) = x + \mu x - x^2$; b) $f(x,\mu) = x + \mu x + x^2$.

in the $x - \mu$ plane the map has two curves of fixed points passing through the origin and existing on both sides of $\mu = 0$.

Consider a $\mathbf{C}^r$ $(r \geq 2)$ map

$$x \mapsto f(x,\mu), \qquad x \in \mathbb{R}^1, \quad \mu \in \mathbb{R}^1 \tag{21.1.27}$$

with

$$\left.\begin{array}{l} f(0,0) = 0 \\ \frac{\partial f}{\partial x}(0,0) = 1 \end{array}\right\} \qquad \text{nonhyperbolic fixed point.} \tag{21.1.28}$$

The fixed points of (21.1.27) are given by

$$f(x,\mu) - x \equiv h(x,\mu) = 0. \tag{21.1.29}$$

Henceforth the argument is very similar to that for the transcritical bifurcation of one-parameter families of one-dimensional vector fields; see Section 20.1d. We want two curves of fixed points to pass through the bifurcation point $(x,\mu) = (0,0)$, so we require that

$$\frac{\partial h}{\partial \mu}(0,0) = \frac{\partial f}{\partial \mu}(0,0) = 0. \tag{21.1.30}$$

Next, we want one of these curves of fixed points to be given by

$$x = 0; \tag{21.1.31}$$

we thus take (21.1.29) of the form

$$h(x,\mu) = xH(x,\mu) = x(F(x,\mu) - 1), \tag{21.1.32}$$

where

$$F(x,\mu) = \left\{ \begin{array}{ll} \frac{f(x,\mu)}{x}, & x \neq 0 \\ \frac{\partial f}{\partial x}(0,\mu), & x = 0 \end{array} \right\} \tag{21.1.33}$$

and, hence,

$$H(x,\mu) = \left\{ \begin{array}{ll} \frac{h(x,\mu)}{x}, & x \neq 0 \\ \frac{\partial h}{\partial x}(0,\mu), & x = 0 \end{array} \right\}. \tag{21.1.34}$$

Now we require $H(x,\mu)$ to have a unique curve of zeros passing through $(x,\mu) = (0,0)$ and existing on both sides of $\mu = 0$. For this it is sufficient to have

$$\frac{\partial H}{\partial \mu}(0,0) = \frac{\partial F}{\partial \mu}(0,0) \neq 0 \tag{21.1.35}$$

and, using (21.1.33), (21.1.35) is the same as

$$\frac{\partial^2 f}{\partial x \partial \mu}(0,0) \neq 0. \tag{21.1.36}$$

By the implicit function theorem, (21.1.36) implies that there exists a unique $\mathbf{C}^r$ function $\mu(x)$ (x sufficiently small) such that

$$H(x,\mu(x)) = F(x,\mu(x)) - 1 = 0. \tag{21.1.37}$$

Hence, we require

$$\frac{d\mu}{dx}(0) \neq 0. \tag{21.1.38}$$

Implicitly differentiating (21.1.37) gives

$$\frac{d\mu}{dx}(0) = \frac{-\frac{\partial H}{\partial x}(0,0)}{\frac{\partial H}{\partial \mu}(0,0)} = \frac{-\frac{\partial F}{\partial x}(0,0)}{\frac{\partial F}{\partial \mu}(0,0)}. \tag{21.1.39}$$

Using (21.1.33), (21.1.39) becomes

$$\frac{d\mu}{dx}(0) = \frac{-\frac{\partial^2 f}{\partial x^2}(0,0)}{\frac{\partial^2 f}{\partial x \partial \mu}(0,0)}. \tag{21.1.40}$$

We now summarize the results. A one-parameter family of $\mathbf{C}^r$ ($r \geq 2$) one-dimensional maps

$$x \mapsto f(x,\mu), \qquad x \in \mathbb{R}^1, \quad \mu \in \mathbb{R}^1 \tag{21.1.41}$$

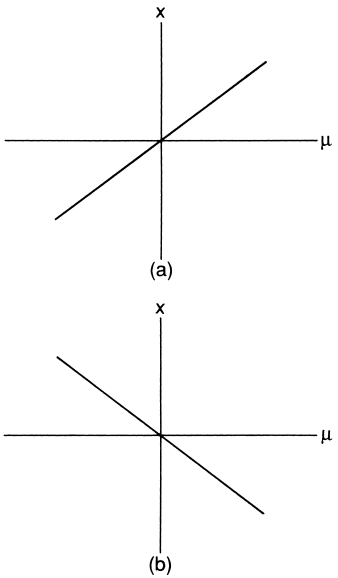

FIGURE 21.1.5.
a) $\left(-\frac{\partial^2 f}{\partial x^2}(0,0)/\frac{\partial^2 f}{\partial x \partial \mu}(0,0)\right) > 0$;
b) $\left(-\frac{\partial^2 f}{\partial x^2}(0,0)/\frac{\partial^2 f}{\partial x \partial \mu}(0,0)\right) < 0$.

having a nonhyperbolic fixed point, i.e.,

$$f(0,0) = 0, \tag{21.1.42}$$

$$\frac{\partial f}{\partial x}(0,0) = 1, \tag{21.1.43}$$

undergoes a transcritical bifurcation at $(x, \mu) = (0,0)$ if

$$\frac{\partial f}{\partial \mu}(0,0) = 0, \tag{21.1.44}$$

$$\frac{\partial^2 f}{\partial x \partial \mu}(0,0) \neq 0, \tag{21.1.45}$$

and

$$\frac{\partial^2 f}{\partial x^2}(0,0) \neq 0. \tag{21.1.46}$$

We remark that the sign of (21.1.40) gives us the slope of the curve of fixed points that is not $x = 0$. In Figure 21.1.5 we show the two cases and leave it as an exercise for the reader to compute the possible stability types for the different curves of fixed points shown in the figure; see Exercise

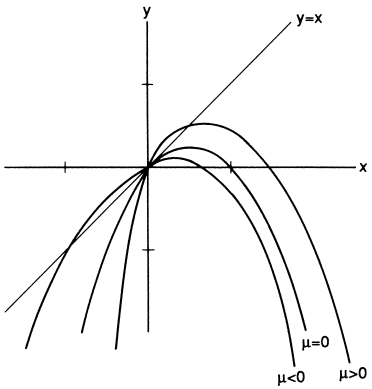

FIGURE 21.1.6.

5. Thus (21.1.21) can be viewed as a normal form for the transcritical bifurcation.

We end our discussion of the transcritical bifurcation by graphically showing the transcritical bifurcation in Figure 21.1.6 for the map

$$x \mapsto x + \mu x - x^2;$$

cf. the discussion at the end of Section 21.1a.

21.1c The Pitchfork Bifurcation

Consider the maps

$$x \mapsto f(x, \mu) = x + \mu x \mp x^3, \qquad x \in \mathbb{R}^1, \quad \mu \in \mathbb{R}^1. \tag{21.1.47}$$

It is easy to verify that $(x, \mu) = (0, 0)$ is a nonhyperbolic fixed point of (21.1.47) with eigenvalue 1, i.e.,

$$f(0, 0) = 0, \tag{21.1.48}$$

$$\frac{\partial f}{\partial x}(0, 0) = 1. \tag{21.1.49}$$

The fixed points of (21.1.47) are given by

$$f(x, \mu) - x = \mu x \mp x^3 = 0. \tag{21.1.50}$$

Thus, there are two curves of fixed points passing through the bifurcation point,

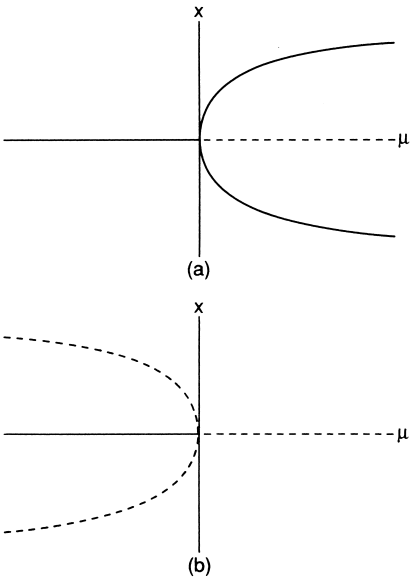

FIGURE 21.1.7. a) $f(x,\mu) = x + \mu x - x^3$, b) $f(x,\mu) = x + \mu x + x^3$.

$$x = 0 \tag{21.1.51}$$

and

$$\mu = \pm x^2 \tag{21.1.52}$$

We illustrate the two cases in Figure 21.1.7 and leave it as an exercise for the reader to verify the stability types of the different branches of fixed points shown in this figure. We refer to this type of bifurcation as a *pitchfork* bifurcation for maps.

We now seek general conditions for a one-parameter family of $\mathbf{C}^r$ $(r \geq 3)$ one-dimensional maps to undergo a pitchfork bifurcation, i.e.,

> in the $x - \mu$ plane the map has two curves of fixed points passing through the bifurcation point; one curve exists on both sides of $\mu = 0$ and the other lies locally to one side of $\mu = 0$.

Consider a $\mathbf{C}^r$ $(r \geq 3)$ map

$$x \mapsto f(x,\mu), \qquad x \in \mathbb{R}^1, \quad \mu \in \mathbb{R}^1 \tag{21.1.53}$$

with

$$\left.\begin{array}{l} f(0,0) = 0 \\ \frac{\partial f}{\partial x}(0,0) = 1 \end{array}\right\} \qquad \text{nonhyperbolic fixed point.} \tag{21.1.54}$$

The fixed points of (21.1.53) are given by

$$f(x,\mu) - x \equiv h(x,\mu) = 0. \tag{21.1.55}$$

Henceforth, the discussion is very similar to the discussion of the pitchfork bifurcation for vector fields (see Section 20.1). In order to have more than one curve of fixed points passing through $(x,\mu) = (0,0)$, we must have

$$\frac{\partial h}{\partial \mu}(0,0) = \frac{\partial f}{\partial \mu}(0,0) = 0. \tag{21.1.56}$$

Since we want one curve of fixed points to be $x = 0$, we take (21.1.55) of the form

$$h(x,\mu) = xH(x,\mu) = x(F(x,\mu) - 1), \tag{21.1.57}$$

where

$$H(x,\mu) = \left\{ \begin{array}{ll} \frac{h(x,\mu)}{x}, & x \neq 0 \\ \frac{\partial h}{\partial x}(0,\mu), & x = 0 \end{array} \right\} \tag{21.1.58}$$

and, hence,

$$F(x,\mu) = \left\{ \begin{array}{ll} \frac{f(x,\mu)}{x}, & x \neq 0 \\ \frac{\partial f}{\partial x}(0,\mu), & x = 0 \end{array} \right\}. \tag{21.1.59}$$

Since we want only one additional curve of fixed points to pass through $(x,\mu) = (0,0)$, we require

$$\frac{\partial H}{\partial \mu}(0,0) = \frac{\partial F}{\partial \mu}(0,0) \neq 0. \tag{21.1.60}$$

Using (21.1.59), (21.1.60) becomes

$$\frac{\partial^2 f}{\partial x \partial \mu}(0,0) \neq 0. \tag{21.1.61}$$

The implicit function theorem and (21.1.61) imply that there is a unique $\mathbf{C}^r$ function, $\mu(x)$ (x sufficiently small), such that

$$H(x,\mu(x)) \equiv F(x,\mu(x)) - 1 = 0. \tag{21.1.62}$$

We require

$$\frac{d\mu}{dx}(0) = 0 \tag{21.1.63}$$

and

$$\frac{d^2\mu}{dx^2}(0) \neq 0. \tag{21.1.64}$$

Implicitly differentiating (21.1.62) gives

$$\frac{d\mu}{dx}(0) = \frac{-\frac{\partial H}{\partial x}(0,0)}{\frac{\partial H}{\partial \mu}(0,0)} = \frac{-\frac{\partial F}{\partial x}(0,0)}{\frac{\partial F}{\partial \mu}(0,0)}, \tag{21.1.65}$$

$$\frac{d^2\mu}{dx^2}(0) = \frac{-\frac{\partial^2 H}{\partial x^2}(0,0)}{\frac{\partial H}{\partial \mu}(0,0)} = \frac{-\frac{\partial^2 F}{\partial x^2}(0,0)}{\frac{\partial F}{\partial \mu}(0,0)}. \tag{21.1.66}$$

Using (21.1.59), (21.1.65) and (21.1.66) become

$$\frac{d\mu}{dx}(0) = \frac{-\frac{\partial^2 f}{\partial x^2}(0,0)}{\frac{\partial^2 f}{\partial x \partial \mu}(0,0)}, \tag{21.1.67}$$

$$\frac{d^2\mu}{dx^2}(0) = \frac{-\frac{\partial^3 f}{\partial x^3}(0,0)}{\frac{\partial^2 f}{\partial x \partial \mu}(0,0)}. \tag{21.1.68}$$

To summarize, a one-parameter family of $\mathbf{C}^r$ $(r \geq 3)$ one-dimensional maps

$$x \mapsto f(x,\mu), \qquad x \in \mathbb{R}^1, \quad \mu \in \mathbb{R}^1 \tag{21.1.69}$$

having a nonhyperbolic fixed point, i.e.,

$$f(0,0) = 0, \tag{21.1.70}$$

$$\frac{\partial f}{\partial x}(0,0) = 1, \tag{21.1.71}$$

undergoes a pitchfork bifurcation at $(x,\mu) = (0,0)$ if

$$\frac{\partial f}{\partial \mu}(0,0) = 0, \tag{21.1.72}$$

$$\frac{\partial^2 f}{\partial x^2}(0,0) = 0, \tag{21.1.73}$$

$$\frac{\partial^2 f}{\partial x \partial \mu}(0,0) \neq 0, \tag{21.1.74}$$

$$\frac{\partial^3 f}{\partial x^3}(0,0) \neq 0. \tag{21.1.75}$$

Moreover, the sign of (21.1.68) tells us on which side of $\mu = 0$ that one of the curves of fixed points lies. We illustrate both cases in Figure 21.1.8 and leave it as an exercise for the reader to compute the possible stability types of the different branches shown in Figure 21.1.8. Thus, we can view (21.1.47) as a normal form for the pitchfork bifurcation.

We end our discussion of the pitchfork bifurcation by graphically showing the bifurcation for

$$x \mapsto x + \mu x - x^3$$

in Figure 21.1.9 in the manner discussed at the end of Section 21.1a.

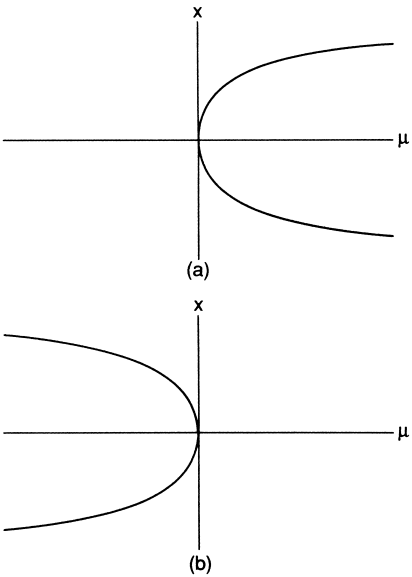

FIGURE 21.1.8.
a) $\left(-\frac{\partial^3 f}{\partial x^3}(0,0)/\frac{\partial^2 f}{\partial x \partial \mu}(0,0)\right) > 0$;
b) $\left(-\frac{\partial^3 f}{\partial x^3}(0,0)/\frac{\partial^2 f}{\partial x \partial \mu}(0,0)\right) < 0$.

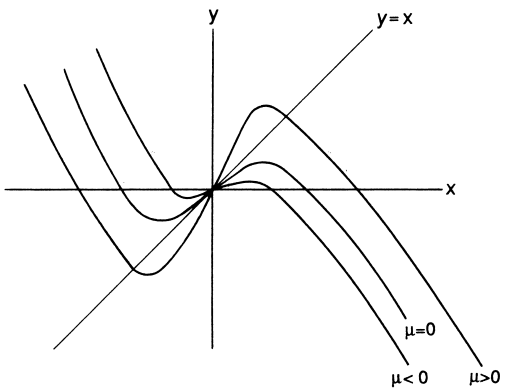

FIGURE 21.1.9.

21.2 An Eigenvalue of −1: Period Doubling

Suppose that our one-parameter family of $\mathbf{C}^r$ $(r \geq 3)$ one-dimensional maps has a nonhyperbolic fixed point, and the eigenvalue associated with

the linearization of the map about the fixed point is -1 rather than 1. Up to this point the bifurcations of one-parameter families of one-dimensional maps have been very much the same as the analogous cases for vector fields. However, the case of an eigenvalue equal to -1 is fundamentally different and does not have an analog with *one-dimensional* vector field dynamics. We begin by studying a specific example.

21.2a Example

Consider the following one-parameter family of one-dimensional maps

$$x \mapsto f(x,\mu) = -x - \mu x + x^3, \qquad x \in \mathbb{R}^1, \quad \mu \in \mathbb{R}^1. \tag{21.2.1}$$

It is easy to verify that (21.2.1) has a nonhyperbolic fixed point at $(x,\mu) = (0,0)$ with eigenvalue -1, i.e.,

$$f(0,0) = 0, \tag{21.2.2}$$

$$\frac{\partial f}{\partial x}(0,0) = -1. \tag{21.2.3}$$

The fixed points of (21.2.1) can be calculated directly and are given by

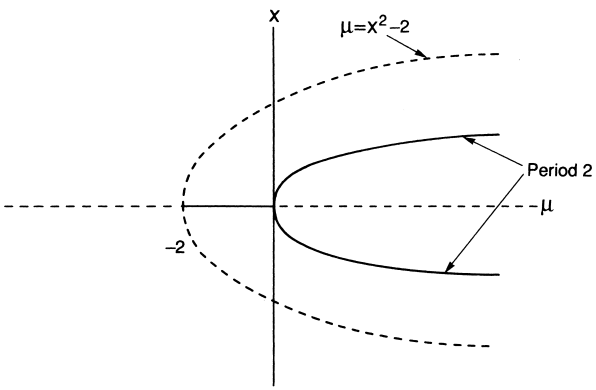

FIGURE 21.2.1.

$$f(x,\mu) - x = x(x^2 - (2+\mu)) = 0. \tag{21.2.4}$$

Thus, (21.2.1) has two curves of fixed points,

$$x = 0 \tag{21.2.5}$$

and

$$x^2 = 2 + \mu, \tag{21.2.6}$$

but only (21.2.5) passes through the bifurcation point $(x, \mu) = (0, 0)$. In Figure 21.2.1

we illustrate the two curves of fixed points and leave it as an exercise for the reader to verify the stability types for the different curves of fixed points shown in the figure. In particular we have

$$x = 0 \text{ is } \begin{cases} \text{unstable for } \mu \leq -2, \\ \text{stable for } -2 < \mu < 0, \\ \text{unstable for } \mu > 0, \end{cases} \tag{21.2.7}$$

and

$$x^2 = 2 + \mu \text{ is } \begin{cases} \text{unstable for } \mu \geq -2, \\ \text{does not exist for } \mu < -2. \end{cases} \tag{21.2.8}$$

From (21.2.7) and (21.2.8) we can immediately see there is a problem, namely, that for $\mu > 0$, the map has exactly three fixed points and all are unstable. (Note: this situation could not occur for one-dimensional vector fields.) A way out of this difficulty would be provided if stable periodic orbits bifurcated from $(x, \mu) = (0, 0)$. We will see that this is indeed the case.

Consider the *second iterate* of (21.2.1), i.e.,

$$x \mapsto f^2(x, \mu) = x + \mu(2 + \mu)x - 2x^3 + \mathcal{O}(4). \tag{21.2.9}$$

It is easy to verify that (21.2.9) has a nonhyperbolic fixed point at $(x, \mu) = (0, 0)$ having an eigenvalue of 1, i.e.,

$$f^2(0, 0) = 0, \tag{21.2.10}$$

$$\frac{\partial f^2}{\partial x}(0, 0) = 1. \tag{21.2.11}$$

Moreover,

$$\frac{\partial f^2}{\partial \mu}(0, 0) = 0, \tag{21.2.12}$$

$$\frac{\partial^2 f^2}{\partial x \partial \mu}(0, 0) = 2, \tag{21.2.13}$$

$$\frac{\partial^2 f^2}{\partial x^2}(0, 0) = 0, \tag{21.2.14}$$

$$\frac{\partial^3 f^2}{\partial x^3}(0, 0) = -12. \tag{21.2.15}$$

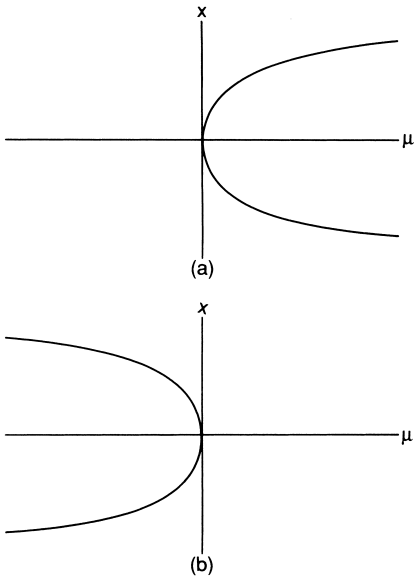

FIGURE 21.2.2.
a) $(-\frac{\partial^3 f^2}{\partial x^3}(0,0)/\frac{\partial^2 f^2}{\partial x \partial \mu}(0,0)) > 0$;
b) $(-\frac{\partial^3 f^2}{\partial x^3}(0,0)/\frac{\partial^2 f^2}{\partial x \partial \mu}(0,0)) < 0$.

Hence, from (21.1.72), (21.1.73), (21.1.74), and (21.1.75), (21.2.12), (21.2.13), (21.2.14), and (21.2.15) imply that the second iterate of (21.2.1) undergoes a pitchfork bifurcation at $(x, \mu) = (0, 0)$. Since the new fixed points of $f^2(x, \mu)$ are not fixed points of $f(x, \mu)$, they must be period two points of $f(x, \mu)$. Hence, $f(x, \mu)$ is said to have undergone a *period-doubling bifurcation* at $(x, \mu) = (0, 0)$.

21.2B The Period-Doubling Bifurcation

Consider a one-parameter family of $\mathbf{C}^r$ $(r \geq 3)$ one-dimensional maps

$$x \mapsto f(x, \mu), \qquad x \in \mathbb{R}^1, \quad \mu \in \mathbb{R}^1. \tag{21.2.16}$$

We seek conditions for (21.2.16) to undergo a period-doubling bifurcation. The previous example will be our guide. It should be clear from the example that conditions sufficient for (21.2.16) to undergo a period-doubling bifurcation are for the map to have a nonhyperbolic fixed point with eigenvalue -1 and for the second iterate of the map to undergo a pitchfork bifurcation at the same nonhyperbolic fixed point. To summarize, using

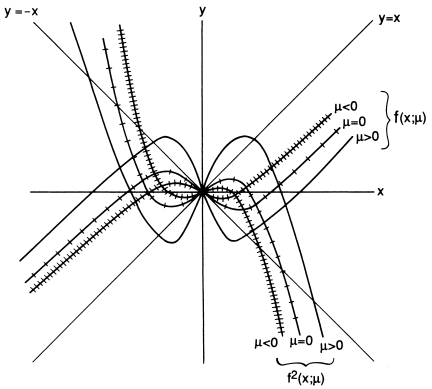

FIGURE 21.2.3.

(21.1.70), (21.1.71), (21.1.72), (21.1.73), (21.1.74), and (21.1.75), it is sufficient for (21.2.16) to satisfy

$$f(0,0) = 0, \tag{21.2.17}$$

$$\frac{\partial f}{\partial x}(0,0) = -1, \tag{21.2.18}$$

$$\frac{\partial f^2}{\partial \mu}(0,0) = 0, \tag{21.2.19}$$

$$\frac{\partial^2 f^2}{\partial x^2}(0,0) = 0, \tag{21.2.20}$$

$$\frac{\partial^2 f^2}{\partial x \partial \mu}(0,0) \neq 0, \tag{21.2.21}$$

$$\frac{\partial^3 f^2}{\partial x^3}(0,0) \neq 0. \tag{21.2.22}$$

Moreover, the sign of $\left(-\frac{\partial^3 f^2(0,0)}{\partial x^3} \Big/ \frac{\partial^2 f^2(0,0)}{\partial x \partial \mu}\right)$ tells us on which side of $\mu = 0$ the period two points lie. We show both cases in Figure 21.2.2 and leave it as an exercise for the reader to compute the possible stability types for the different curves of fixed points shown in the figure; see Exercise 7.

Finally, we demonstrate graphically the period-doubling bifurcation for

$$x \mapsto -x - \mu x + x^3 \equiv f(x, \mu)$$

and the associated pitchfork bifurcation for $f^2(x, \mu)$ in the graphical manner discribed at the end of Section 21.1a in Figure 21.2.3.

21.3 A Pair of Eigenvalues of Modulus 1: The Naimark-Sacker Bifurcation

This section describes the map analog of the Poincaré-Andronov-Hopf bifurcation for vector fields but with some very different twists. Although this bifurcation often goes by the name of "Hopf bifurcation for maps," this is misleading because the bifurcation theorem was first proved independently by Naimark [1959] and Sacker [1965]. Consequently, we will use the term "Naimark-Sacker bifurcation."

We know that in this situation the study of the dynamics of (21.0.1) near the fixed point $(y_0, \lambda_0) \in \mathbb{R}^n \times \mathbb{R}^p$ can be reduced to the study of (21.0.1) restricted to a p-parameter family of two-dimensional center manifolds. We assume that the reduced map has been calculated and is given by

$$x \mapsto f(x, \mu), \qquad x \in \mathbb{R}^2, \quad \mu \in \mathbb{R}^1, \tag{21.3.1}$$

where we take $p = 1$. If there is more than one parameter, we consider all but one as fixed and denote it as μ. In restricting the map to the center manifold, some preliminary transformations have been made so that the fixed point of (21.3.1) is given by $(x, \mu) = (0, 0)$, i.e., we have

$$f(0, 0) = 0, \tag{21.3.2}$$

with the matrix

$$D_x f(0, 0) \tag{21.3.3}$$

having two complex conjugate eigenvalues, denoted $\lambda(0), \bar{\lambda}(0)$, with

$$|\lambda(0)| = 1. \tag{21.3.4}$$

We will also require that

$$\lambda^n(0) \neq 1, \qquad n = 1, 2, 3, 4. \tag{21.3.5}$$

(Note: if $\lambda(0)$ satisfies (21.3.5), then so does $\bar{\lambda(0)}$, and vice versa.)

We showed in Example 19.3a that under these conditions a normal form for (21.3.1) is given by

$$z \mapsto \lambda(\mu) z + c(\mu) z^2 \bar{z} + \mathcal{O}(4), \qquad z \in \mathbb{C}, \quad \mu \in \mathbb{R}^1. \tag{21.3.6}$$

We transform (21.3.6) into polar coordinates by letting

$$z = r e^{2\pi i \theta},$$

and obtain

$$r \mapsto |\lambda(\mu)| \left(r + \left(\mathrm{Re} \left(\frac{c(\mu)}{\lambda(\mu)} \right) \right) r^3 + \mathcal{O}(r^4) \right),$$
$$\theta \mapsto \theta + \phi(\mu) + \frac{1}{2\pi} \left(\mathrm{Im} \left(\frac{c(\mu)}{\lambda(\mu)} \right) \right) r^2 + \mathcal{O}(r^3), \tag{21.3.7}$$

where

$$\phi(\mu) \equiv \frac{1}{2\pi} \tan^{-1} \frac{\omega(\mu)}{\alpha(\mu)} \tag{21.3.8}$$

and

$$c(\mu) = \alpha(\mu) + i\omega(\mu). \tag{21.3.9}$$

We then Taylor expand the coefficients of (21.3.7) about $\mu = 0$ and obtain

$$r \mapsto \left(1 + \frac{d}{d\mu} |\lambda(\mu)| \Big|_{\mu=0} \mu \right) r + \left(\mathrm{Re} \left(\frac{c(0)}{\lambda(0)} \right) \right) r^3 + \mathcal{O}(\mu^2 r, \mu r^3, r^4),$$
$$\theta \mapsto \theta + \phi(0) + \frac{d}{d\mu} (\phi(\mu)) \Big|_{\mu=0} \mu + \frac{1}{2\pi} \left(\mathrm{Im} \frac{c(0)}{\lambda(0)} \right) r^2$$
$$+ \mathcal{O}(\mu^2, \mu r^2, r^3), \tag{21.3.10}$$

where we have used the condition that $|\lambda(0)| = 1$. Note that, since $\lambda^n(0) \neq 1$, where $n = 1, 2, 3, 4$, from (21.3.8) we see that $\phi(0) \neq 0$. We simplify the notation associated with (21.3.10) by setting

$$d \equiv \frac{d}{d\mu} |\lambda(\mu)| \Big|_{\mu=0},$$
$$a \equiv \mathrm{Re} \left(\frac{c(0)}{\lambda(0)} \right),$$
$$\phi_0 \equiv \phi(0),$$
$$\phi_1 \equiv \frac{d}{d\mu} (\phi(\mu)) \Big|_{\mu=0},$$
$$b \equiv \frac{1}{2\pi} \mathrm{Im} \ \frac{c(0)}{\lambda(0)};$$

hence, (21.3.10) becomes

$$r \mapsto r + (d\mu + ar^2) r + \mathcal{O}(\mu^2 r, \mu r^3, r^4),$$
$$\theta \mapsto \theta + \phi_0 + \phi_1 \mu + br^2 + \mathcal{O}(\mu^2, \mu r^2, r^3). \tag{21.3.11}$$

We are interested in the dynamics of (21.3.11) for r small, μ small. Our strategy for understanding this will be the same as in our study of the Poincaré-Andronov-Hopf bifurcation for vector fields (cf. Section 20.2); namely, we will study the dynamics of (21.3.11) *with the higher order terms neglected* (i.e., the truncated normal form) and then try to understand how

the dynamics of the truncated normal form are affected by the higher order terms.

The truncated normal form is given by

$$\begin{aligned} r &\mapsto r + (d\mu + ar^2)r, \\ \theta &\mapsto \theta + \phi_0 + \phi_1\mu + br^2. \end{aligned} \tag{21.3.12}$$

Note that $r = 0$ is a fixed point of (21.3.12) that is

asymptotically stable	for $d\mu < 0$,
unstable	for $d\mu > 0$,
unstable	for $\mu = 0, a > 0$,

and

asymptotically stable	for $\mu = 0, a < 0$.

We recall our study of the truncated normal form for the Poincaré-Andronov-Hopf bifurcation for vector fields (see Section 20.2). In that case, fixed points of the $\dot{r}$ component of the truncated normal form, with $r > 0$, corresponded to periodic orbits. Something geometrically (but *not* dynamically) similar happens for maps also.

Lemma 21.3.1 $\left\{ (r, \theta) \in \mathbb{R}^+ \times S^1 \middle| \, r = \sqrt{\frac{-\mu d}{a}} \right\}$ *is a circle which is invariant under the dynamics generated by (21.3.12).*

Proof: That this set of points is a circle is obvious. The fact that it is invariant under the dynamics generated by (21.3.12) follows from the fact that the r coordinate of points starting on the circle do not change under iteration by (21.3.12). □

It should be clear that the invariant circle can exist for either $\mu > 0$ or $\mu < 0$ depending on the signs of d and a and that there will be only one invariant circle at a distance $\mathcal{O}(\sqrt{\mu})$ from the origin. Stability of the invariant circle is determined by the sign of a. This is a new concept of stability not previously discussed in this book, namely, the stability of an invariant set. Its meaning, hopefully, is intuitively clear. The invariant circle is stable if initial conditions "sufficiently near" the circle stay near the circle under all forward iterations by (21.3.12). It is asymptotically stable if the points actually approach the circle. We summarize this in the following lemma.

Lemma 21.3.2 *The invariant circle is asymptotically stable for $a < 0$ and unstable for $a > 0$.*

Proof: Since the r component of (21.3.12) is independent of θ, this problem reduces to the study of the stability of a fixed point of a one-dimensional map (i.e., the θ dynamics are irrelevant). We leave the details as an exercise for the reader. □

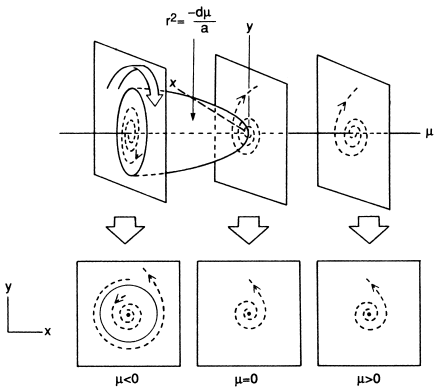

FIGURE 21.3.1. $d > 0$, $a > 0$.

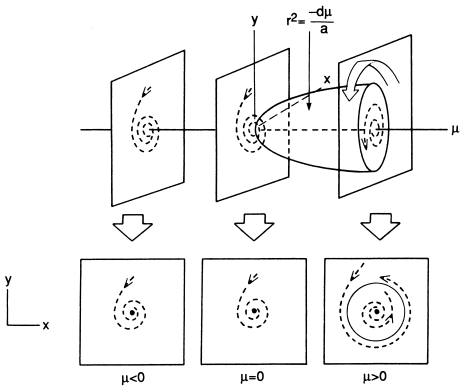

FIGURE 21.3.2. $d > 0$, $a < 0$.

We now describe the four possible cases for the bifurcation of an invariant circle from a fixed point.

Case 1: $d > 0$, $a > 0$. In this case, the origin is an unstable fixed point for $\mu > 0$ and an asymptotically stable fixed point for $\mu < 0$ with an unstable invariant circle for $\mu < 0$; see Figure 21.3.1.

Case 2: $d > 0$, $a < 0$. In this case, the origin is an unstable fixed point for $\mu > 0$ and an asymptotically stable fixed point for $\mu < 0$ with an asymptotically stable invariant circle for $\mu > 0$; see Figure 21.3.2.

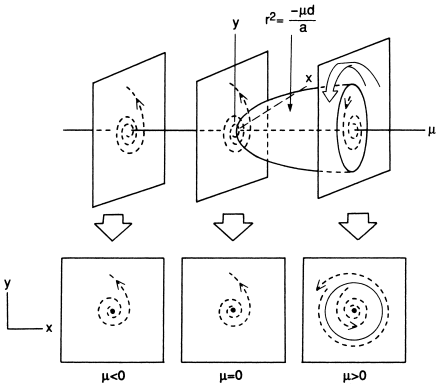

FIGURE 21.3.3. $d < 0$, $a > 0$.

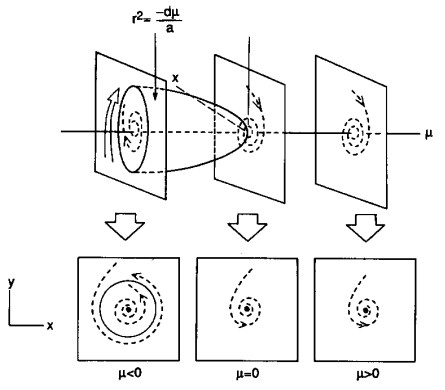

FIGURE 21.3.4. $d < 0$, $a < 0$.

Case 3: $d < 0$, $a > 0$. In this case, the origin is an asymptotically stable fixed point for $\mu > 0$ and an unstable fixed point for $\mu < 0$ with an unstable invariant circle for $\mu > 0$; see Figure 21.3.3.

Case 4: $d < 0$, $a < 0$. In this case, the origin is an asymptotically stable fixed point for $\mu > 0$ and an unstable fixed point for $\mu < 0$ with an asymptotically stable invariant circle for $\mu < 0$; see Figure 21.3.4.

We make the following general remarks.

Remark 1. For $a > 0$, the invariant circle can exist for either $\mu < 0$ (Case 1) or $\mu > 0$ (Case 3) and, in each case, the invariant circle is unstable. Similarly, for $a < 0$, the invariant circle can exist for either $\mu < 0$ (Case 4) or $\mu > 0$ (Case 2) and, in each case, the invariant circle is asymptotically stable. Hence, the quantity a determines the stability of the invariant circle, but it does not tell us on which side of $\mu = 0$ the invariant circle exists.

Remark 2. Recall that

$$d = \frac{d}{d\mu} \left|\lambda(\mu)\right|_{\mu=0}.$$

Hence, for $d > 0$, the eigenvalues cross from inside to outside the unit circle as μ increases through zero and, for $d < 0$, the eigenvalues cross from outside to inside the unit circle as μ increases through zero. Thus, for $d > 0$, it follows that the origin is asymptotically stable for $\mu < 0$ and unstable for $\mu > 0$. Similarly, for $d < 0$, the origin is unstable for $\mu < 0$ and asymptotically stable for $\mu > 0$.

At this point the reader is probably struck by the similarities between the analysis of the truncated normal form (21.3.12) and the analysis for the normal form associated with the Poincaré-Andronov-Hopf bifurcation (see Section 20.2). However, we want to stress that the situation for maps is fundamentally different indeed from this and from all other bifurcations we have studied thus far. In all other bifurcations (either in vector fields or maps) the invariant sets that are created consist of *single orbits* while, in this case, the bifurcation consists of an invariant surface (i.e., a circle) which contains many different orbits. We can study the dynamics on the invariant circle by studying the dynamics of (21.3.12) restricted to the invariant circle (i.e., by considering only initial conditions that start on the invariant circle). Points on the invariant circle have initial r coordinates given by

$$r = \sqrt{\frac{-\mu d}{a}},$$

so that the associated *circle map* is given by

$$\theta \mapsto \theta + \phi_0 + \left(\phi_1 - \frac{d}{a}\right)\mu. \tag{21.3.13}$$

The dynamics of (21.3.12) are easy to understand and depend entirely on the quantity $\phi_0 + (\phi_1 - \frac{d}{a})\mu$. If $\phi_0 + (\phi_1 - \frac{d}{a})\mu$ is rational, then all orbits on the invariant circle are periodic. If $\phi_0 + (\phi_1 - \frac{d}{a})\mu$ is irrational, then all orbits on the invariant circle densely fill the circle. We proved these statements in Chapter 10, Theorem 10.4.2. Thus, as μ is varied, the orbit structure on the invariant circle continually alternates between periodic and quasiperiodic.

Although all of this analysis is for the truncated normal form (21.3.12), our real interest is in the full normal form (21.3.11). For this we have the following theorem.

Theorem 21.3.3 (Naimark-Sacker bifurcation) *Consider the full normal form (21.3.11). Then, for μ sufficiently small, Cases 1, 2, 3, and 4 described above hold.*

Proof: The proof requires more technical machinery than the proof of the Poincaré-Andronov-Hopf bifurcation for vector fields. This should come as no surprise, since the Poincaré-Bendixson theorem and the method of averaging (do not immediately apply to maps. For this reason, we will not state this proof here; excellent expositions of the proof may be found in, e.g., Iooss [1979]. □

We must take care to interpret this theorem correctly. Roughly speaking, it tells us that the "tail" of the normal form does not qualitatively affect the bifurcation of the *invariant circle* exhibited by the truncated normal form. However, it tells us nothing about the dynamics *on the invariant circle*. Indeed, we would expect the higher order terms of the normal form to have a very important affect on the circle map associated with the invariant circle of the full normal form (21.3.11). This is because the circle map associated with the invariant circle of the truncated normal form is structurally unstable.

21.4 The Codimension of Local Bifurcations of Maps

The degeneracy of fixed points of maps can be specified by the concept of codimension as described in Section 20.4. The codimension of a case is computed using exactly the same procedure (cf. Definition 20.4.6). Indeed, for a $\mathbf{C}^r$ vector field

$$\dot{x} = f(x), \qquad x \in \mathbb{R}^n, \tag{21.4.1}$$

we are interested in the local structure of

$$f(x) = 0, \tag{21.4.2}$$

and, for a $\mathbf{C}^r$ map,

$$x \mapsto g(x), \qquad x \in \mathbb{R}^n, \tag{21.4.3}$$

we are interested in the local structure of

$$g(x) - x = 0. \tag{21.4.4}$$

Thus, it should be clear that, mathematically, (21.4.1) and (21.4.3) are the same. We will, therefore, state the results for maps only and leave the verification to the reader.

21.4A One-Dimensional Maps

The maps

$$x \mapsto x + ax^2 + \mathcal{O}(x^3), \tag{21.4.5}$$

$$x \mapsto -x + ax^3 + \mathcal{O}(x^4), \tag{21.4.6}$$

have nonhyperbolic fixed points at $x = 0$. Using the techniques developed in Chapter 20, Section 20.4b it is easy to see that these are *codimension one* fixed points with versal deformations given by

$$x \mapsto x + \mu \mp x^2, \tag{21.4.7}$$

$$x \mapsto -x + \mu x \mp x^3. \tag{21.4.8}$$

Hence, the generic bifurcations of fixed points of one-parameter families of one-dimensional maps are saddle-nodes and period-doublings.

Similarly, the map

$$x \mapsto x + ax^3 + \mathcal{O}(x^4) \tag{21.4.9}$$

has a nonhyperbolic fixed point at $x = 0$. It is easy to show that $x = 0$ is a *codimension two* fixed point, and a versal deformation is given by

$$x \mapsto x + \mu_1 + \mu_2 x \mp x^3. \tag{21.4.10}$$

21.4B Two-Dimensional Maps

Suppose we have a two-dimensional map having a fixed point at the origin with the two eigenvalues of the associated linear map being complex conjugates with modulus one. We denote the two eigenvalues by λ and $\bar{\lambda}$. One can assign a codimension to this nonhyperbolic fixed point using the methods of Section 20.4; the number obtained will depend on λ and $\bar{\lambda}$ (we will do this shortly). We can then construct a candidate for a versal deformation using the same methods. However, these will not give versal deformations. One of the obstructions to this involves the dynamics on invariant circles. As we have seen earlier (see Section 21.3), all of the higher order terms in

the normal form may affect the dynamics on the invariant circle. Nevertheless, we will give the codimension and the associated parametrized families using the techniques of Section 20.4 for the different cases.

The case

$$\lambda^n \neq 1, \qquad n = 1, 2, 3, 4, \tag{21.4.11}$$

is *codimension one*. The associated one-parameter family of normal forms for this bifurcation is

$$z \mapsto (1 + \mu)z + cz^2\bar{z}, \qquad z \in \mathbb{C} \tag{21.4.12}$$

(see Example 19.3a). If we ignore the dynamics on the invariant circle, then (21.4.12) captures all local dynamics.

The cases ruled out by (21.4.11) are referred to as the *strong resonances*. The cases $n = 3$ *and* $n = 4$ are *codimension one* with associated one-parameter families of normal forms given by

$$z \mapsto (1 + \mu)z + c_1\bar{z}^2 + c_2 z^2\bar{z}, \qquad n = 3, \qquad z \in \mathbb{C}, \quad \mu \in \mathbb{R}^1, \tag{21.4.13}$$

$$z \mapsto (1 + \mu)z + c_1\bar{z}^3 + c_2 z^2\bar{z}, \qquad n = 4, \qquad z \in \mathbb{C}, \quad \mu \in \mathbb{R}^1. \tag{21.4.14}$$

The cases $n = 1$ and $n = 2$ correspond to double 1 and double -1 eigenvalues, respectively. If the matrices associated with the linear parts (in Jordan canonical form) are given by

$$\begin{pmatrix} 1 & 1 \\ 0 & 1 \end{pmatrix}, \qquad n = 1, \tag{21.4.15}$$

and

$$\begin{pmatrix} -1 & 1 \\ 0 & -1 \end{pmatrix}, \qquad n = 2, \tag{21.4.16}$$

then these cases are *codimension two* with associated two-parameter families of normal forms given by

$$\begin{aligned} &x \mapsto x + y, \\ &y \mapsto \mu_1 + \mu_2 x + y + ax^2 + bxy, \end{aligned} \qquad n = 1, \tag{21.4.17}$$

$$\begin{aligned} &x \mapsto x + y, \\ &y \mapsto \mu_1 x + \mu_2 y + y + ax^3 + bx^2 y \end{aligned} \qquad n = 2. \tag{21.4.18}$$

Arnold [1983] studied (21.4.13), (21.4.14), (21.4.17), and (21.4.18) in detail by using the important local technique of interpolating a discrete map by a flow. We will work out some of the details in the exercises. The strongly resonant cases arise in applications in, for example, the situation of applying a periodic external force to a system which would freely oscillate with a given frequency. Strong resonance would occur when the forcing frequency and natural frequency were commensurate in the ratios 1/1, 1/2, 1/3, and 1/4. The surprising fact is that, in the cases $n = 1$ and $n = 2$, chaotic motions of the Smale–horseshoe type (see Gambaudo [1985]) may arise.

21.5 Exercises

1. Verify the stability for the branches of fixed points of the maps (21.1.4) shown in Figure 21.1.1. For one dimensional maps (as opposed to one dimensional vector fields) period doubling bifurcations are possible, so this may limit the range in μ for which the stabilities indicated in Figure 21.1.1 are valid.

2. Verify the stability for the branches of fixed points of the maps (21.1.21) shown in Figure 21.1.4. For one dimensional maps (as opposed to one dimensional vector fields) period doubling bifurcations are possible, so this may limit the range in μ for which the stabilities indicated in Figure 21.1.4 are valid.

3. Verify the stability for the branches of fixed points of the maps (21.1.47) shown in Figure 21.1.7. For one dimensional maps (as opposed to one dimensional vector fields) period doubling bifurcations are possible, so this may limit the range in μ for which the stabilities indicated in Figure 21.1.7 are valid.

4. Consider the saddle-node bifurcation for maps and Figure 21.1.2. For the case $\left(-\frac{\partial^2 f}{\partial x^2}(0,0)/\frac{\partial f}{\partial \mu}(0,0)\right) > 0$, give conditions under which the upper part of the curve of fixed points is stable and the lower part is unstable. Alternatively, give conditions under which the upper part of the curve of fixed points is unstable and the lower part is stable.

   Repeat the exercise for the case $\left(-\frac{\partial^2 f}{\partial x^2}(0,0)/\frac{\partial f}{\partial \mu}(0,0)\right) < 0$.

5. Consider the transcritical bifurcation for maps and Figure 21.1.5. For the case $\left(-\frac{\partial^2 f}{\partial x^2}(0,0)/\frac{\partial^2 f}{\partial x \partial \mu}(0,0)\right) > 0$, give conditions for $x = 0$ to be stable for $\mu > 0$ and unstable for $\mu < 0$. Alternatively, give conditions for $x = 0$ to be unstable for $\mu > 0$ and stable for $\mu < 0$.

   Repeat the exercise for the case $\left(-\frac{\partial^2 f}{\partial x^2}(0,0)/\frac{\partial^2 f}{\partial x \partial \mu}(0,0)\right) < 0$.

6. Consider the pitchfork bifurcation for maps and Figure 21.1.8. For the case $\left(-\frac{\partial^3 f}{\partial x^3}(0,0)/\frac{\partial^2 f}{\partial x \partial \mu}(0,0)\right) > 0$, give conditions for $x = 0$ to be stable for $\mu > 0$ and unstable for $\mu < 0$. Alternatively, give conditions for $x = 0$ to be unstable for $\mu > 0$ and stable for $\mu < 0$.

   Repeat the exercise for the case $\left(-\frac{\partial^3 f}{\partial x^3}(0,0)/\frac{\partial^2 f}{\partial x \partial \mu}(0,0)\right) < 0$.

7. Consider the period-doubling bifurcation for maps and Figure 21.2.2. For the case $\left(-\frac{\partial^3 f^2}{\partial x^3}(0,0)/\frac{\partial^2 f^2}{\partial x \partial \mu}(0,0)\right) > 0$, give conditions for the period one points, $x = 0$, to be stable for $\mu > 0$ and unstable for $\mu < 0$. Alternatively, give conditions for $x = 0$ to be unstable for $\mu > 0$ and stable for $\mu < 0$.

   Repeat the exercise for the case $\left(-\frac{\partial^3 f^2}{\partial x^3}(0,0)/\frac{\partial^2 f^2}{\partial x \partial \mu}(0,0)\right) < 0$.

8. In Exercise 6 in Chapter 18 we computed center manifolds near the origin for the following one-parameter families of maps. Describe the bifurcations of the origin. In, for example, a) and a′) the parameter ε multiplies a linear and nonlinear term, respectively. In terms of bifurcations, is there a qualitative difference in the two cases? What kind of general statements can you make?

   a)
   $$\begin{aligned} x &\mapsto -\frac{1}{2}x - y - xy^2, \\ y &\mapsto -\frac{1}{2}x + \varepsilon y + x^2, \end{aligned} \qquad (x, y) \in \mathbb{R}^2.$$

   a′)
   $$\begin{aligned} x &\mapsto -\frac{1}{2}x - y - xy^2, \\ y &\mapsto -\frac{1}{2}y + \varepsilon y^2 + x^2. \end{aligned}$$

b) $\begin{aligned} x &\mapsto x + 2y + x^3, \\ y &\mapsto 2x + y + \varepsilon y, \end{aligned} \qquad (x, y) \in \mathbb{R}^2.$

b′) $\begin{aligned} x &\mapsto x + 2y + x^3, \\ y &\mapsto 2x + y + \varepsilon y^2. \end{aligned}$

c) $\begin{aligned} x &\mapsto -x + y - xy^2, \\ y &\mapsto y + \varepsilon y + x^2 y, \end{aligned} \qquad (x, y) \in \mathbb{R}^2.$

c′) $\begin{aligned} x &\mapsto -x + y - xy^2, \\ y &\mapsto y + \varepsilon y^2 + x^2 y. \end{aligned}$

d) $\begin{aligned} x &\mapsto 2x + y, \\ y &\mapsto 2x + 3y + \varepsilon x + x^4, \end{aligned} \qquad (x, y) \in \mathbb{R}^2.$

d′) $\begin{aligned} x &\mapsto 2x + y + \varepsilon x^2, \\ y &\mapsto 2x + 3y + x^4. \end{aligned}$

e) $\begin{aligned} x &\mapsto x + \varepsilon y, \\ y &\mapsto x + 2y + y^2, \end{aligned} \qquad (x, y) \in \mathbb{R}^2.$

e′) $\begin{aligned} x &\mapsto x + \varepsilon y^2, \\ y &\mapsto x + 2y + y^2. \end{aligned}$

f) $\begin{aligned} x &\mapsto 2x + 3y, \\ y &\mapsto x + \varepsilon y + x^2 + xy^2, \end{aligned} \qquad (x, y) \in \mathbb{R}^2.$

f′) $\begin{aligned} x &\mapsto 2x + 3y, \\ y &\mapsto x + x^2 + \varepsilon y^2 + xy^2. \end{aligned}$

g) $\begin{aligned} x &\mapsto x - z^3, \\ y &\mapsto 2x - y + \varepsilon y, \\ z &\mapsto x + \frac{1}{2} z + x^3, \end{aligned} \qquad (x, y, z) \in \mathbb{R}^3.$

g′) $\begin{aligned} x &\mapsto x - z^3, \\ y &\mapsto 2x - y + \varepsilon y^2, \\ z &\mapsto x + \frac{1}{2} z + x^3. \end{aligned}$

h) $\begin{aligned} x &\mapsto x + \varepsilon z^4, \\ y &\mapsto -x - 2y - x^3, \\ z &\mapsto y - \frac{1}{2} z + y^2, \end{aligned} \qquad (x, y, z) \in \mathbb{R}^3.$

h′) $\begin{aligned} x &\mapsto x + \varepsilon x + z^4, \\ y &\mapsto -x - 2y - x^3, \\ z &\mapsto y - \frac{1}{2} z + y^2. \end{aligned}$

i) $\begin{aligned} x &\mapsto y + \varepsilon x + x^2, \\ y &\mapsto y + xy, \end{aligned} \qquad (x, y) \in \mathbb{R}^2.$

i′) $\begin{aligned} x &\mapsto y + x^2, \\ y &\mapsto y + xy + \varepsilon x^2. \end{aligned}$

j) $\begin{aligned} x &\mapsto \varepsilon x + x^2, \\ y &\mapsto y + xy, \end{aligned} \qquad (x, y) \in \mathbb{R}^2.$

j′) $\begin{aligned} x &\mapsto x^2 + \varepsilon y, \\ y &\mapsto y + xy. \end{aligned}$

9. *Center Manifolds at a Saddle-node Bifurcation Point for Maps*

Following the discussion in Exercise 7 following Section 20.1, develop the center manifold theory for maps so that it applies at a saddle-node bifurcation point.

Apply the resulting theory to the following maps. In each case, compute the center manifold and describe the dynamics near the origin for ε small. Discuss the bifurcations that occur (if any) at $\varepsilon = 0$.

a) $\begin{aligned} x &\mapsto \varepsilon + x + x^2 - y^2, \\ y &\mapsto x^2 + y^2, \end{aligned} \qquad (x, y, \varepsilon) \in \mathbb{R}^3.$

b) $\begin{aligned} x &\mapsto \varepsilon + \varepsilon x + x^2 - y^2, \\ y &\mapsto x^3 + y^2. \end{aligned}$

c) $\begin{aligned} x &\mapsto \varepsilon + x + x^2 - y^2, \\ y &\mapsto \varepsilon + x^2 + y^2. \end{aligned}$

d) $\begin{aligned} x &\mapsto \varepsilon + \frac{1}{2}x - y - x^2, \\ y &\mapsto \frac{1}{2}x + y^2. \end{aligned}$

e) $\begin{aligned} x &\mapsto \varepsilon - x + y + x^3, \\ y &\mapsto y + \varepsilon x - x^2. \end{aligned}$

f) $\begin{aligned} x &\mapsto \varepsilon + x + \varepsilon x + y^3, \\ y &\mapsto x + 2y - x^2. \end{aligned}$

g) $\begin{aligned} x &\mapsto \varepsilon - x + xy + y^2, \\ y &\mapsto 2x - xy - y^2. \end{aligned}$

h) $\begin{aligned} x &\mapsto \varepsilon + 2x + y + x^2 y, \\ y &\mapsto 12x + 3y - xy^2. \end{aligned}$

10. For the Naimark–Sacker bifurcation, compute the expression for the coefficient a analogous to (20.2.14) for vector field. (*Hint:* the answer can be found in Guckenheimer and Holmes [1983]).

11. Consider the following $\mathbf{C}^r$ $(r \geq 1)$ two-dimensional, time-periodic vector field

$$\begin{aligned} \dot{x} &= y, \\ \dot{y} &= f(x, t), \end{aligned} \qquad (x, y) \in \mathbb{R}^2,$$

where $f(x, t)$ has period T in t.

a) Show that the vector field has a (time-dependent) first integral and that the first integral is actually a Hamiltonian for the system.

b) Suppose that the vector field is (constantly) linearly damped as follows

$$\begin{aligned} \dot{x} &= y, \\ \dot{y} &= -\delta y + f(x, t), \end{aligned} \qquad \delta > 0.$$

Show that the associated Poincaré map *cannot* undergo Naimark–Sacker bifurcations.

12. Consider a map of $\mathbb{R}^2$ having a fixed point at the origin where the eigenvalues associated with the linearized map are complex conjugate and of unit modulus. We denote the two eigenvalues by λ and $\overline{\lambda}$. The goal of this exercise is to study the dynamics near the origin in the cases

$$\lambda^q = 1, \qquad q = 1, 2, 3, 4.$$

We will begin by developing a very powerful local technique; namely, interpolating a map by a flow.

a) Prove the following lemma (Arnold [1983]).

Consider a $\mathbf{C}^r$ (r as large as necessary) mapping $f\colon \mathbb{R}^2 \to \mathbb{R}^2$ having a fixed point at the origin with the eigenvalues of the linearization at the origin given by $e^{\pm 2\pi i p/q}$ (and with a Jordan block of order 2 if $q = 1$ or 2). In a sufficiently small neighborhood of the origin the iterate f^q can be represented as follows

$$f^q(z) = \varphi_1(z) + \mathcal{O}(|z|^N), \qquad z \in \mathbb{R}^2,$$

where $\varphi_1(z)$ is the time one map obtained from the flow generated by a vector field, $v(z)$. Moreover, the vector field is invariant under rotations about the origin through the angle $2\pi/q$.

(*Hint:* first put f^q in normal form

$$f^q = \Lambda z + F_2^r(z) + F_3^r(z) + \cdots + F_{N-1}^r(z) + \mathcal{O}(|z|^N).$$

Next consider the vector field

$$\dot{z} = (\Lambda - \mathrm{id})z + F_2^r(z) + F_3^r(z) + \cdots + F_{N-1}^r(z).)$$

Approximate the time one map of this vector field via Picard iteration (justify the use of this method), and show that it gives the desired result. This will show why it is first necessary to put the map in normal form. Moser [1968] gives an alternate proof of this lemma as well as a nice discussion of interpolation of maps by flows.

Next we must deal with versal deformations of these maps.

b) Prove the following lemma (Arnold [1983]).

Consider a deformation f_λ, $\lambda \in \mathbb{R}^p$, of a mapping $f_0 = f$ satisfying the hypotheses of the lemma in Part a). *In a sufficiently small neighborhood of the origin, the iterate f_λ^q can be represented as*

$$f_\lambda^q(z) = \varphi_{1,\lambda}(z) + \mathcal{O}(|z|^N), \qquad z \in \mathbb{R}^2,$$

where $\varphi_{1,\lambda}(z)$ is the time one map obtained from the flow generated by a vector field, v_λ, that is invariant under rotations about the origin through the angle $2\pi/q$. Moreover, $\varphi_{1,0}(z) = \varphi_1(z)$ and $v_0(z) = v(z)$.

(*Hint:* this lemma is a consequence of the fact that the normalizing transformations, up to order N, depend differentiably on the parameters.)

c) A vector field on the plane may have

1. Fixed points (hyperbolic and nonhyperbolic).
2. Periodic orbits.
3. Homoclinic orbits.
4. Heteroclinic orbits.

Suppose the time one map of a vector field having all of these orbits approximates the map f^q in the sense of the lemmas in Part a) and b). How would each of these orbits be affected by the higher order terms (i.e., the $\mathcal{O}(|z|^N)$ terms)?

Now we return to the main problem.

d) Show that the normal forms in the cases $\lambda^q = 1$, $q = 1, 2, 3, 4$, are given by

$$q = 1: \quad \begin{aligned} x &\mapsto x + y + \cdots, \\ y &\mapsto y + ax^2 + bxy + \cdots, \end{aligned} \qquad (x, y) \in \mathbb{R}^2.$$

$$q = 2: \quad \begin{aligned} x &\mapsto x + y + \cdots, \\ y &\mapsto y + ax^3 + bx^2y + \cdots, \end{aligned} \qquad (x, y) \in \mathbb{R}^2.$$

$$q = 3: \quad z \mapsto z + c_1\overline{z}^2 + c_2 z^2\overline{z} + \cdots, \qquad z \in \mathbb{C}.$$

$$q = 4: \quad z \mapsto z + c_1\overline{z}^3 + c_2 z^2\overline{z} + \cdots, \qquad z \in \mathbb{C}.$$

e) Compute the codimension in each case. Argue that candidates for versal deformations are given by

$$q = 1: \quad \begin{aligned} x &\mapsto x + y, \\ y &\mapsto \mu_1 + \mu_2 y + y + ax^2 + bxy, \end{aligned} \qquad (x, y) \in \mathbb{R}^2.$$

$$q = 2: \quad \begin{aligned} x &\mapsto x + y, \\ y &\mapsto \mu_1 x + (1 + \mu_2)y + ax^3 + bx^2y, \end{aligned} \qquad (x, y) \in \mathbb{R}^2.$$

$$q = 3: \quad z \mapsto (1 + \mu)z + c_1\overline{z}^2 + c_2 z^2\overline{z}, \qquad z \in \mathbb{C}.$$

$$q = 4: \quad z \mapsto (1 + \mu)z + c_1\overline{z}^3 + c_2 z^2\overline{z}, \qquad z \in \mathbb{C}.$$

f) Show that the vector fields that interpolate f^q through the order given in Part e) are

$$q = 1: \quad \begin{aligned} \dot{x} &= y, \\ \dot{y} &= \mu_1 + \mu_2 y + a x^2 + b x y, \end{aligned} \qquad (x, y) \in \mathbb{R}^2.$$

$$q = 2: \quad \begin{aligned} \dot{x} &= y, \\ \dot{y} &= \mu_1 x + \mu_2 y + a x^3 + b x^2 y, \end{aligned} \qquad (x, y) \in \mathbb{R}^2.$$

$$q = 3: \quad \dot{z} = \mu z + c_1 \overline{z}^2 + c_2 z^2 \overline{z}, \qquad z \in \mathbb{C}.$$

$$q = 4: \quad \dot{z} = \mu z + c_1 \overline{z}^3 + c_2 z^2 \overline{z}, \qquad z \in \mathbb{C}.$$

g) Describe the complete dynamics of each of the vector fields in Part f).

h) Using the results from Parts g) and c), describe the dynamics of f^q near the origin for $q = 1, 2, 3$, and 4.

We remark that the results of this problem were first obtained by Arnold [1977], [1983]. A very interesting application to a vector field undergoing a Poincaré–Andronov–Hopf bifurcation that is subjected to an external time-periodic perturbation can be found in Gambaudo [1985].

13. Consider the following $\mathbf{C}^r$ (r as large as necessary) one-parameter family of vector fields

$$\dot{x} = f(x, \mu), \qquad (x, \mu) \in \mathbb{R}^n \times \mathbb{R}^1.$$

Suppose this vector field has a fixed point at $(x, \mu) = (0, 0)$.

a) Suppose $n = 1$; can $(x, \mu) = (0, 0)$ undergo a period-doubling bifurcation?

b) Suppose $n = 2$; can $(x, \mu) = (0, 0)$ undergo a period-doubling bifurcation?

c) Suppose $n = 3$; can $(x, \mu) = (0, 0)$ undergo a period-doubling bifurcation?

(*Hint:* consider a linear vector field

$$\dot{x} = Ax, \qquad x \in \mathbb{R}^n,$$

where the flow is given by

$$x = e^{At} x_0,$$

and $\det e^{At} > 0$ for finite t. Use these facts.)

21.6 Maps of the Circle

As we saw in the previous section, the Naimark-Sacker bifurcation gave rise to an invariant circle. Hence, the restriction of the map to the invariant circle gives rise to a *circle map*. In this section we want to establish some of the basic properties of circle maps. First, we establish the setting and notation.

We consider C^1 orientation-preserving homeomorphisms of the circle, S^1, into itself:

$$f : S^1 \to S^1.$$

Our study of circle maps will be aided through the notion of a *lift*. This device will enable us to consider the circle map as defined on the real line

(constructed from the periodic repetition of the unit interval), where issues such as differentiability and order preservation are straightforward. We now define the lift of a circle map.

Definition 21.6.1 (The Lift of a Circle Map) *Consider the following map of the real line* $\mathbb{R}$ *to* S^1*:*

$$\begin{aligned} \Pi : \mathbb{R} &\longrightarrow S^1, \\ x &\longrightarrow e^{2\pi i x} \equiv \theta. \end{aligned}$$

The map $F : \mathbb{R} \longrightarrow \mathbb{R}$ *is said to be a* lift *of* $f : S^1 \longrightarrow S^1$ *if*

$$\Pi \circ F = f \circ \Pi.$$

Through the lift, the property of orientation preservation is manifested by F being an increasing function of x, i.e, $x_1 > x_2$ implies $F(x_1) > F(x_2)$.

> Some authors choose to work with a circle of length one, others choose to work with a circle of length 2π. The difference involves making sure the appropriate factors of 2π are in the right places in the various formulae. For example, in the map Π used in the definition of the lift the factor 2π in the exponent of the exponential implies that we are working on a circle of length one.

We now consider some examples of lifts.

Example 21.6.1. Consider the circle map

$$\begin{aligned} f : S^1 &\longrightarrow S^1, \\ \theta &\longrightarrow \theta + 2\pi\omega. \end{aligned}$$

Then, a lift F of the circle map f satisfies

$$f \circ \Pi = e^{2\pi i(x+\omega)} = \Pi \circ F = e^{2\pi i F(x)},$$

from which it follows that,

$$F(x) = x + \omega + k, \qquad \text{where } k \text{ is some integer.}$$

End of Example 21.6.1

Example 21.6.2. Consider the circle map

$$f : S^1 \longrightarrow S^1,$$
$$\theta \longrightarrow \theta + \epsilon \sin\theta.$$

Then, a lift F of the circle map f satisfies

$$f \circ \Pi = e^{2\pi i\left(x + \frac{\epsilon}{2\pi}\sin 2\pi x\right)} = \Pi \circ F = e^{2\pi i F(x)}$$

from which it follows that,

$$F(x) = x + \frac{\epsilon}{2\pi}\sin 2\pi x + k, \qquad \text{where } k \text{ is some integer.}$$

End of Example 21.6.2

A key quantity in describing the dynamics of circle maps is the *rotation number* associated with a given circle map. We now develop a series of lemmas that will be used in proving some of the important properties of the rotation number.

The following lemma shows that two lifts of the same circle map differ by an integer.

Lemma 21.6.2 *Let $f : S^1 \longrightarrow S^1$ be an orientation preserving homeomorphism of the circle and let F_1 and F_2 be lifts of f. Then $F_1 = F_2 + k$, where k is some integer.*

Proof: The two lifts must satisfy

$$f \circ \Pi = \Pi \circ F_1 = e^{2\pi i F_1(x)},$$
$$f \circ \Pi = \Pi \circ F_2 = e^{2\pi i F_2(x)},$$

from which it follows immediately that $F_1 = F_2 + k$, where k is some integer. □

The following lemma shows that the iterate of the lift of a circle map is the lift of the iterate of the circle map.

Lemma 21.6.3 *If F is a lift of f then F^n is a lift of f^n, $n \geq 1$.*

Proof: By definition of a lift we have

$$\Pi \circ F = f \circ \Pi,$$

and therefore

$$\Pi \circ F \circ F = \Pi \circ F^2 = f \circ \Pi \circ F = f \circ f \circ \Pi = f^2 \circ \Pi.$$

Repeating this argument establishes the result for arbitrary n. □

Lemma 21.6.4 *Let $f : S^1 \longrightarrow S^1$ be an orientation preserving homeomorphism of the circle and let F be a lift. Then*

$$F(x + k) = F(x) + k$$

for any integer k.

Proof: We first consider the case $k = 1$.

Using the definition of the lift we have

$$e^{2\pi i F(x+1)} = \Pi \circ F(x+1) = f \circ \Pi(x+1) = f \circ \Pi(x) = \Pi \circ F(x) = e^{2\pi i F(x)}. \tag{21.6.1}$$

Thus,

$$e^{2\pi i F(x+1)} = e^{2\pi i F(x)}, \tag{21.6.2}$$

which implies that

$$F(x+1) = F(x) + j, \tag{21.6.3}$$

where j is some integer. We now argue that $j = 1$.

We give a proof by contradiction that $j = 1$. Suppose that $j > 1$. Then since $F(x)$ is an increasing function there must exist a point, y, with $x < y < x + 1$, such that

$$F(y) = F(x) + m, \quad 1 \leq m < j.$$

Then

$$f \circ \Pi(y) = e^{2\pi i F(y)} = e^{2\pi i F(x)} = f \circ \Pi(x),$$

from which it follows that

$$y = x + m,$$

where m is some integer $\neq 0$. This contradicts our choice of y.

The case for a general integer k is proved similarly. We can replace $x+1$ by $x+k$ in (21.6.1). Then we can conclude that $F(x+k) = F(x)+j$, where j is some integer. Applying the same argument allows us to conclude that $j = k$. □

Lemma 21.6.5 *Let $f : S^1 \longrightarrow S^1$ be an orientation preserving homeomorphism of the circle and let F be a lift of f. Then $F^n - id$ is a periodic function with period one, $n \geq 1$.*

Proof: First prove the lemma for $n = 1$. Using Lemma 21.6.4, we have

$$F(x+1) - (x+1) = F(x) - x.$$

This proves the lemma for $n = 1$.

Now consider the case $n > 1$. By the chain rule, it follows that f^n is also an orientation preserving homeomorphism of the circle, and by Lemma 21.6.3 F^n is a lift of f^n. Then using Lemma 21.6.4, it follows that

$$F^n(x+1) - (x+1) = F^n(x) - x.$$

This completes the proof of the lemma. □

Lemma 21.6.6 *Let f be an orientation preserving homeomorphism of the circle with lift F. Then there exists an integer k_n such that*

$$k_n < F^n(x) - x < k_n + 3,$$

for every $x \in \mathbb{R}$, $n \geq 1$.

Proof: By Lemma 21.6.5, since $F^n(x) - x$ is periodic with period 1, the result will follow if it is established only for $x \in [0, 1]$.

Now $F^n(0)$ is between two integers m and $m+1$, i.e., $m \leq F^n(0) \leq m+1$. From Lemma 21.6.4 it then follows that $m+1 \leq F^n(1) \leq m+2$. Since F is increasing it follows that $m - 1 < F^n(x) - x < m + 2$. If we let $k_n = m - 1$ the result follows. □

Lemma 21.6.7 *Suppose $f : S^1 \longrightarrow S^1$ is an orientation preserving homeomorphism and F is a lift. Then if $|x-y| < 1$, we have $|F^n(x)-F^n(y)| < 1$, $n \geq 1$.*

Proof: Now $|x - y| < 1$ implies that $-1 < x - y < 1$, or

1. $x < 1 + y$,
2. $y < 1 + x$.

Using Lemma 21.6.4, and the fact that F is increasing, we apply F^n to each of these expressions to obtain

1. $F^n(x) < F^n(1 + y) = F^n(y) + 1 \Rightarrow F^n(x) - F^n(y) < 1$,
2. $F^n(y) < F^n(1 + x) = F^n(x) + 1 \Rightarrow -1 < F^n(x) - F^n(y)$.

Which establishes the desired result. □

We are now at the point where we can develop the definition of rotation number. For an orientation preserving homeomorphism $f : S^1 \longrightarrow S^1$, with F a lift of f, we define the quantity

$$\rho_0(F) \equiv \lim_{n\to\infty} \frac{|F^n(x)|}{n}.$$

First, we show that if this quantity exists, it is independent of x.

Lemma 21.6.8 *If $\rho_0(F)$ exists, then it is independent of x.*

Proof: Let x and y be given points. Then y can be written in the form

$$y = \tilde{y} + k,$$

where k is an integer and $|x - \tilde{y}| < 1$. Using this representation for y, we have

$$\begin{aligned} |F^n(x) - F^n(y)| = |F^n(x) - F^n(\tilde{y} + k)| &= |F^n(x) - F^n(\tilde{y}) - k|, \\ &\leq |F^n(x) - F^n(\tilde{y})| + k. \end{aligned}$$

Using Lemma 21.6.7, since $|x-\tilde{y}|<1$ then $|F^n(x)-F^n(\tilde{y})|<1$. So we get

$$\frac{|F^n(x)-F^n(y)|}{n} \leq \frac{1+k}{n},$$

and therefore

$$\lim_{n\to\infty} \frac{|F^n(x)-F^n(y)|}{n} = 0.$$

This completes the proof. □

Example 21.6.3. Consider the circle map

$$\begin{aligned} f : S^1 &\longrightarrow S^1 \\ \theta &\longrightarrow \theta + 2\pi\omega \end{aligned}$$

with lift

$$\begin{aligned} F : \mathbb{R}^1 &\longrightarrow \mathbb{R}^1, \\ x &\longrightarrow x + \omega + k. \end{aligned}$$

Then we have

$$\rho_0(F) = \lim_{n\to\infty} \frac{x+n\omega+nk}{n} = \omega + k.$$

End of Example 21.6.3

Lemma 21.6.9 *Let $f : S^1 \longrightarrow S^1$ be an orientation preserving homeomorphism and let F_1 and F_2 be lifts such that $\rho_0(F_1)$ and $\rho_0(F_2)$ exist. Then $\rho_0(F_1) = \rho_0(F_2) + k$, where k is an integer.*

Proof: From Lemma 21.6.2,

$$F_1 = F_2 + k.$$

Let T_k denote the translation map, i.e., $T_k : x \mapsto x + k$. Then we can rewrite this equation as

$$F_1 = T_k \circ F_2.$$

Now we want to show that T_k commutes with F_2. We have

$$F_2 \circ T_k = F_2(x+k) = F_2(x) + k, \qquad \text{by Lemma 21.6.4,}$$

and

$$T_k \circ F_2(x) = F_2(x) + k.$$

Hence

$$F_2 \circ T_k = T_k \circ F_2.$$

We use this result in the following way. Since $F_1 = T_k \circ F_2$ it follows that

$$\begin{aligned}
&F_1^n(x) = (T_k \circ F_2)^n (x), \\
&= \underbrace{(T_k \circ F_2) \circ (T_k \circ F_2) \circ \cdots \circ (T_k \circ F_2)(x)}_{\text{n fold composition of } T_k \circ F_2}, \\
&= F_2^n \circ T_k^n(x), \text{ where we have repeatedly commuted "pairwise," } T_k \text{ and } F_2 \\
&= F_2^n(x + nk), \\
&= F_2^n(x) + nk, \text{ by Lemma 21.6.4.}
\end{aligned}$$

Hence

$$F_1^n = F_2^n + nk,$$

From which it immediately follows that

$$\rho_0(F_1) = \rho(F_2) + k.$$

This completes the proof. □

We now prove that $\rho_0(F)$ exists.

Theorem 21.6.10 *Let $f : S^1 \longrightarrow S^1$ be an orientation preserving homeomorphism with lift F. Then*

$$\rho_0(F) = \lim_{n \to \infty} \frac{|F^n(x)|}{n}$$

exists and is independent of x.

Proof: We break the proof down into two cases.

Case 1:

Suppose f has a periodic point, i.e., there exists $\theta \in S^1$ such that $f^m(\theta) = \theta$. Then

$$F^m(x) = x + k,$$

for some fixed x, where k is some integer. Therefore

$$F^{jm}(x) = x + jk,$$

from which it follows that

$$\lim_{j\to\infty} \frac{|F^{jm}(x)|}{jm} = \lim_{j\to\infty} \frac{x+jk}{jm} = \frac{k}{m}.$$

Any integer n can be written in the form

$$n = jm + r, \qquad 0 \le r < m$$

and by Lemma 21.6.6 there exists a constant M such that

$$|F^r(y) - y| \le M,$$

for all $y \in \mathbb{R}$, $0 \le r < m$. So we have

$$\begin{aligned} \frac{|F^n(x) - F^{jm}(x)|}{n} &= \frac{|F^r(F^{jm}(x)) - F^{jm}(x)|}{n} \\ &\le \frac{M}{n}, \end{aligned}$$

from which it follows that

$$\lim_{n\to\infty} \frac{|F^n(x)|}{n} = \lim_{j\to\infty} \frac{|F^{jm}(x)|}{jm+r} = \lim_{j\to\infty} \frac{x+jk}{jm+r} = \frac{k}{m}.$$

So, $\rho_0(F)$ exists whenever f has a periodic point, moreover, in this case $\rho_0(F)$ is rational.

Case 2:

Now we consider the general case. By Lemma 21.6.6 there exists an integer k_n such that

$$k_n < F^n(x) - x < k_n + 3, \tag{21.6.4}$$

for every $x \in \mathbb{R}$, $n \ge 1$. Applying (21.6.4) repeatedly to $x = F^n(x)$, $F^{2n}(x)$, $\cdots$, $F^{(m-1)n}(x)$, we get the following chain of inequalities

$$
\begin{aligned}
&k_n < F^n(x) - x < k_n + 3,\\
&k_n < F^{2n}(x) - F^n(x) < k_n + 3,\\
&k_n < F^{3n}(x) - F^{2n}(x) < k_n + 3,\\
&\quad\vdots\\
&k_n < F^{mn}(x) - F^{(m-1)n}(x) < k_n + 3.
\end{aligned}
$$

Adding these inequalities gives

$$mk_n < F^{mn}(x) - x < m(k_n + 2),$$

or,

$$\frac{k_n}{n} < \frac{F^{mn}(x) - x}{mn} < \frac{k_n + 3}{n}.$$

The first inequality in the chain of inequalities gives

$$\frac{k_n}{n} < \frac{F^n(0)}{n} < \frac{k_n + 3}{n}.$$

Combining these two expressions gives the estimate

$$\left| \frac{F^{mn}(x)}{mn} - \frac{F^n(x)}{n} \right| < \frac{3}{n} \tag{21.6.5}$$

Repeating the above argument with m and n interchanged gives

$$\left| \frac{F^{mn}(x)}{mn} - \frac{F^m(x)}{m} \right| < \frac{3}{m} \tag{21.6.6}$$

Combining (21.6.5) and (21.6.6) gives

$$\left| \frac{F^n(x)}{n} - \frac{F^m(x)}{m} \right| < \frac{3}{n+m}.$$

Hence the sequence $\left\{ \frac{F^n(x)}{n} \right\}$ is a Cauchy sequence in $\mathbb{R}$, so it converges. □

Finally, we define the rotation number of an orientation preserving, homeomorphism of the circle.

Definition 21.6.11 (Rotation Number) *There are two main operational definitions of rotation number. For $f : S^1 \longrightarrow S^1$ an orientation preserving homeomorphism, with F a lift of f:*

1. *Some authors define the rotation number of f, denoted $\rho(f)$, as the fractional part of $\rho_0(F)$ (e.g. Devaney [1986]).*

2. *Other authors define the rotation number of f to be $\rho_0(F)$ (e.g., Katok and Hasselblatt [1995]).*

In either case, we have shown that the rotation number exists, and is independent of the point x.

Next we show that that rotation number depends continuously on f in the C^0 topology.

Theorem 21.6.12 *Let $f : S^1 \longrightarrow S^1$ be an orientation-preserving diffeomorphism. Let $\epsilon > 0$ be given, then there exists a $\delta > 0$ such that if $g : S^1 \longrightarrow S^1$ is also an orientation preserving diffeomorphism which is $C^0 - \delta$ close to f then $|\rho(f) - \rho(g)| < \epsilon$.*

Proof: Choose n such that $\frac{3}{n} < \epsilon$. From Lemma 21.6.6, there exists k_n such that

$$k_n < F^n(0) < k_n + 3$$

for F some lift of f. Choose δ sufficiently small so that for some lift G of g we also have

$$k_n < G^n(0) < k_n + 3$$

Utilizing the same argument as in Theorem 21.6.10, we obtain the inequalities

$$\frac{k_n}{n} < \frac{F^{mn}(0)}{mn} < \frac{k_n + 3}{n}$$

$$\frac{k_n}{n} < \frac{G^{mn}(0)}{mn} < \frac{k_n + 3}{n}$$

Combining these inequalities gives

$$\left| \frac{F^{mn}(0)}{mn} - \frac{G^{mn}(0)}{mn} \right| < \frac{3}{n} < \epsilon$$

and the result follows since

$$\rho_0(F) = \lim_{n\to\infty} = \frac{F^{mn}(0)}{mn},$$

and

$$\rho_0(G) = \lim_{n\to\infty} = \frac{G^{mn}(0)}{mn},$$

and the limit is independent of the point. □

Theorem 21.6.13 *The rotation number is irrational if and only if f has no periodic points.*

Proof: See Devaney [1986]. □

Theorem 21.6.14 *The rotation number is rational if and only if f has a periodic orbit.*

Proof: In our proof of the existence of the rotation number we have shown that if f has a periodic point, then the rotation number is rational. It remains to show that if the rotation number is rational, then f has a periodic point. We leave this to the exercises (or see Katok and Hasselblatt [1995]). □

Here we introduce some terminology. Suppose the rotation number is rational, say $\frac{p}{q}$, with p and q relatively prime integers. We refer to the associated periodic orbit as a "$p-q$" periodic orbit (or a periodic orbit of type "$p-q$"). In terms of the orbit of the point, it is a period q orbit that makes p revolutions around the circle before returning to its original starting point.

The rotation number is invariant under orientation preserving topological conjugacy.

Theorem 21.6.15 *Let f and g be orientation preserving homeomorphisms of S^1, then $\rho(f) = \rho(g^{-1}fg)$.*

Proof: See Katok and Hasselblatt [1995]. □

The Rotation Number and Orbits

While we have seen that an orientation preserving circle homeomorphism has periodic orbits if the rotation number is rational, and it has no periodic orbits if the rotation number is irrational, we have not characterized all possible orbits for the two cases. This is done below, and is referred to as the "Poincaré classification" by Katok and Hasselblatt [1995], where the proof of the statements can be found.

Rational Rotation Number, $\frac{p}{q}$

For any given initial condition, there are three possibilities for the orbit.

- A $\frac{p}{q}$ periodic orbit.
- A homoclinic orbit. The orbit asymptotically approaches a periodic orbit as $n \to -\infty$ and as $n \to +\infty$.
- A heteroclinic orbit. The orbit asymptotically approaches a periodic orbit as $n \to -\infty$ and a different periodic orbit as $n \to +\infty$.

Irrational Rotation Number

For any given initial condition, there are three possibilities for the orbit.

- An orbit that densely fills the circle.
- An orbit that densely fills a Cantor set on the circle.
- An orbit that is homoclinic to a Cantor set on the circle.

21.6A The Dynamics of a Special Class of Circle Maps-Arnold Tongues

The results above are rather general. Now we will study a more specific class of circle maps and obtain more detailed information on the dynamics. In particular, we want to discuss the notion of phase locking and Arnold tongues. The following discussion loosely follows Hall [1984].

Consider the following two-parameter family of C^1 diffeomorphisms of the circle:

$$\theta \longrightarrow \langle \theta + \phi + \alpha\gamma(\theta) \rangle$$

where $\langle \cdot \rangle$ denotes the fractional part, and we have the following assumptions on $\gamma : \mathbb{R}^1 \longrightarrow \mathbb{R}^1$

1. $\gamma \in C^r$, $r \geq 1$, $\left| \frac{d\gamma}{d\theta} \right| \leq 1$,
2. $\forall\ \theta \in \mathbb{R}$, $\gamma(\theta + 1) = \gamma(\theta) + 1$,

3. $\int_0^1 \gamma(\theta)d\theta = 0.$

We will study the following lift of the above circle map:

$$f : \theta \longrightarrow \theta + \phi + \alpha\gamma(\theta) \equiv f(\theta, \phi, \alpha).$$

An example of a map of this type is given by

$$x \mapsto x + \phi + \frac{\alpha}{2\pi} \sin 2\pi x,$$

which is often referred to as *the standard map*, which was studied in detail by Arnold [1965].

The two parameters are ϕ and α. For $\alpha = 0$ the map is just a rigid, linear rotation through the angle ϕ. The parameter α controls the nonlinearity of the map.

We denote the rotation number of the lift by $\rho(\phi, \alpha)$.

Theorem 21.6.16 *For $\phi \in \mathbb{R}$, $\alpha \in [0, 1)$*

1. *$\rho(\phi, \alpha)$ exists and is independent of θ.*
2. *$\rho(\phi, \alpha)$ is continuous in (ϕ, α) and nondecreasing in ϕ.*
3. *If $\rho(\phi, \alpha) = \frac{p}{q}$, with p, q relatively prime positive integers, then there exists $\theta \in [0, 1)$ such that $f^q(\theta, \phi, \alpha) = \theta + p$.*

Proof:

1. In order for this to be true we need only show that f is orientation preserving and increasing, i.e., $\frac{df}{d\theta} > 0$. We have

$$\frac{df}{d\theta}(\theta, \phi, \alpha) = 1 + \alpha \frac{d\gamma}{d\theta}.$$

   Since $\left|\frac{d\gamma}{d\theta}\right| \leq 1$ and $\alpha \in [0, 1)$ the result follows.

2. We have already established that $\rho(\phi, \alpha)$ depends continuously on parameters (cf. Theorem 21.6.12).

We now show that $\rho(\phi, \alpha)$ is nondecreasing in ϕ for each fixed α. Fix α. For $\phi_2 > \phi_1$, we have

$$f(\theta, \phi_2, \alpha) = \theta + \phi_2 + \alpha\gamma(\theta) > f(\theta, \phi_1, \alpha) = \theta + \phi_1 + \alpha\gamma(\theta).$$

Then

$$f^n(\theta, \phi_2, \alpha) > f^n(\theta, \phi_1, \alpha),$$

from which it follows that

$$\rho(\phi_2, \alpha) \geq \rho(\phi_1, \alpha).$$

3. Half of this result was established in Theorem 21.6.10, the other half was left as an exercise.

□

The following lemma will be useful.

Lemma 21.6.17 *For any integer q,*

$$f^q(\theta, \phi, \alpha) = \theta + q\phi + \alpha \sum_{j=0}^{q-1} \gamma(\theta + j\phi) + \alpha h(\theta, \phi, \alpha)$$

where h is as differentiable as γ and $h \to 0$ as $\alpha \to 0$.

Proof: This just involves a direct calculation while introducing the correct notation.

$$\begin{aligned}
q = 1: \quad & f(\theta, \phi, \alpha) = \theta + \phi + \gamma(\theta), \\
q = 2: \quad & f^2(\theta, \phi, \alpha) = \theta + 2\phi + \alpha\gamma(\theta) + \alpha\gamma(\theta + \phi + \alpha\gamma(\theta)), \\
q = 3: \quad & f^3(\theta, \phi, \alpha) = \theta + 3\phi + \alpha\gamma(\theta) + \alpha\gamma(\theta + \phi + \alpha\gamma(\theta)) \\
& \qquad + \alpha\gamma(\theta + 2\phi + \alpha(\gamma(\theta) + \gamma(\theta + \phi + \alpha\gamma(\theta)))).
\end{aligned}$$

Continuing in this manner, the qth iterate has the form

$$\begin{aligned}
f^q(\theta, \phi, \alpha) = \theta + q\phi + \alpha\Big[& \gamma(\theta) + \gamma(\theta + \phi + \alpha\gamma(\theta)) + \gamma\left(\theta + 2\phi + \alpha(\gamma(\theta)\right. \\
& \left. + \gamma(\theta + \phi + \alpha\gamma(\theta)))\right) \\
& + \gamma\left(\theta + 3\phi + \alpha(\gamma(\theta) + \gamma(\theta + \phi + \alpha\gamma(\theta)) + \gamma(\theta + 2\phi + \alpha(\gamma(\theta)\right. \\
& \left. + \gamma(\theta + \phi + \alpha\gamma(\theta)))))\right) + \cdots
\end{aligned}$$

$$+\gamma\left(\theta+(q-1)\phi+\alpha(\gamma(\theta)+\gamma(\theta+\phi+\alpha\gamma(\theta))+\cdots\right.$$
$$+\gamma(\theta+(q-2)\phi+\alpha(\gamma(\theta)+\cdots+\gamma(\theta+(q-3)\phi$$
$$\left.+\ \alpha\gamma(\cdots))))))\right]$$

Since γ is C^1, we can Taylor expand a general term of the form

$$\gamma(\theta+k\phi+\alpha G(\theta,\phi,\alpha))=\gamma(\theta+k\phi)+\alpha\gamma'(\xi)G(\theta,\phi,\alpha).$$

Using this in the expansion for f^q gives

$$f^q(\theta,\phi,\alpha)=\theta+q\phi+\alpha\sum_{j=0}^{q-1}\gamma(\theta+j\phi)+\alpha h(\theta,\phi,\alpha)$$

with $h\in C^1$ and $h\to 0$ as $\alpha\to 0$. □

Definition 21.6.18 *For $\beta\in\mathbb{R}$ we define the set*

$$A_\beta=\{(\phi,\alpha)\,|\,\phi\in\mathbb{R},\alpha\in[0,1),\rho(\phi,\alpha)=\beta\},$$

(note that t $\rho(\phi,0)=\phi$). When $\beta=\frac{p}{q}$, $A_{\frac{p}{q}}$ is called an Arnold Tongue. *If the rotation number is rational the map is said to be* phase-locked *or* mode-locked.

Theorem 21.6.19 (Existence of Arnold Tongues) *For each rational $\frac{p}{q}$ there exists Lipschitz functions ϕ_1, ϕ_2: $[0,1)\longrightarrow\mathbb{R}$ such that*

1. $\forall\ \alpha\in[0,\epsilon),\ \phi_1(\alpha)\le\phi_2(\alpha)$,
2. $\phi_1(0)=\phi_2(0)=\frac{p}{q}$,
3. $(\phi,\alpha)\in A_{\frac{p}{q}}$ *if and only if* $\phi_1(\alpha)\le\phi\le\phi_2(\alpha)$.

The Arnold tongue is illustrated in Figure 21.6.1.

Proof: Consider the equation

$$G(\theta,\phi,\alpha)\equiv f^q(\theta,\phi,\alpha)-\theta-p=0.$$

For fixed ϕ and α, a solution θ of this equation corresponds to a periodic point of period $\frac{p}{q}$. Now for $\alpha=0$, $\phi=\frac{p}{q}$ is a solution, for all θ. We will use

the implicit function theorem to "continue" this solution for $\alpha > 0$. To do this, we must compute the following derivative

$$\begin{aligned}\frac{\partial G}{\partial \phi}(\theta, \phi, \alpha) &= \frac{\partial f^q}{\partial \phi}(\theta, \phi, \alpha) \\ &= q + \alpha \left(\sum_{j=0}^{q-1} \gamma'(\theta + j\phi) \right) + \alpha h'(\theta, \phi, \alpha),\end{aligned}$$

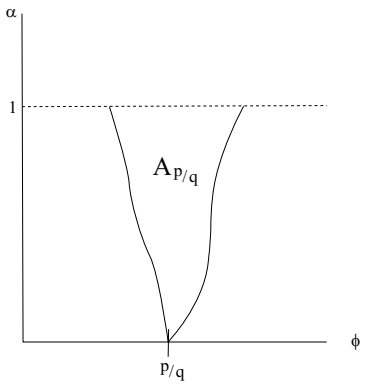

FIGURE 21.6.1. The Arnold tongue $A_{\frac{p}{q}}$.

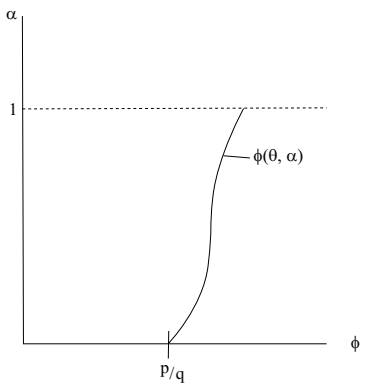

FIGURE 21.6.2. Graph of the function $\phi(\theta, \alpha)$ for some fixed θ.

which is clearly nonzero at $\alpha = 0$, $\phi = \frac{p}{q}$, $\theta \in [0, 1)$. Moreover, since $|\gamma'| \leq 1$, $|h'| \leq \alpha$, it is also nonzero for $0 \leq \alpha < 1$, $\theta \in [0, 1)$. Then by the implicit function theorem there exists a unique C^1 function $\phi(\theta, \alpha)$ with $\theta \in [0, 1)$, $\alpha \in [0, 1)$ such that

$$G(\theta, \phi(\theta, \alpha), \alpha) = f^q(\theta, \phi(\theta, \alpha), \alpha) - \theta - p = 0,$$

with $\phi(\theta, 0) = \frac{p}{q}$, see Figure 21.6.2.

We now take

$$\phi_1(\alpha) = \inf_{\theta \in [0,1)} \phi(\theta, \alpha), \quad \phi_2(\alpha) = \sup_{\theta \in [0,1)} \phi(\theta, \alpha),$$

where $\phi_1(0) = \phi_2(0) = \frac{p}{q}$. For fixed α, the values of ϕ satisfying $\phi_1(\alpha) \leq \phi \leq \phi_2(\alpha)$ correspond to parameter values for which $\rho(\phi, \alpha) = \frac{p}{q}$.

Now we argue that the curve generically opens at $\frac{p}{q}$ as α increases, i.e, as α increases from zero, $\phi_1(\alpha) < \phi_2(\alpha)$. Implicitly differentiating the expression

$$f^q(\theta, \phi(\theta, \alpha), \alpha) - \theta - p = 0,$$

gives

$$\frac{df^q}{d\alpha} = \frac{\partial f^q}{\partial \phi}\frac{\partial \phi}{\partial \alpha} + \frac{\partial f^q}{\partial \alpha} = 0,$$

or

$$\frac{\partial \phi}{\partial \alpha} = -\frac{\frac{\partial f^q}{\partial \alpha}}{\frac{\partial f^q}{\partial \phi}}.$$

Using the expression for f^q given in Lemma 21.6.17, we obtain

$$\left.\frac{\partial \phi}{\partial \alpha}\right|_{\alpha=0} = -\frac{1}{q}\sum_{j=0}^{q-1} \gamma\left(\theta + j\frac{p}{q}\right).$$

From our assumptions, $\gamma(\theta)$ has zero average. It then follows that the average of $\frac{\partial \phi}{\partial \alpha}|_{\alpha=0}$ with respect to θ is zero. Therefore $\frac{\partial \phi}{\partial \alpha}(\theta, 0)$ takes on both positive and negative values. Since generically $\frac{\partial \phi}{\partial \alpha}(\theta, 0)$ is not identically zero, we have $\phi_1(\alpha) < \phi_2(\alpha)$, at least for α near zero. □

The Opening of the Arnold Tongues

We have shown that generically the Arnold tongues open as α increases from zero. In our figures we have illustrated the opening getting wider and wider as α increases to one. However, we stress that this is really just artistic license; we have not proved that the curves behave in this way. McGehee

and Peckham [1995] numerically compute "global" Arnold tongues for a number of examples. Their paper also has a nice literature survey on the subject.

Nonresonance

The Arnold tongues characterize the region in $\alpha - \phi$ for which the rotation number is rational. Herman [1979] has proved a theorem which characterizes irrational rotation numbers.

Theorem 21.6.20 (Herman) *For a given irrational number η there exists a Lipschitz curve $\psi_\eta : [0,1) \longrightarrow \mathbb{R}$ such that $\rho(\phi,\alpha) = \eta$ if and only if $\phi = \psi_\eta(\alpha)$.*

In other words, given an irrational rotation number, it must lie on a Lipschitz curve corresponding to parameter values which give the same irrational rotation number, see Figure 21.6.3.

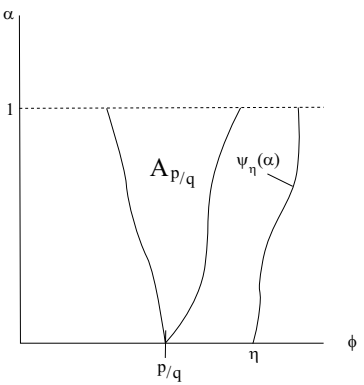

FIGURE 21.6.3. Illustration of an Arnold tongue and a curve $\phi = \psi_\eta(\alpha)$ corresponding to parameter values for which the rotation number is the irrational number η.

The Devils Staircase

Suppose we fix α and graph $\rho(\phi,\alpha)$ as a function of ϕ. The rotation number $\rho(\phi,\alpha)$ is a continuous function of ϕ and α (Theorem 21.6.12) and it is an increasing function of ϕ (Theorem 21.6.16). The graph is constant on

intervals corresponding to rational rotation numbers, and increasing at the points corresponding to irrational rotation numbers. The graph appears as in Figure 21.6.4 and is referred to as a *Devils staircase*.

The Lebesque Measure of the Set of Parameters Corresponding to Rational and Irrational Rotation Numbers

Consider the rotation number $\rho(\alpha, \phi)$ for some fixed $0 \leq \alpha < 1$. For $\alpha = 0$ the rotation number is rational for all rational values of ϕ, and it is irrational otherwise. Hence the Lebesgue measure of ϕ values corresponding to rational rotation numbers is zero and the Lebesgue measure of ϕ values corresponding to irrational rotation numbers is one.

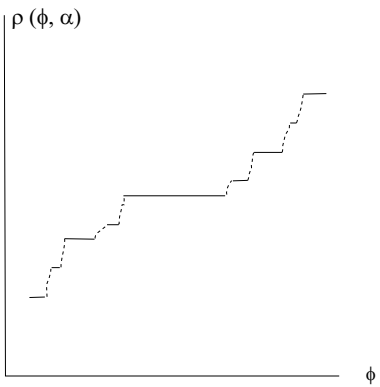

FIGURE 21.6.4. The devils staircase. The graph of $\rho(\alpha, \phi)$ as a function of ϕ, for some fixed $0 < \alpha < 1$.

As α increases from zero (but still remains "small"), one obtains a set of ϕ values having positive measure corresponding to rational rotation numbers. However, the Lebesgue measure of this set is $\mathcal{O}(\alpha)$, and most (in the sense of Lebesgue measure) values of ϕ correspond to irrational rotation numbers. The set of ϕ values corresponding to irrational rotation numbers is a Cantor set; it contains no intervals. From the point of view of applications this seems like a strange situation, since for α small, a ϕ value chose at random will most likely give rise to an irational rotation number, but it can be converted to a rational rotation number by an arbitrarily small perturbation.

Rigorous results on the Lebesgue measure of rotation numbers can be found in Herman [1977].

Phase Locking in a Continuous Time Setting

We remark that phase locking for ordinary differential equations has previously been studied by Loud [1967] and Bushard [1972], [1973].

21.6B Exercises

1. Prove Theorem 21.6.13.
2. Prove that if the rotation number of an orientation preserving homeomorphism of the circle is rational, then it has a periodic orbit (thus completing the proof of Theorem 21.6.14).
3. Prove Theorem 21.6.15.
4. Prove that the curves $\phi_1(\alpha)$ and $\phi_2(\alpha)$ constructed in Theorem 21.6.19 are Lipschitz in α.
5. Prove that the width of the opening of $A_{\frac{p}{q}}$ constructed in Theorem 21.6.19 is $\mathcal{O}(\alpha^q)$.
6. Prove that parameter values on the two bounding curves of the Arnold tongue $A_{\frac{p}{q}}$ (i.e., values of ϕ and α on the curves $\phi_1(\alpha)$ and $\phi_2(\alpha)$) generically correspond to saddle-node bifurcations of $\frac{p}{q}$ periodic orbits. Hint: apply the implicit function theorem to the function

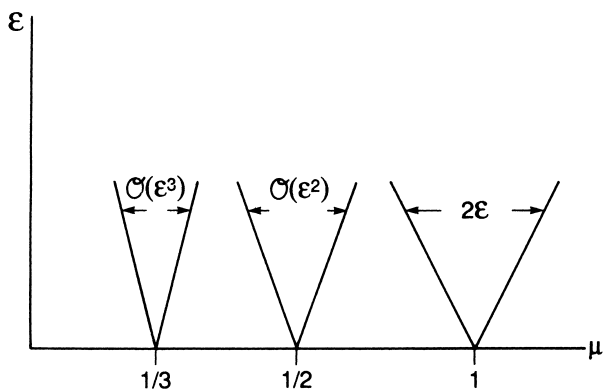

FIGURE 21.6.5.

$$F(\theta, \phi, \alpha) = \left(f^q(\theta, \phi, \alpha) - \theta - p, \frac{\partial f^q}{\partial \theta}(\theta, \phi, \alpha) - 1 \right).$$

7. In this exercise we will compute a few of the Arnold tongues explicitly. The results should give some idea of how the neglected higher order terms in the normal form can affect the dynamics on the invariant circle arising in a Naimark–Sacker bifurcation.

   Consider the two-parameter family of maps

$$x \mapsto x + \mu + \varepsilon \cos 2\pi x \equiv f(x, \mu, \varepsilon), \qquad x \in \mathbb{R}^1, \quad \varepsilon \geq 0, \tag{21.6.7}$$

   where we identify points in $\mathbb{R}_1$ that differ by an integer so that (21.6.7) can be regarded as a map defined on the circle $S^1 = \mathbb{R}^1/\mathbb{Z}$.

a) Discuss the orbit structure of (21.6.7) for $\varepsilon = 0$. In particular, what is the Lebesgue measure of the set of parameter values for which (21.6.7) has periodic orbits?

b) Consider the following regions in the $\mu - \varepsilon$ plane (see Figure 21.6.5).

$$\mu = 1 \pm \varepsilon,$$
$$\mu = \frac{1}{2} \pm \varepsilon^2 \frac{\pi}{2} + \mathcal{O}(\varepsilon^3),$$
$$\mu = \frac{1}{3} + \varepsilon^2 \frac{\sqrt{3}}{6}\pi \pm \varepsilon^3 \frac{\sqrt{7}\pi}{6} + \mathcal{O}(\varepsilon^4).$$

Show that, for parameter values in the interior of these regions, (21.6.7) has a period 1, period 2, and period 3 point, respectively.
Hint: we outline the procedure for the period 2 points.

i. If x is a period 2 point of (21.6.7), then

$$f^2(x, \mu, \varepsilon) - x - 1 = G(x, \mu, \varepsilon) = 0.$$

ii. If $\frac{\partial G}{\partial \mu} \neq 0$, then we have a function $\mu = \mu(x, \varepsilon)$ such that

$$G(x, \mu(x, \varepsilon), \varepsilon) = 0. \tag{21.6.8}$$

iii. Expand the function $\mu(x, \varepsilon)$ as follows

$$\mu(x, \varepsilon) = \mu(x, 0) + \varepsilon \frac{\partial \mu}{\partial \varepsilon}(x, 0) + \frac{\varepsilon^2}{2} \frac{\partial^2 \mu}{\partial \varepsilon^2}(x, 0) + \mathcal{O}(\varepsilon^3).$$

iv. Implicitly differentiating (21.6.8), show that

$$\mu(x, 0) = \frac{1}{2},$$
$$\frac{\partial \mu}{\partial \varepsilon}(x, 0) = 0,$$
$$\frac{\partial^2 \mu}{\partial \varepsilon^2}(x, 0) = 2\pi \sin 4\pi x.$$

v. Taking the infimum and supremum in Step 4, we obtain

$$\mu = \mu(x, \varepsilon) = \frac{1}{2} \pm \varepsilon^2 \frac{\pi}{2} + \mathcal{O}(\varepsilon^3).$$

Justify all steps completely.

Now let us return to the setting of the Naimark–Sacker bifurcation. For $\varepsilon = 0$, (21.6.7) has the form of the truncated Naimark–Sacker normal form restricted to the invariant circle. The term $\varepsilon \cos 2\pi x$ could be viewed as illustrating the possible effects of higher order terms in the normal form. For (21.6.7), at $\varepsilon = 0$ the map has periodic orbits for all rational μ (i.e., a set of Lebesgue measure zero). For ε small and fixed, our results show that the measure of the set of μ values for which (21.6.7) has a periodic orbit is positive. Thus, based on this example, we might expect the higher order terms in the Naimark–Sacker normal form to have a dramatic influence on the dynamics restricted to the bifurcated invariant circle. See Iooss [1979] for more details.

8. For some fixed $0 < \varepsilon < 1$, compute the devils staircase for the following map

$$x \mapsto x + \mu + \varepsilon \cos 2\pi x \equiv f(x, \mu, \varepsilon),$$

where $x \in \mathbb{R}^1$.

22

On the Interpretation and Application of Bifurcation Diagrams: A Word of Caution

At this point, we have seen enough examples so that it should be clear that the term bifurcation refers to the phenomenon of a system exhibiting qualitatively new dynamical behavior as parameters are varied. However, the phrase "as parameters are varied" deserves careful consideration. Let us consider a highly idealized example.

The situation we imagine is wind blowing through Venetian blinds hanging in an open window. The "parameter" in this system will be the wind speed. From experience, most people have observed that nothing much happens when the wind speed is low enough, but, for high enough wind speeds, the blinds begin to oscillate or "flutter." Thus, at some critical parameter value, a Poincaré-Andronov-Hopf bifurcation occurs. However, we must be careful here. In all of our analyses thus far the parameters have been *constant*. Therefore, in order to apply the Poincaré-Andronov-Hopf bifurcation theorem to this problem, the wind speed must be constant. At low constant speeds, the blinds lie flat; at constant speeds above a certain critical value, the blinds oscillate. The point is that we cannot think of the parameter as varying in time, e.g., wind speed increasing over time, even though this is what happens in practice. Dynamical systems having parameters that change in time (no matter how slowly!) and that pass through bifurcation values often exhibit behavior that is very different from the analogous situation where the parameters are constant. Let us consider a more mathematical example due to Haberman [1979, further studied by Schecter [1985]], whose exposition we follow.

Consider the vector field

$$\dot{x} = f(x, \mu), \qquad x \in \mathbb{R}^1, \quad \mu \in \mathbb{R}^1. \tag{22.0.1}$$

We suppose that

$$f(0, \mu) = 0 \tag{22.0.2}$$

so that $x = 0$ is always a fixed point, and that

$$f(x, \mu) = 0 \tag{22.0.3}$$

intersects $x = 0$ at $\mu = b$ and appears as in Figure 22.0.1.

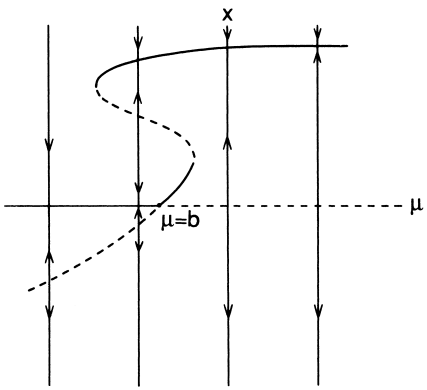

FIGURE 22.0.1.

We further assume that

$$\frac{\partial f}{\partial x}(0, \mu) \quad \text{is} \quad \begin{cases} < 0 & \text{for } x < b, \\ > 0 & \text{for } x > b, \end{cases} \tag{22.0.4}$$

so that the stability of the fixed points is as shown in Figure 22.0.1. Thus, (22.0.1) undergoes a transcritical bifurcation at $\mu = b$. Now, if we think of (22.0.1) as modelling a physical system, we would expect to observe the system in a stable equilibrium state. For $\mu < b$, this would be $x = 0$, and for μ slightly larger than b, x small enough, this would be the upper branch of fixed points bifurcating from the transcritical bifurcation point.

Let us consider the situation in which the parameter is allowed to drift slowly in time as follows

$$\dot{x} = f(x, \mu), \tag{22.0.5}$$

$$\dot{\mu} = \varepsilon, \tag{22.0.6}$$

where ε is viewed as small and positive (so that trajectories always move toward the right).

(Note: Schecter [1985] considers a much more general situation where $\dot{\mu}$ may depend on x and μ.) Now let us consider the fate of an initial condition $(\bar{\mu}, \bar{x})$ with $\bar{\mu} < b$ and $\bar{x} > 0$ sufficiently small; see Figure 22.0.2. This point is attracted strongly toward $x = 0$ (but it can never cross $x = 0$. Why?) and drifts slowly toward the right. Schecter proves that, on passing through $\mu = b$, rather than being repelled from $x = 0$ as would be the case for $\varepsilon = 0$, the trajectory follows closely $x = 0$ (which is an unstable

invariant manifold for $\mu > b$) for awhile before ultimately being repelled away; see Figure 22.0.2.

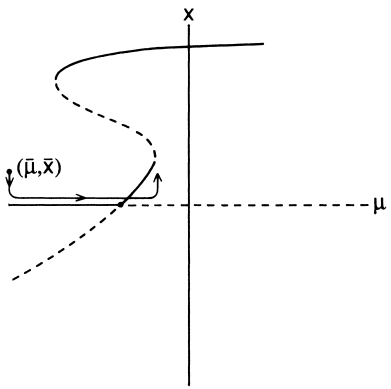

FIGURE 22.0.2.

Thus, what one would observe for $\varepsilon = 0$ differs from that for $\varepsilon \neq 0$; for $\varepsilon \neq 0$, certain trajectories tend to remain in the neighborhood (for awhile) of what are unstable fixed points for $\varepsilon = 0$.

A detailed analysis of problems of this type is beyond the scope of this book (such problems fit very nicely into the context of singular perturbation theory). The point we wish to make is that, within a given system, the behavior of that system on either side of a bifurcation value may be very different in cases when the parameter varies slowly in time (no matter how slowly) through the bifurcation value, as opposed to cases when the parameter is constant. "Slowly varying" saddle-node, transcritical, pitchfork, and Hopf bifurcations for vector fields have all been considered, as well as their Hamiltonian analogs. The reader will find detailed analyses of such problems in Mitropol'skii [1965], Lebovitz and Schaar [1975, 1977], Haberman [1979], Neishtadt [1987], [1988], Baer et al. [1989], Erneux and Mandel [1986], Lebovitz and Pesci [1995], and Raman and Bajaj [1998] . The recent review of Arnold et al. [1994] provides an overview of many of the latest results in this area. Baesens [1991], [1995] considers similar phenomena in maps.

23

The Smale Horseshoe

We will begin our study of "chaotic dynamics" by describing and analyzing a two-dimensional map possessing an invariant set having a delightfully complicated structure. The discussion is virtually the same as the discussion in Wiggins [1988]. Our map is a simplified version of a map first studied by Smale [1963], [1980] and, due to the shape of the image of the domain of the map, is called a *Smale horseshoe.*

We will see that the Smale horseshoe is the prototypical map possessing a chaotic invariant set (note: the phrase "chaotic invariant set" will be precisely defined later on in the discussion). Therefore, we feel that a thorough understanding of the Smale horseshoe is absolutely essential for understanding what is meant by the term "chaos" as it is applied to the dynamics of specific physical systems. For this reason we will first endeavor to define as simple a two-dimensional map as possible that still contains the necessary ingredients for possessing a complicated and chaotic dynamical structure so that the reader may get a feel for what is going on in the map with a minimum of distractions. As a result, our construction may not appeal to those interested in applications, since it may appear rather artificial. However, following our discussion of the simplified Smale horseshoe map, we will give sufficient conditions for the existence of Smale horseshoe–like dynamics in two-dimensional maps that are of a very general nature. We will begin by defining the map and then proceed to a geometrical construction of the invariant set of the map. We will utilize the nature of the geometrical construction in such a way as to motivate a description of the dynamics of the map on its invariant set by symbolic dynamics, following which we will make precise the idea of chaotic dynamics.

23.1 Definition of the Smale Horseshoe Map

We will give a combination geometrical-analytical definition of the map. Consider a map, f, from the square having sides of unit length into $\mathbb{R}^2$

$$f : D \to \mathbb{R}^2, \qquad D = \big\{(x, y) \in \mathbb{R}^2 \,|\, 0 \le x \le 1, 0 \le y \le 1\big\}, \tag{23.1.1}$$

which contracts the x-direction, expands the y-direction, and folds D around, laying it back on itself as shown in Figure 23.1.1.

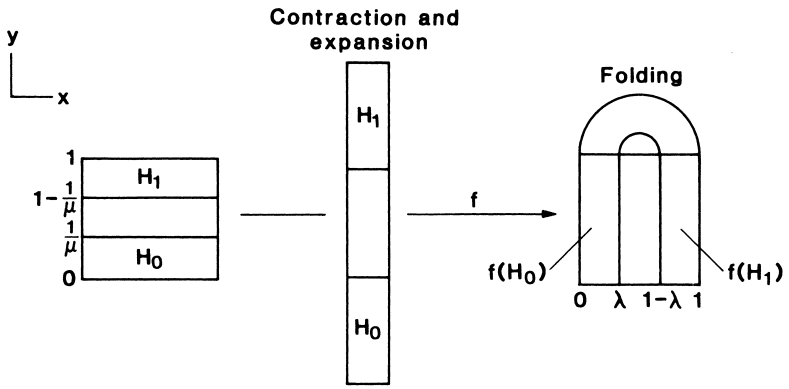

FIGURE 23.1.1.

We will assume that f acts affinely on the "horizontal" rectangles

$$H_0 = \big\{(x, y) \in \mathbb{R}^2 \,|\, 0 \le x \le 1, 0 \le y \le 1/\mu\big\}, \tag{23.1.2}$$

and

$$H_1 = \big\{(x, y) \in \mathbb{R}^2 \,|\, 0 \le x \le 1, 1 - 1/\mu \le y \le 1\big\}, \tag{23.1.3}$$

taking them to the "vertical" rectangles

$$f(H_0) \equiv V_0 = \big\{(x, y) \in \mathbb{R}^2 \,|\, 0 \le x \le \lambda, 0 \le y \le 1\big\}, \tag{23.1.4}$$

and

$$f(H_1) \equiv V_1 = \big\{(x, y) \in \mathbb{R}^2 \,|\, 1 - \lambda \le x \le 1, 0 \le y \le 1\big\}, \tag{23.1.5}$$

with the form of f on H_0 and H_1 given by

$$\begin{aligned} H_0 &: \begin{pmatrix} x \\ y \end{pmatrix} \mapsto \begin{pmatrix} \lambda & 0 \\ 0 & \mu \end{pmatrix} \begin{pmatrix} x \\ y \end{pmatrix}, \\ H_1 &: \begin{pmatrix} x \\ y \end{pmatrix} \mapsto \begin{pmatrix} -\lambda & 0 \\ 0 & -\mu \end{pmatrix} \begin{pmatrix} x \\ y \end{pmatrix} + \begin{pmatrix} 1 \\ \mu \end{pmatrix}, \end{aligned} \tag{23.1.6}$$

and with $0 < \lambda < 1/2$, $\mu > 2$ (note: the fact that, on H_1, the matrix elements are negative means that, in addition to being contracted in the x-direction by a factor λ and expanded in the y-direction by a factor μ, H_1 is also rotated 180°). Additionally, it follows that f^{-1} acts on D as shown in Figure 23.1.2, taking the "vertical" rectangles V_0 and V_1 to the "horizontal" rectangles H_0 and H_1, respectively (note: by "vertical rectangle" we will mean a rectangle in D whose sides parallel to the y axis each have length one, and by "horizontal rectangle" we will mean a rectangle in D whose sides parallel to the x axis each have length one). This serves to define f; however, before proceeding to study the dynamics of f on D, there is a consequence of the definition of f which we want to single out, since it will be very important later.

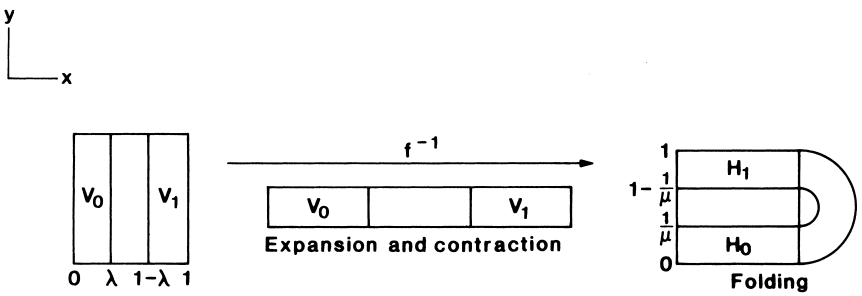

FIGURE 23.1.2.

Lemma 23.1.1 a) *Suppose V is a vertical rectangle; then $f(V) \cap D$ consists of precisely two vertical rectangles, one in V_0 and one in V_1, with their widths each being equal to a factor of λ times the width of V.* b) *Suppose H is a horizontal rectangle; then $f^{-1}(H) \cap D$ consists of precisely two horizontal rectangles, one in H_0 and one in H_1, with their widths being a factor of $1/\mu$ times the width of H.*

Proof: We will prove Case a). Note that from the definition of f, the horizontal and vertical boundaries of H_0 and H_1 are mapped to the horizontal and vertical boundaries of V_0 and V_1, respectively. Let V be a vertical rectangle; then V intersects the horizontal boundaries of H_0 and H_1, and hence, $f(V) \cap D$ consists of two vertical rectangles, one in V_0 and one in V_1. The contraction of the width follows from the form of f on H_0 and H_1, which indicates that the x-direction is contracted uniformly by a factor λ on H_0 and H_1. Case b) is proved similarly. See Figure 23.1.3. □

We make the following remarks concerning this lemma.

Remark 1. The qualitative features of Lemma 23.1.1 are independent of the particular analytical form for f given in (23.1.6); rather, they are more geometrical in nature. This will be important in generalizing the results of this section to arbitrary maps.

Remark 2. Lemma 23.1.1 is concerned only with the behavior of f and f^{-1}. However, we will see in the construction of the invariant set that the behavior described in Lemma 23.1.1 allows us to understand the behavior of f^n for all n.

We now turn to the construction of the invariant set for f.

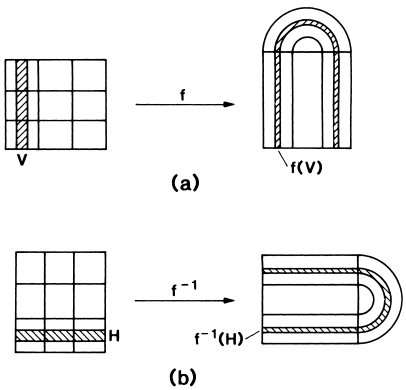

FIGURE 23.1.3.

23.2 Construction of the Invariant Set

We now will geometrically construct the set of points, Λ, which remain in D under all possible iterations by f; thus Λ is defined as

$$\cdots \cap f^{-n}(D) \cap \cdots \cap f^{-1}(D) \cap D \cap f(D) \cap \cdots \cap f^n(D) \cap \cdots$$

or

$$\bigcap_{n=-\infty}^{\infty} f^n(D).$$

We will construct this set inductively, and it will be convenient to construct separately the "halves" of Λ corresponding to the positive iterates and

the negative iterates and then take their intersections to obtain Λ. Before proceeding with the construction, we need some notation in order to keep track of the iterates of f at each step of the inductive process. Let $S = \{0, 1\}$ be an index set, and let s_i denote one of the two elements of S, i.e., $s_i \in S$, $i = 0, \pm 1, \pm 2, \cdots$ (note: the reason for this notation will become apparent later on).

We will construct $\bigcap_{n=0}^{\infty} f^n(D)$ by constructing $\bigcap_{n=0}^{n=k} f^n(D)$ and then determining the nature of the limit as $k \to \infty$.

$\underline{D \cap f(D)}$. By the definition of f, $D \cap f(D)$ consists of the two vertical rectangles V_0 and V_1, which we denote as follows

$$D \cap f(D) = \bigcup_{s_{-1} \in S} V_{s_{-1}} = \{p \in D \,|\, p \in V_{s_{-1}},\ s_{-1} \in S\}, \tag{23.2.1}$$

where $V_{s_{-1}}$ is a vertical rectangle of width λ; see Figure 23.2.1.

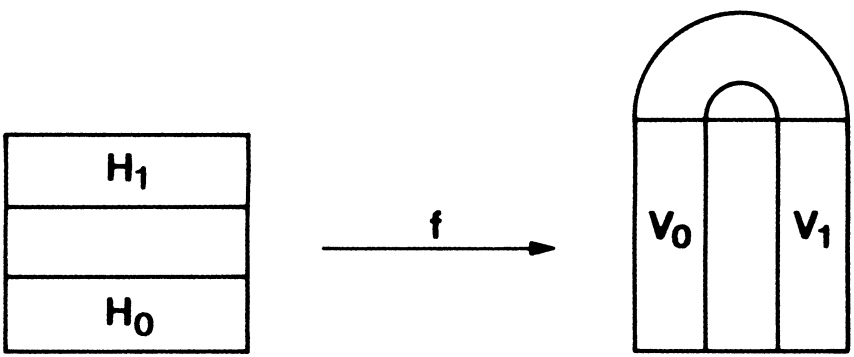

FIGURE 23.2.1.

$\underline{D \cap f(D) \cap f^2(D)}$. It is easy to see that this set is obtained by acting on $\overline{D \cap f(D)}$ with f and taking the intersection with D, since $D \cap f(D \cap f(D)) = D \cap f(D) \cap f^2(D)$. Thus, by Lemma 23.1.1, since $D \cap f(D)$ consists of the vertical rectangles V_0 and V_1 with each intersecting H_0 and H_1 and their respective horizontal boundaries in two components, then $D \cap f(D) \cap f^2(D)$ corresponds to four vertical rectangles, two each in V_0 and V_1, with each of width λ^2. Let us write this out more explicitly. Using (23.2.1) we have

$$D \cap f(D) \cap f^2(D) = D \cap f(D \cap f(D)) = D \cap f\left(\bigcup_{s_{-2} \in S} V_{s_{-2}} \right), \tag{23.2.2}$$

where, in substituting (23.2.1) into (23.2.2), we have changed the subscript s_{-1} on $V_{s_{-1}}$ to $V_{s_{-2}}$. As we will see, this is a notational convenience which will be a counting aid. It should be clear that this causes no problems, since s_{-i} is merely a dummy variable. Using a few set-theoretic manipulations, (23.2.2) becomes

$$D \cap f\Big(\bigcup_{s_{-2}\in S} V_{s_{-2}} \Big) = \bigcup_{s_{-2}\in S} D \cap f(V_{s_{-2}}). \tag{23.2.3}$$

Now, from Lemma 23.1.1, $f(V_{s_{-2}})$ cannot intersect all of D but only $V_0 \cup V_1$, so (23.2.3) becomes

$$\bigcup_{s_{-2}\in S} D \cap f(V_{s_{-2}}) = \bigcup_{\substack{s_{-i}\in S \\ i=1,2}} V_{s_{-1}} \cap f(V_{s_{-2}}). \tag{23.2.4}$$

Putting this all together, we have shown that

$$\begin{aligned} & D \cap f(D) \cap f^2(D) \\ &= \bigcup_{\substack{s_{-i}\in S \\ i=1,2}} (f(V_{s_{-2}}) \cap V_{s_{-1}}) \equiv \bigcup_{\substack{s_{-i}\in S \\ i=1,2}} V_{s_{-1}s_{-2}} \\ &= \big\{ p \in D \,|\, p \in V_{s_{-1}}, f^{-1}(p) \in V_{s_{-2}}, s_{-i} \in S, i = 1,2 \big\}. \end{aligned} \tag{23.2.5}$$

Pictorially, this set is described in Figure 23.2.2.

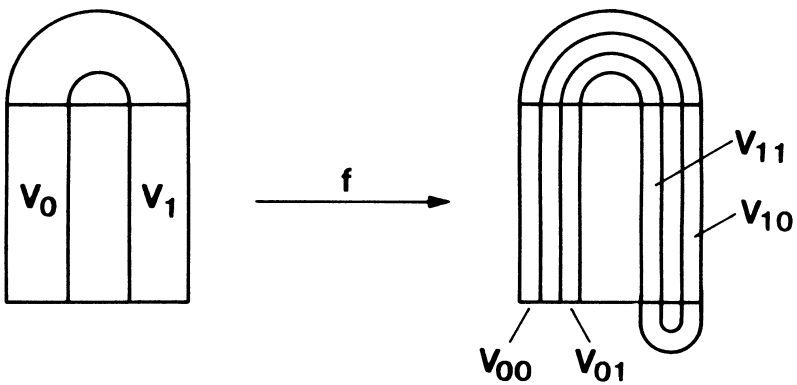

FIGURE 23.2.2.

$D \cap f(D) \cap f^2(D) \cap f^3(D)$. Using the same reasoning as in the previous steps, this set consists of eight vertical rectangles, each having width λ^3,

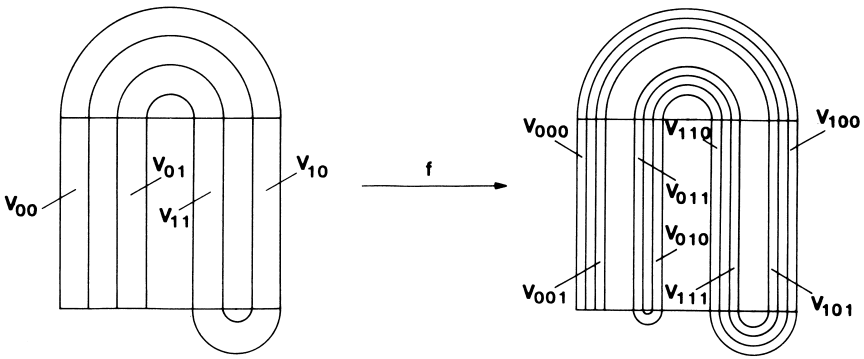

FIGURE 23.2.3.

which we denote as follows

$$\begin{aligned} & D \cap f(D) \cap f^2(D) \cap f^3(D) \\ &= \bigcup_{\substack{s_{-1}\in S \\ i=1,2,3}} (f(V_{s_{-2}s_{-3}}) \cap V_{s_{-1}}) \equiv \bigcup_{\substack{s_{-i}\in S \\ i=1,2,3}} V_{s_{-1}s_{-2}s_{-3}} \\ &= \big\{p \in D \,|\, p \in V_{s-1}, f^{-1}(p) \in V_{s_{-2}}, \\ &\qquad f^{-2}(p) \in V_{s_{-3}}, s_{-i} \in S, i = 1,2,3\big\}, \end{aligned} \tag{23.2.6}$$

and is represented pictorially in Figure 23.2.2.

If we continually repeat this procedure, we almost immediately encounter extreme difficulty in trying to represent this process pictorially, as in Figures 23.2.1 through 23.2.3. However, using Lemma 23.1.1 and our labeling scheme developed above, it is not hard to see that at the k^{th} step we obtain

$$\begin{aligned} & D \cap f(D) \cap \cdots \cap f^k(D) \\ &= \bigcup_{\substack{s_{-i}\in S \\ i=1,2,\ldots,k}} (f(V_{s_{-2}\cdots s_{-k}}) \cap V_{s_{-1}}) \equiv \bigcup_{\substack{s_{-i}\in S \\ i=1,2,\ldots,k}} V_{s_{-1}\cdots s_{-k}} \\ &= \big\{p \in D \,|\, f^{-i+1}(p) \in V_{s_{-i}}, s_{-i} \in S, i = 1,\cdots,k\big\} \end{aligned} \tag{23.2.7}$$

and that this set consists of 2^k vertical rectangles, each of width λ^k.

Before proceeding to discuss the limit as $k \to \infty$, we want to make the following important observation concerning the nature of this construction process. Note that at the k^{th} stage, we obtain 2^k vertical rectangles, and that each vertical rectangle can be labeled by a sequence of 0's and 1's of length k. The important point to realize is that there are 2^k possible distinct

sequences of 0's and 1's having length k and that each of these is realized in our construction process; thus, the labeling of each vertical rectangle is unique at each step. This fact follows from the geometric definition of f and the fact that V_0 and V_1 are disjoint.

Letting $k \to \infty$, since a decreasing intersection of compact sets is nonempty, it is clear that we obtain an infinite number of vertical rectangles and that the width of each of these rectangles is zero, since $\lim_{k\to\infty} \lambda^k = 0$ for $0 < \lambda < 1/2$. Thus, we have shown that

$$\begin{aligned}\bigcap_{n=0}^{\infty} f^n(D) &= \bigcup_{\substack{s_{-i}\in S \\ i=1,2,\ldots}} (f(V_{s_{-2}\cdots s_{-k}\cdots}) \cap V_{s_{-1}}) \\ &\equiv \bigcup_{\substack{s_{-i}\in S \\ i=1,2,\ldots}} V_{s_{-1}\cdots s_{-k}\cdots} \\ &= \left\{p \in D \,|\, f^{-i+1}(p) \in V_{s_{-i}}, s_{-i} \in S, i = 1, 2, \cdots\right\}\end{aligned} \tag{23.2.8}$$

consists of an infinite number of vertical lines and that each line can be labeled by a unique infinite sequence of 0's and 1's (note: we will give a more detailed set-theoretic description of $\cap_{n=0}^{\infty} f^n(D)$ later on).

Next we will construct $\bigcap_{-\infty}^{n=0} f^n(D)$ inductively.

$\underline{D \cap f^{-1}(D)}$. From the definition of f, this set consists of the two horizontal rectangles H_0 and H_1 and is denoted as follows

$$D \cap f^{-1}(D) = \bigcup_{s_0\in S} H_{s_0} = \left\{p \in D \,|\, p \in H_{s_0}, s_0 \in S\right\}. \tag{23.2.9}$$

See Figure 23.2.4.

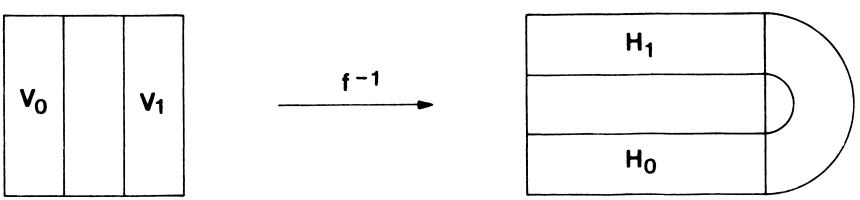

FIGURE 23.2.4.

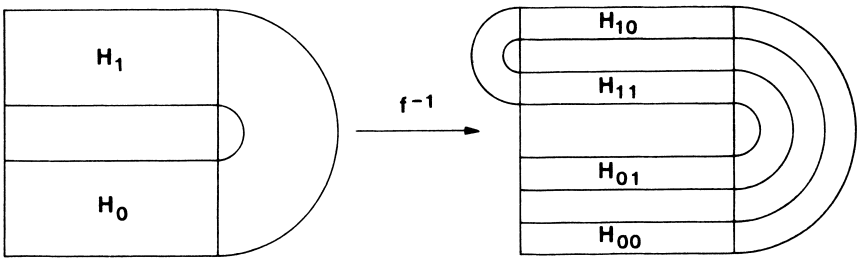

FIGURE 23.2.5.

$D \cap f^{-1}(D) \cap f^{-2}(D)$. We obtain this set from the previously constructed set, $D \cap f^{-1}(D)$, by acting on $D \cap f^{-1}(D)$ with f^{-1} and taking the intersection with D, since $D \cap f^{-1}\big(D \cap f^{-1}(D)\big) = D \cap f^{-1}(D) \cap f^{-2}(D)$. Also, by Lemma 23.1.1, since H_0 intersects both vertical boundaries of V_0 and V_1, as does H_1, $D \cap f^{-1}(D) \cap f^{-2}(D)$ consists of four horizontal rectangles, each of width $1/\mu^2$. Let us write this out more explicitly. Using (23.2.9), we have

$$\begin{aligned} D \cap f^{-1}(D \cap f^{-1}(D)) &= D \cap f^{-1}\Big(\bigcup_{s_1 \in S} H_{s_1}\Big) \\ &= \bigcup_{s_1 \in S} D \cap f^{-1}(H_{s_1}), \end{aligned} \tag{23.2.10}$$

where in substituting (23.2.9) into (23.2.10) we have changed the subscript s_0 on H_{s_0} to s_1. This has no real effect, since s_i is simply a dummy variable. The reason for doing so is that it will provide a useful counting aid.

From Lemma 23.1.1, it follows that $f^{-1}(H_{s_1})$ cannot intersect all of D, only $H_0 \cup H_1$, so that (4.1.14) becomes

$$\bigcup_{s_1 \in S} D \cap f^{-1}(H_{s_1}) = \bigcup_{\substack{s_i \in S \\ i=0,1}} H_{s_0} \cap f^{-1}(H_{s_1}). \tag{23.2.11}$$

Putting everything together, we have shown that

$$\begin{aligned} &D \cap f^{-1}(D) \cap f^{-2}(D) \\ &\quad = \bigcup_{\substack{s_i \in S \\ i=0,1}} \big(f^{-1}(H_{s_1}) \cap H_{s_0}\big) \equiv \bigcup_{\substack{s_i \in S \\ i=0,1}} H_{s_0 s_1} \\ &\quad = \big\{p \in D \,|\, p \in H_{s_0}, f(p) \in H_{s_1}, s_i \in S, i = 0, 1\big\}. \end{aligned} \tag{23.2.12}$$

See Figure 23.2.5.

$D \cap f^{-1}(D) \cap f^{-2}(D) \cap f^{-3}(D)$. Using the same arguments as those given in the previous steps, it is not hard to see that this set consists of eight horizontal rectangles each having width $1/\mu^3$ and that it can be denoted as

$$\begin{aligned} & D \cap f^{-1}(D) \cap f^{-2}(D) \cap f^{-3}(D) \\ &= \bigcup_{\substack{s_i \in S \\ i=0,1,2}} \left(f^{-1}(H_{s_1 s_2}) \cap H_{s_0}\right) \equiv \bigcup_{\substack{s_i \in S \\ i=0,1,2}} H_{s_0 s_1 s_2} \\ &= \left\{p \in D \,|\, p \in H_{s_0}, f(p) \in H_{s_1}, \right. \\ &\qquad \left. f^2(p) \in H_{s_2}, s_i \in S, i = 0, 1, 2\right\}. \end{aligned} \tag{23.2.13}$$

See Figure 23.2.6.

Continuing this procedure, at the k^{th} step we obtain $D \cap f^{-1}(D) \cap \cdots \cap f^{-k}(D)$, which consists of 2^k horizontal rectangles each having width $1/\mu^k$. This set is denoted by

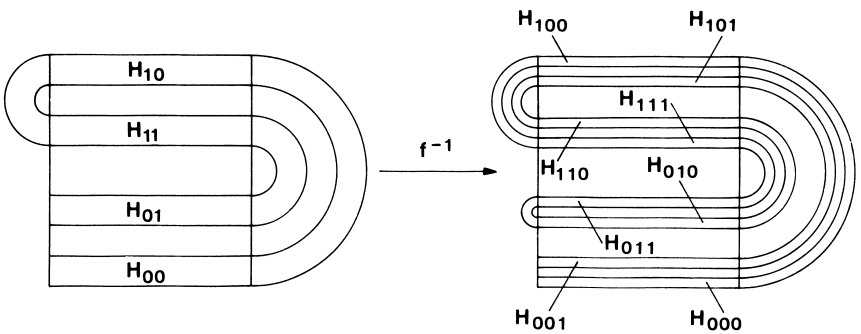

FIGURE 23.2.6.

$$\begin{aligned} & D \cap f^{-1}(D) \cap \cdots \cap f^{-k}(D) \\ &= \bigcup_{\substack{s_i \in S \\ i=0,\cdots,k-1}} \left(f^{-1}(H_{s_1 \cdots s_{k-1}}) \cap H_{s_0}\right) \equiv \bigcup_{\substack{s_i \in S \\ i=0,\cdots,k-1}} H_{s_0 \cdots s_{k-1}} \\ &= \left\{p \in D \,|\, f^i(p) \in H_{s_i}, s_i \in S, i = 0, \cdots, k-1\right\}. \end{aligned} \tag{23.2.14}$$

As in the case of vertical rectangles, we note the important fact that at the k^{th} step of the inductive process, each one of the 2^k vertical rectangles can be labeled uniquely with a sequence of 0's and 1's of length k. Now, as we take the limit as $k \to \infty$, we arrive at $\bigcap_{-\infty}^{n=0} f^n(D)$, which is an infinite

set of horizontal lines, since a decreasing intersection of compact sets is nonempty and the width of each component of the intersection is given by $\lim_{k\to\infty}(1/\mu^k) = 0$, $\mu > 2$. Each line is labeled by a unique infinite sequence of 0's and 1's as follows

$$\begin{aligned}\bigcap_{-\infty}^{n=0} f^n(D) &= \bigcup_{\substack{s_i\in S\\ i=0,1,\cdots}} \big(f(H_{s_1\cdots s_k\cdots}) \cap H_{s_0}\big) \equiv \bigcup_{\substack{s_i\in S\\ i=0,1,\cdots}} H_{s_0\cdots s_k\cdots} \\ &= \big\{p \in D \,|\, f^i(p) \in H_{s_i}, s_i \in S, i = 0, 1, \cdots\big\}. \end{aligned} \tag{23.2.15}$$

Thus, we have

$$\Lambda = \bigcap_{n=-\infty}^{\infty} f^n(D) = \Big[\bigcap_{n=-\infty}^{0} f^n(D)\Big] \cap \Big[\bigcap_{n=0}^{\infty} f^n(D)\Big], \tag{23.2.16}$$

which consists of an infinite set of points, since each vertical line in $\bigcap_{n=0}^{\infty} f^n(D)$ intersects each horizontal line in $\bigcap_{-\infty}^{n=0} f^n(D)$ in a unique point. Furthermore, each point $p \in \Lambda$ can be labeled *uniquely* by a bi-infinite sequence of 0's and 1's which is obtained by concatenating the sequences associated with the respective vertical and horizontal lines that serve to define p. Stated more precisely, let $s_{-1}\cdots s_{-k}\cdots$ be a particular infinite sequence of 0's and 1's; then $V_{s_{-1}\cdots s_{-k}\cdots}$ corresponds to a unique vertical line. Let $s_0\cdots s_k\cdots$ likewise be a particular infinite sequence of 0's and 1's; then $H_{s_0\cdots s_k\cdots}$ corresponds to a unique horizontal line. Now a horizontal line and vertical line intersect in a unique point p; thus, we have a well-defined map from points $p \in \Lambda$ to bi-infinite sequences of 0's and 1's which we call ϕ.

$$p \overset{\phi}{\longmapsto} \cdots s_{-k}\cdots s_{-1}s_0\cdots s_k\cdots\ .$$

Notice that because

$$\begin{aligned} V_{s_{-1}\cdots s_{-k}\cdots} &= \big\{p \in D \,|\, f^{-i+1}(p) \in V_{s_{-i}}, i = 1, \cdots\big\} \\ &= \big\{p \in D \,|\, f^{-i}(p) \in H_{s_{-i}}, i = 1, \cdots\big\} \\ &\qquad \text{since } f(H_{s_i}) = V_{s_i} \end{aligned} \tag{23.2.17}$$

and

$$H_{s_0\cdots s_k\cdots} = \big\{p \in D \,|\, f^i(p) \in H_{s_i}, i = 0, \cdots\big\}, \tag{23.2.18}$$

we have

$$\begin{aligned} p &= V_{s_{-1}\cdots s_{-k}\cdots} \cap H_{s_0\cdots s_k\cdots} \\ &= \big\{p \in D \,|\, f^i(p) \in H_{s_i}, i = 0, \pm1, \pm2, \cdots\big\}. \end{aligned} \tag{23.2.19}$$

Therefore, we see that the unique sequence of 0's and 1's we have associated with p contains information concerning the behavior of p under iteration by f. In particular, the $s_{k^{\text{th}}}$ element in the sequence associated with p indicates that $f^k(p) \in H_{s_k}$. Now, note that for the bi-infinite sequence of 0's and 1's associated with p, the decimal point separates the past iterates from the future iterates; thus, the sequence of 0's and 1's associated with $f^k(p)$ is obtained from the sequence associated with p merely by shifting the decimal point in the sequence associated with p k places to the right if k is positive or k places to the left if k is negative, until s_k is the symbol immediately to the right of the decimal point. We can define a map of bi-infinite sequences of 0's and 1's, called the shift map, σ, which takes a sequence and shifts the decimal point one place to the right. Therefore, if we consider a point $p \in \Lambda$ and its associated bi-infinite sequence of 0's and 1's, $\phi(p)$, we can take any iterate of p, $f^k(p)$, and we can immediately obtain its associated bi-infinite sequence of 0's and 1's given by $\sigma^k(\phi(p))$. Hence, there is a direct relationship between iterating any point $p \in \Lambda$ under f and iterating the sequence of 0's and 1's associated with p under the shift map σ.

Now, at this point, it is not clear where we are going with this analogy between points in Λ and bi-infinite sequences of 0's and 1's since, although the sequence associated with a given point $p \in \Lambda$ contains information on the entire future and past as to whether or not it is in H_0 or H_1 for any given iterate, it is not hard to imagine different points, both contained in the same horizontal rectangle after any given iteration, whose orbits are completely different. The fact that this cannot happen for our map and that the dynamics of f on Λ are completely modeled by the dynamics of the shift map acting on sequences of 0's and 1's is an amazing fact which, to justify, we must digress into symbolic dynamics.

23.3 Symbolic Dynamics

Let $S = \{0, 1\}$ be the set of nonnegative integers consisting of 0 and 1. Let Σ be the collection of all bi-infinite sequences of elements of S, i.e., $s \in \Sigma$ implies

$$s = \{\cdots s_{-n} \cdots s_{-1}.s_0 \cdots s_n \cdots\}, \quad s_i \in S \quad \forall\, i.$$

We will refer to Σ as the space of bi-infinite sequences of two symbols. We wish to introduce some structure on Σ in the form of a metric, $d(\cdot, \cdot)$, which we do as follows. Consider

$$s = \{\cdots s_{-n} \cdots s_{-1}.s_0 \cdots s_n \cdots\},$$

$$\overline{s} = \{\cdots \overline{s}_{-n} \cdots \overline{s}_{-1}.\overline{s}_0 \cdots \overline{s}_n \cdots\} \in \Sigma;$$

we define the distance between s and $\overline{s}$, denoted $d(s, \overline{s})$, as follows

$$d(s, \overline{s}) = \sum_{i=-\infty}^{\infty} \frac{\delta_i}{2^{|i|}} \qquad \text{where } \delta_i = \begin{cases} 0 & \text{if } s_i = \overline{s}_i, \\ 1 & \text{if } s_i \neq \overline{s}_i. \end{cases} \tag{23.3.1}$$

Thus, two sequences are "close" if they agree on a long central block. (Note: the reader should check that $d(\cdot, \cdot)$ does indeed satisfy the properties of a metric. See Devaney [1986] for a proof.)

We consider a map of Σ into itself, which we shall call the shift map, σ, defined as follows: For $s = \{\cdots s_{-n} \cdots s_{-1}.s_0 s_1 \cdots s_n \cdots\} \in \Sigma$, we define

$$\sigma(s) = \{\cdots s_{-n} \cdots s_{-1} s_0.s_1 \cdots s_n \cdots\}$$

or $\sigma(s)_i = s_{i+1}$. Also, σ is continuous; we give a proof of this later in Section 24. Next, we want to consider the dynamics of σ on Σ (note: for our purposes the phrase "dynamics of σ on Σ" refers to the orbits of points in Σ under iteration by σ). It should be clear that σ has precisely two fixed points, namely, the sequence whose elements are all zeros and the sequence whose elements are all ones (notation: bi-infinite sequences which periodically repeat after some fixed length will be denoted by the finite length sequence with an overbar, e.g., $\{\cdots 101010.101010 \cdots\}$ is denoted by $\{\overline{10.10}\}$).

In particular, it is easy to see that the orbits of sequences which periodically repeat are periodic under iteration by σ. For example, consider the sequence $\{\overline{10.10}\}$. We have

$$\sigma\{\overline{10.10}\} = \{\overline{01.01}\},$$

and

$$\sigma\{\overline{01.10}\} = \{\overline{10.10}\};$$

thus,

$$\sigma^2\{\overline{10.10}\} = \{\overline{10.10}\}.$$

Therefore, the orbit of $\{\overline{10.10}\}$ is an orbit of period two for σ. So, from this particular example, it is easy to see that for any fixed k, the orbits of σ having period k correspond to the orbits of sequences made up of periodically repeating blocks of 0's and 1's with the blocks having length

k. Thus, since for any fixed k the number of sequences having a periodically repeating block of length k is finite, we see that σ has a countable infinity of periodic orbits having all possible periods. We list the first few below.

$$\begin{array}{lll}
\text{Period 1} & : & \{\overline{0.0}\}, \{\overline{1.1}\} \\
\text{Period 2} & : & \{\overline{01.01}\} \xrightarrow{\sigma} \{\overline{10.10}\} \xrightarrow{\sigma} \{\overline{01.01}\} \\
\text{Period 3} & : & \{\overline{001.001}\} \xrightarrow{\sigma} \{\overline{010.010}\} \xrightarrow{\sigma} \{\overline{100.100}\} \xrightarrow{\sigma} \{\overline{001.001}\} \\
 & : & \{\overline{110.110}\} \xrightarrow{\sigma} \{\overline{101.101}\} \xrightarrow{\sigma} \{\overline{011.011}\} \xrightarrow{\sigma} \{\overline{110.110}\} \\
\vdots & & \\
\text{etc.} & &
\end{array}$$

Also, σ has an uncountable number of nonperiodic orbits. To show this, we need only construct a nonperiodic sequence and show that there are an uncountable number of such sequences. A proof of this fact goes as follows: we can easily associate an infinite sequence of 0's and 1's with a given bi-infinite sequence by the following rule

$$\cdots s_{-n} \cdots s_{-1} . s_0 \cdots s_n \cdots \;\rightarrow\; . s_0 s_1 s_{-1} s_2 s_{-2} \cdots .$$

Now, we will take it as a known fact that the irrational numbers in the closed unit interval $[0, 1]$ constitute an uncountable set, and that every number in this interval can be expressed in base 2 as a binary expansion of 0's and 1's with the irrational numbers corresponding to nonrepeating sequences. Thus, we have a one-to-one correspondence between an uncountable set of points and nonrepeating sequences of 1's and 0's. As a result, the orbits of these sequences are the nonperiodic orbits of σ, and there are an uncountable number of such orbits.

Another interesting fact concerning the dynamics of σ on Σ is that there exists an element, say $s \in \Sigma$, whose orbit is dense in Σ, i.e., for any given $s' \in \Sigma$ and $\varepsilon > 0$, there exists some integer n such that $d(\sigma^n(s), s') < \varepsilon$. This is easiest to see by constructing s directly. We do this by first constructing all possible sequences of 0's and 1's having length $1, 2, 3, \ldots$. This process is well defined in a set-theoretic sense, since there are only a finite number of possibilities at each step (more specifically, there are 2^k distinct sequences of 0's and 1's of length k). The first few of these sequences would be as follows

$$\begin{array}{lll}
\text{length 1} & : & \{0\}, \{1\} \\
\text{length 2} & : & \{00\}, \{01\}, \{10\}, \{11\} \\
\text{length 3} & : & \{000\}, \{001\}, \{010\}, \{011\}, \{100\}, \{101\}, \{110\}, \{111\} \\
\vdots & & \vdots \\
 & & \text{etc.}
\end{array}$$

We can now introduce an ordering on the collection of sequences of 0's and 1's in order to keep track of the different sequences in the following way. Consider two finite sequences of 0's and 1's

$$s = \{s_1 \cdots s_k\}, \qquad \overline{s} = \{\overline{s}_1 \cdots \overline{s}_{k'}\}.$$

We can then say

$$s < \overline{s} \qquad \text{if} \quad k < k'.$$

If $k = k'$, then

$$s < \overline{s} \qquad \text{if} \quad s_i < \overline{s}_i,$$

where i is the *first* integer such that $s_i \neq \overline{s}_i$. For example, using this ordering we have

$$\begin{aligned} \{0\} &< \{1\}, \\ \{0\} &< \{00\}, \\ \{00\} &< \{01\}, \qquad \text{etc.} \end{aligned}$$

This ordering gives us a systematic way of distinguishing different sequences that have the same length. Thus, we will denote the sequences of 0's and 1's having length k as follows

$$s_1^k < \cdots < s_{2^k}^k,$$

where the superscript refers to the length of the sequence and the subscript refers to a particular sequence of length k which is uniquely specified by the above ordering scheme. This will give us a systematic way of writing down our candidate for a dense orbit.

Now consider the following sequence

$$s = \{\cdots s_8^3 s_6^3 s_4^3 s_2^3 s_4^2 s_2^2 s_2^1 . s_1^1 s_1^2 s_3^2 s_1^3 s_3^3 s_5^3 s_7^3 \cdots\}.$$

Thus, s contains all possible sequences of 0's and 1's of any fixed length. To show that the orbit of s is dense in Σ, we argue as follows: let s' be an arbitrary point in Σ and let $\varepsilon > 0$ be given. An ε-neighborhood of s' consists of all points $s'' \in \Sigma$ such that $d(s', s'') < \varepsilon$, where d is the metric given in (23.3.1). Therefore, by definition of the metric on Σ, there must be some integer $N = N(\varepsilon)$ such that $s'_i = s''_i$, $|i| \leq N$ (note: a proof of this statement can be found in Devaney [1986] or in Chapter 24). By construction, the finite sequence $\{s'_{-N} \cdots s'_{-1} . s'_0 \cdots s'_N\}$ is contained somewhere in

s; therefore, there must be some integer $\tilde{N}$ such that $d\big(\sigma^{\tilde{N}}(s), s'\big) < \epsilon$, and we can then conclude that the orbit of s is dense in Σ.

We summarize these facts concerning the dynamics of σ on Σ in the following theorem.

Theorem 23.3.1 *The shift map σ acting on the space of bi-infinite sequences of 0's and 1's, Σ, has*

i) *a countable infinity of periodic orbits of arbitrarily high period;*

ii) *an uncountable infinity of nonperiodic orbits;*

iii) *a dense orbit.*

23.4 The Dynamics on the Invariant Set

At this point we want to relate the dynamics of σ on Σ, about which we have a great deal of information, to the dynamics of the Smale horseshoe f on its invariant set Λ, about which we know little except for its complicated geometric structure. Recall that we have shown the existence of a well-defined map ϕ which associates to each point, $p \in \Lambda$, a bi-infinite sequence of 0's and 1's, $\phi(p)$. Furthermore, we noted that the sequence associated with any iterate of p, say $f^k(p)$, can be found merely by shifting the decimal point in the sequence associated with p k places to the right if k is positive or k places to the left if k is negative. In particular, the relation $\sigma \circ \phi(p) = \phi \circ f(p)$ holds for every $p \in \Lambda$. Now, if ϕ were invertible and continuous (continuity is necessary since f is continuous), the following relationship would hold

$$\phi^{-1} \circ \sigma \circ \phi(p) = f(p) \qquad \forall\, p \in \Lambda. \tag{23.4.1}$$

Thus, if the orbit $p \in \Lambda$ under f is denoted by

$$\big\{\cdots f^{-n}(p), \cdots, f^{-1}(p), p, f(p), \cdots, f^n(p), \cdots\big\}, \tag{23.4.2}$$

then, since $\phi^{-1} \circ \sigma \circ \phi(p) = f(p)$, we see that

$$\begin{aligned} f^n(p) &= \big(\phi^{-1} \circ \sigma \circ \phi\big) \circ \big(\phi^{-1} \circ \sigma \circ \phi\big) \circ \cdots \circ \big(\phi^{-1} \circ \sigma \circ \phi(p)\big) \\ &= \phi^{-1} \circ \sigma^n \circ \phi(p), \quad n \geq 0. \end{aligned} \tag{23.4.3}$$

Also, from (23.4.1) we have

$$f^{-1}(p) = \phi^{-1} \circ \sigma^{-1} \circ \phi(p) \qquad \forall\, p \in \Lambda,$$

from which we see that

$$\begin{aligned} f^{-n}(p) &= \left(\phi^{-1} \circ \sigma^{-1} \circ \phi\right) \circ \left(\phi^{-1} \circ \sigma^{-1} \circ \phi)\right) \circ \cdots \circ \left(\phi^{-1} \circ \sigma^{-1} \circ \phi(p)\right) \\ &= \phi^{-1} \circ \sigma^{-n} \circ \phi(p), \quad n \geq 0. \end{aligned} \tag{23.4.4}$$

Therefore, using (23.4.2), (23.4.3), and (23.4.4), we see that the orbit of $p \in \Lambda$ under f would correspond directly to the orbit of $\phi(p)$ under σ in Σ. In particular, the entire orbit structure of σ on Σ would be identical to the structure of f on Λ. Hence, in order to verify that this situation holds, we need to show that ϕ is a homeomorphism of Λ and Σ.

Theorem 23.4.1 *The map $\phi : \Lambda \to \Sigma$ is a homeomorphism.*

Proof: We need only show that ϕ is one-to-one and continuous, since continuity of the inverse will follow from the fact that one-to-one, onto, and continuous maps from compact sets into Hausdorff spaces are homeomorphisms (see Dugundji [1966]). We prove each condition separately.

ϕ is one-to-one: This means that given $p, p' \in \Lambda$, if $p \neq p'$, then $\phi(p) \neq \phi(p')$.

We give a proof by contradiction. Suppose $p \neq p'$ and

$$\phi(p) = \phi(p') = \left\{\cdots s_{-n} \cdots s_{-1}.s_0 \cdots s_n \cdots\right\}.$$

Then, by construction of Λ, p and p' lie in the intersection of the vertical line $V_{s_{-1} \cdots s_{-n} \cdots}$ and the horizontal line $H_{s_0 \cdots s_n \cdots}$. However, the intersection of a horizontal line and a vertical line consists of a unique point; therefore $p = p'$, contradicting our original assumption. This contradiction is due to the fact that we have assumed $\phi(p) = \phi(p')$; thus, for $p \neq p'$, $\phi(p) \neq \phi(p')$.

ϕ is onto: This means that given any bi-infinite sequence of 0's and 1's in Σ, say $\{\cdots s_{-n} \cdots s_{-1}.s_0 \cdots s_n \cdots\}$, there is a point $p \in \Lambda$ such that $\phi(p) = \{\cdots s_{-n} \cdots s_{-1}.s_0 \cdots s_n \cdots\}$.

The proof goes as follows: Recall the construction of $\bigcap_{n=0}^{\infty} f^n(D)$ and $\bigcap_{-\infty}^{n=0} f^n(D)$; given any infinite sequence of 0's and 1's, $\{\cdots s_{-n} \cdots s_{-1}.\}$, there is a *unique* vertical line in $\bigcap_{n=0}^{\infty} f^n(D)$ corresponding to this sequence. Similarly, given any infinite sequence of 0's and 1's, $\{.s_0$

$\cdots s_n \cdots\}$, there is a unique horizontal line in $\bigcap_{-\infty}^{n=0} f^n(D)$ corresponding to this sequence. Therefore, we see that for a given horizontal and vertical line, we can associate a unique bi-infinite sequence of 0's and 1's, $\{\cdots s_{-n} \cdots s_{-1}.s_0 \cdots s_n \cdots\}$ and, since a horizontal and vertical line intersect in a unique point, p, to every bi-infinite sequence of 0's and 1's, there corresponds a unique point in Λ.

ϕ is continuous: This means that, given any point $p \in \Lambda$ and $\varepsilon > 0$, we can find a $\delta = \delta(\varepsilon, p)$ such that

$$|p - p'| < \delta \qquad \text{implies} \quad d\big(\phi(p), \phi(p')\big) < \varepsilon,$$

where $|\cdot|$ is the usual distance measurement in $\Re^2$ and $d(\cdot,\cdot)$ is the metric on Σ introduced earlier.

Let $\varepsilon > 0$ be given; then, if we are to have $d(\phi(p), \phi(p')) < \varepsilon$, there must be some integer $N = N(\epsilon)$ such that if

$$\phi(p) = \big\{\cdots s_{-n} \cdots s_{-1}.s_0 \cdots s_n \cdots\big\},$$
$$\phi(p') = \big\{\cdots s'_{-n} \cdots s'_{-1}.s'_0 \cdots s'_n \cdots\big\},$$

then $s_i = s'_i$, $i = 0, \pm 1, \ldots, \pm N$. Thus, by construction of Λ, p and p' lie in the rectangle defined by $H_{s_0 \cdots s_N} \cap V_{s_{-1} \cdots s_{-N}}$; see Figure 23.4.1. Recall that the width and height of this rectangle are λ^N and $1/\mu^{N+1}$, respectively. Thus we have $|p - p'| \le (\lambda^N + 1/\mu^{N+1})$. Therefore, if we take $\delta = \lambda^N + 1/\mu^{N+1}$, continuity is proved. □

We make the following remarks.

Remark 1. Recall from Chapter 12, that the dynamical systems f acting on Λ and σ acting on Σ are said to be *topologically conjugate* if $\phi \circ f(p) = \sigma \circ \phi(p)$. (Note: the equation $\phi \circ f(p) = \sigma \circ \phi(p)$ is also expressed by saying that the following diagram "commutes.")

$$\begin{array}{ccc} \Lambda & \xrightarrow{f} & \Lambda \\ \phi \downarrow & & \downarrow \phi \\ \Sigma & \xrightarrow{\sigma} & \Sigma \end{array}$$

Remark 2. The fact that Λ and Σ are homeomorphic allows us to make several conclusions concerning the set-theoretic nature of Λ. We have already shown that Σ is uncountable, and we state without proof that Σ is a

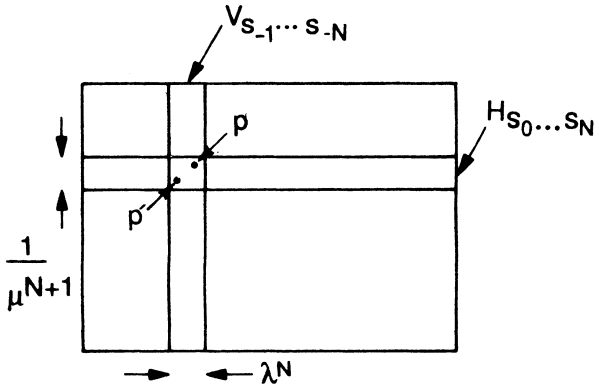

FIGURE 23.4.1.

closed, perfect (meaning every point is a limit point), totally disconnected set and that these properties carry over to Λ via the homeomorphism ϕ. A set having these properties is called a *Cantor set.* We will give more detailed information concerning symbolic dynamics and Cantor sets in Chapter 24.

Now we can state a theorem regarding the dynamics of f on Λ that is almost precisely the same as Theorem 23.3.1, which describes the dynamics of σ on Σ.

Theorem 23.4.2 *The Smale horseshoe, f, has*

i) *a countable infinity of periodic orbits of arbitrarily high period. These periodic orbits are all of saddle type;*

ii) *an uncountable infinity of non-periodic orbits;*

iii) *a dense orbit.*

Proof: This is an immediate consequence of the topological conjugacy of f on Λ with σ on Σ, except for the stability result. The stability result follows from the form of f on H_0 and H_1 given in (23.1.6). □

23.5 Chaos

Now we can make precise the statement that the dynamics of f on Λ is chaotic.

Let $p \in \Lambda$ with corresponding symbol sequence

$$\phi(p) = \{\cdots s_{-n} \cdots s_{-1}.s_0 \cdots s_n \cdots\}.$$

We want to consider points close to p and how they behave under iteration by f as compared with p. Let $\varepsilon > 0$ be given; then we consider an ε-neighborhood of p determined by the usual topology of the plane. Hence there also exists an integer $N = N(\varepsilon)$ such that the corresponding neighborhood of $\phi(p)$ includes the set of sequences $s' = \{\cdots s'_{-n} \cdots s'_{-1}.s'_0 \cdots s'_n \cdots\}$ $\in \Sigma$ such that $s_i = s'_i$, $|i| \leq N$. Now suppose the $N+1$ entry in the sequence corresponding to $\phi(p)$ is 0, and the $N+1$ entry in the sequence corresponding to some s' is 1. Thus, after N iterations, no matter how small ε, the point p is in H_0; the point, say p', corresponding to s' under ϕ^{-1} is in H_1, and they are at least a distance $1-2\lambda$ apart. Therefore, for any point $p \in \Lambda$, no matter how small a neighborhood of p we consider, there is at least one point in this neighborhood such that, after a finite number of iterations, p and this point have separated by some fixed distance. A system displaying such behavior is said to exhibit *sensitive dependence on initial conditions.* A dynamical system displaying sensitive dependence on initial conditions on a closed invariant set (which consists of more than one orbit) will be called *chaotic.*

23.6 Final Remarks and Observations

Now we want to end our discussion of this simplified version of the Smale horseshoe with some final observations.

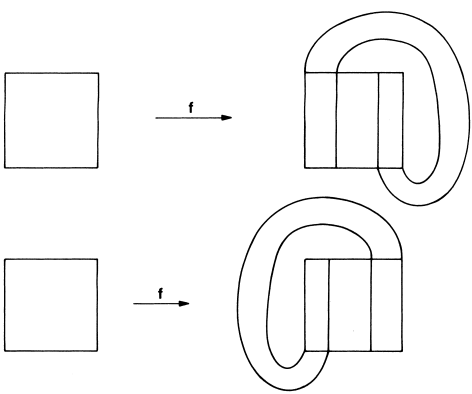

FIGURE 23.6.1.

1. If you consider carefully the main ingredients of f which led to Theorem 23.4.2, you will see that there are two key elements.
   (a) The square is contracted, expanded, and folded in such a way that we can find disjoint regions that are mapped over themselves.
   (b) There exists "strong" stretching and contraction in complementary directions.
2. From observation 1), the fact that the image of the square appears in the shape of a horseshoe is not important. Other possible scenarios are shown in Figure 23.6.1.
3. Notice that, in our study of the invariant set of f, we do not consider the question of the geometry of the points which escape from the square. We remark that this could be an interesting research topic, since this more global question may enable one to determine conditions under which the horseshoe becomes an attractor.
4. Some interesting references related to the Smale horseshoe are Bowen [1975b], Young [1981], Hall [1994] and Kennedy and Yorke[2001].

24

Symbolic Dynamics

In the previous section we saw an example of a two-dimensional map which possessed an invariant Cantor set. The map, restricted to its invariant set, was shown to have a countable infinity of periodic orbits of all periods, an uncountable infinity of nonperiodic orbits, and a dense orbit. Now, in general, the determination of such detailed information concerning the orbit structure of a map is not possible. However, in our example we were able to show that the map restricted to its invariant set behaved the same as the shift map acting on the space of bi-infinite sequences of 0's and 1's (more precisely, these two dynamical systems were shown to be topologically conjugate; thus their orbit structures are identical). The shift map was no less complicated than our original map but, due to its structure, many of the features concerning its dynamics (e.g., the nature and number of its periodic orbits) were more or less obvious. The technique of characterizing the orbit structure of a dynamical system via infinite sequences of "symbols" (in our case 0's and 1's) is known as *symbolic dynamics.* The technique is not new and appears to have originally been applied by Hadamard [1898] in the study of geodesics on surfaces of negative curvature and Birkhoff [1927], [1935] in his studies of dynamical systems. The first exposition of symbolic dynamics as an independent subject was given by Morse and Hedlund [1938]. Applications of this idea to differential equations can be found in Levinson's work on the forced van der Pol equation (Levinson [1949]), from which came Smale's inspiration for his construction of the horseshoe map (Smale [1963], [1980]), and also in the work of Alekseev [1968], [1969], who gives a systematic account of the technique and applies it to problems arising from celestial mechanics. These references by no means represent a complete account of the history of symbolic dynamics or of its applications, and we refer the reader to the bibliographies of the above listed references or to Moser [1973] or Lind and Marcus [1995] for a more complete list of references on the subject and its applications. In recent times (say from about 1965 to the present) there has been a flood of applications of the technique.

Symbolic dynamics will play a key role in explaining the dynamical phenomena we encounter in this chapter. For this reason, we now want to

describe some aspects of symbolic dynamics viewed as an independent subject. Our discussion follows Wiggins [1988].

We let $S = \{1, 2, 3, \cdots, N\}$, $N \geq 2$ be our collection of symbols. We will build our sequences from elements of S. Note that for the purpose of constructing sequences, the elements of S could be anything, e.g., letters of the alphabet, Chinese characters, etc. We will use positive integers since they are familiar, easy to write down, and we have as many of them as we desire.

24.1 The Structure of the Space of Symbol Sequences

We now want to construct the space of all symbol sequences, which we will refer to as Σ^N, from elements of S and derive some properties of Σ^N. It will be convenient to construct Σ^N as a Cartesian product of infinitely many copies of S. This construction will allow us to make some conclusions concerning the properties of Σ^N based only on our knowledge of S, the structure which we give to S, and topological theorems on infinite products.

We now give some structure to S; specifically, we want to make S into a metric space, which can be done with the following metric

$$d(a, b) \equiv \begin{cases} 1 & \text{if} \quad a \neq b, \\ 0 & \text{if} \quad a = b. \end{cases} \tag{24.1.1}$$

It is trivial to check that $d(\cdot, \cdot)$ is a metric.

> The metric (24.1.1) actually induces the discrete topology on S, i.e., the topology defined by the collection of all subsets of S, see Munkres [1975].

Since S consists of a finite number of points, it is trivial to verify that it is compact. Moreover, S is totally disconnected, i.e., its only connected subsets are one-point sets. We summarize the properties of S in the following proposition.

Proposition 24.1.1 *The set S equipped with the metric (24.1.1) is a compact, totally disconnected, metric space.*

We remark that compact metric spaces are automatically complete metric spaces (see Munkres [1975], Section 7-3, Theorem 3.1).

Now we will construct Σ^N as a bi-infinite Cartesian product of copies of S:

$$\Sigma^N \equiv \cdots \times S \times S \times S \times S \times \cdots \equiv \prod_{i=-\infty}^{\infty} S^i \quad \text{where} \quad S^i = S \quad \forall\, i. \tag{24.1.2}$$

Thus, a point in Σ^N is represented as a "bi-infinity-tuple" of elements of S:

$$s \in \Sigma^N \Rightarrow s = \{\cdots, s_{-n}, \cdots, s_{-1}, s_0, s_1, \cdots, s_n, \cdots\} \quad \text{where} \quad s_i \in S \quad \forall\, i,$$

or, more succintly, we will write s as

$$s = \{\cdots s_{-n} \cdots s_{-1}.s_0 s_1 \cdots s_n \cdots\} \qquad \text{where} \quad s_i \in S \quad \forall\, i.$$

A word should be said about the "decimal point" that appears in each symbol sequence and has the effect of separating the symbol sequence into two parts, with both parts being infinite (hence the reason for the phrase "bi-infinite sequence"). At present it does not play a major role in our discussion and could easily be left out with all of our results describing the structure of Σ^N going through just the same. In some sense, it serves as a starting point for constructing the sequences by giving us a natural way of subscripting each element of a sequence. This notation will prove convenient shortly when we define a metric on Σ^N. However, the real significance of the decimal point will become apparent when we define and discuss the shift map acting on Σ^N and its orbit structure.

In order to discuss limit processes in Σ^N, it will be convenient to define a metric on Σ^N. Since S is a metric space, it is also possible to define a metric on Σ^N. There are many possible choices for a metric on Σ^N; however, we will utilize the following. For

$$\begin{aligned} s &= \{\cdots s_{-n} \cdots s_{-1}.s_0 s_1 \cdots s_n \cdots\}, \\ \overline{s} &= \{\cdots \overline{s}_{-n} \cdots \overline{s}_{-1}.\overline{s}_0 \overline{s}_1 \cdots \overline{s}_n \cdots\} \in \Sigma^N, \end{aligned}$$

the distance between s and $\overline{s}$ is defined as

$$d(s, \overline{s}) = \sum_{i=-\infty}^{\infty} \frac{1}{2^{|i|}} \, \frac{d_i(s_i, \overline{s}_i)}{1 + d_i(s_i, \overline{s}_i)}, \tag{24.1.3}$$

where $d_i(\cdot,\cdot)$ is the metric on $S^i \equiv S$ defined in (24.1.1). The reader should verify that (24.1.3) indeed defines a metric. Intuitively, this choice of metric implies that two symbol sequences are "close" if they agree on a long central block. The following lemma makes this precise.

Lemma 24.1.2 *For $s, \overline{s} \in \Sigma^N$,*

i) *Suppose $d(s,\overline{s}) < 1/(2^{M+1})$; then $s_i = \overline{s}_i$ for all $|i| \le M$.*

ii) *Suppose $s_i = \overline{s}_i$ for $|i| \le M$; then $d(s,\overline{s}) \le 1/(2^M)$.*

Proof: The proof of i) is by contradiction. Suppose the hypothesis of i) holds and there exists some j with $|j| \le M$ such that $s_j \neq \overline{s}_j$. Then there exists a term in the sum defining $d(s,\overline{s})$ of the form

$$\frac{1}{2^{|j|}} \frac{d_j(s_j,\overline{s}_j)}{1+d_j(s_j,\overline{s}_j)}.$$

However, since $s_j \neq \overline{s}_j$,

$$\frac{d_j(s_j,\overline{s}_j)}{1+d_j(s_j,\overline{s}_j)} = \frac{1}{2},$$

and each term in the sum defining $d(s,\overline{s})$ is positive so that we have

$$d(s,\overline{s}) \ge \frac{1}{2^{|j|}} \frac{d_j(s_j,\overline{s}_j)}{1+d_j(s_j,\overline{s}_j)} = \frac{1}{2^{|j|+1}} \ge \frac{1}{2^{M+1}},$$

but this contradicts the hypothesis of i).

We now prove ii). If $s_i = \overline{s}_i$ for $|i| \le M$, we have

$$d(s,\overline{s}) = \sum_{-\infty}^{i=-(M+1)} \frac{1}{2^{|i|}} \frac{d_i(s_i,\overline{s}_i)}{1+d_i(s_i,\overline{s}_i)} + \sum_{i=M+1}^{\infty} \frac{1}{2^{|i|}} \frac{d_i(s_i,\overline{s}_i)}{1+d_i(s_i,\overline{s}_i)};$$

however, $\big(d_i(s_i,\overline{s}_i)/(1+d_i(s_i,\overline{s}_i))\big) = 1/2$, so we obtain

$$d(s,\overline{s}) \le 2 \sum_{i=M+1}^{\infty} \frac{1}{2^{i+1}} = \frac{1}{2^M}. \qquad \square$$

Armed with our metric, we can define neighborhoods of points in Σ^N and describe limit processes. Suppose we are given a point

$$\overline{s} = \{\cdots \overline{s}_{-n} \cdots \overline{s}_{-1}.\overline{s}_0\overline{s}_1 \cdots \overline{s}_n \cdots\} \in \Sigma^N, \qquad \overline{s}_i \in S \quad \forall\, i, \tag{24.1.4}$$

and a positive real number $\varepsilon > 0$, and we wish to describe the "ε-neighborhood of $\overline{s}$", i.e., the set of $s \in \Sigma^N$ such that $d(s, \overline{s}) < \varepsilon$. Then, by Lemma 24.1.2, given $\varepsilon > 0$, we can find a positive integer $M = M(\varepsilon)$ such that $d(s, \overline{s}) < \varepsilon$ implies $s_i = \overline{s}_i \ \forall\, |i| \leq M$. Thus, our notation for an ε-neighborhood of an arbitrary $\overline{s} \in \Sigma^N$ will be as follows

$$\mathcal{N}^{M(\varepsilon)}(\overline{s}) = \{s \in \Sigma^N \mid s_i = \overline{s}_i \quad \forall\, |i| \leq M,\ s_i, \overline{s}_i \in S \quad \forall\, i\}.$$

Before stating our theorem concerning the structure of Σ^N we need the following definition.

Definition 24.1.3 *A set is called* perfect *if it is closed and every point in the set is a limit point of the set.*

We are now ready to state our main theorem concerning the structure of Σ^N.

Proposition 24.1.4 *The space Σ^N equipped with the metric (24.1.3) is*

i) *compact,*

ii) *totally disconnected, and*

iii) *perfect.*

Proof: i) Since S is compact, Σ^N is compact by Tychonov's theorem (Munkres [1975], Section 5-1).

ii) By Proposition 24.1.1, S is totally disconnected, and therefore Σ^N is totally disconnected, since the product of totally disconnected spaces is likewise totally disconnected (Dugundji [1966]).

iii) Σ^N is closed, since it is a compact metric space. Let $\overline{s} \in \Sigma^N$ be an arbitrary point in Σ^N; then, to show that $\overline{s}$ is a limit point of Σ^N, we need only show that every neighborhood of $\overline{s}$ contains a point $s \neq \overline{s}$ with $s \in \Sigma^N$. Let $\mathcal{N}^{M(\varepsilon)}(\overline{s})$ be a neighborhood of $\overline{s}$ and let $\hat{s} = \overline{s}_{M(\varepsilon)+1} + 1$ if $\overline{s}_{M(\varepsilon)+1} \neq N$, and $\hat{s} = \overline{s}_{M(\varepsilon)+1} - 1$ if $\overline{s}_{M(\varepsilon)+1} = N$. Then the sequence

$$\{\cdots \overline{s}_{-M(\varepsilon)-2}\hat{s}\overline{s}_{-M(\varepsilon)} \cdots \overline{s}_{-1}.\overline{s}_0\overline{s}_1 \cdots \overline{s}_{M(\varepsilon)}\hat{s}\overline{s}_{M(\varepsilon)+2} \cdots\}$$

is contained in $\mathcal{N}^{M(\varepsilon)}(\overline{s})$ and is not equal to $\overline{s}$; thus Σ^N is perfect. □

We remark that the three properties of Σ^N stated in Proposition 24.1.4 are often taken as the defining properties of a *Cantor set*, of which the classical Cantor "middle-thirds" set is a prime example.

The following theorem of Cantor gives us information concerning the cardinality of perfect sets.

Theorem 24.1.5 *Every perfect set in a complete space has at least the cardinality of the continuum.*

Proof: See Hausdorff [1957]. □

Hence, Σ^N is uncountable.

24.2 The Shift Map

Now that we have established the structure of Σ^N, we define a map on Σ^N, denoted by σ, as follows. For $s = \{\cdots s_{-n} \cdots s_{-1}.s_0 s_1 \cdots s_n \cdots\} \in \Sigma^N$, we define

$$\sigma(s) = \{\cdots s_{-n} \cdots s_{-1} s_0.s_1 \cdots s_n \cdots\},$$

or $[\sigma(s)]_i \equiv s_{i+1}$. The map σ is referred to as the *shift map,* and when the domain of σ is taken to be all of Σ^N, it is often referred to as a *full shift on N symbols.* We have the following proposition concerning some properties of σ.

Proposition 24.2.1 i) $\sigma(\Sigma^N) = \Sigma^N$. ii) σ *is continuous.*

Proof: The proof of i) is obvious. To prove ii) we must show that, given $\varepsilon > 0$, there exists a $\delta(\varepsilon)$ such that $d(s, \overline{s}) < \delta$ implies $d(\sigma(s), \sigma(\overline{s})) < \varepsilon$ for $s, \overline{s} \in \Sigma^N$. Suppose $\varepsilon > 0$ is given; then choose M such that $1/(2^{M-1}) < \varepsilon$. If we then let $\delta = 1/2^{M+1}$, we see by Lemma 24.1.2 that $d(s, \overline{s}) < \delta$ implies $s_i = \overline{s}_i$ for $|i| \leq M$; hence, $[\sigma(s)]_i = [\sigma(\overline{s})]_i$, $|i| \leq M - 1$. Then, also by Lemma 24.1.2, we have $d(\sigma(s), \sigma(\overline{s})) < 1/2^{M-1} < \varepsilon$. □

We now want to consider the orbit structure of σ acting on Σ^N. We have the following proposition.

Proposition 24.2.2 *The shift map σ has*

i) *a countable infinity of periodic orbits consisting of orbits of all periods;*

ii) *an uncountable infinity of nonperiodic orbits; and*

iii) *a dense orbit.*

Proof: i) This is proven in exactly the same way as the analogous result obtained in our discussion of the symbolic dynamics for the Smale horseshoe map in Section 23.3. In particular, the orbits of the periodic symbol sequences are periodic, and there is a countable infinity of such sequences. ii) By Theorem 24.1.5 Σ^N is uncountable; thus, removing the countable infinity of periodic symbol sequences leaves an uncountable number of nonperiodic symbol sequences. Since the orbits of the nonperiodic sequences never repeat, this proves ii). iii) This is proven in exactly the same way as the analogous result obtained in our discussion of the Smale horseshoe map in Section 23; namely, we form a symbol sequence by stringing together all possible symbol sequences of any finite length. The orbit of this sequence is dense in Σ^N since, by construction, some iterate of this symbol sequence will be arbitrarily close to any given symbol sequence in Σ^N. □

24.3 Exercises

1. Compute the *distinct* period k orbits, $k = 1, 2, 3, 4, 5$, for $\sigma : \Sigma^N \to \Sigma^N$, $N = 2, 3, 4, 5$.

2. Prove that $\sigma : \Sigma^N \to \Sigma^N$ has an infinite number of dense orbits. Are these dense orbits countable?

3. Consider a sequence $\bar{s} \in \Sigma^N$. Let $O(\bar{s})$ denote the orbit of $\bar{s}$ under the shift map σ. Then the orbit of a sequence $s \in \Sigma^N$ is said to be *homoclinic to* $O(\bar{s})$ if

$$\lim_{|n|\to\infty} d(\sigma^n(s), O(\bar{s})) = 0.$$

   (a) Prove that any periodic sequence $\bar{s}$ has a countable number of homoclinic orbits.

   (b) Is this true for nonperiodic sequences $\bar{s}$?

   (c) Can a periodic sequence have an infinite number of homoclinic orbits?

4. Consider two sequences $\bar{s}, \tilde{s} \in \Sigma^N$. Then the orbit of any point $s \in \Sigma^N$ is said to be *heteroclinic to* $O(\bar{s})$ *and* $O(\tilde{s})$ if

$$\lim_{n\to\infty} d(\sigma^n(s), O(\bar{s})) = 0 \qquad \text{and} \qquad \lim_{n\to-\infty} d(\sigma^n(s), O(\tilde{s})) = 0.$$

   (a) Prove that any periodic sequences $\bar{s}$, $\tilde{s} \in \Sigma^N$, have a countable number of heteroclinic orbits.

   (b) Is this true for nonperiodic sequences?

   (c) Can two periodic sequences have an infinite number of heteroclinic orbits?

5. Show how the homoclinic orbits in Σ^N can be characterized as the limit of a sequence of periodic orbits with increasing periods.

6. Give a direct proof that Σ^N is totally disconnected. (Hint: using the definition of neighborhood given in (24.1.4), choose any two sequences, s, $\bar{s} \in \Sigma^N$, and construct neighborhoods of each, denoted $\mathcal{N}^M(s), \mathcal{N}^{\bar{M}}(\bar{s})$, that satisfy $\mathcal{N}^M(s) \cap \mathcal{N}^{\bar{M}}(\bar{s}) = \emptyset$ and $\mathcal{N}^M(s) \cup \mathcal{N}^{\bar{M}}(\bar{s}) = \Sigma^N$.)

7. This exercise is concerned with the classical Cantor "middle-thirds" set. This set is constructed inductively as follows: Begin with the unit interval, denoted C_0 for notational purposes, and remove the open interval $(\frac{1}{3}, \frac{2}{3})$ called the "middle third". We refer to the remainder as C_1. Thus

$$C_1 = \left[0, \frac{1}{3}\right] \cup \left[\frac{2}{3}, 1\right].$$

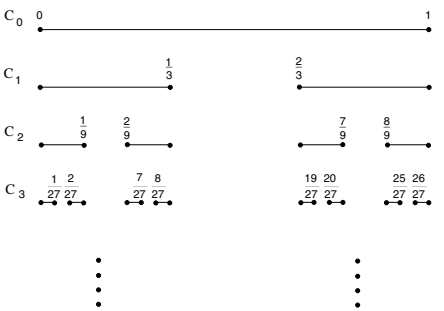

FIGUREE 24.3.1. Graphical illustration of the Cantor set construction.

Next remove the open middle thirds of the two closed intervals in C_1 to obtain

$$C_2 = \left[0, \frac{1}{9}\right] \cup \left[\frac{2}{9}, \frac{1}{3}\right] \cup \left[\frac{2}{3}, \frac{7}{9}\right] \cup \left[\frac{8}{9}, 1\right].$$

Next remove the open middle thirds of the four closed intervals in C_2 to obtain

$$C_3 = \left[0, \frac{1}{27}\right] \cup \left[\frac{2}{27}, \frac{3}{27}\right] \cup \left[\frac{6}{27}, \frac{7}{27}\right] \cup \left[\frac{8}{27}, \frac{1}{3}\right] \cup \left[\frac{2}{3}, \frac{19}{27}\right] \cup \left[\frac{20}{27}, \frac{7}{9}\right] \cup \left[\frac{8}{9}, \frac{25}{27}\right] \cup \left[\frac{26}{27}, 1\right].$$

Continue this procedure, which we illustrate graphically in Fig. 24.3.1.

At the n^{th} step we have 2^n disjoint closed intervals, each of length $\frac{1}{3^n}$. The Cantor set, C, is defined as

$$C \equiv \bigcap_{n=0}^{\infty} C_n.$$

Prove the following:

(a) $C_n = C_{n-1} - \bigcup_{k=0}^{\infty} \left(\frac{1+3k}{3^n}, \frac{2+3k}{3^n}\right)$.

(b) C is compact.
(c) C is closed.
(d) C is uncountable.
(e) C is perfect.
(f) C is totally disconnected.
(g) C has Lebesgue measure zero.

25

The Conley–Moser Conditions, or "How to Prove That a Dynamical System is Chaotic"

In this section we will give sufficient conditions in order for a two-dimensional invertible map to have an invariant Cantor set on which the dynamics are topologically conjugate to a full shift on N symbols ($N \geq 2$). These conditions were first given by Conley and Moser (see Moser [1973]), and we give slight improvements on their estimates. Alekseev [1968], [1969] developed similar criteria. Generalizations to n-dimensions can be found in Wiggins [1988] and Li and Wiggins [1997]. Generalizations to nonautonomous systems can be found in Wiggins [1999].

25.1 The Main Theorem

We begin with several definitions.

Definition 25.1.1 *A* μ_v-vertical curve *is the graph of a function* $x = v(y)$ *for which*

$$0 \leq v(y) \leq 1, \qquad |v(y_1) - v(y_2)| \leq \mu_v |y_1 - y_2| \quad \textit{for} \;\; 0 \leq y_1, \; y_2 \leq 1.$$

Similarly, a μ_h-horizontal curve *is the graph of a function* $y = h(x)$ *for which*

$$0 \leq h(x) \leq 1, \qquad |h(x_1) - h(x_2)| \leq \mu_h |x_1 - x_2| \quad \textit{for} \; 0 \leq x_1, \; x_2 \leq 1;$$

see Figure 25.1.1.

We make the following remarks concerning Definition 25.1.1.

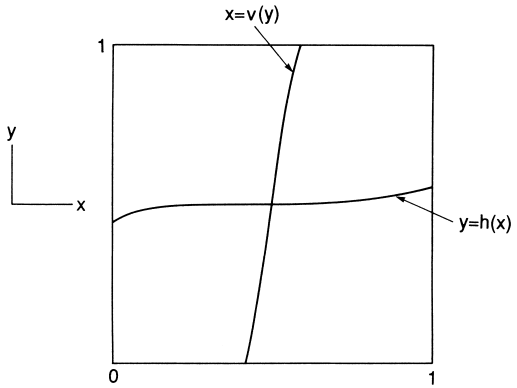

FIGURE 25.1.1.

Remark 1. Functions $x = v(y)$ and $y = h(x)$ satisfying Definition 25.1.1 are called *Lipschitz functions* with Lipschitz constants μ_v and μ_h, respectively.

Remark 2. The constant μ_h can be interpreted as a bound on the slope of the curve defined by the graph of $y = h(x)$. A similar interpretation holds for μ_v and the graph of $x = v(y)$.

Remark 3. For $\mu_v = 0$, the graph of $x = v(y)$ is a vertical line and, for $\mu_h = 0$, the graph of $y = h(x)$ is a horizontal line.

Remark 4. At this point we have put no restrictions on the relationship or magnitudes of μ_v and μ_h.

Next we want to "fatten up" these μ_v-vertical curves and μ_h-horizontal curves into μ_v-vertical strips and μ_h-horizontal strips, respectively.

Definition 25.1.2 *Given two nonintersecting μ_v-vertical curves $v_1(y) < v_2(y)$, $y \in [0,1]$, we define a* μ_v-vertical strip *as*

$$V = \big\{(x,y) \in \mathbb{R}^2 \,|\, x \in [v_1(y), v_2(y)];\ y \in [0,1]\big\}.$$

Similarly, given two nonintersecting μ_h-horizontal curves $h_1(x) < h_2(x)$, $x \in [0,1]$, we define a μ_h-horizontal strip *as*

$$H = \big\{(x,y) \in \mathbb{R}^2 \,|\, y \in [h_1(x), h_2(x)];\ x \in [0,1]\big\};$$

see Figure 25.1.2. The width of horizontal and vertical strips is defined as

$$d(H) = \max_{x\in[0,1]} |h_2(x) - h_1(x)|, \tag{25.1.1}$$

$$d(V) = \max_{y\in[0,1]} |v_2(y) - v_1(y)|. \tag{25.1.2}$$

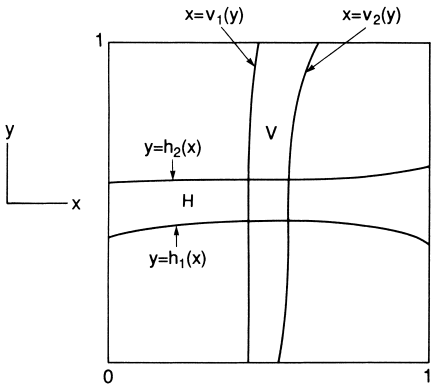

FIGURE 25.1.2.

The following two lemmas will play an important role in the inductive process of constructing the invariant set for the map f.

Lemma 25.1.3 i) *If $V^1 \supset V^2 \supset \cdots \supset V^k \supset \cdots$ is a nested sequence of μ_v-vertical strips with $d(V^k) \to 0$ as $k \to \infty$, then $\bigcap_{k=1}^{\infty} V^k \equiv V^\infty$ is a μ_v-vertical curve.*

ii) *If $H^1 \supset H^2 \supset \cdots \supset H^k \supset \cdots$ is a nested sequence of μ_h-horizontal strips with $d(H^k) \to 0$ as $k \to \infty$, then $\bigcap_{k=1}^{\infty} H^k \equiv H^\infty$ is a μ_h-horizontal curve.*

Proof: We will prove i) only, since the proof of ii) requires only trivial modifications.

Let $C_{\mu_v}[0,1]$ denote the set of Lipschitz functions with Lipschitz constant μ_v defined on the interval $[0,1]$. Then with the metric defined by the maximum norm, $C_{\mu_v}[0,1]$ is a complete metric space (see Arnold [1973] for a proof). Let $x = v_1^k(y)$ and $x = v_2^k(y)$ form the vertical boundaries of the μ_v-vertical strip V^k. Now consider the sequence

$$\{v_1^1(y), v_2^1(y), v_1^2(y), v_2^2(y), \cdots, v_1^k(y), v_2^k(y), \cdots\}. \tag{25.1.3}$$

By definition of the V^k, (25.1.3) is a sequence of elements of $C_{\mu_v}[0,1]$, and since $d(V^k) \to 0$ as $k \to \infty$, it is a Cauchy sequence. Therefore, since

$C_{\mu_v}[0,1]$ is a complete metric space, the Cauchy sequence converges to a unique μ_v-vertical curve. This proves i). □

Lemma 25.1.4 *Suppose* $0 \leq \mu_v \mu_h < 1$. *Then a* μ_v*-vertical curve and a* μ_h*-horizontal curve intersect in a unique point.*

Proof: Let the μ_h-horizontal curve be given by the graph of

$$y = h(x),$$

and let the μ_v-vertical curve be given by the graph of

$$x = v(y).$$

The condition for intersection is that there exists a point (x, y) in the unit square satisfying each relation, i.e., we have

$$y = h(x), \tag{25.1.4}$$

where x in (25.1.4) satisfies

$$x = v(y),$$

in other words, the equation

$$y = h(v(y)) \tag{25.1.5}$$

has a solution. We want to show that this solution is *unique.* We will use the contraction mapping theorem (see Arnold [1973]).

Let us give some background. Consider a map

$$g\colon M \longrightarrow M,$$

where M is a complete metric space. Then g is said to be a *contraction map* if

$$|g(m_1) - g(m_2)| \leq k|m_1 - m_2|, \qquad m_1, m_2 \in M,$$

for some constant $0 \leq k < 1$, where $|\cdot|$ denotes the metric on M. The contraction mapping theorem says that g has a unique fixed point, i.e., there exists *one* point $\overline{m} \in M$ such that

$$g(\overline{m}) = \overline{m}.$$

We now apply this to our situation.

Let I denote the closed unit interval, i.e.,

$$I = \{y \in \mathbb{R}^1 \,|\, 0 \leq y \leq 1\}.$$

Clearly I is a complete metric space. Also, it should be evident that

$$h \circ v : I \longrightarrow I. \tag{25.1.6}$$

Hence, if we show that $h \circ v$ is a contraction map, then by the contraction mapping theorem (25.1.6) has a *unique* solution and we are done. This is just a simple computation. For $y_1, y_2 \in I$ we have

$$\begin{aligned} |h(v(y_1)) - h(v(y_2))| &\leq \mu_h |v(y_1) - v(y_2)| \\ &\leq \mu_h \mu_v |y_1 - y_2|. \end{aligned}$$

Since we have assumed $0 \leq \mu_v \mu_h < 1$, $h \circ v$ is a contraction map. □

With these technical ideas and results established we can now turn to the main business of this section. We consider a map

$$f\colon D \longrightarrow \mathbb{R}^2,$$

where D is the unit square in $\mathbb{R}^2$, i.e.,

$$D = \big\{(x, y) \in \mathbb{R}^2 \,|\, 0 \leq x \leq 1,\ 0 \leq y \leq 1\big\}.$$

Let

$$S = \{1, 2, \cdots, N\}, \qquad (N \geq 2),$$

be an index set, and let

$$H_i, \qquad i = 1, \cdots, N$$

be a set of *disjoint* μ_h-horizontal strips. Finally, let

$$V_i, \qquad i = 1, \cdots, N,$$

be a set of *disjoint* μ_v-vertical strips. Suppose that f satisfies the following two conditions.

Assumption 1. $0 \leq \mu_v \mu_h < 1$ and f maps H_i *homeomorphically* onto V_i, $(f(H_i) = V_i)$ for $i = 1, \cdots, N$. Moreover, the horizontal boundaries of H_i map to the horizontal boundaries of V_i and the vertical boundaries of H_i map to the vertical boundaries of V_i.

Assumption 2. Suppose H is a μ_h-horizontal strip contained in $\bigcup_{i \in S} H_i$. Then

$$f^{-1}(H) \cap H_i \equiv \tilde{H}_i$$

is a μ_h-horizontal strip for every $i \in S$. Moreover,

$$d(\tilde{H}_i) \leq \nu_h d(H) \qquad \text{for some } \ 0 < \nu_h < 1.$$

Similarly, suppose V is a μ_v-vertical strip contained in $\bigcup_{i \in S} V_i$. Then

$$f(V) \cap V_i \equiv \tilde{V}_i$$

is a μ_v-vertical strip for every $i \in S$. Moreover,

$$d(\tilde{V}_i) \leq \nu_v d(V) \qquad \text{for some } \ 0 < \nu_v < 1.$$

Now we can state our main theorem.

Theorem 25.1.5 *Suppose f satisfies Assumptions 1 and 2. Then f has an invariant Cantor set, Λ, on which it is topologically conjugate to a full shift on N symbols, i.e., the following diagram commutes*

$$\begin{array}{ccc} \Lambda & \xrightarrow{f} & \Lambda \\ {\scriptstyle \phi}\downarrow & & \downarrow{\scriptstyle \phi} \\ \Sigma^N & \xrightarrow{\sigma} & \Sigma^N \end{array}$$

where ϕ is a homeomorphism mapping Λ onto Σ^N.

The proof has four steps.

Step 1. Construct Λ.

Step 2. Define the map $\phi \colon \Lambda \longrightarrow \Sigma^N$.

Step 3. Show that ϕ is a homeomorphism.

Step 4. Show that $\phi \circ f = \sigma \circ \phi$.

Proof: Step 1: Construction of the Invariant Set. The construction of the invariant set of the map is very similar to the construction of the invariant set for the Smale horseshoe in Chapter 23. We first construct a set of points that remains in $\bigcup_{i \in S} V_i$ under all backward iterates. This will turn out to be an uncountable infinity of μ_v-vertical curves. Next we construct a set of points that remains in $\bigcup_{i \in S} H_i$ under all forward iterates. This will turn out to be an uncountable infinity of μ_h-horizontal curves. Then the intersection of these two sets is clearly an invariant set contained in $(\bigcup_{i \in S} H_i) \cap (\bigcup_{i \in S} V_i) \subset D$.

The reader may wonder why our terminology here is different than that used in the discussion of the construction of *the* invariant set for the Smale horseshoe. In that case *the* invariant set, Λ, was given by

$$\Lambda = \bigcap_{n=-\infty}^{\infty} f^n(D).$$

However, for the Smale horseshoe we knew how the map acted on all of D. Namely, the part of D not contained in $H_0 \cup H_1$ was "thrown out" of D under the action of f. We have not assumed such behavior in the situation presently under consideration. We know only how the map f acts on $\bigcup_{i \in S} H_i$ and how f^{-1} acts on $\bigcup_{i \in S} V_i$. We will comment more on this following the proof of the theorem.

We begin by inductively constructing the set of points in $\bigcup_{i \in S} V_i$ that remain in $\bigcup_{i \in S} V_i$ under all backwards iterations by f. We denote this set by $\Lambda_{-\infty}$ and Λ_{-n}, $n = 1, 2, \cdots$ denoting the set of points in $\bigcup_{i \in S} V_i$ that remain in $\bigcup_{i \in S} V_i$ under $n-1$ backwards iterations by f.

In the following arguments we will repeatedly use the following set theoretic identities

$$\left(\bigcup_{i \in \mathcal{I}} A_i \right) \cap \left(\bigcup_{j \in \mathcal{J}} B_i \right) = \bigcup_{i \in \mathcal{I}, j \in \mathcal{J}} (A_i \cap B_j)$$

where $\mathcal{I}$ and $\mathcal{J}$ are index sets for the sets A_i and B_j, respectively. Also, for a function $f : A \to B$, with subsets A_1, $A_2 \subset A$ and B_1, $B_2 \subset B$, we have

$$
\begin{aligned}
f(A_1 \cup A_2) &= f(A_1) \cup f(A_2),\\
f^{-1}(B_1 \cup B_2) &= f^{-1}(B_1) \cup f^{-1}(B_2),\\
f(A_1 \cap A_2) &= f(A_1) \cap f(A_2), \quad \text{requires f to be 1-1,}\\
f^{-1}(B_1 \cap B_2) &= f^{-1}(B_1) \cap f^{-1}(B_2).
\end{aligned}
$$

The reader can find proofs in virtually any set theory or topology textbook.

$\underline{\Lambda_{-1}}$. Λ_{-1} is obvious.

$$\Lambda_{-1} = \bigcup_{s_{-1}\in S} V_{s_{-1}}. \tag{25.1.7}$$

$\underline{\Lambda_{-2}}$. It should be clear that

$$\Lambda_{-2} = f(\Lambda_{-1}) \cap \left(\bigcup_{s_{-1}\in S} V_{s_{-1}} \right) \tag{25.1.8}$$

is the set of points in $\bigcup_{s_{-1}\in S} V_{s_{-1}}$ that are mapped into Λ_{-1} under f^{-1}. Then, using (25.1.7), (25.1.8) becomes

$$
\begin{aligned}
\Lambda_{-2} &= \left(\bigcup_{s_{-2}\in S} f(V_{s_{-2}}) \right) \cap \left(\bigcup_{s_{-1}\in S} V_{s_{-1}} \right)\\
&= \bigcup_{\substack{s_{-i}\in S\\ i=1,2}} f(V_{s_{-2}}) \cap V_{s_{-1}} \equiv \bigcup_{\substack{s_{-i}\in S\\ i=1,2}} V_{s_{-1}s_{-2}}.
\end{aligned} \tag{25.1.9}
$$

We note the following.

i) $V_{s_{-1}s_{-2}} = \left\{ p \in D \,|\, p \in V_{s_{-1}}, f^{-1}(p) \in V_{s_{-2}} \right\}$ with $V_{s_{-1}s_{-2}} \subset V_{s_{-1}}$.

ii) It follows from Assumptions 1 and 2 that $V_{s_{-1}s_{-2}}$, $s_{-i} \in S$, $i = 1, 2$, is N^2 μ_v-vertical strips with N of them in each of the V_i, $i \in S$. Note that there are N^2 sequences of length two that are made up of elements of S and that the $V_{s_{-1}s_{-2}}$ can be put in one-to-one correspondence with these sequences.

iii) It follows from Assumption 2 that

$$d(V_{s_{-1}s_{-2}}) \le \nu_v d(V_{s_{-1}}) \le \nu_v. \tag{25.1.10}$$

$\underline{\Lambda_{-3}}$. We construct Λ_{-3} from Λ_{-2} as follows

$$\Lambda_{-3} = f(\Lambda_{-2}) \cap \left(\bigcup_{s_{-1} \in S} V_{s_{-1}} \right). \tag{25.1.11}$$

Hence, (25.1.11) is the set of points in $\bigcup_{s_{-1} \in S} V_{s_{-1}}$ that are mapped into Λ_{-2} under f^{-1}. Using (25.1.9), (25.1.11) becomes

$$\begin{aligned} \Lambda_{-3} &= f \left(\bigcup_{\substack{s_{-i} \in S \\ i=2,3}} f(V_{s_{-3}}) \cap V_{s_{-2}} \right) \cap \left(\bigcup_{s_{-1} \in S} V_{s_{-1}} \right) \\ &= \bigcup_{\substack{s_{-i} \in S \\ i=1,2,3}} f^2(V_{s_{-3}}) \cap f(V_{s_{-2}}) \cap V_{s_{-1}} \\ &\equiv \bigcup_{\substack{s_{-i} \in S \\ i=1,2,3}} V_{s_{-1}s_{-2}s_{-3}}, \end{aligned} \tag{25.1.12}$$

noindent where we have the following.

i) $V_{s_{-1}s_{-2}s_{-3}} = \left\{ p \in D \,|\, p \in V_{s_{-1}}, f^{-1}(p) \in V_{s_{-2}}, f^{-2}(p) \in V_{s_{-3}} \right\}$ with $V_{s_{-1}s_{-2}s_{-3}} \subset V_{s_{-1}s_{-2}} \subset V_{s_{-1}}$.

ii) It follows from Assumptions 1 and 2 that $V_{s_{-1}s_{-2}s_{-3}}$, $s_{-i} \in S$, $i = 1, 2, 3$, is N^3 μ_v-vertical strips with N^2 of them in each of the V_i, $i \in S$. Note that there are N^3 sequences of length three made up of elements of S and that the $V_{s_{-1}s_{-2}s_{-3}}$ can be put in one-to-one correspondence with these sequences.

iii) It follows from Assumption 2 that

$$d(V_{s_{-1}s_{-2}s_{-3}}) \leq \nu_v d(V_{s_{-1}s_{-2}}) \leq \nu_v^2 d(V_{s_{-1}}) \leq \nu_v^2. \tag{25.1.13}$$

This procedure can be carried on indefinitely. At the $(k+1)^{\text{th}}$ step we have

$$\begin{aligned} \Lambda_{-k-1} &= f\left(\Lambda_{-k}\right) \cap \left(\bigcup_{s_{-1} \in S} V_{s_{-1}} \right) \\ &= f \left(\bigcup_{\substack{s_{-i} \in S \\ i=2,\cdots,k+1}} f^{k-1}(V_{s_{-k-1}}) \cap \cdots \cap f(V_{s_{-3}}) \cap V_{s_{-2}} \right) \end{aligned}$$

$$
\begin{aligned}
&\cap \left(\bigcup_{s_{-1}\in S} V_{s_{-1}} \right) \\
&= \bigcup_{\substack{s_{-i}\in S \\ i=1,\ldots,k+1}} f^k(V_{s_{-k-1}}) \cap \cdots \cap f^2(V_{s_3}) \cap f(V_{s_{-2}}) \cap V_{s_{-1}} \\
&\equiv \bigcup_{\substack{s_{-i}\in S \\ i=1,\ldots,k+1}} V_{s_{-1}\cdots s_{k+1}}, \qquad (25.1.14)
\end{aligned}
$$

where we have the following.

i) $V_{s_{-1}\ldots s_{-k-1}} = \left\{ p \in D \,|\, f^{-i+1}(p) \in V_{s_{-i}}, i = 1, 2, \ldots, k+1 \right\}$ with $V_{s_{-1}\cdots s_{-k-1}} \subset V_{s_{-1}\cdots s_{-k}} \subset \cdots \subset V_{s_{-1}s_{-2}} \subset V_{s_{-1}}$.

ii) It follows from Assumptions 1 and 2 that $V_{s_{-1}\cdots s_{-k-1}}$, $s_{-i} \in S$, $i = 1, \cdots, k+1$, is N^{k+1} μ_v-vertical strips with N^k of them in each of the V_i, $i \in S$. Note that there are N^{k+1} sequences of length $k+1$ constructed from elements of S and that these sequences can be put in one-to-one correspondence with the $V_{s_{-1}\cdots s_{-k-1}}$.

iii) From Assumption 2 it follows that

$$
\begin{aligned}
d(V_{s_{-1}\cdots s_{-k-1}}) &\le \nu_v d(V_{s_{-1}\cdots s_{-k}}) \le \nu_v^2 d(V_{s_{-1}\cdots s_{-k+1}}) \\
&\le \nu_v^3 d(V_{s_{-1}\cdots s_{-k+2}}) \le \cdots \le \nu_v^k d(V_{s_{-1}}) \\
&\le \nu_v^k. \qquad (25.1.15)
\end{aligned}
$$

It follows from Assumptions 1 and 2 that in passing to the limit as $k \to \infty$ we obtain

$$
\begin{aligned}
\Lambda_{-\infty} &\equiv \bigcup_{\substack{s_{-i}\in S \\ i=1,2,\ldots}} \cdots \cap f^k(V_{s_{-k-1}}) \cap \cdots \cap f(V_{s_{-2}}) \cap V_{s_{-1}} \\
&\equiv \bigcup_{\substack{s_{-i}\in S \\ i=1,2,\cdots}} V_{s_{-1}\cdots s_{-k}\cdots}, \qquad (25.1.16)
\end{aligned}
$$

which, from Lemma 25.1.3, consists of an infinite number of μ_v-vertical curves. This follows from the fact that given *any* infinite sequence made up of elements of S, say

$$
s_{-1}s_{-2}\cdots s_{-k}\cdots,
$$

we have (by the construction process) an element of $\Lambda_{-\infty}$ which we denote by

$$V_{s_{-1}s_{-2}\cdots s_{-k}\cdots}.$$

Now, by construction, $V_{s_{-1}\cdots s_{-k}\cdots}$ is the intersection of the following nested sequence of sets

$$V_{s_{-1}} \supset V_{s_{-1}s_{-2}} \supset \cdots \supset V_{s_{-1}s_{-2}\cdots s_{-k}} \supset \cdots,$$

where from (25.1.15) it follows that

$$d(V_{s_{-1}\cdots s_{-k}}) \to 0 \quad \text{as} \quad k \to \infty.$$

Thus, by Lemma 25.1.3,

$$V_{s_{-1}s_{-2}\cdots s_{-k}\cdots} = \bigcap_{k=1}^{\infty} V_{s_{-1}\cdots s_{-k}}$$

consists of a μ_v-vertical curve. It also follows by construction that

$$V_{s_{-1}\cdots s_{-k}\cdots} = \left\{p \in D \,|\, f^{-i+1}(p) \in V_{s_{-i}}, i = 1, 2, \cdots\right\}. \tag{25.1.17}$$

We next construct Λ_∞, the set of points in $\bigcup_{i\in S} H_i$ that remain in $\bigcup_{i\in S} H_i$ under all forward iterations by f. We denote the set of points that remain in $\bigcup_{i\in S} H_i$ under n iterations by f by Λ_n. Since the construction of Λ_∞ is very similar to the construction of $\Lambda_{-\infty}$ we will leave out many details that we explicitly noted in the construction of $\Lambda_{-\infty}$.

We have

$$\Lambda_0 = \bigcup_{s_0\in S} H_{s_0}. \tag{25.1.18}$$

$\underline{\Lambda_1}$.

$$\Lambda_1 = f^{-1}(\Lambda_0) \cap \left(\bigcup_{s_0\in S} H_{s_0}\right) \tag{25.1.19}$$

is the set of points in $\bigcup_{s_0\in S} H_{s_0}$ that map into Λ_0 under f. Therefore, using (25.1.18), (25.1.19) becomes

$$\begin{aligned}\Lambda_1 &= f^{-1}\left(\bigcup_{s_1\in S} H_{s_1}\right) \cap \left(\bigcup_{s_0\in S} H_{s_0}\right) \\ &= \bigcup_{\substack{s_i\in S \\ i=0,1}} f^{-1}(H_{s_1}) \cap H_{s_0} \equiv \bigcup_{\substack{s_i\in S \\ i=0,1}} H_{s_0 s_1},\end{aligned} \tag{25.1.20}$$

where we have the following.

i) $H_{s_0 s_1} = \{p \in D \,|\, p \in H_{s_0}, f(p) \in H_{s_1}\}$.

ii) It follows from Assumptions 1 and 2 that Λ_1 consists of N^2 μ_h-horizontal strips with N of them in each of the H_i, $i \in S$. Moreover, there are N^2 sequences of length two made up of elements of S and these can be put in one-to-one correspondence with the $H_{s_0 s_1}$.

iii) From Assumption 2 we have

$$d(H_{s_0 s_1}) \leq \nu_h d(H_{s_0}) \leq \nu_h. \tag{25.1.21}$$

Continuing the construction in this manner and repeatedly appealing to Assumptions 1 and 2 allows us to conclude that

$$\begin{aligned} \Lambda_k &= f^{-1}(\Lambda_{k-1}) \cap \left(\bigcup_{s_0 \in S} H_{s_0} \right) \\ &= \bigcup_{\substack{s_i \in S \\ i=0,\cdots,k}} f^{-k}(H_{s_k}) \cap \cdots \cap f^{-1}(H_{s_1}) \cap H_{s_0} \\ &\equiv \bigcup_{\substack{s_i \in S \\ i=0,\cdots,k}} H_{s_0 \cdots s_k} \end{aligned} \tag{25.1.22}$$

consists of N^{k+1} μ_h-horizontal strips with N^k of them in each of the H_i, $i \in S$. Moreover,

$$d(H_{s_0 \cdots s_k}) \leq \nu_h^{k+1}.$$

It should also be clear that

$$H_{s_0 \cdots s_k} = \{p \in D \,|\, f^i(p) \in H_{s_i}, i = 0, 1, \cdots, k\}$$

and that there are N^{k+1} sequences of length $k+1$ made up of elements of S which can be put in a one-to-one correspondence with the $H_{s_0 \cdots s_k}$.

Thus, in passing to the limit as $k \to \infty$, we obtain

$$\begin{aligned} \Lambda_\infty &= \bigcup_{\substack{s_i \in S \\ i=0,1,\cdots}} \cdots \cap f^{-k}(H_{s_k}) \cap \cdots \cap f^{-1}(H_{s_1}) \cap H_{s_0} \\ &= \bigcup_{\substack{s_i \in S \\ i=0,1,\cdots}} H_{s_0 s_1 \cdots s_k \cdots} \end{aligned} \tag{25.1.23}$$

and

$$H_{s_0 s_1 \cdots s_k \cdots} = \left\{ p \in D \,|\, f^i(p) \in H_{s_i}, i = 0, 1, \cdots \right\}. \tag{25.1.24}$$

By Lemma 25.1.3, Λ_∞ consists of an infinite number of μ_h-horizontal curves. This follows from the fact that given any infinite sequence made up of elements of S, say

$$s_0 s_1 \cdots s_k \cdots ,$$

the construction process implies that there is an element of Λ_∞ which we denote by

$$H_{s_0 s_1 \cdots s_k \cdots}.$$

Now, by construction, $H_{s_0 s_1 \cdots s_k \cdots}$ is the intersection of the following nested sequence of sets

$$H_{s_0} \supset H_{s_0 s_1} \supset \cdots \supset H_{s_0 s_1 \cdots s_k} \supset \cdots ,$$

and from (25.1.23) it follows that

$$d(H_{s_0 s_1 \cdots s_k}) \to 0 \quad \text{as} \quad k \to \infty.$$

Hence, by Lemma 25.1.3, $H_{s_0 s_1 \cdots s_k \cdots}$ is a μ_h-horizontal curve.

It follows that an invariant set, i.e., a set of points that remains in D under *all* iterations by f is given by

$$\Lambda = \{\Lambda_{-\infty} \cap \Lambda_\infty\} \subset \left\{ \left(\bigcup_{i \in S} H_i \right) \cap \left(\bigcup_{i \in S} V_i \right) \right\} \subset D.$$

Moreover, by Lemma 25.1.4, since $0 \leq \mu_v \mu_h < 1$, Λ is a set of discrete points. It should be clear that Λ is uncountable, and shortly we will show that it is a Cantor set.

Step 2: The Definition of $\phi: \Lambda \to \Sigma^N$. Choose any point $p \in \Lambda$; then by construction there exist two (and only two) infinite sequences

$$\begin{array}{l} s_0 s_1 \cdots s_k \cdots , \\ s_{-1} s_{-2} \cdots s_{-k} \cdots , \end{array} \qquad s_i \in S, \quad i = 0, \pm 1, \pm 2, \cdots ,$$

such that

$$p = V_{s_{-1} s_{-2} \cdots s_{-k} \cdots} \cap H_{s_0 s_1 \cdots s_k \cdots}. \tag{25.1.25}$$

We thus associate with every point $p \in \Lambda$ a bi-infinite sequence made up of elements of S, i.e., an element of Σ^N, as follows

$$\begin{aligned} \phi\colon \Lambda &\longrightarrow \Sigma^N, \\ p &\longmapsto (\cdots s_{-k}\cdots s_{-1}.s_0 s_1 \cdots s_k \cdots) \end{aligned} \tag{25.1.26}$$

where the bi-infinite sequence associated with p, $\phi(p)$, is constructed by concatenating the infinite sequence associated with the μ_v-vertical curve and the infinite sequence associated with the μ_h-horizontal curve whose intersection gives p, as indicated in (25.1.25). Since a μ_h-horizontal curve and a μ_v-vertical curve can only intersect in one point (for $0 \le \mu_v\mu_h < 1$ by Lemma 4.3.2), the map ϕ is well defined.

Now recall from (25.1.17) that

$$V_{s_{-1}s_{-2}\cdots s_{-k}\cdots} = \{p \in D \,|\, f^{-i+1}(p) \in V_{s_{-i}}, i = 1, 2, \cdots\}, \tag{25.1.27}$$

and by assumption we have

$$f(H_{s_i}) = V_{s_i};$$

thus, (25.1.27) is the same as

$$V_{s_{-1}s_{-2}\cdots s_{-k}\cdots} = \{p \in D \,|\, f^{-i}(p) \in H_{s_{-i}}, i = 1, 2, \cdots\}. \tag{25.1.28}$$

Also, by (25.1.24) we have

$$H_{s_0 s_1 \cdots s_k \cdots} = \{p \in D \,|\, f^i(p) \in H_{s_i}, i = 0, 1, 2, \cdots\}. \tag{25.1.29}$$

Therefore, from (25.1.26), (25.1.28), and (25.1.29) we see that the bi-infinite sequence associated with any point $p \in \Lambda$ contains information concerning the behavior of the orbit of p. In particular, from $\phi(p)$ we can determine which H_i, $i \in S$ contains $f^k(p)$, i.e., $f^k(p) \in H_{s_k}$.

Alternatively, we could have arrived at the definition of ϕ in a slightly different manner. By construction, the orbit of any $p \in \Lambda$ must remain in $\bigcup_{i\in S} H_i$. Hence, we can associate with any $p \in \Lambda$ a bi-infinite sequence made up of elements of S, i.e., an element of Σ^N, as follows

$$p \longrightarrow \phi(p) = \{\cdots s_{-k}\cdots s_{-1}.s_0 s_1 \cdots s_k \cdots\}$$

by the rule that the k^{th} element of the sequence $\phi(p)$ is chosen to be the subscript of the H_i, $i \in S$, which contains $f^k(p)$, i.e., $f^k(p) \in H_{s_k}$. This gives a well-defined map of Λ into Σ^N since the H_i are disjoint.

Step 3: ϕ is a Homeomorphism.

We must show that ϕ is one-to-one, onto, and continuous. Continuity of ϕ^{-1} will follow from the fact that one-to-one, onto, and continuous maps from compact sets into Hausdorff spaces are homeomorphisms (see Dugundji [1966]). The proof is virtually the same as for the analogous situation in Theorem 23.4.1; however, continuity presents a slight twist so, for the sake of completeness, we will give all of the details.

$\boxed{\phi \text{ is One-to-One.}}$ This means that given $p, p' \in \Lambda$, if $p \neq p'$, then $\phi(p) \neq \phi(p')$.

We give a proof by contradiction. Suppose $p \neq p'$ and

$$\phi(p) = \phi(p') = \{\cdots s_{-n} \cdots s_{-1}.s_0 \cdots s_n \cdots\},$$

then, by construction of Λ, p and p' lie in the intersection of a μ_v-vertical curve $V_{s_{-1}\cdots s_{-n}\cdots}$ and a μ_h-horizontal curve $H_{s_0\cdots s_n\cdots}$. However, by Lemma 25.1.4, the intersection of a μ_h-horizontal curve and a μ_v-vertical curve consists of a unique point; therefore, $p = p'$, contradicting our original assumption. This contradiction is due to the fact that we have assumed $\phi(p) = \phi(p')$; thus, for $p \neq p'$, $\phi(p) \neq \phi(p')$.

$\boxed{\phi \text{ is Onto.}}$ This means that, given any bi-infinite sequence in Σ^N, say $\{\cdots s_{-n} \cdots s_{-1}.s_0 \cdots s_n \cdots\}$, there is a point $p \in \Lambda$ such that $\phi(p) = \{\cdots s_{-n} \cdots s_{-1}.s_0 \cdots s_n \cdots\}$.

The proof goes as follows. Choose $\{\cdots s_{-k} \cdots s_{-1}.s_0 s_1 \cdots s_k \cdots\} \in \Sigma^N$. Then, by construction of $\Lambda = \Lambda_{-\infty} \cap \Lambda_{\infty}$, we can find a μ_h-horizontal curve in Λ_{∞} denoted $H_{s_0 s_1 \cdots s_k \cdots}$ and a μ_v-vertical curve in $\Lambda_{-\infty}$ denoted $V_{s_{-1}s_{-2}\cdots s_{-k}\cdots}$. Now, by Lemma 4.3.2, $H_{s_0 s_1 \cdots s_k \cdots}$ and $V_{s_{-1}\cdots s_{-k}\cdots}$ intersect in a unique point $p \in \Lambda$ and, by definition of ϕ, the sequence associated with p, $\phi(p)$, is given by $\{\cdots s_{-k} \cdots s_{-1}.s_0 s_1 \cdots s_k \cdots\}$.

$\boxed{\phi \text{ is Continuous.}}$ This means that given any point $p \in \Lambda$ and $\varepsilon > 0$, we can find a $\delta = \delta(\varepsilon, p)$ such that

$$|p - p'| < \delta \qquad \text{implies} \quad d(\phi(p), \phi(p')) < \varepsilon,$$

where $|\cdot|$ is the usual distance measurement in R^2 and $d(\cdot, \cdot)$ is the metric on Σ^N introduced in Section 24.1.

Let $\varepsilon > 0$ be given; then, by Lemma 24.1.2, if we are to have $|\phi(p) - \phi(p')| < \varepsilon$ there must be some integer $N = N(\varepsilon)$ such that if

$$\phi(p) = \{\cdots s_{-n} \cdots s_{-1}.s_0 \cdots s_n \cdots\},$$
$$\phi(p') = \{\cdots s'_{-n} \cdots s'_{-1}.s'_0 \cdots s'_n \cdots\},$$

then $s_i = s'_i$, $i = 0, \pm 1, \cdots, \pm N$. Thus, by construction of Λ, p and p' lie in the set defined by $H_{s_0 \cdots s_N} \cap V_{s_{-1} \cdots s_{-N}}$. We denote the μ_v-vertical curves defining the boundary of $V_{s_{-1} \cdots s_{-N}}$ by the graphs of $x = v_1(y)$ and $x = v_2(y)$. Similarly, we denote the μ_h-horizontal curves defining the boundary of $H_{s_0 \cdots s_N}$ by the graphs of $y = h_1(x)$ and $y = h_2(x)$; see Figure 25.1.3. Note from (25.1.23) and (25.1.15) that we have

$$d(H_{s_0 \cdots s_N}) \leq \nu_h^N, \tag{25.1.30}$$
$$d(V_{s_{-1} \cdots s_{-N}}) \leq \nu_v^{N-1}. \tag{25.1.31}$$

Hence, from Definition 25.1.2 we have

$$\max_{y \in [0,1]} |v_1(y) - v_2(y)| \equiv \|v_1 - v_2\| \leq \nu_v^{N-1}, \tag{25.1.32}$$
$$\max_{x \in [0,1]} |h_1(x) - h_2(x)| \equiv \|h_1 - h_2\| \leq \nu_h^N. \tag{25.1.33}$$

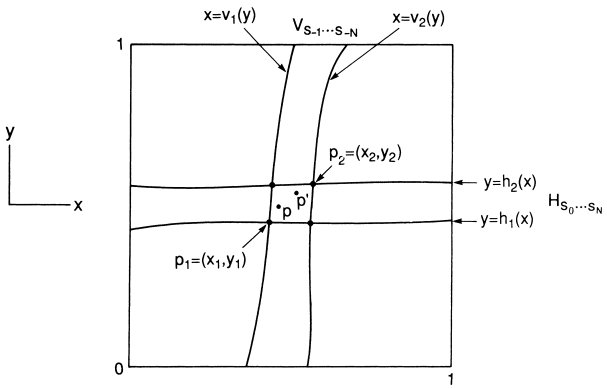

FIGURE 25.1.3.

The following lemma will prove useful in proving continuity of ϕ.

Lemma 25.1.6

$$|x_1 - x_2| \leq \frac{1}{1 - \mu_v \mu_h} \big[\|v_1 - v_2\| + \mu_v \|h_1 - h_2\|\big], \tag{25.1.34}$$
$$|y_1 - y_2| \leq \frac{1}{1 - \mu_v \mu_h} \big[\|h_1 - h_2\| + \mu_h \|v_1 - v_2\|\big]. \tag{25.1.35}$$

Proof: This follows from the following simple calculations.

$$\begin{aligned} |x_1 - x_2| &= |v_1(y_1) - v_2(y_2)| \\ &\le |v_1(y_1) - v_1(y_2)| + |v_1(y_2) - v_2(y_2)| \\ &\le \mu_v |y_1 - y_2| + \|v_1 - v_2\| \end{aligned} \tag{25.1.36}$$

and

$$\begin{aligned} |y_1 - y_2| &= |h_1(x_1) - h_2(x_2)| \\ &\le |h_1(x_1) - h_1(x_2)| + |h_1(x_2) - h_2(x_2)| \\ &\le \mu_h |x_1 - x_2| + \|h_1 - h_2\|. \end{aligned} \tag{25.1.37}$$

Substituting (25.1.37) into (25.1.36) gives (25.1.34), and substituting (25.1.36) into (25.1.37) gives (25.1.35). Note that these algebraic manipulations require $1 - \mu_v \mu_h > 0$. This proves Lemma 25.1.6. □

Now we can complete the proof that ϕ is continuous. Let p_1 denote the intersection of the graph of $h_1(x)$ with $v_1(y)$ and p_2 denote the intersection of the graph of $h_2(x)$ with $v_2(y)$. Now it follows that

$$|p - p'| \le |p_1 - p_2|. \tag{25.1.38}$$

We denote the coordinates of p_1 and p_2 by (x_1, y_1) and (x_2, y_2), respectively. Using (25.1.38), we obtain

$$|p - p'| \le |x_1 - x_2| + |y_1 - y_2|, \tag{25.1.39}$$

and using Lemma 25.1.6, we obtain

$$\begin{aligned} |x_1 - x_2| + |y_1 - y_2| \le \frac{1}{1 - \mu_v \mu_h} \big[&(1 + \mu_h) \|v_1 - v_2\| \\ &+ (1 + \mu_v) \|h_1 - h_2\| \big]. \end{aligned} \tag{25.1.40}$$

Using (25.1.39), (25.1.40), (25.1.32), and (25.1.33) we obtain

$$|p - p'| \le \frac{1}{1 - \mu_v \mu_h} \big[(1 + \mu_h) \nu_v^{N-1} + (1 + \mu_v) \nu_h^N \big].$$

Hence, if we take

$$\delta = \frac{1}{1 - \mu_v \mu_h} \big[(1 + \mu_h) \nu_v^{N-1} + (1 + \mu_v) \nu_h^N \big],$$

continuity is proved.

Step 4: $\phi \circ f = \sigma \circ \phi$. Choose any $p \in \Lambda$ and let

$$\phi(p) = \{\cdots s_{-k} \cdots s_{-1}.s_0 s_1 \cdots s_k \cdots\};$$

then

$$\sigma \circ \phi(p) = \{\cdots s_{-k} \cdots s_{-1} s_0.s_1 \cdots s_k \cdots\}. \tag{25.1.41}$$

Now, by definition of ϕ, it follows that

$$\phi \circ f(p) = \{\cdots s_{-k} \cdots s_{-1} s_0.s_1 \cdots s_k \cdots\}; \tag{25.1.42}$$

hence, from (25.1.41) and (25.1.42), we see that

$$\phi \circ f(p) = \sigma \circ \phi(p)$$

and p is arbitrary. This completes our proof of Theorem 25.1.5. □

25.2 Sector Bundles

In Chapters 26 and 27 we will see that certain orbits called homoclinic orbits give rise to the geometrical conditions that allow Assumption 1 to hold in a two-dimensional map. However, a direct verification of Assumption 2 is not easy. When one thinks of stretching and contraction rates of maps, it is natural to think of the properties of the derivative of the map at different points. We now want to derive a condition that is equivalent to Assumption 2 that is based solely on properties of the derivative of f (hence we must assume that f is at least $\mathbf{C}^1$). We begin by establishing some notation.

We define

$$f(H_i) \cap H_j \equiv V_{ji} \tag{25.2.1}$$

and

$$H_i \cap f^{-1}(H_j) \equiv H_{ij} = f^{-1}(V_{ji}) \tag{25.2.2}$$

for $i, j \in S$ where $S = \{1, \ldots, N\}$ $(N \geq 2)$ is an index set; see Figure 25.2.1. We further define

$$\mathcal{H} = \bigcup_{i,j \in S} H_{ij}$$

and

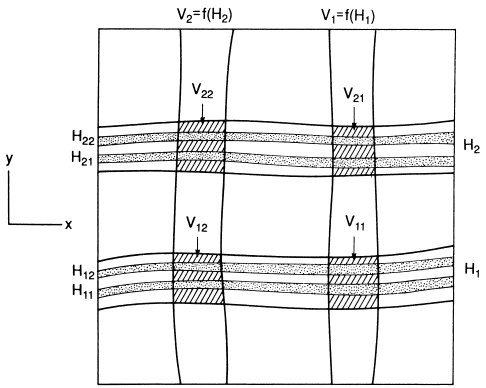

FIGURE 25.2.1. $N = 2$ for illustrative purposes.

$$\mathcal{V} = \bigcup_{i,j \in S} V_{ji}.$$

It should be clear that

$$f(\mathcal{H}) = \mathcal{V}.$$

We now want to strengthen our requirements on f by assuming that f *maps* $\mathcal{H}$ $\mathbf{C}^1$ *diffeomorphically onto* $\mathcal{V}$.

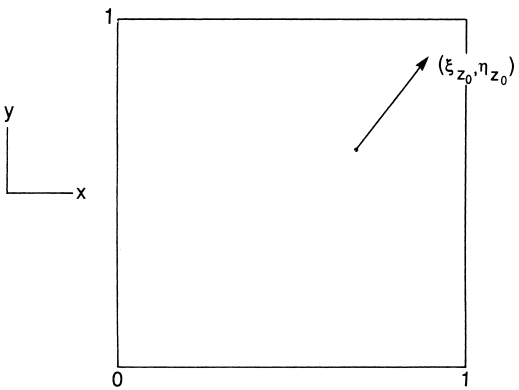

FIGURE 25.2.2.

For any point $z_0 = (x_0, y_0) \in \mathcal{H} \bigcup \mathcal{V}$, we denote a vector emanating from this point by $(\xi_{z_0}, \eta_{z_0}) \in \mathbb{R}^2$; see Figure 25.2.2. We define the *stable sector at* z_0 as follows

$$\mathcal{S}^s_{z_0} = \left\{ (\xi_{z_0}, \eta_{z_0}) \in \mathbb{R}^2 \,|\, |\eta_{z_0}| \leq \mu_h |\xi_{z_0}| \right\}. \tag{25.2.3}$$

Geometrically, $\mathcal{S}^s_{z_0}$ defines a cone of vectors emanating from z_0, where μ_h is the maximum of the absolute value of the slope of any vector in the cone and slope is measured with respect to the x-axis; see Figure 25.2.3. Similarly, the *unstable sector at* z_0 is defined as

$$\mathcal{S}^u_{z_0} = \left\{(\xi_{z_0}, \eta_{z_0}) \in \mathbb{R}^2 \,|\, |\xi_{z_0}| \leq \mu_v |\eta_{z_0}|\right\}. \tag{25.2.4}$$

Geometrically, $\mathcal{S}^u_{z_0}$ defines a cone of vectors emanating from z_0, where μ_v is the maximum of the absolute value of the slope of any vector in the cone and slope is measured with respect to the y-axis; see Figure 25.2.3. We will put restrictions on μ_v and μ_h shortly.

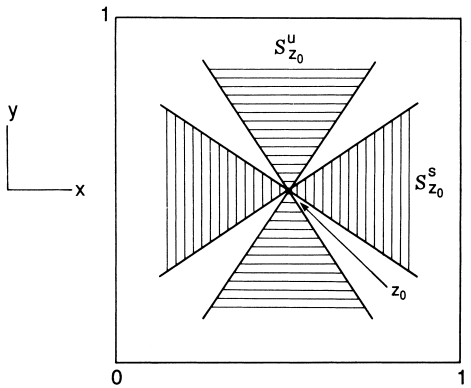

FIGURE 25.2.3.

We take the union of the stable and unstable sectors over points in $\mathcal{H}$ and $\mathcal{V}$ to form *sector bundles* as follows

$$\mathcal{S}^s_{\mathcal{H}} = \bigcup_{z_0 \in \mathcal{H}} \mathcal{S}^s_{z_0},$$
$$\mathcal{S}^s_{\mathcal{V}} = \bigcup_{z_0 \in \mathcal{V}} \mathcal{S}^s_{z_0},$$
$$\mathcal{S}^u_{\mathcal{H}} = \bigcup_{z_0 \in \mathcal{H}} \mathcal{S}^u_{z_0},$$
$$\mathcal{S}^u_{\mathcal{V}} = \bigcup_{z_0 \in \mathcal{V}} \mathcal{S}^u_{z_0}.$$

We refer to $\mathcal{S}^s_{\mathcal{H}}$ as the *stable sector bundle over* $\mathcal{H}$, $\mathcal{S}^s_{\mathcal{V}}$ as the *stable sector bundle over* $\mathcal{V}$, $\mathcal{S}^u_{\mathcal{H}}$ as the *unstable sector bundle over* $\mathcal{H}$, and $\mathcal{S}^u_{\mathcal{V}}$ as the *unstable sector bundle over* $\mathcal{V}$.

Now we can state our alternative to Assumption 2.

Assumption 3. $Df(\mathcal{S}^u_{\mathcal{H}}) \subset \mathcal{S}^u_{\mathcal{V}}$ and $Df^{-1}(\mathcal{S}^s_{\mathcal{V}}) \subset \mathcal{S}^s_{\mathcal{H}}$.

Moreover, if $(\xi_{z_0}, \eta_{z_0}) \in \mathcal{S}^u_{z_0}$ and $Df(z_0)(\xi_{z_0}, \eta_{z_0}) \equiv (\xi_{f(z_0)}, \eta_{f(z_0)}) \in \mathcal{S}^u_{f(z_0)}$, then we have

$$|\eta_{f(z_0)}| \geq \left(\frac{1}{\mu}\right) |\eta_{z_0}|.$$

Similarly, if $(\xi_{z_0}, \eta_{z_0}) \in \mathcal{S}^s_{z_0}$ and $Df^{-1}(z_0)(\xi_{z_0}, \eta_{z_0}) \equiv (\xi_{f^{-1}(z_0)}, \eta_{f^{-1}(z_0)}) \in \mathcal{S}^s_{f^{-1}(z_0)}$, then

$$|\xi_{f^{-1}(z_0)}| \geq \left(\frac{1}{\mu}\right) |\xi_{z_0}|,$$

where $0 < \mu < 1 - \mu_v \mu_h$; see Figure 25.2.4. We remark that the notation $Df(\mathcal{S}^u_{\mathcal{H}}) \subset \mathcal{S}^u_{\mathcal{V}}$ is somewhat abbreviated. More completely, it means that for every $z_0 \in \mathcal{H}$, $(\xi_{z_0}, \eta_{z_0}) \in \mathcal{S}^u_{z_0}$, we have $Df(z_0)(\xi_{z_0}, \eta_{z_0}) \equiv (\xi_{f(z_0)}, \eta_{f(z_0)}) \in \mathcal{S}^u_{f(z_0)}$; similarly for $Df^{-1}(\mathcal{S}^s_{\mathcal{V}}) \subset \mathcal{S}^s_{\mathcal{H}}$. We now state the main theorem.

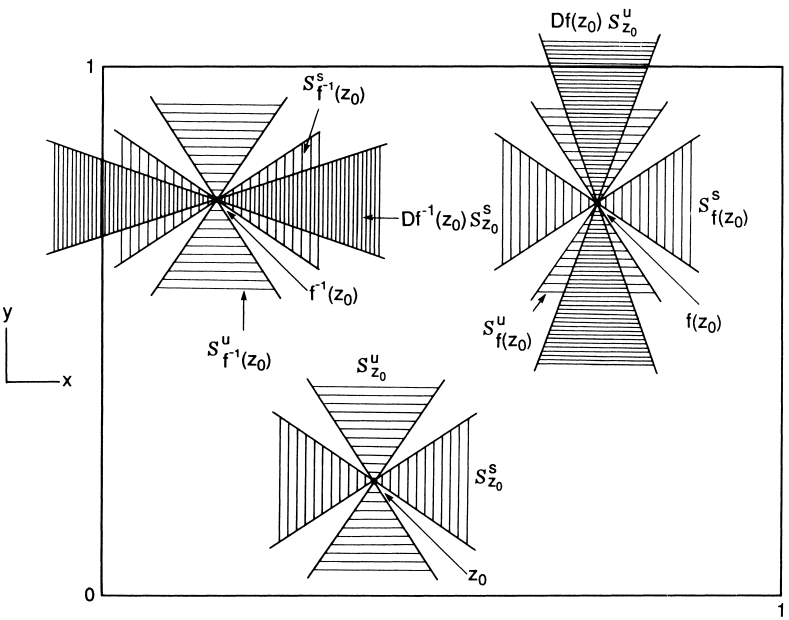

FIGURE 25.2.4.

Theorem 25.2.1 *If Assumptions 1 and 3 hold with* $0 < \mu < 1 - \mu_v \mu_h$, *then Assumption 2 holds with* $\nu_h = \nu_v = \mu/(1 - \mu_v \mu_h)$.

Proof: We will prove only the part concerning horizontal strips; the part concerning vertical strips is proven similarly. The proof consists of several steps.

Step 1. Let $\overline{H}$ be a μ_h-horizontal curve contained in $\bigcup_{j\in S} H_j$. Then show $f^{-1}(\overline{H}) \cap H_i \equiv \overline{H}_i$ is a μ_h-horizontal curve contained in H_i for all $i \in S$.

Step 2. Let H be a μ_h-horizontal strip contained in $\bigcup_{j\in S} H_j$. Then use Step 1 to show that $f^{-1}(H) \cap H_i \equiv \tilde{H}_i$ is a μ_h-horizontal strip for each $i \in S$.

Step 3. Show that $d(\tilde{H}_i) \leq (\mu/(1-\mu_v\mu_h))\ d(H)$. We begin with Step 1.

Step 1. Let $\overline{H} \subset \bigcup_{j\in S} H_j$ be a μ_h-horizontal curve. Then $\overline{H}$ intersects both vertical boundaries of each V_i $\forall\, i \in S$. Hence, $f^{-1}(\overline{H}) \cap H_i$ is a curve for each $i \in S$ by Assumption 1.

Next we argue that $f^{-1}(\overline{H}) \cap H_i$ is a μ_h-horizontal curve $\forall\, i \in S$.

This follows from Assumption 3, since Df^{-1} maps $\mathcal{S}^s_{\mathcal{V}}$ into $\mathcal{S}^s_{\mathcal{H}}$. Let (x_1, y_1), (x_2, y_2) be any two points on $f^{-1}(\overline{H}) \cap H_i$, i fixed; then by the mean value theorem

$$|y_1 - y_2| \leq \mu_h |x_1 - x_2|.$$

Thus, $f^{-1}(\overline{H}) \cap H_i$ is the graph of a μ_h-horizontal curve $y = h(x)$.

Step 2. Let $H \subset \bigcup_{j\in S} H_j$ be a μ_h-horizontal strip. Then applying Step 1 to the horizontal boundaries of H shows that $f^{-1}(H) \cap H_i$ is a μ_h-horizontal strip for every $i \in S$.

Step 3. Fix i and choose points p_0 and p_1 on the horizontal boundary of $\tilde{H}_i$ *having the same x-components* such that

$$d(\tilde{H}_i) = |p_0 - p_1|. \tag{25.2.5}$$

Consider the vertical line connecting p_0 and p_1 defined as follows

$$p(t) = tp_1 + (1-t)p_0, \qquad 0 \leq t \leq 1;$$

see Figure 25.2.5. Then it should be obvious that

$$\dot{p}(t) = p_1 - p_0 \in \mathcal{S}^u_{\mathcal{H}} \qquad \forall\, 0 \leq t \leq 1.$$

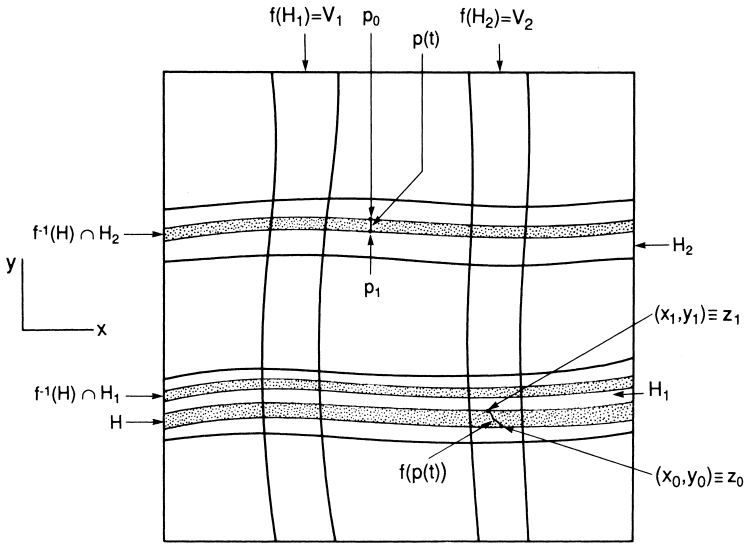

FIGURE 25.2.5.

Next we consider the image of $p(t)$ under f, which we denote by

$$f(p(t)) \equiv z(t) = (x(t), y(t)), \qquad 0 \le t \le 1.$$

It should be clear the $z(t)$ is a curve connecting the two horizontal boundaries of H as shown in Figure 25.2.5. We denote the endpoints of the curve by

$$f(p(0)) \equiv z_0 = (x_0, y_0)$$

and

$$f(p(1)) \equiv z_1 = (x_1, y_1).$$

Moreover, since H is μ_h-horizontal, z_0 lies on a μ_h-horizontal curve that we denote by $y = h_0(x)$ and z_1 lies on a μ_h-horizontal curve that we denote by $y = h_1(x)$. Tangent vectors to $z(t)$ are given by

$$\dot{z}(t) = Df(p(t))\dot{p}(t). \tag{25.2.6}$$

Using (25.2.6) and the fact that from Assumption 3 $Df(\mathcal{S}^u_{\mathcal{H}}) \subset \mathcal{S}^u_{\mathcal{V}}$, we conclude that $z(t)$ is a μ_v-vertical curve. Therefore, applying Lemma 25.1.6 to $z(t)$, $y = h_0(x)$, and $y = h_1(x)$ we obtain

$$|y_0 - y_1| \le \frac{1}{1 - \mu_v\mu_h}\|h_0 - h_1\| = \frac{1}{1 - \mu_v\mu_h}d(H). \tag{25.2.7}$$

Also by Assumption 3 we have

$$|\dot{y}(t)| \geq \frac{1}{\mu}|\dot{p}(t)| = \frac{1}{\mu}|p_1 - p_0|. \tag{25.2.8}$$

Integrating (25.2.8) gives

$$|p_1 - p_0| \leq \mu \int_0^1 |\dot{y}(t)|dt \leq \mu|y_1 - y_0|. \tag{25.2.9}$$

Finally, (25.2.7) and (25.2.9) along with (25.2.5) give

$$d(\tilde{H}_i) \leq \frac{\mu}{1 - \mu_v\mu_h} d(H). \qquad \square$$

25.3 Exercises

1. Prove Eq. (25.1.38).

2. This problem was first studied in detail by Philip Holmes (see Guckenheimer and Holmes [1983] for additional references). We consider the mechanical system consisting of a small ball bouncing vertically on a massive vibrating table, where each impact is governed by the relationship

$$V(t_j) - W(t_j) = -\alpha\,(U(t_j) - W(t_j))$$

where U, V, and W are, respectively, the absolute velocities of the approaching ball, the departing ball, and the table, $0 < \alpha \leq 1$ is the coefficient of restitution, and $t = t_j$ is the time of the j^{th} impact. We assume that the distance the ball travels between impacts under the influence of gravity , g, is large compared with the overall displacement of the table, then the time interval between impacts is approximated by

$$t_{j+1} - t_j = \frac{2V(t_j)}{g}$$

and the velocity of approach at the $(j+1)^{\text{st}}$ impact is

$$U(t_{j+1}) = -V(t_j).$$

Combining these relationships, we obtain a recurrence relationship relating the state of the system at the $(j+1)^{\text{st}}$ impact to that at the j^{th} of the following form:

$$\begin{aligned} t_{j+1} &= t_j + \frac{2V_j}{g}, \\ V_{j+1} &= \alpha V_j + (1+\alpha)W(t_j + \frac{2V_j}{g}), \end{aligned}$$

where we use the notation $V(t_j) \equiv V_j$, etc.

Assuming that the table motion is sinusoidal of the form $-\beta \sin \omega t$, and nondimensionalizing, the map, which we henceforth refer to as f, takes the form

$$f : \begin{cases} \phi_{j+1} = \phi_j + v_j \\ v_{j+1} = \alpha v_j - \gamma \cos(\phi_j + v_j) \end{cases} \tag{25.3.1}$$

where $\phi = \omega t$, $v = \frac{2\omega V}{g}$, and $\gamma = 2\omega^2(1+\alpha)\beta/g$.

(a) Verify that the inverse of the map is given by

$$f^{-1} : \begin{cases} \phi_{j-1} = \phi_j - \frac{1}{\alpha}(\gamma \cos \phi_j + v_j) \\ v_{j-1} = \frac{1}{\alpha}(\gamma \cos \phi_j + v_j) \end{cases} \tag{25.3.2}$$

(b) Verify that the map is area preserving for $\alpha = 1$ and contracts areas uniformly for $\alpha < 1$.

(c) Prove the following lemma, which establishes assumption 1 of the Conley-Moser conditions.

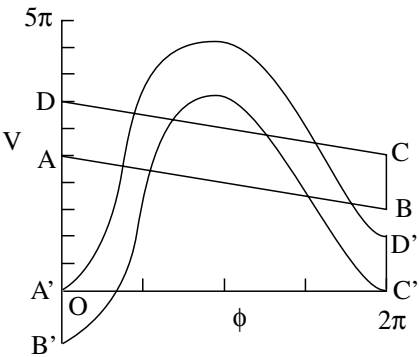

FIGURE 25.3.1.

Lemma 25.3.1 *For $\alpha = 1$ and $\gamma \geq 4\pi$ one can find horizontal and vertical strips H_i, V_i such that $f(H_i) = V_i$, $i = 1, 2$. Moreover horizontal boundaries of H_i map to horizontal boundaries of V_i and vertical boundaries of H_i map to vertical boundaries of V_i, $i = 1, 2$.*

Hint: In Fig. 25.3.1 consider the parallelogram $ABCD$ bounded by the lines

$$\begin{aligned} \phi + v &= 0 \quad (AB) \\ \phi + v &= 2\pi \quad (CD) \\ \phi &= 0 \quad (AD) \\ \phi &= 2\pi \quad (BC) \end{aligned}$$

The parallelogram is foliated by the lines $\phi + v = k$, $k \in [0, 2\pi]$. Show that the image of such lines under f are the vertical lines $\phi = k$, $v \in [k - 2\pi - \gamma \cos k, k - \gamma \cos k]$. The images of the boundaries $\phi = 0$ and $\phi = 2\pi$ are the curves $v = \phi - \gamma \cos \phi$, $v = \phi - 2\pi - \gamma \cos \phi$.

(d) Prove the following lemma, which establishes assumption 3 of the Conley-Moser conditions.

Lemma 25.3.2 *For γ sufficiently large (5π is sufficient), there are sector bundles $S^u(p)$, $S^s(p)$ based at points $p \in \bigcup_{i,j=1,2}(H_i \cap V_j)$ centered on the lines $\phi =$ constant and $\phi + v =$ constant, respectively, and each of angular extent $\frac{\pi}{4}$, such that $Df(S^u(p)) \subset S^u(p)$ and $Df^{-1}(S^s(p)) \subset S^s(p)$. Moreover, $Df(p)$ expands vertical distances by a factor of at least 5.5 and Df^{-1} expands horizontal distances by a factor of at least 4.5.*

Hint: let

$$Df = \begin{pmatrix} 1 & 1 \\ r & 1+r \end{pmatrix}, \qquad Df^{-1} = \begin{pmatrix} 1+r & -1 \\ -r & 1 \end{pmatrix}$$

where $r = \gamma \sin(\phi + v)$ or $\gamma \sin \phi$, and see Fig. 25.3.2.

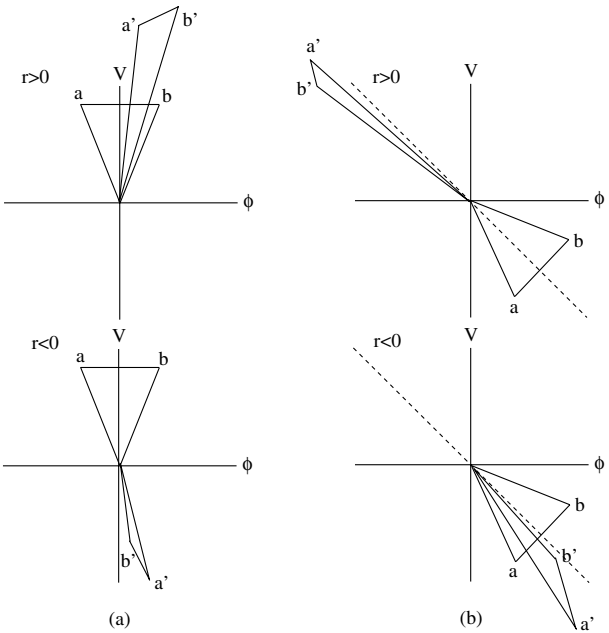

FIGURE 25.3.2. a) Behavior of unstable sectors under Df. b) Behavior of stable sectors under Df^{-1}.

(e) Use the previously proved results to establish the following theorem.

Theorem 25.3.3 *For $\gamma \geq 5\pi$ and $\alpha = 1$ the map possesses an invariant, hyperbolic Cantor set Λ on which $f|_\Lambda$ is topologically conjugate to the shift on two symbols.*

(f) Give a physical description of the dynamics in the invariant Cantor set for this problem.

3. This problem is concerned with the Hénon map,

$$H : \begin{cases} x_{n+1} = a - by_n - x_n^2, \\ y_{n+1} = x_n. \end{cases} , \tag{25.3.3}$$

which is studied in detail in Devaney and Nitecki [1979].

(a) Let R be the larger root of $\rho^2 - (|b|+1)\rho - a = 0$. Let S be the square centered at the origin with vertices $(\pm R, \pm R)$. Show that for

$$a > \frac{(5+2\sqrt{5})(1+|b|)^2}{4} \tag{25.3.4}$$

the condition

$$|x| \geq \lambda \frac{1+|b|}{2}$$

divides S into two vertical strips, V_1 and V_2, and the condition

$$|y| \geq \lambda \frac{1+|b|}{2}$$

divides S into two horizontal strips, H_1 and H_2, which obey assumption 1 of the Conley-Moser conditions.

(b) Consider the sectors

$$\begin{aligned} \mathcal{S}^u_{z_0} &= \{(\xi_{z_0}, \eta_{z_0}) \,|\, |\xi_{z_0}| \geq \lambda |\eta_{z_0}|\}\,, \\ \mathcal{S}^s_{z_0} &= \{(\xi_{z_0}, \eta_{z_0}) \,|\, |\eta_{z_0}| \geq \lambda |\xi_{z_0}|\}\,. \end{aligned}$$

Prove that if (25.3.4) holds then we can choose $\lambda > 2$ so that in V_1 and V_2 $\mathcal{S}^u$ is invariant under $DH(x,y)$ and in the H_1 and H_2 $\mathcal{S}^s$ is invariant under $DH^{-1}(x,y)$. Thus, conclude that assumption 3 of the Conley-Moser Conditions hold.

(c) Prove that the Hénon map has a hyperbolic invariant Cantor set on which it is topologically conjugate to the shift on two symbols.

4. *Horseshoes are Structurally Stable.* Suppose that a map $f: D \to \mathbb{R}^2$ satisfies the hypothesis of Theorem 25.2.1. Then it possesses an invariant Cantor set Λ. Show that, for ε sufficiently small, the map $f + \varepsilon g$ (with g $\mathbf{C}^r$, $r \geq 1$, on D) also possesses an invariant Cantor set Λ_ε. Moreover, show that Λ_ε can be constructed so that $(f+\varepsilon g)\Big|_{\Lambda_\varepsilon}$ is topologically conjugate to $f\Big|_{\Lambda}$.

26

Dynamics Near Homoclinic Points of Two-Dimensional Maps

In Chapter 25 we gave sufficient conditions for a two-dimensional map to possess an invariant Cantor set on which it is topologically conjugate to a full shift on N symbols. In this section we want to show that the existence of certain orbits of a two-dimensional map, specifically, transverse homoclinic orbits to a hyperbolic fixed point, imply that in a sufficiently small neighborhood of a point on the homoclinic orbit, the conditions given in Chapter 25 hold. There are two very similar theorems which deal with this situation; Moser's theorem (see Moser [1973]) and the Smale–Birkhoff homoclinic theorem (see Smale [1963]). We will prove Moser's theorem and describe how the Smale–Birkhoff theorem differs.

The situation that we are considering is as follows: let

$$f: \mathbb{R}^2 \longrightarrow \mathbb{R}^2$$

be a $\mathbf{C}^r$ $(r \geq 1)$ diffeomorphism satisfying the following hypotheses.

Hypothesis 1. f has a hyperbolic periodic point, p.

Hypothesis 2. $W^s(p)$ and $W^u(p)$ intersect transversely.

Without loss of generality we can assume that the hyperbolic periodic point, p, is a fixed point, for if p has period k, then $f^k(p) = p$ and the following arguments can be applied to f^k. A point that is in $W^s(p) \cap W^u(p)$ is said to be *homoclinic to* p. If $W^s(p)$ intersects $W^u(p)$ transversely in a point, then the point is called a *transverse homoclinic point.* Our goal is to show that in a neighborhood of a transverse homoclinic point there exists an invariant Cantor set on which the dynamics are topologically conjugate to a full shift on N symbols. Before formulating this as a theorem, a few preliminary steps need to be taken.

Step 1: Local Coordinates for f. Without loss of generality we can assume that the hyperbolic fixed point, p, is located at the origin (cf. Section 3). Let U be a neighborhood of the origin. Then, in U, f can be written in the form

$$\begin{aligned} \xi &\longmapsto \lambda\xi + g_1(\xi,\eta), \\ \eta &\longmapsto \mu\eta + g_2(\xi,\eta), \end{aligned} \qquad (\xi,\eta) \in U \subset \mathbb{R}^2, \tag{26.0.1}$$

where $0 < |\lambda| < 1$, $|\mu| > 1$, and g_1, g_2 are $\mathcal{O}(2)$ in ξ and η. Hence, $\eta = 0$ and $\xi = 0$ are the stable and unstable manifolds, respectively, of the *linearized* map. However, in the proof of the theorem we will find it more convenient to use the local stable and unstable manifolds of the origin as coordinates. This can be done by utilizing a simple (nonlinear) change of coordinates.

We know from Theorem 3.2.1 that the local stable and unstable manifolds of the hyperbolic fixed point can be represented as the graphs of $\mathbf{C}^r$ functions, i.e.,

$$\begin{aligned} W^s_{\text{loc}}(0) &= \text{graph } h^s(\xi), \\ W^u_{\text{loc}}(0) &= \text{graph } h^u(\eta), \end{aligned} \tag{26.0.2}$$

where $h^s(0) = h^u(0) = Dh^s(0) = Dh^u(0) = 0$. If we define the coordinate transformation

$$(x,y) = (\xi - h^u(\eta), \eta - h^s(\xi)), \tag{26.0.3}$$

then (26.0.1) takes the form

$$\begin{aligned} x &\longmapsto \lambda x + f_1(x,y), \\ y &\longmapsto \mu y + f_2(x,y), \end{aligned} \tag{26.0.4}$$

with

$$\begin{aligned} f_1(0,y) &= 0, \\ f_2(x,0) &= 0. \end{aligned} \tag{26.0.5}$$

Equation (26.0.5) implies that $y = 0$ and $x = 0$ are the stable and unstable manifolds, respectively, of the origin. We emphasize that the transformation (26.0.3) is only locally valid; therefore (26.0.4) has meaning only in a "sufficiently small" neighborhood of the origin. Despite the bad notation, we refer to this neighborhood, as above, by U.

Step 2: Global Consequences of a Homoclinic Orbit. By assumption, $W^s(0)$ and $W^u(0)$ intersect at, say, q. Then, since $q \in W^s(0) \cap W^u(0)$,

$$\begin{aligned} \lim_{n\to\infty} f^n(q) &= 0, \\ \lim_{n\to-\infty} f^n(q) &= 0. \end{aligned} \tag{26.0.6}$$

Therefore, we can find positive integers k_0 and k_1 such that

$$\begin{aligned} &f^{k_0}(q) \equiv q_0 \in U, \\ &f^{-k_1}(q) = q_1 \in U. \end{aligned} \tag{26.0.7}$$

In the coordinates in U we denote

$$\begin{aligned} q_0 &= (x_0, 0), \\ q_1 &= (0, y_1). \end{aligned}$$

It follows from (26.0.7) that

$$f^k(q_1) = q_0,$$

where $k = k_0 + k_1$; see Figure 26.0.1.

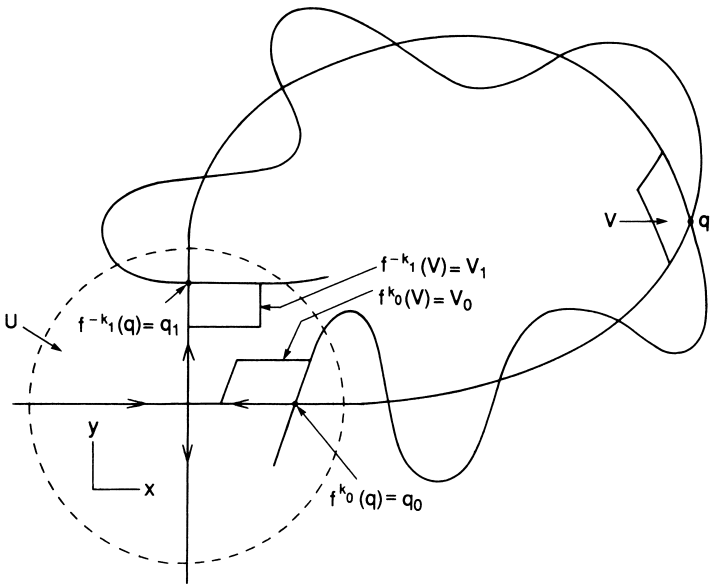

FIGURE 26.0.1.

Next we choose a region V as shown in Figure 26.0.1 with one side along $W^s(0)$ emanating from q, one side along $W^u(0)$ emanating from q, and the remaining two sides parallel to the tangent vectors of $W^s(0)$ and $W^u(0)$ at q. Now V can be chosen to lie on the appropriate sides of $W^s(0)$ and $W^u(0)$ and taken sufficiently small so that

$$f^{-k_1}(V) \equiv V_1 \subset U$$

and

$$f^{k_0}(V) \equiv V_0 \subset U \tag{26.0.8}$$

appear as in Figure 26.0.1. From (26.0.8) it follows that we have

$$f^{k}(V_1) = V_0. \tag{26.0.9}$$

Let us make an important comment concerning Figure 26.0.1. The important aspect is that we can choose V and (large) positive integers k_0 and k_1 such that $f^{k_0}(V)$ and $f^{-k_1}(V)$ are *both in the first quadrant, and disjoint.* This can always be done and is left as one of the exercises at the end of this section. (Note: Certainly k depends on the size of U as U shrinks to a point $k \to \infty$.) We remark that in Figure 26.0.1 we depict $W^s(0)$ and $W^u(0)$ as winding amongst each other. We will discuss the geometrical aspects of this more fully later on; for the proof of this theorem a detailed knowledge of the geometry of the "homoclinic tangle" is not so important. However, the one aspect of the intersection of $W^s(0)$ and $W^u(0)$ *at* q that will be of importance is the assumption that the intersection is *transversal at* q. Since f is a diffeomorphism, this implies that $W^s(0)$ and $W^u(0)$ also intersect transversely at $f^{k_0}(q) = q_0$ and $f^{-k_1}(q) = q_1$ (or, more generally, at $f^k(q)$ for any integer k).

The next step involves gaining an understanding of the dynamics near the hyperbolic fixed point.

Step 3: Dynamics Near the Origin. We first state a well-known lemma that describes some geometric aspects of the dynamics of a curve as it passes near the hyperbolic fixed point under iteration by f.

Let $\bar{q} \in W^s(0) - \{0\}$, and let C be a curve intersecting $W^s(0)$ transversely at $\bar{q}$. Let C^N denote the connected component of $f^N(C) \cap U$ to which $f^N(\bar{q})$ belongs; see Figure 26.0.2. Then we have the following lemma.

Lemma 26.0.4 (The lambda lemma) *Given $\varepsilon > 0$ and U sufficiently small there exists a positive integer N_0 such that for $N \geq N_0$ C^N is $\mathbf{C}^1$ ε-close to $W^u(0) \cap U$.*

Proof: Proofs can be found in Palis and de Melo [1982] or Newhouse [1980]. Here we give a proof for two-dimensional diffeomorphisms.

Without loss of generality we can assume $\bar{q} \in U$. Moreover, we will take U of the form

$$U \equiv I_x \times I_y,$$

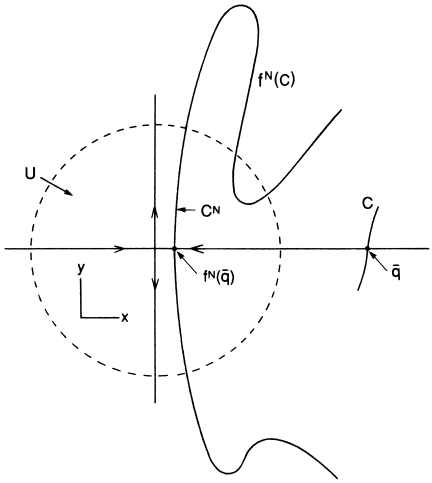

FIGURE 26.0.2.

where I_x is an interval on the x axis containing the origin and I_y is an interval on the y axis containing the origin. We denote the partial derivatives of f_1 and f_2 by f_{1x}, f_{1y}, f_{2x}, f_{2y}. Since they are zero at the origin, for U sufficiently small we can find a constant k such that

$$1 > k \geq \sup_U \left\{ |\frac{1}{\lambda} f_{1x}|, |f_{1y}|, |f_{2x}|, |f_{2y}| \right\}, \tag{26.0.10}$$

and

$$\frac{|\lambda|}{|\mu|}\frac{1+k}{1-k} < \frac{|\lambda|}{|\mu|}\frac{1+k}{1-5k} < 1, \tag{26.0.11}$$

$$1 < |\mu| - 2k, \tag{26.0.12}$$

$$\frac{k}{|\mu| - k}\left(\frac{1}{1 - \frac{|\lambda|}{|\mu|}\frac{1+k}{1-k}}\right) < 2. \tag{26.0.13}$$

Let $v_0 = (v_0^x, v_0^y)$ denote a unit vector tangent to C at $\bar{q}$. Since we are assuming that C intersects the x axis transversely at $\bar{q}$ we have $v_0^y \neq 0$. We denote the slope of v_0 by $\lambda_0 = \frac{|v_0^x|}{|v_0^y|}$, and we denote iterates of $\bar{q}$ and v_0 by

$$\begin{aligned} q_1 &= f(\bar{q}), & v_1 &= Df(\bar{q})v_0, \\ q_2 &= f(q_1), & v_2 &= Df(q_1)v_1, \\ &\vdots & &\vdots \\ q_n &= f(q_{n-1}), & v_n &= Df(q_{n-1})v_{n-1}. \end{aligned} \tag{26.0.14}$$

The steps in the proof of the lemma are as follows.

Step 1. Estimate the slopes of the iterates of v_0 under Df and show that they are bounded for all $n \geq n_0$.

Step 2. The estimates of step 1 are for a vector tangent to C at $\bar{q}$. Using continuity of tangent vectors with respect to the point of tangency, we extend the estimates of step 1 to all tangent vectors in some smaller curve, $\tilde{C}$, contained in $f^{n_0}(C)$ that passes through $f^{n_0}(\bar{q})$. We then estimate the slopes of an arbitrary vector on $\tilde{C}$ under iteration by Df.

Step 3. Once the estimates for the slopes of iterates of tangent vectors to $\tilde{C}$ are obtained we then show that $\tilde{C}$ stretches in the direction of $W^u(0) \cap U$ under iteration by f.

We begin with the first step. We estimate the evolution of the slope of v_0 under iteration by Df. We have

$$\begin{aligned} Df(\bar{q})v_0 &= \begin{pmatrix} \lambda + f_{1x}(\bar{x},0) & f_{1y}(\bar{x},0) \\ 0 & \mu + f_{2y}(\bar{x},0) \end{pmatrix} \begin{pmatrix} v_0^x \\ v_0^y \end{pmatrix}, \\ &= \begin{pmatrix} (\lambda + f_{1x}(\bar{x},0))\, v_0^x + f_{1y}(\bar{x},0) v_0^y \\ (\mu + f_{2y}(\bar{x},0))\, v_0^y \end{pmatrix} \equiv \begin{pmatrix} v_1^x \\ v_1^y \end{pmatrix}, \end{aligned} \tag{26.0.15}$$

where the zero entry in the matrix arises since $f_2(x,0) = f_{2x}(x,0) = 0$. Using (26.0.15) and (26.0.10), we obtain the following estimates

$$\begin{aligned} \lambda_1 = \frac{|v_1^x|}{|v_1^y|} &= \frac{|\lambda v_0^x + f_{1x} v_0^x + f_{1y} v_0^y|}{|\mu v_0^y + f_{2y} v_0^y|}, \\ &\leq \frac{|\lambda v_0^x + f_{1x} v_0^x|}{|\mu v_0^y + f_{2y} v_0^y|} + \frac{|f_{1y}|}{|\mu + f_{2y}|}, \\ &\leq \frac{|\lambda|}{|\mu|} \frac{|v_0^x|}{|v_0^y|} \frac{|1 + \frac{f_{1x}}{\lambda}|}{|1 + \frac{f_{2y}}{\mu}|} + \frac{|f_{1y}|}{|\mu + f_{2y}|}, \\ &\leq \frac{|\lambda|}{|\mu|} \lambda_0 \frac{1+k}{1-k} + \frac{k}{|\mu| - k}. \end{aligned} \tag{26.0.16}$$

Henceforth we will not explicitly denote the arguments of the partial derivatives $f_{1x}, f_{1y}, f_{2x}, f_{2y}$ as we will always estimate them using the uniform estimate in (26.0.10). This will always apply since they will always be evaluated on points in U.

Repeating the calculation in (26.0.15), and the estimates used in (26.0.16) gives

$$\lambda_2 = \frac{|v_2^x|}{|v_2^y|} = \frac{|\lambda v_1^x + f_{1x} v_1^x + f_{1y} v_1^y|}{|\mu v_1^y + f_{2y} v_1^y|},$$
$$\leq \frac{|\lambda|}{|\mu|}\lambda_1 \frac{1+k}{1-k} + \frac{k}{|\mu|-k}, \tag{26.0.17}$$

Repeating these same calculations and estimates, at the n^{th} step we obtain the following estimate

$$\lambda_n \leq \frac{|\lambda|}{|\mu|}\lambda_{n-1} \frac{1+k}{1-k} + \frac{k}{|\mu|-k}, \tag{26.0.18}$$

or,

$$\lambda_n \leq \left(\frac{|\lambda|}{|\mu|}\frac{1+k}{1-k}\right)^n \lambda_0 + \frac{k}{|\mu|-k}\sum_{i=0}^{n-1}\left(\frac{|\lambda|}{|\mu|}\frac{1+k}{1-k}\right)^i,$$
$$\leq \left(\frac{|\lambda|}{|\mu|}\frac{1+k}{1-k}\right)^n \lambda_0 + \frac{k}{|\mu|-k}\left(\frac{1}{1-\frac{|\lambda|}{|\mu|}\frac{1+k}{1-k}}\right). \tag{26.0.19}$$

Since, by (26.0.11), $\left(\frac{|\lambda|}{|\mu|}\frac{1+k}{1-k}\right)^n \to 0$ as $n \to \infty$ we can find an integer n_0 such that

$$\lambda_n \leq 3 \quad \text{for all} \quad n \geq n_0. \tag{26.0.20}$$

This completes step 1.

In step 2 we begin by considering a smaller neighborhood of the origin, but one that is only shrunk in the x direction. Let δ be a small positive real number and let δI_x denote I_x multiplied or "scaled" by δ. Let

$$U_1 \equiv \delta I_x \times I_y.$$

Then we can choose δ so small that

$$\sup_{U_1} |f_{1y}| \leq k_1 \tag{26.0.21}$$

where

$$k_1 \leq \frac{\epsilon}{2}(|\mu| - 5k)\left(1 - \frac{|\lambda|}{|\mu|}\frac{1+k}{1-5k}\right). \tag{26.0.22}$$

By continuity of tangent vectors, we can find a curve in $f^{n_0}(C)$, $\tilde{C}$, containing $f^{n_0}(\bar{q})$, such that the slope λ of any unit vector on this curve obeys

$$\lambda_{n_0} \leq 4, \tag{26.0.23}$$

see Fig. 26.0.3.

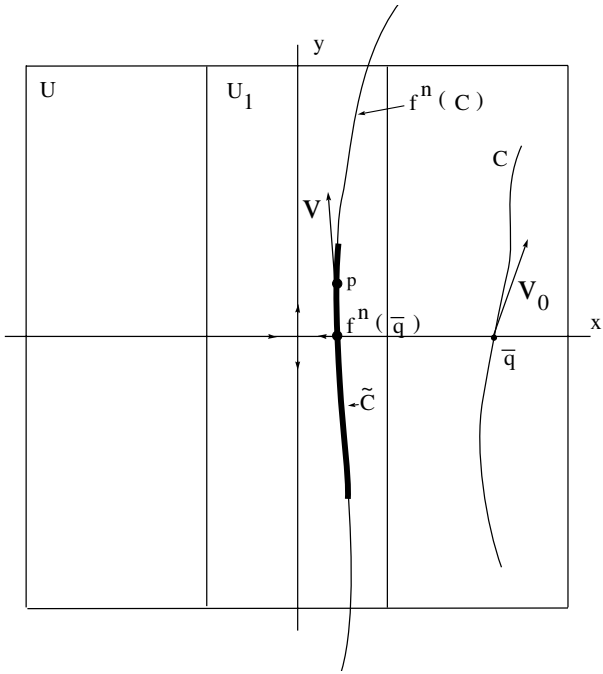

FIGURE 26.0.3.

Let p denote any point in $\tilde{C}$ and let v denote a vector tangent to $\tilde{C}$ at p. We calculate the iterates of the slope of v. As earlier, we have

$$Df(p) = \begin{pmatrix} \lambda v^x + f_{1x} v^x + f_{1y} v^y \\ f_{2x} v^x + \mu v^y + f_{2y} v^y \end{pmatrix} \equiv \begin{pmatrix} v^x_{n_0+1} \\ v^y_{n_0+1} \end{pmatrix}, \tag{26.0.24}$$

which is used to obtain the following estimates

$$\begin{aligned} \lambda_{n_0+1} &= \frac{|\lambda v^x + f_{1x} v^x + f_{1y} v^y|}{|f_{2x} v^x + \mu v^y + f_{2y} v^y|} \\ &\leq \frac{|\lambda v^x + f_{1x} v^x|}{|f_{2x} v^x + \mu v^y + f_{2y} v^y|} + \frac{|f_{1y} v^y|}{|f_{2x} v^x + \mu v^y + f_{2y} v^y|} \\ &\leq \frac{|\lambda|}{|\mu|} \frac{|v^x|}{|v^y|} \frac{|1 + \frac{f_{1x}}{\lambda}|}{|1 + \frac{f_{2y}}{\mu} + \frac{f_{2x}}{\mu} \frac{v^x}{v^y}|} + \frac{k_1}{|\mu + f_{2y} + f_{2x} \frac{v^x}{v^y}|} \\ &\leq \frac{|\lambda|}{|\mu|} \lambda_{n_0} \frac{1+k}{1-k-k\lambda_{n_0}} + \frac{k_1}{|\mu| - k - k\lambda_{n_0}} \end{aligned} \tag{26.0.25}$$

or, using (26.0.23),

$$\lambda_{n_0+1} \le \frac{|\lambda|}{|\mu|}\lambda_{n_0}\frac{1+k}{1-5k} + \frac{k_1}{|\mu|-5k}. \tag{26.0.26}$$

Iterating these calculations as above gives

$$\lambda_{n_0+n} \le \left(\frac{|\lambda|}{|\mu|}\frac{1+k}{1-5k}\right)^n \lambda_{n_0} + \frac{k_1}{\mu-5k}\left(\frac{1}{1-\frac{|\lambda|}{|\mu|}\frac{1+k}{1-5k}}\right). \tag{26.0.27}$$

Since $\left(\frac{|\lambda|}{|\mu|}\frac{1+k}{1-5k}\right)^n \to 0$ as $n \to \infty$, and λ_{n_0} is bounded by (26.0.23), we can find an integer $\bar{n}$ such that

$$\left(\frac{|\lambda|}{|\mu|}\frac{1+k}{1-5k}\right)^n \lambda_{n_0} \le \frac{\epsilon}{2}$$

for $n \ge \bar{n}$. Using this, along with (26.0.22), gives

$$\lambda_{n_0+n} \le \epsilon \tag{26.0.28}$$

for $n \ge \bar{n}$. Note that this calculation is valid for *any* tangent vector in $f^n(\tilde{C})$. We can take N_0 in the statement of the lemma to be $n_0 + \bar{n}$. This completes step 2.

In step 3 we compare the norm of a tangent vector to that of its image under Df, i.e., we estimate

$$\sqrt{\frac{|v^x_{n+1}|^2 + |v^y_{n+1}|^2}{|v^x_n|^2 + |v^y_n|^2}} = \frac{|v^y_{n+1}|}{|v^y_n|}\sqrt{\frac{\lambda^2_{n+1}+1}{\lambda^2_n+1}}. \tag{26.0.29}$$

For n sufficiently large this expression is arbitrarily close to $\frac{|v^y_{n+1}|}{|v^y_n|}$ since $\lambda_n \to 0$ as $n \to \infty$. We also have that

$$\begin{aligned}\frac{|v^y_{n+1}|}{|v^y_n|} &= \frac{|f_{2x}v^x_n + \mu v^y_n + f_{2y}v^y_n|}{|v^y_n|} \\ &= |f_{2x}\lambda_n + \mu + f_{2y}| > |\mu| - 2k > 1\end{aligned} \tag{26.0.30}$$

for n large by (26.0.12) and (26.0.28). Thus we see that the norms of the iterates of nonzero tangent vectors are growing by a ratio that approaches $|\mu| - 2k > 1$. Hence, $f^n(\tilde{C})$ is stretching in the direction of $W^u(0) \cap U$. This, together with (26.0.28), proves the lemma. □

We make several remarks regarding the lambda lemma.

Remark 1. The lambda lemma is valid in n-dimensions (Palis and de Melo [1982], Newhouse [1980]) and even ∞-dimensions (Hale and Lin [1986], Lerman and Silnikov [1989], Walther [1987]). However, the statement of the lemma requires some technical modifications. A continuous time version of the lambda lemma can be found in Deng [1989a, b].

Remark 2. The phrase $\mathbf{C}^1$ ε-close implies that tangent vectors on C^N are ε-close to tangent vectors on $W^u(0) \cap U$. By our choice of coordinates in U, all vectors tangent to $W^u(0) \cap U$ are parallel to $(0, 1)$.

Remark 3. It should be clear from step 3 of the proof that the estimates involved in proving the lambda lemma give us information on the stretching of tangent vectors. In particular, let $z_0 \in f^{-N}(C^N)$ with (ξ_{z_0}, η_{z_0}) a vector tangent to $f^{-N}(C^N)$ at z_0. It follows that $Df^N(z_0)(\xi_{z_0}, \eta_{z_0}) \equiv (\xi_{f^N(z_0)}, \eta_{f^N(z_0)})$ is a vector tangent to C^N at $f^N(z_0)$. Then

$$|\xi_{f^N(z_0)}|$$

can be made arbitrarily *small* by taking N large enough, and

$$|\eta_{f^N(z_0)}|$$

can be made arbitrarily large by taking N large enough; see Figure 26.0.4.

We now define the *transversal map,* f^T, of V_0 into V_1 as follows. Let $D(f^T)$ denote the domain of f^T and choose $p \in V_0$. We then say that $p \in D(f^T)$ if there exists an integer $n > 0$ such that

$$f^n(p) \in V_1$$

and

$$f(p), f^2(p), \cdots, f^{n-1}(p) \in U. \tag{26.0.31}$$

Next we define

$$f^T(p) = f^n(p) \in V_1, \tag{26.0.32}$$

where n is the smallest integer such that (26.0.32) holds.

Step 4: The Dynamics Outside of U. Recall from (26.0.9) that we have

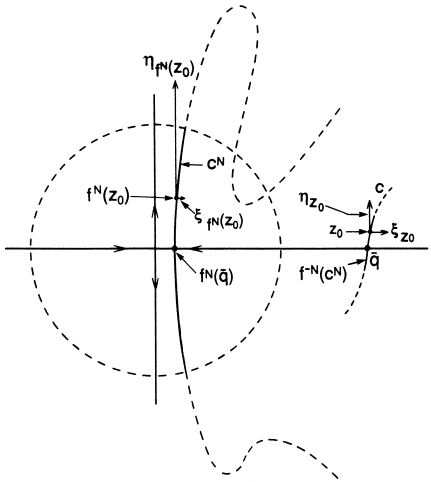

FIGURE 26.0.4.

$$f^k(V_1) = V_0.$$

Hence, since $V_1 \subset U$, f^k can be represented in the $x - y$ coordinates as follows

$$f^k(x,\overline{y}) = \begin{pmatrix} x_0 \\ 0 \end{pmatrix} + \begin{pmatrix} a & b \\ c & d \end{pmatrix} \begin{pmatrix} x \\ \overline{y} \end{pmatrix} + \begin{pmatrix} \phi_1(x,\overline{y}) \\ \phi_2(x,\overline{y}) \end{pmatrix}, \quad (x,\overline{y}) \in V_1, \tag{26.0.33}$$

where $\overline{y} = y - y_1$, $\phi_1(x,\overline{y})$ and $\phi_2(x,\overline{y})$ are $\mathcal{O}(2)$ in x and $\overline{y}$, a, b, c, d are constants, and, from (26.0.7), $q_0 \equiv (x_0, 0)$ and $q_1 \equiv (0, y_1)$.

Step 5: The Transversal Map of V_0 into V_0. Using Steps 3 and 4 we have that

$$f^k \circ f^T : D(f^T) \subset V_0 \to V_0 \tag{26.0.34}$$

is a transversal map of $D(f^T) \subset V_0$ into V_0.

Now we can finally state Moser's theorem.

Theorem 26.0.5 (Moser [1973]) *For k sufficiently large the map $f^k \circ f^T$ has an invariant Cantor set on which it is topologically conjugate to a full shift on N symbols.*

Proof: The strategy is to find μ_h-horizontal strips in V_0 that are mapped homeomorphically onto μ_v-vertical strips in V_0 with proper behavior of the

boundaries such that Assumptions 1 and 3 of Chapter 25 hold. Theorem 26.0.5 will then follow from Theorem 25.2.1. We remark that we will take as the horizontal boundaries of V_0 the two segments of the boundary of V_0 that are "parallel" to $W^s(0)$ and as the vertical boundary of V_0 the remaining two segments of the boundary of V_0. Similarly, the horizontal boundary of V_1 is taken to be the two segments of the boundary of V_1 parallel to $W^s(0)$, and the horizontal boundary of V_1 is taken to be the remaining two segments of the boundary of V_1; see Figure 26.0.5.

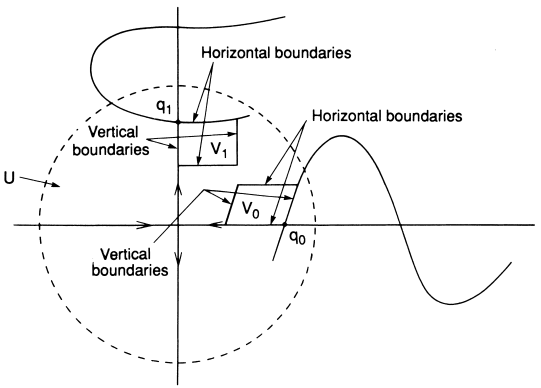

FIGURE 26.0.5.

We begin by choosing a set of μ_h-horizontal strips in V_0 such that Assumption 1 of Section 25.1 holds. First we make the observation that it follows from the lambda lemma that there exists a positive integer N_0 such that for $N \geq N_0$ both vertical boundaries of the component of $f^N(V_0) \cap U$ containing $f^N(q_0)$ intersect both horizontal boundaries of V_1 as shown in Figure 26.0.6.

Let $\tilde{V}_N \equiv f^N(V_0) \cap V_1$ denote this set. Then, for N_0 sufficiently large, it follows by applying the lambda lemma to f^{-1} that $f^{-N}(\tilde{V}_N) \equiv H_N$ is a μ_h-horizontal strip stretching across V_0 with the vertical boundaries of H_N contained in the vertical boundaries of V_0 as shown in Figure 26.0.6.

(Note: since the tangent vectors at each point on the horizontal boundaries of H_N can be made arbitrarily close to the tangent vector of $W^s(0) \cap U$, it follows that the horizontal boundaries of H_N are graphs over x.) It should be clear from the definition of f^T that $H_N \subset D(f^T)$.

Now we choose a sequence of integers, $N_0 + j_1$, $N_0 + j_2, \cdots$ with

$$\tilde{V}_i \equiv f^{N_0+j_i}(V_0) \cap V_1 \tag{26.0.35}$$

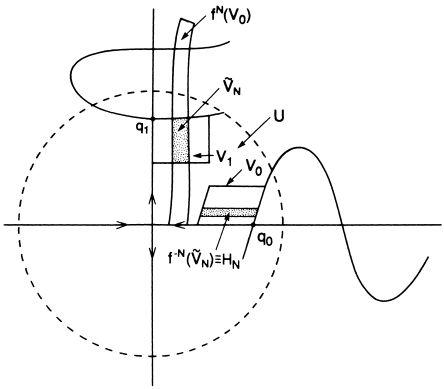

FIGURE 26.0.6.

as described above. The sequence $\{j_1, j_2, \cdots, j_n, \cdots\}$ is chosen such that the $\tilde{V}_i$ are disjoint. Then

$$f^{-N_0-j_i}(\tilde{V}_i) \equiv H_i, \qquad i = 1, 2, \cdots, \tag{26.0.36}$$

are a set of disjoint μ_h-horizontal strips contained in V_0. It follows by applying the lambda lemma to f^{-1} that, for N_0 sufficiently large, μ_h is arbitrarily close to zero. We choose a finite number of the H_i

$$\{H_1, \cdots, H_N\}.$$

Then $f^k \circ f^T(H_i) \equiv V_i$, $i = 1, \cdots, N$ appear as in Figure 26.0.7. A consideration of the manner in which the boundary of V_1 maps to the boundary of V_0 under f^k shows that horizontal (resp. vertical) boundaries of the H_i map to horizontal (resp. vertical) boundaries of the V_i under $f^k \circ f^T$.

We now need to argue that the V_i are μ_v-vertical strips with $0 \leq \mu_v \mu_h < 1$. This goes as follows. By the lambda lemma, for N_0 sufficiently large, the vertical boundaries of the V_i are arbitrarily close to $W^u(0) \cap U$. Hence, by the form of f^k given in Step 4, the vertical boundaries of $f^k(\tilde{V}_i) \equiv V_i$ are arbitrarily close to the tangent vector to $W^u(0)$ at q_0. Therefore, the vertical boundaries of the V_i can be represented as graphs over the y variables. Moreover, by the remark above, μ_h can be taken as small as we like (by taking N_0 large); it follows that we can satisfy $0 \leq \mu_h \mu_v < 1$, where μ_v is taken to be *twice the absolute value* of the slope of the tangent vector of $W^u(0)$ at q_0. (Note: the reason for taking this choice for μ_v will be apparent when we define stable sectors and verify Assumption 3.) Hence, Assumption 1 holds.

Next we need to show that Assumption 3 holds. We will show this for

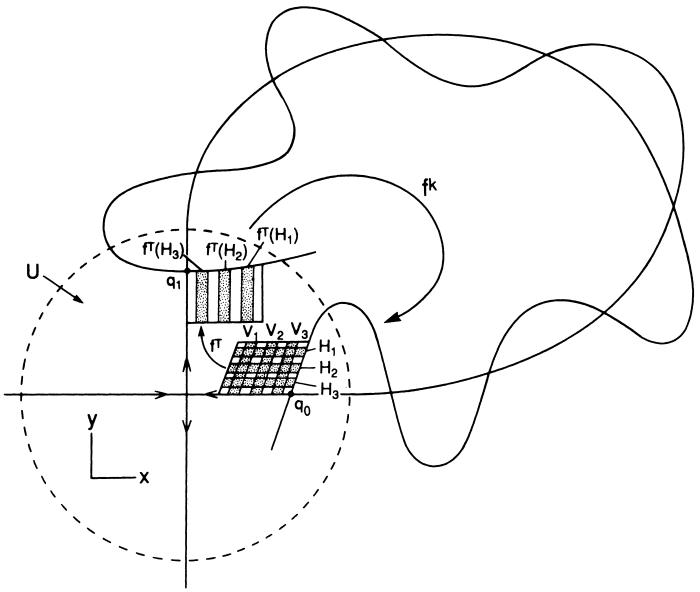

FIGURE 26.0.7.

the unstable sectors and leave it as an exercise for the reader to verify the part of Assumption 3 dealing with the stable sectors. First we must define the unstable sector bundle.

Recall from Section 25.2 that

$$f^k \circ f^T(H_i) \cap H_j \equiv V_{ji},$$

$$H_i \cap (f^k \circ f^T)^{-1}(H_j) \equiv H_{ij} = (f^k \circ f^T)^{-1}(V_{ji}), \tag{26.0.37}$$

with

$$\mathcal{H} = \bigcup_{i,j \in S} H_{ij} \quad \text{and} \quad \mathcal{V} = \bigcup_{i,j \in S} V_{ji}, \tag{26.0.38}$$

where $S = \{1, \cdots, N\}$ $(N \geq 2)$ is the index set. We choose $z_0 \equiv (x_0, y_0) \in \mathcal{H} \cup \mathcal{V}$; then the unstable sector at z_0 is denoted by

$$\mathcal{S}^u_{z_0} = \left\{(\xi_{z_0}, \eta_{z_0}) \in R^2 \,|\, |\xi_{z_0}| \leq \mu_v |\eta_{z_0}|\right\}, \tag{26.0.39}$$

and we have the sector bundles

$$\mathcal{S}^u_{\mathcal{H}} = \bigcup_{z_0 \in \mathcal{H}} \mathcal{S}^u_{z_0} \quad \text{and} \quad \mathcal{S}^u_{\mathcal{V}} = \bigcup_{z_0 \in \mathcal{V}} \mathcal{S}^u_{z_0}. \tag{26.0.40}$$

We make the important remark that by our choice of μ_v a vector parallel to the tangent vector of $W^u(0)$ at q_0 is contained in the interior of $\mathcal{S}^u_{z_0}$; see Figure 26.0.8.

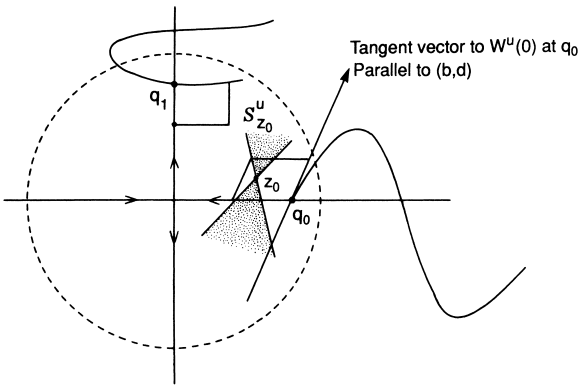

FIGURE 26.0.8.

We must show that

$$1) \qquad D(f^k \circ f^T)(\mathcal{S}^u_{\mathcal{H}}) \subset \mathcal{S}^u_{\mathcal{V}} \tag{26.0.41}$$

and

$$2) \qquad |\eta_{f^k \circ f^T(z_0)}| \geq \left(\frac{1}{\mu}\right) |\eta_{z_0}|; \tag{26.0.42}$$

where $0 < \mu < 1 - \mu_v \mu_h$.

Before showing that 1) and 2) hold we make the following observations.

Observation 1.

$$D(f^k \circ f^T) = Df^k Df^T \tag{26.0.43}$$

and, from (26.0.33),

$$Df^k = \begin{pmatrix} a & b \\ c & d \end{pmatrix} + \begin{pmatrix} \phi_{1x} & \phi_{1\overline{y}} \\ \phi_{2x} & \phi_{2\overline{y}} \end{pmatrix}. \tag{26.0.44}$$

Now, since $\phi_1(x, \overline{y})$ and $\phi_2(x, \overline{y})$ are $\mathcal{O}(2)$ in x and $\overline{y}$, by choosing U sufficiently small ϕ_{1x}, $\phi_{1\overline{y}}$, ϕ_{2x}, and $\phi_{2\overline{y}}$ can be made arbitrarily small compared to a, b, c, and d.

Observation 2: Consequences of Transversality. From Step 2, $W^s(0)$ and $W^u(0)$ intersect transversely at q_0 and q_1. We have

$$f^k(q_1) = q_0,$$

$$Df^k(q_1) = \begin{pmatrix} a & b \\ c & d \end{pmatrix}, \tag{26.0.45}$$

and

$$Df^{-k}(q_0) = (Df^k(q_1))^{-1} = \frac{1}{ad-bc}\begin{pmatrix} d & -b \\ -c & a \end{pmatrix}. \tag{26.0.46}$$

In our choice of coordinates a vector tangent to $W^u(0)$ at q_1 is parallel to $(0,1)$, and a vector tangent to $W^s(0)$ at q_0 is parallel to $(1,0)$. Hence, if $W^s(0)$ and $W^u(0)$ intersect transversely at q_0 and q_1, we must have that

$$Df^k(q_1)\begin{pmatrix} 0 \\ 1 \end{pmatrix} = \begin{pmatrix} a & b \\ c & d \end{pmatrix}\begin{pmatrix} 0 \\ 1 \end{pmatrix} = \begin{pmatrix} b \\ d \end{pmatrix}$$

is not parallel to

$$\begin{pmatrix} 1 \\ 0 \end{pmatrix},$$

and

$$\begin{aligned} Df^{-k}(q_0)\begin{pmatrix} 1 \\ 0 \end{pmatrix} &= \frac{1}{ad-bc}\begin{pmatrix} d & -b \\ -c & a \end{pmatrix}\begin{pmatrix} 1 \\ 0 \end{pmatrix} \\ &= \frac{1}{ad-bc}\begin{pmatrix} d \\ -c \end{pmatrix} \end{aligned}$$

is not parallel to

$$\begin{pmatrix} 0 \\ 1 \end{pmatrix}.$$

It is easy to see that these conditions will be satisfied provided

$$d \neq 0.$$

Note that (b, d) is a vector parallel to the tangent vector to $W^u(0)$ at q_0. We will use this later on.

Now we return to showing that Assumption 3 holds for the unstable sector bundle. We must demonstrate the following.

1. $D(f^k \circ f^T)(\mathcal{S}^u_{\mathcal{H}}) \subset \mathcal{S}^u_{\mathcal{V}}$, and
2. $|\eta_{f^k \circ f^T(z_0)}| > \frac{1}{\mu}|\eta_{z_0}|$; $0 < \mu < 1 - \mu_v \mu_h$.

$\boxed{D(f^k \circ f^T)(\mathcal{S}^u_{\mathcal{H}}) \subset \mathcal{S}^u_{\mathcal{V}}}$

We choose $z_0 \in \mathcal{H}$ and let $(\xi_{z_0}, \eta_{z_0}) \in \mathcal{S}^u_{z_0}$ and

$$Df^T(z_0)(\xi_{z_0}, \eta_{z_0}) = \big(\xi_{f^T(z_0)}, \eta_{f^T(z_0)}\big). \tag{26.0.47}$$

Then, using (26.0.43) and (26.0.44), we have

$$\begin{aligned} Df^k(f^T(z_0))Df^T(z_0)(\xi_{z_0}, \eta_{z_0}) &= \begin{pmatrix} (a+\phi_{1x})\xi_{f^T(z_0)} + (b+\phi_{1\overline{y}})\eta_{f^T(z_0)} \\ (c+\phi_{2x})\xi_{f^T(z_0)} + (d+\phi_{2\overline{y}})\eta_{f^T(z_0)} \end{pmatrix} \\ &\equiv \begin{pmatrix} \xi_{f^k \circ f^T(z_0)} \\ \eta_{f^k \circ f^T(z_0)} \end{pmatrix}, \end{aligned} \tag{26.0.48}$$

where all partial derivatives are evaluated at $z_0 = (x_0, y_0)$. We must show that

$$\begin{aligned} \frac{|\xi_{f^k \circ f^T(z_0)}|}{|\eta_{f^k \circ f^T(z_0)}|} = \frac{|(a+\phi_{1x})(\xi_{f^T(z_0)})/(\eta_{f^T(z_0)}) + (b+\phi_{1\overline{y}})|}{|(c+\phi_{2x})(\xi_{f^T(z_0)})/(\eta_{f^T(z_0)}) + (d+\phi_{2\overline{y}})|} \\ \in \ \mathcal{S}^u_{f^k \circ f^T(z_0)}. \end{aligned} \tag{26.0.49}$$

From Remark 3 following the lambda lemma, for N_0 sufficiently large,

$$\frac{|\xi_{f^T(z_0)}|}{|\eta_{f^T(z_0)}|}$$

can be made arbitrarily small. Also, from Observation 1 above, for V sufficiently small,

$$\phi_{1x}, \phi_{1\overline{y}}, \phi_{2x}, \phi_{2\overline{y}}$$

can be made arbitrarily small. Hence, using these two results we see that

$$\frac{|\xi_{f^k \circ f^T(z_0)}|}{|\eta_{f^k \circ f^T(z_0)}|}$$

can be made arbitrarily close to

$$\frac{|b|}{|d|},$$

where, as shown in Observation 2 above, (b, d) is a vector parallel to the tangent vector of $W^u(0)$ at q_0; see Figure 26.0.9. Since this holds for any $z_0 \in \mathcal{H}$, we have $D(f^k \circ f^T)(\mathcal{S}^u_{\mathcal{H}}) \subset \mathcal{S}^u_{\mathcal{V}}$.

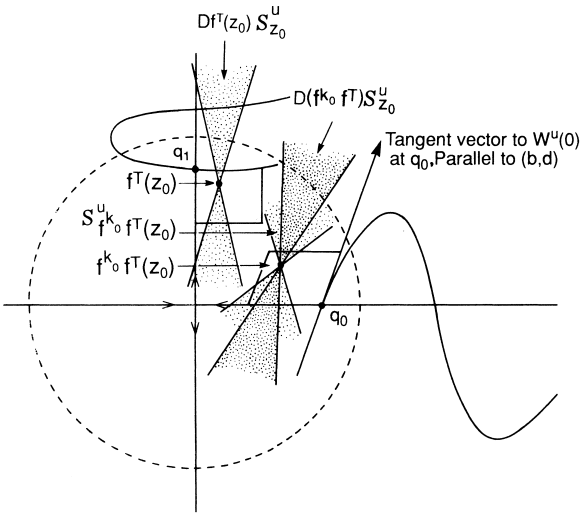

FIGURE 26.0.9.

$$\boxed{|\eta_{f^k \circ f^T(z_0)}| \geq \tfrac{1}{\mu}|\eta_{z_0}|; 0 < \mu < 1 - \mu_v \mu_h}$$

Using (26.0.48) we have

$$\frac{|\eta_{f^k \circ f^T(z_0)}|}{|\eta_{z_0}|} = \frac{|(c + \phi_{2x})\xi_{f^T(z_0)} + (d + \phi_{2\overline{y}})\eta_{f^T(z_0)}|}{|\eta_{z_0}|}. \tag{26.0.50}$$

Again, as a result of the lambda lemma, for N_0 sufficiently large, $|\eta_{f^T(z_0)}|$ can be made arbitrarily large, $|\xi_{f^T(z_0)}|$ can be made arbitrarily small, and by transversality of the intersection of $W^u(0)$ and $W^s(0)$ at q, $d \neq 0$ (with $\phi_{1\overline{y}}$ small compared to d). Thus, (26.0.50) can be made as large as we desire by choosing N_0 big enough. □

The Smale–Birkhoff Homoclinic Theorem

The Smale–Birkhoff homoclinic theorem is very similar to Moser's theorem. We will state the theorem and describe briefly how it differs. The assumptions and set-up are the same as for Moser's theorem.

Theorem 26.0.6 (Smale [1963]) *There exists an integer $n \geq 1$ such that f^n has an invariant Cantor set on which it is topologically conjugate to a full shift on N symbols.*

Proof: We will only give the barest outline in order to show the difference between the Smale–Birkhoff homoclinic theorem and Moser's theorem and leave the details as an exercise for the reader.

Choose a "rectangle," V_0, containing a homoclinic point *and* the hyperbolic fixed point as shown in Figure 26.0.10. Then, for n sufficiently large, $f^n(V_0)$ intersects V_0 a finite number of times as shown in Figure 26.0.10.

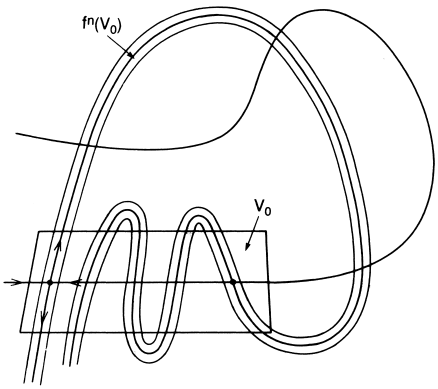

FIGURE 26.0.10.

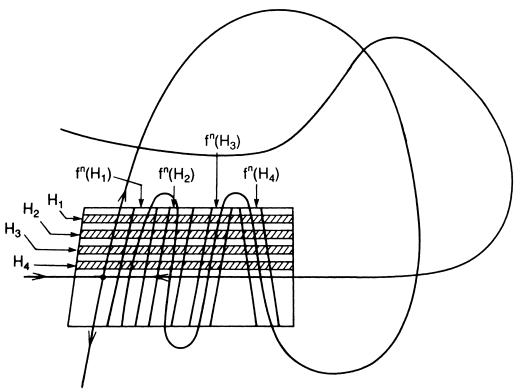

FIGURE 26.0.11. Horizontal strips $H_1, \cdots, H_4$ and their image under f^n.

Now, one can find μ_h-horizontal strips in V_0 that map over themselves in μ_v-vertical strips such that Assumptions 1 and 3 of Chapter 25 hold;

see Figure 26.0.11. The details needed to prove these statements are very similar to those needed for the proof of Moser's theorem, and it will be an instructive exercise for the reader to give a rigorous proof. □

From the outline of the proof of the Smale–Birkhoff homoclinic theorem, one can see how it differs from Moser's theorem. In both cases the invariant Cantor set is constructed near a homoclinic point sufficiently close to the hyperbolic fixed point. However, in the Smale–Birkhoff theorem, all points leave the Cantor set and return *at the same time* (i.e., after n iterates of f); in Moser's construction, points leave the Cantor set and may return *at different times* (recall the definition of f^T). What are the dynamical consequences of the two different constructions?

26.1 Heteroclinic Cycles

In this subsection we apply the lambda lemma to show that transverse heteroclinic cycles (to be defined shortly) imply the existence of transverse homoclinic orbits. Hence, Moser's theorem or the Smale-Birkhoff homoclinic theorem apply. Our proof will be for the two-dimensional case, and it follows the general n-dimensional result that can be found in Palis and de Melo [1982]. We begin with a preliminary result.

Proposition 26.1.1 *Let $f : \mathbb{R}^2 \to \mathbb{R}^2$ be a $\mathbf{C}^r$, $r \geq 1$ diffeomorphism, and suppose that p_1, p_2, and p_3 are hyperbolic fixed points. Furthermore, suppose $W^u(p_1)$ transversely intersects $W^s(p_2)$ and $W^u(p_2)$ transversely intersects $W^s(p_3)$. Then $W^u(p_1)$ transversely intersects $W^s(p_3)$.*

Proof: Let q_3 denote a point of transversal intersection of $W^u(p_2)$ and $W^s(p_3)$, and consider a curve $D_{23} \in W^u(p_2)$ containing p_2 and q_3 (see Fig. 26.1.1). First, note the following consequence of the persistence of transverse intersections.

> The fact that D_{23} transversely intersects $W^s(p_3)$ implies that there exists $\epsilon > 0$ such that if $\tilde{D}$ is a curve $\mathbf{C}^1$ close to D_{23} then $\tilde{D}$ also has a point of transverse intersection with $W^s(p_3)$.

Let q_2 denote a point of transversal intersection of $W^u(p_1)$ and $W^s(p_2)$, and consider a curve $D_{12} \in W^u(p_1)$ containing q_2(see Fig. 26.1.1). Then it follows from the lambda lemma that there exists N_0 such that $f^{N_0}(D_{12})$ contains a curve $\tilde{D}_{12}$ that is $\mathbf{C}^1$ ϵ-close to D_{23}. By the persistence of

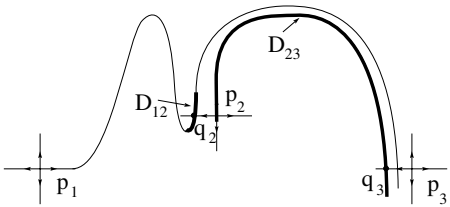

FIGURE 26.1.1.

transversal intersections, for ϵ sufficiently small there exists a point of transversal intersection of $\tilde{D}_{12}$ with $W^s(p_3)$. Since $W^u(p_1)$ is invariant $f^{N_0}(D_{12}) \subset W^u(p_1)$. Hence, $W^u(p_1)$ has a point of transverse intersection with $W^s(p_3)$. □

Next we define the notion of a heteroclinic cycle.

Definition 26.1.2 (Heteroclinic Cycle.) *Let $f : \mathbb{R}^2 \to \mathbb{R}^2$ be a $\mathbf{C}^r$, $r \geq 1$ diffeomorphism, and suppose that $p_0, p_1, \cdots, p_{n-1}, p_n \equiv p_0$ are hyperbolic fixed points such that $W^u(p_i)$ transversely intersects $W^s(p_{i+1})$, $i = 0, \cdots, n-1$. Then the fixed points, along with their stable and unstable manifolds, are said to form a* heteroclinic cycle. *See Fig. 26.1.2.*

Theorem 26.1.3 *Let $f : \mathbb{R}^2 \to \mathbb{R}^2$ be a $\mathbf{C}^r$, $r \geq 1$ diffeomorphism, and suppose that $p_0, p_1, \cdots, p_{n-1}, p_n \equiv p_0$ are hyperbolic fixed points that form a heteroclinic cycle. Then $W^u(p_i)$ transversely intersects $W^s(p_i)$, $i = 0, \cdots, n-1$.*

Proof: This is an immediate consequence of Proposition 26.1.1. □

26.2 Exercises

1. Consider the map
$$\begin{aligned} \xi &\mapsto \lambda\xi + g_1(\xi, \eta), \\ \eta &\mapsto \mu\eta + g_2(\xi, \eta), \end{aligned} \qquad (\xi, \eta) \in U \subset \mathbb{R}^2, \tag{26.2.1}$$
defined in (26.0.1). Under the transformation given in (26.0.3)

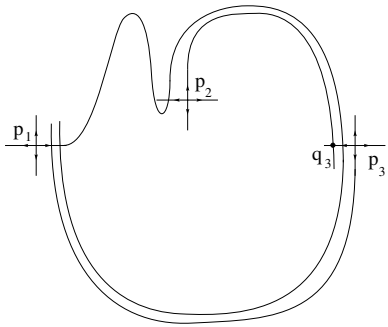

FIGURE 26.1.2. Heteroclinic cycles imply homoclinic orbits.

$$(x, y) = (\xi - h^u(\eta), \eta - h^s(\xi)),$$

with

$$W^s_{\text{loc}}(0) = \text{graph} \quad h^s(\xi),$$
$$W^u_{\text{loc}}(0) = \text{graph} \quad h^u(\eta).$$

Show that (26.2.1) takes the form

$$x \mapsto \lambda x + f_1(x, y),$$
$$y \mapsto \mu y + f_2(x, y),$$

with

$$f_1(0, y) = 0,$$
$$f_2(x, 0) = 0.$$

What are the specific forms of f_1 and f_2 in terms of g_1 and g_2?

2. Consider the region V shown in Figure 26.0.1. Show that V can be chosen so that $f^{k_0}(V)$ and $f^{-k_1}(V_1)$ appear as in Figure 26.0.1. In particular, show that for some positive integers $k_0, k_1 > 0$, both $f^{k_0}(V)$ and $f^{k_1}(V)$ lie in the first quadrant with their sides coinciding with the particular pieces of $W^s(0)$ and $W^u(0)$ as shown in Figure 26.0.1.

3. Concerning step 2 of the set-up for the proof of Theorem 26.0.5, prove that if $W^s(0)$ and $W^u(0)$ intersect transversely at a point q, then they also intersect transversely at $f^k(q)$ for any integer k.

4. This exercise is concerned with the choosing of the μ_h-horizontal strips in the proof of Theorem 26.0.5. Consider the sequence of integers, $N_0 + j_1$, $N_0 + j_2, \cdots$ with

$$\tilde{V}_i \equiv f^{N_0 + j_i}(V_0) \cap V_1. \tag{26.2.2}$$

Show that the sequence $\{j_1, j_2, \cdots, j_n, \cdots\}$ can be chosen such that the $\tilde{V}_i$ are disjoint.

5. Following the outline given after Theorem 26.0.6, prove the Smale–Birkhoff homoclinic theorem.

6. Discuss the dynamical similarities and differences between Moser's theorem (Theorem 26.0.5) and the Smale–Birkhoff homoclinic theorem (Theorem 26.0.6). In particular, how do orbits differ in the invariant sets constructed in each theorem?

7. Suppose $f\colon \mathbb{R}^2 \to \mathbb{R}^2$ is $\mathbf{C}^r$ $(r \geq 1)$, having a hyperbolic fixed point at p_0 whose stable and unstable manifolds intersect transversely as shown in Figure 26.2.1a.

   We are interested in the dynamics near p_0. Suppose that in local coordinates (x, y) near p_0 the linearization of f has the form

$$Df(p_0)\colon \begin{pmatrix} x \\ y \end{pmatrix} \mapsto \begin{pmatrix} \lambda & 0 \\ 0 & \mu \end{pmatrix} \begin{pmatrix} x \\ y \end{pmatrix}, \qquad \begin{matrix} \lambda < 1, \\ \mu > 1, \end{matrix}$$

   so that orbits near p_0 appear as in Figure 26.2.1b. However, we know that the stable and unstable manifolds near p_0 oscillate infinitely often as shown in Figure 26.2.1a.

   Are Figures 26.2.1a and 26.2.1b contradictory? If not, show how orbits in Figure 26.2.1b are manifested in Figure 26.2.1a.

8. Consider a $\mathbf{C}^r$ $(r \geq 1)$ diffeomorphism

$$f\colon \mathbb{R}^2 \to \mathbb{R}^2$$

   having hyperbolic fixed points at p_0 and p_1, respectively. Suppose $q \in W^s(p_0) \cap W^u(p_1)$; then q is called a *heteroclinic* point, and if $W^s(p_0)$ intersects $W^u(p_1)$ transversely at q, q is called a *transverse heteroclinic point.* In order to be more descriptive, sometimes q is referred to as being *heteroclinic to* p_0 *and* p_1; see Figure 26.2.2a.

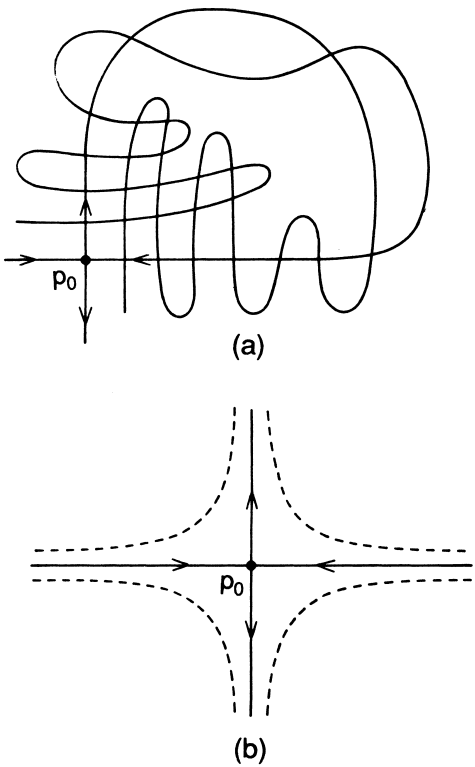

FIGURE 26.2.1.

(a) Does the existence of a transverse heteroclinic point imply the existence of a Cantor set on which some iterate of f is topologically conjugate to a full shift on N ($N \geq 2$) symbols?

(b) Additionally, suppose that $W^u(p_0)$ intersects $W^s(p_1)$ transversely to form a *heteroclinic cycle* as shown in Figure 26.2.2b. Show that in this case one can find an invariant Cantor set on which some iterate of f is topologically conjugate to a full shift on N ($N \geq 2$) symbols. (*Hint:* mimic the proof of Theorem 26.0.5.)

(c) Suppose that a branch of $W^u(p_0)$ coincides with a branch of $W^s(p_0)$, yet $W^s(p_0)$ intersects $W^u(p_1)$ transversely at q; see Figure 26.2.2c. Does it follow that you can find an invariant Cantor set on which some iterate of f is topologically conjugate to a full shift on N ($N \geq 2$) symbols?

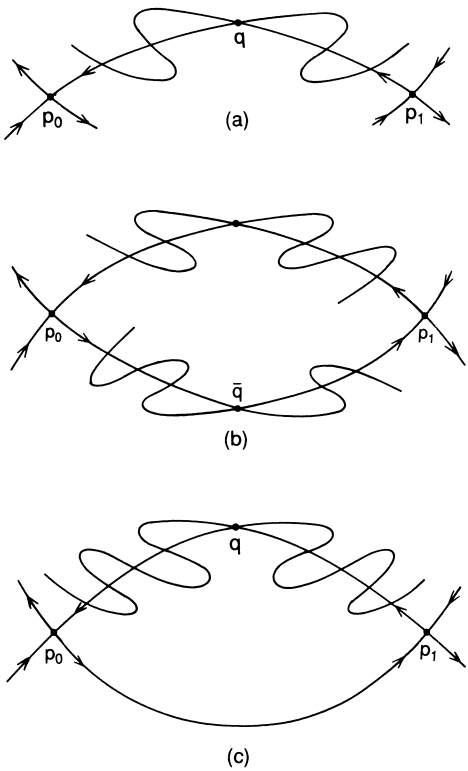

FIGURE 26.2.2.

27

Orbits Homoclinic to Hyperbolic Fixed Points in Three-Dimensional Autonomous Vector Fields

In this chapter we will study the orbit structure near orbits homoclinic to hyperbolic fixed points of three-dimensional autonomous vector fields. The term "near" refers to both phase space and parameter space. We will see that in some cases Smale horseshoe–type behavior may arise. In parametrized systems the creation of the horseshoes may be accompanied by cascades of period-doubling and saddle-node bifurcations as described in Theorem 32.1.2, or the horseshoes may "explode" into creation at a critical parameter value. We will see that the nature of the orbit structure near the homoclinic orbits depends mainly on two properties of the vector field:

1. the nature of the eigenvalues of the linearized vector field at the fixed point;
2. the existence of multiple homoclinic orbits to the same hyperbolic fixed point which could be a consequence of *symmetries* of the vector field;
3. the global geometry of the stable and unstable manifolds (roughly speaking, how they "twist" in phase space).

Regarding Property 1, it should be clear that there are only two possibilities for the three eigenvalues associated with the linearized vector field.

1. *Saddle* λ_1, λ_2, λ_3 real with $\lambda_1, \lambda_2 < 0$, $\lambda_3 > 0$.
2. *Saddle-focus* $\rho \pm i\omega$, λ with $\rho < 0$, $\lambda > 0$.

All other possibilities for hyperbolic fixed points follow from these two via time reversal. We will analyze each situation individually, but first we

want to describe the general technique of analysis that will apply to both cases.

The study of homoclinic and heteroclinic bifurcations has exploded in the past 10 years and it is impossible to do it justice in one book in any detail. Our approach will be more elementary so as to develop some intuition about the key issues that are involved. We will also give an extensive literature survey.

27.1 The Technique of Analysis

Consider a three-dimensional autonomous $\mathbf{C}^r$ $(r \geq 2)$ vector field having a hyperbolic fixed point at the origin with a two-dimensional stable manifold and a one-dimensional unstable manifold such that a homoclinic orbit connects the origin to itself (i.e., $W^u(0) \cap W^s(0) \neq \emptyset$) (see Figure 27.1.1 for the two possibilities according to the nature of the linearized flow near the origin).

The strategy will be to define a two-dimensional cross-section to the vector field near the homoclinic orbit, and to construct a map of the cross-

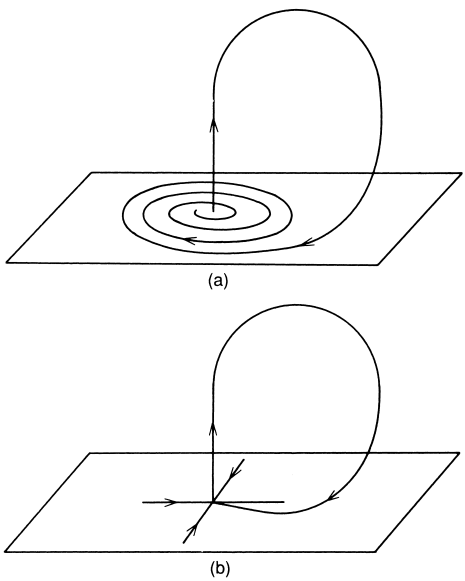

FIGURE 27.1.1. a) Saddle-focus. b) Saddle with purely real eigenvalues.

section into itself from the flow generated by the vector field. This is exactly the same idea that was used in Chapter 10 and was used to prove Moser's theorem in Chapter 26. Let us be more precise.

Consider cross-sections Π_0 and Π_1 transverse to the homoclinic orbit and located in a "sufficiently small neighborhood of the origin" as shown in Figure 27.1.2.

We construct a Poincaré map of Π_0 into itself

$$P: \Pi_0 \longrightarrow \Pi_0,$$

which will be the composition of two maps, one constructed from the flow near the origin

$$P_0: \Pi_0 \longrightarrow \Pi_1$$

and the other constructed from the flow defined outside a neighborhood of the origin

$$P_1: \Pi_1 \longrightarrow \Pi_0.$$

Then we have

$$P \equiv P_1 \circ P_0: \Pi_0 \longrightarrow \Pi_0;$$

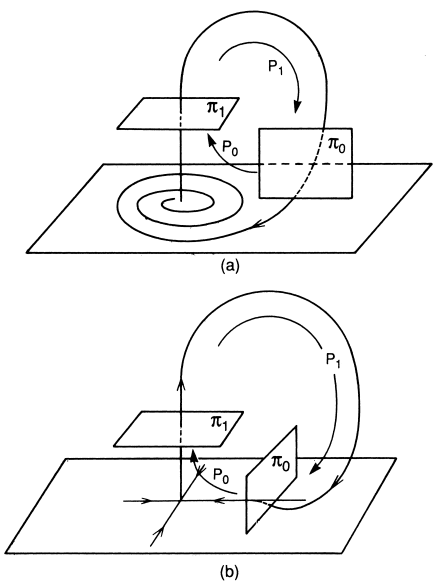

FIGURE 27.1.2. Poincaré map near the homoclinic orbit. a) Saddle-focus. b) Saddle with real eigenvalues.

see Figure 27.1.2. Thus, the entire construction requires four steps.

Step 1: Define Π_0 *and* Π_1. We will do this in each of the cases individually. As is typical, the choice of a cross-section on which to define a Poincaré map requires some knowledge of the geometrical structure of the phase space. A clever choice can often simplify the computations considerably.

Step 2: Construction of P_0. For Π_0 and Π_1 located sufficiently close to the origin, the map of Π_0 into Π_1 is "essentially" given by the flow generated by the linearized vector field. We put "essentially" in quotes, because using the linearized vector field to construct P_0 does introduce an error. However, the error can be made arbitrarily small by taking Π_0 and Π_1 sufficiently small and close to the origin; see Wiggins [1988] and Bakaleinikov and Silbergleit [1995a], [1995b]. Moreover, this error is truly negligible in the sense that it does not affect our results. Therefore, we will construct P_0 from the flow generated by the linearized vector field in order to avoid unnecessary technical distractions.

Step 3: Construction of P_1. Let $p_0 \equiv W^u(0) \cap \Pi_0$ and $p_1 \equiv W^u(0) \cap \Pi_1$. Then the time of flight from p_0 to p_1 is finite, since we are outside of a neighborhood of the fixed point. We will assume that, except for the origin, the homoclinic orbit is bounded away from all other possible fixed points of the vector field. Then, by continuity with respect to initial conditions, for Π_0 sufficiently small, the flow generated by the vector field maps Π_0 onto Π_1. This implies that the map P_1 is defined for Π_0 sufficiently small.

Thus, P_0 is defined, but how is it computed? Taylor expanding P_1 about p_0 gives

$$P_1(h) = p_0 + DP_1(p_1)h + \mathcal{O}(|h|^2),$$

where h represents coordinates on Π_1 centered at p_1. Now for Π_1 sufficiently small the $\mathcal{O}(|h|^2)$ term in this expression can be made arbitrarily small. Therefore, for $P_1 : \Pi_1 \to \Pi_0$, we will take

$$P_1(h) = p_0 + DP_1(p_1)h.$$

Of course, this approximation to P_1 introduces an error. However, in Wiggins [1988] and Bakaleinikov and Silbergleit [1995a,b] it is shown that the error is truly negligible in the sense that it does not affect our results. In some cases it will be necessary to assume that $DP_1(p_1)$ is a diffeomorphism.

Step 4: Construction of $P \equiv P_1 \circ P_0$. With P_0 and P_1 defined the construction of P is obvious.

Let us now make some heuristic remarks. Our analysis will give us information on the orbit structure in a sufficiently small neighborhood of the homoclinic orbit. The map P_0 can be constructed exactly from the linearized vector field (since we can "solve" linear, constant coefficient ordinary differential equations). Hence, we can compute how Π_0 is stretched, contracted, and, possibly, folded as it passes near the fixed point. Now P_1 might appear to present a problem, since we cannot even compute $DP_1(p_1)$ without solving for the flow generated by the nonlinear vector field. Fortunately, and perhaps surprisingly, it will turn out that we do not need to know $DP_1(p_1)$ exactly, only that it is *compatible with the geometry of the homoclinic orbit.* This will be made clear in the examples to which we now turn.

27.2 Orbits Homoclinic to a Saddle-Point with Purely Real Eigenvalues

Consider the following

$$\begin{aligned} \dot{x} &= \lambda_1 x + f_1(x, y, z; \mu), \\ \dot{y} &= \lambda_2 y + f_2(x, y, z; \mu), \\ \dot{z} &= \lambda_3 z + f_3(x, y, z; \mu), \end{aligned} \qquad (x, y, z, \mu) \in \mathbb{R}^1 \times \mathbb{R}^1 \times \mathbb{R}^1 \times \mathbb{R}^1, \quad (27.2.1)$$

where the f_i are $\mathbf{C}^2$ and they vanish at $(x, y, z, \mu) = (0, 0, 0, 0)$ and are nonlinear in x, y, and z. Hence, (4.8.1) has a fixed point at the origin with eigenvalues given by λ_1, λ_2, and λ_3. We make the following assumptions.

Assumption 1. $\lambda_1, \lambda_2 < 0$, $\lambda_3 > 0$.

Assumption 2. At $\mu = 0$, (27.2.1) possesses a homoclinic orbit Γ connecting $(x, y, z) = (0, 0, 0)$ to itself. Moreover, we assume that the homoclinic orbit breaks as shown in Figure 27.2.1 for $\mu > 0$ and $\mu < 0$.

The following remarks are now in order.

Remark 1. We assume that the parameter dependence is contained in the f_i and not in the eigenvalues λ_1, λ_2, and λ_3. This is mainly for convenience and does not affect the generality of our results.

Remark 2. In Figure 27.2.1 we drew the homoclinic orbit entering a neighborhood of the origin along a curve that is tangent to the y-axis at the origin. This assumes that $\lambda_2 > \lambda_1$ and that the system is *generic.* We deal with these issues in the exercises. Our results will not change for generic systems if $\lambda_1 \geq \lambda_2$.

We will analyze the orbit structure in a neighborhood of Γ in the standard way by computing a Poincaré map on an appropriately chosen cross-section. We choose two rectangles transverse to the flow, which are defined as follows

$$\begin{aligned} \Pi_0 &= \big\{(x,y,z) \in \mathbb{R}^3 \,|\, |x| \leq \varepsilon, y = \varepsilon, 0 < z \leq \varepsilon\big\}, \\ \Pi_1 &= \big\{(x,y,z) \in \mathbb{R}^3 \,|\, |x| \leq \varepsilon, |y| \leq \varepsilon, z = \varepsilon\big\}, \end{aligned} \tag{27.2.2}$$

for some $\varepsilon > 0$; see Figure 27.2.2.

Computation of P_0

The flow linearized at the origin is given by

$$\begin{aligned} x(t) &= x_0 e^{\lambda_1 t}, \\ y(t) &= y_0 e^{\lambda_2 t}, \\ z(t) &= z_0 e^{\lambda_3 t}, \end{aligned} \tag{27.2.3}$$

and the time of flight from Π_0 to Π_1 is given by

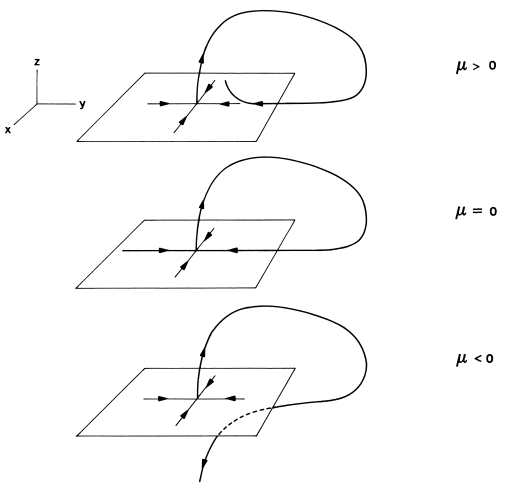

FIGURE 27.2.1.

$$t = \frac{1}{\lambda_3} \log \frac{\varepsilon}{z_0}. \tag{27.2.4}$$

Hence, the map

$$P_0 \colon \Pi_0 \to \Pi_1$$

is given by (leaving off the subscript 0's)

$$\begin{pmatrix} x \\ \varepsilon \\ z \end{pmatrix} \mapsto \begin{pmatrix} x\left(\frac{\varepsilon}{z}\right)^{\lambda_1/\lambda_3} \\ \varepsilon\left(\frac{\varepsilon}{z}\right)^{\lambda_2/\lambda_3} \\ \varepsilon \end{pmatrix}. \tag{27.2.5}$$

Computation of P_1

Following the discussion of Step 3 in our general analysis above, we take as P_1 the following affine map

$$P_1 \colon \Pi_1 \longrightarrow \Pi_0$$

$$\begin{pmatrix} x \\ y \\ \varepsilon \end{pmatrix} \mapsto \begin{pmatrix} 0 \\ \varepsilon \\ 0 \end{pmatrix} + \begin{pmatrix} a & b & 0 \\ 0 & 0 & 0 \\ c & d & 0 \end{pmatrix} \begin{pmatrix} x \\ y \\ 0 \end{pmatrix} + \begin{pmatrix} e\mu \\ 0 \\ f\mu \end{pmatrix}, \tag{27.2.6}$$

where a, b, c, d, e, and f are constants. Note from Figure 27.2.1 that we have $f > 0$, so we may rescale the parameter μ so that $f = 1$. Henceforth, we will assume that this has been done. Let us briefly explain the form of (27.2.6). On Π_0 the y coordinate is fixed at $y = \varepsilon$. This explains why there are only zeros in the middle row of the linear part of (27.2.6). Also, the z coordinate of Π_1 is fixed at $z = \varepsilon$. This explains why there are only zeros in the third column of the matrix in (27.2.6).

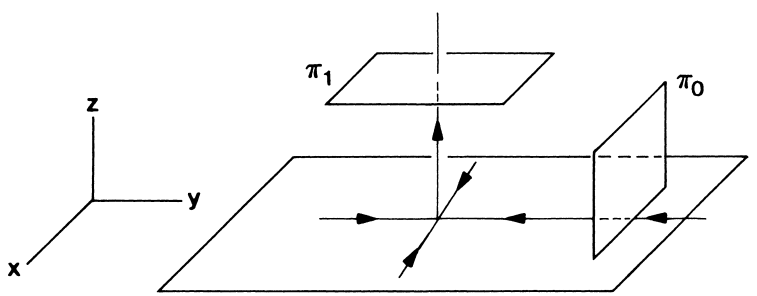

FIGURE 27.2.2.

The Poincaré Map $P \equiv P_1 \circ P_0$

Forming the composition of P_0 and P_1, we obtain the Poincaré map defined in a neighborhood of the homoclinic orbit having the following form.

$$P \equiv P_1 \circ P_0 \colon \Pi_0 \to \Pi_0,$$

$$\begin{pmatrix} x \\ z \end{pmatrix} \mapsto \begin{pmatrix} ax\left(\frac{\varepsilon}{z}\right)^{\lambda_1/\lambda_3} + b\varepsilon\left(\frac{\varepsilon}{z}\right)^{\lambda_2/\lambda_3} + e\mu \\ cx\left(\frac{\varepsilon}{z}\right)^{\lambda_1/\lambda_3} + d\varepsilon\left(\frac{\varepsilon}{z}\right)^{\lambda_2/\lambda_3} + \mu \end{pmatrix}, \tag{27.2.7}$$

where Π_0 is chosen sufficiently small so that $P_1 \circ P_0$ is defined.

We reiterate that the approximate Poincaré map (27.2.7) is valid for ε sufficiently small and x and z sufficiently small. For ε sufficiently small, the approximation of P_0 by the linearized flow is valid and, for x and z sufficiently small, the approximation of P_1 by the affine map P_1 is valid. Note that ε, x, and z are independent.

Calculation of Fixed Points of P

Now we look for fixed points of the Poincaré map (which will correspond to periodic orbits of (27.2.1). First some notation; let

$$A = a\varepsilon^{\lambda_1/\lambda_3}, \quad B = b\varepsilon^{1+(\lambda_2/\lambda_3)}, \quad C = c\varepsilon^{\lambda_1/\lambda_3}, \quad D = d\varepsilon^{1+(\lambda_2/\lambda_3)}.$$

Then the condition for fixed points of (27.2.7) is

$$x = Axz^{|\lambda_1|/\lambda_3} + Bz^{|\lambda_2|/\lambda_3} + e\mu, \tag{27.2.8}$$

$$z = Cxz^{|\lambda_1|/\lambda_3} + Dz^{|\lambda_2|/\lambda_3} + \mu. \tag{27.2.9}$$

Solving (27.2.8) for x as a function of z gives

$$x = \frac{Bz^{|\lambda_2|/\lambda_3} + e\mu}{1 - Az^{|\lambda_1|/\lambda_3}}. \tag{27.2.10}$$

We will restrict ourselves to a sufficiently small neighborhood of the homoclinic orbit so that z can be taken sufficiently small in order that the denominator of (27.2.10) can be taken to be 1. Substituting this expression for x into (27.2.9) gives the following condition for fixed points of (27.2.7) in terms of z and μ only

$$z - \mu = CBz^{|\lambda_1+\lambda_2|/\lambda_3} + Ce\mu z^{|\lambda_1|/\lambda_3} + Dz^{|\lambda_2|/\lambda_3}. \tag{27.2.11}$$

We will graphically display the solutions of (27.2.11) for μ sufficiently small and near zero by graphing the left-hand side of (27.2.11) and the right-hand side of (27.2.11) and seeking intersections of the curves.

First, we want to examine the slope of the right-hand side of (27.2.11) at $z = 0$. This is given by the following expression

$$\begin{aligned}
&\frac{d}{dz}\left(CBz^{|\lambda_1+\lambda_2|/\lambda_3} + Ce\mu z^{|\lambda_1|/\lambda_3} + Dz^{|\lambda_2|/\lambda_3}\right) \\
&= \frac{|\lambda_1+\lambda_2|}{\lambda_3} CBz^{\frac{|\lambda_1+\lambda_2|}{\lambda_3}-1} + \frac{|\lambda_1|}{\lambda_3} Ce\mu z^{\frac{|\lambda_1|}{\lambda_3}-1} \\
&+ \frac{|\lambda_2|}{\lambda_3} Dz^{\frac{|\lambda_2|}{\lambda_3}-1}. \qquad (27.2.12)
\end{aligned}$$

If we assume that P_1 is invertible then $ad - bc \neq 0$. This implies that $AD - BC \neq 0$ so that C and D cannot both be zero. Therefore, at $z = 0$, (27.2.12) takes the values

$$\begin{array}{ll}
\infty & \text{if } |\lambda_1| < \lambda_3 \quad \text{or } |\lambda_2| < \lambda_3 \\
0 & \text{if } |\lambda_1| > \lambda_3 \quad \text{and } |\lambda_2| > \lambda_3.
\end{array}$$

There are four possible cases, two each for both the infinite-slope and zero-slope situations. The differences in these situations depend mainly on global effects, i.e., the relative signs of A, B, C, D, e, and μ. We will consider this more carefully shortly. Figure 27.2.3 illustrates the graphical solution of (27.2.11) in the zero-slope case. The two-slope cases illustrated in Figure 27.2.3 give the same result, namely, that for $\mu > 0$ a periodic orbit bifurcates from the homoclinic orbit.

In the infinite-slope case the two possible situations are illustrated in Figure 27.2.4. Interestingly, in the infinite-slope case we get two different results; namely, in one case we get a periodic orbit for $\mu < 0$, and in the other case a periodic orbit for $\mu > 0$. So what is going on? As we will shortly see, there is a global effect in this case that our local analysis does not detect. Now we want to explain this global effect.

Let τ be a tube beginning and ending on Π_0 and Π_1, respectively, which contains Γ. Then $\tau \cap W^s(0)$ is a two-dimensional strip which we denote as $\mathcal{R}$. Suppose, *without twisting* $\mathcal{R}$, that we join together the two ends of $\mathcal{R}$. Then there are two possibilities: 1) $W^s(0)$ experiences an even number of half-twists inside τ, in which case, when the ends of $\mathcal{R}$ are joined together it is homeomorphic to a cylinder, or 2) $W^s(0)$ experiences an odd number of half-twists inside τ, in which case, when the ends of $\mathcal{R}$ are joined together it is homeomorphic to a Mobius strip; see Figure 27.2.5. The reader should verify this experimentally with a strip of paper.

We now want to discuss the dynamical consequences of these two situations. First, consider the rectangle $\mathcal{D} \subset \Pi_0$ shown in Figure 27.2.6, which has its lower horizontal boundary in $W^s(0)$. We want to consider the shape of the image of $\mathcal{D}$ under P_0. From (27.2.5), P_0 is given by

$$\begin{pmatrix} x \\ \varepsilon \\ z \end{pmatrix} \mapsto \begin{pmatrix} x\left(\frac{\varepsilon}{z}\right)^{\lambda_1/\lambda_3} \\ \varepsilon\left(\frac{\varepsilon}{z}\right)^{\lambda_2/\lambda_3} \\ \varepsilon \end{pmatrix} \equiv \begin{pmatrix} x' \\ y' \\ \varepsilon \end{pmatrix}, \tag{27.2.13}$$

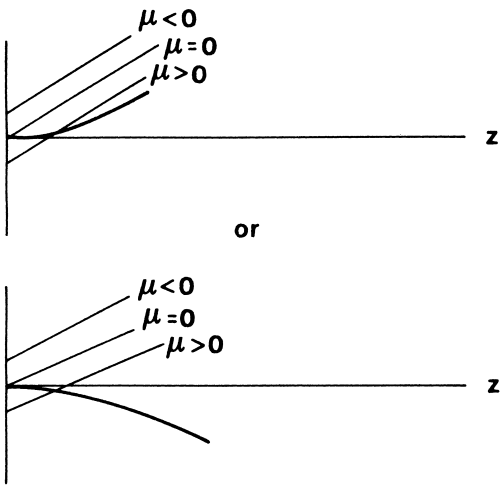

FIGURE 27.2.3. Graphical solution of (27.2.11) in the zero-slope case.

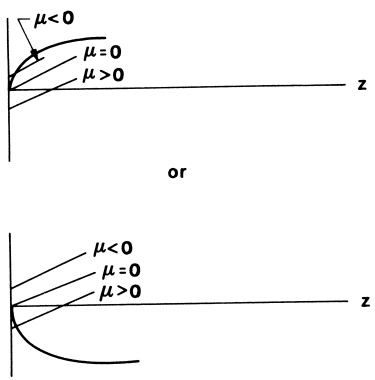

FIGURE 27.2.4. Graphical solution of (27.2.11) in the infinite-slope case.

where, to avoid confusion, we label the coordinates in Π_1 by x' and y'. Now consider a horizontal line in $\mathcal{D}$, i.e., a line with $z =$ constant. From (27.2.13) we see that this line is mapped to a line in Π_1 given by

$$y' = \varepsilon \left(\frac{\varepsilon}{z}\right)^{\lambda_2/\lambda_3} = \text{constant}. \tag{27.2.14}$$

However, the length of this line is not preserved, since

$$\frac{x'}{x} = \left(\frac{\varepsilon}{z}\right)^{\lambda_1/\lambda_3} \longrightarrow 0 \quad \text{as} \quad z \to 0 \tag{27.2.15}$$

because $\lambda_1 < 0 < \lambda_3$. Next consider a vertical line in $\mathcal{D}$, i.e., a line with $x =$ constant. From (27.2.13) we see that

$$\frac{y'}{z} = \varepsilon^{1+\frac{\lambda_2}{\lambda_3}} z^{-\frac{\lambda_2}{\lambda_3}-1}. \tag{27.2.16}$$

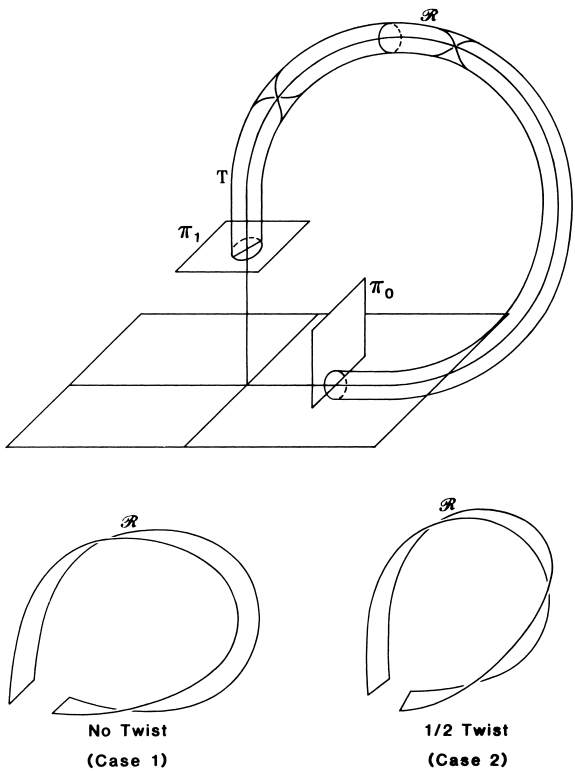

FIGURE 27.2.5.

Hence, for $-\lambda_2 > \lambda_3$, the length of vertical lines is contracted under P_0 as $z \to 0$ and, for $-\lambda_2 < \lambda_3$, the length of vertical lines is expanded under P_0 as $z \to 0$. Now, (27.2.15) implies that a horizontal line in $\mathcal{D}$ on the stable manifold of the origin is contracted to a point (i.e., P_0 is not defined here). From these remarks we thus see that $\mathcal{D}$ is mapped to the "half-bowtie" shape as shown in Figure 27.2.6. Note that for $\lambda_2 > \lambda_1$ the "vertical" boundary of the "half-bowtie" is tangent to the y-axis at the origin. If $\lambda_2 < \lambda_1$, it would be tangent to the x-axis at the origin. Since we are assuming $\lambda_2 > \lambda_1$ for the purpose of illustrating the construction and geometry of the maps, we show only the first case.

Under the map P_1 the half-bowtie $P_0(\mathcal{D})$ is mapped back around Γ with the sharp tip of $P_0(\mathcal{D})$ coming back near $\Gamma \cap \Pi_0$. In the case where $\mathcal{R}$ is homeomorphic to a cylinder, $P_0(\mathcal{D})$ twists around an even number of times in its journey around Γ and comes back to Π_0 lying above $W^s(0)$. In the case where $\mathcal{R}$ is homeomorphic to a mobius strip, $P_0(\mathcal{D})$ twists around an odd number of times in its journey around Γ and returns to Π_0 lying below $W^s(0)$; see Figure 27.2.7.

At this point, we will return to the four different cases that arose in locating the bifurcated periodic orbits and see which particular global effect occurs.

Recall from (27.2.11) that the z components of the fixed points were

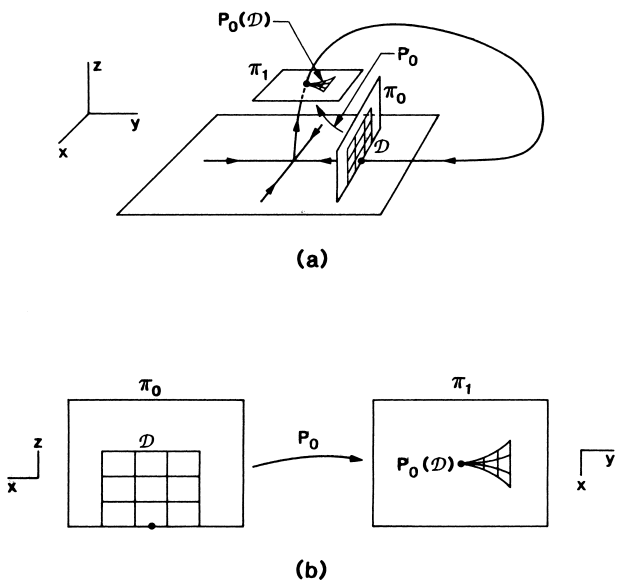

FIGURE 27.2.6.

obtained by solving

$$z = CBz^{\frac{|\lambda_1+\lambda_2|}{\lambda_3}} + Ce\mu z^{\frac{|\lambda_1|}{\lambda_3}} + Dz^{\frac{|\lambda_2|}{\lambda_3}} + \mu. \tag{27.2.17}$$

The right-hand side of this equation thus represents the z-component of the first return of a point to Π_0. Then, at $\mu = 0$, the first return will be positive if we have a cylinder (C) and negative if we have a mobius band (M). Using this remark, we can go back to the four cases and label them as in Figure 27.2.8.

We now address the question of stability of the bifurcated periodic orbits.

Stability of the Periodic Orbits

The derivative of (27.2.7) is given by

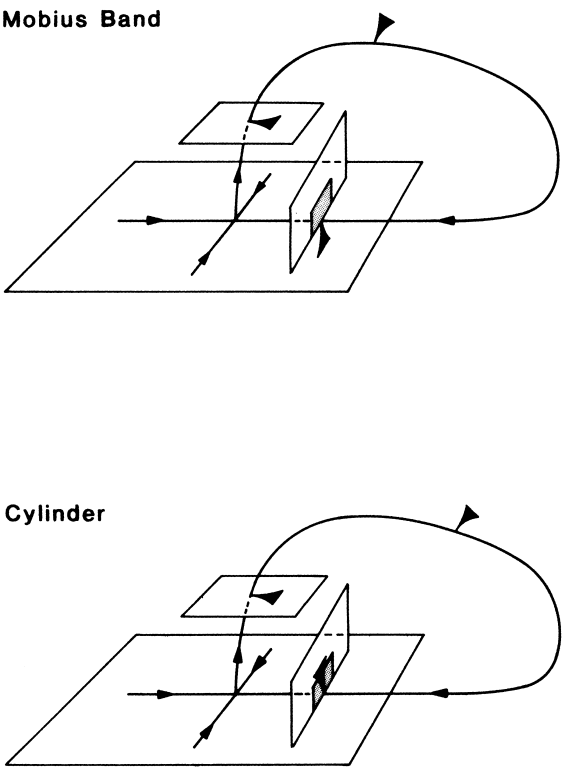

FIGURE 27.2.7.

$$DP = \begin{pmatrix} Az^{\frac{|\lambda_1|}{\lambda_3}} \dfrac{|\lambda_1|}{\lambda_3} Axz^{\frac{|\lambda_1|}{\lambda_3}-1} + \dfrac{|\lambda_2|}{\lambda_3} Bz^{\frac{|\lambda_2|}{\lambda_3}-1} \\ \\ Cz^{\frac{|\lambda_1|}{\lambda_3}} \dfrac{|\lambda_1|}{\lambda_3} Cxz^{\frac{|\lambda_1|}{\lambda_3}-1} + \dfrac{|\lambda_2|}{\lambda_3} Dz^{\frac{|\lambda_2|}{\lambda_3}-1} \end{pmatrix}. \tag{27.2.18}$$

Stability is determined by considering the nature of the eigenvalues of (27.2.18). The eigenvalues of DP are given by

$$\gamma_{1,2} = \frac{\operatorname{tr} DP}{2} \pm \frac{1}{2}\sqrt{(\operatorname{tr} DP)^2 - 4\det(DP)}, \tag{27.2.19}$$

where

$$\begin{aligned} \det DP &= \frac{|\lambda_2|}{\lambda_3}(AD - BC)z^{\frac{|\lambda_1+\lambda_2|-\lambda_3}{\lambda_3}}, \\ \operatorname{tr} DP &= Az^{\frac{|\lambda_1|}{\lambda_3}} + \frac{|\lambda_1|}{\lambda_3} Cxz^{\frac{|\lambda_1|}{\lambda_3}-1} + \frac{|\lambda_2|}{\lambda_3} Dz^{\frac{|\lambda_2|}{\lambda_3}-1}. \end{aligned} \tag{27.2.20}$$

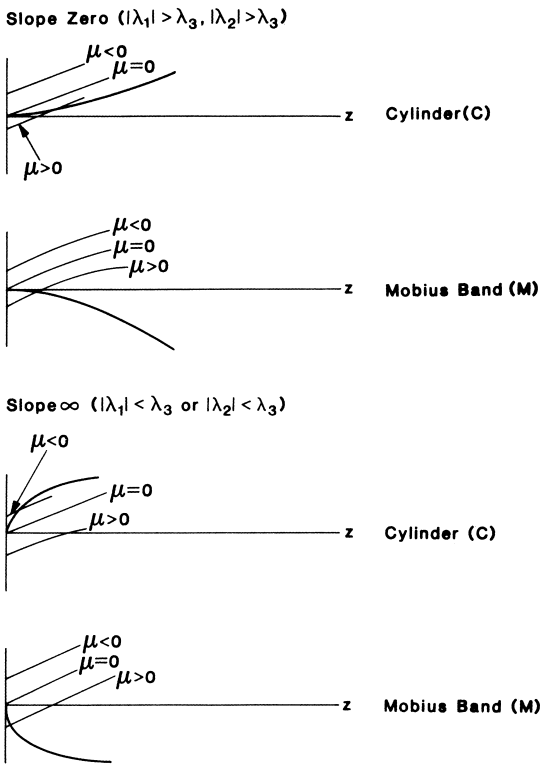

FIGURE 27.2.8.

Substituting equation (27.2.10) for x at a fixed point into the expression for $\operatorname{tr} DP$ gives

$$\operatorname{tr} DP = Az^{\frac{|\lambda_1|}{\lambda_3}} + \frac{|\lambda_1|}{\lambda_3} CBz^{\frac{|\lambda_1+\lambda_2|}{\lambda_3}-1} + \frac{|\lambda_2|}{\lambda_3} Dz^{\frac{|\lambda_2|}{\lambda_3}-1} + \frac{|\lambda_1|}{\lambda_3} Ce\mu z^{\frac{|\lambda_1|}{\lambda_3}-1}. \tag{27.2.21}$$

Let us note the following important facts.

For z sufficiently small

$$\det DP \text{ is } \begin{cases} \text{a) arbitrarily large for } |\lambda_1 + \lambda_2| < \lambda_3; \\ \text{b) arbitrarily small for } |\lambda_1 + \lambda_2| > \lambda_3. \end{cases}$$

$$\operatorname{tr} DP \text{ is } \begin{cases} \text{a) arbitrarily large for } |\lambda_1| < \lambda_3 \text{ or } |\lambda_2| < \lambda_3; \\ \text{b) arbitrarily small for } |\lambda_1| > \lambda_3 \text{ and } |\lambda_2| > \lambda_3. \end{cases}$$

Using these facts along with (27.2.19) and (27.2.20) we can conclude the following.

1. For $|\lambda_1| > \lambda_3$ and $|\lambda_2| > \lambda_3$, both eigenvalues of DP can be made arbitrarily small by taking z sufficiently small.
2. For $|\lambda_1 + \lambda_2| > \lambda_3$ and $|\lambda_1| < \lambda_3$ and/or $|\lambda_2| < \lambda_3$, one eigenvalue can be made arbitrarily small and the other eigenvalue can be made arbitrarily large by taking z sufficiently small.
3. For $|\lambda_1 + \lambda_2| < \lambda_3$, either both eigenvalues can be made arbitrarily large, or one eigenvalue can be made arbitrarily large and the other arbitrarily small, by taking z sufficiently small.

We summarize our results in the following theorem.

Theorem 27.2.1 *For $\mu \neq 0$ and sufficiently small, a periodic orbit bifurcates from Γ in (27.2.1). The periodic orbit is a*

i) *sink for $|\lambda_1| > \lambda_3$ and $|\lambda_2| > \lambda_3$;*

ii) *saddle for $|\lambda_1 + \lambda_2| > \lambda_3$, $|\lambda_1| < \lambda_3$, and/or $|\lambda_2| < \lambda_3$;*

iii) *saddle or source for $|\lambda_1 + \lambda_2| < \lambda_3$.*

We remark that the construction of the Poincaré map used in the proof of Theorem 27.2.1 was for the case $\lambda_2 > \lambda_1$ (see Figure 27.2.1); however,

the same result holds for $\lambda_2 < \lambda_1$ and $\lambda_1 = \lambda_2$. We leave the details to the reader in the exercises.

Next we consider the case of two homoclinic orbits connecting the saddle type fixed point to itself and show how under certain conditions chaotic dynamics may arise.

27.2A Two Orbits Homoclinic to a Fixed Point Having Real Eigenvalues

We consider the same system as before; however, we now replace Assumption 2 with Assumption 2′ given below.

Assumption 2′. Equation (27.2.1) has a pair of orbits, Γ_r, Γ_ℓ, homoclinic to $(0,0,0)$ at $\mu = 0$, and Γ_r and Γ_ℓ lie in separate branches of the unstable manifold of $(0,0,0)$. There are thus two possible generic pictures illustrated in Figure 27.2.9.

Note that the coordinate axes in Figure 27.2.9 have been rotated with respect to those in Figure 27.2.1. This is merely for artistic convenience. We will consider only the configuration of Case a in Figure 27.2.9; however, the same analysis (and most of the resulting dynamics) will go through for Case b. Our goal will be to establish that the Poincaré map constructed near the homoclinic orbits contains the chaotic dynamics of the Smale horseshoe or, more specifically, that it contains an invariant Cantor set on which it is homeomorphic to the full shift on two symbols (see Chapter 24).

We begin by constructing the local cross-sections to the vector field near the origin. We define

$$\begin{aligned}
\Pi_0^r &= \big\{(x,y,z) \in \mathbb{R}^3 \,|\, y = \varepsilon,\ |x| \le \varepsilon,\ 0 < z \le \varepsilon\big\},\\
\Pi_0^\ell &= \big\{(x,y,z) \in \mathbb{R}^3 \,|\, y = \varepsilon,\ |x| \le \varepsilon,\ -\varepsilon \le z < 0\big\},\\
\Pi_1^r &= \big\{(x,y,z) \in \mathbb{R}^3 \,|\, z = \varepsilon,\ |x| \le \varepsilon,\ 0 < y \le \varepsilon\big\},\\
\Pi_1^\ell &= \big\{(x,y,z) \in \mathbb{R}^3 \,|\, z = -\varepsilon,\ |x| \le \varepsilon,\ 0 < y \le \varepsilon\big\},
\end{aligned} \tag{27.2.22}$$

for $\varepsilon > 0$ and small; see Figure 27.2.10 for an illustration of the geometry near the origin.

Now recall the global twisting of the stable manifold of the origin. We want to consider the effect of this in our construction of the Poincaré map. Let τ_r (resp. τ_ℓ) be a tube beginning and ending on Π_1^r (resp. Π_1^ℓ) and Π_0^r (resp. Π_0^ℓ) which contains Γ_r (resp. Γ_ℓ) (see Figure 27.2.5). Then $\tau_r \cap W^s(0)$

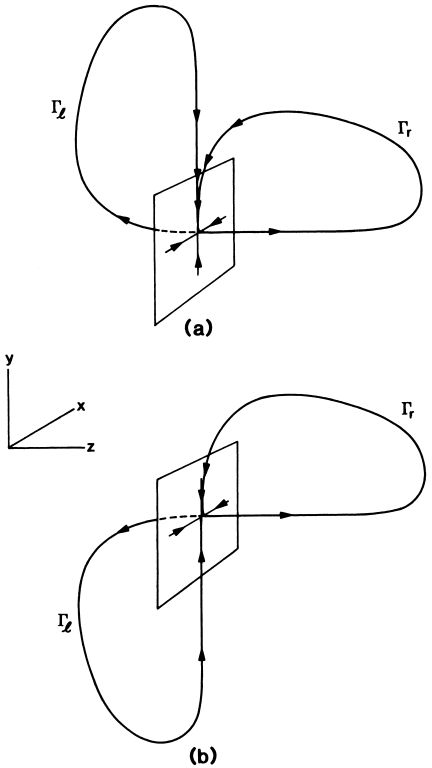

FIGURE 27.2.9.

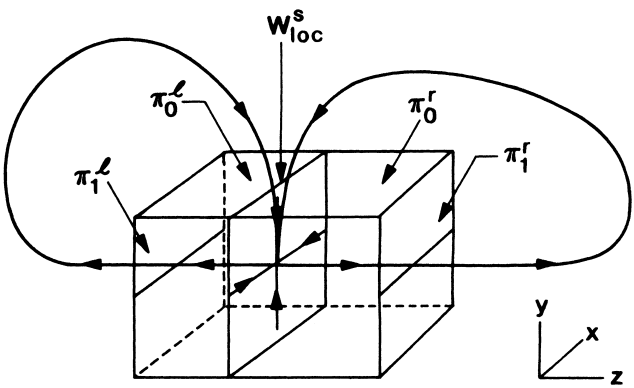

FIGURE 27.2.10.

(resp. $\tau_\ell \cap W^s(0)$) is a two-dimensional strip, which we denote as $\mathcal{R}_r$ (resp. $\mathcal{R}_\ell$). If we join together the two ends of $\mathcal{R}_r$ (resp. $\mathcal{R}_\ell$) *without twisting* $\mathcal{R}_r$ (resp. $\mathcal{R}_\ell$), then $\mathcal{R}_r$ (resp. $\mathcal{R}_\ell$) is homeomorphic to either a cylinder or a mobius strip (see Figure 27.2.5). Thus, this global effect gives rise to three distinct possibilities.

1. $\mathcal{R}_r$ and $\mathcal{R}_\ell$ are homeomorphic to cylinders.
2. $\mathcal{R}_r$ is homeomorphic to a cylinder and $\mathcal{R}_\ell$ is homeomorphic to a mobius strip.
3. $\mathcal{R}_r$ and $\mathcal{R}_\ell$ are homeomorphic to mobius strips.

These three cases manifest themselves in the Poincaré map as shown in Figure 27.2.11.

We now want to motivate how we might expect a horseshoe to arise in these situations. Consider Case 1. Suppose we vary the parameter μ so

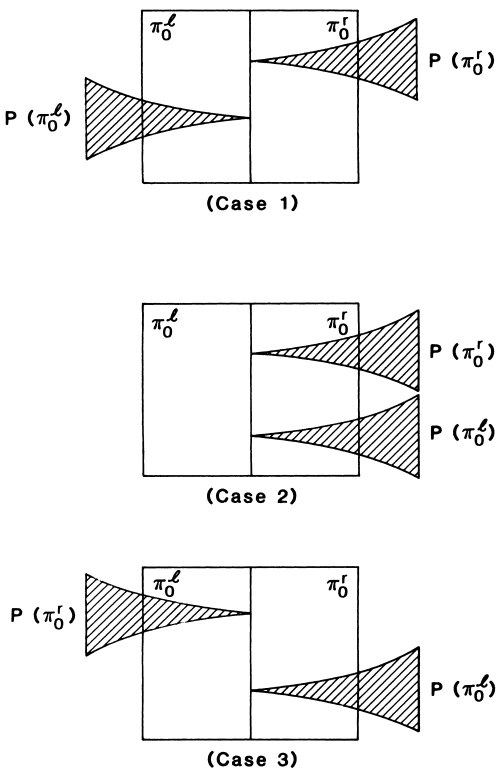

FIGURE 27.2.11.

that the homoclinic orbits break, with the result that the images of Π_0^r and Π_0^ℓ move in the manner shown in Figure 27.2.12. The question of whether or not we would expect such behavior in a one-parameter family of three-dimensional vector fields will be addressed shortly.

From Figure 27.2.12 one can begin to see how we might get horseshoe-like dynamics in this system. We can choose μ_h-horizontal strips in Π_0^r and Π_0^ℓ, which are mapped over themselves in μ_v-vertical strips as μ is varied, as shown in Figure 27.2.13. The conditions on the relative magnitudes of the eigenvalues at the fixed point will insure the appropriate stretching and contracting directions. Note that no horseshoe behavior is possible at $\mu = 0$.

Of course, many things need to be justified in Figure 27.2.13, namely,

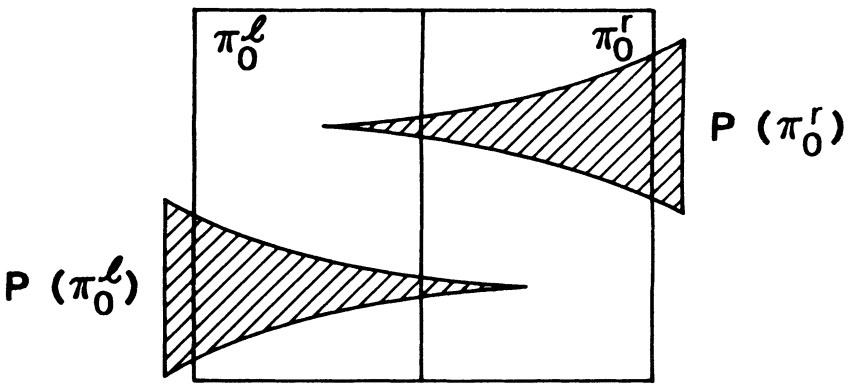

FIGURE 27.2.12.

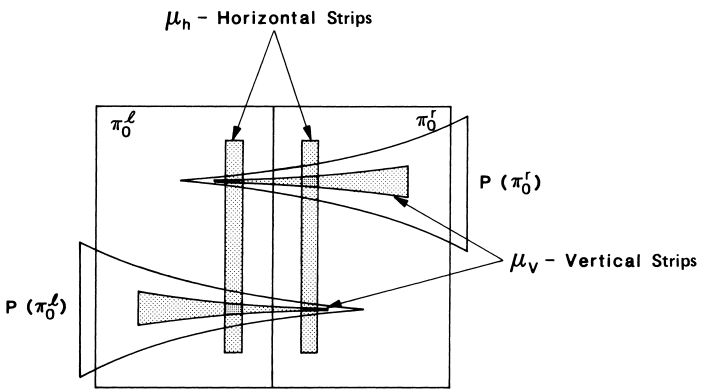

FIGURE 27.2.13.

the stretching and contraction rates and also that the little "half-bowties" behave correctly as the homoclinic orbits are broken. However, rather than go through the three cases individually, we will settle for studying a specific example and refer the reader to Afraimovich, Bykov, and Silnikov [1983] for detailed discussions of the general case. However, first we want to discuss the role of parameters.

In a three-dimensional vector field one would expect that varying a parameter would result in the destruction of a particular homoclinic orbit. In the case of two homoclinic orbits we cannot expect that the behavior of both homoclinic orbits can be controlled by a single parameter resulting in the behavior shown in Figure 27.2.11. For this we would need two parameters where each parameter could be thought of as "controlling" a particular homoclinic orbit. In the language of bifurcation theory this is a global codimension-two bifurcation problem. However, if the vector field contains a symmetry, e.g., (27.2.1) is invariant under the change of coordinates $(x, y, z) \to (-x, y, -z)$, which represents a 180° rotation about the y axis, then the existence of one homoclinic orbit necessitates the existence of another so that one parameter controls both. For simplicity, we will treat the symmetric case and refer the reader to Afraimovich, Bykov, and Silnikov [1983] for a discussion of the nonsymmetric cases. The symmetric case is of historical interest, since this is precisely the situation that arises in the much-studied Lorenz equations; see Sparrow [1982].

The case we will consider is characterized by the following properties.

Assumption 1′. $0 < -\lambda_2 < \lambda_3 < -\lambda_1$, $d \neq 0$.

Assumption 2′. Equation (27.2.1) is invariant under the coordinate transformation $(x, y, z) \to (-x, y, -z)$, and the homoclinic orbits break for μ near zero in the manner shown in Figure 27.2.14.

Assumption A1′ insures that the Poincaré map has a strongly contracting direction and a strongly expanding direction (recall from (27.2.6) that d is an entry in the matrix defining P_1, and $d \neq 0$ is a generic condition). The reader should recall the discussion of Figure 27.2.6, which explains the geometry behind these statements.

Now, the Poincaré map P of $\Pi_0^r \cup \Pi_0^\ell$ into $\Pi_0^r \cup \Pi_0^\ell$ consists of two parts

$$P_r \colon \Pi_0^r \to \Pi_0^r \cup \Pi_0^\ell, \tag{27.2.23}$$

with P_r given by (27.2.7), and

$$P_\ell \colon \Pi_0^\ell \to \Pi_0^r \cup \Pi_0^\ell, \tag{27.2.24}$$

where by the symmetry we have

$$P_\ell(x, z; \mu) = -P_r(-x, -z; \mu). \tag{27.2.25}$$

Our goal is to show that, for $\mu < 0$, P contains an invariant Cantor set on which it is topologically conjugate to the full shift on two symbols. This is done in the following theorem.

Theorem 27.2.2 *There exists $\mu_0 < 0$ such that, for $\mu_0 < \mu < 0$, P possesses an invariant Cantor set on which it is topologically conjugate to the full shift on two symbols.*

Proof: The method behind the proof of this theorem is the same as that used in the proof of Moser's theorem (see Chapter 26). In $\Pi_0^r \cup \Pi_0^\ell$ we locate two disjoint μ_h-horizontal strips that are mapped over themselves in two μ_v-vertical strips so that Assumptions 1 and 3 of Section 25 hold.

We choose $\mu < 0$ fixed. Then we choose two μ_h-horizontal strips, one in Π_0^r and one in Π_0^ℓ, where the "horizontal" coordinate is the z axis. We choose the horizontal sides of the strips to be parallel to the x-axis so that $\mu_h = 0$. Then, under the Poincaré map P defined in (27.2.23) and (27.2.24), since $\lambda_3 < -\lambda_1$ and μ is fixed, we can choose the two μ_h-horizontal strips

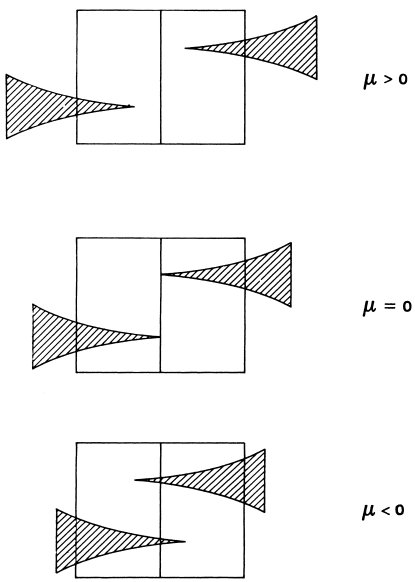

FIGURE 27.2.14.

sufficiently close to $W^s(0)$ so that the image of each μ_h-horizontal strip intersects both horizontal boundaries of each of the μ_h-horizontal strips as shown in Figure 27.2.15. Thus, it follows that Assumption 1 holds.

Next we must verify that Assumption 3 holds. This follows from a calculation very similar to that which we performed to show that Assumption 3 holds in the proof of Moser's theorem in Chapter 26. It uses the fact that $-\lambda_2 < \lambda_3 < -\lambda_1$ and $d \neq 0$. We leave the details as an exercise for the reader. □

We left out many of the details of the proof of Theorem 27.2.2. In the exercises we outline how one would complete the missing details.

The dynamical consequences of Theorem 27.2.2 are stunning. For $\mu \geq 0$, there is nothing spectacular associated with the dynamics near the (broken) homoclinic orbits. However, for $\mu < 0$, the horseshoes and their attendant chaotic dynamics appear seemingly out of nowhere. This particular type of global bifurcation has been called a *homoclinic explosion.*

27.2B Observations and Additional References

We have barely scratched the surface of the possible dynamics associated with orbits homoclinic to a fixed point having real eigenvalues in a third-order ordinary differential equation. There are several issues which deserve a more thorough investigation.

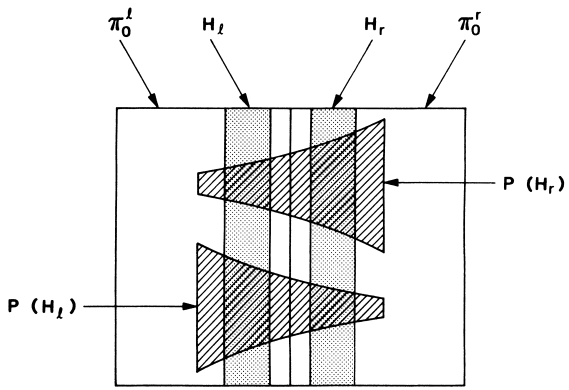

FIGURE 27.2.15.

1. *Two Homoclinic Orbits without Symmetry.* See Afraimovich, Bykov, and Silnikov [1983] and the references therein.

2. *The Existence of Strange Attractors.* Horseshoes are chaotic invariant sets, yet all the orbits in the horseshoes are unstable of saddle type. Nevertheless, it should be clear that horseshoes may exhibit a striking effect on the dynamics of any system. In particular, they are often the chaotic heart of numerically observed strange attractors. For work on the "strange attractor problem" associated with orbits homoclinic to fixed points having real eigenvalues in a third-order ordinary differential equation, see Afraimovich, Bykov, and Silnikov [1983] and Shashkov and Shil'nikov [1994]. Most of the work done on such systems has been in the context of the Lorenz equations. References for Lorenz attractors include Sparrow [1982], Guckenheimer and Williams [1980], and Williams [1980]. Recently, some breakthroughs have been made in proving the existence of strange attractors in such equations by Rychlik [1990] and Robinson [1989]. Recently, an elegant computer assisted proof of the existence of a strange attractor for the Lorenz equations was given by Tucker [1999]; see also Morales et al. [1998] and the popular articles of Stewart [2000] and Viana [2000].

3. *Bifurcations Creating the Horseshoe.* In the homoclinic explosion an infinite number of periodic orbits of all possible periods are created. The question arises concerning precisely how these periodic orbits were created and how they are related to each other. This question also has relevance to the strange attractor problem. See Robinson [2000], Gonchenko et al. [1996], [1997], and Silnikov and Turaev [1997].

   In recent years Birman, Williams, and Holmes have been using the *knot type* of a periodic orbit as a bifurcation invariant in order to understand the appearance, disappearance, and interrelation of periodic orbits in third-order ordinary differential equations. Roughly speaking, a periodic orbit in three dimensions can be thought of as a knotted closed loop. As system parameters are varied, the periodic orbit may never intersect itself due to uniqueness of solutions. Hence, the knot type of a periodic orbit cannot change as parameters are varied. The knot type is therefore a bifurcation invariant as well as a key tool for developing a classification scheme for periodic orbits. For references, see Birman and Williams [1983a,b], Holmes [1986], [1987], Holmes and Williams [1985], Ghrist et al. [1997], Gilmore [1998], and Plumecoq and Lefranc [2000a,b].

27.3 Orbits Homoclinic to a Saddle-Focus

We now consider the dynamics near an orbit homoclinic to a fixed point of saddle-focus type in a third-order ordinary differential equation. This has become known as the *Silnikov phenomenon,* since it was first studied by Silnikov [1965].

We consider an equation of the following form

$$\begin{aligned} \dot{x} &= \rho x - \omega y + P(x, y, z), \\ \dot{y} &= \omega x + \rho y + Q(x, y, z), \\ \dot{z} &= \lambda z + R(x, y, z), \end{aligned} \tag{27.3.1}$$

where P, Q, R are $\mathbf{C}^2$ and $\mathcal{O}(2)$ at the origin. It should be clear that $(0, 0, 0)$ is a fixed point and that the eigenvalues of (27.3.1) linearized about $(0, 0, 0)$ are given by $\rho \pm i\omega$, λ (note that there are no parameters in this problem at the moment; we will consider bifurcations of (27.3.1) later). We make the following assumptions on the system (27.3.1).

Assumption 1. Equation (27.3.1) possesses a homoclinic orbit Γ connecting $(0, 0, 0)$ to itself.

Assumption 2. $\lambda > -\rho > 0$.

Thus, $(0, 0, 0)$ possesses a two-dimensional stable manifold and a one-dimensional unstable manifold which intersect nontransversely; see Figure 27.3.1.

In order to determine the nature of the orbit structure near Γ, we construct a Poincaré map defined near Γ in the manner described at the be-

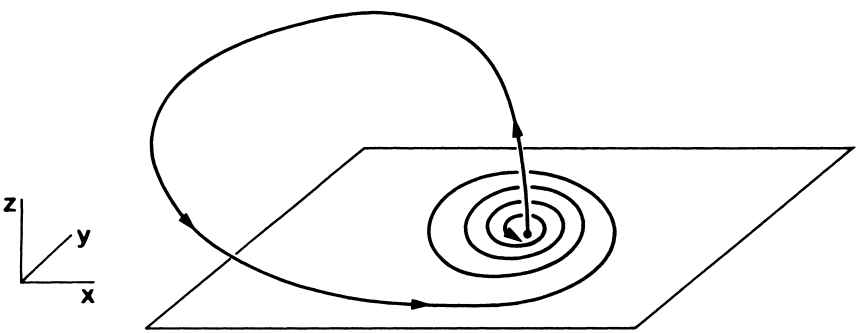

FIGURE 27.3.1.

ginning of this section.

Computation of P_0

Let Π_0 be a rectangle lying in the $x - z$ plane, and let Π_1 be a rectangle parallel to the $x - y$ plane at $z = \varepsilon$; see Figure 27.3.2. As opposed to the case of purely real eigenvalues, Π_0 will require a more detailed description. However, in order to do this we need to better understand the dynamics of the flow near the origin.

The flow generated by (27.3.1) linearized about the origin is given by

$$\begin{aligned} x(t) &= e^{\rho t}(x_0 \cos \omega t - y_0 \sin \omega t), \\ y(t) &= e^{\rho t}(x_0 \sin \omega t + y_0 \cos \omega t), \\ z(t) &= z_0 e^{\lambda t}. \end{aligned} \tag{27.3.2}$$

The time of flight for points starting on Π_0 to reach Π_1 is found by solving

$$\varepsilon = z_0 e^{\lambda t} \tag{27.3.3}$$

or

$$t = \frac{1}{\lambda} \log \frac{\varepsilon}{z_0}. \tag{27.3.4}$$

Thus, P_0 is given by (omitting the subscript 0's)

$$P_0 \colon \Pi_0 \to \Pi_1,$$

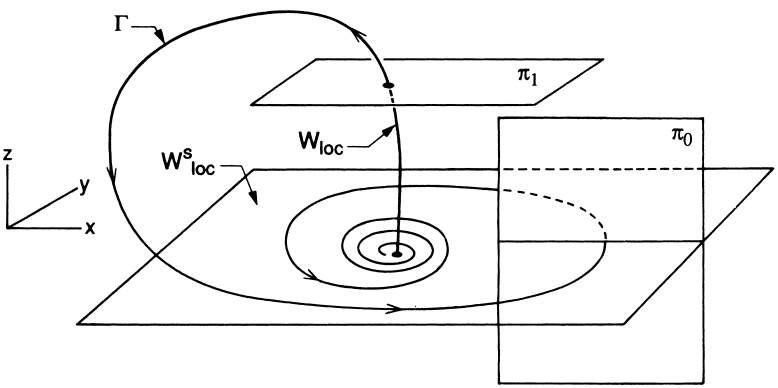

FIGURE 27.3.2.

$$\begin{pmatrix} x \\ 0 \\ z \end{pmatrix} \mapsto \begin{pmatrix} x\left(\frac{\varepsilon}{z}\right)^{\rho/\lambda} \cos\left(\frac{\omega}{\lambda} \log \frac{\varepsilon}{z}\right) \\ x\left(\frac{\varepsilon}{z}\right)^{\rho/\lambda} \sin\left(\frac{\omega}{\lambda} \log \frac{\varepsilon}{z}\right) \\ \varepsilon \end{pmatrix}. \tag{27.3.5}$$

We now consider Π_0 more carefully. For Π_0 arbitrarily chosen it is possible for points on Π_0 to intersect Π_0 many times before reaching Π_1. In this case, P_0 would not map Π_0 diffeomorphically onto $P_0(\Pi_0)$. We want to avoid this situation, since the conditions for a map to possess the dynamics of the shift map described in Section 25 are given for diffeomorphisms. According to (27.3.2), it takes time $t = 2\pi/\omega$ for a point starting in the $x - z$ plane with $x > 0$ to return to the $x - z$ plane with $x > 0$. Now let $x = \varepsilon$, $0 < z \leq \varepsilon$ be the right-hand boundary of Π_0. Then if we choose $x = \varepsilon e^{2\pi\rho/\omega}$, $0 < z \leq \varepsilon$ to be the left-hand boundary of Π_0, no point starting in the interior of Π_0 returns to Π_0 before reaching Π_1. We take this as the definition of Π_0:

$$\Pi_0 = \left\{(x, y, z) \in \mathbb{R}^3 \,|\, y = 0,\ \varepsilon e^{2\pi\rho/\omega} \leq x \leq \varepsilon,\ 0 < z \leq \varepsilon\right\}. \tag{27.3.6}$$

Π_1 is chosen large enough to contain $P_0(\Pi_0)$ in its interior.

We now want to describe the geometry of $P_0(\Pi_0)$. Π_1 is coordinatized by x and y, which we will label as x', y' to avoid confusion with the coordinates of Π_0. Then, from (27.3.5), we have

$$(x', y') = \left(x\left(\frac{\varepsilon}{z}\right)^{\rho/\lambda} \cos\left(\frac{\omega}{\lambda} \log \frac{\varepsilon}{z}\right), x\left(\frac{\varepsilon}{z}\right)^{\rho/\lambda} \sin\left(\frac{\omega}{\lambda} \log \frac{\varepsilon}{z}\right)\right). \tag{27.3.7}$$

Polar coordinates on Π_1 give a clearer picture of the geometry. Let

$$r = \sqrt{x'^2 + y'^2}, \qquad \frac{y'}{x'} = \tan\theta.$$

Then (27.3.7) becomes

$$(r, \theta) = \left(x\left(\frac{\varepsilon}{z}\right)^{\rho/\lambda}, \frac{\omega}{\lambda} \log \frac{\varepsilon}{z}\right). \tag{27.3.8}$$

Now consider a vertical line in Π_0, i.e., a line with $x =$ constant. By (27.3.8) it gets mapped into a logarithmic spiral. A horizontal line in Π_0, i.e., a line with $z =$ constant, gets mapped onto a radial line emanating from $(0, 0, \varepsilon)$. Consider the rectangles

$$\begin{aligned} R_k = \big\{(x, y, z) \in \mathbb{R}^3 \,|\, y = 0,\ & \varepsilon e^{\frac{2\pi\rho}{\omega}} \leq x \leq \varepsilon, \\ & \varepsilon e^{\frac{-2\pi(k+1)\lambda}{\omega}} \leq z \leq \varepsilon e^{\frac{-2\pi k\lambda}{\omega}}\big\}. \end{aligned} \tag{27.3.9}$$

Then we have

$$\Pi_0 = \bigcup_{k=0}^{\infty} R_k.$$

We study the geometry of the image of a rectangle R_k by determining the behavior of its horizontal and vertical boundaries under P_0. We denote these four line segments as

$$\begin{aligned}
h^u &= \left\{(x,y,z) \in \mathbb{R}^3 \,|\, y = 0,\ z = \varepsilon e^{\frac{-2\pi k\lambda}{\omega}}, \varepsilon e^{\frac{2\pi\rho}{\omega}} \le x \le \varepsilon\right\},\\
h^\ell &= \left\{(x,y,z) \in \mathbb{R}^3 \,|\, y = 0,\ z = \varepsilon e^{\frac{-2\pi(k+1)\lambda}{\omega}}, \varepsilon e^{\frac{2\pi\rho}{\omega}} \le x \le \varepsilon\right\},\\
v^r &= \left\{(x,y,z) \in \mathbb{R}^3 \,|\, y = 0,\ x = \varepsilon, \varepsilon e^{\frac{-2\pi(k+1)\lambda}{\omega}} \le z \le \varepsilon e^{\frac{-2\pi k\lambda}{\omega}}\right\},\\
v^\ell &= \left\{(x,y,z) \in \mathbb{R}^3 \,|\, y = 0,\ x = \varepsilon e^{\frac{2\pi\rho}{\omega}}, \varepsilon e^{\frac{-2\pi(k+1)\lambda}{\omega}} \le z \le \varepsilon e^{\frac{-2\pi k\lambda}{\omega}}\right\};
\end{aligned} \tag{27.3.10}$$

see Figure 27.3.3. The images of these line segments under P_0 are given by

$$\begin{aligned}
P_0(h^u) &= \left\{(r,\theta,z) \in \mathbb{R}^3 \,|\, z = \varepsilon, \theta = 2\pi k, \varepsilon e^{\frac{2\pi(k+1)\rho}{\omega}} \le r \le \varepsilon e^{\frac{2\pi k\rho}{\omega}}\right\},\\
P_0(h^\ell) &= \left\{(r,\theta,z) \in \mathbb{R}^3 \,|\, z = \varepsilon, \theta = 2\pi(k+1), \varepsilon e^{\frac{2\pi(k+2)\rho}{\omega}} \le r \le \varepsilon e^{\frac{2\pi(k+1)\rho}{\omega}}\right\},\\
P_0(v^r) &= \left\{(r,\theta,z) \in \mathbb{R}^3 \,|\, z = \varepsilon, 2\pi k \le \theta \le 2\pi(k+1), r(\theta) = \varepsilon e^{\frac{\rho\theta}{\omega}}\right\},\\
P_0(v^\ell) &= \left\{(r,\theta,z) \in \mathbb{R}^3 \,|\, z = \varepsilon, 2\pi k \le \theta \le 2\pi(k+1), r(\theta) = \varepsilon e^{\frac{\rho(2\pi+\theta)}{\omega}}\right\},
\end{aligned} \tag{27.3.11}$$

so that $P_0(R_k)$ appears as in Figure 27.3.3.

The geometry of Figure 27.3.3 should give a strong indication that horseshoes may arise in this system.

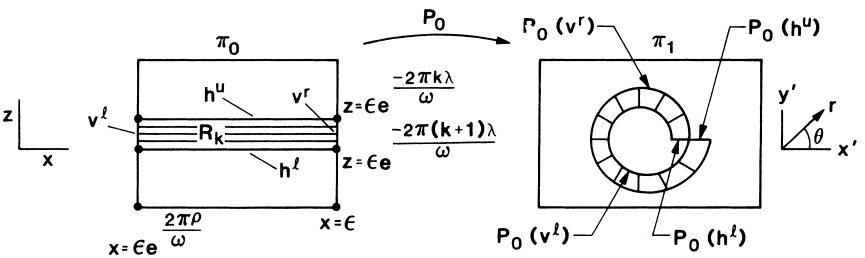

FIGURE 27.3.3.

Computation of P_1

From the discussion at the beginning of this section, we approximate P_1 by an affine map as follows

$$P_1 : \Pi_1 \to \Pi_0,$$
$$\begin{pmatrix} x \\ y \\ \varepsilon \end{pmatrix} \mapsto \begin{pmatrix} a & b & 0 \\ 0 & 0 & 0 \\ c & d & 0 \end{pmatrix} \begin{pmatrix} x \\ y \\ 0 \end{pmatrix} + \begin{pmatrix} \overline{x} \\ 0 \\ 0 \end{pmatrix}, \tag{27.3.12}$$

where $(\overline{x}, 0, 0) \equiv \Gamma \cap \Pi_0$ is the intersection of the homoclinic orbit with Π_0 (note: by our choice of Π_0, Γ intersects Γ_0 only once). We remark that the structure of the 3×3 matrix in (27.3.12) comes from the fact that the coordinates of Π_1 are x and y with $z = \varepsilon =$ constant and the coordinates of Π_0 are x and z with $y = 0$.

The Poincaré Map $P \equiv P_1 \circ P_0$

Composing (27.3.5) and (27.3.12) gives

$$P \equiv P_1 \circ P_0 : \Pi_0 \to \Pi_0,$$
$$\begin{pmatrix} x \\ z \end{pmatrix} \mapsto \begin{pmatrix} x \left(\frac{\varepsilon}{z}\right)^{\rho/\lambda} \left[a \cos\left(\frac{\omega}{\lambda} \log \frac{\varepsilon}{z}\right) + b \sin\left(\frac{\omega}{\lambda} \log \frac{\varepsilon}{z}\right)\right] + \overline{x} \\ x \left(\frac{\varepsilon}{z}\right)^{\rho/\lambda} \left[c \cos\left(\frac{\omega}{\lambda} \log \frac{\varepsilon}{z}\right) + d \sin\left(\frac{\omega}{\lambda} \log \frac{\varepsilon}{z}\right)\right] \end{pmatrix}, \tag{27.3.13}$$

where Π_0 is chosen sufficiently small (by taking ε small). Thus, $P(\Pi_0)$ appears as in Figure 27.3.4.

Our goal is to show that P contains an invariant Cantor set on which it is topologically conjugate to a full shift on (at least) two symbols.

Consider the rectangle R_k shown in Figure 27.3.5. In order to verify the proper behavior of horizontal and vertical strips in R_k, it will be necessary to verify that the inner and outer boundaries of $P(R_k)$ both intersect the upper boundary of R_k as shown in Figure 27.3.5 or, in other words, the upper horizontal boundary of R_k intersects (at least) two points of the inner boundary of $P(R_k)$. Additionally, it will be useful to know how many rectangles above R_k $P(R_k)$ also intersects in this manner. We have the following lemma.

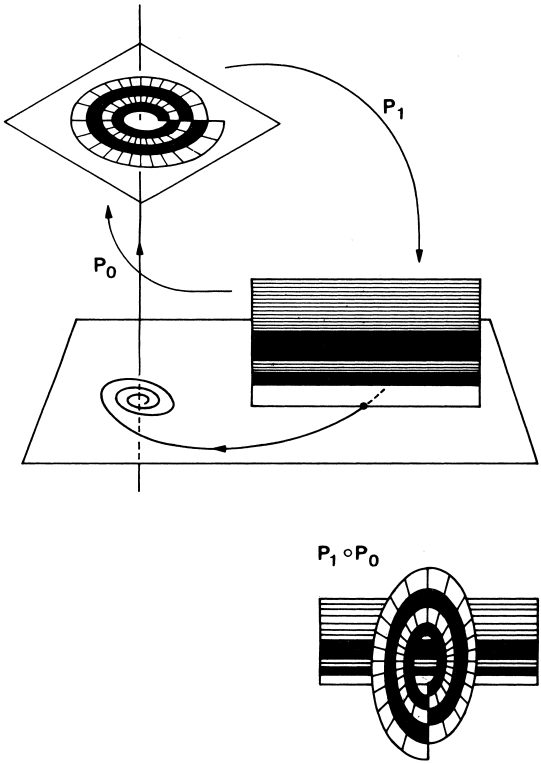

FIGURE 27.3.4.

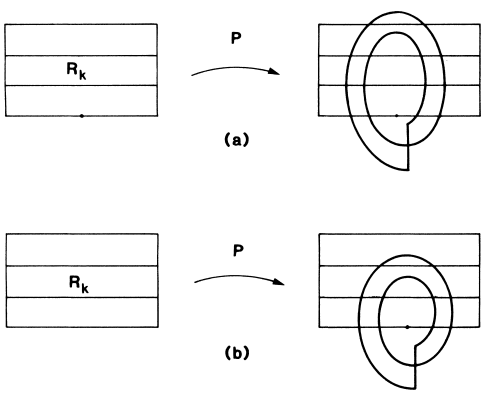

FIGURE 27.3.5. Two possibilities for $P(R_k) \cap R_k$.

Lemma 27.3.1 *Consider R_k for fixed k sufficiently large. Then the inner boundary of $P(R_k)$ intersects the upper horizontal boundary of R_i in (at least) two points for $i \geq k/\alpha$ where $1 \leq \alpha < -\lambda/\rho$. Moreover, the preimage of the vertical boundaries of $P(R_k) \cap R_i$ is contained in the vertical boundary of R_k.*

Proof: The z coordinate of the upper horizontal boundary of R_i is given by

$$\overline{z} = \varepsilon e^{\frac{-2\pi i\lambda}{\omega}}, \tag{27.3.14}$$

and the point on the inner boundary of $P_0(R_k)$ closest to $(0, 0, \varepsilon)$ is given by

$$r_{\min} = \varepsilon e^{\frac{4\pi\rho}{\omega}} e^{\frac{2\pi k\rho}{\omega}}. \tag{27.3.15}$$

Since P_1 is an affine map, the bound on the inner boundary of $P(R_k) = P_1 \circ P_0(R_k)$ can be expressed as

$$\overline{r}_{\min} = K\varepsilon e^{\frac{4\pi\rho}{\omega}} e^{\frac{2\pi k\rho}{\omega}} \tag{27.3.16}$$

for some $K > 0$. The inner boundary of $P(R_k)$ will intersect the upper horizontal boundary of R_i in (at least) two points provided

$$\frac{\overline{r}_{\min}}{\overline{z}} > 1. \tag{27.3.17}$$

Using (27.3.14) and (27.3.16), we compute this ratio explicitly and find

$$\frac{\overline{r}_{\min}}{\overline{z}} = Ke^{\frac{4\pi\rho}{\omega}} e^{\frac{2\pi}{\omega}(k\rho+i\lambda)}. \tag{27.3.18}$$

Because $Ke^{4\pi\rho/\omega}$ is a fixed constant, the size of (27.3.18) is controlled by the $e^{(2\pi/\omega)(k\rho+i\lambda)}$ term. In order to make (27.3.18) larger than one, it is sufficient that $k\rho + i\lambda$ is taken sufficiently large. By Assumption 2 we have $\lambda + \rho > 0$, so for $i \geq k/\alpha$, $1 \leq \alpha < -\lambda/\rho$, $k\rho + i\lambda$ is positive, and for k sufficiently large, (27.3.18) is larger than one.

We now describe the behavior of the vertical boundaries of R_k. Recall Figure 27.3.5a. Under P_0 the vertical boundaries of R_k map to the inner and outer boundaries of an annulus-like object. P_1 is an invertible affine map; hence, the inner and outer boundaries of $P_0(R_k)$ correspond to the inner and outer boundaries of $P(R_k) = P_1 \circ P_0(R_k)$. Therefore, the preimage of the vertical boundary of $P(R_k) \cap R_i$ is contained in the vertical boundary of R_k. □

Lemma 27.3.1 points out the necessity of Assumption 2, since, if we had instead $-\rho > \lambda > 0$, then the image of R_k would fall below R_k for k sufficiently large, as shown in Figure 27.3.5b.

We now can state our main theorem.

Theorem 27.3.2 *For k sufficiently large, R_k contains an invariant Cantor set, Λ_k, on which the Poincaré map P is topologically conjugate to a full shift on two symbols.*

Proof: The proof is very similar to the proof of both Moser's theorem (see Section 26) and Theorem 27.2.2. In R_k we must find two disjoint μ_h-horizontal strips that are mapped over themselves in μ_v-vertical strips on which Assumptions 1 and 3 of Section 25 hold.

The fact that such μ_h-horizontal strips can be found on which Assumption 1 holds follows from Lemma 27.3.1. The fact that Assumption 3 holds follows from a calculation similar to that given in Moser's theorem and Theorem 27.2.2. In the exercises we outline how one fills in the details of this proof. □

We make several remarks.

Remark 1. The dynamics of P are often described by the phrase "P has a countable infinity of horseshoes."

Remark 2. Note from Lemma 27.3.1 that the horseshoes in the different R_k can interact. This would lead to different ways of setting up the symbolic dynamics. We will deal with this issue in the exercises.

Remark 3. If one were to break the homoclinic orbit with a perturbation, then only a finite number of the Λ_k would survive. We deal with this issue in the exercises.

27.3A The Bifurcation Analysis of Glendinning and Sparrow

Now that we have seen how complicated the orbit structure is in the neighborhood of an orbit homoclinic to a fixed point of saddle-focus type, we want to get an understanding of how this situation occurs as the homoclinic orbit is created. In this regard, the analysis given by Glendinning and Sparrow [1984] is insightful.

Suppose that the homoclinic orbit in (27.3.1) depends on a scalar parameter μ in the manner shown in Figure 27.3.6.

We construct a parameter-dependent Poincaré map in the same manner as when we discussed the case of a fixed point with all real eigenvalues. This map is given by

$$\begin{pmatrix} x \\ z \end{pmatrix} \mapsto \begin{pmatrix} x\left(\frac{\varepsilon}{z}\right)^{\rho/\lambda}\left[a\cos\frac{\omega}{\lambda}\log\frac{\varepsilon}{z} + b\sin\frac{\omega}{\lambda}\log\frac{\varepsilon}{z}\right] + e\mu + \overline{x} \\ \\ x\left(\frac{\varepsilon}{z}\right)^{\rho/\lambda}\left[c\cos\frac{\omega}{\lambda}\log\frac{\varepsilon}{z} + d\sin\frac{\omega}{\lambda}\log\frac{\varepsilon}{z}\right] + f\mu \end{pmatrix}, \quad (27.3.19)$$

where, from Figure 27.3.6, we have $f > 0$. We have already seen that this map possesses a countable infinity of horseshoes at $\mu = 0$, and we know that each horseshoe contains periodic orbits of all periods. To study how the horseshoes are formed in this situation as the homoclinic orbit is formed is a difficult (and unsolved) problem. We will tackle a more modest

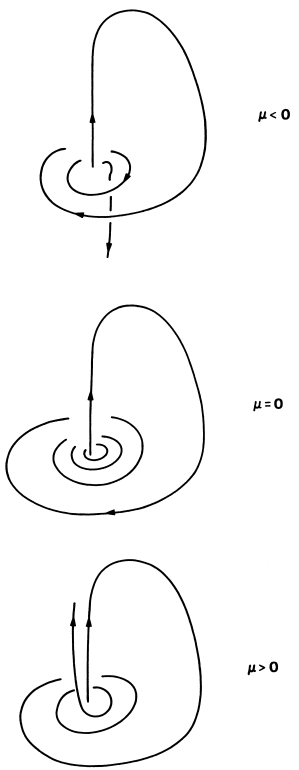

FIGURE 27.3.6.

problem which will still give us a good idea about some things that are happening; namely, we will study the fixed points of the above map. Recall that the fixed points correspond to periodic orbits which pass through a neighborhood of the origin *once* before closing up. First we put the map in a form which will be easier to work with. The map can be written in the form

$$\begin{pmatrix} x \\ z \end{pmatrix} \mapsto \begin{pmatrix} x\left(\frac{\varepsilon}{z}\right)^{\rho/\lambda} p\cos\left(\frac{\omega}{\lambda}\log\frac{\varepsilon}{z}+\phi_1\right)+e\mu+\overline{x} \\ \\ x\left(\frac{\varepsilon}{z}\right)^{\rho/\lambda} q\cos\left(\frac{\omega}{\lambda}\log\frac{\varepsilon}{z}+\phi_2\right)+\mu \end{pmatrix}, \tag{27.3.20}$$

where we have rescaled μ so that $f = 1$ (note that f must be positive).

Now let

$$-\delta = \frac{\rho}{\lambda}, \quad \alpha = p\varepsilon^{-\delta}, \quad \beta = q\varepsilon^{-\delta},$$
$$\xi = -\frac{\omega}{\lambda}, \quad \Phi_1 = \frac{\omega}{\lambda}\log\varepsilon + \phi_1, \quad \Phi_2 = \frac{\omega}{\lambda}\log\varepsilon + \phi_2.$$

Then the map takes the form

$$\begin{pmatrix} x \\ z \end{pmatrix} \mapsto \begin{pmatrix} \alpha x z^\delta \cos(\xi\log z + \Phi_1) + e\mu + \overline{x} \\ \beta x z^\delta \cos(\xi\log z + \Phi_2) + \mu \end{pmatrix}. \tag{27.3.21}$$

Now we will study the fixed points of this map and their stability and bifurcations.

Fixed Points

The fixed points are found by solving

$$x = \alpha x z^\delta \cos(\xi\log z + \Phi_1) + e\mu + \overline{x}, \tag{27.3.22}$$

$$z = \beta x z^\delta \cos(\xi\log z + \Phi_2) + \mu. \tag{27.3.23}$$

Solving (27.3.22) for x as a function of z gives

$$x = \frac{e\mu + \overline{x}}{1 - \alpha z^\delta \cos(\xi\log z + \Phi_1)}. \tag{27.3.24}$$

Substituting (27.3.24) into (27.3.23) gives

$$(z-\mu)(1-\alpha z^{\delta}\cos(\xi\log z+\Phi_1)) = (e\mu+\overline{x})\beta z^{\delta}\cos(\xi\log z+\Phi_2). \quad (27.3.25)$$

Solving (27.3.25) gives us the z-component of the fixed point; substituting this into (27.3.22) gives us the x-component of the fixed point. In order to obtain an idea about the solutions of (27.3.25) we will assume that z is so small that

$$1-\alpha z^{\delta}\cos(\xi\log z+\Phi_1)\sim 1; \quad (27.3.26)$$

then the equation of the z component of the fixed point will be

$$(z-\mu) = (e\mu+\overline{x})\beta z^{\delta}\cos(\xi\log z+\Phi_2). \quad (27.3.27)$$

We solve (27.3.27) graphically by drawing the graph of both the right- and left-hand sides of (27.3.27) and looking for points of intersection. There are various cases shown in Figure 27.3.7.

$\underline{\delta<1}$. In the the case $\delta<1$, we have

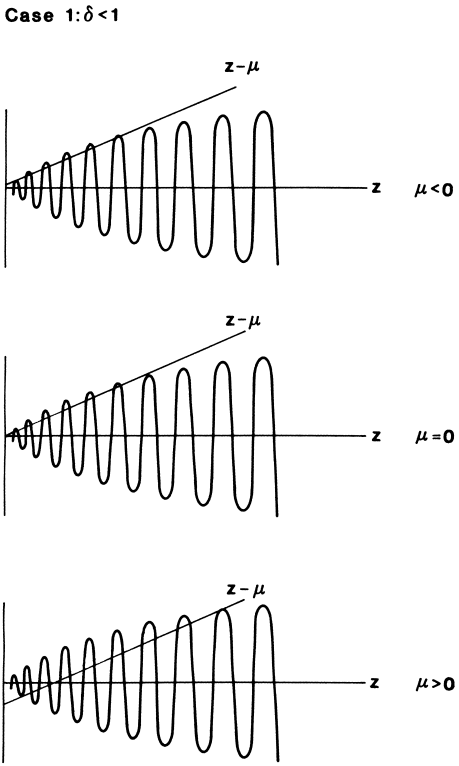

FIGURE 27.3.7. Graphical construction of the solutions of (27.3.27) for $\delta<1$.

$\mu < 0$**:** finite number of fixed points;

$\mu = 0$**:** countable infinity of fixed points;

$\mu > 0$**:** finite number of fixed points.

$\underline{\delta > 1}$. The next case is $\delta > 1$, i.e., Assumption 2 does not hold. We show the results in Figure 27.3.8. In the case $\delta > 1$, we have

$\mu \leq 0$**:** there are no fixed points except the one at $z = \mu = 0$ (i.e., the homoclinic orbit).

$\mu > 0$**:** For $z > 0$, there is one fixed point for each μ. This can be seen as follows: the slope of the wiggly curve is of order $z^{\delta-1}$, which is small for z small, since $\delta > 1$. Thus, the $z - \mu$ line intersects it only once.

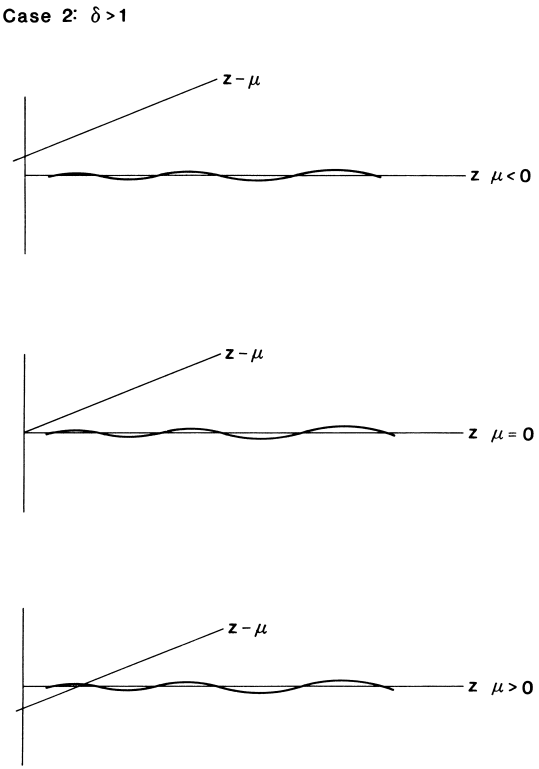

FIGURE 27.3.8. Graphical construction of the solutions of (27.3.27) for $\delta > 1$.

Again, the fixed points which we have found correspond to periodic orbits of the parametrized version of (27.3.1) which pass *once* through a neighborhood of zero before closing up. Our knowledge of these fixed points allows us to draw the following bifurcation diagrams in Figure 27.3.9.

The $\delta > 1$ diagram should be clear; however, the $\delta < 1$ diagram may be confusing. The wiggly curve in the diagram above represents periodic orbits. It should be clear from Figure 27.3.9 that periodic orbits are born in pairs, and the one with the lower z value has the higher period (since it passes closer to the fixed point). We will worry more about the structure of this curve as we proceed.

Stability of the Fixed Points

The Jacobian of the map is given by

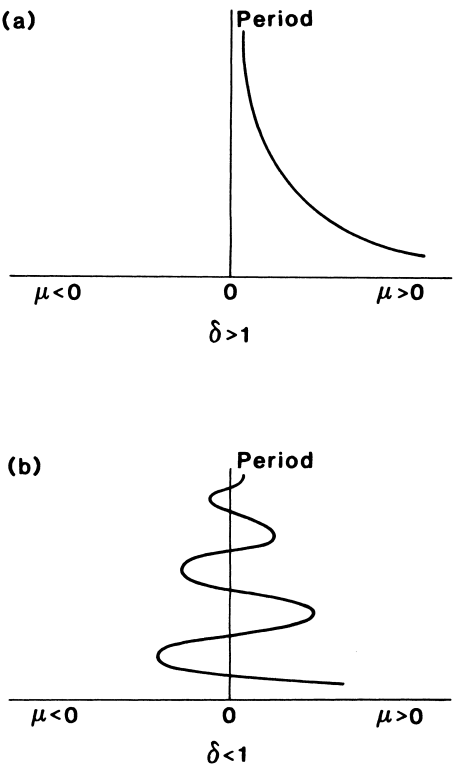

FIGURE 27.3.9. a) $\delta > 1$. b) $\delta < 1$.

$$\begin{pmatrix} A & C \\ D & B \end{pmatrix},$$

where

$$\begin{aligned} A &= \alpha z^{\delta} \cos(\xi \log z + \Phi_1), \\ B &= \beta x z^{\delta-1}[\delta \cos(\xi \log z + \Phi_2) - \xi \sin(\xi \log z + \Phi_2)], \\ C &= \alpha x z^{\delta-1}[\delta \cos(\xi \log z + \Phi_1) - \xi \sin(\xi \log z + \Phi_1)], \\ D &= \beta z^{\delta} \cos(\xi \log z + \Phi_2). \end{aligned} \tag{27.3.28}$$

The eigenvalues of the matrix are given by

$$\lambda_{1,2} = \frac{1}{2}\left\{(A+B) \pm \sqrt{(A+B)^2 - 4(AB-CD)}\right\}. \tag{27.3.29}$$

$\underline{\delta > 1}$. For $\delta > 1$, it should be clear that the eigenvalues will be small if z is small (since both z^{δ} and $z^{\delta-1}$ are small). Hence, for $\delta > 1$, the one periodic orbit existing for $\mu > 0$ is stable for μ small, and the homoclinic orbit at $\mu = 0$ is an attractor.

The case $\delta < 1$ is more complicated.

$\underline{\delta < 1}$. First notice that the determinant of the matrix given by $AB - CD$ only contains terms of order $z^{2\delta-1}$, so the map will be

area-contracting	$\frac{1}{2} < \delta < 1$,
area-expanding	$0 < \delta < \frac{1}{2}$,

for z sufficiently small.

We would thus expect different results in these two different δ ranges.

Now recall that the wiggly curve whose intersection with $z - \mu$ gave the fixed points was given by

$$(e\mu + \overline{x})\beta z^{\delta} \cos(\xi \log z + \Phi_2).$$

Thus, from (27.3.28), a fixed point corresponding to a maximum of this curve corresponds to $B = 0$, and a fixed point corresponding to a zero crossing of this curve corresponds to $D = 0$. We now want to look at the stability of fixed points satisfying these conditions.

$\underline{D = 0}$. In this case $\lambda_1 = A$, $\lambda_2 = B$. Thus, for z small, λ_1 is small and λ_2 is always large; hence, the fixed point is a saddle. Note in particular that,

for $\mu = 0$, D is very close to zero; hence all periodic orbits will be saddles as expected.

$\underline{B = 0}$. The eigenvalues are given by

$$\lambda_{1,2} = \frac{1}{2}\left[A \pm \sqrt{A^2 + 4CD}\right],$$

and both eigenvalues will have large or small modulus depending on whether CD is large or small, since

$A^2 \sim z^{2\delta}$ can be neglected compared with $CD \sim z^{2\delta-1}$,
$A \sim z^{\delta}$ can be neglected compared with $\sqrt{CD} \sim z^{\delta-(1/2)}$.

Whether or not CD is small depends on whether $0 < \delta < \frac{1}{2}$ or $\frac{1}{2} < \delta < 1$. Hence, we have

stable fixed points for $\frac{1}{2} < \delta < 1$.
unstable fixed points for $0 < \delta < \frac{1}{2}$.

Now we want to put everything together for other z values (i.e., for z such that $B, D \neq 0$).

Consider Figure 27.3.10, which is a blow-up of Figure 27.3.7 for various parameter values. In this figure the intersection of the two curves gives us the z coordinate of the fixed points.

Now we describe what happens at each parameter value shown in Figure 27.3.10.

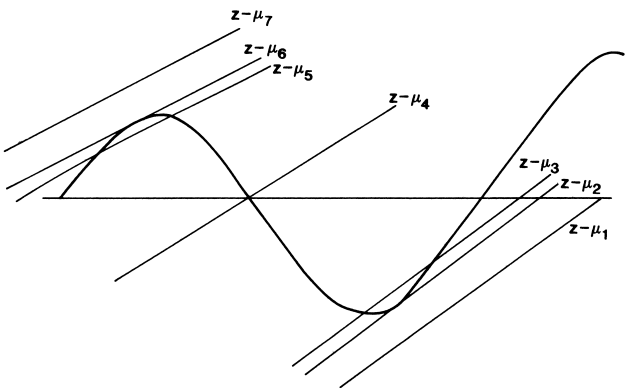

FIGURE 27.3.10.

$\mu = \mu_6$**:** At this point we have a tangency, and we know that a saddle-node pair will be born in a saddle-node bifurcation.

$\mu = \mu_5$**:** At this point we have two fixed points; the one with the lower z value has the larger period. Also, the one at the maximum of the curve has $B = 0$; therefore, it is stable for $\delta > \frac{1}{2}$, unstable for $\delta < \frac{1}{2}$. The other fixed point is a saddle.

$\mu = \mu_4$**:** At this point the stable (unstable) fixed point has become a saddle since $D = 0$. Therefore, it must have changed its stability type via a period-doubling bifurcation.

$\mu = \mu_3$**:** At this point $B = 0$ again; therefore, the saddle has become either purely stable or unstable again. This must have occurred via a reverse period-doubling bifurcation.

$\mu = \mu_2$**:** A saddle-node bifurcation occurs.

Hence, we finally arrive at Figure 27.3.11.

Next we want to get an idea of the size of the "wiggles" in Figure 27.3.11 because, if the wiggles are small, that implies that the one-loop periodic orbits are only visible for a narrow range of parameters. If the wiggles are large, we might expect there to be a greater likelihood of observing the periodic orbits.

Let us denote the parameter values at which the tangent to the curve in Figure 27.3.11 is vertical by

$$\mu_i, \mu_{i+1}, \cdots, \mu_{i+n}, \cdots \to 0, \tag{27.3.30}$$

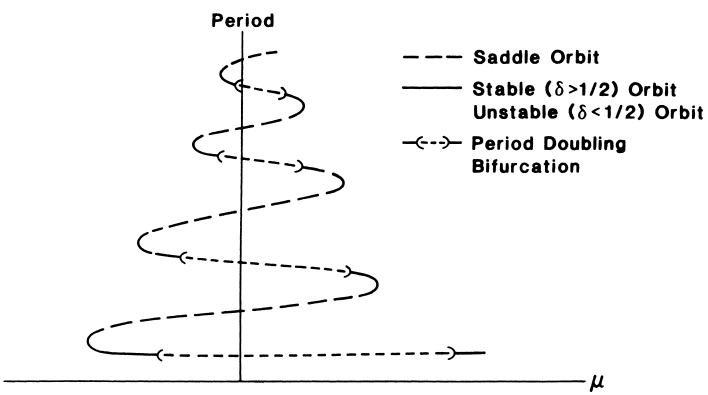

FIGURE 27.3.11.

where the μ_i alternate in sign. Now recall that the z component of the fixed point was given by the solutions to the equations

$$z - \mu = (e\mu + \overline{x})\beta z^{\delta} \cos(\xi \log z + \Phi_2). \tag{27.3.31}$$

Thus, we have

$$z_i - \mu_i = (e\mu_i + \overline{x})\beta z_i^{\delta} \cos(\xi \log z_i + \Phi_2), \tag{27.3.32}$$

$$z_{i+1} - \mu_{i+1} = (e\mu_{i+1} + \overline{x})\beta z_{i+1}^{\delta} \cos(\xi \log z_{i+1} + \Phi_2). \tag{27.3.33}$$

From (27.3.32) and (27.3.33), we obtain

$$\mu_i = \frac{z_i - \overline{x}\beta z_i^{\delta} \cos(\xi \log z_i + \Phi_2)}{1 + e\beta z_i^{\delta} \cos(\xi \log z_i + \Phi_2)}, \tag{27.3.34}$$

$$\mu_{i+1} = \frac{z_{i+1} - \overline{x}\beta z_{i+1}^{\delta} \cos(\xi \log z_{i+1} + \Phi_2)}{1 + e\beta z_{i+1}^{\delta} \cos(\xi \log z_{i+1} + \Phi_2)}. \tag{27.3.35}$$

Now note that we have

$$\xi \log z_{i+1} - \xi \log z_i \approx \pi \Rightarrow \frac{z_{i+1}}{z_i} \approx \exp \frac{\pi}{\xi}, \tag{27.3.36}$$

and we assume that $z << 1$ so that

$$1 + e\beta z_{i(i+1)}^{\delta} \cos(\xi \log z_{i(i+1)} + \Phi_2) \sim 1. \tag{27.3.37}$$

Finally, we obtain

$$\frac{\mu_{i+1}}{\mu_i} = \frac{z_{i+1} + [\overline{x}\beta \cos(\xi \log z_i + \Phi_2)] z_{i+1}^{\delta}}{z_i - [\overline{x}\beta \cos(\xi \log z_i + \Phi_2)] z_i^{\delta}}. \tag{27.3.38}$$

Now, in the limit as $z \to 0$, (27.3.38) becomes

$$\frac{\mu_{i+1}}{\mu_i} \approx -\left(\frac{z_{i+1}}{z_i}\right)^{\delta} \approx -\exp\left(\frac{\pi\delta}{\xi}\right). \tag{27.3.39}$$

Recall that $\delta = -\rho/\lambda$, $\xi = -\omega/\lambda$. We thus obtain

$$\lim_{i \to \infty} \frac{\mu_{i+1}}{\mu_i} = -\exp \frac{\rho\pi}{\omega}. \tag{27.3.40}$$

This quantity governs the size of the oscillations we see in Figure 27.3.11.

27.3B Double-Pulse Homoclinic Orbits

Now we will show that, as we break our original homoclinic orbit (the *principal* homoclinic orbit), other homoclinic orbits of a different nature arise, and the Silnikov picture is repeated for these new homoclinic orbits. This phenomenon was first noted by Hastings [1982], Evans et al. [1982], Gaspard [1983], and Glendinning and Sparrow [1984]. We follow the argument of Gaspard.

When we break the homoclinic orbit, the unstable manifold intersects Π_0 at the point $(e\mu + \overline{x}, \mu)$. Thus, if $\mu > 0$, this point can be used as an initial condition for our map. Now, if the z component of the image of this point is zero, we will have found a new homoclinic orbit which passes once through a neighborhood of the origin before falling back into the origin. This condition is given by

$$0 = \beta(e\mu + \overline{x})\mu^{\delta} \cos(\xi \log \mu + \Phi_2) + \mu \tag{27.3.41}$$

or

$$-\mu = \beta(e\mu + \overline{x})\mu^{\delta} \cos(\xi \log \mu + \Phi_2). \tag{27.3.42}$$

We find the solutions for this graphically for $\delta > 1$ and $\delta < 1$ in the same manner as we investigated the equations for the fixed points; see Figure 27.3.12.

Thus, for $\underline{\delta > 1}$, the only homoclinic orbit is the principal homoclinic orbit which exists at $\mu = 0$.

For $\underline{\delta < 1}$, we get a countable infinity of μ values

$$\mu_i, \mu_{i+1}, \cdots, \mu_{i+n}, \cdots \to 0, \tag{27.3.43}$$

for which these *subsidiary* or *double-pulse* homoclinic orbits exist, as shown in Figure 27.3.13.

Note for each of these homoclinic orbits, we can reconstruct our original Silnikov picture of a countable infinity of horseshoes. For a reference dealing with double-pulse homoclinic orbits for the case of real eigenvalues, see Yanagida [1987].

27.3C Observations and General Remarks

We end this section with some final observations and remarks.

Remark 1: Comparison Between the Saddle with Real Eigenvalues and the Saddle-Focus. Before leaving three dimensions, we want to re-emphasize the main differences between the two cases studied.

Real Eigenvalues. In order to have horseshoes it was necessary to start with two homoclinic orbits. Even so, there were no horseshoes near the homoclinic orbits until the homoclinic orbits were broken such as might happen by varying a parameter. It was necessary to know the global twisting of orbits around the homoclinic orbits in order to determine how the horseshoe was formed.

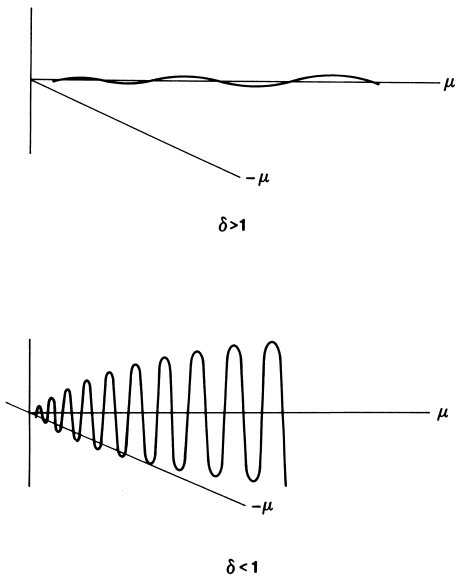

FIGURE 27.3.12. Graphical construction of the solutions of (27.3.42).

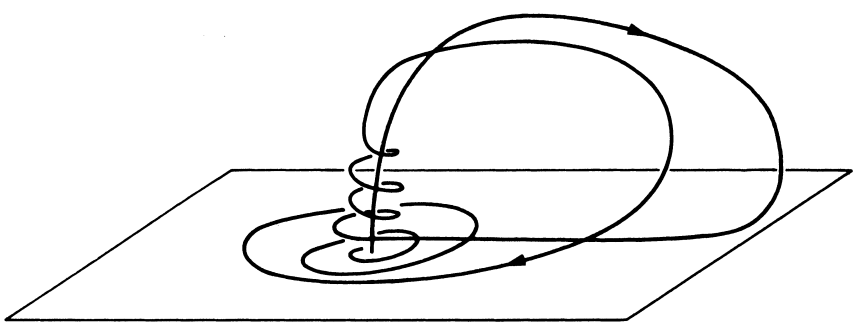

FIGURE 27.3.13.

Complex Eigenvalues. One homoclinic orbit is sufficient for a countable infinity of horseshoes whose existence does not require first breaking the homoclinic connection. Knowledge of global twisting around the homoclinic orbit is unnecessary, since the spiralling associated with the imaginary part of the eigenvalues tends to "smear" trajectories uniformly around the homoclinic orbit.

There is an extensive amount of work on Silnikov's phenomenon. Below we give some references.

Remark 2: Strange Attractors. Silnikov-type attractors have not attracted the great amount of attention that has been given to Lorenz attractors. The topology of the spiralling associated with the imaginary parts of the eigenvalues makes the Silnikov problem more difficult, but see Gonchenko et al. [1997] and Homburg [2002].

Remark 3: Creation of the Horseshoes and Bifurcation Analysis. We have given part of the bifurcation analysis of Glendinning and Sparrow [1984]. Their paper also contains some interesting numerical work and conjectures. The reader should also consult Gaspard, Kapral, and Nicolis [1984] and Gonchenko et al. [1997].

Remark 4: Nonhyperbolic Fixed Points. See Deng [1990], Deng [1992], Lyubimov and Byelousova [1993], Hirschberg and Knobloch [1993], Champneys, Harterich, and Sandstede [1996], and Champneys and Rodriguez-Luis [1999].

Remark 5: Applications. The Silnikov phenomenon arises in a variety of applications. See, for example, Arneodo, Coullet, and Tresser [1981a,b], [1985], Arneodo, Coullet, Spiegel, and Tresser [1985], Arneodo, Coullet, and Spiegel [1982], Gaspard and Nicolis [1983], Hastings [1982], Pikovskii, Rabinovich, and Trakhtengerts [1979], Rabinovich [1978], Rabinovich and Fabrikant [1979], Roux, Rossi, Bachelart, and Vidal [1981], Vyshkind and Rabinovich [1976], Arnéodo et al. [1993], and Wang [1993].

Remark 6: The General Technique for Analyzing the Orbit Structure Near Homoclinic Orbits. The reader should note the similarities between the analyses of the orbit structure near orbits homoclinic to 1) hyperbolic periodic points of two-dimensional diffeomorphisms (or, equivalently, hyperbolic periodic orbits of autonomous, three-dimensional vector fields); 2) hyperbolic fixed points of three-dimensional autonomous vector fields having purely real eigenvalues; and 3) hyperbolic fixed points of three-dimensional autonomous vector fields having a pair of complex conjugate eigenvalues. In

all three cases a return map was constructed in a neighborhood of a point along the homoclinic orbit that consisted of the composition of two maps. One map described the dynamics near the hyperbolic invariant set (i.e., periodic orbit or fixed point) and the other map described the dynamics near the homoclinic orbit outside of a neighborhood of the hyperbolic invariant set. Due to the fact that the fixed point is hyperbolic, the first map is well approximated from the linearization of the dynamical system (either map or vector field) about the hyperbolic invariant set (either periodic orbit or fixed point). The second map, if we restrict ourselves to a sufficiently small neighborhood of the homoclinic orbit, is well approximated by an affine map. In all cases, in order to show that chaotic invariant sets (more precisely, an invarant Cantor set on which the dynamics are topologically conjugate to a full shift on N symbols) are present near the homoclinic orbit, we find N μ_h-horizontal strips that are mapped over themselves in μ_v-vertical strips so that Assumptions 1 and 3 of Chapter 25 hold. The nature of the map near the hyperbolic invariant set is responsible for the verification of Assumption 3 (i.e., expansion and contraction in the appropriate directions). The nature of the map outside of the hyperbolic invariant set is responsible for the verification of Assumption 1. However, note that in the case of transversal orbits homoclinic to hyperbolic periodic orbits of n-dimensional diffeomorphisms, we did not need any special assumptions on the eigenvalues of the periodic orbit or the nature of the intersection of the stable and unstable manifolds (hyperbolicity and transversality were sufficient). This is very different from the situation of orbits homoclinic to hyperbolic fixed points of autonomous vector fields, where special assumptions on the relative magnitudes of the eigenvalues at the fixed point and the nature of the (nontransversal) homoclinic orbit(s) were necessary.

Remark 7: Higher Dimensional Results. For generalizations to orbits homoclinic to hyperbolic fixed points of n-dimensional ($n \geq 4$) autonomous vector fields, the reader should consult Turaev and Silnikov [1987], Ovsyannikov and Silnikov [1987], Deng [1989a], [1989b], [1993], Chow, Deng, and Fiedler [1990], Ovsyannikov and Silnikov [1992], Arnold et al. [1994],and Homburg [1996], Glendinning [1997], Ashwin [1997], Ragazzo [1997], Laing and Glendinning [1997], Fowler [1990], Chernyshev [1985], and Glendinning and Laing [1996].

Remark 8: Numerical Methods. See Champneys, Kuznetsov, and Sandstede [1996] for a review of numerical methods for computing homoclinic orbits. See also Beyn and Kleinkauf [1997], Liu et al. [1997], and Doedel and Friedman [1989].

Remark 9: N-Pulse Homoclinic Orbits. In recent years there has been a great deal of work on N-pulse homoclinic orbits or "multi-bump" orbits. See

Champneys [1994], Zelati and Nolasco [1999], Camassa et al. [1998], Bolotin and MacKay [1997], Rabinowitz [1997], Soto Trevino and Kaper [1996], Kaper and Kovacic [1996], Haller and Wiggins [1995], and Glendinning [1989].

Remark 10: Global Center Manifold Techniques. Recently generalizations of the local center manifold techniques to a global setting valid in the neighborhood of a homoclinic orbit have been developed. See Sandstede [1993], Homburg [1996], Shaskov and Turaev [1999], and Chow et al. [2000].

Remark 10: Heteroclinic Cycles. See Wiggins [1988] and Tresser [1984] for some general results in $\mathbb{R}^3$. Devaney [1976] discusses some heteroclinic cycles in Hamiltonian systems. Heteroclinic cycles frequently arise in applications. For example, they appear to be the mechanism giving rise to "bursting" in a model for the interaction of eddies in the boundary layer of fluid flow near a wall, see Aubry, Holmes, and Lumley [1988] and Guckenheimer and Holmes [1988]. See also Tian and Du [2000], Koon et al. [2000], Homburg [2000], Ashwin and Field [1999], Chossat et al. [1999], Woods and Champneys [1999], Chow et al [1999], Sun and Kooij [1998], Qi and Jing [1998], Han [1998], Ashwin and Chossat [1998], Belykh and Bykov [1998], Zimmermann and Natiello [1998], Chernyshev [1997], Krupa [1997], Hou and Golubitsky [1997], Chossat et al. [1997], Maxwell [1997], Zhu [1996], Lauterbach et al. [1996], Worfolk [1996], Blazquez and Tuma [1996], Batteli [1994], Krupa and Melbourne [1995], Lauterbach and Roberts [1992], McCord and Mischaikow [1992], Field and Swift [1991], Feng [1991], Chossat and Armbruster [1991], Campbell and Holmes [1991], Armbruster and Chossatt [1991], and Deng [1991].

Remark 11: Homoclinic Orbits in Hamiltonian and Reversible Systems. Early work on homoclinic orbits in Hamiltonian systems can be found in Devaney [1976], [1978], Holmes [1980], and Wiggins [1988]. There has been a great deal of additional work in these areas over the past 10 years. See Champneys and Harterich [2000], Zhang [2000], Bolle and Buffoni [1999], Arioli and Szulkin [1999], Ding and Willem [1999], Ding and Girardi [1999], Koltsova and Lerman [1998], Ding [1998], Koltsova and Lerman [1996], Koltsova and Lerman [1995], Ragazzo [1997], Mielke et al. [1992], Lerman [1991], Buffoni [1993], Champneys and Toland [1993], Lerman [1989], and Turaev and Silnikov [1989] . For some results for reversible systems see Afendikov and Mielke [1999], Iooss [1997], and Chirchill and Rod [1986].

27.4 Exercises

1. Recall the discussion in Section 27.2 and specifically the vector field (27.2.1). Would there be any qualitative changes in the results of these sections if the eigenvalues depended on the parameter μ? How would this situation best be handled?

2. Show that *generically* for $\lambda_2 > \lambda_1$, the homoclinic orbit in (27.2.1) for $\mu = 0$ is tangent to the y axis in the $x - y$ plane at the origin.

   Construct a *nongeneric* example where this does not occur and explain why your example is not generic. (*Hint:* find an appropriate symmetry.)

3. In Equation (27.2.10) we took

$$\frac{1}{1 - Az^{|\lambda_1|/\lambda_3}} \sim 1 \qquad \text{as} \quad z \to 0.$$

   Show that if instead we take

$$\frac{1}{1 - Az^{|\lambda_1|/\lambda_3}} = 1 + Az^{|\lambda_1|/\lambda_3} + \cdots$$

   our results are not affected for z sufficiently small.

4. From Section 27.2, consider the case $\lambda_2 < \lambda_1$. Show that in this case the homoclinic orbit of (27.2.1) is tangent to the x-axis at the origin in the $x - y$ plane. Construct a Poincaré map near the homoclinic orbit following Section 27.2 and show that Theorem 27.2.1 still holds. In describing the "half-bowtie" shape of $P_0(\Pi_0)$ in Π_1, compare it with the case $\lambda_1 < \lambda_2$.

5. From Section 27.2, consider the case $\lambda_2 = \lambda_1$. Describe the geometry of the return of the homoclinic orbit to the origin. Construct a Poincaré map following Section 27.2 and show that Theorem 27.2.1 still holds. In describing the "half-bowtie" shape of $P_0(\Pi_0)$ in Π_1, compare it with the cases $\lambda_1 > \lambda_2$ and $\lambda_2 < \lambda_1$.

6. Argue that if (27.2.1) possesses only one homoclinic orbit, then the Poincaré map defined near the homoclinic orbit cannot possess an invariant Cantor set on which it is topologically conjugate to a full shift on N ($N \geq 2$) symbols.

7. Recall the discussion in Section 27.2a. In Assumption $1'$, discuss the necessity and geometry behind the requirement $d \neq 0$.

8. Work out all of the details in the proof of Theorem 27.2.2. (*Hint:* mimic the proof of Moser's theorem in Section 26.)

9. Recall the discussion in Section 27.2a. Suppose we instead chose configuration b) in Figure 27.2.9 with Assumption $1'$ and Assumption $2'$ still holding. Is Theorem 27.2.2 still valid in this case? If so, what modifications must be made in order to carry out the proof?

10. Work out all of the details in the proof of Theorem 27.3.2. (*Hint:* mimic the proof of Moser's theorem in Section 26.)

11. In Theorem 27.3.2 we proved the existence of an invariant Cantor set $\Lambda_k \subset R_k$ such that the Poincaré map restricted to Λ_k was topologically conjugate to a full shift on two symbols. This was true for all k sufficiently large. Show that Theorem 27.3.2 can be modified (in particular, the choice of μ_h-horizontal and μ_v-vertical strips) so that Π_0 contains an invariant Cantor set on which the Poincaré map is topologically conjugate to a full shift on N symbols with N arbitrarily large. (*Hint:* use Lemma 27.3.1 and see Wiggins [1988] if you need help.)

    Is there a difference in the dynamics of this invariant set and the dynamics in $\bigcup_{k \geq k_0} \Lambda_k$ constructed in Theorem 27.3.2?

12. Recall the construction in Theorem 27.3.2. Suppose the Poincaré map P is perturbed (as might occur in a one-parameter family). Show that, for sufficiently small perturbations, an infinite number of the Λ_k are destroyed yet a finite number survive. Does this contradict the fact that horseshoes are structurally stable?

13. Recall the discussion in Section 27.3. Suppose (27.3.1) is invariant under the coordinate transformation
$$(x, y, z) \to (-x, -y, -z)$$
with Assumptions 1 and 3 still holding.

    a) Show that (27.3.1) must possess two orbits homoclinic to the origin. Draw the two homoclinic orbits in the phase space. Denote the homoclinic orbits by Γ_0 and Γ_1.
    b) Construct a Poincaré map in a neighborhood of $\Gamma_0 \cup \Gamma_1 \cup \{(0, 0, 0)\}$ and show that the map has an invariant Cantor set on which the dynamics are topologically conjugate to a full shift on two symbols.
    c) If we denote the two symbols by 0 and 1, show that the motion in phase space is such that a '0' corresponds to a trajectory following close to Γ_0 and a '1' corresponds to a trajectory following close to Γ_1. Hence, give a geometrical description of the manifestation of chaos in phase space. (See Wiggins [1988] if you need help.)

14. Consider our description of the bifurcation analysis of Glendinning and Sparrow. Justify the curves shown in Figure 27.3.9.

15. Consider the sequence of bifurcations discussed in Figure 27.3.10. Explain why a period-doubling bifurcation occurs after μ_5 and a reverse period-doubling bifurcation occurs before μ_3.

16. Suppose we reverse the direction of time in (27.3.1), i.e., we let
$$t \to -t,$$
with Assumptions 1 and 2 still holding. Describe the dynamics near the homoclinic orbit.

17. Consider the vector field (27.3.1). Suppose that Assumption 1 holds but Assumption 2 is replaced by the following.

    Assumption 2′. $-\rho > \lambda > 0$.

    Describe the dynamics near the homoclinic orbit. (See Holmes [1980] for help.)

18. Consider a $\mathbf{C}^r$ (r as large as necessary) autonomous vector field in $\mathbb{R}^3$. We denote coordinates in $\mathbb{R}^3$ by $x - y - z$. Suppose the vector field has two hyperbolic fixed points, p_1 and p_2, respectively, in the $x - y$ plane.

    Local Assumption: The vector field linearized at p_1 has the form
$$\begin{aligned} \dot{x} &= \lambda_1 x, \\ \dot{y} &= \lambda_2 y, \\ \dot{z} &= \lambda_3 z, \end{aligned}$$
    with $\lambda_1 > 0$, $\lambda_3 < \lambda_2 < 0$.

    The vector field linearized at p_2 has the form
$$\begin{aligned} \dot{x} &= \rho x - \omega y, \\ \dot{y} &= \omega x + \rho y, \\ \dot{z} &= \lambda z, \end{aligned}$$
    with $\rho < 0$, $\lambda > 0$, $\omega \neq 0$.

    Global Assumption: p_1 and p_2 are connected by a heteroclinic orbit, denoted Γ_{12} that lies in the $x - y$ plane.

    p_2 and p_1 are connected by a heteroclinic orbit, Γ_{21}, that lies outside the plane; see Figure 27.4.1.

    Thus, $\Gamma_{12} \cup \Gamma_{21} \cup \{p_1\} \cup \{p_2\}$ form a heteroclinic cycle. The goal is to construct a Poincaré map, P, in a neighborhood of the heteroclinic cycle and prove the following theorem.

Theorem 27.4.1 (Tresser) *P possesses a countable number of horseshoes provided*

$$\frac{\rho\lambda_2}{\lambda\lambda_1} < 1.$$

(*Hint:* P will be constructed from the composition of four maps. Define cross sections Π_{01}, Π_{11}, Π_{12}, and Π_{02} appropriately; see Figure 27.4.1. $\Pi_{0,1}$ and Π_{11} should be sufficiently close to p_1, and Π_{12} and Π_{02} should be chosen sufficiently close to p_2. If the coordinates on these cross-sections are chosen appropriately, then we can derive maps as follows

$$P_{01}\colon\ \Pi_{01} \to \Pi_1,$$
$$\begin{pmatrix} x_1 \\ \varepsilon \\ z_1 \end{pmatrix} \mapsto \begin{pmatrix} \varepsilon \\ \varepsilon \left(\frac{\varepsilon}{x_1}\right)^{\lambda_2/\lambda_1} \\ z_1 \left(\frac{\varepsilon}{x_1}\right)^{\lambda_3/\lambda_1} \end{pmatrix},$$

$$P_{02}\colon\ \Pi_{02} \to \Pi_{12},$$
$$\begin{pmatrix} x_2 \\ 0 \\ z_2 \end{pmatrix} \mapsto \begin{pmatrix} x_2 \left(\frac{\varepsilon}{z_2}\right)^{\rho/\lambda} \cos\frac{\omega}{\lambda}\log\frac{\varepsilon}{z_2} \\ x_2 \left(\frac{\varepsilon}{z_2}\right)^{\rho/\lambda} \sin\frac{\omega}{\lambda}\log\frac{\varepsilon}{z_2} \\ \varepsilon \end{pmatrix},$$

$$P_{12}\colon\ \Pi_{12} \to \Pi_{01},$$
$$\begin{pmatrix} x_2 \\ y_2 \\ \varepsilon \end{pmatrix} \mapsto \begin{pmatrix} 0 \\ 0 \\ \varepsilon \end{pmatrix} + \begin{pmatrix} a_2 & b_2 & 0 \\ c_2 & d_2 & 0 \\ 0 & 0 & 0 \end{pmatrix} \begin{pmatrix} x_2 \\ y_2 \\ 0 \end{pmatrix},$$

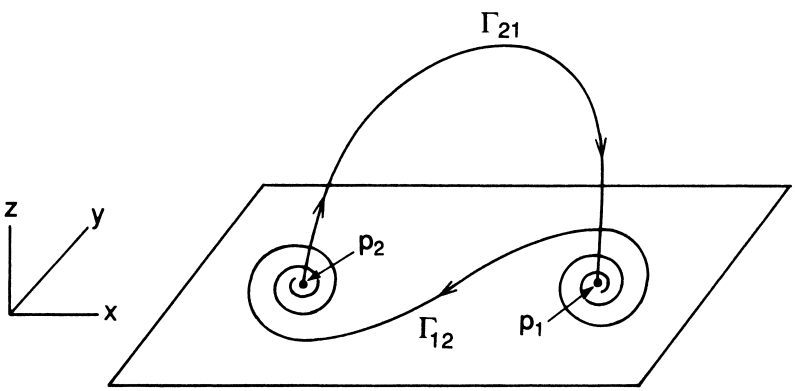

FIGURE 27.4.1.

$$P_{11}\colon\ \Pi_{11} \to \Pi_{02},$$
$$\begin{pmatrix} \varepsilon \\ y_1 \\ z_2 \end{pmatrix} \mapsto \begin{pmatrix} \varepsilon \\ 0 \\ 0 \end{pmatrix} + \begin{pmatrix} 0 & 0 & 0 \\ a & a_1 & b_1 \\ 0 & c_1 & d_1 \end{pmatrix} \begin{pmatrix} 0 \\ y_1 \\ z_1 \end{pmatrix},$$

where $x_1 - y_1 - z_1$ denote coordinates near p_1, and $x_2 - y_2 - z_2$ denote coordinates near p_2. These maps are approximations (see the discussion at the beginning of this chapter; discuss their validity and specify all steps in their derivation.

Then the Poincaré map near the heteroclinic cycle is defined as

$$P \equiv P_{11} \circ P_{01} \circ P_{12} \circ P_{02}\colon \Pi_{02} \to \Pi_{02}.$$

The rest of the proof is very much the same as Theorem 27.3.2. (See Wiggins [1988] for additional help.)

19. Consider a $\mathbf{C}^r$ (r as large as necessary) autonomous vector field in $\mathbb{R}^3$. We denote coordinates in $\mathbb{R}^3$ by $x - y - z$. Suppose the vector field has two hyperbolic fixed points, denoted p_1 and p_2, respectively, which lie in the $x - y$ plane.

Local Assumption: The vector field linearized at p_1 has the form

$$\begin{aligned} \dot{x} &= \rho_1 x - \omega_1 y, \\ \dot{y} &= \omega_1 x + \rho_1 y, \\ \dot{z} &= \lambda_1 z, \end{aligned}$$

with

$$\lambda_1 > 0,\ \rho_1 < 0 \qquad \text{and} \qquad \omega_1 \neq 0.$$

The vector field linearized at p_2 has the form

$$\begin{aligned} \dot{x} &= \rho_2 x - \omega_2 y, \\ \dot{y} &= \omega_2 x + \rho_2 y, \\ \dot{z} &= \lambda_2 z, \end{aligned}$$

with $\lambda_2 < 0$, $\rho_2 > 0$, and $\omega_2 \neq 0$.

Global Assumption: There exists a trajectory Γ_{12} in the $x - y$ plane connecting p_1 to p_2.

There exists a trajectory Γ_{21} connecting p_2 to p_1.

See figure 27.4.2 for an illustration of the geometry. Γ_{12} and Γ_{21} are examples of *heteroclinic orbits,* i.e., an orbit that is biasymptotic to two different fixed points. $\Gamma_{12} \cup \Gamma_{21} \cup \{p_1\} \cup \{p_2\}$ is said to form a *heteroclinic cycle.*

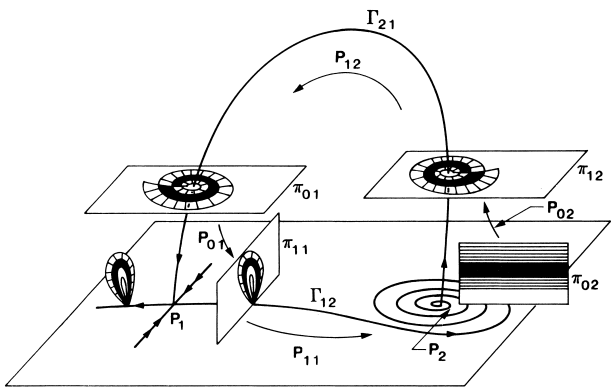

FIGURE 27.4.2.

a) Define a Poincaré map in the neighborhood of the heteroclinic cycle and determine if there are conditions on the eigenvalues (i.e., ρ, ρ, λ, and λ) such that the map possesses an invariant Cantor set on which the dynamics are topologically conjugate to a full shift on N ($N \geq 2$) symbols.

b) Consider the case

$$\begin{aligned} |\rho_2| &= |\rho_1|, \\ |\lambda_2| &= |\lambda_1|, \\ |\omega_2| &= |\omega_1|. \end{aligned}$$

Can horseshoes exist in this case? What is the relevance of this case to Case III of the *truncated* (hence symmetric) three-dimensional normal form discussed in Section 33.2?

20. Recall the motivational example for deriving Poincaré maps near homoclinic orbits described in Chapter 10. We now describe the analog of that example for heteroclinic orbits.

Consider a $\mathbf{C}^r$ (r as large as necessary) two-parameter family of vector fields in the plane having a hyperbolic fixed points p_1 and p_2, respectively.

Local Assumption: The vector field linearized at p_1 is given by

$$\begin{aligned} \dot{x}_1 &= \alpha_1 x_1, \\ \dot{y}_1 &= \beta_1 y_1, \end{aligned} \qquad \alpha_1 < 0,\ \beta_1 > 0,$$

and the vector field linearized at p_2 is given by

$$\begin{aligned} \dot{x}_2 &= \alpha_2 x_2, \\ \dot{y}_2 &= \beta_2 y_2, \end{aligned} \qquad \alpha_2 > 0,\ \beta_2 < 0,$$

where α_i, β_i, $i = 1, 2$ are constants.

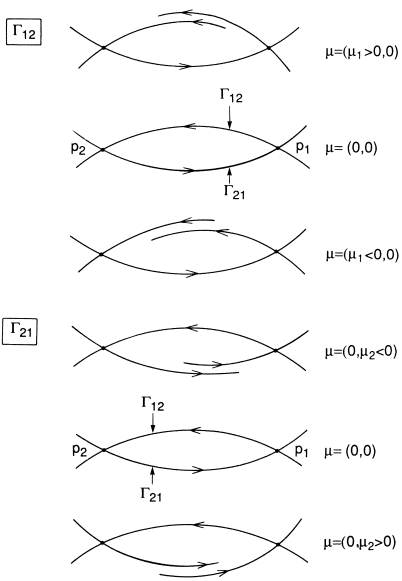

FIGURE 27.4.3.

Global Assumption. p_1 and p_2 are connected by a heteroclinic cycle. We denote the heteroclinic orbit going from p_1 to p_2 in positive time by Γ_{12} and the heteroclinic orbit going from p_2 to p_1 in positive time by Γ_{21}.

The heteroclinic cycle depends on the parameters as follows. For $\mu \equiv (\mu_1, \mu_2)$, let $\mathcal{N}$ be a neighborhood of zero in the μ_1, μ_2 plane; then we assume the following.

1) Γ_{12} exists for all $\mu \in \{(\mu_1, \mu_2) \mid \mu_1 = 0\} \cap \mathcal{N} \equiv \mathcal{N}_1$.
2) Γ_{21} exists for all $\mu \in \{(\mu_1, \mu_2) \mid \mu_2 = 0\} \cap \mathcal{N} \equiv \mathcal{N}_2$.

Furthermore, we assume that Γ_{12} and Γ_{21} break "transversely" as shown in Figure 27.4.3.

Construct a two-parameter family of Poincaré maps near the heteroclinic cycle and study the bifurcation and stability of periodic orbits.

28

Melnikov's Method for Homoclinic Orbits in Two-Dimensional, Time-Periodic Vector Fields

We have seen that transverse homoclinic orbits to hyperbolic periodic points of two-dimensional maps gives rise to chaotic dynamics in the sense of Theorems 26.0.5 and 26.0.6. We will now develop a perturbation method originally due to Melnikov [1963] for proving the existence of transverse homoclinic orbits to hyperbolic periodic orbits in a class of two-dimensional, time-periodic vector fields; then by considering a Poincaré map, Theorems 26.0.5 and 26.0.6 can be applied to conclude that the system possesses chaotic dynamics.

28.1 The General Theory

We consider the following class of systems:

$$\begin{aligned} \dot{x} &= \frac{\partial H}{\partial y}(x,y) + \varepsilon g_1(x,y,t,\epsilon), \\ \dot{y} &= -\frac{\partial H}{\partial x}(x,y) + \varepsilon g_2(x,y,t,\varepsilon), \qquad (x,y) \in \mathbb{R}^2; \end{aligned} \tag{28.1.1}$$

or, in vector form,

$$\dot{q} = JDH(q) + \varepsilon g(q,t,\varepsilon), \tag{28.1.2}$$

where $q = (x,y)$, $DH = (\frac{\partial H}{\partial x}, \frac{\partial H}{\partial y})$, $g = (g_1, g_2)$, and

$$J = \begin{pmatrix} 0 & 1 \\ -1 & 0 \end{pmatrix}.$$

We assume that (28.1.1) is sufficiently differentiable ($\mathbf{C}^r$, $r \geq 2$ will do) on

the region of interest. Most importantly, we also assume that g is periodic in t with period $T = 2\pi/\omega$.

We referred to (28.1.1) with $\varepsilon = 0$ as the unperturbed system

$$\begin{aligned} \dot{x} &= \frac{\partial H}{\partial y}(x, y), \\ \dot{y} &= -\frac{\partial H}{\partial x}(x, y), \end{aligned} \tag{28.1.3}$$

or, in vector form,

$$\dot{q} = JDH(q), \tag{28.1.4}$$

and we had the following assumptions on the structure of the phase space of the unperturbed system (see Figure 28.1.1).

Assumption 1. The unperturbed system possesses a hyperbolic fixed point, p_0, connected to itself by a homoclinic orbit $q_0(t) \equiv (x_0(t), y_0(t))$.

Assumption 2. Let $\Gamma_{p_0} = \{q \in \mathbb{R}^2 \mid q = q_0(t), t \in \mathbb{R}\} \cup \{p_0\} = W^s(p_0) \cap W^u(p_0) \cup \{p_0\}$. The interior of Γ_{p_0} is filled with a continuous family of periodic orbits $q^\alpha(t)$ with period T^α, $\alpha \in (-1, 0)$. We assume that $\lim_{\alpha \to 0} q^\alpha(t) = q_0(t)$, and $\lim_{\alpha \to 0} T^\alpha = \infty$.

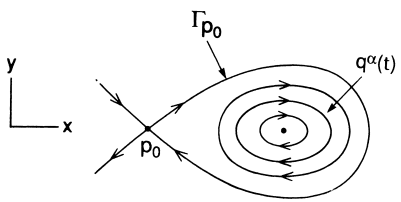

FIGURE 28.1.1.

The subharmonic Melnikov theory enabled us to understand how the periodic orbits $q^\alpha(t)$ were affected by the perturbation; now we will develop a technique to see how the homoclinic orbit, Γ_{p_0}, is so affected. Geometrically, the homoclinic Melnikov method is a bit different from the subharmonic Melnikov method. However, there is an important relationship between the two as $\alpha \to 0$ (i.e., as the periodic orbits limit on the homoclinic orbit) that we want to point out later on in this section. We remark that it is possible to develop the homoclinic Melnikov method for a more general class of two-dimensional, time-periodic systems than (28.1.1); in particular, we do not have to assume that the unperturbed system is Hamiltonian. We will deal with these generalizations in the exercises.

Our development of the homoclinic Melnikov method will consist of several steps, which we briefly describe.

Step 1. Develop a parametrization of the homoclinic "manifold" of the unperturbed system.

Step 2. Develop a measure of the "splitting" of the manifolds for the perturbed system using the unperturbed "homoclinic coordinates."

Step 3. Derive the Melnikov function and show how it is related to the distance between the manifolds.

Before beginning with Step 1 we want to rewrite (28.1.1) as an autonomous three-dimensional system (cf. Chapter 7) as follows

$$\begin{aligned} \dot{x} &= \frac{\partial H}{\partial y}(x,y) + \varepsilon g_1(x,y,\phi,\varepsilon), \\ \dot{y} &= -\frac{\partial H}{\partial x}(x,y) + \varepsilon g_2(x,y,\phi,\varepsilon), \qquad (x,y,\phi) \in \mathbb{R}^1 \times \mathbb{R}^1 \times S^1, \\ \dot{\phi} &= \omega, \end{aligned} \tag{28.1.5}$$

or, in vector form,

$$\begin{aligned} \dot{q} &= JDH(q) + \varepsilon g(q,\phi;\varepsilon), \\ \dot{\phi} &= \omega. \end{aligned} \tag{28.1.6}$$

The unperturbed system is obtained from (28.1.6) by setting $\varepsilon = 0$, i.e.,

$$\begin{aligned} \dot{q} &= JDH(q), \\ \dot{\phi} &= \omega. \end{aligned} \tag{28.1.7}$$

We will see that this apparently trivial trick offers several geometrical advantages. In particular, the perturbed system is of a very different character than the unperturbed system, and this trick forces us to treat them on a more equal footing. Also, the relationship between the splitting of the manifolds "in time" and the splitting of the manifolds on a particular Poincaré section and how this is manifested by the Melnikov function will be more apparent.

Step 1: Phase Space Geometry of the Unperturbed Vector Field: A Parametrization of the Homoclinic Manifold. When viewed in the three-dimensional phase space $\mathbb{R}^2 \times S^1$, the hyperbolic fixed point p_0 of the q component of the unperturbed system (28.1.7) becomes a periodic orbit

$$\gamma(t) = (p_0, \phi(t) = \omega t + \phi_0). \tag{28.1.8}$$

We denote the two-dimensional stable and unstable manifolds of $\gamma(t)$ by $W^s(\gamma(t))$ and $W^u(\gamma(t))$, respectively. Because of Assumption 1 above, $W^s(\gamma(t))$ and $W^u(\gamma(t))$ coincide along a two-dimensional *homoclinic manifold.* We denote this homoclinic manifold by Γ_γ; see Figure 28.1.2. We remark that the structure of this figure should not be surprising; it reflects the fact that the unperturbed phase space is independent of time (ϕ).

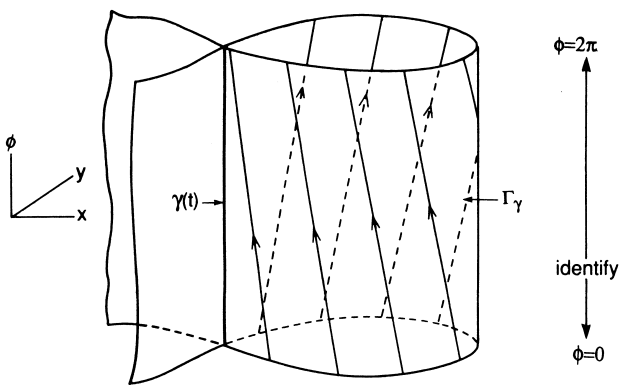

FIGURE 28.1.2. The homoclinic manifold, Γ_γ. The lines on Γ_γ represent a typical trajectory.

Our goal is to determine how Γ_γ "breaks up" under the influence of the perturbation. We now want to describe what we mean by this statement, which will serve to motivate the following discussion.

The homoclinic manifold Γ_γ is formed by the coincidence of two two-dimensional surfaces, a branch of $W^s(\gamma(t))$ and a branch of $W^u(\gamma(t))$. In three dimensions, one would not expect two two-dimensional surfaces to coincide in this manner but, rather, one would expect them to intersect in one-dimensional curves as shown in Figure 28.1.3. (Note: as mentioned in Chapter 12, if two invariant manifolds of a *vector field* intersect, they must intersect along (at least) a one-dimensional trajectory of the vector field if we have uniqueness of solutions; we will explore this in more detail later.) Figure 28.1.3 illustrates what we mean by the term "break up" of Γ_γ. Now we want to analytically quantify Figure 28.1.3. In order to do this we will develop a measurement of the deviation of the perturbed stable and unstable manifolds of $\gamma(t)$ from Γ_γ. This will consist of measuring the distance between the perturbed stable and unstable manifolds along the direction normal to Γ_γ. Evidently, this measurement will vary from point-to-point on Γ_γ so we first need to describe a parametrization of Γ_γ.

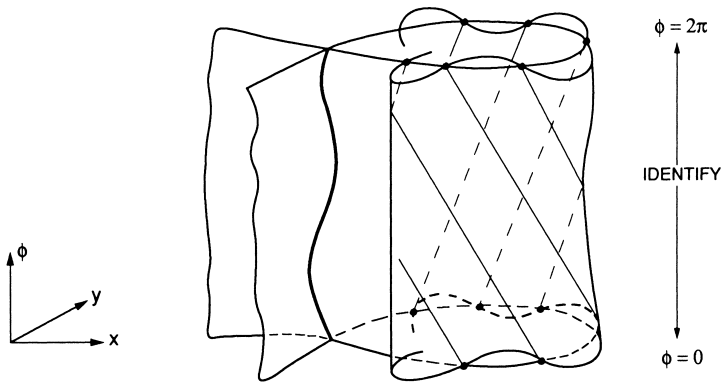

FIGURE 28.1.3.

Parametrization of Γ_γ*: Homoclinic Coordinates.* Every point on Γ_γ can be represented by

$$(q_0(-t_0), \phi_0) \in \Gamma_\gamma \tag{28.1.9}$$

for $t_0 \in \mathbb{R}^1$, $\phi_0 \in (0, 2\pi]$. The interpretation of t_0 is the time of flight from the point $q_0(-t_0)$ to the point $q_0(0)$ along the unperturbed homoclinic trajectory $q_0(t)$. Since the time of flight from $q_0(-t_0)$ to $q_0(0)$ is unique, the map

$$(t_0, \phi_0) \longmapsto (q_0(-t_0), \phi_0) \tag{28.1.10}$$

is one-to-one so that for a given $(t_0, \phi_0) \in \mathbb{R}^1 \times S^1$, $(q_0(-t_0), \phi_0)$ corresponds to a unique point on Γ_γ (see Exercise 1). Hence, we have

$$\Gamma_\gamma = \big\{(q, \phi) \in \mathbb{R}^2 \times S^1 \,|\, q = q_0(-t_0), t_0 \in \mathbb{R}^1; \phi = \phi_0 \in (0, 2\pi]\big\}. \tag{28.1.11}$$

The geometrical meaning of the parameters t_0 and ϕ_0 should be clear from Figure 28.1.2.

At each point $p \equiv (q_0(-t_0), \phi_0) \in \Gamma_\gamma$ we construct a vector, π_p, normal to Γ_γ that is defined as follows

$$\pi_p = \left(\frac{\partial H}{\partial x}(x_0(-t_0), y_0(-t_0)), \frac{\partial H}{\partial y}(x_0(-t_0), y_0(-t_0)), 0\right) \tag{28.1.12}$$

or, in vector form,

$$\pi_p \equiv (DH(q_0(-t_0)), 0). \tag{28.1.13}$$

Thus, varying t_0 and ϕ_0 serves to move π_p to every point on Γ_γ; see Figure 28.1.4. We make the important remark that at each point $p \in \Gamma_\gamma$, $W^s(\gamma(t))$

and $W^u(\gamma(t))$ intersect π_p transversely at p. Finally, when considering the behavior of Γ_γ near p under perturbation, we will be interested only in the points on π_p that are $\mathcal{O}(\varepsilon)$ close to p. This will be further clarified in Step 2.

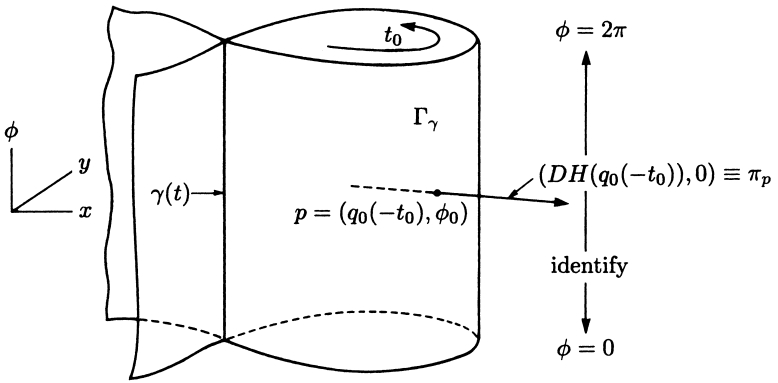

FIGURE 28.1.4. Homoclinic coordinates.

Step 2: Phase Space Geometry of the Perturbed Vector Field: "The Splitting of the Manifolds." We now turn our attention to describing how Γ_γ is affected by the perturbation. However, first we need some preliminary results concerning the persistence of $\gamma(t)$ along with its stable and unstable manifolds.

Proposition 28.1.1 *For ε sufficiently small, the periodic orbit $\gamma(t)$ of the unperturbed vector field (28.1.7) persists as a periodic orbit, $\gamma_\varepsilon(t) = \gamma(t) + \mathcal{O}(\varepsilon)$, of the perturbed vector field (28.1.6) having the same stability type as $\gamma(t)$ with $\gamma_\varepsilon(t)$ depending on ε in a $\mathbf{C}^r$ manner. Moreover, $W^s_{loc}(\gamma_\varepsilon(t))$ and $W^u_{loc}(\gamma_\varepsilon(t))$ are $\mathbf{C}^r$ ε-close to $W^s_{loc}(\gamma(t))$ and $W^u_{loc}(\gamma(t))$, respectively.*

Proof: Using the idea of a Poincaré map and appealing to the stable and unstable manifold theorem for maps, proof of this theorem is an easy exercise that we leave for the reader (see Exercise 2). □

The global stable and unstable manifolds of $\gamma_\varepsilon(t)$ can be obtained from the local stable and unstable manifolds of $\gamma_\varepsilon(t)$ by time evolution as follows. Let $\phi_t(\cdot)$ denote the flow generated by (28.1.6) (note: do not confuse the notation for the flow, $\phi_t(\cdot)$, with the angle ϕ). Then we define the global stable and unstable manifolds of $\gamma_\varepsilon(t)$ as follows

$$W^s(\gamma_\varepsilon(t)) = \bigcup_{t\le 0} \phi_t(W^s_{\rm loc}(\gamma_\varepsilon(t)),$$
$$W^u(\gamma_\varepsilon(t)) = \bigcup_{t\ge 0} \phi_t(W^u_{\rm loc}(\gamma_\varepsilon(t)). \tag{28.1.14}$$

If we restrict ourselves to compact sets in $\mathbb{R}^2 \times S^1$ containing $W^s(\gamma_\varepsilon(t))$ and $W^u(\gamma_\varepsilon(t))$, then $W^s(\gamma_\varepsilon(t))$ and $W^u(\gamma_\varepsilon(t))$ are $\mathbf{C}^r$ functions of ε on these compact sets. This follows from the fact that $\phi_t(\cdot)$ is a $\mathbf{C}^r$ diffeomorphism that is also $\mathbf{C}^r$ in ε (see Theorem 7.3.1). Our analysis of the splitting of the manifolds will be restricted to an $\mathcal{O}(\varepsilon)$ neighborhood of Γ_γ.

Let us describe Proposition 28.1.1 more geometrically. The content of the proposition is that, for some ε_0 small, we can find a neighborhood $\mathcal{N}(\varepsilon_0)$ in $\mathbb{R}^2 \times S^1$ containing $\gamma(t)$ with the distance from $\gamma(t)$ to the boundary of $\mathcal{N}(\varepsilon_0)$ being $\mathcal{O}(\varepsilon_0)$. Moreover, for $0 < \varepsilon < \varepsilon_0$, $\gamma_\varepsilon(t)$ is also contained in $\mathcal{N}(\varepsilon_0)$ with $W^s(\gamma(t)) \cap \mathcal{N}(\varepsilon_0) \equiv W^s_{\rm loc}(\gamma(t))$ and $W^u(\gamma(t)) \cap \mathcal{N}(\varepsilon_0) \equiv W^u_{\rm loc}(\gamma(t))$ $\mathbf{C}^r$ ε-close to $W^s(\gamma_\varepsilon(t)) \cap \mathcal{N}(\varepsilon_0) \equiv W^s_{\rm loc}(\gamma_\varepsilon(t))$ and $W^u(\gamma_\varepsilon(t)) \cap \mathcal{N}(\varepsilon_0) \equiv W^u_{\rm loc}(\gamma_\varepsilon(t))$, respectively. We can choose $\mathcal{N}(\varepsilon_0)$ to be a solid torus as follows

$$\mathcal{N}(\varepsilon_0) = \big\{(q,\phi) \in \mathbb{R}^2 \,|\, |q - p_0| \le C\varepsilon_0, \phi \in (0, 2\pi]\big\}, \tag{28.1.15}$$

where C is some positive constant; see Figure 28.1.5.

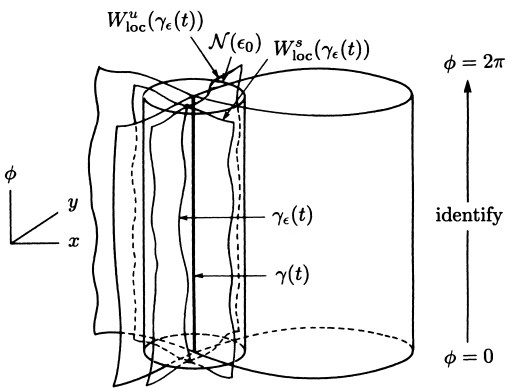

FIGURE 28.1.5.

In some of our geometrical arguments we will be comparing individual trajectories of the unperturbed vector field with trajectories of the perturbed vector field. For this it will often be easier to consider the projection of these trajectories into the q-plane or a plane parallel to the q-plane. Let

us show how this is done. Consider the following cross-section of the phase space (don't think about Poincaré maps yet)

$$\Sigma^{\phi_0} = \big\{(q,\phi) \in \mathbb{R}^2 \,|\, \phi = \phi_0\big\}. \tag{28.1.16}$$

It should be clear that Σ^{ϕ_0} is parallel to the q-plane and coincides with the q-plane for $\phi_0 = 0$; see Figure 28.1.6. Note that

$$\gamma(t) \cap \Sigma^{\phi_0} = p_0 \tag{28.1.17}$$

and

$$\Gamma_\gamma \cap \Sigma^{\phi_0} = \big\{q \in \mathbb{R}^2 \,|\, q = q_0(t), t \in \mathbb{R}\big\} = \Gamma_{p_0}. \tag{28.1.18}$$

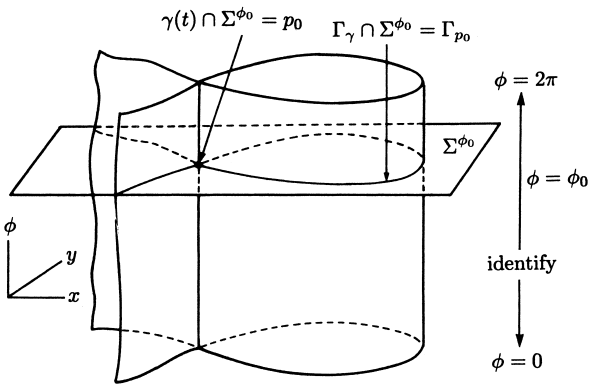

FIGURE 28.1.6.

In particular, (28.1.17) and (28.1.18) are independent of ϕ_0; this simply reflects the fact that the unperturbed vector field is autonomous. Now let $(q(t), \phi(t))$ and $(q_\varepsilon(t), \phi(t))$ be trajectories of the unperturbed and perturbed vector fields, respectively. Then the projections of these trajectories onto Σ^{ϕ_0} are given by

$$(q_0(t), \phi_0) \tag{28.1.19}$$

and

$$(q_\varepsilon(t), \phi_0). \tag{28.1.20}$$

We remark that $q_\varepsilon(t)$ actually depends on ϕ_0 (as opposed to $q(t)$), since the q-component of the perturbed vector field (28.1.6) depends on ϕ, i.e., the perturbed vector field is nonautonomous. Therefore, (28.1.20) could be a very complicated curve in Σ^{ϕ_0}, possibly intersecting itself many times. This tends to obscure much of the dynamical content of the trajectory. We will

remedy this situation later on when we consider a Poincaré map constructed from the flow generated by the perturbed vector field; see Figures 28.1.7 and 28.1.8 for an illustration of the geometry behind the projections (28.1.19) and (28.1.20).

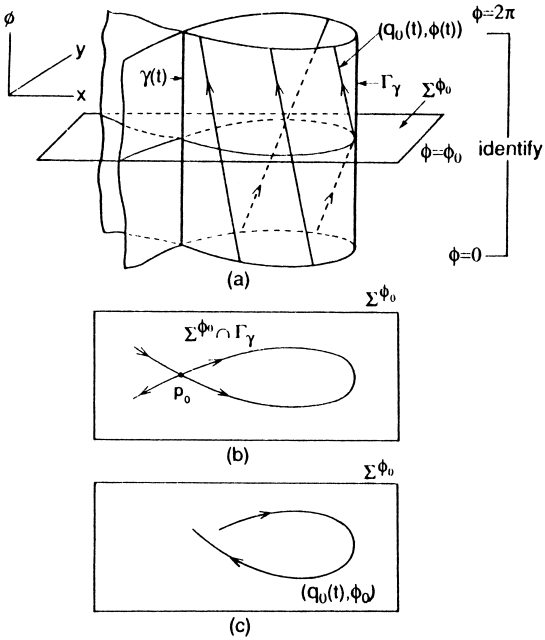

FIGURE 28.1.7.

We are now at the point where we can define the splitting of $W^s(\gamma_\varepsilon(t))$ and $W^u(\gamma_\varepsilon(t))$. Choose any point $p \in \Gamma_\gamma$. Then $W^s(\gamma(t))$ and $W^u(\gamma(t))$ intersect π_p transversely at p. Hence, by the persistence of transversal intersections and the fact that $W^s(\gamma_\varepsilon(t))$ and $W^u(\gamma_\varepsilon(t))$ are $\mathbf{C}^r$ in ε, for ε sufficiently small $W^s(\gamma_\varepsilon(t))$ and $W^u(\gamma_\varepsilon(t))$ intersect π_p transversely in the points p^s_ε and p^u_ε, respectively. It is therefore natural to define *the distance between* $W^s(\gamma_\varepsilon(t))$ *and* $W^u(\gamma_\varepsilon(t))$ *at the point* p, denoted $d(p,\varepsilon)$, to be

$$d(p,\varepsilon) \equiv |p^u_\varepsilon - p^s_\varepsilon|; \tag{28.1.21}$$

see Figure 28.1.9. We will find it convenient in the next step to redefine (28.1.21) in an equivalent, but slightly less natural manner as follows

$$d(p,\varepsilon) = \frac{(p^u_\varepsilon - p^s_\varepsilon)\cdot(DH(q_0(-t_0)),0)}{\|DH(q_0(-t_0))\|} \tag{28.1.22}$$

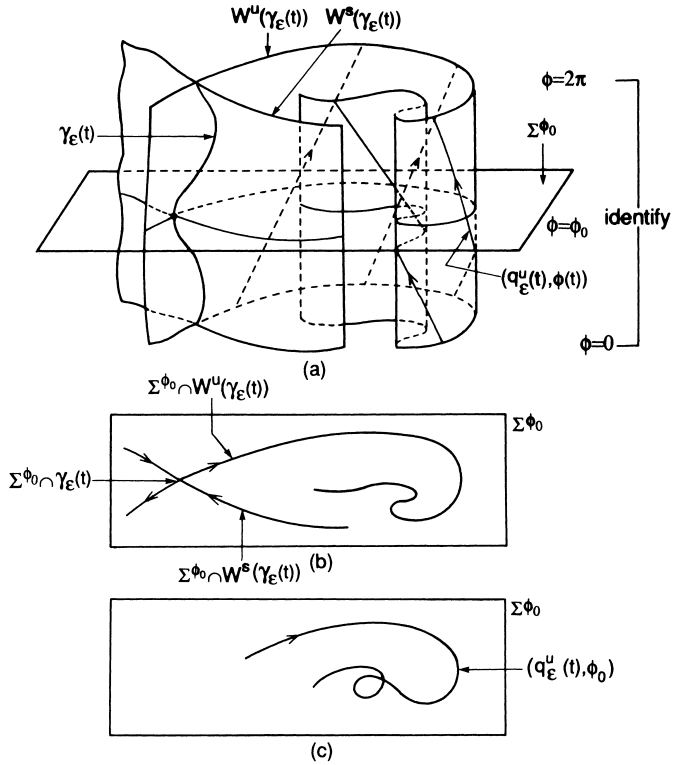

FIGURE 28.1.8.

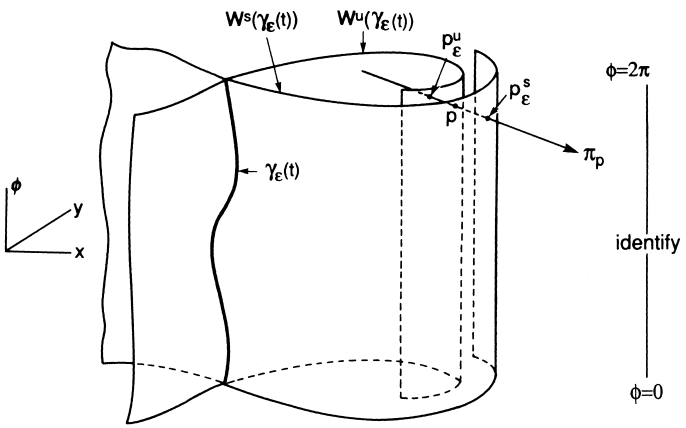

FIGURE 28.1.9.

where "$\cdot$" denotes the vector scalar product and

$$\|DH(q_0(-t_0))\| = \sqrt{\left(\frac{\partial H}{\partial x}(q_0(-t_0))\right)^2 + \left(\frac{\partial H}{\partial y}(q_0(-t_0))\right)^2}.$$

Because p_ε^u and p_ε^s are chosen to lie on the vector $(DH(q_0(-t_0)), 0)$, it should be clear that the magnitude of (28.1.22) is equal to the magnitude of (28.1.21). However, (28.1.22) is a signed measure of the distance and reflects the relative orientations of $W^s(\gamma_\varepsilon(t))$ and $W^u(\gamma_\varepsilon(t))$ near p; see Figure 28.1.10. Note that since p_ε^u and p_ε^s lie on π_p, we can write

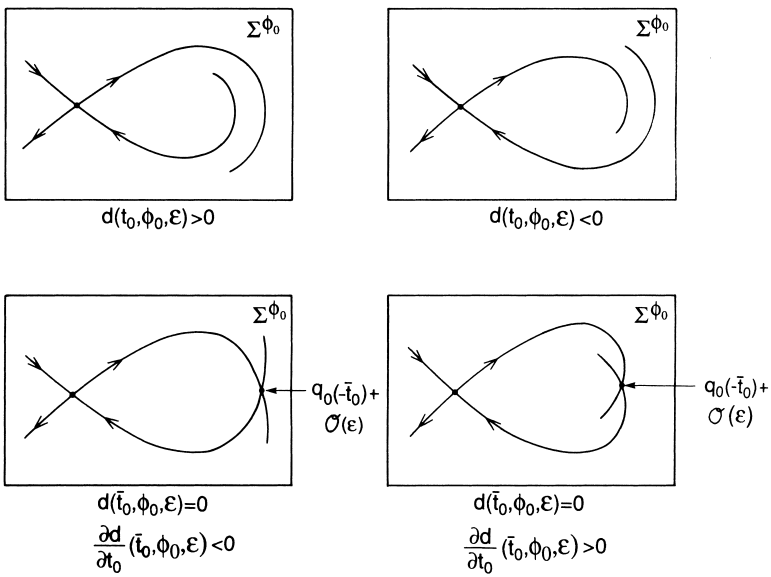

FIGURE 28.1.10.

$$p_\varepsilon^u = (q_\varepsilon^u, \phi_0) \tag{28.1.23}$$

and

$$p_\varepsilon^s = (q_\varepsilon^s, \phi_0), \tag{28.1.24}$$

i.e., p_ε^u and p_ε^s have the same ϕ_0 coordinate. Thus, (28.1.22) is the same as

$$d(t_0, \phi_0, \varepsilon) = \frac{DH(q_0(-t_0)) \cdot (q_\varepsilon^u - q_\varepsilon^s)}{\|DH(q_0(-t_0))\|}, \tag{28.1.25}$$

where we are now denoting $d(p, \varepsilon)$ by $d(t_0, \phi_0, \varepsilon)$, since every point $p \in \Gamma_\gamma$ can be uniquely represented by the parameters (t_0, ϕ_0), $t_0 \in \mathbb{R}$, $\phi_0 \in (0, 2\pi]$, according to the parametrization $p = (q_0(-t_0), \phi_0)$ described in Step 1.

Before deriving a computable approximation to (28.1.25) in Step 3, we want to address a technical issue involving the choice of p^u_ε and p^s_ε. Certainly by transversality and $\mathbf{C}^r$ dependence on ε, for ε sufficiently small, $W^s(\gamma_\varepsilon(t))$ and $W^u(\gamma_\varepsilon(t))$ intersect π_p. However, these manifolds may intersect π_p in more than one point (indeed, an infinite number of points is possible), as shown in Figure 28.1.11. The question then arises as to which points p^u_ε and p^s_ε are chosen so as to define (28.1.25). We first give a definition.

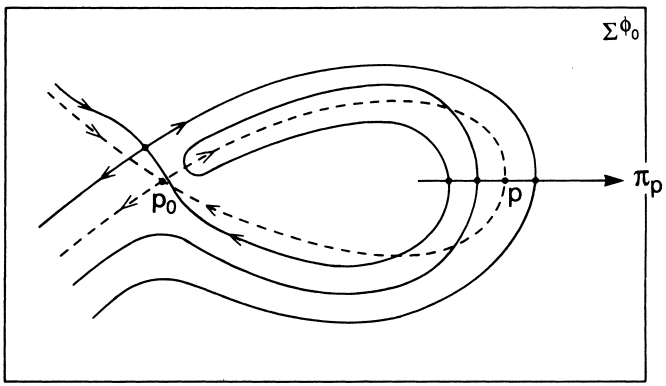

FIGURE 28.1.11.

Definition 28.1.2 *Let $p^s_{\varepsilon,i} \in W^s(\gamma_\varepsilon(t)) \cap \pi_p$ and $p^u_{\varepsilon,i} \in W^u(\gamma_\varepsilon(t)) \cap \pi_p$, $i \in \mathcal{I}$, where $\mathcal{I}$ is some index set. Let $(q^s_{\varepsilon,i}(t), \phi(t)) \in W^s(\gamma_\varepsilon(t))$ and $(q^u_{\varepsilon,i}(t), \phi(t)) \in W^u(\gamma_\varepsilon(t))$ denote orbits of the perturbed vector field (28.1.6) satisfying $(q^s_{\varepsilon,i}(0), \phi(0)) = p^s_{\varepsilon,i}$ and $(q^u_{\varepsilon,i}(0), \phi(0)) = p^u_{\varepsilon,i}$, respectively. Then we have the following (see Figure 28.1.12).*

1. *For some $i = \bar{i} \in \mathcal{I}$ we say that $p^s_{\varepsilon,\bar{i}}$ is the point in $W^s(\gamma_\varepsilon(t)) \cap \pi_p$ that is closest to $\gamma_\varepsilon(t)$ in terms of positive time of flight along $W^s(\gamma_\varepsilon(t))$ if, for all $t > 0$, $(q^s_{\varepsilon,\bar{i}}(t), \phi_0) \cap \pi_p = \emptyset$.*

2. *For some $i = \bar{i} \in \mathcal{I}$ we say that $p^u_{\varepsilon,\bar{i}}$ is the point in $W^u(\gamma_\varepsilon(t)) \cap \pi_p$ that is closest to $\gamma_\varepsilon(t)$ in terms of negative time of flight along $W^u(\gamma_\varepsilon(t))$ if, for all $t < 0$, $(q^u_{\varepsilon,\bar{i}}(t), \phi_0) \cap \pi_p = \emptyset$.*

We make the following remarks regarding this definition.

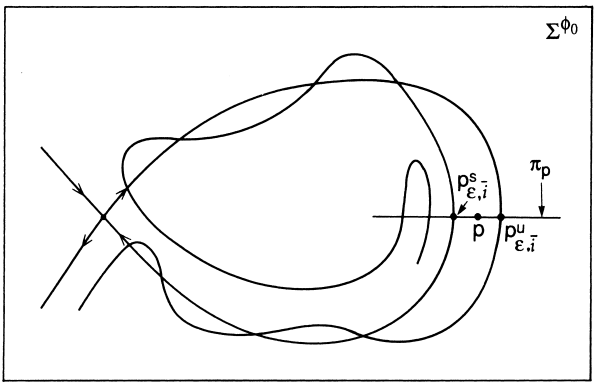

FIGURE 28.1.12.

Remark 1. For p fixed, we are interested only in the points in $W^s(\gamma_\varepsilon(t)) \cap \pi_p$ and $W^u(\gamma_\varepsilon(t)) \cap \pi_p$ that are $\mathcal{O}(\varepsilon)$ close to p. This is because our methods are perturbative.

Remark 2. For the unperturbed system, the orbit through p leaves π_p in positive and negative time and enters a neighborhood of the hyperbolic orbit without ever returning to π_p. The orbits through π_p described in Definition 28.1.2 are the perturbed orbits that most closely behave in this manner.

Remark 3. The points $p^s_{\varepsilon,\bar{i}}$ and $p^u_{\varepsilon,\bar{i}}$ are unique. This will follow from the proof of Lemma 28.1.3.

The points p^s_ε and p^u_ε used in defining (28.1.25) are chosen to be closest to $\gamma_\varepsilon(t)$ in the sense of positive time of flight along $W^s(\gamma_\varepsilon(t))$ and negative time of flight along $W^u(\gamma_\varepsilon(t))$, respectively, as described in Definition 28.1.2. Still, the question remains as to why this choice. The consequences of the following lemma will answer this question.

Lemma 28.1.3 *Let $p^s_{\varepsilon,\bar{i}}$ (resp. $p^u_{\varepsilon,\bar{i}}$) be a point on $W^s(\gamma_\varepsilon(t)) \cap \pi_p$ (resp. $W^u(\gamma_\varepsilon(t)) \cap \pi_p$) that is* not *closest to $\gamma_\varepsilon(t)$ in the sense of Definition 28.1.2, and let $\mathcal{N}(\varepsilon_0)$ denote the neighborhood of $\gamma(t)$ and $\gamma_\varepsilon(t)$ described following Proposition 28.1.1. Let $(q^s_{\varepsilon,\bar{i}}(t), \phi(t))$ (resp. $(q^u_{\varepsilon,\bar{i}}(t), \phi(t))$) be a trajectory in $W^s(\gamma_\varepsilon(t))$ (resp. $W^u(\gamma_\varepsilon(t))$) satisfying $(q^s_{\varepsilon,\bar{i}}(0), \phi(0)) = p^s_{\varepsilon,\bar{i}}$ (resp. $(q^u_{\varepsilon,\bar{i}}(0), \phi(0)) = p^u_{\varepsilon,\bar{i}}$). Then, for ε sufficiently small,* before *$(q^s_{\varepsilon,\bar{i}}(t), \phi_0)$, $t > 0$, (resp. $(q^u_{\varepsilon,\bar{i}}(t), \phi_0)$, $t < 0$) can intersect π_p (as it must by Definition 28.1.2), it must pass through $\mathcal{N}(\varepsilon_0)$* (see Figure 28.1.13).

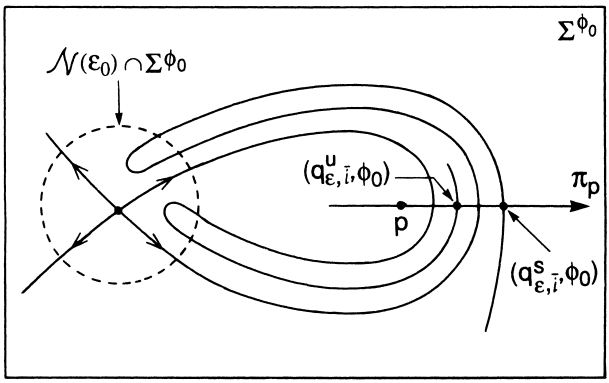

FIGURE 28.1.13.

Proof: We give the argument for trajectories in $W^s(\gamma_\varepsilon(t))$; the argument for trajectories in $W^u(\gamma_\varepsilon(t))$ will follow immediately by considering the time-reversed vector field.

First we consider the unperturbed vector field. Consider any point (q_0^s, ϕ_0) on $W^s(\gamma(t)) \cap \mathcal{N}(\varepsilon_0)$; see Figure 28.1.14. Let $(q_0^s(t), \phi(t)) \in W^s(\gamma(t))$ satisfy $(q_0^s(0), \phi(0)) = (q_0^s, \phi_0)$. Then there exists a *finite time,* $-\infty < T^s < 0$, such that $(q_0^s(T^s), \phi(T^s)) \in W^s(\gamma(t)) \cap \mathcal{N}(\varepsilon_0)$. In other words, T^s is the time that it takes a trajectory leaving $\mathcal{N}(\varepsilon_0)$ in $W^s(\gamma(t))$ to reenter $\mathcal{N}(\varepsilon_0)$; see Figure 28.1.14.

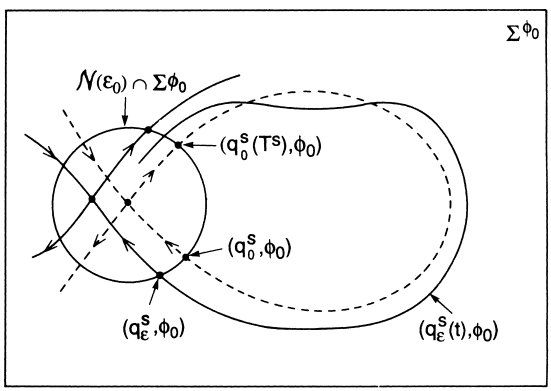

FIGURE 28.1.14.

We now want to compare trajectories in $W^s(\gamma(t))$ with trajectories in $W^s(\gamma_\varepsilon(t))$. Choose points

$$(q_0^s, \phi_0) \in W^s_{\text{loc}}(\gamma(t)) \cap \mathcal{N}(\varepsilon_0)$$

and

$$(q_\varepsilon^s, \phi_0) \in W^s_{\text{loc}}(\gamma_\varepsilon(t)) \cap \mathcal{N}(\varepsilon_0),$$

and consider trajectories

$$(q_0^s(t), \phi(t)) \in W^s(\gamma(t))$$

and

$$(q_\varepsilon^s(t), \phi(t)) \in W^s(\gamma_\varepsilon(t))$$

satisfying

$$(q_0^s(0), \phi(0)) = (q_0^s, \phi_0)$$

and

$$(q_\varepsilon^s(0), \phi(0)) = (q_\varepsilon^s, \phi_0);$$

see Figure 28.1.14. Then

$$|(q_\varepsilon^s(t), \phi(t)) - (q_0^s(t), \phi(t))| = \mathcal{O}(\varepsilon_0) \tag{28.1.26}$$

for $0 \leq t \leq \infty$ and, by Gronwall's inequality (see Hale [1980]),

$$|(q_\varepsilon^s(t), \phi(t)) - (q_0^s(t), \phi(t)| = \mathcal{O}(\varepsilon) \tag{28.1.27}$$

for $T^s \leq t \leq 0$. Therefore, a trajectory in $W^s(\gamma_\varepsilon(t))$ leaving $\mathcal{N}(\varepsilon_0)$ in *negative time* must follow $\mathcal{O}(\varepsilon)$ close to a trajectory in $W^s(\gamma(t))$ until it reenters $\mathcal{N}(\varepsilon_0)$ (since we only have a finite time estimate outside of $\mathcal{N}(\varepsilon_0)$).

Hence, this argument shows that $(q_0^s(t), \phi(t))$ and $(q_\varepsilon^s(t), \phi(t))$ remain ε-close for $T^s \leq t < \infty$, i.e., until $(q_\varepsilon^s(t), \phi(t))$ enters $\mathcal{N}(\varepsilon_0)$ under the negative time flow. However, this argument does not rule out the fact that $(q_\varepsilon^s(t), \phi(t))$ can develop "kinks" and therefore re-intersect π_p (while remaining ε-close to $(q_0^s(t), \phi(t))$), as shown in Figure 28.1.15.

This *does not* happen since tangent vectors of $(q_\varepsilon^s(t), \phi(t))$ and $(q_0^s(t), \phi(t))$ are $\mathcal{O}(\varepsilon)$ close for $T^s \leq t < \infty$. This can be seen as follows; we have just shown that on $T^s \leq t < \infty$ we have

$$(q_\varepsilon^s(t), \phi(t)) = (q_0^s(t) + \mathcal{O}(\varepsilon), \phi(t)), \tag{28.1.28}$$

and a vector tangent to $(q_\varepsilon^s(t), \phi(t))$ is given by

$$\begin{aligned} \dot{q}_\varepsilon^s &= JDH(q_\varepsilon^s) + \varepsilon g(q_\varepsilon^s, \phi(t)), \\ \dot{\phi} &= \omega. \end{aligned} \tag{28.1.29}$$

Substituting (28.1.28) into the right-hand side of (28.1.29) and Taylor expanding about $\varepsilon = 0$ gives

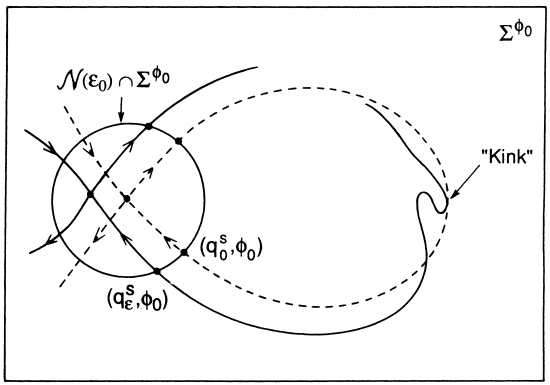

FIGURE 28.1.15.

$$\begin{aligned} \dot{q}_\varepsilon^s &= JDH(q_0^s) + \mathcal{O}(\varepsilon), \\ \dot{\phi} &= \omega. \end{aligned} \tag{28.1.30}$$

Now, a vector tangent to $(q_0^s(t), \phi(t))$ is given by

$$\begin{aligned} \dot{q}_0^s &= JDH(q_0^s), \\ \phi &= \omega. \end{aligned} \tag{28.1.31}$$

Clearly, (28.1.30) and (28.1.31) are $\mathcal{O}(\varepsilon)$ close on $T^s \leq t < \infty$ so that the situation shown in Figure 28.1.15 *cannot* occur on this time interval for ε sufficiently small.

Now let $p_{\varepsilon,\bar{i}}^s \in W^s(\gamma_\varepsilon(t)) \cap \pi_p$ be a point that is *not* closest to $\gamma_\varepsilon(t)$ in terms of positive time of flight as defined in Definition 28.1.2. Let $(q_{\varepsilon,\bar{i}}^s(t), \phi(t)) \in W^s(\gamma_\varepsilon(t))$ satisfy $(q_{\varepsilon,\bar{i}}^s(0), \phi(0)) = p_{\varepsilon,\bar{i}}^s$. Then, by Definition 28.1.2, for some $\bar{t} > 0$, $(q_{\varepsilon,\bar{i}}^s(\bar{t}), \phi_0) \in W^s(\gamma_\varepsilon(t)) \cap \pi_p$. Hence, by the argument given above, for ε sufficiently small, somewhere in $0 < t < \bar{t}$, $(q_{\varepsilon,\bar{i}}^s(t), \phi(t))$ must have entered $\mathcal{N}(\varepsilon_0)$. □

We make the following remarks regarding Lemma 28.1.3.

Remark 1. The reader should note that $T^s = T^s(\varepsilon_0)$. That is why it was necessary to consider a fixed neighborhood containing $\gamma(t)$ and $\gamma_\varepsilon(t)$.

Remark 2. From the proof of Lemma 28.1.3 it follows that the points closest to $\gamma_\varepsilon(t)$ in the sense described in Definition 28.1.2 are unique. We leave the details to Exercise 4.

Remark 3. Let $p_\varepsilon^s = (q_\varepsilon^s, \phi_0) \in W^s(\gamma_\varepsilon(t)) \cap \pi_p$, and let $(q_\varepsilon^s(t), \phi(t)) \in W^s(\gamma_\varepsilon(t))$ satisfy $(q_\varepsilon^s(0), \phi(0)) = (q_\varepsilon^s, \phi_0)$. Then if p_ε^s is the point closest to $\gamma_\varepsilon(t)$ in the sense of Definition 28.1.2, it follows from the proof of Lemma 28.1.3 that

$$|q_\varepsilon^s(t) - q_0(t - t_0)| = \mathcal{O}(\varepsilon), \qquad t \in [0, \infty), \tag{28.1.32}$$

$$|\dot{q}_\varepsilon^s(t) - \dot{q}_0(t - t_0)| = \mathcal{O}(\varepsilon), \qquad t \in [0, \infty). \tag{28.1.33}$$

A similar statement can be made for points in $W^u(\gamma_\varepsilon(t)) \cap \pi_p$ and solutions in $W^u(\gamma_\epsilon(t))$. In deriving the Melnikov function in the next step we will need to approximate perturbed solutions in $W^s(\gamma_\varepsilon(t))$ and $W^u(\gamma_\varepsilon(t))$ by unperturbed solutions in $W^s(\gamma(t))$ and $W^u(\gamma(t))$ for semi-infinite time intervals with $\mathcal{O}(\varepsilon)$ accuracy. This is why the Melnikov function will only detect points on $W^s(\gamma_\varepsilon(t)) \cap \pi_p \cap W^u(\gamma_\varepsilon(t))$ that are closest to $\gamma_\varepsilon(t)$ in the sense of Definition 28.1.2.

Step 3: Derivation of the Melnikov Function. Taylor expanding (28.1.25) about $\varepsilon = 0$ gives

$$d(t_0, \phi_0, \varepsilon) = d(t_0, \phi_0, 0) + \varepsilon \frac{\partial d}{\partial \varepsilon}(t_0, \phi_0, 0) + \mathcal{O}(\varepsilon^2), \tag{28.1.34}$$

where

$$d(t_0, \phi_0, 0) = 0 \tag{28.1.35}$$

and]

$$\frac{\partial d}{\partial \varepsilon}(t_0, \phi_0, 0) = \frac{DH(q_0(-t_0)) \cdot \left(\frac{\partial q_\varepsilon^u}{\partial \varepsilon}|_{\varepsilon=0} - \frac{\partial q_\varepsilon^s}{\partial \varepsilon}|_{\varepsilon=0} \right)}{\|DH(q_0(-t_0))\|}. \tag{28.1.36}$$

The *Melnikov function* is defined to be

$$M(t_0, \phi_0) \equiv DH(q_0(-t_0)) \cdot \left(\frac{\partial q_\varepsilon^u}{\partial \varepsilon}\bigg|_{\varepsilon=0} - \frac{\partial q_\varepsilon^s}{\partial \varepsilon}\bigg|_{\varepsilon=0} \right). \tag{28.1.37}$$

Now, since

$$DH(q_0(-t_0)) = \left(\frac{\partial H}{\partial x}(q_0(-t_0)), \frac{\partial H}{\partial y}(q_0(-t_0)) \right)$$

is not zero on $q_0(-t_0)$, for t_0 finite, we see that

$$M(t_0, \phi_0) = 0 \Rightarrow \frac{\partial d}{\partial \varepsilon}(t_0, \phi_0) = 0. \tag{28.1.38}$$

Therefore, up to a nonzero normalization factor ($\|DH(q_0(-t_0))\|$), the Melnikov function is the lowest order nonzero term in the Taylor expansion for the distance between $W^s(\gamma_\varepsilon(t))$ and $W^u(\gamma_\varepsilon(t))$ at the point p.

We now want to derive an expression for $M(t_0, \phi_0)$ that can be computed without needing to know the solution of the perturbed vector field. We do this by utilizing Melnikov's original trick. We define a time-dependent Melnikov function using the flow generated by both the unperturbed vector field and the perturbed vector field. We have to be careful here since we do not have any a priori knowledge of arbitrary orbits generated by the perturbed vector field. However, the persistence and differentiability of $\gamma(t)$, $W^s(\gamma(t))$, and $W^u(\gamma(t))$ as described in Proposition 28.1.1 are all that we need, since Definition 28.1.2 and Lemma 28.1.3 allow us to characterize the orbits of interest for determining the splitting of $W^s(\gamma_\varepsilon(t))$ and $W^u(\gamma_\varepsilon(t))$. We then derive an ordinary differential equation which the time-dependent Melnikov function must satisfy. The ordinary differential equation turns out to be first order and linear; hence it is trivially solvable. The solution evaluated at the appropriate time will yield the Melnikov function.

We begin by defining the time-dependent Melnikov function as follows

$$M(t; t_0, \phi_0) \equiv DH(q_0(t - t_0)) \cdot \left(\left. \frac{\partial q_\varepsilon^u(t)}{\partial \varepsilon} \right|_{\varepsilon=0} - \left. \frac{\partial q_\varepsilon^s(t)}{\partial \varepsilon} \right|_{\varepsilon=0} \right). \tag{28.1.39}$$

We want to take some care in describing precisely what we mean by (28.1.39). We denote orbits in $W^s(\gamma_\varepsilon(t))$ and $W^u(\gamma_\varepsilon(t))$ by $q_\varepsilon^s(t)$ and $q_\varepsilon^u(t)$, respectively. Then in (28.1.39) the expressions

$$\left. \frac{\partial q_\varepsilon^u(t)}{\partial \varepsilon} \right|_{\varepsilon=0} \tag{28.1.40}$$

and

$$\left. \frac{\partial q_\varepsilon^s(t)}{\partial \varepsilon} \right|_{\varepsilon=0} \tag{28.1.41}$$

are simply the derivatives with respect to ε (evaluated at $\varepsilon = 0$) of $q_\varepsilon^u(t)$ and $q_\varepsilon^s(t)$, respectively, where $q_\varepsilon^u(t)$ and $q_\varepsilon^s(t)$ satisfy

$$q_\varepsilon^u(0) = q_\varepsilon^u, \tag{28.1.42}$$

$$q_\varepsilon^s(0) = q_\varepsilon^s. \tag{28.1.43}$$

The expression $q_0(t-t_0)$ denotes the unperturbed homoclinic orbit. Thus, we see that (28.1.39) is a bit unusual; part of it, $(DH(q_0(t-t_0)))$, evolves in time under the dynamics of the unperturbed vector field with the remaining part

$$\left(\frac{\partial q_\varepsilon^u(t)}{\partial \varepsilon}\bigg|_{\varepsilon=0} - \frac{\partial q_\varepsilon^s(t)}{\partial \varepsilon}\bigg|_{\varepsilon=0} \right)$$

evolving in time under the dynamics of the perturbed vector field. It should be obvious that the relationship between the time-dependent Melnikov function and the Melnikov function is given by

$$M(0; t_0, \phi_0) = M(t_0, \phi_0). \tag{28.1.44}$$

Next we turn to deriving an ordinary differential equation that $M(t; t_0, \phi_0)$ must satisfy. The expressions we derive will be a bit cumbersome, so for the sake of a more compact notation we define

$$\frac{\partial q_\varepsilon^u(t)}{\partial \varepsilon}\bigg|_{\varepsilon=0} \equiv q_1^u(t),$$

$$\frac{\partial q_\varepsilon^s(t)}{\partial \varepsilon}\bigg|_{\varepsilon=0} \equiv q_1^s(t).$$

Then (28.1.39) can be rewritten as

$$M(t; t_0, \phi_0) = DH(q_0(t-t_0)) \cdot (q_1^u(t) - q_1^s(t)). \tag{28.1.45}$$

We want to introduce a further definition to compactify the notation as follows

$$M(t; t_0, \phi_0) \equiv \Delta^u(t) - \Delta^s(t), \tag{28.1.46}$$

where

$$\Delta^{u,s}(t) \equiv DH(q_0(t-t_0)) \cdot q_1^{u,s}(t). \tag{28.1.47}$$

Differentiating (28.1.47) with respect to t gives

$$\begin{aligned} \frac{d}{dt}(\Delta^{u,s}(t)) = &\left(\frac{d}{dt}(DH(q_0(t-t_0))) \right) \cdot q_1^{u,s}(t) \\ &+ DH(q_0(t-t_0)) \cdot \frac{d}{dt} q_1^{u,s}(t). \end{aligned} \tag{28.1.48}$$

The term $\frac{d}{dt}(q_1^{u,s}(t))$ in (28.1.48) needs some explanation. Recall from above that we have defined

$$q_1^{u,s}(t) \equiv \left.\frac{\partial q_\varepsilon^{u,s}(t)}{\partial \varepsilon}\right|_{\varepsilon=0},$$

and $q_\varepsilon^{u,s}(t)$ solves

$$\frac{d}{dt}(q_\varepsilon^{u,s}(t)) = JDH(q_\varepsilon^{u,s}(t)) + \varepsilon g(q_\varepsilon^{u,s}(t), \phi(t), \varepsilon), \tag{28.1.49}$$

where $\phi(t) = \omega t + \phi_0$. Since $q_\varepsilon^{u,s}(t)$ is $\mathbf{C}^r$ in ε and t (see Theorem 7.3.1), we can differentiate (28.1.49) with respect to ε and interchange the order of the ε and t differentiations to obtain

$$\begin{aligned}\frac{d}{dt}\left(\left.\frac{\partial q_\varepsilon^{u,s}(t)}{\partial \varepsilon}\right|_{\varepsilon=0}\right) = {} & JD^2H(q_0(t-t_0))\left.\frac{\partial q_\varepsilon^{u,s}(t)}{\partial \varepsilon}\right|_{\varepsilon=0(t)} \\ & + g(q_0(t-t_0), \phi(t), 0)\end{aligned} \tag{28.1.50}$$

or

$$\frac{d}{dt}q_1^{u,s}(t) = JD^2H(q_0(t-t_0))q_1^{u,s}(t) + g(q_0(t-t_0), \phi(t), 0). \tag{28.1.51}$$

Equation (28.1.51) is referred to as the *first variational equation*. We remark that $q_1^u(t)$ solves (28.1.51) for $t \in (-\infty, 0]$, and $q_1^s(t)$ solves (4.5.51) for $t \in (0, \infty]$; see the remarks following Lemma 28.1.3. Substituting (28.1.51) into (28.1.48) gives

$$\begin{aligned}\frac{d}{dt}(\Delta^{u,s}(t)) = {} & \left(\frac{d}{dt}(DH(q_0(t-t_0)))\right) \cdot q_1^{u,s}(t) \\ & + DH(q_0(t-t_0)) \cdot JD^2H(q_0(t-t_0))q_1^{u,s}(t) \\ & + DH(q_0(t-t_0)) \cdot g(q_0(t-t_0), \phi(t), 0).\end{aligned} \tag{28.1.52}$$

Now a wonderful thing happens.

Lemma 28.1.4

$$\begin{aligned}&\left(\frac{d}{dt}(DH(q_0(t-t_0)))\right) \cdot q_1^{u,s}(t) \\ &\quad + DH(q_0(t-t_0)) \cdot \ JD^2H(q_0(t-t_0))q_1^{u,s}(t) = 0.\end{aligned}$$

Proof: First note that

$$\frac{d}{dt}\big(DH(q_0(t-t_0))\big) = D^2H(q_0(t-t_0))\dot{q}_0(t-t_0)$$
$$= \big(D^2H(q_0(t-t_0))\big)\big(JDH(q_0(t-t_0))\big). \tag{28.1.53}$$

Let $q_1^{u,s}(t) = (x_1^{u,s}(t), y_1^{u,s}(t))$. Then we have

$$(D^2H)(JDH)\cdot q_1^{u,s} = \begin{pmatrix} \frac{\partial^2 H}{\partial x^2} & \frac{\partial^2 H}{\partial x \partial y} \\ \frac{\partial^2 H}{\partial x \partial y} & \frac{\partial^2 H}{\partial y^2} \end{pmatrix} \begin{pmatrix} \frac{\partial H}{\partial y} \\ -\frac{\partial H}{\partial x} \end{pmatrix} \cdot \begin{pmatrix} x_1^{u,s} \\ \\ y_1^{u,s} \end{pmatrix}$$
$$= x_1^{u,s}\left[\frac{\partial^2 H}{\partial x^2}\frac{\partial H}{\partial y} - \frac{\partial^2 H}{\partial x \partial y}\frac{\partial H}{\partial x}\right]$$
$$+ y_1^{u,s}\left[\frac{\partial^2 H}{\partial x \partial y}\frac{\partial H}{\partial y} - \frac{\partial^2 H}{\partial y^2}\frac{\partial H}{\partial x}\right] \tag{28.1.54}$$

and

$$DH\cdot(JD^2H)q_1^{u,s} = \begin{pmatrix} \frac{\partial H}{\partial x} \\ \frac{\partial H}{\partial y} \end{pmatrix} \cdot \begin{pmatrix} \frac{\partial^2 H}{\partial x \partial y} & \frac{\partial^2 H}{\partial y^2} \\ -\frac{\partial^2 H}{\partial x^2} & \frac{\partial^2 H}{\partial x \partial y} \end{pmatrix} \begin{pmatrix} x_1^{u,s} \\ \\ y_1^{u,s} \end{pmatrix}$$
$$= x_1^{u,s}\left[\frac{\partial^2 H}{\partial x \partial y}\frac{\partial H}{\partial x} - \frac{\partial^2 H}{\partial x^2}\frac{\partial H}{\partial y}\right]$$
$$+ y_1^{u,s}\left[\frac{\partial^2 H}{\partial y^2}\frac{\partial H}{\partial x} - \frac{\partial^2 H}{\partial x \partial y}\frac{\partial H}{\partial y}\right], \tag{28.1.55}$$

where we have left out the argument $q_0(t-t_0) = (x_0(t-t_0), y_0(t-t_0))$ for the sake of a less cumbersome notation. Adding (28.1.54) and (28.1.55) gives the result. □

Therefore, using Lemma 28.1.4, (28.1.48) becomes

$$\frac{d}{dt}(\Delta^{u,s}(t)) = DH(q_0(t-t_0))\cdot g(q_0(t-t_0), \phi(t), 0). \tag{28.1.56}$$

Integrating $\Delta^u(t)$ and $\Delta^s(t)$ individually from $-\tau$ to 0 and 0 to τ ($\tau > 0$), respectively, gives

$$\Delta^u(0) - \Delta^u(-\tau) = \int_{-\tau}^{0} DH(q_0(t-t_0))\cdot g(q_0(t-t_0), \omega t + \phi_0, 0)dt \tag{28.1.57}$$

and

$$\Delta^s(\tau) - \Delta^s(0) = \int_0^\tau DH(q_0(t-t_0)) \cdot g(q_0(t-t_0), \omega t + \phi_0, 0)dt \quad (28.1.58)$$

where we have substituted $\phi(t) = \omega t + \phi_0$ into the integrand. Adding (28.1.57) and (28.1.58) and referring to (28.1.44) and (28.1.46) gives

$$\begin{aligned} M(t_0, \phi_0) = M(0, t_0, \phi_0) &= \Delta^u(0) - \Delta^s(0) \\ &= \int_{-\tau}^{\tau} DH(q_0(t-t_0)) \cdot g(q_0(t-t_0), \omega t + \phi_0, 0)dt \\ &\quad + \Delta^s(\tau) - \Delta^u(-\tau). \end{aligned} \quad (28.1.59)$$

We now want to consider the limit of (28.1.59) as $\tau \to \infty$.

Lemma 28.1.5

$$\lim_{\tau\to\infty} \Delta^s(\tau) = \lim_{\tau\to\infty} \Delta^u(-\tau) = 0.$$

Proof: Recall from (28.1.47) that

$$\Delta^{u,s}(t) = DH(q_0(t-t_0)) \cdot q_1^{u,s}(t).$$

Now, as $t \to \infty$ (resp. $-\infty$), $DH(q_0(t-t_0))$ goes to zero *exponentially* fast, since $q_0(t-t_0)$ approaches a *hyperbolic* fixed point. Also, as $t \to \infty$ (resp. $-\infty$), $q_1^s(t)$ (resp. $q_1^u(t)$) is bounded (see Exercise 6). Hence, $\Delta^s(\tau)$ (resp. $\Delta^u(-\tau)$) goes to zero as $\tau \to \infty$. □

Lemma 28.1.6 *The improper integral*

$$\int_{-\infty}^{\infty} DH(q_0(t-t_0)) \cdot g(q_0(t-t_0), \omega t + \phi_0, 0)dt$$

converges absolutely.

Proof: This result follows from the fact that $g(q_0(t-t_0), \omega t + \phi_0, 0)$ is bounded for all t and $DH(q_0(t-t_0))$ goes to zero exponentially fast as $t \to \pm\infty$. □

Hence, combining Lemma 28.1.5 and Lemma 28.1.6, (28.1.59) becomes

$$M(t_0, \phi_0) = \int_{-\infty}^{\infty} DH(q_0(t-t_0)) \cdot g(q_0(t-t_0), \omega t + \phi_0, 0)dt. \quad (28.1.60)$$

Before giving the main theorem we want to point out an interesting property of the Melnikov function. If we make the transformation

$$t \longrightarrow t + t_0,$$

then (28.1.60) becomes

$$M(t_0, \phi_0) = \int_{-\infty}^{\infty} DH(q_0(t)) \cdot g(q_0(t), \omega t + \omega t_0 + \phi_0, 0) dt. \tag{28.1.61}$$

Recall that $g(q, \cdot, 0)$ is periodic, which implies that $M(t_0, \phi_0)$ is periodic in t_0 with period $2\pi/\omega$ *and* periodic in ϕ_0 with period 2π. The geometry of this will be explained shortly. However, it should be clear from (28.1.61) that varying t_0 and varying ϕ_0 have the same effect. Moreover, from (28.1.61) and the periodicity of $g(q, \cdot, 0)$, it follows that

$$\frac{\partial M}{\partial \phi_0}(t_0, \phi_0) = \frac{1}{\omega} \frac{\partial M}{\partial t_0}(t_0, \phi_0); \tag{28.1.62}$$

hence, $\frac{\partial M}{\partial t_0} = 0$ if and only if $\frac{\partial M}{\partial \phi_0} = 0$. In Theorem 28.1.7 we will need to have $\frac{\partial M}{\partial t_0} \neq 0$ or $\frac{\partial M}{\partial \phi_0} \neq 0$. However, from (28.1.62), if one is nonzero, then so is the other; hence, we will state the theorem in terms of $\frac{\partial M}{\partial t_0} \neq 0$.

Theorem 28.1.7 *Suppose we have a point* $(t_0, \phi_0) = (\bar{t}_0, \bar{\phi}_0)$ *such that*

i) $M(\bar{t}_0, \bar{\phi}_0) = 0$ *and*

ii) $\left.\frac{\partial M}{\partial t_0}\right|_{(\bar{t}_0, \bar{\phi}_0)} \neq 0.$

Then, for ε *sufficiently small,* $W^s(\gamma_\varepsilon(t))$ *and* $W^u(\gamma_\varepsilon(t))$ *intersect transversely at* $(q_0(-\bar{t}_0) + \mathcal{O}(\varepsilon), \bar{\phi}_0)$. *Moreover, if* $M(t_0, \phi_0) \neq 0$ *for all* $(t_0, \phi_0) \in \mathbb{R}^1 \times S^1$, *then* $W^s(\gamma_\varepsilon(t)) \cap W^u(\gamma_\varepsilon(t)) = \emptyset$.

Proof: Recall from (28.1.34), (28.1.36), and (28.1.37) that we have

$$d(t_0, \phi_0, \varepsilon) = \varepsilon \frac{M(t_0, \phi_0)}{\|DH(q_0(-t_0))\|} + \mathcal{O}(\varepsilon^2). \tag{28.1.63}$$

Note that if we define

$$d(t_0, \phi_0, \varepsilon) = \varepsilon \tilde{d}(t_0, \phi_0, \varepsilon), \tag{28.1.64}$$

where

$$\tilde{d}(t_0, \phi_0, \varepsilon) = \frac{M(t_0, \phi_0)}{\|DH(q_0(-t_0))\|} + \mathcal{O}(\varepsilon), \tag{28.1.65}$$

then

$$\tilde{d}(t_0, \phi_0, \varepsilon) = 0 \Rightarrow d(t_0, \phi_0, \varepsilon) = 0. \tag{28.1.66}$$

Therefore, we will work with $\tilde{d}(t_0, \phi_0, \varepsilon)$.

Now at $(t_0, \phi_0, \varepsilon) = (\bar{t}_0, \bar{\phi}_0, 0)$ we have

$$\tilde{d}(\bar{t}_0, \bar{\phi}_0, 0) = \frac{M(\bar{t}_0, \bar{\phi}_0)}{\|DH(q_0(-\bar{t}_0))\|} = 0, \tag{28.1.67}$$

with

$$\left.\frac{\partial \tilde{d}}{\partial t_0}\right|_{(\bar{t}_0, \bar{\phi}_0, 0)} = \frac{1}{\|DH(q_0(-\bar{t}_0))\|} \left.\frac{\partial M}{\partial t_0}\right|_{(\bar{t}_0, \bar{\phi}_0)} \neq 0. \tag{28.1.68}$$

By the implicit function theorem, there thus exists a function

$$t_0 = t_0(\phi_0, \varepsilon) \tag{28.1.69}$$

for $|\phi - \phi_0|$, ε sufficiently small, such that

$$\tilde{d}(t_0(\phi_0, \varepsilon), \phi_0, \varepsilon) = 0. \tag{28.1.70}$$

This shows that $W^s(\gamma_\varepsilon(t))$ and $W^u(\gamma_\varepsilon(t))$ intersect $\mathcal{O}(\varepsilon)$ close to $(q_0(-t_0), \phi_0)$. Next we need to worry about transversality.

Suppose that $W^s(\gamma_\varepsilon(t))$ and $W^u(\gamma_\varepsilon(t))$ intersect at some point p. Then recall from Chapter 12 that the intersection is said to be transversal if

$$T_p W^s(\gamma_\varepsilon(t)) + T_p W^u(\gamma_\varepsilon(t)) = \mathbb{R}^3. \tag{28.1.71}$$

Now, for ε sufficiently small, the points on $W^s(\gamma_\varepsilon(t))$ and $W^u(\gamma_\varepsilon(t))$ that are closest to $\gamma_\varepsilon(t)$ in the sense of Definition 28.1.2 can be parametrized by t_0 and ϕ_0. Hence,

$$\left(\frac{\partial q^u_\varepsilon}{\partial t_0}, \frac{\partial q^u_\varepsilon}{\partial \phi_0}\right) \tag{28.1.72}$$

and

$$\left(\frac{\partial q^s_\varepsilon}{\partial t_0}, \frac{\partial q^s_\varepsilon}{\partial \phi_0}\right) \tag{28.1.73}$$

are a basis for $T_p W^u(\gamma_\varepsilon(t))$ and $T_p W^s(\gamma_\varepsilon(t))$, respectively.

(Note: it is important for the reader to understand how (28.1.72) and (28.1.73) are computed. By definition, $p = (q^s_\varepsilon, \phi_0) = (q^u_\varepsilon, \phi_0)$, and q^s_ε and q^u_ε are the points satisfying $q^s_\varepsilon(0) = q^s_\varepsilon$, $q^u_\varepsilon(0) = q^u_\varepsilon$, where $q^s_\varepsilon(t)$ and $q^u_\varepsilon(t)$

are trajectories in $W^s(\gamma_\varepsilon(t))$ and $W^u(\gamma_\varepsilon(t))$, respectively. Since those trajectories depend parametrically on t_0 and ϕ_0, (28.1.72) and (28.1.73) are simply the derivatives of the respective trajectories with respect to t_0 and ϕ_0 evaluated at $t = 0$.)

$T_pW^s(\gamma_\varepsilon(t))$ and $T_pW^u(\gamma_\varepsilon(t))$ will not be tangent at p provided

$$\frac{\partial q_\varepsilon^u}{\partial t_0} - \frac{\partial q_\varepsilon^s}{\partial t_0} \neq 0 \tag{28.1.74}$$

or

$$\frac{\partial q_\varepsilon^u}{\partial \phi_0} - \frac{\partial q_\varepsilon^u}{\partial \phi_0} \neq 0. \tag{28.1.75}$$

Differentiating $d(t_0, \phi_0, \varepsilon)$ with respect to t_0 and ϕ_0 and evaluating at the intersection point given by $(\bar{t}_0 + \mathcal{O}(\varepsilon), \bar{\phi}_0)$ (where $M(\bar{t}_0, \bar{\phi}_0) = 0$) gives

$$\begin{aligned}\frac{\partial d}{\partial t_0}(\bar{t}_0, \bar{\phi}_0, \varepsilon) &= \frac{DH(q_0(-\bar{t}_0)) \cdot ((\partial q_\varepsilon^u)/(\partial t_0) - (\partial q_\varepsilon^s)/(\partial t_0))}{\|DH(q_0(-\bar{t}_0))\|} \\ &= \varepsilon \frac{(\partial M/\partial t_0)(\bar{t}_0, \bar{\phi}_0)}{\|DH(q_0(-t_0))\|} + \mathcal{O}(\varepsilon^2),\end{aligned} \tag{28.1.76}$$

$$\begin{aligned}\frac{\partial d}{\partial \phi_0}(\bar{t}_0, \bar{\phi}_0, \varepsilon) &= \frac{DH(q_0(-\bar{t}_0)) \cdot ((\partial q_\varepsilon^u)/(\partial \phi_0) - (\partial q_\varepsilon^s)/(\partial \phi_0))}{\|DH(q_0(-\bar{t}_0))\|} \\ &= \varepsilon \frac{(\partial M/\partial \phi_0)(\bar{t}_0, \bar{\phi}_0)}{\|DH(q_0(-\bar{t}_0))\|} + \mathcal{O}(\varepsilon^2).\end{aligned} \tag{28.1.77}$$

Hence, it should be clear from (28.1.76) and (28.1.77) that, for ε sufficiently small, a sufficient condition for transversality is

$$\frac{\partial M}{\partial \phi_0}(\bar{t}_0, \bar{\phi}_0) = \frac{1}{\omega}\frac{\partial M}{\partial t_0}(\bar{t}_0, \bar{\phi}_0) \neq 0. \tag{28.1.78}$$

Finally, we leave the fact that $M(t_0, \phi_0) \neq 0$ implies $W^s(\gamma_\varepsilon(t)) \cap W^u(\gamma_\varepsilon(t)) = \emptyset$ as an exercise for the reader (see Exercise 7). □

28.2 Poincaré Maps and the Geometry of the Melnikov Function

We now want to describe the geometry associated with the independent variables, t_0 and ϕ_0, of the Melnikov function.

Consider the following cross-section to the phase space $\mathbb{R}^2 \times S^1$

$$\Sigma^{\phi_0} = \big\{(q,\phi) \in \mathbb{R}^2 \times S^1 \,|\, \phi = \phi_0\big\}. \tag{28.2.1}$$

Since $\dot{\phi} = \omega > 0$, it follows that the vector field is transverse to Σ^{ϕ_0}. Then the Poincaré map of Σ^{ϕ_0} into itself defined by the flow generated by the perturbed vector field (28.1.6) is given by

$$\begin{aligned} P_\varepsilon : \Sigma^{\phi_0} &\longrightarrow \Sigma^{\phi_0}, \\ q_\varepsilon(0) &\longmapsto q_\varepsilon(2\pi/\omega), \end{aligned} \tag{28.2.2}$$

where $(q_\varepsilon(t), \phi(t) = \omega t + \phi_0)$ denotes the flow generated by the perturbed vector field (28.1.6). Now the periodic orbit $\gamma_\varepsilon(t)$ intersects Σ^{ϕ_0} in a point which we denote as

$$p_{\varepsilon,\phi_0} = \gamma_\varepsilon(t) \cap \Sigma^{\phi_0}. \tag{28.2.3}$$

It should be clear that p_{ε,ϕ_0} is a hyperbolic fixed point for the Poincaré map having a one-dimensional stable manifold, $W^s(p_{\varepsilon,\phi_0})$ and a one-dimensional unstable manifold, $W^u(p_{\varepsilon,\phi_0})$ given by

$$W^s(p_{\varepsilon,\phi_0}) \equiv W^s(\gamma_\varepsilon(t)) \cap \Sigma^{\phi_0}$$

and

$$W^u(p_{\varepsilon,\phi_0}) \equiv W^u(\gamma_\varepsilon(t)) \cap \Sigma^{\phi_0}, \tag{28.2.4}$$

respectively; see Figure 28.2.1.

Now let us return to the Melnikov function. From our parametrization of the homoclinic manifold, Γ_γ, it follows that *fixing* ϕ_0 and varying t_0 corresponds to restricting our distance measurement to a fixed cross-section Σ^{ϕ_0}. In this case, $M(t_0, \phi_0)$, ϕ_0 fixed, is a measurement of the distance between $W^s(p_{\varepsilon,\phi_0})$ and $W^u(p_{\varepsilon,\phi_0})$. In this case also zeros of the Melnikov function correspond to homoclinic points of a two-dimensional map, and Moser's theorem or the Smale–Birkhoff homoclinic theorem may be applied to conclude that the dynamics are chaotic (provided the homoclinic points are transverse).

Alternately, we can *fix* t_0 and vary ϕ_0 in the Melnikov function. This would correspond to fixing π_p at a specific point $(q_0(-t_0), \phi_0)$ on Γ_γ and varying the cross-section Σ^{ϕ_0}. The Melnikov function would be a measure of the distance between $W^s(\gamma_\varepsilon(t))$ and $W^u(\gamma_\varepsilon(t))$ at a fixed location in q but on different cross-sections Σ^{ϕ_0}. Since the vector field has no fixed points on $W^s(\gamma_\varepsilon(t)) \cup W^u(\gamma_\varepsilon(t))$, as the cross-section is varied all orbits in $W^s(\gamma_\varepsilon(t)) \cup W^u(\gamma_\varepsilon(t))$ must pass through π_p with $q_0(-t_0)$ fixed. Hence, no homoclinic orbits would be "missed" by the Melnikov function.

However, recall the form of the Melnikov function given in (28.1.61)

$$M(t_0, \phi_0) = \int_{-\infty}^{\infty} DH(q_0(t)) \cdot g(q_0(t), \omega t + \omega t_0 + \phi_0, 0) dt. \tag{28.2.5}$$

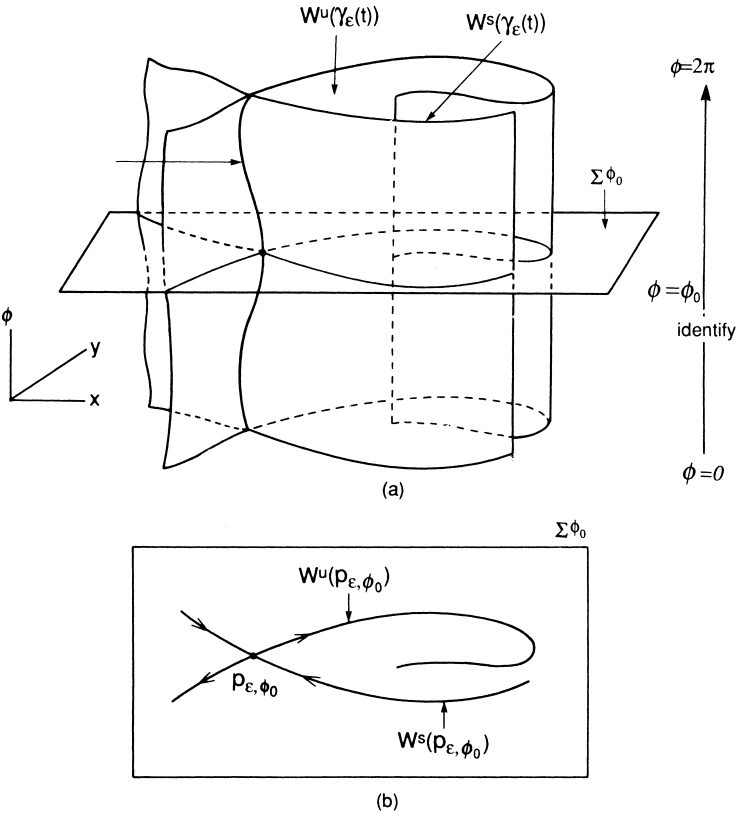

FIGURE 28.2.1.

It is clear from (28.2.5) that, analytically, the variation of t_0 with ϕ_0 fixed is equivalent to the variation of ϕ_0 with t_0 fixed. The underlying reason for this is that if $W^s(\gamma_\varepsilon(t))$ and $W^u(\gamma_\varepsilon(t))$ intersect, by uniqueness of solutions they cannot intersect at isolated points but, rather, must intersect along a trajectory (solution of (28.1.6)) that is asymptotic to $\gamma_\varepsilon(t)$ in both positive and negative time.

28.3 Some Properties of the Melnikov Function

Here we collect some basic properties and characteristics of the Melnikov function.

1. As mentioned earlier, $M(t_0, \phi_0)$ is a signed measure of the distance.

We now want to explore this in more detail. Let us restrict ourselves to the Poincaré map defined on the cross-section Σ^{ϕ_0} and view ϕ_0 as fixed; then $d(t_0, \phi_0, \varepsilon)$ measures the distance between $W^s(p_{\varepsilon,\phi_0})$ and $W^u(p_{\varepsilon,\phi_0})$ (see Section 28.2). We recall that the *distance between* $W^s(p_{\varepsilon,\phi_0})$ *and* $W^u(p_{\varepsilon,\phi_0})$ *at the point* $p = (q_0(-t_0), \phi_0)$ is given by

$$\begin{aligned} d(t_0, \phi_0, \varepsilon) &= \frac{DH(q_0(-t_0)) \cdot (q^u_\varepsilon - q^s_\varepsilon)}{\|DH(q_0(-t_0))\|} \\ &= \varepsilon \frac{M(t_0, \phi_0)}{\|DH(q_0(-t_0))\|} + \mathcal{O}(\varepsilon^2) \end{aligned} \tag{28.3.1}$$

where q^u_ε and q^s_ε are defined in Definition 28.1.2. Hence, for ε sufficiently small

$$M(t_0, \phi_0) \begin{matrix} > \\ < \end{matrix} 0 \Rightarrow d(t_0, \phi_0, \varepsilon) \begin{matrix} > \\ < \end{matrix} 0. \tag{28.3.2}$$

Thus, using (28.3.1) and (28.3.2), Figure 28.1.10 holds if we replace $d(t_0, \phi_0, \varepsilon)$ with $M(t_0, \phi_0)$.

2. $M(t_0, \phi_0)$ is periodic in t_0 with period $2\pi/\omega$ and periodic in ϕ_0 with period 2π. This follows from the fact that the perturbation, $\varepsilon g(q, t, \varepsilon)$, is periodic in t with period $2\pi/\omega$ as well as from the form of $M(t_0, \phi_0)$ given in (28.1.61).

3. Recall from (28.3.1) that the distance between $W^s(\gamma_\varepsilon(t))$ and $W^u(\gamma_\varepsilon(t))$ is given by

$$d(t_0, \phi_0, \varepsilon) = \varepsilon \frac{M(t_0, \phi_0)}{\|DH(q_0(-t_0))\|} + \mathcal{O}(\varepsilon^2). \tag{28.3.3}$$

We want to focus on the denominator, $\|DH(q_0(-t_0))\|$, in the $\mathcal{O}(\varepsilon)$ term of (28.3.3). Let us consider the situation with ϕ_0 fixed so that $d(t_0, \phi_0, \varepsilon)$ measures the distance between the stable and unstable manifolds of a hyperbolic fixed point of the Poincaré map (see Section 28.2). Then, as $t_0 \to \pm\infty$, the measurement of distance is being made close to the hyperbolic fixed point (since $q_0(-t_0)$ approaches the unperturbed hyperbolic fixed point as $t_0 \to \pm\infty$). Also, as $t_0 \to \pm\infty$, $\|DH(q_0(-t_0))\| \to 0$, indicating that $d(t_0, \phi_0, \varepsilon) \to \infty$. Geometrically, this means that the distance between the manifolds is oscillating unboundedly near the hyperbolic fixed point. The reader should compare this analytic result with the geometrical picture given by the lambda lemma (Lemma 26.0.4).

4. Suppose that the perturbation is autonomous, i.e., $\varepsilon g(q)$ does not depend explicitly on time. Then the Melnikov function is given by

$$M = \int_{-\infty}^{\infty} DH(q_0(t)) \cdot g(q_0(t), 0) dt. \tag{28.3.4}$$

In this case M is just a number, i.e., it is not a function of t_0 and ϕ_0. This makes sense, since, for autonomous two-dimensional vector fields, either the stable and unstable manifolds of a hyperbolic fixed point coincide or they do not intersect at all. In Exercise 11 we will deal more fully with the geometry of the Melnikov function for autonomous problems.

5. Suppose the vector field is Hamiltonian, i.e., we have a $\mathbf{C}^{r+1}$ $(r \geq 2)$ function periodic in t with period $T = 2\pi/\omega$ given by

$$H_\varepsilon(x, y, t) = H(x, y) + \varepsilon H_1(x, y, t, \varepsilon) \tag{28.3.5}$$

such that the perturbed vector field (28.1.1) is given by

$$\begin{aligned} \dot{x} &= \frac{\partial H}{\partial y}(x, y) + \varepsilon \frac{\partial H_1}{\partial y}(x, y, t, \varepsilon), \\ \dot{y} &= -\frac{\partial H}{\partial x}(x, y) - \varepsilon \frac{\partial H_1}{\partial x}(x, y, t, \varepsilon). \end{aligned} \tag{28.3.6}$$

In this case, using (28.1.61) and (28.3.6), it is easy to see that the Melnikov function is given by

$$M(t_0, \phi_0) = -\int_{-\infty}^{\infty} \{H, H_1\}(q_0(t), \omega t + \omega t_0 + \phi_0, 0) dt, \tag{28.3.7}$$

where

$$\{H, H_1\} \equiv \frac{\partial H}{\partial x}\frac{\partial H_1}{\partial y} - \frac{\partial H}{\partial y}\frac{\partial H_1}{\partial x} \tag{28.3.8}$$

is the *Poisson bracket* of H with H_1.

28.4 Homoclinic Bifurcations

Suppose the vector field (28.1.6) depends on a scalar parameter μ, i.e.,

$$\begin{aligned} \dot{q} &= JDH(q) + \varepsilon g(q, \phi, \mu, \varepsilon), \\ \dot{\phi} &= \omega, \qquad (q, \phi, \mu) \in \mathbb{R}^2 \times S^1 \times \mathbb{R}^1. \end{aligned} \tag{28.4.1}$$

If, in a specific problem, there is more than one parameter, then consider all but one as fixed. In this case the Melnikov functions depend on the parameter μ. In particular, we write

$$M(t_0, \phi_0, \mu). \tag{28.4.2}$$

We will consider ϕ_0 as fixed, i.e., the Poincaré map associated with (28.4.1) is defined on the cross-section Σ^{ϕ_0}. We have the following bifurcation theorem for the Melnikov function.

Theorem 28.4.1 *Suppose we have* $(\bar{t}_0, \overline{\mu})$ *such that*

i) $M(\bar{t}_0, \phi_0, \overline{\mu}) = 0$,

ii) $\dfrac{\partial M}{\partial t_0}(\bar{t}_0, \phi_0, \overline{\mu}) = 0$,

iii) $\dfrac{\partial M}{\partial \mu}(\bar{t}_0, \phi_0, \overline{\mu}) \neq 0$,

iv) $\dfrac{\partial^2 M}{\partial t_0^2}(\bar{t}_0, \phi_0, \overline{\mu}) \neq 0$.

Then the stable and unstable manifolds of the hyperbolic fixed point on the cross-section Σ^{ϕ_0} *are quadratically tangent at* $(q_0(-\bar{t}_0)) + \mathcal{O}(\varepsilon)$ *for* $\mu = \overline{\mu} + \mathcal{O}(\varepsilon)$.

Proof: Tangency of the manifolds implies

$$\begin{aligned} d(t_0, \phi_0, \mu, \varepsilon) &= 0, \\ \frac{\partial d}{dt_0}(t_0, \phi_0, \mu, \varepsilon) &= 0. \end{aligned} \tag{28.4.3}$$

Let $d(t_0, \phi_0, \mu, \varepsilon) = \varepsilon \tilde{d}(t_0, \phi_0, \mu, \varepsilon)$ with

$$\tilde{d}(t_0, \phi_0, \mu, \varepsilon) = \frac{M(t_0, \phi_0, \mu)}{\|DH(q_0(-t_0))\|} + \mathcal{O}(\varepsilon), \tag{28.4.4}$$

as in the proof of Theorem 28.1.7. Then a solution of

$$\begin{aligned} \tilde{d}(t_0, \phi_0, \mu, \varepsilon) &= 0, \\ \frac{\partial \tilde{d}}{\partial t_0}(t_0, \phi_0, \mu, \varepsilon) &= 0, \end{aligned} \tag{28.4.5}$$

is a solution of (28.4.3). Now by Hypotheses i) and ii) of the theorem, (28.4.5) has a solution at $(\bar{t}_0, \phi_0, \overline{\mu}, 0)$. Hypotheses iii) and iv) allow us to apply the implicit function theorem to show that the solution persits for ε sufficiently small; the details follow exactly as in the proof of Theorem 28.1.7 and are left as an exercise for the reader. □

We remark that the condition $\frac{\partial^2 M}{\partial t_0^2}(\bar{t}_0, \phi_0, \overline{\mu}) \neq 0$ implies that the tangency is quadratic.

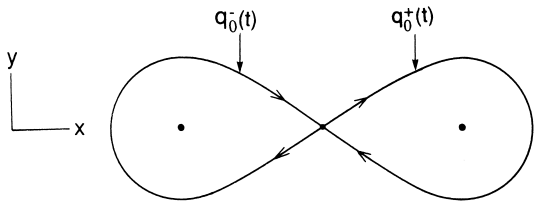

FIGURE 28.4.1.

28.5 Application to the Damped, Forced Duffing Oscillator

The damped, forced Duffing oscillator is given by

$$\begin{aligned} \dot{x} &= y, \\ \dot{y} &= x - x^3 + \varepsilon(\gamma \cos\phi - \delta y), \\ \dot{\phi} &= \omega. \end{aligned} \tag{28.5.1}$$

For $\varepsilon = 0$, (28.5.1) has a pair of homoclinic orbits (see Exercise 1.2.29) given by

$$q_0^{\pm}(t) = (x_0^{\pm}(t), y_0^{\pm}(t)) = \big(\pm\sqrt{2}\,\mathrm{sech}\,t, \mp\sqrt{2}\,\mathrm{sech}\,t\,\tanh t\big); \tag{28.5.2}$$

see Figure 28.4.1.

The homoclinic Melnikov function is given by

$$\begin{aligned} &M^{\pm}(t_0, \phi_0) \\ &\quad = \int_{-\infty}^{\infty} [-\delta(y^{\pm}(t))^2 \pm \gamma y^{\pm}(t) \cos(\omega t + \omega t_0 + \phi_0)]dt. \end{aligned} \tag{28.5.3}$$

Substituting (28.5.2) into (28.5.3) gives

$$M^{\pm}(t_0, \phi_0) = -\frac{4\delta}{3} \pm \sqrt{2}\gamma\pi\omega\,\mathrm{sech}\frac{\pi\omega}{2}\sin(\omega t_0 + \phi_0). \tag{28.5.4}$$

Fixing ϕ_0 defines a cross-section

$$\Sigma^{\phi_0} = \big\{(x, y, \phi) \in \mathbb{R} \times \mathbb{R} \times S^1 \,|\, \phi = \phi_0\big\}, \tag{28.5.5}$$

where the Melnikov function describes the splitting of the stable and unstable manifolds of the hyperbolic fixed point defined on the cross-section. Let $P_{\varepsilon}^{\phi_0}$ denote the Poincaré map of the cross-section Σ^{ϕ_0} defined by the flow generated by (28.5.1) and consider the case $\delta = 0$. Then, using the Melnikov function (28.5.4) and Remark 1 of Section 28.3, it is easy to verify that the stable and unstable manifolds of the hyperbolic fixed point P_{ϕ_0}

intersect as in Figure 28.5.1 for $\phi_0 = 0$, $\pi/2$, π, and $3\pi/2$. Figure 28.5.1 illustrates an important point; namely, that altering the cross-section on which the Poincaré map is defined can change the symmetry properties of the Poincaré map. This can often result in substantial savings in computer time in the numerical computation of Poincaré maps. We will explore these issues in Exercise 10 as well as consider how Figure 28.5.1 changes for $\delta \neq 0$.

From (28.5.4) it is easy to see that the condition for the manifolds to intersect in terms of the parameters (δ, ω, γ) is given by

$$\delta < \left(\frac{3\pi\omega \operatorname{sech} \frac{\pi\omega}{2}}{2\sqrt{2}} \right) \gamma. \tag{28.5.6}$$

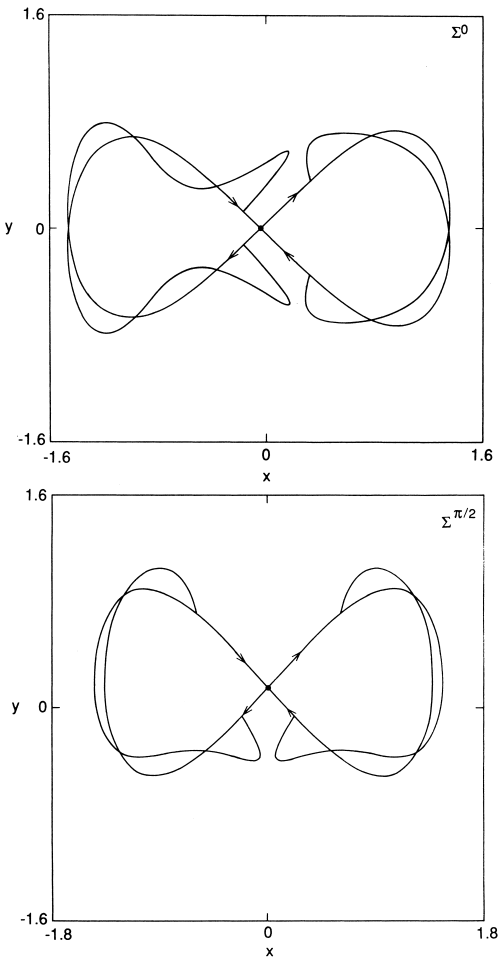

FIGURE 28.5.1.

In Figure 28.5.2 we graph the critical surface $\delta = \left(\frac{3\pi\omega \operatorname{sech}(\pi\omega/2)}{2\sqrt{2}}\right)\gamma$, and we note the following.

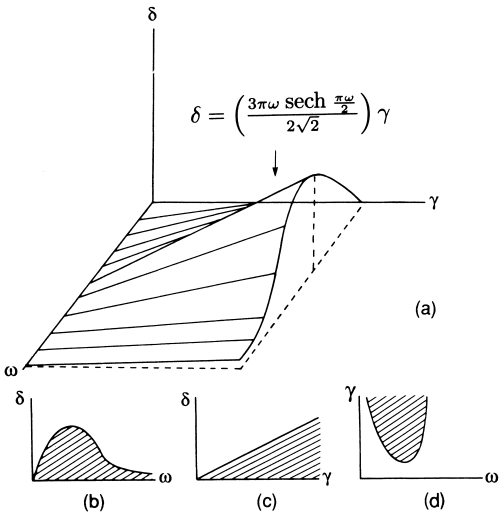

FIGURE 28.5.2. a) Graph of the critical surface $\delta = \left(\frac{3\pi\omega \operatorname{sech}(\pi\omega/2)}{2\sqrt{2}}\right)\gamma$. b) Cross-section of the critical surface for γ = constant. c) Cross-section of the critical surface for ω = constant. d) Cross-section of the critical surface for δ = constant.

1. The condition (28.5.6) for intersection of the manifolds is independent of the particular cross-section Σ^{ϕ_0} (as it should be).

2. If the "right-hand" branches of the stable and unstable manifolds intersect, then the "left-hand" branches also intersect, and vice-versa. However, as seen in Figure 28.5.1, the geometry of intersections of the right-hand branches and left-hand branches may differ.

Thus, (28.5.6) is a criterion for chaos in the damped, forced Duffing oscillator as a function of the parameters (δ, ω, γ).

Finally we remark that Melnikov-type methods have been developed for multi-degree-of-freedom systems and for systems having more general time dependencies. These techniques also deal with orbits homoclinic to invariant sets other than periodic orbits. A complete exposition of this theory can be found in Wiggins [1988].

28.6 Exercises

1. Consider the parametrization of the homoclinic manifold given in (28.1.9). Show that the map
$$(t_0, \phi_0) \mapsto (q_0(-t_0), \phi_0), \qquad (t_0, \phi_0) \in \mathbb{R}^1 \times S^1,$$
is $\mathbf{C}^r$, one-to-one, and onto.

2. Recall Proposition 28.1.1. Prove that, for ε sufficiently small, $\gamma_\varepsilon(t)$ persists as a periodic orbit of period $T = 2\pi/\omega$ having the same stability type as $\gamma(t)$. For information concerning the persistence of the local stable and unstable manifolds, see Fenichel [1971] or Wiggins [1994].

3. Suppose that Γ_γ intersects π_p transversely at some $p = (q_0(-t_0), \phi_0)$. Show that, for ε sufficiently small, $W^s(\gamma_\varepsilon(t))$ and $W^u(\gamma_\varepsilon(t))$ each intersect Π_p transversely at a distance $\mathcal{O}(\varepsilon)$ from p.

4. Recall Definition 28.1.2. Show that the points $p^s_{\varepsilon,\bar{t}}$ and $p^u_{\varepsilon,\bar{t}}$ "closest" to $\gamma_\varepsilon(t)$ in the sense of Definition 28.1.2 are unique. (*Hint:* study the proof of Lemma 28.1.3.)

5. Recall the set-up for the proof of Lemma 28.1.3. Choose
$$(q^s_0, \phi_0) \in W^s_{\text{loc}}(\gamma(t)) \cap \mathcal{N}(\varepsilon_0)$$
and
$$(q^s_\varepsilon, \phi_0) \in W^s_{\text{loc}}(\gamma_\varepsilon(t)) \cap \mathcal{N}(\varepsilon_0),$$
with the trajectories
$$(q^s_0(t), \phi(t)) \in W^s(\gamma(t))$$
and
$$(q^s_\varepsilon(t), \phi(t)) \in W^s(\gamma_\varepsilon(t))$$
satisfying
$$(q^s_0(0), \phi(0)) = (q^s_0, \phi_0)$$
and
$$(q^s_\varepsilon(0), \phi(0)) = (q^s_\varepsilon, \phi_0).$$
Prove that
$$\left|(q^s_\varepsilon(t), \phi(t)) - (q^s_0(t), \phi(t))\right| = \mathcal{O}(\varepsilon_0)$$
for $0 < t < \infty$.

6. Suppose $q^s_\varepsilon(t) \in W^s(\gamma_\varepsilon(t))$ is a solution of (28.1.6). Then show that
$$\left.\frac{\partial q^s_\varepsilon(t)}{\partial \varepsilon}\right|_{\varepsilon=0} \equiv q^s_1(t)$$
is bounded in t as $t \to \infty$. (*Hint:* as $t \to \infty$, $q^s_1(t)$ should behave as $\left.\frac{\partial \gamma_\varepsilon(t)}{\partial \varepsilon}\right|_{\varepsilon=0}$.
Does the same result hold for solutions in $W^u(\gamma_\varepsilon(t))$ as $t \to -\infty$?

7. Recall Theorem 28.1.7. Show that if $M(t_0, \phi_0) \neq 0$ for all $(t_0, \phi_0) \in \mathbb{R}^1 \times S^1$, then $W^s(\gamma_\varepsilon(t)) \cap W^u(\gamma_\varepsilon(t)) = \emptyset$. (*Hint:* study the proof of Lemma 28.1.3.)

8. Consider the Poincaré maps associated with the damped, periodically forced Duffing equation on the cross-sections Σ^0, $\Sigma^{\pi/2}$, Σ^π, and $\Sigma^{3\pi/2}$ shown in Figure 28.5.1 for $\delta = 0$. Describe in detail how the geometry of the stable and unstable manifolds changes on each cross-section for $\delta \neq 0$. (*Hint:* use the Melnikov function.)

9. *Melnikov's Method for Autonomous Perturbations*

Suppose we consider the $\mathbf{C}^r$ $(r \geq 2)$ vector field

$$\dot{x} = \frac{\partial H}{\partial y}(x, y) + \varepsilon g_1(x, y; \mu, \varepsilon),$$
$$\dot{y} = -\frac{\partial H}{\partial x}(x, y) + \varepsilon g_2(x, y; \mu, \varepsilon), \qquad (x, y, \mu) \in \mathbb{R}^3,$$

or

$$\dot{q} = JDH(q) + \varepsilon g(q; \mu, \varepsilon), \tag{28.6.1}$$

where

$$q \equiv (x, y),$$

$$DH = \begin{pmatrix} \frac{\partial H}{\partial x} \\ \frac{\partial H}{\partial y} \end{pmatrix},$$

$$J = \begin{pmatrix} 0 & 1 \\ -1 & 0 \end{pmatrix},$$

$$g = (g_1, g_2),$$

with ε small and μ regarded as a parameter.

Suppose that the unperturbed system (i.e., (28.6.1) with $\varepsilon = 0$) satisfies Assumptions 1 and 2 of Section 28.1. Discuss the geometrical meaning of

$$M(\mu) = \int_{-\infty}^{\infty} (DH \cdot g)(q_0(t), \mu) dt.$$

Compare $M(\mu)$ with $M(t_0, \phi_0)$ derived in Section 28.

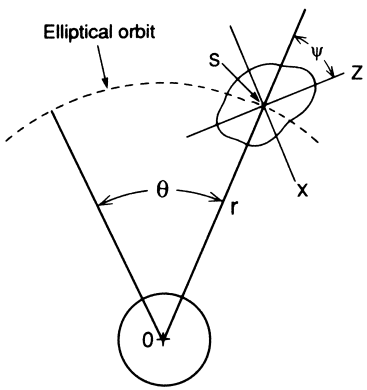

FIGURE 28.6.1.

10. The equation of motion describing the librational motion of an arbitrarily shaped satellite in a planar, elliptical orbit is

$$(1 + \varepsilon\mu \cos\theta)\psi'' - 2\varepsilon\mu \sin\theta(\psi' + 1) + 3K_i \sin\psi \cos\psi = 0$$

where $\psi' \equiv \frac{\partial \psi}{\partial \theta}$, $K_i = \frac{I_{xx} - I_{zz}}{I_{yy}}$, ε is small, and $\varepsilon\mu$ is the eccentricity of the orbit; see Modi and Brereton [1969]. The geometry is illustrated in Figure 28.6.1. For ε small, this equation can be written in the form (using the fact that $\frac{1}{1+\varepsilon\mu\cos\theta} = 1 - \varepsilon\mu\cos\theta + \mathcal{O}(\varepsilon^2)$)

$$\psi'' + 3K_i \sin\psi\cos\psi = \varepsilon[2\mu\sin\theta(\psi' + 1) + 3\mu K_i \sin\psi\cos\psi\cos\theta] + \mathcal{O}(\varepsilon^2).$$

Use Melnikov's method to study orbits homoclinic to hyperbolic periodic orbits for $\varepsilon \neq 0$. Describe the physical manifestation of any chaotic dynamics that arise in this problem.

11. The driven *Morse oscillator* is an equation frequently used in theoretical chemistry to describe the photodissociation of molecules (see, e.g., Goggin and Milonni [1988]). The equation is given by

$$\begin{aligned} \dot{x} &= y, \\ \dot{y} &= -\mu\left(e^{-x} - e^{-2x}\right) + \varepsilon\gamma\cos\omega t, \end{aligned} \tag{28.6.2}$$

with μ, γ, $\omega > 0$.

For $\varepsilon = 0$, the equation is Hamiltonian with Hamiltonian function

$$H(x, y) = \frac{y^2}{2} + \mu\left(-e^{-x} + \frac{1}{2}e^{-2x}\right).$$

a) Show that for $\varepsilon = 0$, $(x, y) = (\infty, 0)$ is a nonhyperbolic fixed point of (28.6.2) that is connected to itself by a homoclinic orbit.

We would like to apply Melnikov's theory to (28.6.2) in order to see if (28.6.2) has horseshoes; however, the fixed point having the homoclinic orbit is nonhyperbolic. Therefore, the theory developed in this chapter does not immediately apply. Schecter [1987a], [1987b] has extended Melnikov's method so that it applies to nonhyperbolic fixed points. However, we will not develop his technique.

Instead, we introduce the following transformation of variables

$$x = -2\log u, \qquad y = v, \tag{28.6.3}$$

and reparametrize time as follows

$$\frac{ds}{dt} = -\frac{u}{2}.$$

b) Rewrite (28.6.2) in these new variables and show that the resulting equation, for $\varepsilon = 0$, has a *hyperbolic* fixed point at the origin that is connected to itself by a homoclinic orbit. Apply Melnikov's method in order to study homoclinic orbits for $\varepsilon \neq 0$.

c) Describe the resulting chaotic dynamics in both the $x - y$ and $u - v$ coordinate systems.

This problem was originally solved by Bruhn [1989]. The transformation (28.6.3) is known as a "McGehee transformation" in honor of Richard McGehee, who first cooked it up in order to study a degenerate fixed point at infinity in a celestial mechanics problem (see McGehee [1974]). Such singularities frequently arise in mechanics and coordinate transformations such as (28.6.3) can greatly facilitate the analysis. An excellent introduction to such problems can be found in Devaney [1982].

12. Consider the $\mathbf{C}^r$ $(r \geq 2)$ vector field

$$\begin{aligned} \dot{x} &= f_1(x, y) + \varepsilon g_1(x, y, t; \varepsilon), \\ \dot{y} &= f_2(x, y) + \varepsilon g_2(x, y, t; \varepsilon), \qquad (x, y) \in \mathbb{R}^2, \end{aligned}$$

or

$$\dot{q} = f(q) + \varepsilon g(q, t; \varepsilon), \tag{28.6.4}$$

where

$$\begin{aligned} q &\equiv (x, y), \\ f &\equiv (f_1, f_2), \\ g &\equiv (g_1, g_2), \end{aligned}$$

with ε small and $g(q, t; \varepsilon)$ periodic in t with period $T = 2\pi/\omega$.

Assumption: For $\varepsilon = 0$, (28.6.4) has a hyperbolic fixed point at p_0 that is connected to itself by a homoclinic orbit, $q_0(t)$, i.e., $\lim_{t\to\pm\infty} q_0(t) = p_0$.

a) Derive a measure of the distance between the stable and unstable manifolds of the hyperbolic periodic orbit that persists in (28.6.4) for ε sufficiently small. (*Hint:* follow the steps in this chapter as closely as possible. If you need help, see Melnikov [1963].)

b) Using the parametrization of the unperturbed homoclinic orbit in terms of $(t_0, \phi_0) \in \mathbb{R}^1 \times S^1$ as defined in (28.1.9), is the Melnikov function obtained in part a) periodic in both t_0 and ϕ_0? Explain fully the reasons behind your answer.

13. How is the Melnikov theory modified if in the unperturbed vector field we instead had two hyperbolic fixed points, p_1 and p_2, connected by a heteroclinic orbit, $q_0(t)$, i.e., $\lim_{t\to\infty} q_0(t) = p_1$ and $\lim_{t\to-\infty} q_0(t) = p_2$? (*Hint:* follow the development of the homoclinic Melnikov theory in this chapter. You should arrive at the same formula for the distance between the stable and unstable manifolds; however, the geometrical interpretation will be different.)

14. Consider the vector field

$$\begin{aligned} \dot{\theta} &= \varepsilon v, \\ \dot{v} &= -\varepsilon \sin\theta + \varepsilon^2 \gamma \cos\omega t, \qquad (\theta, v) \in S^1 \times \mathbb{R}^1, \quad \varepsilon \text{ small}. \end{aligned}$$

Apply Melnikov's method to show that the Poincaré map associated with this equation has transverse homoclinic orbits. What problems arise? Can any conclusions be drawn for homoclinic orbits arising in the following vector field?

$$\dot{\theta} = \varepsilon v, \tag{28.6.5}$$

$$\dot{v} = -\varepsilon \sin\theta + \varepsilon^2(-\delta v + \gamma \cos\omega t). \tag{28.6.6}$$

What implications do these examples have for applying Melnikov's method to vector fields

$$\dot{x} = \varepsilon f(x, t), \qquad f - T\text{-periodic in } t, \quad x \in \mathbb{R}^2,$$

that are transformed into

$$\dot{y} = \overline{f}(y) + \varepsilon g(y, t), \qquad y \in \mathbb{R}^2, \quad \overline{f}(y) = \frac{1}{T}\int_0^T f(y, t)dt,$$

by the method of averaging?

We refer the reader to Holmes, Marsden, and Scheurle [1988] and Delshams and Seara [1992] for more examples of problems of this type along with some rigorous results.

15. Consider the following vector field :

$$\begin{aligned} \dot{x} &= y, \\ \dot{y} &= x - x^2 - \varepsilon\delta y + \varepsilon\gamma \cos\omega t. \end{aligned}$$

Compute the Melnikov function and describe the surface in $\gamma - \delta - \omega$ space where the bifurcation to homoclinic orbits occurs.

16. *Fluid Transport and the Dynamical Systems Point of View.* Consider the Navier–Stokes equations for three-dimensional viscous, incompressible fluid

$$\frac{\partial v}{\partial t} + (v \cdot \nabla)v = -\nabla p + \frac{1}{R}\nabla^2 v,$$

where p denotes the pressure and R the Reynolds number. Additionally, boundary and initial conditions may be specified. The solution of this highly nonlinear partial differential equation gives a velocity field, $v(x,t)$. Suppose we are interested in the transport of infinitesimal fluid elements (referred to as fluid particles) in this flow. The fluid particles move under the influence of two processes: convection (or advection) due to the velocity field and molecular diffusion (since the fluid is not really a continuum). The motion of fluid particles due to convection is determined by

$$\dot{x} = v(x,t), \qquad x \in \mathbb{R}^3.$$

This is simply a finite-dimensional dynamical system where the phase space is actually the physical space occupied by the fluid.

If we consider two-dimensional incompressible inviscid fluid flow, the velocity field can be determined from a stream function, $\psi(x_1, x_2; t)$, where

$$v(x_1, x_2, t) = \left(\frac{\partial \psi}{\partial x_2}, -\frac{\partial \psi}{\partial x_1} \right);$$

see Chorin and Marsden [1979] for background on these statements. The equations for fluid particle motions in this case become

$$\begin{aligned} \dot{x}_1 &= \frac{\partial \psi}{\partial x_2}(x_1, x_2, t), \\ \dot{x}_2 &= -\frac{\partial \psi}{\partial x_1}(x_1, x_2, t). \end{aligned}$$

The reader should note that this is simply a Hamiltonian dynamical system where the stream function plays the role of the Hamiltonian. The study of the transport and mixing of fluids along these lines using the framework of dynamical systems theory is a topic of much current interest; the reader should consult Ottino [1989] for a good introduction and Rom-Kedar, Leonard, and Wiggins [1990] for a specific example.

We will consider the situation of fluid particle transport in modulated traveling waves in a binary fluid mixture heated from below; see Weiss and Knobloch [1989] and Moses and Steinberg [1988]. The stream function (in a moving frame) near an instability leading to time-dependent oscillations is given by

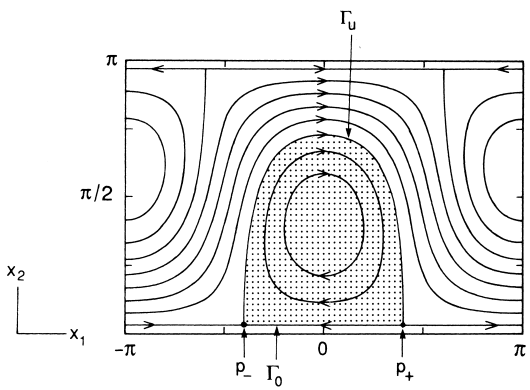

FIGURE 28.6.2.

$$\psi(x_1, x_2, t) = \psi_0(x_1, x_2) + \varepsilon\psi_1(x_1, x_2, t),$$

where

$$\psi_0(x_1, x_2) = -x_2 + R\cos x_1 \sin x_2,$$

$$\psi_1(x_1, x_2, t) = \frac{\gamma}{2}\left[\left(1 - \frac{2}{\omega}\right)\cos(x_1 + \omega t + \theta) + \left(1 + \frac{2}{\omega}\right)\cos(x_1 - \omega t - \theta)\right]\sin x_2.$$

In the above $\omega > 0$, θ is a phase, and R, γ, and ε are parameters (amplitude depending on the temperature) with $0 < \varepsilon << 1$; see Weiss and Knobloch [1989] for a detailed discussion. The equations for fluid particle motions are given by

$$\dot{x}_1 = \frac{\partial\psi_0}{\partial x_2}(x_1, x_2) + \varepsilon\frac{\partial\psi_1}{\partial x_2}(x_1, x_2, t),$$
$$\dot{x}_2 = -\frac{\partial\psi_0}{\partial x_1}(x_1, x_2) - \varepsilon\frac{\partial\psi_1}{\partial x_1}(x_1, x_2, t).$$

For $\varepsilon = 0$, $R > 1$, the streamlines of the flow (corresponding to the level sets of $\psi_0(x_1, x_2)$) appear as in Figure 28.6.2. Note the two hyperbolic fixed points on the x_1-axis, denoted p_+ and p_-, respectively. The fixed points are connected by a pair of heteroclinic orbits denoted Γ_0 and Γ_u. This heteroclinic cycle forms a region of trapped fluid that is shaded in Figure 28.6.2.

a) For $\varepsilon \neq 0$ show that Γ_0 persists and results in a barrier which fluid cannot cross.

b) Show that for $\varepsilon \neq 0$, Γ_u breaks up giving rise to transverse heteroclinic orbits. This provides a mechanism for fluid to mix between the two regions in the time-dependent fluid flow.

c) Show that a horseshoe exists in the heteroclinic tangle for $\varepsilon \neq 0$. (*Hint:* see Rom-Kedar et al. [1990].) Hence, chaotic fluid particle trajectories exist.

29

Liapunov Exponents

A positive Liapunov exponent is often taken as a signature of chaos. We will address this specific question in Chapter 30. But in this chapter we discuss Liapunov exponents following Oseledec [1968] and Benettin *et al.* [1980a, b].

29.1 Liapunov Exponents of a Trajectory

Consider the $\mathbf{C}^r$ $(r \geq 1)$ vector field

$$\dot{x} = f(x), \qquad x \in \mathbb{R}^n. \tag{29.1.1}$$

Let $x(t, x_0)$ be a trajectory of (29.1.1) satisfying $x(0, x_0) = x_0$. We want to describe the orbit structure of (29.1.1) near $x(t, x_0)$. In particular, we want to know the geometry associated with the attraction and/or repulsion of orbits of (29.1.1) relative to $x(t, x_0)$. For this it is natural to first consider the orbit structure of the linearization of (29.1.1) about $x(t, x_0)$ given by

$$\dot{\xi} = Df(x(t))\xi, \qquad \xi \in \mathbb{R}^n. \tag{29.1.2}$$

Let $X(t; x(t, x_0))$ be the fundamental solution matrix of (29.1.2) and let $e \neq 0$ be a vector in $\mathbb{R}^n$. Then the *coefficient of expansion in the direction* e *along the trajectory through* x_0 is defined to be

$$\lambda_t(x_0, e) \equiv \frac{\|X(t; x(t, x_0))e\|}{\|e\|}, \tag{29.1.3}$$

where $\|\cdot\| = \sqrt{\langle \cdot, \cdot \rangle}$ with $\langle \cdot, \cdot \rangle$ denoting the standard scalar product on $\mathbb{R}^n$. Note that $\lambda_t(x_0, e)$ is a time-dependent quantity that also depends on a particular orbit of (29.1.1) (through the fundamental solution matrix $X(t; x(t, x_0))$), a particular point along this orbit, and a particular direction along this orbit. The *Liapunov characteristic exponent* (or just Liapunov

exponent) *in the direction* e *along the trajectory through* x_0 is defined to be

$$\chi(X(t;x(t,x_0)),x_0,e) \equiv \overline{\lim_{t\to\infty}}\frac{1}{t}\log\lambda_t(x_0,e). \tag{29.1.4}$$

We make several remarks concerning this definition.

1. Equation (29.1.4) is an asymptotic quantity. Therefore, in order for it to make sense, we must at least know that $x(t,x_0)$ exists for all $t>0$. This will be true if the phase space is a compact, boundaryless manifold or if x_0 lies in a positively invariant region.

2. For the zero vector we define $\chi(X(t;x(t,x_0)),x_0,0)=-\infty$.

3. The fundamental solution matrix, $X(t;x(t,x_0))$, of (29.1.2) is associated with a particular trajectory, $x(t,x_0)$, of (29.1.1). Thus, if we considered a different trajectory, $\tilde{x}(t,\tilde{x}_0)$, of (29.1.1), then the fundamental solution matrix associated with the vector field linearized about $\tilde{x}(t,\tilde{x}_0)$ may (and most probably will) have different properties.

4. The Liapunov exponent in the direction e along the orbit through x_0 is unchanged if the initial condition of the trajectory along the orbit is varied. In particular, for any $t_1\in\mathbb{R}$, let $x(t_1,x_0)\equiv x_1$; then $\chi(X(t;x(t,x_0)),x_0,e)=\chi(X(t;x(t,x_0)),x_1,e)$. This should be intuitively clear from the fact that the exponents are limits as $t\to\infty$; see Exercise 1.

5. In light of the previous remark it makes sense to drop the initial condition of the trajectory from the notation for a Liapunov exponent, i.e., $\chi(X(t;x(t,x_0)),x_0,e)=\chi(X(t;x(t,x_0)),e)$. Moreover, our discussions in this subsection will be concerned with Liapunov exponents associated with a given trajectory, and, hence, a given fundamental solution matrix $X(t;x(t,x_0))$. In this setting we will further simplify the notation by dropping the explicit dependence on the fundamental solution matrix $X(t;x(t,x_0))$, i.e., $\chi(X(t;x(t,x_0)),e)=\chi(e)$.

6. In general, Liapunov exponents are *not* continuous functions of the orbits. This can be seen from Example 29.2.3.

Next we want to develop some geometrical properties of the Liapunov exponents associated with a given trajectory. The following lemma is fundamental in this regard.

Lemma 29.1.1 *For any vectors* $f,\ g\in\mathbb{R}^n$, *and nonzero constant* $c\in\mathbb{R}$,

$$\chi(f+g) \leq \max\{\chi(f), \chi(g)\}, \tag{29.1.5}$$

$$\chi(cg) = \chi(g). \tag{29.1.6}$$

Proof: This follows immediately from the definition of Liapunov exponents given in (29.1.4). □

This lemma, along with the standard definition of a vector space, implies the following proposition.

Proposition 29.1.2 *For any* $r \in \mathbb{R}$

$$\{g \in \mathbb{R}^n \,|\, \chi(g) \leq r\}$$

is a vector subspace of $\mathbb{R}^n$.

From this proposition we can conclude that there are at most n (i.e., the dimension of the phase space) distinct Liapunov exponents associated with a trajectory. More precisely, we have the following result.

Proposition 29.1.3 *The set of numbers*

$$\{\chi(g)\}_{\substack{g\in\mathbb{R}^n \\ g\neq 0}},$$

takes at most $n = dim\,\mathbb{R}^n$ *values, which we denote by*

$$\nu_1 > \cdots > \nu_s, \quad 1 \leq s \leq n.$$

Proof: See Exercise 2. □

Associated with the s distinct values for the Liapunov exponents we have $s+1$ nested subspaces.

Proposition 29.1.4 *Let* $L_i = \{g \in \mathbb{R}^n \,|\, \chi(g) \leq \nu_i\}$. *Then*

$$\{0\} \equiv L_{s+1} \subset L_s \subset \cdots \subset L_1 = \mathbb{R}^n$$

with $L_{i+1} \neq L_i$ *and* $\chi(g) = \nu_i$ *if and only if* $g \in L_i \backslash L_{i+1}$, $1 \leq i \leq s$.

Proof: This is an immediate consequence of Proposition 29.1.2 and Proposition 29.1.3. □

Next we define the notion of the *spectrum* of Liapunov exponents associated with $X(t; x(t, x_0))$.

Definition 29.1.5 (Spectrum of $X(t; x(t, x_0))$) *The numbers $\nu_1, \cdots, \nu_s$ are referred to as the* spectrum of Liapunov exponents associated with $X(t; x(t, x_0))$, *and denoted by sp $(X(t; x(t, x_0)))$. The multiplicity of ν_i is denoted by k_i, and is given by $k_i \equiv dim\, L_i - dim\, L_{i+1}$, $1 \leq i \leq s$.*

Next we want to consider conditions under which the limit, rather than the lim sup, in (29.1.4) exists. First we need two definitions.

Definition 29.1.6 (Normal Basis) *A basis $\{e_1, \cdots, e_n\}$ of $\mathbb{R}^n$ is said to be a* normal basis *if*

$$\sum_{i=1}^{n} \chi(e_i) \leq \sum_{i=1}^{n} \chi(f_i),$$

where $\{f_1, \cdots, f_n\}$ is any other basis of $\mathbb{R}^n$.

Definition 29.1.7 (Regular Family) *The fundamental solution matrix $X(t; x(t, x_0))$ is called* regular as $t \to \infty$ *if*

1. $\lim_{t\to\infty} \frac{1}{t} \log |\det X(t; x(t, x_0))|$ *exists and is finite, and*
2. *for each normal basis $\{e_1, \cdots, e_n\}$*

$$\sum_{i=1}^{n} \chi(e_i) = \lim_{t\to\infty} \frac{1}{t} \log |\det X(t; x(t, x_0))|.$$

Now we can state the main existence theorem due to Liapunov [1966].

Theorem 29.1.8 *If $X(t; x(t, x_0))$ is regular as $t \to \infty$, then*

$$\chi(e) = \lim_{t\to\infty} \frac{1}{t} \log \lambda_t(x_0, e) \tag{29.1.7}$$

exists and is finite for any vector $e \in \mathbb{R}^n$.

Proof: See Liapunov [1966], Oseledec [1968], or Benettin *et al.* [1980a]. □

This immediately raises the question of whether or not a particular fundamental solution matrix is regular. This problem was addressed by Oseledec [1968] and is answered (in a sense) in the *Oseledec multiplicative ergodic theorem*. Oseledec showed that, with respect to some invariant measure, almost all trajectories give rise to regular fundamental solution matrices. There are a number of technical issues associated with stating this fundamental theorem, and we refer the reader to Oseledec [1968] and Benettin *et al.* [1980a] for more details.

Liapunov exponents are just one type of spectra one can associate with a linear, time-varying system. There are others (e.g., we introduced the notion of exponential dichotomy in Chapter 3). A survey of different spectra for linear systems is given in Dieci and van Vleck [2002].

Some new insights into the behavior of Liapunov exponents, and their generalizations, have been obtained by Colonius and Kliemann by combining methods of nonlinear geometric control theory with dynamical systems theory. See Colonius and Kliemann [1996b], and references therein.

29.2 Examples

Let us now consider a few examples.

Example 29.2.1 (A Linear, Homogeneous, Constant Coefficient System). Consider the linear, scalar vector field

$$\dot{x} = ax, \qquad x \in \mathbb{R}^1, \tag{29.2.1}$$

where a is a constant. Equation (29.2.1) has three orbits, $x = 0$, $x > 0$, and $x < 0$, but the fundamental solution matrix associated with each orbit is given by

$$X(t) = e^{at}. \tag{29.2.2}$$

Thus, using (29.2.2) and (29.1.7), we see that each orbit of (29.2.1) has only one Liapunov exponent, and the Liapunov exponent of each orbit is a. Thus, if $a > 0$, trajectories of (29.2.1) separate exponentially as $t \to \infty$.

End of Example 29.2.1

Example 29.2.2 (An Integrable System). Consider a planar, Hamiltonian system in a region of phase space where the vector field is given in action-angle

variables as follows

$$\begin{aligned} \dot{I} &= 0, \\ \dot{\theta} &= \Omega(I), \end{aligned} \qquad (I, \theta) \in \mathbb{R}^+ \times S^1. \tag{29.2.3}$$

Then, a trajectory of (29.2.3) is given by

$$\begin{aligned} I &= \text{constant}, \\ \theta(t) &= \Omega(I)t + \theta_0. \end{aligned} \tag{29.2.4}$$

Linearizing (29.2.3) about (29.2.4) gives

$$\begin{pmatrix} \dot{\xi}_1 \\ \dot{\xi}_2 \end{pmatrix} = \begin{pmatrix} 0 & 0 \\ \frac{\partial \Omega}{\partial I}(I) & 0 \end{pmatrix} \begin{pmatrix} \xi_1 \\ \xi_2 \end{pmatrix}. \tag{29.2.5}$$

The fundamental solution matrix of (29.2.5) is easily computed and found to be

$$X(t) = \begin{pmatrix} C & C \\ C\frac{\partial \Omega}{\partial I}(I)t & 0 \end{pmatrix}, \tag{29.2.6}$$

where C is a constant. Letting $\delta\theta$ represent a vector tangent to a trajectory and δI a vector normal to a trajectory using (29.2.6) and (29.1.7), we easily obtain

$$\begin{aligned} \chi(I, \delta I) &= 0, \\ \chi(I, \delta\theta) &= 0, \end{aligned}$$

for any I labeling a trajectory of (29.2.3) defined by (29.2.4).

End of Example 29.2.2

Example 29.2.3 (A Two-Dimensional, Autonomous, Nonlinear System). Consider the vector field

$$\begin{aligned} \dot{x} &= x - x^3, \\ \dot{y} &= -y. \end{aligned} \tag{29.2.7}$$

In Example 8.2.2 of Chapter 8, we saw that (29.2.7) has a saddle at $(x, y) = (0, 0)$ and sinks at $(\pm 1, 0)$. Moreover, the closed interval $[-1, 1]$ on the x-axis is an attracting set; see Figure 29.2.1.

We want to compute the Liapunov exponents associated with orbits in this attracting set. The attracting set $[-1, 1]$ contains five orbits, the fixed points $(x, y) = (0, 0)$, $(\pm 1, 0)$ and the open intervals $(-1, 0)$ and $(0, 1)$. Each orbit has two Liapunov exponents. We will compute the Liapunov exponents of each orbit individually. We let $\delta x \equiv (1, 0)$ denote a tangent vector in the x direction and $\delta y \equiv (0, 1)$ denote a tangent vector in the y direction. It should be clear that

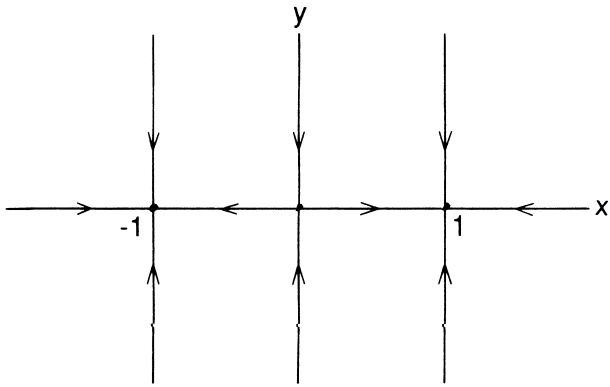

FIGURE 29.2.1.

at each point of the attracting set δx and δy are a basis of $\mathbb{R}^2$. The Liapunov exponents for the three fixed points are trivial to obtain and we merely state the results.

$$\begin{aligned} (0,0) \qquad & \chi((0,0),\delta x) = +1, \\ & \chi((0,0),\delta y) = -1. \end{aligned}$$

$$\begin{aligned} (-1,0) \qquad & \chi((-1,0),\delta x) = -2, \\ & \chi((-1,0),\delta y) = -1. \end{aligned}$$

$$\begin{aligned} (+1,0) \qquad & \chi((1,0),\delta x) = -2, \\ & \chi((1,0),\delta y) = -1. \end{aligned}$$

The Liapunov exponents for the orbits $0 < x < 1$, $y = 0$, and $-1 < x < 0$, $y = 0$, require a little more work. Note that (29.2.7) is unchanged under the coordinate transformation $x \to -x$. Therefore, the Liapunov exponents for the orbit $0 < x < 1$, $y = 0$, are the same as for the orbit $-1 < x < 0$, $y = 0$.

Linearizing (29.2.7) about $(x(t), 0)$ gives

$$\begin{pmatrix} \dot{\xi}_1 \\ \dot{\xi}_2 \end{pmatrix} = \begin{pmatrix} 1 - 3x^2(t) & 0 \\ 0 & -1 \end{pmatrix} \begin{pmatrix} \xi_1 \\ \xi_2 \end{pmatrix}, \tag{29.2.8}$$

where $x(t)$ is a trajectory in $0 < x < 1$, $y = 0$. Integrating the x-component of (29.2.7) gives

$$x^2(t) = \frac{e^{2t}}{e^{2t} + 1}. \tag{29.2.9}$$

Substituting (29.2.9) into (29.2.8), we obtain the fundamental solution matrix

$$X(t) = \begin{pmatrix} e^{-2t}(1+e^{-2t})^{-3/2} & 0 \\ 0 & e^{-t} \end{pmatrix}. \tag{29.2.10}$$

Using (29.1.7) and (29.2.10), we obtain the Liapunov exponents

$$\begin{aligned} 0 < x < 1,\ y = 0 \qquad & \chi((0 < x < 1, y = 0), \delta x) = -2, \\ & \chi((0 < x < 1, y = 0), \delta y) = -1, \\ -1 < x < 0,\ y = 0 \qquad & \chi((-1 < x < 0, y = 0), \delta x) = -2, \\ & \chi((-1 < x < 0, y = 0), \delta y) = -1. \end{aligned}$$

End of Example 29.2.3

We end this section with some final remarks.

Remark 1. We can view the Liapunov exponents of a given orbit as the long time average of the real parts of the eigenvalues of the fundamental solution matrix associated with the linearization of the vector field about the orbit. Therefore, they give us information concerning local expansion and contraction of phase space only and nothing about twisting and folding.

Remark 2. It should be clear that if the orbit is a fixed point or periodic orbit, then the Liapunov exponents are, in the first case, the real parts of the eigenvalues associated with the matrix of the vector field linearized about the fixed point and, in the second case, the real parts of the Floquet exponents. Thus, in some sense the theory of Liapunov exponents is a generalization of linear stability theory for arbitrary trajectories (but see Goldhirsch et al. [1987]).

This brings up an interesting point. Associated with the linear eigenspaces associated with vector fields linearized about fixed points and periodic orbits are manifolds invariant under the full nonlinear dynamics where orbits have the same asymptotic behavior as in the linearized system. We refer to these as the stable and unstable manifolds. Might an *arbitrary* orbit possess stable and unstable manifolds having dimension equal to the number of negative and positive Liapunov exponents, respectively, associated with the orbit? The answer to this question is yes, and it has been proved by Pesin [1976], [1977], but see also Sacker and Sell [1974], [1976a], [1976b], [1978], and [1980].

We have only hinted in this section at the various properties of Liapunov exponents. For more information the reader should consult Liapunov

[1966], Bylov et al. [1966], Oseledec [1968], Ledrappier and Young [1991], and Young [1982]. We develop many additional properties of Liapunov exponents in the exercises.

29.3 Numerical Computation of Liapunov Exponents

In applications the Liapunov exponents of a trajectory will need to be computed numerically. There has been much rigorous work in recent years involving the accurate computation of Liapunov exponents. Two papers that discuss this problem with great detail and rigour are Dieci et al. [1997] and Bridges and Reich [2001]. The paper of Dieci et al. [1997] is notable for providing error estimates for the finite time computations[1]. Dieci [2002] describes algorithms for computing Liapunov exponents that do not require the computation of a Jacobian. Related work can be found in Rangarajan *et al.* [1998] and Janaki *et al.* [1999]. These numerical approaches involve either a QR or a singular value decomposition (SVD) of the fundamental solution matrix. While the theory of QR and SVD for *constant* matrices is well-known, the fundamental solution matrix varies in time. The theory for QR and SVD of time varying matrices is developed in Dieci and Eirola [1999] amd Dieci and van Vleck [1999]. Methods for computing Liapunov exponents that are specific to Hamiltonian systems can be found in Partovi [1999] and Yamaguchi and Iwai [2001]. The paper of Ramasubramanian and Sriram [2000] provides a comparative study between different algorithms for the computation of Liapunov exponents. The work of Udwadia and von Bremen [2001], [2002] is also notable.

29.4 Exercises

1. Recall the discussion earlier in this chapter. Show that

$$\chi(x_0, e) = \chi(x(T), e)$$

for any finite T.

2. Prove Proposition 29.1.3.

3. Consider a planar, Hamiltonian vector field. Must all Liapunov exponents of *every* orbit be zero?

[1]Liapunov exponents are asymptotic quantities. They are defined in the limit as time approaches infinity. Obviously, this limit cannot be realized on a computer, and therefore some error is incurred.

4. Show that any trajectory of a vector field that remains bounded and does not terminate on a fixed point must have at least one zero Liapunov exponent. (*Hint:* consider the direction tangent to the orbit.)

5. In any realistic example, the Liapunov exponents of an orbit must be calculated numerically. In this case, you can see that a problem may arise. Namely, a Liapunov exponent is a number obtained in the limit $t \to \infty$, and, in practice, one can only compute for a finite amount of time.

   Recall Example 29.2.3. Consider an initial condition

   $$(x, y) = (\varepsilon, 0),$$

   and the direction

   $$\delta x = (1, 0).$$

   Let

   $$\chi_t(x_0, e) = \frac{1}{t} \log \lambda_t(x_0, e),$$

   and compute

   $$\chi_t((\varepsilon, 0), \delta x)$$

   for this example. It should follow from the discussion in the example that for some T we have

   $$\chi_t((\varepsilon, 0), \delta x) \leq 0, \qquad t \in [T, \infty).$$

   Let $T_0(\varepsilon)$ be the value of t such that

   $$\chi_{T_0(\varepsilon)}((\varepsilon, 0), \delta x) = 0.$$

   a) Compute $T_0(\varepsilon)$ and graph it as a function of ε.

   b) What can you conclude from this example concerning the numerical computation of Liapunov exponents?

6. Consider a linear velocity field given by:

   $$\begin{pmatrix} \dot{x}_1 \\ \dot{x}_2 \end{pmatrix} = \begin{pmatrix} \cos 4t & \sin 4t - 2 \\ \sin 4t + 2 & -\cos 4t \end{pmatrix} \begin{pmatrix} x_1 \\ x_2 \end{pmatrix}. \tag{29.4.1}$$

   Verify that the solution of (29.4.1) is given by:

   $$\begin{aligned} x_1(t) &= x_{10} e^t \cos 2t - x_{20} e^{-t} \sin 2t, \\ x_2(t) &= x_{10} e^t \sin 2t + x_{20} e^{-t} \cos 2t. \end{aligned} \tag{29.4.2}$$

   (a) What is the fundamental solution matrix associated with (29.4.1)?

   (b) Compute the Liapunov exponents associated with this fundamental solution matrix.

30

Chaos and Strange Attractors

In this chapter we want to examine what is meant by the term "chaos" as applied to deterministic dynamical systems as well as the notion of a "strange attractor." We will begin by giving several definitions of properties that should be characteristic of "chaos" and then consider several examples that possess one, several, or all of these properties.

We consider $\mathbf{C}^r$ $(r \geq 1)$ autonomous vector fields and maps on $\mathbb{R}^n$ denoted as follows

$$\text{vector field} \qquad \dot{x} = f(x), \tag{30.0.1}$$

$$\text{map} \qquad x \mapsto g(x). \tag{30.0.2}$$

We denote the flow generated by (30.0.1) by $\phi(t, x)$ and we assume that it exists for all $t > 0$. We assume that $\Lambda \subset \mathbb{R}^n$ is a compact set invariant under $\phi(t, x)$ (resp. $g(x)$), i.e., $\phi(t, \Lambda) \subset \Lambda$ for all $t \in \mathbb{R}$ (resp. $g^n(\Lambda) \subset \Lambda$ for all $n \in \mathbb{Z}$, except that if g is not invertible, we must take $n \geq 0$). Then we have the following definitions.

Definition 30.0.1 (Sensitive Dependence on Initial Conditions) *The flow $\phi(t, x)$ (resp. $g(x)$) is said to have* sensitive dependence on initial conditions on Λ *if there exists $\varepsilon > 0$ such that, for any $x \in \Lambda$ and any neighborhood U of x, there exists $y \in U$ and $t > 0$ (resp. $n > 0$) such that $|\phi(t, x) - \phi(t, y)| > \varepsilon$ (resp. $|g^n(x) - g^n(y)| > \varepsilon$).*

Roughly speaking, Definition 30.0.1 says that for any point $x \in \Lambda$, there is (at least) one point arbitrarily close to Λ that diverges from x. Some authors require the rate of divergence to be exponential; for reasons to be explained later, we will not do so. As we will see in the examples, taken by itself sensitive dependence on initial conditions is a fairly common feature in many dynamical systems.

Definition 30.0.2 (Chaotic Invariant Set) *Λ is said to be* chaotic *if*

1. *$\phi(t,x)$ (resp. $g(x)$) has sensitive dependence on initial conditions on Λ.*

2. *$\phi(t,x)$ (resp. $g(x)$) is topologically transitive on Λ.*

Some authors (e.g., Devaney [1986]) add an additional requirement to Definition 30.0.2. For further discussions of the definition of chaos see Glasner and Weiss [1993] and Banks *et al.* [1992].

3. The periodic orbits of $\phi(t,x)$ (resp. $g(x)$) are dense in Λ.

We will not explicitly include point 3 as part of the definition of a chaotic invariant set, but we will examine its importance and relationship to "chaos."

We will now consider several examples that exhibit the properties described in these two definitions.

Example 30.0.1. Consider the following vector field on $\mathbb{R}^1$

$$\dot{x} = ax, \qquad x \in \mathbb{R}^1, \tag{30.0.3}$$

with $a > 0$. The flow generated by (30.0.3) is given by

$$\phi(t,x) = e^{at}x. \tag{30.0.4}$$

From (30.0.4) we conclude the following.

1. $\phi(t,x)$ has no periodic orbits.
2. $\phi(t,x)$ is topologically transitive on the *noncompact* sets $(0,\infty)$ and $(-\infty,0)$.
3. $\phi(t,x)$ has sensitive dependence on initial conditions on $\mathbb{R}^1$ since for any $x_0, x_1 \in \mathbb{R}^1$, with $x_0 \neq x_1$,

$$|\phi(t,x_0) - \phi(t,x_1)| = e^{at}|x_0 - x_1|.$$

Hence, the distance between any two points grows (exponentially) in time.

End of Example 30.0.1

Example 30.0.2. Consider the vector field

$$\begin{aligned} \dot{r} &= \sin\frac{\pi}{r}, \\ \dot{\theta} &= r, \qquad (r,\theta) \in \mathbb{R}^+ \times S^1. \end{aligned} \tag{30.0.5}$$

The flow generated by (30.0.5) has a countable infinity of periodic orbits given by

$$(r(t),\theta(t)) = \left(\frac{1}{n}, \frac{t}{n} + \theta_0\right), \qquad n = 1,2,3,\cdots . \tag{30.0.6}$$

It is easy to verify that the periodic orbits are stable for n even and unstable for n odd. Hence, in a compact region of the phase space, (30.0.5) has a countable infinity of unstable periodic orbits. We leave it as an exercise for the reader to verify that (30.0.5) may exhibit sensitive dependence on initial conditions in (open) annuli bounded by adjacent stable periodic orbits (see Exercise 2). However, (30.0.5) is only topologically transitive in the (open) annuli bounded by adjacent stable and unstable periodic orbits.

End of Example 30.0.2

Example 30.0.3. Consider the vector field on the two torus, $T^2 \equiv S^1 \times S^1$

$$\begin{aligned} \dot{\theta}_1 &= \omega_1, \\ \dot{\theta}_2 &= \omega_2, \qquad (\theta_1,\theta_2) \in T^2, \end{aligned} \tag{30.0.7}$$

with

$$\frac{\omega_1}{\omega_2} = \text{irrational}. \tag{30.0.8}$$

Then, it follows from Chapter 10, Section 10.4a, that the flow generated by (30.0.7) is topologically transitive on T^2. From (30.0.8) it is easy to see that the flow generated by (30.0.7) has no periodic orbits. We leave it as an exercise for the reader (see Exercise 3) to show that on T^2 the flow generated by (30.0.7) does *not* have sensitive dependence on initial conditions.

End of Example 30.0.3

Example 30.0.4. Consider the following integrable twist map

$$\begin{pmatrix} I \\ \theta \end{pmatrix} \mapsto \begin{pmatrix} I \\ 2\pi\Omega(I) + \theta \end{pmatrix} \equiv \begin{pmatrix} f_1(I,\theta) \\ f_2(I,\theta) \end{pmatrix}, \qquad (I,\theta) \in \mathbb{R}^+ \times S^1, \tag{30.0.9}$$

and

$$\frac{\partial\Omega}{\partial I}(I) \neq 0 \qquad \text{(twist condition)}. \tag{30.0.10}$$

The n^{th} iterate of (30.0.9) is easily calculated and is given by

$$\begin{pmatrix} I \\ \theta \end{pmatrix} \mapsto \begin{pmatrix} I \\ 2\pi n\Omega(I) + \theta \end{pmatrix} \equiv \begin{pmatrix} f_1^n(I,\theta) \\ f_2^n(I,\theta) \end{pmatrix}. \tag{30.0.11}$$

The simple form of (30.0.9) and (30.0.11) enable us to easily verify the following.

1. Equation (30.0.9) is *not* topologically transitive, since all orbits remain on invariant circles.
2. The periodic orbits of (30.0.9) are dense in the phase space. This uses the twist condition.
3. Equation (30.0.9) has sensitive dependence on initial conditions due to the twist condition. This can be seen as follows. For (I_0, θ_0), $(I_1, \theta_1) \in \mathbb{R}^+ \times S^1$, with $I_0 \neq I_1$, we have

$$\begin{aligned} &|(f_1^n(I_0,\theta_0) - f_1^n(I_1,\theta_1)), (f_2^n(I_0,\theta_0) - f_2^n(I_1,\theta_1))| \\ = \ &|((I_0 - I_1), (2\pi n(\Omega(I_0) - \Omega(I_1)) + (\theta_0 - \theta_1))|. \end{aligned} \tag{30.0.12}$$

Therefore, from (30.0.10), $\Omega(I_0) - \Omega(I_1) \neq 0$. Thus, we see from (30.0.12) that as n increases, the θ components of nearby points drift apart. However, the rate of separation is *not* exponential.

End of Example 30.0.4

Example 30.0.5. Consider

$$\sigma\colon \Sigma^N \longrightarrow \Sigma^N, \tag{30.0.13}$$

where Σ^N is the space of bi-infinite sequences of N symbols and σ is the shift map as described in Chapter 24. Then we have proven the following.

1. Σ^N is compact and invariant (see Proposition 24.1.4).
2. σ is topologically transitive, i.e., σ has an orbit that is dense in Σ^N (see Proposition 24.2.2).
3. σ has sensitive dependence on initial conditions (see Section 23.5).
4. σ has a countable infinity of periodic orbits (see Proposition 24.2.2) that are dense in Σ^N (see Exercise 4).

Thus, Σ^N is a chaotic, compact invariant set for σ. From Chapters 25, 26, and 27 we know that two-dimensional maps and three-dimensional autonomous vector fields may possess compact invariant sets on which the dynamics are topologically conjugate to (30.0.13). In all of these cases, homoclinic (and possibly

heteroclinic) orbits are the underlying mechanism that gives rise to such behavior. This is important, because this knowledge enables us to develop techniques (e.g., Melnikov's method) that predict (in terms of the system parameters) when chaotic dynamics occur in specific dynamical systems.

End of Example 30.0.5

We make the following remarks concerning these examples.

Remark 1. Example 30.0.1 illustrates why we require chaotic invariant sets to be compact.

Remark 2. Example 30.0.2 illustrates why having an infinite number of unstable periodic orbits in a compact, invariant region of phase space is not by itself a sufficient condition for chaotic dynamics.

Remark 3. Example 30.0.3 describes a vector field having a compact invariant set (which is actually, the entire phase space) on which the dynamics are topologically transitive, but it does not have sensitive dependence on initial conditions.

Remark 4. Example 30.0.4 describes a two-dimensional integrable map that has sensitive dependence on initial conditions and the periodic orbits are dense in the phase space, but it is not topologically transitive.

Thus, taken together, Examples 30.0.1 through 30.0.4 show the importance of Definition 30.0.2 being satisfied completely. Example 30.0.5 shows how chaotic dynamics can arise in many dynamical systems. However, it does not address the question of observability.

Definition 30.0.3 (Strange Attractor) *Suppose $\mathcal{A} \subset \mathbb{R}^n$ is an attractor. Then $\mathcal{A}$ is called a* strange attractor *if it is chaotic.*

Hence, if we want to prove that a dynamical system has a strange attractor we might proceed as follows.

Step 1. Find a trapping region, $\mathcal{M}$, in the phase space (see Definition 8.2.2 in Chapter 8).

Step 2. Show that $\mathcal{M}$ contains a chaotic invariant set Λ. In practice, this means showing that inside $\mathcal{M}$ is a homoclinic orbit (or heteroclinic

cycle) which has associated with it an invariant Cantor set on which the dynamics are topologically conjugate to a full shift on N symbols (recall Chapters 26 and 27).

Step 3. Then, from Definition 8.2.1 in Chapter 8,

$$\bigcap_{t>0} \phi(t, \mathcal{M}) \quad \left(\text{resp.} \bigcap_{n>0} g^n(\mathcal{M}) \right) \equiv \mathcal{A} \tag{30.0.14}$$

is an attracting set. Moreover, $\Lambda \subset \mathcal{A}$ (see Exercise 5) so that $\mathcal{A}$ contains a mechanism that gives rise to sensitive dependence on initial conditions; in order to conclude that $\mathcal{A}$ is a strange attractor we need only demonstrate the following.

1. The sensitive dependence on initial conditions on Λ extends to $\mathcal{A}$;
2. $\mathcal{A}$ is topologically transitive.

Hence, in just three steps we can show that a dynamical system possesses a strange attractor. In this book we have developed techniques and seen examples of how to carry out Steps 1 and 2. However, the third step is the killer, namely, showing that $\mathcal{A}$ is topologically transitive. This is because a single, *stable* orbit in $\mathcal{A}$ will destroy topological transitivity and, in Chapter 32, we will see that periodic sinks are always associated with quadratic homoclinic tangencies. Moreover, as a result of Newhouse's work, at least for two-dimensional dissipative maps, these homoclinic tangencies are persistent in the sense that if we destroy a particular tangency we will create another elsewhere in the homoclinic tangle. This is largely the reason why there is yet to be an analytical proof of the existence of a strange attractor for the periodically forced, damped Duffing oscillator, despite an enormous amount of numerical evidence. However, Wang and Young [2002] give a result that proves the existence of a strange attractor for "sufficently large damping".

At present, there exist rigorous results concerning strange attractors (by our Definition 30.0.3) in the following areas.

1. *One-Dimensional Non-Invertible Maps.* For maps such as

$$x \mapsto \mu x(1 - x)$$

or

$$x \mapsto x^2 - \mu$$

with μ a parameter there now exists a fairly complete existence theory for strange attractors. The reader should consult Jakobsen [1981], Misiurewicz [1981], Johnson [1987], Guckenheimer and Johnson [1990], and de Melo and van Strien [1993].

2. *Hyperbolic Attractors of Two-Dimensional Maps.* Plykin [1974], Nemytskii and Stepanov [1989] and Newhouse [1980] have constructed examples of hyperbolic attracting sets which satisfy Definition 30.0.2. These examples are somewhat artificial in the sense that one would not expect them to arise in Poincaré maps of ordinary differential equations that arise in typical applications.

3. *Lorenz-Like Systems.* The topology associated with the Lorenz equations (see Sparrow [1982]) avoids many of the problems associated with Newhouse sinks. Consequently, in the past few years there has been much progress in proving that the Lorenz equations (along with slightly modified versions of the Lorenz equations) possess a strange attractor. The reader is referred to Sinai and Vul [1981], Afraimovich, Bykov, and Silnikov [1983], Rychlik [1990], and Robinson [1989]. Recently, an elegant computer assisted proof of the existence of a strange attractor for the Lorenz equations was given by Tucker [1999]; see also Morales et al. [1998] and the popular articles of Stewart [2000] and Viana [2000].

4. *The Hénon Map.* The Hénon map is defined to be

$$\begin{aligned} x &\mapsto y, \\ y &\mapsto -\varepsilon x + \mu - y^2, \end{aligned} \tag{30.0.15}$$

where ε and μ are parameters. Over the past ten years a large amount of numerical evidence has suggested the existence of a strange attractor in this map. Recently, Benedicks and Carleson [1991] have proven that, for ε small, (30.0.15) does indeed possess a strange attractor.

5. *Recent Results on Strange Attractors.* For recent work on strange attractors see Palis and Takens [1993], Mora and Viana [1993], Diaz et al. [1996], Naudot [1996], and Turaev and Silnikov [1998].

6. *Strange Attractors for Nonautonomous Vector Fields.* If the nonautonomous vector field is time-periodic, then its study can be reduced to an associated Poincaré map (Chapter 10) and strange attractor results for maps can be applied. A very thorough discussion of this can be found in Wang and Young [2002].

   If the vector field is *not* time-periodic, then many new issues arise. The notion of an attractor for general nonautonomous systems was described in Chapter 8, Section 8.4. In addition to the notion of attractors for such vector fields, a definition and characterization of

chaos must be given. This has been considered in Scheurle [1986], Wiggins [1988], [1999], Stoffer [1988a,b], Meyer and Sell [1989], and Lerman and Silnikov [1992]. With notions of "attraction" and "chaos" in hand for nonautonomous vector fields with arbitrary time dependence one should be able to develop a notion of "strange attractor". Nevertheless, this is a subject which has not been developed, both from the point of view of rigorous mathematical results, and specific examples.

Thus, the "strange attractor problem" is still far from being solved in general. In particular, there is a need for thoroughly studied examples in higher dimensions, for vector fields in dimensions larger than three and for maps of dimension larger than two. A variety of examples of systems undergoing (rigorously proven) chaotic behavior in high dimensions can be found; however, the attractive nature of the chaos in these examples has not been studied.

If a dynamical system possesses a chaotic invariant set, then an obvious question arises: namely, how is the chaos manifested in terms of "random" or "unpredictable" behavior of the system? The answer to this question depends on the geometry of the construction of the chaotic invariant set and, thus, the answer varies from problem to problem (as we should expect). Let us consider an example, our old friend the periodically forced, damped Duffing oscillator.

This system is given by

$$\begin{aligned} \dot{x} &= y, \\ \dot{y} &= x - x^3 + \varepsilon(-\delta y + \gamma \cos \omega t). \end{aligned} \tag{30.0.16}$$

We know from Chapter 28 that, for ε sufficiently small and $\delta < \left(\frac{3\pi\omega \operatorname{sech}(\pi\omega/2)}{2\sqrt{2}}\right)\gamma$, the Poincaré map associated with (30.0.16) possesses transverse homoclinic orbits to a hyperbolic fixed point. Theorem 26.0.5 implies that (30.0.16) has chaotic dynamics. However, we want to interpret this chaos specifically in terms of the dynamics of (30.0.16). We will do this by constructing the chaotic invariant set geometrically and describing the associated symbolic dynamics geometrically. Our discussion will be heuristic, but, at this stage, the reader should easily be able to supply the necessary rigor (see Exercise 7).

Consider the two "horizontal" strips labeled H_+ and H_- in Figure 30.0.1.

Under the Poincaré map, denoted P, H_+ and H_- are mapped over themselves in iterates as shown heuristically in Figure 30.0.1. It should be clear that the horizontal (resp. vertical) boundaries of H_+ and H_- map to hor-

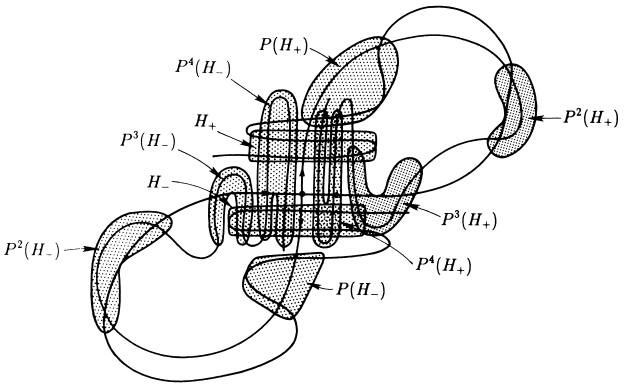

FIGURE 30.0.1.

izontal (resp. vertical) boundaries of $P^4(H_+)$ and $P^4(H_-)$, respectively. Thus, one can show that Assumptions 1 and 3 of Chapter 25 hold (see Exercise 7). Therefore, $H_+ \cup H_-$ contains an invariant Cantor set, Λ, on which the dynamics are topologically conjugate to a full shift on two symbols. A point starting in $\Lambda \cap H_+$ makes a circuit around the right-hand homoclinic tangle before returning to Λ. A point starting in $\Lambda \cap H_-$ makes a circuit around the left-hand homoclinic tangle before returning to Λ. A symbol sequence such as

$$(\cdots + + + - - - + \cdot - + - - \cdots)$$

thus corresponds to an initial condition starting in H_-, going to H_+ under P^4 (hence making a circuit around the left-hand homoclinic tangle), and then going back to H_- under P^4 (hence making a circuit around the right-hand homoclinic tangle), etc. The geometrical meaning of "chaos" should be clear for this system, but the reader should do Exercise 7.

We end this section with some final remarks.

Remark 1. The dynamics of the full shift on N symbols best describes what we mean by the term "chaos" as applied to deterministic dynamical systems. The system is purely deterministic; however, the dynamics are such that our inability to *precisely* specify the initial conditions results in behavior that appears random or unpredictable.

Remark 2. We did not include in our definition of the chaotic invariant set (Definition 30.0.2) the requirement of density of periodic points. If the chaotic invariant set is hyperbolic, then, by the shadowing lemma (see, e.g., Shub [1987]), it follows immediately that the periodic points are dense.

Moreover, Grebogi et al. [1985] have obtained numerical evidence for the existence of chaotic attractors in maps of the N-torus which have the property that orbits in the attractor densely cover the N-torus.

Remark 3. In our definition of sensitive dependence on initial conditions (Definition 30.0.1) we did not require the separation rate to be exponential. This is because it appears now that the strange attractors observed in numerical experiments of typical dynamical systems arising in applications will not, in general, be hyperbolic. Hence, one should expect parts of the attractor to exhibit nonexponential contraction or expansion rates. This is an area where new analytical techniques need to be developed.

Remark 4. Positive Liapunov exponents have been a standard criterion for deciding when a dynamical system is "chaotic" over the past few years. Examples 29.2.1 and 29.2.3 show that this criterion should be interpreted with caution; see also Exercise 5 following Chapter 29.

Remark 5. In an interesting series of papers, Brown and Chua [1996a,b], [1998] describe relationships between different characterizations of chaos in great detail.

30.1 Exercises

1. Can a $\mathbf{C}^r$ map or flow depend on initial conditions in a $\mathbf{C}^r$ manner and also exhibit sensitive dependence on initial conditions? Explain.

2. Recall Example 30.0.2. Do all or only some orbits in the open annuli bounded by adjacent stable periodic orbits exhibit sensitive dependence on initial conditions?

3. Recall Example 30.0.3. Show that the flow generated by (30.0.7) is topologically transitive on T^2.

4. Show that for the dynamical system

$$\sigma\colon \Sigma^N \to \Sigma^N$$

the periodic orbits are dense in Σ^N.

5. Let

$$x \mapsto g(x), \qquad x \in \mathbb{R}^n,$$

be a $\mathbf{C}^r$ $(r \geq 1)$ map. Suppose $\mathcal{M} \subset \mathbb{R}^n$ is a trapping region with $\Lambda \subset \mathcal{M}$ a chaotic invariant set. Then defining

$$\mathcal{A} \equiv \bigcap_{n>0} g^n(\mathcal{M}),$$

show that

$$\Lambda \subset \mathcal{A}.$$

6. Very often one hears the phrase,

A dynamical system is chaotic if it has one positive Liapunov exponent.

Discuss what this phrase means in light of the discussion in Sections 29 and 30. Consider both dissipative and nondissipative systems.

7. Recall the discussion of chaos in the phase space of the damped, periodically forced Duffing oscillator at the end of Section 30. The goal of this exercise is to make the heuristic arguments given in that discussion rigorous.

   a) Draw the homoclinic tangle correctly for the Poincaré map on a given cross-section (say Σ^0). You may want to use a computer.

   b) Find candidates for two μ_h-horizontal strips, denoted H_0 and H_1, which map over themselves in μ_v-vertical strips under some iterate of the Poincaré map so that Assumptions 1 and 3 of Chapter 25 are satisfied. Choose the horizontal strips so that the relationship between the motion in phase space and the dynamics on the invariant set is as described in Chapter 30.

   c) Describe the relationship between the number of iterates needed to form the chaotic invariant set and the parameters $\gamma - \delta - \omega$ (see Holmes and Marsden [1982] for help).

8. Often one hears the phrase,

   For diffeomorphisms of dimension two and larger and for vector fields of dimension three and larger, homoclinic orbits produce chaos.

   Is this statement generally true? Give a complete discussion with examples.

9. For Example 30.0.4 prove that the periodic orbits are dense.

31

Hyperbolic Invariant Sets: A Chaotic Saddle

We now want to show that the invariant Cantor set Λ constructed in Chapter 25 has a very special structure. In particular, it is an example of a *hyperbolic invariant set.* Hyperbolic invariant sets are examples of *chaotic saddles*, a terminology that has developed over the past 10 years. We will comment more on this at the end of this chapter.

The notion of *hyperbolicity* played a central role in the development of dynamical systems theory. We will begin this chapter by giving the necessary definitions and constructions in the context of two dimensional diffeomorphisms (we follow Moser [1973]). This has the advantage of allowing us to give rather complete proofs of results using fairly simple mathematics (the mathematical tools are simple, the *reasoning and constructions* with those tools is more complicated). Afterwards we will discuss the general n-dimensional result.

31.1 Hyperbolicity of the Invariant Cantor Set Λ Constructed in Chapter 25

We begin with the following definition.

Definition 31.1.1 *Let $f: \mathbb{R}^2 \to \mathbb{R}^2$ be a $\mathbf{C}^r$ $(r \geq 1)$ diffeomorphism and let $\Lambda \subset \mathbb{R}^2$ be a compact set that is invariant under f. Then we say that Λ is a* hyperbolic invariant set *if*

1. *At each point $z_0 \in \Lambda$ there exists a pair of lines, $E^s_{z_0}$ and $E^u_{z_0}$, that are invariant under $Df(z_0)$ in the sense that*

$$Df(z_0)E^s_{z_0} = E^s_{f(z_0)}$$

and

$$Df(z_0)E^u_{z_0} = E^u_{f(z_0)}.$$

2. *There exists a constant* $0 < \lambda < 1$ *such that if*

$$\zeta_{z_0} = (\xi_{z_0}, \eta_{z_0}) \in E^s_{z_0}, \qquad \textit{then} \quad |Df(z_0)\zeta_{z_0}| < \lambda|\zeta_{z_0}|$$

and if

$$\zeta_{z_0} = (\xi_{z_0}, \eta_{z_0}) \in E^u_{z_0}, \qquad \textit{then} \quad |Df^{-1}(z_0)\zeta_{z_0}| < \lambda|\zeta_{z_0}|,$$

where $|\zeta_{z_0}| = \sqrt{(\xi_{z_0})^2 + (\eta_{z_0})^2}$.

3. $E^s_{z_0}$ *and* $E^u_{z_0}$ *vary continuously with* $z_0 \in \Lambda$.

We make the following remarks concerning this definition.

Remark 1. It should be clear that hyperbolic fixed points and hyperbolic periodic orbits are examples of hyperbolic invariant sets.

Remark 2. $E^s \equiv \bigcup_{z_0 \in \Lambda} E^s_{z_0}$ and $E^u \equiv \bigcup_{z_0 \in \Lambda} E^u_{z_0}$ are called the invariant stable and unstable line bundles over Λ, respectively.

We now state the theorem that Λ is a hyperbolic invariant set.

Theorem 31.1.2 (Moser [1973]) *Consider the* $\mathbf{C}^r$ $(r \geq 1)$ *diffeomorphism* f *and its invariant set* Λ *described in Theorem 25.2.1. Let* $\Delta = \sup_\Lambda(\det Df)$. *Then if*

$$\Delta, \Delta^{-1} \leq \mu^{-2},$$

where $0 < \mu < 1 - \mu_v\mu_h$, Λ *is a hyperbolic invariant set.*

Proof: We begin by constructing the unstable invariant line bundle over Λ, $E^u \equiv \bigcup_{z_0 \in \Lambda} E^u_{z_0}$. First, we want to recall some important points from the hypotheses of Theorem 25.2.1.

i)
$$\mathcal{S}^u_{z_0} = \big\{(\xi_{z_0}, \eta_{z_0}) \in R^2 \,|\, |\xi_{z_0}| \leq \mu_v|\eta_{z_0}|\big\}. \tag{31.1.1}$$

ii)
$$Df(\mathcal{S}^u_{\mathcal{H}}) \subset \mathcal{S}^u_{\mathcal{V}}. \tag{31.1.2}$$

iii) For $(\xi_{z_0}, \eta_{z_0}) \in \mathcal{S}^u_{z_0}$, $Df(z_0)(\xi_{z_0}, \eta_{z_0}) \equiv (\xi_{f(z_0)}, \eta_{f(z_0)}) \in \mathcal{S}^u_{f(z_0)}$, we have

$$|\eta_{f(z_0)}| \geq \frac{1}{\mu}|\eta_{z_0}|, \tag{31.1.3}$$

where $0 < \mu < 1 - \mu_v\mu_h$.

The construction of E^u will be by the contraction mapping principle. We define

$$\mathcal{L}^u_\Lambda = \{\text{continuous line bundles over } \Lambda \text{ contained in } \mathcal{S}^u_\Lambda\}.$$

"Points" in $\mathcal{L}^u_\Lambda$ will be denoted by

$$\begin{aligned}\mathcal{L}^u_\Lambda(\alpha(z_0)) &\equiv \bigcup_{z_0\in\Lambda} L^u_{\alpha(z_0)},\\ \mathcal{L}^u_\Lambda(\beta(z_0)) &\equiv \bigcup_{z_0\in\Lambda} L^u_{\beta(z_0)},\end{aligned} \tag{31.1.4}$$

where

$$\begin{aligned}L^u_{\alpha(z_0)} &= \big\{(\xi_{z_0},\eta_{z_0})\in\mathbb{R}^2 \,|\, \xi_{z_0} = \alpha(z_0)\eta_{z_0}\big\},\\ L^u_{\beta(z_0)} &= \big\{(\xi_{z_0},\eta_{z_0})\in\mathbb{R}^2 \,|\, \xi_{z_0} = \beta(z_0)\eta_{z_0}\big\},\end{aligned} \tag{31.1.5}$$

with $\alpha(z_0)$, $\beta(z_0)$ continuous functions on Λ and

$$\sup_{z_0\in\Lambda} |\alpha(z_0)| \le \mu_v,$$

$$\sup_{z_0\in\Lambda} |\beta(z_0)| \le \mu_v.$$

As notation for a line in a line bundle, say $\mathcal{L}^u_\Lambda(\alpha(z_0))$, at a point $z_0\in\Lambda$ we have

$$\big(\mathcal{L}^u_\Lambda(\alpha(z_0))\big)_{z_0} \equiv L^u_{\alpha(z_0)}.$$

$\mathcal{L}^u_\Lambda$ is a complete metric space with metric defined by

$$\|\mathcal{L}^u_\Lambda(\alpha(z_0)) - \mathcal{L}^u_\Lambda(\beta(z_0))\| \equiv \sup_{z_0\in\Lambda} |\alpha(z_0)-\beta(z_0)|. \tag{31.1.6}$$

From (31.1.6), the geometrical meaning of the continuity of a line bundle should be clear.

We define a map on $\mathcal{L}^u_\Lambda$ as follows. For any $\mathcal{L}^u_\Lambda(\alpha(z_0))\in\mathcal{L}^u_\Lambda$ we have

$$\big(F(\mathcal{L}^u_\Lambda(\alpha(z_0)))\big)_{z_0} \equiv Df(f^{-1}(z_0))L^u_{\alpha(f^{-1}(z_0))}. \tag{31.1.7}$$

From the fact that $Df(\mathcal{S}^u_{\mathcal{H}})\subset\mathcal{S}^u_{\mathcal{V}}$, it follows that

$$F(\mathcal{L}^u_\Lambda)\subset\mathcal{L}^u_\Lambda. \tag{31.1.8}$$

We now show that F is a contraction map. Choose $\mathcal{L}^u_\Lambda(\alpha(z_0))$, $\mathcal{L}^u_\Lambda(\beta(z_0)) \in \mathcal{L}^u_\Lambda$; then we must show that

$$\|F(\mathcal{L}^u_\Lambda(\alpha(z_0))) - F(\mathcal{L}^u_\Lambda(\beta(z_0)))\| \le k\|\mathcal{L}^u_\Lambda(\alpha(z_0)) - \mathcal{L}^u_\Lambda(\beta(z_0))\|, \quad (31.1.9)$$

where $0 < k < 1$.

From (31.1.8),

$$F(\mathcal{L}^u_\Lambda(\alpha(z_0))) = \mathcal{L}^u_\Lambda(\alpha^*(z_0)) \in \mathcal{L}^u_\Lambda,$$
$$F(\mathcal{L}^u_\Lambda(\beta(z_0))) = \mathcal{L}^u_\Lambda(\beta^*(z_0)) \in \mathcal{L}^u_\Lambda,$$

and we must compute $\alpha^*(z_0)$ and $\beta^*(z_0)$ in order to verify (31.1.9).

Let us denote, for simplicity of notation,

$$Df \equiv \begin{pmatrix} a & b \\ c & d \end{pmatrix}, \quad (31.1.10)$$

where, of course, a, b, c, and d are the appropriate partial derivatives of $f \equiv (f_1, f_2)$ and are therefore functions of z_0. However, to carry this along in the formulae would result in very cumbersome expressions. Hence, we remind the reader to think of the partial derivatives a, b, c, and d as being evaluated at the same point as $Df(\cdot)$ even though we will not explicitly display this dependence.

Using (31.1.10), we have

$$a\xi_{z_0} + b\eta_{z_0} = \xi_{f(z_0)},$$
$$c\xi_{z_0} + d\eta_{z_0} = \eta_{f(z_0)}. \quad (31.1.11)$$

Consider an arbitrary line

$$L^u_{\alpha(z_0)} = \left\{(\xi_{z_0}, \eta_{z_0}) \in \mathbb{R}^2 \,|\, \xi_{z_0} = \alpha(z_0)\eta_{z_0}\right\} \in \mathcal{L}^u_\Lambda(\alpha(z_0)); \quad (31.1.12)$$

then

$$Df(f^{-1}(z_0))L^u_{\alpha(f^{-1}(z_0))} \equiv L^u_{\alpha^*(z_0)} \quad (31.1.13)$$

and, using (31.1.11) and (31.1.12), we have

$$\xi_{z_0} = \left(\frac{a\alpha(f^{-1}(z_0)) + b}{c\alpha(f^{-1}(z_0)) + d}\right)\eta_{z_0} \equiv \alpha^*(z_0)\eta_{z_0}. \quad (31.1.14)$$

Thus,

$$\alpha^*(z_0) \equiv \frac{a\alpha(f^{-1}(z_0)) + b}{c\alpha(f^{-1}(z_0)) + d} \tag{31.1.15}$$

is also continuous over Λ. We have thus shown that

$$F\big(\mathcal{L}^u_\Lambda(\alpha(z_0))\big) = \mathcal{L}^u_\Lambda(\alpha^*(z_0)),$$

where

$$\alpha^*(z_0) = \frac{a\alpha(f^{-1}(z_0)) + b}{c\alpha(f^{-1}(z_0)) + d}.$$

Similarly,

$$F\big(\mathcal{L}^u_\Lambda(\beta(z_0))\big) = \mathcal{L}^u_\Lambda(\beta^*(z_0)),$$

where

$$\beta^*(z_0) = \frac{a\beta(f^{-1}(z_0)) + b}{c\beta(f^{-1}(z_0)) + d}. \tag{31.1.16}$$

Now, using (31.1.6), we have

$$\|F\big(\mathcal{L}^u_\Lambda(\alpha(z_0))\big) - F\big(\mathcal{L}^u_\Lambda(\beta(z_0))\big)\| = \sup_{z_0\in\Lambda} |\alpha^*(z_0) - \beta^*(z_0)|. \tag{31.1.17}$$

Using (31.1.15) and (31.1.16), we obtain

$$|\alpha^*(z_0) - \beta^*(z_0)| \le \Delta \frac{|\alpha(f^{-1}(z_0)) - \beta(f^{-1}(z_0))|}{|c\alpha(f^{-1}(z_0)) + d|\,|c\beta(f^{-1}(z_0)) + d|}. \tag{31.1.18}$$

From (31.1.3) and (31.1.11) we have

$$\frac{|\eta_{z_0}|}{|\eta_{f^{-1}(z_0)}|} = \left| c\frac{\xi_{f^{-1}(z_0)}}{\eta_{f^{-1}(z_0)}} + d \right| \ge \frac{1}{\mu} \tag{31.1.19}$$

and, therefore, since $\xi_{f^{-1}(z_0)} = \alpha(f^{-1}(z_0))\eta_{f^{-1}(z_0)}$, we have

$$|c\alpha(f^{-1}(z_0)) + d|, \quad |c\beta(f^{-1}(z_0)) + d| \ge \frac{1}{\mu} \tag{31.1.20}$$

where $0 < \mu < 1 - \mu_v\mu_h$.

Combining (31.1.18) and (31.1.20) gives

$$|\alpha^*(z_0) - \beta^*(z_0)| \le \mu^2 \Delta |\alpha(f^{-1}(z_0)) - \beta(f^{-1}(z_0))|. \tag{31.1.21}$$

Note that since Λ is invariant under f, we have

$$\sup_{z_0 \in \Lambda} |\alpha(f^{-1}(z_0)) - \beta(f^{-1}(z_0))| = \sup_{z_0 \in \Lambda} |\alpha(z_0) - \beta(z_0)|. \tag{31.1.22}$$

Taking the supremum of (31.1.21) over $z_0 \in \Lambda$ and using (31.1.22), (31.1.6), and (31.1.17) gives

$$\begin{aligned} &\|F\big(\mathcal{L}^u_\Lambda(\alpha(z_0))\big) - F\big(\mathcal{L}^u_\Lambda(\beta(z_0))\big)\| \\ &\qquad \le \mu^2 \Delta \|\mathcal{L}^u_\Lambda(\alpha(z_0)) - \mathcal{L}^u_\Lambda(\beta(z_0))\|; \end{aligned} \tag{31.1.23}$$

thus F is a contraction map provided

$$\mu^2 \Delta < 1. \tag{31.1.24}$$

Therefore, by the contraction mapping principle, F has a unique, continuous fixed point. We denote this fixed point by

$$E^u = \bigcup_{z_0 \in \Lambda} E^u_{z_0}. \tag{31.1.25}$$

Thus we have

$$F(E^u) = E^u$$

or, from (31.1.13),

$$(F(E^u))_{z_0} = Df(f^{-1}(z_0)) E^u_{f^{-1}(z_0)} = E^u_{z_0},$$

which is what we wanted to construct. The construction of the stable line bundle over Λ is virtually identical and we leave it as an exercise for the reader.

This shows that Λ satisfies Part 1 of Definition 31.1.1. Part 3 follows from continuity of the fixed point of F (by the contraction mapping principle). Continuity is measured with respect to the metric (31.1.6) so the geometrical meaning should be clear. Part 2 of Definition 31.1.1, expansion and contraction rates, is a trivial consequence of Assumption 3 that we leave as an exercise for the reader. □

31.1A Stable and Unstable Manifolds of the Hyperbolic Invariant Set

Theorem 31.1.2 gives us information on the linearization of f at each point of Λ, but we can also obtain information on f itself. Recall from the proof of Theorem 25.2.1 that

$$\Lambda = \Lambda_{-\infty} \cap \Lambda_{\infty},$$

with

$$\Lambda_{-\infty} = \bigcup_{\substack{s_{-i} \in S \\ i=1,2,\cdots}} V_{s_{-1}\cdots s_{-k}\cdots},$$

$$\Lambda_{\infty} = \bigcup_{\substack{s_i \in S \\ i=0,1,\cdots}} H_{s_0\cdots s_k\cdots},$$

where, for each infinite sequence of elements of S, $V_{s_{-1}\cdots s_{-k}\cdots}$ and $H_{s_0\cdots s_k\cdots}$ are μ_v-vertical and μ_h-horizontal curves, respectively, with $0 \le \mu_v\mu_h < 1$. Thus, for any $z_0 \in \Lambda$, there exists a unique μ_v-vertical curve in $\Lambda_{-\infty}$, $V_{s_{-1}\cdots s_{-k}\cdots}$, and a unique μ_h-horizontal curve in Λ_{∞}, $H_{s_0\cdots s_k\cdots}$, such that

$$z_0 = V_{s_{-1}\cdots s_{-k}\cdots} \cap H_{s_0\cdots s_k\cdots}.$$

Moreover, we can prove the following theorem.

Theorem 31.1.3 (Moser [1973]) *Consider the* $\mathbf{C}^r$ $(r \ge 1)$ *diffeomorphism* f *and its invariant set* Λ *described in Theorem 25.2.1. Let* $\Delta = \sup_{\Lambda}(\det Df)$. *Then if*

$$0 < \mu \le \min\left(\sqrt{|\Delta|}, \frac{1}{\sqrt{|\Delta|}}\right),$$

the curves in $\Lambda_{-\infty}$ *and* Λ_{∞} *are* $\mathbf{C}^1$ *curves whose tangents at points in* Λ *coincide with* E^u *and* E^s, *respectively.*

Proof: The proof follows the same ideas as Theorem 31.1.2; in Exercise 2 we outline the steps one must complete to establish the theorem. □

In some sense we can think of these curves as defining the stable and unstable manifolds of points in Λ. The details of this are worked out in the exercises. But first we must first give some definitions. We will give these definitions in the general n-dimensional setting.

31.2 Hyperbolic Invariant Sets in $\mathbb{R}^n$

Consider a C^r $(r \geq 1)$ diffeomorphism

$$f : \mathbb{R}^n \to \mathbb{R}^n,$$

and let Λ be a compact invariant set for f.

Definition 31.2.1 (Hyperbolic Invariant Set) *Λ is said to be a* hyperbolic invariant set *if for each $p \in \Lambda$ there is a splitting*

$$\mathbb{R}^n = E_p^s + E_p^u,$$

which varies continuously with $p \in \Lambda$, and constants $C > 0$, $0 < \lambda < 1$ such that

1. *(***Invariance of the Splitting***)*

$$Df(p)E_p^s = E_{f(p)}^s,$$

$$Df(p)E_p^u = E_{f(p)}^u.$$

2. *(***Contraction and Expansion***)*

$$|Df^n(p)v| \leq C\lambda^n|v|, \quad \forall\, v \in E_p^s,\, p \in \Lambda,$$

$$|Df^{-n}(p)v| \leq C\lambda^n|v|, \quad \forall\, v \in E_p^u,\, p \in \Lambda.$$

For any point $p \in \Lambda$, $\varepsilon > 0$, the stable and unstable sets of p of size ε are defined as follows

$$W_\varepsilon^s(p) = \big\{p' \in \Lambda \,|\, |f^n(p) - f^n(p')| \leq \varepsilon \text{ for } n \geq 0\big\},$$
$$W_\varepsilon^u(p) = \big\{p' \in \Lambda \,|\, |f^{-n}(p) - f^{-n}(p')| \leq \varepsilon \text{ for } n \geq 0\big\}.$$

From Chapter 3, we have seen that if p is a hyperbolic fixed point the following hold.

1. For ε sufficiently small, $W_\varepsilon^s(p)$ is a $\mathbf{C}^r$ manifold tangent to E_p^s at p and having the same dimension as E_p^s. $W_\varepsilon^s(p)$ is called the local stable manifold of p.

2. The stable manifold of p is defined as follows

$$W^s(p) = \bigcup_{n=0}^{\infty} f^{-n}(W^s_\varepsilon(p)).$$

Similar statements hold for $W^u_\varepsilon(p)$.

The invariant manifold theorem for hyperbolic invariant sets (see Hirsch, Pugh, and Shub [1977]) tells us that a similar structure holds for each point in Λ.

Theorem 31.2.2 *Let Λ be a hyperbolic invariant set of a $\mathbf{C}^r$ $(r \geq 1)$ diffeomorphism f. Then, for $\varepsilon > 0$ sufficiently small and for each point $p \in \Lambda$, the following hold.*

i) *$W^s_\varepsilon(p)$ and $W^u_\varepsilon(p)$ are $\mathbf{C}^r$ manifolds tangent to E^s_p and E^u_p, respectively, at p and having the same dimension as E^s_p and E^u_p, respectively.*

ii) *There are constants $C > 0$, $0 < \lambda < 1$, such that if $p' \in W^s_\varepsilon(p)$, then*

$$|f^n(p) - f^n(p')| \leq C\lambda^n |p - p'|, \quad \text{for} \quad n \geq 0$$

and if $p' \in W^u_\varepsilon(p)$, then

$$|f^{-n}(p) - f^{-n}(p')| \leq C\lambda^n |p - p'| \quad \text{for} \quad n \geq 0.$$

iii)

$$f(W^s_\varepsilon(p)) \subset W^s_\varepsilon(f(p)),$$
$$f^{-1}(W^u_\varepsilon(p)) \subset W^u_\varepsilon(f^{-1}(p)).$$

iv) *$W^s_\varepsilon(p)$ and $W^u_\varepsilon(p)$ vary continuously with p.*

Proof: See Hirsch, Pugh, and Shub [1977]. □

With Theorem 31.2.2 in hand, one can then define the global stable and unstable manifolds of any point $p \in \Lambda$ as follows

$$W^s(p) = \bigcup_{n=0}^{\infty} f^{-n}(W^s_\varepsilon(f^n(p))),$$
$$W^u(p) = \bigcup_{n=0}^{\infty} f^{n}(W^u_\varepsilon(f^{-n}(p))).$$

We refer the reader to the exercises for more detailed studies of the issues raised here in the context of the hyperbolic invariant set constructed in Theorem 31.1.2 and we end this section with some final remarks.

Remark 1: Structural Stability. Hyperbolic invariant sets (like hyperbolic fixed points and periodic orbits) are structurally stable; see Hirsch, Pugh, and Shub [1977].

Remark 2: History. The reason for discussing the concept of hyperbolic invariant sets is that they have played a central role in the development of modern dynamical systems theory. The definitions of Anosov diffemorphisms and Axiom A diffeomorphisms rely crucially on hyperbolicity, and their study has been important for the development of many concepts and theorems in dynamical systems theory. For example, the ideas of Markov partitions, pseudo orbits, shadowing, etc., were all developed initially in these contexts and all utilize crucially the notion of a hyperbolic invariant set[1].

Indeed, the existence of a hyperbolic invariant set is often assumed a priori. This has caused the applied scientist great difficulty since, in order to utilize many of the techniques or theorems of dynamical systems theory, he or she must first show that the system under study possesses a hyperbolic invariant set. The techniques developed here, specifically the preservation of sector bundles, allow one to explicitly construct hyperbolic invariant sets. For more information on the consequences and utilization of hyperbolic invariant sets see Smale [1967], Nitecki [1971], [1978], Conley [1978], Palis and de Melo [1982], Shub [1987], Franks [1982], Palis and Takens [1993], and Katok and Hasselblatt [1995].

Remark 3: Chaotic Saddles. Hyperbolic invariant sets were studied in great detail in the 1960's; well before the term "chaos" was popularized in the context of dynamics. Hyperbolic invariant sets are examples of *chaotic saddles*; a notion around which many papers have been published over the past 10 years. See, for example, Lai *et al.* [1993], Thompson *et al.* [1994], Ashwin *et al.* [1996], Dhamala and Lai [1999], Kapitaniak *et al.* [1999], Kapitaniak [2001], and Robert *et. al* [1998], [2000]. Most of these works are numerical in nature and fail to recognize the related pioneering work of the 60's and 70's. Much can be learned about "chaotic saddles" by studying the seminal works of Bowen [1970a,b], [1972], [1973], [1975a] and Newhouse [1972].

[1] Anosov diffeomorphisms are those where the entire phase space is a hyperbolic invariant set for the diffeomorphism. Axiom A diffeomorphisms are those having the property that their set of nonwandering points (cf. Definition 8.1.5) is hyperbolic and the the set of nonwandering points is the closure of the set of periodic orbits.

Nevertheless, the numerical studies of the last 10 years on chaotic saddles do go beyond the previous work in that they consider the more complex issues of loss of hyperbolicity and bifurcation. This is an important area of research for which there are not many theorems, at the moment.

31.2A Sector Bundles for Maps on $\mathbb{R}^n$

In this section we state the higher dimensional analog of Theorem 31.1.2. As above, let $f: \mathbb{R}^n \to \mathbb{R}^n$ be a C^r $(r \geq 1)$ diffeomorphism and let Λ be a closed set which is invariant under f. Let $\mathbb{R}^n = E_p^s \oplus E_p^u$ be a splitting of $\mathbb{R}^n$ for $p \in \Lambda$ and let $\mu(p)$ be a positive real valued function defined on Λ. We define the $\mu(p)$ sector, denoted $S_{\mu(p)}$, as follows

$$S_{\mu(p)} = \left\{ (\xi_p, \eta_p) \in E_p^s \oplus E_p^u \mid |\xi_p| \leq \mu(p) |\eta_p| \right\} \tag{31.2.1}$$

and we define the complementary sector, $S'_{\mu(p)}$, as follows

$$S'_{\mu(p)} = \mathbb{R}^n - S_{\mu(p)}. \tag{31.2.2}$$

Then we have the following theorem.

Theorem 31.2.3 *Let $f: \mathbb{R}^n \to \mathbb{R}^n$ be a C^r $(r \geq 1)$ diffeomorphism and let $\Lambda \subset \mathbb{R}^n$ be a closed set which is invariant under f. Then Λ is a hyperbolic invariant set if and only if there exists a splitting $\mathbb{R}^n = E_p^s \oplus E_p^u$ for each $p \in \Lambda$, an integer $n > 0$, constants $C > 0$, $0 < \lambda < 1$ with $C\lambda^n < 1$, and a real valued function $\mu: \Lambda \to \mathbb{R}^+$ such that the following conditions are satisfied:*

1)

$$\sup_{p \in \Lambda} \left\{ \max(\mu(p), \mu(p)^{-1}) \right\} < \infty. \tag{31.2.3}$$

2) *For each $p \in \Lambda$, we have*

$$\begin{aligned} &\textbf{a)}\ Df^n(p) \cdot S_{\mu(p)} \subset S_{\mu(f^n(p))} \\ &\textbf{b)} \qquad \text{if } \xi_p \in S'_{\mu(p)}, \qquad |Df^n(p)\xi_p| \leq C\lambda^n |\xi_p| \\ &\textbf{c)} \qquad \text{if } \xi_p \in S_{\mu(p)}, \qquad \left|Df^{-n}(p)\xi_p\right| \leq C\lambda^n |\xi_p|. \end{aligned} \tag{31.2.4}$$

The proof of this theorem can be found in Newhouse and Palis [1973]. Theorem 31.2.3 tells us that in order to establish hyperbolicity for Λ we

need only find bundles of sectors $S = \bigcup_{p\in\Lambda} S_{\mu(p)}$, $S' = \bigcup_{p\in\Lambda} S'_{\mu(p)}$, such that Df maps S into S while expanding each vector in S and Df maps S' into S' while contracting each vector in S'.

Now regarding Theorem 25.2.1 from Chapter 25, the reader should notice that if A1 and A3 hold then the invariant set Λ is a hyperbolic invariant set since the conditions of A3 are weakened versions of the necessary and sufficient conditions for a set to be hyperbolic given in Theorem 31.2.3.

31.3 A Consequence of Hyperbolicity: The Shadowing Lemma

We will end this section by discussing the shadowing property associated with hyperbolic invariant sets. Two recent monographs on shadowing are Lani-Wayda [1995] and Pilyugin [1999]. We follow the proof of Robinson [1977]. First we need some defintions.

Definition 31.3.1 (ϵ pseudo orbit) *An infinite ϵ pseudo orbit is a doubly infinite sequence of points*

$$\{x_i, \mid i \in \mathbb{Z}\}$$

such that

$$|f(x_i) - x_{i+1}| < \epsilon.$$

Definition 31.3.2 *Suppose U is a neighborhood of a hyperbolic invariant set Λ where the hyperbolic splitting holds. Then we say that U is a set where f is hyperbolic.*

Lemma 31.3.3 (Shadowing Lemma) *Let $U \in \mathbb{R}^n$ be a region where f is hyperbolic. Given $\delta > 0$ there exists $\epsilon > 0$ such that if $\{x_i, \mid i \in \mathbb{Z}\}$ is an ϵ pseudo orbit in U then there exists a unique y such that*

$$|f^i(y) - x_i| < \delta$$

for all $i \in \mathbb{Z}$, i.e. every ϵ pseudo orbit is δ shadowed by an orbit of f.

Proof: Consider a neighborhood U of Λ where f is hyperbolic. Then the invariant splitting of $\mathbb{R}^n$ over Λ (i.e., $\mathbb{R}^n = E^s_x + E^u_x$, $x \in \Lambda$) extends to an "almost invariant" splitting" over U.

For each $x \in U$ consider the disks of radius $\delta/2$ in E^s_x and E^u_x. The cartesian product of these disks gives a neighborhood $B(x)$ of x.

For δ sufficiently small, f is close to Df in $B(x)$. Thus, in $B(x)$ the contraction and expansion properties of f are close to those of Df.

If ϵ is small enough, and $\{x_i \,|\, i \in \mathbb{Z}\}$ is an ϵ pseudo orbit in U, then $f(B(x_{j-1}))$ stretches across $B(x_j)$ in the unstable directions and is contracted in the stable directions. Then $f\left(f\left(B(x_{j-1})\right) \cap B(x_{j-1})\right) \cap B(x_j)$ is an even thinner strip that crosses $B(x_j)$ in the unstable directions. Continuing this construction:

$$\bigcap_{n\geq 0} f^n\left(B(x_{j-n})\right) \equiv D^u(x_j, \{x_i\})$$

is a disk that stretches across $B(x_j)$ in the unstable direction. We call it *the unstable disk at x_j for the ϵ pseudo orbit*. It does not necessarily contain x_j and it is the same dimension as $E^u_{x_j}$.

By construction, a point $y \in D^u(x_j, \{x_i\})$ if and only if $y \in f^n\left(B(x_{j-n})\right)$ for all $n \geq 0$, i.e., $f^{-n}(y) \in B(x_{j-n})$ for all $n \geq 0$. This gives the "backward half" of the shadowing orbit. Next we construct the "forward half".

From the stable manifold theorem it follows that $D^u(x_j, \{x_i\})$ is C^1 and almost tangent to $E^u_{x_j}$. Moreover, f expands $D^u(x_j, \{x_i\})$ across $D^u(x_{j+1}, \{x_i\})$. Thus $f^{-1} : D^u(x_{j+1}, \{x_i\}) \to D^u(x_j, \{x_i\})$ is a uniform contraction. Hence, the contraction mapping principle implies that

$$\bigcap_{n\geq 0} \left\{f^{-n}\left(D^u(x_n, \{x_i\}\, 0)\right)\right\},$$

is the unique point y such that $y \in f^{-n}(B(x_n))$ for all n, i.e. such that $f^n(y) \in B(x_n)$ for all n. Hence, the orbit of y δ shadows the ϵ pseudo orbit. □

31.3A Applications of the Shadowing Lemma

Applications of the shadowing lemma present themselves immediately. In many settings our dynamical systems are not "perfect". The imperfection can arise from modelling errors or uncertainties. They could arise in the process of numerical simulation of the trajectories of a dynamical system through round-off errors. In each of these situations we would like to know that the trajectories of our "approximate" dynamical system are "close"

to a trajectory of the "real" dynamical system. The shadowing lemma provides a compelling framework for thinking about such issues. Results along these lines can be found in Nusse and Yorke [1988], Grebogi *et al.* [1990], Coomes *et al.* [1993], [1994a,b], [1995a, b], [1997], Coomes [1997], Palmer [1996], Sauer *et al.* [1997], Stoffer and Palmer [1999], van Vleck [1995], [2000], Corless [1992], Fryska and Zohdy [1992], Sauer and Yorke [1991], and Palmore and McCauley [1987].

However, it must be understood that shadowing only rigorously holds in the setting of hyperbolic dynamics–a setting the is extremely rare in applications. Numerical simulations on the effect of the loss of hyperbolicity on shadowing can be found in Dawson *et al.* [1994]. A rigorous result has recently been obtained by Bonatti et al. [2000].

Applications of shadowing in partial differential equations can be found in Larsson and Sanz-Serna [1999], Ostermann and Palencia [2000], Angenent [1987], and Chow *et al.* [1989].

Applications of shadowing in perturbation theory can be found in Murdock [1990], [1995], [1996], and Lin [1989], [1996].

Applications of shadowing in fluid mechanics can be found in Klapper [1992], [1993] and Ghosh *et al.* [1998].

An application of shadowing to predictability can be found in Pearson [2001].

A shadowing lemma for random maps is developed in Chow and van Vleck [1992/93].

Alternate proofs of the shadowing lemma can be found in Meyer and Sell [1987], Fečkan [1991], and Hadeler [1996].

Other interesting references concerning shadowing are Chu and Koo [1996], Henry [1994], Krüger and Troubetzkoy [1992], Blank [1991], Steinlein and Walther [1991], and Palmer [1988].

31.4 Exercises

1. Recall from the proof of Theorem 31.1.2 that

$$\mathcal{L}^u_\Lambda = \left\{\text{continuous line bundles over } \Lambda \text{ contained in } \mathcal{S}^u_\Lambda\right\}$$

with typical "points" in $\mathcal{L}^u_\Lambda$ denoted by

$$\mathcal{L}^u_\Lambda(\alpha(z_0)) \equiv \bigcup_{z_0 \in \Lambda} L^u_{\alpha(z_0)},$$

$$\mathcal{L}^u_\Lambda(\beta(z_0)) \equiv \bigcup_{z_0\in\Lambda} L^u_{\beta(z_0)},$$

where

$$L^u_{\alpha(z_0)} = \Big\{(\xi_{z_0},\eta_{z_0})\in\mathbb{R}^2 \mid \xi_{z_0} = \alpha(z_0)\eta_{z_0}\Big\},$$
$$L^u_{\beta(z_0)} = \Big\{(\xi_{z_0},\eta_{z_0})\in\mathbb{R}^2 \mid \xi_{z_0} = \beta(z_0)\eta_{z_0}\Big\}.$$

We defined a metric on $\mathcal{L}^u_\Lambda$ as follows

$$\|\mathcal{L}^u_\Lambda(\alpha(z_0)) - \mathcal{L}^u_\Lambda(\beta(z_0))\| = \sup_{z_0\in\Lambda} |\alpha(z_0)-\beta(z_0)|. \tag{31.4.1}$$

a) Prove that (31.4.1) is indeed a metric.

b) Prove that $\mathcal{L}^u_\Lambda$ is a complete metric space with the metric (31.4.1).

c) Recall the unstable invariant line bundle constructed in Theorem 31.1.2 that we denoted

$$E^u = \bigcup_{z_0\in\Lambda} E^u_{z_0}.$$

For $\zeta_{z_0} = (\xi_{z_0},\eta_{z_0}) \in E^u_{z_0}$ prove that

$$|Df^{-1}(z_0)\zeta_{z_0}| < \lambda|\zeta_{z_0}|$$

where $0<\lambda<1$.

2. Prove Theorem 31.1.3. *Hints:* 1) show that the map F defined on $\mathcal{L}^u_\Lambda$ in (31.1.7) can be extended to a map on line bundles over $\Lambda_{-\infty}$ (the μ_v-vertical curves) and not just Λ.

2) Next, let the graph of $x = v(y)$ be a μ_v-vertical curve in $\Lambda_{-\infty}$ and let $z_0 = (x_0,y_0)$ be a point on that curve. Let T_{z_0} denote the set of lines $\xi = \alpha(z_0)\eta$ with

$$\alpha(z_0) = \lim_{n\to\infty} \frac{v(y_n) - v(y'_n)}{y_n - y'_n},$$

where $y_n \neq y'_n$ are two sequences approaching y_0 for which this limit exists. Show that $|\alpha(z_0)| \le \mu_v$ and that the set of $\alpha(z_0)$, z_0 fixed, satisfying this is closed.

3) Let

$$\omega(T_{z_0}) = \max\alpha(z_0) - \min\alpha(z_0) \le 2\mu_v,$$

where the maximum and minimum is taken over the set defined above. Show that *if* $\omega(T_{z_0}) = 0$, then the curve has a derivative at z_0 and that, since the two sequences, y_n and y'_n, were arbitrary, the derivative is continuous.

4) Finally, we will be through if, from Step 3, we show that $\omega(T_{z_0}) = 0$. This is done as follows. First show that $F(T_{z_0}) = T_{z_0}$, $z_0\in\Lambda_{-\infty}$, by using the mean value theorem. Next use the contraction property to show that $\omega(T_{z_0}) = \omega(F(T_{z_0})) \le \frac{1}{2}\omega(T_{z_0})$ and from this conclude that $\omega(T_{z_0}) = 0$. Does it follow that $E^u_{z_0}$ agrees with the tangent to this $\mathbf{C}^1$ curve?

If you need help see Moser [1973].

3. Consider the invariant set Λ constructed in Theorem 25.2.1. Using Theorems 31.1.2, 31.1.3, and 31.2.2 describe in detail the stable and unstable manifolds of Λ.

4. *Horseshoes are Structurally Stable.* Suppose that a map $f\colon D\to\mathbb{R}^2$ satisfies the hypothesis of Theorem 25.2.1. Then it possesses an invariant Cantor set Λ. Show that, for ε sufficiently small, the map $f+\varepsilon g$ (with g $\mathbf{C}^r$, $r\ge 1$, on D) also possesses an invariant Cantor set Λ_ε. Moreover, show that Λ_ε can be constructed so that $(f+\varepsilon g)\Big|_{\Lambda_\varepsilon}$ is topologically conjugate to $f\Big|_\Lambda$.

32

Long Period Sinks in Dissipative Systems and Elliptic Islands in Conservative Systems

Long period sinks in dissipative systems and elliptic islands in conservative systems are the "demons" that thwart proofs of the existence of strange attractors in dissipative systems and sets of positive measure on which the dynamics is chaotic in conservative systems. In this chapter we describe some aspects of these phenomena.

32.1 Homoclinic Bifurcations: Cascades of Period-Doubling and Saddle-Node Bifurcations

In Chapter 26 we described some aspects of the complex dynamics associated with a transverse homoclinic orbit to a hyperbolic fixed point. In particular, the map possessed a countable infinity of unstable periodic orbits of all periods. We now want to consider the situation of a bifurcation to transverse homoclinic orbits. Specifically, we consider a one-parameter family of diffeomorphisms of the plane having a hyperbolic periodic orbit (which, without loss of generality, we can assume is a fixed point). Referring to the parameter as μ, suppose, for $\mu > \mu_0$, the stable and unstable manifolds of the fixed point do not intersect and, for $\mu < \mu_0$, they intersect transversely (the reader might peek ahead to Figure 32.1.2). Hence, a natural question arises; as we go from $\mu > \mu_0$ (i.e., no horseshoe) to $\mu < \mu_0$ (i.e., many horseshoes), how are all the unstable periodic orbits created? We will see that under certain conditions the creation of the complicated dynamics associated with a transverse homoclinic orbit to a hyperbolic periodic orbit is an infinite sequence (or cascade) of period-doubling and saddle-node bifurcations. The set-up for the analysis will be very similar

to that given in Chapter 26 for the proof of Moser's theorem. Specifically, we will analyze a sufficiently large iterate of the map that is defined in a neighborhood (in both phase and parameter space) of a homoclinic point. We begin by stating our assumptions.

We consider a one-parameter family of two-dimensional $\mathbf{C}^r$ $(r \geq 3)$ diffeomorphisms

$$z \mapsto f(z;\mu), \qquad z \in \mathbb{R}^2, \quad \mu \in I \subset \mathbb{R}^1, \tag{32.1.1}$$

where I is some interval in $\mathbb{R}^1$. We have the following assumption on the map.

Assumption 1: Existence of a Hyperbolic Fixed Point. For all $\mu \in I$,

$$f(0,\mu) = 0. \tag{32.1.2}$$

Moreover, $z = 0$ is a hyperbolic fixed point with the eigenvalues of $Df(0,\mu)$ given by $\rho(\mu)$, $\lambda(\mu)$, with

$$0 < \rho(\mu) < 1 < \lambda(\mu) < \frac{1}{\rho(\mu)}. \tag{32.1.3}$$

We remark that since (32.1.3) is satisfied for all $\mu \in I$, we will often omit denoting the explicit dependence of the eigenvalues ρ and λ on μ unless it is relevant to the specific argument being discussed. We denote the stable and unstable manifolds of the hyperbolic fixed point by $W^s_\mu(0)$ and $W^u_\mu(0)$, respectively.

Assumption 2: Existence of a Homoclinic Point. At $\mu = 0$, $W^s_0(0)$ and $W^u_0(0)$ intersect.

Assumption 3: Behavior Near the Fixed Point. There exists some neighborhood $\mathcal{N}$ of the origin such that the map takes the form

$$f(x,y;\mu) = (\rho x, \lambda y), \tag{32.1.4}$$

where x and y are local coordinates in $\mathcal{N}$.

Note that Assumption 3 implies that $W^s_\mu(0) \cap \mathcal{N}$ and $W^u_\mu(0) \cap \mathcal{N}$ are given by the local coordinate axes.

Our final assumption will place more specific conditions on the geometry of the intersection of $W^s_\mu(0)$ with $W^u_\mu(0)$ at $\mu = 0$. This is most conveniently

done in terms of the local return map in a neighborhood of a homoclinic point which we now derive.

We are interested in the dynamics near a homoclinic point. Therefore, using the same construction as that given in the proof of Moser's theorem in Chapter 26, we will derive a map of a neighborhood of a homoclinic point into itself, which is given by f^N, for some N (large). The construction proceeds as follows. Assumption 3 implies that there exists a point $(0, y_0) \in W_0^u(0) \cap \mathcal{N}$ and a point $(x_0, 0) \in W_0^s(0) \cap \mathcal{N}$ such that $f^k(0, y_0; 0) = (x_0, 0)$ for some $k \geq 1$. Thus, following the construction in Chapter 26, we can find a neighborhood of $(0, y_0)$, $U_{y_0} \subset \mathcal{N}$, and a neighborhood of $(x_0, 0)$, $U_{x_0} \subset \mathcal{N}$, such that $f^k(U_{y_0}; 0) = U_{x_0}$; see Figure 32.1.1 (for all the details, see the construction in Chapter26) Note that by continuity, $f^k(\cdot; \mu)$ will be defined in U_{y_0} for μ sufficiently small. We can now state our final assumption.

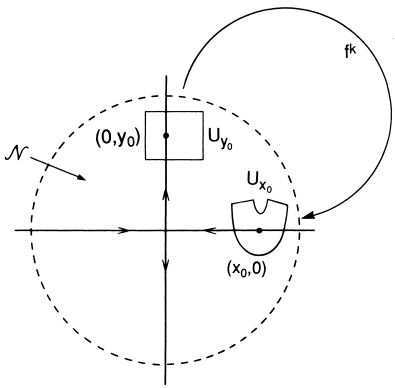

FIGURE 32.1.1.

Assumption 4: Quadratic Homoclinic Tangency at $\mu = 0$. We assume that, in U_{y_0}, $f^k(\cdot; \mu)$ has the form

$$\begin{aligned} f^k : U_{y_0} &\longrightarrow U_{x_0} \\ (x, y) &\longmapsto (x_0 - \beta(y - y_0), \mu + \gamma x + \delta(y - y_0)^2), \end{aligned} \tag{32.1.5}$$

with $\beta, \gamma, \delta > 0$. Hence, for μ near zero, $W_\mu^s(0)$ and $W_\mu^u(0)$ behave as in Figure 32.1.2.

From Lemma 26.0.4 and the arguments given in Chapter 26 it follows that there exists an integer N_0 such that, for all $n \geq N_0$, we can find subsets $U_{x_0}^n \subset U_{x_0}$ such that $f^n(x, y; \mu) = (\rho^n x, \lambda^n y)$ maps $U_{x_0}^n$ into U_{y_0}, i.e.,

$$f^n(U_{x_0}^n; \mu) \subset U_{y_0} \tag{32.1.6}$$

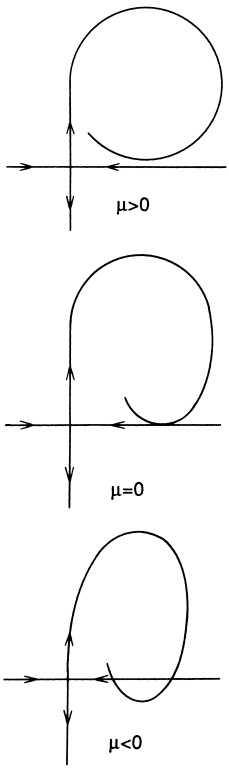

FIGURE 32.1.2.

for μ sufficiently small (note: this can be trivially verified due to the fact that we have assumed f is linear in $\mathcal{N}$). Therefore,

$$f^n \circ f^k \equiv f^{n+k}\colon f^{-k}(U^n_{x_0};\mu) \longrightarrow U_{y_0},$$
$$(x,y) \longmapsto (\rho^n(x_0 - \beta(y-y_0)), \lambda^n(\mu + \gamma x + \delta(y-y_0)^2)), \qquad (32.1.7)$$

is well defined for μ sufficiently small (note: in general $n = n(\mu)$).

We now give our first result.

Theorem 32.1.1 (Gavrilov and Silnikov [1973]) *At $\mu = 0$ there exists an integer N_0 such that, for all $n \geq N_0$, there exists a set $\Lambda_{n+k} \subset \mathcal{N}$, invariant under f^{n+k}, such that $f^{n+k}|_{\Lambda_{n+k}}$ is topologically conjugate to a full shift on two symbols.*

Proof: The proof can be found in Gavrilov and Silnikov [1973] or Guckenheimer and Holmes [1983]. The basic idea is to choose a neighborhood of

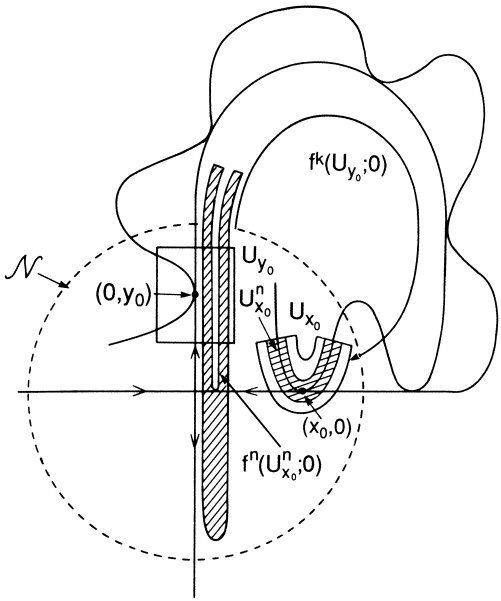

FIGURE 32.1.3.

$(0, y_0)$ so that $f^{n+k}(\cdot;\mu)$ maps it back over itself and Assumptions 1 and 3 of Chapter 25 hold; see Figure 32.1.3. In Exercise 1 we outline the steps necessary to prove this theorem. □

The next theorem tells us how the periodic orbits in the sets Λ_{n+k}, $n \geq N_0$, are created as μ decreases through zero.

Theorem 32.1.2 (Gavrilov and Silnikov [1973]) *There exists an integer N_0 and infinite sequences of parameter values*

$$\{\mu_{SN}^{n+k}\}, \qquad n \geq N_0,$$

$$\{\mu_{PD}^{n+k}\}, \qquad n \geq N_0$$

with $\mu_{SN}^{n+k} > 0$, $\mu_{PD}^{n+k} > 0$ and $\mu_{SN}^{n+k} \; n \overrightarrow{\to}\infty \; 0$, $\mu_{PD}^{n+k} \; n \overrightarrow{\to}\infty \; 0$ such that μ_{SN}^{n+k} corresponds to a saddle-node bifurcation value for f^{n+k}, and μ_{PD}^{n+k} corresponds to a period-doubling bifurcation value for f^{n+k}. Moreover,

$$\mu_{SN}^{N_0+k} > \mu_{PD}^{N_0+k} > \mu_{SN}^{N_0+1+k} > \mu_{PD}^{N_0+1+k} > \cdots > \mu_{SN}^{N_0+m+k} > \mu_{PD}^{N_0+m+k} > \cdots \tag{32.1.8}$$

with

$$\mu_{SN}^{n+k} \sim \lambda^{-n} \quad as \quad n \to \infty \tag{32.1.9}$$

and

$$\mu_{PD}^{n+k} \sim \lambda^{-n} \quad as \quad n \to \infty. \tag{32.1.10}$$

Before proving Theorem 32.1.2 we want to make several remarks.

Remark 1. In the saddle-node bifurcation at $\mu = \mu_{SN}^{n+k}$, the node is actually a sink. The two orbits created are period $n + k$ orbits for f. The sink created in the saddle-node bifurcation subsequently loses stability in a period-doubling bifurcation at $\mu = \mu_{PD}^{n+k}$ (hence, we must have $\mu_{PD}^{n+k} < \mu_{SN}^{n+k}$), resulting in the creation of a period $2(n + k)$ sink for f. This bifurcation scenario will be verified in the course of the proof of Theorem 32.1.2.

Remark 2. Theorem 32.1.2 tells us how the countable infinity of periodic orbits in the horseshoes for $\mu \leq 0$ are created; namely, the periodic orbits are created in saddle-node bifurcations, and the period is increased through period-doubling bifurcations.

Remark 3. Equations (32.1.9) and (32.1.10) gives us the rate by which the period-doubling and saddle-node bifurcation values accumulate on $\mu = 0$. This rate is *not* universal but depends on the size of the unstable eigenvalue of the hyperbolic fixed point.

Remark 4. Theorems 32.1.1 and 32.1.2 are stated explicitly for dissipative or nonconservative maps, i.e., $\lambda\rho < 1$. However, similar results will hold for area-preserving maps where we have $\lambda\rho = 1$; see Newhouse [1983] and Exercise 3.

We now begin the proof of Theorem 32.1.2.

Proof: The proof is constructive. The condition for fixed points of f^{n+k} is given by

$$x = \rho^n x_0 - \beta\rho^n(y - y_0), \tag{32.1.11}$$

$$y = \mu\lambda^n + \gamma\lambda^n x + \delta\lambda^n(y - y_0)^2, \tag{32.1.12}$$

where it is important to recall that x_0, y_0, γ, β, δ, and $\rho > 0$. By substituting (32.1.11) into (32.1.12) we obtain

$$\begin{aligned}\delta\lambda^n y^2 - (\beta\gamma\lambda^n\rho^n + 2\delta\lambda^n y_0 + 1)y + \delta\lambda^n y_0^2 \\ + \beta\gamma\lambda^n\rho^n y_0 + \gamma\rho^n\lambda^n x_0 + \mu\lambda^n = 0.\end{aligned} \tag{32.1.13}$$

Solving (32.1.13) yields

$$y = \frac{\beta\gamma\lambda^n\rho^n + 2\delta\lambda^n y_0 + 1}{2\delta\lambda^n} \pm \frac{1}{2\delta\lambda^n}\big[((\beta\gamma\lambda^n\rho^n + 2\delta\lambda^n y_0 + 1)^2 - 4\delta\lambda^n(\delta\lambda^n y_0^2 + \beta\gamma\lambda^n\rho^n y_0 + \gamma\lambda^n\rho^n x_0 + \mu\lambda^n)\big]^{1/2}. \tag{32.1.14}$$

After some algebra, the expression under the radical in (32.1.15) can be simplified so that (32.1.15) becomes

$$y = \frac{\beta\gamma\lambda^n\rho^n + 2\delta\lambda^n y_0 + 1}{2\delta\lambda^n} \pm \frac{1}{2\delta\lambda^n} \times \sqrt{4\delta\lambda^{2n}\big[\frac{(\beta\gamma\rho^n + \lambda^{-n})^2}{4\delta} + (y_0\lambda^{-n} - \gamma\rho^n x_0) - \mu\big]}. \tag{32.1.15}$$

Note that (32.1.15) is a function of n and μ. Thus, (32.1.15) gives the y coordinate of a fixed point which can be substituted into (32.1.11) to obtain the x coordinate. Note that since (32.1.11) is linear in x, for a fixed y coordinate there is a unique x coordinate for the fixed point. Thus, in studying the numbers of fixed points and their bifurcations, it suffices to study only (32.1.15).

From (32.1.15) we can easily see that there are *no fixed points* for

$$\mu > \frac{(\beta\gamma\rho^n + \lambda^{-n})^2}{4\delta} + (y_0\lambda^{-n} - \gamma\rho^n x_0) \tag{32.1.16}$$

and *two fixed points* for

$$\mu < \frac{(\beta\gamma\rho^n + \lambda^{-n})^2}{4\delta} + (y_0\lambda^{-n} - \gamma\rho^n x_0). \tag{32.1.17}$$

Therefore,

$$\mu = \frac{(\beta\gamma\rho^n + \lambda^{-n})^2}{4\delta} + (y_0\lambda^{-n} - \gamma\rho^n x_0) \tag{32.1.18}$$

is a *bifurcation value* for f^{n+k}.

Next, we verify that this is a saddle-node bifurcation. This can be shown directly. From (32.1.7), the matrix associated with the linearized map is given by

$$Df^{n+k} = \begin{pmatrix} 0 & -\beta\rho^n \\ \gamma\lambda^n & 2\delta\lambda^n(y - y_0) \end{pmatrix}; \tag{32.1.19}$$

hence we have

$$\det Df^{n+k} = \gamma\beta\rho^n\lambda^n, \tag{32.1.20}$$
$$\operatorname{tr} Df^{n+k} = 2\delta\lambda^n(y - y_0), \tag{32.1.21}$$

with eigenvalues, χ_1 and χ_2, of (4.7.17) given by

$$\chi_{1,2} = \frac{\operatorname{tr} Df^{n+k}}{2} \pm \frac{1}{2}\sqrt{(\operatorname{tr} Df^{n+k})^2 - 4\det Df^{n+k}}. \tag{32.1.22}$$

At the bifurcation value (32.1.18) there is only one fixed point where, using (32.1.20), (32.1.21), and (32.1.22), the eigenvalues of (32.1.19) are given by

$$\chi_1 = 1, \qquad \chi_2 = \gamma\beta\rho^n\lambda^n. \tag{32.1.23}$$

Note that since $\rho\lambda < 1$, by taking n sufficiently large, χ_2 can be made arbitrarily small.

At this point we want to check the stability of the bifurcating fixed points. From (32.1.20), (32.1.21) and using $\rho\lambda < 1$, we see that for n sufficiently large, the eigenvalues of (32.1.19) are approximately given by

$$\chi_1 \approx \operatorname{tr} Df^{n+k}, \tag{32.1.24}$$
$$\chi_2 \approx 0, \tag{32.1.25}$$

and by substituting (32.1.15) into (32.1.21) (and neglecting terms of $\mathcal{O}(\rho^n\lambda^n)$) we have

$$\chi_1 \approx 1 \pm \sqrt{4\delta\lambda^{2n}\left(\frac{(\gamma\beta\rho^n + \lambda^{-n})^2}{4\delta} + (y_0\lambda^{-n} - \gamma x_0\rho^n) - \mu\right)}. \tag{32.1.26}$$

Thus, for the branch of fixed points with y coordinate given by

$$y = \frac{\beta\gamma\lambda^n\rho^n + 2\delta\lambda^n y_0 + 1}{2\delta\lambda^n} + \frac{1}{2\delta\lambda^n} \times \sqrt{4\delta\lambda^{2n}\left(\frac{(\beta\gamma\rho^n + \lambda^{-n})^2}{4\delta} + (y_0\lambda^{-n} - \gamma\rho^n x_0) - \mu\right)}, \tag{32.1.27}$$

the eigenvalues associated with the linearized map are, for n sufficiently large, approximately given by

$$\chi_1 \approx 1 + \sqrt{4\delta\lambda^{2n}\left(\frac{(\gamma\beta\rho^n + \lambda^{-n})^2}{4\delta} + (y_0\lambda^{-n} - \gamma x_0\rho^n) - \mu\right)},$$
$$\chi_2 \approx 0. \tag{32.1.28}$$

Hence, for

$$\mu < \frac{(\gamma\beta\rho^n + \lambda^{-n})^2}{4\delta} + (y_0\lambda^{-n} - \gamma x_0\rho^n) \tag{32.1.29}$$

(which, from (32.1.18), is the saddle-node bifurcation value), it is easy to see that this fixed point is always a *saddle.* Similarly, for the branch of fixed points given by

$$y = \frac{\beta\gamma\lambda^n\rho^n + 2\delta\lambda^n y_0 + 1}{2\delta\lambda^n} - \frac{1}{2\delta\lambda^n}\sqrt{4\delta\lambda^n\left(\frac{(\beta\gamma\rho^n + \lambda^{-n})^2}{4\delta} + (y_0\lambda^{-n} - \gamma\rho^n x_0) - \mu\right)}, \tag{32.1.30}$$

the eigenvalues associated with the linearized map are, for n sufficiently large, approximately given by

$$\chi_1 \approx 1 - \sqrt{4\delta\lambda^{2n}\left(\frac{(\beta\gamma\rho^n + \lambda^{-n})^2}{4\delta} + (y_0\lambda^{-n} - \gamma\rho^n x_0) - \mu\right)},$$
$$\chi_2 \approx 0. \tag{32.1.31}$$

Therefore, for μ "slightly" less than $\frac{(\beta\gamma\rho^n + \lambda^{-n})^2}{4\delta} + (y_0\lambda^{-n} - \gamma\rho^n x_0)$, it is easy to see that this fixed point is a *sink.* However, as μ decreases further, it is possible for χ_1 to decrease through -1 and, consequently, for this branch of fixed points to undergo a period-doubling bifurcation. We now want to study this possibility.

We are considering the branch of fixed points with y coordinate given by

$$y = \frac{\beta\gamma\lambda^n\rho^n + 2\delta\lambda^n y_0 + 1}{2\delta\lambda^n} - \frac{1}{2\delta\lambda^n} \times\sqrt{4\delta\lambda^{2n}\left(\frac{(\beta\gamma\rho^n + \lambda^{-n})^2}{4\delta} + (y_0\lambda^{-n} - \gamma\rho^n x_0) - \mu\right)}. \tag{32.1.32}$$

From (32.1.22), the condition for an eigenvalue of Df^{n+k} to be -1 is

$$1 + \det Df^{n+k} = -\mathrm{tr}\, Df^{n+k}. \tag{32.1.33}$$

Substituting (32.1.20) and (32.1.21) into (32.1.33) yields

$$1 + \gamma\beta\rho^n\lambda^n = 2\delta\lambda^n y_0 - 2\delta\lambda^n y, \tag{32.1.34}$$

and substituting (32.1.32) into (32.1.34) yields

$$1 + \gamma\beta\rho^n\lambda^n = \sqrt{\delta\lambda^{2n}\left(\frac{(\beta\gamma\rho^n + \lambda^{-n})^2}{4\delta} + (y_0\lambda^{-n} - \gamma\rho^n x_0) - \mu\right)}. \tag{32.1.35}$$

By solving (32.1.35) for μ, we obtain

$$\mu = -\frac{3}{4\delta}(\gamma\beta\rho^n + \lambda^{-n})^2 + (y_0\lambda^{-n} - \gamma\rho^n x_0). \tag{32.1.36}$$

Hence, (32.1.36) is the bifurcation value for the period-doubling bifurcation of the sink created in the saddle-node bifurcation. We leave it as an exercise for the reader to verify that the period-doubling bifurcation is "generic" (see Exercise 2).

Let us summarize what we have shown thus far. The map f^{n+k}, for n sufficiently large, undergoes a *saddle-node* bifurcation at

$$\mu_{SN}^{n+k} = \frac{(\beta\gamma\rho^n + \lambda^{-n})^2}{4\delta} + (y_0\lambda^{-n} - \gamma\rho^n x_0). \tag{32.1.37}$$

In this bifurcation two fixed points of f^{n+k} are created, a saddle and a sink. As μ decreases below μ_{SN}^{n+k}, the saddle remains a saddle but the sink undergoes a period-doubling bifurcation at

$$\mu_{PD}^{n+k} = -\frac{3(\beta\gamma\rho^n + \lambda^{-n})^2}{4\delta} + (y_0\lambda^{-n} - \gamma\rho^n x_0). \tag{32.1.38}$$

It is easy to see from (32.1.37) and (32.1.38) that we have

$$\mu_{PD}^{n+k} < \mu_{SN}^{n+k}.$$

Also, for n sufficiently large, we have

$$y_0\lambda^{-n} - \gamma\rho^n x_0 >> (\beta\gamma\rho^n + \lambda^{-n})^2. \tag{32.1.39}$$

Using (32.1.39) along with the fact that

$$(y_0\lambda^{-n} - \gamma\rho^n x_0) = \lambda^{-n}(y_0 - \gamma\rho^n\lambda^n x_0) \tag{32.1.40}$$

with $\rho\lambda < 1$ implies that

$$\mu_{SN}^{n+k} > 0$$

and

$$\mu_{PD}^{n+k} > 0$$

for n sufficiently large. Next we need to show that

$$\mu_{SN}^{n+1+k} < \mu_{PD}^{n+k}.$$

From (32.1.37) and (32.1.38), we have

$$\mu_{SN}^{n+1+k} = \frac{(\beta\gamma\rho^{n+1} - \lambda^{-n-1})^2}{4\delta} + \lambda^{-n-1}(y_0 - \gamma\rho^{n+1}\lambda^{-n-1}x_0) \tag{32.1.41}$$

and

$$\mu_{PD}^{n+k} = -\frac{3(\beta\gamma\rho^n - \lambda^{-n})^2}{4\delta} + \lambda^{-n}(y_0 - \gamma\rho^n\lambda^n x_0). \tag{32.1.42}$$

Using (32.1.39) and (32.1.40), along with the fact that $\lambda > 1$, we can easily see from (32.1.41) and (32.1.42) that, for n sufficiently large, we have

$$\mu_{SN}^{n+1+k} < \mu_{PD}^{n+k}. \tag{32.1.43}$$

Equation (32.1.8) now follows from (32.1.43) by induction. Finally, it follows from (32.1.39), (32.1.37) and (32.1.38) that

$$\mu_{SN}^{n+k} \sim \lambda^{-n} \quad \text{as} \quad n \to \infty$$

and

$$\mu_{PD}^{n+k} \sim \lambda^{-n} \quad \text{as} \quad n \to \infty. \qquad \square$$

Let us now comment on the generality of our results. In particular, in Assumption 2 we assumed that our map is linear in a neighborhood, $\mathcal{N}$, of the origin, and in Assumption 3 we assumed that the form of the map defined outside of a neighborhood of the origin is given as in (32.1.5). It follows from the work of Gavrilov and Silnikov [1972], [1973] that our results are not restricted by these assumptions in the sense that if we assume the most general forms for f in $\mathcal{N}$ and for f^k, Theorems 32.1.1 and 32.1.2 are unchanged. We remark that this generally holds for the study of the orbit structure near orbits homoclinic to hyperbolic periodic points. A return map defined near a homoclinic point constructed as the composition of an iterate of the *linearized map* near the origin with low-order terms in the

Taylor expansion of an iterate of the map outside of a neighborhood of the origin is sufficient to capture the qualitative dynamics in a sufficiently small neighborhood of the homoclinic point. Let us now briefly describe the set-up considered by Gavrilov and Silnikov.

In local coordinates in $\mathcal{N}$, Gavrilov and Silnikov showed that a general $\mathbf{C}^r$ $(r \geq 3)$ diffeomorphism can be written in the form

$$\begin{pmatrix} x \\ y \end{pmatrix} \longmapsto \begin{pmatrix} \lambda(\mu)x + f(x, y; \mu)x \\ \rho(\mu)y + g(x, y; \mu)y \end{pmatrix}. \tag{32.1.44}$$

For the form of f^k acting outside of $\mathcal{N}$ (but mapping a neighborhood of a homoclinic point on the local unstable manifold in $\mathcal{N}$ to a neighborhood of the local stable manifold in $\mathcal{N}$), they assumed the completely general form

$$f^k\colon \begin{pmatrix} x \\ y \end{pmatrix} \longmapsto \begin{pmatrix} x_0 + F(x, y - y_0; \mu) \\ G(x, y - y_0; \mu) \end{pmatrix}. \tag{32.1.45}$$

The assumption of quadratic homoclinic tangency at $\mu = 0$ requires

$$G_y(0, 0, 0) = 0, \tag{32.1.46}$$

$$G_{yy}(0, 0, 0) \neq 0 \tag{32.1.47}$$

(note: since f is a diffeomorphism, then (32.1.46) implies that we must have $G_x(0, 0, 0) \neq 0$ and $F_y(0, 0, 0) \neq 0$). Gavrilov and Silnikov then simplify (32.1.45) as follows; letting

$$y - y_0 = \phi(x, \mu) \tag{32.1.48}$$

be the (unique) solution of

$$G_y(x, y - y_0, \mu) = 0 \tag{32.1.49}$$

(which can be solved by the implicit function theorem as a result of (32.1.47)), (32.1.45) can be rewritten as

$$\begin{pmatrix} x \\ y \end{pmatrix} \longmapsto \begin{pmatrix} x_0 + F(x, y - y_0; \mu) \\ E(\mu) + C(x, \mu)x + D(x, \mu)(y - y_0 - \phi(x, \mu))^2 \end{pmatrix}, \tag{32.1.50}$$

where

$$\begin{aligned} E(\mu) &\equiv G(0, \phi(0, \mu), \mu), \quad E(0) = 0, \\ C(0, 0) &\equiv c, \\ 2D(0, y_0, 0) &\equiv d. \end{aligned}$$

The reader should note the similarity of (32.1.50) and (32.1.5). The numbers c and d in (32.1.50) describe the geometry of the tangency of the stable

and unstable manifolds. Gavrilov and Silnikov show that there are ten cases to consider depending on the signs of λ, ρ, c, and d. (Note: yes, there are 16 possible combinations of signs of these parameters, but Gavrilov and Silnikov show how to reduce the number of possibilities.)

Five of the cases correspond to orientation-preserving maps with the remaining five corresponding to orientation-reversing maps. The example we treated corresponds to one of the five orientation-preserving maps with λ, ρ, $c, d > 0$. The structure of the period-doubling and saddle-node cascades can be different for the remaining cases, and we refer the reader to Gavrilov and Silnikov [1972], [1973] for the details.

32.2 Newhouse Sinks in Dissipative Systems

The following corollary is an obvious consequence of the proof of Theorem 32.1.2.

Corollary 32.2.1 *Let p_0 denote a point of quadratic tangency of $W_0^s(0)$ and $W_0^u(0)$. Then for all n sufficiently large there is a parameter value, μ^{n+k}, with $\mu^{n+k} \to 0$ as $n \to \infty$, such that f has a periodic sink, p_n, of period $n + k$ with $p_n \to p_0$ as $n \to \infty$.*

The reason for pulling out this corollary from Theorem 32.1.2 is that if we put it together with some deep results of Newhouse concerning the persistence of quadratic homoclinic tangencies, we get a very provocative result. (Note: Newhouse's results do not require our more restrictive Assumptions 3 and 4 given above but, rather, they apply to any two-dimensional diffeomorphism having a *dissipative* hyperbolic periodic point whose stable and unstable manifolds have a quadratic tangency.) We now want to give a brief description of the implications of Newhouse's results in the context of this section.

It should be clear that a specific point of tangency of $W_0^s(0)$ and $W_0^u(0)$ can easily be destroyed by the slightest perturbation. However, Newhouse [1974] has proven the following result.

Theorem 32.2.2 *For $\varepsilon > 0$, let $I_\varepsilon = \{\mu \in I \,|\, |\mu| < \varepsilon\}$. Then, for every $\varepsilon > 0$, there exists a nontrivial interval $\hat{I}_\varepsilon \subset I_\varepsilon$ such that $\hat{I}_\varepsilon$ contains a dense set of points at which $W_\mu^s(0)$ and $W_\mu^u(0)$ have a quadratic homoclinic tangency.*

Proof: This "parametrized" version of Newhouse's theorem is due to Robinson [1983]. □

Heuristically, Theorem 32.2.2 says that if we destroy the quadratic homoclinic tangency at $\mu = 0$ by varying μ slightly, then for a dense set of parameter values containing $\mu = 0$, we have a quadratic homoclinic tangency somewhere else in the homoclinic tangle. Thus, Corollary 32.2.1 can be applied to each of these tangencies so that Corollary 32.2.1 and Theorem 32.2.2 together imply that there are parameter values at which the map has infinitely many periodic attractors which coexist with Smale horseshoe–type dynamics. This phenomenon is at the heart of the difficulties encountered in proving that a two-dimensional map possesses a "strange attractor." We will discuss this in much more detail in Chapter 30.

We close with some final remarks.

Remark 1: For higher dimensional generalizations of the Newhouse sink phenomenon see Palis and Viana [1994].

Remark 2: The Codimension of a Homoclinic Bifurcation. By the term "homoclinic bifurcation," we mean the creation of transverse homoclinic orbits to a hyperbolic periodic point of a two-dimensional diffeomorphism as parameters are varied. Since the stable and unstable manifolds of the hyperbolic periodic point are codimension one, their transversal intersection occurs stably in a one-parameter family of maps. Now recall the definition of "codimension of a bifurcation" given in Chapter 20. Roughly speaking, the codimension is the number of parameters in which the corresponding parametrized family is stable under perturbations. We have seen in this section that there is an infinity of saddle-node and period-doubling bifurcation values accumulating on the quadratic homoclinic tangency parameter value. Thus the type of bifurcation is codimension infinity by the standard definitions. In particular, one cannot find a versal deformation for this type of bifurcation satisfying the standard definitions given in Chapter 20.

Remark 3. There have been a number of papers by the Maryland group over the last few years that have shed much light on the creation of horseshoes. In particular, we refer the reader to Yorke and Alligood [1985] and Alligood et al. [1987]. In Tedeschini-Lalli and Yorke [1986] the question of the measure of the set of parameter values for which the map possesses an infinite number of coexisting periodic sinks is addressed. For a "generic" map, the measure of the set is shown to be zero.

Remark 4. For additional recent work on the dynamical consequences associated with homoclinic tangencies see Diaz et al. [1999], Diaz and Rocha [1997a, b], Diaz [1995] and Diaz and Ures [1994].

32.3 Islands of Stability in Conservative Systems

There is a conservative analog of the Newhouse sink phenomenon. Early results along these lines are due to Newhouse [1977]. An analysis similar in spirit to the Gavrilov and Silnikov work described in this chapter is given in Gonchenko and Silnikov [2000]. See also Duarte [1999].

32.4 Exercises

1. Prove Theorem 32.1.1. (*Hints:* the idea is to find a region S_n in U_{y_0} such that Assumptions 1 and 3 of Chapter 25 hold for f^{n+k}. 1) Let $S_n = \{(x, y) \mid |y - y_0| \leq \varepsilon, 0 \leq x \leq \nu^n\}$ where $\rho < \nu < \frac{1}{\lambda}$. The idea is to show that $f^{n+k}(S_n; 0)$ intersects S_n in two μ_v-vertical strips. Then the pre-image of these two μ_v-vertical strips will be μ_h-horizontal strips with proper boundary behavior and $0 \leq \mu_h \mu_v < 1$. This can be accomplished in several steps. First show that under $f^k(\cdot; 0)$, vertical lines in S_n (i.e., lines with $x = c$ = constant) map to parabolas in U_{x_0} given by the graph of $y = \gamma c + \frac{\delta}{\beta^2}(x - x_0)^2$. 2) Show that for n sufficiently large, the x-components of points in $f^{n+k}(\cdot; \mu)$ are smaller than ν^n. 3) Finally, show that for $\varepsilon = \varepsilon(n) \sim (y_0 \lambda^{-n}/\delta)^{1/2}$, $f^{n+k}(S_n; 0)$ cuts through the top and bottom horizontal boundaries of S_n. From these three facts you should be able to find μ_h-horizontal and μ_v-vertical strips so that Assumption 1 is satisfied.

   The proof that Assumption 3 holds is very similar to the same step carried out in Theorem 26.0.5. Use the fact that

$$Df^{n+k}(x, y; 0) = \begin{pmatrix} 0 & -\beta\rho^n \\ \gamma\lambda^n & 2\delta\lambda^n(y - y_0) \end{pmatrix}$$

   and that, for $|y - y_0| \sim (y_0 \lambda^{-n}/\delta)^{1/2}$ and n sufficiently large, this Jacobian is essentially

$$Df^{n+k}(x, y; 0) \sim \begin{pmatrix} 0 & 0 \\ \gamma\lambda^n & 2(y_0 \delta \lambda^n)^{1/2} \end{pmatrix}.$$

   (Drawing figures in each case should help.)

2. Recall the proof of Theorem 32.1.2. In showing that the sink created in the saddle-node bifurcation of f^{n+k} subsequently underwent a period-doubling bifurcation at

$$\mu = -\frac{3}{4\delta}(\gamma\beta\rho^n + \lambda^{-n})^2 + (y_0\lambda^{-n} - \gamma\rho^n x_0),$$

   we only showed that the map had an eigenvalue of -1 at this parameter value. Examine the nonlinear terms (possibly do a center manifold reduction) to show that this period-doubling bifurcation is indeed nondegenerate or "generic."

3. Show that Theorem 32.1.2 holds for area-preserving maps. (*Hint:* use the implicit function theorem proof given in Tedeschini-Lalli and Yorke [1986].)

4. Does the result of Theorem 32.1.1 hold for area-preserving maps?

33

Global Bifurcations Arising from Local Codimension—Two Bifurcations

In Section 20.6 we studied the bifurcation of a fixed point of a vector field in the situation where the matrix associated with the linearization of the vector field at the bifurcation point had two zero eigenvalues, and in Section 20.7 we studied the situation where the matrix had a zero and a pure imaginary pair of eigenvalues (with any remaining eigenvalues having nonzero real part). In both cases we saw that dynamical phenomena arose which could not be explained by any local bifurcation analysis, and in this section we want to attempt to complete the analysis. In the case of the double-zero eigenvalue we will succeed completely. In the case of the zero-pure imaginary pair we will only achieve partial success. We begin with the double-zero eigenvalue.

33.1 The Double-Zero Eigenvalue

Recall from Section 20.6 that the truncated normal form associated with this bifurcation is given by

$$\begin{aligned} \dot{x} &= y, \\ \dot{y} &= \mu_1 + \mu_2 y + x^2 + bxy, \qquad b = \pm 1. \end{aligned} \tag{33.1.1}$$

Equation (33.1.1) applies to generic vector fields, i.e., there are no symmetries and we treat the case $b = +1$.

Recall that (33.1.1) has no periodic orbits for $\mu_1 > 0$ and, for $\mu_1 < 0$, periodic orbits are created in a Poincaré-Andronov-Hopf bifurcation. Therefore, there must be some other bifurcation occurring which accounts for the destruction of the periodic orbits as μ_1 increases through zero. In Section 20.6 we gave some heuristic arguments as to why this should be

a *homoclinic or saddle-connection* bifurcation, and now we want to prove this.

We begin by rescaling the dependent variables and parameters of (33.1.1) as follows

$$x = \varepsilon^2 u, \quad y = \varepsilon^3 v, \quad \mu_1 = -\varepsilon^4, \quad \mu_2 = \varepsilon^2 \nu_2 \quad (\varepsilon > 0), \tag{33.1.2}$$

and we rescale the independent variable time as follows

$$t \longrightarrow \frac{t}{\varepsilon},$$

so that (33.1.1) becomes

$$\begin{aligned} \dot{u} &= v, \\ \dot{v} &= -1 + u^2 + \varepsilon(\nu_2 v + uv). \end{aligned} \tag{33.1.3}$$

Notice that, in the original variables, we are interested in $\mu_1 < 0$ and that our rescaling allows us to interpret our results in this parameter regime. (Note: the reader should be somewhat irritated that we have simply pulled this particular rescaling "out of the air." For now, we will proceed with the analysis, but at the end of this section we will discuss "why it works.")

The single most important characteristic of this rescaling is that, for $\varepsilon = 0$, the rescaled equations (33.1.3) become a completely integrable Hamiltonian system with Hamiltonian function given by

$$H(u, v) = \frac{v^2}{2} + u - \frac{u^3}{3}. \tag{33.1.4}$$

Melnikov's method can then be used to perform a global analysis that includes the effects of the higher order terms of the normal form. The phase space of this completely integrable Hamiltonian system is shown in Figure 33.1.1. Thus, the vector field

$$\begin{aligned} \dot{u} &= v, \\ \dot{v} &= -1 + u^2, \end{aligned} \tag{33.1.5}$$

has a hyperbolic fixed point at

$$(u, v) = (1, 0),$$

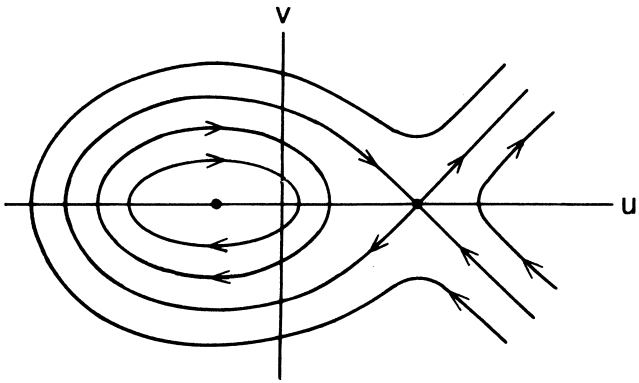

FIGURE 33.1.1.

an elliptic fixed point at

$$(u, v) = (-1, 0),$$

and a one-parameter family of periodic orbits surrounding the elliptic fixed point. We denote the latter by

$$(u^\alpha(t), v^\alpha(t)), \qquad \alpha \in [-1, 0) \tag{33.1.6}$$

with period T^α where

$$(u^{-1}(t), v^{-1}(t)) = (-1, 0) \tag{33.1.7}$$

and

$$\begin{aligned} \lim_{\alpha \to 0} (u^\alpha(t), v^\alpha(t)) &= (u_0(t), v_0(t)) \\ &= \left(1 - 3\text{sech}^2 \frac{t}{\sqrt{2}}, 3\sqrt{2}\text{sech}^2 \frac{t}{\sqrt{2}} \tanh \frac{t}{\sqrt{2}}\right) \end{aligned} \tag{33.1.8}$$

is a homoclinic orbit connecting the hyperbolic fixed point to itself.

The Melnikov theory can now be used to determine the effect of the $\mathcal{O}(\varepsilon)$ part of (33.1.3) on this integrable structure. The homoclinic Melnikov function is given by

$$M(\nu_2) = \int_{-\infty}^{\infty} v_0(t) \big[\nu_2 v_0(t) + u_0(t) v_0(t)\big] dt. \tag{33.1.9}$$

Using the expression for $u_0(t)$ and $v_0(t)$ given in (33.1.8), (33.1.9) becomes

$$M(\nu_2) = 7\nu_2 - 5$$

or

$$M(\nu_2) = 0 \Rightarrow \nu_2 = \frac{5}{7}; \tag{33.1.10}$$

hence, a bifurcation curve on which the stable and unstable manifolds of the hyperbolic fixed point coincide is given by

$$\nu_2 = \frac{5}{7} + \mathcal{O}(\varepsilon). \tag{33.1.11}$$

We now want to translate (33.1.11) back into our original parameter values. Using (33.1.2) and (33.1.11), we obtain

$$\mu_1 = -\left(\frac{49}{25}\right)\mu_2^2 + \mathcal{O}(\mu_2^{5/2}) \tag{33.1.12}$$

for the homoclinic bifurcation curve. Note that we have

$$M > 0 \qquad \text{for} \quad \mu_1 > -\frac{49}{25}\mu_2^2, \tag{33.1.13}$$

and

$$M < 0 \qquad \text{for} \quad \mu_1 < -\frac{49}{25}\mu_2^2, \tag{33.1.14}$$

which give us the relative orientations of the stable and unstable manifolds of the hyperbolic fixed points that we show in Figure 33.1.2.

Thus, we have shown the existence of a global mechanism for periodic orbits to be created and destroyed. Can we now actually claim that the periodic orbit created in the Poincaré–Andronov–Hopf bifurcation is the one that is destroyed in the homoclinic bifurcation? No, we cannot, because it is possible for nonlocal saddle-node bifurcations of periodic orbits to occur in the parameter region between the Poincaré–Andronov–Hopf and homoclinic bifurcation curves. We can check whether or not such bifurcations occur by computing the Melnikov function for the periodic orbits. This is given by

$$M(\alpha;\nu_2) = \nu_2 \int_0^{T^\alpha} (v^\alpha(t))^2 dt + \int_0^{T^\alpha} u^\alpha(t)(v^\alpha(t))^2 dt. \tag{33.1.15}$$

The condition $M(\alpha;\nu_2) = 0$ implies the existence of a periodic orbit for (33.1.3). Using (33.1.15), this is equivalent to

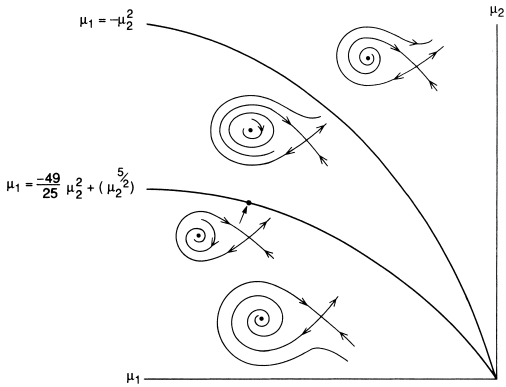

FIGURE 33.1.2.

$$\nu_2 = \frac{\int_0^{T^\alpha} u^\alpha(t)(v^\alpha(t))^2 dt}{\int_0^{T^\alpha} (v^\alpha(t))^2 dt} \equiv f(\alpha). \tag{33.1.16}$$

Now, if $f(\alpha)$ is a monotone function on $[-1, 0]$, we can conclude that (33.1.3) has a unique periodic orbit created in a Poincaré–Andronov–Hopf bifurcation and destroyed in a homoclinic bifurcation. It turns out that $f(\alpha)$ is indeed monotone. This can be verified by computing the expressions for $(u^\alpha(t), v^\alpha(t))$ directly in terms of elliptic functions and then analytically evaluating $f(\alpha)$ from (33.1.16). Once this is done, monotonicity properties of $f(\alpha)$ may be studied. This is a fairly messy (but, in principle, straightforward) calculation that we leave as an exercise for the interested reader. We note that this result was obtained by Bogdanov [1975], Takens [1974], and Carr [1981]. Therefore, the complete bifurcation diagram for (33.1.1) with $b = +1$ is as shown in Figure 33.1.3 and we end with the following remarks.

Remark 1. The local bifurcation analysis of (33.1.1) did not require any smallness restrictions on μ_1 and μ_2. The global bifurcation analysis does require μ_1 and μ_2 to be "sufficiently small."

Remark 2. It is now fairly easy to show that restoring the higher order terms in the normal form (33.1.1) does not qualitatively affect the bifurcation diagram. We will outline the necessary arguments in Exercise 2.

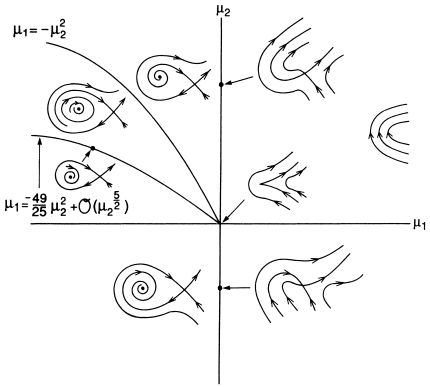

FIGURE 33.1.3.

33.2 A Zero and a Pure Imaginary Pair of Eigenvalues

The normal form associated with this bifurcation is three-dimensional. However, the symmetry in the linear part associated with the pure imaginary eigenvalues enabled us to decouple one of the coordinates from the remaining two so that we could begin our analysis using phase plane techniques. In some sense, the dynamics in this phase plane can be viewed as an approximation to a Poincaré map of the full three-dimensional normal form. This is also a result of the symmetry of the linear part. Our analysis will proceed in the following steps.

Step 1. Analyze global bifurcations of the associate truncated, two-dimensional normal form.

Step 2. Interpret in terms of the truncated, three-dimensional normal form.

Step 3. Discuss the effects of higher order terms in the normal form.

Step 1. Recall from Section 20.7 that the associated two-dimensional normal form of interest is given by

$$\begin{aligned} \dot{r} &= \mu_1 r + arz, \\ \dot{z} &= \mu_2 + br^2 - z^2, \end{aligned} \tag{33.2.1}$$

where $a \neq 0$ and $b = \pm 1$. There were essentially only four distinct cases to study, and only two admitted the possibility of global bifurcations (for r, z small). They were denoted by

$$\begin{array}{ll} \text{Case IIa,b} & a < 0, b = +1, \\ \text{Case III} & a > 0, b = -1. \end{array}$$

In Case IIa,b we are interested in the dynamics near the μ_2-axis for $\mu_2 < 0$. In Case III we are interested in the dynamics near the μ_2-axis for $\mu_2 > 0$. In both cases the normal form was integrable on the μ_2-axis (with the appropriate sign of μ_2); thus, we would expect higher order terms in the normal form to drastically affect the dynamics in this parameter regime. Our strategy will be to include the cubic terms in the normal form and to introduce a scaling of the variables so that we obtain a perturbed Hamiltonian system. Then a Melnikov-type analysis can be used to determine the number of periodic orbits and possible homoclinic bifurcations.

From (20.4.44), restoring the cubic terms to (33.2.1) gives

$$\begin{aligned} \dot{r} &= \mu_1 r + arz + (cr^3 + dr^2 z), \\ \dot{z} &= \mu_2 + br^2 - z^2 + (er^2 z + fz^3). \end{aligned} \tag{33.2.2}$$

In Guckenheimer and Holmes [1983] it is shown that coordinate changes can be introduced so that all cubic terms except for z^3 in (33.2.2) can be eliminated (see Exercise 3 where we outline this procedure). Hence, without loss of generality, we can analyze the following normal form

$$\begin{aligned} \dot{r} &= \mu_1 r + arz, \\ \dot{z} &= \mu_2 + br^2 - z^2 + fz^3. \end{aligned} \tag{33.2.3}$$

We next rescale the dependent variables and parameters as follows

$$r = \varepsilon u, \quad z = \varepsilon v, \quad \mu_1 = \varepsilon^2 \nu_1, \quad \mu_2 = \varepsilon^2 \nu_2, \tag{33.2.4}$$

and we rescale time as follows

$$t \longrightarrow \varepsilon t,$$

so that (33.2.2) becomes

$$\begin{aligned} \dot{u} &= auv + \varepsilon \nu_1 u, \\ \dot{v} &= \nu_2 + bu^2 - v^2 + \varepsilon f v^3. \end{aligned} \tag{33.2.5}$$

At $\varepsilon = 0$, the vector field has the first integral (for $a \neq 1$)

$$F(u, v) = \frac{a}{2} u^{2/a} \left[\nu_2 + \frac{b}{1+a} u^2 - v^2 \right]. \tag{33.2.6}$$

Unfortunately, it is not Hamiltonian, but can be made Hamiltonian (Guckenheimer and Holmes [1983]) by multiplying the right-hand side of (33.2.5) by the integrating factor $u^{(2/a)-1}$ to obtain

$$\begin{aligned}\dot{u} &= au^{2/a}v + \varepsilon\nu_1 u^{2/a},\\ \dot{v} &= -bu^{(2/a)-1} + bu^{(2/a)+1} - u^{(2/a)-1}v^2 + \varepsilon f u^{(2/a)-1}v^3,\end{aligned} \tag{33.2.7}$$

where we let $\nu_2 = \mp 1$ when $b = \pm 1$ since, for Case IIa,b, we are interested in $\mu_2 < 0$ and, for Case III, we are interested in $\mu_2 > 0$. For $\varepsilon = 0$, (33.2.7) is Hamiltonian with Hamiltonian function

$$H(u,v) = \frac{1}{2}u^{2/a}v^2 + \frac{ab}{2}u^{2/a} - \frac{ab}{2(a+1)}u^{(2/a)+2}, \qquad a+1 \neq 0$$

or

$$H(u,v) = -\frac{1}{2}u^{-2}v^2 - \frac{b}{2}u^{-2} - b\log u, \qquad a+1 = 0. \tag{33.2.8}$$

In Figure 33.2.1 we show the level sets of the Hamiltonian (i.e., the orbits of (33.2.7) for $\varepsilon = 0$) for the relevant cases. We see from this figure that, for Case IIa,b, the integrable Hamiltonian system has a one-parameter family of periodic orbits surrounding an elliptic fixed point with the orbits becoming unbounded in amplitude. In Case III the integrable Hamiltonian system has a one-parameter family of periodic orbits surrounding an elliptic fixed point that limit on a heteroclinic cycle. In both cases we denote the one-parameter family of orbits by

$$(u^\alpha(t), v^\alpha(t)), \qquad \alpha \in [-1, 0),$$

with period T^α, where $(u^{-1}(t), v^{-1}(t))$ is an elliptic fixed point in both Case IIa,b and Case III, and $\lim_{\alpha\to 0}(u^\alpha(t), v^\alpha(t))$ is an unbounded periodic orbit in Case IIa,b and a heteroclinic cycle in Case III.

The Melnikov functions are given by

$$\begin{aligned}&M(\alpha;\nu_1)\\ &= af\int_0^{T^\alpha} (u^\alpha(t))^{(4/a)-1}(v^\alpha(t))^4 dt\\ &- \nu_1\int_0^{T^\alpha} \big[b(u^\alpha(t))^{(4/a)+1} - b(u^\alpha(t))^{(4/a)-1}\\ &+ (u^\alpha(t))^{(4/a)-1}(v^\alpha(t))^2\big]dt.\end{aligned} \tag{33.2.9}$$

Therefore, $M(\alpha;\nu_1) = 0$ is equivalent to

$$\nu_1 = \frac{af\int_0^{T^\alpha}(u^\alpha(t))^{(4/a)-1}(v^\alpha(t))^4 dt}{\int_0^{T^\alpha}[b(u^\alpha(t))^{(4/a)+1} - b(u^\alpha(t))^{(4/a)-1} + (u^\alpha(t))^{(4/a)-1}(v^\alpha(t))^2]dt}$$
$$\equiv f(\alpha). \tag{33.2.10}$$

We are interested in

Case IIa,b	$a < 0, b = 1, f \neq 0, \nu_1 < 0,$
Case III	$a > 0, b = -1, f \neq 0, \nu_1 > 0.$

Thus, if $f(\alpha)$ is a monotone function of α (for a, b, and f fixed as above), then (33.2.7) has a unique periodic orbit which is born in a Poincaré-Andronov-Hopf bifurcation (we consider stability in Exercise 4) and grows monotonically in amplitude in Case IIa,b and disappears in a heteroclinic bifurcation in Case III. However, proof that (33.2.10) is monotonic in α is a formidable and difficult problem, since the integrals cannot be evaluated explicitly in terms of elementary integrals. Fortunately, it has recently

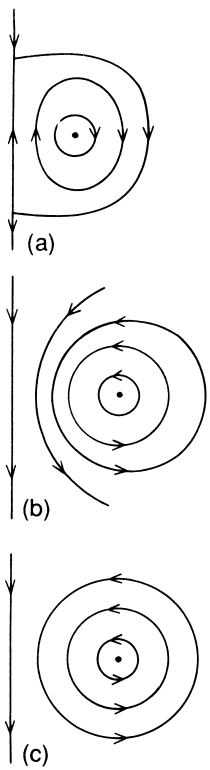

FIGURE 33.2.1. Integrable structure of (4.9.22) for $\varepsilon = 0$. a) Case III; b) Case IIa,b, $-1 < a < 0$; c) Case IIa,b, $a \leq -1$.

been proven by Zoladek [1984], [1987] (see also Carr et al. [1985], van Gils [1985] and Chow et al. [1989]) that (33.2.10) is indeed monotone in α. The techniques in these papers for proving monotonicity involve complicated estimates that we will not go into here. In Figure 33.2.2 we show an example of a possible bifurcation for Case III with $a = 2$, $f < 0$.

Step 2. We now turn to Step 2, interpreting the dynamics of the two-dimensional vector field in terms of the three-dimensional dynamics. The truncated, three-dimensional normal form is given by

$$\begin{aligned} \dot{r} &= \mu_1 r + arz, \\ \dot{z} &= \mu_2 + br^2 - z^2 + fz^3, \\ \dot{\theta} &= \omega + \cdots . \end{aligned} \tag{33.2.11}$$

Thus, the r and z components of (33.2.11) are independent of θ, and the discussion in Section 20.7 still holds. Namely, it is the case that the periodic orbits become invariant two tori in the full three-dimensional phase space and, in Case III, the heteroclinic cycle becomes such that the two-dimensional stable manifold and one-dimensional unstable manifold of the hyperbolic fixed point with $z < 0$ coincides with the two-dimensional unstable manifold and one-dimensional stable manifold of the hyperbolic fixed point with $z > 0$ creating the invariant sphere (with invariant axis), as shown in Figure 33.2.3. Both situations are radically altered by the addition of the higher order terms in the normal form and we now turn to a

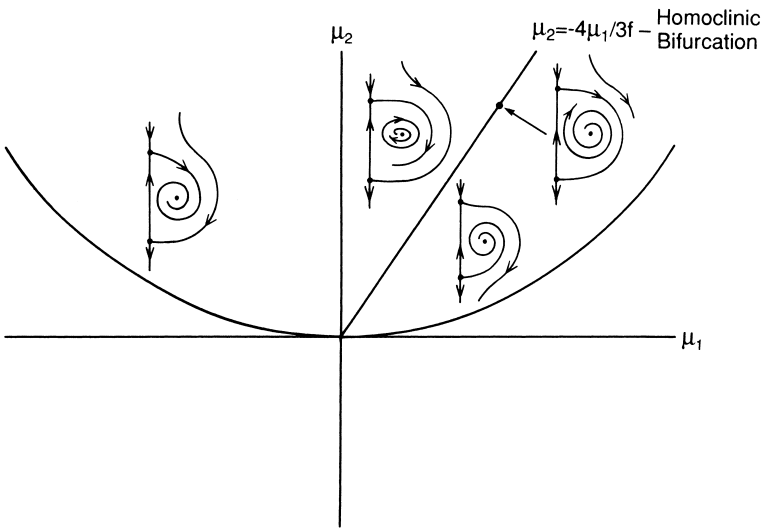

FIGURE 33.2.2.

discussion of this situation in Step 3.

Step 3. The problem of how the invariant two-tori of the truncated normal form in Cases IIa,b and III and the heteroclinic cycle in Case III are affected by the higher order terms of the normal form is difficult, and the full story is not yet known. We will briefly summarize the main issues and known results.

Invariant Two-Tori

Concerning the invariant two-tori of the truncated normal form in Cases IIa,b and Case III there are two main questions that arise.

1. Do the two-tori persist when the effects of the higher order terms of the normal form are considered?
2. In the truncated normal form the orbits on the invariant two-tori are either periodic or quasiperiodic, densely covering the torus. Do invariant two-tori having quasiperiodic flow persist when the effects of the higher order terms of the normal form are considered?

In answering the first question techniques from the persistence theory of normally hyperbolic invariant manifolds are used (see, e.g., Fenichel [1971], [1979], [1977], Hirsch, Pugh, and Shub [1977], and Wiggins [1994]). The application of these techniques is not straightforward, since the strength of the normal hyperbolicity depends on the bifurcation parameter. Results

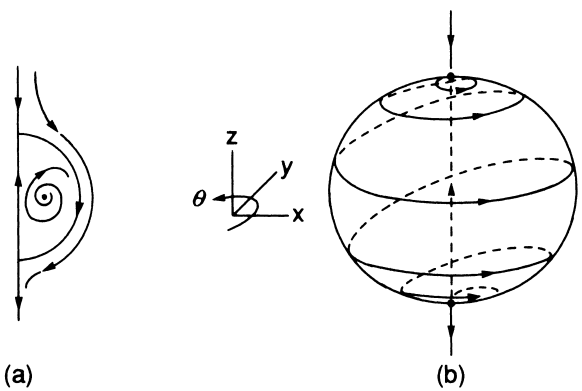

FIGURE 33.2.3. a) Cross-section of the heteroclinic cycle for the truncated normal form. b) Heteroclinic cycle for the truncated normal form.

showing that invariant two-tori persist have been obtained by Iooss and Langford [1980] and Scheurle and Marsden [1984].

In answering the second question small divisor problems arise which necessitate the use of KAM-type techniques (see, e.g., Siegel and Moser [1971]). This is very much beyond the scope of this book. However, we mention that some results along these lines have been obtained by Scheurle and Marsden [1984]. Their results imply that on a Cantor set of parameter values having positive Lebesgue measure one has invariant two-tori having quasiperiodic flow. Many of these issues are discussed in the section on circle maps in Section 21.6.

Heteroclinic Cycle

In Case III the truncated normal form has two saddle-type fixed points on the z axis; p_1 having a two-dimensional stable manifold and a one-dimensional unstable manifold and p_2 having a two-dimensional unstable manifold and a one-dimensional stable manifold with $W^s(p_1)$ coinciding with $W^u(p_2)$ to form the invariant sphere as shown in Figure 33.2.3. The axis of the sphere is formed from the coincidence of a branch of $W^u(p_1)$ with a branch of $W^s(p_2)$.

We expect the effects of the higher order terms of the normal form to drastically alter this situation. Generically, we would expect the one-dimensional unstable manifold of p_1 and the one-dimensional stable manifold of p_2 to *not* intersect in the three-dimensional phase space. Similarly, generically we would expect the two-dimensional stable manifold of p_2 and the two-dimensional unstable manifold of p_1 to intersect along one-dimensional orbits in three-dimensional phase space. We illustrate these two solutions in Figure 33.2.4.

Now it may happen that when this degenerate structure is broken the branch of $W^u(p_1)$ inside the sphere falls into $W^s(p_1)$, or, similarly, the branch of $W^s(p_2)$ inside the sphere falls into $W^u(p_2)$; see Figure 33.2.5.

If this happens, then from Section 27.3 the reader should realize that it is possible for a return map defined near one or the other of these homoclinic orbits to possess a countable infinity of Smale horseshoes, i.e., Silnikov's phenomenon may occur. Moreover, from Section 27.3 a countable infinity of period-doubling and saddle-node bifurcation values would accumulate on the parameter value at which the homoclinic orbit was formed. Thus, this particular local codimension-two bifurcation would actually be codimension-infinity when all of the dynamical effects are included (see the comments at the end of Chapter 32).

The fact that this local codimension-two bifurcation point can exhibit Silnikov's phenomenon in its versal deformation has been proved by Broer and Vegter [1984]. They prove that the full normal form possesses orbits homoclinic to a hyperbolic fixed point. Their result is very delicate in the sense that, due to the rotational symmetry of the linear part of the normal form, the symmetry is preserved to all orders in the normal form (i.e., the r and z components of the normal form are independent of θ). Thus, the homoclinic orbits are a result of exponentially small terms that are not picked up in the Taylor expansion and subsequent normal form transformation of the vector field.

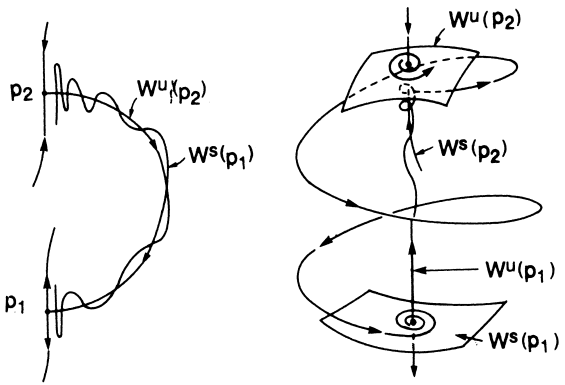

FIGURE 33.2.4. a) Cross-section of the manifolds for the full normal form. b) Homoclinic orbit for the full normal form.

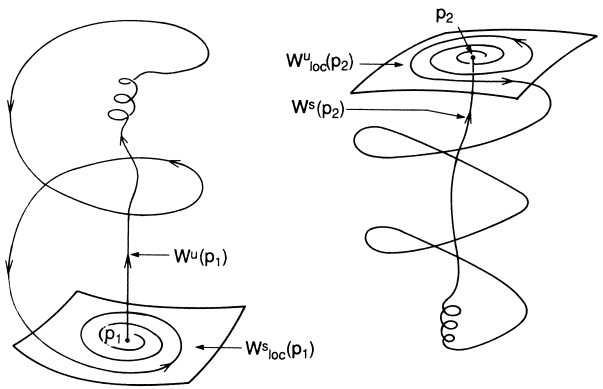

FIGURE 33.2.5. Possible homoclinic orbits for the full normal form.

The Hamiltonian-Dissipative Decomposition

The key aspect that enabled the preceeding analyses to go through was the fact that one could find an "inspired" rescaling that transformed the normal form into a perturbation of an integrable Hamiltonian system with the higher order terms in the normal form part of the perturbation (note: the perturbation need *not* also be Hamiltonian). Once this has been accomplished, a wealth of techniques for the global analysis of nonlinear dynamical systems can then be employed; for example, Melnikov theory, perturbation theory for normally hyperbolic invariant manifolds, and KAM theory. However, the real question is, "in a given problem, how can we find the rescalings which turn the problem into a perturbation of a completely integrable Hamiltonian system?"

The rescalings in this section are due to the cleverness of Takens [1974], Bogdanov [1975], Guckenheimer and Holmes [1983], Kopell and Howard [1975], and Iooss and Langford [1980]. However, in recent years there has been an effort to understand the structure of the normal form that leads to a splitting of the normal form into a Hamiltonian part and a dissipative part so that the appropriate rescalings can be generated by some computational procedure. We refer the reader to Lewis and Marsden [1989] and Olver and Shakiban [1988].

33.3 Exercises

1. Show that the function $f(\alpha)$ defined in (33.1.16) is monotone.

2. Show that the two-parameter family

$$\begin{aligned} \dot{x} &= y, \\ \dot{y} &= \mu_1 + \mu_2 y + x^2 + bxy, \qquad b = \pm 1, \end{aligned} \tag{33.3.1}$$

   is a versal deformation of a fixed point of a planar vector field at which the matrix associated with the linearization has the form

$$\begin{pmatrix} 0 & 1 \\ 0 & 0 \end{pmatrix}.$$

   (*Hint:* the idea is to show that the neglected higher order terms in the normal form do not introduce any qualitatively new dynamics in the sense that the bifurcation diagram in Figure 33.1.3 is unchanged. Begin by considering the fixed points and local bifurcations and show that these are qualitatively unchanged. Next, consider the global behavior, i.e., homoclinic orbits and "large amplitude" periodic orbits. The Melnikov theory can be used here.

   Once all of these results are established, does it then follow that (33.3.1) is a versal deformation?)

3. Recall Exercise 1 following Section 20.6, the double-zero eigenvalue with the symmetry $(x, y) \to (-x, -y)$. The normal form was given by

$$\begin{aligned}\dot{x} &= y,\\ \dot{y} &= \mu_1 x + \mu_2 y + cx^3 - x^2 y, \qquad c = \pm 1.\end{aligned} \tag{33.3.2}$$

In this exercise we want to analyze possible global behavior that might occur.

a) For $c = +1$, using the rescaling

$$x = \varepsilon u, \quad y = \varepsilon^2 v, \quad \mu_1 = -\varepsilon^2, \quad \mu_2 = \varepsilon^2 \nu_2$$

and $t \to \frac{t}{\varepsilon}$, show that (33.3.2) becomes

$$\begin{aligned}\dot{u} &= v,\\ \dot{v} &= -u + u^3 + \varepsilon(\nu_2 v - u^2 v).\end{aligned} \tag{33.3.3}$$

b) Show that (33.3.3) is Hamiltonian for $\varepsilon = 0$ and draw the phase portrait.

c) Use the Melnikov theory to show that (33.3.3) has a heteroclinic connection on

$$\mu_2 = -\frac{\mu_1}{5} + \cdots . \tag{33.3.4}$$

What is the form of the higher order terms in (33.3.4) (i.e., $\mathcal{O}(\mu_1^\alpha)$, where α is some number)? This is important for determining the behavior of the bifurcation curves at the origin.

d) Show that (33.3.3) has a unique periodic orbit for $\mu_1 < 0$ between $\mu_2 = 0$ and $\mu_2 = -\frac{\mu_1}{5} + \cdots$.

e) Draw the complete bifurcation diagram for (33.3.2) with $c = +1$. Is (33.3.2) a versal deformation for $c = +1$?

f) For $c = -1$, using the rescaling

$$x = \varepsilon u, \quad y = \varepsilon^2 v, \quad \mu_1 = \varepsilon^2, \quad \mu_2 = \varepsilon^2 \nu_2,$$

and $t \to \frac{t}{\varepsilon}$, show that (33.3.2) becomes

$$\begin{aligned}\dot{u} &= v,\\ \dot{v} &= u - u^3 + \varepsilon(\nu_2 v - u^2 v).\end{aligned} \tag{33.3.5}$$

g) Show that (33.3.5) is Hamiltonian for $\varepsilon = 0$ and draw the phase portrait.

h) Using the Melnikov theory, show that (33.3.5) undergoes a homoclinic bifurcation on

$$\mu_2 = \frac{4}{5}\mu_1 + \cdots , \tag{33.3.6}$$

and a saddle-node bifurcation of periodic orbits on

$$\mu_2 = c\mu_1 + \cdots , \tag{33.3.7}$$

with $c \approx .752$. Hence, for $\mu_1 > 0$, between $\mu_2 = \mu_1$ and $\mu_2 = \frac{4}{5}\mu_1 + \cdots$, (33.3.2) has three periodic orbits for $c = -1$. What are their stabilities? Between $\mu_2 = \frac{4}{5}\mu_1 + \cdots$ and $\mu_2 = c\mu_1 + \cdots$ (33.3.2) has two periodic orbits for $c = -1$. What are their stabilities? Below $\mu_2 = c\mu_1 + \cdots$ there are no periodic orbits for $c = -1$.

In (33.3.6) and(33.3.7) what is the form of the higher order terms (i.e., $\mathcal{O}(\mu_1^\alpha)$ where α is some number).

1. Draw the complete bifurcation diagram for (33.3.2) with $c = -1$. Is (33.3.2) a versal deformation for $c = -1$?

(*Hint:* the Melnikov theory for autonomous systems is developed in Exercise 11 and the Melnikov theory for heteroclinic orbits is developed in Exercise 16 following Chapter 28.)

4. Show that all the cubic terms, *except* z^3, can be eliminated from (33.2.2) so that it takes the form of (33.2.3). (*Hint:* this result is due to J. Guckenheimer.

   Consider the following coordinate transformation

$$\begin{aligned} s &= r(1+gz), \\ w &= z + hr^2 + iz^2, \\ \tau &= (1+jz)^{-1}t, \end{aligned}$$

   where g, h, i, j are unspecified constants, they will be chosen to make the equations simpler. In these new coordinates (33.2.2) becomes

$$\begin{aligned} \frac{ds}{d\tau} &= \mu_1 s + asw + (c + bg - ah)s^3 + (d - g - ai + aj)sw^2 \\ &\quad + R_s(s, w, \mu_1, \mu_2), \\ \frac{dw}{d\tau} &= \mu_2 + bs^2 - w^2 + (e - 2bg + 2(a+1)h + 2bi + bj)s^2 w \\ &\quad + (f - j)w^3 + R_w(s, w, \mu_1, \mu_2), \end{aligned}$$

   where the remainder terms are $\mathcal{O}(4)$ in s, w, μ_1, μ_2. We will ignore R_s and R_w and choose g, h, i, j so as to make the cubic terms as simple as possible. If we think of the cubic terms as being in a vector space spanned by

$$\begin{pmatrix} s^3 \\ 0 \end{pmatrix}, \begin{pmatrix} sw^2 \\ 0 \end{pmatrix}, \begin{pmatrix} 0 \\ s^2 w \end{pmatrix}, \begin{pmatrix} 0 \\ w^3 \end{pmatrix},$$

   the problem of annihilating the cubic terms reduces to solving the linear problem

$$Ax = \theta,$$

   where

$$x = \begin{pmatrix} g \\ h \\ i \\ j \end{pmatrix}, \qquad \theta = \begin{pmatrix} -c \\ -d \\ -e \\ -f \end{pmatrix},$$

$$A = \begin{pmatrix} b & -a & 0 & 0 \\ -1 & 0 & -a & a \\ -2b & 2a+2 & 2b & b \\ 0 & 0 & 0 & -1 \end{pmatrix}.$$

   It is not hard to show that A has rank 3 and that we can eliminate all cubic terms except $\begin{pmatrix} 0 \\ w^3 \end{pmatrix}$. Thus, since our transformation did not change our equation at $\mathcal{O}(2)$ and below, we can write our normal form in the r, z coordinates as

$$\begin{aligned} \dot{r} &= \mu_1 r + arz, \\ \dot{z} &= \mu_2 + br^2 - z^2 + fz^3 \end{aligned}$$

   (where f can take on all values).)

5. Once the cubic terms have been restored, study the Poincaré–Andronov–Hopf bifurcation in Case IIa,b and Case III.

6. Verify that the homoclinic bifurcation shown in Figure 33.2.2 occurs for $a = 2$, $f < 0$.

7. Suppose that $W^u(p_1)$ falls into $W^s(p_1)$ as shown in Figure 33.2.5. What are the conditions on the normal form in order that the hypotheses of Theorem 27.3.2 hold.

   Suppose $W^s(p_2)$ falls into $W^u(p_2)$ as shown in Figure 33.2.5. Can horseshoes also occur in this case? What conditions must the normal form satisfy?

34

Glossary of Frequently Used Terms

Absorbing set: A positive invariant compact subset $B \subset \mathbb{R}^n$ is called an *absorbing set* if there exists a bounded subset of $\mathbb{R}^n$, U, with $U \supset B$, and:

flows: $t_U > 0$ such that $\phi(t, U) \subset B$, $\forall t \geq t_U$.

maps: $n_U > 0$ such that $g^n(U) \subset B$, $\forall n \geq n_U$.

Action: The functional

$$\int_{t_0}^{t_1} L(q_1, \ldots, q_N, \dot{q}_1, \ldots, \dot{q}_N, t)dt,$$

defined on curves in configuration space (such that the endpoints of each curve are fixed) and where L is the Lagrangian, is referred to as the *action*.

Action-Angle Coordinates, or Variables: These coordinates can be constructed for completely integrable Hamiltonian systems that satisfy the hypotheses of the Liouville-Arnold theorem, and they are denoted by (θ, I), $\theta \in T^n$, $I \in \mathbb{R}^n$. In these coordinates the Hamiltonian is a function of only the action variable, I, i.e., $H = H(I)$, and Hamilton's equations become:

$$\begin{aligned} \dot{\theta} &= \frac{\partial H}{\partial I}, \\ \dot{I} &= -\frac{\partial H}{\partial \theta} = 0. \end{aligned}$$

These equations can be easily integrated to yield the trajectories:

$$\begin{aligned} \theta(t) &= \frac{\partial H}{\partial I}(I_0)t + \theta(0), \\ I(t) &= I_0 = \text{constant}. \end{aligned}$$

Hence, these are the trajectories on the n dimensional tori described by the Liouville-Arnold theorem. $\frac{\partial H}{\partial I}(I_0)$ is referred to as the frequency of the torus $I = I_0$.

Asymptotically Autonomous Vector Field: A vector field $\dot{x} = f(x, t)$, $x \in \mathbb{R}^n$, is said to be *asymptotically autonomous* if $\lim_{t\to\infty} f(x, t) = g(x)$ exists.

Asymptotic Stability: Roughly, a trajectory is said to be *asymptotically stable* if it is Liapunov stable and, at a given time, trajectories starting close enough to the specified trajectory approach the trajectory as time increases.

Attracting Set: Let $\phi(t, x)$ denote the flow generated by a vector field and let $x \mapsto g(x)$ denote a map. A closed invariant set $A \subset \mathbb{R}^n$ is called an *attracting set* if there is some neighborhood U of A such that:

flows: $\forall t \geq 0$, $\quad \phi(t, U) \subset U \quad$ and $\quad \bigcap_{t>0} \phi(t, U) = A$.

maps: $\forall n \geq 0$, $\quad g^n(U) \subset U \quad$ and $\quad \bigcap_{n>0} g^n(U) = A$.

Attractor: An *attractor* is a topologically transitive attracting set.

Autonomous System: A dynamical system that does not depend explicitly on the independent variable (which is often referred to as "time").

Basin of Attraction: Let $\phi(t,x)$ denote the flow generated by a vector field and let $x \mapsto g(x)$ denote a map. The *domain or basin of attraction* of an attracting set A is given by

flows: $\displaystyle\bigcup_{t\leq 0} \phi(t,U),$

maps: $\displaystyle\bigcup_{n\leq 0} g^n(U),$

where U is any trapping region.

Bifurcation of a Fixed Point: A fixed point $(x,\mu) = (0,0)$ of a one-parameter family of one-dimensional vector fields, $\dot{x} = f(x,\mu)$, or maps, $x \mapsto f(x,\mu)$, is said to undergo a *bifurcation* at $\mu = 0$ if the flow for μ near zero and x near zero is *not* qualitatively the same as the flow near $x = 0$ at $\mu = 0$. A necessary, but not sufficient, condition for bifurcation of a fixed point is that the fixed point is non-hyperbolic.

Cantor Set: A compact, totally disconnected, perfect set.

Center Manifold of a Fixed Point: The center manifold of a fixed point is an invariant manifold passing through a fixed point which is tangent to the center subspace at the fixed point, and has the same dimension as the center subspace.

Center Subspace of a Fixed Point: Consider an (autonomous) ordinary differential equation (resp. map) linearized about a fixed point, and the Jacobian matrix associated with this linearization. The center subspace associated with the fixed point is the span of the generalized eigenvectors corresponding to eigenvalues of the Jacobian matrix having zero real part (resp. modulus one). It is an invariant manifold under the linearized dynamics.

Chaotic Invariant Set: A compact set Λ invariant under a flow $\phi(t,x)$ (or map $g(x)$) is said to be *chaotic* if

1. $\phi(t,x)$ (resp. $g(x)$) has sensitive dependence on initial conditions on Λ.
2. $\phi(t,x)$ (resp. $g(x)$) is topologically transitive on Λ.

Cocycle: Let P denote a *parameter space*. Let $\Theta = \{\theta_t \mid t \in \mathbb{R}\}$ denote a one-parameter family of mappings of P into itself, i.e.,

$$\begin{aligned} \theta_t &: P \to P, \\ &p \mapsto \theta_t p, \end{aligned}$$

with

$$\theta_t \circ \theta_s = \theta_{t+s}, \quad \forall t,\ s \in \mathbb{R},$$

and

$$\theta_0 = \mathrm{id}.$$

Then a family of mappings

$$\phi_{t,p} : \mathbb{R}^n \to \mathbb{R}^n, \quad t \in \mathbb{R},\ p \in P,$$

is called a *cocycle on* $\mathbb{R}^n$ *with respect to a group* Θ *of mappings on* P if:

1. $\phi_{0,p} = \mathrm{id}$,
2. $\phi_{t+s,p} = \phi_{t,\theta_s p} \circ \phi_{s,p}$,

for all $t, s \in \mathbb{R}$, $p \in P$.

Codimension of a Submanifold: Let M be an m-dimensional manifold and let N be an n-dimensional submanifold contained in M; then the codimension of N is defined to be $m - n$. Equivalently, in a coordinate setting, the codimension of N is the number of independent equations needed to define N. Thus, the codimension of a submanifold is a measure of the avoidability of the submanifold as one moves about the ambient space; in particular, the codimension of a submanifold N is equal to the minimum dimension of a submanifold $P \subset M$ that intersects N such that the intersection is transversal. This is the definition of codimension in a finite-dimensional setting, which permits some intuition to be gained; now we move to the infinite-dimensional setting. Let M be an infinite-dimensional manifold and let N be a submanifold contained in M. Roughly speaking, an infinite-dimensional manifold is a set which is locally diffeomorphic to an infinite-dimensional Banach space. Because infinite-dimensional manifolds are discussed in this section only, and then mainly in a heuristic fashion, we refer the reader to the literature for the proper definitions.) We say that N is of codimension k if every point of N is contained in some open set in M which is diffeomorphic to $U \times \mathbb{R}^k$, where U is an open set in N. This implies that k is the smallest dimension of a submanifold $P \subset M$ that intersects N such that the intersection is transversal. Thus, the definition of codimension in the infinite-dimensional case has the same geometrical connotations as in the finite-dimensional case. Now we return to our main discussion. (For the case of "codimension ∞", $\mathbb{R}^k$ in this definition is replaced with an infinite dimensional Banach space.)

Completely Integrable Hamiltonian System: Hamilton's equations, for n degrees-of-freedom, are said to be *completely integrable* if there exists n functions (called *integrals*)

$$F_1 \equiv H, F_2, \cdots, F_n, \quad (H \text{ is the Hamiltonian}),$$

which satisfy the following conditions.

1. The F_i, $i = 1, \cdots, n$, are functionally independent on U, with the possible exception of sets of measure zero.
2. $\{F_i, F_j\} = 0$, for all i and j, where $\{\cdot, \cdot\}$ denotes the Poisson bracket.

Configuration Space: The space of generalized coordinates of a system is often referred to as the *configuration space* of the system.

Conjugacy: A change of variables, or coordinates. Consider two C^r diffeomorphisms $f\colon \mathbb{R}^n \to \mathbb{R}^n$ and $g\colon \mathbb{R}^n \to \mathbb{R}^n$, and a C^k diffeomorphism $h\colon \mathbb{R}^n \to \mathbb{R}^n$. f and g are said to be C^k *conjugate* ($k \leq r$) if there exists a C^k diffeomorphism $h\colon \mathbb{R}^n \to \mathbb{R}^n$ such that $g \circ h = h \circ f$. If $k = 0$, f and g are said to be *topologically conjugate*.

The conjugacy of two diffeomorphisms is often represented by the following diagram.

$$\begin{array}{ccc} \mathbb{R}^n & \xrightarrow{f} & \mathbb{R}^n \\ \Big\downarrow{\scriptstyle h} & & \Big\downarrow{\scriptstyle h}. \\ \mathbb{R}^n & \xrightarrow{g} & \mathbb{R}^n \end{array}$$

The diagram is said to *commute* if the relation $g \circ h = h \circ f$ holds, meaning that you can start at a point in the upper left-hand corner of the diagram and reach the same point in the lower right-hand corner of the diagram by either of the two possible routes. We note that h need not be defined on all of $\mathbb{R}^n$ but possibly only locally about a given point. In such cases, f and g are said to be *locally* C^k *conjugate*.

Conley-Moser Conditions: A set of geometrical and analytical criteria for a map that, if satisfied, imply that the map behaves like a Smale horseshoe.

C^r Function: A function is said to be C^r if it is r times differentiable, and if each of the deriviatives is a continuous function. For $r = 0$ the function is merely continuous.

C^r Diffeomorphism: A function is said to be a C^r diffeomorphism if the function is invertible, and if both the function and its inverse are C^r functions. For $r = 0$ the function is said to be a *homeomorphism*.

Cyclic Coordinate: A synonym for ignorable coordinate.

Degrees of Freedom: The phrase *degrees of freedom* has its origins in mechanics. The number of degrees of freedom of a mechanical system is the number of independent coordinates

that are required to describe the configuration of the system (i. e., "position coordinates"). Thus, the number of degrees of freedom is half the dimension of the phase space of the corresponding Hamiltonian dynamical system. If an n degree of freedom system also depends explicitly on time (i.e., the vector field is nonautonomous), the the phrase $n + \frac{1}{2}$ *degree of freedom system* is often used.

Diophantine Frequency: A frequency vector $\omega \in \mathbb{R}^n$ is said to be *diophantine* if there exists constants τ, $\gamma > 0$ such that the following infinite number of inequalities hold:

$$|\omega \cdot k| \geq \gamma |k|^{-\tau} \quad \forall k \in \mathbf{Z}^n - \{0\}$$

where

$$|k| \equiv \sup_i |k_i|.$$

Distance Between a Point and a Set: Let $S \in \mathbb{R}^n$ be an arbitrary set and $p \in \mathbb{R}^n$ be an arbitrary point. Then the distance between the point p and the set S is denoted and defined as:

$$d(p, S) = \inf_{x \in S} |p - x|. \tag{34.0.1}$$

Double-Hopf Bifurcation: The bifurcation associated with a nonhyperbolic equilibrium point of an autonomous vector field where the matrix associated with the linearization of the the vector field about the equilibrium point has the following Jordan canonical form:

$$\begin{pmatrix} 0 & \omega_1 & 0 & 0 \\ \omega_1 & 0 & 0 & 0 \\ 0 & 0 & 0 & -\omega_2 \\ 0 & 0 & \omega_2 & 0 \end{pmatrix}.$$

Duffing Equation: The second order, ordinary differential equation:

$$\ddot{x} - x + x^3 = 0, \qquad x \in \mathbb{R},$$

or, written as a system

$$\begin{aligned} \dot{x} &= y, \\ \dot{y} &= x - x^3, \qquad (x, y) \in \mathbb{R}^2. \end{aligned}$$

Sometimes damping and external driving (time-dependence) are added

$$\begin{aligned} \dot{x} &= y, \\ \dot{y} &= x - x^3 - \delta y + \gamma f(t), \qquad (x, y) \in \mathbb{R}^2, \end{aligned}$$

in this case it is referred to as the damped (δy), driven ($\gamma f(t)$) Duffing equation, where δ and γ are parameters.

Dynamical System: A system that changes in time; usually described by differential equations (continuous time) or difference equations (sometimes called "maps) (discrete time), or, possibly, some combination of the two.

Elliptic Equilibrium Point: An equilibrium point of an autonomous Hamiltonian system is said to be *elliptic* if all of the eigenvalues of the matrix associated with the linearization about the equilibrium point are purely imaginary, and nonzero.

Equilibrium Solution: A constant solution of a vector field, i.e. a point in phase space where the vector field is zero, also referred to as a *fixed point*.

Exponential Dichotomy: The linear field $\dot{x} = A(t)x$, $x \in \mathbb{R}^n$ is said to possess an *exponential dichotomy* if each of the n linear independent solutions exhibit exponential growth or decay as $t \to \infty$. More precisely, suppose $X(t)$ is the *fundamental solution matrix* of this linear vector field, i.e., for any initial condition ξ_0, $\xi(t) = X(t)\xi_0$ is the solution of the vector field passing through ξ_0 at $t = 0$, $X(0) = \mathrm{id}$. Let $\| \cdot \|$ denote a norm on $\mathbb{R}^n$. Then the linear vector field is said to possess an *exponential dichotomy* if there exists a projection operator P, $P^2 = P$, and constants K_1, K_2, λ_1, $\lambda_2 > 0$, such that

$$\| X(t)PX^{-1}(\tau) \| \leq K_1 \exp\left(-\lambda_1(t-\tau)\right), \quad t \geq \tau,$$
$$\| X(t)\left(\mathrm{id} - P\right)X^{-1}(\tau) \| \leq K_2 \exp\left(\lambda_2(t-\tau)\right), \quad t \leq \tau.$$

Extended Phase Space: The cartesian product of the phase space with the independent variable (which is often referred to as "time").

Fold Bifurcation: Another term for a saddle-node bifurcation.

Γ-Equivariant Map: Let $f : V \to V$ denote a mapping of a vector space V into V. Let Γ denote a compact Lie group with a specified action on V. We say that f is Γ-*equivariant with respect to this action* if

$$f(\gamma x) = \gamma f(x), \quad \forall \gamma \in \Gamma,\ x \in V.$$

Γ-Invariant Function: Now let $f : V \to \mathbb{R}$ denote a mapping of a vector space V into $\mathbb{R}$. Let Γ denote a compact Lie group with a specified action on V. We say that f is Γ-*invariant with respect to this action* if

$$f(\gamma x) = f(x), \quad \forall \gamma \in \Gamma,\ x \in V.$$

If f is a vector field then we will refer to it as a Γ- equivariant vector field. It follows that if $x(t)$ is a solution of a Γ-equivariant vector field $\dot{x} = f(x)$, then $\gamma x(t)$ is also a solution, for each $\gamma \in \Gamma$.

General Linear Group, $GL(\mathbb{R}^n)$: $GL(\mathbb{R}^n)$ is the group of linear, invertible transformations of $\mathbb{R}^n$ into $\mathbb{R}^n$, which we can view as the group of nonsingular $n \times n$ matrices over $\mathbb{R}$.

Generalized Coordinates: A set of coordinates that contain the minimum number of independent coordinates needed to specify all the positions of a set of particles is referred to as *generalized coordinates*, and denoted by $(q_1, \ldots, q_N)$. Generalized coordinates may be distances, angles, or quantities relating them. The integer N is referred to as the number of *degrees-of-freedom* of a system. So a system is said to have N degrees-of-freedom if the positions of all its components can be described by N independent (generalized) coordinates.

Generalized Momentum: $p_i = \frac{\partial L}{\partial \dot{q}_i}$ is referred to as the ith component of generalized momentum.

Generalized Velocity: $(\dot{q}_1, \ldots, \dot{q}_N)$ are referred to as *generalized velocities*, where $(q_1, \ldots, q_N)$ are generalized coordinates.

Generating Function: Consider the Hamiltonian

$$H(q, p, t),$$

and the associated Hamilton's equations:

$$\dot{q} = \frac{\partial H}{\partial p}(q, p, t),$$
$$\dot{p} = -\frac{\partial H}{\partial q}(q, p, t).$$

Suppose we have a transformation of coordinates of the form

$$Q = Q(q, p, t),$$
$$P = P(q, p, t),$$

which we assume can be inverted (viewing t as fixed) to yield

$$q = q(Q, P, t),$$
$$p = p(Q, P, t).$$

The Hamiltonian in the original (q, p) coordinates can be written as a function of the (Q, P) coordinates:

$$H(q,p,t) = \bar{H}(Q,P,t).$$

In the $Q-P$ coordinates Hamilton's equations will hold, i.e.,

$$\dot{Q} = \frac{\partial \bar{H}}{\partial P}(Q,P,t),$$
$$\dot{P} = -\frac{\partial \bar{H}}{\partial Q}(Q,P,t).$$

provided the coordinate transformation satisfies:

$$p_i = \frac{\partial F}{\partial q_i},$$
$$P_i = -\frac{\partial F}{\partial Q_i},$$
$$\bar{H} = H + \frac{\partial F}{\partial t},$$

where the function F satisfies:

$$dF(q,Q,t) = \sum_{i=1}^{N} p_i dq_i - \sum_{i=1}^{N} P_i dQ_i + (H - \bar{H})dt.$$

The function F is referred to as a generating function.

Generic Property: A property of a map (resp. vector field) is said to be C^k *generic* if the set of maps (resp. vector fields) possessing that property contains a residual subset in the C^k topology.

Gradient Vector Field: A gradient vector field is a vector field having the form $\dot{x} = \nabla V(x)$, $x \in \mathbb{R}^n$, where $V(x)$ is a scalar valued function.

Group: A group is a set, G, equipped with a binary operation on the group elements, denoted "$*$" and referred to as *group multiplication*, which satisfies the following three properties.

1. G is closed under group multiplication, i.e., $g_1,\ g_2 \in G \Rightarrow g_1 * g_2 \in G$.
2. There exists a multiplicative identity element in G, i.e., there exists an element $e \in G$ such that $e * g = g * g = g$, for any $g \in G$.
3. For every element of G there exists a multiplicative inverse, i.e., for every $g \in G$, there exists an element, denoted g^{-1}, such that $g * g^{-1} = g^{-1} * g = e$.
4. Multiplication is associative, i.e., $(g_1 * g_2) * g_3 = g_1 * (g_2 * g_3)$, for any $g_1,\ g_2,\ g_3 \in G$.

Hamilton's Equations: The ordinary differential equations:

$$\dot{q}_i = \frac{\partial H}{\partial p_i},$$
$$\dot{p}_i = -\frac{\partial H}{\partial q_i}, \quad i = 1, \ldots, N,$$

are referred to as Hamilton's equations, where $H = H(q,p)$ is a scalar valued function called the *Hamiltonian*.

Hamilton-Jacobi Equation: The partial differential equation

$$\frac{\partial S}{\partial t} + H\left(q, \frac{\partial S}{\partial q}, t\right) = 0,$$

for some scalar valued function H ($q \in \mathbb{R}^N$) is referred to as the Hamilton-Jacobi equation.

Hausdorff Metric: Let A and B be two nonempty, compact subsets of $\mathbb{R}^n$. The Hausdorff metric defined on the set of nonempty, compact subsets of $\mathbb{R}^n$ is defined as:

$$H(A,B) \equiv \max\left(H^*(A,B), H^*(B,A)\right).$$

Hausdorff Separation: Let A and B be two nonempty, compact subsets of $\mathbb{R}^n$. The Hausdorff separation of A and B, denoted $H^*(A,B)$, is defined as:

$$H^*(A,B) \equiv \max_{a\in A} \operatorname{dist}(\mathrm{a},\mathrm{B}) = \max_{\mathrm{a}\in\mathrm{A}} \min_{\mathrm{b}\in\mathrm{B}} \parallel \mathrm{a}-\mathrm{b} \parallel .$$

Heteroclinic Orbit: An orbit is said to be *heteroclinic to the two invariant sets* Λ_1 *and* Λ_2 if it approaches Λ_1 asymptotically under time evolution as time goes to $-\infty$ and approaches Λ_2 asymptotically under time evolution as time goes to $+\infty$. If the invariant sets have stable and unstable manifolds then a heteroclinic orbit lies in the intersection of the unstable manifold of Λ_1 and the stable manifold of Λ_2.

Homoclinic Orbit: An orbit is said to be *homoclinic to an invariant set* if it approaches the invariant set asymptotically under time evolution as time goes to $\pm\infty$. If the invariant set has stable and unstable manifolds then a homoclinic orbit lies in the intersection of the stable and unstable manifolds.

Hopf Bifurcation: See Poincaré-Andronov-Hopf bifurcation.

Hopf-Steady State Bifurcation: The bifurcation associated with a nonhyperbolic equilibrium point of an autonomous vector field where the matrix associated with the linearization of the the vector field about the equilibrium point has the following Jordan canonical form:

$$\begin{pmatrix} 0 & -\omega & 0 \\ \omega & 0 & 0 \\ 0 & 0 & 0 \end{pmatrix}.$$

Hyperbolic Fixed Point: A fixed point of a vector field that has the property that none of the eigenvalues of the matrix associated with the linearization of the vector field at the fixed point lie on the imaginary axis. A fixed point of a map or difference equation that has the property that none of the eigenvalues of the matrix associated with the linearization of the map at the fixed point lie on the unit circle.

Hyperbolic Trajectory: The trajectory $\bar{x}(t)$ of the vector field $\dot{x} = f(x,t)$ is said to be *hyperbolic* if the associated linear equation, $\dot{\xi} = D_x f(\bar{x}(t),t)\xi$, possesses and exponential dichotomy.

Ignorable Coordinate: A generalized coordinate that does not appear in the Lagrangian (although the generalized velocity corresponding to the coordinate may appear in the Lagrangian).

Index of a Closed Curve: Consider an autonomous vector field defined in some simply connected region, $\mathcal{R}$, of the plane (this is a two-dimensional idea only). Let Γ be any closed loop in $\mathcal{R}$ *which contains no fixed points* of the vector field. You can imagine at each point, p, on the loop Γ that there is an arrow representing the value of the vector field at p.

Now as you move around Γ in the counter-clockwise sense (call this the positive direction), the vectors on Γ rotate, and when you get back to the point at which you started, they will have rotated through an angle $2\pi k$, where k is some integer. This integer, k, is called the *index of* Γ.

The index of a closed curve containing no fixed points can be calculated by integrating the change in the angle of the vectors at each point on Γ around Γ (this angle is measured with respect to some chosen coordinate system). For a vector field defined on some simply connected region, $\mathcal{R}$, of the plane given by

$$\begin{aligned} \dot{x} &= f(x,y), \\ \dot{y} &= g(x,y), \qquad (x,y) \in \mathcal{R} \subset \mathbb{R}^2, \end{aligned}$$

the index of Γ, k, is found by computing

$$k = \frac{1}{2\pi}\oint_\Gamma d\phi = \frac{1}{2\pi}\oint_\Gamma d\left(\tan^{-1}\frac{g(x,y)}{f(x,y)}\right) = \frac{1}{2\pi}\oint_\Gamma \frac{f\,dg - g\,df}{f^2+g^2}.$$

Infinitesimally Symplectic Transformations: Consider a C^r, $r \geq 1$, map $f : \mathbb{R}^{2n} \to \mathbb{R}^{2n}$. Then f is said to be an *infinitesimally symplectic* or Ω *skew* transformation if

$$\Omega(Df(x)u, v) = -\Omega(u, Df(x)v), \qquad \forall x, u, v \in \mathbb{R}^{2n},$$

where Ω denotes a symplectic form on $\mathbb{R}^{2n}$. In terms of the canonical symplectic form this relation takes the form:

$$JDf(x) + Df(x)^T J = 0.$$

Infinitesimally symplectic maps arise in the study of the linearization of Hamiltonian vector fields at equilibria.

Infinitesimally Reversible Linear Map: Suppose $G : \mathbb{R}^n \to \mathbb{R}^n$ is a linear involution and $A : \mathbb{R}^n \to \mathbb{R}^n$ is a linear map. Then A is said to be *infinitesimally reversible* if

$$AG + GA = 0.$$

This linearization condition is defined at a *symmetric* fixed point. Infinitesimally reversible linear maps arise in the study of the linearization of reversible vector fields at symmetric fixed points.

Integral Curve: A trajectory in extended phase space.

Invariant Manifold: An invariant set, which is also a manifold.

Invariant Set: A set of points in phase space that has the property that trajectories with initial conditions in the set remain in the set forever.

Involution: Consider a C^r map

$$G : \mathbb{R}^n \mapsto \mathbb{R}^n,$$

satisfying

$$G \circ G = id,$$

where id stands for the identity map. G is called an *involution*

Kolmogorov-Arnold-Moser (KAM) Theorem: This is a perturbation theorem that applies to perturbations of completely integrable Hamiltonian systems expressed in action-angle coordinates. It states that for sufficiently small perturbations the tori in the unperturbed, completely integrable system corresponding to diophantine frequency vector persist for the perturbed system.

Lagrangian: The scalar valued function $L = T - V$ is referred to as the *Lagrangian* of a systems, where T is the kinetic energy and V is the potential energy.

Lagrange's Equations: $\frac{d}{dt}\frac{\partial L}{\partial \dot{q}_i} - \frac{\partial L}{\partial q_i} = 0$, $i = 1, \ldots, N$, are referred to as Lagrange's equations for an N degree-of-freedom system, where $q_1, \ldots, q_N$ are generalized coordinates, and L is the Lagrangian.

Liapunov Function: A scalar valued function, defined on the phase space (or, possibly just some subset thereof) whose level sets define trapping regions for the trajectories of a dynamical system.

Liapunov Stability: Roughly, a trajectory is said to be *Liapunov stable* if, at a given time, trajectories starting close enough to the specified trajectory remain close for all later time.

Lie Group: A Lie group is a closed subgroup of $GL(\mathbb{R}^n)$, which we will denote by Γ.

A subgroup is a subset of a group, which obeys the same axioms as a group (but with the important point that it is the subset that is closed with respect to group multiplication). The term "closed" in the definition of a Lie group needs clarification. We can identify the space of all $n \times n$ matrices with R^{n^2}. Then $GL(\mathbb{R}^n)$ is an open subset of R^{n^2}. Γ is said to be a *closed subgroup* if it is a closed subset of $GL(\mathbb{R}^n)$, as well as a subgroup of $GL(\mathbb{R}^n)$.

If this closed subset is *compact* or *connected* then the associated Lie group is also said to be compact or connected.

Lie Group Action on a Vector Space: Let Γ denote a Lie group and V a vector space. We say that Γ acts linearly on V if there is a continuous mapping, referred to as the *action*:

$$\begin{aligned} &\Gamma \times V \to V, \\ &(\gamma, v) \mapsto \gamma \cdot v, \end{aligned}$$

such that

1. For each $\gamma \in \Gamma$ the mapping

$$\begin{aligned} \rho_\gamma \; : \; & V \to V, \\ & v \mapsto \gamma \cdot v \equiv \rho_\gamma(v). \end{aligned}$$

   is linear.

2. (a) For any $\gamma_1, \gamma_2 \in \Gamma$,

$$\gamma_1 \cdot (\gamma_2 \cdot v) = (\gamma_1 * \gamma_2) \cdot v.$$

   (b) $e \cdot v = v$.

The Lift of a Circle Map: Consider the following map of the real line $\mathbb{R}$ to S^1:

$$\begin{aligned} \Pi : \mathbb{R} &\longrightarrow S^1, \\ x &\longrightarrow e^{2\pi i x} \equiv \theta. \end{aligned}$$

The map $F : \mathbb{R} \longrightarrow \mathbb{R}$ is said to be a *lift* of $f : S^1 \longrightarrow S^1$ if

$$\Pi \circ F = f \circ \Pi.$$

Linearization: The procedure of Taylor expanding a dynamical system in the dependent variable about a specific solution, or invariant set, and throwing away all but the terms linear in the dependent variable.

Liouville-Arnold Theorem: This theorem describes the phase space structure of certain n degree-of-freedom completely integrable Hamiltonian systems. Suppose $F_1, \ldots, F_n$ are n integrals satisfying the definition of complete integrability. Then we examine the (in general) n dimensional sets defined by

$$\begin{aligned} F_1 &= f_1, \\ &\vdots \quad \vdots \\ F_n &= f_n, \end{aligned}$$

where the f_i, $i = 1, \ldots, n$ are constants. The Liouville-Arnold theorem states that if these sets are compact and connected, then they are actually n-tori.

Multiplicity of a Resonance: A resonant frequency vector $\omega \in \mathbb{R}^n$ is said to be of multiplicity $m < n$ if there exist independent $k^i \in \mathbb{Z}^n - \{0\}, i = 1, \ldots, m$, such that $k^i \cdot \omega = 0$.

Naimark-Sacker Torus Bifurcation: A bifurcation of a fixed point of a map where the linearization has a pair of eigenvalues on the unit circle. The eigenvalues satisfy a non-resonance condition in the sense that they are no one of the first four roots of unity, i.e., if λ denotes one of the eigenvalues then $\lambda^n \neq 1$, $n = 1, 2, 3, 4$. The bifurcation of the fixed point gives rise to an invariant circle. This bifurcation is sometimes referred to as the "Hopf bifurcation for maps".

Negative Invariant Manifold: A negative invariant set that is also a manifold.

Negative Invariant Set: A set of points in phase space that has the property that trajectories with initial conditions in the set remain in the set for all negative time.

Nekhoroshev's Theorem: This is a perturbation theorem that applies to perturbations of completely integrable Hamiltonian systems expressed in action-angle coordinates. It states that for sufficiently small perturbations the action variable change by a small amount over an exponentially long time interval.

Node: An equilibrium point of a vector field having the property that the matrix associated with the linearization at the fixed point has all eigenvalues either in the right or the left half plane. Hence, a node is a hyperbolic fixed point that is either attracting or repelling.

Nonautonomous System: A dynamical system that depends explicitly on the independent variable (which is often referred to as "time").

Nonwandering Points: Let $\phi(t,x)$ denote the flow generated by a vector field and let $x \mapsto g(x)$ denote a map. A point x_0 is called *nonwandering* if the following holds.

Flows: For *any* neighborhood U of x_0 and $T > 0$, there exists some $|t| > T$ such that

$$\phi(t, U) \cap U \neq \emptyset.$$

Maps: For *any* neighborhood U of x_0, there exists some $n \neq 0$ such that

$$g^n(U) \cap U \neq \emptyset.$$

Note that if the map is noninvertible, then we must take $n > 0$.

Nonwandering Set: The set of all nonwandering points of a map or flow is called the *nonwandering set* of that particular map or flow.

ω and α Limit Points of Trajectories: Let $\phi(t,x)$ denote the flow generated by a vector field. A point $x_0 \in \mathbb{R}^n$ is called an ω *limit point* of $x \in \mathbb{R}^n$, denoted $\omega(x)$, if there exists a sequence $\{t_i\}$, $t_i \longrightarrow \infty$, such that

$$\phi(t_i, x) \longrightarrow x_0.$$

α *limit points* are defined similarly by taking a sequence $\{t_i\}$, $t_i \longrightarrow -\infty$.

ω and α Limit Sets of a Flow: The set of all ω limit points of a flow or map is called the ω *limit set*. The α limit set is similarly defined.

Normal Form: A local theory that applies in the neighborhood of an orbit of a vector field or map. The theory provides an algorithmic way to generate a sequence of nonlinear coordinate changes that eliminate as much of the nonlinearity as possible at each order (where "order" refers to the terms in a Taylor expansion about the orbit). Interestingly, the form of the nonlinearity that cannot be eliminated by such coordinate changes is determined by the structure of the linear part of the vector field or map.

Orbit: The set of points in phase space through which a trajectory passes.

Orbital Derivative: Consider a dynamical system, with its phase space, and a function defined on this phase space. The orbital derivative of the function is the derivative of the function along trajectories of this dynamical system.

Order of a Resonance: Suppose $\omega \in \mathbb{R}^n$ is a frequency vector and $k \cdot \omega = 0$ for some $k \in \mathbb{Z}^n - \{0\}$. Then the order of this resonance is defined to be $|k| = \sum_i |k_i|$.

Perfect Set: A set is called *perfect* if it is closed and every point in the set is a limit point of the set.

Period-Doubling Bifurcation: A bifurcation of a fixed point of a map where the linearization at the fixed point has an eigenvalue of -1. In this bifurcation the fixed point (i.e., period one point) changes its stability type and a period two orbit is created (or destroyed).

Phase Curve: The solution of an ordinary differential equation, synonomous with the term trajectory.

Phase Space: The space of *dependent variables* of an ordinary differential equation or map.

Poincaré-Andronov-Hopf Bifurcation: A bifurcation of a fixed point of a vector field where the linearization has a pair of purely imaginary eigenvalues (which are not zero). Provided a nondegeneracy condition involving the quadratic and cubic nonlinear terms holds, this bifurcation gives rise to a unique periodic orbit.

Poincaré-Bendixson Theorem: A theorem that applies to two- dimensional, autonomous vector fields on the sphere, or on a compact, positively invariant subset of $\mathbb{R}^2$. It states that the omega limit sets are either equilibrium points, periodic orbits, or a collection of orbits made up of fixed points and orbits connecting fixed points (heteroclinic orbits) that form a closed path.

Poincaré Map: A map obtained from the trajectories of an ordinary differential equation. There are many ways in which this can be done. However, a guiding principle is that the dynamics of the map must correspond to the dynamics of the vector field.

Poisson Bracket: Let H, $G : U \to \mathbb{R}$, $U \subset \mathbb{R}^{2n}$, denote two C^r, $r \geq 2$, functions. Then the *Poisson bracket* of these two functions is another function, and it is defined through the symplectic form Ω on $\mathbb{R}^{2n}$ as follows:

$$\{H, G\} \equiv \Omega(X_H, X_G) \equiv \langle X_H, JX_G \rangle,$$

where X_H and X_G denote the Hamiltonian vector fields corresponding to the Hamiltonian functions H and G, respectively.

Positive Invariant Manifold: A positive invariant set that is also a manifold.

Positive Invariant Set: A set of points in phase space that has the property that trajectories with initial conditions in the set remain in the set for all positive time.

Pullback Absorbing Family: A family

$$\hat{B} = \{B_p,\, p \in P\}\,,$$

of compact subsets of $\mathbb{R}^n$ is called a pullback absorbing family for a cocycle $\{\phi_{t,p},\, t \in \mathbb{R}, p \in P\}$ on $\mathbb{R}^n$ if for each $p \in P$ there is a bounded subset of $\mathbb{R}^n$, U_p, satisfying $U_p \supset B_p$, and a time $t_{U_p} > 0$ such that:

$$\phi_{t,\theta_{-t}p}(U_{\theta_{-t}p}) \subset B_p, \quad \text{for all} \quad t \geq t_{U_p}\,.$$

Pullback Attracting Set: A family $\hat{A} = \{A_p,\, p \in P\}$ of compact subsets of $\mathbb{R}^n$ is called a *pullback attracting set of a cocycle* $\{\phi_{t,p},\, t \in \mathbb{R}, p \in P\}$ *on* $\mathbb{R}^n$ if it is invariant in the sense that:

$$\phi_{t,p}\,(A_p) = A_{\theta_t p},\, t \in \mathbb{R},\, p \in P,$$

and *pullback attracting* in the sense that for every A_p there exists a bounded subset of $\mathbb{R}^n$, $D_p \supset A_p$, such that

$$\lim_{t \to \infty} H^* \left(\phi_{t,\theta_{-t}p}(D_{\theta_{-t}p}), A_p \right) = 0.$$

Principle of Least Action: The principle of least action states that extrema of the action functional are solutions of Lagrange's equations, and vice-versa.

Quasiperiodic Motion: A function

$$\begin{aligned} h: \quad & \mathbb{R}^1 \to \mathbb{R}^m \\ & t \mapsto h(t) \end{aligned}$$

is called *quasiperiodic* if it can be represented in the form

$$h(t) = H(\omega_1 t, \ldots, \omega_n t),$$

where $H(x_1, \ldots, x_n)$ is a function of period 2π in $x_1, \ldots, x_n$. The real numbers $\omega_1, \ldots, \omega_n$ are called the *basic frequencies*. We shall denote by $C^r(\omega_1, \ldots, \omega_n)$ the class of $h(t)$ for which $H(x_1, \ldots, x_n)$ is r times continuously differentiable.

For example, the function

$$h(t) = \gamma_1 \cos \omega_1 t + \gamma_2 \sin \omega_2 t$$

is a quasiperiodic function.

(Note: There exists a more general class of functions called *almost periodic functions* which can be viewed as quasiperiodic functions having an infinite number of basic frequencies. These will not be considered in this book, see Hale [1980] for a discussion and rigorous definitions.)

A *quasiperiodic solution* $\phi(t)$, of an ordinary differential equation is a solution which is quasiperiodic in time. A *quasiperiodic orbit* is the orbit of any point through which $\phi(t)$ passes. A quasiperiodic orbit may be interpreted geometrically as lying on an n dimensional torus. This can be seen as follows. Consider the equation

$$y = H(x_1, \ldots, x_n).$$

Then, if $m \geq n$ and $D_x H$ has rank n for all $x = (x_1, \ldots, x_n)$, then this equation can be viewed as an embedding of an n-torus in m space with $x_1, \ldots, x_n$ serving as coordinates on the torus. Now, viewing $h(t)$ as a solution of an ordinary differential equation, since $x_i = \omega_i t$, $i = 1, \ldots, n$, $h(t)$ can be viewed as tracing a curve on the n-torus as t varies.

Representation of Γ on V: Let $GL(V)$ denote the group of invertible linear transformations of V into V. The map

$$\rho : \Gamma \to GL(V),$$
$$\gamma \mapsto \rho_\gamma,$$

is called a representation of Γ on V.

Resonance: The frequency vector $\omega \in \mathbb{R}^n$ is said to be *resonant* if there exists $k \in \mathbb{Z}^n - \{0\}$ such that $k \cdot \omega = 0$. If no such $k \in \mathbb{Z}^n - \{0\}$ exists, ω is said to be *nonresonant*.

Residual Set: Let X be a topological space, and let U be a subset of X. U is called a *residual set* if it is the intersection of a countable number of sets each of which are open and dense in X. If every residual set in X is itself dense in X, then X is called a *Baire space*.

Reversible Dynamical System: Let $\dot{x} = f(x)$, $x \in \mathbb{R}^n$ be a vector field and let $G : \mathbb{R}^n \to bbR^n$ be an involution. Then the vector field is said to be *reversible* if $\frac{d}{dt}(G(x)) = -f(G(x))$. A map $x_{n+1} = g(x_n)$ is said to be reversible if $g(G(x_{n+1})) = G(x_n)$.

Reversible Linear Map: Suppose $G : \mathbb{R}^n \to \mathbb{R}^n$ is a linear involution and $A : \mathbb{R}^n \to \mathbb{R}^n$ is a linear map. Then A is said to be *reversible* if

$$AGA = G.$$

Note that this linearization condition is defined at a *symmetric* fixed point. Reversible linear maps arise in the study of the linearization of reversible maps at symmetric fixed points.

Rotation Number: Consider an orientation preserving homeomorphism $f : S^1 \longrightarrow S^1$, with F a lift of f, we define the quantity

$$\rho_0(F) \equiv \lim_{n \to \infty} \frac{|F^n(x)|}{n}.$$

There are two main operational definitions of rotation number. For $f : S^1 \longrightarrow S^1$ an orientation preserving homeomorphism, with F a lift of f:

1. Some authors define the rotation number of f, denoted $\rho(f)$, as the fractional part of $\rho_0(F)$ (e.g. Devaney [1986]).
2. Other authors define the rotation number of f to be $\rho_0(F)$ (e.g., Katok and Hasselblatt [1995]).

In either case, the rotation number exists, and is independent of the point x.

Saddle-Node Bifurcation: A bifurcation of a fixed point where one goes from zero to two fixed points as a parameter is varied through the bifurcation point. At the bifurcation point the linearization has a zero eigenvalue for vector fields and an eigenvalue of one for maps. This bifurcation is also referred to as a tangent or fold bifurcation.

Sensitive dependence on initial conditions: Consider $\mathbf{C}^r$ $(r \geq 1)$ autonomous vector fields and maps on $\mathbb{R}^n$ denoted as follows

$$\text{vector field} \qquad \dot{x} = f(x), \tag{34.0.2}$$

$$\text{map} \qquad x \mapsto g(x). \tag{34.0.3}$$

Denote the flow generated by (34.0.2) by $\phi(t,x)$ and we assume that it exists for all $t > 0$. We assume that $\Lambda \subset \mathbb{R}^n$ is a compact set invariant under $\phi(t,x)$ (resp. $g(x)$), i.e., $\phi(t,\Lambda) \subset \Lambda$ for all $t \in \mathbb{R}$ (resp. $g^n(\Lambda) \subset \Lambda$ for all $n \in \mathbb{Z}$, except that if g is not invertible, we must take $n \geq 0$). The flow $\phi(t,x)$ (resp. $g(x)$) is said to have *sensitive dependence on initial conditions on* Λ if there exists $\varepsilon > 0$ such that, for any $x \in \Lambda$ and any neighborhood U of x, there exists $y \in U$ and $t > 0$ (resp. $n > 0$) such that $|\phi(t,x) - \phi(t,y)| > \varepsilon$ (resp. $|g^n(x) - g^n(y)| > \varepsilon$).

Shift Map: A map defined on the space of bi-infinite sequences of N symbols (see symbol sequence). It acts by shifting the sequence one place to the left of the point separating the sequence into two infinite halves. More precisely, if we denote the shift map by σ, and a symbol sequence by

$$s = \left\{ \cdots s_{-n} \cdots s_{-1} . s_0 s_1 \cdots s_n \cdots \right\}$$

$$\text{where} \quad s_i \in \{1, 2, \ldots, N\} \quad \forall\, i.$$

Then

$$\sigma\left(\left\{ \cdots s_{-n} \cdots s_{-1} . s_0 s_1 \cdots s_n \cdots \right\}\right)$$

$$= \left\{ \cdots s_{-n} \cdots s_{-1} s_0 . s_1 \cdots s_n \cdots \right\}.$$

Skew-Product Flow: This is a formalism that can be applied to nonautonomous vector fields which allows one to retain the flow property. The crucial observation leading to the development of the approach is the following. Suppose $x(t)$ is a solution of $\dot{x} = f(x,t)$. Then $x_\tau(t) \equiv x(t+\tau)$ is a solution of $\dot{x}_\tau(t) = f_\tau(x_\tau(t), t) \equiv f(x(t+\tau), t+\tau)$

We first define the space of nonautonomous vector fields whose time translates remain within the space, i.e.,

$$\mathcal{F} \equiv \{\text{Space of functions } f : \mathbb{R}^n \times \mathbb{R} \to \mathbb{R}^n \text{ such that} \\ f_\tau(\cdot,\cdot) \equiv f(\cdot, \cdot + \tau) \in \mathcal{F} \text{ for all } \tau \in \mathbb{R}.\}$$

We then define the group of shift operators on $\mathcal{F}$:

$$\theta_\tau : \mathcal{F} \to \mathcal{F},$$
$$f \mapsto \theta_\tau f \equiv f_\tau, \quad \forall \tau \in \mathbb{R},$$

and we define the product space:

$$\mathcal{X} \equiv \mathbb{R}^n \times \mathcal{F}.$$

Let $x(t, x_0, f)$ denote a solution of $\dot{x} = f(x,t)$ with $x(0, x_0, f) = x_0$. Finally, we define the family of mappings:

$$\Psi_t : \mathcal{X} \to \mathcal{X},$$
$$(x_0, f) \mapsto (x(t, x_0, f), \theta_t f)\,.$$

It can then be shown that Ψ_t is a one-parameter family of mappings of $\mathcal{X}$ into $\mathcal{X}$, or flow:

$$\Psi_{t+s}(x_0, f) = \Psi_t \circ \Psi_s(x_0, f).$$

Smale Horseshoe: As originally conceived by Smale, a two-dimensional, nonlinear, invertible map possessing an invariant set with a remarkable structure. The invariant set has the structure of a Cantor set. In addition, it has a countable infinity of periodic orbits of all possible periods, an uncountable infinity of nonperiodic orbits, and an orbit that is dense in the invariant set. The dynamics on the invariant set is chaotic. The map has since been

generalized to many other settings (n dimensions as well as infinite dimensions, and in also in the context of noninvertible maps).

Space of Vector-Valued Homogeneous Polynomials of Degree k, H_k: Let $\{s_1, \cdots, s_n\}$ denote a basis of $\mathbb{R}^n$, and let $y = (y_1, \cdots, y_n)$ be coordinates with respect to this basis. Now consider those basis elements with coefficients consisting of homogeneous polynomials of degree k, i.e.,

$$(y_1^{m_1} y_2^{m_2} \cdots y_n^{m_n}) s_i, \quad \sum_{j=1}^{n} m_j = k,$$

where $m_j \geq 0$ are integers. We refer to these objects as *vector-valued homogeneous polynomials of degree k*. The set of all vector-valued homogeneous polynomials of degree k forms a linear vector space, which we denote by H_k. A basis for H_k consists of elements formed by considering all possible homogeneous polynomials of degree k that multiply each s_i.

Stable Manifold of a Fixed Point: The stable manifold of a fixed point is an invariant manifold passing through a fixed point which is tangent to the stable subspace at the fixed point, and has the same dimension as the stable subspace. Trajectories starting in the stable manifold have qualitatively the same dynamics as trajectories in the stable subspace under the linearized dynamics. Namely, they approach the fixed point asymptotically as $t \to \infty$ at an exponential rate.

Stable Subspace of a Fixed Point: Consider an (autonomous) ordinary differential equation (resp. map) linearized about a fixed point, and the Jacobian matrix associated with this linearization. The stable subspace associated with the fixed point is the span of the generalized eigenvectors corresponding to eigenvalues of the Jacobian matrix having negative real part (resp. modulus less than one). It is an invariant manifold under the linearized dynamics. Trajectories starting in the stable subspace approach the fixed point at an exponential rate as $t \to \infty$.

Strange Attractor: Suppose $\mathcal{A} \subset \mathbb{R}^n$ is an attractor. Then $\mathcal{A}$ is called a *strange attractor* if it is also a chaotic invariant set.

Structural Stability: Let $C^r(\mathbb{R}^n, \mathbb{R}^n)$ denote the space of C^r maps of $\mathbb{R}^n$ into $\mathbb{R}^n$. In terms of dynamical systems, we can think of the elements of $C^r(\mathbb{R}^n, \mathbb{R}^n)$ as being vector fields. We denote the subset of $C^r(\mathbb{R}^n, \mathbb{R}^n)$ consisting of the C^r diffeomorphisms by $\mathrm{Diff}^r(\mathbb{R}^n, \mathbb{R}^n)$. Two elements of $C^r(\mathbb{R}^n, \mathbb{R}^n)$ are said to be C^r ε-close ($k \leq r$), or just C^k close, if they, along with their first k derivatives, are within ε as measured in some norm. Consider a map $f \in \mathrm{Diff}^r(M, M)$ (resp. a C^r vector field in $C^r(M, M)$); then f is said to be *structurally stable* if there exists a neighborhood $\mathcal{N}$ of f in the C^k topology such that f is C^0 conjugate (resp. C^0 equivalent) to every map (resp. vector field) in $\mathcal{N}$.

Symbol Sequence: The space of bi-infinite symbol sequences, denoted Σ^N, is the set of sequences of the form:

$$s = \left\{ \cdots s_{-n} \cdots s_{-1} . s_0 s_1 \cdots s_n \cdots \right\}$$

$$\text{where} \quad s_i \in \{1, 2, \ldots, N\} \quad \forall\, i.$$

The term "bi-infinite" comes from the fact that two infinite sequences are concatenated, with the two "halves" separated by a period.

Symbolic Dynamics: An approach for "modeling" the dynamics of a map or flow (or even a more general type of dynamical system) by the shift map acting on the space of symbol sequences. The symbols can often be thought of for labels of different regions in the phase space of the dynamical system and the shift dynamics describes the visitation of points to the different regions under the dynamics.

Symmetric Fixed Point: In the study of reversible system we say that a point, say x_0, is a symmetric fixed point if it is a fixed point of the dynamical system and if $G(x_0) = x_0$, where G is the involution used to define reversibility.

Symplectic Form: By a *symplectic form* on $\mathbb{R}^{2n}$ we mean a skew-symmetric, nondegenerate bilinear form. By nondegenerate we mean that the matrix representation of the bilinear form is nonsingular. A vector space equipped with a symplectic form is called a *symplectic vector space*. For our phase space $\mathbb{R}^{2n}$ a symplectic form is given by

$$\Omega(u, v) \equiv \langle u, Jv \rangle, \qquad u, v \in \mathbb{R}^{2n},$$

where $\langle \cdot, \cdot \rangle$ denotes the standard Euclidean inner product on $\mathbb{R}^{2n}$ and

$$J = \begin{pmatrix} 0 & \mathrm{id} \\ -\mathrm{id} & 0 \end{pmatrix},$$

where "id" denotes the $n \times n$ identity matrix. This particular symplectic form is referred to as the *canonical symplectic form*.

Topological Transitivity: Let $\phi(t, x)$ denote the flow generated by a vector field and let $x \mapsto g(x)$ denote a map. A closed invariant set A is said to be *topologically transitive* if, for any two open sets $U, V \subset A$

flows: $\exists\ t \in \mathbb{R} \ni \phi(t, U) \cap V \neq \emptyset$,

maps: $\exists\ n \in \mathbb{Z} \ni g^n(U) \cap V \neq \emptyset$.

Symplectic or Canonical Transformations: Consider a C^r, $r \geq 1$, diffeomorphism $f : \mathbb{R}^{2n} \to \mathbb{R}^{2n}$. Then f is said to be a *canonical* or *symplectic* transformation if

$$\Omega(u, v) = \Omega(Df(x)u, Df(x)v), \qquad \forall x, u, v \in \mathbb{R}^{2n},$$

where Ω is a symplectic form on $\mathbb{R}^{2n}$. Equivalently, a canonical transformation is one that is defined by a generating function.

Takens-Bogdanov Bifurcation: The bifurcation associated with a nonhyperbolic equilibrium point of an autonomous vector field where the matrix associated with the linearization of the the vector field about the equilibrium point has the following Jordan canonical form:

$$\begin{pmatrix} 0 & 1 \\ 0 & 0 \end{pmatrix}.$$

Tangent Bifurcation: Another term for a saddle-node bifurcation.

Transcritical Bifurcation: A bifurcation of a fixed point where one goes from two fixed points, to one at the bifurcation point, and back to two as one varies the parameter through the bifurcation point. In this scenario one observes the fixed points colliding and then moving apart, but interchanging stability types. At the bifurcation point the linearization has a zero eigenvalue for vector fields and an eigenvalue of one for maps.

Transversality: Let M and N be differentiable (at least C^1) manifolds in $\mathbb{R}^n$. Let p be a point in $\mathbb{R}^n$; then M and N are said to be *transversal at* p if $p \notin M \cap N$; or, if $p \in M \cap N$, then $T_pM + T_pN = \mathbb{R}^n$, where T_pM and T_pN denote the tangent spaces of M and N, respectively, at the point p. M and N are said to be *transversal* if they are transversal at every point $p \in \mathbb{R}^n$.

Trapping Region: The open set U in the definition of *attracting set* is referred to as a *trapping region*. That is, points starting in U remain in U for all later times.

Trajectory: The solution of an ordinary differential equation, synonomous with the phrase phase curve.

Unstable Manifold of a Fixed Point: The unstable manifold of a fixed point is an invariant manifold passing through a fixed point which is tangent to the unstable subspace at the fixed point, and has the same dimension as the unstable subspace. Trajectories starting in the unstable manifold have qualitatively the same dynamics as trajectories in the unstable subspace under the linearized dynamics. Namely, they approach the fixed point asymptotically as $t \to -\infty$ at an exponential rate.

Unstable Subspace of a Fixed Point: Consider an (autonomous) ordinary differential equation (resp. map) linearized about a fixed point, and the Jacobian matrix associated with this linearization. The unstable subspace associated with the fixed point is the span of the generalized eigenvectors corresponding to eigenvalues of the Jacobian matrix having positive real part (resp. modulus greater than one). It is an invariant manifold under the linearized dynamics. Trajectories starting in the unstable subspace approach the fixed point at an exponential rate as $t \to -\infty$.

Versal Deformation: Roughly speaking, a versal deformation of a degenerate "object", such as a vector field, map, or matrix, is a parametrized family of such "objects" that contains the degenerate object such that the parameterized *family* itself is structurally stable. The minimum number of parameters needed for a versal deformation is referred to as "the

codimension" of the degenerate object, which may be interpreted as a bifurcation point in the appropriate space.

Volume Preserving Map: The map $x \mapsto f(x)$ is said to be volume preserving if $\det Df(x) = 1$.

Volume Preserving Vector Field: The vector field $\dot{x} = f(x,t)$ is said to be volume preserving of $\nabla \cdot f(x,t) = 0$. Sometimes the phrase "divergence free vector field" is used.

Bibliography

Abraham, R.H. and Marsden, J.E. [1978]. *Foundations of Mechanics.* Benjamin/Cummings: Menlo Park, CA.

Abraham, R.H., Marsden, J.E., and Ratiu, T. [1988]. *Manifolds, Tensor Analysis, and Applications.* Springer-Verlag: New York, Heidelberg, Berlin.

Aeyels, D. [1995] Asymptotic stability of nonautonomous systems by Liapunov's direct method. *Systems & Control Letters*, **25**, 273-280.

Afendikov, A., Mielke, A. [1999] Bifurcation of homoclinic orbits to a saddle-focus in reversible systems with SO(2)-symmetry. *J. Diff. Eq.*, **159**(2), 370-402.

Afraimovich, V.S., Bykov, V.V., and Silnikov, L.P. [1983]. On structurally unstable attracting limit sets of Lorenz attractor type. *Trans. Moscow Math. Soc.* **2**, 153–216.

Alekseev, V.M. [1968a]. Quasirandom dynamical systems, I. *Math. USSR-Sb.* **5**, 73–128.

Alekseev, V.M. [1968b]. Quasirandom dynamical systems, II. *Math. USSR-Sb.* **6**, 505–560.

Alekseev, V.M. [1969]. Quasirandom dynamical systems, III. *Math. USSR-Sb.* **7**, 1–43.

Algaba, A., Freire, E., Gamero, E., Rodriguez-Luis, A.J. [1998] Analysis of Hopf and Takens-Bogdanov bifurcations in a modified van der Pol-Duffing oscillator. *Non. Dyn.*,**16**(4), 369-404.

Algaba, A., Freire, E., Gamero, E., Rodriguez-Luis, A.J. [1999a] On a codimension-three unfolding of the interaction of degenerate Hopf and pitchfork bifurcations. *Int. J. Bif. Chaos*, **9**(7), 1333-1362.

Algaba, A., Merino, M., Rodriguez-Luis, A.J. [1999b] Evolution of Arnold's tongues in a Z(2)-symmetric electronic circuit. *J IEICE Trans. Fund. Elect. Comm. Comp. Sci.***E82A** (9), 1714-1721.

Algaba, A., Freire, E., Gamero, E., Rodriguez-Luis, A.J. [1999c] On the Takens-Bogdanov bifurcation in the Chua's equation. *J IEICE Trans. Fund. Elect. Comm. Comp. Sci.***E82A** (9), 1722-1728.

Algaba, A., Freire, E., Gamero, E., Rodriguez-Luis, A.J. [1999d] A three-parameter study of a degenerate case of the Hopf- pitchfork bifurcation *Nonlinearity*, **12**(4), 1177-1206.

Allen, T., Moroz, I.M. [1997] Hopf-Hopf and Hopf-Steady mode interactions with O(2) symmetry in Langmuir circulations. *J. Geo. Astro. Fluid Dyn.*, **85**(3-4), 243-278.

Andronov, A.A. [1929]. Application of Poincaré's theorem on "bifurcation points" and "change in stability" to simple auto-oscillatory systems. *C.R. Acad. Sci. Paris* **189** (15), 559–561.

Andronov, A. A., Pontryagin, L. [1937] Systèmes Grossiers. *Dokl. Akad. Nauk. SSSR*, **14**, 247-251.

Andronov, A.A., Leontovich, E.A., Gordon, I.I., and Maier, A.G. [1971]. *Theory of Bifurcations of Dynamic Systems on a Plane.* Israel Program of Scientific Translations: Jerusalem.

Angenent, S. [1987] The shadowing lemma for elliptic PDE. Dynamics of infinite-dimensional systems (Lisbon, 1986), 7–22, NATO Adv. Sci. Inst. Ser. F Comput. Systems Sci., 37, Springer, Berlin.

Aranson, S. Kh., Zhuzhoma, E. V., Medvedev, V. S. [1997] Strengthening the C^r-Closing Lemma for Dynamical Systems and Foliations of the Torus. *Mathematical Notes*, **61**(3), 265-271.

Arecchi, F. T. [1987] The physics of laser chaos. *Nucl. Phys. B (Proc. Suppl.)*, **2**, 13-24.

Arioli, G., Szulkin, A. [1999] Homoclinic solutions of Hamiltonian systems with symmetry. *J. Diff. Eq.*, **158**(2), 291-313.

Armbruster, D., Chossat, P. [1991] Heteroclinic Orbits in a Spherically Invariant System. *Physica D*, **50**(2), 155-176.

Arnéodo, A., Coullet, P., and Tresser, C. [1981a]. A possible new mechanism for the onset of turbulence. *Phys. Lett.* **81A**, 197–201.

Arnéodo, A., Coullet, P., and Tresser, C. [1981b]. Possible new strange attractors with spiral structure. *Comm. Math. Phys.* **79**, 573–579.

Arnéodo, A., Coullet, P., and Tresser, C. [1982]. Oscillators with chaotic behavior: An illustration of a theorem by Shil'nikov. *J. Statist. Phys.* **27**, 171–182.

Arnéodo, A., Coullet, P., and Spiegel, E. [1982]. Chaos in a finite macroscopic system. *Phys. Lett.* **92A**, 369–373.

Arnéodo, A., Coullet, P., Spiegel, E., and Tresser, C. [1985]. Asymptotic chaos. *Physica* **14D**, 327–347.

Arnéodo, A., Argoul, F., Elezgaray, J., Richetti, P. [1993] Homoclinic chaos in chemical systems. *Physica D*, **62**, 134-169.

Arnold, L. [1998] *Random Dynamical Systems.* Springer-Verlag: New York, Heidelberg, Berlin.

Arnold, V.I. [1961] The stability of the equilibrium position of a Hamiltonian system of ordinary differential equations in the general elliptic case. *Soviet Math. Dokl.*, **2**, 247-249.

Arnold, V. I. [1963] Small Denominators and Problems of Stability of Motion in Classical and Celestial Mechanics. *Russ. Math. Surv.*, **18**(6), 85-191.

Arnold, V.I. [1963] Proof of A. N. Kolmogorov's theorem on the preservation of quasiperodic motions under small perturbations of the Hamiltonian, *Russ. Math. Surveys*, **18**(5), 9-36.

Arnold, V. I. [1965] Small Denominators I. Mappings of the Circumference onto Itself. *AMS Translations, Series 2*, **46**, pp 213-284. American Mathematical Society: Providence.

Arnold, V.I. [1972]. Lectures on bifurcations in versal families. *Russian Math. Surveys* **27**, 54–123.

Arnold, V.I. [1973]. *Ordinary Differential Equations.* M.I.T. Press: Cambridge, MA.

Arnold, V.I. [1977]. Loss of stability of self oscillations close to resonances and versal deformations of equivariant vector fields. *Functional Anal. Appl.* **11**(2), 1–10.

Arnold, V.I. [1978]. *Mathematical Methods of Classical Mechanics.* Springer-Verlag: New York, Heidelberg, Berlin.

Arnold, V.I. [1983]. *Geometrical Methods in the Theory of Ordinary Differential Equations.* Springer-Verlag: New York, Heidelberg, Berlin.

Arnold,V.I., Kozlov,V.V., and Neishtadt, A.I. [1988] *Mathematical Aspects of Classical and Celestial Mechanics* in *Dynamical Systems III*, V.I. Arnold (ed.), Springer-Verlag: New York, Heidelberg, Berlin.

Arnold, V. I., Afrajmovich, V.S., Il'yashenko, Yu. S., and Shilnikov, L. P. [1994] *Bifurcation Theory and Catastrophe Theory* in *Dynamical Systems V*, V.I. Arnold (ed.), Springer-Verlag: New York, Heidelberg, Berlin.

Ashwin, P., Buescu, J., Stewart, I. [1996] From attractor to chaotic saddle: a tale of transverse instability. *Nonlinearity*, **9**, 703-737.

Ashwin, P. [1997] Cycles homoclinic to chaotic sets; Robustness and resonance. *Chaos*, **7**(2), 207-220.

Ashwin, P., Chossat, P. [1998] Attractors for robust heteroclinic cycles with continue of connection. *J. Nonlin. Sci.*, **8**(2), 103-129.

Ashwin, P., Field, M. [1999] Heteroclinic networks in coupled cell systems. *Arch. Rat. Mech. Anal.*, **148**(2), 107-143.

Aubry, N., Holmes, P., Lumley, J. L. [1988] The dynamics od coherent structures in the wall region of a turbulent boundary layer. *J. Fluid Mech.*, **192**, 115-173.

Aubry, S. [1983a]. The twist map, the extended Frenkel–Kontorova model and the devil's staircase. *Physica* **7D**, 240–258.

Aubry, S. [1983b]. Devil's staircase and order without periodicity in classical condensed matter. *J. Physique* **44**, 147–162.

Baer, S.M., Erneux, T., and Rinzel, J. [1989]. The slow passage through a Hopf bifurcation: Delay, memory effects, and resonance. *SIAM J. Appl. Math.* **49**, 55–71.

Baesens, C. [1991] Slow Sweep Through a Period-Doubling Cascade-Delayed Bifurcations and Renormalization. *Physica D*, **53**(2-4), 319-375.

Baesens, C. [1995] Gevrey Series and Dynamic Bifurcations for Analytic Slow-Fast Mappings. *Nonlinearity*, **8**(2), 179-201.

Baider, A. [1989]. Unique normal forms for vector fields and Hamiltonians. *J. Differential Equations* **78**, 33–52.

Baider, A. and Churchill, R.C. [1988]. Uniqueness and non-uniqueness of normal forms for vector fields. *Proc. Roy. Soc. Edinburgh Sect. A* **108**, 27–33.

Bakaleinikov, L. A., Silbergleit, A. S. [1995a] On the applicability of the approximate Poincaré mapping to the analysis of dynamics induced by ODE systems I. Proximity of mappings. *Physica D*, **83**, 326-341.

Bakaleinikov, L. A., Silbergleit, A. S. [1995b] On the applicability of the approximate Poincaré mapping to the analysis of dynamics induced by ODE systems II. Proximity of coordinate partial derivatives of Poincaré mappings. *Physica D*, **83**, 342-354.

Banks, J., Brooks, J., Cairns, G., Davis, G., Stacey, P. [1992] On Devaney's definition of chaos. *Am. Math. Mon.*, **99**, 332-334.

Bargmann, V. [1961] On a Hilbert Space of Analytic Functions and an Associated Integral Transform, Part I. *Comm. Pure Appl. Math.* **14**, 187-214.

Barles, G. [1994] *Solutions de viscosité des equations de Hamilton-Jacobi*. Springer-Verlag: Berlin.

Barles, G., Sougandis, P. E. [2000a] On the large time behavior of solutions of Hamilton-Jacobi equations. *SIAM J. Math. Anal.*, **31**(4), 925-939.

Barles, G., Sougandis, P. E. [2000b] Some counterexamples on the asymptotic behavior of the solutions of Hamilton-Jacobi equations. *C. R. Acad. Sci. Paris*, **330**, Série 1, 963-968.

Batiste, O., Mercader, I., Net, M., Knobloch, E. [1999] Onset of oscillatory binary fluid convection in finite containers. *Phys. Rev. E.*, **59** (6), 6730-6741.

Batteli, F. [1994] Bifurcation from Heteroclinic Orbits with Semi-Hyperbolic Equilibria. *Ann. di Mat. Pura ed App.*, **166**,267-289.

Bazzani, A., S. Marmi, and G. Turchetti [1990] Nekhoroshev estimates for isochronous non resonant symplectic maps. *Celest. Mech.*, **47**, 333-359.

Belhaq, M., Houssni, M., Freire, E., Rodriguez-Luis, A.J. [2000] Asymptotics of homoclinic bifurcation in a three-dimensional system. *J. Nonlinear. Dyn.*,**21**(2), 135-155.

Belykh, V.N., Bykov, V.V. [1998] Bifurcations for heteroclinic orbits of a periodic motion and a saddle-focus and dynamical chaos. *Chaos, Solitons, Fractals*, **9**(1-2), 1-18.

Benedicks, M. and Carleson, L. [1991]. The Dynamics of the Hénon Map. *Annals of Mathematics*, **133**(1), 73-170.

Benettin, G., Galgani, L., Giorgilli, A., and Strelcyn, J.-M. [1980a]. Lyapunov characteristic exponents for smooth dynamical systems and for Hamiltonian systems; a method for computing all of them, Part 1: Theory. *Meccanica* **15**, 9–20.

Benettin, G., Galgani, L., Giorgilli, A., and Strelcyn, J.-M. [1980b]. Lyapunov characteristic exponents for smooth dynamical systems and for Hamiltonian systems; a method for computing all of them, Part II: Numerical application. *Meccanica* **15**, 21–30.

Benton, S. H. [1977] *The Hamilton-Jacobi Equation: A Global Approach*. Academic Press: New York.

Bessi, U. [1997] Arnold's example with three rotators. *Nonlinearity*, **10**, 763-781.

Beyn, W.J., Kleinkauf, J.M. [1997] Numerical approximation of homoclinic chaos. *Num. Alg.*, **14**(1-3), 25-53.

Beyn, W. J., Kless, W. [1998] Numerical expansions of invariant manifolds in large dynamical systems. *Numer. Math.*, **80**, 1-38.

Bi, Q.S., Yu, P. [1999b] Symbolic software development for computing the normal form of double Hopf bifurcation. *J. Math. Comp. Model.* , **29**(9), 49-70.

Birkhoff, G.D. [1927]. *Dynamical Systems*. A.M.S. Coll. Publications, vol. 9, reprinted 1966. American Mathematical Society: Providence.

Birkhoff, G.D. [1935]. Nouvelles Recherches sur les systèmes dynamiques. *Mem. Point. Acad. Sci. Novi. Lyncaei* **1**, 85–216.

Birman, J.S. and Williams, R.F. [1983a]. Knotted periodic orbits in dynamical systems I: Lorenz's equations. *Topology* **22**, 47–82.

Birman, J.S. and Williams, R.F. [1983b]. Knotted periodic orbits in dynamical systems II: Knot holders for fibred knots. *Contemp. Math.* **20**, 1–60.

Bishop, A.R., Flesch, R., Forest, M.G., McLaughlin, D.W., and Overman, E.A. [1990] Correlations between chaos in a perturbed Sine-Gordon equation and a truncated model system, *SIAM J. Math. Anal.* **21**, 1511-1536.

Blank, M. L. [1991] Shadowing of ϵ-trajectories of general multidimensional mappings. *Wiss. Z. Tech. Univ. Dresden*, **40**(2), 157–159.

Blazquez, M., Tuma, E. [1996] Chaotic behavior of orbits close to a heteroclinic contour. *Int. J. Bif. Chaos*, **6**(1), 69-79.

Bogdanov, R.I. [1975]. Versal deformations of a singular point on the plane in the case of zero eigenvalues. *Functional Anal. Appl.* **9**(2), 144–145.

Bolle, P., Buffoni, B. [1999] Multibump homoclinic solutions to a centre equilibrium in a class of autonomous Hamiltonian systems. *Nonlinearity*, **12**(6), 1699-1716.

Bolotin, S., MacKay, R. [1997] Multibump orbits near the anti-integrable limit for Lagrangian systems. *Nonlinearity*, **10**(5), 1015-1029.

Bonatti, C., Diaz, L. J., Turcat, G. [2000] There is no "shadowing lemma" for partially hyperbolic dynamics. *Comp. Rend. Acad. Sci. ser. I–Math.*, **330**(7), 587-592.

Bowen, R. [1970a] Markov partitions for Axiom *A* diffeomorphisms. *Amer. J. Math.*, **92**(3), 725-747.

Bowen, R. [1970b] Markov partitions and minimal sets for Axiom *A* diffeomorphisms. *Amer. J. Math.*, **92**(4), 907-918.

Bowen, R. [1972] Periodic orbits for hyperbolic flows. *Amer. J. Math.*, **94**(1), 1-30.

Bowen, R. [1973] Symbolic dynamics for hyperbolic flows. *Amer. J. Math.*, **95**(2), 429-460.

Bowen, R. [1975a] *Equilibrium states and the ergodic theory of Anosov diffeomorphisms.* Springer Lecture Notes in Mathematics. No. 470, Springer-Verlag: Berlin.

Bowen, R. [1975b] A horseshoe with positive measure. *Invent. Math.*, **293**, 203–204.

Bowen, R. [1978]. *On Axiom A Diffeomorphisms.* CBMS Regional Conference Series in Mathematics, vol. 35. A.M.S. Publications: Providence.

Boxler, P. [1989] A Stochastic Version of Center Manifold Theory. *Probab. Th. Rel. Fields*, **83**, 509-545.

Boxler, P. [1991] How to Construct Stochastic Center Manifolds on the Level of Vector Fields. *Springer-Verlag Lecture Notes in Mathematics*, **1486**, 141-158.

Boyce, W.E. and DiPrima, R.C. [1977]. *Elementary Differential Equations and Boundary Value Problems.* Wiley: New York.

Bridges, T. J., Reich, S. [2001] Computing Lyapunov exponents on a Stiefel manifold. *Physica D*, **156**, 219-238.

Broer, H.W. and Vegter, G. [1984]. Subordinate Sil'nikov bifurcations near some singularities of vector fields having low codimension. *Ergodic Theory and Dynamical Systems* **4**, 509–525.

Bronstein, I. U. and A. Ya. Kopanskii [1994]. *Smooth Invariant Manifolds and Normal Forms.* World Scientific: Singapore.

Brown, R. and L. O. Chua [1996a] Clarifying Chaos: Examples and Counterexamples. *Int. J. Bif. Chaos*, **6**(1), 219-249.

Brown, R. and L. O. Chua [1996b] From Almost Periodic to Chaotic: The Fundamental Map. *Int. J. Bif. Chaos*, **6**(6), 1111-1125.

Brown, R. and L. O. Chua [1998] Clarifying Chaos II: Bernoulli Chaos, Zero Lyapunov Exponents and Strange Attractors. *Int. J. Bif. Chaos*, **8**(1), 1-32.

Bryuno, A.D. [1988]. The normal form of a Hamiltonian system. *Russian Math. Surveys*, **43**(1), 25-66.

Bryuno, A.D. [1989a]. *Local Methods in Nonlinear Differential Equations. Part I. The Local Method of Nonlinear Analysis of Differential Equations. Part II. The Sets of Analyticity of a Normalizing Transformation.* Springer-Verlag: New York, Heidelberg, Berlin.

Bryuno, A.D. [1989b]. Normalization of a Hamiltonian system near an invariant cycle or torus. *Russian Math. Surveys*, **44**(2), 53-89.

Bryuno, A.D. [1989c]. On the Question of Stability in a Hamiltonian System. Dynamical Systems and Ergodic Theory, Banach Center Publications, vol. 23. PWN-Polish Scientific Publishers:Warsaw.

Buffoni, B. [1993] Cascade of homoclinic orbits for Hamiltonian systems-further results. *Nonlinearity*, **6**(6), 1091-1092.

Burgoyne, N., Cushman, R. [1977a] Normal forms for real linear Hamiltonian systems, in "the 1976 NASA Conference on Geometric Control Theory", pp. 483-529, Math. Sci. Press, Brookline, MA, 1977.

Burgoyne, N., Cushman, R. [1977b] Conjugacy classes in linear groups. *J. Algebra*, **44**, 339-362.

Bushard, L. B. [1973] Periodic Solutions and Locking in on the Periodic Surface. *Int. J. Nonlinear Mech.*, **8**, 129-141.

Bushard, L. B. [1972] Behavior of the Periodic Surface for a Periodically Perturbed Autonomous System and Periodic Solutions. *J. Diff. Eq.*, **12**, 487-503.

Bylov, B.F., Vinograd, R.E., Grobman, D.M., and Nemyckii, V.V. [1966]. *Theory of Liapunov Characteristic Numbers.* Moscow (Russian).

Byrd, P.F. and Friedman, M.D. [1971]. *Handbook of Elliptic Integrals for Scientists and Engineers.* Springer-Verlag: New York, Heidelberg, Berlin.

Camassa, R., Kovacic, G., Tin, S.K.[1998] A Melnikov method for homoclinic orbits with many pulses. *Arch. Rat. Mech. Anal.*, **143**(2), 105-193.

Campbell, S. A., Holmes, P. [1991] Bifurcation from O(2) Symmetrical Heteroclinic Cycles with 3 Interacting Modes. *Nonlinearity*, **4**(3), 697-726.

Campbell, S.A. [1999] Stability and bifurcation in the harmonic oscillator with multiple, delayed feedback loops. *Dyn. Cont. Disc. Imp. Sys.*, **5**(1-4), 225-235.

Carr, J. [1981]. *Applications of Center Manifold Theory.* Springer-Verlag: New York, Heidelberg, Berlin.

Carr, J., Chow, S.-N., and Hale, J.K. [1985]. Abelian integrals and bifurcation theory. *J. Differential Equations* **59**, 413–436.

Carroll, T. L. [1999] Approximating Chaotic Time Series Through Unstable Periodic Orbits. *Phys. Rev. E.*, **59**(2), 1615-1621.

Cassels, J. W. S. [1957] *An Introduction to Diophantine Approximation.* Cambridge University Press: Cambridge.

Celletti, A. and Chierchia, L. [1988]. Construction of analytic KAM surfaces and effective stability bounds. *Comm. Math. Phys.* **118**, 119–161.

Champneys, A. R. [1994] Subsidiary Homoclinic Orbits to a Saddle-Focus for Reversible Systems. *Int. J. Bif. Chaos*, **4**(6), 1447-1482.

Champneys, A. R., Toland, J. F. [1993] Bifurcation of a plethora of multimodal homoclinic orbits for autonomous Hamiltonian systems. *Nonlinearity*, **6**(5), 665-721.

Champneys, A. R., Harterich, J., Sandstede, B. [1996] A nontransverse homoclinic orbit to a saddle-node equilibrium. *Ergod. Th. Dyn. Sys.*, **16**(3), 431-450.

Champneys, A. R., Kuznetsov, Y. A., Sandstede, B. [1996] A numerical toolbox for homoclinic bifurcation analysis. *Int. J. Bif. Chaos*, **6**(5), 867-887.

Champneys, A.R., Rodriguez-Luis, A.J. [1999] The non-transverse Shil'nikov-Hopf bifurcation: uncoupling of homoclinic orbits and homoclinic tangencies. *Physica D*, **128**(2-4), 130-158.

Champneys, A.R., Harterich, J. [2000] Cascades of homoclinic orbits to a saddle-centre for reversible and perturbed Hamiltonian systems. *Dyn. Stab. Sys* **15**(3), 231-252.

Chen, G., Della Dora, J. [1999] Normal forms for differentiable maps near a fixed point. *Numerical Algorithms*, **22**, 213-230.

Chernyshev, V. E. [1985] Structure of the neighborhood of a homoclinic contour with a saddle-point flow. *Diff. Eq.*, **21**(9), 1038-1042.

Chernyshev, V.E. [1997] Perturbation of heteroclinic cycles containing saddle-foci. *Diff. Eq.*, **33**(5), 717-719.

Chicone, C. [1999] *Ordinary Differential Equations with Applications.* Springer-Verlag: New York, Heidelberg, Berlin.

Chillingworth, D.R.J. [1976]. *Differentiable Topology with a View to Applications.* Pitman: London.

Chorin, A.J. and Marsden, J.E. [1979]. *A Mathematical Introduction to Fluid Mechanics.* Springer-Verlag: New York, Heidelberg, Berlin.

Chossat, P., Armbruster, D. [1991] Structurally Stable Heteroclinic Cycles in a System with O(3) Symmetry. *Springer-Verlag Lecture Notes in Mathematics*, **1463**, 38-62.

Chossat, P., Krupa, M., Melbourne, I., Scheel, A. [1997] Transverse bifurcations of homoclinic cycles.*Physica D*, **100**(1-2), 85-100.

Chossat, P., Guyard, F., Lauterbach, R. [1999] Generalized heteroclinic cycles in spherically invariant systems and their perturbations. *J. Nonlin. Sci.*,**9**(5), 479-524.

Chow, S.-N. and Hale, J.K. [1982]. *Methods of Bifurcation Theory.* Springer-Verlag: New York, Heidelberg, Berlin.

Chow, S.-N., Li, C., and Wang, D. [1989]. Uniqueness of periodic orbits of some vector fields with codimension two singularities. *J. Differential Equations* **77**, 231–253.

Chow, S.-N., Lin, X.-B., and Palmer, K. J. [1989]. A shadowing lemma with applications to semilinear parabolic equations. *SIAM J. Math. Anal.*, **20**(3), 547-557.

Chow, S. -N., Drachman, B., Wang, D. [1990] Computation of Normal Forms. *J. Comp. Appl. Math.*, **29**, 129-143.

Chow, S.-N., Deng, B., Terman, D. [1990] The bifurcation of homoclinic and periodic orbits from two heteroclinic orbits. *SIAM. J. Math. Anal.*, **21**(1), 179-204.

Chow, S.-N., Deng, B., Terman, D. [1991] The bifurcation of homoclinic orbits from two heteroclinic orbits-a topological approach.*Applicable Analysis*, **42**, 275-299.

Chow, S.-N.,Van Vleck, E. S. [1992/93] A shadowing lemma for random diffeomorphisms. *Random Comput. Dynam.*, **1**(2), 197–218.

Chow, S.-N., Yi, Y. [1994] Center manifold and stability for skew-product flows. *J. Dynam. Differential Equations* **6**(4), 543–582.

Chow, S.N., Deng, B., Friedman, M.J. [1999] Theory and application of a nongeneric heteroclinic loop bifurcation. *SIAM J. App. Math.*, **59**(4), 1303-1321.

Chow, S. N., Liu, W., Yi, Y. F. [2000] Center manifolds for smooth invariant manifolds. *Trans. Am. Math. Soc.*, **352**(11), 5179-5211.

Chu, C.-K., Koo, K.-S. [1996] Recurrence and the shadowing property. *Topology Appl.*, **71**(3), 217–225.

Churchill, R. C., M. Kummer, and D. L. Rod [1983] On Averaging, Reduction, and Symmetry in Hamiltonian Systems. *J. Diff. Eq.*, **49**, 359-414.

Churchill, R. C., Rod, D. L. [1986] Homoclinic and heteroclinic orbits of reversible vector-fields under perturbation. *P. Roy. Soc. Edinb. A*, —bf 102, 345-363, part 3-4.

Churchill, R. C., Kummer, M. [1999] A unified approach to linear and nonlinear normal forms for Hamiltonian systems. *J. Symbolic Computation*, **27**, 49-131.

Coddington, E. A., Levinson, N. [1955] *Theory of Ordinary Differential Equations.* McGraw-Hill: New York.

Colonius, F., Kliemann, W. [1996a] The Morse spectrum of linear flows on vector bundles. *Trans. AMS*, **348**(11), 4355-4388.

Colonius, F., Kliemann, W. [1996b] The Lyapunov spectrum of families of time-varying matrices. *Trans. AMS*, **348**(11), 4389-4408.

Conley, C. [1978]. *Isolated Invariant Sets and the Morse Index.* CBMS Regional Conference Series in Mathematics, vol. 38.
American Mathematical Society: Providence.

Coomes, B. A., Kocak, H.,Palmer, K. J. [1993] Periodic shadowing. Chaotic numerics (Geelong, 1993), 115–130, *Contemp. Math.*, 172, Amer. Math. Soc., Providence, RI.

Coomes, B. A., Kocak, H.,Palmer, K. J. [1994a] Shadowing in discrete dynamical systems. Six lectures on dynamical systems (Augsburg, 1994), 163–211, World Sci. Publishing, River Edge, NJ.

Coomes, B. A., Kocak, H.,Palmer, K. J. [1994b] Shadowing orbits of ordinary differential equations. Oscillations in nonlinear systems: applications and numerical aspects. *J. Comput. Appl. Math.*, **52**(1-3), 35–43.

Coomes, B. A., Kocak, H.,Palmer, K. J. [1995a] Rigorous computational shadowing of orbits of ordinary differential equations. *Numer. Math.*, **69**(4), 401–421.

Coomes, B. A., Kocak, H.,Palmer, K. J. [1995b] A shadowing theorem for ordinary differential equations. *Z. Angew. Math. Phys.*, **46**(1), 85–106.

Coomes, B.A., Kocak, H., Palmer, K. J. [1997] Long periodic shadowing. Dynamical numerical analysis (Atlanta, GA, 1995). *Numer. Algorithms*, **14**(1-3), 55–78.

Coomes, B. A. [1997] Shadowing orbits of ordinary differential equations on invariant submanifolds. *Trans. Amer. Math. Soc.*, **349**(1), 203–216.

Coppel, W. A. [1978] *Dichotomies in Stability Theory.* Springer Lecture Notes in Mathematics, vol. 629. Springer-Verlag: New York, Heidelberg, Berlin.

Corless, R. M. [1992] Defect-controlled numerical methods and shadowing for chaotic differential equations. Experimental mathematics: computational issues in nonlinear science (Los Alamos, NM, 1991). *Phys. D*, **60**(1-4), 323–334.

Coullet, P. and Spiegel, E.A. [1983]. Amplitude equations for systems with competing instabilities. *SIAM J. Appl. Math.* **43**, 774–819.

Courant, R., Hilbert, D. [1962] *Methods of Mathematical Physics. Volume II. Partial Differential Equations.* Wiley: New York.

Cushman, R. and Sanders, J.A. [1986]. Nilpotent normal forms and representation theory of $sl(2, R)$. In *Multi-Parameter Bifurcation Theory,* M. Golubitsky and J. Guckenheimer (eds.) Contemporary Mathematics, vol. 56. American Mathematical Society, Providence.

Cvitanović, P. [1995] Dynamical Averaging in Terms of Periodic Orbits. *Physica D*, **83**, 109-123.

Dawes, J.H.P. [2000] The $1 : \sqrt{2}$ Hopf/steady-state mode interaction in three- dimensional magnetoconvection. *Physica D*, **139**(1-2), 109-136.

Dawson, S., Grebogi, C., Sauer, T., Yorke, J. A. [1994] Obstructions to shadowing when a Lyapunov exponent fluctuates about zero. *Phys. Rev. Lett.*, **73**(14), 1927-1930.

de Blasi, F. S., Schinas, J. [1973] On the stable manifold theorem for discrete time dependent processes in Banach spaces. *Bull. London Math. Soc.*, **5**, 275-282.

Degtiarev, E.V., Wataghin, V. [1998] Takens-Bogdanov bifurcation in a two-component nonlinear optical system with diffractive feedback. *J. Mod. Opt.*, **45**(9), 1927-1942.

Deng, B. [1989a] Exponential expansion with Silnikov's saddle-focus. *J. Diff. Eq.*, **82**, 156-173.

Deng, B. [1989b] The Silnikov problem, exponential expansion, strong λ-lemma, C^1-linearization, and homoclinic bifurcation. *J. Diff. Eq.*, **79**, 189-231.

Deng, B. [1990] Homoclinic bifurcations with nonhyperbolic equilibria. *SIAM J. Math. Anal.*, **21**(3), 693-720.

Deng, B. [1991] The bifurcations of countable connections from a twisted heteroclinic loop. *SIAM J. Math. Anal.*, **22**(3), 653-679.

Deng, B. [1992] The transverse homoclinic dynamics and their bifurcations at nonhyperbolic fixed-points. *T. Am. Math. Soc*, **331**(1), 15-53.

Deng, B. [1993] On Silnikov's homoclinic-saddle-focus theorem. *J. Diff. Eq.*, **102**, 305-329.

Devaney, R. [1976] Homoclinic orbits in Hamiltonian systems. *J. Diff. Eq.*, **21**, 431-438.

Devaney, R. [1978] Transversal homoclinic orbits in an integrable system. *Amer. J. Math.*, **100**, 631-642.

Devaney, R. L., Nitecki, Z. [1979] Shift automorphisms in the Hénon mapping. *Comm. Math. Phys.*, **67**, 137-148.

Devaney, R.L. [1986]. *An Introduction to Chaotic Dynamical Systems.* Benjamin/Cummings: Menlo Park, CA.

Dhamala, M., Lai, Y.-C. [1999] Unstable periodic orbits and the natural measure of nonhyperbolic chaotic saddles. *Phys. Rev. E*, **60**(5), 6176-6179.

Diaz, L. J., Ures, R. [1994] Persistent homoclinic tangencies and the unfoldingof cycles. *Ann. Inst. Henri Poincaré–An. Nonlin.*, **11**(6), 643-659.

Diaz, L. J. [1995] Persistence of cycles and nonhyperbolic dynamics at heteroclinic bifurcations. *Nonlinearity*, **8**(5), 693-713.

Diaz, L. J., Rocha, J., Viana, M. [1996] Strange attractors in saddle-node cycles: prevalence and globality. *Inv. Math.*, **125**(1), 37-74.

Diaz, L. J., Rocha, J. [1997a] Large measure of hyperbolic dynamics when unfolding heteroclinic cycles. *Nonlinearity*, **10**(4), 857-884.

Diaz, L. J., Rocha, J. [1997b] Non-critical saddle-node cycles and robust non-hyperbolic dynamics. *Dyn. Stab. Sys.*, **12**(2), 109-135.

Diaz, L. J., Pujals, E. R., Ures, R. [1999] Partial hyperbolicity and robust transitivity. *Act. Math.*, **183**(1), 1-43.

Dieci, L., Rusell, R. D., Van Vleck, E. S. [1997] On the computation of Lyapunov exponents for continuous dynamical systems. *SIAM J. Numer. Anal.*, **34**(1), 402-423.

Dieci, L., Eirola, T. [1999] On smooth decompositions of matrices. *SIAM J. Matrix Anal. Appl.*, **20**(3), 800-819.

Dieci, L., Van Vleck, E. S. [1999] Computation of orthonormal factors for fundamental solution matrices. *Numer. Math.*, **83**, 599-620.

Dieci, L. [2002] Jacobian free computation of Lyapunov exponents. *J. Dyn. Diff. Eq.*, **14**(3), 697-717.

Dieci, L., Van Vleck, E. S. [2002] Lyapunov spectral intervals: Theory and Computation. *SIAM J. Numer. Anal.*, **40**(2), 516-542.

Ding, Y.H.[1998] Infinitely many homoclinic orbits for a class of Hamiltonian systems with symmetry. *Chin. Ann. Math., ser. B*, **19**(2), 167-178.

Ding, Y.H., Willem, M. [1999] Homoclinic orbits of a Hamiltonian system. *Z. Angew. Math. Phys.*, **50**(5), 759-778.

Ding, Y.H., Girardi, M. [1999] Infinitely many homoclinic orbits of a Hamiltonian system with symmetry. *Nonlin. Anal.-Th., Meth., App.*, **38**(3), 391-415.

Dodson, M. M., Rynne, B. P., and Vickers, J. A. G. [1989] Averaging in Multifrequency Systems. *Nonlinearity*, **2**, 137-148.

Doedel, E. J., Friedman, M. J. [1989] Numerical Computation of Heteroclinic Orbits. *J. Comp. App. Math.*, **26**(1-2), 155-170.

Douady, R. [1982] Une démonstration directe de l'équivalence des théoremes de tores invariants pour difféomorphismes et champs de vecteurs. *C. R. Acad. Sc. Paris*, **295**, 201-204.

Duarte, P. [1999] Abundance of elliptic isles at conservative bifurcations. *Dyn. Stab. Sys.*, **14**(4), 339-356.

Dubrovin, B.A., Fomenko, A.T., and Novikov, S.P. [1984]. *Modern Geometry—Methods and Applications, Part I. The Geometry of Surfaces, Transformation Groups, and Fields.* Springer-Verlag: New York, Heidelberg, Berlin.

Dugundji, J. [1966]. *Topology.* Allyn and Bacon: Boston.

Easton, R.W. [1986]. Trellises formed by stable and unstable manifolds in the plane. *Trans. Amer. Math. Soc.* **294**, 714–732.

Eckmann, J.-P., Ruelle, D. [1985] Ergodic theory of chaos and strange attractors. *Rev. Mod. Phys.*, **57**(3), 617-656.

Eliasson, L.H. [1988] Perturbations of stable invariant tori, *Ann. Sci. Norm. Super. Pisa Cl. Sci. IV.*, Ser. **15**,115.

Ellison, J. A., Saenz, A. W., and Dumas, S. [1990] Improved N^{th} order averaging theory for periodic systems. *J. Diff. Eq.*, **84**(2), 383-403.

Elphick, C., Tirapegui, E., Brachet, M.E., Coullet, P., and Iooss, G. [1987]. A simple global characterization for normal forms of singular vector fields. *Physica* **29D**, 95–127.

Erneux, T. and Mandel, P. [1986]. Imperfect bifurcation with a slowly varying control parameter. *SIAM J. Appl. Math.* **46**, 1–16.

Evans, J.W., Fenichel, N., and Feroe, J.A. [1982]. Double impulse solutions in nerve axon equations. *SIAM J. Appl. Math.* **42**(2), 219–234.

Evans, L. C., Gomes, D. [2001] Effective Hamiltonians and Averaging for Hamiltonian Dynamics I. *Arch. Rat. Mech. Anal.*, **157**, 1-33.

Farmer, J. D., Sidorowich, J. J. [1991] Optimal shadowing and noise reduction. *Phys. D*, **47**(3), 373–392.

Fasso, F., Guzzo, M., Benettin, G. [1998] Nekhoroshev-stability of elliptic equilibria of Hamiltonian systems. *Comm. Math. Phys.*, **197**(2), 347-360.

Fathi, A. [1997] Solutions KAM faibles conjuguées et barrières de Peierls. *C. R. Acad. Sci. Paris*, **325**, Série 1, 649-652.

Fathi, A. [1998] Orbites hétéroclines et ensemble de Peierls. *C. R. Acad. Sci. Paris*, **326**, Série 1, 1213-1216.

Fečkan, M. [1991] A remark on the shadowing lemma. *Funkcial. Ekvac.*, **34**(3), 391–402.

Feng, B. Y. [1991] The Stability of a Heteroclinic Cycles for the Critical Case. *Sci. China ser. A-Math., Phys., Astron.*, **34**(8), 920-934.

Feng, Z.C. and Wiggins, S. [1993] On the existence of chaos in a class of two-degree-of-freedom, damped, strongly parametrically forced mechanical systems with broken $O(2)$ symmetry, *ZAMP*, **44**, 201-248.

Fenichel, N. [1971]. Persistence and smoothness of invariant manifolds for flows. *Indiana Univ. Math. J.* **21**, 193–225.

Fenichel, N. [1974] Asymptotic stability with rate conditions. *Ind. Univ. Math. J.*, **23**, 1109–1137.

Fenichel, N. [1977] Asymptotic stability with rate conditions, II. *Ind. Univ. Math. J.*, **26**, 81–93.

Fenichel, N. [1979] Geometric singular perturbation theory for ordinary differential equations. *J. Diff. Eqns.*, **31**, 53–98.

Ferrer, S., Lara, M., Palacián, J., San Juan, J. F., Viartola, A., Yanguas, P. [1998] The Hénon-Heiles Problem in Three Dimensions. I. Periodic Orbits Near the Origin. *Int. J. Bif. Chaos.*, **8** (6), 1199-1213.

Field, M., Swift, J. W. [1991] Stationary Bifurcation to Limit Cycles and Heteroclinic Cycles. *Nonlinearity*, **4**(4), 1001-1043.

Fowler, A. C., Sparrow, C. T. [1990] Bifocal homoclinic orbits in 4 dimensions. *Nonlinearity*, **4**(4), 1159-1182.

Fowler, A. C. [1990] Homoclinic orbits in N dimensions. *Stud. Appl. Math.*, **83**(3), 193-209.

Franks, J.M. [1982]. *Homology and Dynamical Systems.* CBMS Regional Conference Series in Mathematics, vol. 49. A.M.S. Publications: Providence.

Friedlin, M. I. and Wentzell, A. D. [1984] *Random Perturbations of Dynamical Systems.* Springer-Verlag: New York, Heidelberg, Berlin.

Fryska, S.T., Zohdy, M. A.[1992] Computer dynamics and shadowing of chaotic orbits. *Phys. Lett. A*, **166**(5-6), 340–346.

Galin, D. M. [1972] On real matrices depending on parameters. *Uspekhi Math. Nauka*, **27**(1), 241-242.

Galin, D.M. [1982]. Versal deformations of linear Hamiltonian systems. *Amer. Math. Soc. Trans.* **118**, 1–12.

Gallavotti, G., Gentile, G., Mastropietro, V. [2000] Hamilton-Jacobi equation, heteroclinic chains, and Arnol'd diffusion in three time scale systems. *Nonlinearity*, **13**(2), 323-340.

Gambaudo, J.M. [1985]. Perturbation of a Hopf bifurcation by external time-periodic forcing. *J. Differential Equations* **57**, 172–199.

Gantmacher, F.R. [1977]. *Theory of Matrices,* vol. 1. Chelsea: New York.

Gantmacher, F.R. [1989]. *Theory of Matrices,* vol. 2. Chelsea: New York.

Gaspard, P. [1983]. Generation of a countable set of homoclinic flows through bifurcation. *Phys. Lett.* **97A**, 1–4.

Gaspard, P. and Nicolis, G. [1983]. What can we learn from homoclinic orbits in chaotic systems? *J. Statist. Phys.* **31**, 499–518.

Gaspard, P., Kapral, R., and Nicolis, G. [1984]. Bifurcation phenomena near homoclinic systems: A two parameter analysis. *J. Statist. Phys.* **35**, 697–727.

Gavrilov, N.K. and Silnikov, L.P. [1972]. On three dimensional dynamical systems close to systems with a structurally unstable homoclinic curve, I. *Math. USSR-Sb.* **17**, 467–485.

Gavrilov, N.K. and Silnikov, L.P. [1973]. On three dimensional dynamical systems close to systems with a structurally unstable homoclinic curve, II. *Math. USSR-Sb.* **19**, 139–156.

Ghosh, S., Leonard, A., Wiggins [1998] Diffusion of a passive scalar from a no-slip boundary into a two-dimensional chaotic advection field. *Journal of Fluid Mechanics*, **372**, 119-163.

Ghrist, R. W., Holmes, P. J., Sullivan, M. C. [1997] Knots and links in three-dimensional flows. Lecture Notes in Mathematics, **1654**. Springer-Verlag:Berlin.

Gibson, C.G. [1979]. *Singular Points of Smooth Mappings.* Pitman: London.

Gilmore, R. [1998] Topological analysis of chaotic dynamical systems. *Rev. Mod. Phys.*, **70**(4), 1455-1529.

Gils, S. A. van [1984] *Some Studies in Dynamical Systems Theory.* Thesis, Vrije Universitet, Amsterdam.

Glasner, E., Weiss, B. [1993] Sensitive dependence on initial conditions. *Nonlinearity*, **6**, 1067-1075.

Glendinning, P. and Sparrow, C. [1984]. Local and global behavior near homoclinic orbits. *J. Statist. Phys.* **35**, 645–696.

Glendinning, P., Tresser, C. [1985]Heteroclinic Loops Leading to Hyperchaos. *J. de Phys. Lett.*, **46**(8), L347-L352.

Glendinning, P. [1987] Asymmetric perturbations of Lorenz-like equations. *Dyn. Stab. Sys.*, **2**(1), 43–53.

Glendinning, P. [1989] Subsidiary bifurcations near bifocal homoclinic orbits. *Math. Proc. Cambridge*, **105**:597-605, part 3.

Glendinning, P., Laing, C. [1996] A homoclinic hierarchy. *Phys. Lett. A*, **211**(3), 155-160.

Glendinning, P [1997] Differential equations with bifocal homoclinic orbits. . *Int. J. Bif. Chaos*, **7**(1), 27-37.

Goggin, M.E. and Milonni, P.W. [1988]. Driven Morse oscillator: Classical chaos, quantum theory, and photodissociation. *Phys. Rev. A* **37**, 796–806.

Goldhirsch, I., Sulem, P.-L., and Orszag, S.A. [1987]. Stability and Lyapunov stability of dynamical systems: A differential approach and a numerical method. *Physica* **27D**, 311–337.

Goldstein, H. [1980]. *Classical Mechanics,* 2nd ed. Addison-Wesley: Reading, MA.

Golubitsky, M. and Guillemin, V. [1973]. *Stable Mappings and Their Singularities.* Springer-Verlag: New York, Heidelberg, Berlin.

Golubitsky, M. and Schaeffer, D.G. [1985]. *Singularities and Groups in Bifurcation Theory,* vol. 1. Springer-Verlag: New York, Heidelberg, Berlin.

Golubitsky, M. and Stewart, I. [1987]. Generic bifurcation of Hamiltonian systems with symmetry. *Physica* **24D**, 391–405.

Golubitsky, M., Stewart, I., and Schaeffer, D.G. [1988]. *Singularities and Groups in Bifurcation Theory,* vol. 2. Springer-Verlag: New York, Heidelberg, Berlin.

Golubitsky, M. and J. E. Marsden [1983] The Morse Lemma in Infinite Dimensions via the Deformation Method. *SIAM J. Math. Anal.*, **14**(6), 1037-1044.

Golubitsky, M., M. Krupa, C. Lim [1991] Time-reversibility and particle sedimentation. *SIAM J. Appl. Math.* **51**, 49-72.

Golubitsky, M. G., J. E. Marsden, I. Stewart, M. Dellnitz [1995] The Constrained Lyapunov-Schmidt Procedure and Periodic Orbits. *Fields Institute Communications*, **4**, pp. 81-127, W. F. Langford and W. Nagata, eds. American Mathematical Society: Providence.

Golubitsky, M., LeBlanc, V.G., Melbourne, I. [1997] Meandering of the spiral tip: An alternative approach. *J. Non. Sci.*, **7**(6), 557-586.

Gomes, D. A. [2001a] A stochstic analog of Aubry-Mather theory. preprint.

Gomes, D. A. [2001b] Viscosity solutions of Hamilton-Jacobi Equations, and Asymptotics for Hamiltonian Systems. preprint.

Gomes, D. A. [2001c] Regularity theory for Hamilton-Jacobi equations. preprint.

Gonchenko, S. V., Silnikov, L. P., Turaev, D. V. [1996] Dynamical phenomena in systems with structurally unstable Poincaré homoclinic orbits. [*Chaos*, **6**(1), 15-31.

Gonchenko, S. V., Turaev, D. V., Gaspard, P., Nicolis, G. [1997] Complexity in the bifurcation structure of homoclinic loops to a saddle focus. *Nonlinearity*, **10**, 409-423.

Gonchenko, S. V., Silnikov, L. P., Turaev, D. V. [1997] Quasiattractors and homoclinic tangencies. *Comp. Math. App*, **34**(2-4), 195-227.

Gonchenko, S. V., Silnikov, L. P. [2000] On two-dimensional area-preserving diffeomorphisms with infinitely many elliptic islands. *J. Stat. Phys.*, **101**(1/2), 321-356.

Grebogi, C., Ott, E., and Yorke, J.A. [1985]. Attractors on an N-torus: Quasiperiodicity versus chaos. *Physica* **15D**, 354–373.

Grebogi, C., Hammel, S. M., Yorke, J. A., Sauer, T. [1990] Shadowing of physical trajectories in chaotic dynamics–containment and refinement. *Phys. Rev. Lett.*, **65**(13), 1527-1530.

Grobman, D.M. [1959]. Homeomorphisms of systems of differential equations. *Dokl. Akad. Nauk SSSR* **128**, 880.

Grüne, L., Kloeden, P. E. [2001] Discretization, inflation, and perturbation of attractors. in *Ergodic Theory, Analysis, and Efficient Simulation of Dynamical Systems*. B. Fiedler, ed., pp. 399- 416. Springer-Verlag:Berlin.

Guckenheimer, J. and Williams, R.F. [1980]. Structural stability of the Lorenz attractor. *Publ. Math. IHES* **50**, 73–100.

Guckenheimer, J. and Holmes, P.J. [1983]. *Nonlinear Oscillations, Dynamical Systems, and Bifurcations of Vector Fields*. Springer-Verlag: New York, Heidelberg, Berlin.

Guckenheimer, J., Holmes, P. [1988] Structurally Stable Heteroclinic Cycles. *Math. Proc. Camb. Phil. Soc.*, **103**, 189-192.

Guckenheimer, J. [1981]. On a codimension two bifurcation. In *Dynamical Systems and Turbulence,* D.A. Rand and L.S. Young (eds.), pp. 99–142. Springer Lecture Notes in Mathematics, vol. 898. Springer-Verlag: New York, Heidelberg, Berlin.

Guckenheimer, J. and Johnson, S. [1990]. Distortion of S-unimodal maps. *Annals of Mathematics*, **132**(1), 71-130.

Guillemin, V. and Pollack, A. [1974] *Differential Topology*. Prentice Hall, inc.:Englewood Cliffs.

Guillemin, V. and S. Sternberg [1984] *Symplectic Techniques in Phys ics*. Cambridge University Press: Cambridge.

Gustavson, F. G. [1966] On Constructing Formal Integrals Near of an Hamiltonian System Near an Equilibrium Point. *Astron. J.*, **71**, 670-686.

Haberman, R. [1979]. Slowly varying jump and transition phenomena associated with algebraic bifurcation problems. *SIAM J. Appl. Math.* **37**, 69–105.

Hadamard, J. [1898]. Les surfaces à curbures opposés et leurs lignes géodesiques. *Journ. de Math.* **5**, 27–73.

Hadamard, J. [1901]. Sur l'iteration et les solutions asymptotiques des equations différentielles. *Bull. Soc. Math. France*, **29**, 224–228.

Hadeler, K. P. [1996] Shadowing orbits and Kantorovich's theorem. *Numer. Math.*, **73**(1), 65–73.

Hale, J. [1980]. *Ordinary Differential Equations*. Robert E. Krieger Publishing Co., Inc.: Malabar, Florida.

Hale, J.K. and Lin, X.-B. [1986]. Symbolic dynamics and nonlinear semiflows. *Ann. Mat. Pura Appl.* **144**(4), 224–259.

Hall, G. R. [1984]. Resonance Zones in Two Parameter Families of Circle Homeomorphisms. *SIAM J. Math. Anal.*, **15**, 1075-1081.

Hall, T. [1994] The creation of horseshoes. *Nonlinearity*, **7**, 861-924.

Haller, G., and Wiggins, S. [1993] Orbits Homoclinic to Resonances: The Hamiltonian Case. *Physica D*, **66**, 298-346.

Haller, G., and Wiggins, S. [1995] N-Pulse Homoclinic Orbits in Perturbations of Hyperbolic Manifolds of Hamiltonian Equilibria. *Arch. Rat. Mech. Anal.***130**, 25-101.

Haller, G., and Wiggins, S. [1996] Geometry and Chaos Near Resonant Equilibria of 3- DOF Hamiltonian Systems, *Physica D*, **90**, 319-365.

Han, M.A. [1998] Bifurcations of limit cycles from a heteroclinic cycle of Hamiltonian systems. *Chin. Ann. Math. ser. B*, **19**(2), 189-196.

Hardy, G. H. and E. M. Wright [1938] *An Introduction to the Theory of Numbers.* Oxford University Press: Oxford.

Hartman, P. [1964] *Ordinary Differential Equations.* Wiley: New York.

Hassard, B.D., Kazarinoff, N.D., and Wan, Y.-H. [1980]. *Theory and Applications of the Hopf Bifurcation.* Cambridge University Press: Cambridge.

Hastings, S. [1982]. Single and multiple pulse waves for the Fitzhugh–Nagumo equations. *SIAM J. Appl. Math.* **42**, 247–260.

Hausdorff, [1962]. *Set Theory.* Chelsea: New York.

Hayashi, S. [1997] Connecting Invariant Manifolds and the Solution of the C^1 Stability and Ω-Stability Conjectures for Flows. *Ann. Math.*, **145**, 81-137. See also the correction in *Ann. Math.*, **150**, 1999, 353-356.

Haykin, S. [1994] *Neural Networks, A Comprehensive Introduction.* Macmillan:New York.

Henrard, J. [1970]. Periodic Orbits Emanating From a Resonant Equilibrium. *Celestial Mechanics*, **1**, 437-466.

Henry, D. [1981]. *Geometric Theory of Semilinear Parabolic Equations.* Springer Lecture Notes in Mathematics, vol. 840. Springer-Verlag: New York, Heidelberg, Berlin.

Henry, D.B. [1994] Exponential dichotomies, the shadowing lemma and homoclinic orbits in Banach spaces. Dynamical phase transitions (São Paulo, 1994). *Resenhas*, **1**(4), 381–401.

Herman, M. R. [1977] Mesure de Lebesgue et nombre de rotation. *Lecture Notes in Mathematics*, **597**, pp. 271-293. Springer-Verlag: New York.

Herman, M. R. [1979] Sur la conjugaison differentiable des diffeomorphismes du cercle á des rotations. *Publ. Math. I.H.E.S.*, **49**, 5-234.

Herman, M.R. [1988]. Existence et non existence de Tores Invariants par des diffeomorphismes symplectiques, preprint.

Herman, M. R. [1991] Examples of Hamiltonian Flows such that no C^∞ Perturbation has a Periodic Orbit on an Open Set of Energy Surfaces. *C. R. Acad. Sci. Paris*, **t. 312**, *Série I*, 989-994.

Hirsch, M.W. [1976]. *Differential Topology.* Springer-Verlag: New York, Heidelberg, Berlin.

Hirsch, M.W., Pugh, C.C., and Shub, M. [1977]. *Invariant Manifolds.* Springer Lecture Notes in Mathematics, vol. 583. Springer Verlag: New York, Heidelberg, Berlin.

Hirsch, M.W. and Smale, S. [1974]. *Differential Equations, Dynamical Systems, and Linear Algebra.* Academic Press: New York.

Hirschberg, P., Knobloch, E. [1993] Silnikov-Hopf Bifurcation. *Physica D*, **62**, 202-216.

Holmes, P.J. and Rand, D.A. [1978]. Bifurcations of the forced van der Pol oscillator. *Quart. Appl. Math.* **35**, 495–509.

Holmes, P.J. [1980]. A strange family of three-dimensional vector fields near a degenerate singularity. *J. Differential Equations* **37**, 382–404.

Holmes, P. J. [1980] Periodic, nonperiodic, and irregular motions in a Hamiltonian system. *Rocky Mountain J. Math*, **10**, 679-693.

Holmes, P.J. and Moon, F.C. [1983]. Strange attractors in nonlinear mechanics. *Trans. ASME J. Appl. Mech.* **50**, 1021–1032.

Holmes, C.A. and Wood, D. [1985]. Studies of a complex Duffing equation in nonlinear waves on plane Poiseuille flow, preprint, Imperial College, London.

Holmes, P.J. and Williams, R.F. [1985]. Knotted periodic orbits in suspensions of Smale's horseshoe: Torus knots and bifurcation sequences. *Arch. Rational Mech. Anal.* **90**, 115–194.

Holmes, P.J. [1986]. Spatial structure of time-periodic solutions of the Ginzburg–Landau equation. *Physica* **23D**, 84–90.

Holmes, P.J. [1986]. Knotted periodic orbits in suspensions of Smale's horseshoe: Period multiplying and cabled knots. *Physica* **21D**, 7–41.

Holmes, P.J. [1987]. Knotted periodic orbits in suspensions of annulus maps. *Proc. Roy. Soc. London Ser. A* **411**, 351–378.

Holmes, P. J., and C. A. Stuart [1992] Homoclinic Orbits for Eventually Autonomous Planar Flows. *Z. angew. Math. Phys. (ZAMP)*, **43**, 598-625.

Homburg, A. J. [1996] Global aspects of homoclinic bifurcation of vector fields-introduction. *Mem. AMS*, **121**(578), 1.

Homburg, A.J. [2000] Singular heteroclinic cycles. *J. Diff. Eq.*, **161**, 358-402.

Homburg, A.J. [2002] Periodic attractors, strange attractors, and hyperbolic dynamics near homoclinic orbits to saddle-focus equilibria. *Nonlinearity*, **15**, 1029-1050.

Hoover, W. G., H. A. Posch, B. L. Holian, M. J. Gillan, M. Mareschal, and C. Massobrio [1987] Dissipative irreversibility from Nosé's reversible mechanics. *Mol. Simulation* **1**, 79-86.

Hopf, E. [1942]. Abzweigung einer periodischen Lösung von einer station- ären Lösung eines Differentialsystems. *Ber. Math. Phys. Sächsische Akademie der Wissenschaften Leipzig* **94**, 1–22 (see also the English translation in Marsden and McCracken [1976]).

Hou, C.Z. Golubitsky, M. [1997] An example of symmetry breaking to heteroclinic cycles. *J. Diff. Eq,*, **133**(1), 30-48.

Hoveijn, I. [1992] *Aspects of resonance in dynamical systems*, Ph.D. thesis, University of Utrecht.

Hoveijn, I. [1996] Versal Deformations and Normal Forms for Reversible and Hamiltonian Linear Systems. *J. Diff. Eq.*, **126**, 408-442.

Iooss, G. [1979]. *Bifurcation of Maps and Applications.* North Holland: Amsterdam.

Iooss, G. and Langford, W.F. [1980]. Conjectures on the routes to turbulence via bifurcation. In *Nonlinear Dynamics,* R.H.G. Helleman (ed.), pp. 489–505. New York Academy of Sciences: New York City, NY.

Iooss, G. [1988] Global Characterization of the Normal Form for a Vector Field Near a Closed Orbit. *J. Diff. Eq.*, **76**, 47-76.

Iooss, G. [1997] Existence of orbits homoclinic to an elliptic equilibrium, for a reversible system. *Comptes Rend. de L. Acad. Sci. ser. I. Math*, **324**(9), 993-997.

Irwin, M. C. [1973] Hyperbolic time-dependent processes. *Bull. London Math. Soc.*, **5**, 209-217.

Ito, H. [1989] Convergence of Birkhoff Normal Forms for Integrable Systems. *Comment. Math. Helvetici*, **64**, 412-461.

Jakobson, M.V. [1981]. Absolutely continuous invariant measures for one-parameter families of one-dimensional maps. *Comm. Math. Phys.* **81**, 39–88.

Janaki, T. M., Rangarajan, G., Habib, S., Ryne, R. D. [1999] Computation of the Lyapunov spectrum for continuous -time dynamical systems and discrete maps. *Phys. Rev. E.*, **60**(6), 6614-6626.

Johnson, R.A. [1986]. Exponential dichotomy, rotation number, and linear differential operators with bounded coefficients. *J. Differential Equations* **61**, 54–78.

Johnson, S. [1987]. Singular measures without restrictive intervals. *Comm. Math. Phys.* **110**, 185–190.

Johnson, R.A. [1987]. m-Functions and Floquet exponents for linear differential systems. *Ann. Mat. Pura Appl. (4)* vol. CXLVII, 211–248.

Johnson, R. A.,Kloeden, P. E. [2001] Nonautonomous attractors of skew-product flows with digitized driving systems. *Electron, J. Diff. Eqns.*, Vol. 2001, No. 58, pp. 1-16.

Jorba, A., and Simo, C. [1992] On the reducibility of linear differential equations with quasiperiodic coefficients. *J. Diff. Eq.*, **98**, 111-124.

Jorba, A., Ramírez-Ros, R., and Villanueva, J. [1997] Effective reducibility of quasi-periodic linear equations close to constant coefficients. *SIAM J. Math. Anal.*, **28**(1), 178-188.

Kaper, T. J. [1992] On the structure of separatrix swept regions of slowly modulated Hamiltonian systems. On the quantification of mixing in chaotic Stokes flows: the eccentric journal bearing. Caltech Ph. D. thesis.

Kaper, T. J., Wiggins, S. [1992] On the Structure of Separatrix-Swept Regions in Singularly-Perturbed Hamiltonian Systems. *Differential and Integral Equations*, **5**(6), 1363-1381.

Kaper, T.J., Kovacic, G. [1996] Multi-bump orbits homoclinic to resonance bands. *Trans. Am. Math. Soc.*, **348**(10), 3835-3887.

Kapitaniak, T., Lai, Y.-C., Grebogi, C. [1999] Metamorphosis of chaotic saddle. *Phys. Lett. A*, **259**, 445-450.

Kapitaniak, T. [2001] Partially nearly riddled basins in systems with chaotic saddle. *Chaos, Solitons, & Fractals*, **12**, 2363-2367.

Kaplan, B.Z. and Kottick, D. [1983]. Use of a three-phase oscillator model for the compact representation of synchronomous generators. *IEEE Trans. Magn.,* vol. MAG-19, 1480–1486.

Kaplan, B.Z. and Kottick, D. [1985]. A compact representation of synchronous motors and unregulated synchronous generators. *IEEE Trans. Magn.,* vol. MAG-21, 2657–2663.

Kaplan, B.Z. and Kottick, D. [1987]. Employment of three-phase compact oscillator models for representing comprehensively two synchronous generator systems. *Elect. Mach. Power Systems* **12**, 363–375.

Kaplan, B.Z. and Yardeni, D. [1989]. Possible chaotic phenomenon in a three-phase oscillator. *IEEE Trans. Circuits and Systems* **36**(8), 1148–1151.

Kaplan, L., Heller, E. J. [1999] Measuring Scars of Periodic Orbits. *Phys. Rev. E.*, **59**(6), 6609-6628.

Katok, A. and Bernstein, D. [1987]. Birkhoff periodic orbits for small perturbations of completely integrable Hamiltonian systems with convex Hamiltonians. *Invent. Math.* **88**, 225–241.

Katok, A. and Hasselblatt, B. [1995] *Introduction to the Modern Theory of Dynamical systems.* Cambridge University Press: Cambridge.

Kelley, A. [1967]. The stable, center-stable, center, center-unstable, unstable manifolds. An appendix in *Transversal Mappings and Flows,* R. Abraham and J. Robbin. Benjamin: New York.

Kennedy, J,. Yorke, J. A. [2001] Topological horseshoes. *Trans. Amer. Math. Soc.*, **353**(6), 2513-2530.

Kertesz, V. [1997] Codimension $n \geq 2$ bifurcations of nilpotent singularities on the plane. *Non. Lin. Anal.-TMA*, **30**(8), 5121-5126.

Kertesz, V. [2000] Bifurcation problems with high codimensions *J Math. Comp. Modelling*, **31** (4-5), 99-108.

Kirchgraber, U. and K. J. Palmer [1990] *Geometry in the Neighborhood of Invariant Manifolds of Maps and Flows and Linearization.* Pitman Research Notes in Mathematics Series. Longman Scientific & Technical. published in the United States with John Wiley & Sons, Inc.: New York.

Kirk, V., Marsden, J. E., and M. Silber [1996]. New Solution Branches for an Equivariant Normal Form Using Hamiltonian Methods. Caltech preprint.

Klapper, I. [1992] Shadowing and the role of small diffusivity in the chaotic advection of scalars. *Phys. Fluids A*, **4**(5), 861–864.

Klapper, I. [1993] Shadowing and the diffusionless limit in fast dynamo theory. *Nonlinearity*, **6**(6), 869–884.

Kloeden, P.E., Schmalfuss, B. [1997] Nonautonomous systems, cocycle attractors, and variable time-step discretization. *Numerical Algorithms*, **14**, 141-152.

Kloeden, P. E., Stonier, D. J. [1998] Cocycle attractors in nonautonomously perturbed differential equations. *Dynamics of Continuous, Discrete, and Impulsive Systems*, **4**(2), 211-226.

Knobloch, E. [1986a]. Normal Forms for Bifurcations at a Double-Zero Eigenvalue. *Phys. Lett. A*. **115** (5), 199-201.

Knobloch, E. [1986b]. Normal Form Coefficients for the Nonresonant Double Hopf Bifurcation. *Phys. Lett. A*. **116** (8), 365-369.

Knyazhishche, L. B., Shavel, N. A. [1995] Nonautonomous Systems: Asymptotical Stability Conditions Using Localization of the Limit Sets. *Differential Equations*, **31**(3), 389-399.

Kocak, H. [1984]. Normal forms and versal deformations of linear Hamiltonian systems. *J. Differential Equations* **51**, 359–407.

Kolmogorov, A. N. [1954] On conservation of conditionally periodic motions under small perturbations of the Hamiltonian. *Dokl. Akad. Nauk. USSR*, **98**(4), 527-530.

Koltsova, O.Y., Lerman, L.M. [1995] Periodic and Homoclinic Orbits in a 2-Parameter Unfolding of a Hamiltonian System with a Homoclinic Orbit to a Saddle-Center. *Int. J. Bif. Chaos*, **5**(2), 397-408.

Koltsova, O.Y., Lerman, L.M.[1996] Families of transverse Poincare homoclinic orbits in 2N-dimensional Hamiltonian systems close to the system with a loop to a saddle-center. *Int. J. Bif. Chaos*, **6**(6), 991-1006.

Koltsova, O.Y., Lerman, L.M. [1998] Transverse Poincare homoclinic orbits in 2N-dimensional Hamiltonian systems close to the system with a loop to a saddle-center. *Dokl. Akad. Nauk.*, **359**(4), 448-451.

Koon, W.S., Lo, M.W., Marsden, J.E., Ross, S.D. [2000] Heteroclinic connections between periodic orbits and resonance transitions in celestial mechanics. *Chaos*, **10**(2), 427-469.

Kopell, N. and Howard, L.N. [1975]. Bifurcations and trajectories joining critical points. *Adv. in Math.* **18**, 306–358.

Kovačič, G. and S. Wiggins [1992] Orbits Homoclinic to Resonances, with an Application to Chaos in a Model of the Forced and Damped Sine-Gordon Equation, *Physica D*, **57**, 185-225.

Kozlov, V. V. [1985] Calculus of variations in the large and classical mechanics. *Russian Math. Surveys*,**40**(2), 37-71.

Krasnosel'skii, M. A.[1968] *The Operator of Translation Along Trajectories of Differential Equations*, Translations of Mathematical Monographs, Vol. 19, American Mathematical Society: Providence.

Krüger, T., Troubetzkoy, S. [1992] Markov partitions and shadowing for non-uniformly hyperbolic systems with singularities. *Ergodic Theory Dynam. Systems*, **12**(3), 487–508.

Krupa, M., Melborne, I. [1995] Asymptotic Stability of Heteroclinic Cycles in Systems with Symmetry. *Erg. Th. Dyn. Sys.*, **15**, 121-147.

Krupa, M.[1997] Robust heteroclinic cycles. *J. Nonlin. Sci.*, **7**(2), 129-176.

Kuksin, S. and J. Pöschel [1994] On the Inclusion of Analytic Symplectic Maps in Analytic Hamiltonian Flows and its Applications. in *Seminar on Dynamical Systems*, S. Kuksin, V. Lazutkin, J. Pöschel, eds., Birkhäuser: Basel.

Kummer, M. [1971]. How to avoid "secular" terms in classical and quantum mechanics. *Nuovo Cimento B,* 123–148.

Kummer, M. [1990]. On resonant classical Hamiltonians with n frequencies. *J. Diff. Eq.*, **83**, 220-243.

Labate, A., Ciofini, M., Meucci, R., Boccaletti, S., Arecchi, F.T. [1997] Pattern dynamics in a large Fresnel number laser close to threshold. *Phys. Rev. A.*, *56*(3), 2237-2241.

Lahiri, A., Roy, M. S. [2001] The Hamiltonian Hopf bifurcation: an elementary perturbative approach. *Int. J. Nonlinear Mechanics*, **36**, 787-802.

Lai, Y.-C., Grebogi, C., Yorke, J. A., Kan, I. [1993] How often are chaotic saddles nonhyperbolic? *Nonlinearity*, **6**, 779-797.

Lai, Y.-C., Nagai, Y., Grebogi, C. [1997] Characterization of the Natural Measure by Unstable Periodic Orbits in Chaotic Attractors. *Phys. Rev. Lett.*, **79**(4), 649-652.

Laing, C., Glendinning, P. [1997] Bifocal homoclinic bifurcations. *Physica D*, **102**(1-2), 1-14.

Landau, L.D. and Lifschitz, E.M. [1976]. *Mechanics.* Pergamon: Oxford.

Landman, M.J. [1987]. Solutions of the Ginzburg–Landau equation of interest in shear flow transition. *Stud. Appl. Math.* **76**(3), 187–238.

Langford, W.F. [1979]. Periodic and steady mode interactions lead to tori. *SIAM J. Appl. Math.* **37**(1), 22–48.

Langford, W.F. [1985]. A review of interactions of Hopf and steady-state bifurcations. In *Nonlinear Dynamics and Turbulence,* G. Barenblatt, G. Iooss, and D.D. Joseph (eds.), pp. 215–237. Pitman: London.

Lani-Wayda, B. [1995] *Hyperbolic sets, shadowing and persistence for noninvertible mappings in Banach spaces.* Pitman Research Notes in Mathematics Series, 334. Longman, Harlow; copublished in the United States with John Wiley & Sons, Inc., New York.

Larsson, S., Sanz-Serna, J.-M. [1999] A shadowing result with applications to finite element approximation of reaction-diffusion equations, *Math. Comp.*, **68**, 55–72.

LaSalle, J.P. and Lefschetz, S. [1961]. *Stability by Liapunov's Direct Method.* Academic Press: New York.

LaSalle, J.P. [1968] Stability Theory for Ordinary Differential Equations. *J. Diff. Eq.*, **4**, 57-65.

Laub, A. J. , Meyer, K. [1974] Canonical forms for symplectic and Hamiltonian matrices. *Celestial Mech.*, **9**, 213-238.

Lauterbach, R., Roberts, M. [1992] Heteroclinic Cycles in Dynamic Systems with Broken Spherical Symmetry. *J. Diff. Eq.*, **100**(1), 22-48.

Lauterbach, R., Maier Paape, S., Reissner, E. [1996] A systematic study of heteroclinic cycles in dynamical systems with broken symmetries. *Proc. Roy. Soc. Ed. sec. A-Math.*, **126**, 885-909.

Lebovitz, N.R. and Schaar, R.J. [1975]. Exchange of stabilities in autonomous systems. *Stud. Appl. Math.* **54**, 229–260.

Lebovitz, N.R. and Schaar, R.J. [1977]. Exchange of stabilities in autonomous systems, II. Vertical bifurcations. *Stud. Appl. Math.* **56**, 1–50.

Lebovitz, N. R., Pesci, A. I. [1995] Dynamic bifurcation in Hamiltonian systems with one degree of freedom. *SIAM J. Appl. Math.*, **55**(4), 1117-1133.

Ledrappier, F., Young, L.-S. [1991] Stability of Lyapunov exponents. *Ergodic Theory Dynam. Systems*, **11**(3), 469–484.

Leen, T. K. [1993] A coordinate-independent center manifold reduction. *Physics Letters A*, **174**, 89-93.

Lerman, L. M. [1989] On the behavior of a Hamiltonian system in the neighborhood of the transversal homoclinic orbit of saddle-focus type. *Russ. Math. Surv.*, **44**(2), 285-286.

Lerman, L.M. and Silnikov, L.P. [1989]. Homoclinic structures in infinite-dimensional systems. *Siberian Math. J.* **29**(3), 408–417.

Lerman, L. M. [1991] Hamiltonian systems with loops of a separatrix of a saddle-center. *Selecta Mathematica Sovietica*, **10**(3), 297-306.

Lerman, L.M. and Šilnikov, L.P. [1992] Homoclinical structures in nonautonomous systems: Nonautonomous chaos, *Chaos*, **2**(3), 447-454.

Lesher, S., Spano, M. L., Mellen, N. M., Guan, L., Dykstra, S., Cohen, A. H. [1999] Stable Lamprey Swimming on a Skeleton of Unstable Periodic Orbits. *Neurocomputing*, **26-27**, 779-788.

Levinson, N. [1949]. A second order differential equation with singular solutions. *Ann. Math.* **50**, 127–153.

Lewis, D. and Marsden, J. [1989]. A Hamiltonian-dissipative decomposition of normal forms of vector fields, in *Bifurcation Theory and its Num. An.*, Li Kaitai, ed., pp 51-78. Xi'an Jaitong University Press.

Lewis, H. R.,Kostelec, P.J. [1996] The use of Hamilton's principle to derive time-advance algorithms for ordinary differential equations. *Comput. Phys. Comm.* **96** (2-3), 129–151.

Li, Y., Wiggins, S. [1997] Homoclinic orbits and chaos in discretized perturbed NLS systems. II. Symbolic dynamics. *J. Nonlinear Sci.*, **7**(4), 315–370.

Liapunov, A. M. [1947] *Probleme general de la stabilite du movement.* Princeton University Press: Princeton.

Liapunov, A.M. [1966]. *Stability of Motion.* Academic Press: New York.

Lin, X.-B. [1989] Shadowing lemma and singularly perturbed boundary value problems. *SIAM J. Appl. Math.*, **49**(1), 26–54.

Lin, X.-B. [1996] Shadowing matching errors for wave-front-like solutions. *J. Differential Equations*, **129**(2), 403–457.

Lind, D., Marcus, B. [1995] *An Introduction to Symbolic Dynamics and Coding.* Cambridge University Press: Cambridge.

Lions, P.-L. [1982] *Generalized solutions of Hamilton-Jacobi Equations.* Pitman: Boston.

Liu, X. [1993] On Attractivity fro Nonautonomous Systems. *Quart. Appl. Math.*, **51**(2), 319-327.

Liu, L.X., Moore, G., Russell, R.D. [1997] Computation and continuation of homoclinic and heteroclinic orbits with arclength parameterization. *SIAM J. Sci. Comp.*, **18**(1), 69-93.

de la Llave, R. and Wayne, C.E. [1990] Whiskered and low dimensional tori in nearly integrable Hamiltonian systems, University of Texas, Austin preprint.

de la Llave, R. and Rana, D. [1990]. Accurate strategies for small divisor problems. *Bull. Am. Math. Soc.*, **22**(1), 85-90.

Lochak, P. [1992] Canonical perturbation theory via simultaneous approximation. *Russian Math. Surveys*, **47**(6),57-133.

Lochak, P., Neishtadt, A. [1992] Estimates of stability time for nearly integrable systems with a quasiconvex Hamiltonian. *Chaos*, **4**(2), 495-500.

Loud, W. S. [1967] Phase Shift and Locking in Regions. *Quart. J. Appl. Math.*. **25**, 222-227.

Lyubimov, D. V., Byelousova, S. L. [1993] Onset of homoclinic chaos due to degeneracy in the spectrum of the saddle. *Physica D*, **62**, 317-322.

MacKay, R.S. [1990]. A criterion for non-existence of invariant tori for Hamiltonian systems. *Physica D*, **36**(1-2), 64-82.

MacKay, R.S., Meiss, J.D., and Stark, J. [1989]. Converse KAM theory for symplectic twist maps. *Nonlinearity*, **2**, 555-570.

MacKay, R.S. and Percival, I.C. [1985]. Converse KAM: Theory and practice. *Comm. Math. Phys.* **98**, 469–512.

Mandel, P. and Erneux, T. [1987]. The slow passage through a steady bifurcation: Delay and memory effects. *J. Statist. Phys.* **48**, 1059–1070.

Mañé, R. [1982] An Ergodic Closing Lemma. *Ann. Math.*, **116**, 503-540.

Markus, L. [1956] Asymptotically Autonomous Differential Systems. In: Contributions to the Theory of Nonlinear Oscillations III, S. Lefschetz, ed. (*Ann. Math. Stud.*, vol. 36, pp 17-29), Princeton University Press: Princeton.

Marsden, J.E. and McCracken, M. [1976]. *The Hopf Bifurcation and Its Applications.* Springer-Verlag: New York, Heidelberg, Berlin.

Mather, J. [1982]. Existence of quasi-periodic orbits for twist maps of the annulus, *Topology* **21**(4), 457–467.

Mather, J. [1984]. Non-existence of invariant circles. *Ergodic Theory Dynamical Systems* **4**, 301–311.

Mather, J. [1986]. A criterion for the non-existence of invariant circles. *Publ. Math. IHES* **63**, 153–204.

Mather, J. [1993] Variational construction of connecting orbits. *Ann. Inst. Fourier, Grenoble*, **43**(5), 1349-1386.

Maxwell, T.O. [1997] Heteroclinic chains for a reversible Hamiltonian system. *Nonlin. Anal.-Th., Meth., App*, **28**(5), 871-887.

McCord, C., Mischaikow, K. [1992] Connected Simple Systems, Transition Matrices, and Heteroclinic Bifurcations. *Trans. Am. Math. Soc.*, **333**(1), 397-422.

McGehee, R. P. [1973] A stable manifold theorem for degenerate fixed points with applications to celestial mechanics. *J. Differential Equations*, **14**, 70–88.

McGehee, R. P., Peckham, B. B. [1995] Determining the global topology of resonance surfaces for periodically forced oscillator families, in *Normal Forms and Homoclinic Chaos*, W. F. Langford and W. Nagata, eds., pp 233-251. Fields Institute Communications: American Mathematical Society: Providence.

McLaughlin, D., Overman II, E.A., Wiggins, S. and Xiong, X. [1996] Homoclinic Orbits in a Four Dimensional Model of a Perturbed NLS Equation: A Geometric Singular Perturbation Study. *Dynamics Reported*, **5**(New Series), 190-287.

Meinsma, G. [1995] Elementary proof of the Routh-Hurwitz test. *Systems & Control Letters*, **25**, 237-242.

Melbourne, I. and Dellnitz, M. [1993] Normal forms for linear Hamiltonian vector fields commuting with the action of a compact Lie group. *Math. Proc. Camb. Phil. Soc.*, **114**, 235-268.

Melnikov, V.K. [1963]. On the stability of the center for time periodic perturbations. *Trans. Moscow Math. Soc.* **12**, 1–57.

Melo, W.d., Strien, S. v., [1993] *One dimensional dynamics*. Springer-Verlag: New York.

Menck, J. [1993]. Real Birkhoff Normal Forms and Complex Coordinates. *Z. angew. Math. Phys. (ZAMP)*, **44**, 131-146.

Meyer, K. R. [1975] Generic bifurcations in Hamiltonian systems. Springer Lecture Notes in Mathematics, volume 468. Springer-Verlag: New York, Heidelberg, Berlin.

Meyer, K.R. [1986]. Counter-examples in dynamical systems via normal form theory. *SIAM Rev.* **28**, 41–51.

Meyer, K. R. and D. S. Schmidt [1986] The Stability of the Lagrange Triangular Point and a Theorem of Arnold. *J. Diff. Eq.*, **62**, 222-236.

Meyer, K. R., Sell, G. R. [1987] An analytic proof of the shadowing lemma. *Funkcial. Ekvac.*, **30**(1), 127–133.

Meyer, K. R., Sell, G. R. [1989] Melnikov transforms, Bernoulli bundles, and almost periodic perturbations. *Trans. Amer. Math. Soc.*, **314**(1), 63-105.

Meyer, K. R. [1990] The geometry of harmonic oscillators. *Amer. Math. Monthly*, **97**(6) (1990), 457–465.

Meyer, K. R. and G. R. Hall [1992] *Introduction to Hamiltonian Dynamical Systems and the N-Body Problem*. Springer-Verlag: New York, Heidelberg, Berlin.

Meyer, K. R., Zhang, X. [1996] Stability of skew dynamical systems. *J. Differential Equations*, **132**(1), 66–86.

Mielke, A. [1991] *Hamiltonian and Lagrangian flows on center manifolds : with applications to elliptic variational problems*. Springer Lecture Notes in Mathematics, vol 1489. Springer-Verlag: New York.

Mielke, A., Holmes, P., O'Reilly, O. [1992] Cascades of homoclinic orbits to, and chaos near, a Hamiltonian saddle-center. *J. Dyn. Diff. Eq.*, **4**(1), 95-126.

Milnor, J. [1985]. On the concept of attractor. *Comm. Math. Phys.* **99**, 177–195.

Misiurewicz, M. [1981]. The structure of mapping of an interval with zero entropy. *Publ. Math. IHES* **53**, 5–16.

Mitropol'skii, Y.A. [1965]. *Problems of the Asymptotic Theory of Nonstationary Vibrations*. Israel Program for Scientific Translations.

Modi, V.S. and Brereton, R.C. [1969]. Periodic solutions associated with the gravity–gradient-oriented system: Part I. Analytical and numerical determination. *AIAA J.* **7**, 1217–1225.

Moore, D.R. Weiss, N.O. [2000] Resonant interactions in thermosolutal convection. *Proc. Roy.Soc. Lond. Ser. A-Math. Phys. Eng. Sci.*, **456**(1993), 39-62.

Moore, G., Hubert, E. [1999] Algorithms for constructing stable manifolds of stationary solutions. *IMA J. Num. Anal.*, **19**, 375-424.

Mora, L., Viana, M. [1993] Abundance of strange attractors. *Acta. Math.*, **171**(1), 1-71.

Morales, C. A., Pacifico, M. J., Pujals, E.R. [1998] on C^1 robust singular transitive sets for three-dimensional flows. *Comp. Rend. Acad. Sci. ser. I- Math.*, **326**(1), 81-86.

Morse, M. and Hedlund, G.A. [1938]. Symbolic dynamics. *Amer. J. Math.* **60**, 815–866.

Moser, J. [1958] On a Generalization of a Theorem of A. Liapounoff. *Comm. Pure App. Math.*, **11**, 257-271.

Moser, J. [1962] On invariant curves of an area preserving mappings of an annulus. *Nachr. Akad. Wiss. Gött., II. Math.-Phys. Kl.*, 1-20.

Moser, J. [1968]. Lectures on Hamiltonian systems. *Mem. Amer. Math. Soc.* **81**, American Mathematical Society: Providence.

Moser, J. [1973]. *Stable and Random Motions in Dynamical Systems*. Princeton University Press: Princeton.

Moser, J. [1976] Periodic orbits near an equilibrium and a theorem by Alan Weinstein. *Comm. Pure. Appl. Math.*, **29**, 727-747.

Moser, J. [1978] "Addendum to "Periodic orbits near an equilibrium and a theorem by Alan Weinstein." *Comm. Pure. App. Math.*, **31**, 529-530.

Moses, E. and Steinberg, V. [1988]. Mass transport in propagating patterns of convection. *Phys. Rev. Lett.* **60**(20), 2030–2033.

Munkres, J. R. [1975] *Topology, a first course.* Prentice Hall-Englewood Cliffs.

Murdock, J. [1995] Shadowing multiple elbow orbits: an application of dynamical systems to perturbation theory. *J. Differential Equations*, **119**(1), 224–247.

Murdock, J. [1996] Shadowing in perturbation theory. *Appl. Anal.*, **62**(1-2), 161–179.

Murdock, J. A. [1990] A shadowing approach to passage through resonance. *Proc. Roy. Soc. Edinburgh Sect. A*, **116**(1-2), 1–22.

Murphy, K.D., Lee, C.L. [1998] The 1 : 1 internally resonant response of a cantilever beam attached to a rotating body. *J. Sound Vib.*, **211**(2), 179-194.

Naimark, J. [1959]. On some cases of periodic motions depending on parameters. *Dokl. Akad. Nauk. SSSR* **129**, 736–739.

Namachchivaya, N. S., Leng, G. [1990] Equivalence of Stochastic Averaging and Stochastic Normal Forms. *J. Appl. Mech.*, **57**, 1011-1017.

Namachchivaya, N. S., Lin, Y. K. [1991] Method of Stochastic Normal Forms. *Int. J. Non-Linear Mechanics*, **26** (6), 931-943.

Namachchivaya, N. S., Doyle, M. M., Langford, W. F., Evans, N. W. [1994] Normal Form for Generalized Hopf Bifurcation with Non-Semisimple 1:1 Resonance. *Z. angew. Math. Phys. (ZAMP)*, **45**, 312-335.

Naudot, V. [1996] Strange attractor in the unfolding of an inclination-flip homoclinic orbit. *Erg. Th. Dyn. Sys.*, **16**, 1071-1086.

Nayfeh, A.H. and Mook, D.T. [1979]. *Nonlinear Oscillations.* John Wiley: New York.

Needham, D.J., McAllister, S. [1998] Centre families in two-dimensional complex holomorphic dynamical systems. *Proc. Roy. Soc. of London Ser. A.-Math. Phys. Eng. Sci.*, **454**(1976), 2267-2278.

Neishtadt, A.I. [1987]. Persistence of stability loss for dynamical bifurcations, I. *Differential Equations* **23**, 1385–1391.

Neishtadt, A.I. [1988]. Persistence of stability loss for dynamical bifurcations, II. *Differential Equations* **24**, 171–176.

Nekhorosev, N.N. [1977] An exponential estimate on the time of stabilty of nearly-integrable Hamiltonian systems, *Russ. Math. Surv.* **32**, 1.

Nemytskii, V.V. and Stepanov, V.V. [1989]. *Qualitative Theory of Differential Equations.* Dover: New York.

Newell, A.C. [1985]. *Solitons in Mathematics and Physics.* CBMS-NSF Regional Conference Series in Applied Mathematics, vol. 48, SIAM: Philadelphia.

Newhouse, S. E. [1972] Hyperbolic Limit Sets. *Trans. Amer. Math. Soc.*, **167**, 125-150.

Newhouse, S. and Palis, J. [1973]. Bifurcations of Morse–Smale dynamical systems. In *Dynamical Systems,* M.M. Peixoto (ed.). Academic Press: New York, London.

Newhouse, S.E. [1974]. Diffeomorphisms with infinitely many sinks. *Topology* **13**, 9–18.

Newhouse, S. E. [1977] Quasi-elliptic Periodic Points in Conservative Dynamical Systems. *Amer. J. Math.*, **99**(5), 1061-1087.

Newhouse, S.E. [1979]. The abundance of wild hyperbolic sets and non-smooth stable sets for diffeomorphisms. *Publ. Math. IHES* **50**, 101–151.

Newhouse, S.E. [1980]. Lectures on dynamical systems. In *Dynamical Systems.* C.I.M.E. Lectures, Bressanone, Italy, June 1978, pp. 1–114. Birkhauser: Boston.

Newhouse, S.E. [1983]. Generic properties of conservative systems. In *Chaotic Behavior of Deterministic Systems.* Les Houches 1981, G. Iooss, R.H.G. Helleman, and R. Stora (eds.). North-Holland: Amsterdam, New York.

Newhouse, S. and Palis, J. [1973]. Bifurcations of Morse–Smale dynamical systems. In *Dynamical Systems,* M.M. Peixoto (ed.). Academic Press: New York, London.

Newton, P.K. and Sirovich, L. [1986a]. Instabilities of the Ginzburg–Landau equation: Periodic solutions. *Quart. Appl. Math.* **44**(1), 49–58.

Newton, P.K. and Sirovich, L. [1986b]. Instabilities of the Ginzburg–Landau equation: Part II, secondary bifurcation. *Quart. Appl. Math.* **44**(2), 367–374.

Niederman, L. [1998] Nonlinear stability around an elliptic equilibrium point in a Hamiltonian system. *Nonlinearity*, **11**, (6), 1465-1479.

Nikolaev, I.P., Larichev, A.V., Wataghin, V. Degtiarev, E.V., Peirolo, R. [1999] Experimental observation of steady and drifting roll patterns in a nonlinear optical system near a codimension-two point. *J. Opt. Comm.*, **159**(1-3), 184-190.

Nitecki, Z. [1971]. *Differentiable Dynamics.* M.I.T. Press: Cambridge.

Nusse, H.E., Yorke, J.A. [1988] Is every approximate trajectory of some process near and exact trajectory of a nearby process? *Comm. Math. Phys.*, **114**(3), 363-379.

Olver, P.J. [1986]. *Applications of Lie Groups to Differential Equations.* Springer-Verlag: New York, Heidelberg, Berlin.

Olver, P.J. and Shakiban, C. [1988]. Dissipative decomposition of ordinary differential equations. *Proc. Roy. Soc. Edinburgh Sect. A* **109**, 297–317.

Oseledec, V.I. [1968]. A multiplicative ergodic theorem. Liapunov characteristic numbers for dynamical systems. *Trans. Moscow Math. Soc.* **19**, 197–231.

Osinga, H. [1996] *Computing Invariant Manifolds: Variations of the Graph Transform.* Ph. D. Thesis, Groningen University.

Ostermann, A., Palencia, C. [2000] Shadowing for nonautonomous parabolic problems with applications to long-time error bounds. *SIAM J. Numer. Anal.*, **37**(5), 1399–1419.

Ottino, J.M. [1989]. *The Kinematics of Mixing: Stretching, Chaos, and Transport.* Cambridge University Press: Cambridge.

Ovsyannikov, I. M., Shil'nikov, L. P. [1987] On systems with a saddle-focus homoclinic curve. *Math. USSR. Sb.*, **58**(2), 557-574.

Ovsyannikov, I. M., Shil'nikov, L. P. [1992] Systems with a homoclinic curve of multidimensional saddle-focus type, and spiral chaos. *Math. USSR Sb.*, **73**(2), 415-443.

Palis, J. and de Melo, W. [1982]. *Geometric Theory of Dynamical Systems: An Introduction.* Springer-Verlag: New York, Heidelberg, Berlin.

Palis, J. and F. Takens [1993] *Hyperbolicity & Sensitive Chaotic Dynamics at Homoclinic Bifurcations.* Cambridge University Press: Cambridge.

Palis, J., Viana, M. [1994] High dimension diffeomorphisms displaying infinitely many periodic attractors. *Ann. Math.*, **140**(1), 207-250.

Palmer, K. J. [1988] Exponential dichotomies, the shadowing lemma and transversal homoclinic points.*Dynamics reported*, Vol. 1, 265–306, Dynam. Report. Ser. Dynam. Systems Appl., 1, Wiley, Chichester.

Palmer, K. J. [1996] Shadowing and Silnikov chaos. *Nonlinear Anal.*, **27**(9), 1075–1093.

Palmore, J. I., McCauley, J. L. [1987] Shadowing by computable chaotic orbits. *Phys. Lett. A*, **122**(8), 399–402.

Partovi, H. [1999] Reduced tangent dynamics and Lyapunov spectrum for Hamiltonian systems. *Phys. Rev. Lett.*, **82**(17), 3424-3427.

Pearson, D. W. [2001]Shadowing and prediction of dynamical systems. *Math. Comput. Modelling*, **34** (7-8), 813–820.

Peixoto, M.M. [1962]. Structural stability on two-dimensional manifolds. *Topology* **1**, 101–120.

Percival, I.C. [1979]. Variational principles for invariant tori and cantori. In *Nonlinear Dynamics and the Beam-Beam Interaction,* in M. Month and J.C. Herrera (eds.), *Am. Inst. of Phys. Conf. Proc.* **57**, 302–310.

Percival, I. and Richards, D. [1982]. *Introduction to Dynamics.* Cambridge University Press: Cambridge.

Perron, O. [1928]. Über stabilität und asymptotisches verhalten der Integrale von Differentialgleichungssystem. *Math. Z.*, **29**, 129–160.

Perron, O. [1929] Über stabilität und asymptotisches verhalten der Lösungen eines systems endlicher differenzengleichungen. *J. Reine Angew. Math.*, **161**, 41-64.

Perron, O. [1930] Die stabilitätsfrage bei differentialgleichungen. *Math. Z.*, **1930**, 703-728.

Pikovskii, A.S., Rabinovich, M.I., and Trakhtengerts, V.Yu. [1979]. Onset of stochasticity in decay confinement of parametric instability. *Soviet Phys. JETP* **47**, 715–719.

Pilyugin, S. Yu. [1999] *Shadowing in dynamical systems.* Lecture Notes in Mathematics, 1706. Springer-Verlag: Berlin.

Pliss, V.A. [1964]. The reduction principle in the theory of stability of motion. *Soviet Math.* **5**, 247–250.

Plumecoq, J., Lefranc, M. [2000a] From template analysis to generating partitions I: Periodic orbits, knots and symbolic encodings. *Physica D*, **144**(3-4), 231-258.

Plumecoq, J., Lefranc, M. [2000b] From template analysis to generating partitions II: Characterization of the symbolic encodings. *Physica D*, **144**(3-4), 259-278.

Plykin, R. [1974]. Sources and sinks for A-diffeomorphisms. *Math. USSR-Sb.* **23**, 233–253.

Poincaré, H. [1899]. *Les Méthodes Nouvelles de la Mécanique Céleste,* 3 vols. Gauthier-Villars: Paris.

Poincaré, H. [1892]. *Les Méthodes Nouvelles de la Mécanique Céleste,* vol. I. Gauthier-Villars: Paris.

Poincaré, H. [1929]. Sur les propriétés des fonctions définies par les équations aux différences partielles. *Oeuvres,* Gauthier-Villars: Paris, pp. XCIX–CX.

Politi, A., G. L. Oppo, R. Badii [1986] Coexistence of conservative and dissipative behavior in reversible dynamical systems. *Phys. Rev. A*, **33**, 4055-4060.

Pöschel, J. [1989] On elliptic lower dimensional tori in Hamiltonian systems, *Math. Z.*, **202**, 559.

Pöschel, J. [1993] Nekhoroshev estimates for quasi-convex Hamiltonian systems, *Math. Z.*, **213**(2), 187-216.

Pugh, C. [1967] The closing lemma. *Amer. J. Math.*, **89**, 956- 1009.

Pugh, C., Robinson, C [1983] The C^1 closing lemma, including Hamiltonians. *Ergod. Th. & Dynam. Sys.*, **3**, 261-313.

Qi, D.W., Jing, Z.J. [1998] Bifurcations of a pair of nonorientable heteroclinic cycles. *J. Math. Anal. App.*, **222**(2), 319-338.

Rabinovich, M.I. [1978]. Stochastic self-oscillations and turbulence. *Soviet Phys. Uspekhi* **21**, 443–469.

Rabinovich, M.I. and Fabrikant, A.L. [1979]. Stochastic self-oscillation of waves in non-equilibrium media. *Soviet Phys. JETP* **50**, 311–323.

Rabinowitz, P. [1978] Periodic solutions of Hamiltonian systems. *Comm. Pure App. Math.*, **31**, 157-184.

Rabinowitz, P.H. [1997] A multibump construction in a degenerate setting. *Calc. Var. Part. Diff. Eq.*, **5**(2), 159-182.

Ragazzo, C. G. [1997] Irregular dynamics and homoclinic orbits to Hamiltonian saddle-centers. *Comm. Pure. App. Math.*, **50**(2), 105-147.

Ragazzo, C.G. [1997] On the stability of double homoclinic loops. *Comm. Math. Phys.*, **184**(2), 251-272.

Raman, A., Bajaj, A. [1998] On the non-stationary passage through bifurcations in resonantly forced Hamiltonian oscillators. *Int. J. Non-Linear Mechanics*, **33**(5), 907-933.

Ramanan, V.V., Kumar, K.A., Graham, M.D. [1999] Stability of viscoelastic shear flows subjected to steady or oscillatory transverse flow. *J. Fluid Mech.*. **379**, 255-277.

Ramasubramanian, K., Sriram, M. N. [2000] A comparative study of computation of Lyapunov spectra with different algorithms. *Physica D*, **139**, 72-86.

Rand, R.H. and Armbruster, D. [1987]. *Perturbation Methods, Bifurcation Theory and Computer Algebra.* Springer-Verlag: New York, Heidelberg, Berlin.

Rangarajan, G., Habib, S., Ryne, R. D. [1998] Lyapunov exponents without rescaling and reorthogonalization. *Phys. Rev. Lett.*, **80**(17), 3747-3750.

Renardy, Y.Y., Renardy, M., Fujimura, K. [1999] Takens-Bogdanov bifurcation on the hexagonal lattice for double-layer convection. *Physica D*, **129**(3-4), 171-202.

Robert, C., Alligood, K. T., Ott, E., Yorke, J. A. [1998] Outer tangency bfurcations of chaotic sets. *Phys. Rev. Lett.*, **80**(22), 4867-4870.

Robert, C., Alligood, K. T., Ott, E., Yorke, J. A. [2000] Explosions of chaotic sets. *Phys. D*, **144**, 44-61.

Roberts, J. A. G. and G. R. W. Quispel [1992] Chaos and Time-Reversal Symmetry. Order and Chaos in Reversible Dynamical Systems. *Phys. Rep.*, **216** (2 & 3), 63-177.

Robinson, R. C. [1970a] Generic properties of conservative systems. *Amer. J. Math.*, **92**(3), 562-603.

Robinson, R. C. [1970b] Generic properties of conservative systems II. *Amer. J. Math.*, **92**(4), 897-906.

Robinson, C. [1977] Stability theorems and hyperbolicity in dynamical systems. Proceedings of the Regional Conference on the Application of Topological Methods in Differential Equations (Boulder, Colo., 1976). *Rocky Mountain J. Math.*, **7**(3), 425-437.

Robinson, C. [1978] Introduction to the closing lemma, in *The Structure of Attractors in Dynamical Systems*. Springer Lecture Notes in Mathematics, **668**. Springer-Verlag: New York, Heidelberg, Berlin.

Robinson, C. [1983]. Bifurcation to infinitely many sinks. *Comm. Math. Phys.* **90**, 433–459.

Robinson,C. [1989] Homoclinic bifurcation to a transitive attractor of Lorenz type. *Nonlinearity*, **2** (1989), 495-518.

Robinson, C. [2000] Nonsymmetric Lorenz attractors from homoclinic bifurcation. *SIAM J. Math. Anal.*, **32**(1), 119-141.

Roels, J. [1971a] An extension to resonant cases of Lyapunov's theorem concerning the periodic solutions near a Hamiltonian equilibrium. *J. Diff. Eq.*, **9**(2), 300-324.

Roels, J. [1971b] Families of periodic solutions near a Hamiltonian equlibrium when the ratio of two eigenvalues is 3. *J. Diff. Eq.*, **10**(3), 431-447.

Rom-Kedar, V., Leonard, A., and Wiggins, S. [1990]. An analytical study of transport, mixing, and chaos in an unsteady vortical flow. *J. Fluid Mech.*, **214**, 347-394.

Rom-Kedar, V. and Wiggins, S. [1990]. Transport in two-dimensional maps. *Arch. Rational Mech. Anal.*, **109**, 239-298.

Rom-Kedar, V. [1990] Transport rates of a family of two dimensional maps and flows. *Physica D*, **43**, 229-268.

Rom-Kedar, V. [1994] Homoclinic tangles-classification and applications. *Nonlinearity*, **7**, 441-473.

Roquejoffre, J.-M. [2001] Convergence to steady states or periodic solutions of a class of Hamilton-Jacobi equations. *J. MAth. Pures Appl.*, **80**(1), 85-104.

Roux, J.C., Rossi, A., Bachelart, S., and Vidal, C. [1981]. Experimental observations of complex dynamical behavior during a chemical reaction. *Physica* **2D**, 395–403.

Rudnev, M.,Wiggins, S. [1999] On a partially hyperbolic KAM theorem. *Regul. Chaotic Dyn.* **4**(4), 39–58.

Rudnev, M., Wiggins, S. [2000] On a homoclinic splitting problem. *Regul. Chaotic Dyn.* **5**(2), 227–242.

Ruelle, D. [1973]. Bifurcations in the presence of a symmetry group. *Arch. Rational Mech. Anal.* **51**, 136–152.

Ruelle, D. [1981]. Small random perturbations of dynamical systems and the definition of attractors. *Comm. Math. Phys.* **82**, 137–151.

Rund, H. [1966] *The Hamilton-Jacobi Theory in the Calculus of Variations: Its Role in Mathematics and Physics*. Van Nostrand: London.

Rüssmann. H. [1964] Über das Verhalten analytischer Hamiltonscher Differentialgleichungen in der Nähe einer Gleichgewichtslösung. *Math. Ann.*, **154**, 285-300.

Rüssmann, H. [1975] On Optimal Estimates for the Solutions of Linear Partial Differential Equations of First Order with Constant Coefficients on the Torus. Springer Lecture Notes in Physics, vol. 38. Springer-Verlag: New York, Heidelberg, Berlin.

Rychlik, M. [1990]. Lorenz attractors through Silnikov type bifurcations. Part I. *Ergod. Th. & Dynam. Sys.*, **10**, 793-821.

Sacker, R.S. [1965]. On invariant surfaces and bifurcations of periodic solutions of ordinary differential equations. *Comm. Pure Appl. Math.* **18**, 717–732.

Sacker, R. J. [1969] A perturbation theorem for invariant manifolds and Hölder continuity. *J. Math. Mech.*, **18**, 187-198.

Sacker, R. J., and Sell G. R. [1974] Existence of dichotomies and invariant splittings for linear differential systems. *J. Diff. Eqns.*, **15**, 429–458.

Sacker, R. J. [1976] Skew-product dynamical systems. Dynamical systems (Proc. Internat. Sympos., Brown Univ., Providence, R.I., 1974), Vol. II, pp. 175–179. Academic Press: New York.

Sacker, R. J., Sell, G. R. [1977] Lifting properties in skew-product flows with applications to differential equations. *Mem. Amer. Math. Soc.*, **11**(190) iv+67 pp.

Sáenz, A. W., W. W. Zachary, and R. Cawley (eds.) [1986] *Local and Global Methods of Nonlinear Dynamics*. Lecture Notes in Physics, vol. 252. Springer-Verlag: New York, Heidelberg, Berlin.

Salamon, D., Zehnder, E. [1989] KAM theory in configuration space. *Comm. Math. Helv.*, **64**(1), 84-132.

Sauer, T. , Yorke, J. A. [1991] Shadowing trajectories of dynamical systems. *Computer aided proofs in analysis* (Cincinnati, OH, 1989), 229–234, IMA Vol. Math. Appl., 28, Springer, New York.

Sauer T., Grebogi C., Yorke J.A. [1997] How long do numerical chaotic solutions remain valid? *Phys. Rev. Lett.*, **79** (1), 59-62.

Sauzin, D. [2001] A new method for measuring the splitting of invariant manifolds. *Ann. Sci. École Norm. Sup.*, **34**(2), 159–221.

Schecter, S. [1985]. Persistent unstable equilibria and closed orbits of a singularly perturbed system. *J. Differential Equations* **60**, 131–141.

Schecter, S. [1988]. Stable manifolds in the method of averaging. *Trans. Amer. Math. Soc.* **308**, 159–176.

Scheurle, J. and Marsden, J.E. [1984]. Bifurcation to quasi-periodic tori in the interaction of steady state and Hopf bifurcations. *SIAM J. Math. Anal.* **15**(6), 1055–1074.

Scheurle, J. [1986] Chaotic solutions of systems with almost periodic forcing. *Z. Angew. Math. Phys.*, **37**(1), 12-26.

Schmalfuss, B. [1998] A random fixed point theorem and the random graph transformation. *J. Math. Anal. App.*, **225**, 91-113.

Schmidt, W. M. [1980] *Diophantine Approximation. Lecture Notes in Mathematics.* Springer-Verlag: New York, Heidelberg, Berlin.

Schwartz, A. J. [1963]. A generaliztion of a Poincaré–Bendixson theorem to closed two-dimensional manifolds. *Amer. J. Math.* **85**, 453–458; errata, ibid. **85**, 753.

Sell, G. R. [1967a] Nonautonomous differential equations and topological dynamics. I. The basic theory, *Trans. Amer. Math. Soc.* **127**, 241–262.

Sell, G. R. [1967b] Nonautonomous differential equations and topological dynamics. II. Limiting equations, *Trans. Amer. Math. Soc.* **127**, 263–283.

Sell, G.R. [1971]. *Topological Dynamics and Differential Equations.* Van Nostrand-Reinhold: London.

Sell, G.R. [1978]. The structure of a flow in the vicinity of an almost periodic motion. *J. Differential Equations* **27**, 359–393.

Séré, E. [1993] Looking for the Bernoulli shift. *Ann. Inst. Henri Poincaré*, **10**(5), 561-590.

Sethna, P. R. and Feng, Z. C. [1991] On Nonautonomous Problems with Broken D_4 Symmetry. University of Minnesota preprint.

Sevryuk, M. B. [1986] *Reversible Systems.* Springer Lecture Notes in Mathematics, vol. 1211. Springer-Verlag: New York.

Sevryuk, M. B. [1991] Lower dimensional tori in reversible systems. *Chaos*, **1**(2), 160-167.

Sevryuk, M. B. [1992] Reversible Linear Systems and Their Versal Deformations. *Journal of Soviet Mathematics*, **60**, 1663-1680.

Shashkov, M. V., Shil'nikov, L. P. [1994] The existence of a smooth invariant foliation for Lorentz-type maps. *Differential Equations*, **30**(4), 536-544.

Shen, W., Yi, Y. [1998] Almost automorphic and almost periodic dynamics in skew-product semiflows. *Mem. Amer. Math. Soc.* **136**(647), x+93 pp.

Shub, M. [1987]. *Global Stability of Dynamical Systems.* Springer-Verlag: New York, Heidelberg, Berlin.

Siegel, C.L. [1941]. On the Integrals of Canonical Systems. *Ann. Math.* **42**, 806–822.

Siegel, C.L. [1954]. Über die Existenz einer Normalform analytischer Hamiltonscher Differentialgleichungen in der Nähe einer Gleichgewichtslösung. *Math. Ann.*, **128**, 144-170.

Siegel, C.L. and Moser, J.K. [1971]. *Lectures on Celestial Mechanics.* Springer-Verlag: New York, Heidelberg, Berlin.

Siegmund, S. [2002] Normal forms for nonautonomous differential equations. *J. Diff. Eq.*,**178**, 541-573.

Sijbrand, J. [1985]. Properties of center manifolds. *Trans. Amer. Math. Soc.* **289**, 431–469.

Silnikov, L.P. [1965] A Case of the Existence of a Denumerable Set of Periodic Motions. *Sov. Math. Dokl.* **6**, 163–166.

Silnikov, L. P., Turaev, D. V. [1997] Simple bifurcations leading to hyperbolic attractors *Comp. Math. App.*, **34**(2-4), 173-193.

Simó, C. [1990] Analytical and numerical computation of invariant manifolds, in *Modern Methods in Celestial Mechanics, Editions Frontières*, D, Benest and C, Froeschlé, eds. pp. 285-330.

Sinai, J.G. and Vul, E. [1981]. Hyperbolicity conditions for the Lorenz model. *Physica* **2D**, 3-7.

Skeldon, A.C., Moroz, I.M. [1998] On a codimension-three bifurcation arising in a simple dynamo model *Physica D*, **117**(1-4), 117-127.

Smale, S. [1963]. Diffeomorphisms with many periodic points. In *Differential and Combinatorial Topology,* S.S. Cairns (ed.), pp. 63–80. Princeton University Press: Princeton.

Smale, S. [1966]. Structurally stable systems are not dense. *Amer. J. Math.* **88**, 491–496.

Smale, S. [1967]. Differentiable dynamical systems. *Bull. Amer. Math. Soc.* **73**, 747–817.

Smale, S. [1980]. *The Mathematics of Time: Essays on Dynamical Systems, Economic Processes and Related Topics.* Springer-Verlag: New York, Heidelberg, Berlin.

Smoller, J. [1983]. *Shock Waves and Reaction-Diffusion Equations.* Springer-Verlag: New York, Heidelberg, Berlin.

So, P., Francis, J. T., Netoff, T. I., Gluckman, B. J., Schiff, S. J. [1998] Periodic Orbits: A New Language for Neuronal Dynamics. *Biophysical Journal*, **74**, 2776-2785.

Solari, H.G., Oppo, G.L. [1994] Laser with injected signal-perturbation of an invariant circle. *Opt. Comm.*, **111**(1-2), 173-190.

Šošitaĭšvili, A.N. [1975]. Bifurcations of topological type of a vector field near a singular point. *Trudy Sem. Petrovsk.* **1**, 279–309.

Soto Trevino, C., Kaper, T.J. [1996] Higher-order Melnikov theory for adiabatic systems. *J, Math. Phys.*, **37**(12), 6220-6249.

Sparrow, C. [1982]. *The Lorenz Equations.* Springer-Verlag: New York, Heidelberg, Berlin.

Stark, J. [1988]. An exhaustive criterion for the non-existence of invariant circles for area-preserving twist maps. *Comm. Math. Phys.* **117**, 177–189.

Steinlein, H., Walther, H.-O. [1989] Hyperbolic sets and shadowing for noninvertible maps. *Advanced topics in the theory of dynamical systems* (Trento, 1987), 219–234, Notes Rep. Math. Sci. Engrg., 6, Academic Press, Boston, MA, 1989.

Sternberg, S. [1957]. On local C^n contractions of the real line. *Duke Math. J.* **24**, 97–102.

Sternberg, S. [1957]. Local contractions and a theorem of Poincaré. *Amer. J. Math.* **79**, 809–824.

Sternberg, S. [1958]. On the structure of local homeomorphisms of Euclidean n-space, II. *Amer. J. Math.* **80**, 623–631.

Stewart, I. [2000] The Lorenz attractor exists. *Nature*, **406**(6799), 948-949.

Stoffer, D. [1988a]. Transversal homoclinic points and hyperbolic sets for non-autonomous maps I. *J. Appl. Math. and Phys. (ZAMP)*, **39**, 518-549.

Stoffer, D. [1988b]. Transversal homoclinic points and hyperbolic sets for non-autonomous maps II. *J. Appl. Math. and Phys. (ZAMP)*, **39**, 783-812.

Stoffer, D. Palmer, K. J. [1999] Rigorous verification of chaotic behaviour of maps using validated shadowing. *Nonlinearity*, **12**(6), 1683–1698.

Struwe, M. [1990] *Variational methods: applications to nonlinear partial differential equations and Hamiltonian systems.* Springer-Verlag: New York, Heidelberg, Berlin.

Summers, J.L., Savage, M.D. [1992] 2 Timescale harmonic-balance. 1. Application to autonomous one-dimensional nonlinear oscillators. *Phil Trans. Roy. Soc. Lond. ser. A-Math. Phys. Eng. Sci.*, **340**(1659), 473-501.

Sun, J.H., Kooij, R.E. [1998] Bifurcations to a heteroclinic manifold with nonhyperbolic equilibria in R^n. *Acta. Math. Sci.*, **18**(3), 293-302.

Szeri, A., Leal, L.G., Wiggins, S. [1991] On the Dynamics of Suspended Microstructure in Unsteady, Spatially Inhomogeneous Two-Dimensional Fluid Flows. *Journal of Fluid Mechanics*, **228**, 207-241.

Takens, F. [1970] Hamiltonian systems: generic properties of closed orbits and local perturbations. *Math. Ann.*, **188**, 304-312.

Takens, F. [1972] Homoclinic points in conservative systems. *Inv. Math.*, **18**, 267-292.

Takens, F. [1974]. Singularities of vector fields. *Publ. Math. IHES* **43**, 47–100.

Takens, F. [1979]. Forced oscillations and bifurcations. *Comm. Math. Inst. Rijksuniv. Utrecht* **3**, 1–59.

Tedeschini-Lalli, L. and Yorke, J.A. [1986]. How often do simple dynamical processes have infinitely many coexisting sinks? *Comm. Math. Phys.* **106**, 635–657.

Thieme, H. R. [1992] Convergence Results and a Poincaré-Bendixson Trichotomy for Asymptotically Autonomous Differential Equations. *J. Math. Bio.*, **30**, 755-763.

Thieme, H. R. [1994] Asymptotically Autonomous Differential Equations in the Plane. *Rocky Mountain J. Math.*, **24**(1), 351-380.

Thompson, J. M. T., Stewart, H. B., Ueda, Y. [1994] Safe, explosive, and dangerous bifurcations in dissipative dynamical systems. *Phys. Rev. E*, **49**(2), 1019-1027.

Tian, Q.P., Zhu, D.M. [2000] Bifurcations of nontwisted heteroclinic loop. *Sci. Chin. ser. A-Math., Phys., Astron.*, *43*(8), 818-828.

Tracy, E.R., Tang, X.Z. [1998] Anomalous scaling behavior in Takens-Bogdanov bifurcations. *Phys. Lett. A*, **242**(4-5), 239-244.

Tracy, E.R., Tang, X.Z., Kulp, C. [1998] Takens-Bogdanov random walks. *Phys. Rev. E*, **57**(4), 3749-3756.

Treshchev, D.V. [1991] The mechanism of destruction of resonant tori of Hamiltonian systems, *Math. USSR Sb.*, **68**, 181.

Treshchev, D.V. [1995] An estimate of irremovable nonconstant terms in the reducibility problem, in *Dynamical Systems in Classical Mechanics*, V.V. Kozlov, ed. Advances in the Mathematical Science. AMS Translations, Series 2, vol. 168. AMS: Providence

Tresser, C. [1984]. About some theorems by L.P. Silnikov. *Ann. Inst. H. Poincaré* **40**, 440–461.

Tsang, K.Y., R. E. Mirollo, S. H. Strogatz, K. Wiesenfeld [1991] Dynamics of a globally coupled oscillator array. *Physica D*, **48**, 102-112.

Tucker, W. [1999] The Lorenz attractor exists. *Comp. Rend. Acad. Sci. ser. I- Math.*, **328**(12), 1197-1202.

Turaev, D. V. [1988] On bifurcations of a homoclinic figure 8 of a multi-dimensional saddle. *Russ. Math. Surv.*, **44**(5), 264-265.

Turaev, D. V., Shil'nikov, L. P. [1987] On bifurcations of a homoclinic "figure-eight" for a saddle with a negative saddle value. *Sov. Math. Dokl.*,**34**(2), 397-401.

Turaev, D. V., Shil'nikov, L. P. [1989] On Hamiltonian systems with homoclinic saddle curves. *Sov. Math. Dokl.*,**39**(1), 165-168.

Turaev, D. V., Silnikov, L. P. [1998] An example of a wild strange attractor. *Sb. Math.*, **189**(1-2), 291-314.

Udwadia, F. E., von Bremen, H. F. [2001] An efficient and stable approach for computation of Lyapunov characteristic exponents of continuous dynamical systems. *Appl. Math. Comput.* , **121**(2-3), 219-259.

Udwadia, F. E., von Bremen, H.F. [2002] Computation of Lyapunov characteristic exponents for continuous dynamical systems. *Z. Angew. Math. Phys.*, **53** (1), 123-146.

van Gils, S.A. [1984] *Some Studies in Dynamical Systems Theory*. Thesis, Vrije Universitet, Amsterdam.

van Gils, S.A. [1985]. A note on "Abelian integrals and bifurcation theory." *J. Differential Equations* **59**, 437–441.

van der Meer, J.-C. [1985]. *The Hamiltonian Hopf Bifurcation.* Springer Lecture Notes in Mathematics, vol. 1160. Springer-Verlag: New York, Heidelberg, Berlin.

Van Vleck, E.S. [2000] Numerical shadowing using component wise bounds and a sharper fixed point result. *SIAM J. Sci. Comput.*, **22**(3), 787–801.

Van Vleck, E. S. [1995] Numerical shadowing near hyperbolic trajectories. *SIAM J. Sci. Comput.*, **16**(5), 1177–1189.

Viana, M. [2000] What's new on Lorenz strange attractors? *Math. Intell.*, **22**(3), 6-19.

Walther, H.-O. [1987]. Inclination lemmas with dominated convergence. *ZAMP*, **32**, 327-337.

Wan, Y.-H. [1977] On the Uniqueness of Invariant Manifolds. *J. Diff. Eqn.*, **24**, 268-273.

Wang, X.-J. [1993] Genesis of bursting oscillations in the Hindmarsh-Rose model and homoclinicity to a chaotic saddle. *Physica D*, **62**, 263-274.

Wang, Q., Young, L.-S. [2002] From invariant curves to strange attractors. *Comm. Math. Phys.*, **225**(2), 275-304.

Weinstein, A. [1973] Normal modes for non-linear Hamiltonian systems. *Invent. Math.*, **45**, 47-57.

Weiss, J.B. and Knobloch, E. [1989]. Mass transport and mixing by modulated traveling waves. *Phys. Rev. A*, **40**(5), 2579-2589.

Whittaker, E. T. [1904] *A Treatise on the Analytical Dynamics of Particles and Rigid Bodies*. Cambridge University Press: Cambridge.

Wiggins, S. and Holmes, P.J. [1987a]. Periodic orbits in slowly varying oscillators. *SIAM J. Math. Anal.* **18**, 542–611.

Wiggins, S. and Holmes, P.J. [1987b]. Homoclinic orbits in slowly varying oscillators. *SIAM J. Math. Anal.* **18**, 612–629. (See also 1988, *SIAM J. Math. Anal.* **19**, 1254–1255, errata.)

Wiggins, S. [1988] *Global Bifurcations and Chaos – Analytical Methods*. Springer-Verlag: New York, Heidelberg, Berlin.

Wiggins, S. [1990] On the Geometry of Transport in Phase Space, I. Transport in k-Degree-of-Freedom Hamiltonian Systems, $2 \leq k < \infty$, Physica D, **44**, 471-501.

Wiggins, S. [1992] *Chaotic Transport in Dynamical Systems*. Springer-Verlag: New York, Heidelberg, Berlin.

Wiggins, S. [1994] *Normally Hyperbolic Invariant Manifolds in Dynamical Systems*. Springer-Verlag: New York, Heidelberg, Berlin.

Wiggins, S. [1999] Chaos in the dynamics generated by sequences of maps, with applications to chaotic advection in flows with aperiodic time dependence. *Z. angew. Math. Phys.*, **50**, 585-616.

Williams, R.F. [1980]. Structure of Lorenz attractors. *Publ. Math. IHES* **80**, 59–72.

Williamson, J [1936] On the algebraic problem concerning the normal forms of linear dynamical systems. *Amer. J. Math.*, **58**, 141-163.

Wittenberg, R. W., Holmes, P. J. [1997] The Limited Effectiveness of Normal Forms: A Critical Review and Extension of Local Bifurcation Studies of the Brusselator PDE. *Physica D*, **100**, 1-40.

Woods, P.D., Champneys, A.R. [1999] Heteroclinic tangles and homoclinic snaking in the unfolding of a degenerate reversible Hamiltonian-Hopf bifurcation. *Physica D*, **129**(3-4), 147-170.

Worfolk, P.A.[1996] An equivariant, inclination-flip, heteroclinic bifurcation. *Nonlinearity*, **9**(3), 631-647.

Wu, B.S., Kupper, T. [1996] Computation of hopf branches bifurcating from a class of Hopf/steady-state points. *Comp. Meth. App. Mech. Eng.*, **131**(1-2), 159-172.

Wu, B.S., Kupper, T. [1998] Computation of Hopf branches bifurcating from a Hopf/Pitchfork point for problems with Z(2)-symmetry. *J. Comp. Math.*, **16**(5), 403-416.

Yamaguchi, Y. Y., Iwai, T. [2001] Geometric approach to Lyapunov analysis in Hamiltonian dynamics. *Phys. Rev. E.*, **64**, 066206.

Yanagida, E. [1987]. Branching of double pulse solutions from single pulse solutions in nerve axon equations. *J. Differential Equations* **66**, 243–262.

Yang, X.-S. [2001] Remarks on three types of asymptotic stability. *Systems & Control Letters*, **42**, 299-302.

Yi, Y. [1993a] A Generalized Integral Manifold Theorem. *J. Diff. Eq.*, **102**(1), 153-187.

Yi, Y. [1993b] Stability of integral manifold and orbital attraction of quasi-periodic motion. *J. Differential Equations*, **103**(2), 278–322.

Yorke, J.A. and Alligood, K.T. [1985]. Period doubling cascades of attractors: A prerequisite for horseshoes. *Comm. Math. Phys.* **101**, 305–321.

Yoshizawa, T. [1985] Attractivity in Non-Autonomous Systems. *Int. J. Non-Linear Mechanics*, **20**(5/6), 519-528.

Young, L.-S. [1981] On the prevalence of horseshoes. *Trans. Amer. Math. Soc.*, **263**(1), 75–88.

Young, L.-S. [1982] Dimension, entropy and Lyapunov exponents. *Ergodic Theory Dynamical Systems*, **2**(1), 109–124.

Zelati, V. C., Ekeland, I., Séré, E. [1990] A variational approach to homoclinic orbits in Hamiltonian systems. *Math. Ann.*, **288**, 133-160.

Zelati, V.C., Nolasco, M. [1999] Multibump solutions for Hamiltonian systems with fast and slow forcing.*Boll. della Uni. Mat. Ital.*, **2B**(3), 585-608.

Zhang, S.Q. [2000] Symmetrically homoclinic orbits for symmetric Hamiltonian systems Source. *J. Math. Anal. App.*, **247**(2), 645-652.

Zhu, D.M. [1996] Transversal heteroclinic orbits in general degenerate cases. *Sci. Chin. ser. A-Math., Phys., Astr.*, **39**(2), 113-121.

Zimmermann, M.G., Natiello, M.A., Solari, H.G. [1997] Sil'nikov-saddle-node interaction near a codimension-2 bifurcation: Laser with injected signal. *Physica D*, **109**(3-4), 293-314.

Zimmermann, M.G., Natiello, M.A. [1998] Homoclinic and heteroclinic bifurcations close to a twisted heteroclinic cycle. *Int. J. Bif. Chaos*, **8**(2), 359-375.

Zoladek, H. [1984]. On the versality of symmetric vector fields in the plane. *Math. USSR-Sb.* **48**, 463–492.

Zoladek, H. [1987]. Bifurcations of certain family of planar vector fields tangent to axes. *Differential Equations* **67**, 1–55.

Zoldi, S., Greenside, H. S. [1998] Spatially Localized Unstable Periodic Orbits of a High Dimensional Chaotic System. *Phys. Rev. E.*, **57**(3), R2511-R2514.

Index

ϵ pseudo orbit, 758
ω Limit Set of A Nonautonomous System, 242
ω and α Limit Points of Trajectories, 104
ω and α limit sets, 104
k-jet Extension of a Map, 400
k-jet of a Map, 398
n-degree-of-freedom integrable Hamiltonian systems, 82
integrable Hamiltonian system, 82
integrable vector field, 77
separatrix, 80
1-torus, 77
1:1 Resonance, 328
1:2 Resonance, 330
1:3 Resonance, 331

full shift on N symbols, 612

absorbing set, 108
Action Principle in Phase Space, 182
Action Space, 220
Adjoint Action, 420, 485
affine map, 130
Anosov diffeomorphisms, 756
Arnold Tongues, 542
Asymptotic Orbital Stability, 9
Asymptotic Stability, 7
asymptotically autonomous vector fields, 242
asymptotically stable, 11
Attracting Sets, 107
Attraction in Nonautonomous Systems, 111
Attractor, 110
Attractors, 107
autonomous, 2
Autonomous Vector Fields, 92
Axiom A diffeomorphisms, 756

Banach space, 394
Basin of Attraction, 108
Basins of Attraction, 107
Bendixson's criterion, 72
bifurcation, 359
Bifurcation of a Fixed Point, 361, 362
Bifurcation of Fixed Points of Vector Fields, 356
bifurcation value, 359
Bifurcations Creating the Horseshoe, 658
Bifurcations Near Resonant Elliptic Equilibrium Points, 495
Bifurcations of Fixed Points of Maps, 498
Birkhoff Normal Form, 333
Birkhoff normal form, 333
Birkhoff's theorem, 334

canonical symplectic form, 199
center, 16
Center Manifold, 246
Center Manifolds, 245
Center Manifolds at a Saddle-node Bifurcation Point for Vector Fields, 375
Center Manifolds Depending on Parameters, 251
Center Manifolds for Maps, 257
Center Manifolds for Vector Fields, 246
Centralizer, 487
Centralizer of a Matrix, 421
Chaos, 573, 736
chaotic attractors, 75

chaotic dynamics, 555, 687
Chaotic Invariant Set, 736
Chaotic Saddle, 747
circle, 77
closing lemma, 74
Cocycle, 97
Codimension of a Bifurcation, 392
Codimension of a Fixed Point, 403
Codimension of a Homoclinic Bifurcation, 775
Codimension of a Local Bifurcation, 402
Codimension of a Submanifold, 393
Codimension of Local Bifurcations of Maps, 523
Complete Integral of the Hamilton-Jacobi Equation, 188
Completely Integrable Hamiltonian Systems, 210
complex coordinates, 333
Complexification of a Real Linear Map, 31
Complexification of a Subspace, 31
Computation of Normal Forms, 354
configuration space, 171
Conjugacy, 152
Conley-Moser Conditions, 585
constraints, 169
Construction of a Versal Deformation, 407
Continuation of Solutions, 91
critical point, 5
Cyclic Coordinates, 178
cylinder, 82

Definition of the Smale Horseshoe Map, 555
Deformation of a Matrix, 418
degree theory, 88
Derivation of Lagrange's Equations, 172
Descartes' Rule of Signs, 13
Devils Staircase, 548
difference equation, 1
Differentiability of the Unstable Manifold, 48
Differentiability with Respect to Parameters, 91
Dihedral Group of Order $2n$, 309
Diophantine Frequencies, 217
Dirichlet's theorem, 26
Divergence of the Normalizing Transformations, 354
double-Hopf bifurcation, 305, 416
Double-Pulse Homoclinic Orbits, 676
Double-Zero Eigenvalue, 413, 777
Double-Zero Eigenvalue with Symmetry, 446
Dulac, 72
Dynamical Averaging, 75
dynamical systems, 1
Dynamics of Completely Integrable Hamiltonian Systems in Action-Angle Coordinates, 211

Eigenvalue of -1, 512
Eigenvalues of Infinitesimally Symplectic Matrices, 206
Eigenvalues of Symplectic Matrices, 203
Elementary Hamiltonian Bifurcations, 491
elliptic, 16
Elphick-Tirapegui-Brachet-Coullet-Iooss Normal Form, 290
Energy Integral, 176
Equilibria of Vector Fields, 5
equilibrium solution, 5
Equivalence of Deformations, 418, 486
Equivariant Map, 312
exchange of stability, 360

existence, 90
Existence of Arnold Tongues, 545
Existence of Invariant Manifolds, 43
Exponential Dichotomy, 53
exponential map, 318
extended phase space, 56

Family Induced from a Deformation, 407, 418
feedback control systems, 479
first integral, 77
first variational equation, 706
fixed point, 5
flow, 93
Fluid Transport, 724
Foliation of Resonant Tori, 213
Foliations of Stable, Unstable, and Center Manifolds, 61
forced van der Pol equation, 576
forward convergence, 112
frequency map, 212
Frequency Space, 220
frozen time vector field, 5
fundamental solution matrix, 726
Fundamental Theorem of Algebra, 13

Generalized Coordinates, 170
generalized force, 173
generalized momentum, 177
generalized velocities, 171
Geometry of the Melnikov Function, 711
Geometry of the Resonances, 220
Global Bifurcations, 777
Global Unstable Manifold, 48
Green's theorem on the plane, 72
Group, 306
Group Action, 338
Gustavson normal form, 333

Hénon map, 241
Hénon Map, 742
Hadamard's Method, 44
Hamilton's canonical equations, 200
Hamilton's Equations, 177
Hamilton's equations, 177
Hamilton's Equations in Poisson Bracket Form, 201
Hamilton's Principle of Least Action, 182
Hamilton's Principle of Least Action in Phase Space, 183
Hamilton-Jacobi Equation, 187
Hamiltonian Normal Forms, 316
Hamiltonian Normal Forms and Symmetries, 338
Hamiltonian Pitchfork, 492
Hamiltonian Saddle Node, 491
Hamiltonian-Dissipative Decomposition, 790
Harmonic Response, 132
Hartman-Grobman Theorem, 350
Hausdorff Metric, 113
Hausdorff Separation, 113
Heteroclinic Cycle, 632, 788
Heteroclinic Cycles, 476, 631
heteroclinic orbit, 542
holonomic constraints, 169
Homoclinic Bifurcations, 762
homoclinic orbit, 542
homoclinic orbits, 448
Homological Equation, 354
Hopf bifurcation theorem, 385
Hopf fibration, 85
Hopf- steady state, 416
Hopf-Steady State Bifurcation, 477
Hopf-steady state interaction, 416
Hyperbolic Attractors, 742
Hyperbolic Fixed Point, 12
Hyperbolic Invariant Set, 754
Hyperbolic Invariant Sets, 747
Hyperbolic Trajectories, 53
Hyperbolic Trajectory, 55
hyperbolic trajectory in the extended phase space, 56

implicit function theorem, 356, 364, 367, 368
Inclusion of Linearly Unstable Directions, 263
index theory, 87, 443
Induced Family, 486
infinite-dimensional space of dynamical systems, 397
infinitesimally reversible, 236
Infinitesimally Symplectic Transformations, 204
Inner Product on H_k, 291
integral, 77
integral curve, 2
Invariance of the Graph of a Function, 39
invariant Cantor set, 576
Invariant Manifold, 28
Invariant Manifolds, 28
Invariant Manifolds for Stochastic Dynamical Systems, 62
Invariant Set, 28
invariant subspaces, 245
Invariant Two-Tori, 787
involution, 234
Irrational Rotation Number, 542

KAM theorem, 221, 223
KAM Theorem for Symplectic Maps, 225
kinetic energy, 173
Kronecker flow, 212

Lagrangian, 174
Lagrangian dynamical systems, 169
Lagrangian function, 174
lambda lemma, 615, 631
LaSalle Invariance Principle, 110
Liapunov exponent in the direction e, 727
Liapunov Exponents, 726
Liapunov function, 107
Liapunov Functions, 20
Liapunov Stability, 7
Liapunov stability, 222
Liapunov's theorem, 26
Liapunov- Perron Method, 44
Liapunov-Perron Method, 49
Liapunov-Perron operator, 50
Lie algebra theory, 273
Lie Group, 307
Lie Group Action on a Vector Space, 307
Lie Group Actions, 306
Lie Group Actions on Vector Spaces, 310
Lie Groups, 306
Lie transforms, 319
Lift of a Circle Map, 531
line bundle, 748
Linearization, 10
Linearization of Reversible Dynamical Systems, 236
Linearly Unstable Directions, 256
Liouville's Theorem, 99
Lipschitz functions, 586
Lorenz Equations, 253
Lorenz equations, 658
Lyapunov Subcenter Theorem, 334, 335

map, 1
Maps, 15
Maps of the Circle, 530
Markov partitions, 756
Melnikov Function, 703
Melnikov theory, 779
Melnikov's Method, 687
Melnikov's Method for Autonomous Perturbations, 721
Method of Amplitude Expansions, 354
miniversal, 419, 487
mode interaction, 416
Momentum Integrals, 177
Morse Function, 222
Morse oscillator, 722
Moser's Theorem, 334, 336

Moser's theorem, 612, 622
multiple homoclinic orbits, 636
Multiplicity of a Resonance, 213

n-dimensional Orthogonal Group, 308
n-dimensional Unitary Group, 309
Naimark-Sacker Bifurcation, 517
Nekhoroshev, 221
Nekhoroshev Theorem for Symplectic Maps, 224
Nekoroshev's theorem, 223
non- resonant double-Hopf bifurcation, 416
Non-Semisimple Double Zero Eigenvalue, 314
nonautonomous, 2
Nonautonomous Systems, 354
Nonautonomous Vector Fields, 94
Nondegenerate Critical Point, 222
nonhyperbolic fixed points, 246
Nonresonance, 548
Nonuniqueness of Normal Forms, 353
Nonwandering Points, 106
Nonwandering Set, 107
Normal Basis, 729
Normal Form Coefficients, 314
Normal Form for a Map Near a Fixed Point, 303
Normal Form for a Vector Field Near a Periodic Orbit, 303
Normal Form for the Naimark-Sacker Torus Bifurcation, 285
normal form for the pitchfork bifurcation, 511
Normal Form for The Poincaré-Andronov-Hopf Bifurcation, 279
normal form for the transcritical bifurcation, 508
Normal Form of a Vector Field Depending on Parameters, 302
normal form theorem, 318
Normal Forms, 270
Normal Forms for Resonant Elliptic Fixed Points of Two Degree-of-Freedom Systems, 327
Normal Forms for Stochastic Systems, 355
Normal Forms for Vector Fields, 270
Normal Forms for Vector Fields with Parameters, 278
Normal Forms Near Elliptic Fixed Points, 322

One-Dimensional Maps, 524
One-Dimensional Non-Invertible Maps, 741
Orbit Under the Adjoint Action, 420, 486
orbital derivative, 22
Orbital Stability, 9
Orbits Homoclinic to a Saddle-Focus, 659
Orbits Homoclinic to a Saddle-Point with Purely Real Eigenvalues, 640
Orbits Homoclinic to Hyperbolic Fixed Points, 636
Order of a Resonance, 213
order of the resonance, 322, 352
ordinary differential equation, 1
orientation preserving topological conjugacy, 541
orientation-preserving homeomorphisms, 530
Oseledec multiplicative ergodic theorem, 730

Pair of Eigenvalues of Modulus 1, 517
Pair of Pure Imaginary Pairs of Eigenvalues, 316

Parametric Version of $\mathbf{C}^0$-Equivalence, 406
Parametrized Families of Maps, 263
Pendulum, 174
pendulum, 82
Period Doubling, 512
Period-Doubling Bifurcation, 515
period-doubling bifurcation, 767
Periodic Orbits, 71, 475
Periodically Forced Linear Oscillators, 128
phase curve, 2
phase flow, 93
Phase Locking, 550
phase space, 1
photodissociation of molecules, 722
Pitchfork Bifurcation, 370, 389, 508
pitchfork bifurcation, 360, 372
Poincaré Maps, 122
Poincaré maps, 94
Poincaré Recurrence Theorem, 101
Poincaré-Andronov-Hopf Bifurcation, 384, 392, 410
Poincaré-Andronov-Hopf bifurcation, 450, 461, 467, 493, 518
Poincaré-Andronov-Hopf normal form, 468, 470
Poincaré-Bendixson, 117
Poincaré-Bendixson Theorem, 384
Poincaré Map Associated with a Two Degree-of-Freedom Hamiltonian System, 144
Poincaré Map Near a Periodic Orbit, 123
Poincaré Maps, 711
Poincaré–Andronov–Hopf, 439
Poincaré–Andronov–Hopf bifurcation, 283
Poincaré-Andronov-Hopf bifurcation, 442, 777
Poisson Brackets, 200
potential, 79
potential function, 173
power system dynamics, 478
Principle of Least Action, 180
Properties of ω Limit Points, 105
Properties of Center Manifolds, 263
Properties of Reversible Dynamical Systems, 239
Properties of the Melnikov Function, 713
pseudo orbits, 756
Pullback Absorbing Family, 114
Pullback Attracting Set, 113
pullback convergence, 112

Quasiconvexity, 222
quasilinear partial differential equation, 248
Quasiperiodic Response, 137

Rational Rotation Number, 542
Real Hamiltonians as Functions of Complex Variables, 324
Real Normal Forms and Complex Coordinates, 355
reduced to quadratures, 210
reduction principle, 246
Regular Family, 729
Representation, 308
representation of a group, 308
Resonance, 212
resonant double- Hopf bifurcation, 416
Resonant Normal Form, 334
rest point, 5
Reversible, 238
Reversible Dynamical Systems, 234
Rotation Number, 539
rotation number, 532
Routh table, 14
Routh's Equations, 178

Routh's function, 179
Routh-Hurwitz criterion, 13
Routhian, 179

saddle, 16
Saddle-Node Bifurcation, 363, 387, 500
saddle-node bifurcation, 359, 364, 366, 371, 503, 767
satellite, 721
Sector Bundles, 602, 757
sector bundles, 625
Semiclassical Mechanics, 75
Sensitive Dependence on Initial Conditions, 736
Shadowing Lemma, 758
Shift Map, 581
Silnikov phenomenon, 659
singularity, 5
sink, 16
Skew-Product Flow, 95
Smale Horseshoe, 555
Smale horseshoe, 636
Smale–Birkhoff Homoclinic Theorem, 629
Smale–Birkhoff homoclinic theorem, 612
Smooth Linearization, 355
solution, 2
source, 16
Space of k-jets, 399
Space of Vector-Valued Homogeneous Polynomials of Degree k, 273
Special Orthogonal Group, 308
Special Unitary Group, 309
Stability of Bifurcations Under Perturbations, 387
Stability of Elliptic Equilibria, 222
Stability of Trajectories, 7
Stable and Unstable Manifolds of Hyperbolic Trajectories, 56
stable node, 16
Standard map, 241
stationary point, 5
steady state, 5
Strange Attractor, 740
Strange Attractors, 658, 736, 742
strong resonances, 525
structurally stable, 356, 756
subcritical, 383
subharmonic Melnikov theory, 688
Subharmonic Response of Order m, 133
Subharmonics, 131
supercritical, 383
Symbolic Dynamics, 566, 576
Symmetric Dynamical Systems, 312
symmetric fixed point, 236
Symmetries, 306
Symmetries of the Normal Form, 296
Symplectic Forms, 199
symplectic Group, 309
symplectic maps, 223
symplectic polar coordinates, 333
symplectic structure, 199
symplectic transformation, 207

Takens-Bogdanov Bifurcation, 436
Takens-Bogdanov Normal Form, 276
Tangency of the Vector Field to the Graph, 39
Tangent Space Approximation, 250
The "Double-Hopf" Bifurcation, 298
The Graph Transform, 44
The Kinetic Energy, 175
The Normal Form Theorem, 275
The Poincaré Map of a Time-Periodic Ordinary Differential Equation, 127
Thom transversality theorem, 401, 407
three-spheres, 83

three-tori, 478
time dependent, 2
time independent, 2
time series, 75
Time-Dependent Hyperbolic Trajectories, 52
time-dependent Melnikov function, 704
Topological Transitivity, 110
topologically transitive, 737, 739
trajectory, 2
Transcritical Bifurcation, 366, 389, 504
transcritical bifurcation, 360, 369, 370
Transformation of Hamilton's Equations Under Symplectic Transformations, 208
Transversality, 627
Transversality of a Map, 420
Transversality of a Map to a Submanifold, 400
transverse heteroclinic point, 634
transverse homoclinic orbits, 687
Trapping Region, 107
Two Homoclinic Orbits without Symmetry, 658
Two-Dimensional Maps, 524
Two-Manifolds, 77

Ultraharmonic Response of Order n, 134
Ultraharmonics, 131
Ultrasubharmonic Response of Order m, n, 136
Ultrasubharmonics, 131
unforced Duffing oscillator, 77
uniqueness, 90
Uniqueness of Stable, Unstable, and Center Manifolds, 39
universal, 419, 487
unstable node, 16

van der Pol equation, 448
Variation of the Cross-Section, 154, 155
Variational Methods, 180
vector field, 1
versal, 487
Versal Deformation, 407
Versal Deformations, 406
Versal Deformations of Families of Matrices, 417
Versal Deformations of Linear Hamiltonian Systems, 482
Versal Deformations of Linear, Reversible Dynamical Systems, 490
Versal Deformations of Quadratic Hamiltonians of Codimension ≤ 2, 488
Versal Deformations of Real Matrices, 431
Volume Preserving Vector Fields, 101

Williamson's Theorem, 482

Zero and a Pair of Pure Imaginary Eigenvalues, 315
Zero and a Pure Imaginary Pair of Eigenvalues, 449
Zero Eigenvalue, 357